



NUREG/CR-7272

NRC ATWS-I Stability Tests with Downskew Axial Power Profile

KATHY Test Series STS123

AVAILABILITY OF REFERENCE MATERIALS IN NRC PUBLICATIONS

NRC Reference Material

As of November 1999, you may electronically access NUREG-series publications and other NRC records at the NRC's Library at www.nrc.gov/reading-rm.html. Publicly released records include, to name a few, NUREG-series publications; *Federal Register* notices; applicant, licensee, and vendor documents and correspondence; NRC correspondence and internal memoranda; bulletins and information notices; inspection and investigative reports; licensee event reports; and Commission papers and their attachments.

NRC publications in the NUREG series, NRC regulations, and Title 10, "Energy," in the *Code of Federal Regulations* may also be purchased from one of these two sources:

1. The Superintendent of Documents

U.S. Government Publishing Office
Washington, DC 20402-0001
Internet: www.bookstore.gpo.gov
Telephone: (202) 512-1800
Fax: (202) 512-2104

2. The National Technical Information Service

5301 Shawnee Road
Alexandria, VA 22312-0002
Internet: www.ntis.gov
1-800-553-6847 or, locally, (703) 605-6000

A single copy of each NRC draft report for comment is available free, to the extent of supply, upon written request as follows:

Address: **U.S. Nuclear Regulatory Commission**
Office of Administration
Multimedia, Graphics, and Storage &
Distribution Branch
Washington, DC 20555-0001
E-mail: distribution.resource@nrc.gov
Facsimile: (301) 415-2289

Some publications in the NUREG series that are posted at the NRC's Web site address www.nrc.gov/reading-rm/doc-collections/nuregs are updated periodically and may differ from the last printed version. Although references to material found on a Web site bear the date the material was accessed, the material available on the date cited may subsequently be removed from the site.

Non-NRC Reference Material

Documents available from public and special technical libraries include all open literature items, such as books, journal articles, transactions, *Federal Register* notices, Federal and State legislation, and congressional reports. Such documents as theses, dissertations, foreign reports and translations, and non-NRC conference proceedings may be purchased from their sponsoring organization.

Copies of industry codes and standards used in a substantive manner in the NRC regulatory process are maintained at—

The NRC Technical Library

Two White Flint North
11545 Rockville Pike
Rockville, MD 20852-2738

These standards are available in the library for reference use by the public. Codes and standards are usually copyrighted and may be purchased from the originating organization or, if they are American National Standards, from—

American National Standards Institute

11 West 42nd Street
New York, NY 10036-8002
Internet: www.ansi.org
(212) 642-4900

Legally binding regulatory requirements are stated only in laws; NRC regulations; licenses, including technical specifications; or orders, not in NUREG-series publications. The views expressed in contractor prepared publications in this series are not necessarily those of the NRC.

The NUREG series comprises (1) technical and administrative reports and books prepared by the staff (NUREG-XXXX) or agency contractors (NUREG/CR-XXXX), (2) proceedings of conferences (NUREG/CP-XXXX), (3) reports resulting from international agreements (NUREG/IA-XXXX), (4) brochures (NUREG/BR-XXXX), and (5) compilations of legal decisions and orders of the Commission and the Atomic and Safety Licensing Boards and of Directors' decisions under Section 2.206 of the NRC's regulations (NUREG-0750).

DISCLAIMER: This report was prepared as an account of work sponsored by an agency of the U.S. Government. Neither the U.S. Government nor any agency thereof, nor any employee, makes any warranty, expressed or implied, or assumes any legal liability or responsibility for any third party's use, or the results of such use, of any information, apparatus, product, or process disclosed in this publication, or represents that its use by such third party would not infringe privately owned rights.

NRC ATWS-I Stability Tests with Downskew Axial Power Profile

KATHY Test Series STS123

Manuscript Completed: September 2020

Date Published: September 2020

Prepared by:

D. Tinkler¹, K. Greene¹, K. Quick¹

J. Kronenberg², R. Velton², F. Wehle²

A. Beisiegel³, T. Berger³, F. El Rharbaoui³

P. Yarsky⁴

¹Framatome Inc.
Richland, WA 99354, USA

²Framatome GmbH
91001 Erlangen, Germany

³Framatome GmbH
63787 Karlstein, Germany

⁴U.S. Nuclear Regulatory Commission
Washington DC, 20555

Tarek Zaki, NRC Project Manager

Office of Nuclear Regulatory Research

ABSTRACT

Natural circulation instability tests were performed in the Multifunction Thermal Hydraulic Test Facility KATHY in Karlstein, Germany. One type of test involved stepping up test assembly power in oscillating flow until failure to rewet occurs based on temperature observation. A second type of test introduced a simulated neutronic feedback to dynamically change the power, again with flow oscillations up to the point of failure to rewet. Two tests featured a transient inlet temperature. The largest flow oscillations in the test program ranged from ~ -7 kilograms per second (kg/s) to 13 kg/s. The tests varied system pressure (7 and 8 megapascals), water level in the steam-water separator (0.4 and 1.1 meters), and inlet subcooling (20 Kelvin and 35 Kelvin). A full-scale boiling-water reactor rod bundle was simulated in these tests. Before the dynamic instability tests, the rod bundle was characterized with single-phase- and two-phase pressure drop tests. Steady-state critical power tests were also performed to characterize the conditions under which steady-state dryout occurs. This report describes the tests performed as part of this program. This research effort supported the continued development and benchmarking of the U.S. Nuclear Regulatory Commission (NRC) reactor systems analysis computer code with state-of-the-art, realistic modeling capabilities thereby enabling more effective use of confirmatory calculations in licensing reviews.

TABLE OF CONTENTS

ABSTRACT	iii
LIST OF FIGURES	ix
LIST OF TABLES	ix
EXECUTIVE SUMMARY	xi
ABBREVIATIONS AND ACRONYMS	xiii
1 INTRODUCTION	1-1
1.1 Steady-State Tests STS-123.01 and STS-123.02	1-1
1.2 Instability Tests STS-123.03.....	1-1
2 TEST LOOP	2-1
2.1 Steady-State Tests STS-123.01 and STS-123.02	2-2
2.2 Instability Test STS-123.03.....	2-2
2.3 Test Bundle	2-4
2.4 Radial Power Distribution and Thermocouple Positions STS-123.01	2-6
2.5 Radial Power Distribution and Thermocouple Positions STS-123.02 and STS-123.03	2-11
2.6 Heater Rod Characteristics (Specified).....	2-16
2.7 Pressure Taps Along the Test Bundle	2-17
2.8 Pressure Taps Along the Loop and Instrumentation	2-18
2.9 Hydraulic Characteristics	2-19
3 STEADY-STATE TEST RESULTS	3-1
3.1 Critical Heat Flux Tests	3-1
3.2 Pressure Drop Tests.....	3-5
3.2.1 Single-Phase Pressure Drop Tests.....	3-5
3.2.2 Two-Phase Pressure Drop Tests.....	3-7
3.3 Heat Balance Measurement	3-11
3.4 Replicate Test Procedure	3-13
4 INSTABILITY TEST RESULTS	4-1
4.1 Natural Circulation Instability Tests.....	4-1
4.2 Test Matrix	4-1
4.2.1 Non-SINAN Tests	4-2
4.2.2 SINAN Tests.....	4-2
4.2.3 Transient Tests.....	4-2
4.3 Summary of Test Data.....	4-2
4.4 Replicate Test Procedure	4-3
5 TEST RUN IDENTIFICATION CONVENTION	5-1
6 EVALUATION OF THE MEASURED DATA	6-1
6.1 Pressure Drop Results over the Test Bundle.....	6-1
6.1.1 Measurement Range	6-1
6.1.2 Geodetic Correction.....	6-2
6.1.3 Irreversible Correction	6-2

6.2	Pressure Drop Results over the Test Loop	6-2
6.2.1	Geodetic Correction.....	6-2
6.2.2	Irreversible Correction	6-3
6.3	System Pressure	6-4
6.4	Water Level in the Steam-Water Separator	6-4
6.5	Inlet Mass Flow Instability Test STS-123.03	6-4
6.5.1	Turbine Flow Meter S73 CF08.....	6-4
6.5.2	Mass Evaluation by Inlet Pressure Drop S73 CP12	6-6
6.6	Inlet Subcooling.....	6-7
7	MEASUREMENT UNCERTAINTIES.....	7-1
7.1	Electrical Power Uncertainty	7-1
7.2	Fluid Flow by Nozzle Uncertainty	7-1
7.3	System Pressure Uncertainty	7-3
7.4	Differential Pressure Uncertainty	7-3
7.5	Inlet Subcooling Uncertainty	7-3
8	CONCLUSION.....	8-1
9	NOTES	9-1
9.1	Steady-State Tests STS-123.01, STS-123.02	9-1
9.2	Instability Test STS-123.03.....	9-1
APPENDIX A	REQUIREMENTS FOR STEADY-STATE AND	
	ATWS-I TESTS	A-1
APPENDIX B	LIST OF ATWS-I TEST DATA	B-1
APPENDIX C	TEST MATRIX INSTABILITY TEST STS-123.03	
	INITIAL CONDITIONS	C-1
APPENDIX D	PLOTS OF INSTABILITY TEST STS-123.03-101.01	D-1
APPENDIX E	PLOTS OF INSTABILITY TEST STS-123.03-102.01	E-1
APPENDIX F	PLOTS OF INSTABILITY TEST STS-123.03-103.01	F-1
APPENDIX G	PLOTS OF INSTABILITY TEST STS-123.03-104.01	G-1
APPENDIX H	PLOTS OF INSTABILITY TEST STS-123.03-104.02	H-1
APPENDIX I	PLOTS OF INSTABILITY TEST STS-123.03-104.03	I-1
APPENDIX J	PLOTS OF INSTABILITY TEST STS-123.03-105.01	J-1
APPENDIX K	PLOTS OF INSTABILITY TEST STS-123.03-105.02	K-1
APPENDIX L	PLOTS OF INSTABILITY TEST STS-123.03-106.01	L-1
APPENDIX M	PLOTS OF INSTABILITY TEST STS-123.03-107.01	M-1
APPENDIX N	PLOTS OF INSTABILITY TEST STS-123.03-108.01	N-1
APPENDIX O	PLOTS OF INSTABILITY TEST STS-123.03-109.01	O-1
APPENDIX P	PLOTS OF INSTABILITY TEST STS-123.03-110.01	P-1
APPENDIX Q	PLOTS OF INSTABILITY TEST STS-123.03-201.01	Q-1
APPENDIX R	PLOTS OF INSTABILITY TEST STS-123.03-202.01	R-1
APPENDIX S	PLOTS OF INSTABILITY TEST STS-123.03-203.01	S-1
APPENDIX T	PLOTS OF INSTABILITY TEST STS-123.03-203.02	T-1
APPENDIX U	PLOTS OF INSTABILITY TEST STS-123.03-204.01	U-1
APPENDIX V	PLOTS OF INSTABILITY TEST STS-123.03-205.01	V-1
APPENDIX W	PLOTS OF INSTABILITY TEST STS-123.03-206.01	W-1

APPENDIX X	PLOTS OF INSTABILITY TEST STS-123.03-207.01	X-1
APPENDIX Y	PLOTS OF INSTABILITY TEST STS-123.03-207.02	Y-1
APPENDIX Z	PLOTS OF INSTABILITY TEST STS-123.03-207.03	Z-1
APPENDIX AA	PLOTS OF INSTABILITY TEST STS-123.03-A01.01	AA-1
APPENDIX BB	PLOTS OF INSTABILITY TEST STS-123.03-F01.01	BB-1
APPENDIX CC	PLOTS OF INSTABILITY TEST STS-123.03-G01.01	CC-1
APPENDIX DD	PLOTS OF INSTABILITY TEST STS-123.03-C01.01	DD-1
APPENDIX EE	PLOTS OF INSTABILITY TEST STS-123.03-D01.01	EE-1
APPENDIX FF	PLOTS OF INSTABILITY TEST STS-123.03-B01.01	FF-1
APPENDIX GG	PLOTS OF INSTABILITY TEST STS-123.03-401.01	GG-1
APPENDIX HH	PLOTS OF INSTABILITY TEST STS-123.03-402.01	HH-1
APPENDIX II	PLOTS OF INSTABILITY TEST STS-123.03-403.01	II-1
APPENDIX JJ	PLOTS OF INSTABILITY TEST STS-123.03-404.01	JJ-1
APPENDIX KK	PLOTS OF INSTABILITY TEST STS-123.03-405.01	KK-1
APPENDIX LL	PLOTS OF INSTABILITY TEST STS-123.03-406.01	LL-1
APPENDIX MM	PLOTS OF INSTABILITY TEST STS-123.03-407.01	MM-1
APPENDIX NN	PLOTS OF INSTABILITY TEST STS-123.03-301.01	NN-1
APPENDIX OO	PLOTS OF INSTABILITY TEST STS-123.03-302.01	OO-1
APPENDIX PP	PLOTS OF INSTABILITY TEST STS-123.03-303.01	PP-1
APPENDIX QQ	PLOTS OF INSTABILITY TEST STS-123.03-304.01	QQ-1
APPENDIX RR	PLOTS OF INSTABILITY TEST STS-123.03-305.01	RR-1
APPENDIX SS	PLOTS OF INSTABILITY TEST STS-123.03-306.01	SS-1
APPENDIX TT	PLOTS OF INSTABILITY TEST STS-123.03-307.01	TT-1
APPENDIX UU	PLOTS OF INSTABILITY TEST STS-123.03-308.01	UU-1
APPENDIX VV	PLOTS OF INSTABILITY TEST STS-123.03-309.01	VV-1
APPENDIX WW	PLOTS OF INSTABILITY TEST STS-123.03-310.01	WW-1
APPENDIX XX	PLOTS OF INSTABILITY TEST STS-123.03-A11.01	XX-1
APPENDIX YY	PLOTS OF INSTABILITY TEST STS-123.03-B11.01	YY-1
APPENDIX ZZ	PLOTS OF INSTABILITY TEST STS-123.03-C11.01	ZZ-1
APPENDIX AAA	PLOTS OF INSTABILITY TEST STS-123.03-D11.01	AAA-1
APPENDIX BBB	PLOTS OF INSTABILITY TEST STS-123.03-F11.01	BBB-1
APPENDIX CCC	PLOTS OF INSTABILITY TEST STS-123.03-G11.01	CCC-1
APPENDIX DDD	PLOTS OF INSTABILITY TEST STS-123.03-F11.02	DDD-1
APPENDIX EEE	PLOTS OF INSTABILITY TEST STS-123.03-F11.03	EEE-1
APPENDIX FFF	PLOTS OF INSTABILITY TEST STS-123.03-E11.01	FFF-1
APPENDIX GGG	PLOTS OF INSTABILITY TEST STS-123.03-E01.01	GGG-1
APPENDIX HHH	PLOTS OF INSTABILITY TEST STS-123.03-A01.02	HHH-1
APPENDIX III	PLOTS OF INSTABILITY TEST STS-123.03-101.02	III-1
APPENDIX JJJ	PLOTS OF INSTABILITY TEST STS-123.03-T01.01	JJJ-1
APPENDIX KKK	PLOTS OF INSTABILITY TEST STS-123.03-T01.02	KKK-1
APPENDIX LLL	MASS FLOW RATES FROM DP-INLET S73 CP12A	LLL-1

LIST OF FIGURES

Figure 2-1	KATHY Thermal-Hydraulic Loop	2-3
Figure 2-2	Spacer Example 1.....	2-4
Figure 2-3	Spacer Example 2.....	2-5
Figure 2-4	Radial Power Distribution, STS-123.01, Revision 1, Global	2-7
Figure 2-5	Radial Power Distribution, STS-123.01, Revision 1, Axial Zone 1	2-8
Figure 2-6	Radial Power Distribution, STS-123.01, Revision 1, Axial Zone 2	2-9
Figure 2-7	TC Positions, STS-123.01.....	2-10
Figure 2-8	Radial Power Distributions, STS-123.02 and STS-123.03, Revision 0, Global	2-12
Figure 2-9	Radial Power Distributions, STS-123.02 and STS-123.03, Revision 0, Axial Zone 1	2-13
Figure 2-10	Radial Power Distributions, STS-123.02 and STS-123.03, Revision 0, Axial Zone 2.....	2-14
Figure 2-11	TC Positions, STS-123.02 and STS-123.03	2-15

LIST OF TABLES

Table 2-1	Measurement Transducer Channel Names and Pressure Tap Elevations	2-17
Table 3-1	Critical Bundle Power, STS-123.01	3-2
Table 3-2	Single-Phase Pressure Drops, STS-123.02	3-6
Table 3-3	Two-Phase Pressure Drops, STS-123.02	3-8
Table 3-4	Heat Balance Measurement, STS-123.01	3-12

EXECUTIVE SUMMARY

A variety of critical heat flux (CHF), pressure drop, and flow instability tests were performed in the Multifunction Thermal Hydraulic Test Facility KATHY of the laboratories of Framatome GmbH, located in Karlstein, Germany, in 2016. These tests were performed on a boiling-water reactor test bundle configuration. This research effort supported the continued development and benchmarking of the U.S. Nuclear Regulatory Commission (NRC) reactor systems analysis computer code with state-of-the-art, realistic modeling capabilities thereby enabling more effective use of confirmatory calculations in licensing reviews.

Steady-state CHF tests were performed with the test bundle STS-123.01 from August 22 to 24, 2016. The thermal-hydraulic conditions covered pressures from 5.5 megapascals (MPa) to 8.3 MPa, flow rates from 3.0 to 12.6 kilograms per second (kg/s) and inlet temperatures from 224 degrees Celsius (C) to 289 degrees C. Six high-powered heater rods with a maximum radial peaking factor of ~ 1.26 were placed in the test bundle.

Most CHF events were observed at rod position 69, at thermocouple (TC)-level 1 for flow rates up to ~ 7 kg/s and with a transition to TC-level 3 for larger flow rates. Less frequent CHF events were observed at rod position 23 TC-level 1 and rod position 87 TC-level 1.

Single- and two-phase pressure drop tests were performed with the test bundle STS-123.02 on September 23, 2016. The nominal system pressure was 6.9 MPa. The flow rates ranged from 3.2 to 18.9 kg/s at an inlet temperature of 260 degrees C for single-phase and 274 degrees C for two-phase pressure drop tests.

The largest single-phase pressure drop was ~ 700 millibar (mbar) at the measurement points S73 CP1013 and S73 CP210 for a flow rate of 18.9 kg/s. The parallel installed "K" (narrow measurement range) and "G" (wide measurement range) differential pressure transducers showed good agreement.

The largest two-phase pressure drop was close to 1500 mbar at the measurement points S73 CP1013 and S73 CP210 for a flow rate of 15.8 kg/s and a bundle power of 8 megawatts. The parallel installed "K" and "G" differential pressure transducers showed good agreement as long as the end of measurement range for the "K" transducers was not reached (S73 CP210K and S73 CP219K).

Natural circulation instability tests were performed with the test bundle STS-123.03 from December 10 to 20, 2016. The nominal thermal-hydraulic conditions varied from 7.0 to 8.0 MPa in pressure, 20 to 35 Kelvin in subcooling at the inlet, and 0.4- to 1.1-meter level in the separator. Two types of tests were performed. In the first type, the test bundle power was increased stepwise until a failure to rewet was observed based on temperature excursion. In the second type, a separate neutronic feedback power module calculated online an additional dynamic power contribution.

In total, 41 test runs were performed without simulated neutronic feedback and 19 test runs were performed with simulated neutronic feedback. These tests also include two tests with transient inlet temperature. The largest mass flow oscillation was observed ranging from ~ -7 kg/s to ~ 13 kg/s during test run T01.02.

ABBREVIATIONS AND ACRONYMS

ATWS-I	anticipated transient without scram instability
BOHL	beginning of heated length
CHF	critical heat flux
DAkks	Deutsche Akkreditierungsstelle GmbH (the national accreditation body for the Federal Republic of Germany)
DAQ	Data Acquisition System
DIN	Deutsches Institut für Normung (the German Institute for Standardization)
DR	decay ratio
EN	English
EOHL	end of heated length
ID	channel name
ISA	International Federation of the National Standardizing Associations
ISO	International Organization for Standardization
KATHY	Karlstein Thermal Hydraulic Test Loop
NRC	U.S. Nuclear Regulatory Commission
PC	personal computer
PLHR	part-length heater rod
Rhosub	harmonic mode subcriticality in \$
SINAN	An online power feedback module uses a measured inlet flow rate to simulate a realistic power response. This calculated power response is then output as a power demand to the loop.
STS	“ <i>Siedewasser Test Strecke</i> ” = boiling-water reactor test section
Tau	fuel thermal time constant in s
TC	thermocouple
Vrcmul	void reactivity coefficient multiplying factor
ΔT	change in temperature from initial temperature

1 INTRODUCTION

1.1 Steady-State Tests STS-123.01 and STS-123.02

From August 22 to 24, 2016, and on September 23, 2016, steady-state critical heat flux (CHF) tests as well as single- and two-phase pressure drop tests were performed according to the test specification with the test bundles STS-123.01 and STS-123.02 in the Multifunction Thermal Hydraulic Test Facility KATHY of the laboratories of Framatome GmbH in Karlstein, Germany.

STS-123.01 (CHF tests)

Date of tests	August 22 to 24, 2016
Test specification	see Appendix A
Pressure	5.5, 6.9, and 8.3 megapascals (MPa)
Mass flow rate	3 to 12.6 kilograms per second (kg/s)
Inlet temperature	224.4 to 288.6 ° Celsius (C)
Inlet subcooling	50 to 220 kilojoules per kilogram (kJ/kg)
Customers attendant	J. Kronenberg, Framatome GmbH (August 22 to 24, 2016) P. Yarsky, U.S. Nuclear Regulatory Commission (NRC) (August 22 to 24, 2016) T. Zaki, NRC (August 22 to 24, 2016) S. Brown, Orano (August 22 to 24, 2016)

STS-123.02 (Pressure drop tests)

Date of tests	September 23, 2016
Test specification	see Appendix A
Pressure	6.9 MPa
Mass flow rate	3.15 to 18.9 kg/s
Inlet temperatures	260 °C (Single-phase) / 273.8 °C (Two-phase)
Inlet subcooling	127.8 kJ/kg (Single-phase) / 58.2 kJ/kg (Two-phase)
Customers attendant	J. Kronenberg, Framatome GmbH (September 23, 2016)

The test results are only valid for the tested bundles STS-123.01 to STS-123.02.

1.2 Instability Tests STS-123.03

From December 10 to 20, 2016, natural circulation instability tests were performed according to the test specification in Appendix A with the test bundle STS-123.03 in the Multifunction Thermal Hydraulic Test Facility KATHY of the laboratories of Framatome GmbH in Karlstein, Germany. Section 2.2 describe the natural circulation setup.

At each subcooling, the test bundle power was increased stepwise until a failure to rewet was observed based on temperature excursion.

Appendix B indicates in the column “*Feedback active*” when an online power feedback module (described in Appendix A) was used to measure the inlet flow rate and to simulate a realistic power response. This calculated power response was then dynamically output as an additional power demand to the stationary loop base power.

STS-123.03 (Instability tests)

Date of commissioning	December 7, 2016
Date of tests	December 10 to 20, 2016
Test specification	see Appendix A
Pressure	7.0 and 7.9 MPa
Mass flow rate	Natural circulation
Inlet temperature	~275 °C to ~248 °C
Inlet subcooling	~100 to ~193 kJ/kg
Customers attendant	P. Yarsky, NRC (December 7, December 12 to 20, 2016) T. Zaki, NRC (December 7, December 12 to 16, 2016) D. Tinkler, Framatome Inc. (December 7, December 12 to 20, 2016) J. Kronenberg, Framatome GmbH (December 12 to 16, 2016) S. Brown, Orano (December 12 to 20, 2016) R. Velten, Framatome GmbH (December 7, December 10 to 20, 2016) F. Wehle, Framatome GmbH (December 12 to 20, 2016) D. Kreuter, Framatome GmbH (December 20, 2016)

Appendix C provides the initial thermal-hydraulic test conditions of the instability measurements.

2 TEST LOOP

Figure 2-1 shows that the thermal-hydraulic test facility is a high-pressure water heat transfer loop containing a test vessel with the test assembly and upper and lower electrical bus bars, high-pressure coolers, a direct contact condenser, an electrically heated pressurizer, and the main circulation pumps. The figure shows two inlet flow lines of different sizes. The different sizes allow fine control of the flow rate over a broad range. The direct current power supply consists of four thyristor controlled rectifiers.

As shown in Figure 2-1, the forced flow loop may be reconfigured into a natural circulation loop. The natural circulation loop consists of the test vessel housing, the test bundle with the electric power supply system, and the riser that connects the upper plenum of the test section with the steam-water separator, and the downcomer. This configuration has no circulation pump. To measure the mass flow rate oscillations, a turbine flow meter is installed in the horizontal inlet pipe coming from the downcomer. Inside the steam-water separator, the two-phase flow mixture is passively separated. The saturated water leaves the separator at the bottom and is mixed in the vertical feed water injector with colder feed water to adjust the specified inlet subcooling. To discharge the saturated steam generated in the test bundle and to adjust the inlet subcooling, the natural circulation loop is connected to the 22-megawatt high-pressure boiler system of the Karlstein laboratory. The saturated steam leaves the separator at the top and flows to the condenser of the boiler system.

The Data Acquisition System (DAQ) samples the analog signals of the loop instrumentation, digitizing them with 16-bit analog-to-digital converters and stores the signals on hard disk. The hardware of the DAQ is based on National Instruments SCXI-bus components.¹ Six personal computers (PCs) are used: one controls the acquisition and data flow; three provide display and visualization of selected channels, including thermocouples (TCs), during tests; one is used to display test results following each test run; and one computer is used by the test monitoring engineer to access results directly. The data acquisition software is based on the programming language of "LabView." Evaluation software is applied to transfer the raw data (voltage) into physical values (e.g., pressure, temperature) is written in "C."

The same direct current power supply provides power to each of the test bundles STS-123.01, STS-123.02, and STS-123.03. The design power is ~ 20 megawatts. The current is measured by DynAmp transformer and redundantly by shunts, which leads to several measurement points of bundle power:

- S73_FC01: Measured gross bundle power. Current is measured by shunts (S73CE03IS).
- P_FC01Net: Measured net bundle power. Current is measured by shunts (S73CE03IS).
- S73_FC02: Measured gross bundle power. Current is measured by the DynAmp-transformer (S73_CE09IWA).
- P_FC02Net: Measured net bundle power. Current is measured by the DynAmp-transformer (S73_CE09IWA).

¹ "Getting Started with SCXI," National Instruments Corporation, Report No. 320515F-01, July 2000 edition.

The gross bundle power *includes* the power consumption of the external compensation rods (P_Comp_Bundle) for the part-length heater rods. The net bundle power *excludes* the power consumption of the external compensation rods for the part-length heater rods. Finally, the alias POWER points to the measurement point P_FC02Net.

2.1 Steady-State Tests STS-123.01 and STS-123.02

The bundles STS-123.01 and STS-123.02 were tested in the steady-state test setup of the Multifunction Thermal Hydraulic Test Facility KATHY of the Karlstein laboratories of Framatome GmbH.

2.2 Instability Test STS-123.03

The bundle STS-123.03 was tested in the natural circulation loop configuration setup of the Multifunction Thermal Hydraulic Test Facility KATHY.

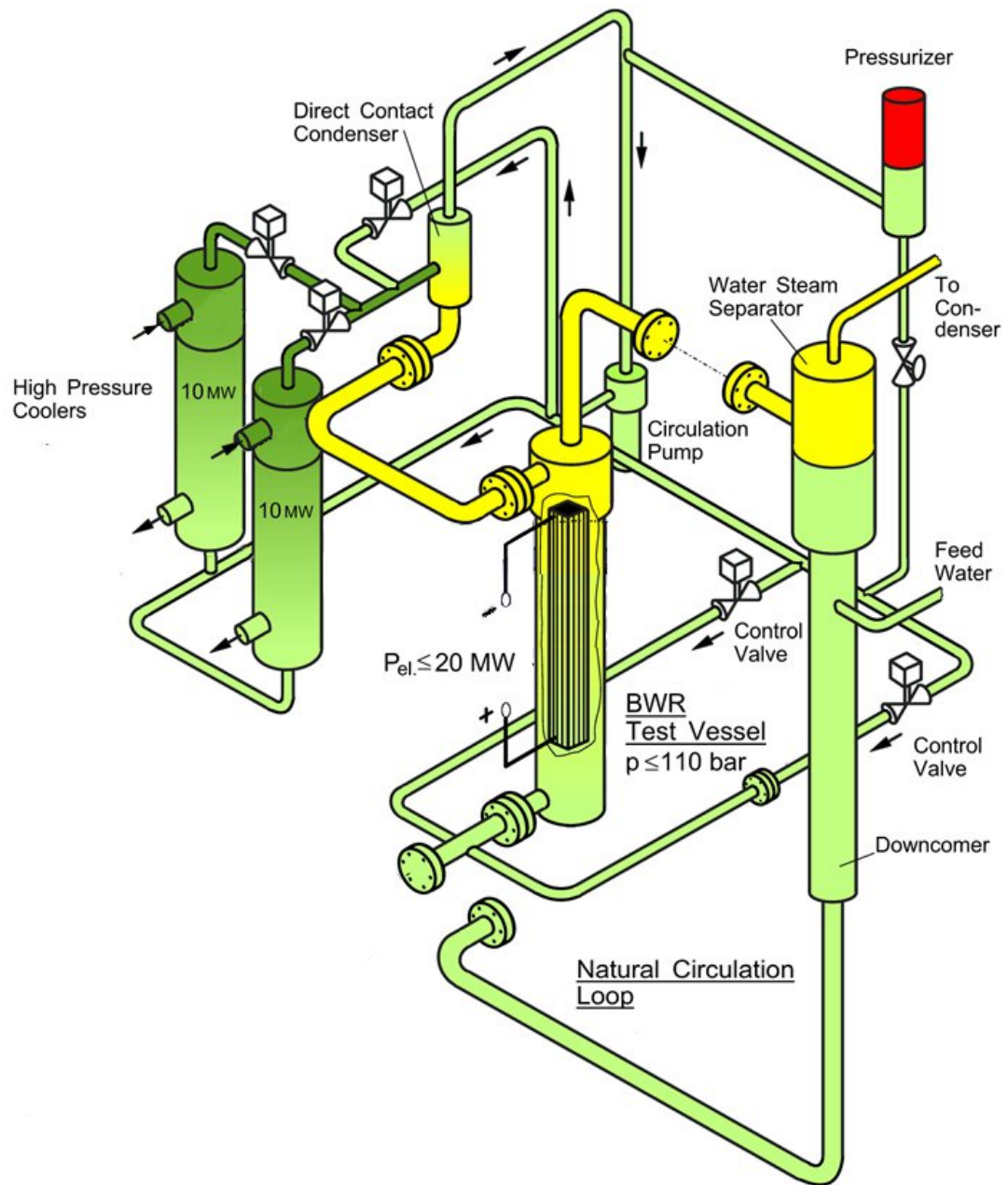


Figure 2-1 KATHY Thermal-Hydraulic Loop

2.3 Test Bundle

STS-123.01, STS-123.02 and STS-123.03

Lattice arrangement		10x10 square array
Spacer type	AH00–AH0 and AH10	AH62/18
	AH1–AH5	AH61/24
	AH6–AH9	AH61/22
Number of spacers within heated length		9
Total number of spacers		12

The tested bundle design was never commercially operated but does contain features that are common to modern boiling-water reactor fuel—flow channel, rods, and spacers with swirl vanes. Photos showing examples of the test spacers are provided in Figure 2-2 and Figure 2-3.

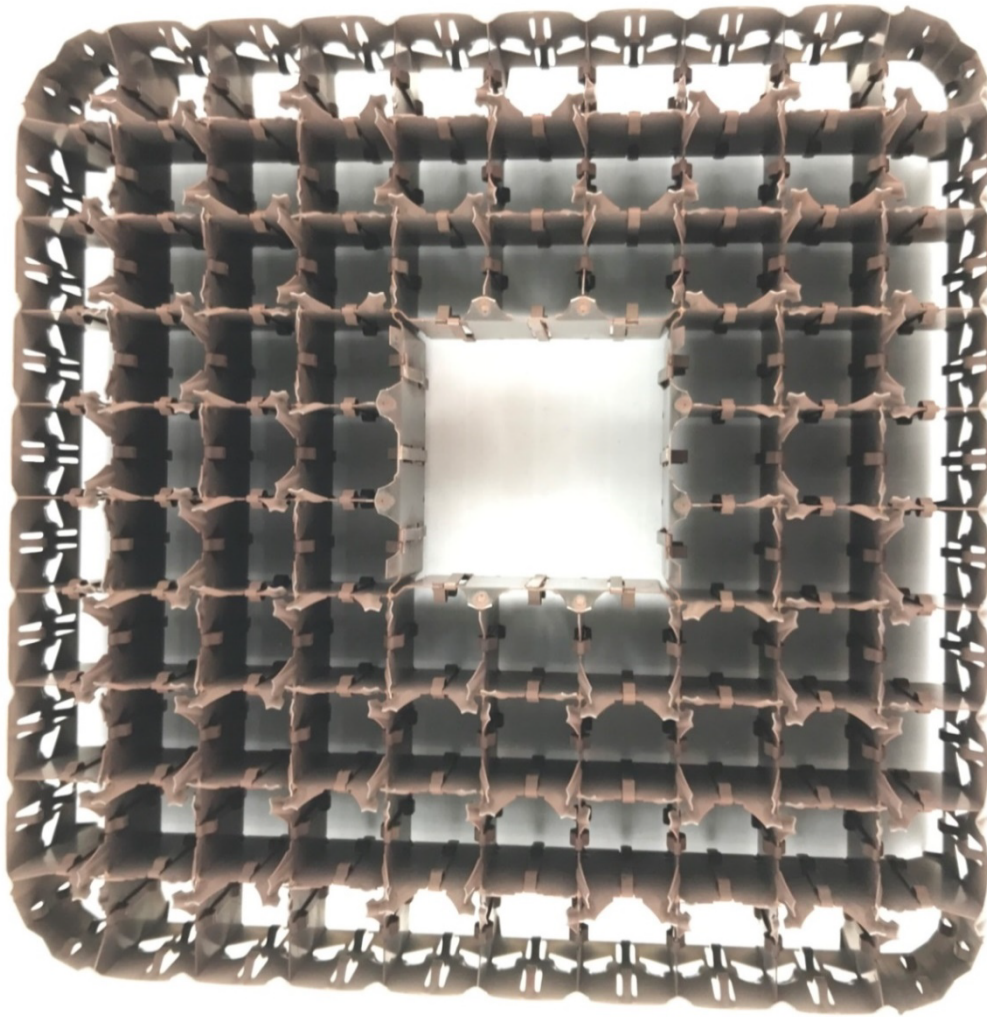


Figure 2-2 Spacer Example 1

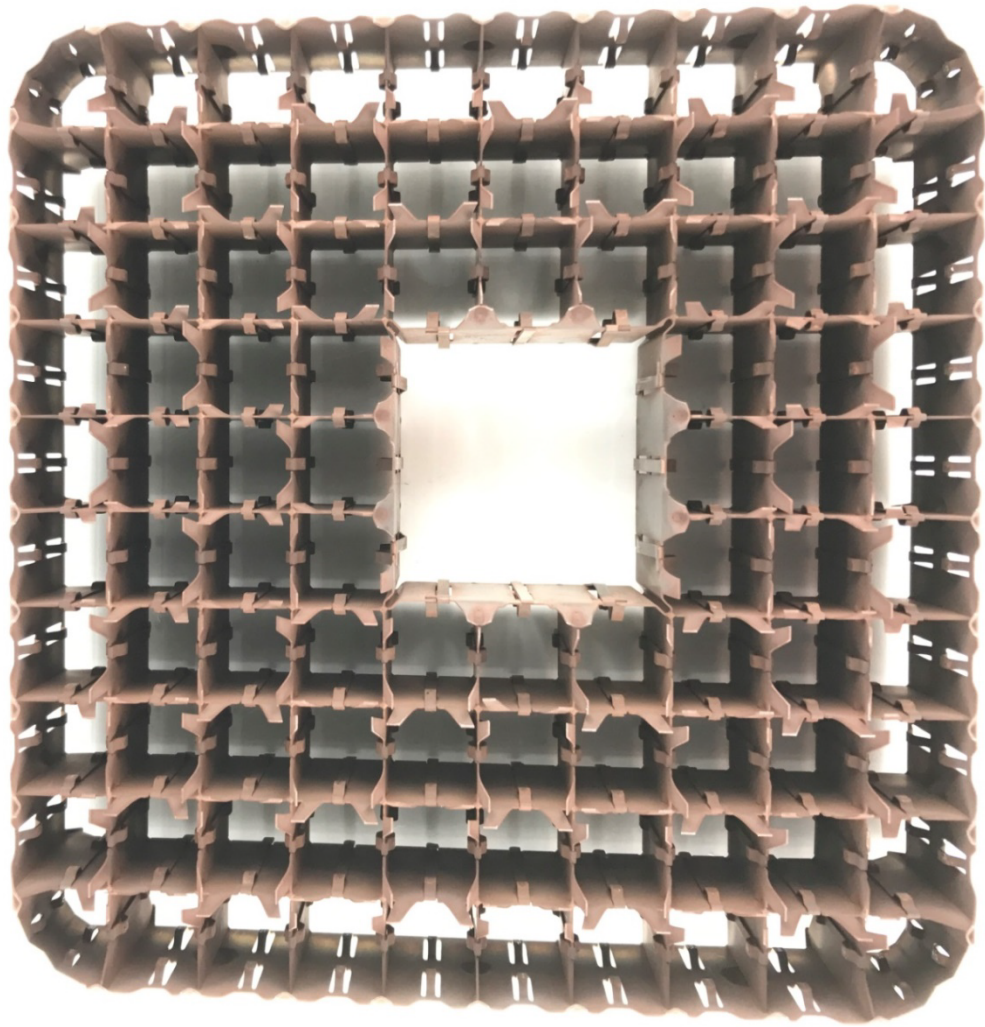


Figure 2-3 Spacer Example 2

2.4 Radial Power Distribution and Thermocouple Positions STS-123.01

The CHF tests were performed with the test bundle STS-123.01.

Figure 2-4 to Figure 2-6 show the radial power distribution of STS-123.01.

Figure 2-7 shows the TC positions of STS-123.01.

The nonoperational TCs during STS-123.01 were as follows:

8/1Z	From test run 412.01
29/4X	From test run 296.01
54/5Z	From test run 411.02
58/1Z, 58/3Z, 58/5X, 58/6Z	From test run 311.03
58/2Z, 58/4X	From beginning to end
58/3X	From test run 311.02
58/4Z	From test run 301.01
58/5Z	From test run 311.01
59/1Z	From beginning to end
78/3Z	From test run 300.01
80/5Z	From beginning to end
98/4Z	From test run 311.02
98/5X	From test run 295.01

Rod-No. Rodname P-Factor

1 W3006 1.056	2 W2D01B 1.173	3 W3007 1.049	4 W2D05B 1.171	5 W3008 1.056	6 W2D07B 1.172	7 W3009 1.049	8 W2D08B 1.171	9 W3010 1.052	10 W3011 1.055
11 W2D09B 1.172	12 W6003K B 0.682	13 W4006 0.915	14 W4008 0.919	15 W6005K B 0.675	16 W4009 0.923	17 W3012 1.051	18 W4010 0.921	19 W6006K B 0.680	20 W2D10B 1.173
21 W3013 1.057	22 W4011 0.920	23 W3D08B 1.075	24 W4003B 0.934	25 W4012 0.915	26 W4014 0.916	27 W4015 0.917	28 W4045B 0.929	29 W3D09B 1.081	30 W3014 1.051
31 W2D11B 1.174	32 W4016 0.917	33 W4017 0.920	34 W4018 0.920	35 W4019 0.920	36 W3016 1.055	37 W4020 0.921	38 W4022 0.918	39 W4023 0.912	40 W3017 1.050
41 W3018 1.058	42 W6008K B 0.674	43 W4024 0.920	44 W4025 0.919				48 W6009K B 0.680	49 W4026 0.912	50 W3020 1.061
51 W2D12B 1.173	52 W4027 0.921	53 W4028 0.917	54 W3D16B 1.074				58 W3D07B 1.077	59 W1D07B 1.259	60 W3D10B 1.072
61 W3021 1.055	62 W3D11B 1.076	63 W4031 0.918	64 W4047B 0.934				68 W6020K B 0.676	69 W1D08B 1.258	70 W3D12B 1.081
71 W2D13B 1.166	72 W4032 0.915	73 W4037 0.915	74 W4040 0.923	75 W6012K B 0.679	76 W3D13B 1.080	77 W6014K B 0.674	78 W3D14B 1.077	79 W1D09B 1.258	80 W3D15B 1.075
81 W3022 1.056	82 W6015K B 0.673	83 W3023 1.057	84 W4049B 0.948	85 W4041 0.925	86 W1D11B 1.268	87 W1D12B 1.260	88 W1D13B 1.267	89 W6016K B 0.677	90 W3024 1.054
91 W3025 1.056	92 W2D14B 1.172	93 W3026 1.056	94 W3027 1.055	95 W3030 1.045	96 W3D02B 1.078	97 W3D04B 1.077	98 W3D06B 1.077	99 W3032 1.056	100 W3033 1.050

Figure 2-4 Radial Power Distribution, STS-123.01, Revision 1, Global

Rod-No. Rodname P-Factor

1 W3006 1.009	2 W2D01B 1.121	3 W3007 1.003	4 W2D05B 1.119	5 W3008 1.009	6 W2D07B 1.120	7 W3009 1.003	8 W2D08B 1.119	9 W3010 1.005	10 W3011 1.008
11 W2D09B 1.120	12 W6003K B 1.058	13 W4006 0.875	14 W4008 0.878	15 W6005K B 1.046	16 W4009 0.882	17 W3012 1.005	18 W4010 0.880	19 W6006K B 1.054	20 W2D10B 1.121
21 W3013 1.010	22 W4011 0.879	23 W3D08B 1.027	24 W4003B 0.893	25 W4012 0.874	26 W4014 0.876	27 W4015 0.876	28 W4045B 0.888	29 W3D09B 1.033	30 W3014 1.005
31 W2D11B 1.122	32 W4016 0.877	33 W4017 0.879	34 W4018 0.879	35 W4019 0.879	36 W3016 1.008	37 W4020 0.880	38 W4022 0.878	39 W4023 0.872	40 W3017 1.004
41 W3018 1.011	42 W6008K B 1.046	43 W4024 0.879	44 W4025 0.879				48 W6009K B 1.054	49 W4026 0.871	50 W3020 1.014
51 W2D12B 1.121	52 W4027 0.880	53 W4028 0.876	54 W3D16B 1.026				58 W3D07B 1.030	59 W1D07B 1.203	60 W3D10B 1.024
61 W3021 1.009	62 W3D11B 1.028	63 W4031 0.877	64 W4047B 0.892				68 W6020K B 1.048	69 W1D08B 1.202	70 W3D12B 1.033
71 W2D13B 1.115	72 W4032 0.875	73 W4037 0.875	74 W4040 0.882	75 W6012K B 1.054	76 W3D13B 1.033	77 W6014K B 1.045	78 W3D14B 1.029	79 W1D09B 1.203	80 W3D15B 1.027
81 W3022 1.009	82 W6015K B 1.043	83 W3023 1.010	84 W4049B 0.906	85 W4041 0.884	86 W1D11B 1.212	87 W1D12B 1.204	88 W1D13B 1.211	89 W6016K B 1.049	90 W3024 1.007
91 W3025 1.010	92 W2D14B 1.120	93 W3026 1.009	94 W3027 1.008	95 W3030 0.999	96 W3D02B 1.031	97 W3D04B 1.029	98 W3D06B 1.029	99 W3032 1.009	100 W3033 1.004

Figure 2-5 Radial Power Distribution, STS-123.01, Revision 1, Axial Zone 1

Rod-No. Rodname P-Factor

1 W3006 1.015	2 W2D01B 1.128	3 W3007 1.009	4 W2D05B 1.126	5 W3008 1.015	6 W2D07B 1.127	7 W3009 1.009	8 W2D08B 1.126	9 W3010 1.012	10 W3011 1.014
11 W2D09B 1.127		13 W4006 0.880	14 W4008 0.883		16 W4009 0.887	17 W3012 1.011	18 W4010 0.885		20 W2D10B 1.128
21 W3013 1.016	22 W4011 0.884	23 W3D08B 1.034	24 W4003B 0.898	25 W4012 0.880	26 W4014 0.881	27 W4015 0.882	28 W4045B 0.893	29 W3D09B 1.039	30 W3014 1.011
31 W2D11B 1.129	32 W4016 0.882	33 W4017 0.885	34 W4018 0.884	35 W4019 0.885	36 W3016 1.014	37 W4020 0.886	38 W4022 0.883	39 W4023 0.877	40 W3017 1.010
41 W3018 1.017		43 W4024 0.885	44 W4025 0.884					49 W4026 0.877	50 W3020 1.021
51 W2D12B 1.128	52 W4027 0.886	53 W4028 0.882	54 W3D16B 1.033				58 W3D07B 1.036	59 W1D07B 1.211	60 W3D10B 1.031
61 W3021 1.015	62 W3D11B 1.034	63 W4031 0.883	64 W4047B 0.898					69 W1D08B 1.210	70 W3D12B 1.040
71 W2D13B 1.122	72 W4032 0.880	73 W4037 0.880	74 W4040 0.888		76 W3D13B 1.039		78 W3D14B 1.035	79 W1D09B 1.210	80 W3D15B 1.034
81 W3022 1.015		83 W3023 1.016	84 W4049B 0.912	85 W4041 0.889	86 W1D11B 1.219	87 W1D12B 1.212	88 W1D13B 1.219		90 W3024 1.013
91 W3025 1.016	92 W2D14B 1.127	93 W3026 1.016	94 W3027 1.014	95 W3030 1.005	96 W3D02B 1.037	97 W3D04B 1.036	98 W3D06B 1.036	99 W3032 1.016	100 W3033 1.010

Figure 2-6 Radial Power Distribution, STS-123.01, Revision 1, Axial Zone 2

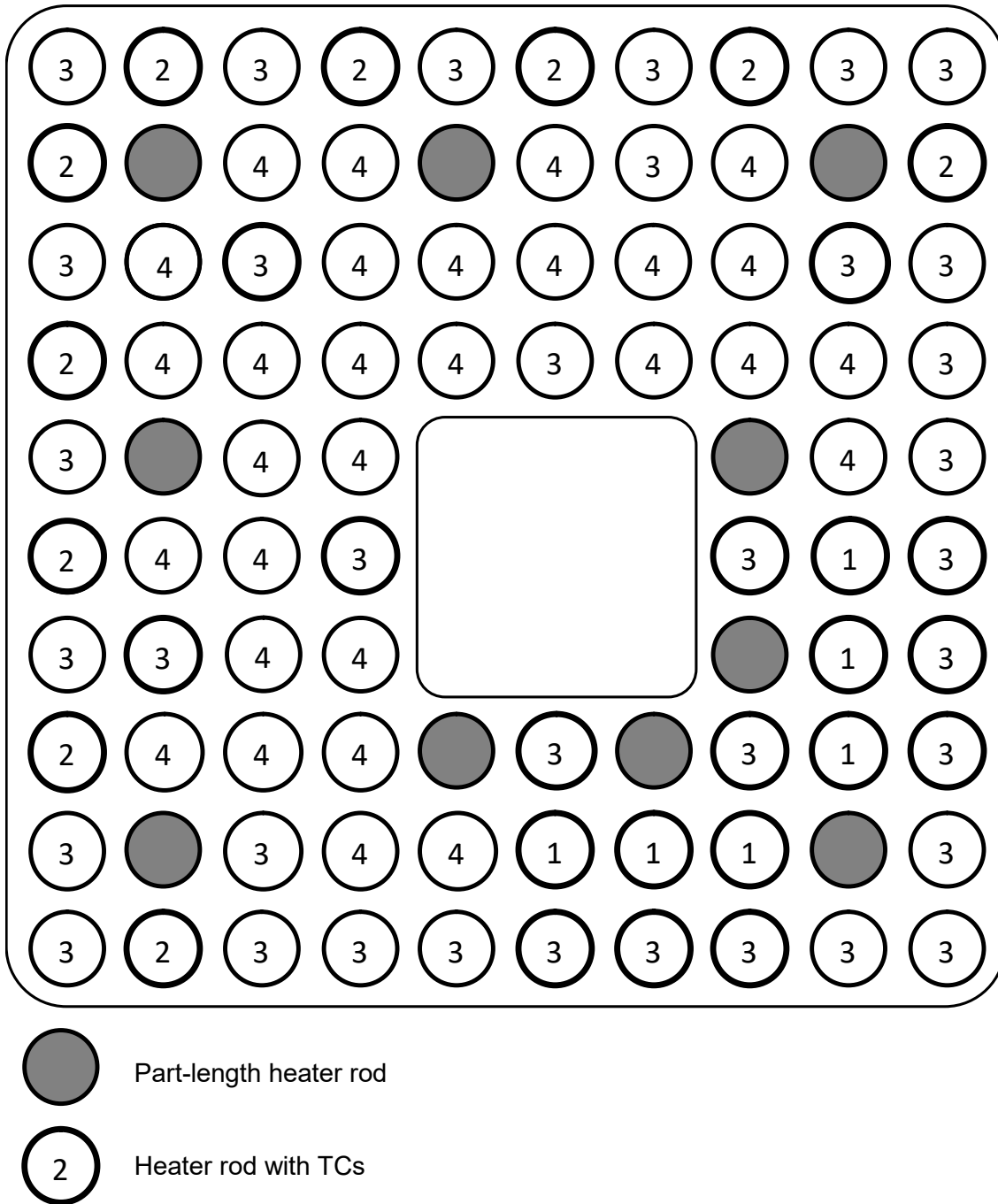


Figure 2-7 TC Positions, STS-123.01

2.5 Radial Power Distribution and Thermocouple Positions STS-123.02 and STS-123.03

The pressure drop tests were performed with the test bundle STS-123.02.

The instability tests were performed with the test bundle STS-123.03.

The test bundle STS-123.01 was inspected after completing the CHF tests and reassembled before the pressure drop tests on STS-123.02.

Together with the reassembling of STS-123.02, several heater rods were replaced to increase the number of available heater rod TCs.

The reassembling resulted in the following differences:

Pos.	STS-123.01		STS-123.02/STS-123.03
17	W3012	→	W3C02B
23	W3D08B	→	W3C01B
36	W3016	→	W3C03B
58	W3D07B	→	W3D08B
59	W1D07B	→	W1D11B
62	W3D11B	→	W3D06B
83	W3023	→	W3C04B
86	W1D11B	→	W1D14B
98	W3D06B	→	W3D11B

The test bundles STS-123.02 and STS-123.03 have the same radial power distributions and TC positions.

Figure 2-8 to Figure 2-10 show the radial power distribution.

Figure 2-11 shows the TC positions.

Of the TCs monitored during test STS-123.02, the following nonoperational TCs were observed:

17/2Z	From beginning to end
69/2Z	From beginning to end
88/4Z	From beginning to end
96/4Z	From beginning to end
97/4X	From beginning to end
98/5Z	From beginning to end

Of the TCs monitored during test STS-123.03, the following nonoperational TCs were observed:

6/3X	From beginning to end
17/2Z	From beginning to end
88/4Z	From beginning to end
98/5Z	From beginning to end

Between tests, repairs to TCs were attempted and were sometimes successful. This is the reason that the number of nonoperational TCs in test STS-123.03 is lower than in STS-123.02.

Rod-No.
Rodname
P-Factor

1 W3006 1.056	2 W2D01B 1.172	3 W3007 1.049	4 W2D05B 1.170	5 W3008 1.055	6 W2D07B 1.172	7 W3009 1.049	8 W2D08B 1.171	9 W3010 1.052	10 W3011 1.054
11 W2D09B 1.171	12 W6003K B 0.683	13 W4006 0.915	14 W4008 0.918	15 W6005K B 0.675	16 W4009 0.923	17 W3C02B 1.065	18 W4010 0.920	19 W6006K B 0.680	20 W2D10B 1.173
21 W3013 1.056	22 W4011 0.919	23 W3C01B 1.063	24 W4003B 0.934	25 W4012 0.915	26 W4014 0.916	27 W4015 0.917	28 W4045B 0.929	29 W3D09B 1.080	30 W3014 1.051
31 W2D11B 1.173	32 W4016 0.917	33 W4017 0.920	34 W4018 0.919	35 W4019 0.920	36 W3C03B 1.063	37 W4020 0.921	38 W4022 0.918	39 W4023 0.912	40 W3017 1.050
41 W3018 1.058	42 W6008K B 0.675	43 W4024 0.920	44 W4025 0.919				48 W6009K B 0.680	49 W4026 0.912	50 W3020 1.061
51 W2D12B 1.173	52 W4027 0.921	53 W4028 0.917	54 W3D16B 1.073				58 W3D08B 1.075	59 W1D11B 1.267	60 W3D10B 1.072
61 W3021 1.055	62 W3D06B 1.077	63 W4031 0.918	64 W4047B 0.933				68 W6020K B 0.676	69 W1D08B 1.257	70 W3D12B 1.081
71 W2D13B 1.166	72 W4032 0.915	73 W4037 0.915	74 W4040 0.923	75 W6012K B 0.680	76 W3D13B 1.080	77 W6014K B 0.674	78 W3D14B 1.076	79 W1D09B 1.258	80 W3D15B 1.075
81 W3022 1.056	82 W6015K B 0.673	83 W3C04B 1.065	84 W4049B 0.948	85 W4041 0.924	86 W1D14B 1.262	87 W1D12B 1.260	88 W1D13B 1.267	89 W6016K B 0.677	90 W3024 1.053
91 W3025 1.056	92 W2D14B 1.171	93 W3026 1.056	94 W3027 1.054	95 W3030 1.045	96 W3D02B 1.078	97 W3D04B 1.077	98 W3D11B 1.075	99 W3032 1.056	100 W3033 1.050

Figure 2-8 Radial Power Distributions, STS-123.02 and STS-123.03, Revision 0, Global

Rod-No. Rodname P-Factor

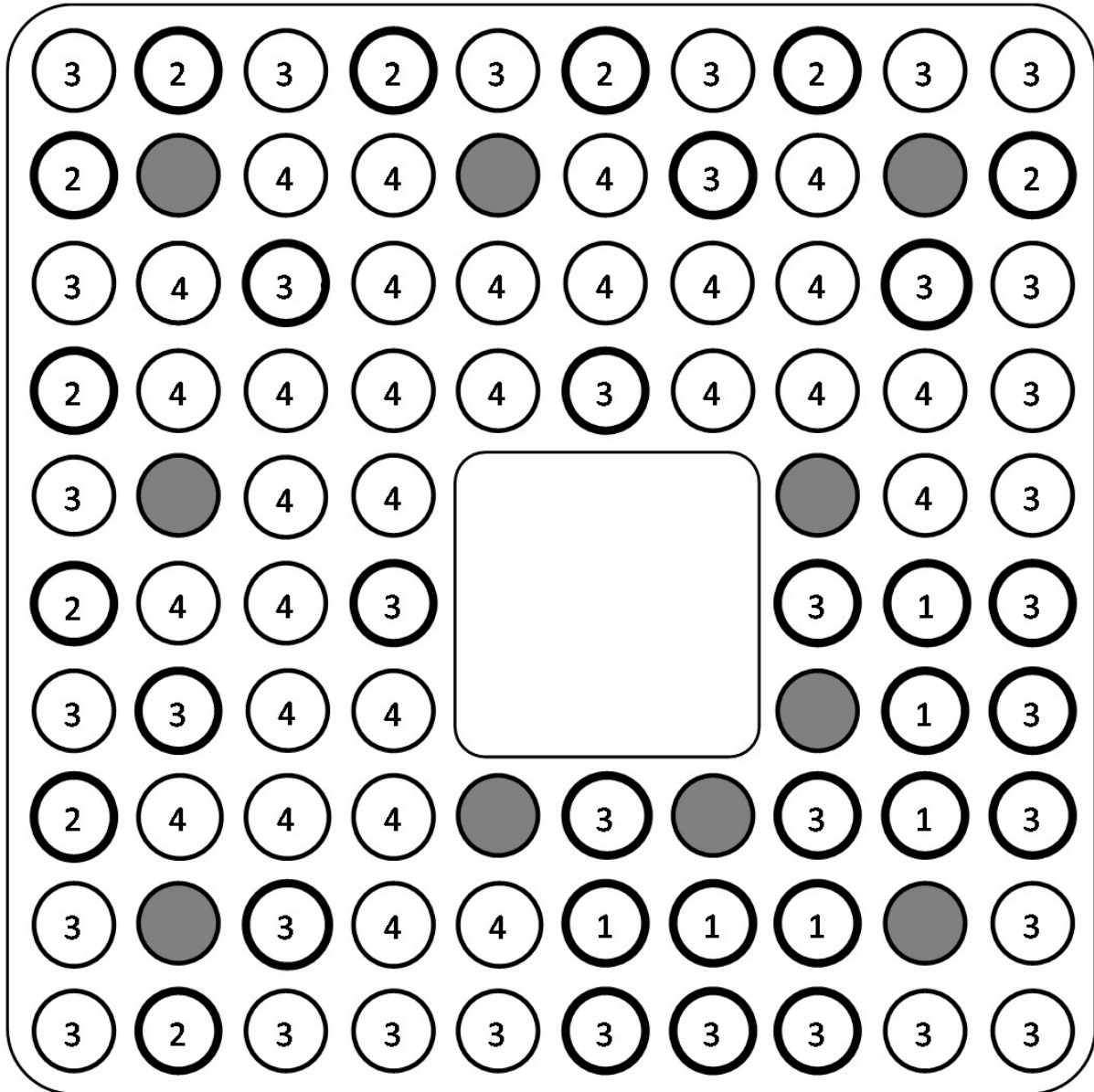
1 W3006 1.009	2 W2D01B 1.120	3 W3007 1.003	4 W2D05B 1.118	5 W3008 1.009	6 W2D07B 1.120	7 W3009 1.003	8 W2D08B 1.119	9 W3010 1.005	10 W3011 1.008
11 W2D09B 1.119	12 W6003K B 1.058	13 W4006 0.875	14 W4008 0.878	15 W6005K B 1.046	16 W4009 0.882	17 W3C02B 1.018	18 W4010 0.880	19 W6006K B 1.055	20 W2D10B 1.121
21 W3013 1.010	22 W4011 0.879	23 W3C01B 1.016	24 W4003B 0.892	25 W4012 0.874	26 W4014 0.876	27 W4015 0.876	28 W4045B 0.888	29 W3D09B 1.033	30 W3014 1.005
31 W2D11B 1.121	32 W4016 0.876	33 W4017 0.879	34 W4018 0.879	35 W4019 0.879	36 W3C03B 1.016	37 W4020 0.880	38 W4022 0.877	39 W4023 0.871	40 W3017 1.003
41 W3018 1.011	42 W6008K B 1.046	43 W4024 0.879	44 W4025 0.878				48 W6009K B 1.054	49 W4026 0.871	50 W3020 1.014
51 W2D12B 1.121	52 W4027 0.880	53 W4028 0.876	54 W3D16B 1.026				58 W3D08B 1.027	59 W1D11B 1.211	60 W3D10B 1.024
61 W3021 1.008	62 W3D06B 1.029	63 W4031 0.877	64 W4047B 0.892				68 W6020K B 1.048	69 W1D08B 1.202	70 W3D12B 1.033
71 W2D13B 1.114	72 W4032 0.875	73 W4037 0.875	74 W4040 0.882	75 W6012K B 1.054	76 W3D13B 1.032	77 W6014K B 1.045	78 W3D14B 1.029	79 W1D09B 1.202	80 W3D15B 1.027
81 W3022 1.009	82 W6015K B 1.043	83 W3C04B 1.018	84 W4049B 0.906	85 W4041 0.883	86 W1D14B 1.206	87 W1D12B 1.204	88 W1D13B 1.211	89 W6016K B 1.050	90 W3024 1.007
91 W3025 1.009	92 W2D14B 1.120	93 W3026 1.009	94 W3027 1.008	95 W3030 0.999	96 W3D02B 1.030	97 W3D04B 1.029	98 W3D11B 1.028	99 W3032 1.009	100 W3033 1.004

Figure 2-9 Radial Power Distributions, STS-123.02 and STS-123.03, Revision 0, Axial Zone 1

Rod-No. Rodname P-Factor

1 W3006 1.015	2 W2D01B 1.127	3 W3007 1.009	4 W2D05B 1.125	5 W3008 1.015	6 W2D07B 1.127	7 W3009 1.009	8 W2D08B 1.126	9 W3010 1.011	10 W3011 1.014
11 W2D09B 1.126		13 W4006 0.880	14 W4008 0.883		16 W4009 0.887	17 W3C02B 1.025	18 W4010 0.885		20 W2D10B 1.128
21 W3013 1.016	22 W4011 0.884	23 W3C01B 1.022	24 W4003B 0.898	25 W4012 0.880	26 W4014 0.881	27 W4015 0.881	28 W4045B 0.893	29 W3D09B 1.039	30 W3014 1.011
31 W2D11B 1.128	32 W4016 0.882	33 W4017 0.885	34 W4018 0.884	35 W4019 0.884	36 W3C03B 1.023	37 W4020 0.885	38 W4022 0.883	39 W4023 0.877	40 W3017 1.010
41 W3018 1.017		43 W4024 0.884	44 W4025 0.884					49 W4026 0.877	50 W3020 1.020
51 W2D12B 1.128	52 W4027 0.886	53 W4028 0.882	54 W3D16B 1.032				58 W3D08B 1.033	59 W1D11B 1.219	60 W3D10B 1.031
61 W3021 1.015	62 W3D06B 1.035	63 W4031 0.883	64 W4047B 0.898					69 W1D08B 1.209	70 W3D12B 1.039
71 W2D13B 1.121	72 W4032 0.880	73 W4037 0.880	74 W4040 0.887		76 W3D13B 1.039		78 W3D14B 1.035	79 W1D09B 1.210	80 W3D15B 1.033
81 W3022 1.015		83 W3C04B 1.024	84 W4049B 0.912	85 W4041 0.889	86 W1D14B 1.214	87 W1D12B 1.212	88 W1D13B 1.218		90 W3024 1.013
91 W3025 1.016	92 W2D14B 1.126	93 W3026 1.015	94 W3027 1.014	95 W3030 1.005	96 W3D02B 1.037	97 W3D04B 1.035	98 W3D11B 1.034	99 W3032 1.015	100 W3033 1.010

Figure 2-10 Radial Power Distributions, STS-123.02 and STS-123.03, Revision 0, Axial Zone 2



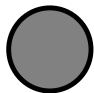

-  Part-length heater rod
-  Heater rod with TCs

Figure 2-11 TC Positions, STS-123.02 and STS-123.03

2.6 Heater Rod Characteristics (Specified)

Heater rod types used	W*D**B W**** W4***B W6***KB	heater rods equipped with TC heater rods, without TC heater rods, equipped with voltage taps part-length heater rods
Axial heat flux profile	downskew	
Axial peaking factor	1.6	
Number of full-length heater rods	81	
Heated length of full-length heater rods	3708.4 millimeters (mm)	
Number of part-length heater rods	10	
Heated length of part-length heater rods	1851.2 mm	
Rod to rod pitch	12.95 mm	
Rod to rod gap	2.67 mm	
Outer diameter of heater rods	10.28 mm	
Total heated area	10.299 square meters (m ²)	

The functionality of the heater rods was checked before the STS-123 test program. The conclusion was that the number of heater rods available was sufficient to assemble the test bundles.

The bottom of the ceramic liner is located at 0 mm and the beginning of heated length (BOHL) at 301.7 mm.

2.7 Pressure Taps Along the Test Bundle

Table 2-1 gives the location of the pressure taps of the level-corrected data channels. The position of the lower tap and the upper tap refer to the lower end of the ceramic liner.

Table 2-1 Measurement Transducer Channel Names and Pressure Tap Elevations

Measurement transducer (level corrected)	Lower tap pos. [mm]	Upper tap pos. [mm]	Span between taps [mm]
S73 CP222K Korr	290	794	504
S73 CP222G Korr	290	794	504
S73 CP2227K Korr	794	2207	1413
S73 CP2227G Korr	794	2207	1413
S73 CP2728K Korr	2207	2600	393
S73 CP2728G Korr	2207	2600	393
S73 CP2829K Korr	2600	3347	747
S73 CP2829G Korr	2600	3347	747
S73 CP2930K Korr	3347	3700	353
S73 CP2930G Korr	3347	3700	353
S73 CP309K Korr	3700	4127	427
S73 CP309G Korr	3700	4127	427
S73 CP1012K Korr	4185	4597	412
S73 CP1012G Korr	4185	4597	412
S73 CP1013K Korr	4185	4738	553
S73 CP1013G Korr	4185	4738	553
S73 CP210K Korr	290	4185	3895
S73 CP210G Korr	290	4185	3895
S73 CP219K Korr	282	4127	3845
S73 CP219G Korr	282	4127	3845
S73 CP3013 Korr	3700	4738	1038
S73 CP10CP05 Korr	4185	5214	1029

2.8 Pressure Taps Along the Loop and Instrumentation

The differential pressure drops measurement channel names (IDs) along the test loop are as follows:

S73_CP11:	Upper and lower taps of downcomer
S73_CP12:	Lower tap of downcomer and BOHL A: Standard transformer B: "Faster" transformer with different sensor design
S73 CP14:	End of heated length (EOHL) to steam-water separator
S73 CP15:	Lower tap of steam-water separator to upper tap of downcomer
S73 CP16:	Along the riser

The measurement points given in the plots provided in Appendix D are derived by the following measurement points:

T_Inlet:	S73_CT03B, Temperature at inlet pipeline
p_system:	S73_CP05B, Pressure at test bundle outlet
M_flow:	S73_CF08, Turbine flow meter measurement. Remark: The turbine is a relatively "slow" device. Section 6.5.2 provides a separate transient mass flow evaluation.
Sync_SINAN:	Sync_SINAN (Voltage input). Timestamp between the KATHY and SINAN-DAQs
LEVEL_SEP:	Calculated water level in the steam-water separator, based on differential pressure S73_CL01B

2.9 Hydraulic Characteristics

Axial zone 1 characterizes the full-rod section, and axial zone 2 provides the characteristics downstream of the end of the part-length heater rod (PLHR).

Axial Zone 1: BOHL—End of PLHR

Beginning of axial zone 1	301.7 mm from the lower end of ceramic liner
End of axial zone 1	2393.2 mm from the lower end of ceramic liner
Flow channel width	134.0 mm
Flow channel corner radius	10.15 mm
Flow area	9097.3 square millimeters (mm ²)
Water channel simulator	35.0 mm (without internal flow)
Hydraulic diameter	10.13 mm

Axial Zone 2: End of PLHR—EOHL

Beginning of axial zone 2	2393.2 mm from the lower end of ceramic liner
End of axial zone 2	4010.1 mm from the lower end of ceramic liner
Flow channel width	134.0 mm
Flow channel corner radius	10.15 mm
Flow area	9927.3 mm ²
Water channel simulator	35.0 mm (without internal flow)
Hydraulic diameter	12.15 mm

3 STEADY-STATE TEST RESULTS

3.1 Critical Heat Flux Tests

Appendix A gives the nominal CHF test conditions.

STS-123.01

Date of tests	August 22 to 24, 2016
Test runs (in total)	71
(Thereof) replicate test runs	15

Table 3-1 shows the CHF test results.

Table 3-1 Critical Bundle Power, STS-123.01

TCs indicating boiling transition are referenced in descending order of the magnitude of the temperature increase.

TC1 (highest increase) → TC6 (lowest increase)

Run No.	p_system [bar]	M_flow [kg/s]	Inlet M_Flux [kg/m ² *s]	Power [kW]	T_Inlet [GrdC]	dh Inlet1 [kJ/kg]	dh Inlet2 [kJ/kg]	TC 1	TC 2	TC 3	TC 4	TC 5	TC 6	Remark on TC condition
200.01	55.0	2.99	328	4297	260.9	48.6	45.7	23/1Z						
201.01	55.1	2.99	329	4407	252.3	91.7	88.6	62/1Z	87/1Z	79/1Z				
202.01	55.1	3.01	331	4557	243.7	133.1	130.2	23/1Z	87/1Z					
203.01	55.2	2.97	327	4671	235.0	174.5	171.8	87/1Z	23/1Z					
204.01	55.0	2.99	329	4786	225.5	218.3	215.3	87/1Z						
205.01	55.1	4.98	548	6913	260.7	52.6	47.3	23/1Z						
206.01	55.0	4.99	549	7076	252.9	90.1	84.9	23/1Z						
207.01	55.3	4.97	546	7236	244.9	130.6	125.5	23/1Z						
208.01	55.1	4.96	545	7366	236.7	168.5	163.1	23/1Z						
209.01	55.1	4.98	547	7633	225.7	219.9	214.7	23/1Z						
209.02	55.2	4.96	546	7647	225.2	222.8	217.9	23/1Z	69/1Z	59/2Z				
210.01	55.1	7.03	773	9179	262.1	48.9	40.8	69/1Z						
211.01	55.0	7.01	770	9399	253.2	91.8	83.8	69/1Z	23/1Z					
212.01	55.1	7.04	774	9623	244.4	134.7	126.8	69/1Z						8/1Z later defective
213.01	55.2	7.07	777	9834	236.9	170.5	162.6	69/1Z	79/2Z					
213.02	55.2	7.03	772	9793	236.7	171.3	163.7	69/1Z						
214.01	55.1	7.02	771	10107	225.8	222.6	214.7	79/2Z	69/1Z	69/3X				
214.02	55.1	7.01	771	10061	224.4	228.8	221.1	69/1Z						8/1Z later defective
214.03	55.2	7.04	774	10052	225.7	223.1	215.4	69/1Z						
294.01	82.9	9.50	1045	9903	278.1	111.7	105.4	69/3X	87/4Z	69/5X	97/2Z			
295.01	54.8	9.50	1044	11330	252.4	98.0	86.2	69/3X						
296.01	69.3	7.99	878	9609	267.9	97.4	90.2	69/3X	69/1Z					
297.01	69.3	9.44	1038	10562	267.4	101.0	92.4	69/3X	69/5X					
298.01	69.4	11.01	1210	11308	267.9	100.1	90.2	69/5X	69/3X					29/4X later defective
299.01	69.3	12.63	1388	11959	268.1	100.5	89.0	69/5X						58/5Z later defective
299.02	68.8	12.60	1385	12009	267.5	100.8	89.2	69/5X						78/3Z later defective

Run No.	p_system [bar]	M_flow [kg/s]	Inlet M_Flux [kg/m ² *s]	Power [kW]	T_Inlet [GrdC]	dh Inlet1 [kJ/kg]	dh Inlet2 [kJ/kg]	TC 1	TC 2	TC 3	TC 4	TC 5	TC 6	Remark on TC condition
299.03	69.1	12.62	1388	12143	266.9	105.5	93.7	69/5X	69/3X	59/5Z				
299.04	69.1	12.67	1392	12139	266.6	107.3	95.7	69/5X	69/3X					
300.01	68.7	2.97	327	4176	275.5	50.4	47.9	87/1Z	79/1Z	23/1Z				
301.01	69.4	3.00	329	4278	268.6	89.1	86.7	87/1Z	79/1Z	23/1Z				58/1Z, 58/3Z later defective
302.01	68.6	2.98	328	4380	259.2	132.3	129.6	87/1Z						
303.01	68.7	2.97	326	4484	251.9	168.7	166.0	87/1Z						79/1Z, 79/2Z, 62/1Z, 23/1Z late response
304.01	68.9	2.97	327	4602	241.7	218.1	215.7	87/1Z	79/1Z					79/2Z, 23/1Z late response
305.01	69.4	5.00	549	6623	276.4	50.9	46.8	69/1Z	23/1Z					
306.01	69.5	5.00	550	6752	268.8	90.1	86.3	69/1Z						
307.01	69.4	5.01	551	6952	260.8	129.5	125.7	69/1Z	79/1Z					58/3X later defective
308.01	69.3	4.99	549	7108	252.2	171.9	168.0	69/1Z						
309.01	69.3	5.00	549	7311	241.7	221.7	217.9	69/1Z						
310.01	69.2	7.01	771	8555	276.9	49.7	43.7	69/1Z						
311.01	69.3	7.01	770	8771	269.1	89.5	83.7	69/1Z						
311.02	69.3	6.97	766	8756	269.1	89.6	83.8	69/1Z						58/1Z later defective
311.03	68.9	7.03	773	8775	268.3	91.4	85.3	69/1Z						78/3Z later defective
311.04	69.1	7.00	769	8717	268.0	94.1	88.2	69/1Z						
311.05	69.0	7.02	772	8847	267.5	96.3	90.3	69/1Z						29/4X is defective
311.06	69.1	7.03	773	8812	268.5	91.7	85.8	69/1Z						
311.07	69.0	7.02	772	8800	267.2	98.3	92.2	69/1Z						
312.01	69.4	7.07	777	9005	260.9	131.6	125.6	69/1Z						
313.01	69.4	6.97	766	9167	252.3	173.0	167.3	69/1Z						
314.01	69.4	6.98	767	9433	242.3	221.0	215.4	69/1Z						
314.02	68.7	6.99	768	9453	241.6	221.7	215.7	69/1Z						8/1Z later defective
315.01	69.2	9.02	992	10073	275.8	56.9	48.6	69/3X						
316.01	69.0	9.03	992	10322	268.5	93.4	85.1	69/3X						
317.01	69.1	9.02	991	10573	260.0	136.5	128.4	69/3X						
318.01	69.1	9.02	991	10861	252.0	175.7	167.3	69/3X	97/2Z					
319.01	69.1	9.01	991	11169	240.6	229.8	221.9	69/3X						
400.01	83.0	3.00	330	3967	288.9	50.7	48.2	23/1Z	79/1Z					
401.01	83.0	3.00	330	4074	281.4	90.6	88.3	79/1Z	87/1Z	23/1Z	62/1Z			

Run No.	p_system [bar]	M_flow [kg/s]	Inlet M_Flux [kg/m ² *s]	Power [kW]	T_Inlet [GrdC]	dh Inlet1 [kJ/kg]	dh Inlet2 [kJ/kg]	TC 1	TC 2	TC 3	TC 4	TC 5	TC 6	Remark on TC condition
402.01	83.1	2.99	329	4174	273.6	131.8	129.4	87/1Z	79/1Z					
403.01	83.0	3.00	330	4273	266.1	169.2	166.8	87/1Z	79/1Z					
404.01	83.0	2.99	328	4387	255.5	221.7	219.1	87/1Z						
405.01	83.1	5.00	550	6195	288.5	54.4	50.8	69/1Z						
406.01	83.0	5.00	550	6347	281.1	93.6	90.1	69/1Z						
407.01	83.0	5.01	551	6528	273.1	134.9	131.3	69/1Z						
408.01	82.9	5.01	550	6724	264.7	176.5	173.1	69/1Z						
409.01	83.1	5.01	551	6940	254.6	227.4	224.0	69/1Z						
410.01	83.0	7.03	772	8039	288.3	56.4	51.4	69/1Z						
411.01	82.8	7.09	780	8285	281.5	92.2	87.1	69/1Z						
411.02	82.9	7.00	769	8192	281.9	90.8	85.6	69/1Z						
412.01	83.0	7.01	770	8447	273.6	134.0	129.1	69/1Z						8/1Z later defective
413.01	83.0	7.01	770	8657	265.9	172.2	167.4	69/1Z						
414.01	83.0	7.01	770	8954	254.5	228.6	224.1	69/1Z						

dh Inlet1: Assembly inlet subcooling determined based on the inlet pressure

dh Inlet2: Assembly inlet subcooling determined based on the exit pressure

3.2 Pressure Drop Tests

Appendix A gives the nominal pressure drop test conditions.

The steady-state test loop setup has a small (“1”) and a large inlet flow line (“2”). The column headers (“Flow line [1 / 2]”) in Table 3-2 and Table 3-3 refer to this.

The test bundle Δp -gauge lines are equipped with a purging system that injects small amounts of subcooled water to compensate for potential water evaporation. The column headers (“Purging [off / on]”) in Table 3-2 and Table 3-3 indicate whether purging was activated.

3.2.1 Single-Phase Pressure Drop Tests

STS-123.02

Date of tests	September 23, 2016
Test runs (in total)	10
(Thereof) replicate test runs	3

Table 3-2 shows the single-phase pressure drop test results.

Table 3-2 Single-Phase Pressure Drops, STS-123.02

Run No.	p_syste m [bar]	M_flow [kg/s]	Inlet_ M_flux [kg/m ² s]	Power [kW]	T_inlet [GrDC]	X_Outlet [-]	Flow line [1 / 2]	Purging [OFF / ON]	S73 CP222K Korr [mbar]	S73 CP222G Korr [mbar]	S73 CP2227 K Korr [mbar]	S73 CP2227 G Korr [mbar]	S73 CP2728 K Korr [mbar]	S73 CP2728 G Korr [mbar]	S73 CP2728 K Korr [mbar]	S73 CP2829 K Korr [mbar]	S73 CP2829 G Korr [mbar]
001.01	68.9	3.15	346	0	260.5	-0.08	1	OFF	38.9	39.2	113.6	113.4	32.0	32.2	59.1	59.0	
002.01	68.9	4.50	494	0	260.4	-0.08	1	OFF	40.3	40.6	117.9	117.8	33.0	33.2	60.8	60.8	
002.02	68.9	4.57	503	0	261.7	-0.08	2	OFF	40.3	40.5	117.7	117.6	33.0	33.1	60.7	60.6	
003.01	68.9	6.32	695	0	260.2	-0.08	1	OFF	42.9	43.1	125.5	125.5	34.8	35.0	63.9	63.8	
003.02	68.9	6.34	697	0	261.6	-0.08	2	OFF	42.8	43.1	125.2	125.1	34.8	34.9	63.7	63.6	
004.01	68.9	9.53	1048	0	262.2	-0.08	2	OFF	49.1	49.3	143.9	143.8	39.2	39.4	71.1	71.1	
005.01	68.9	12.74	1400	0	260.9	-0.08	2	OFF	57.6	57.9	169.3	169.3	45.1	45.3	81.5	81.4	
006.01	68.9	15.92	1750	0	260.1	-0.08	2	OFF	68.4	68.6	201.2	201.2	52.5	52.7	94.4	94.4	
007.01	68.9	18.87	2075	0	259.2	-0.09	2	OFF	80.1	80.3	235.6	235.6	60.6	60.8	108.3	108.3	
007.02	69.0	18.86	2073	0	259.5	-0.09	2	ON	79.5	79.6	234.7	234.8	63.5	63.9	104.1	104.1	

Run No.	S73 CP2930K Korr [mbar]	S73 CP2930G Korr [mbar]	S73 CP309K Korr [mbar]	S73 CP309G Korr [mbar]	S73 CP1012K Korr [mbar]	S73 CP1012G Korr [mbar]	S73 CP1013K Korr [mbar]	S73 CP1013G Korr [mbar]	S73 CP210K Korr [mbar]	S73 CP210G Korr [mbar]	S73 CP219K Korr [mbar]	S73 CP219G Korr [mbar]	S73 CP3013 Korr [mbar]	S73 CP10CP05 Korr [mbar]
001.01	28.5	28.3	34.0	33.3	32.4	33.1	44.0	44.0	309.9	310.1	306.3	306.0	82.3	86.5
002.01	29.3	29.2	35.0	34.3	33.2	33.9	45.0	44.9	320.2	320.4	316.4	316.1	84.2	87.3
002.02	29.3	29.1	34.9	34.3	33.2	33.9	45.1	45.0	319.9	320.1	315.9	315.7	84.4	86.5
003.01	30.8	30.7	36.6	36.0	34.8	35.5	46.8	46.7	338.6	338.8	334.7	334.4	87.7	90.3
003.02	30.7	30.6	36.5	35.9	34.7	35.4	46.7	46.7	337.8	338.0	334.0	333.8	87.6	89.9
004.01	34.4	34.3	40.6	40.0	38.5	39.2	51.1	51.1	382.6	382.9	378.5	378.4	96.6	98.4
005.01	39.5	39.4	46.2	45.6	43.6	44.3	57.0	57.0	443.7	444.1	439.2	439.2	108.3	110.4
006.01	45.8	45.7	53.2	52.6	50.0	50.7	64.4	64.4	520.4	520.9	515.4	515.5	123.1	125.5
007.01	52.7	52.6	60.7	60.1	56.9	57.6	72.3	72.4	603.3	603.9	597.8	598.0	139.1	142.0
007.02	52.1	52.2	61.5	61.1	57.0	57.7	72.3	72.1	601.5	601.9	595.6	596.0	139.5	144.9

3.2.2 Two-Phase Pressure Drop Tests

STS-123.02

Date of tests	September 23, 2016
Test runs (in total)	30
(Thereof) replicate test runs	9

Table 3-3 shows the two-phase pressure drop test results.

Table 3-3 Two-Phase Pressure Drops, STS-123.02

Run No.	p_syste m [bar]	M_flow [kg/s]	Inlet_ M_flux [kg/m²s]	Power [kW]	T_inlet [GrdC]	X_Outlet [-]	Flow line [1 / 2]	Purging [OFF / ON]	S73 CP222K Korr [mbar]	S73 CP222G Korr [mbar]	S73 CP2227 K Korr [mbar]	S73 CP2227 G Korr [mbar]	S73 CP2278 K Korr [mbar]	S73 CP2278 G Korr [mbar]	S73 CP2829 K Korr [mbar]	S73 CP2829 G Korr [mbar]
009.21	68.8	6.27	690	6999	274.4	0.70	2	OFF	46.2	46.4	225.5	225.5	74.6	74.9	130.3	130.4
009.22	68.9	6.17	678	7007	274.6	0.72	1	ON	45.3	45.3	220.1	220.1	77.5	78.0	122.2	122.2
009.23	69.0	6.29	691	6998	273.7	0.70	2	ON	45.9	46.0	223.3	223.4	78.3	78.7	125.3	125.4
010.21	69.0	9.46	1040	2006	273.5	0.10	2	ON	48.6	48.6	155.8	155.9	46.4	46.9	72.2	72.2
011.21	69.0	9.53	1048	4002	274.0	0.24	2	OFF	52.2	52.4	211.3	211.3	66.8	67.0	120.4	120.4
011.22	69.0	9.46	1040	4006	273.8	0.24	2	ON	51.5	51.6	207.6	207.7	69.6	70.0	115.0	115.0
012.21	69.0	9.47	1041	6005	273.7	0.38	2	ON	55.0	55.1	272.7	272.8	96.0	96.5	161.7	161.8
013.21	69.0	9.49	1043	7000	273.7	0.45	2	OFF	57.1	57.3	309.2	309.3	105.4	105.7	189.8	190.0

Run No.	S73 CP2930K Korr [mbar]	S73 CP2930G Korr [mbar]	S73 CP309K Korr [mbar]	S73 CP309G Korr [mbar]	S73 CP1012K Korr [mbar]	S73 CP1012G Korr [mbar]	S73 CP1013K Korr [mbar]	S73 CP1013G Korr [mbar]	S73 CP210K Korr [mbar]	S73 CP210G Korr [mbar]	S73 CP219K Korr [mbar]	S73 CP219G Korr [mbar]	S73 CP3013 Korr [mbar]	S73 CP10CP05 Korr [mbar]
009.21	67.6	67.5	73.3	72.8	67.3	68.1	82.7	82.7	624.0	624.3	617.8	618.0	162.3	159.2
009.22	65.7	65.9	72.5	72.2	66.1	66.7	81.1	81.1	608.4	609.3	603.1	603.5	159.4	160.6
009.23	67.2	67.3	74.6	74.2	67.6	68.3	83.0	82.8	620.2	620.7	614.4	615.0	163.6	164.1
010.21	38.3	38.3	44.1	43.7	39.9	40.5	50.5	50.3	408.7	409.1	405.3	405.4	98.3	103.3
011.21	63.3	63.1	70.3	69.7	63.8	64.6	78.4	78.5	589.5	590.0	584.4	584.5	154.5	154.4
011.22	61.9	62.0	70.2	69.8	63.3	64.0	77.6	77.5	581.0	581.5	575.5	575.8	153.4	156.5
012.21	87.6	87.7	98.7	98.4	89.3	90.1	107.7	107.6	779.1	780.0	771.8	772.3	214.3	216.9
013.21	100.8	100.8	111.4	111.0	101.5	102.4	122.6	122.8	883.0	883.7	874.0	874.9	243.4	239.5

Run No.	p_syste m [bar]	M_flow [kg/s]	Inlet_ M_flux [kg/m²s]	Power [kW]	T_inlet [GrdC]	X_Outlet [-]	Flow line [1 / 2]	Purging [OFF / ON]	S73 CP222K Korr [mbar]	S73 CP222G Korr [mbar]	S73 CP2227 K Korr [mbar]	S73 CP2227 G Korr [mbar]	S73 CP2728 K Korr [mbar]	S73 CP2728 G Korr [mbar]	S73 CP2829 K Korr [mbar]	S73 CP2829 G Korr [mbar]
013.22	69.0	9.46	1040	6998	273.6	0.45	2	ON	56.6	56.7	306.2	306.4	108.5	109.0	184.6	184.6
014.21	69.0	9.45	1039	8002	273.8	0.52	2	ON	58.5	58.5	342.4	342.7	121.2	121.8	207.1	207.3
015.21	69.0	12.63	1388	2006	273.6	0.07	2	ON	56.9	56.9	188.7	188.7	56.4	56.8	91.9	91.8
016.21	69.0	12.63	1388	4007	274.0	0.17	2	ON	60.5	60.6	259.1	259.2	86.4	86.9	148.2	148.3

Run No.	p_syste m [bar]	M_flow [kg/s]	Inlet_ M_flux [kg/m²s]	Power [kW]	T_inlet [GrdC]	X_Outlet [-]	Flow line [1 / 2]	Purging [OFF / ON]	S73 CP222K Korr [mbar]	S73 CP222G Korr [mbar]	S73 CP2227 Korr [mbar]	S73 CP2227 G Korr [mbar]	S73 CP2728 K Korr [mbar]	S73 CP2728 G Korr [mbar]	S73 CP2829 K Korr [mbar]	S73 CP2829 G Korr [mbar]
017.21	69.0	12.63	1389	6006	273.8	0.28	2	ON	65.3	65.4	342.5	342.7	120.1	120.6	209.3	209.5
018.21	69.0	12.62	1387	6999	273.6	0.33	2	OFF	67.9	68.1	386.1	386.4	132.5	132.8	243.5	243.9
018.22	69.0	12.64	1389	7000	274.1	0.33	2	ON	68.0	68.0	387.5	387.7	136.8	137.3	240.1	240.4
019.21	69.0	12.64	1389	8003	274.0	0.38	2	ON	70.5	70.6	432.1	432.4	152.9	153.4	270.2	270.6

Run No.	S73 CP2930K Korr [mbar]	S73 CP2930G Korr [mbar]	S73 CP309K Korr [mbar]	S73 CP309G Korr [mbar]	S73 CP1012K Korr [mbar]	S73 CP1012G Korr [mbar]	S73 CP1013K Korr [mbar]	S73 CP1013G Korr [mbar]	S73 CP210K Korr [mbar]	S73 CP210G Korr [mbar]	S73 CP219K Korr [mbar]	S73 CP219G Korr [mbar]	S73 CP3013 Korr [mbar]	S73 CP3013 Korr [mbar]	S73 CP2829 G Korr [mbar]
013.22	99.7	99.8	112.4	112.1	101.0	101.9	121.9	122.1	876.2	877.8	867.9	869.0	243.4	243.4	242.5
014.21	111.0	111.2	125.5	125.2	112.5	113.2	135.8	135.9	912.9*	976.2	909.7*	967.0	271.4	271.4	268.3
015.21	48.1	48.1	55.1	54.7	50.0	50.6	62.6	62.3	501.1	501.6	496.6	496.9	122.3	122.3	128.2
016.21	79.6	79.8	90.3	90.0	81.8	82.5	99.1	99.1	731.2	731.8	724.1	724.5	196.8	196.8	200.0
017.21	113.4	113.6	127.9	127.7	116.1	116.8	138.5	138.5	912.8*	989.4	909.7*	979.1	276.7	276.7	278.9
018.21	129.9	129.9	144.9	144.4	132.0	132.9	157.5	157.8	911.6*	1117.3	908.5*	1105.9	314.2	314.2	312.2
018.22	129.8	130.0	147.3	147.1	132.3	133.2	157.9	158.0	912.8*	1121.5	909.5*	1110.2	316.9	316.9	317.6
019.21	145.5	145.7	165.3	165.1	147.9	148.7	176.6	176.8	912.8*	1250.1	909.6*	1237.4	355.1	355.1	353.0

*End of measuring range

Run No.	p_syste m [bar]	M_flow [kg/s]	Inlet_ M_flux [kg/m²s]	Power [kW]	T_inlet [GrdC]	X_Outlet [-]	Flow line [1 / 2]	Purging [OFF / ON]	S73 CP222K Korr [mbar]	S73 CP222G Korr [mbar]	S73 CP2227 Korr [mbar]	S73 CP2227 G Korr [mbar]	S73 CP2728 K Korr [mbar]	S73 CP2728 G Korr [mbar]	S73 CP2829 K Korr [mbar]	S73 CP2829 G Korr [mbar]
020.21	69.0	15.75	1732	2006	274.0	0.05	2	ON	67.3	67.3	221.6	221.6	66.1	66.6	110.8	110.8
021.21	69.0	15.78	1734	4003	274.1	0.13	2	OFF	71.2	71.4	308.7	308.8	98.7	99.0	183.1	183.3
021.22	69.0	15.75	1731	4007	274.3	0.13	2	ON	71.0	71.0	308.0	308.1	102.3	102.8	179.6	179.8
022.21	69.1	15.77	1733	6008	273.8	0.21	2	ON	76.3	76.4	406.8	407.0	142.3	142.8	253.6	254.0
023.21	69.0	15.81	1738	7000	274.2	0.26	2	OFF	80.0	80.2	465.0	465.3	159.5	159.9	296.9	297.4
023.22	69.1	15.76	1733	7001	274.0	0.26	2	ON	79.6	79.7	461.9	462.3	163.2	163.2	291.5	291.8
024.21	69.0	15.75	1731	7995	273.8	0.30	2	ON	82.4	82.5	513.4	513.8	181.4	181.9	327.2	327.7
025.21	69.0	18.88	2076	2005	273.9	0.03	2	ON	79.7	79.7	254.3	254.4	74.8	75.3	128.6	128.7

Run No.	S73 CP2930K Korr [mbar]	S73 CP2930G Korr [mbar]	S73 CP309K Korr [mbar]	S73 CP309G Korr [mbar]	S73 CP1012K Korr [mbar]	S73 CP1012G Korr [mbar]	S73 CP1013K Korr [mbar]	S73 CP1013G Korr [mbar]	S73 CP210K Korr [mbar]	S73 CP210G Korr [mbar]	S73 CP219K Korr [mbar]	S73 CP219G Korr [mbar]	S73 CP3013 Korr [mbar]	S73 CP10CP05 Korr [mbar]
020.21	57.7	57.8	65.8	65.5	59.8	60.5	74.3	74.1	594.6	595.2	588.9	589.4	145.7	153.1
021.21	97.6	97.5	108.9	108.3	99.3	100.1	120.0	120.2	877.1	877.9	868.5	869.0	238.3	238.4
021.22	96.8	97.0	109.6	109.3	99.4	100.2	120.0	120.0	876.1	876.8	867.1	867.8	238.9	242.6
022.21	138.0	138.1	155.6	155.4	141.2	142.0	168.0	168.1	912.9*	1185.6	909.7*	1173.5	336.1	337.4
023.21	159.5	159.6	178.1	177.7	162.5	163.5	192.8	193.2	911.3*	1354.4	908.5*	1340.4	385.3	382.3
023.22	158.2	158.4	179.9	179.6	161.5	162.3	191.8	192.0	912.8*	1348.9	909.7*	1335.0	385.7	386.2
024.21	177.3	177.4	201.5	201.2	180.5	181.4	214.1	214.4	912.6*	1499.4	909.5*	1484.3	431.4	431.6
025.21	66.5	66.6	75.9	75.6	68.9	69.6	85.1	85.0	686.1	686.8	679.6	680.1	167.5	175.5

*End of measuring range

Run No.	p_syste m [bar]	M_flow [kg/s]	Inlet_ M_flux [kg/m²s]	Power [kW]	T_inlet [GrDC]	X_Outlet [-]	Flow line [1 / 2]	Purging [OFF / ON]	S73 CP222K Korr [mbar]	S73 CP222G Korr [mbar]	S73 CP2227 K Korr [mbar]	S73 CP2227 G Korr [mbar]	S73 CP2227 K Korr [mbar]	S73 CP2278 K Korr [mbar]	S73 CP2278 G Korr [mbar]	S73 CP2278 K Korr [mbar]	S73 CP2829 K Korr [mbar]	S73 CP2829 G Korr [mbar]
026.21	69.0	18.87	2074	4004	273.7	0.10	2	OFF	83.1	83.4	351.7	351.9	112.3	112.3	112.6	210.6	210.9	210.9
026.22	69.0	18.88	2075	4007	273.9	0.10	2	ON	83.2	83.3	351.7	351.9	116.0	116.0	116.6	207.7	208.0	208.0
027.21	69.0	18.90	2078	6008	274.5	0.17	2	ON	89.7	89.7	474.5	474.7	165.5	165.5	166.1	299.5	299.8	299.8
028.21	69.0	18.88	2075	7003	274.1	0.21	2	OFF	92.4	92.7	534.6	535.0	184.2	184.2	184.6	346.0	346.5	346.5
028.22	69.0	18.90	2078	7001	274.2	0.21	2	ON	92.6	92.7	533.4	533.9	188.0	188.0	188.7	341.6	342.2	342.2
029.21	69.0	18.91	2079	7997	273.9	0.24	2	ON	95.7	95.8	592.2	592.7	209.6	210.3	210.3	383.1	383.9	383.9

Run No.	S73 CP2930K Korr [mbar]	S73 CP2930G Korr [mbar]	S73 CP309K Korr [mbar]	S73 CP309G Korr [mbar]	S73 CP1012K Korr [mbar]	S73 CP1012G Korr [mbar]	S73 CP1013K Korr [mbar]	S73 CP1013G Korr [mbar]	S73 CP210K Korr [mbar]	S73 CP210G Korr [mbar]	S73 CP219K Korr [mbar]	S73 CP219G Korr [mbar]	S73 CP3013 Korr [mbar]	S73 CP10CP05 Korr [mbar]
026.21	113.0	113.0	126.0	125.5	115.0	115.9	138.9	139.2	911.7*	1008.3	908.8*	997.7	275.8	277.7
026.22	112.5	112.6	127.1	126.9	115.5	116.3	139.4	139.4	912.9*	1009.6	909.8*	999.0	277.4	284.0
027.21	163.7	163.9	184.2	184.1	167.1	168.1	199.2	199.6	912.3*	1392.7	909.2*	1378.8	398.4	400.4
028.21	187.2	187.3	209.3	209.0	190.1	191.2	225.8	226.4	911.3*	1571.3	908.6*	1555.1	452.1	448.5
028.22	186.8	187.0	212.1	211.9	190.1	190.9	225.8	226.1	912.7*	1572.2	909.6*	1555.8	454.7	455.0
029.21	209.0	209.3	237.4	237.3	212.4	213.4	252.1	252.5	912.6*	1746.7	909.5*	1728.6	508.0	508.4

*End of measuring range

3.3 Heat Balance Measurement

The heat balance measurements were performed before the test for both flow lines to check the measurement equipment. The measured electric power is compared with a calorimetric calculation according to the following formula:

$$\dot{Q}_{loss} = P_{el} - \dot{Q}_{thermal}$$

$$\dot{Q}_{thermal} = \dot{m} \cdot (h_{out} - h_{in})$$

$$h_{out}, h_{in} = f_{(p,T)} \quad (\text{Applying IAPWS-IF97})$$

STS-123.01

Date of tests	August 22, 2016
Test runs (in total)	4
(Thereof) replicate test runs	0

Table 3-4 shows the heat balance test results.

Table 3-4 Heat Balance Measurement, STS-123.01

Run No.	p_system [bar]	M_flow [kg/s]	Inlet_M_flux [kg/m ² *s]	Power [kW]	T_inlet [GrdC]	T_outlet [GrdC]	X_Outlet [-]	P_Loss [kW]
HB.01	69.5	6.29	692	0	199.0	198.4	-0.27	-17
HB.02	69.5	12.61	1386	0	200.4	200.3	-0.27	-6
HB.03	69.6	6.29	691	1007	199.2	233.2	-0.17	-34
HB.04	69.6	12.60	1385	2004	199.4	233.7	-0.17	-34

3.4 Replicate Test Procedure

Replicate CHF tests (repetition of a predefined test point to demonstrate stable loop operation) were performed several times a test day as a standard or after abnormal occurrences in the test loop.

4 INSTABILITY TEST RESULTS

4.1 Natural Circulation Instability Tests

The module simulating neutronic feedback (SINAN) is based on the measured inlet flow rate. Without this feedback module active, the power is held constant.

STS-123.03

Date of tests	December 10 to 20, 2016
Test runs	41 without SINAN feedback 19 with SINAN feedback
(Thereof) replicate test runs	1
(Thereof) transient test runs	2

4.2 Test Matrix

Appendix A specifies the test program.

Appendix B documents the test matrix of the performed instability tests, their initial thermal-hydraulic conditions, and SINAN module parameters of Tau, Rhosub, and Vrcmul. Tau is a parameter in the SINAN module that characterizes the fuel thermal inertia, Rhosub is a parameter that characterizes modal harmonics in the neutron kinetics model, and Vrcmul is a parameter that characterizes the strength of the simulated void reactivity feedback.

The enveloping instability test conditions were as follows:

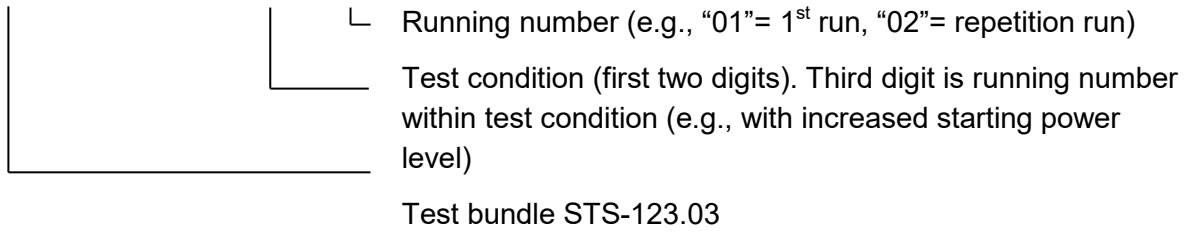
- System pressure 7.0 MPa and 8.0 MPa
- Inlet subcooling 20 Kelvin (K) and 35 K
- Water level 0.4 meter (m) and 1.1 m (in the steam-water separator)
- Tau* 2.0 second (s), 2.5 s, and 3.7 s
- Rhosub* 0.0 dollars (\$), 0.8 \$, 1.0 \$, and 1.2 \$
- Vrcmul* 0.05 to 0.30

* Only for test runs with applied SINAN module.

The nomenclature of the test run names is shown below.

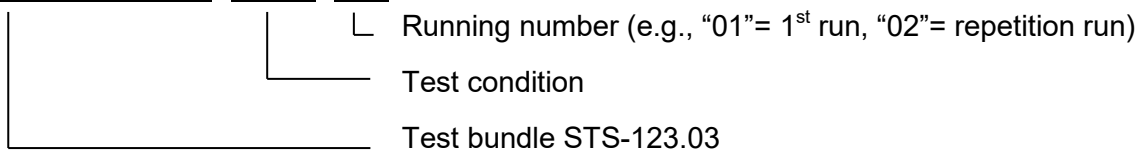
4.2.1 Non-SINAN Tests

S T S - 1 2 3 . 0 3 - 1 0 1 . 0 1



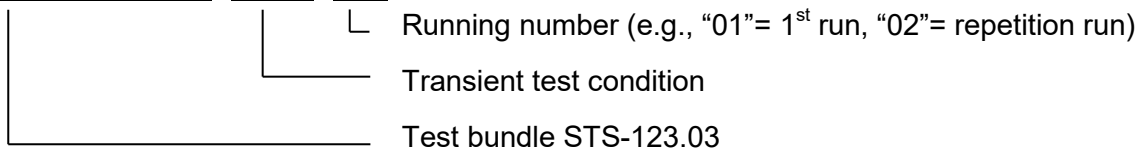
4.2.2 SINAN Tests

S T S - 1 2 3 . 0 3 - A 0 1 . 0 1



4.2.3 Transient Tests

S T S - 1 2 3 . 0 3 - T 0 1 . 0 1



4.3 Summary of Test Data

According to the test matrix, the non-SINAN tests were started at a certain power level. In the subsequent test runs, the initial power level was increased in small increments.

The SINAN tests applied a neutronic feedback power module. It was independently operated on a separate PC.

Appendix B and the 9th plot of Appendix D through Appendix KKK give a rough overview of the parametrized SINAN coefficients (e.g., Vrcmul, Rhosub, and Tau) over the time. Nevertheless, for detailed evaluation, the corresponding values as a function of time have to be used.

The measurement point "Sync_SINAN" (1st plot in Appendix D through Appendix KKK) indicates the time when SINAN was set active.

Also, two tests were performed with transient inlet temperatures ("transient tests"). Due to the nature of these tests, the water level inside the separator was not constant.

Appendix C summarizes the initial test conditions, the separator water level, and whether SINAN was active.

Appendix D through Appendix KKK show eight or nine plots for each test run, using the following nomenclature:

- 1st Plot: System data
 - t_inlet [°C] Inlet temperature
 - p_system [bar] System pressure (absolute)
 - M_flow [kg/s] Bundle mass flow measured by the turbine in the inlet section
 - Sync_SINAN [V] Status of the neutronic feedback power module (0 V => OFF, 5 V => ON)
 - LEVEL_SEP[m] Water level in the steam-water separator
- 2nd Plot: Differential pressures inlet and feedwater temperature
 - CP12A_irr [mbar] Differential pressure inlet geometry (“slow” transformer)
 - CP12B_irr [mbar] Differential pressure inlet geometry (“fast” transformer)
 - S73_CT19 [°C] Temperature feedwater into downcomer
- 3rd to 8th Plot: TC temperatures
 - 59\1Z [°C] Temperature TC heater rod pos. 59, 1st level, Z-direction
(Sequence continues for heaters in positions 59, 69, 79, 86, 87, and 88.)
 - 88\6Z [°C] Temperature TC heater rod positions 88, 6th level, Z-direction
- 9th Plot: SINAN conditions (only for SINAN tests)
 - Vrcmul [-] Void reactivity coefficient multiplying factor
 - Tau [s] Fuel thermal time constant
 - Rhosub [\$] Harmonic mode subcriticality

The 9th plot is plotted versus the “relative time” of the data.

4.4 Replicate Test Procedure

As part of the instability measurements, one repeatability test was performed. The first test performed without SINAN feedback was agreed upon to be the repeatability point and was performed on the final day of testing. The repeatability measurement used the same power search as was used in the first test. The acceptance criteria for this test were the power level at the point of oscillation inception being within 2 percent and the oscillation magnitude at the time of initial dryout being within 2 percent.

The repeatability measurements were made and showed very good agreement to the initial tests. Results were well within the agreed-upon acceptance criteria and show no noticeable changes in loop behavior over the test campaign.

5 TEST RUN IDENTIFICATION CONVENTION

The nomenclature is as follows:

- “STS-123.03...”: Data of the KATHY DAQ
- “SIN-123.03...”: Data of the separate neutronic feedback power PC (e.g., Vrcmul-, Rho-, Tau-coefficients). The SINAN software used the KATHY loop data recorded with this DAQ (e.g., “flow_new,” “dhin_new,” “power Kathy”) to derive the transient power.

6 EVALUATION OF THE MEASURED DATA

6.1 Pressure Drop Results over the Test Bundle

The positions of the lower and the upper tap refer to the lower end of the ceramic liner.

Appendix A gives the nominal boundary conditions (test matrix) for the pressure drop tests.

The differential pressure drop measurement IDs along the test bundle are as follows:

- S73 CP222
- S73 CP2227
- S73 CP2728
- S73 CP2829
- S73 CP2930
- S73 CP309
- S73 CP1012
- S73 CP1013
- S73 CP210
- S73 CP219
- S73 CP3013
- S73 CP10CP05

6.1.1 Measurement Range

As measured pressure drops (the asterisk "*" is the placeholder for the above-mentioned measurement IDs):

- *K: narrow measurement range
- *G: wide measurement range

6.1.2 Geodetic Correction

Geodetically corrected pressure drops with regard to the density of the pressure gauge line inside the annular space outside of the flow channel and inside the test vessel. This report does not include the geodetic correction of the water column inside the flow channel because the axial density distribution inside the test bundle is unknown.

The total pressure drop is defined as follows (sample measurement ID: S73_CP1012):

$$S73_CP1012K_Korr = S73_CP1012K + \rho_{1012} * g * \Delta h_{1012}$$

where S73_CP1012K	=	measured value
Δh_{1012}	=	difference of level of pressure taps (e.g., tap 10 and tap 12)
ρ_{1012}	=	average density of the relevant pressure gauge tube, calculated from temperature measurements on the surface of the pressure gauge tube
1012	=	pressure tap numbers (10 and 12)
g	=	gravity constant = 9.81 (m/s ²)

6.1.3 Irreversible Correction

The local quality inside the test bundle is not evaluated. As such, void distributions within the bundle are not known. Therefore, the irreversible pressure loss needs to be separately evaluated, consistent with the methodology that uses these data.

6.2 Pressure Drop Results over the Test Loop

6.2.1 Geodetic Correction

Geodetically corrected pressure drops (IDs ending with “*Korr”) are calculated with regard to the difference in density of the pressure gauge line and the fluid.

The calculation is based on the assumption that the velocity is equal at both pressure taps in a single flow regime.

The total pressure drop is defined as follows (sample measurement ID: S73_CP15):

$$CP15_Korr = S73_CP15 + g * \Delta h_{15} * (\rho_1 - \rho_{15})$$

where S73_CP15	=	measured value
Δh_{15}	=	difference of level of pressure taps
ρ_{15}	=	actual fluid density = f (t, p system)
ρ_1	=	density in the pressure gauge line = f (20 °C, p system)
15	=	pressure tap number
g	=	gravity constant = 9.81 (m/s ²)

The exception is CP14_Korr, due to the unknown fluid density differences inside the riser compared to the water level inside the separator. It was determined as:

$$CP14_Korr = S73_CP14 + \rho_{14} * g * \Delta h_{14}$$

If further evaluations are performed on CP14_Korr, this has to be taken into account.

The densities were calculated from the following fluid temperatures:

- ρ_{11} = f (S73_CT20, p_system) used for measurement ID: S73_CP11
- ρ_{12} = Rho_inlet = f (T_inlet, p_system) used for measurement ID: S73_CP12
- ρ_{14} = f (20 °C, p_system) used for measurement ID: S73_CP14
- ρ_{15} = $\rho_{separator} * 0.33 + \rho_{Downcomer} * 0.67$ used for measurement ID: S73_CP15, with:
- $\rho_{separator}$ = f (S73_CT18, p system)
- $\rho_{Downcomer}$ = f (S73_CT20, p system)

The temperature within the span of height Δh_{15} (along the feedwater injector) shows a temperature profile. The upstream section temperature (before the feedwater injector) is measured by S73_CT18. The downstream section (after the feedwater injector) is measured by S73_CT20. The ratio 0.33 to 0.67 represents the normalized lengths of the two sections.

- ρ_{16} = f (X_Outlet, p_system) used for measurement ID: S73 CP16, with:
 - X_Outlet = f (H_Outlet)
 - H_Outlet = H_Inl + (power / M_flow)
 - H_Inl = f (S73 CP04, T_inlet)

6.2.2 Irreversible Correction

These pressure drops (ending with “*irr”) are calculated as the (“*Korr”) pressure drops as described before but with respect to the calculated medium (steam/water) velocities at both pressure taps due to possibly different flow areas at the pressure taps.

The measurement channels ending on “*irr” were calculated with these flow areas:

- CP11_irr: Upper and lower taps of downcomer
- CP12(A or B)_irr: Lower tap of downcomer and BOHL
- CP14_irr: EOHL to steam-water separator; not calculated due to the unknown velocities
- CP15_irr: Lower tap of steam-water separator to upper tap of downcomer
- CP16_irr: Along the riser

6.3 System Pressure

The system pressure “p_system” is an alias of S73 CP05B and is measured by a gauge pressure transducer. Therefore, the absolute pressure is obtained by:

$$p_{abs} = p_m + k$$

where

p_{abs}	=	absolute system pressure at test section outlet in bar
p_m	=	pressure measured by the gauge pressure transducer
k	=	1.0 bar

6.4 Water Level in the Steam-Water Separator

The water level in the steam-water separator is determined with the following formula:

$$LEVEL_SEP = \frac{H \cdot (\rho_1 - \rho'') \cdot g - \Delta p_m}{(\rho' - \rho'') \cdot g}$$

where

LEVEL_SEP	=	separator level in m
H	=	distance between the pressure taps
Δp_m	=	value of differential pressure S73_CL01B
ρ', ρ''	=	density of saturated water (SEP_LIQUID) and steam (SEP_STEAM) of separator pressure (S73_CP08B)
ρ_1	=	density in the measuring gauge line of S73_CL01B = f (20 °C, p_system)
g	=	gravity constant = 9.81 m/s ²

6.5 Inlet Mass Flow Instability Test STS-123.03

6.5.1 Turbine Flow Meter S73 CF08

The instability test loop cannot be equipped with a flow measurement by means of a nozzle at the inlet, as its pressure drop would influence the natural circulation characteristics. Therefore, the instability test STS-123.03 volumetric flow S73 CF08 is measured by a turbine flow meter at the inlet of the test vessel.

The output value of the turbine flow meter is a function of the measured impulses. The turbine meter was calibrated in a DAKks (Deutsche Akkreditierungsstelle GmbH)-accredited laboratory (test certificate: 17-001, D-PL-15108-01-00- 2016-05, dated May 20, 2016).

The mass flow was calculated as:

$$S73_CM08 = S73_CF08 * \text{Rho_CF08}, \text{ (with: Rho_CF08 = f [S73_CP04, T_inlet])}$$

A redundant and diversified check at stationary mass flows was performed during the commissioning of steady-state CHF test STS-123.01 to check the turbine flow meter against the mass flow reference M_CF03G (by means of nozzle flow measurement) of the KATHY test loop. Therefore, the turbine flow meter was installed during STS-123.01 in the inlet pipeline. Two measurement channels of the turbine flow meter are available: S73 CF06 in liters per second l/s and M_CF06 in kg/s. Both channels are calculated and measured by the spinning of the turbine.

These were the comparable results:

Test No.	Time	Date	M_CF03G [kg/s] Reference Nozzle	M_CF06 [kg/s] Turbine	Delta %
STS-123.01-IBS.14	10:02:00	08/16/16	0.498059	0.500926	0.6
STS-123.01-IBS.15	10:04:00	08/16/16	1.039101	1.049549	1.0
STS-123.01-IBS.16	10:06:00	08/16/16	1.551450	1.552297	0.1
STS-123.01-IBS.17	10:09:00	08/16/16	1.999344	1.989529	-0.5
STS-123.01-IBS.18	10:12:00	08/16/16	2.501765	2.491899	-0.4
STS-123.01-IBS.19	10:14:00	08/16/16	2.989212	2.986041	-0.1
STS-123.01-IBS.20	10:15:00	08/16/16	3.515385	3.504891	-0.3
STS-123.01-IBS.21	10:17:00	08/16/16	3.975415	3.969369	-0.2
STS-123.01-IBS.22	10:21:00	08/16/16	4.480199	4.479612	0.0
STS-123.01-IBS.23	10:23:00	08/16/16	5.010063	5.008858	0.0
STS-123.01-IBS.24	10:24:00	08/16/16	5.489166	5.493779	0.1
STS-123.01-IBS.25	10:26:00	08/16/16	5.987362	5.995006	0.1
STS-123.01-IBS.26	10:31:00	08/16/16	6.466621	6.485505	0.3
STS-123.01-IBS.27	10:33:00	08/16/16	6.692286	6.715189	0.3

The mass flow M_CF06 (by turbine flow meter) compared to M_CF03G (by nozzle) was in good agreement (-0.5 percent to 1.0 percent) for stationary mass flows ranging from 0.5 kg/s to 6.7 kg/s.

Before instability test STS-123.03, the turbine flow meter was then installed in the inlet pipeline of the instability test loop.

The turbine flow meter should be evaluated only for (semi-) stationary mass flow conditions. Because of its measurement principle, it shows a lag/slip for transient mass flows.

6.5.2 Mass Evaluation by Inlet Pressure Drop S73 CP12

The inlet pressure drop S73 CP12B was separately postprocessed to derive the dynamic inlet mass flows during the instability test STS-123.03.

The inlet flow is measured by a turbine device that is accurate for steady-state and slow transients. For oscillatory flow, the measurement suffers from the inertia problem that underestimates the magnitude of flow oscillations and displays a time delay. This problem is solved by relying on pressure drop measurements across two points in the inlet piping. Since the two pressure taps are not close to each other, flow inertia must be taken into account. The flow is determined by solving the differential equation:

$$I \frac{d\dot{m}}{dt} = \Delta p(t) - \frac{k}{2\rho A^2} \dot{m}(t) |\dot{m}(t)|$$

- Where
- I = Flow inertia, sum of length-to-area for all pipe segments, [m⁻¹]
 - \dot{m} = Mass flow rate, [kg/s]
 - t = Time, [s]
 - Δp = Pressure drop, [pascals]
 - k = Loss coefficient [-]
 - ρ = Fluid density, [kg/m³]
 - A = Reference area for the definition of loss coefficient, taken as 0.0064516 m² (10 square inches)

The differential equation above assumes the form losses to be symmetrical in the forward and reverse directions. The absolute value of the flow rate in the last term is needed to obtain flow in either direction. A central-differencing scheme (semi-implicit) is used to obtain the flow rate. Thus,

$$I \frac{\dot{m}(t + \Delta t) - \dot{m}(t)}{\Delta t} = \frac{1}{2} (\Delta p(t + \Delta t) + \Delta p(t)) - \frac{k}{8\rho A^2} (\dot{m}(t + \Delta t) + \dot{m}(t)) |\dot{m}(t + \Delta t) + \dot{m}(t)|$$

Solution of the algebraic equation resulting from the central differencing scheme requires a priori knowledge of the flow direction. This is done by using the sign of the mass flow rate produced by an explicit method (identified with a tilde). The solution is reduced to solving a quadratic equation with the coefficients:

$$a = \frac{k}{8\rho A^2 I} \text{sign} [\tilde{m}(t + \Delta t) + \dot{m}(t)]$$

$$b = 1 + 2a \dot{m}(t)$$

$$c = a \dot{m}^2(t) - \dot{m}(t) - \frac{\Delta t}{2I} (\Delta p(t + \Delta t) + \Delta p(t))$$

The new time step mass flow rate is obtained from:

$$\dot{m}(t + \Delta t) = \frac{-b + \sqrt{b^2 - 4ac}}{2a}$$

Appendix LLL gives the results of the postprocessed mass flows.

6.6 Inlet Subcooling

The inlet subcooling DH_Inlet is = f (S73 CP04, T_inlet). T_inlet is derived by the measured inlet temperature measurement point S73_CT03B.

7 MEASUREMENT UNCERTAINTIES

The measurement uncertainties are as follows:

- electrical power ± 0.2 percent (full scale)
- fluid flow ± 1.1 percent (full scale), by nozzle
- system pressure ± 0.2 percent (full scale)
- differential pressure ± 0.2 percent (full scale)
- inlet temperature ± 0.4 K
- inlet subcooling ± 2.8 kJ/kg

7.1 Electrical Power Uncertainty

The bundle power measurement is based upon the multiplication of bundle current and voltage drop of the heated length. The systematic saturation error of the current measurement is eliminated by calibration and polynomial fit.

Bundle Power Uncertainty Source	Estimated Uncertainty
1. Uncertainty current transducer	0.1 %
2. Calibration device setup of current transducers	0.1 %
3. Uncertainty power analyzer (including voltage measurement)	0.1 %
4. Calibration device setup	0.1 %
Total estimated bundle power measurement uncertainty*	0.2 %

* Assuming uncertainties are statistically independent.

7.2 Fluid Flow by Nozzle Uncertainty

The bundle mass flow measurement is performed by sensing the pressure drop across an ISA² 1932 nozzle. The mass flow measurement uncertainty was calculated according to ISO³ 5167 ("Measurement of Fluid Flow by Means of Pressure Differential Devices Inserted in Circular Cross-section Conduits Running Full," International Standards Organization, 2003) by considering the following functional relationship:

$$q_m = \frac{C}{\sqrt{1-\beta^4}} \cdot \varepsilon \cdot \frac{\pi}{4} \cdot d^2 \cdot \sqrt{2 \cdot \Delta p \cdot \rho}$$

where

- q_m = bundle mass flow in kg/s
- C = nozzle flow coefficient according to DIN EN⁴ ISO 5167 Part 1
- β = diameter ratio $\beta = d/D$
- d = nozzle throat diameter at operating temperature
- D = inner diameter of pipe
- Δp = nozzle differential pressure drop

² ISA is the International Federation of the National Standardizing Associations.

³ ISO is International Organization for Standardization.

⁴ DIN is Deutsches Institut für Normung, the German institute for standardization; EN is English.

ε = expansion factor = 1 (for water flow)
 ρ = density at nozzle

The static mass flow measurement uncertainty was calculated by applying the following equation, provided by ISO 5167.

$$e_{qm,static} = \sqrt{e_c^2 + e_\varepsilon^2 + 4 e_d^2 \left(1 + \frac{\beta^4}{1 - \beta^4}\right)^2 + 4 e_D^2 \cdot \left(\frac{\beta^4}{1 - \beta^4}\right)^2 + \frac{1}{4} e_p^2 + \frac{1}{4} e_{\Delta p}^2}$$

The total mass flow measurement uncertainty is calculated by the static and the oscillating flow measurement uncertainties:

$$e_{qm,total} = \sqrt{e_{qm,static}^2 + e_{qm,oscillation}^2} = \sqrt{0.01^2 + 0.005^2}$$

$$e_{qm,total} = 1.1 \%$$

The estimated magnitudes of the various sources of mass flow uncertainty and of the total mass flow measurement uncertainty are indicated as follows:

Bundle Mass Flow Uncertainty Source	Estimated Uncertainty
1. Flow coefficient, e_c	0.8 %
2. Expansion factor, e_ε	0.0 % (single phase flow)
3. Nozzle throat diameter, e_d	0.2 %
4. Upstream inner pipe diameter, e_D	0.2 %
5. Density, e_p	0.4 %
6. Differential pressure drop, $e_{\Delta p}$	0.2 % (static)
7. Oscillation of mass flow, $e_{qm,oscillation}$	0.5 %
Total estimated mass flow measurement uncertainty $e_{qm,total}$	1.1 %

7.3 System Pressure Uncertainty

The system pressure is measured by pressure transducer. This device is calibrated against a high-precision reference transducer, which in turn is calibrated against standards-traceable national standards.

The sources of uncertainty in the measurement of system pressure are given as follows:

System Pressure Measurement Uncertainty Source	Estimated Uncertainty
1. Calibration of reference transducer	0.1 %
2. Calibration of pressure transducer vs. reference transducer	0.1 %
3. Calibration of reference device	0.1 %
4. Measuring channel vs. reference device	0.1 %
Total estimated pressure measurement uncertainty	0.2 %

7.4 Differential Pressure Uncertainty

The differential pressure is measured by differential pressure transducers. This device is calibrated against a high-precision reference transducer, which in turn is calibrated against standards-traceable national standards.

The sources of uncertainty in the measurement of differential pressure are given as follows:

Differential Pressure Measurement Uncertainty Source	Estimated Uncertainty
1. Calibration of reference transducer	0.1 %
2. Calibration of differential pressure transducer vs. reference transducer	0.1 %
3. Calibration of reference device	0.1 %
4. Measuring channel vs. reference device	0.1 %
Total estimated differential pressure measurement uncertainty	0.2 %

7.5 Inlet Subcooling Uncertainty

The test section inlet subcooling is a derived parameter based upon the fluid temperature at the test section inlet and the system pressure. The uncertainty associated with the system pressure is ± 0.4 bar (measurement range 0–200 bar). The fluid inlet temperature is measured to within ± 0.4 K by a 100 ohm platinum resistance thermometer. Through application of steam-water tables, the inlet subcooling uncertainty was estimated for 69 bar as indicated below:

Uncertainty Source	Estimated Uncertainty	Inlet Subcooling Uncertainty
1. System pressure	0.4 bar	2.0 kJ/kg
2. Inlet temperature	0.4 K	1.9 kJ/kg
Total estimated inlet subcooling measurement uncertainty*		2.8 kJ/kg

* Assuming uncertainties in pressure and temperature are statistically independent.

8 CONCLUSION

The test results are valid.

The test results are related to the tested bundles STS-123.01, STS-123.02, and STS-123.03.

Following the tests, the bundle was disassembled. Observations made of the disassembled test section components did not indicate any issues with the measurements.

9 NOTES

9.1 Steady-State Tests STS-123.01, STS-123.02

During steady-state test STS-123.01, analysts noticed that some differential pressure taps over the test bundle were blocked at hot conditions. The test bundle STS-123.01 was inspected and the blockages were removed. Afterwards, the pressure drop tests were run with the test bundle STS-123.02.

TC 59/1Z was defective through STS-123.01. Position 59 was a high-powered heater rod and 1Z is the most downstream TC location. Level 1 is expected to show CHF with small mass flow rates. Therefore, the STS-123.01 CHF tests were started with several additional scoping CHF tests to demonstrate that rod position 59 was not the leading position in the test bundle. These scoping CHF tests were the test runs STS-123.01-294.01 to -299.04. For these tests, the mass flow rate was increased to force CHF detections to TC levels 2 to 5. No CHF was monitored at the upstream TCs of the heater rod on position 59.

9.2 Instability Test STS-123.03

On December 7, 2016, during the commissioning of the instability test loop, condensation hammers were noticed in the steam-water mixing chamber. Analysts assumed that the steam quencher pipe inside was damaged.

From December 8 to 9, 2016, a second steam-water mixing chamber was routed and connected to the instability test loop. This new setup was successfully commissioned on December 10, 2016.

The high subcooling test runs were performed at approximately 30 K–35 K.

APPENDIX A REQUIREMENTS FOR STEADY-STATE AND ATWS-I TESTS

A.1 Introduction and Summary

This document defines the test hardware and the test program for the steady-state part of the anticipated transient without SCRAM instability (ATWS-I) test. The steady-state part is considered as the pretest to the instability test. Test data will be applied to evaluate the pressure loss coefficients of the spacers and the bundle dryout performance at steady-state conditions.

A.2 Pressure Drop and Boiling Transition Test Program

A.2.1 Program Scope

Framatome will supply the test equipment.

A.2.2 Experimental Measurements

The following measurements shall be recorded simultaneously for each set of tests performed in this experimental program:

- bundle power (kilowatts (kW))
- assembly inlet flow (kilograms per second (kg/s))
- assembly inlet temperature (degrees Celsius (°C))
- assembly inlet subcooling determined based on the exit pressure as used for the previous tests (kilojoules per kilogram (kJ/kg))
- assembly inlet subcooling determined based on the inlet pressure (kJ/kg)
- assembly exit pressure (bar)
- differential pressures along the test assembly (millibar (mbar))
- rod and thermocouple experiencing boiling transition

A.2.3 Dryout Tests STS-123.01

Tests shall be conducted with an electrically heated bundle using a downskew axial power profile for the determination of the boiling transition behavior. The tests shall specifically determine the radial and axial location of boiling transition and the test assembly power at which boiling transition is detected.

Figure 2-4 to Figure 2-11 in the main body of this report show the bundle average local peaking pattern (distribution of rod types) and rod positions with thermocouple instrumentation (bold circles). Rod type 1 includes heater rods with the highest radial power peaking of about 1.3. The radial power peaking of type 2 heater rods is about 1.2, type 3 rods 1.1, and type 4 rods about 1.0.

The test matrix and pressure variation shown shall be followed for the peaking pattern given in Figure 2-4 to Figure 2-6. A minimum of two replicate points shall have been repeated at the end of each day. One of these points will be a repeat of the first data point taken during the day's testing. One of these points shall include the following state point: assembly exit pressure 69 bar, inlet mass flow rate of 7 kg/s, inlet subcooling of 90 kJ/kg. After the completion of measurements for every mass flow, one replicate point shall be repeated to confirm the tested performance. Replicate points shall also be repeated after every occurrence in the loop (e.g., trip of power or failure of a bundle component). The table below shows the total estimated number of steady-state critical power data points, including replicates.

Assembly performance can affect these criteria. If necessary, these criteria can be changed by the test team with the concurrence of Framatome GmbH. The criteria applied for each critical power measurement shall be reported.

Test matrix for the standard map at assembly exit pressure 69 bar

Flow rate (kg/s)	Inlet subcooling (kJ/kg)				
	50	90	130	170	220
7	X	X	X	X	X
5	X	X	X	X	X
3	X	X	X	X	X

Note: The test results can affect the actual test matrix. The test matrix can be changed with concurrence of Framatome GmbH by signature in the test procedure or test logs.

Pressure variation

Flow rate (kg/s)	Pressure (bar)		
	55	69	83
7	X	X	X
5	X	X	X
3	X	X	X

Note: For each mass flow rate, measurements are taken at each inlet subcooling of 50, 90, 130, 170, and 220 kJ/kg.

Total number of data points in the tests with the downskew power profile

	Pressure			TOTAL
	55 bar	69 bar	83 bar	
# of data points	15	15	15	45
# of repeat points	3	8	3	14
Σ	18	23	18	59

A.2.4 Pressure Drop Measurements STS-123.02

Pressure drop measurements shall be made to determine component (mainly spacer grid) pressure loss for conditions of single- and two-phase flow. The single-phase pressure drop shall be determined at a pressure of 69 bar, inlet temperature of 260 degrees C and mass flow rates given in the table below. Single- and two-phase pressure drop measurements at 4.50 kg/s and 6.30 kg/s shall be performed twice: once with the low flow line and once with the high flow line.

The two-phase pressure drop tests shall be performed on the test bundle at 69 bar and an inlet subcooling of 58 kJ/kg. The single- and two-phase test matrices show the flow rates and bundle powers. Figure 2-8 to Figure 2-10 show the peaking pattern. For the two-phase pressure drop measurements, the bundle power shall not exceed 90 percent of the bundle critical power. The table below shows the total number of pressure drop measurements.

The overall pressure drop shall be measured by two separate devices with different measurement ranges to provide assurance that the measurements are correct.

Single-phase pressure drop test matrix

Flow rate (kg/s)	3.15	4.50	6.30	9.45	12.60	15.75	18.90
69 bar, 260 °C	X	X	X	X	X	X	X

Two-phase pressure drop test matrix

Flow rate (kg/s)	Power (megawatts)					
	2	3	4	6	7	8
18.90	X		X	X	X	X
15.75	X		X	X	X	X
12.60	X		X	X	X	X
9.45	X		X	X	X	X
6.30	X		X	X	X	
4.50	X	X	X			
3.15	X	X				

Note: The results can affect the actual test matrix. The test matrix can be changed with concurrence of Framatome GmbH. Concurrence may be indicated by signature in the test procedure or test logs.

Number of single- and two-phase pressure drop data points

Single phase	Two phase	Replicates	Total state points
7	29	9	45

Note: The results can affect the actual test matrix. The test matrix can be changed with concurrence of Framatome GmbH. Concurrence may be indicated by signature in the test procedure or test logs.

A.3 STS-123.03 Requirements for ATWS-I Instability Tests

A.3.1 Introduction and Summary

The present specification defines the test hardware and test program for ATWS-I stability measurements for the U.S. Nuclear Regulatory Commission. It contains the definition of the test program, discussion of the test hardware, and documentation requirements.

The purpose of the measurements is to collect data for the stability performance of the bundle under natural circulation conditions to be used for subsequent thermal-hydraulic code validation. The flow oscillation magnitude will be allowed to increase to collect cyclical dryout and rewetting data, without violating the loop safety limits.

The test bundle is a full scale mockup of a noncommercial 10x10 boiling-water reactor bundle design. It consists of a square array of rods supported at fixed axial positions by spacers. The bundle contains 81 full-length rods and 10 part-length heater rods that are 10.28 millimeters (mm) in diameter. A square cross section inner water channel occupies a 3x3 array with an outer dimension of 35 mm. The inner water channel has no internal fluid flow. The test bundle has a ceramic liner, which serves to simulate the flow channel and to electrically insulate the spacers from each other. The ceramics are housed in a stainless steel outer channel.

A.3.2 Stability Test Program

The stability measurements to collect decay ratio and frequency data are taken under steady-state conditions and also under transient conditions with oscillating flow. The latter extends to large oscillation magnitudes such that cyclical dryout and rewetting and failure to rewet are observed. Some tests will be performed while a feedback module simulating neutron kinetics and pin conduction takes the inlet flow signal as input and provides a power demand signal as output. The following sections outline the projected test series; however, this test matrix may be modified during the actual tests to fit within the allotted time frame.

A.3.3 Range of Parameters

The test matrix is created by varying the operating parameters in the following ranges:

- Pressure: 7–8 megapascals
- Subcooling: 20–45 Kelvin (K)
- Flow rate: Natural circulation
- Feedback Parameters: For the measurements with feedback module, the main decay ratio search parameter is the feedback gain representing a void-reactivity coefficient. Subcritical reactivity and fuel thermal time constant will also be varied to test their effect.

A.3.4 Test Matrix without Feedback Module

The table below gives the proposed matrix.

Test No.	Pressure bar	Inlet Subcooling K	Example Initial Power megawatts	Water Level
1	70	20.0	3.0	Nominal
2	70	20.0	3.0	Reduced
3	70	45.0	3.0	Nominal
4	80	20.0	3.0	Nominal

Based on a specific initial power corresponding to a precalculated decay ratio of 0.5, for each test run, the power shall be increased in steps defined by Framatome GmbH.

A.3.5 Test Matrix with Feedback Module

The table below gives the test sequences for the measurements with feedback for one subcooling point. Limit cycle amplitude limits are also indicated. The test sequences with feedback in the table below are repeated for the subcooling values 20 K and 45 K.

An initial state point will be established (i.e., pressure, subcooling, and initial power) and individual feedback parameters will be varied within that state point, as shown in the table below. The varied parameters are the following:

- Subcritical reactivity, ρ_{sub}
- Fuel thermal time constant, τ

Feedback		Pressure (bar)	Fuel Thermal Time Constant	Expected DR ⁵		Oscillation Magnitude		Record Time [min]	Comments	
ρ_{sub}	gain			Hyd.	System	Flow%	Power%			
0	0	70	2.5	0.5	-	Noise	Noise	10	Dryout inception Dryout/rewetting, $\Delta T < 100$ K	
	Small			0.5	<1.0	Coherent	Coherent	3		
	Increase			0.5	~1.0	20%		3		
	Increase			0.5	>1.0	Large		1		
				0.5	>1.0	Large	Decay	Short		2
0	0	80	2.5	0.5	-	Noise	Noise	10	Dryout inception Dryout/rewetting, $\Delta T < 100$ K ⁶	
	Small			0.5	<1.0	Coherent	Coherent	3		
	Increase			0.5	~1.0	20%		3		
	Increase			0.5	>1.0	Large		1		
				0.5	>1.0	Large	Decay	Short		2
1.0	Same	70	2.5	0.5	<1.0	Noise	Noise	10	Dryout inception Dryout/rewetting, $\Delta T < 100$ K	
	Increase			0.5	~1.0	Coherent	Coherent	3		
	Increase			0.5	>1.0	20%		3		
	Increase			0.5	>1.0	Large		1		
	Increase			0.5	>1.0	Large		Short		
	0			0.5	-	Decay	Short	2		

⁵ DR is decay ratio

⁶ ΔT is the change in temperature from initial temperature

Feedback		Pressure (bar)	Fuel Thermal Time Constant	Expected DR ⁵		Oscillation Magnitude		Record Time [min]	Comments
ρ_{sub}	gain			Hyd.	System	Flow%	Power%		
0.8	Same	70	2.5	0.5	<1.0	Noise	Noise	10	Dryout inception Dryout/rewetting, $\Delta T < 100$ K
	Increase			0.5	~1.0	Coherent	Coherent	3	
	Increase			0.5	>1.0	20%		3	
	Increase			0.5	>1.0	Large		1	
	Increase			0.5	>1.0	Large		Short	
	0			0.5	-	Decay		2	
1.2	Same	70	2.5	0.5	<1.0	Noise	Noise	10	Dryout inception Dryout/rewetting, $\Delta T < 100$ K
	Increase			0.5	~1.0	Coherent	Coherent	3	
	Increase			0.5	>1.0	20%		3	
	Increase			0.5	>1.0	Large		1	
	Increase			0.5	>1.0	Large		Short	
	0			0.5	-	Decay		2	
0.0	Same	70	2.0	0.5	<1.0	Noise	Noise	10	Dryout inception Dryout/rewetting, $\Delta T < 100$ K
	Increase			0.5	~1.0	Coherent	Coherent	3	
	Increase			0.5	>1.0	20%		3	
	Increase			0.5	>1.0	Large		1	
	Increase			0.5	>1.0	Large		Short	
	0			0.5	-	Decay		2	
0.0	Same	70	4.0	0.5	<1.0	Noise	Noise	10	Dryout inception Dryout/rewetting, $\Delta T < 100$ K
	Increase			0.5	~1.0	Coherent	Coherent	3	
	Increase			0.5	>1.0	20%		3	
	Increase			0.5	>1.0	Large		1	
	Increase			0.5	>1.0	Large		Short	
	0			0.5	-	Decay		2	

Test results can affect the actual test matrix. The test matrix can be changed with concurrence of Framatome GmbH indicated by signature in the test procedure or test logs.

APPENDIX B LIST OF ATWS-I TEST DATA

- Tests without Feedback

Test No.	Pressure bar	Inlet Subcooling K	Inlet Temp °C	Water Level	Run Number (STS-123.03 -xxx.xx)	Date Complete	Time Notes Comments
pretest	69	20	265	Nominal	101.01	10.12.2016	
pretest	69	20	265	Nominal	102.01	10.12.2016	
pretest	69	20	265	Nominal	103.01	10.12.2016	
pretest	69	20	265	Nominal	104.01	10.12.2016	
1	70	20	265	Nominal	104.02	12.12.2016	
				Nominal	104.03	12.12.2016	
				Nominal	105.01	12.12.2016	
				Nominal	105.02	12.12.2016	
				Nominal	106.01	12.12.2016	
				Nominal	107.01	12.12.2016	
				Nominal	108.01	12.12.2016	
				Nominal	109.01	12.12.2016	
				Nominal		12.12.2016	4 min
				Nominal		12.12.2016	5.3 min
				Nominal	110.01	12.12.2016	
				Nominal		12.12.2016	30s
				Nominal		12.12.2016	4 min
Nominal	12.12.2016	6 min/dryout					
2	70	20	265	Reduced	201.01	12.12.2016	
				Reduced	202.01	12.12.2016	
				Reduced	203.01	12.12.2016	
				Reduced	203.02	13.12.2016	start 9:53
				Reduced	204.01	13.12.2016	start 10:10
				Reduced	205.01	13.12.2016	
				Reduced	206.01	13.12.2016	
				Reduced	207.01	13.12.2016	
				Reduced		13.12.2016	start 10:54
				Reduced		13.12.2016	start 11:01
				Reduced	207.02	13.12.2016	
				Reduced		13.12.2016	start 12:06
				Reduced		13.12.2016	start 12:09

Test No.	Pressure bar	Inlet Subcooling K	Inlet Temp °C	Water Level	Run Number (STS-123.03 -xxx.xx)	Date Complete	Time Notes Comments
				Reduced		13.12.2016	start 12:11
				Reduced		13.12.2016	start 12:13
				Reduced		13.12.2016	start 12:15
				Reduced		13.12.2016	start 12:17
				Reduced		13.12.2016	start 12:28
				Reduced	207.03	13.12.2016	start 12:29
				Reduced		13.12.2016	start 12:31
				Reduced		13.12.2016	start 12:33
				Reduced		13.12.2016	start 12:35
				Reduced		13.12.2016	start 12:37
				Reduced		13.12.2016	start 12:39
				Reduced		13.12.2016	start 12:42/dryout
3	70	45		Nominal	310.01	16.12.2016	start 15:42
				Nominal		16.12.2016	start 15:48
				Nominal		16.12.2016	start 15:51
				Nominal		16.12.2016	start 15:54
				Nominal		16.12.2016	start 15:57
				Nominal		16.12.2016	start 15:59
				Nominal		16.12.2016	start 16:02
				Nominal		16.12.2016	start 16:04
				Nominal		16.12.2016	start 16:06
				Nominal		16.12.2016	start 16:08
				Nominal		16.12.2016	start 16:09/dryout
4	80	20	275	Nominal	401.01	14.12.2016	
				Nominal	402.01	14.12.2016	
				Nominal	403.01	14.12.2016	
				Nominal	404.01	14.12.2016	
				Nominal	405.01	15.12.2016	
				Nominal	406.01	15.12.2016	dryout—reapproach
				Nominal	407.01	15.12.2016	start 16:29
				Nominal		15.12.2016	start 16:30
				Nominal		15.12.2016	start 16:35
				Nominal		15.12.2016	start 16:40/dryout

Test No.	Pressure bar	Inlet Subcooling K	Inlet Temp °C	Water Level	Run Number (STS-123.03 -xxx.xx)	Date Complete	Time Notes Comments
5	70	20	265	Nominal	101.02	20.12.2016	Repeatability test

• Tests with Feedback, Inlet Subcooling 20 K

Feedback	Pressure (bar)	Fuel Thermal Time Constant	Expected DR		Oscillation Magnitude		Record Time	Comments	Run Number	Date Complete	Posttest Comments
			Hyd.	System	Flow%	Power%					
ρ_{sub} Gain	0	70	2.5	0.5	-	Noise	Noise	10	123.03-A01.01	13.12.2016	Repeat of test
	Small			0.5	<1.0	Coherent	Coherent	3	123.03-A01.02	20.12.2016	
	Increase			0.5	~1.0	20%		3			
	Increase			0.5	>1.0	Large	Large	1			
						Large	Dryout inception	Short			
						Decay	Dryout/rewetting, $\Delta T < 100$ K	2			
0	80	2.5	0.5	0.5	-	Noise	Noise	10	123.03-E01.01	20.12.2016	
	Small			0.5	<1.0	Coherent	Coherent	3			
	Increase			0.5	~1.0	20%		3			
	Increase			0.5	>1.0	Large	Large	1			
						Large	Dryout inception	Short			
						Decay	Dryout/rewetting, $\Delta T < 100$ K	2			
1	70	2.5	0.5	0.5	<1.0	Noise	Noise	10	123.03-C01.01	14.12.2016	
	Increase			0.5	~1.0	Coherent	Coherent	3			
	Increase			0.5	>1.0	20%		3			
	Increase			0.5	>1.0	Large	Large	1			
						Large	Dryout inception	Short			
						Decay	Dryout/rewetting, $\Delta T < 100$ K	2			
0.8	70	2.5	0.5	0.5	<1.0	Noise	Noise	10	123.03-D01.01	14.12.2016	
	Increase			0.5	~1.0	Coherent	Coherent	3			
	Increase			0.5	>1.0	20%		3			
	Increase			0.5	>1.0	Large	Large	1			
						Large	Dryout inception	Short			
						Decay	Dryout/rewetting, $\Delta T < 100$ K	2			

Feedback	Pressure (bar)	Fuel Thermal Time Constant	Expected DR		Oscillation Magnitude		Record Time	Comments	Run Number	Date Complete	Posttest Comments
			Hyd.	System	Flow%	Power%					
ρ_{sub} Gain	70	2.5	0.5	<1.0	Noise	Noise	10	Dryout inception Dryout/rewetting, $\Delta T < 100$ K	123.03-B01.01	14.12.2016	
			0.5	~1.0	Coherent	Coherent	3				
			0.5	>1.0	20%		3				
			0.5	>1.0	Large		1				
			0.5	>1.0	Large		Short				
			0.5	-	Decay		2				
0	70	2	0.5	<1.0	Noise	Noise	10	Dryout inception Dryout/rewetting, $\Delta T < 100$ K	123.03-F01.01	13.12.2016	
			0.5	~1.0	Coherent	Coherent	3				
			0.5	>1.0	20%		3				
			0.5	>1.0	Large		1				
			0.5	>1.0	Large		Short				
			0.5	-	Decay		2				
0	70	4	0.5	<1.0	Noise	Noise	10	Dryout inception Dryout/rewetting, $\Delta T < 100$ K	123.03-G01.01	13.12.2016	
			0.5	~1.0	Coherent	Coherent	3				
			0.5	>1.0	20%		3				
			0.5	>1.0	Large		1				
			0.5	>1.0	Large		Short				
			0.5	-	Decay		2				

• Tests with Feedback, Inlet Subcooling 45K Target (30K–35K actual)

Feedback	Pressure (bar)	Fuel thermal Time Constant	Expected DR		Oscillation Magnitude		Record Time	Comments	Run Number	Date Complete	Posttest Comments
			Hyd.	System	Flow%	Power%					
ρ_{sub} Gain							[min]		SIN/STS*		
0	70	2.5	0.5	-	Noise	Noise	10		123.03-A11.01	19.12.2016	
Small			0.5	<1.0	Coherent	Coherent	3				
Increase			0.5	~1.0	20%		3				
Increase			0.5	>1.0	Large		1	Dryout inception			
					Large		Short	Dryout/rewetting, $\Delta T < 100$ K			
					Decay		2				
0	80	2.5	0.5	-	Noise	Noise	10		123.03-E11.01	20.12.2016	
Small			0.5	<1.0	Coherent	Coherent	3				
Increase			0.5	~1.0	20%		3				
Increase			0.5	>1.0	Large		1	Dryout inception			
					Large		Short	Dryout/rewetting, $\Delta T < 100$ K			
					Decay		2				
1	70	2.5	0.5	<1.0	Noise	Noise	10		123.03-C11.01	19.12.2016	
Same			0.5	~1.0	Coherent	Coherent	3				
Increase			0.5	>1.0	20%		3				
Increase			0.5	>1.0	Large		1	Dryout inception			
Increase			0.5	>1.0	Large		Short	Dryout/rewetting, $\Delta T < 100$ K			
0			0.5	-	Decay		2				
0.8	70	2.5	0.5	<1.0	Noise	Noise	10		123.03-D11.01	19.12.2016	
Same			0.5	~1.0	Coherent	Coherent	3				
Increase			0.5	>1.0	20%		3				
Increase			0.5	>1.0	Large		1	Dryout inception			
Increase			0.5	>1.0	Large		Short	Dryout/rewetting, $\Delta T < 100$ K			
0			0.5	-	Decay		2				

Feedback	Pressure (bar)	Fuel thermal Time Constant	Expected DR		Oscillation Magnitude		Record Time	Comments	Run Number	Date Complete	Posttest Comments
			Hyd.	System	Flow%	Power%					
ρ_{sub} Gain	70	2.5	0.5	<1.0	Noise	Noise	10	Dryout inception Dryout/rewetting, $\Delta T < 100$ K	123.03-B11.01	19.12.2016	
			0.5	~1.0	Coherent	Coherent	3				
			0.5	>1.0	20%		3				
			0.5	>1.0	Large		1				
			0.5	>1.0	Large		Short				
			0.5	-	Decay		2				
0	70	2	0.5	<1.0	Noise	Noise	10	Dryout inception Dryout/rewetting, $\Delta T < 100$ K	123.03-F11.03	20.12.2016	
			0.5	~1.0	Coherent	Coherent	3				
			0.5	>1.0	20%		3				
			0.5	>1.0	Large		1				
			0.5	>1.0	Large		Short				
			0.5	-	Decay		2				
0	70	4	0.5	<1.0	Noise	Noise	10	Dryout inception Dryout/rewetting, $\Delta T < 100$ K	123.03-G11.01	19.12.2016	
			0.5	~1.0	Coherent	Coherent	3				
			0.5	>1.0	20%		3				
			0.5	>1.0	Large		1				
			0.5	>1.0	Large		Short				
			0.5	-	Decay		2				

• Transient test conditions

Feedback	Pressure (bar)	Fuel thermal Time Constant	Expected DR		Oscillation Magnitude		Record Time	Comments	Run Number	Date Complete	Posttest Comments
			Hyd.	System	Flow%	Power%					
ρ_{sub} Gain							[min]		SIN/STS*		
**	**	**	**	**	**	**	**	**	123.03-T01.01	20.12.2016	Transient test— Initial No failure to rewet Transient retest— Failure to rewet observed
									123.03-T01.02	20.12.2016	

* - Each of the tests generated two data sets, SIN- for the SINAN data and STS- for the KATHY test loop data. In some cases, a posttest processing file was generated for graphics.

** - The test engineer and the U.S. Nuclear Regulatory Commission defined the transient runs, which were negotiated before the test runs.

APPENDIX C

**TEST MATRIX INSTABILITY TEST STS-123.03
INITIAL CONDITIONS**

Run No.	Date	Time	System Pressure [bar]	Subcooling [kJ/kg] ⁷⁾	Mass Flow [kg/s] ³⁾	Level Separator [m]	Feedback Active [-]	Tau [s]	Rhosub [\$]	Vrcmul [-]	Leading TC [-]
101.01	Dec 10, 2016	12:41	70.5	125.8	6.0	1.13	No	--	--	--	--
102.01	Dec 10, 2016	13:43	70.8	113.4	5.4	1.14	No	--	--	--	--
103.01	Dec 10, 2016	14:33	69.7	108.6	5.1	1.13	No	--	--	--	--
104.01	Dec 10, 2016	14:46	70.2	109.4	5.0	1.12	No	--	--	--	--
104.02	Dec 12, 2016	11:00	70.1	108.3	5.0	1.10	No	--	--	--	--
104.03	Dec 12, 2016	11:32	70.8	108.3	5.0	1.12	No	--	--	--	--
105.01	Dec 12, 2016	12:12	70.1	103.5	4.7	1.11	No	--	--	--	--
105.02	Dec 12, 2016	12:45	70.3	111.9	4.8	1.13	No	--	--	--	--
106.01	Dec 12, 2016	12:59	69.6	105.9	4.5-5.0	1.13	No	--	--	--	--
107.01	Dec 12, 2016	13:13	70.5	110.6	4.5-5.0	1.13	No	--	--	--	--
108.01	Dec 12, 2016	13:28	70.2	103.3	3.9-5.2	1.12	No	--	--	--	--
109.01	Dec 12, 2016	13:58	70.3	107.4	3.0-6.0	1.12	No	--	--	--	--
110.01	Dec 12, 2016	14:08	70.0	103.9	2.0-7.0	1.12	No	--	--	--	59/5X, 59/5Z
201.01	Dec 12, 2016	14:32	70.3	108.6	5.1	0.40	No	--	--	--	--
202.01	Dec 12, 2016	15:31	70.0	111.3	5.0	0.42	No	--	--	--	--
203.01	Dec 12, 2016	15:56	70.7	106.9	4.7	0.40	No	--	--	--	--
203.02	Dec 13, 2016	09:48	70.4	103.8	4.7	0.40	No	--	--	--	--
204.01	Dec 13, 2016	10:10	70.6	107.0	4.6	0.39	No	--	--	--	--
205.01	Dec 13, 2016	10:25	70.5	105.1	3.5-5.1	0.40	No	--	--	--	--
206.01	Dec 13, 2016	10:45	70.7	103.9	2.0-6.5	0.39	No	--	--	--	--
207.01 ⁴⁾	Dec 13, 2016	10:55	70.1	106.8	1.6-6.9	0.42	No	--	--	--	--
207.02	Dec 13, 2016	11:54	70.5	106.0	2.0-6.5	0.42	No	--	--	--	--
207.03	Dec 13, 2016	12:20	70.3	102.6	3.8-4.7	0.42	No	--	--	--	87/5X 87/5Z
A01.01	Dec 13, 2016	14:00	70.5	106.2	5.2	1.10	Yes	2.5	0.0	0.10-0.17	88/6Z
F01.01	Dec 13, 2016	15:31	70.1	103.9	5.2	1.12	Yes	2.0	0.0	0.10-0.15	88/6Z

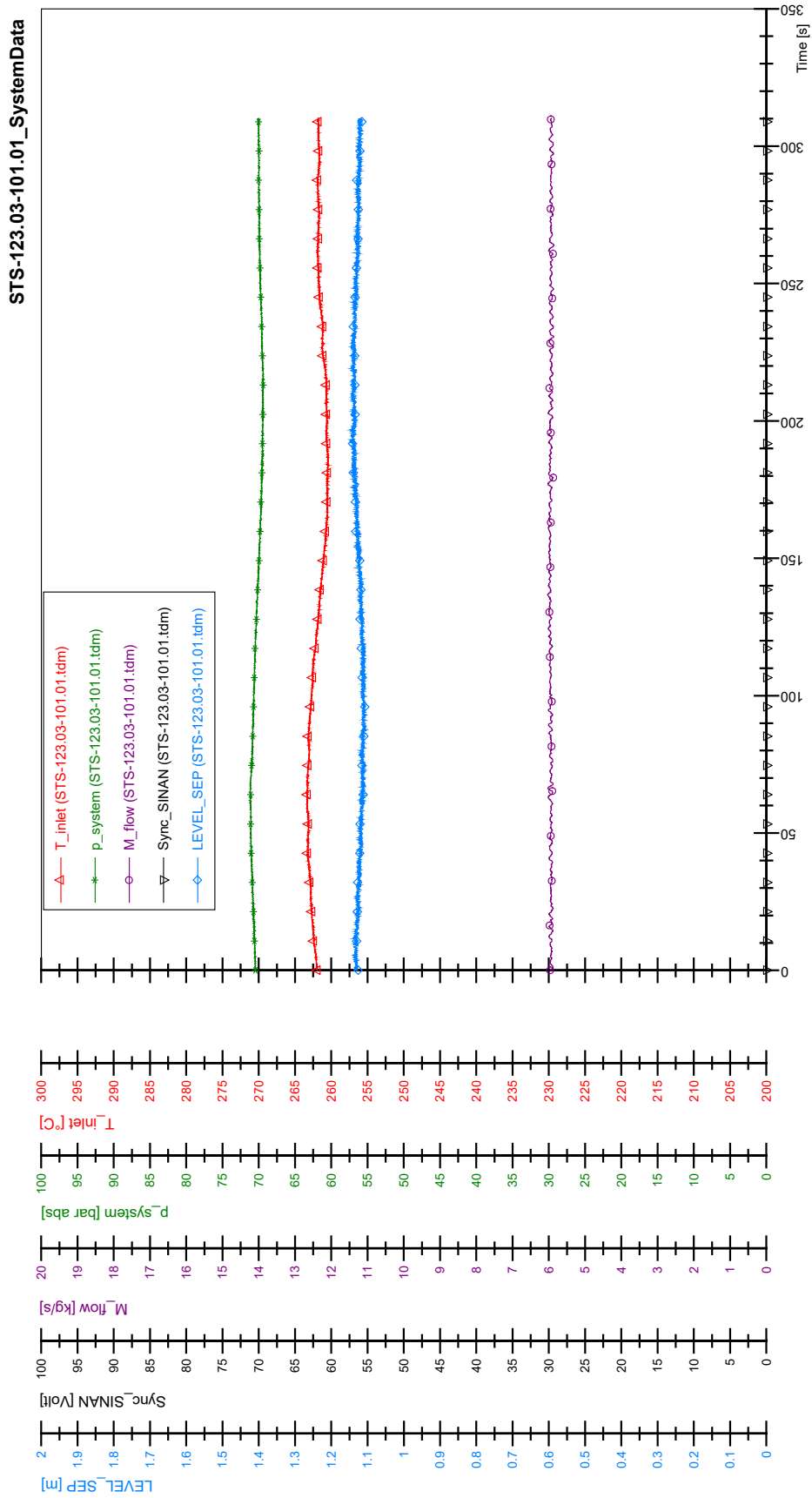
Run No.	Date	Time	System Pressure [bar]	Subcooling [kJ/kg] ⁷⁾	Mass Flow [kg/s] ³⁾	Level Separator [m]	Feedback Active [-]	Tau [s]	Rhosub [\$]	Vrcmul [-]	Leading TC [-]
G01.01	Dec 13, 2016	16:08	70.2	101.5	5.1	1.10	Yes	2.0	0.0	0.10–0.16	88/6Z
C01.01	Dec 14, 2016	10:24	70.2	100.8	5.2	1.09	Yes	2.5	1.0	0.05–0.30	88/6Z
D01.01	Dec 14, 2016	12:11	69.8	103.3	5.1	1.11	Yes	2.5	0.8	0.10–0.27	88/6Z
B01.01	Dec 14, 2016	13:30	69.9	102.3	5.2	1.12	Yes	2.5	1.2	0.10–0.30	88/6Z
401.01	Dec 14, 2016	15:21	79.4	96.9	5.6	1.12	No	--	--	--	--
402.01	Dec 14, 2016	15:32	79.3	105.4	5.5	1.10	No	--	--	--	--
403.01	Dec 14, 2016	16:00	79.4	107.9	5.1	1.13	No	--	--	--	--
404.01	Dec 14, 2016	16:40	78.4	102.9	4.8	1.14	No	--	--	--	--
405.01	Dec 15, 2016	15:22	79.2	101.3	4.5	1.10	No	--	--	--	--
406.01 ⁴⁾	Dec 15, 2016	15:35	78.8	105.5	oscillating	1.13	No	--	--	--	--
407.01	Dec 15, 2016	16:24	78.9	101.8	4.6	1.11	No	--	--	--	59/5X, 59/5Z, 79/5Z, 79/5X, 87/5Z, 87/5X
301.01	Dec 16, 2016	11:25	70.2	171.0	5.9	1.11	No	--	--	--	--
302.01	Dec 16, 2016	12:42	70.4	192.8 ⁵⁾	5.7	1.15	No	--	--	--	--
303.01	Dec 16, 2016	13:42	70.1	178.7 ⁵⁾	5.7	1.11	No	--	--	--	--
304.01	Dec 16, 2016	14:40	70.0	150.3	5.6	1.11	No	--	--	--	--
305.01	Dec 16, 2016	14:58	70.6	158.4	5.4	1.08	No	--	--	--	--
306.01	Dec 16, 2016	15:05	70.6	161.8	5.4	1.08	No	--	--	--	--
307.01	Dec 16, 2016	15:16	70.8	167.6	4.7–5.9	1.12	No	--	--	--	--
308.01	Dec 16, 2016	15:27	70.0	170.4	3.6–6.9	1.14	No	--	--	--	--
309.01	Dec 16, 2016	15:37	70.1	175.1	3.0–7.5	1.12	No	--	--	--	--
310.01	Dec 16, 2016	15:47	70.1	177.6	2.1–8.1	1.11	No	--	--	--	88/5X, 88/5Z 88/6Z
A11.01	Dec 19, 2016	11:07	69.6	150.1	5.4	1.13	Yes	2.5	0.0	0.05–0.14	88/6Z

Run No.	Date	Time	System Pressure [bar]	Subcooling [kJ/kg] ⁷⁾	Mass Flow [kg/s] ³⁾	Level Separator [m]	Feedback Active [-]	Tau [s]	Rhosub [\$]	Vrcmul [-]	Leading TC [-]
B11.01	Dec 19, 2016	13:10	70.2	152.9	5.5	1.09	Yes	2.5	1.2	0.10–0.24	88/6Z
C11.01	Dec 19, 2016	14:20	70.4	141.9	5.3	1.08	Yes	2.5	1.0	0.10–0.24	88/6Z
D11.01	Dec 19, 2016	15:23	69.7	148.6	5.5	1.10	Yes	2.5	0.8	0.10–0.22	88/6Z
F11.01 ⁶⁾	Dec 19, 2016	16:01	69.8	148.3	5.4	1.14	Yes				--
G11.01	Dec 19, 2016	16:21	69.8	149.3	5.4	1.10	Yes	3.7	0.0	0.08–0.17	88/6Z
F11.02 ⁴⁾	Dec 20, 2016	09:50	69.9	149.7	5.4	1.10	Yes	2.0	0.0	0.06	--
F11.03	Dec 20, 2016	10:20	69.8	152.2	5.3	1.10	Yes	2.0	0.0	0.06–0.14	88/6Z
E11.01	Dec 20, 2016	11:26	79.6	153.2	5.8	1.12	Yes	2.5	0.0	0.05–0.27	88/6Z
E01.01	Dec 20, 2016	14:00	78.8	105.2	5.4	1.08	Yes	2.5	0.0	0.15–0.23	88/6Z
A01.02	Dec 20, 2016	15:01	70.1	97.7	5.3	1.12	Yes	2.5	0.0	0.10–0.23	88/6Z
101.02	Dec 20, 2016	16:30	70.3	110.8	4.8	1.11	No	--	--	--	59/6Z, 59/5X 59/5Z
T01.01 ¹⁾	Dec 20, 2016	18:02	69.8	101.1	5.3	1.12 ¹⁾	Yes	2.5	0.0	0.10–0.09	--
T01.02 ¹⁾	Dec 20, 2016	18:47	69.6	106.3	5.3	1.09 ¹⁾	Yes	2.5	0.0	0.11–0.28	²⁾

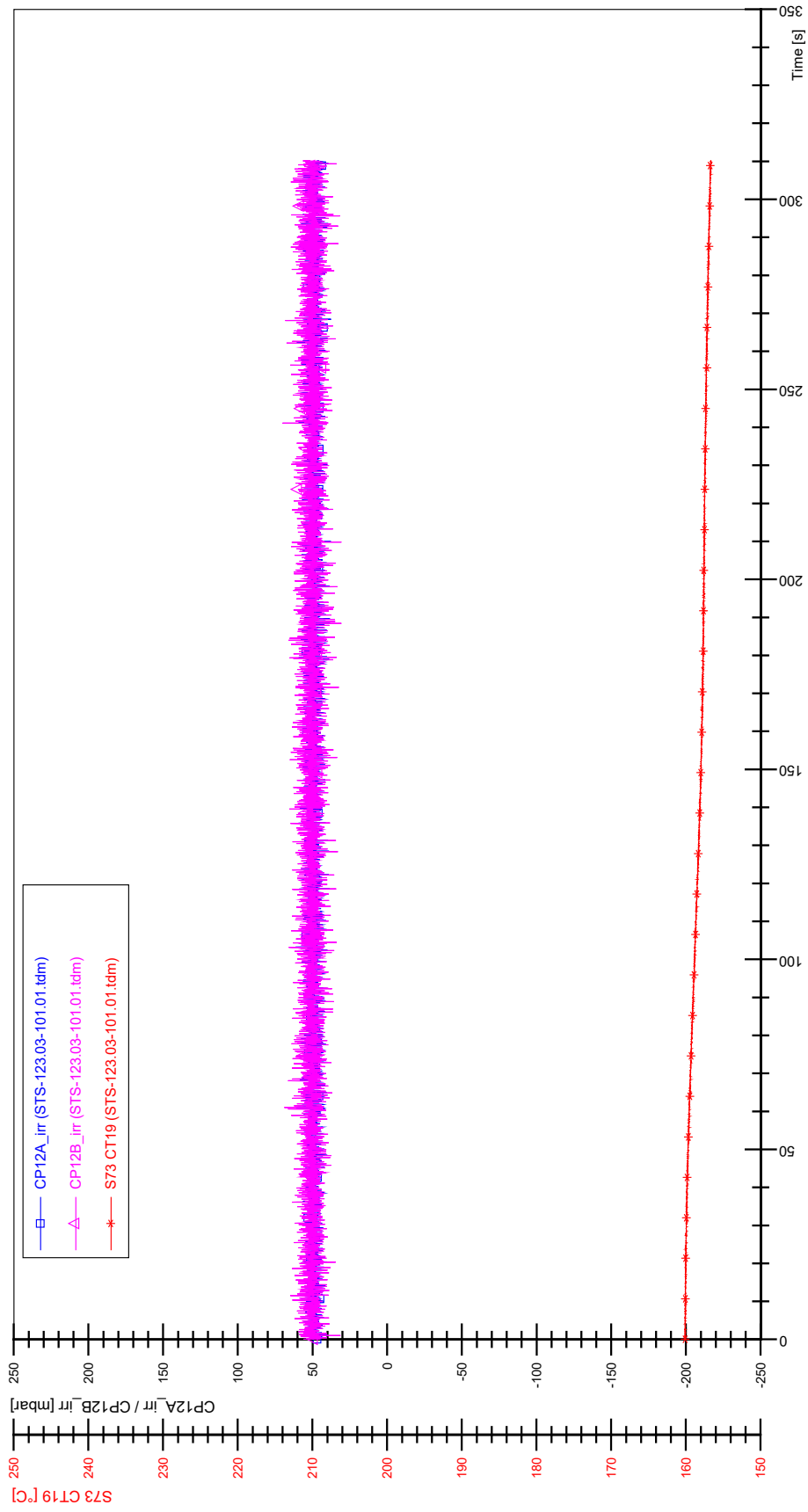
Remarks:

- 1) Transient inlet temperature test: => level separator is not constant
- 2) Nominal thermocouple (TC) temperature threshold was not activated. Oscillating temperature increases were monitored on high-powered rods.
- 3) Approximate turbine flow meter value, see explanations in Section 6.5
- 4) Power trip during test
- 5) Inlet subcooling is not constant
- 6) Strong power increase by SINAN module
- 7) Related to p_system [outlet]

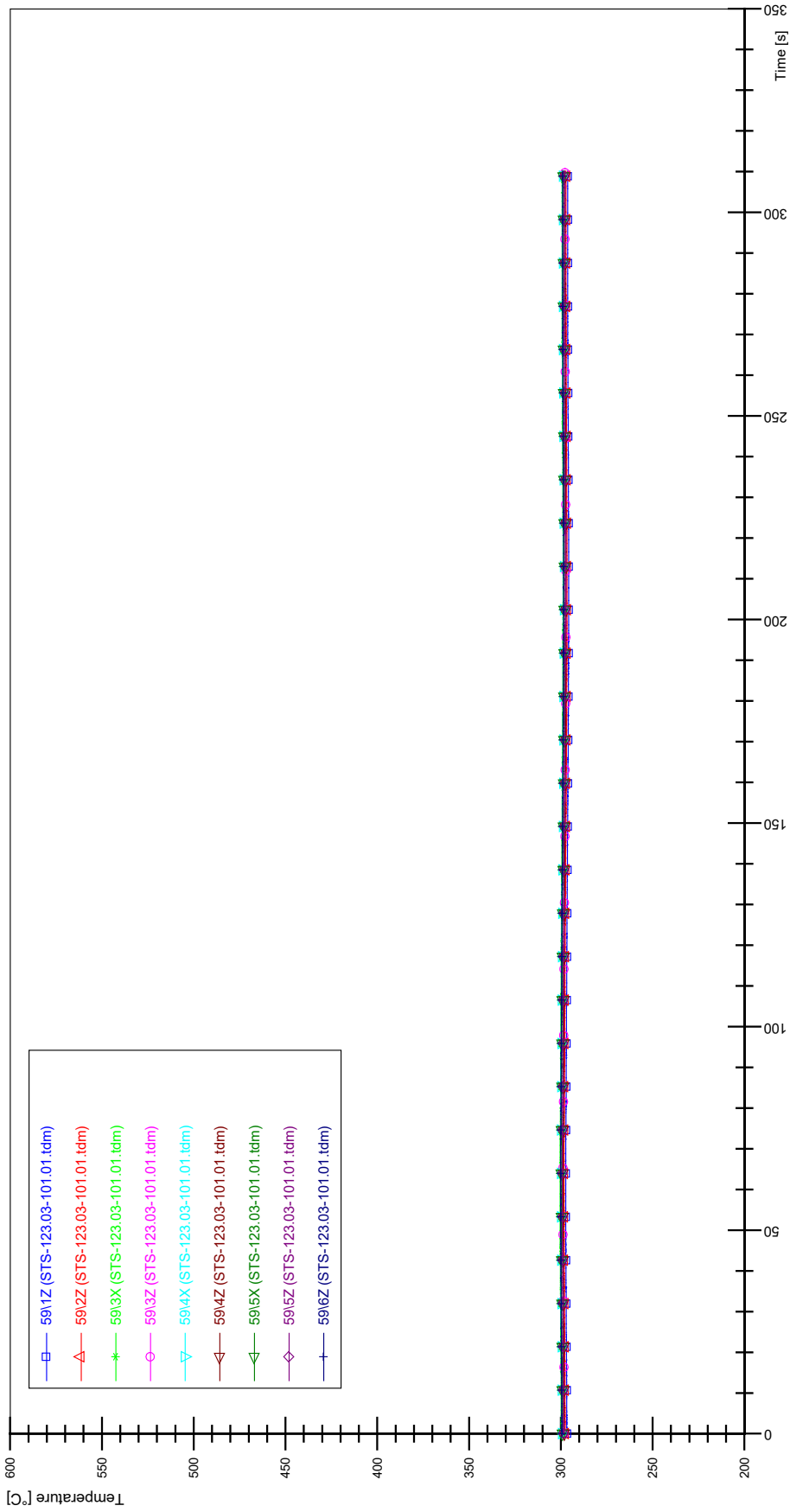
APPENDIX D PLOTS OF INSTABILITY TEST STS-123.03-101.01



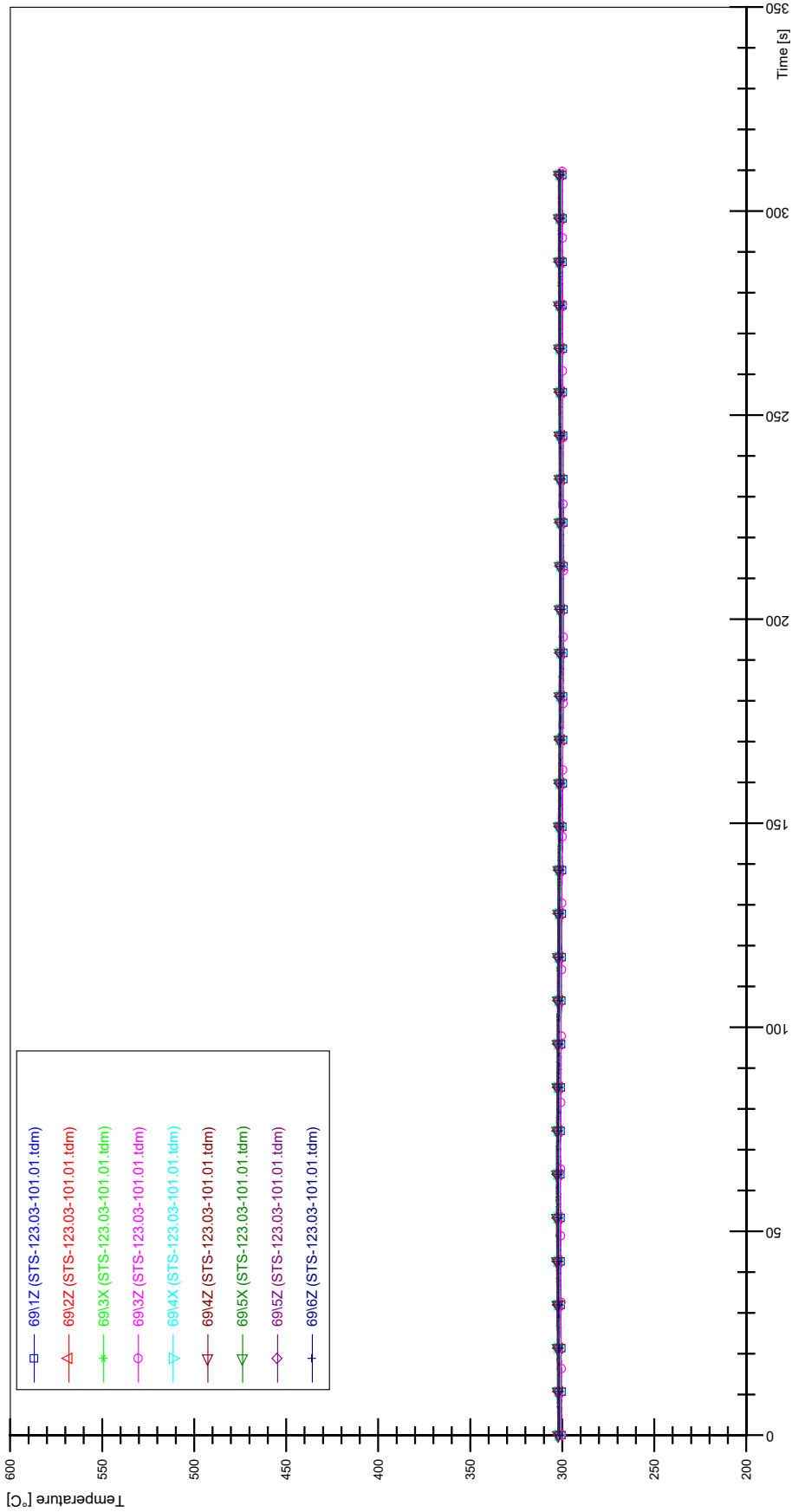
STS-123.03-101.01_CP12_CT19



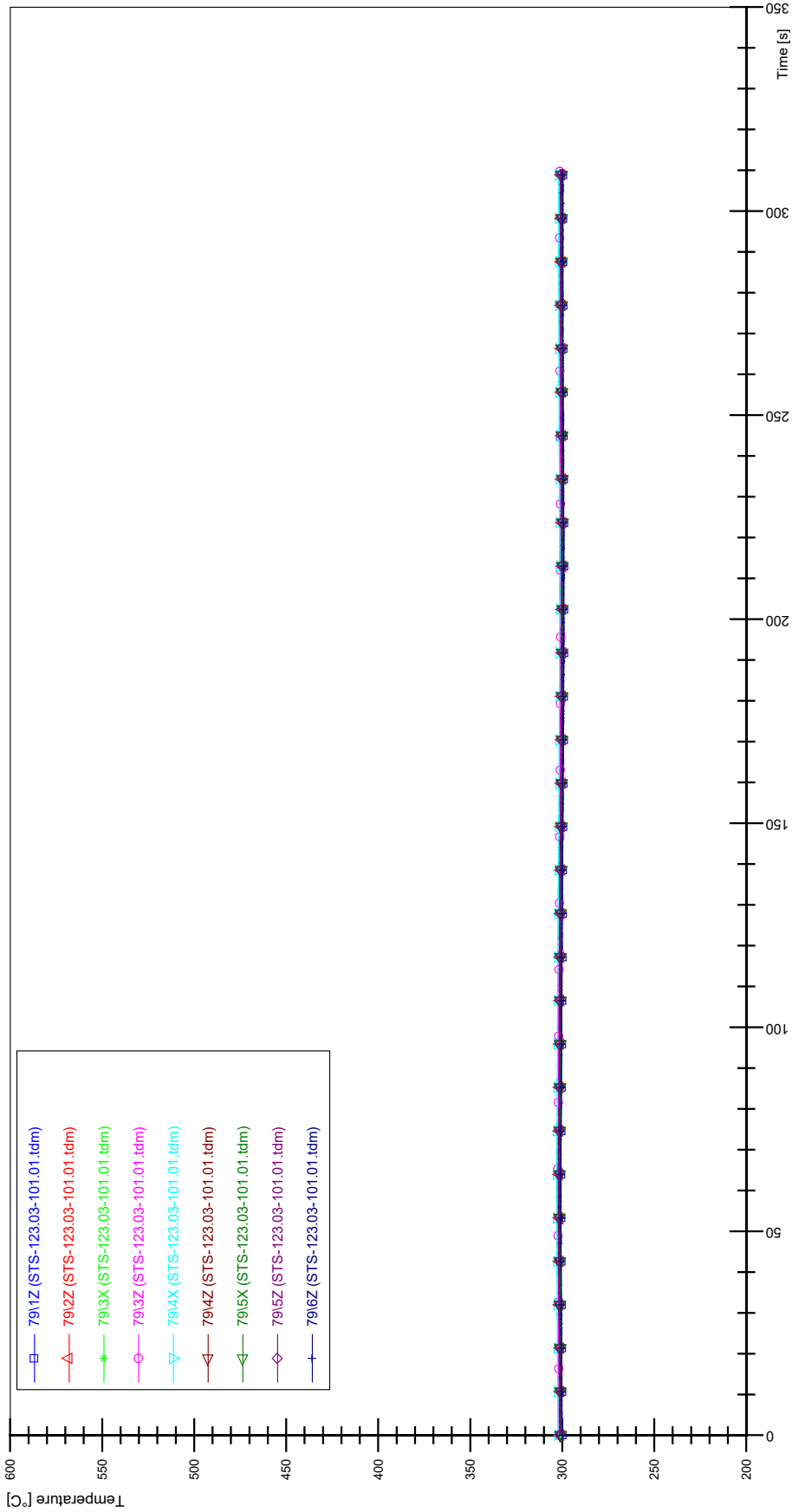
STS-123.03-101.01_Rod_59



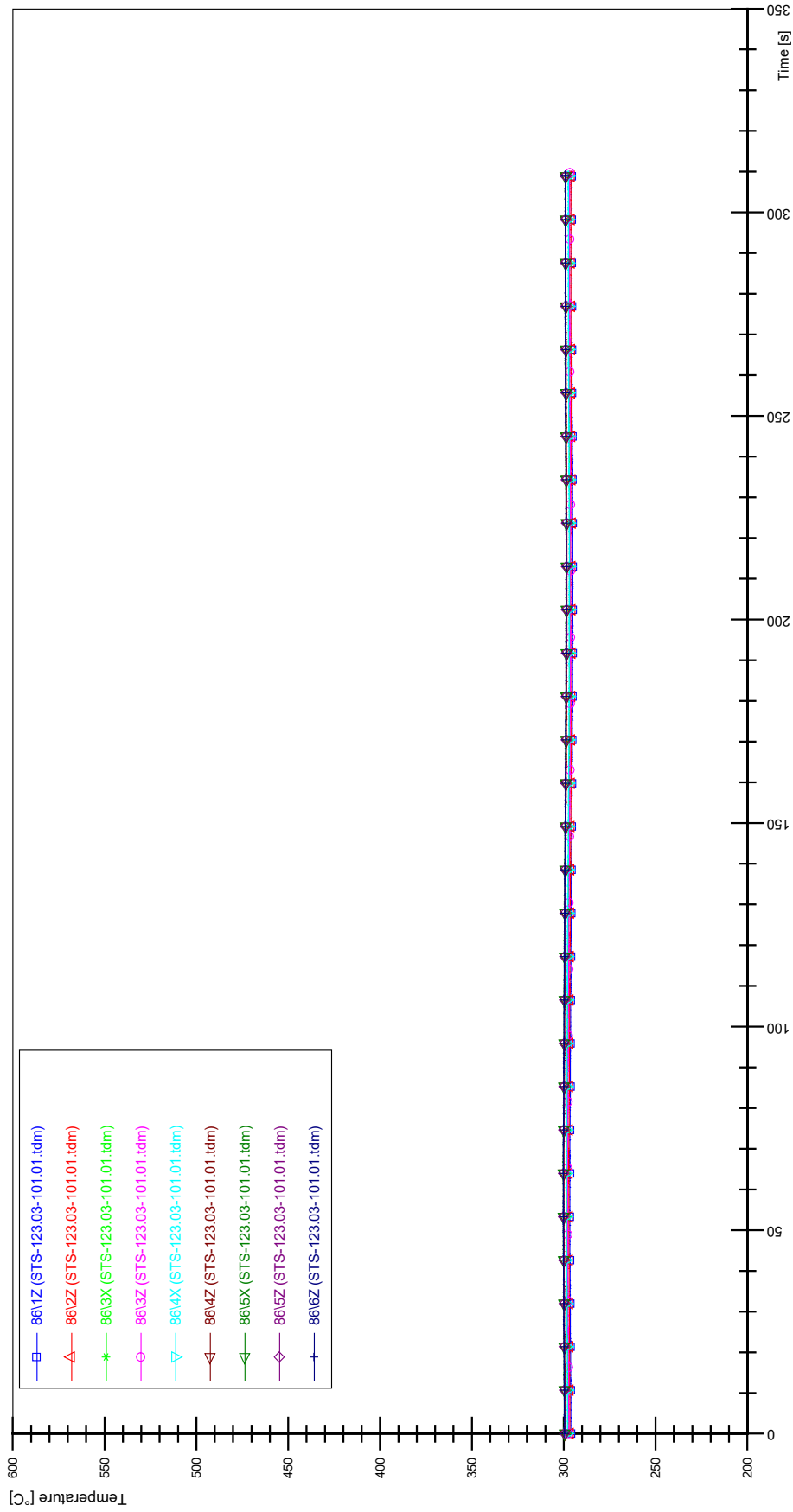
STS-123.03-101.01_Rod_69



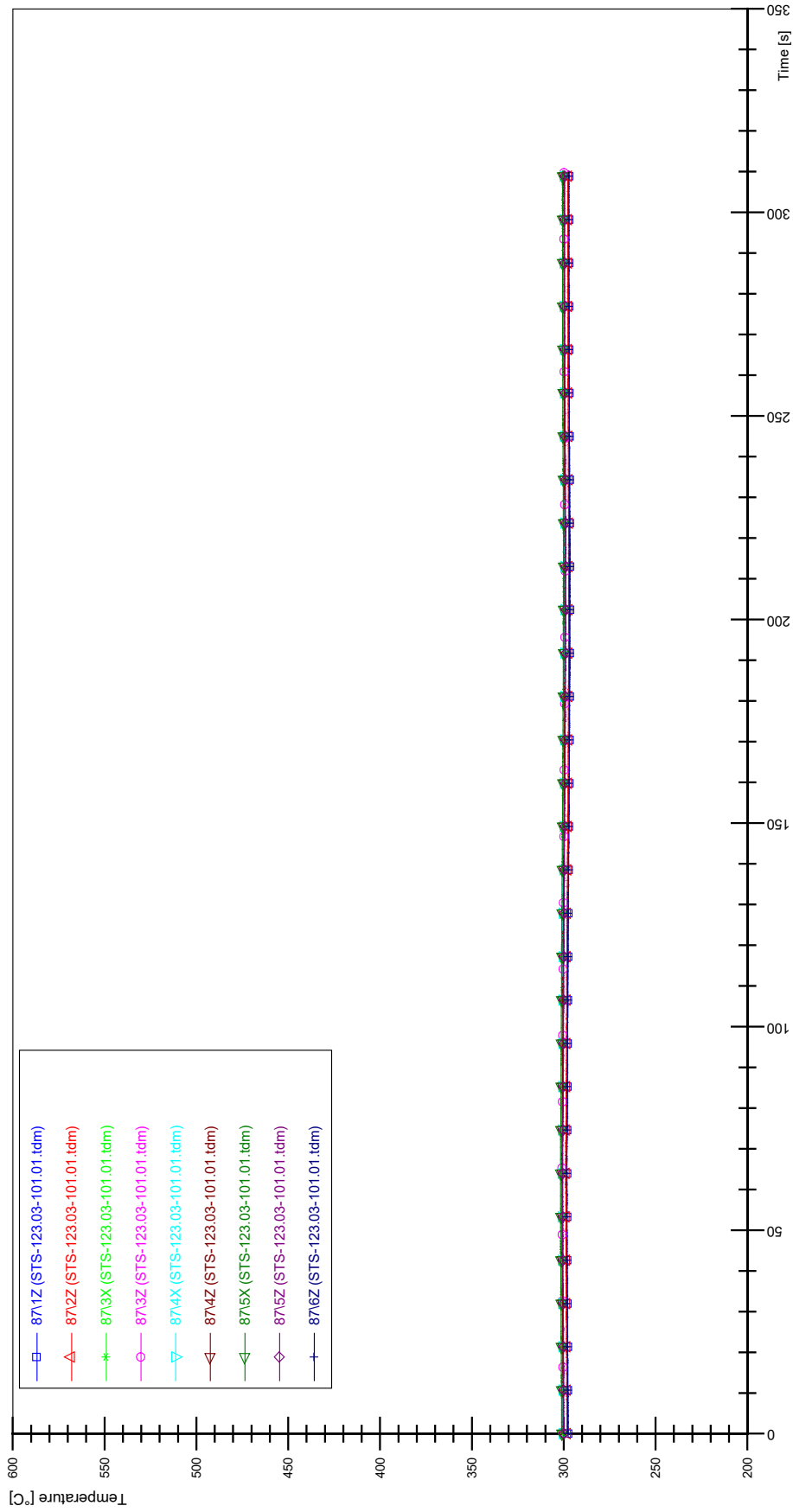
STS-123.03-101.01_Rod_79



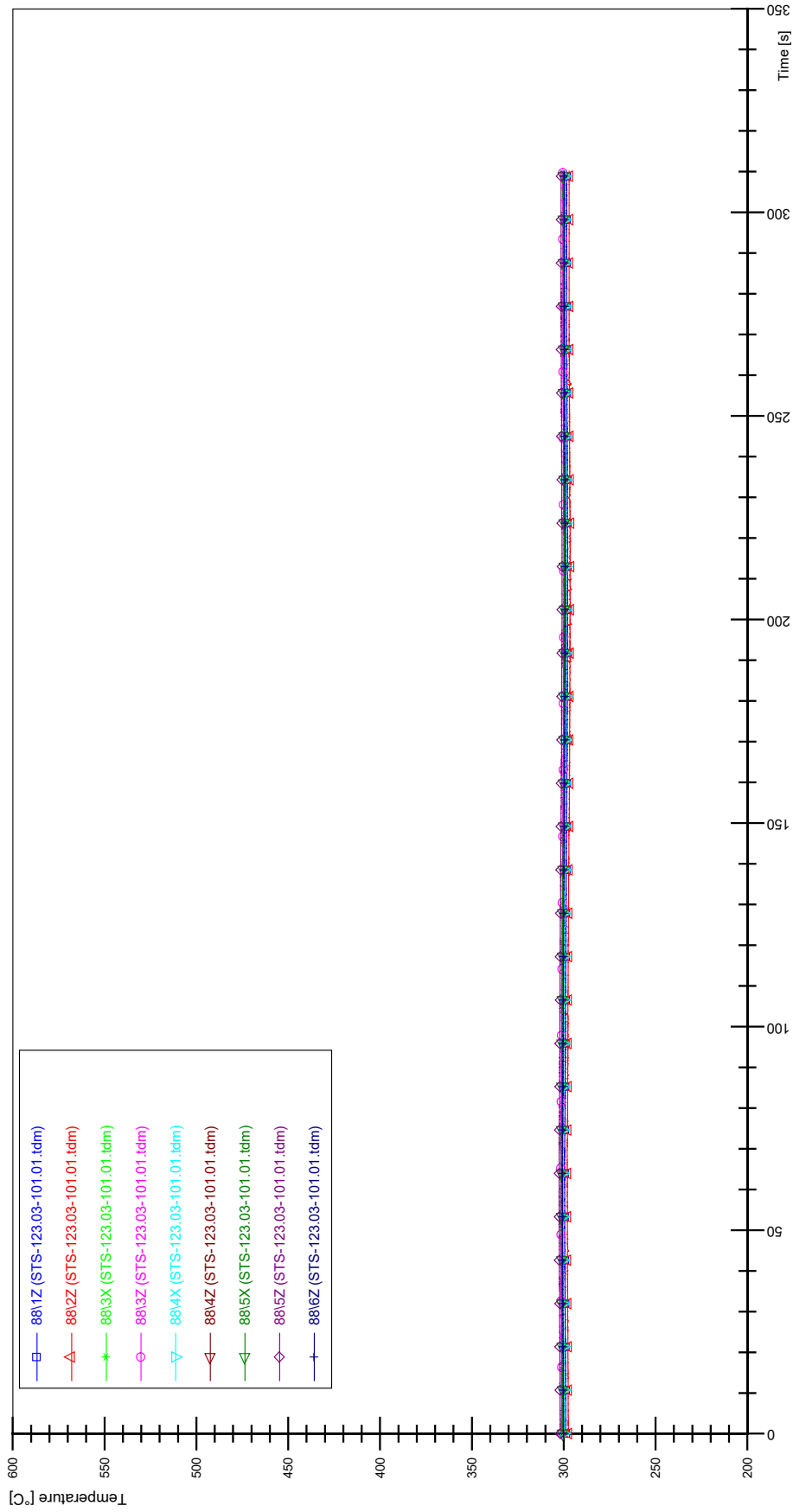
STS-123.03-101.01_Rod_86



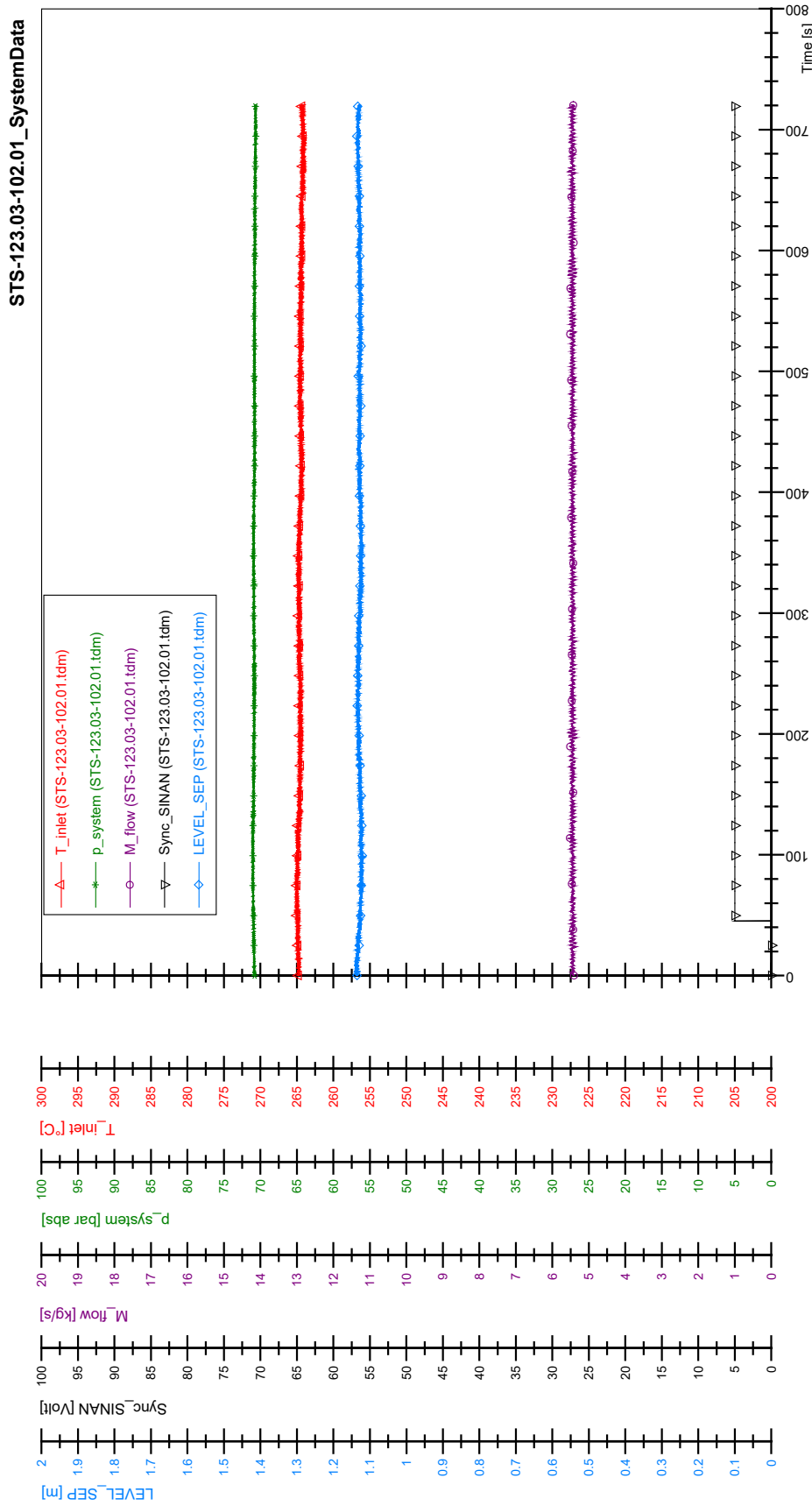
STS-123.03-101.01_Rod_87

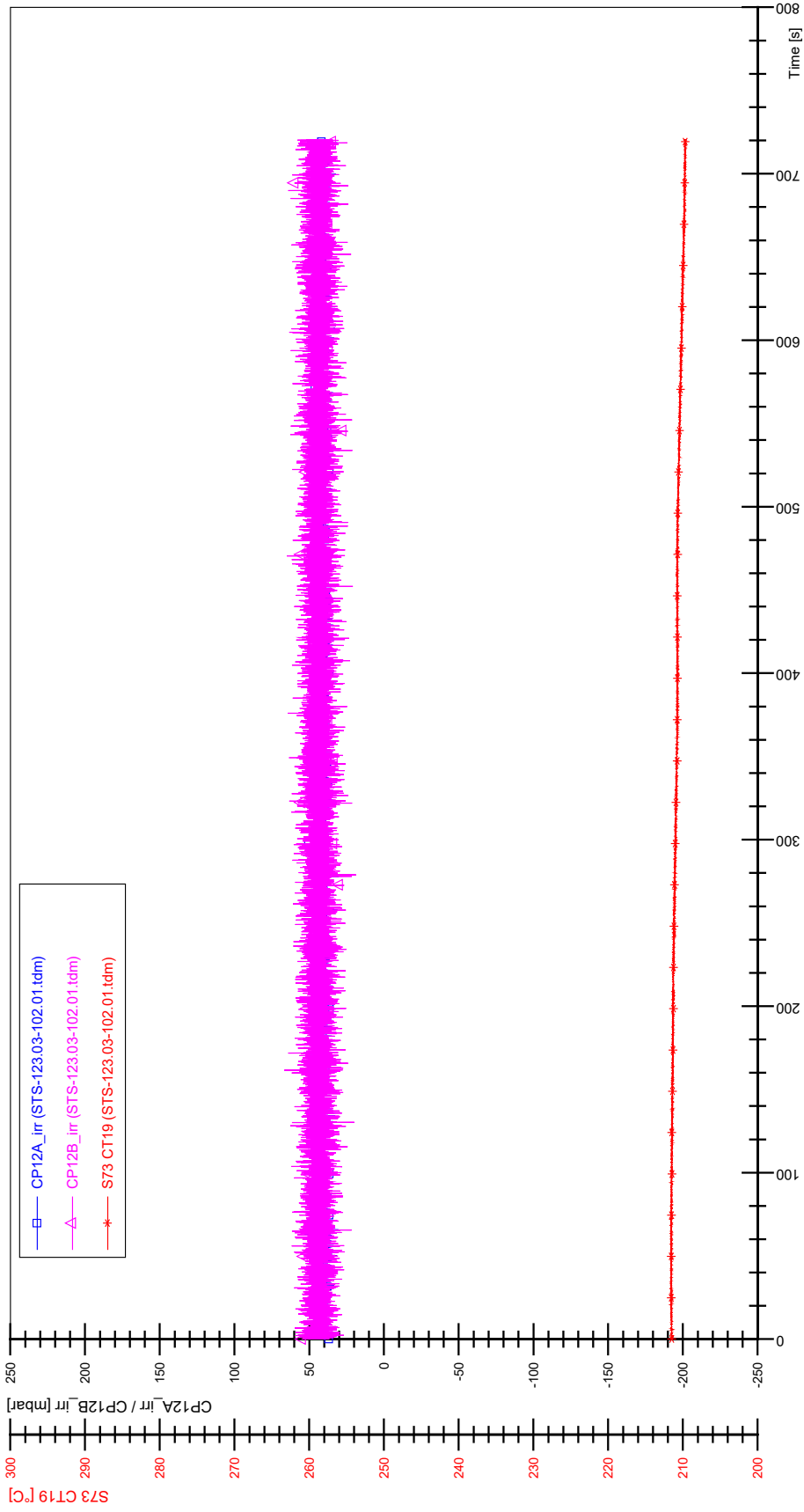


STS-123.03-101.01_Rod_88

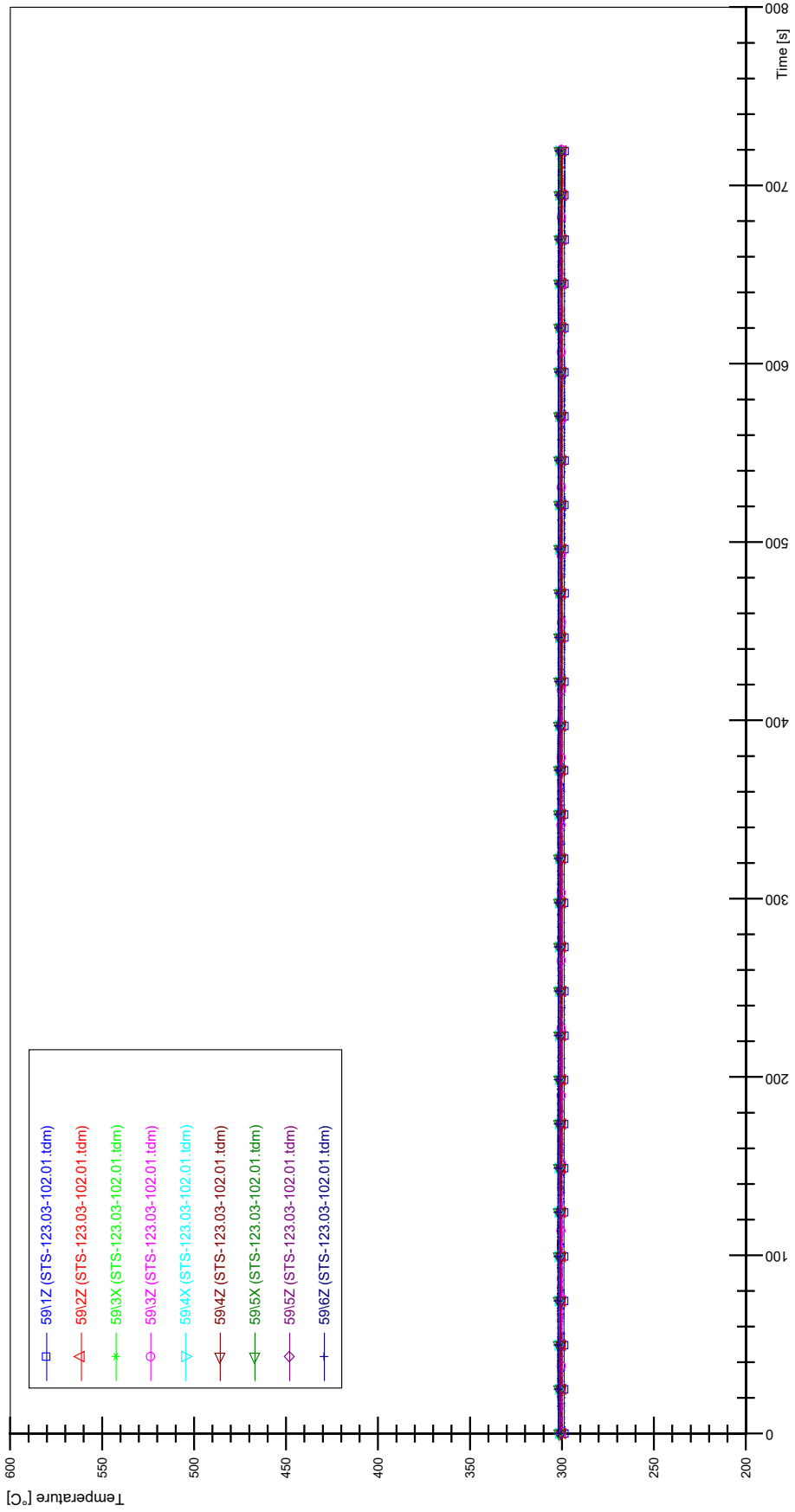


APPENDIX E PLOTS OF INSTABILITY TEST STS-123.03-102.01

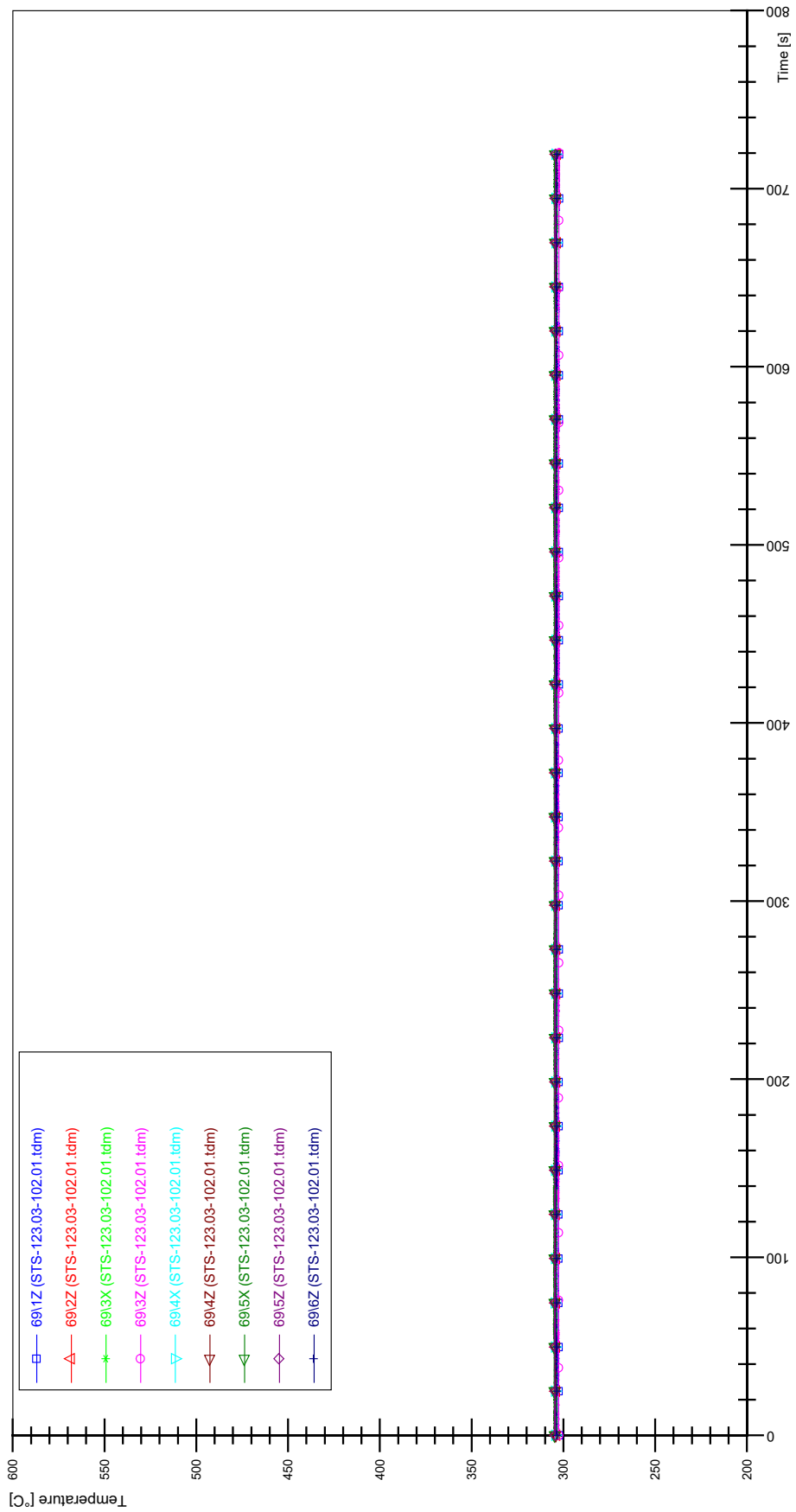




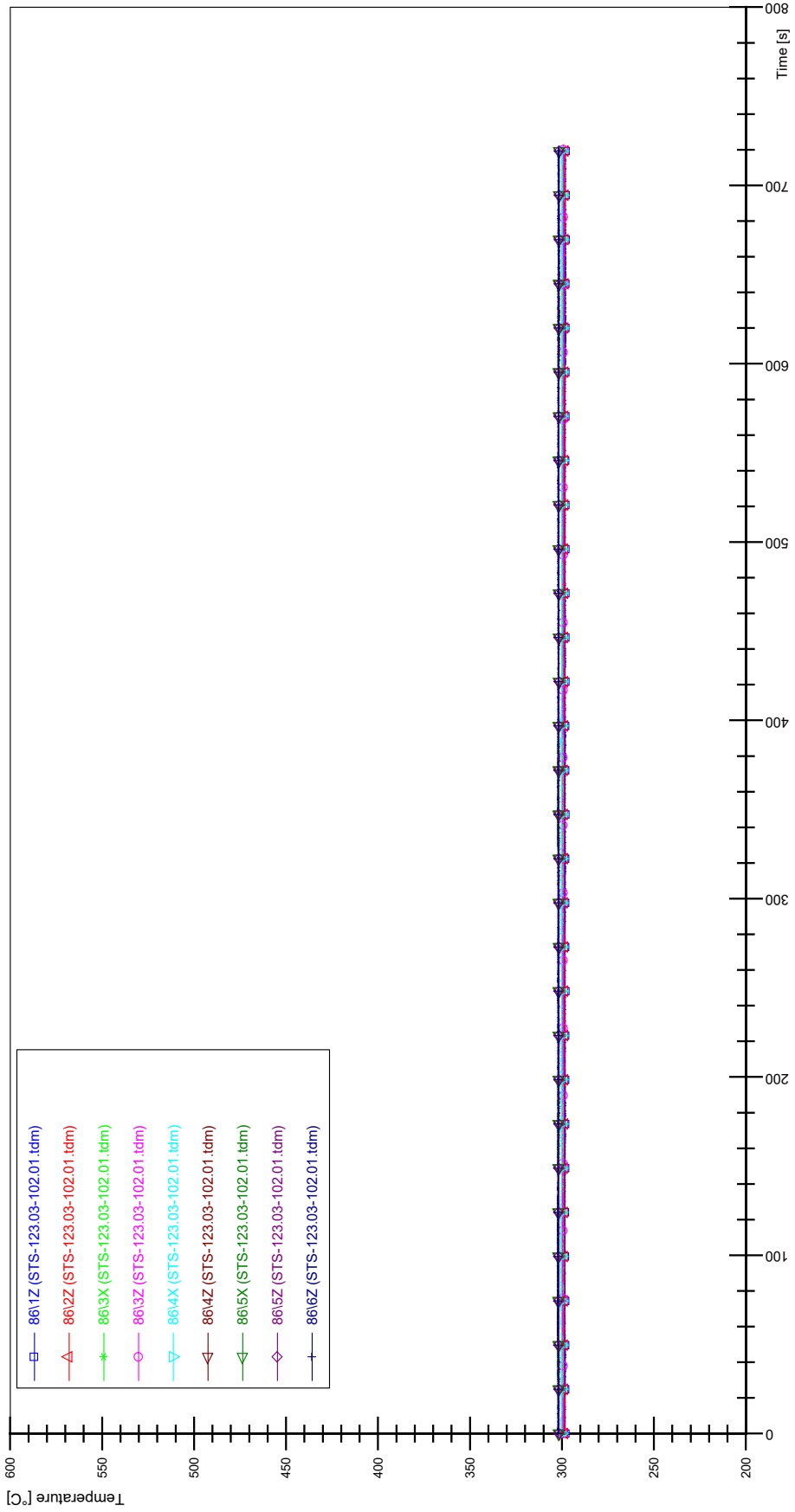
STS-123.03-102.01_Rod_59



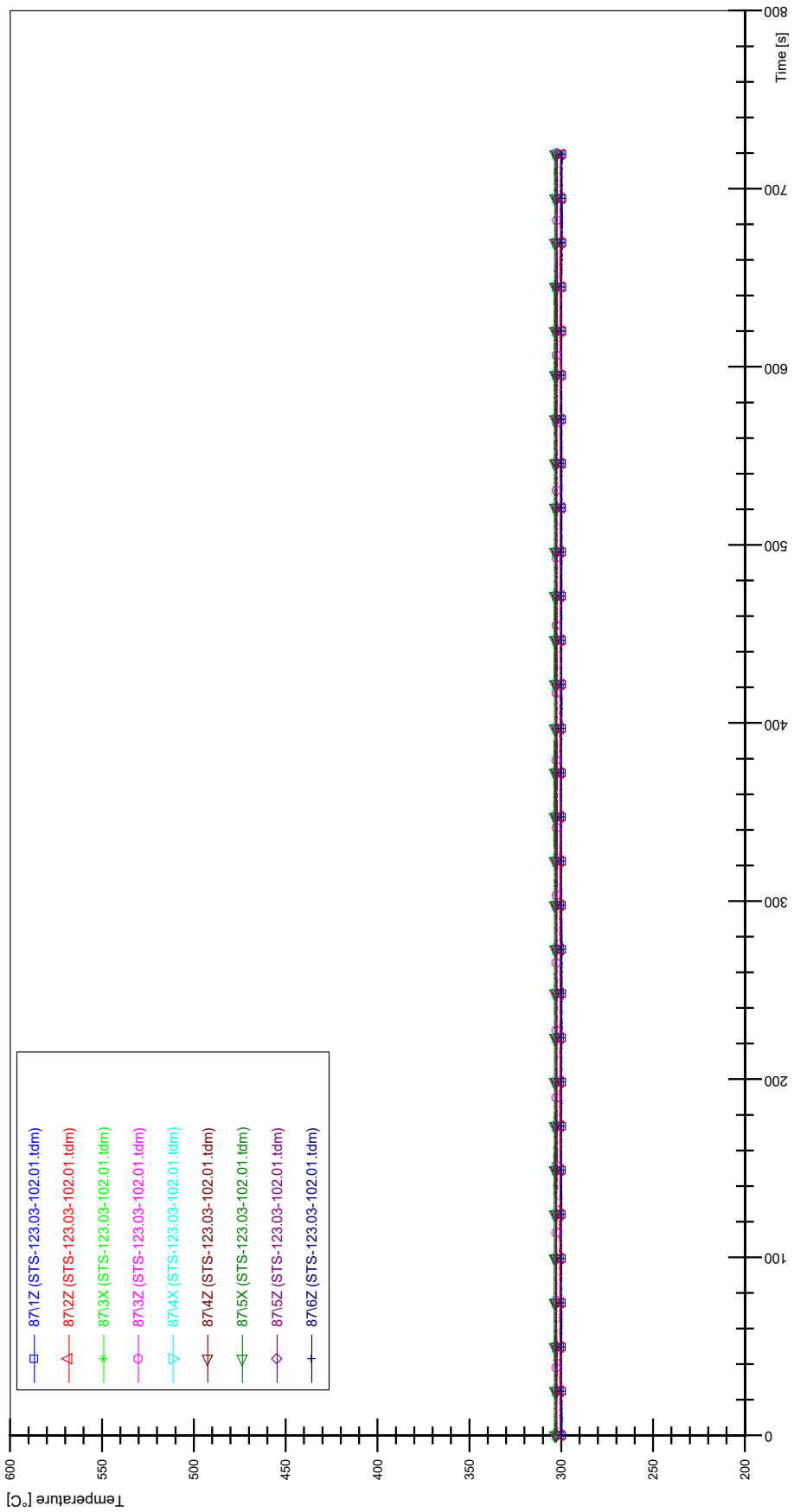
STS-123.03-102.01_Rod_69



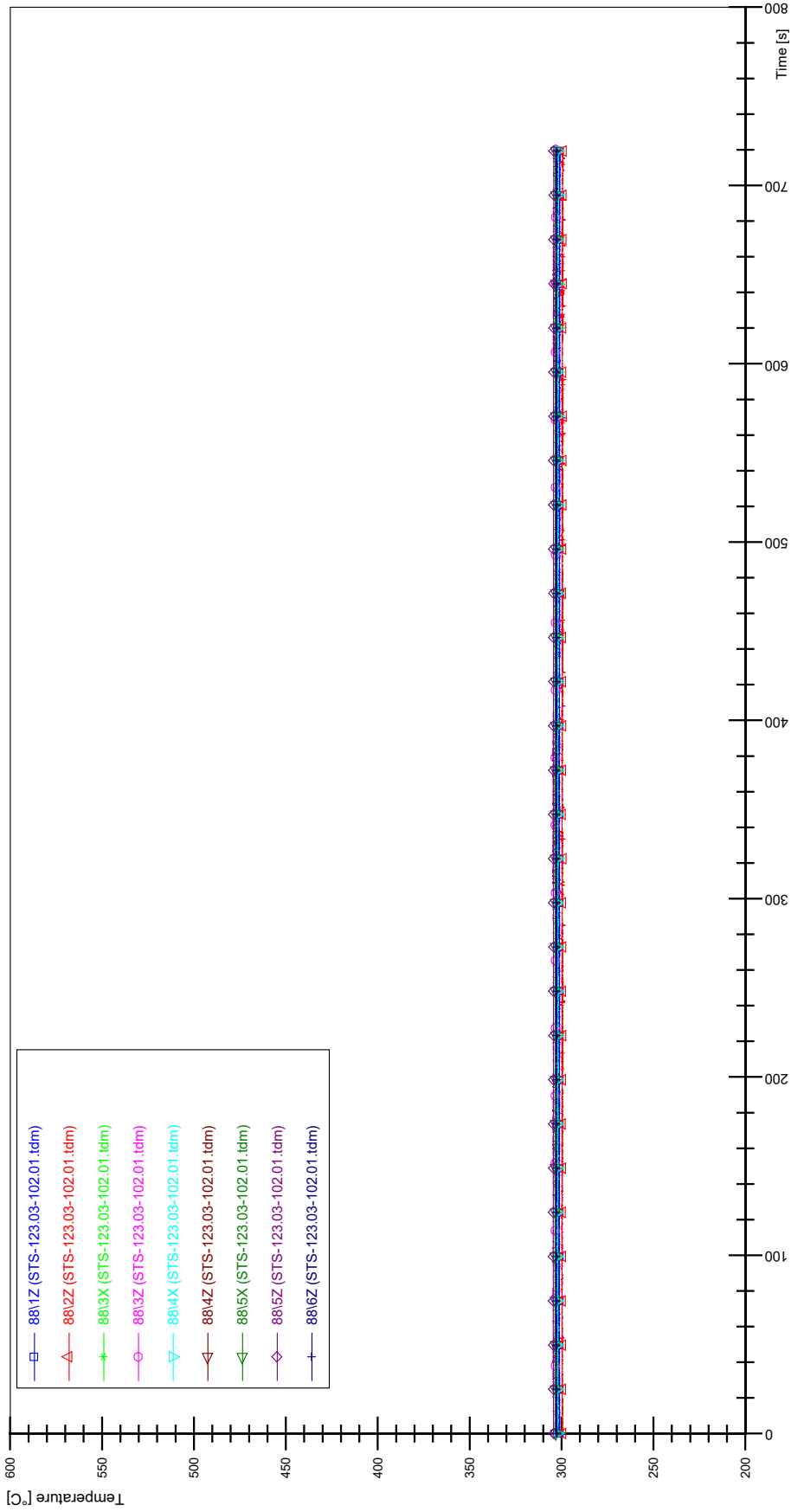
STS-123.03-102.01_Rod_86



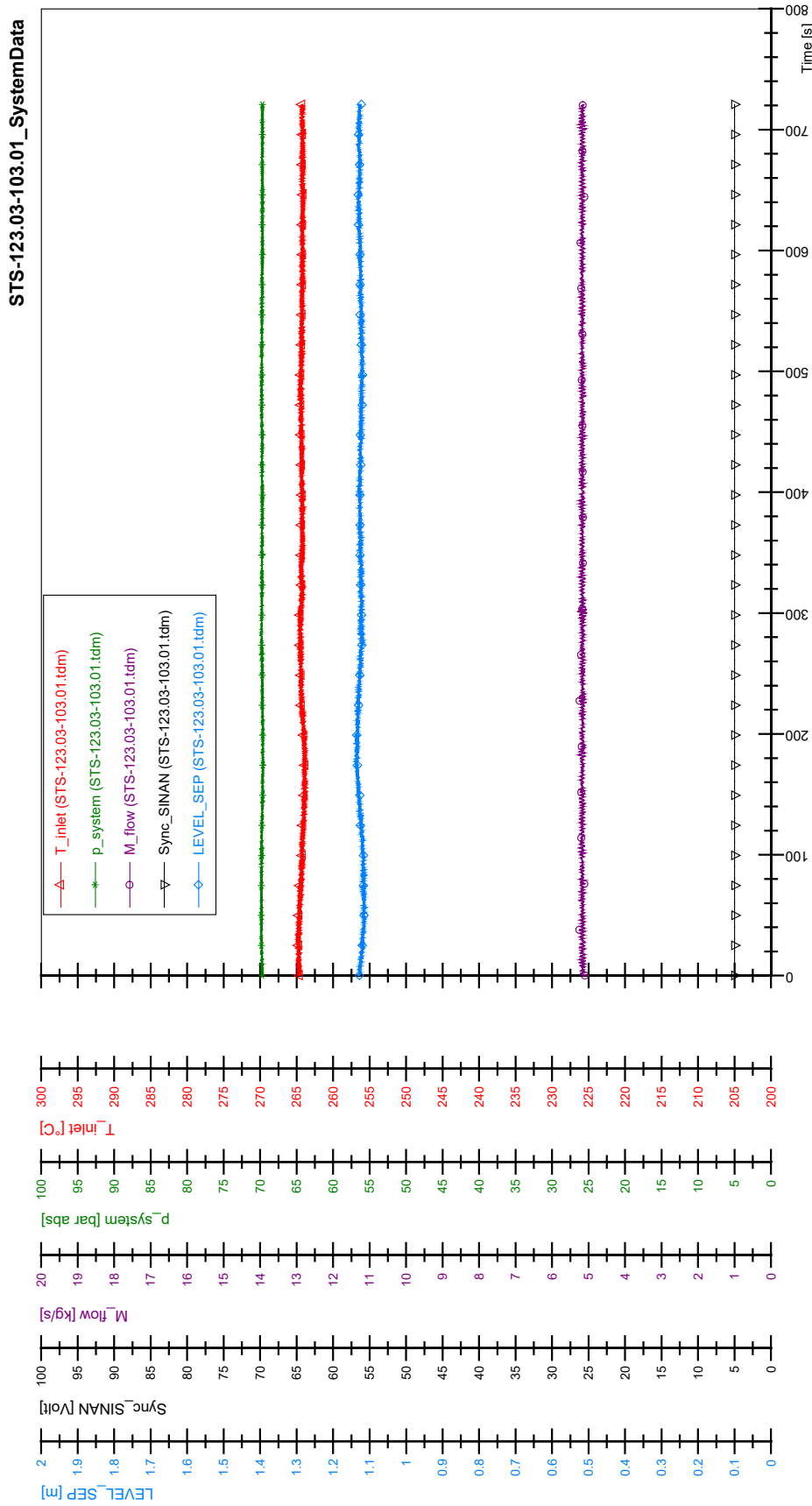
STS-123.03-102.01_Rod_87

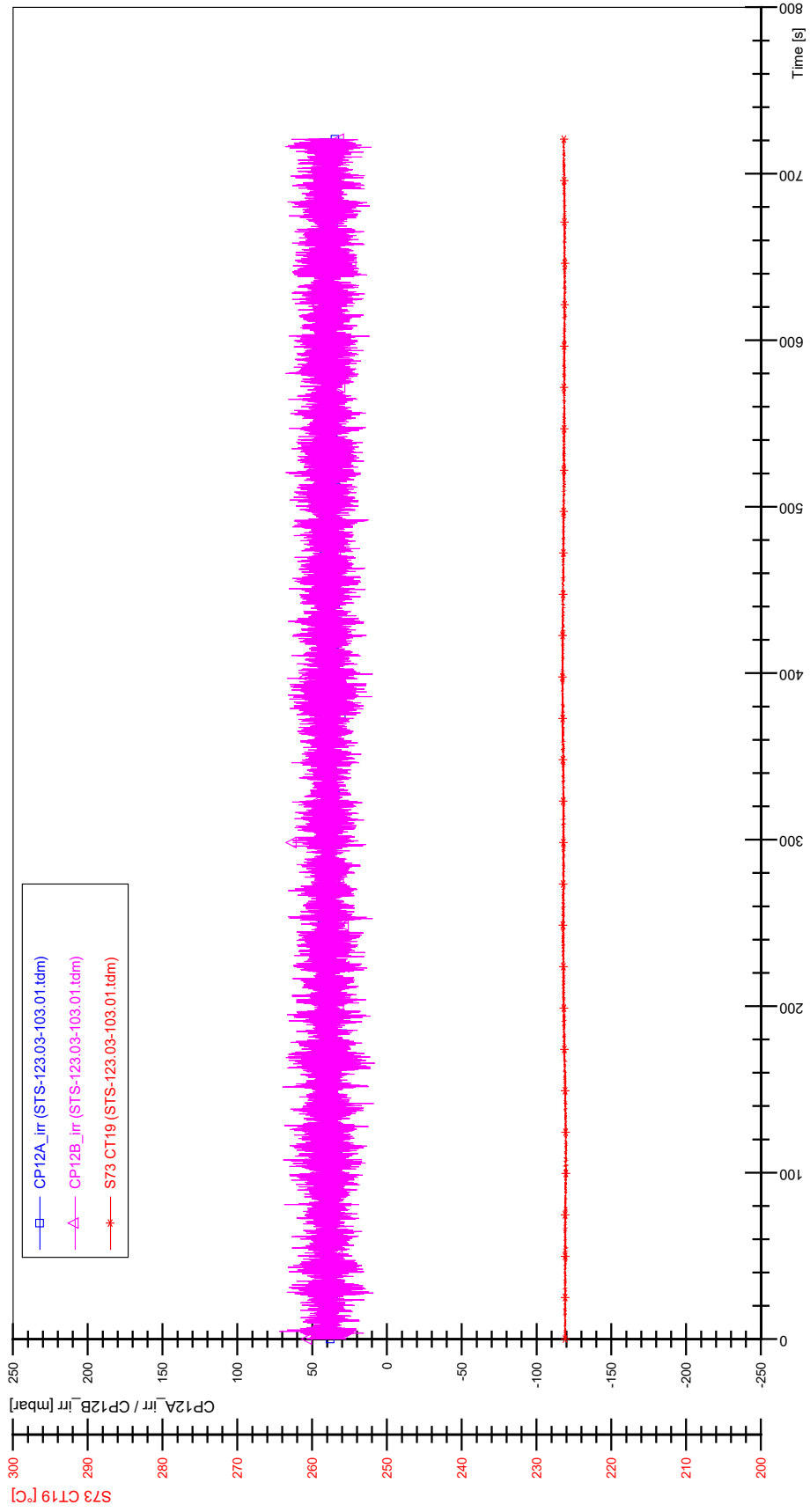


STS-123.03-102.01_Rod_88

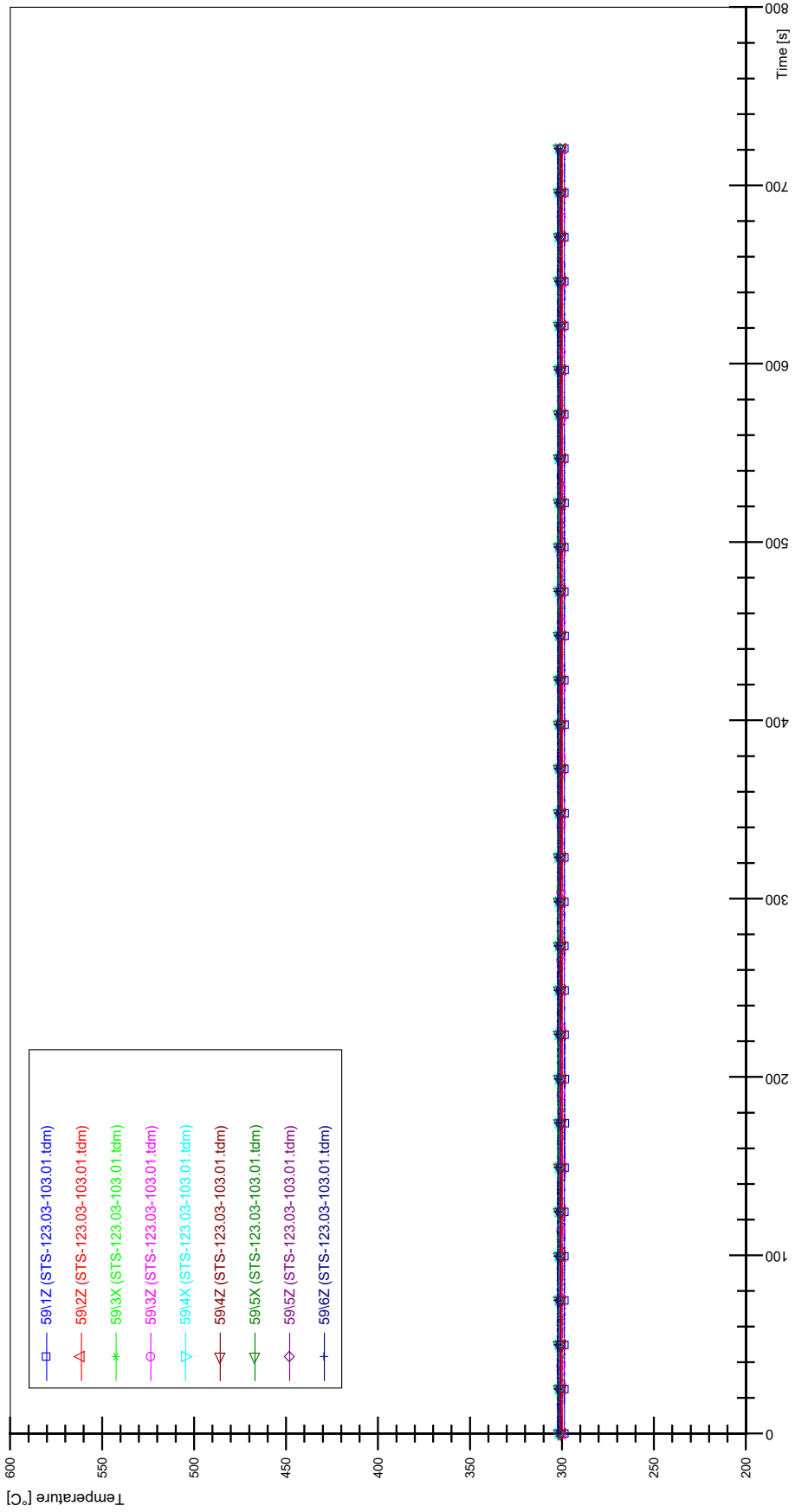


APPENDIX F PLOTS OF INSTABILITY TEST STS-123.03-103.01

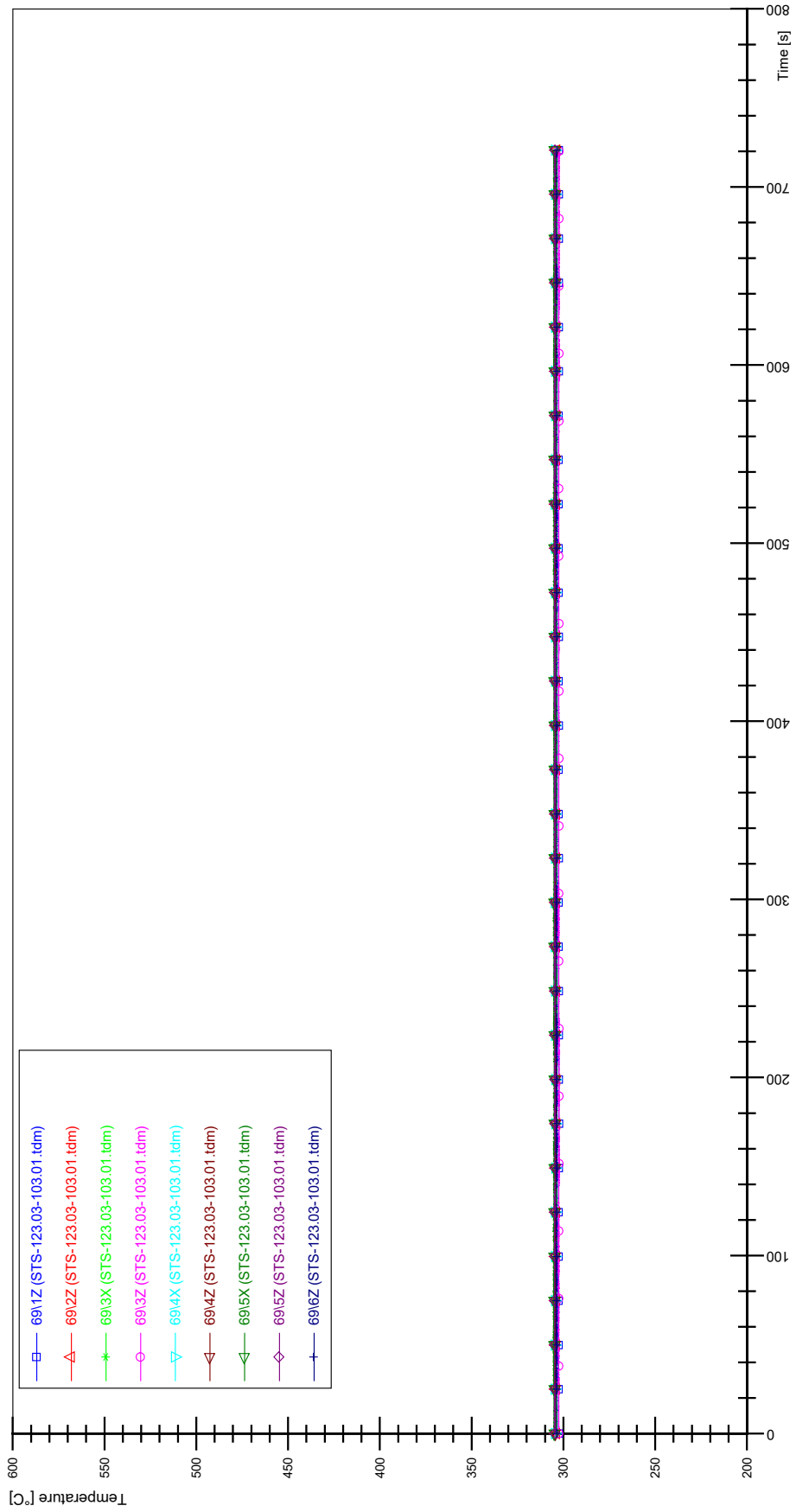




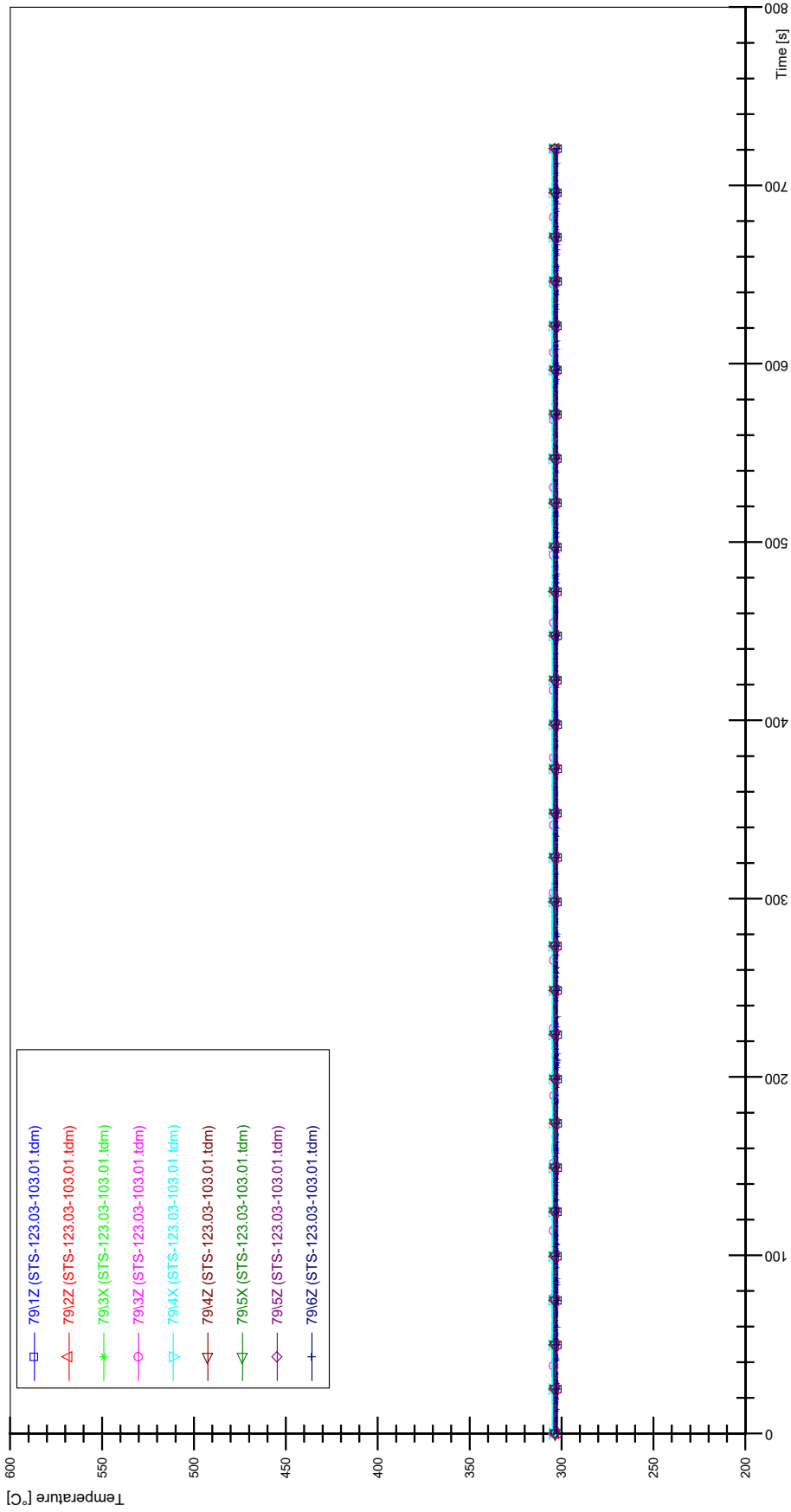
STS-123.03-103.01_Rod_59



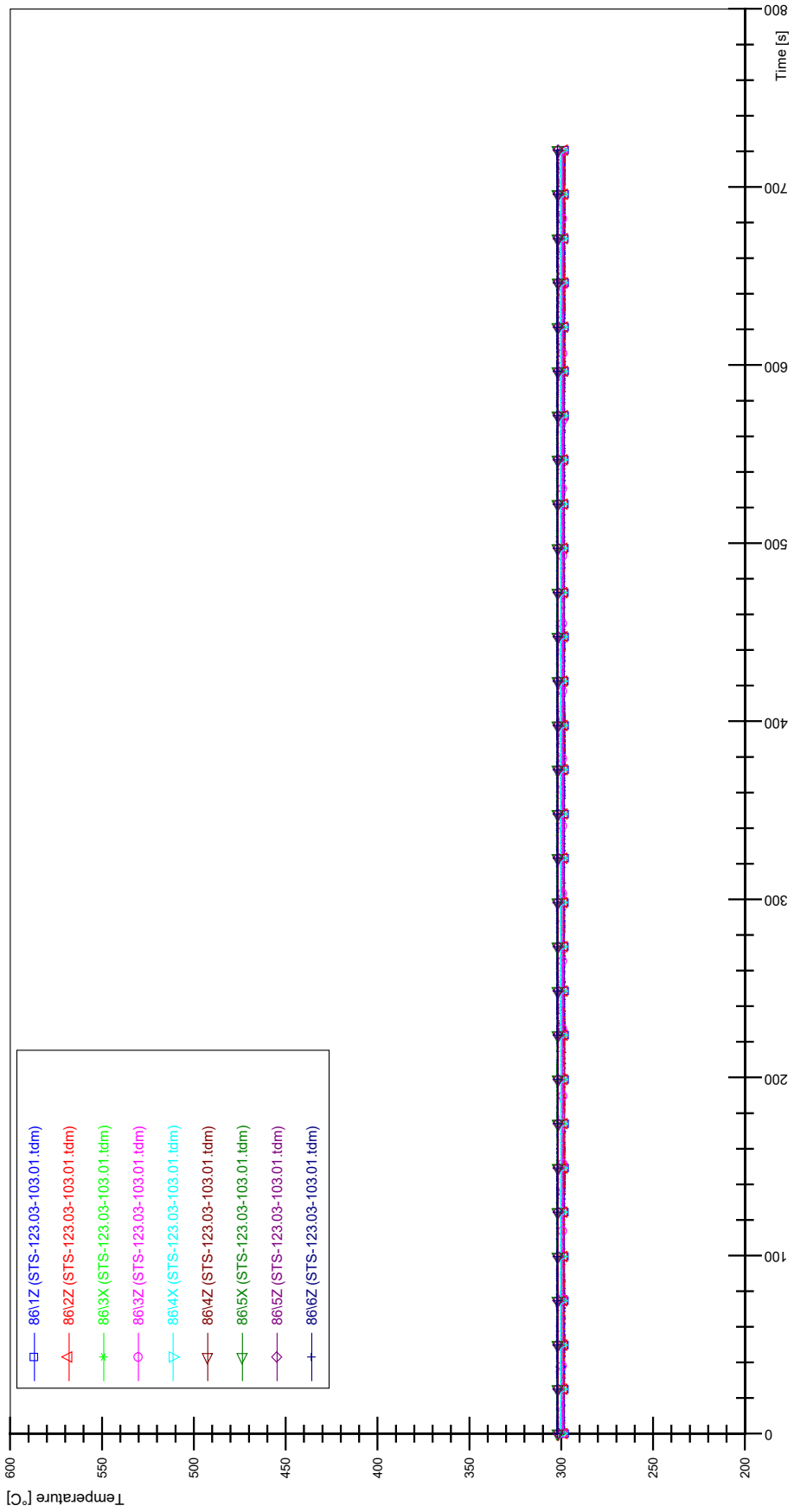
STS-123.03-103.01_Rod_69



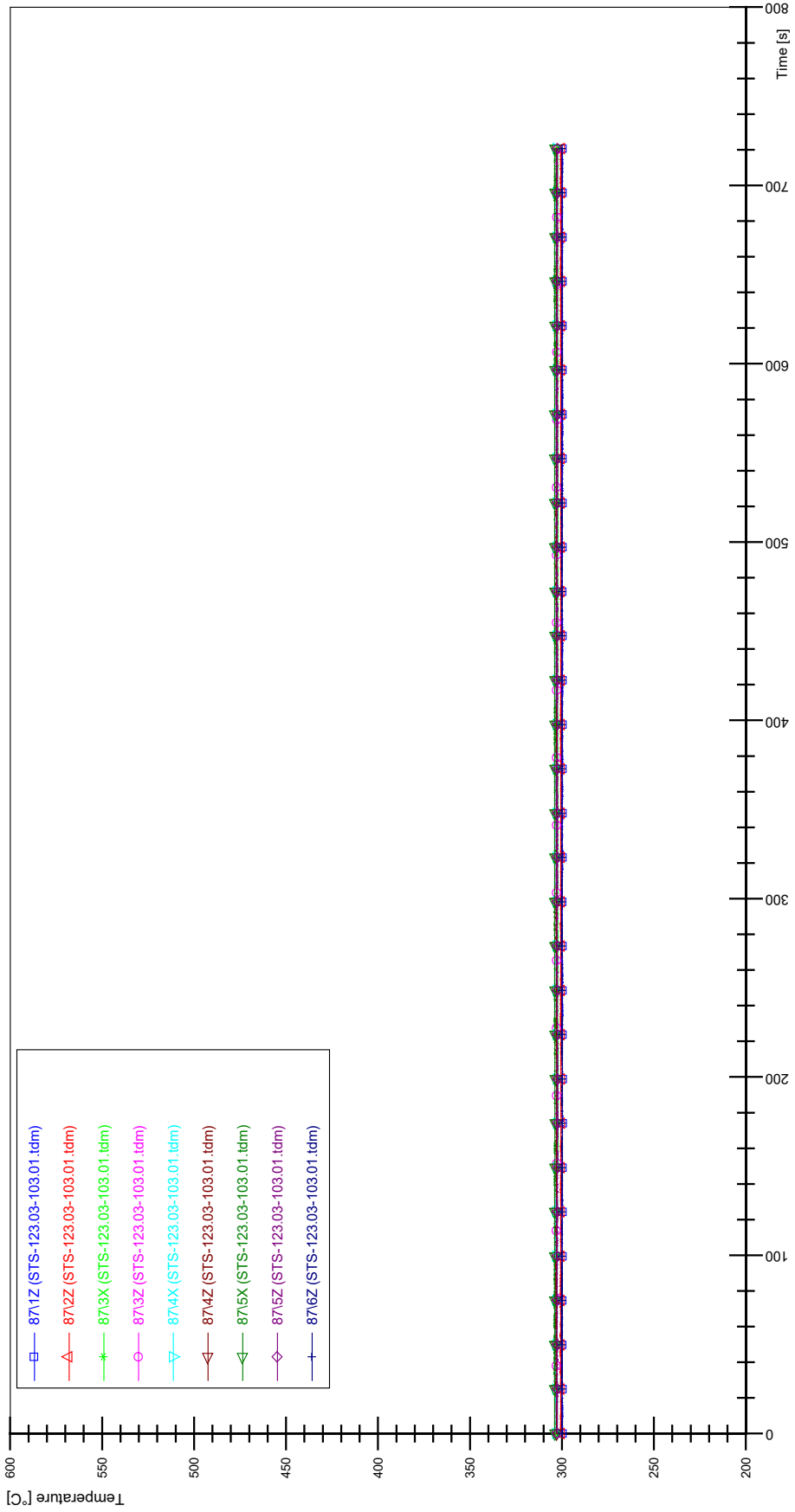
STS-123.03-103.01_Rod_79



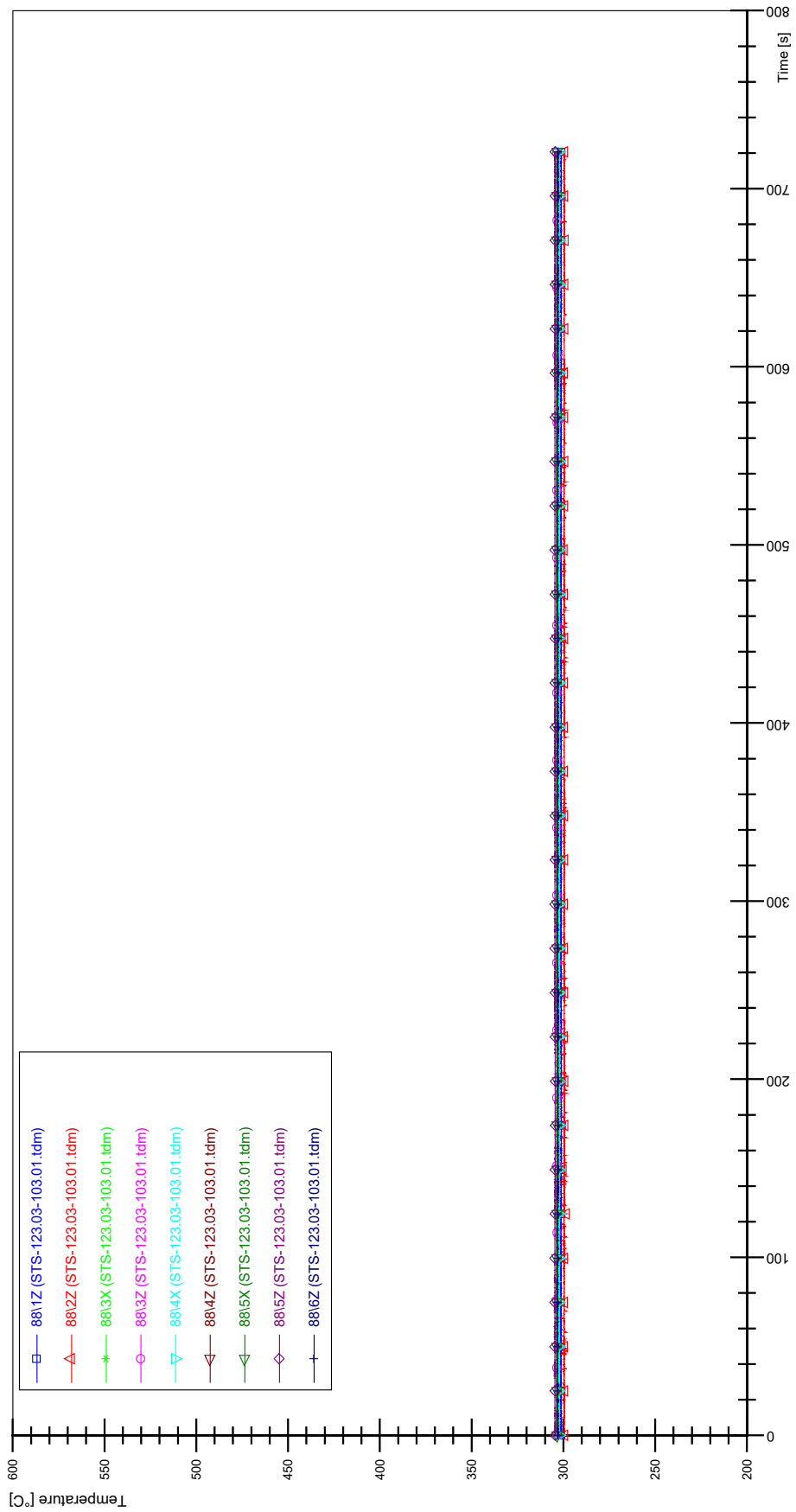
STS-123.03-103.01_Rod_86



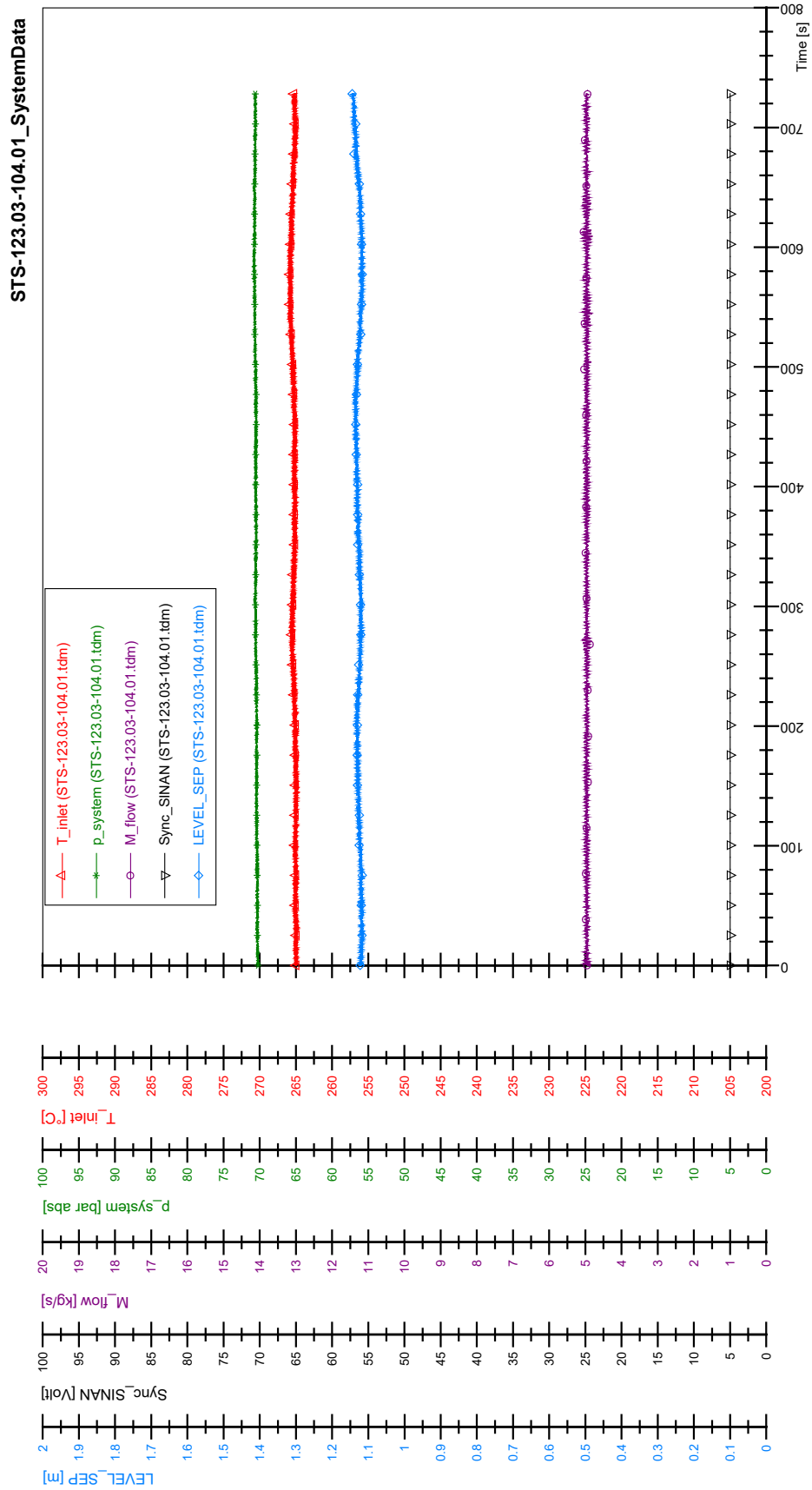
STS-123.03-103.01_Rod_87



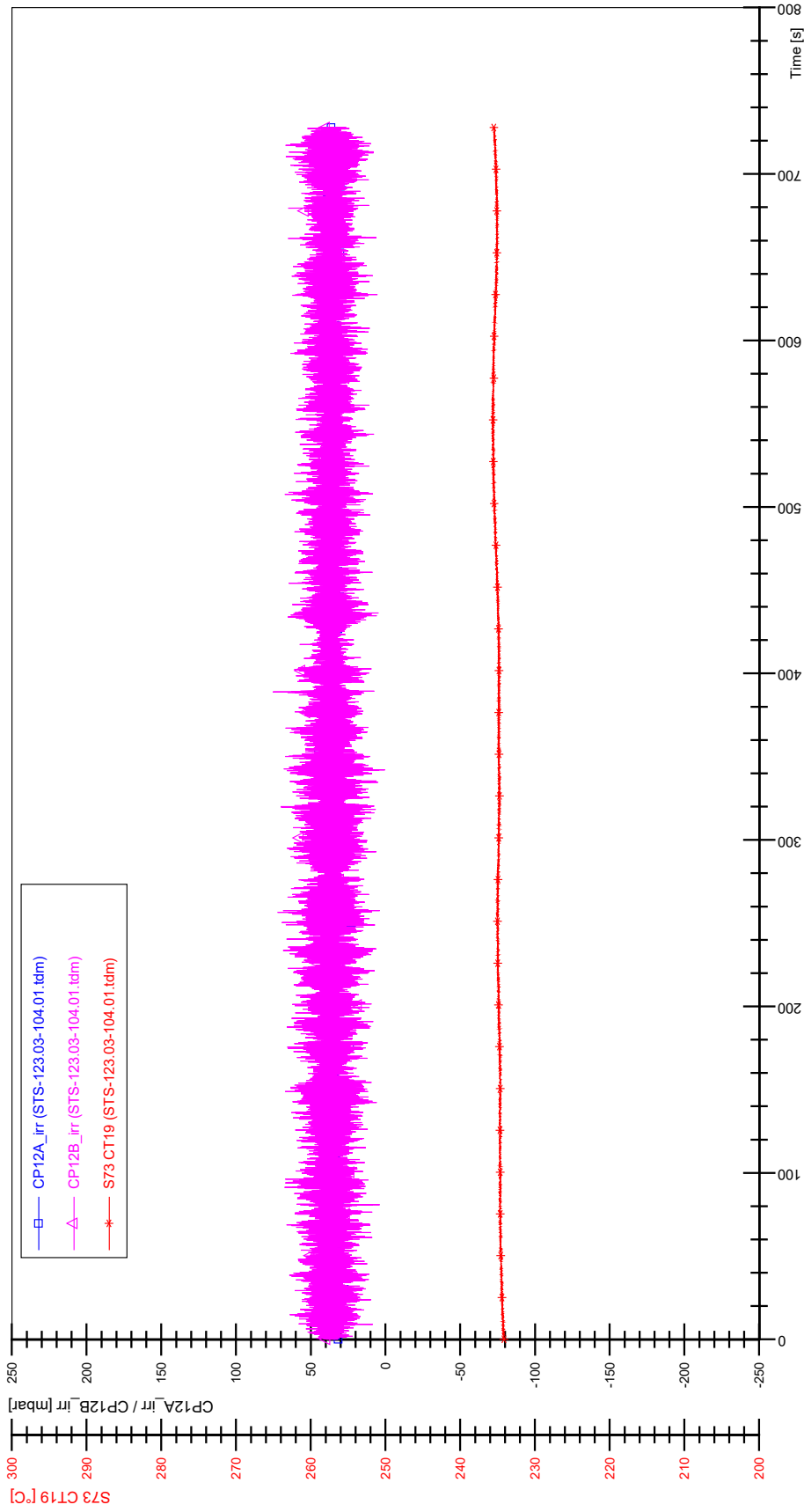
STS-123.03-103.01_Rod_88



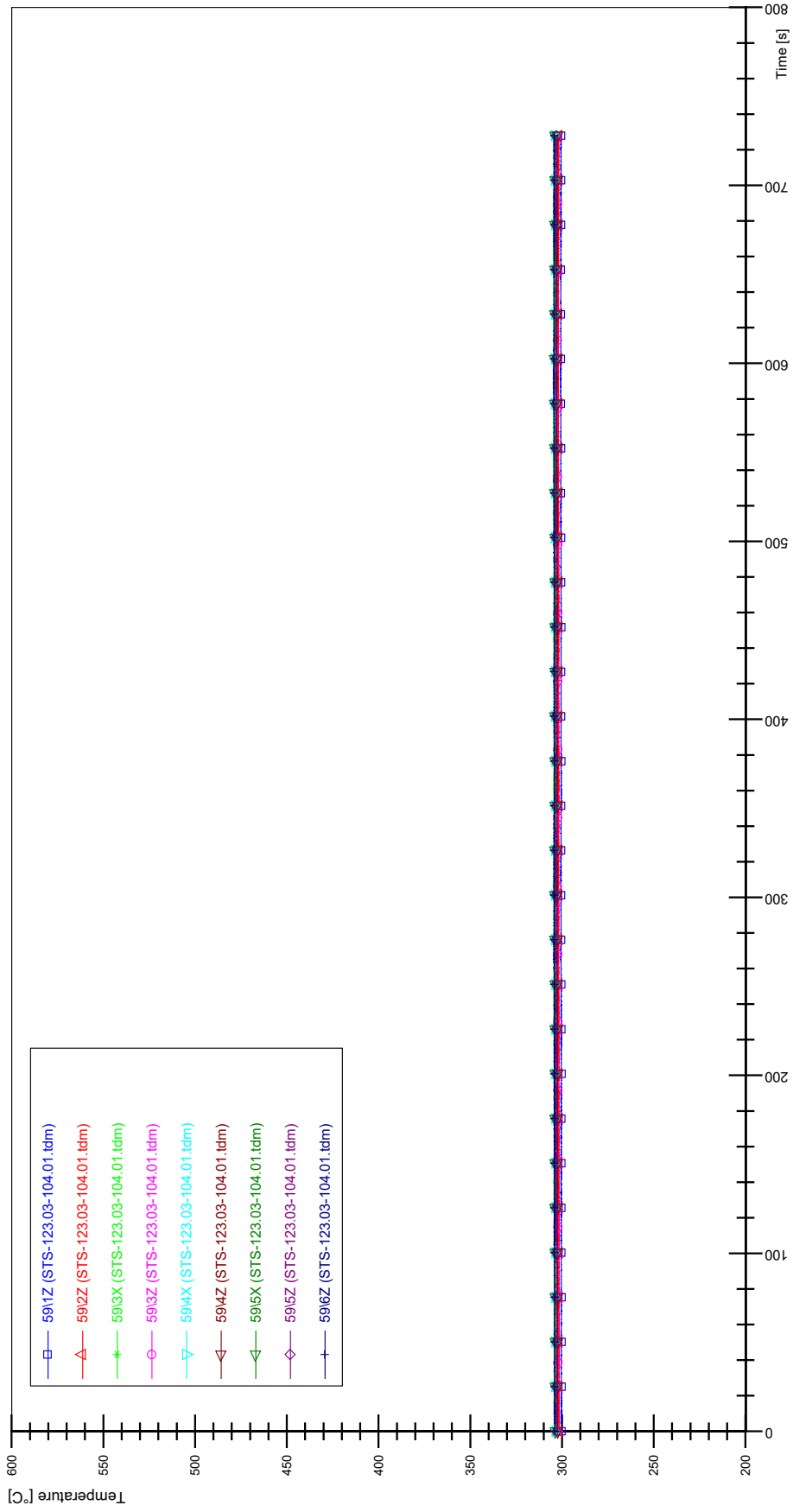
APPENDIX G PLOTS OF INSTABILITY TEST STS-123.03-104.01



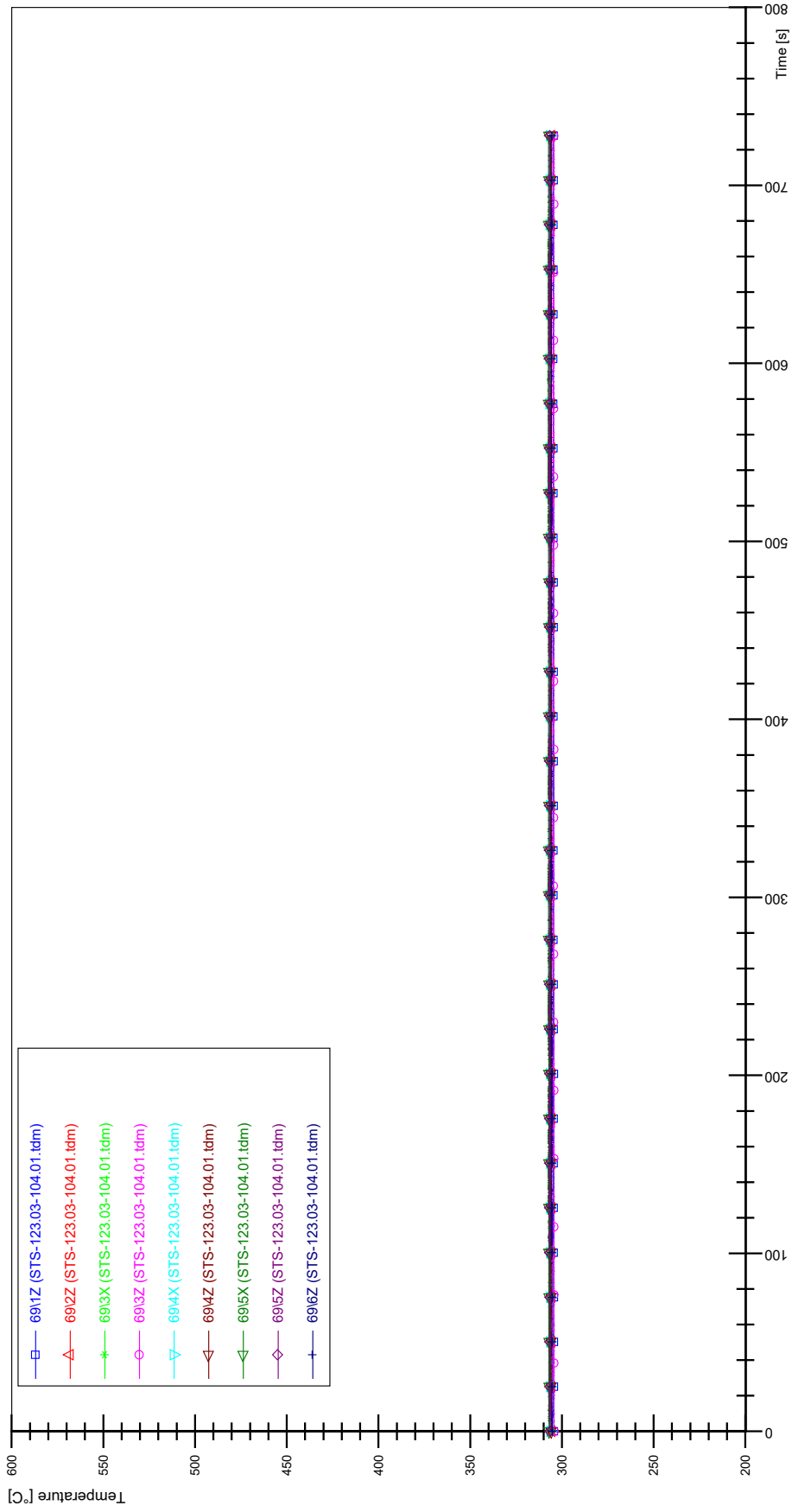
STS-123.03-104.01_CP12_CT19



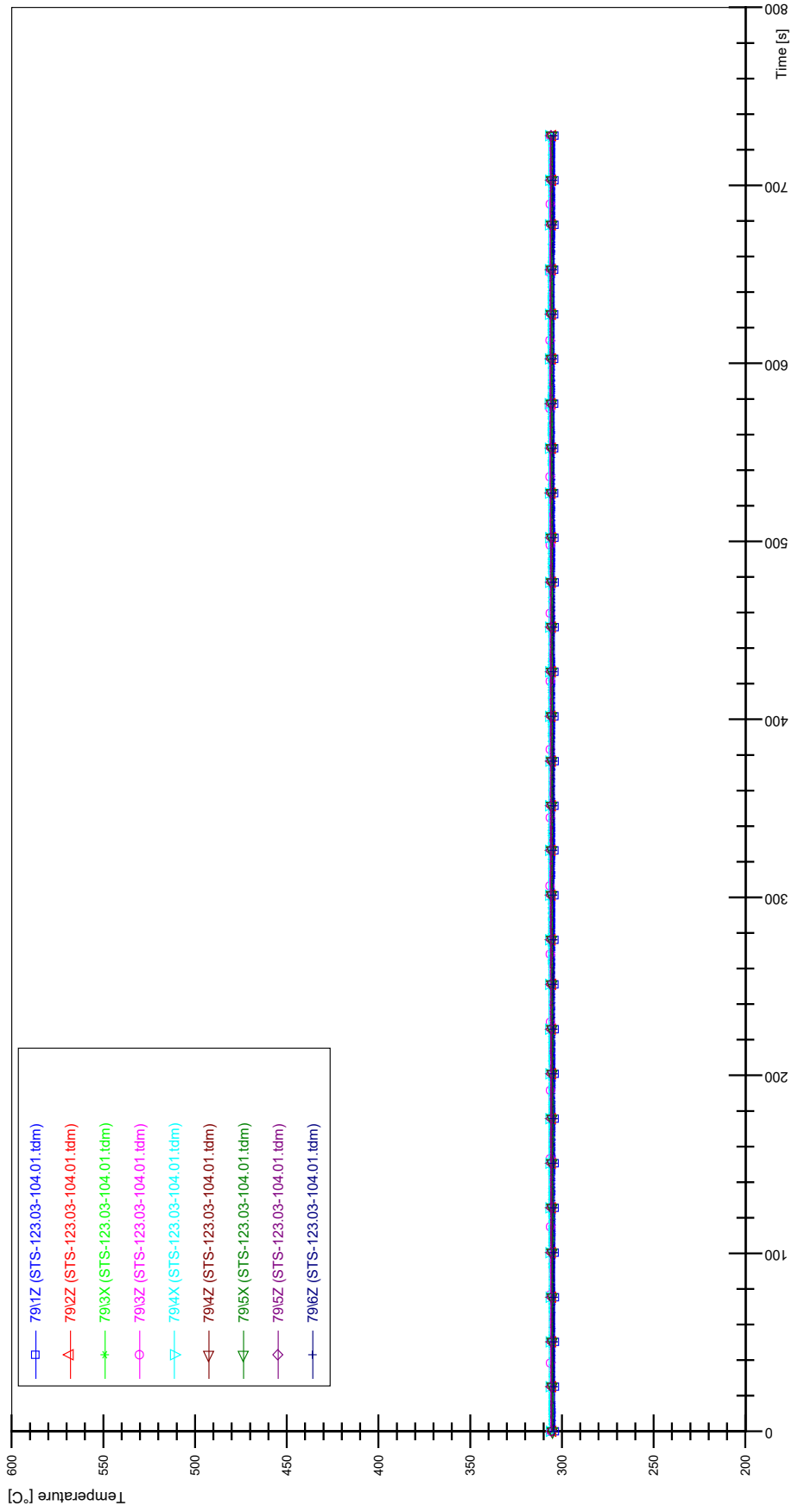
STS-123.03-104.01_Rod_59



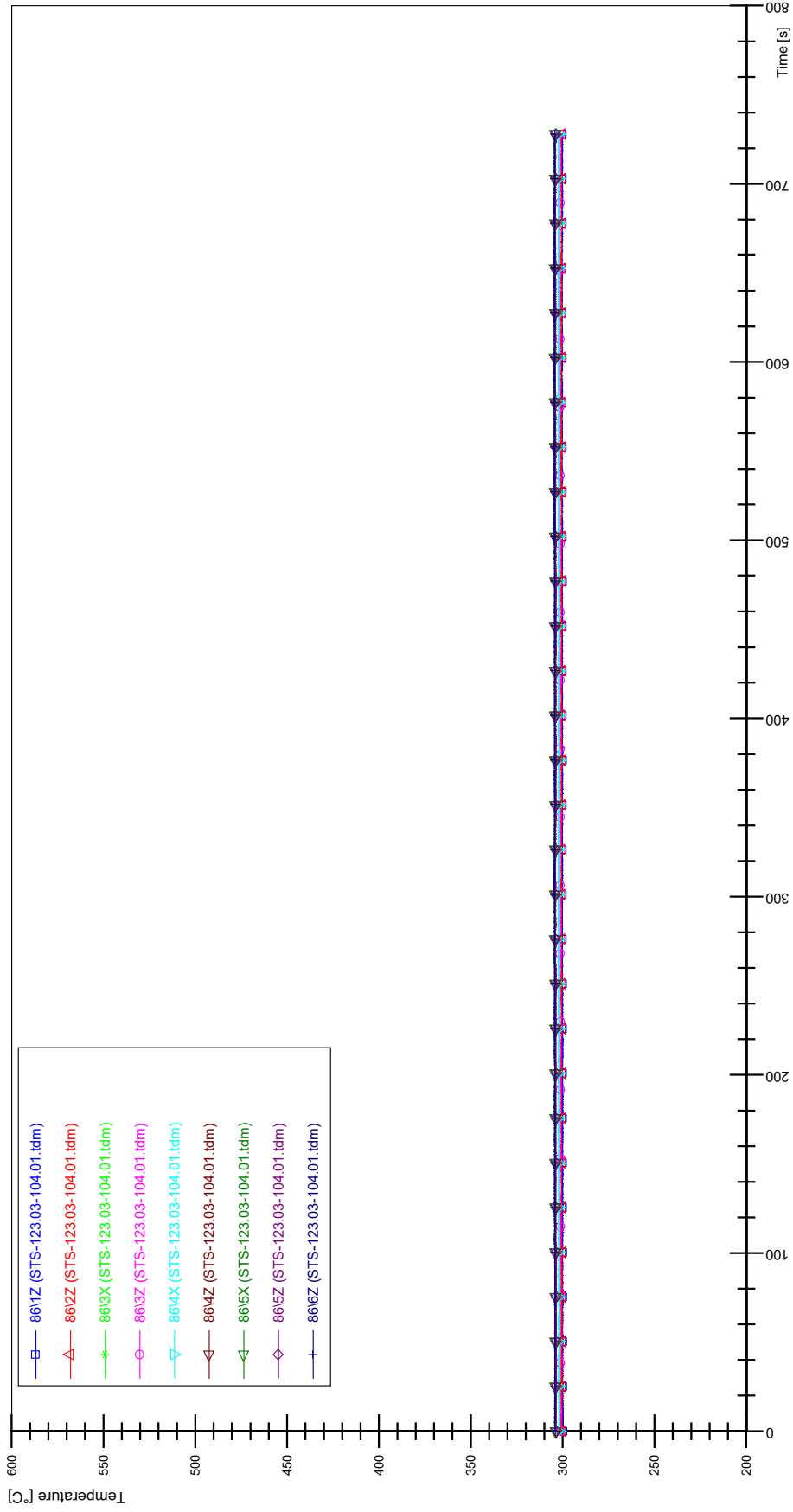
STS-123.03-104.01_Rod_69



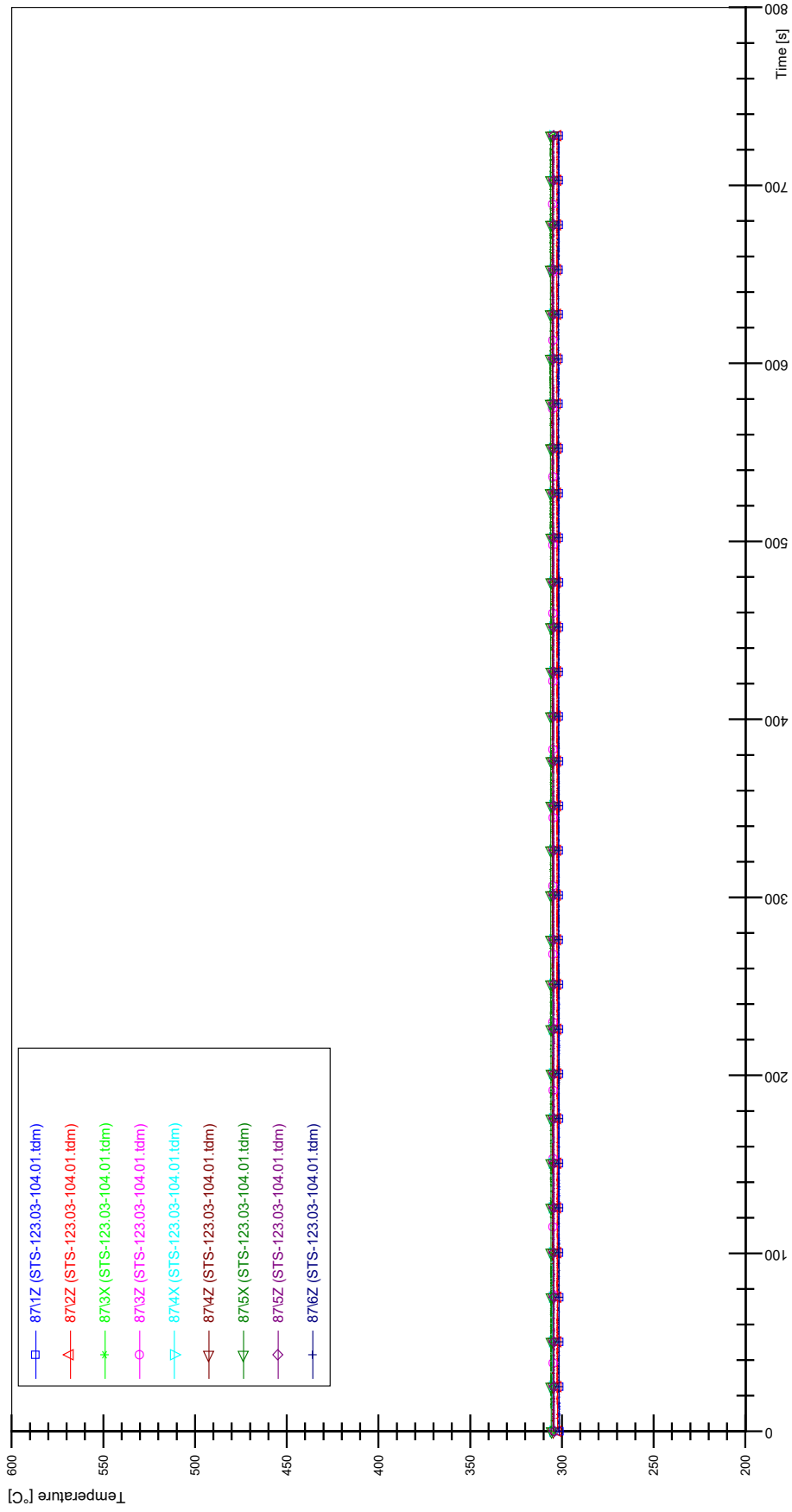
STS-123.03-104.01_Rod_79



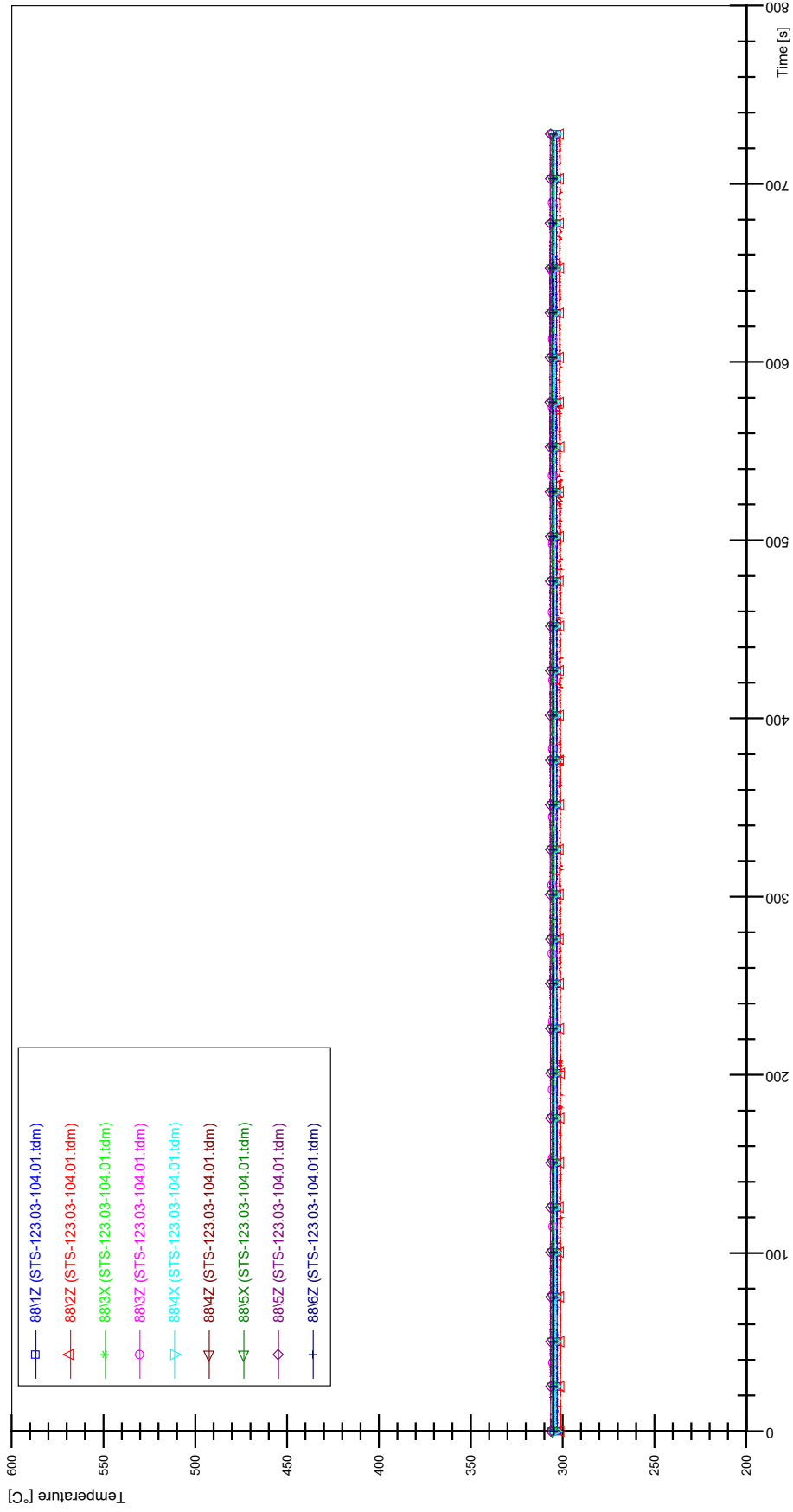
STS-123.03-104.01_Rod_86



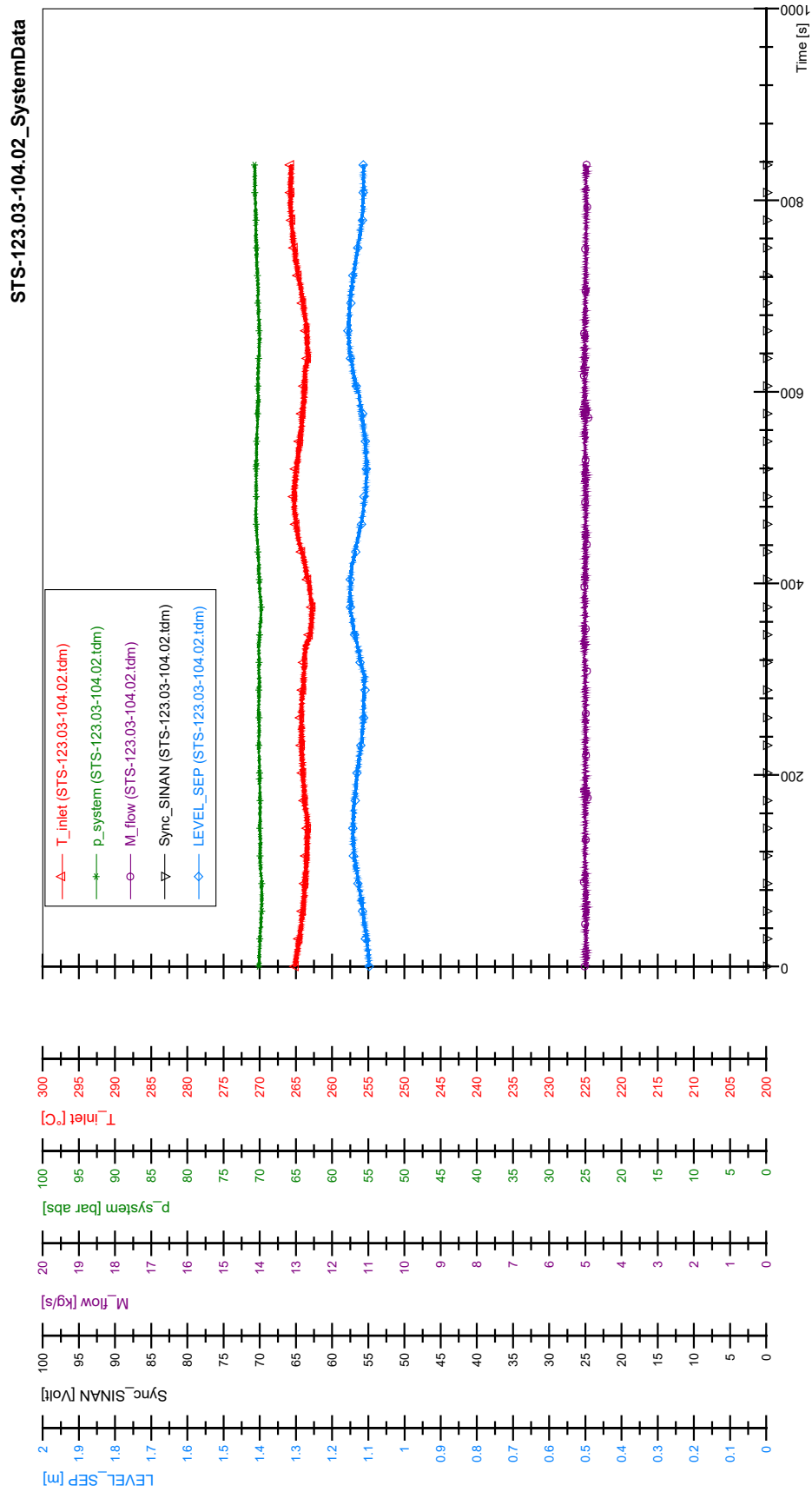
STS-123.03-104.01_Rod_87

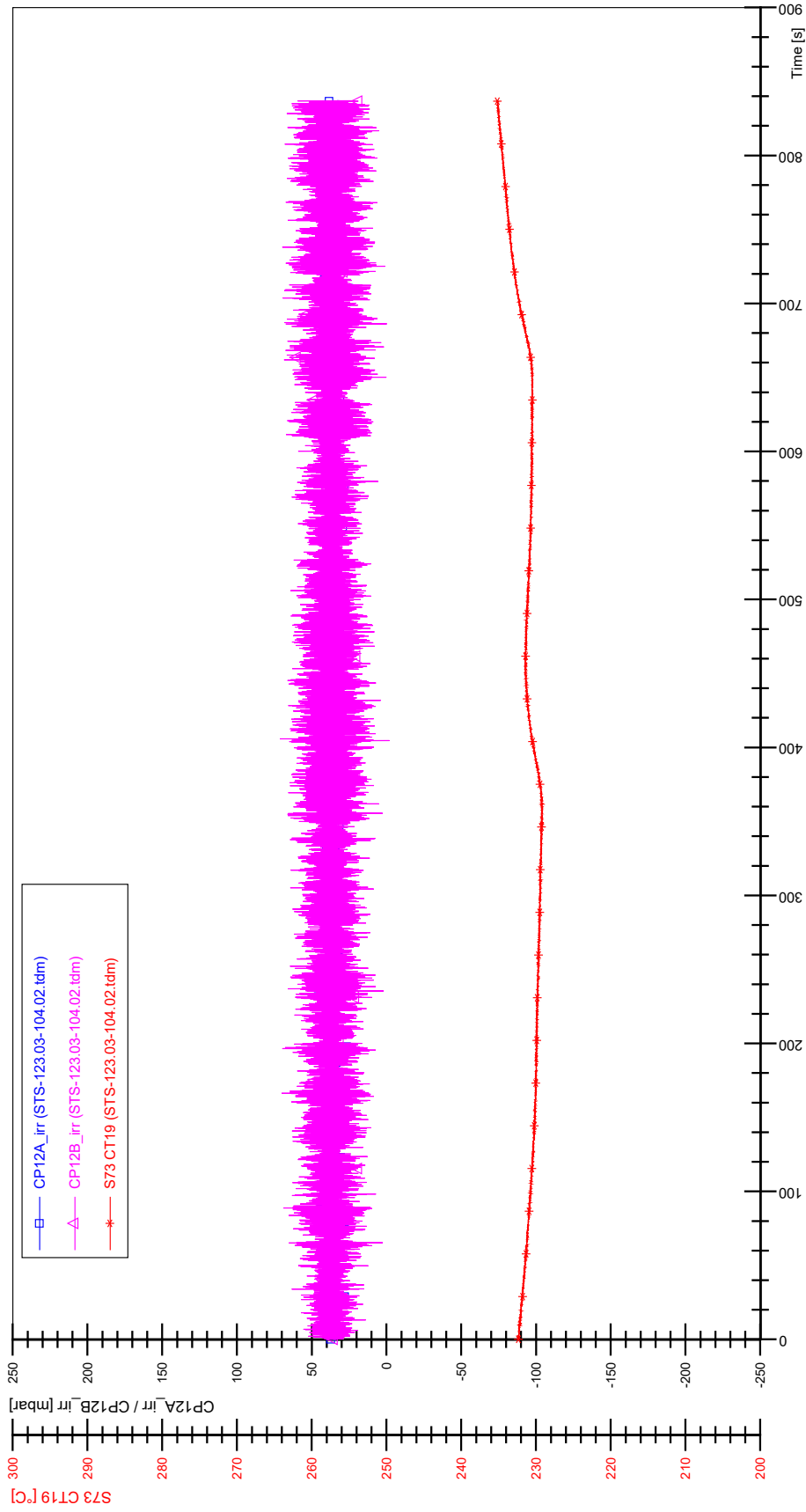


STS-123.03-104.01_Rod_88

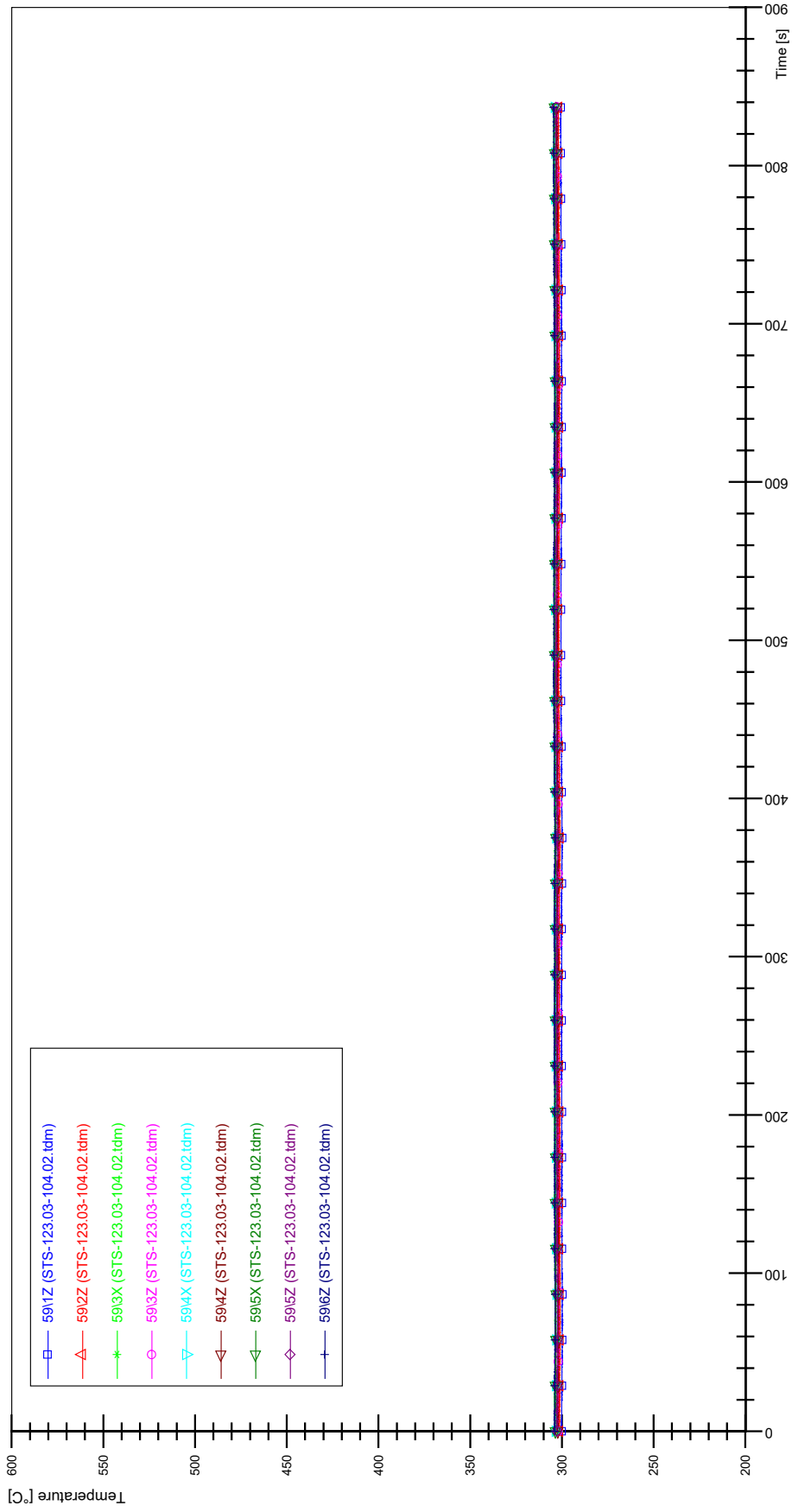


APPENDIX H PLOTS OF INSTABILITY TEST STS-123.03-104.02

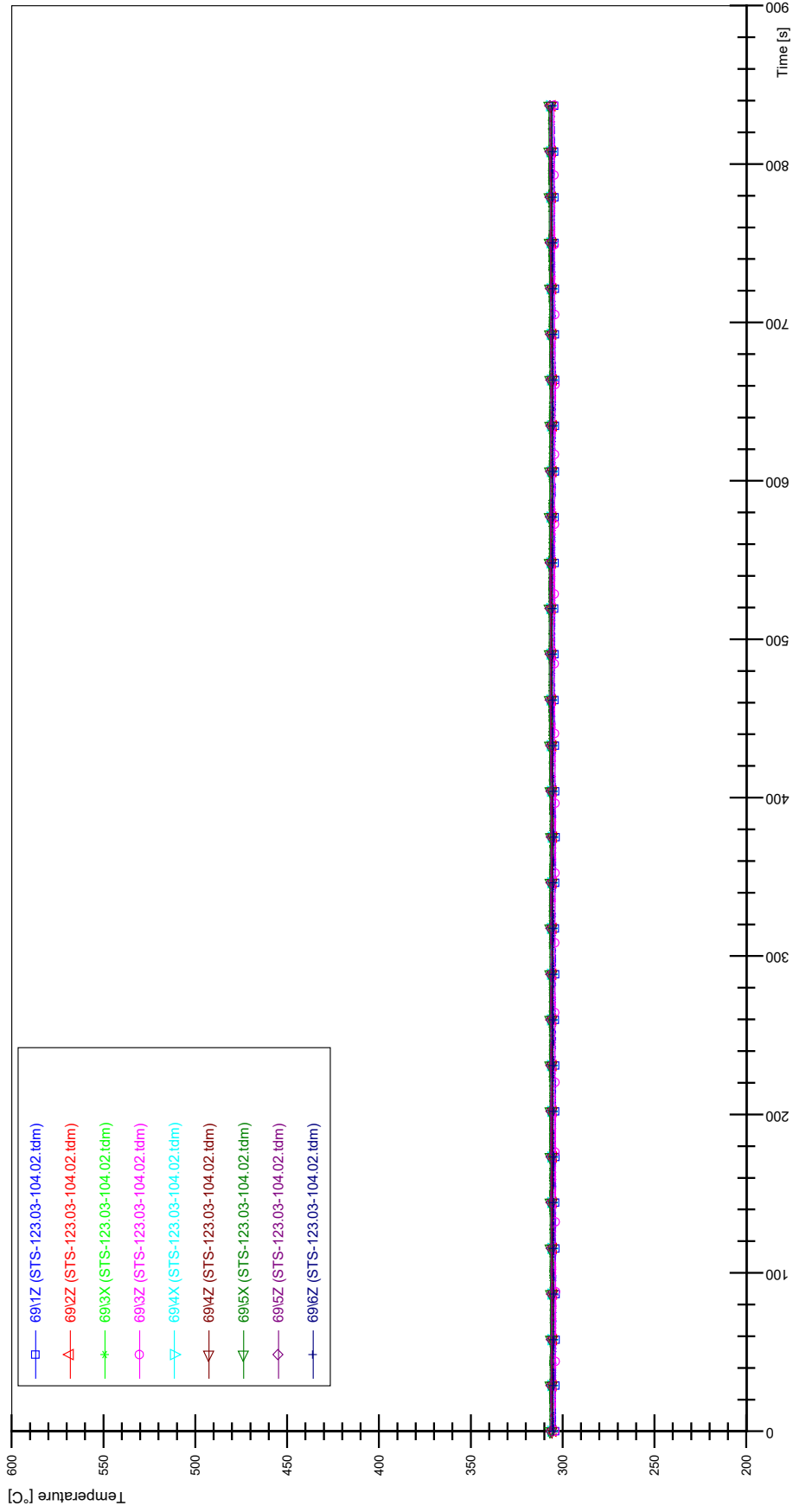




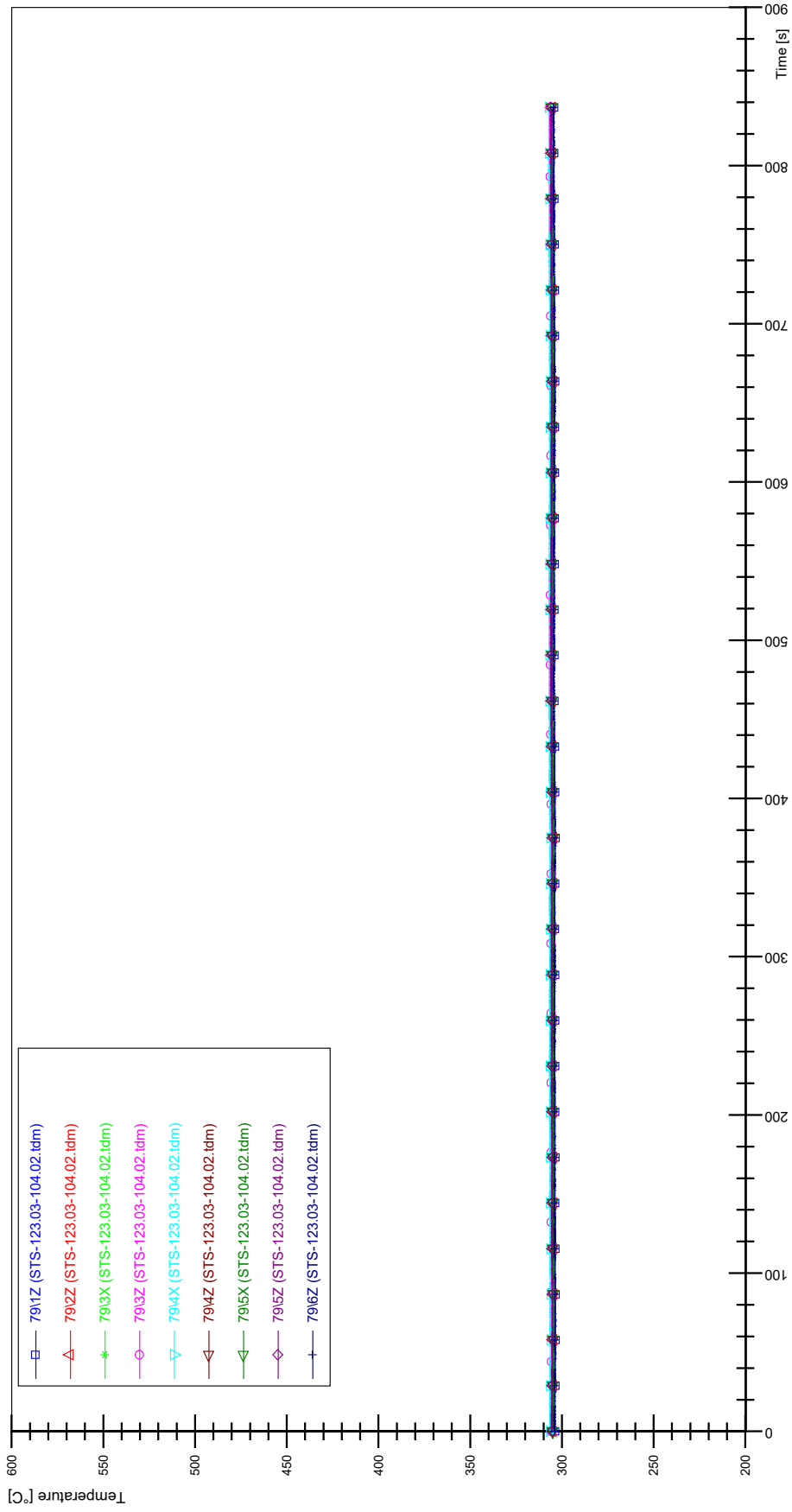
STS-123.03-104.02_Rod_59



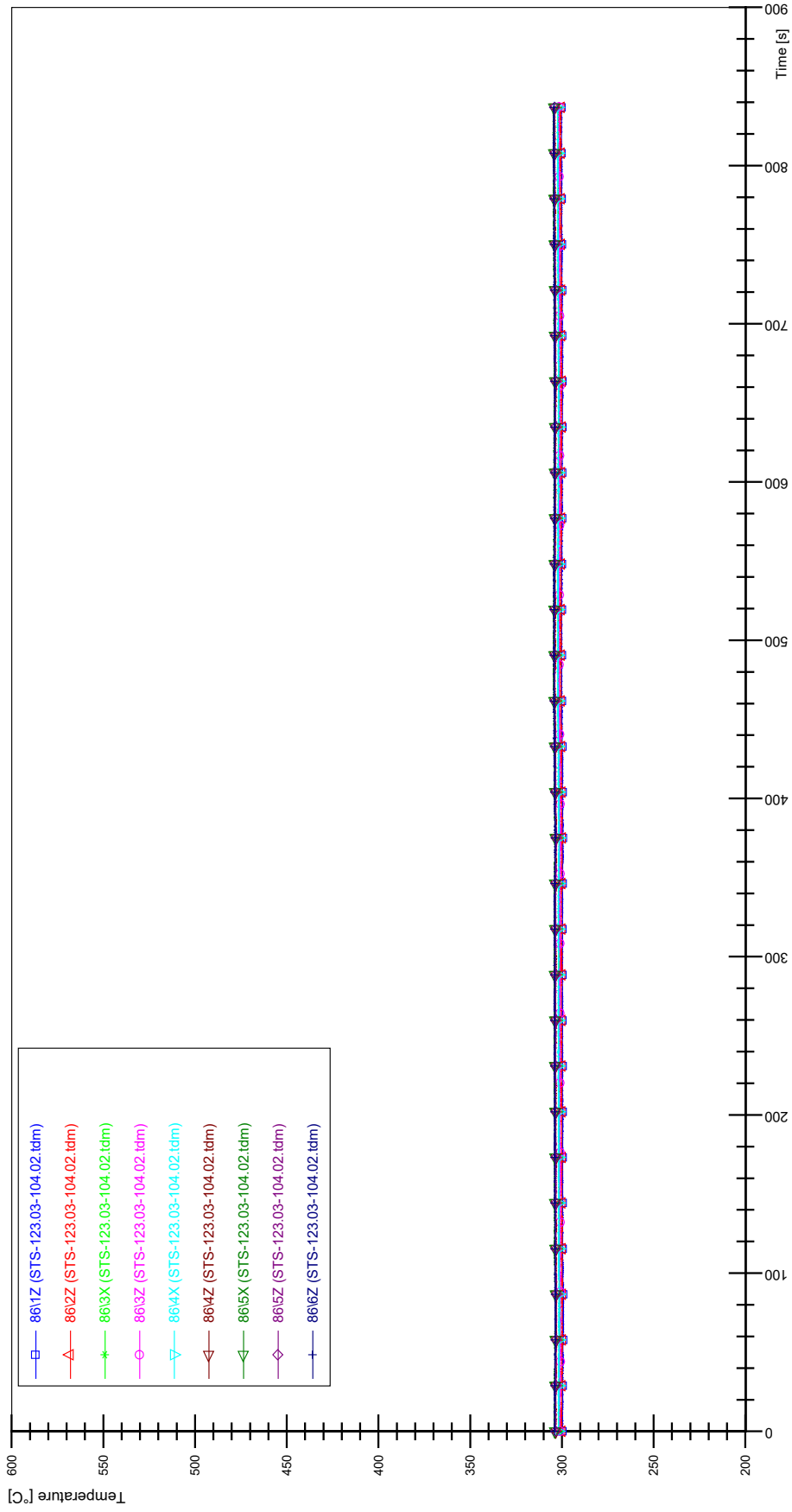
STS-123.03-104.02_Rod_69



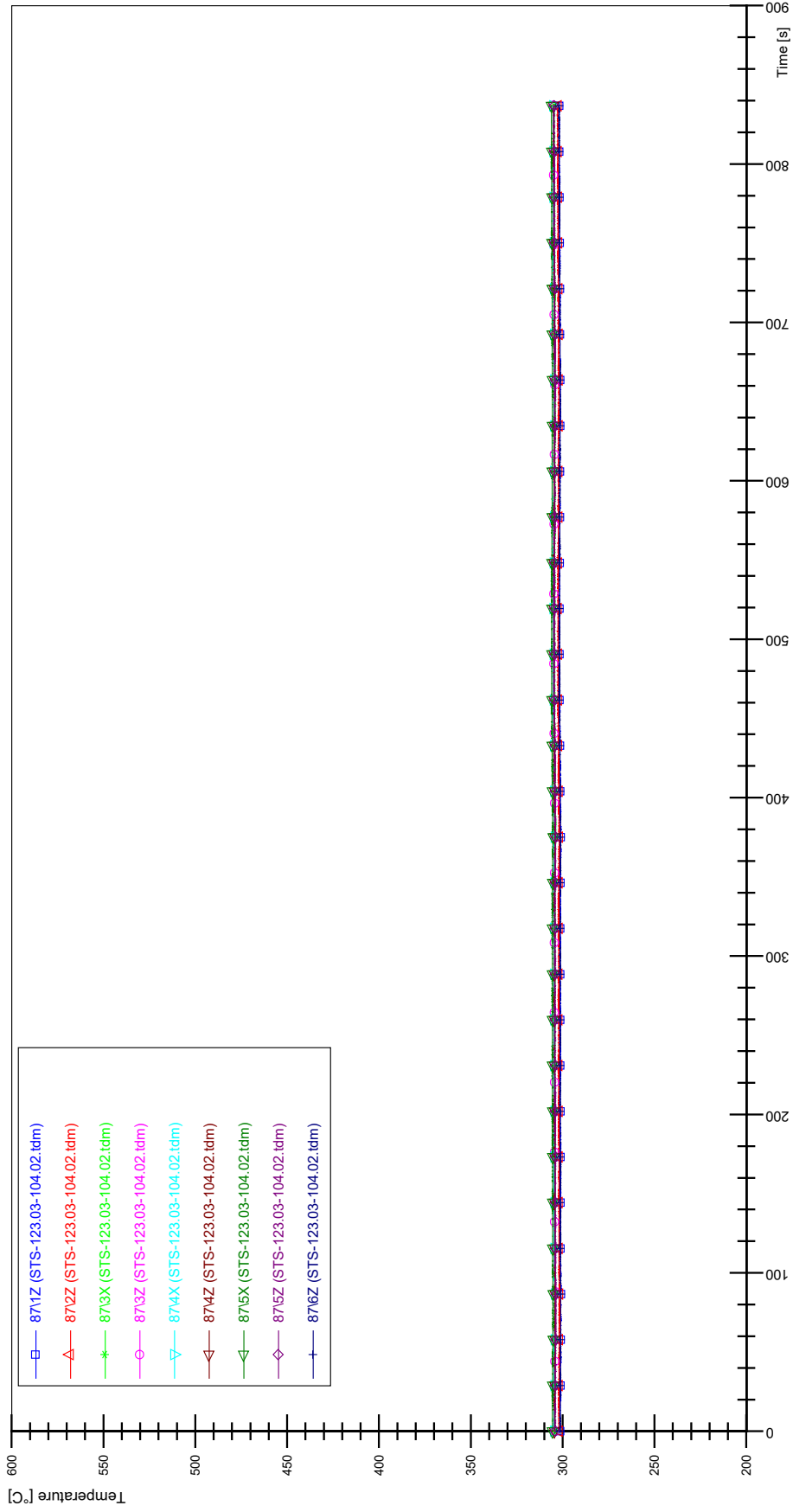
STS-123.03-104.02_Rod_79



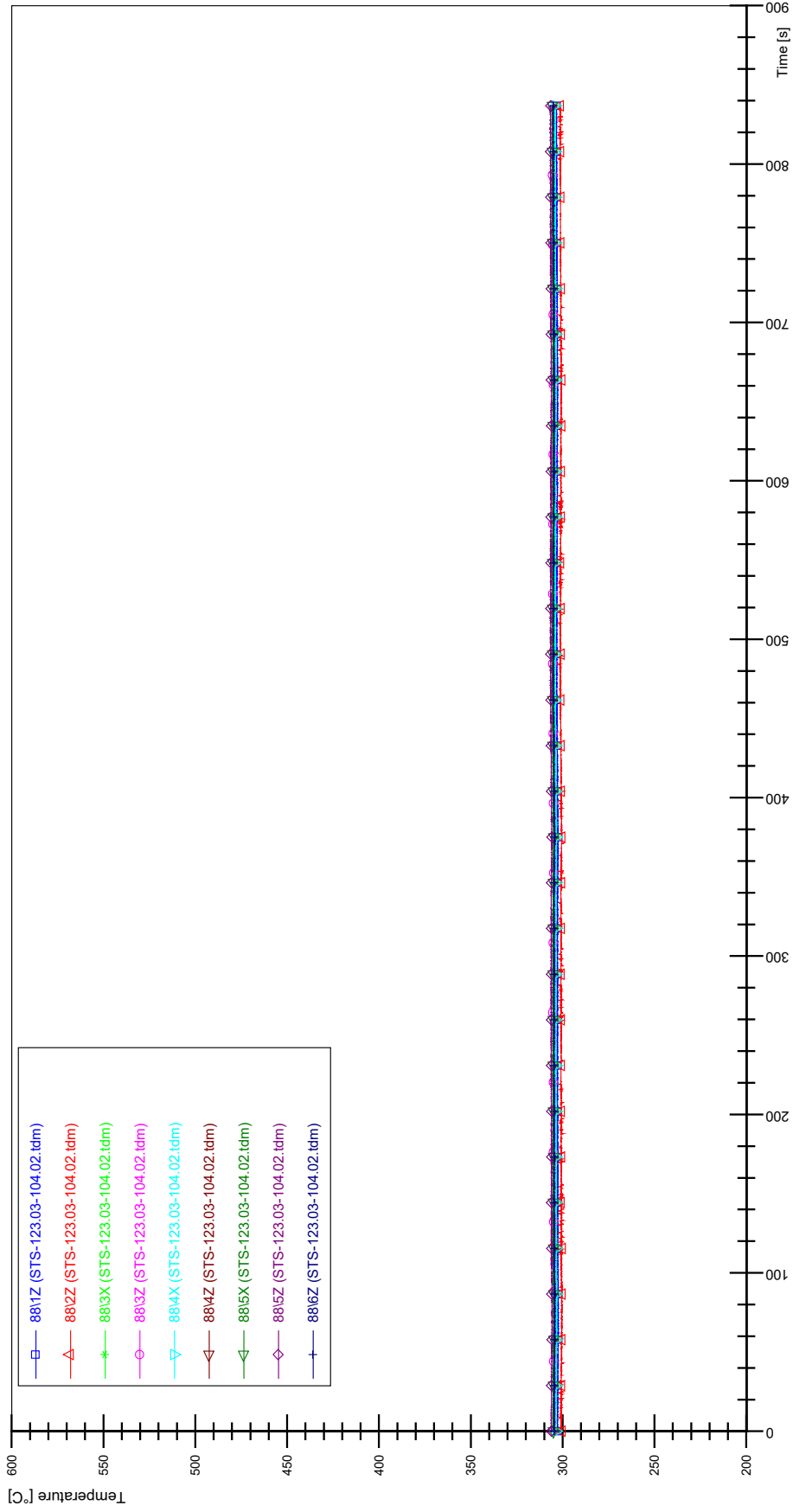
STS-123.03-104.02_Rod_86



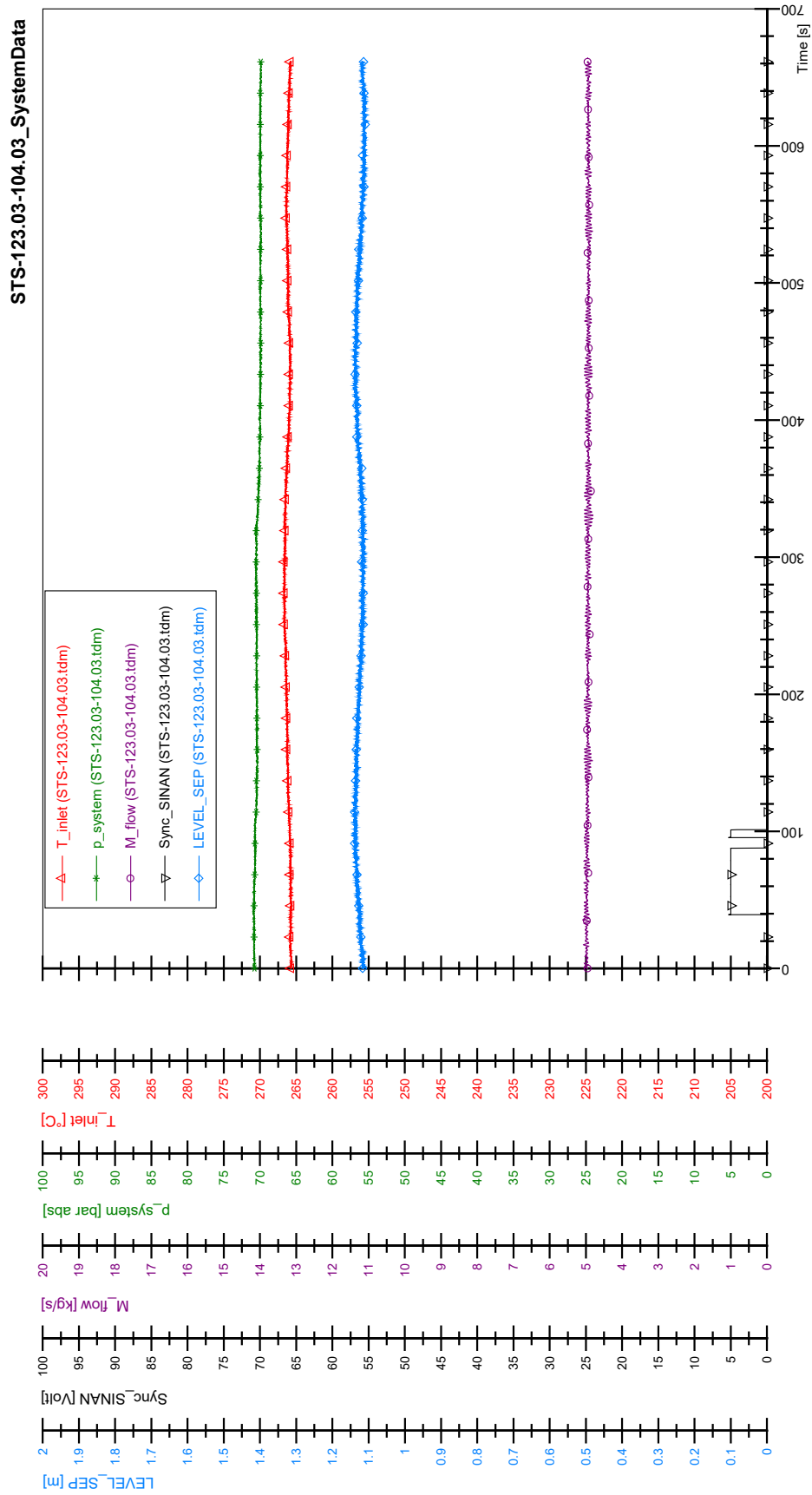
STS-123.03-104.02_Rod_87



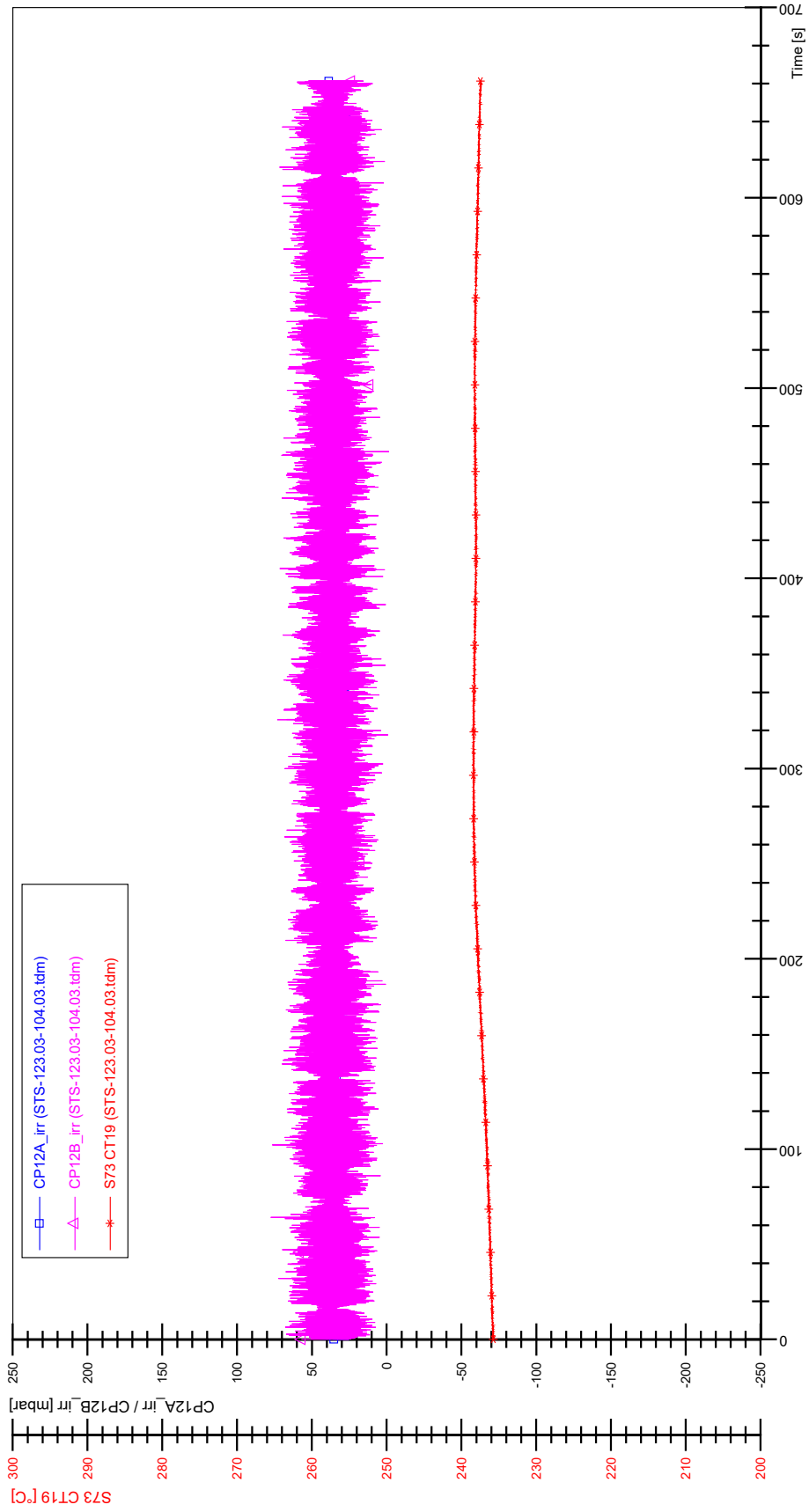
STS-123.03-104.02_Rod_88



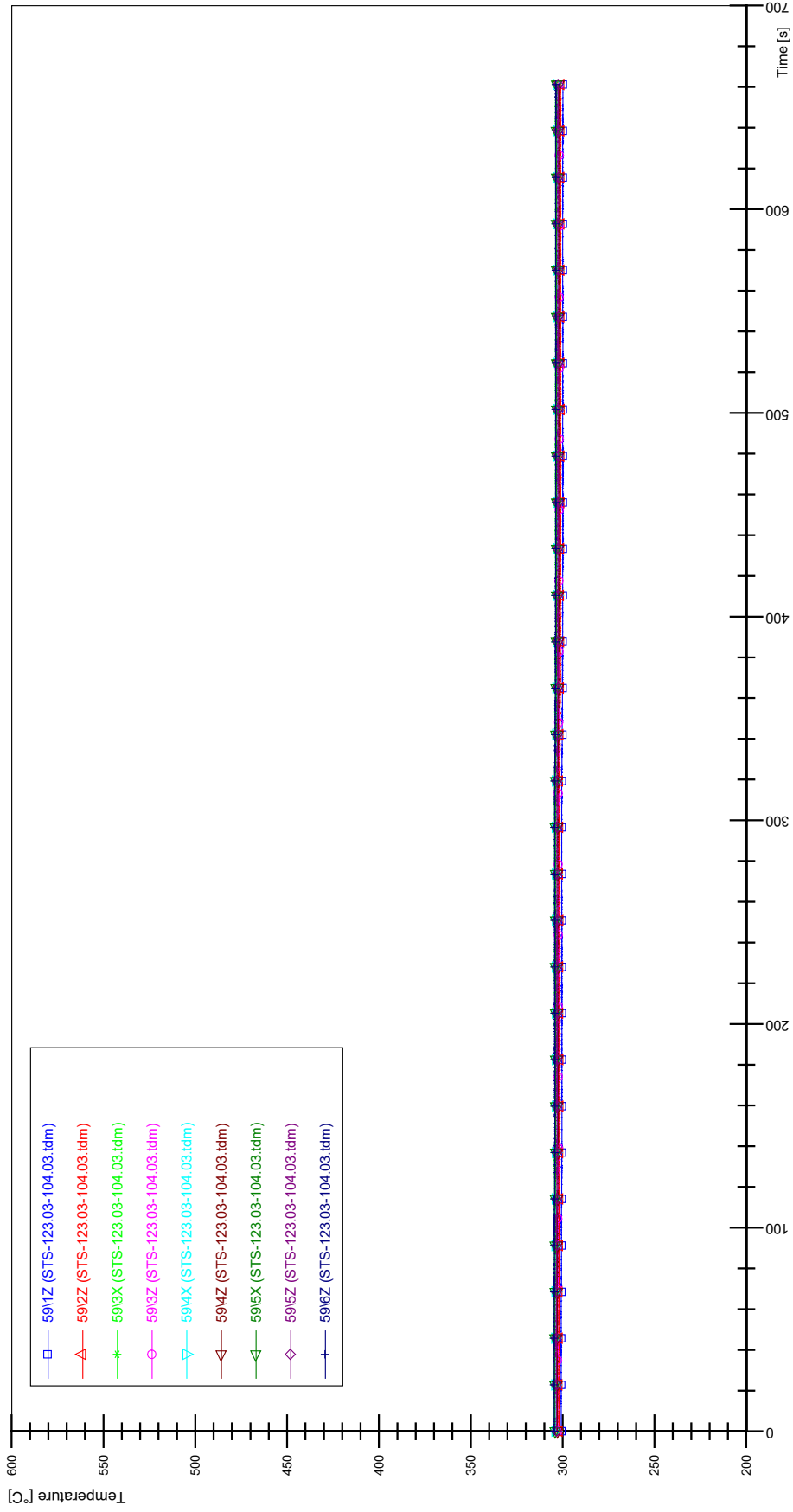
APPENDIX I PLOTS OF INSTABILITY TEST STS-123.03-104.03



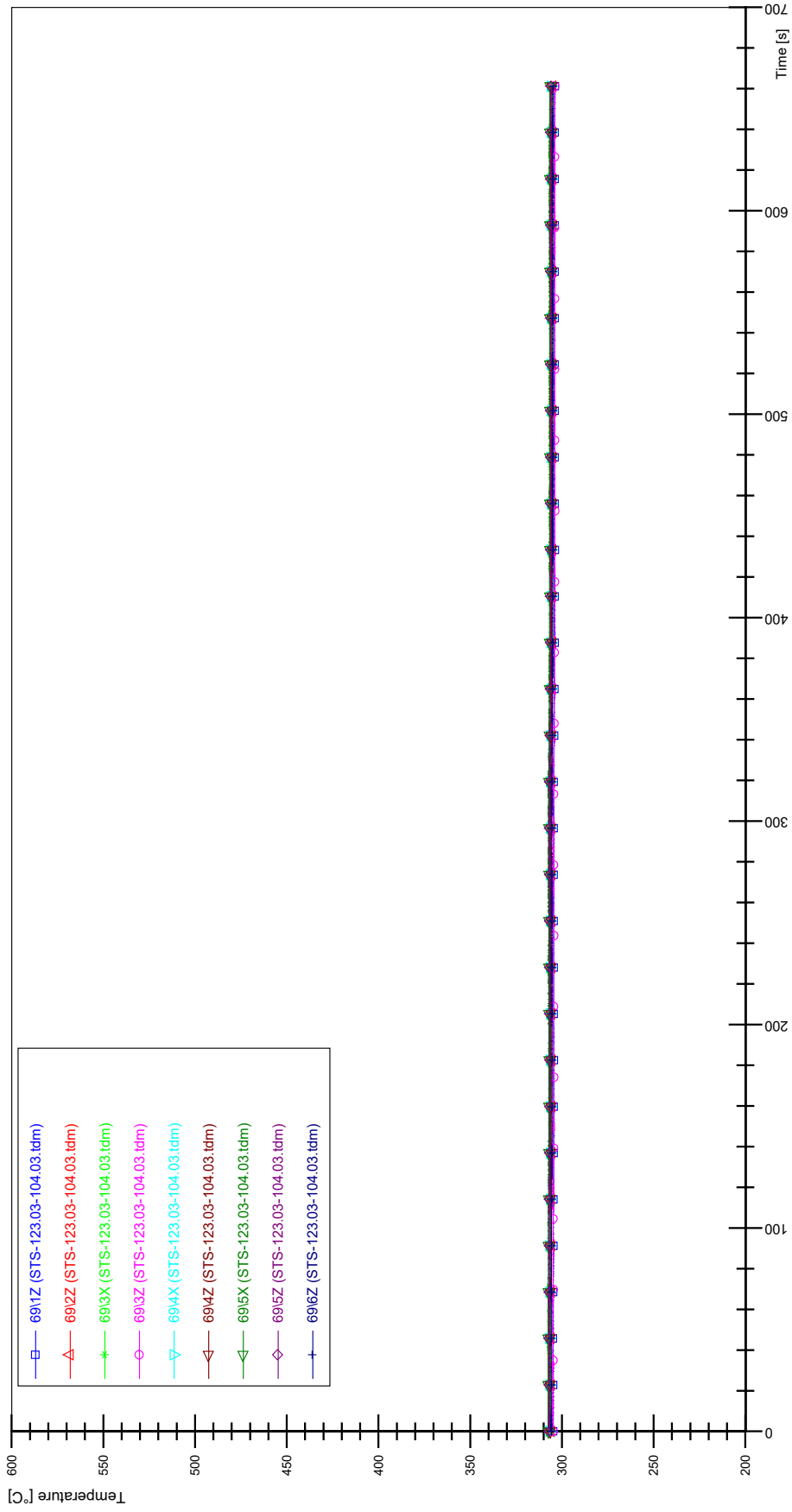
STS-123.03-104.03_CP12_CT19



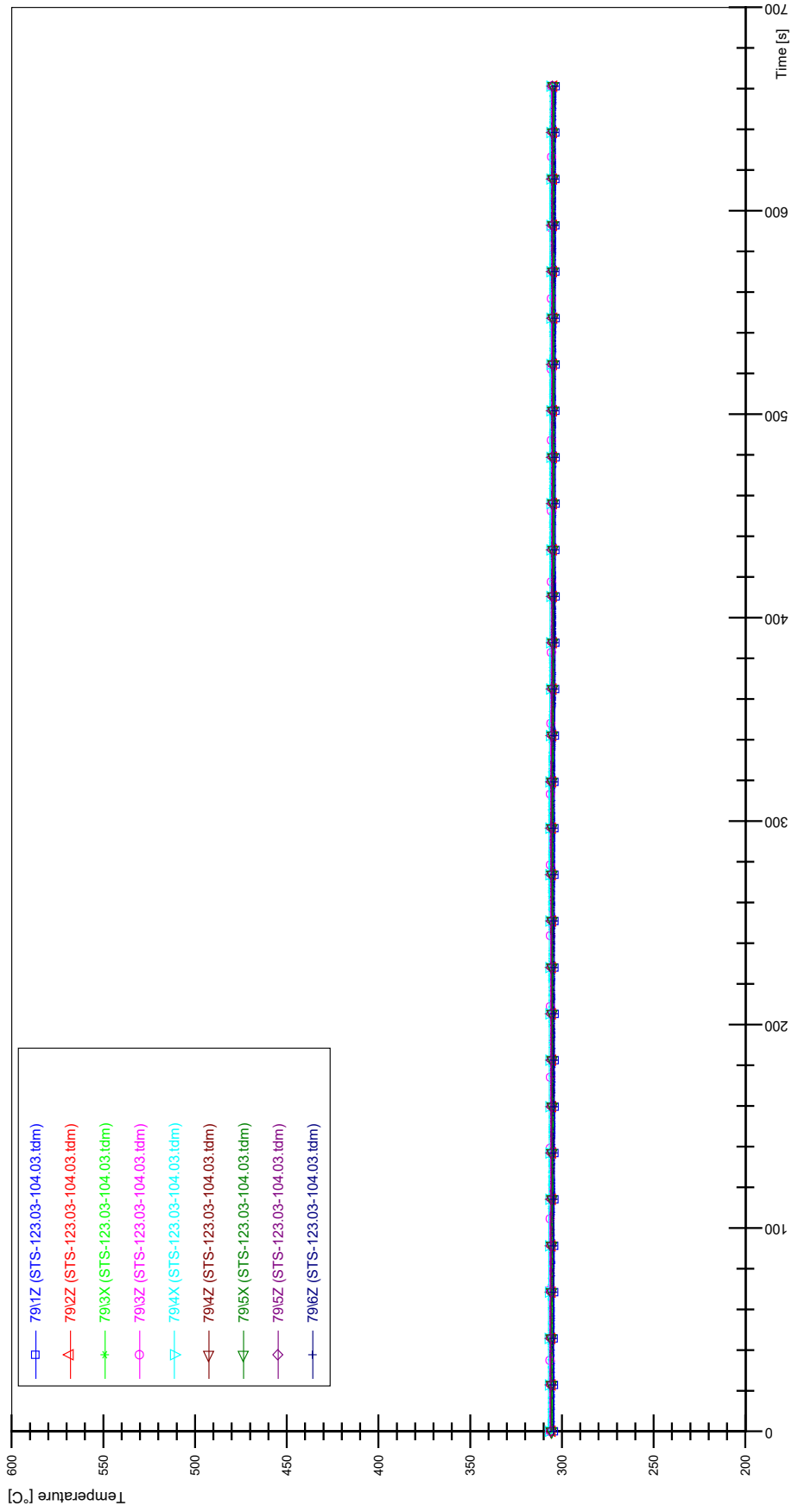
STS-123.03-104.03_Rod_59



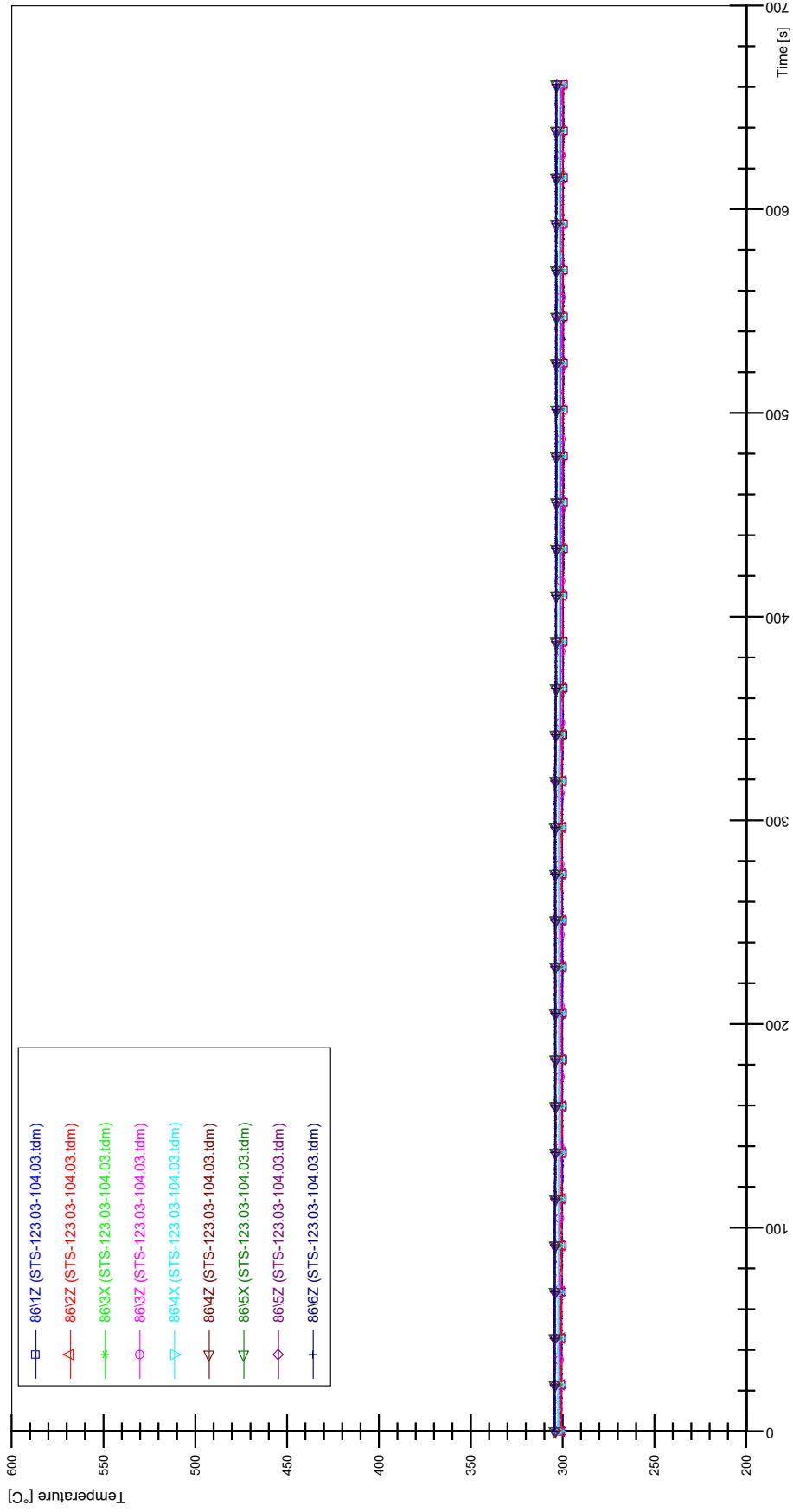
STS-123.03-104.03_Rod_69



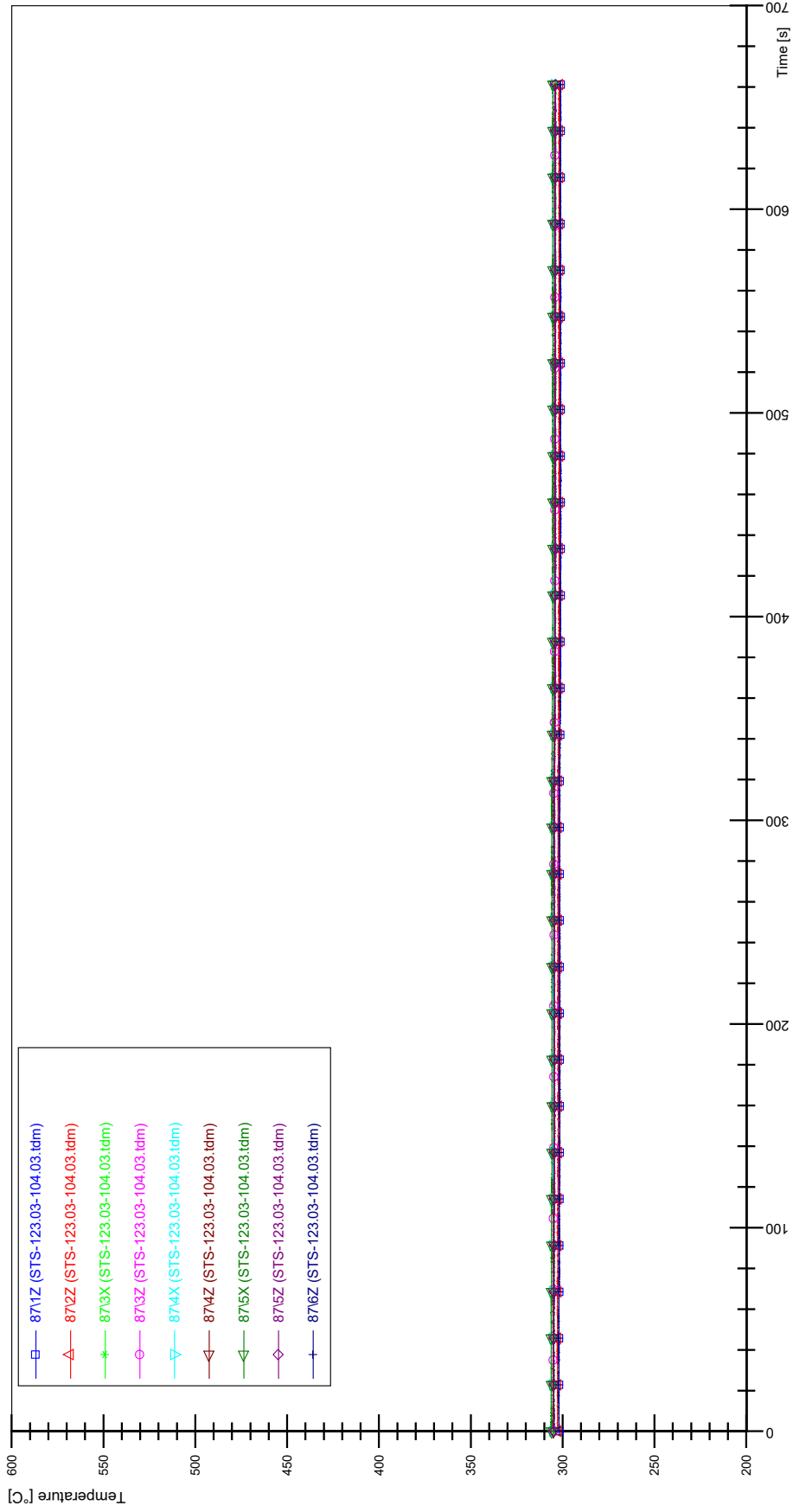
STS-123.03-104.03_Rod_79



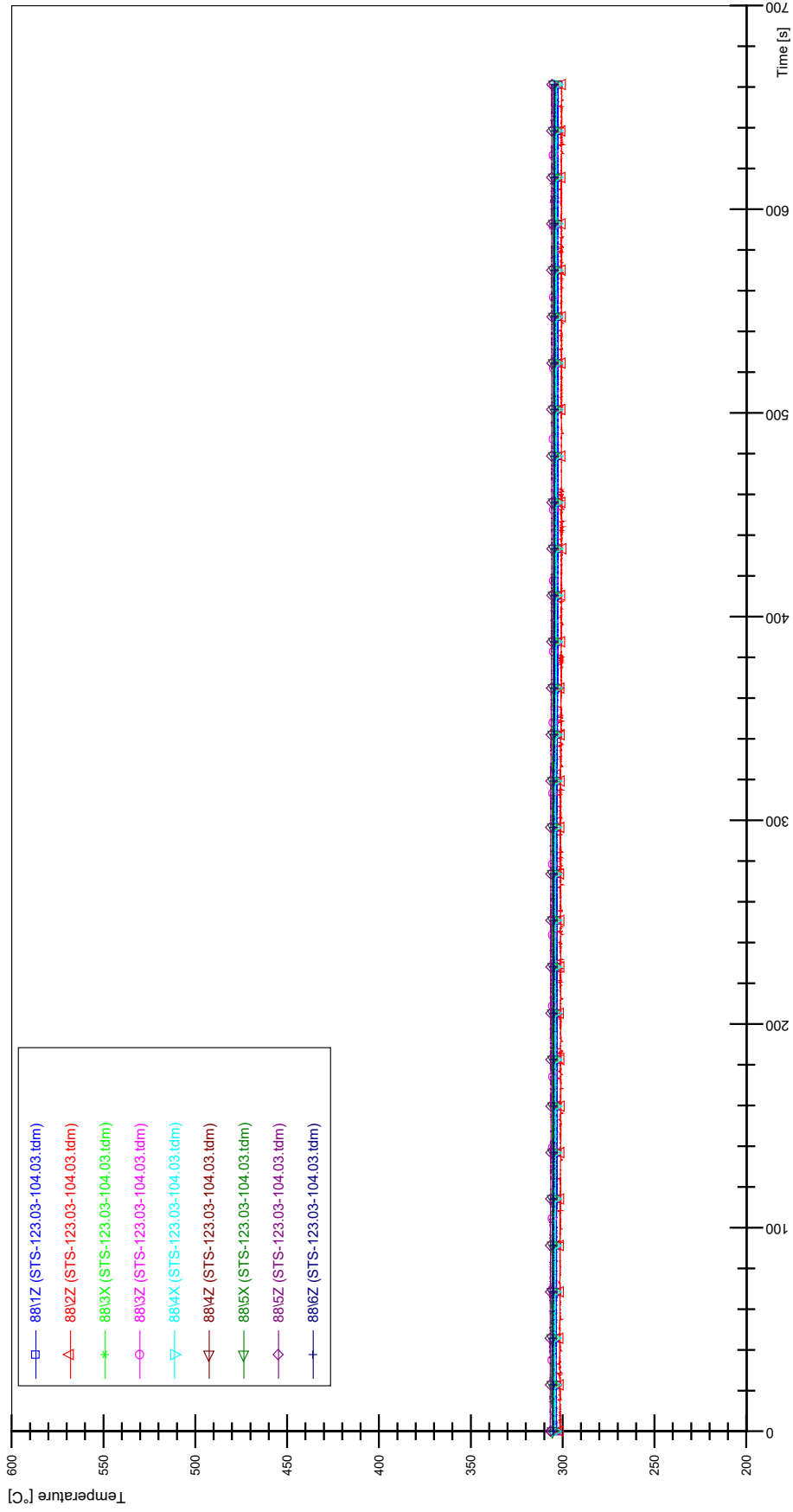
STS-123.03-104.03_Rod_86



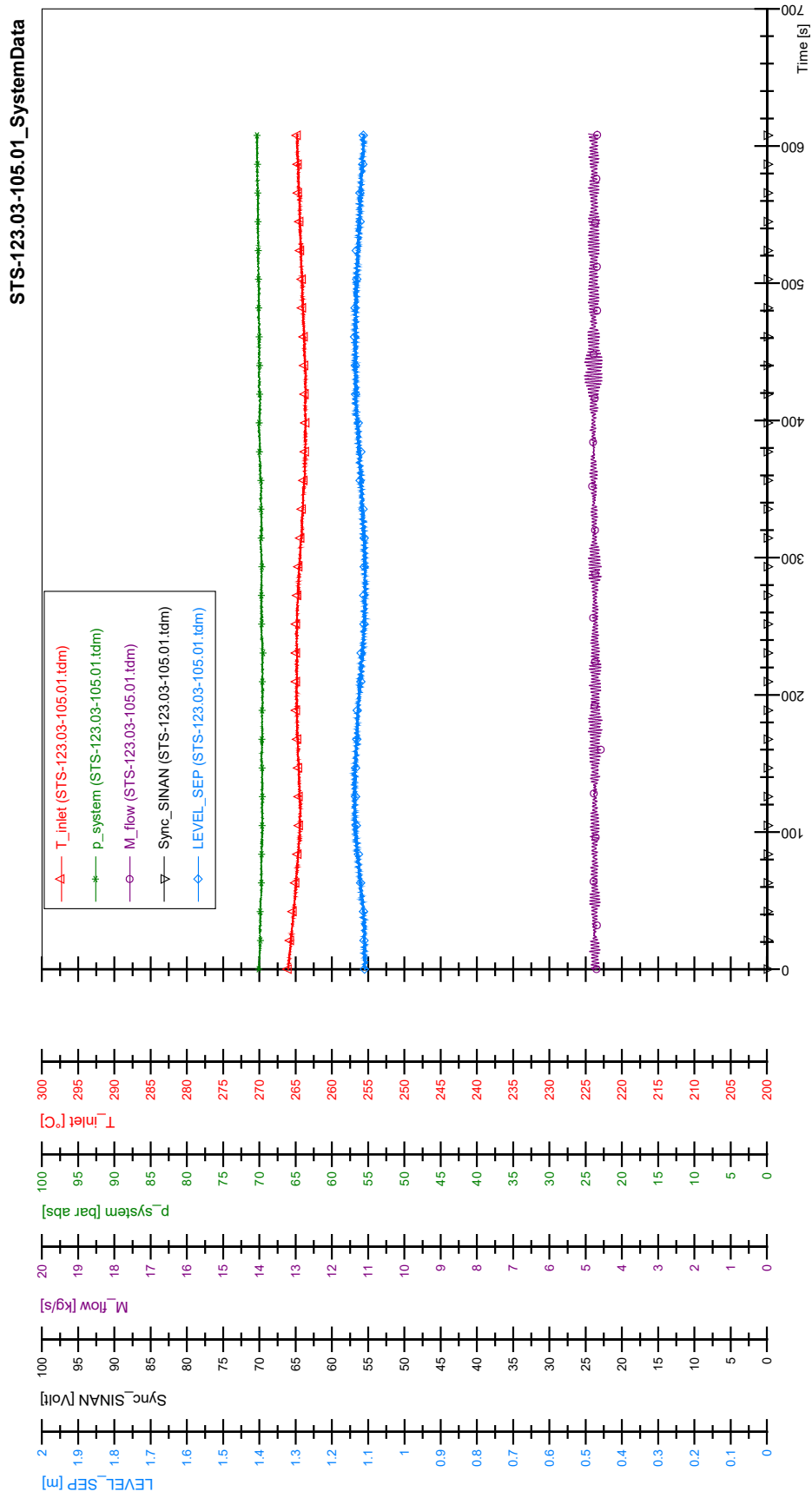
STS-123.03-104.03_Rod_87



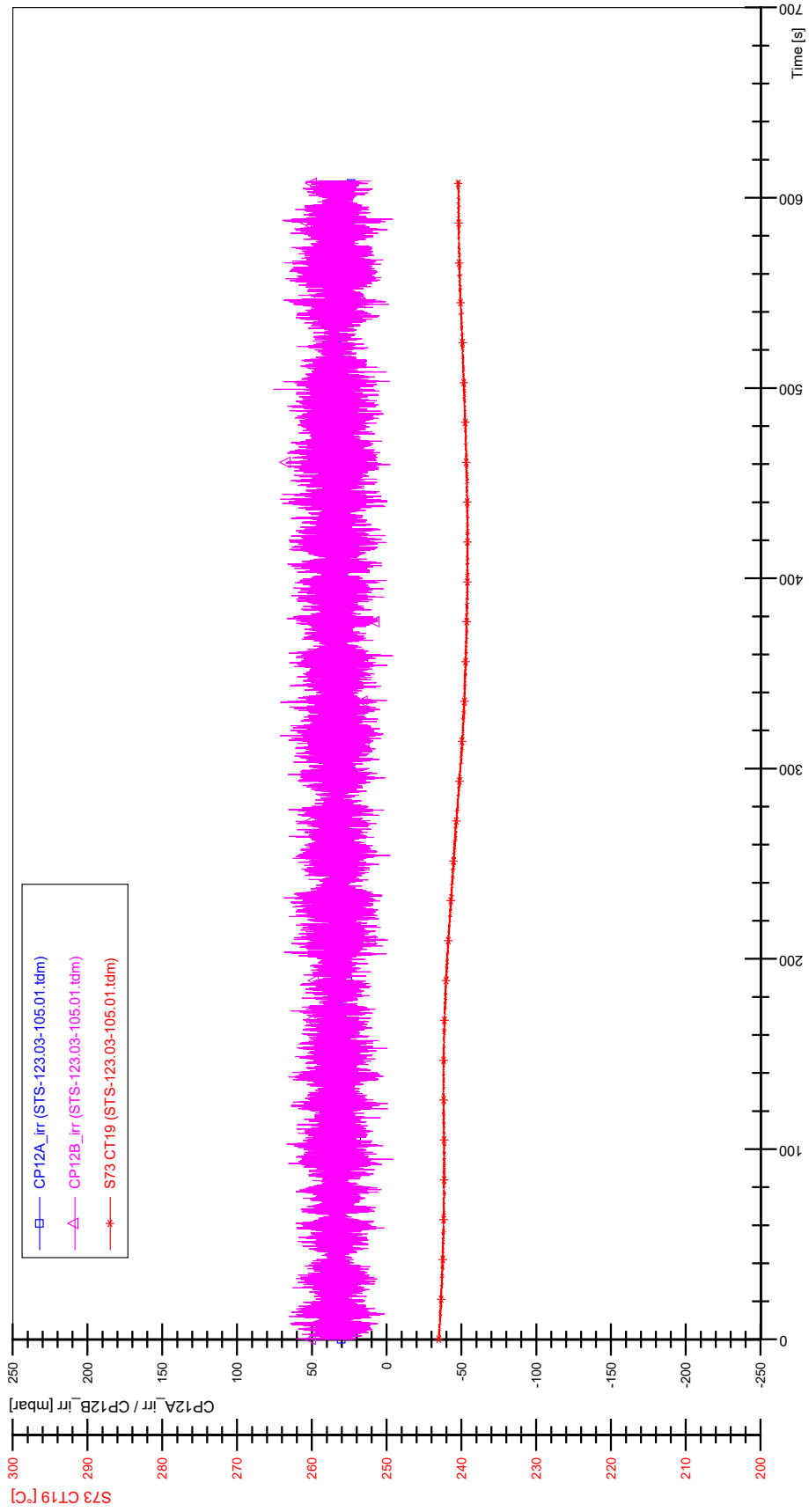
STS-123.03-104.03_Rod_88



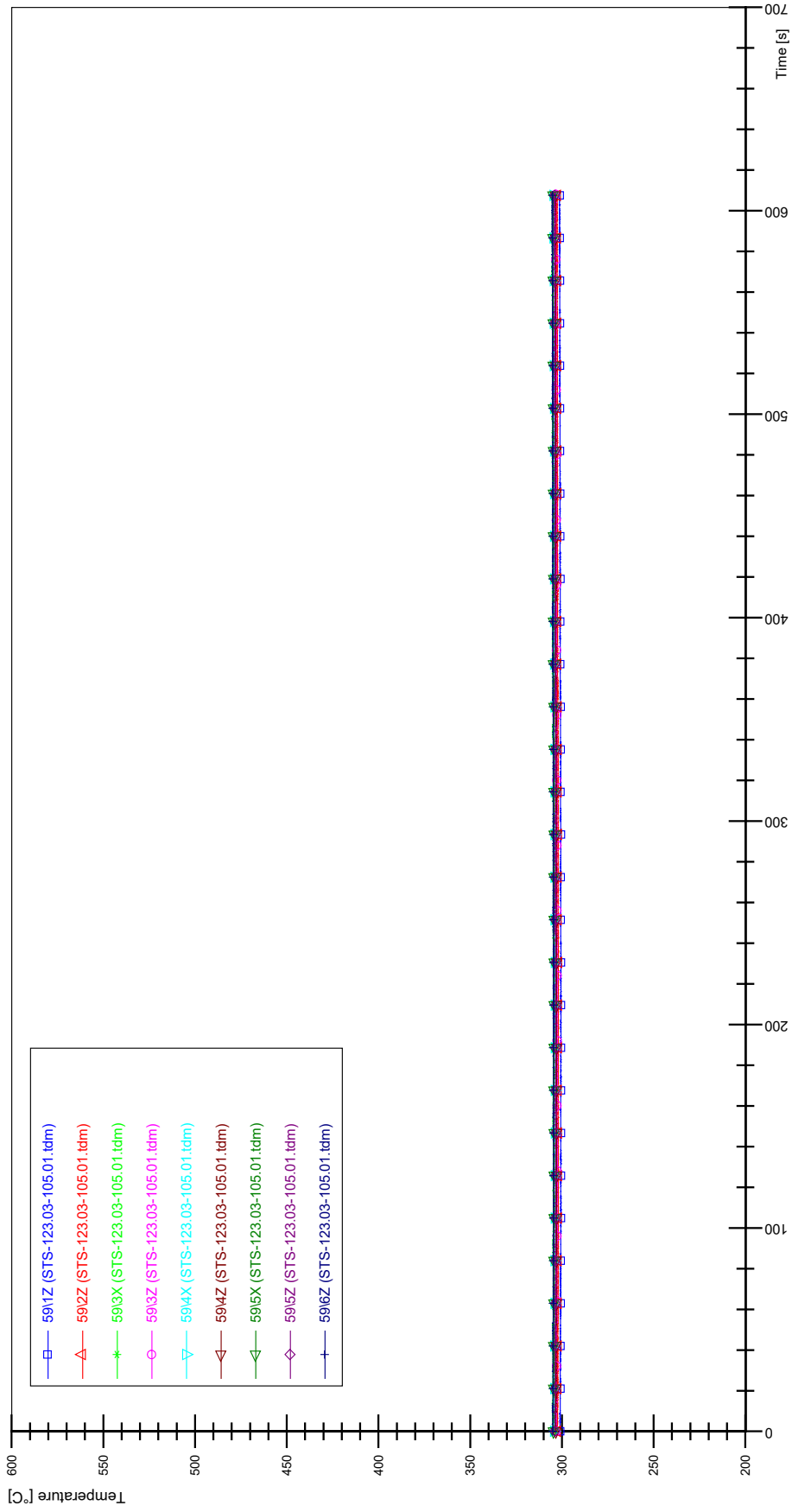
APPENDIX J PLOTS OF INSTABILITY TEST STS-123.03-105.01



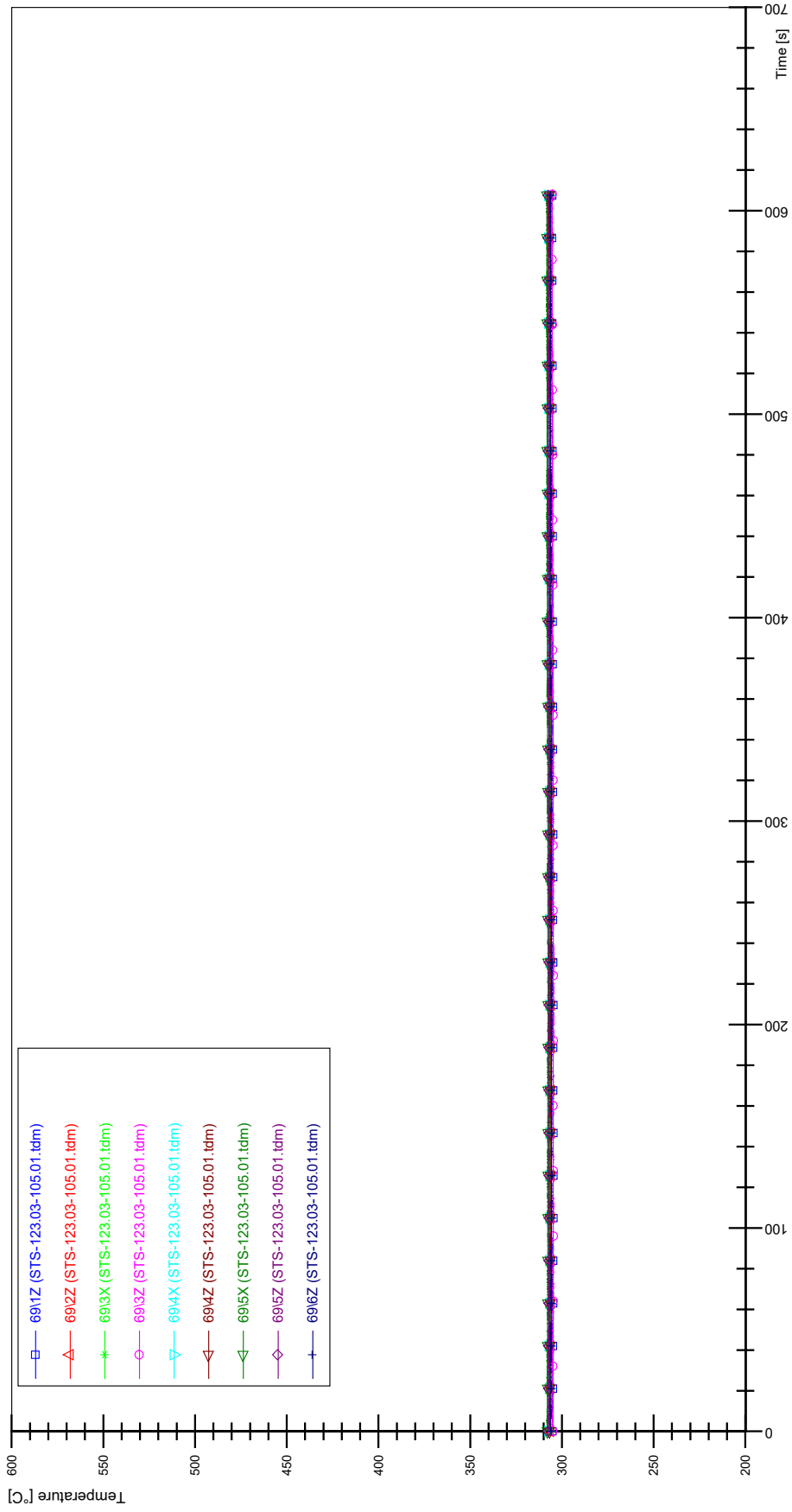
STS-123.03-105.01_CP12_CT19



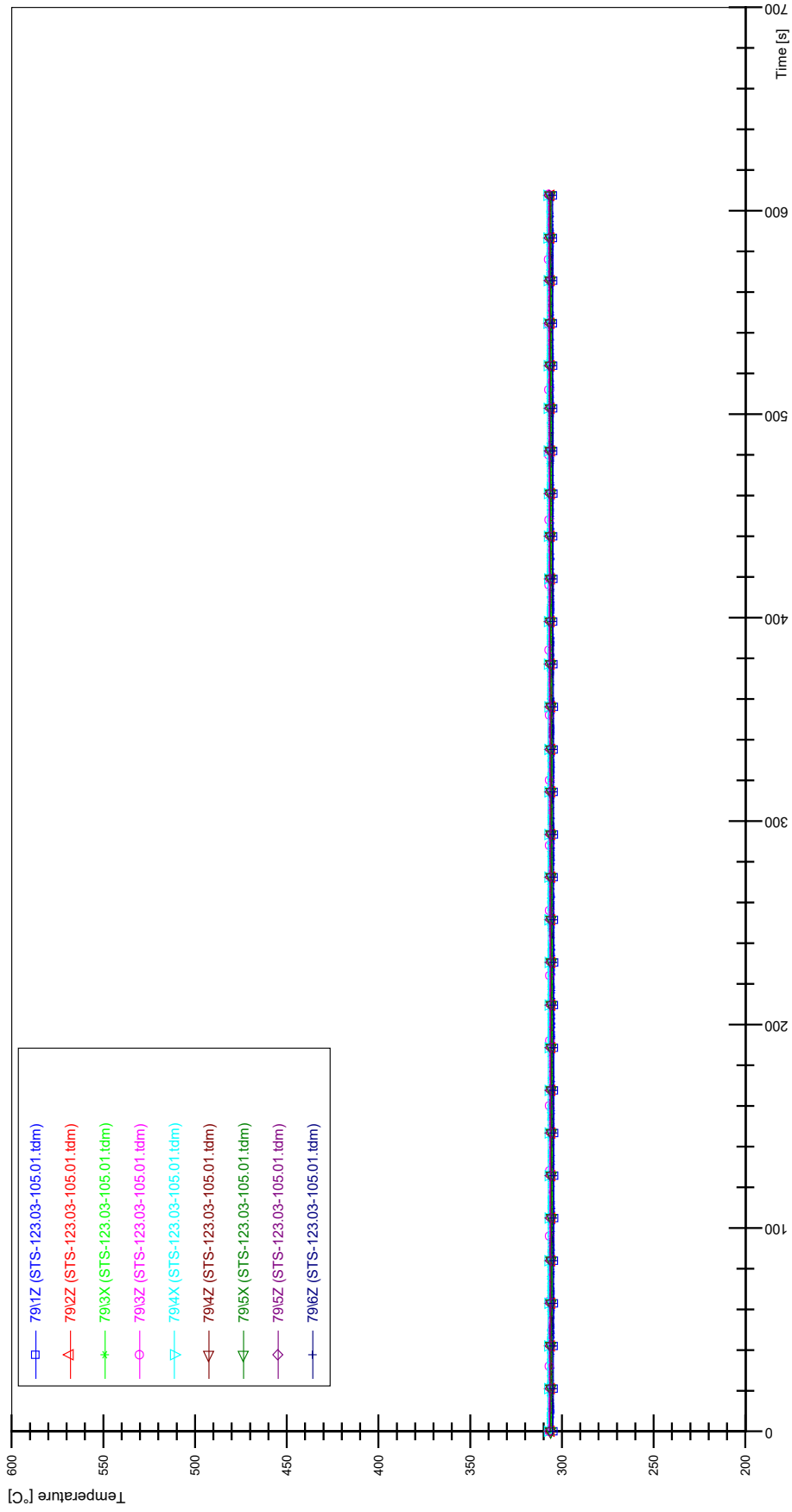
STS-123.03-105.01_Rod_59



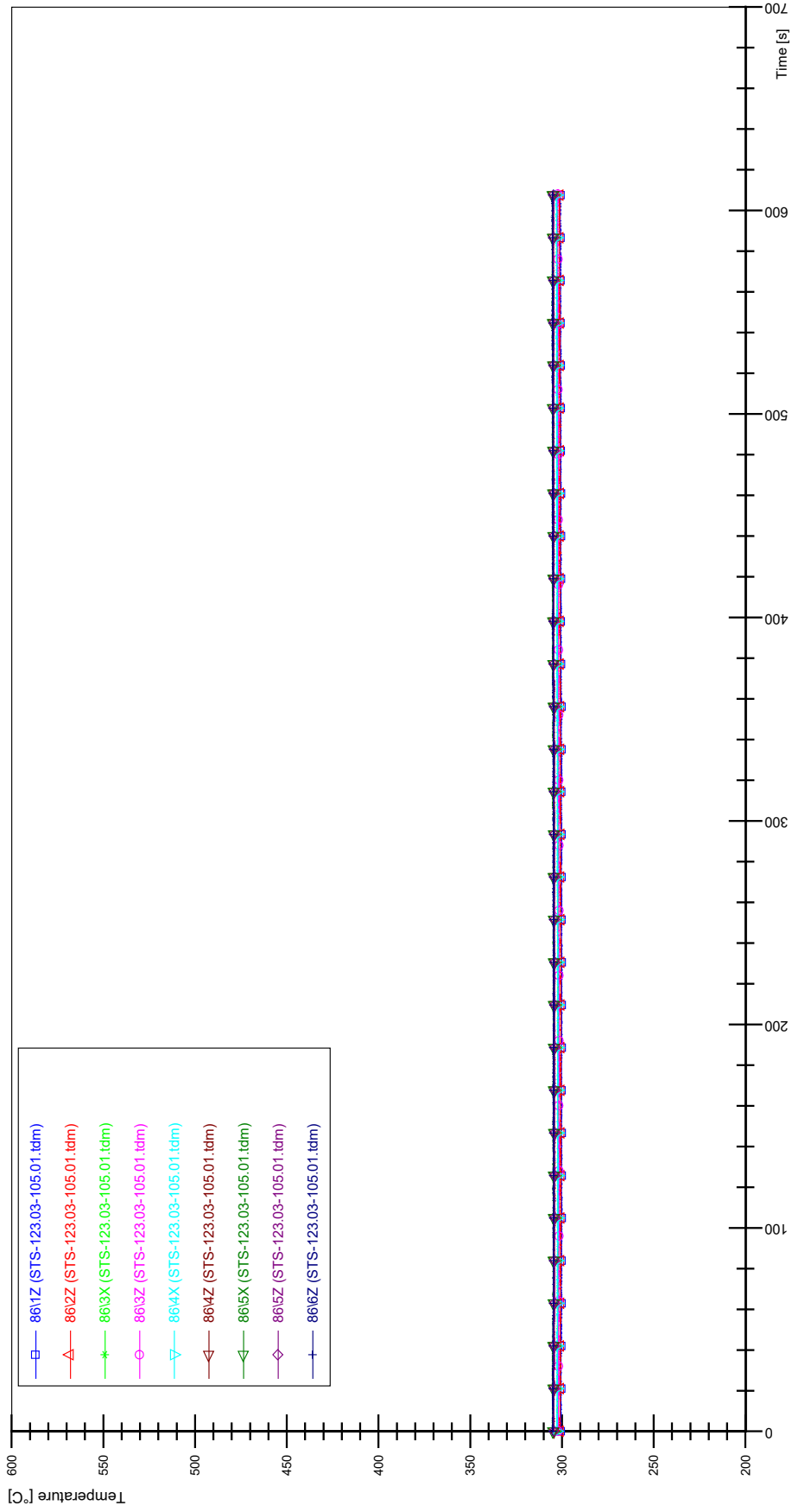
STS-123.03-105.01_Rod_69



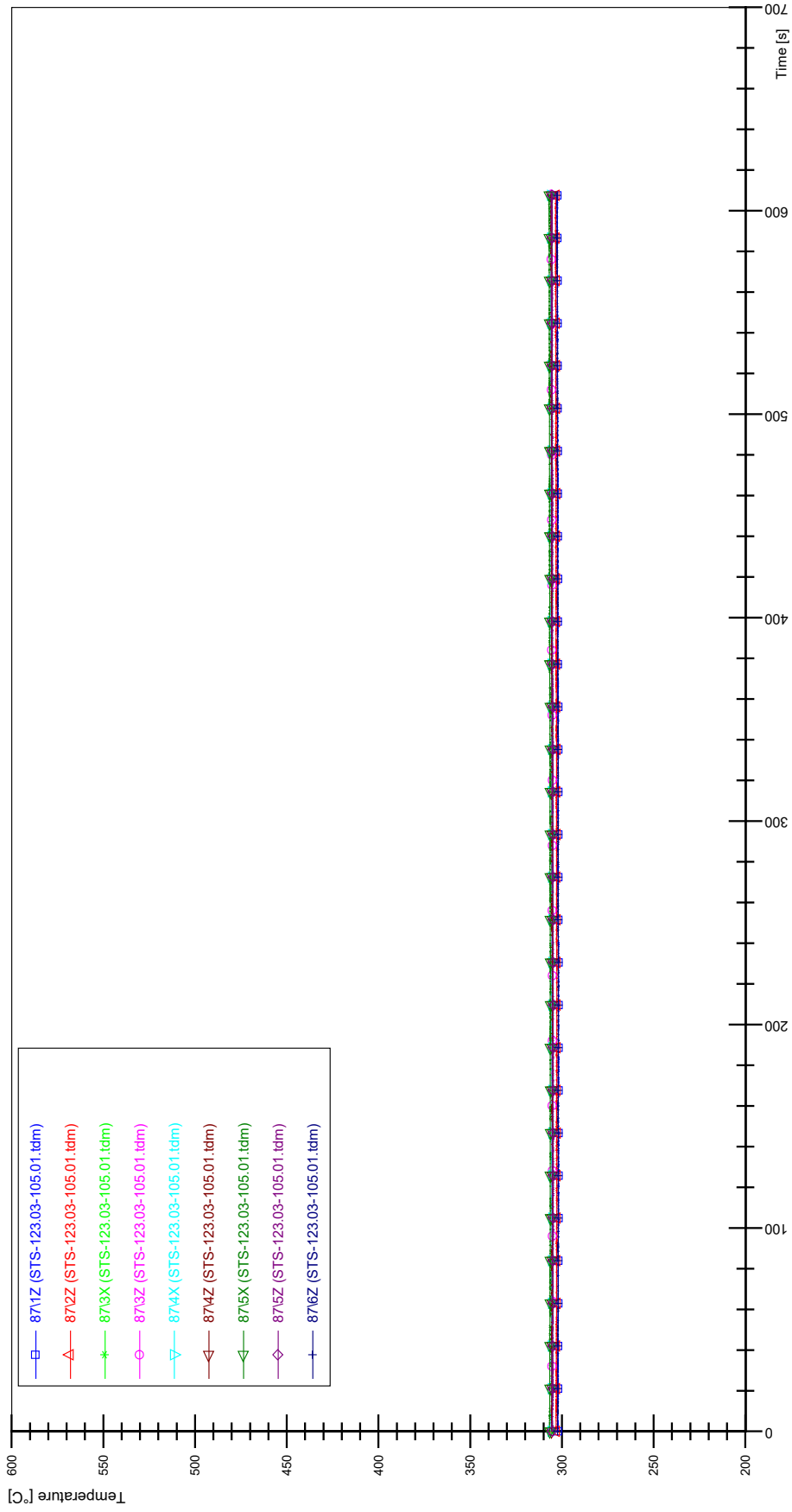
STS-123.03-105.01_Rod_79



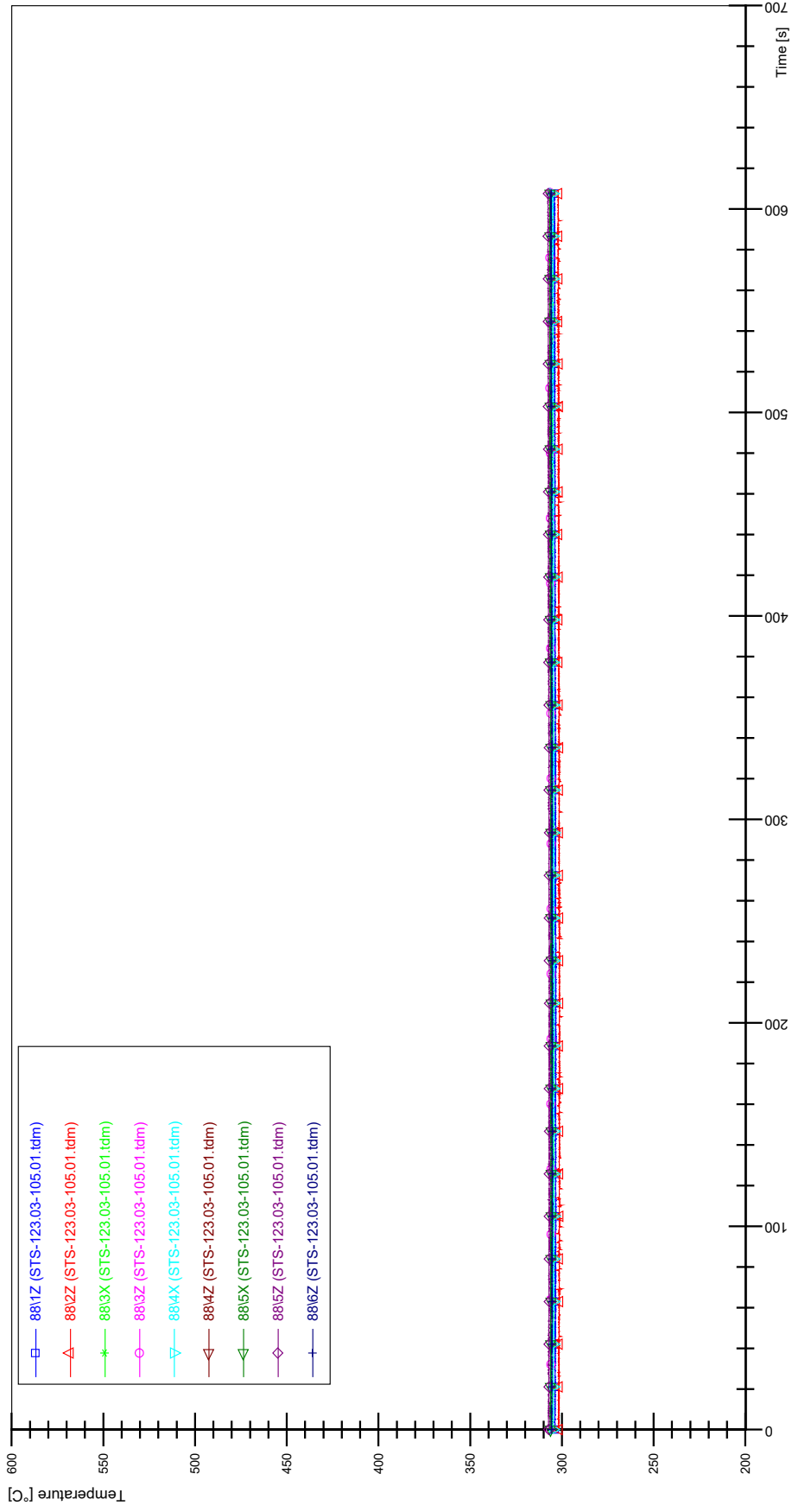
STS-123.03-105.01_Rod_86



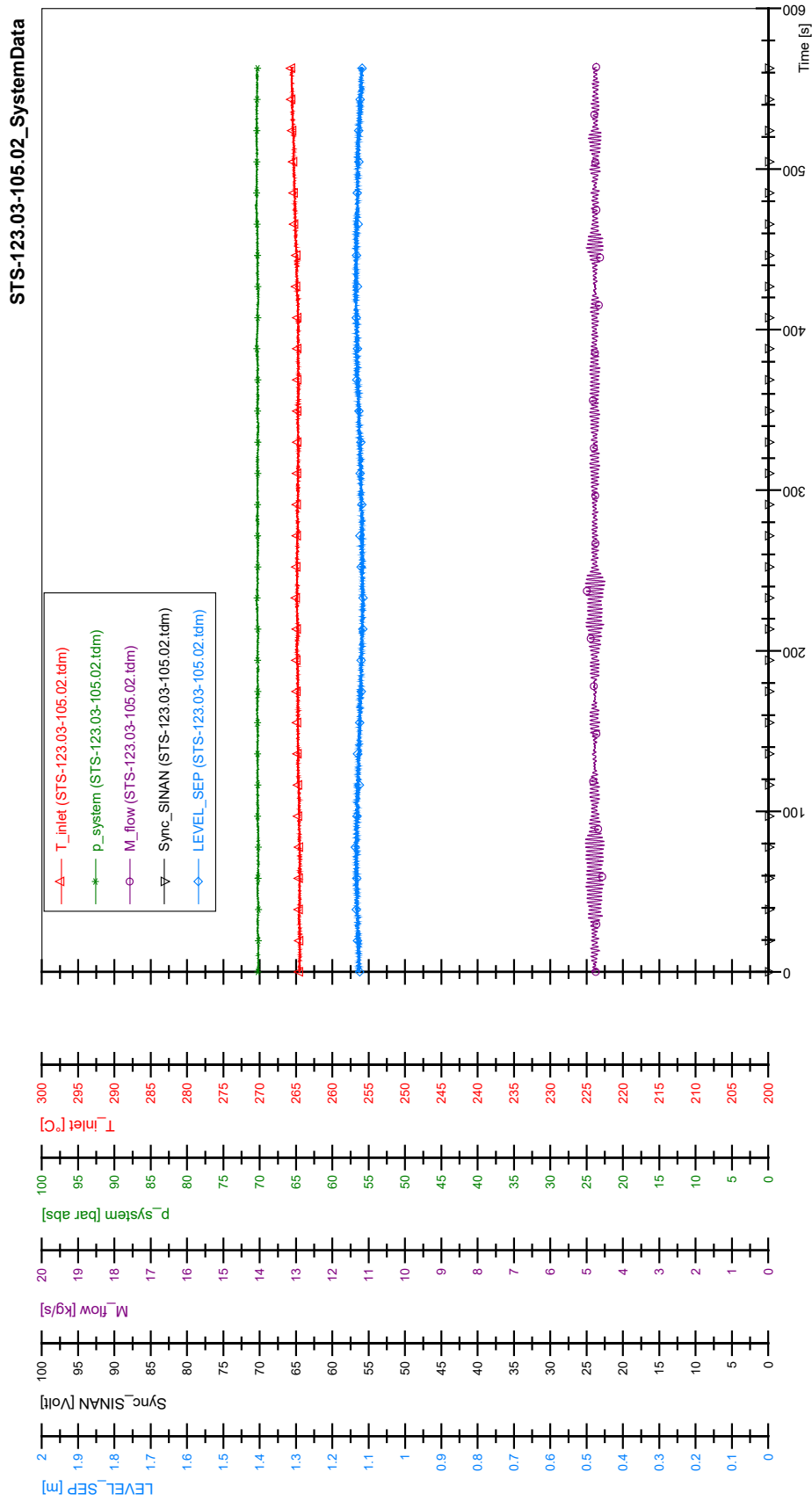
STS-123.03-105.01_Rod_87

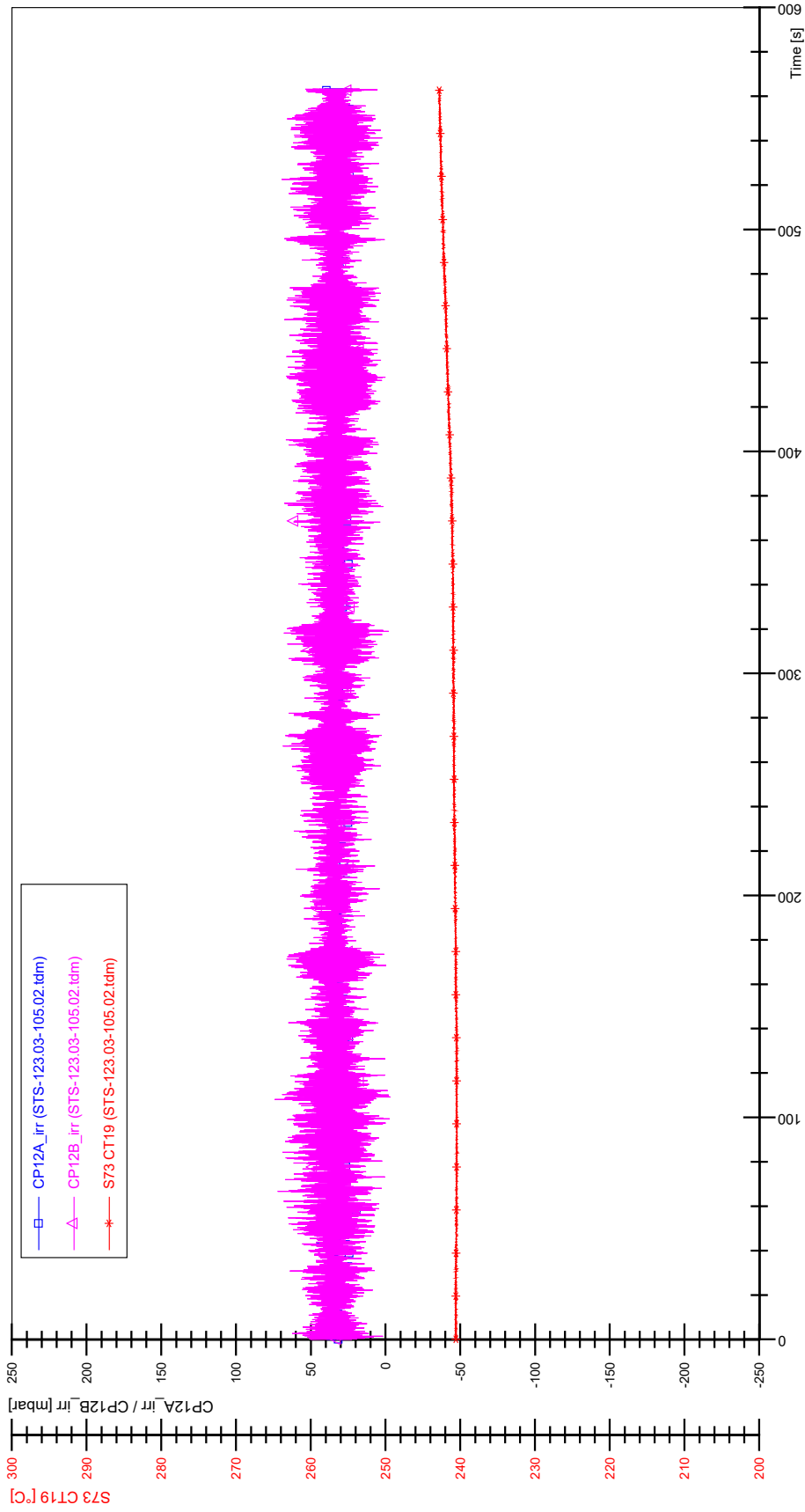


STS-123.03-105.01_Rod_88

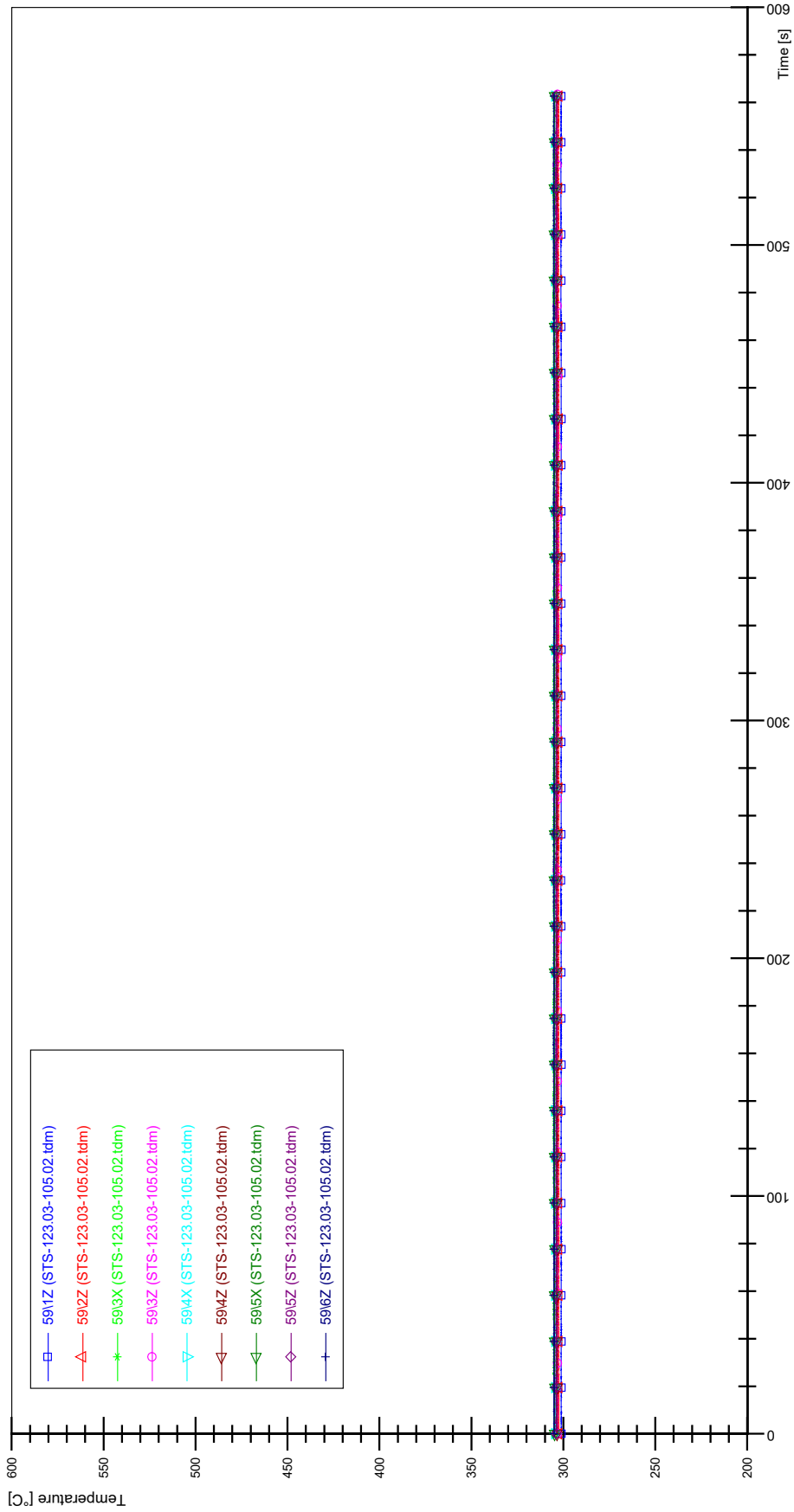


APPENDIX K PLOTS OF INSTABILITY TEST STS-123.03-105.02

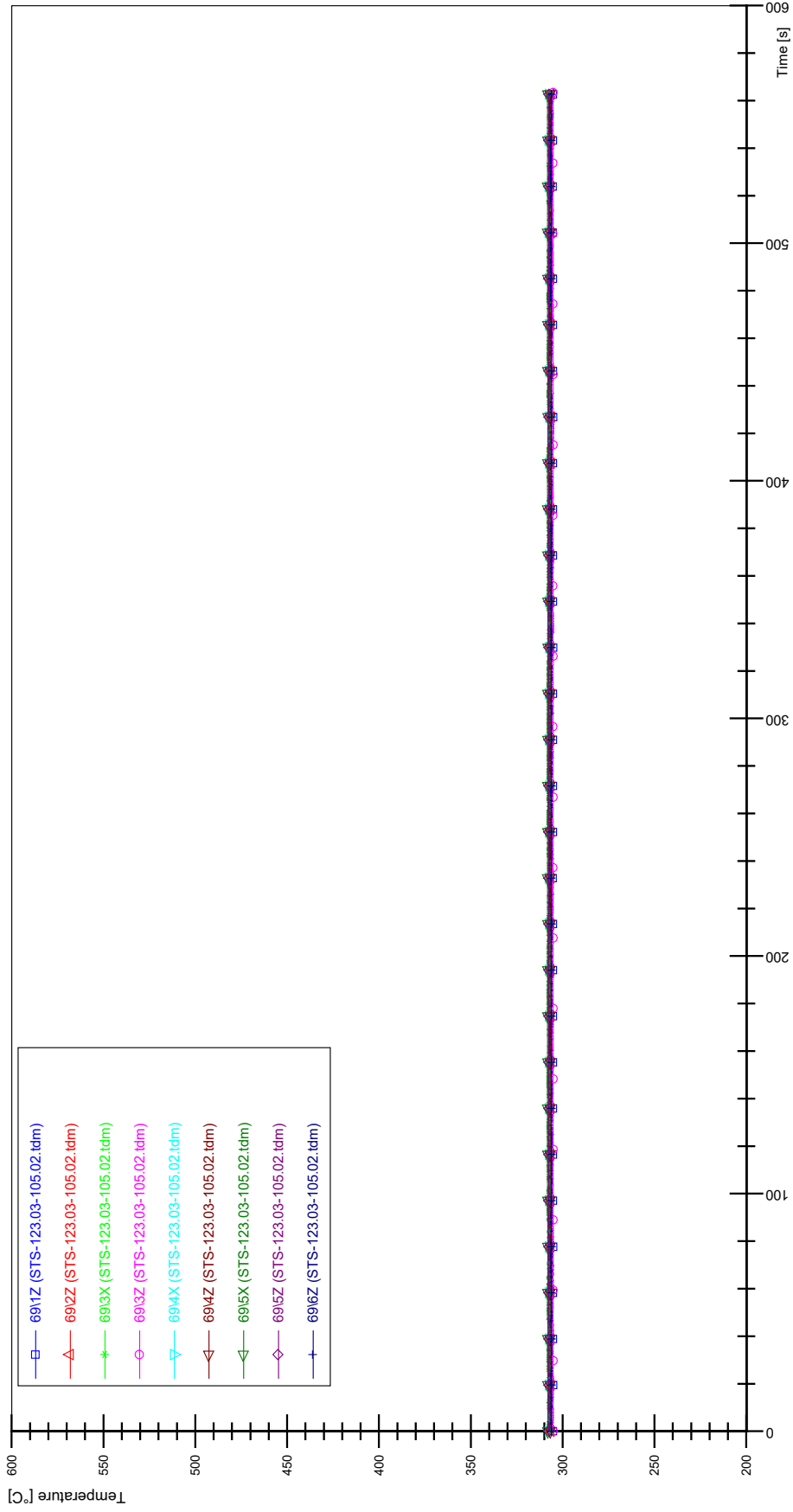




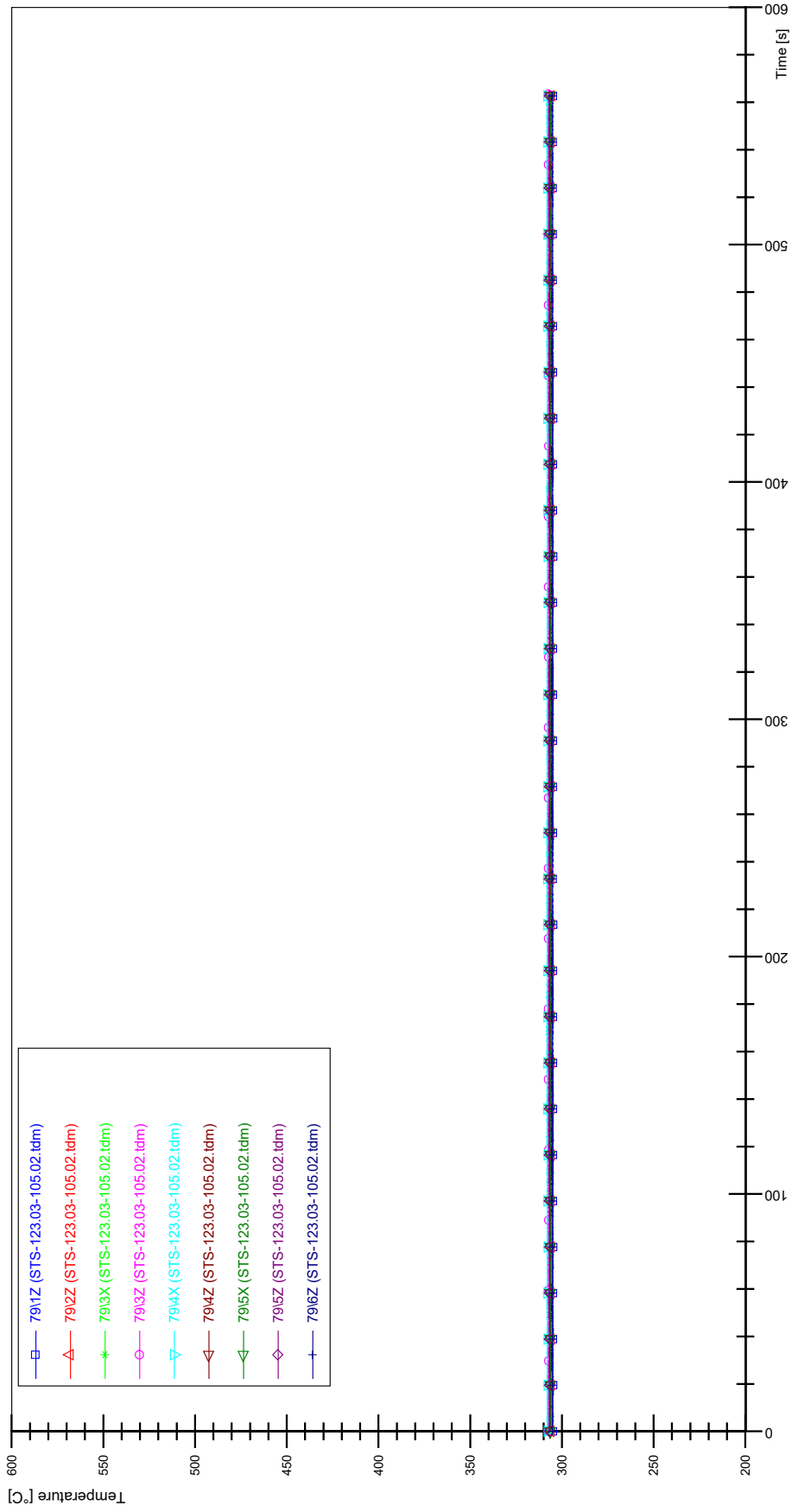
STS-123.03-105.02_Rod_59



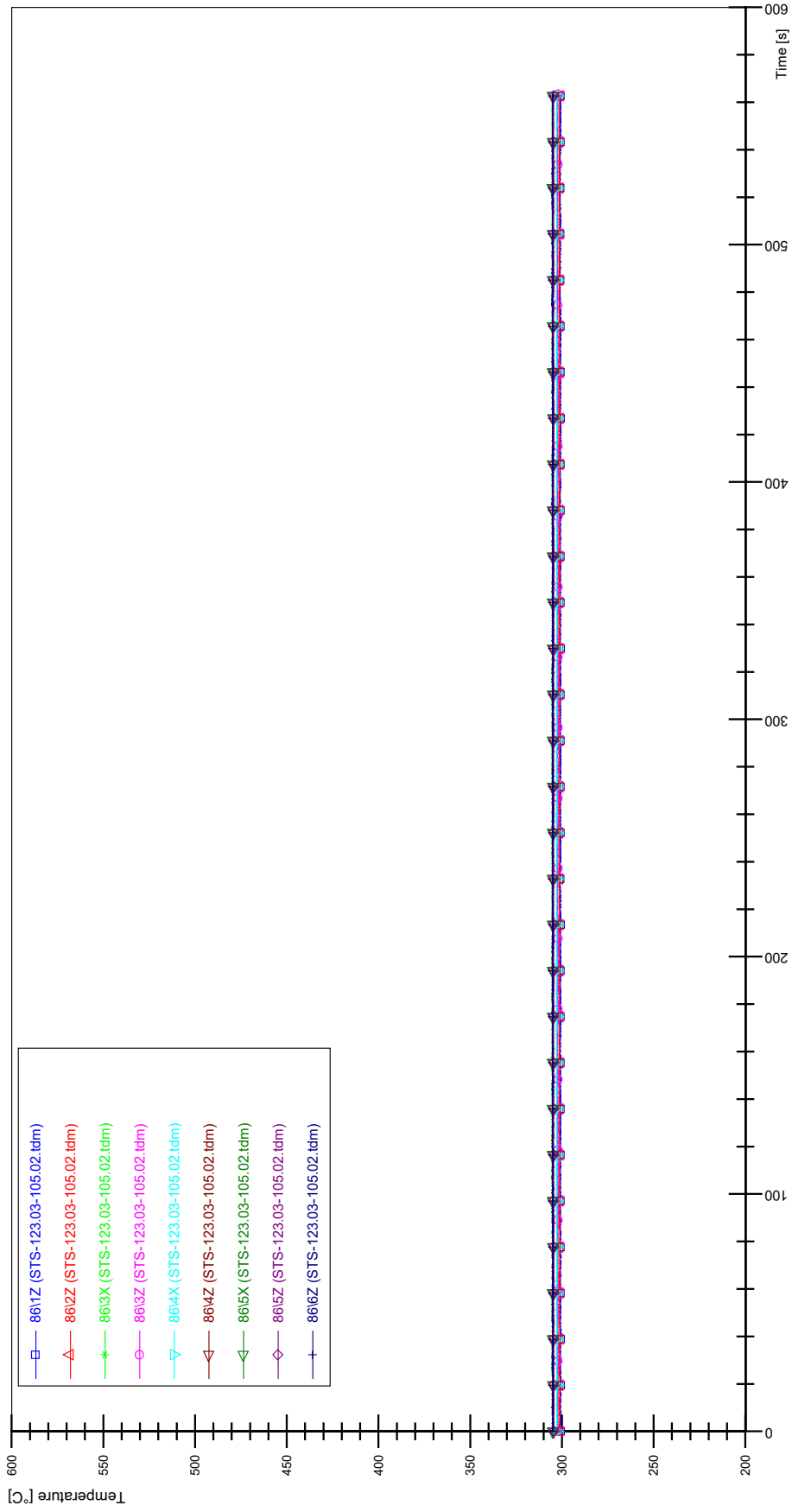
STS-123.03-105.02_Rod_69



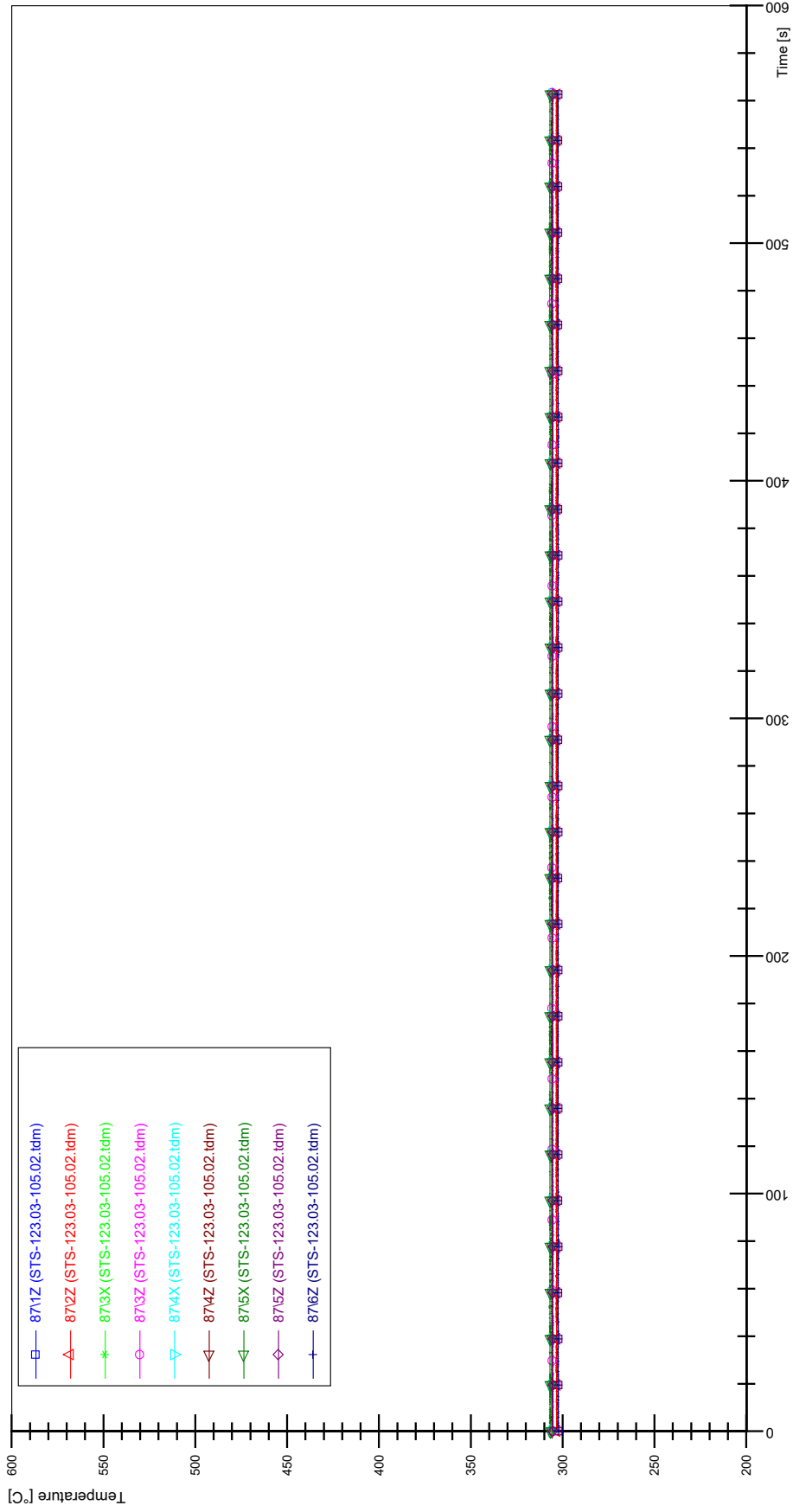
STS-123.03-105.02_Rod_79



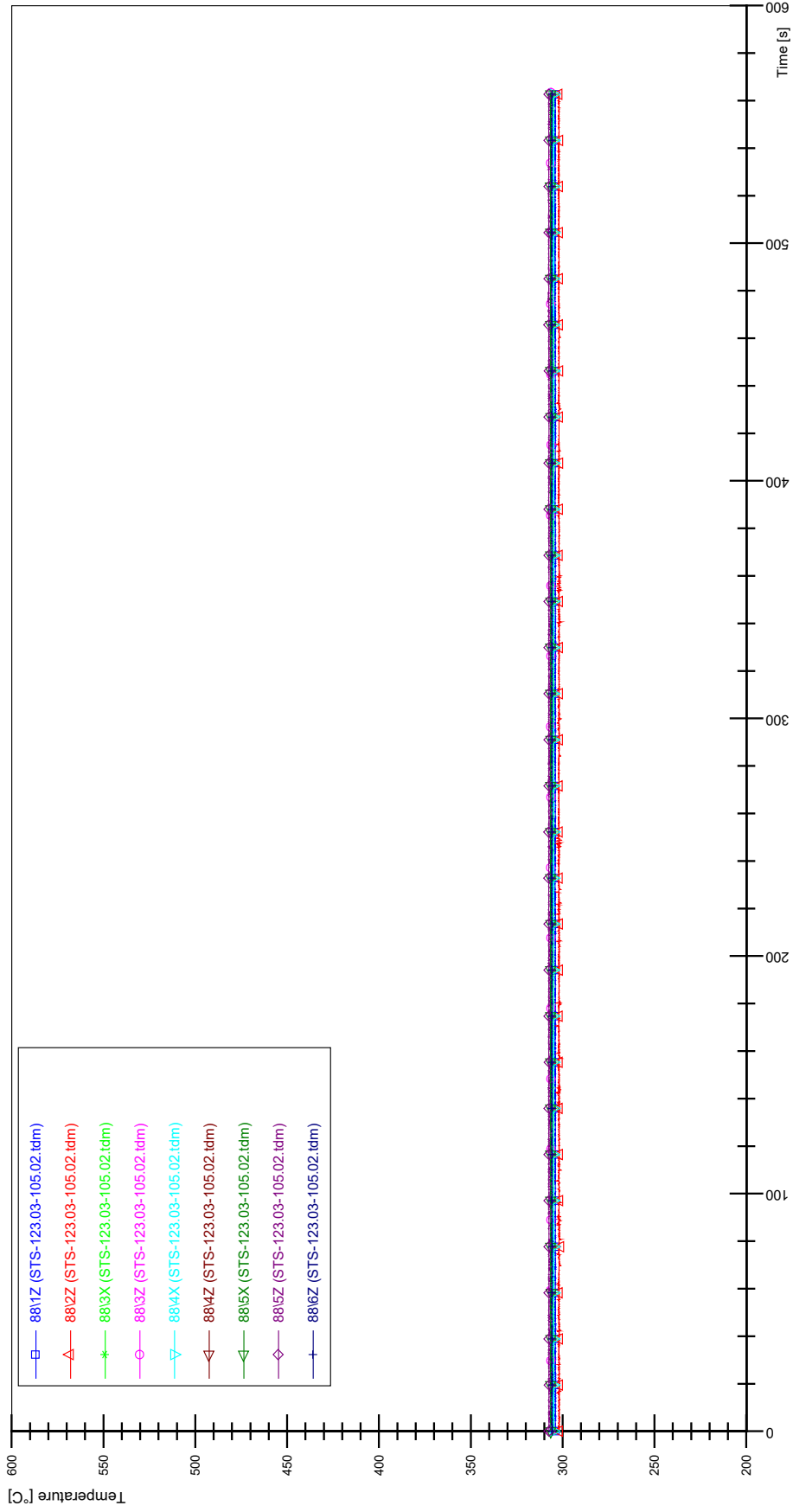
STS-123.03-105.02_Rod_86



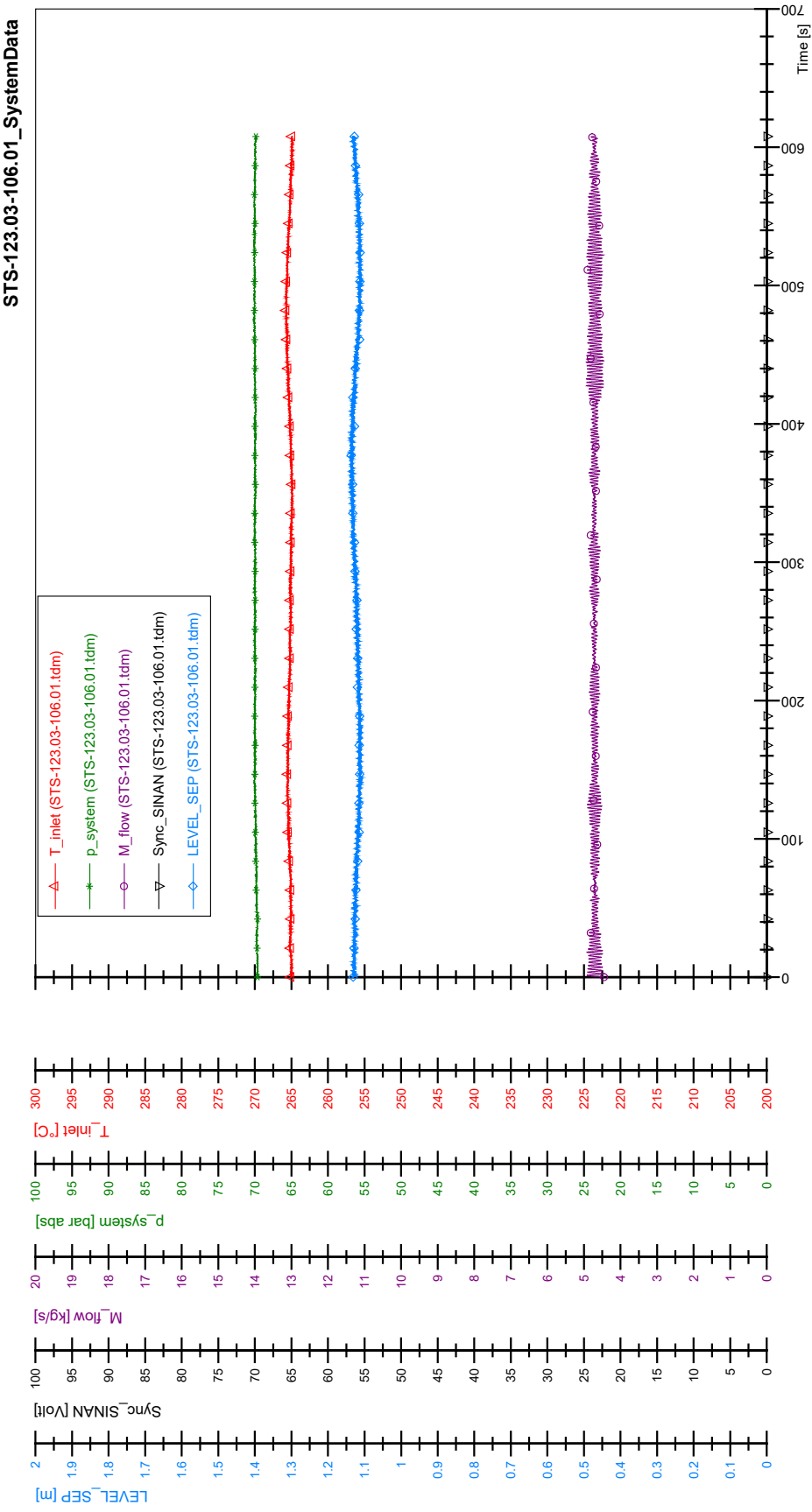
STS-123.03-105.02_Rod_87

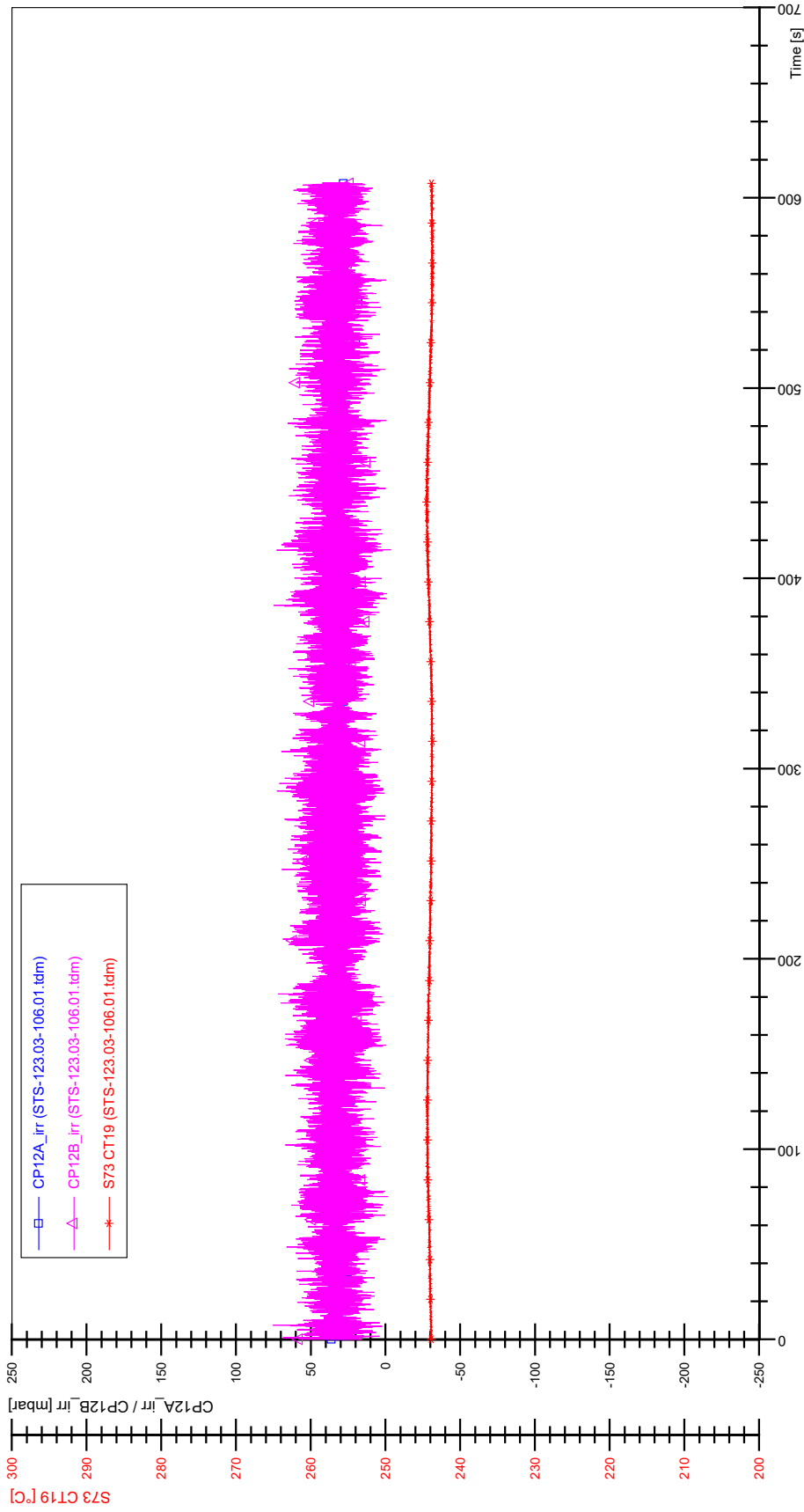


STS-123.03-105.02_Rod_88

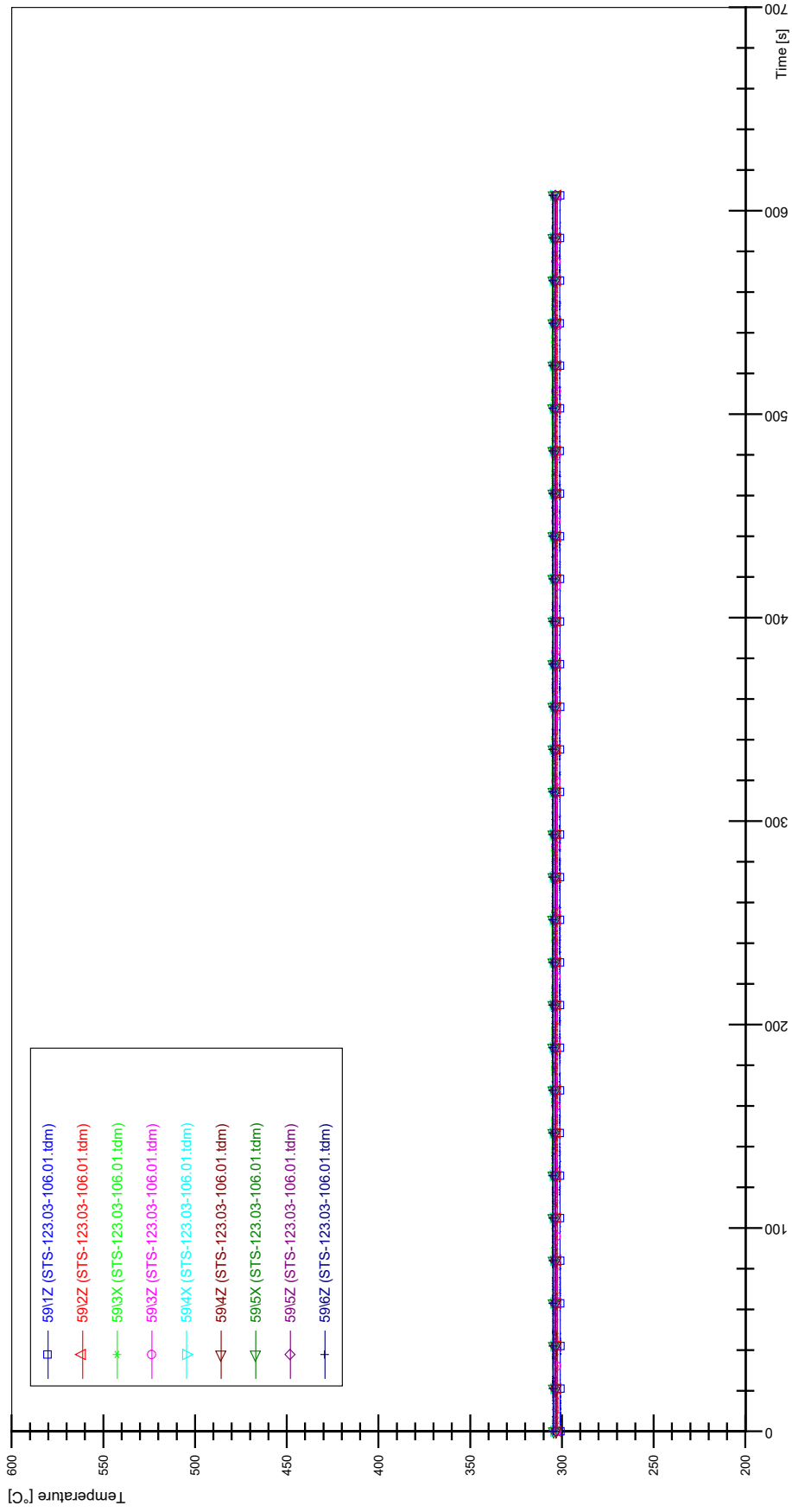


APPENDIX L PLOTS OF INSTABILITY TEST STS-123.03-106.01

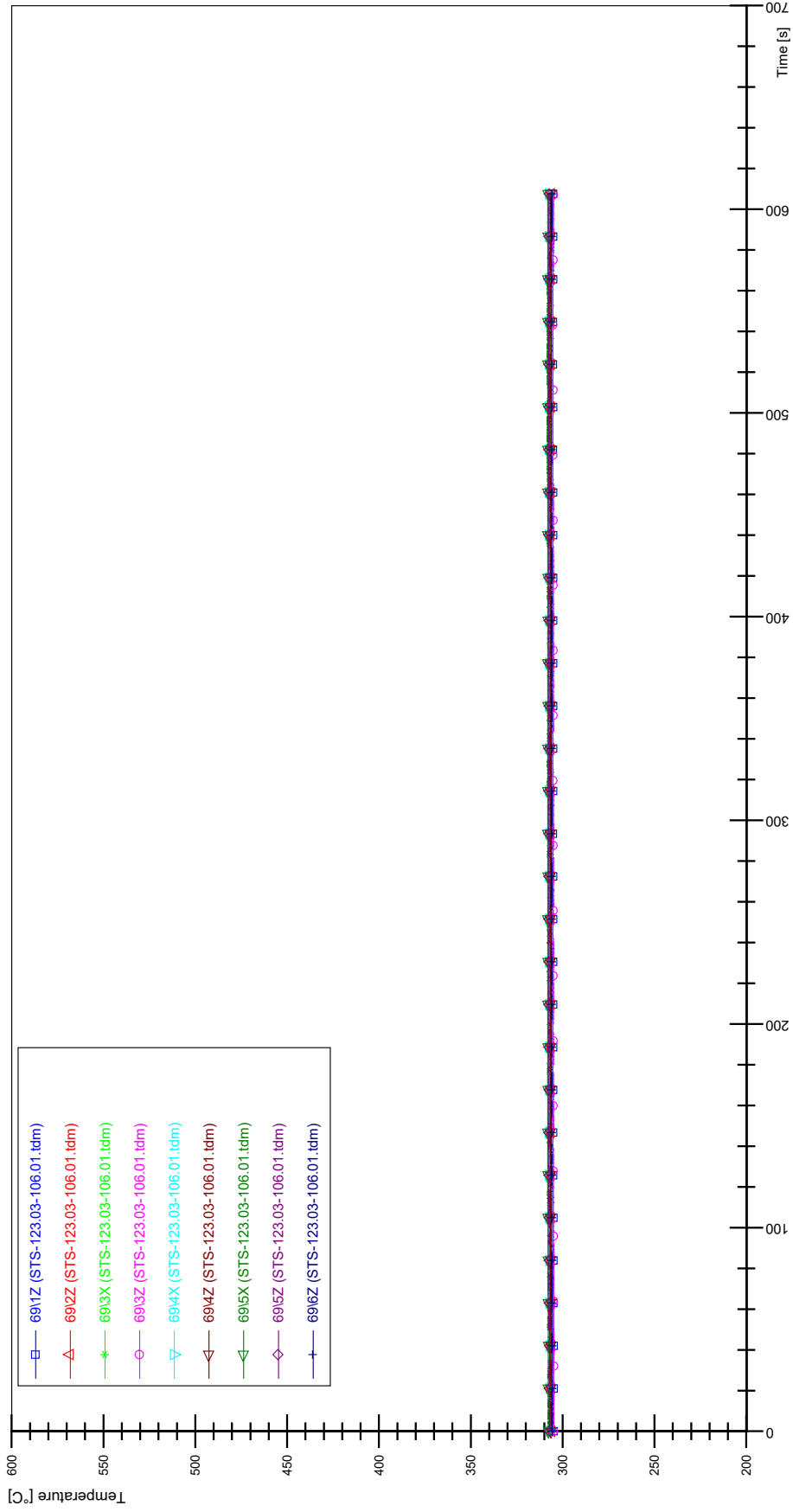




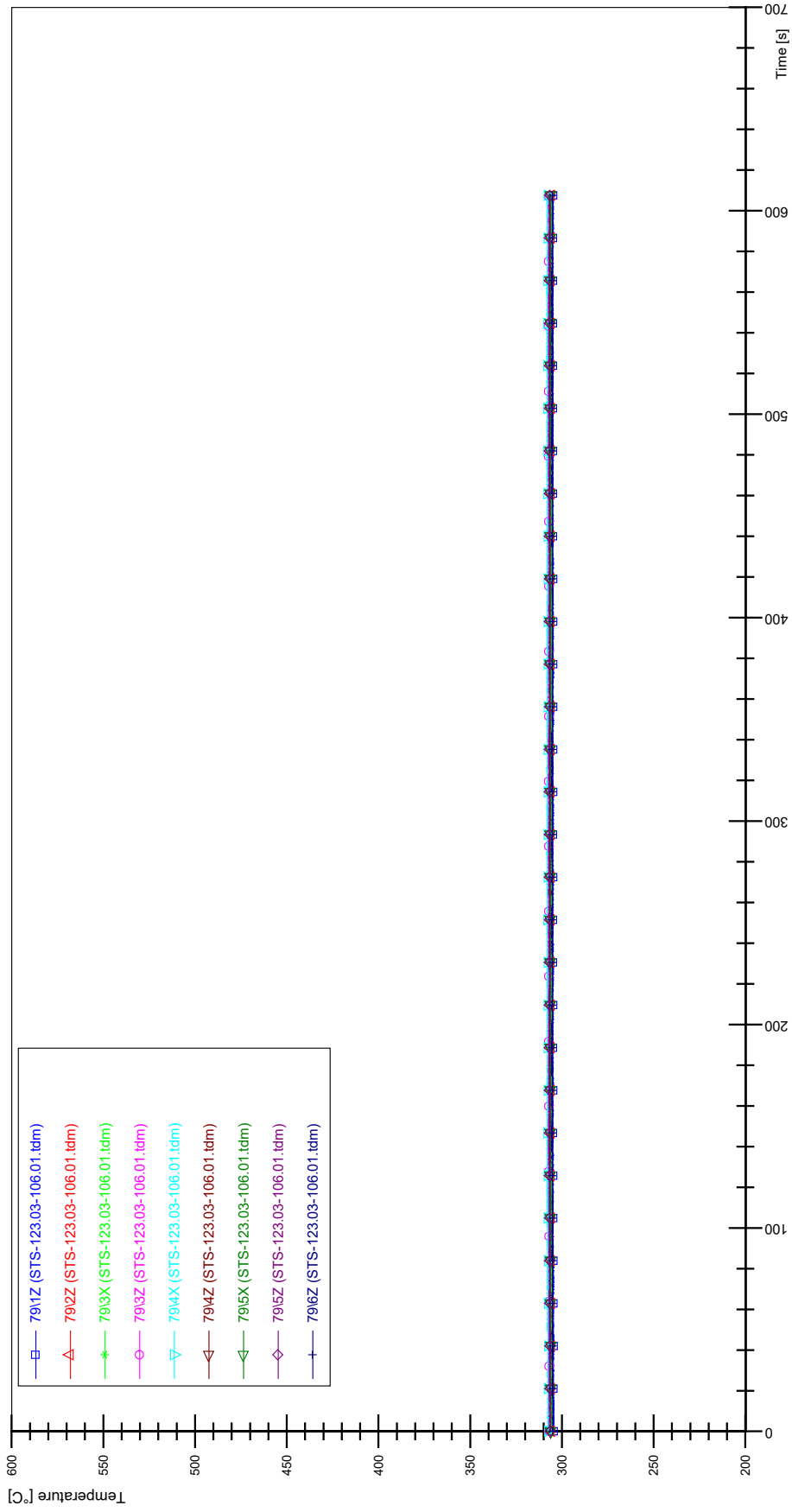
STS-123.03-106.01_Rod_59



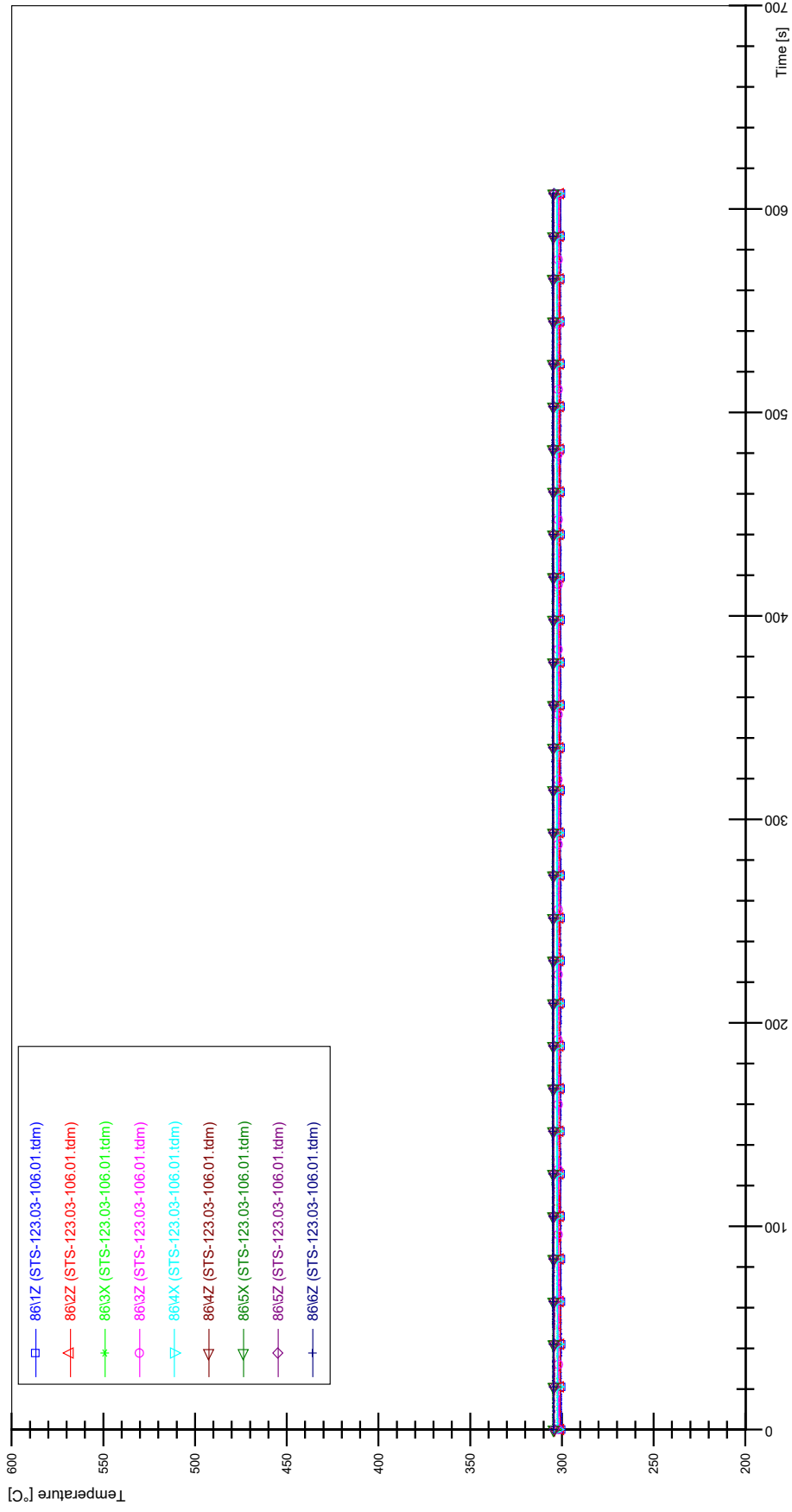
STS-123.03-106.01_Rod_69



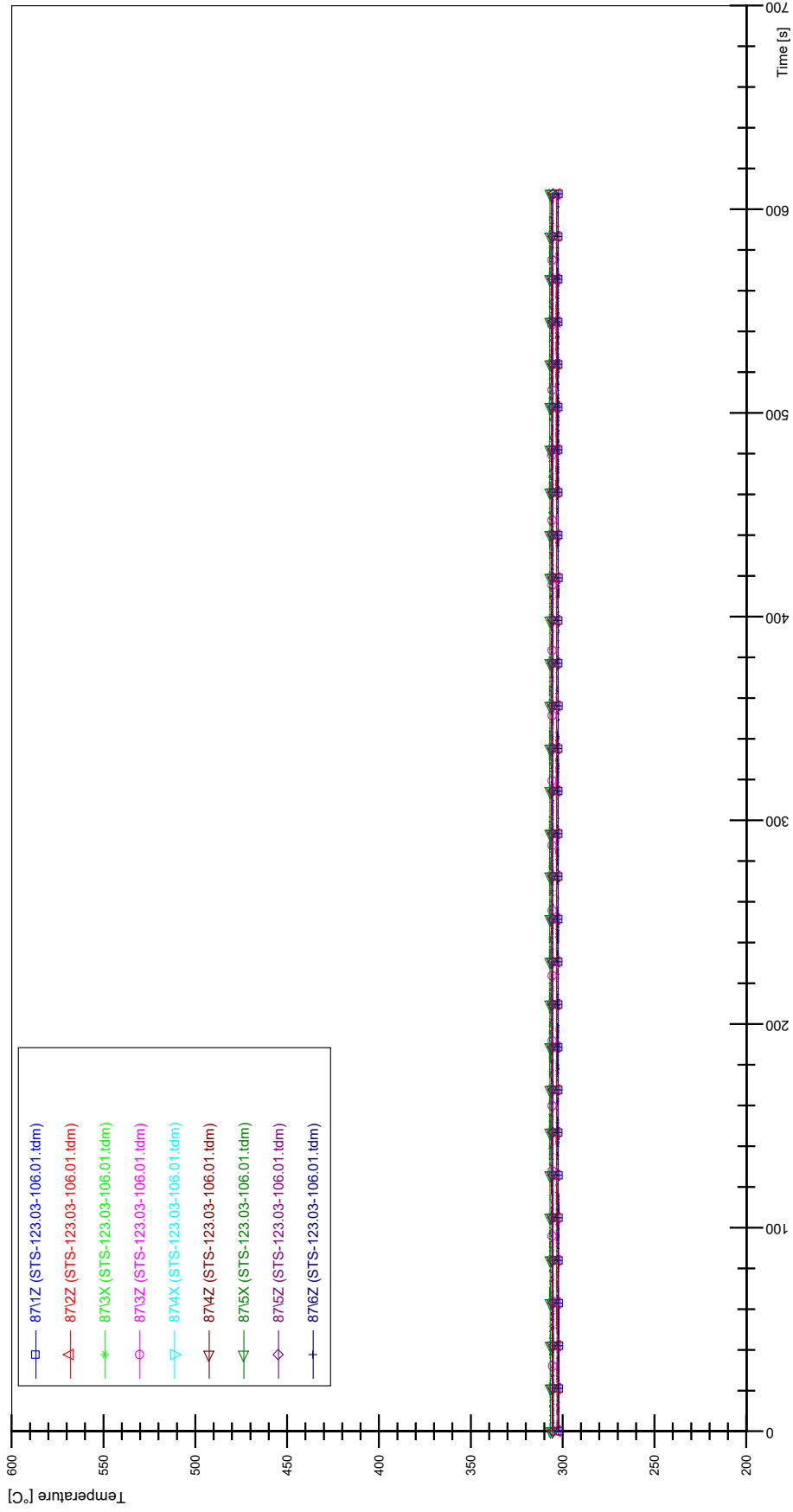
STS-123.03-106.01_Rod_79



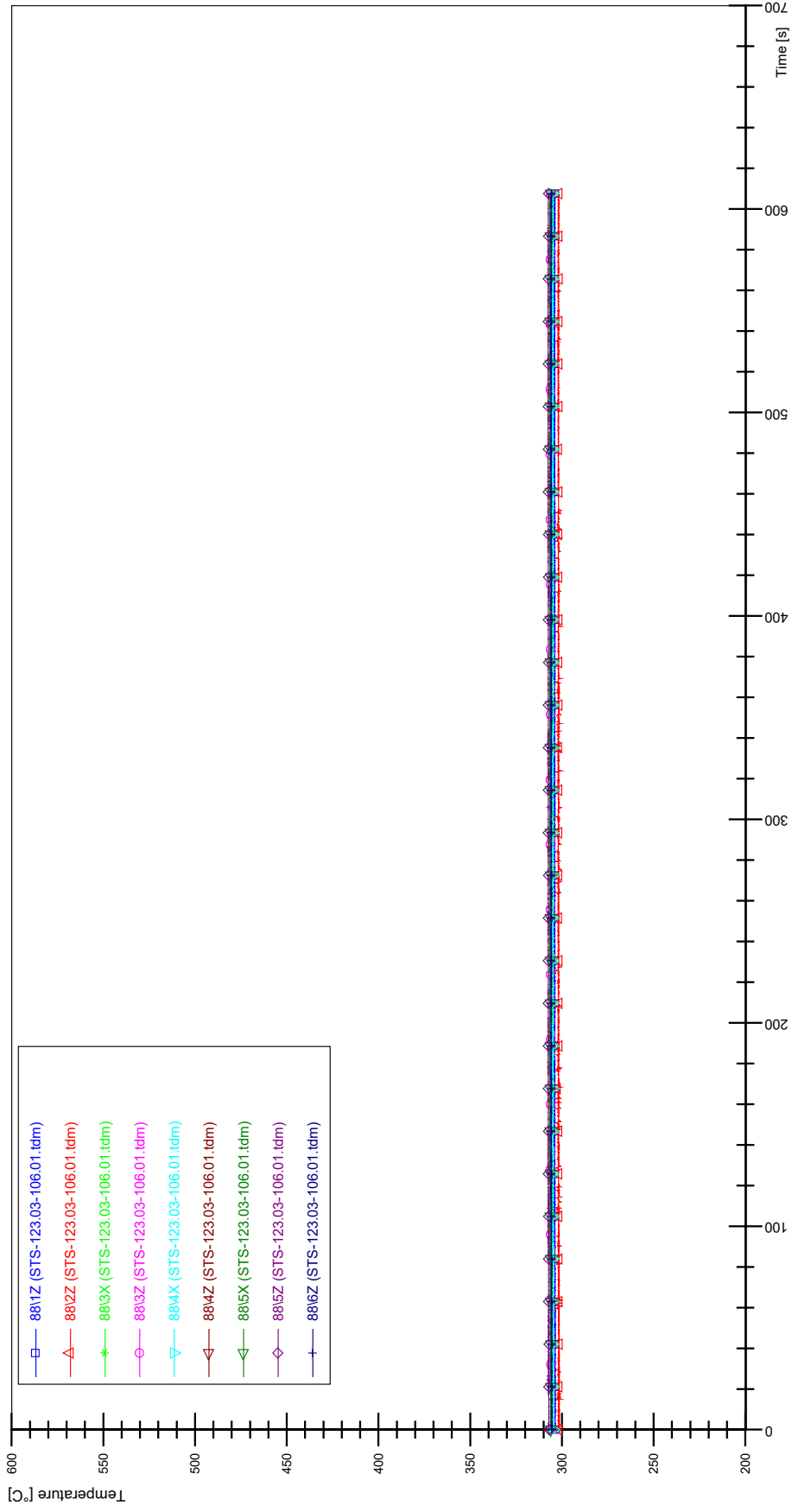
STS-123.03-106.01_Rod_86



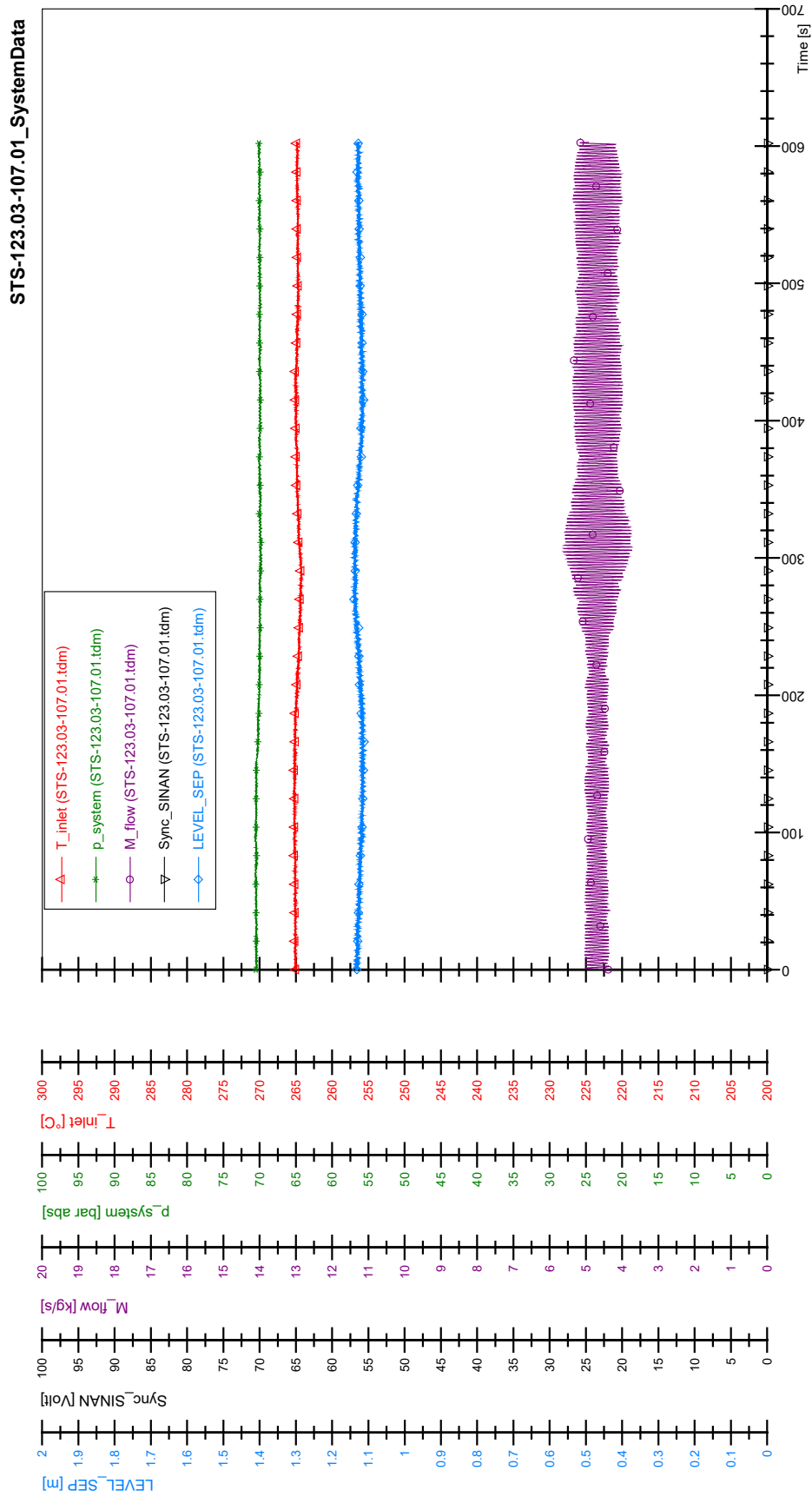
STS-123.03-106.01_Rod_87

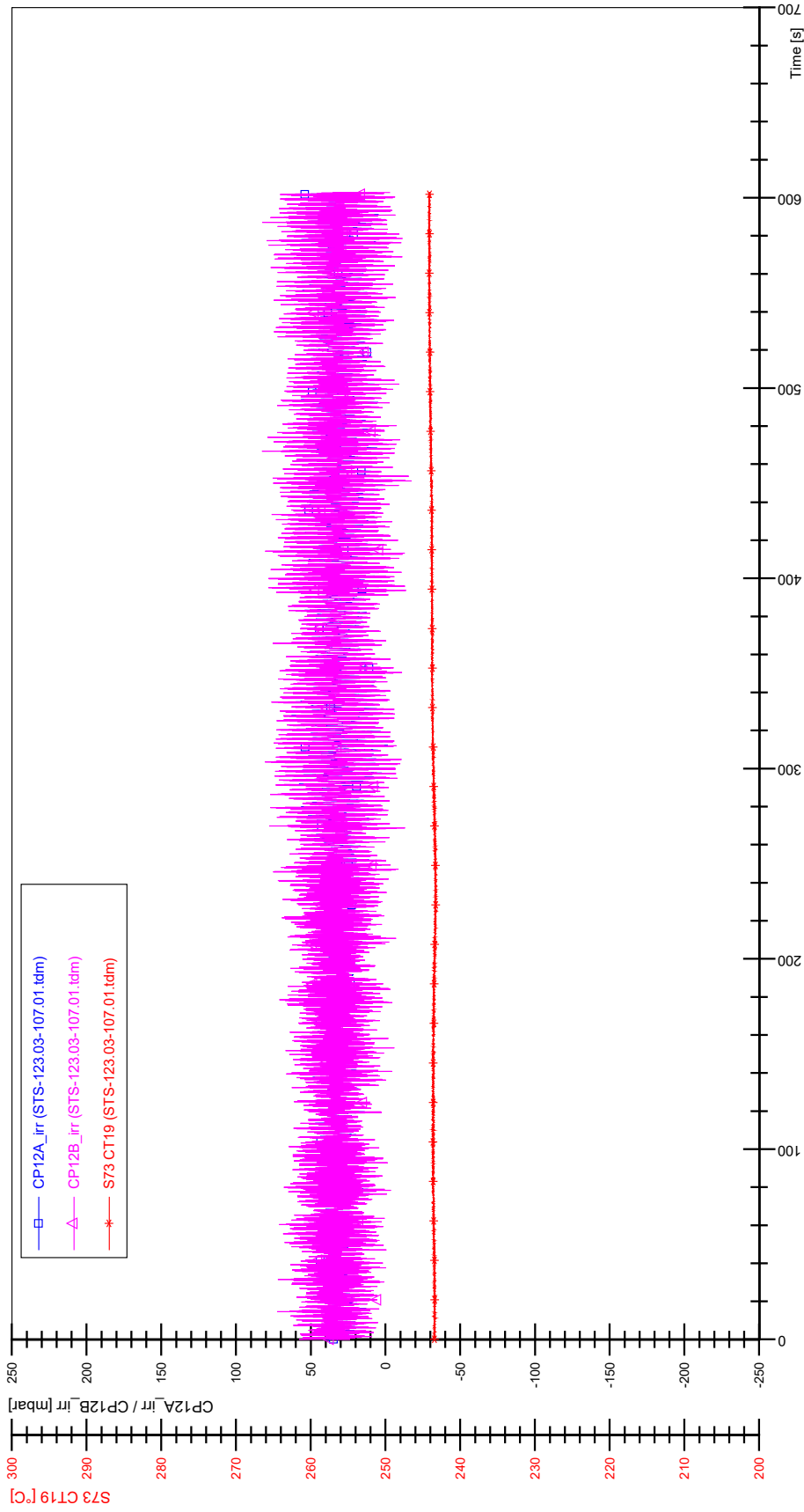


STS-123.03-106.01_Rod_88

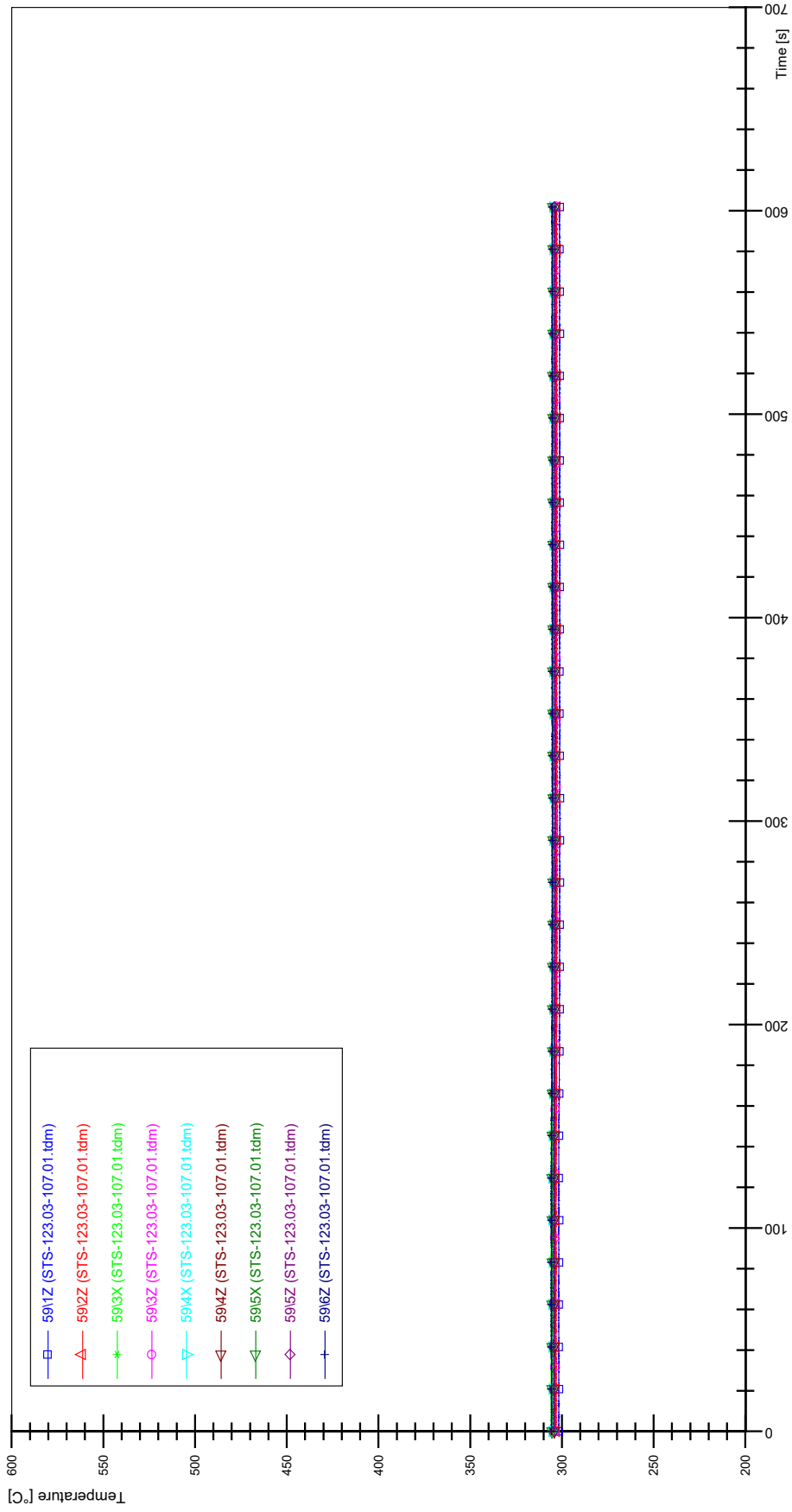


APPENDIX M PLOTS OF INSTABILITY TEST STS-123.03-107.01

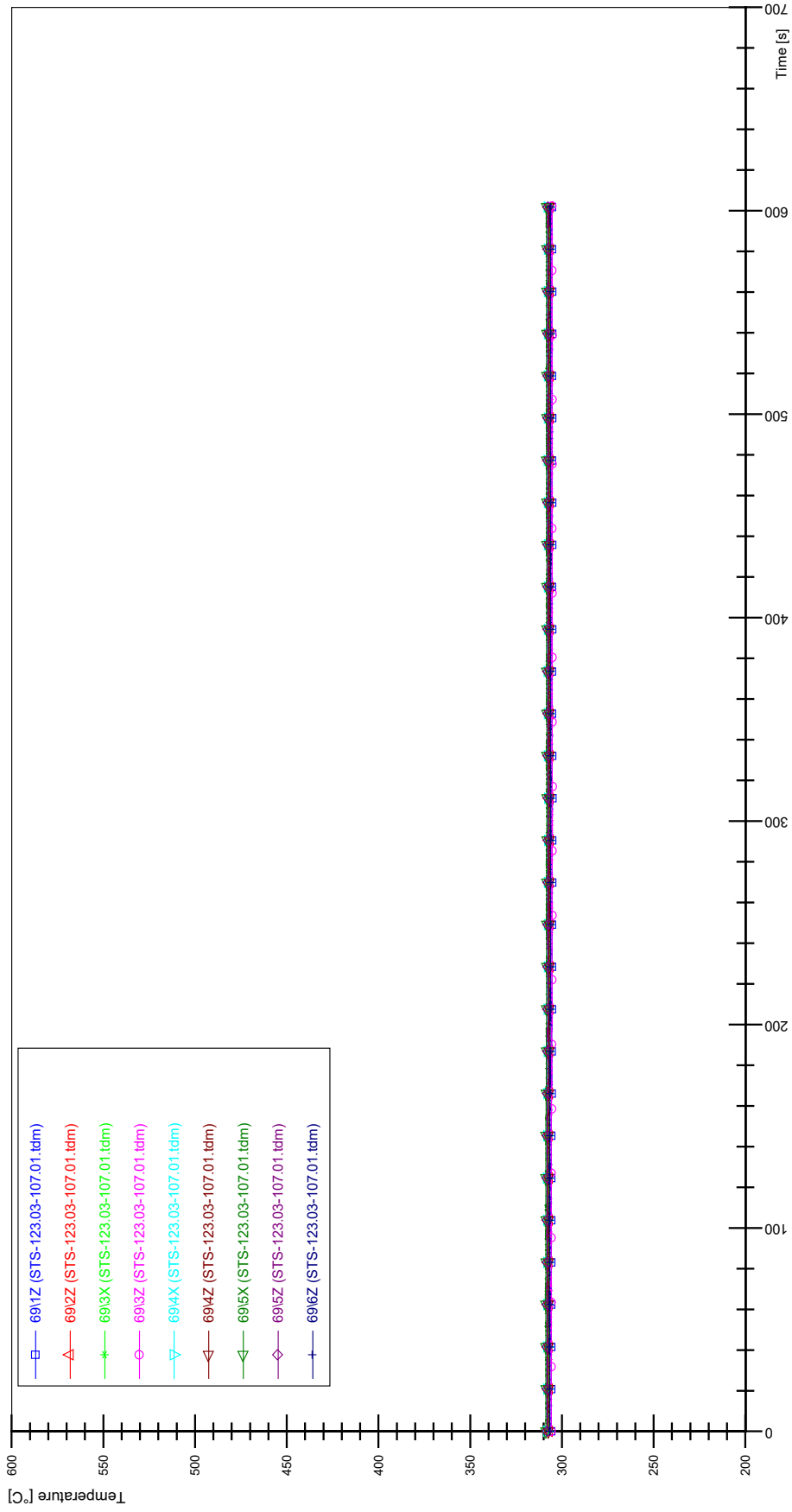




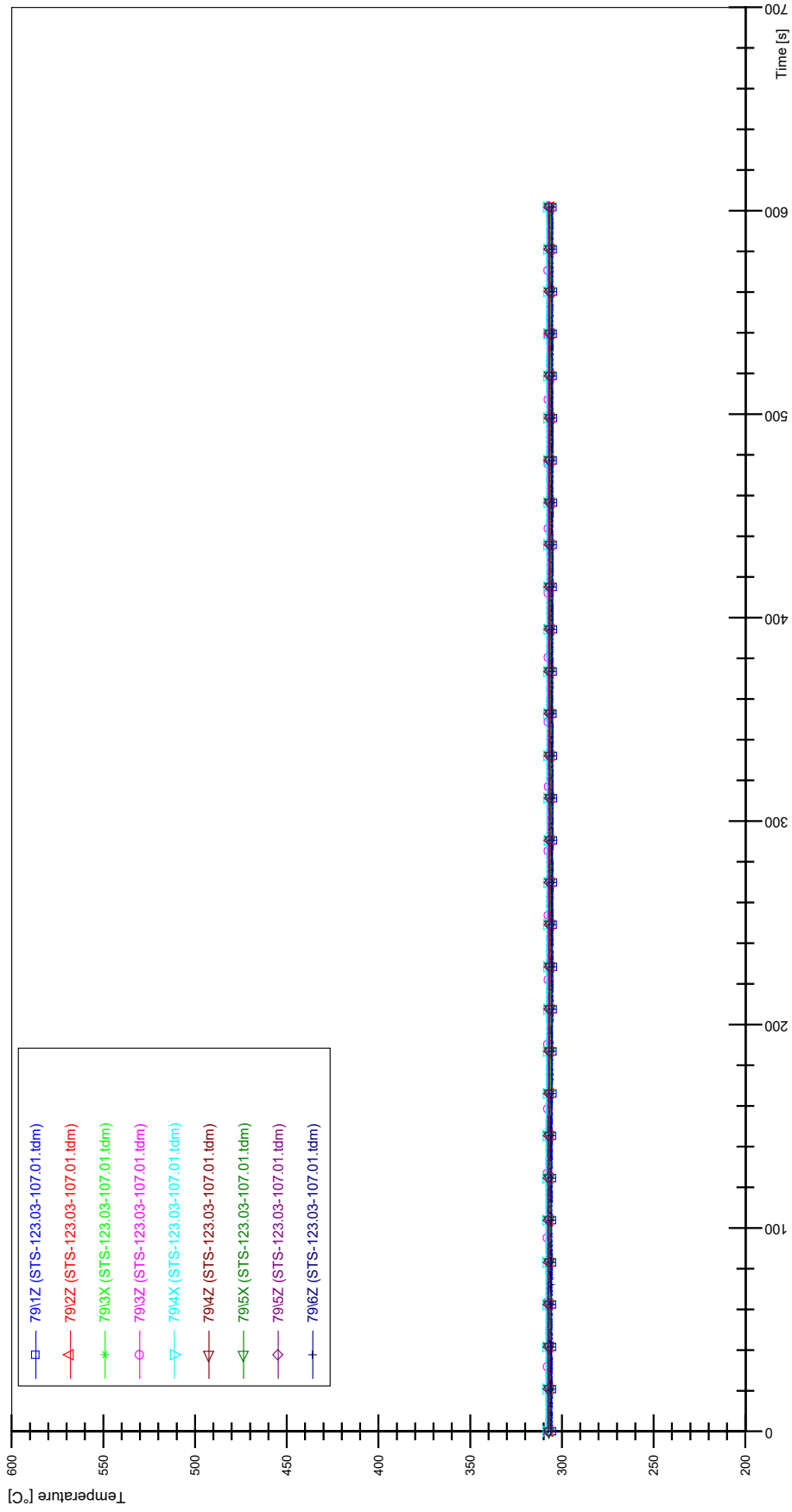
STS-123.03-107.01_Rod_59



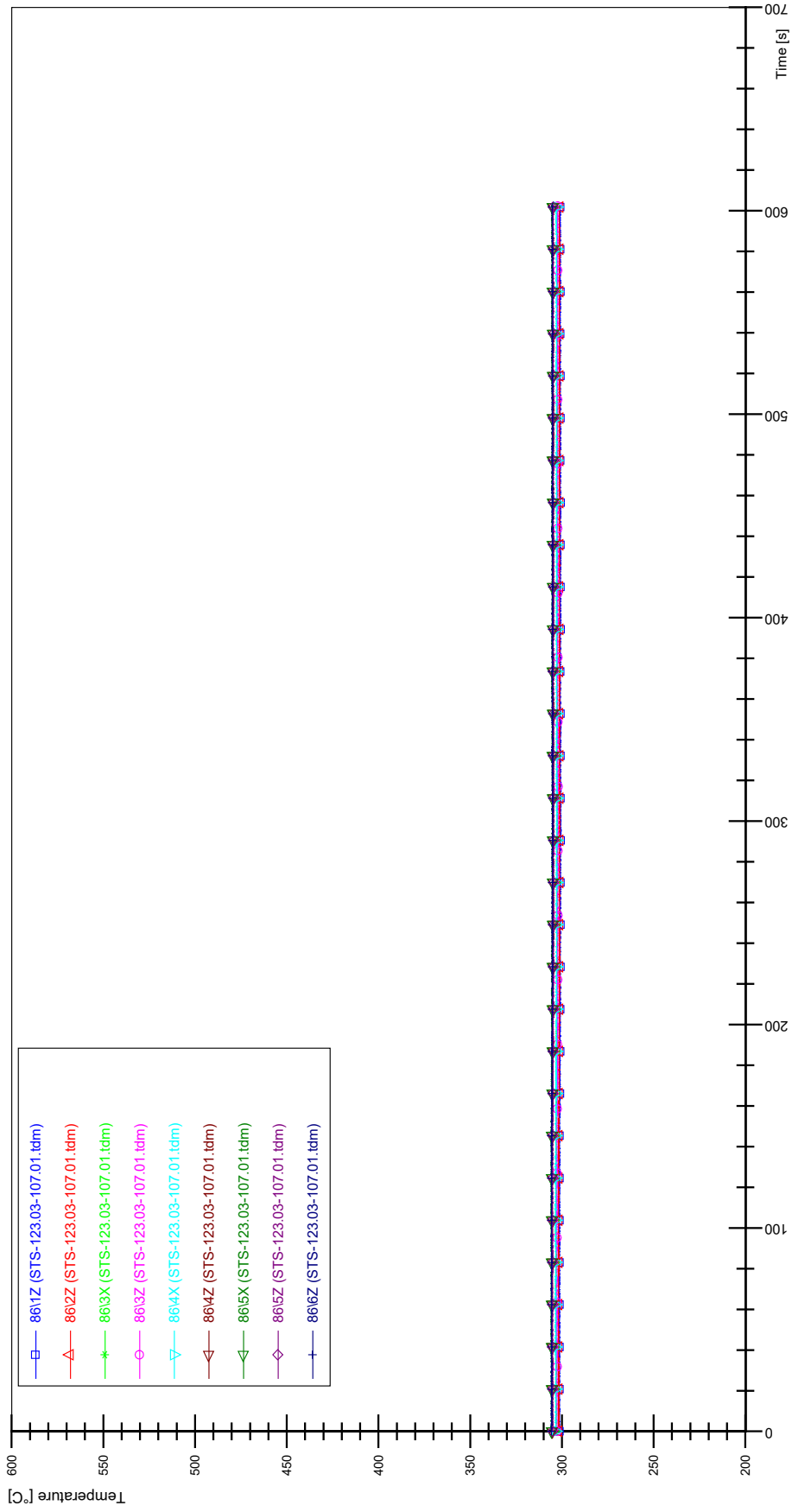
STS-123.03-107.01_Rod_69



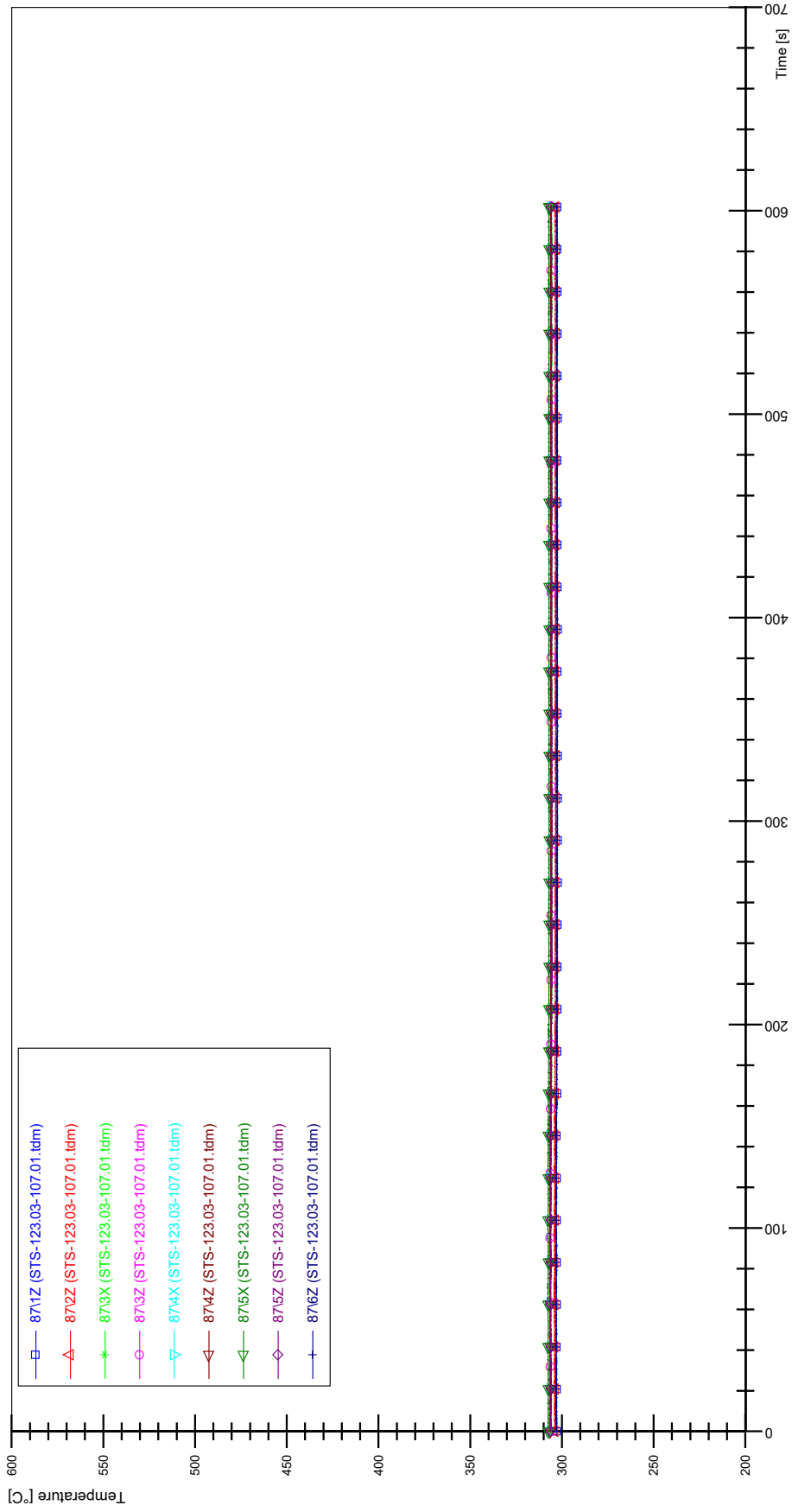
STS-123.03-107.01_Rod_79



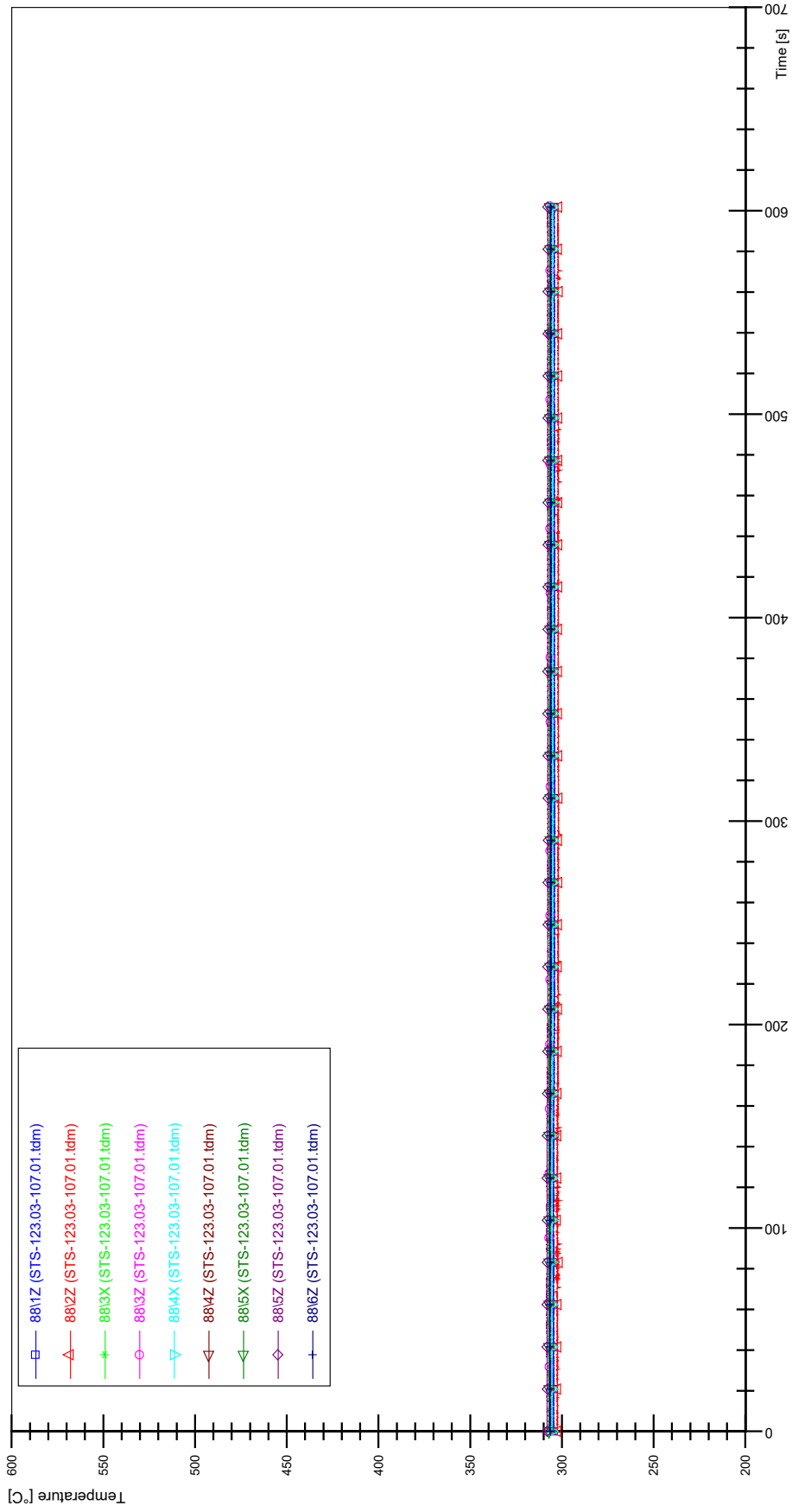
STS-123.03-107.01_Rod_86



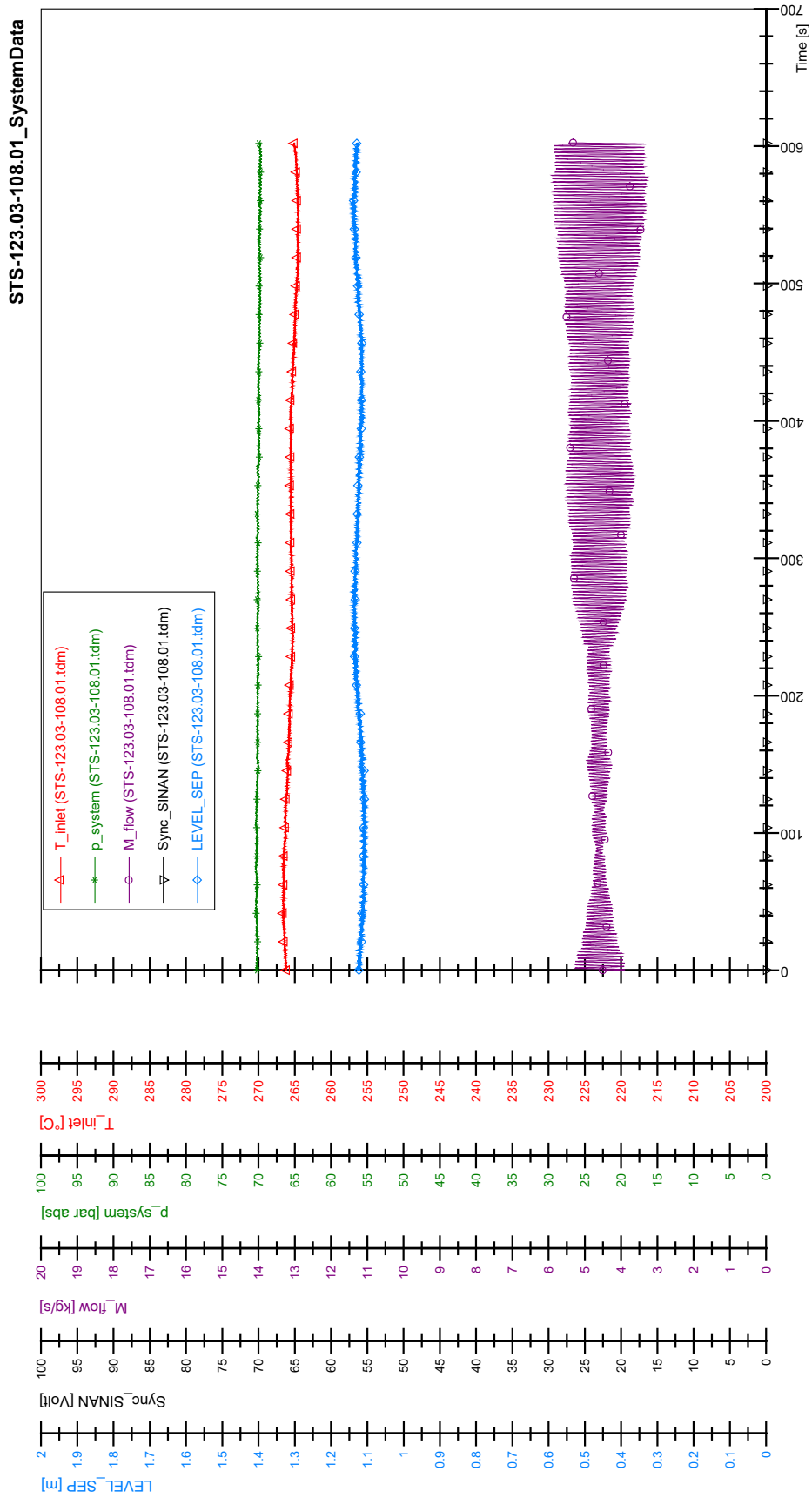
STS-123.03-107.01_Rod_87



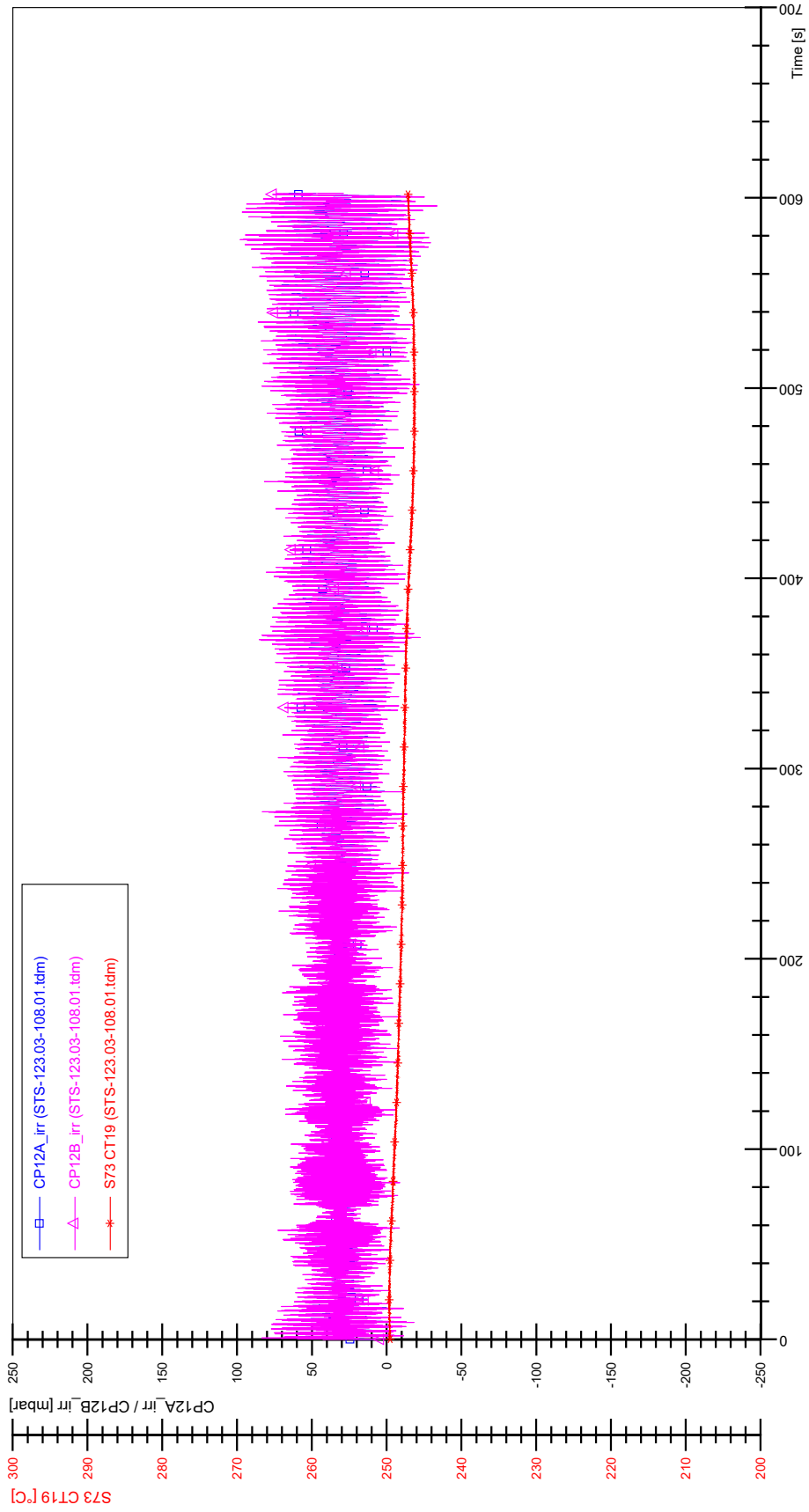
STS-123.03-107.01_Rod_88



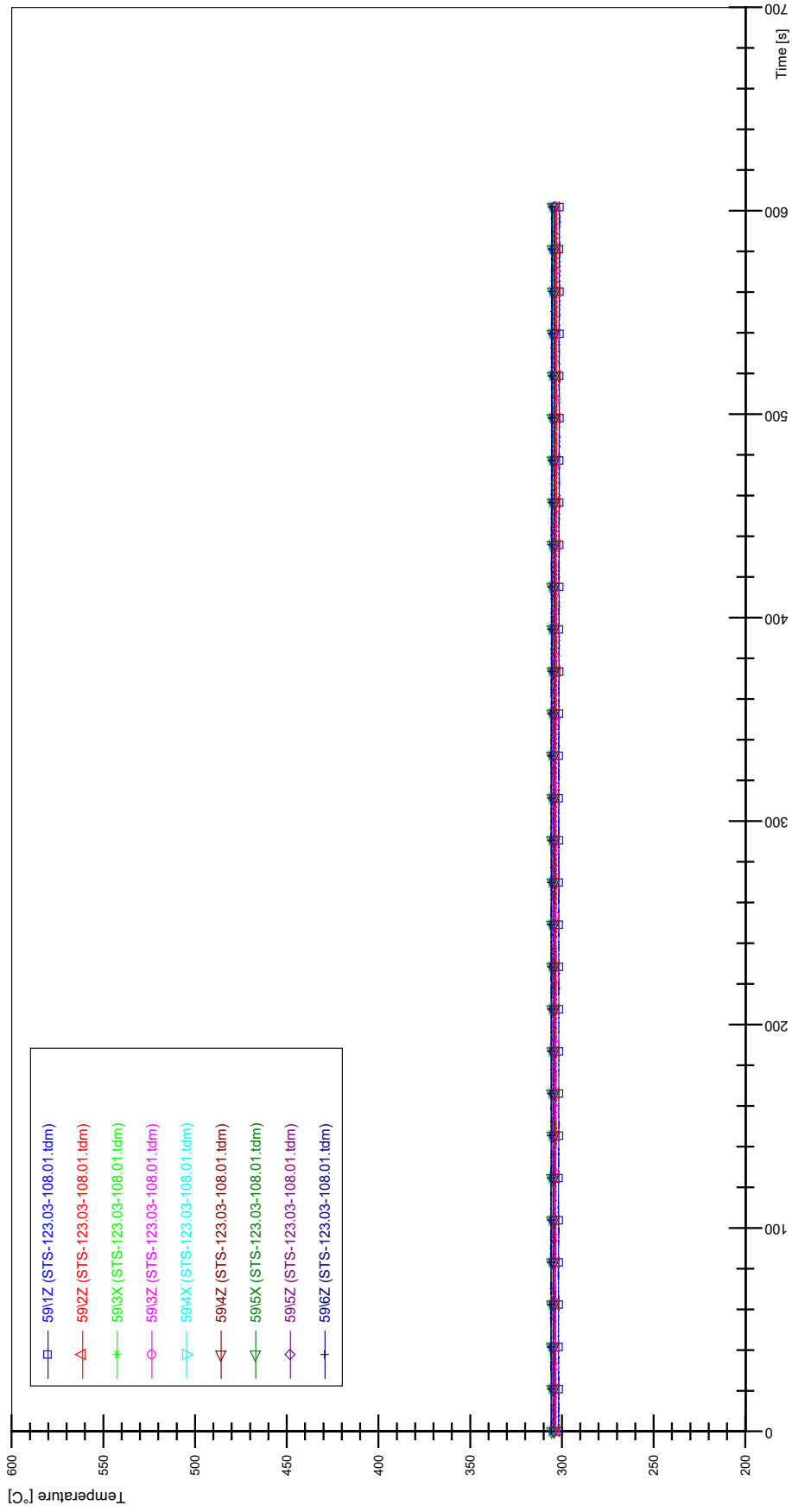
APPENDIX N PLOTS OF INSTABILITY TEST STS-123.03-108.01



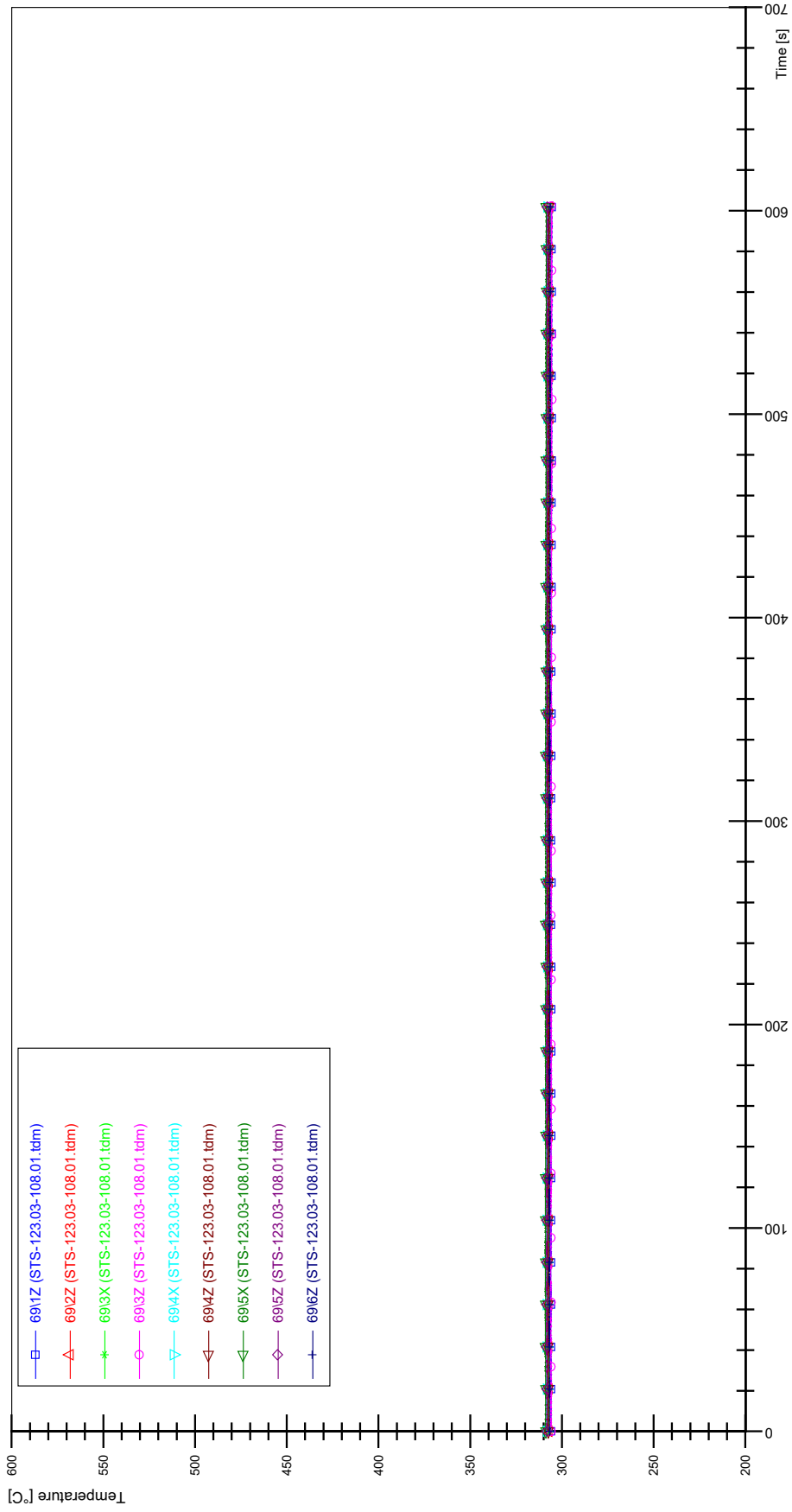
STS-123.03-108.01_CP12_CT19



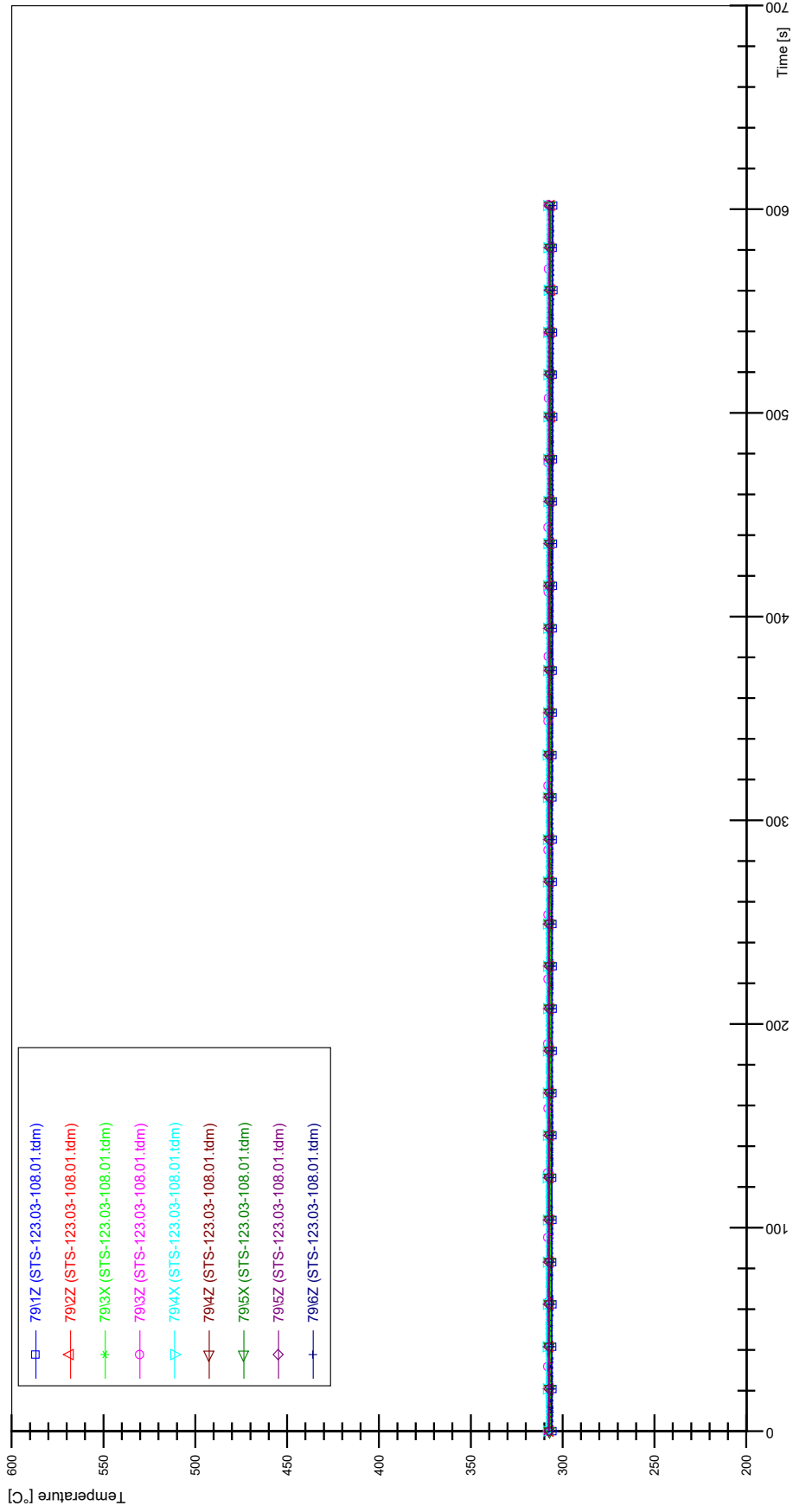
STS-123.03-108.01_Rod_59



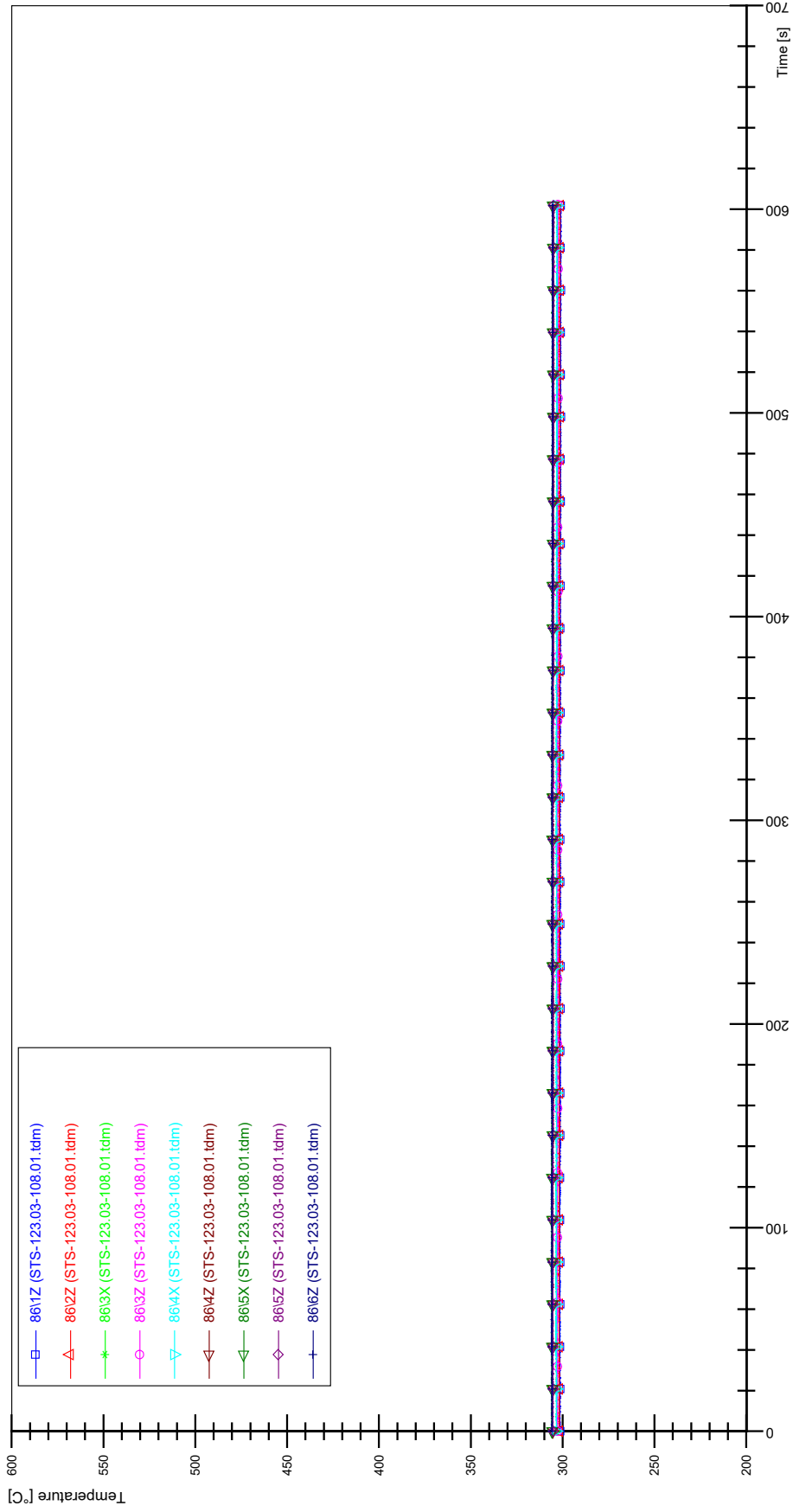
STS-123.03-108.01_Rod_69



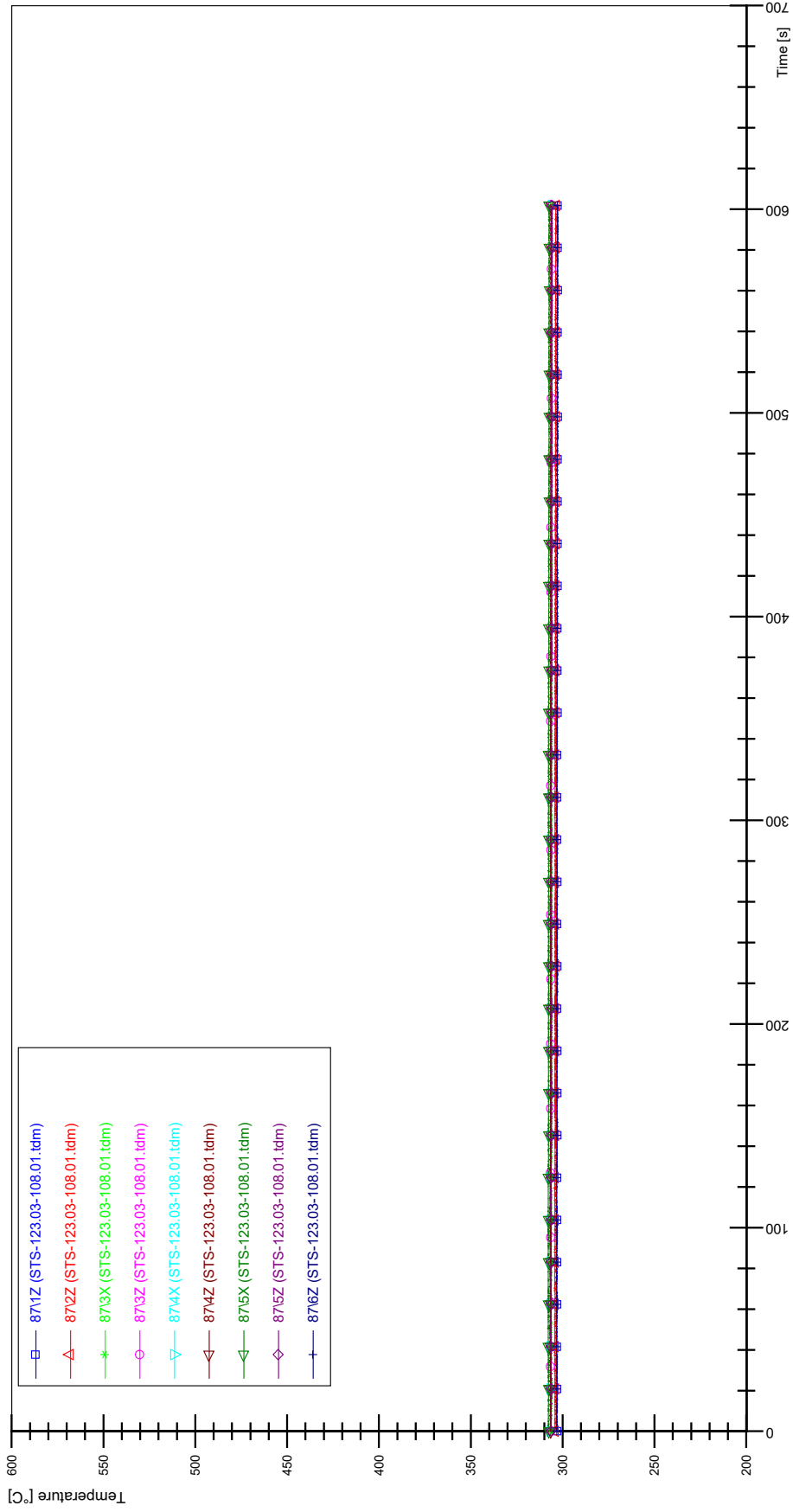
STS-123.03-108.01_Rod_79



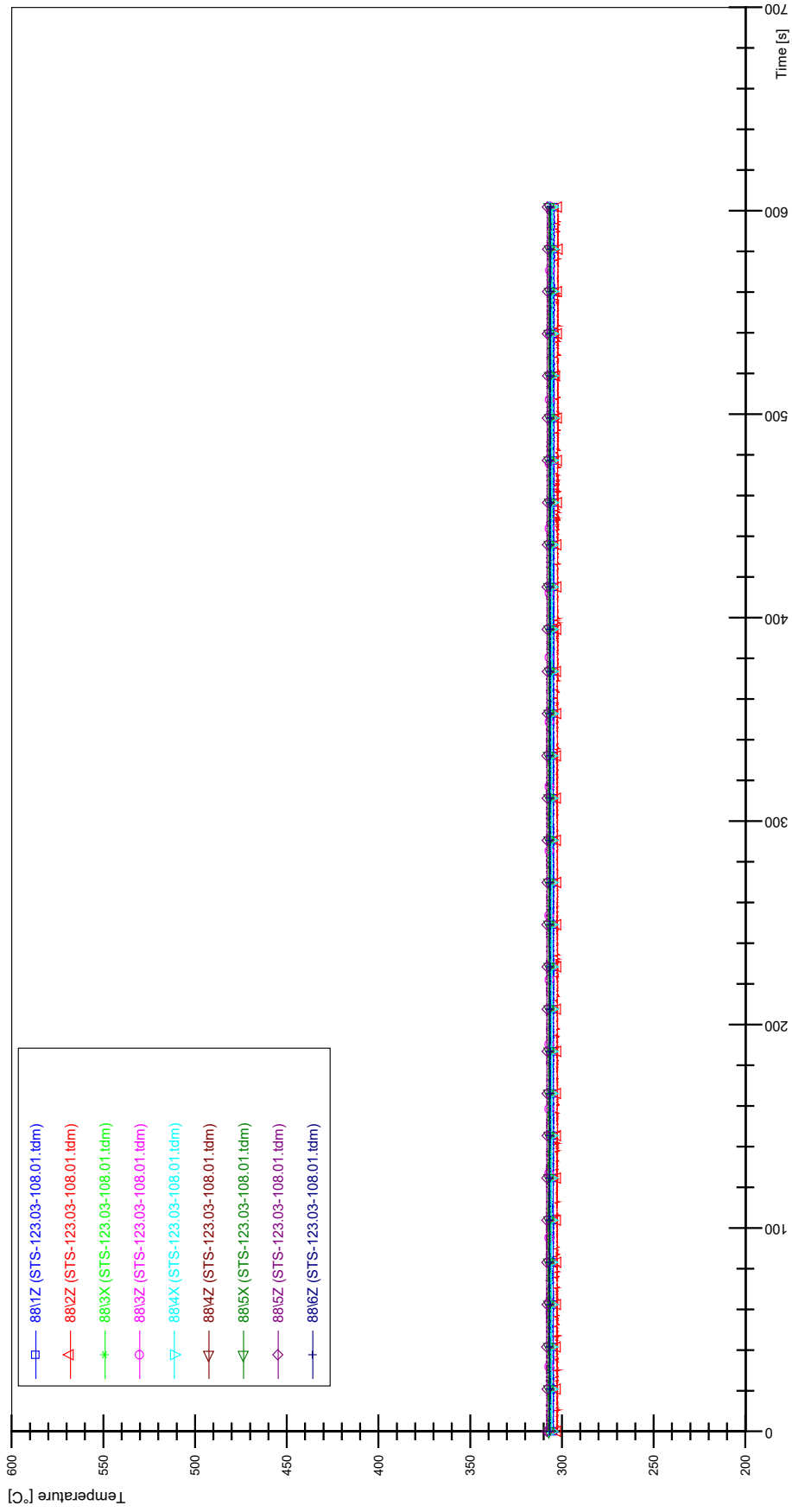
STS-123.03-108.01_Rod_86



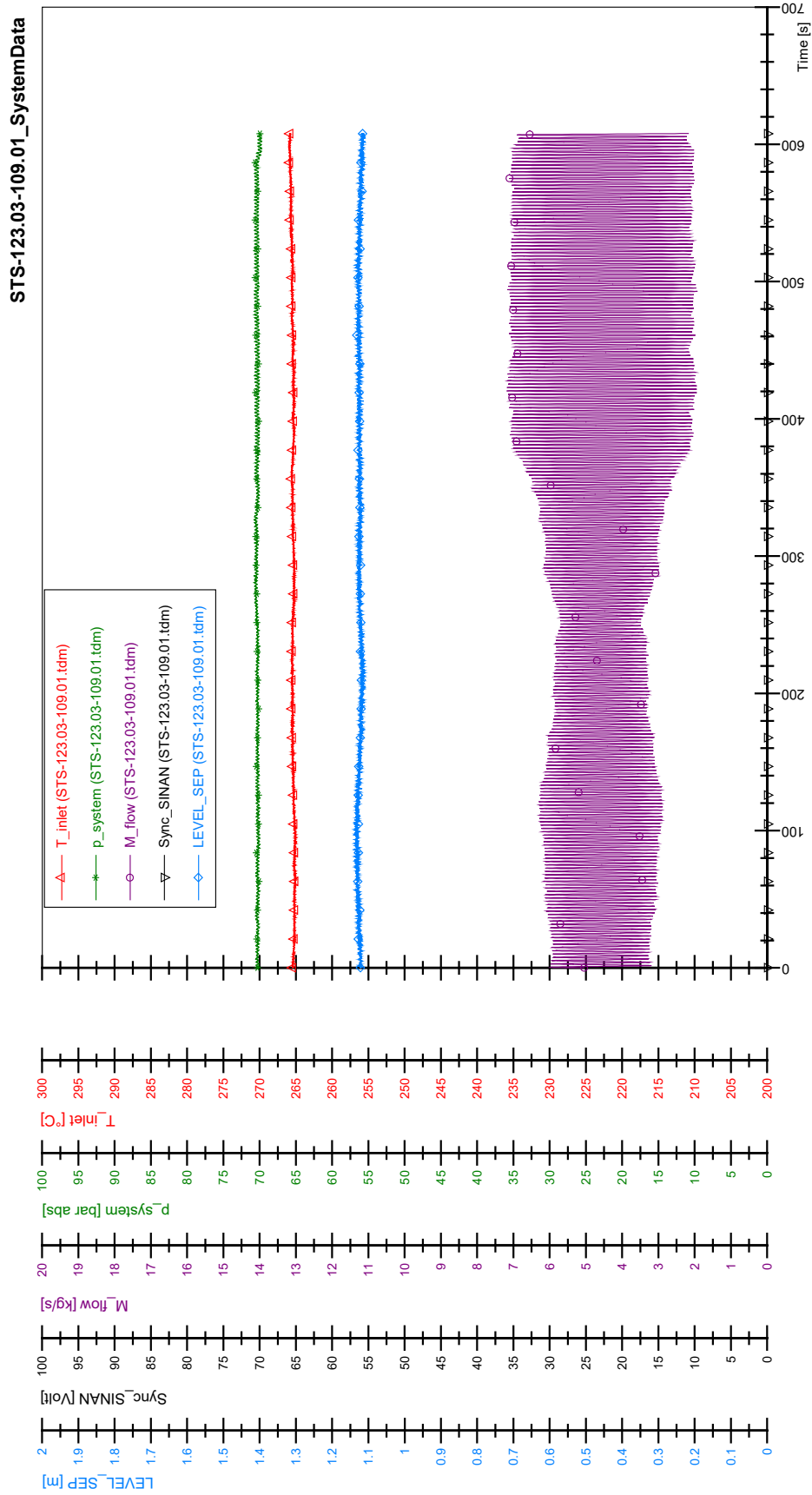
STS-123.03-108.01_Rod_87

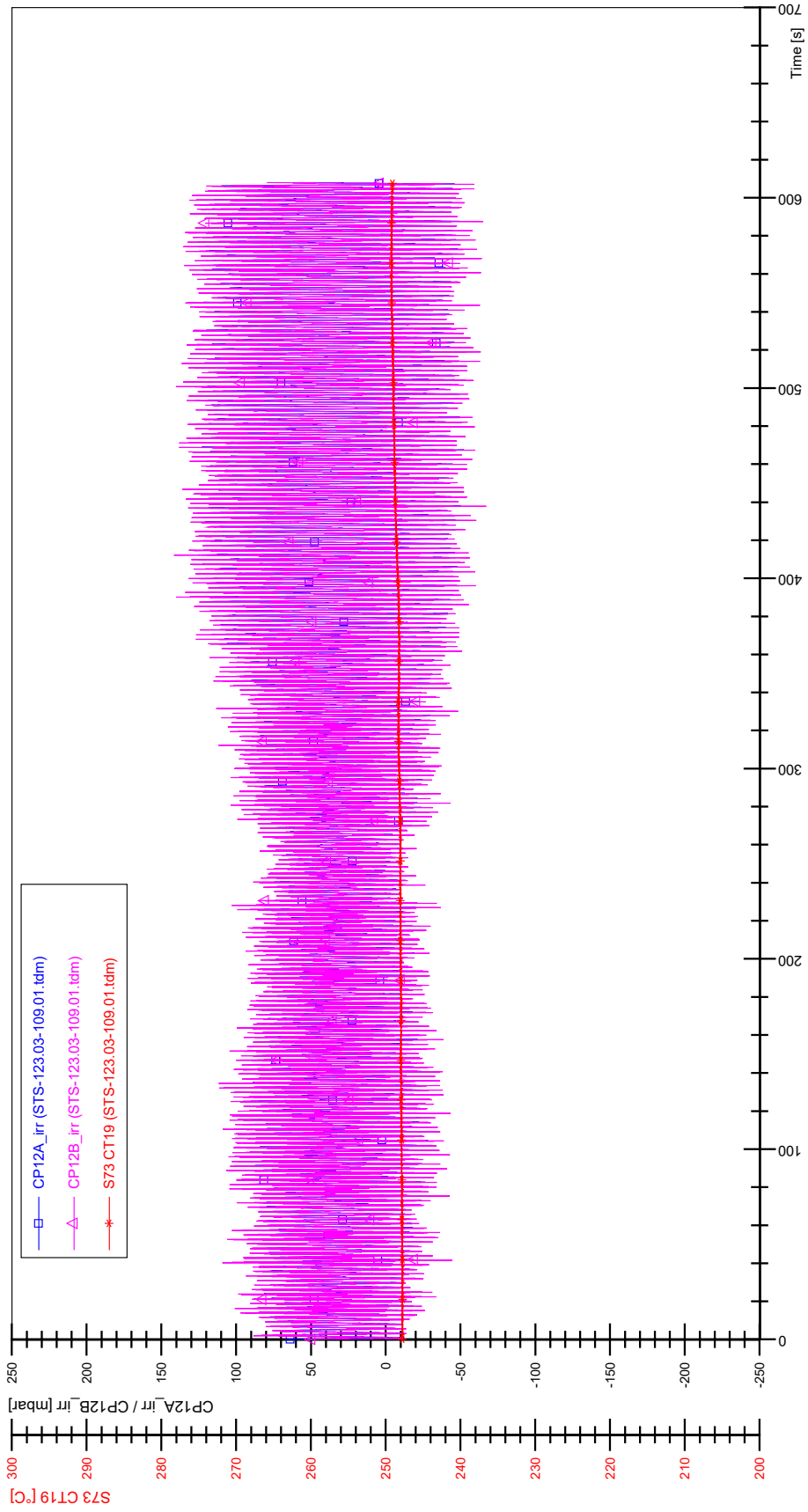


STS-123.03-108.01_Rod_88

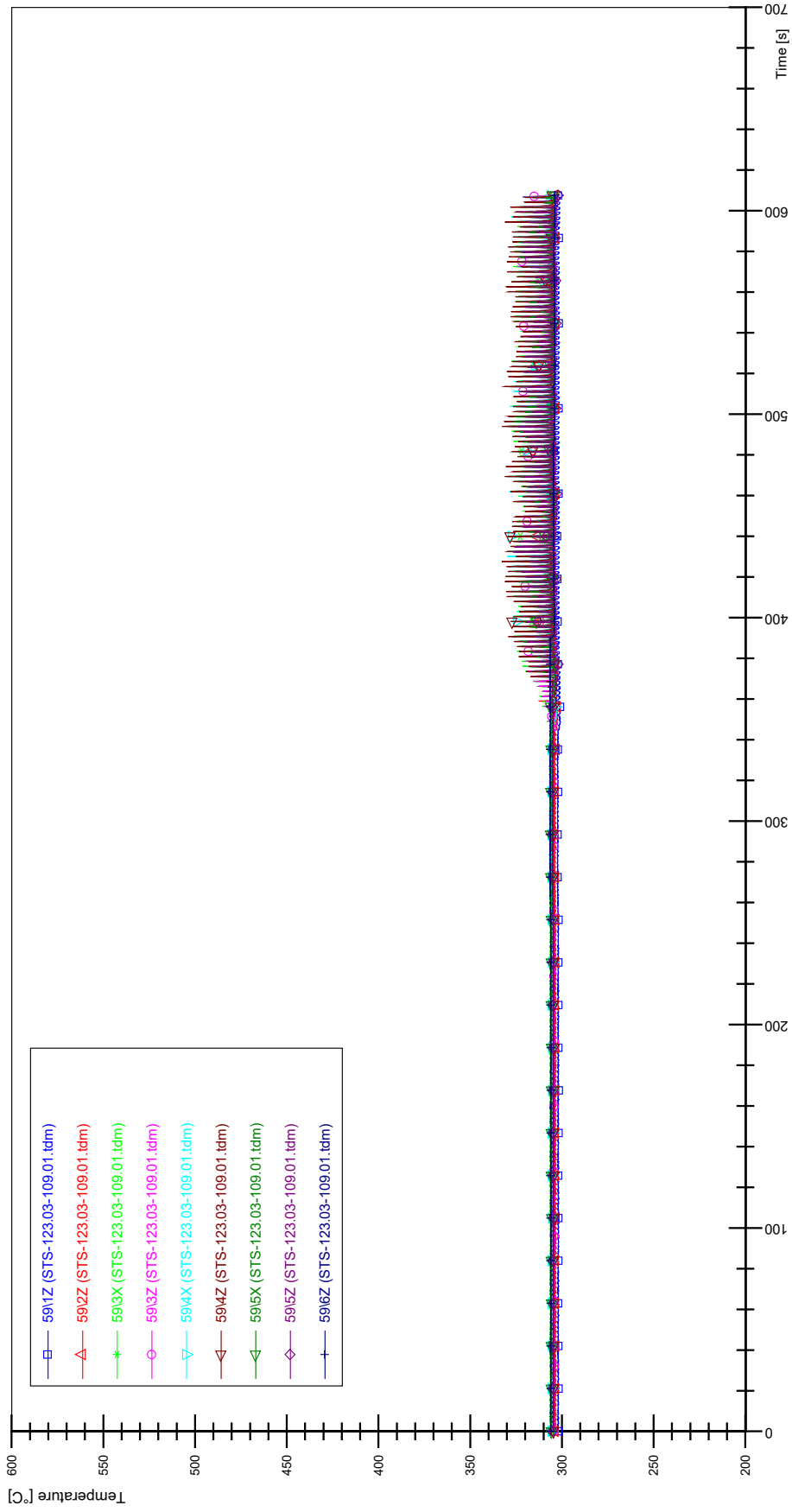


APPENDIX O PLOTS OF INSTABILITY TEST STS-123.03-109.01

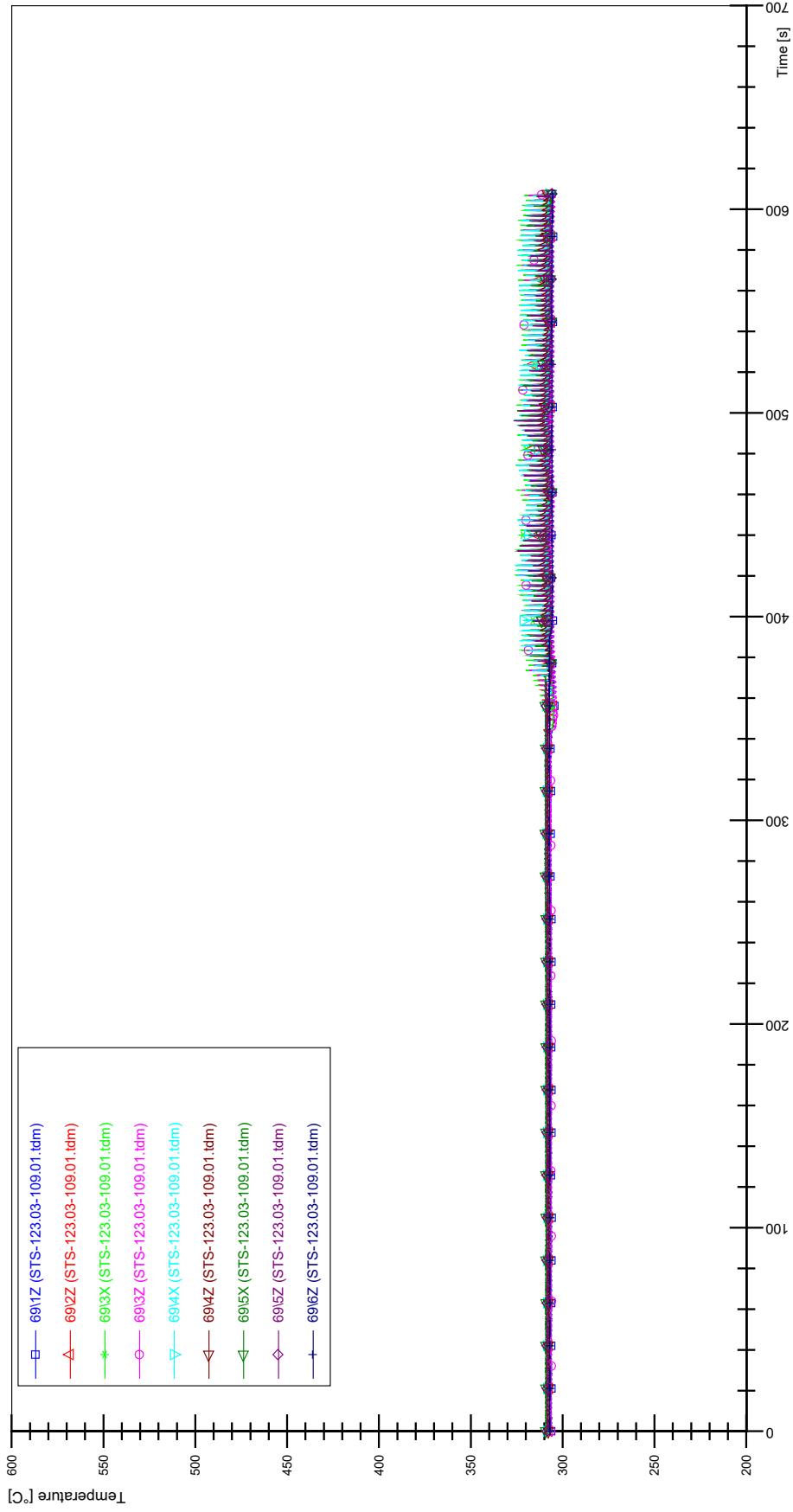




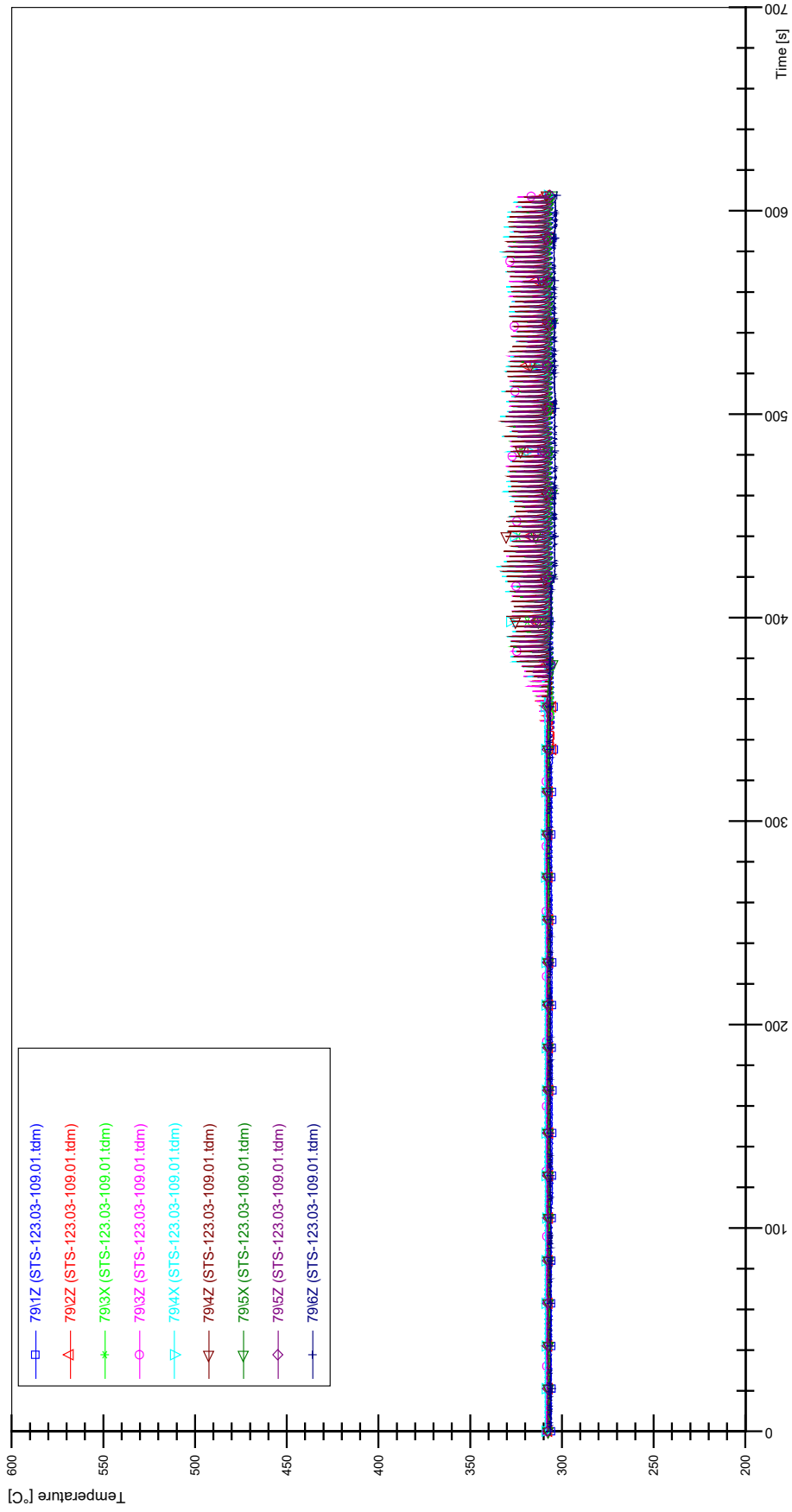
STS-123.03-109.01_Rod_59



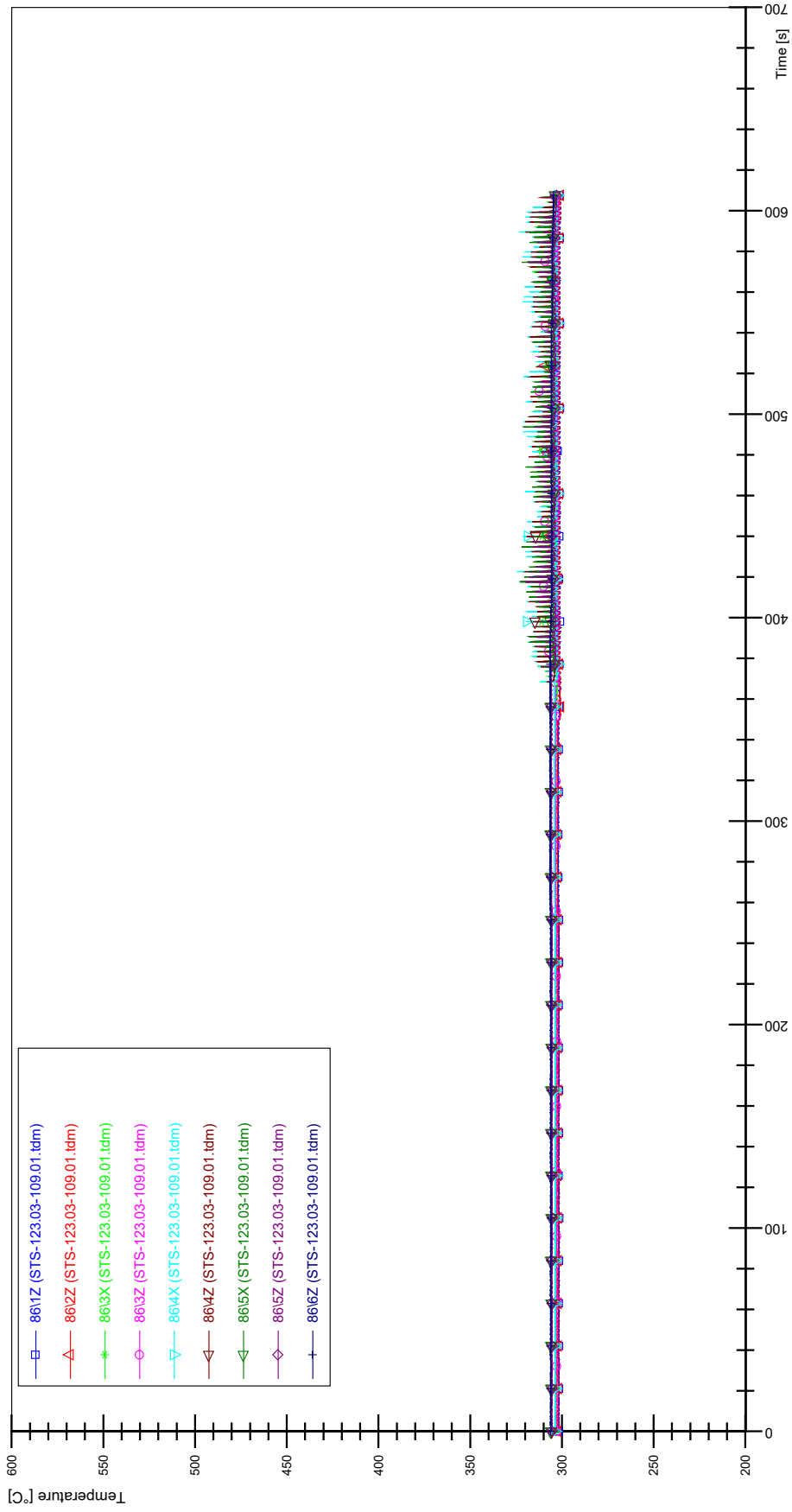
STS-123.03-109.01_Rod_69



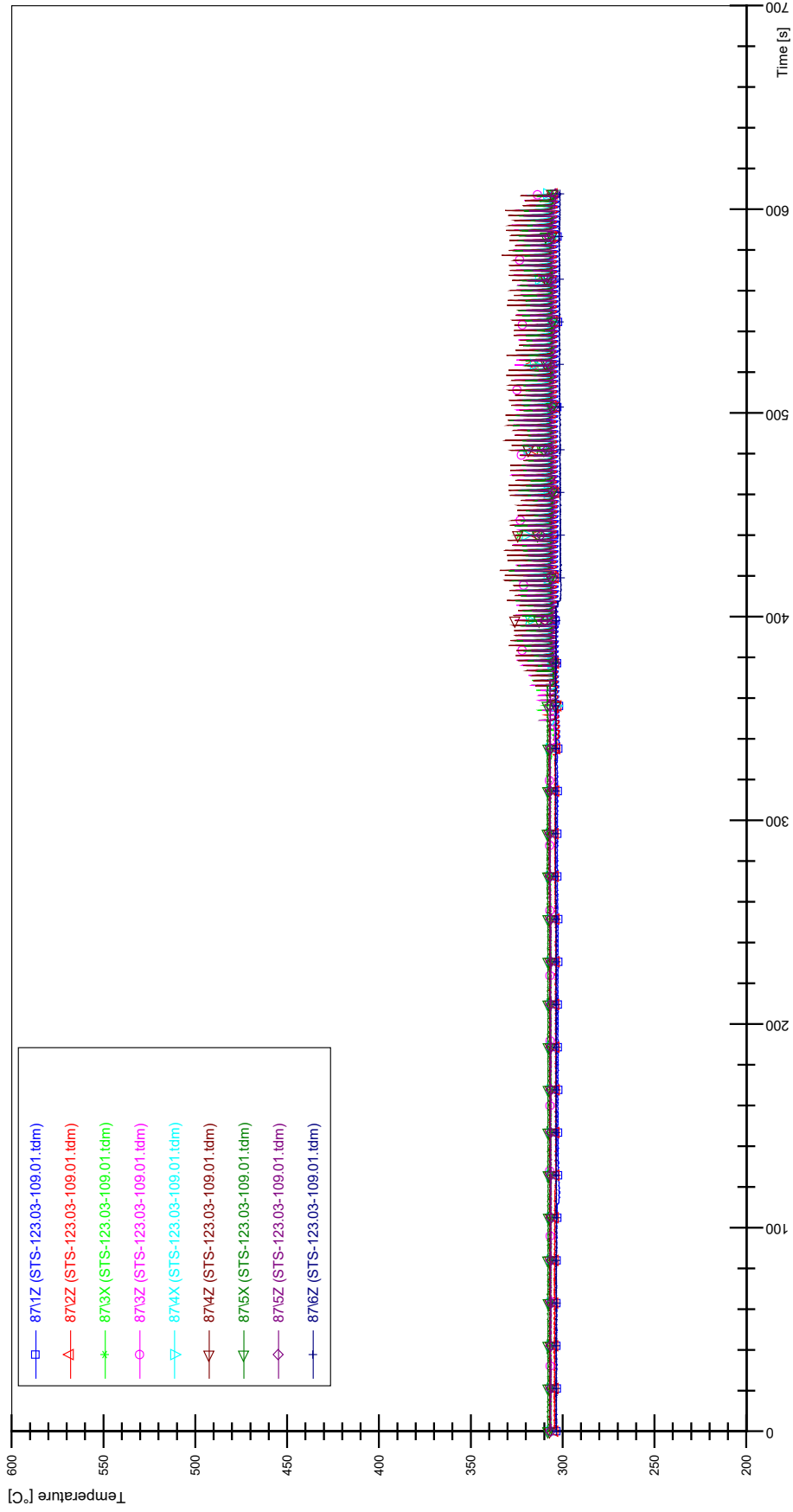
STS-123.03-109.01_Rod_79



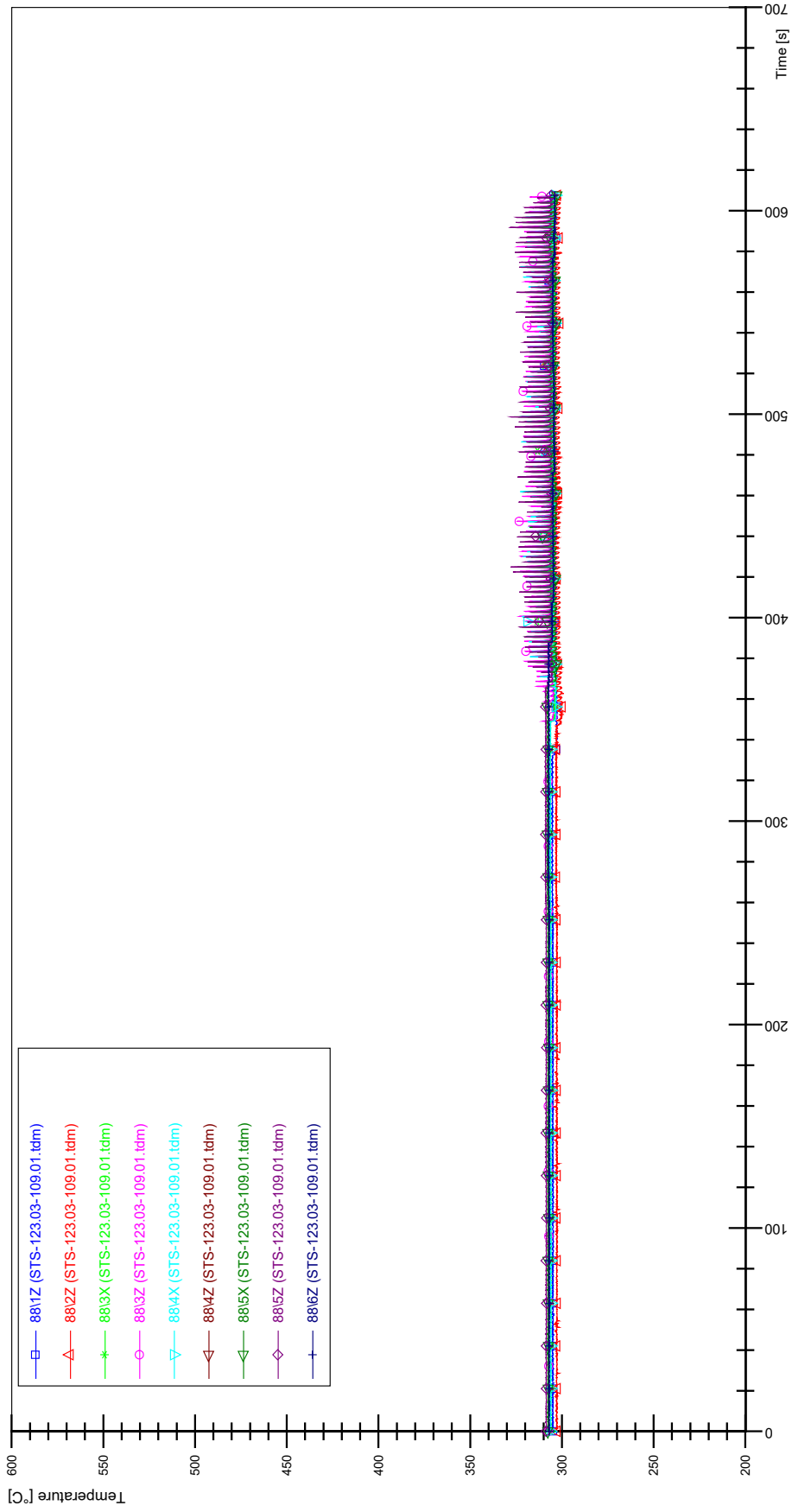
STS-123.03-109.01_Rod_86



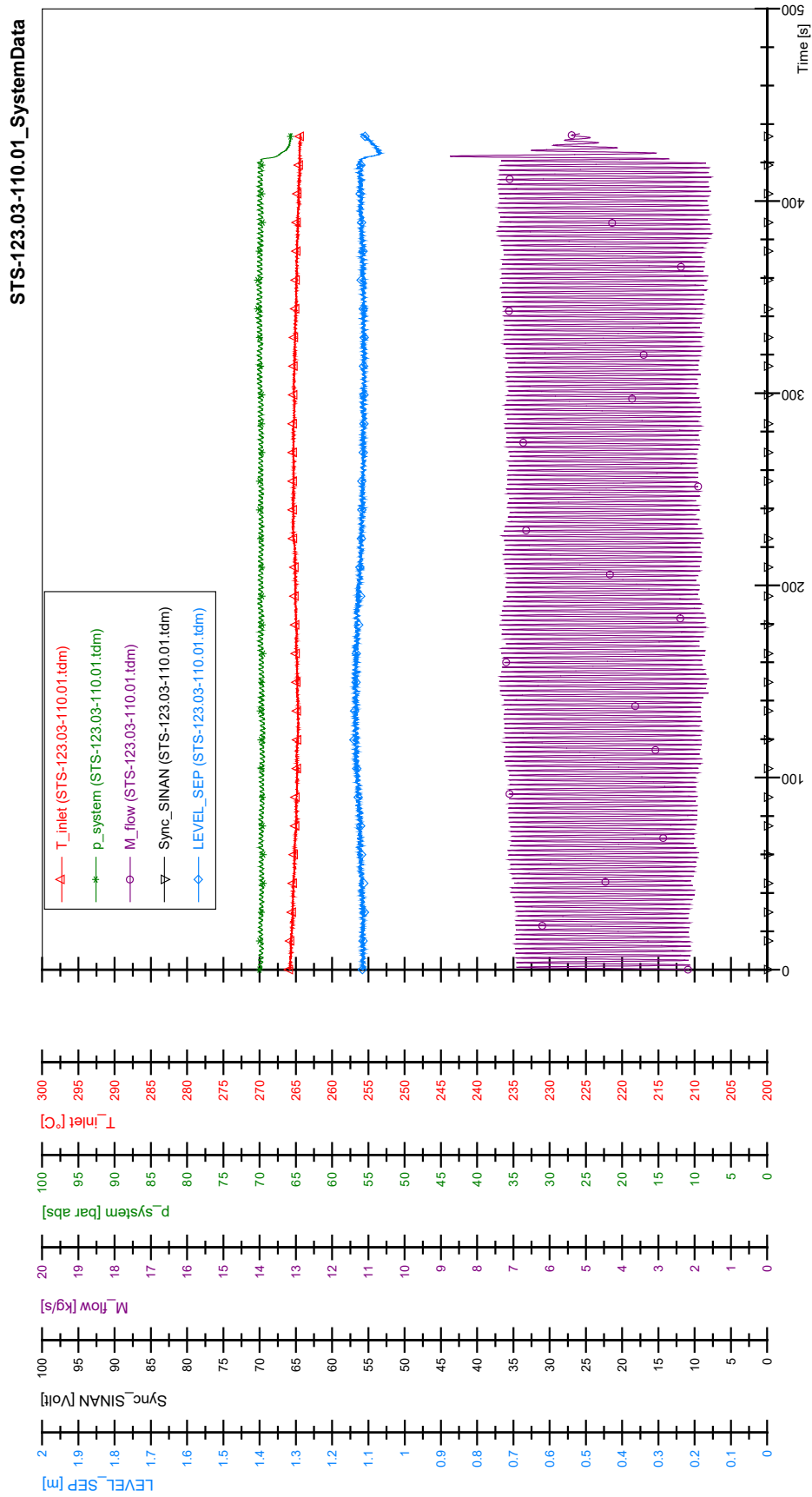
STS-123.03-109.01_Rod_87

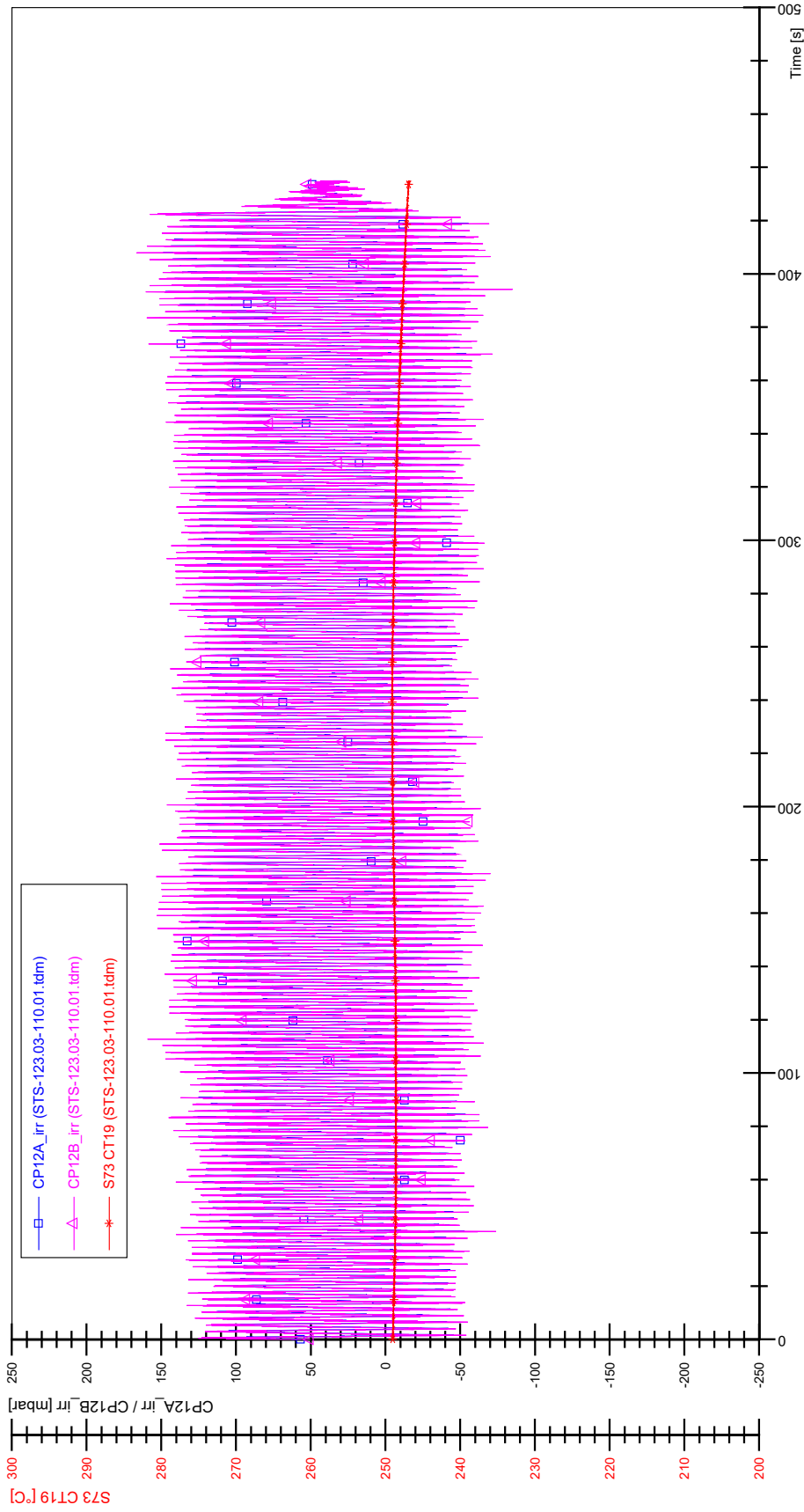


STS-123.03-109.01_Rod_88

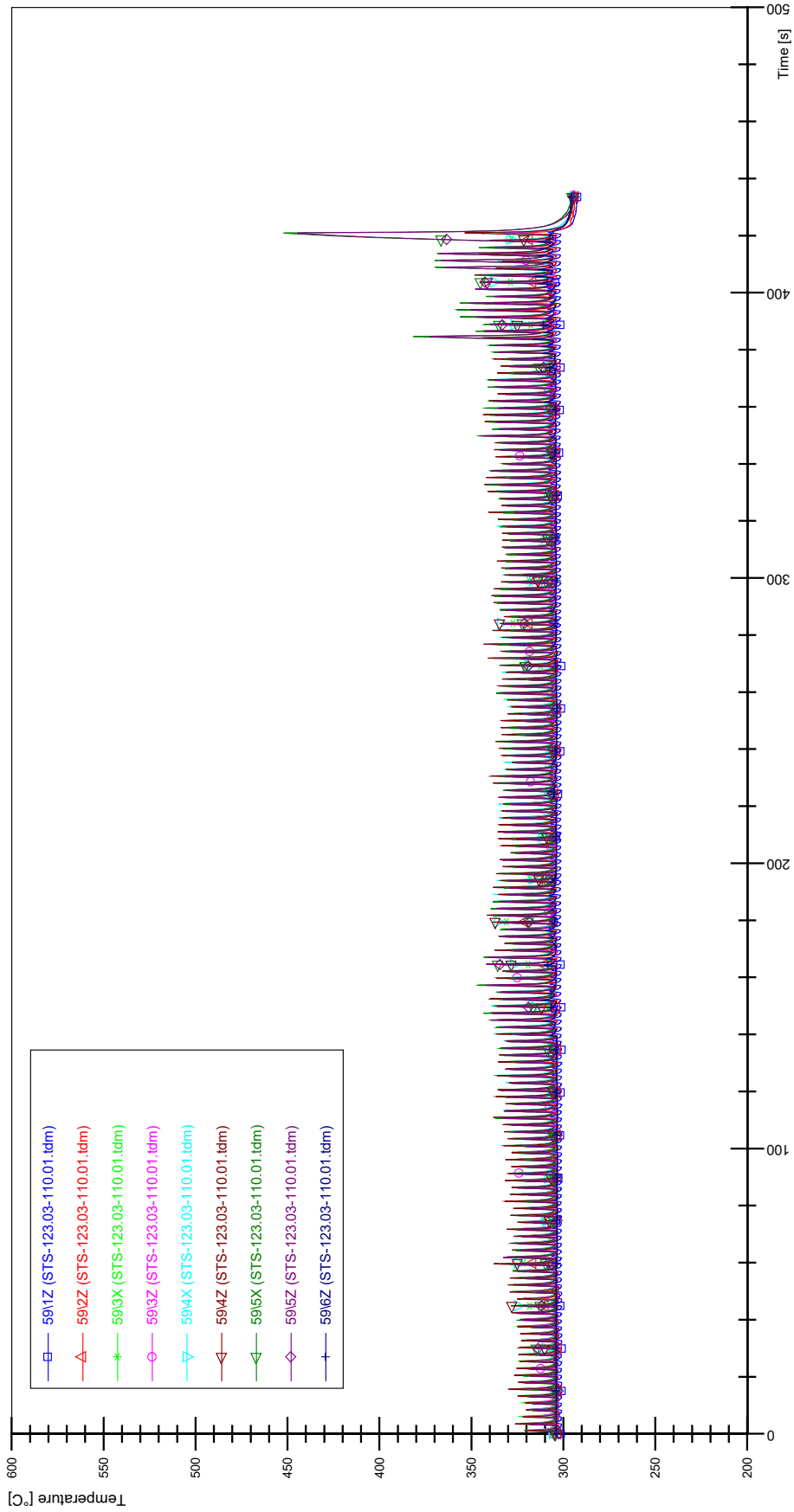


APPENDIX P PLOTS OF INSTABILITY TEST STS-123.03-110.01

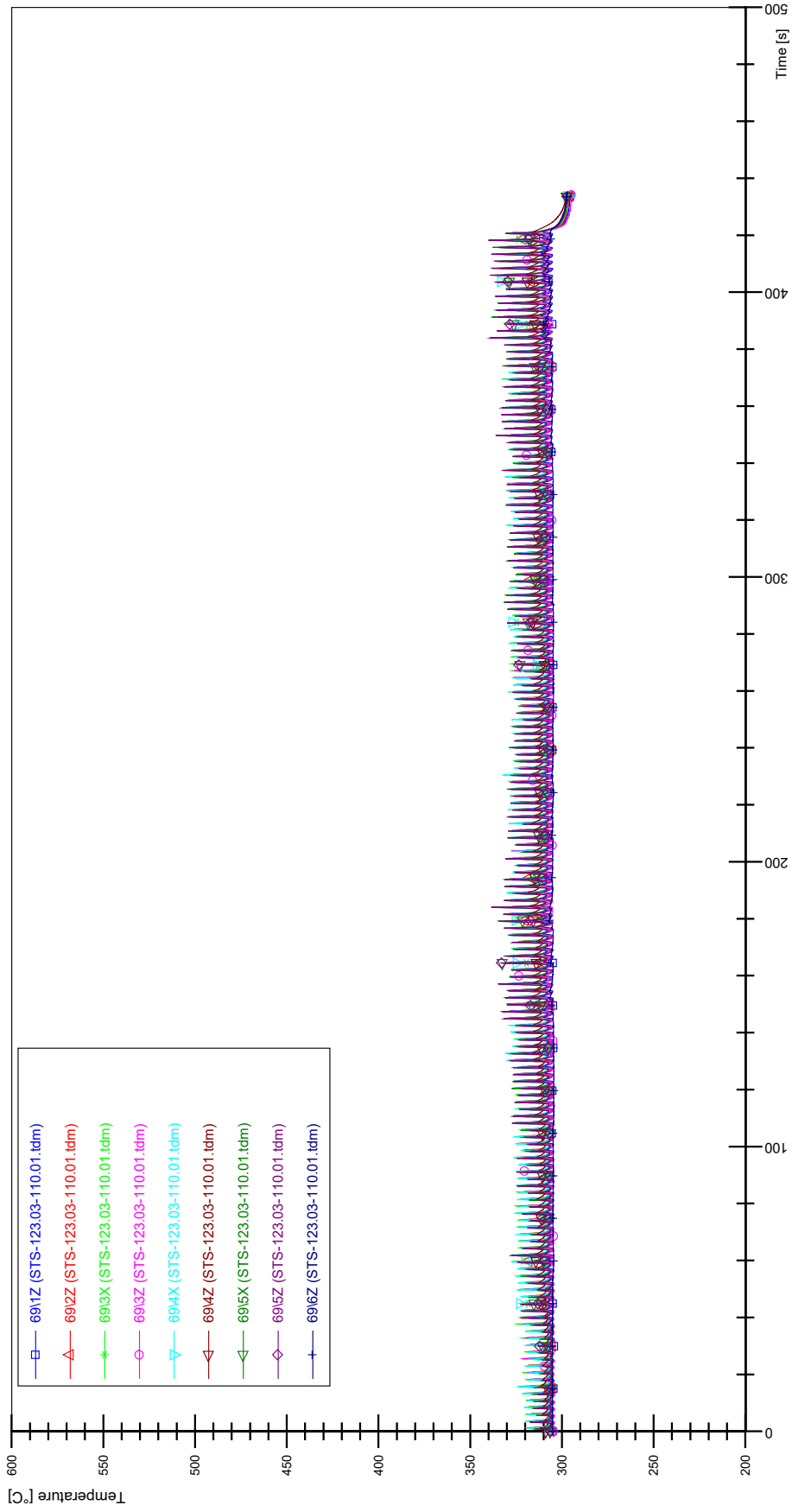




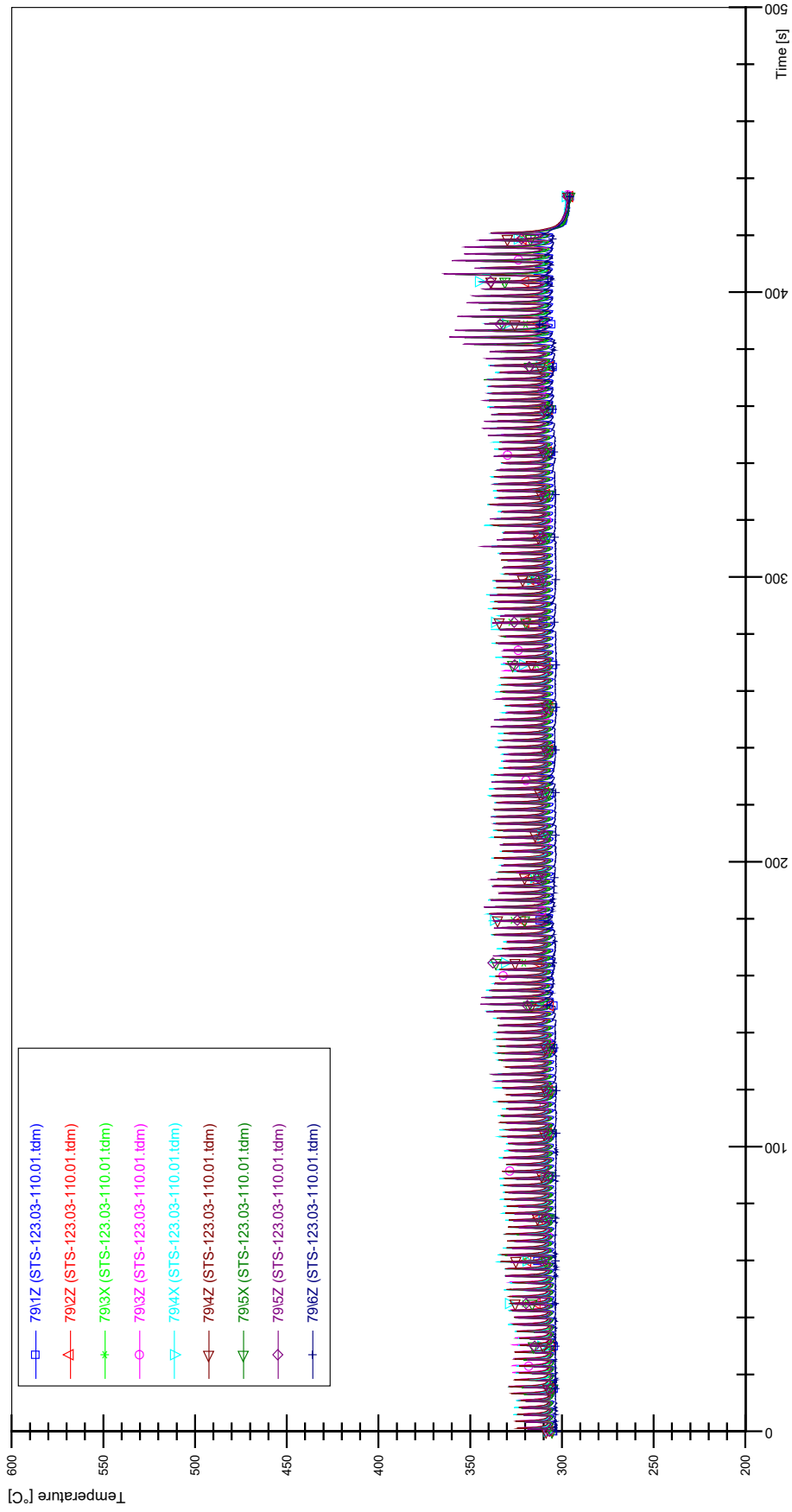
STS-123.03-110.01_Rod_59



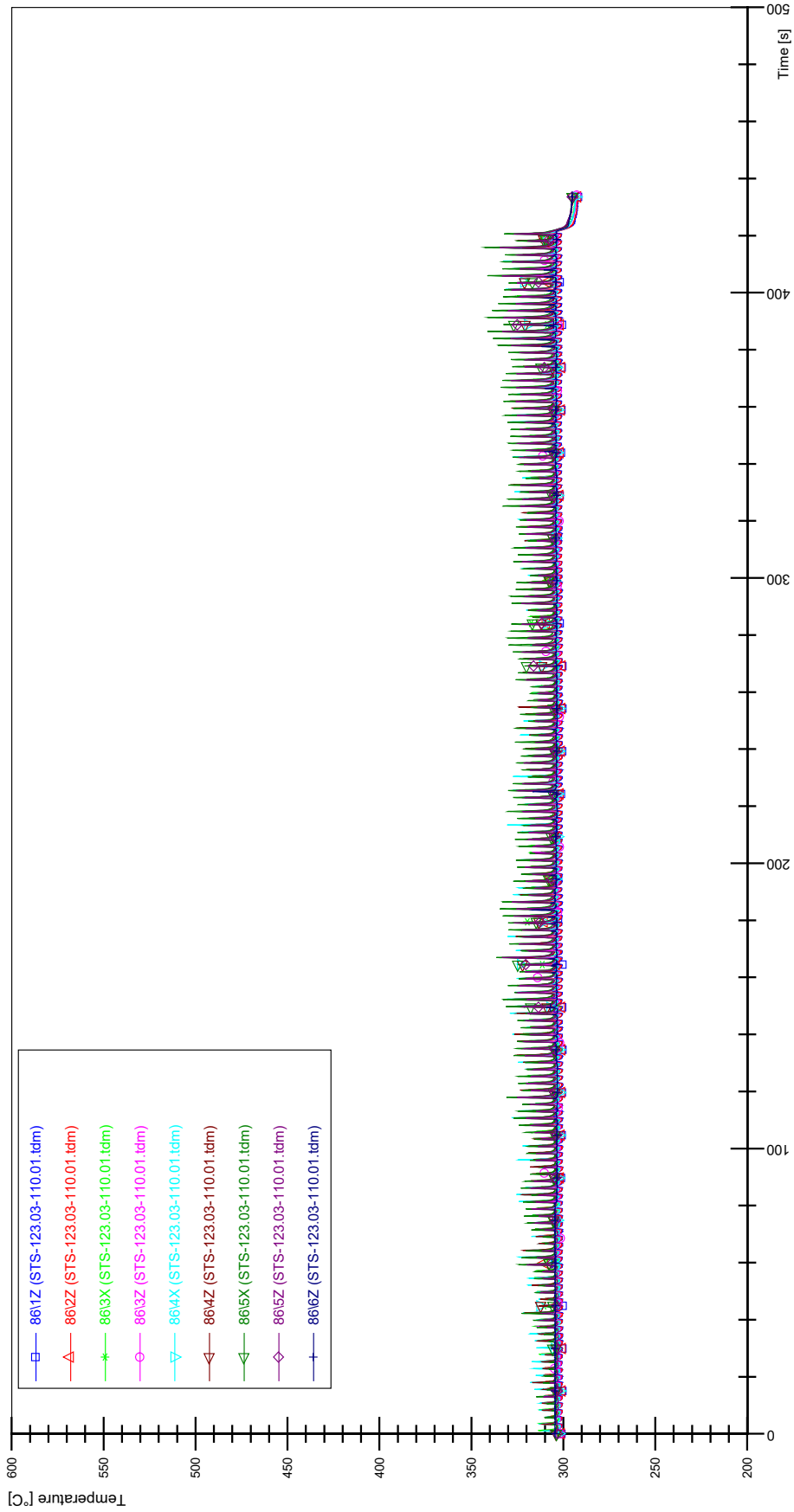
STS-123.03-110.01_Rod_69



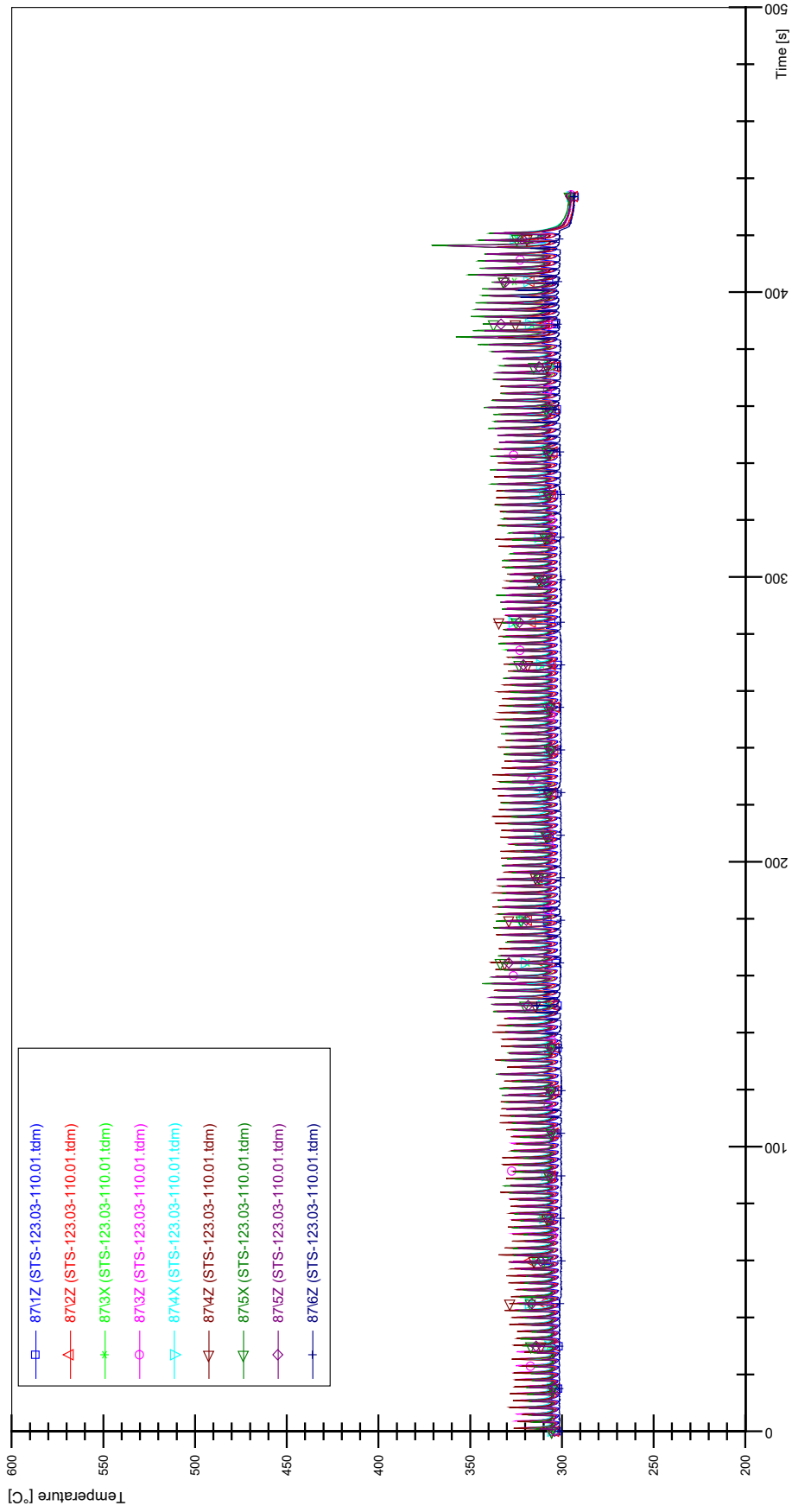
STS-123.03-110.01_Rod_79



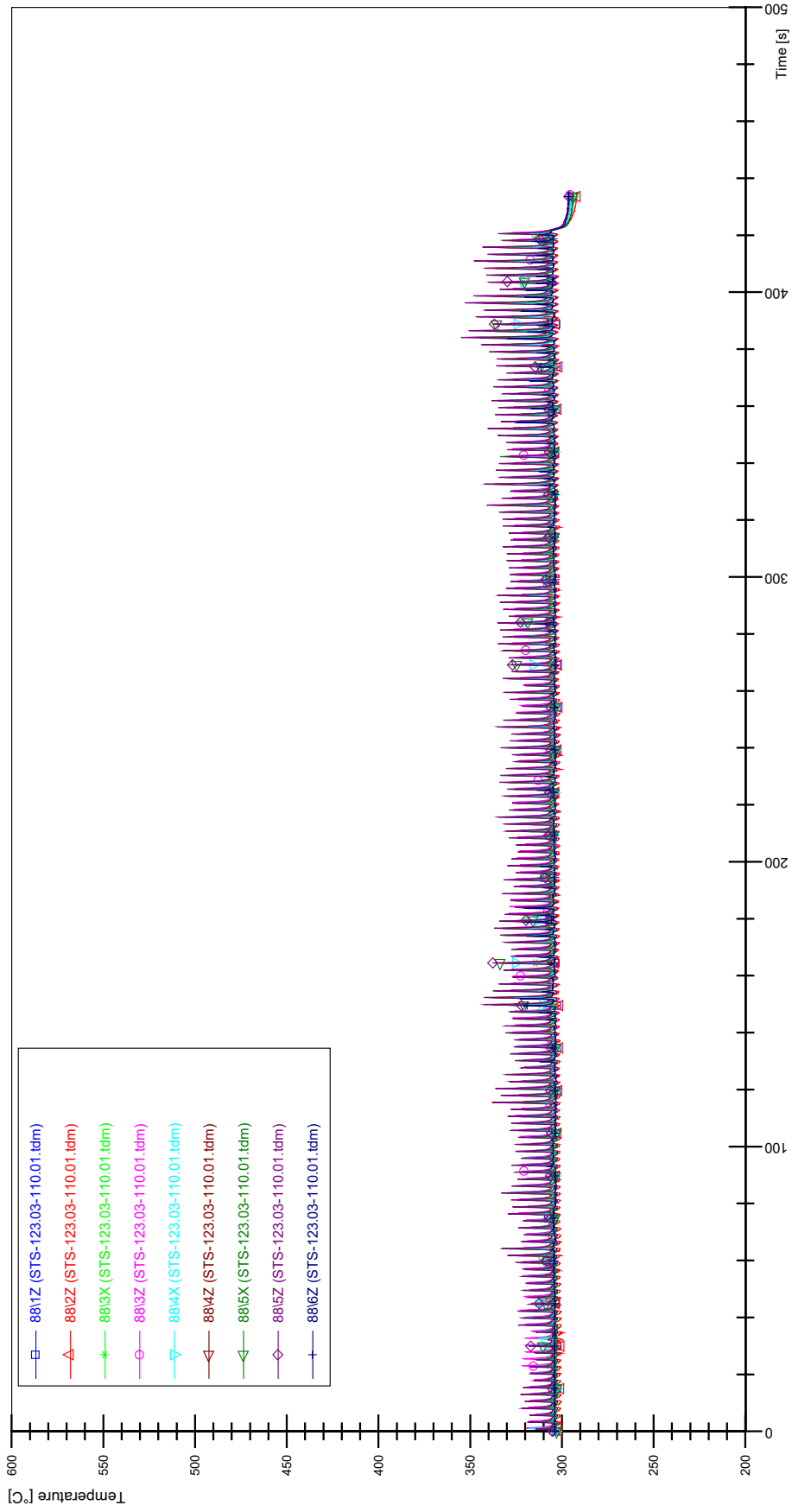
STS-123.03-110.01_Rod_86



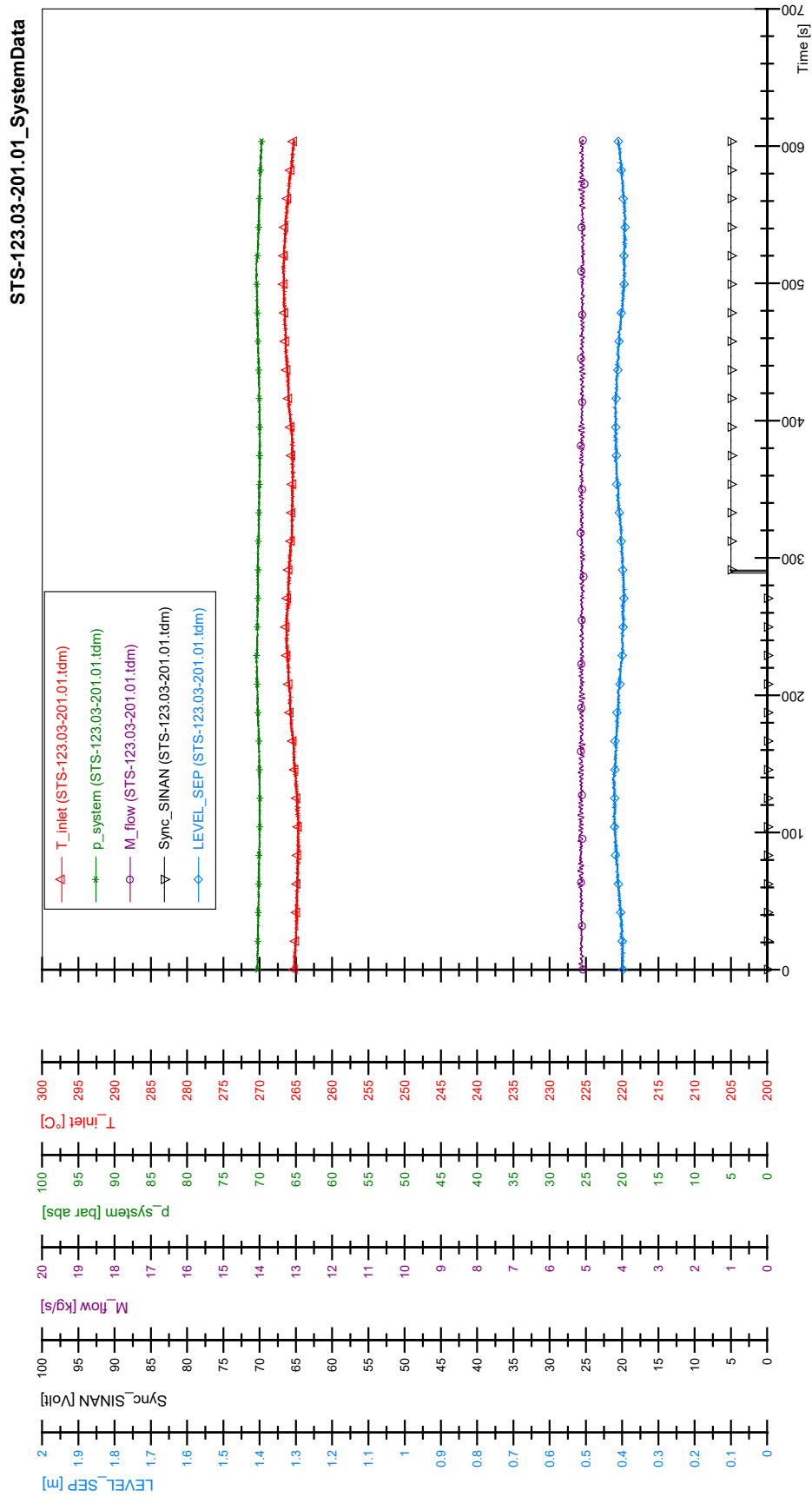
STS-123.03-110.01_Rod_87



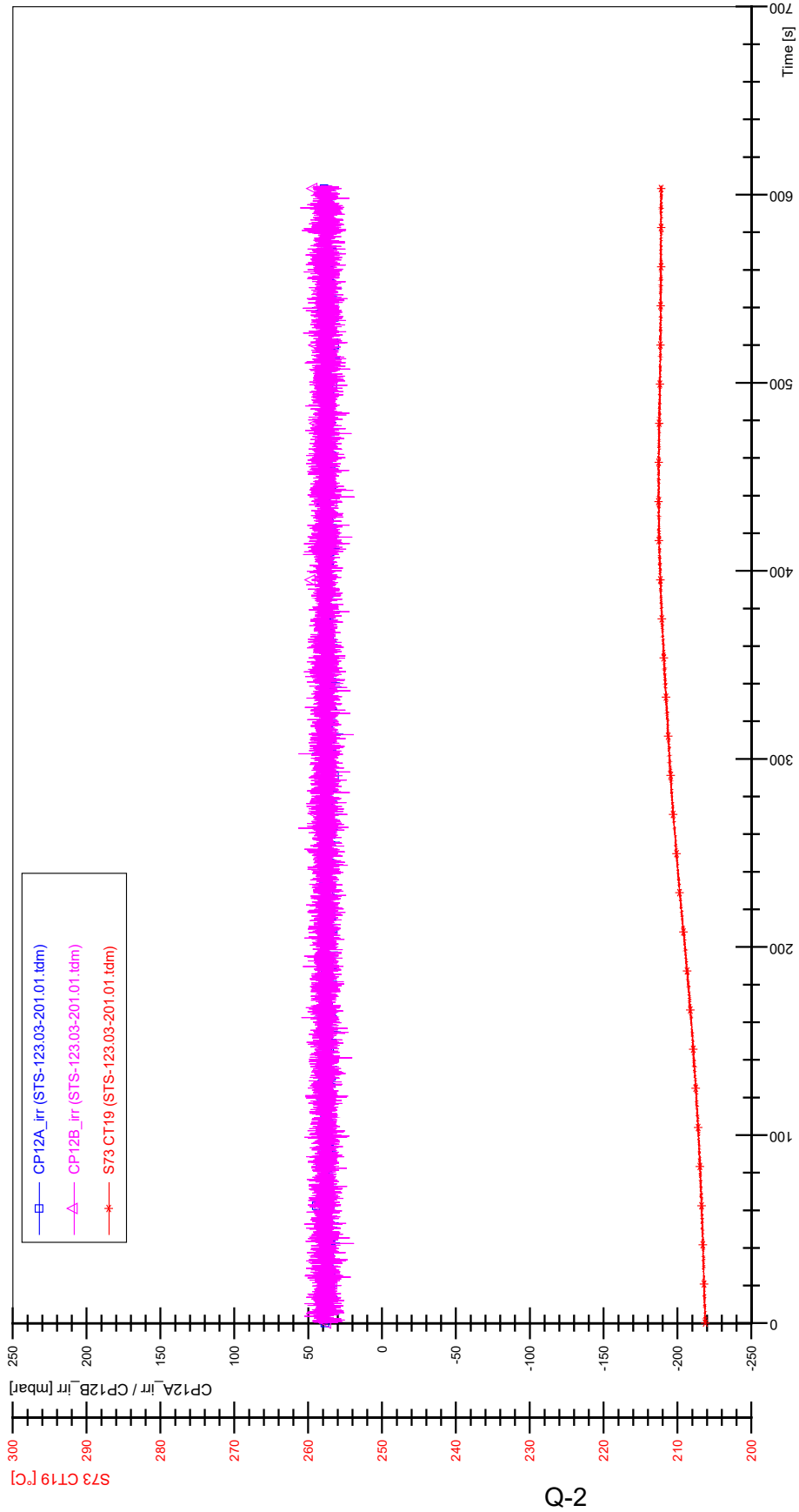
STS-123.03-110.01_Rod_88



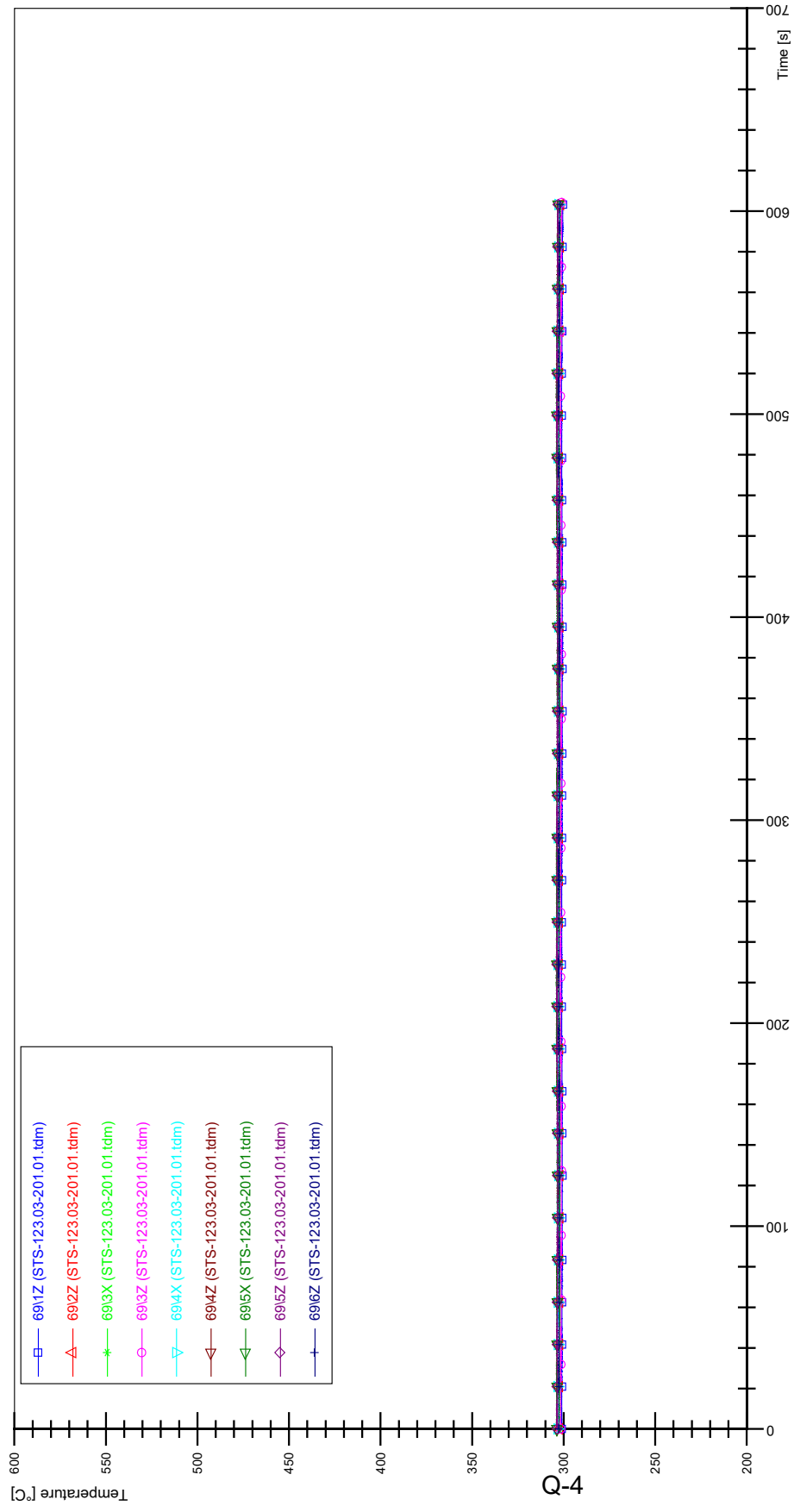
APPENDIX Q PLOTS OF INSTABILITY TEST STS-123.03-201.01



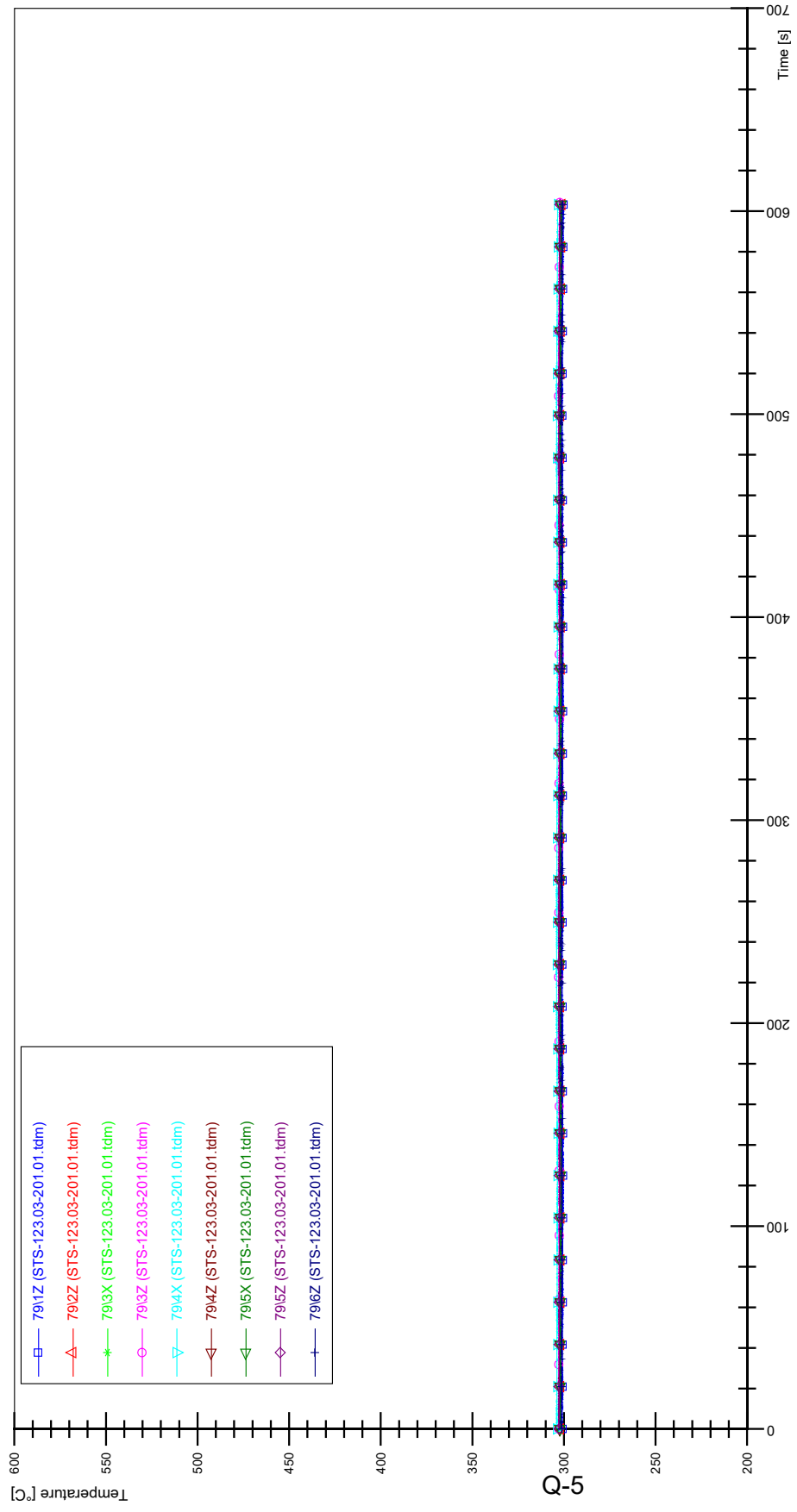
STS-123.03-201.01_CP12_CT19



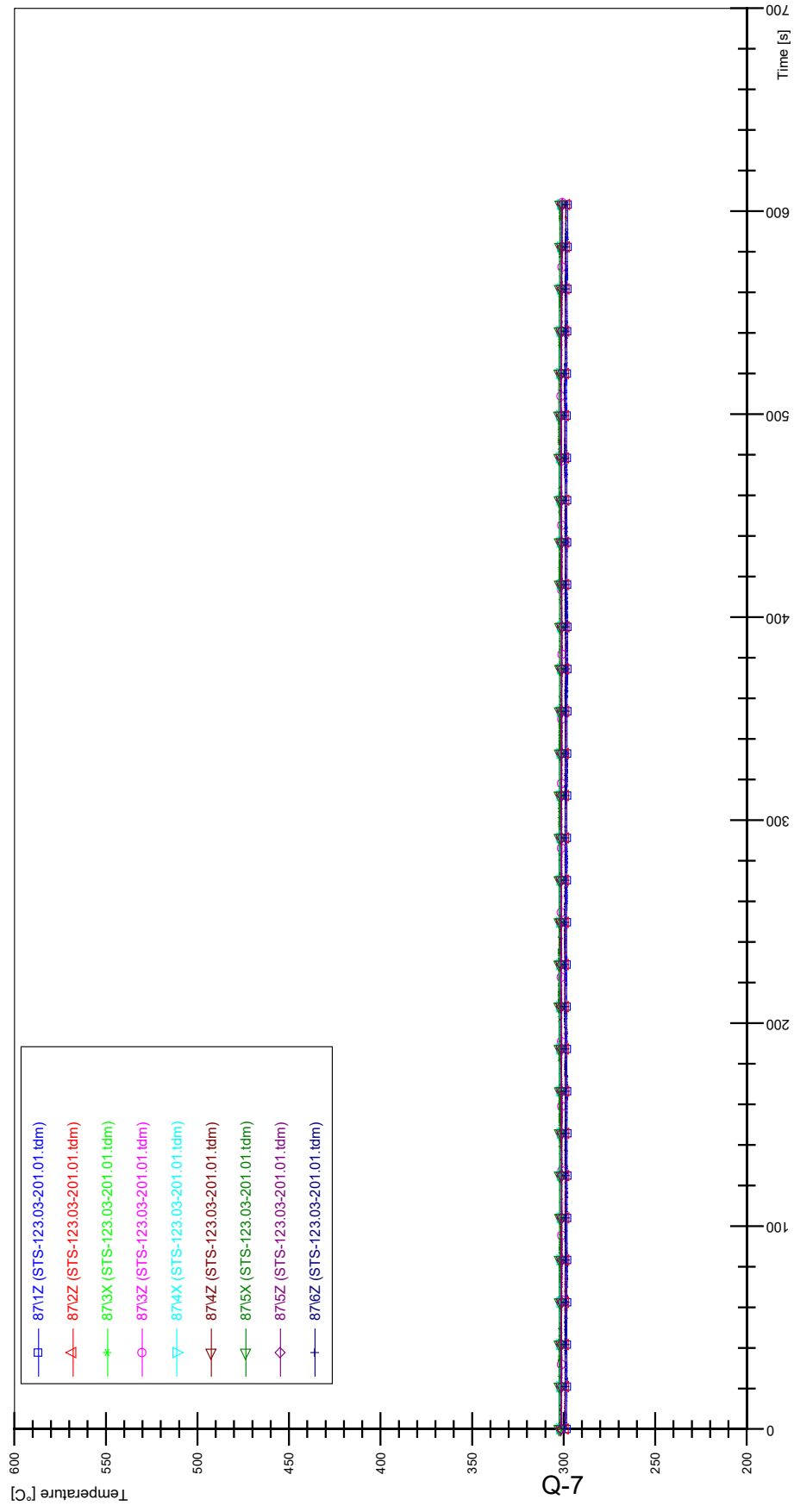
STS-123.03-201.01_Rod_69



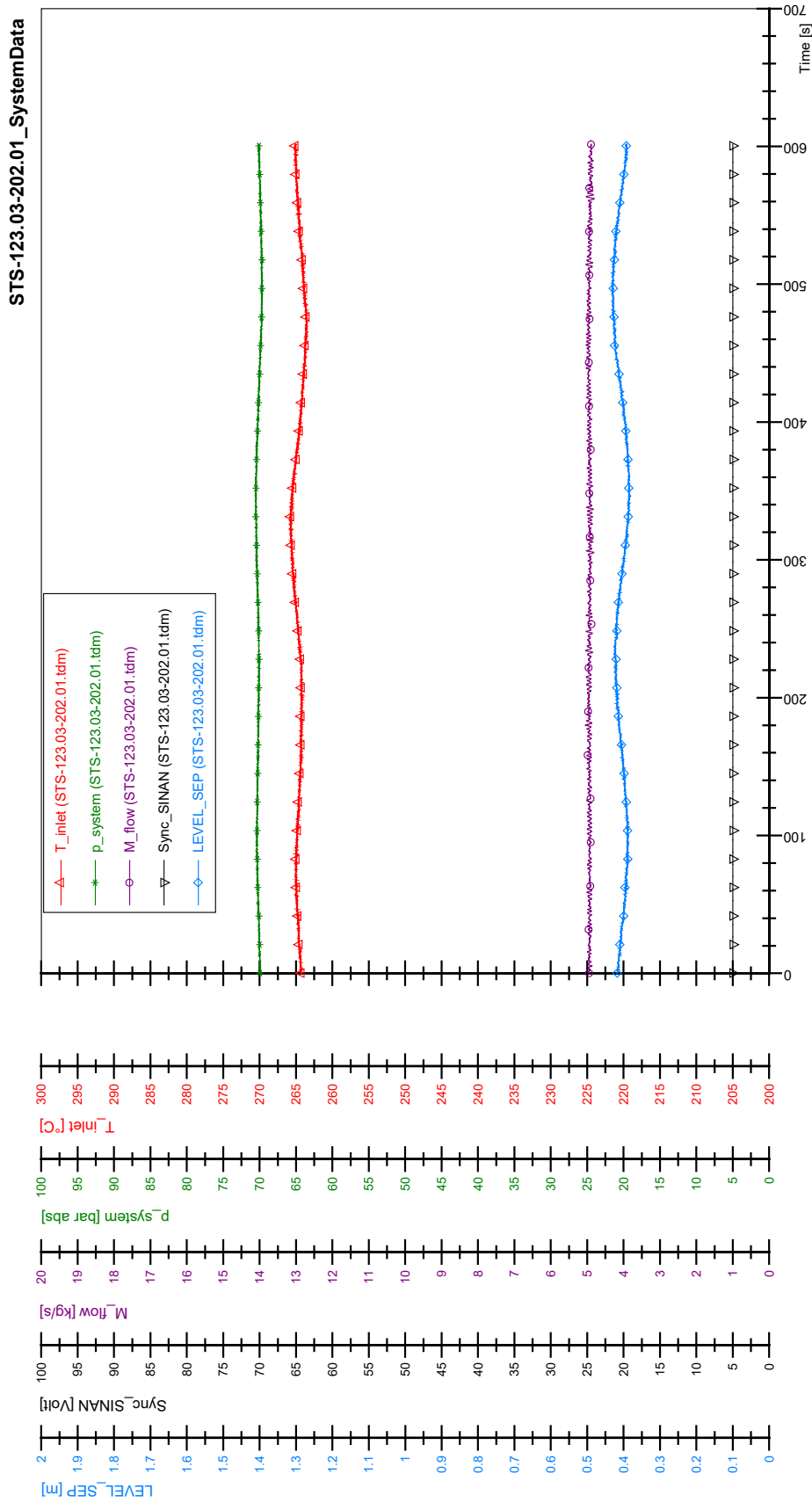
STS-123.03-201.01_Rod_79

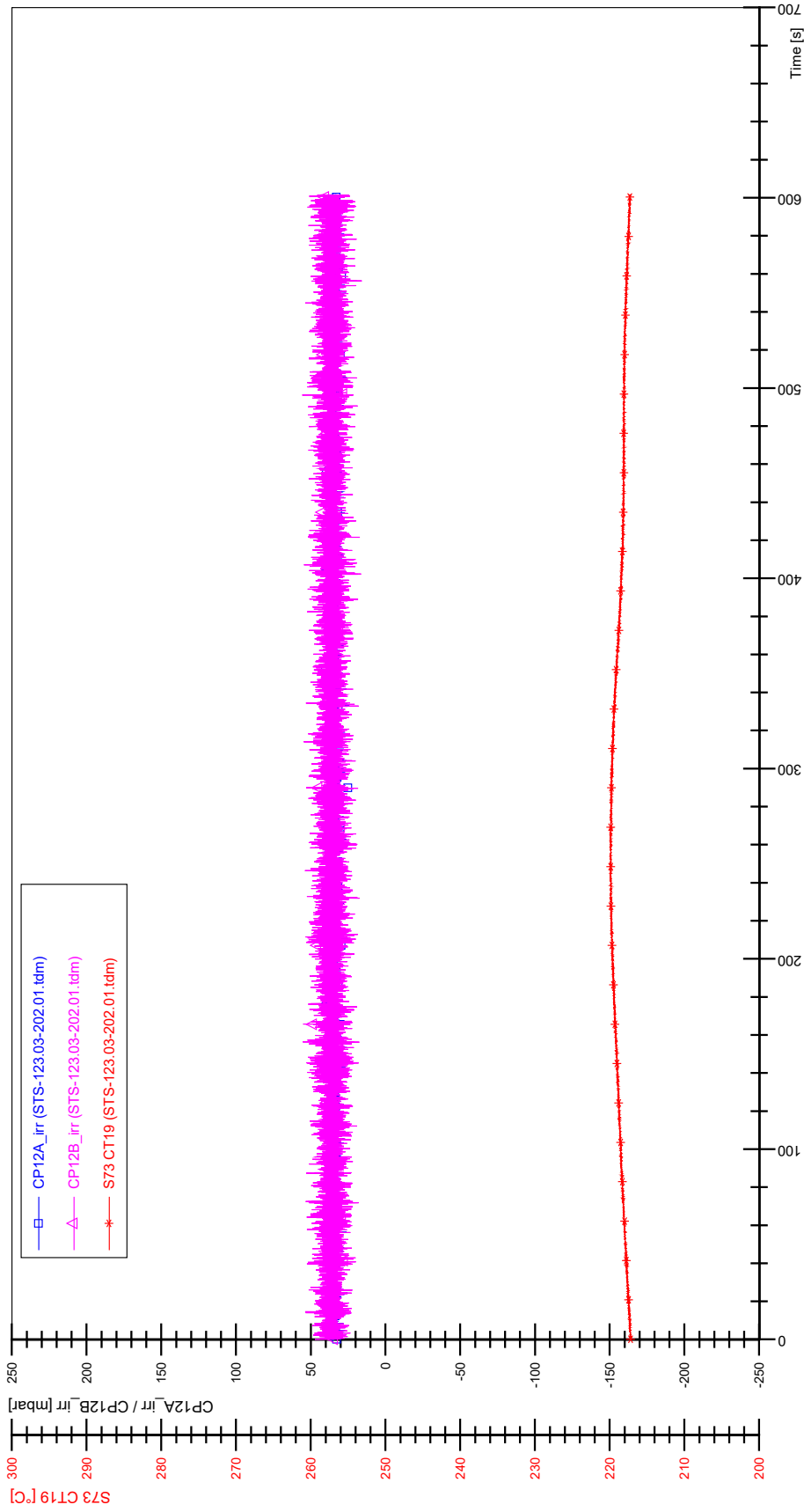


STS-123.03-201.01_Rod_87

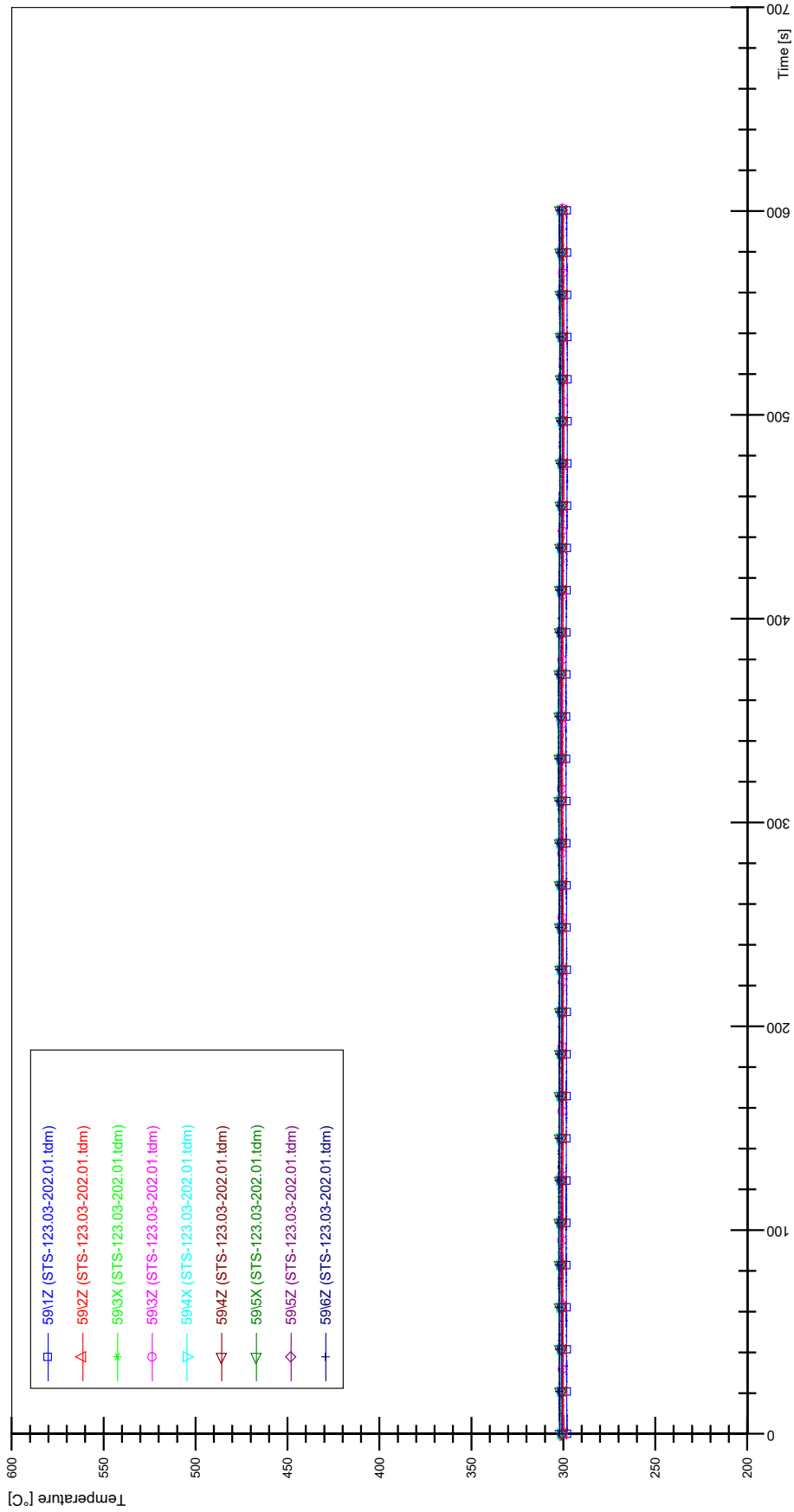


APPENDIX R PLOTS OF INSTABILITY TEST STS-123.03-202.01

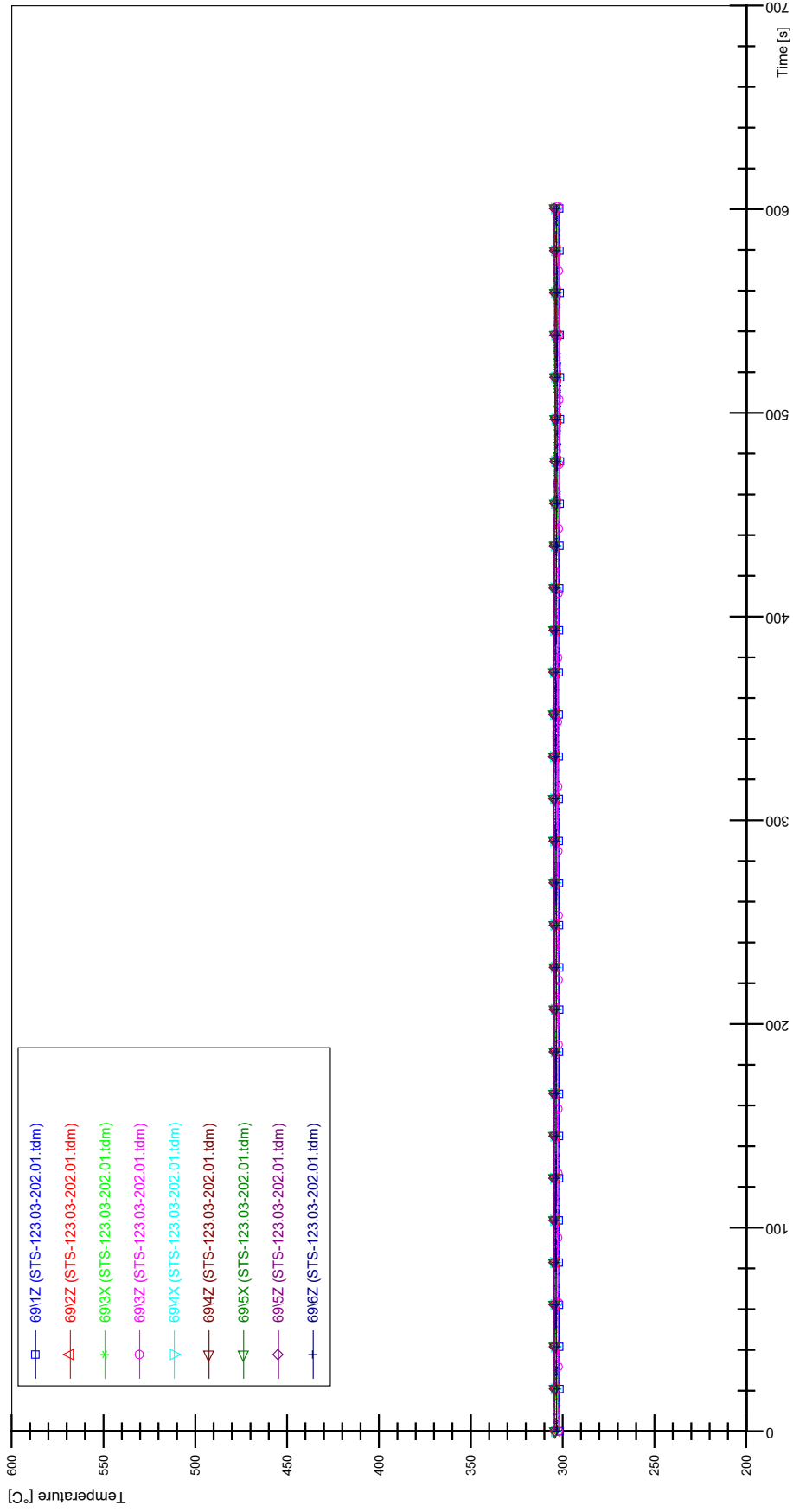




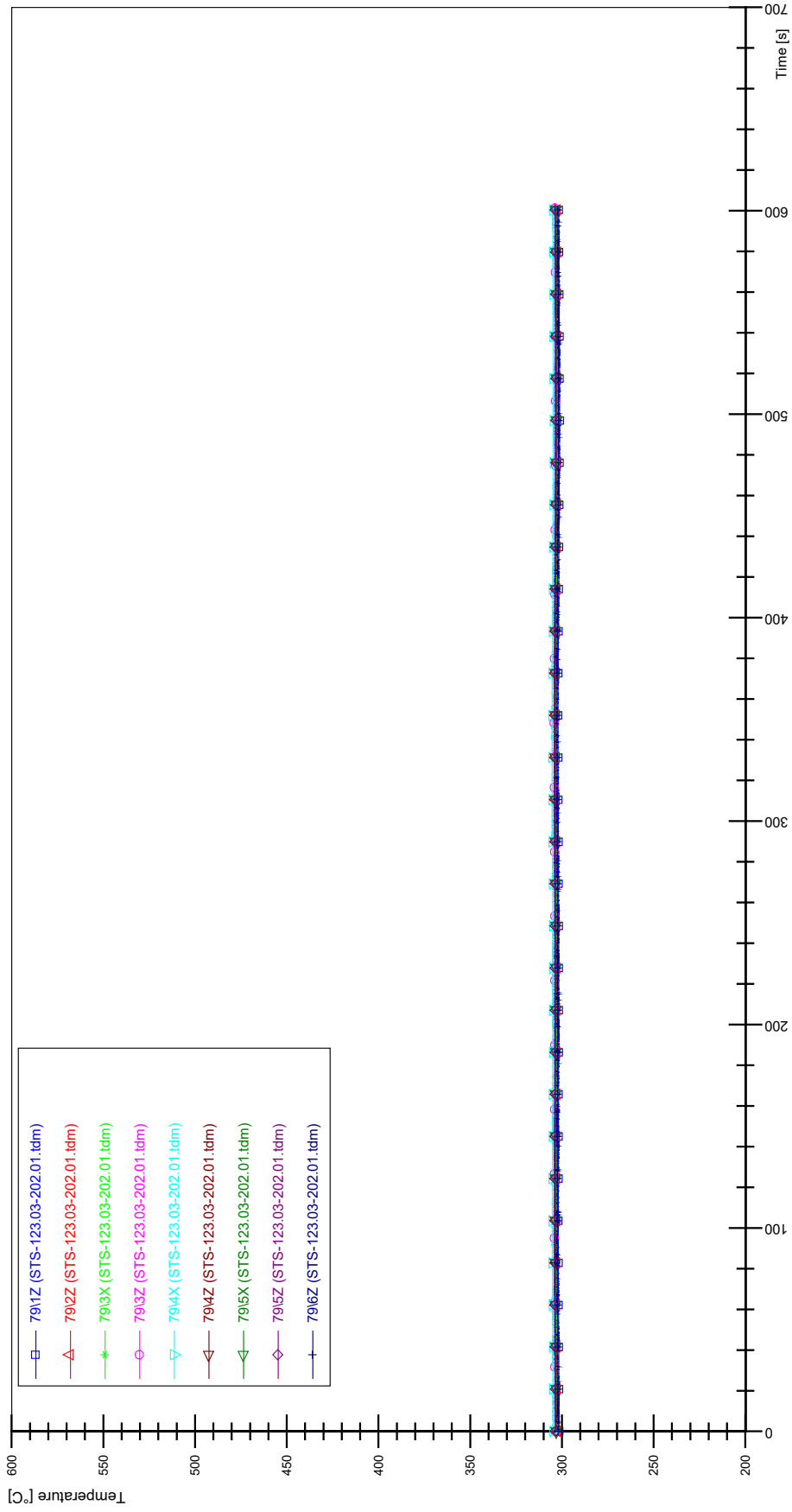
STS-123.03-202.01_Rod_59



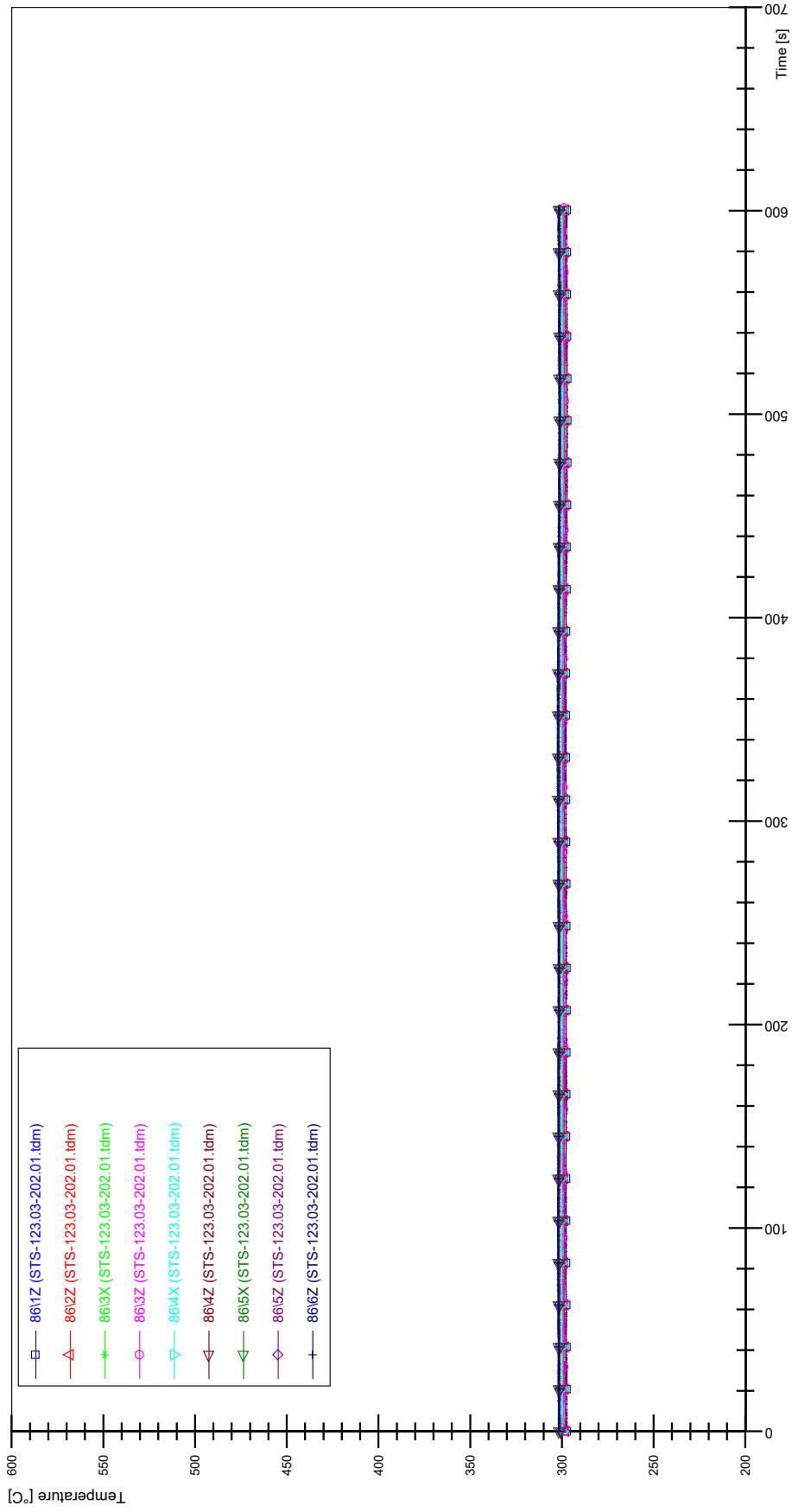
STS-123.03-202.01_Rod_69



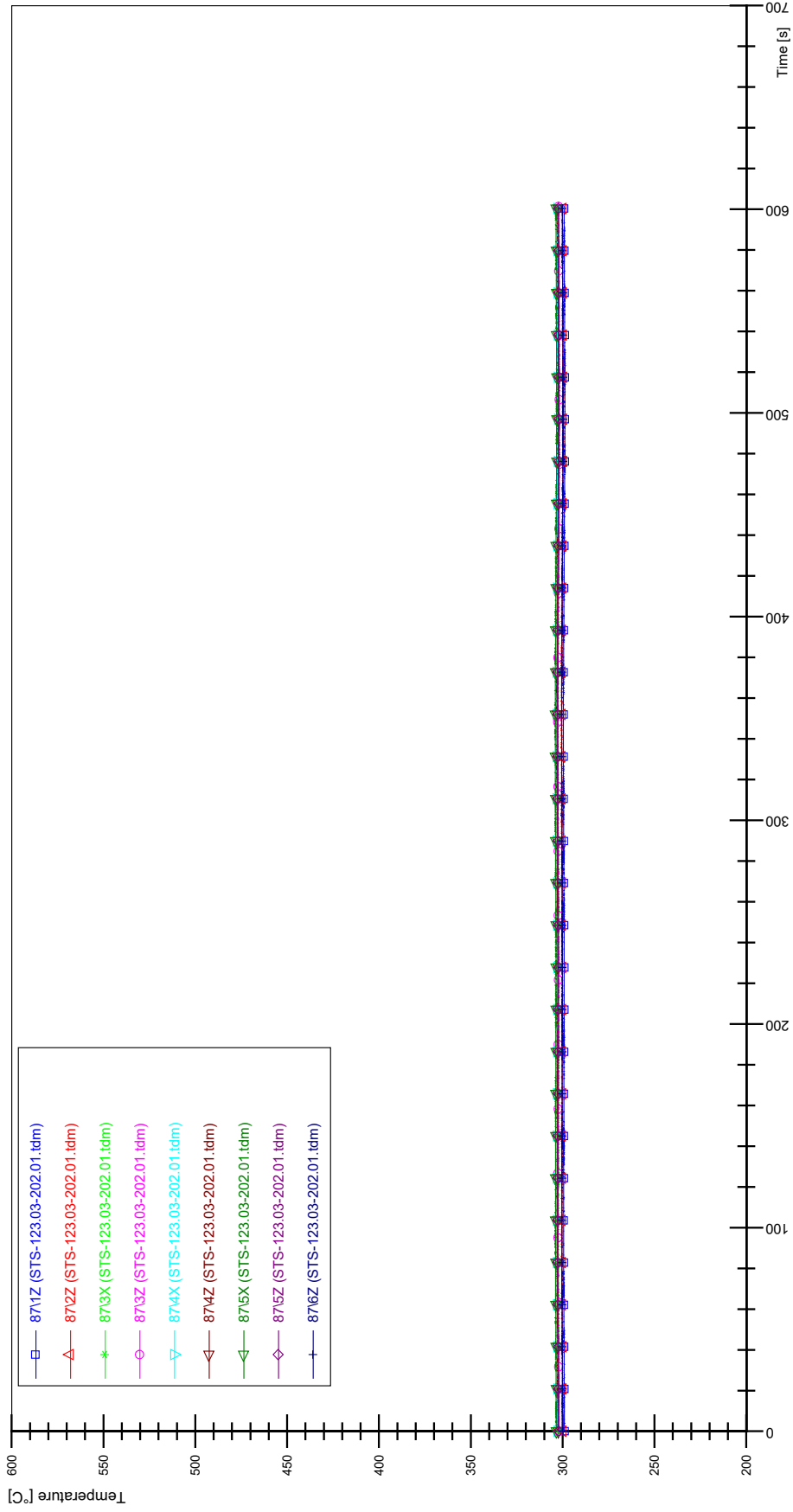
STS-123.03-202.01_Rod_79



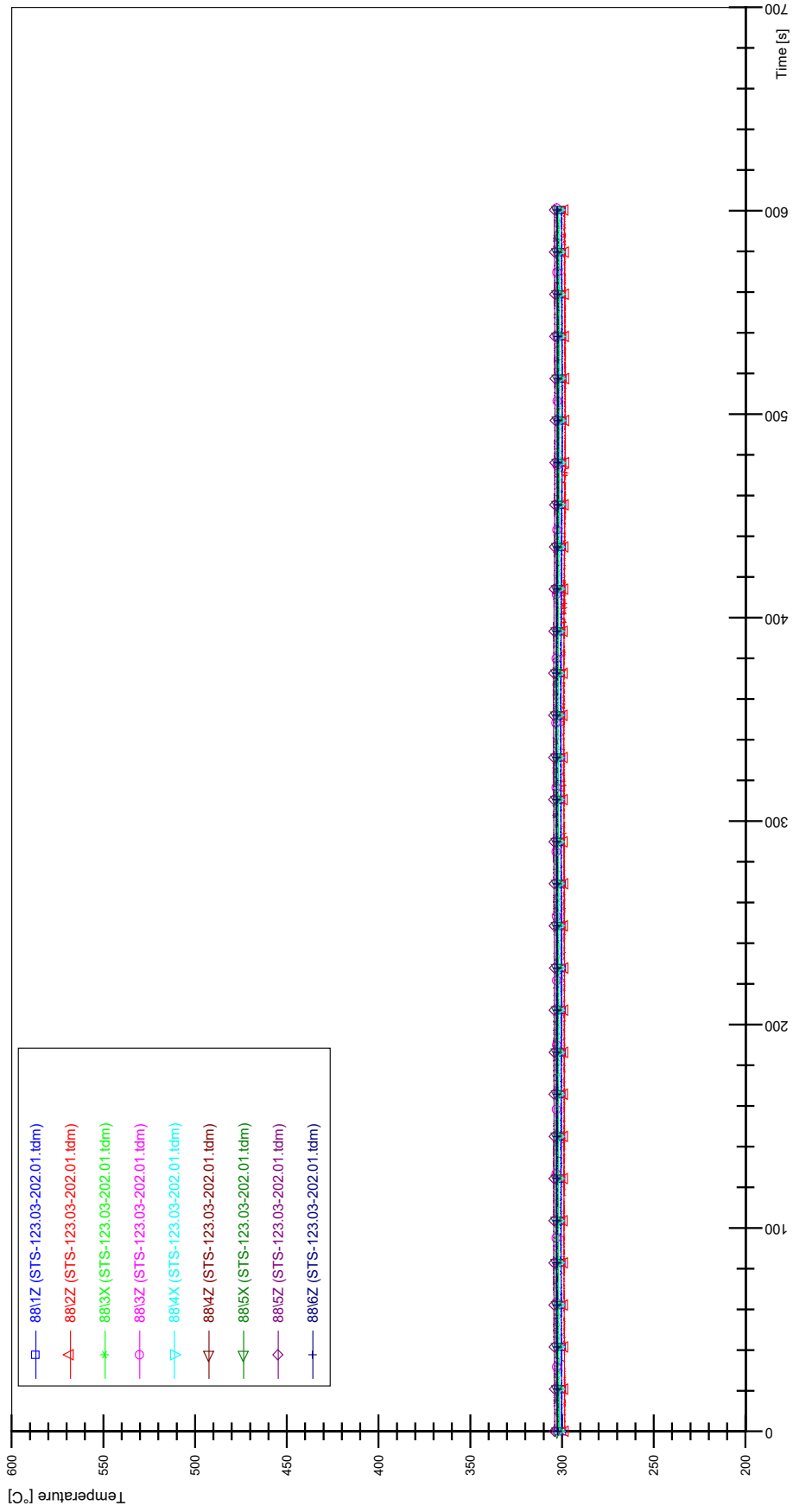
STS-123.03-202.01_Rod_86



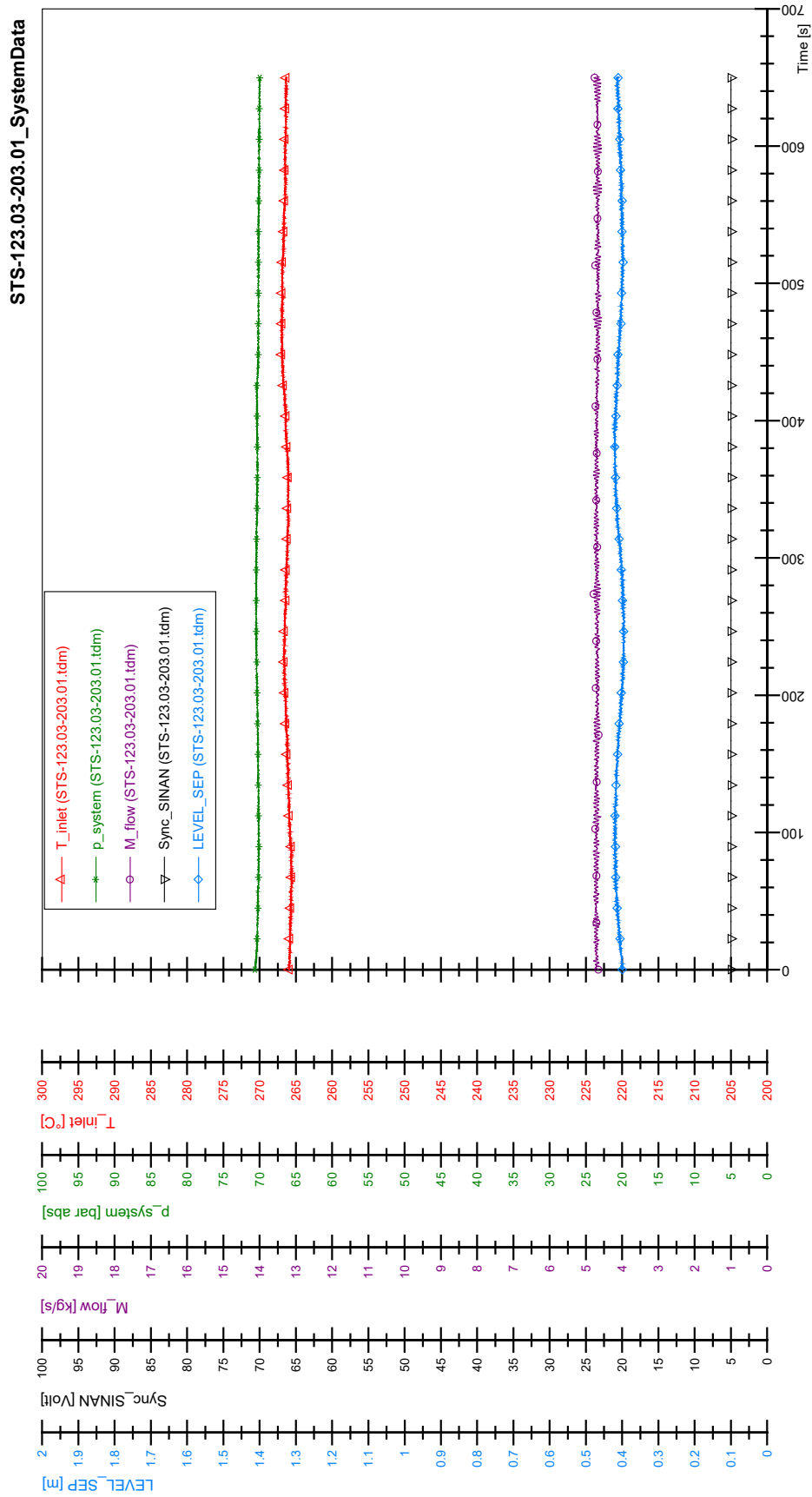
STS-123.03-202.01_Rod_87

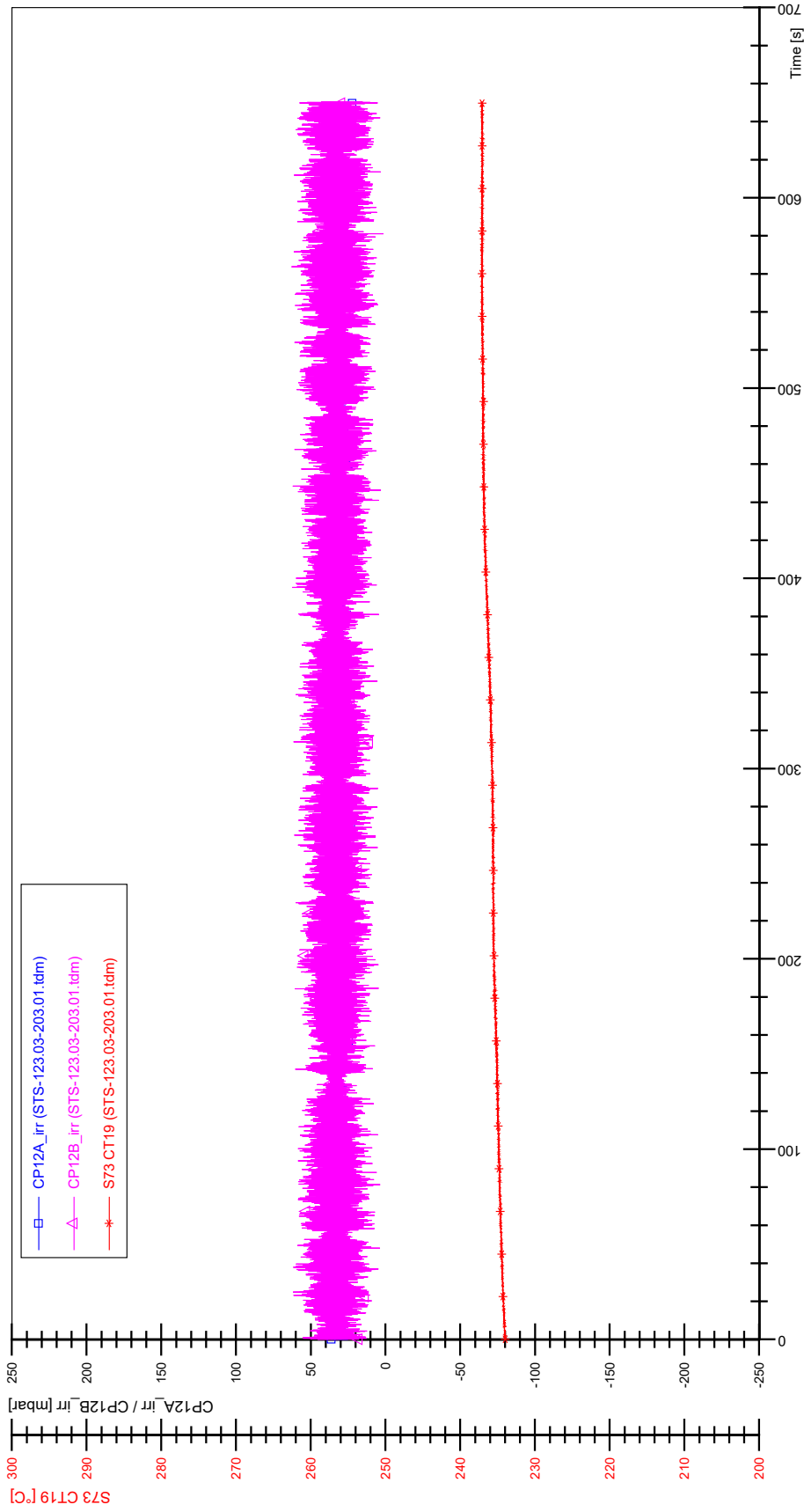


STS-123.03-202.01_Rod_88

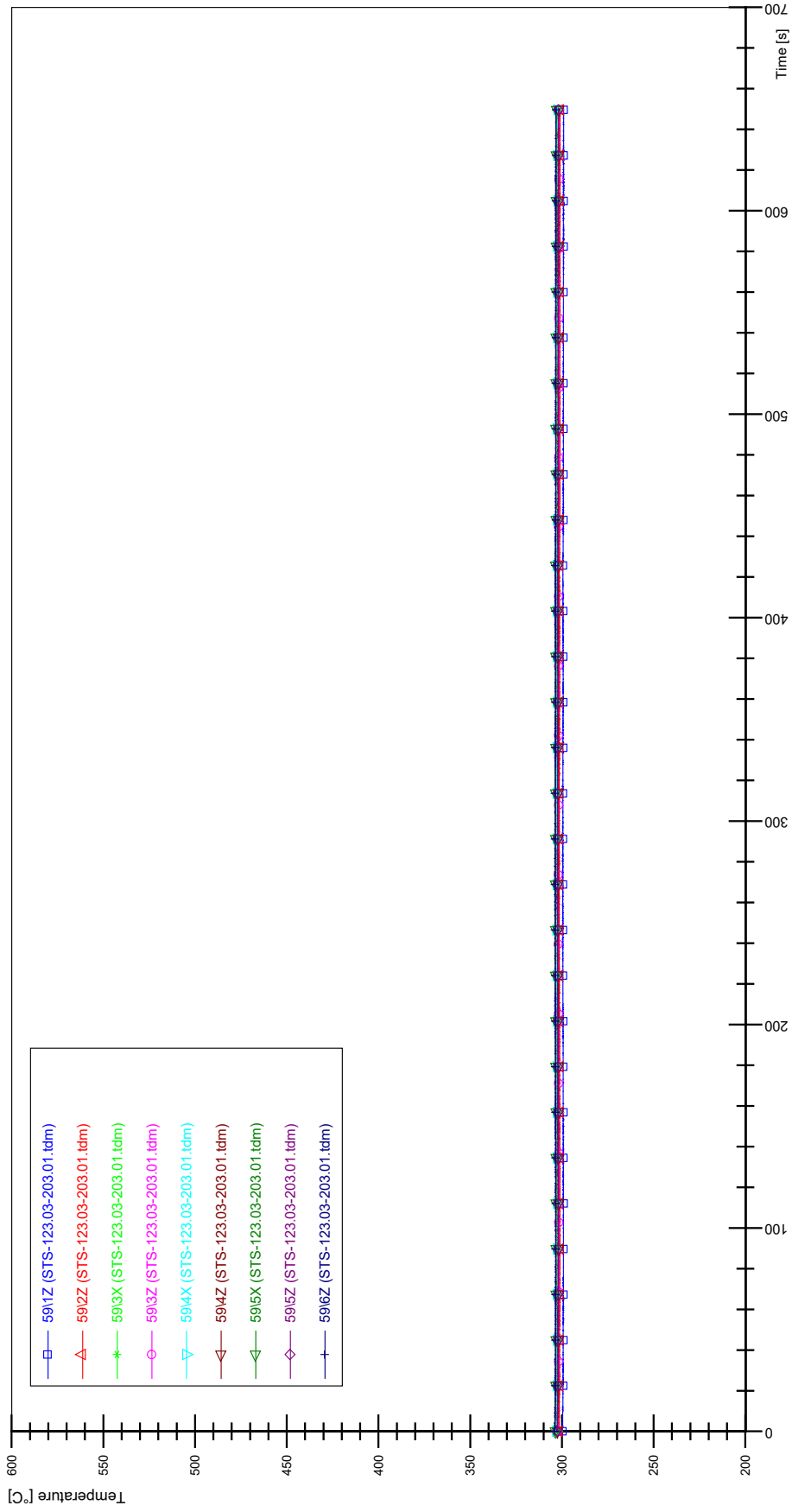


APPENDIX S PLOTS OF INSTABILITY TEST STS-123.03-203.01

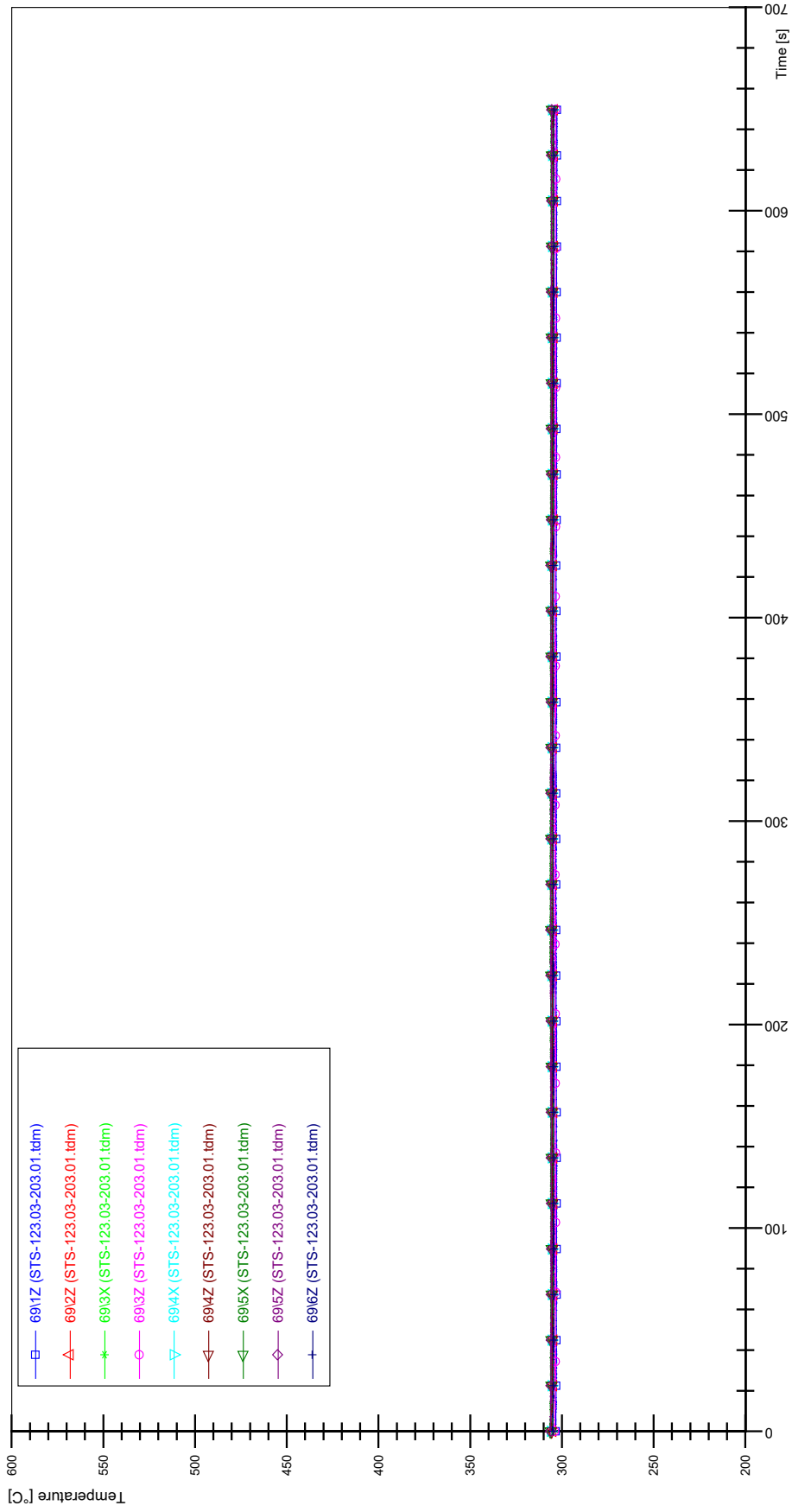




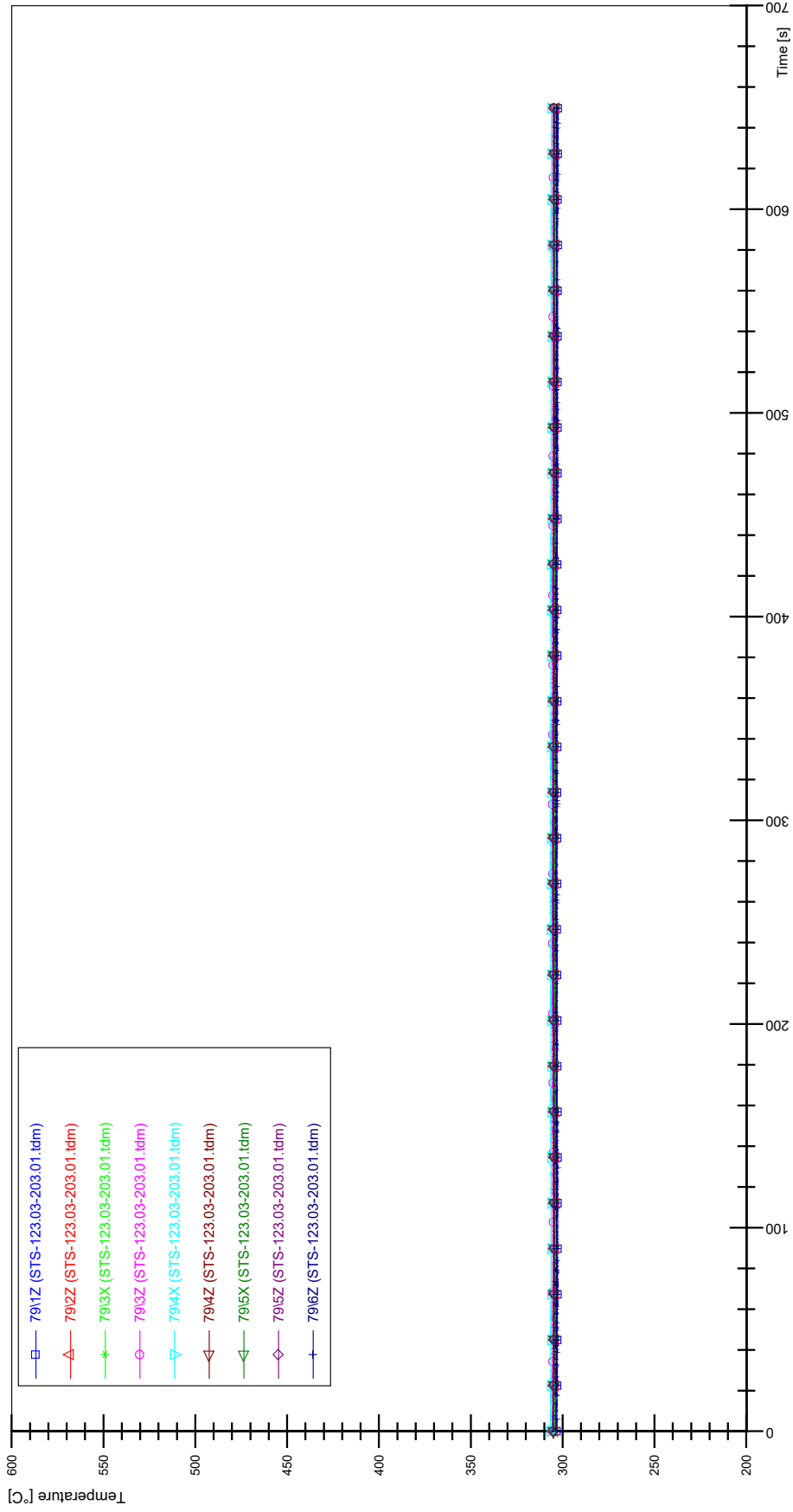
STS-123.03-203.01_Rod_59



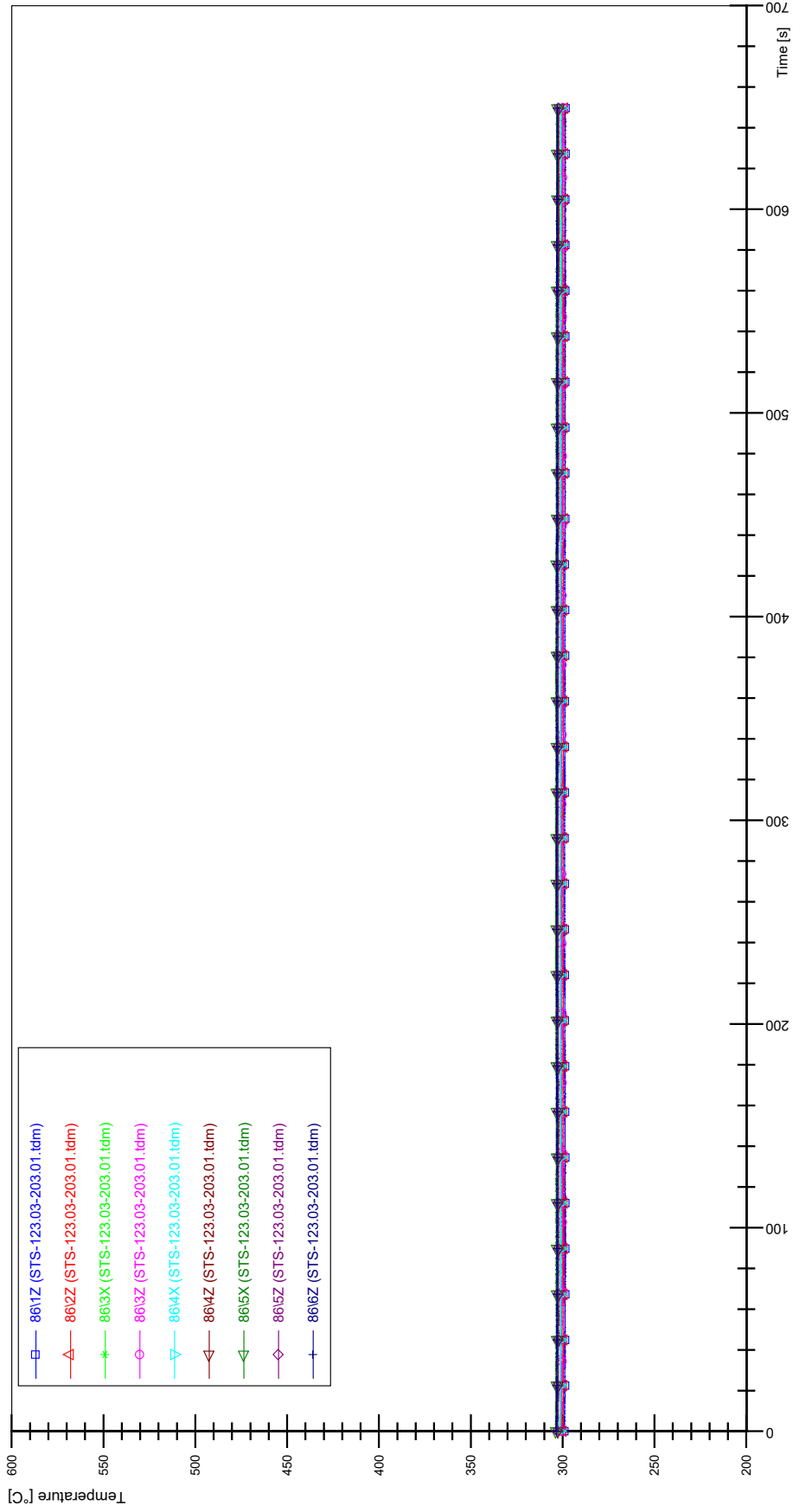
STS-123.03-203.01_Rod_69



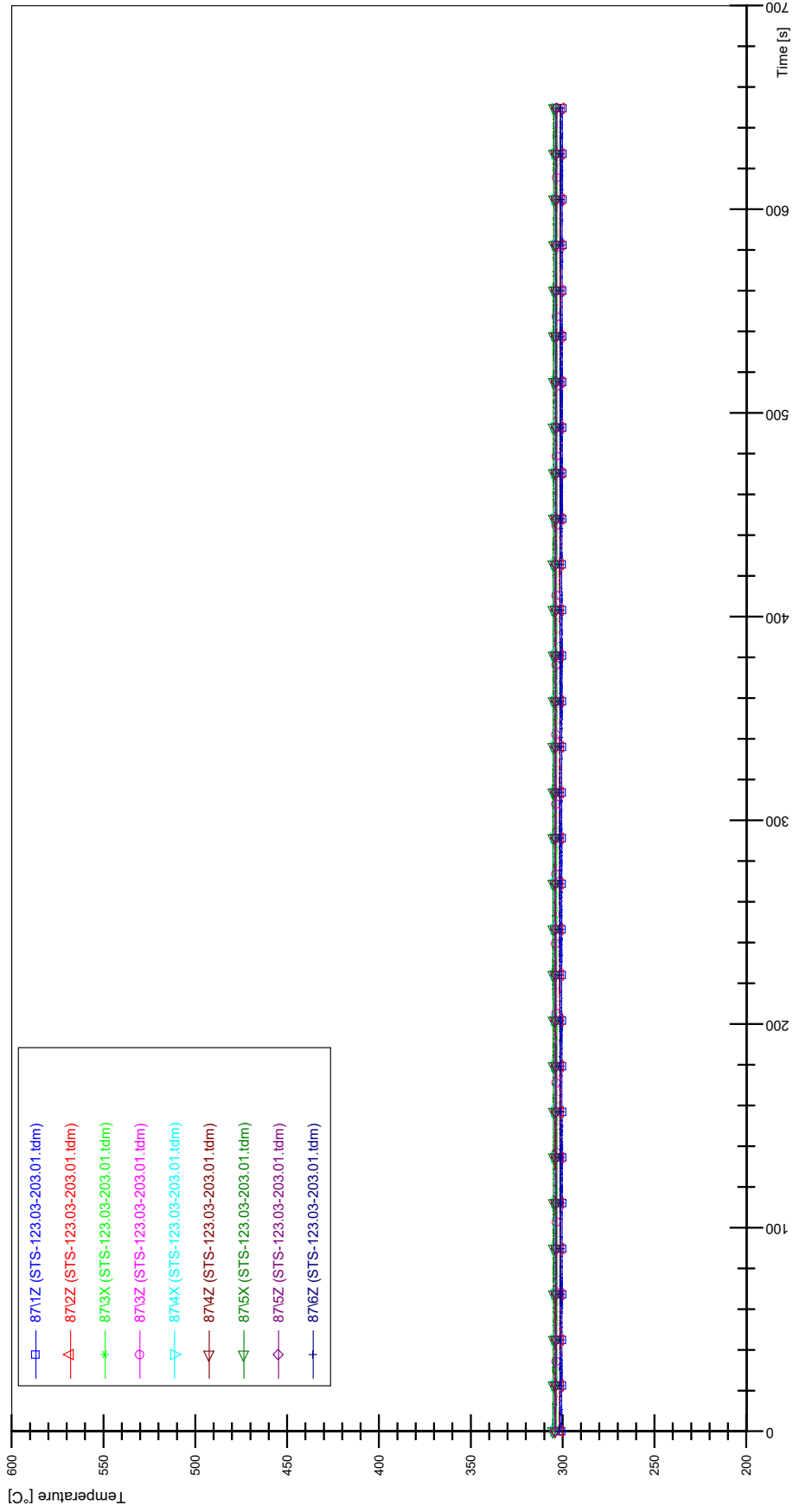
STS-123.03-203.01_Rod_79



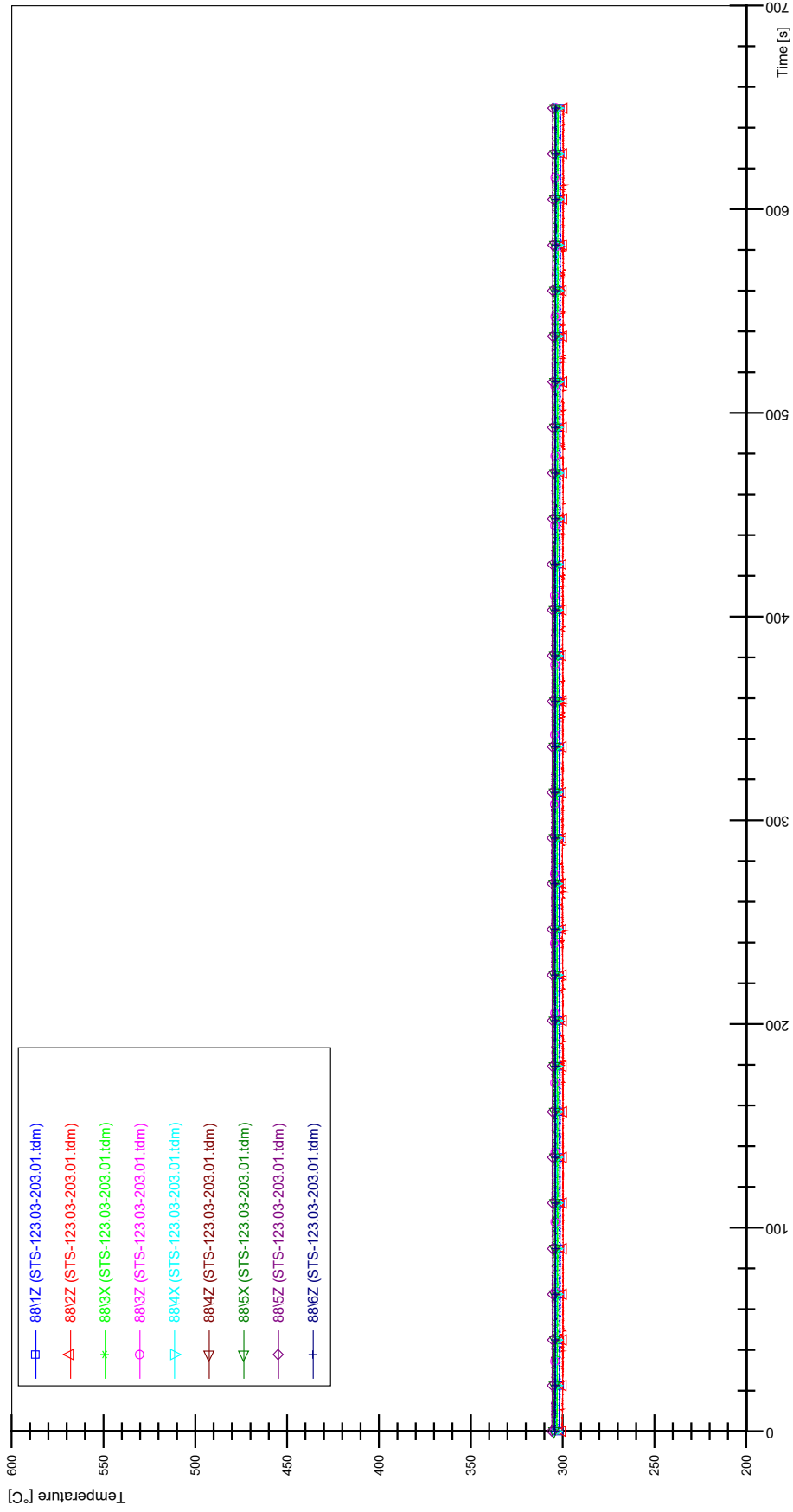
STS-123.03-203.01_Rod_86



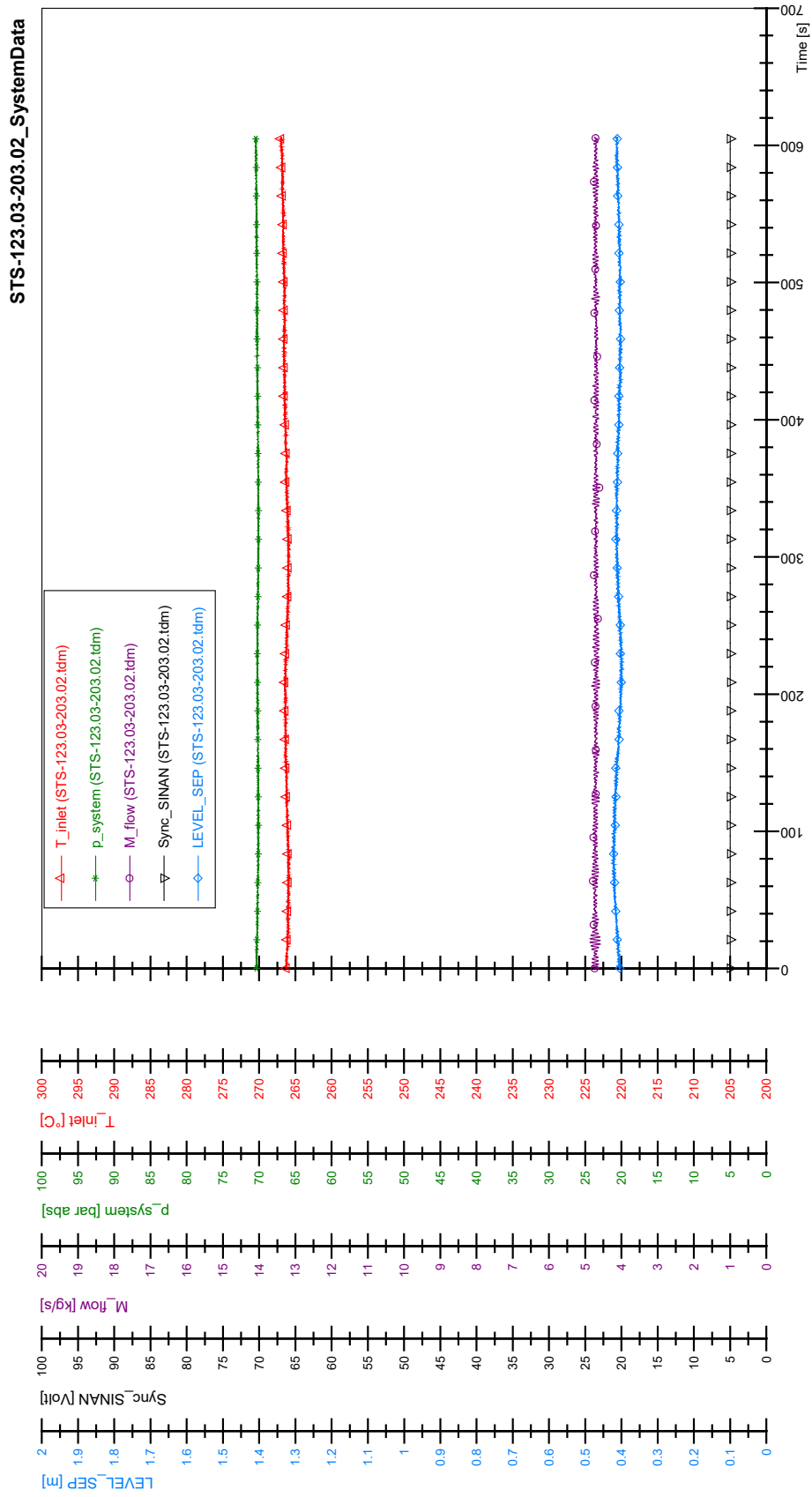
STS-123.03-203.01_Rod_87

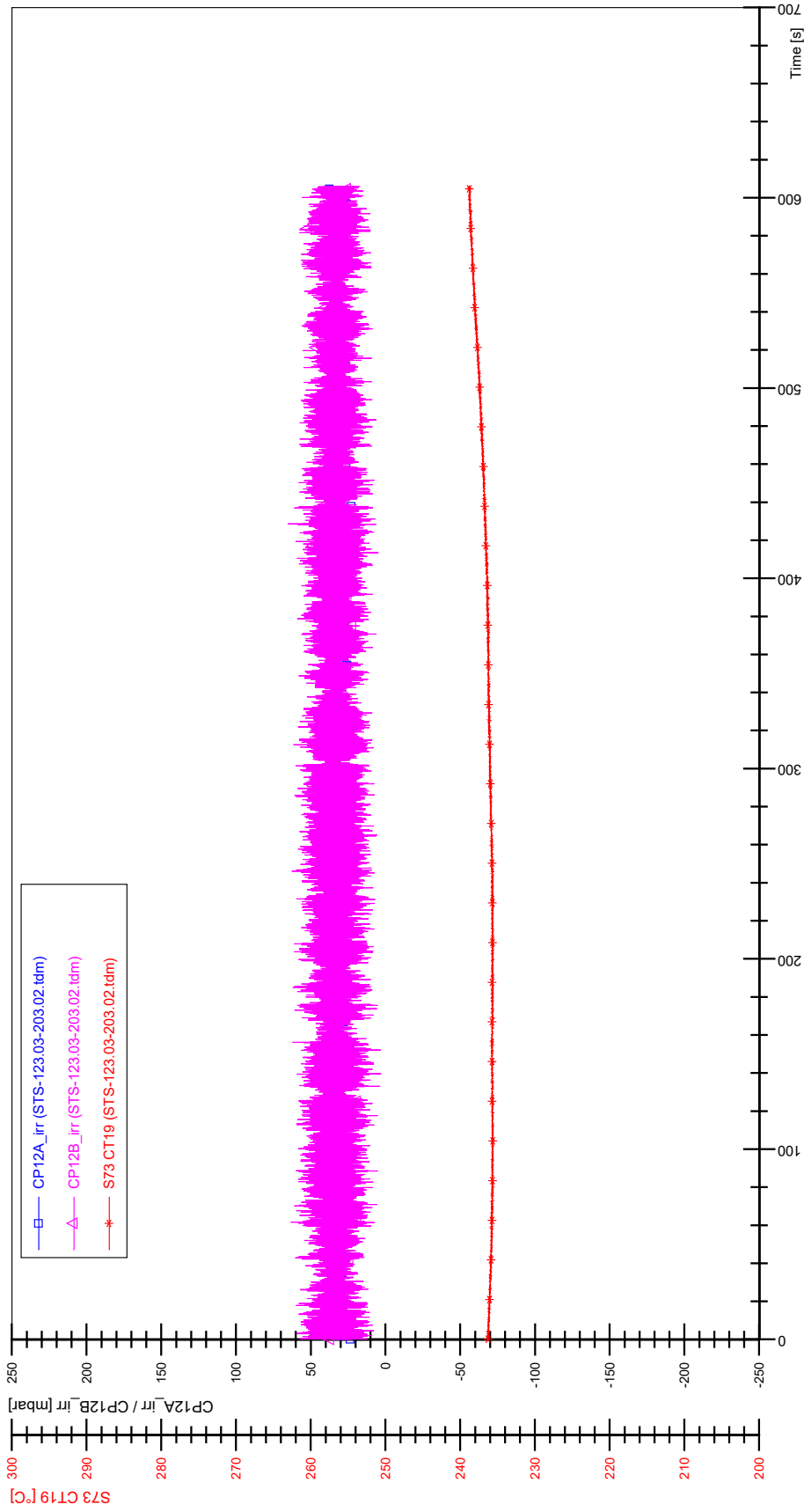


STS-123.03-203.01_Rod_88

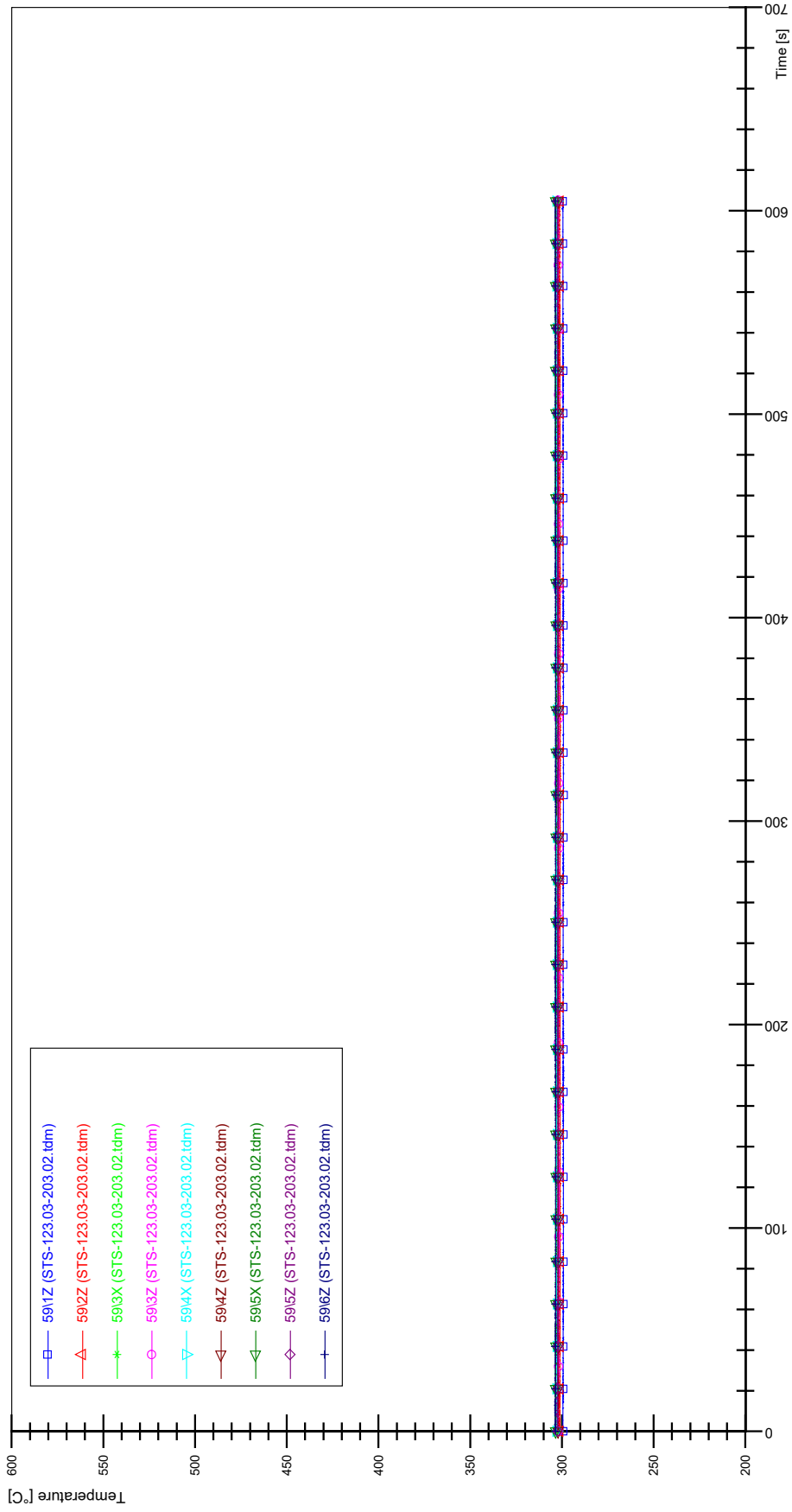


APPENDIX T PLOTS OF INSTABILITY TEST STS-123.03-203.02

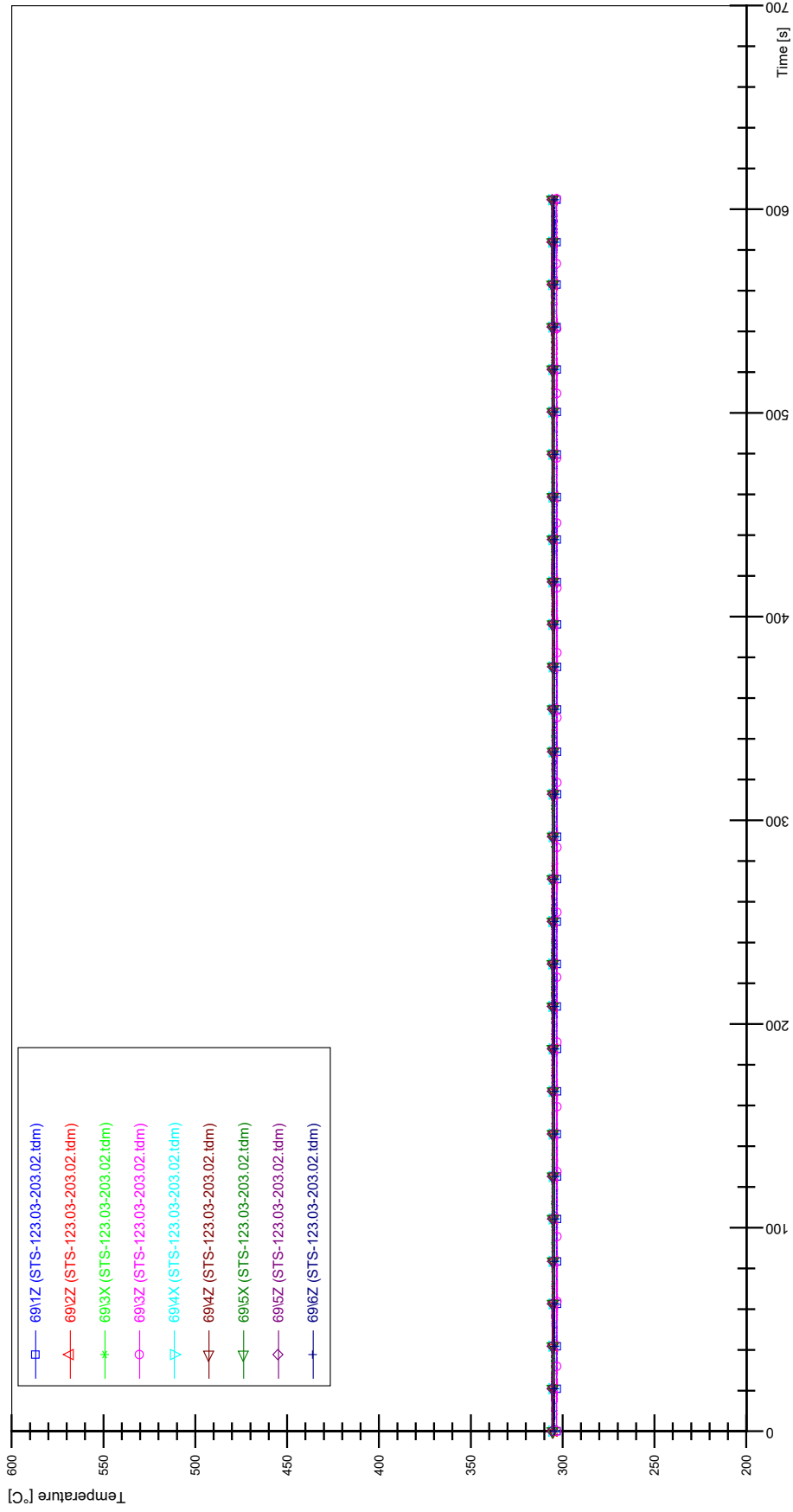




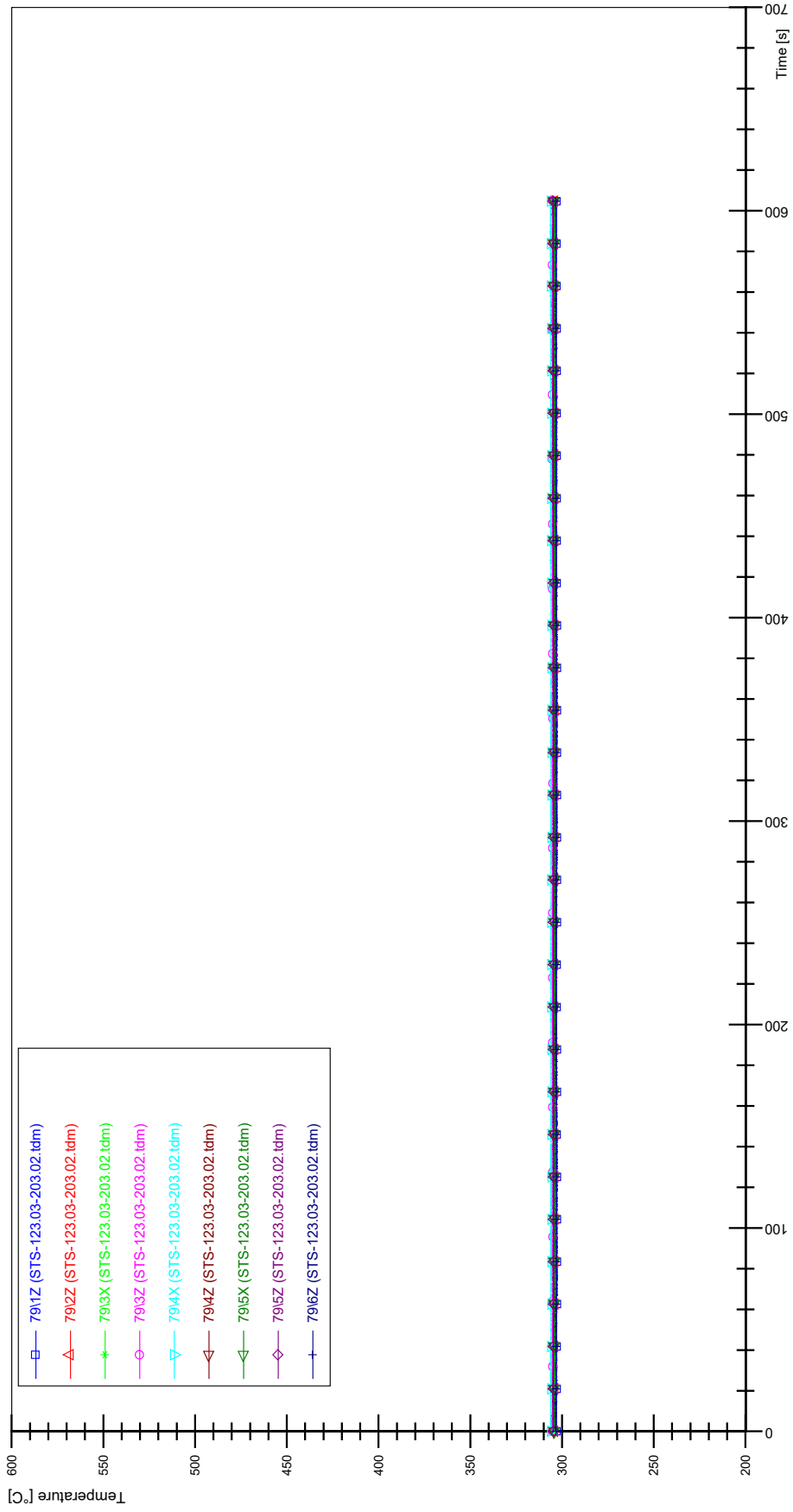
STS-123.03-203.02_Rod_59



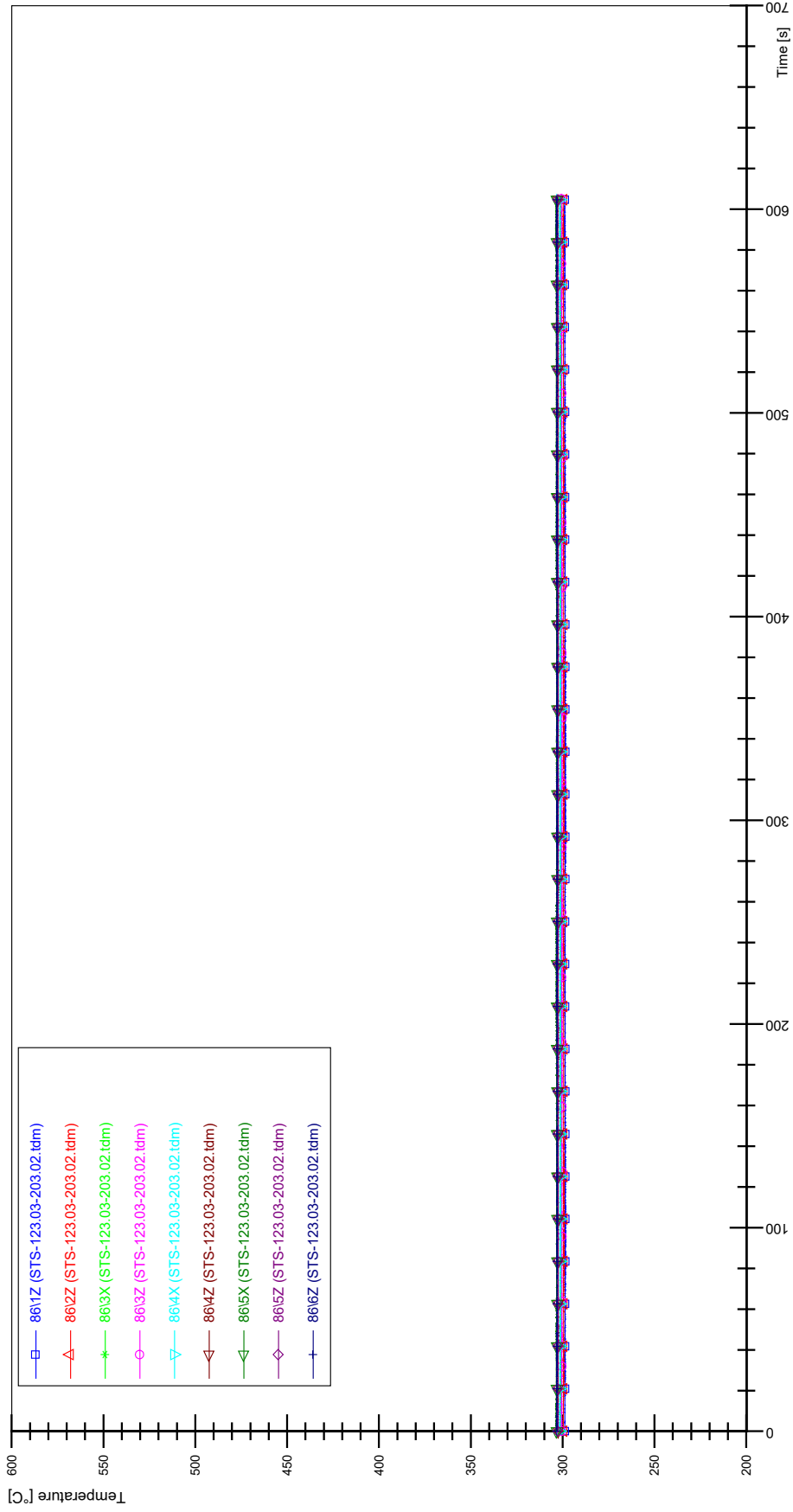
STS-123.03-203.02_Rod_69



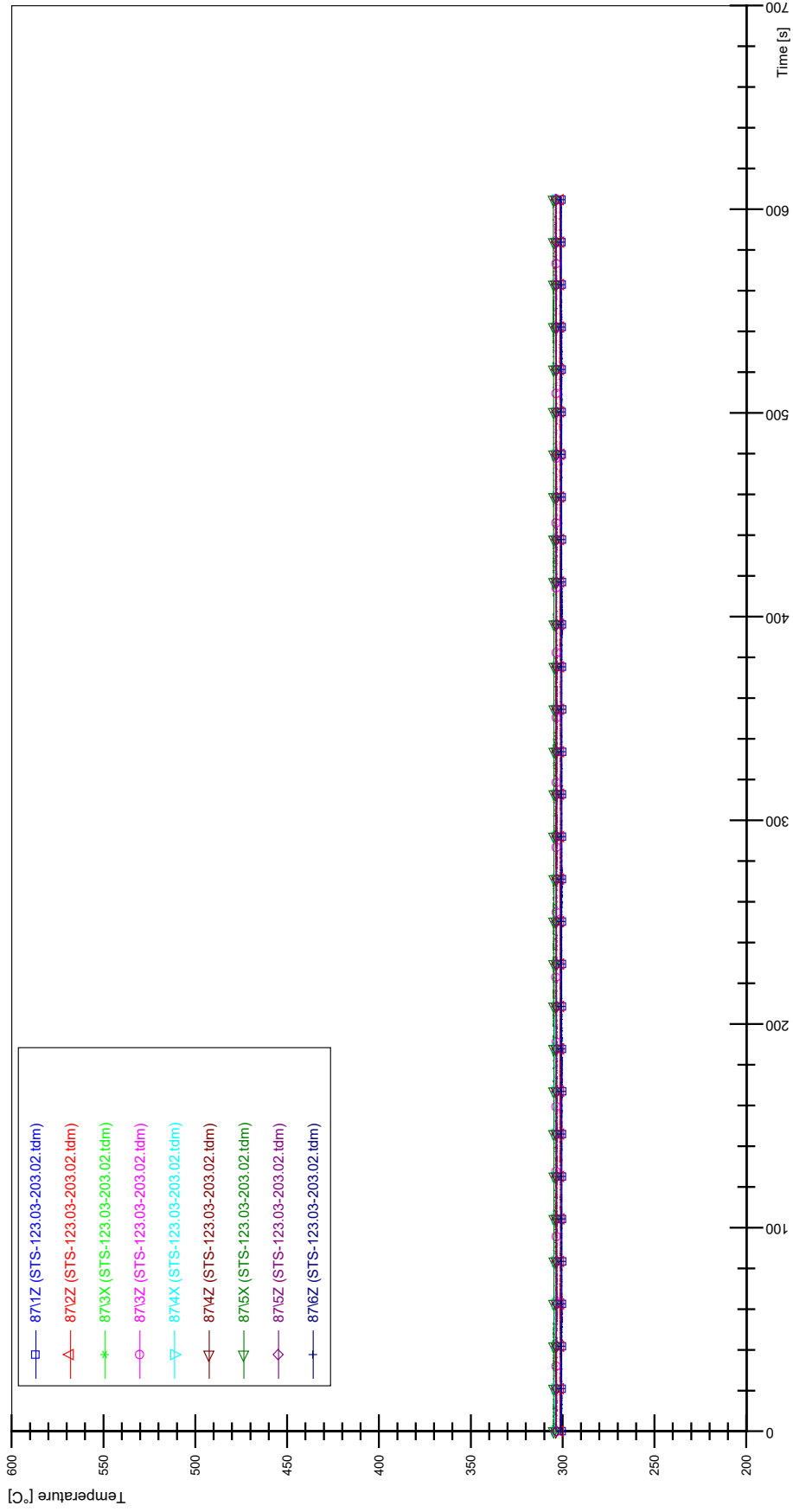
STS-123.03-203.02_Rod_79



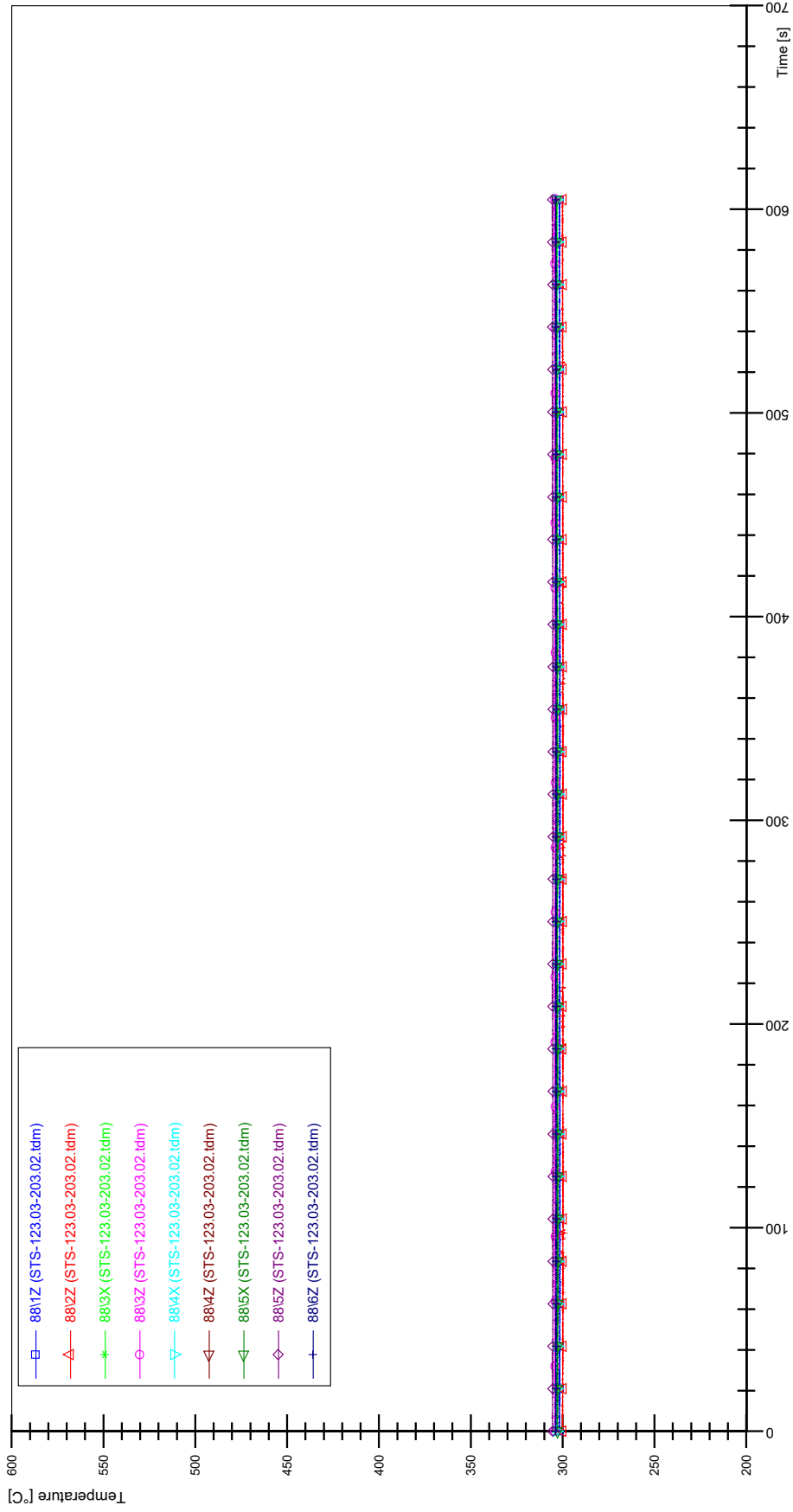
STS-123.03-203.02_Rod_86



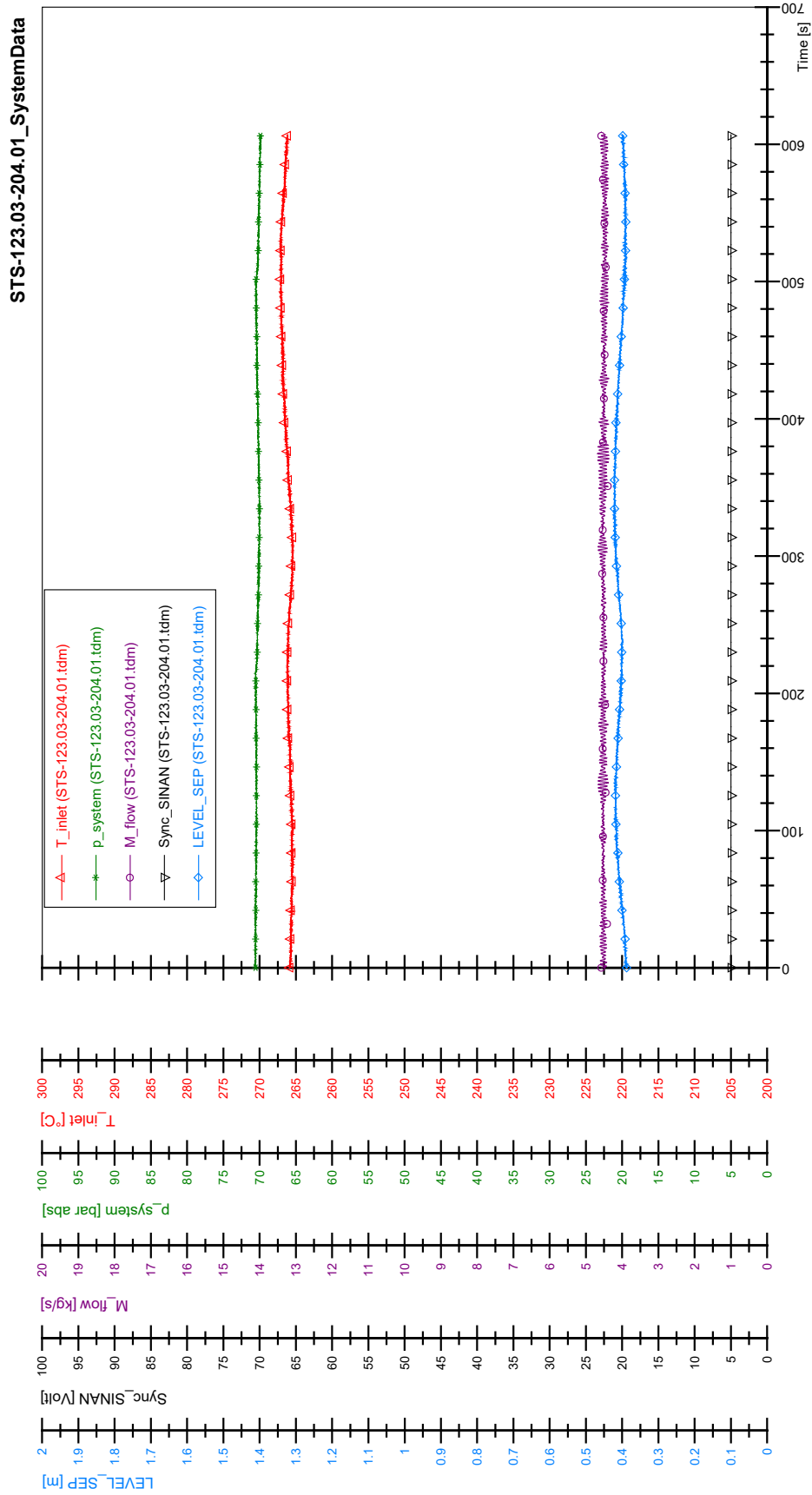
STS-123.03-203.02_Rod_87



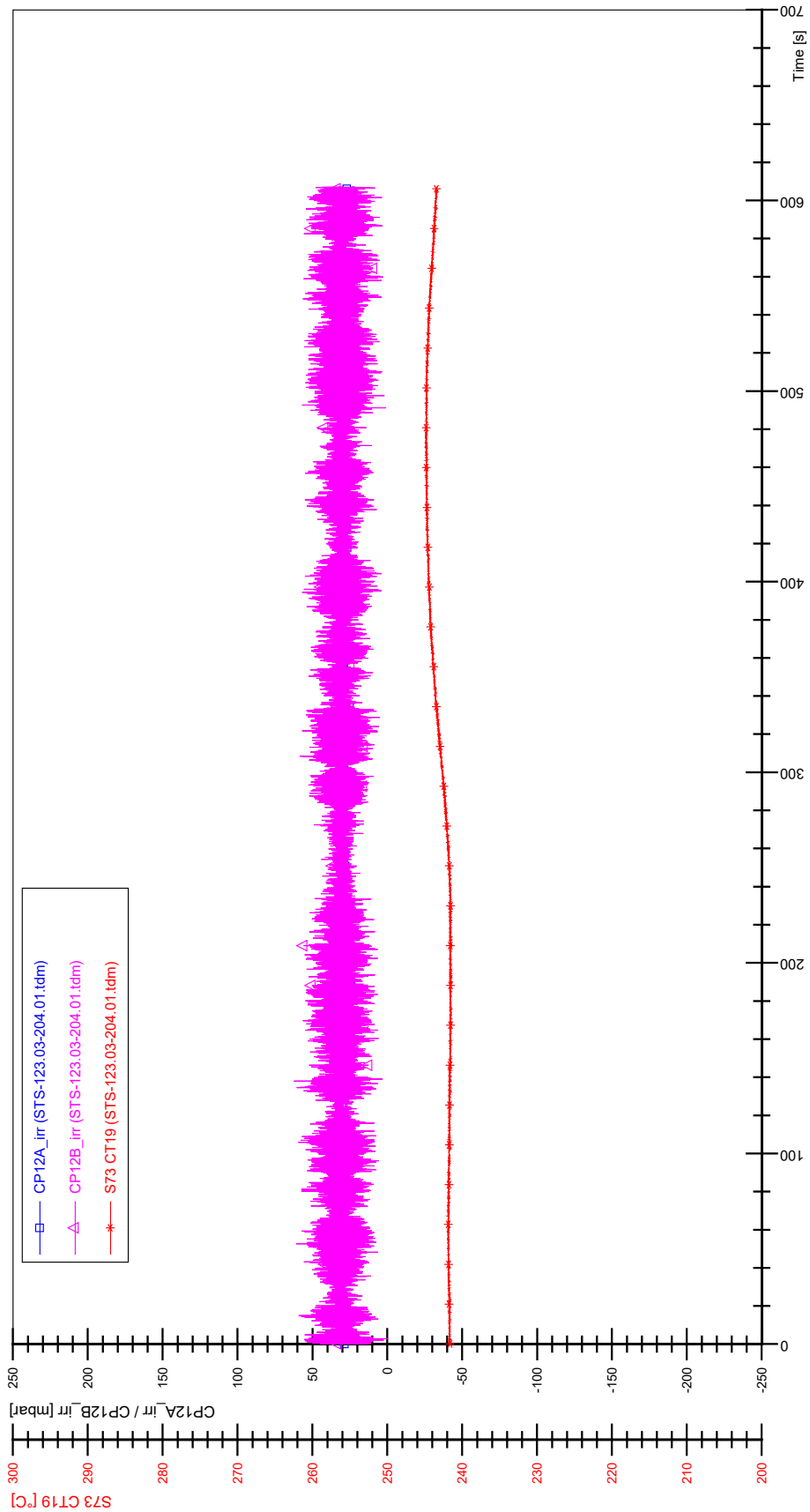
STS-123.03-203.02_Rod_88



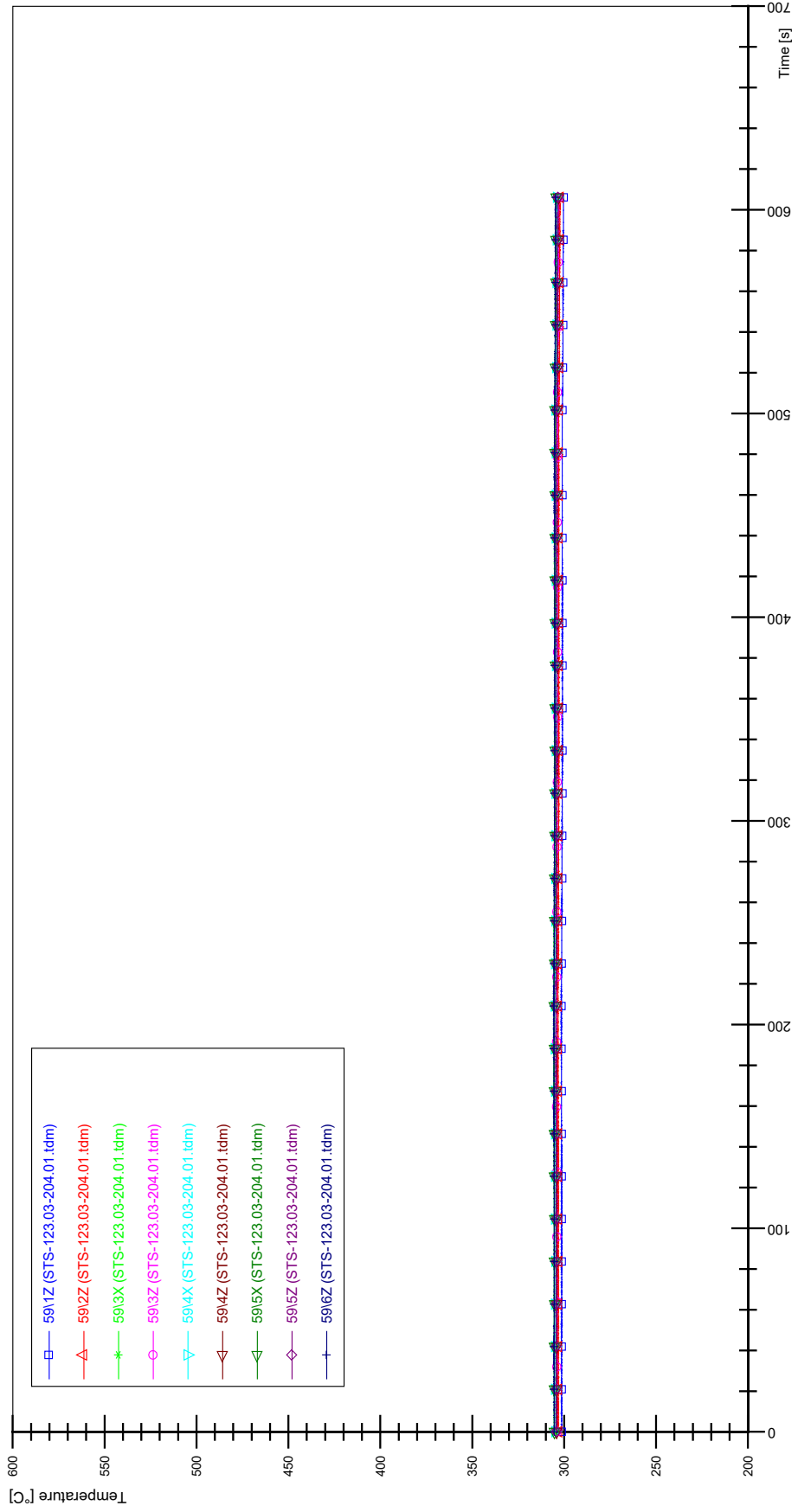
APPENDIX U PLOTS OF INSTABILITY TEST STS-123.03-204.01



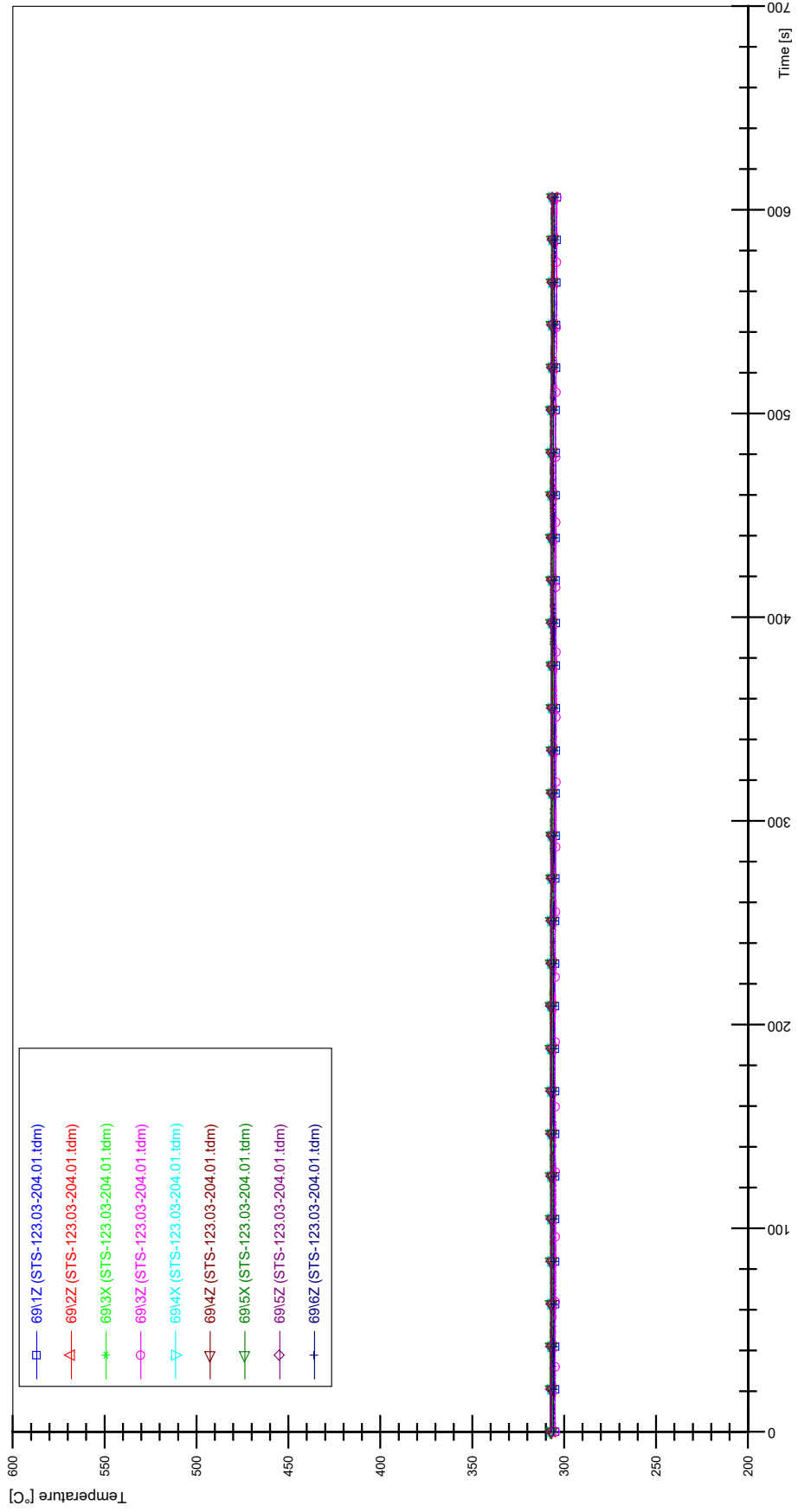
STS-123.03-204.01_CP12_CT19



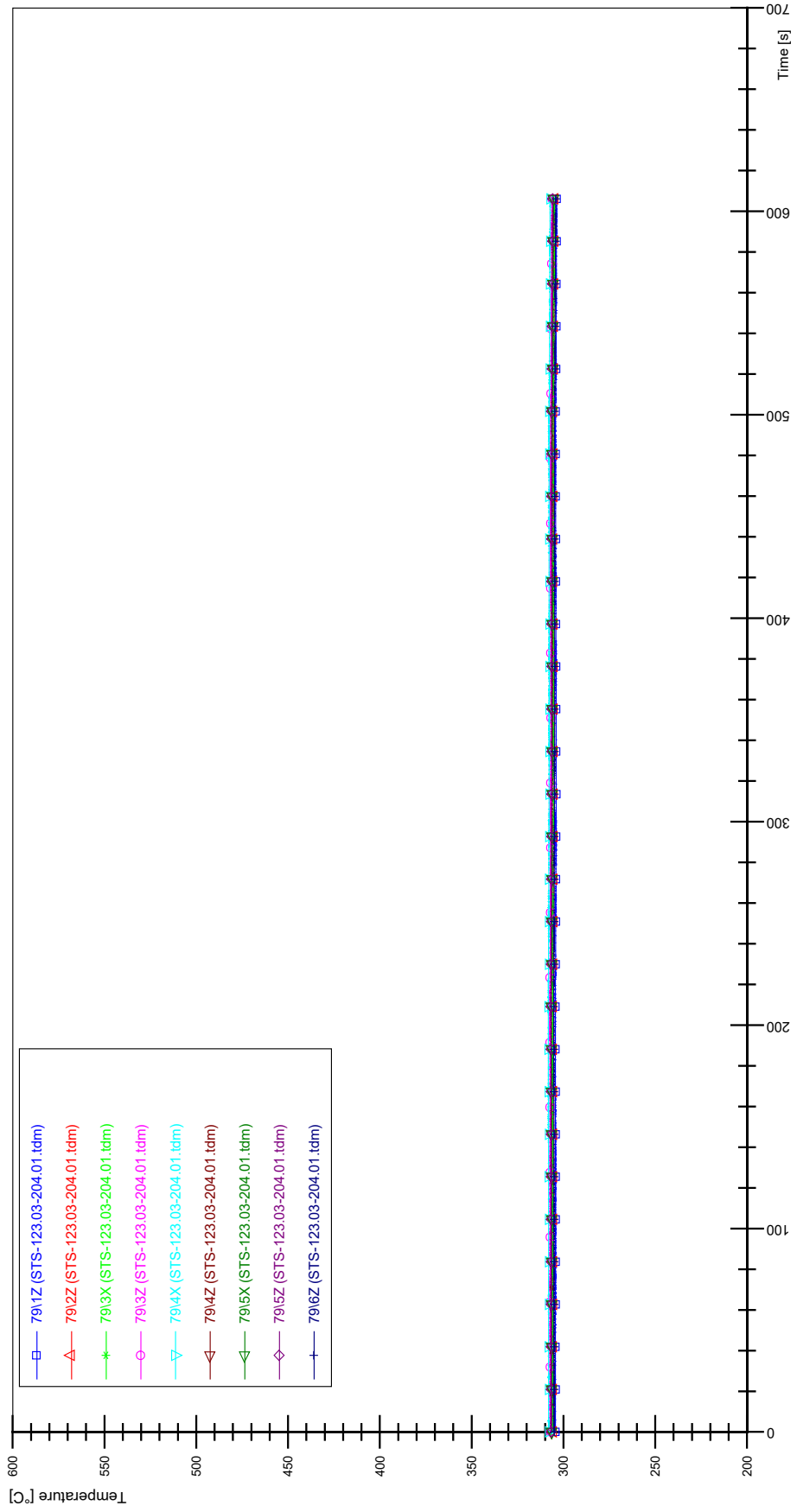
STS-123.03-204.01_Rod_59



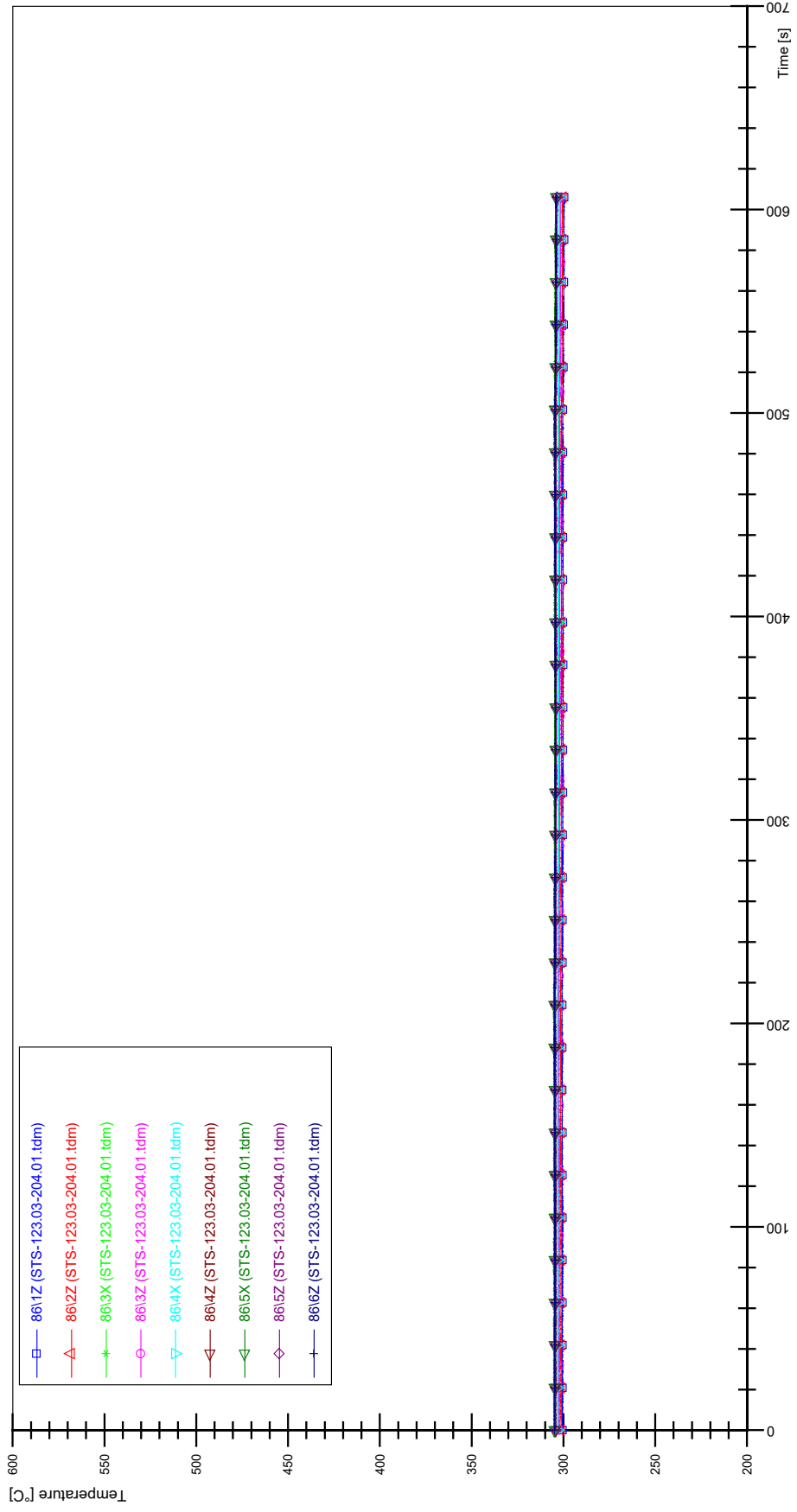
STS-123.03-204.01_Rod_69



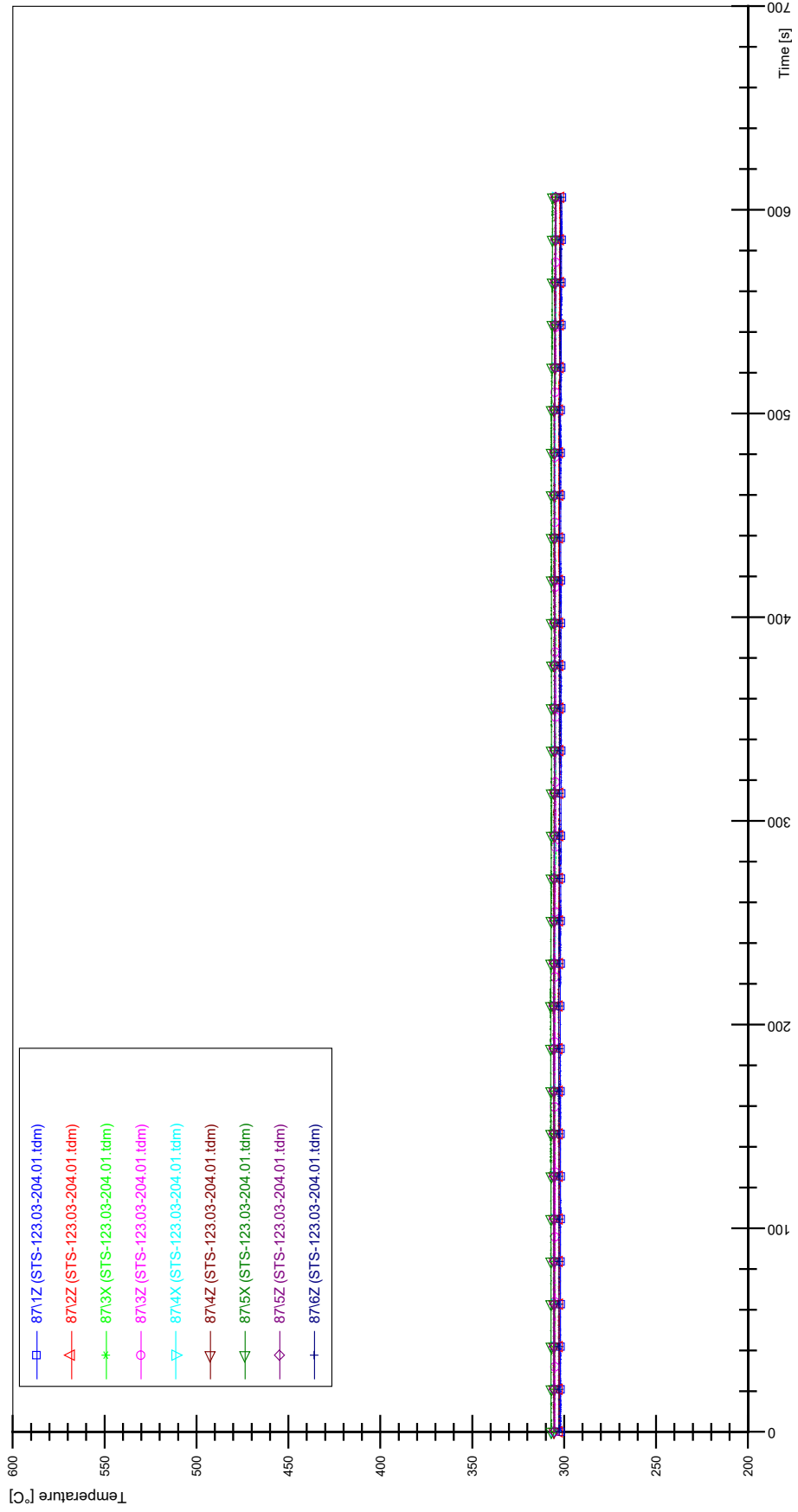
STS-123.03-204.01_Rod_79



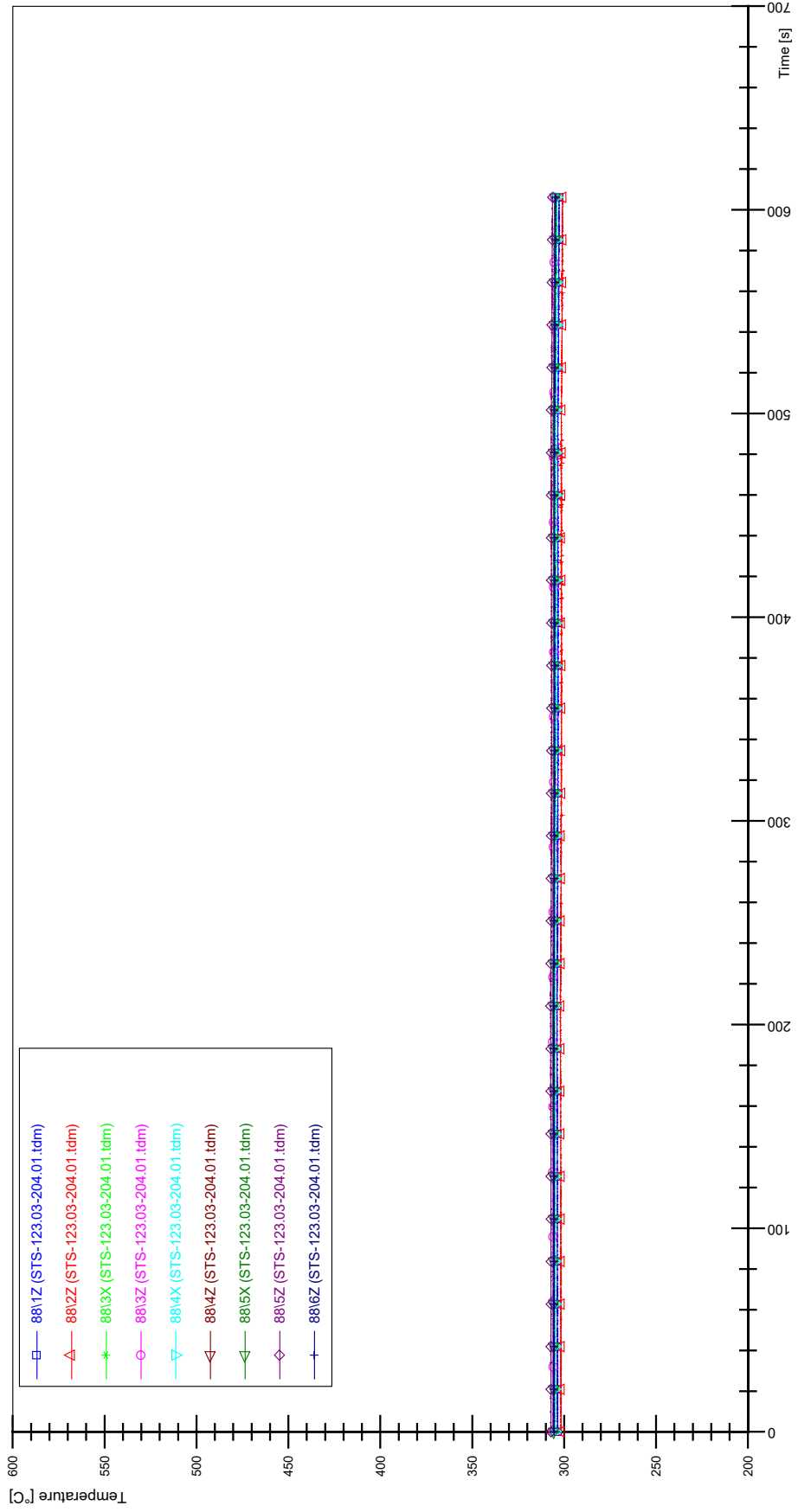
STS-123.03-204.01_Rod_86



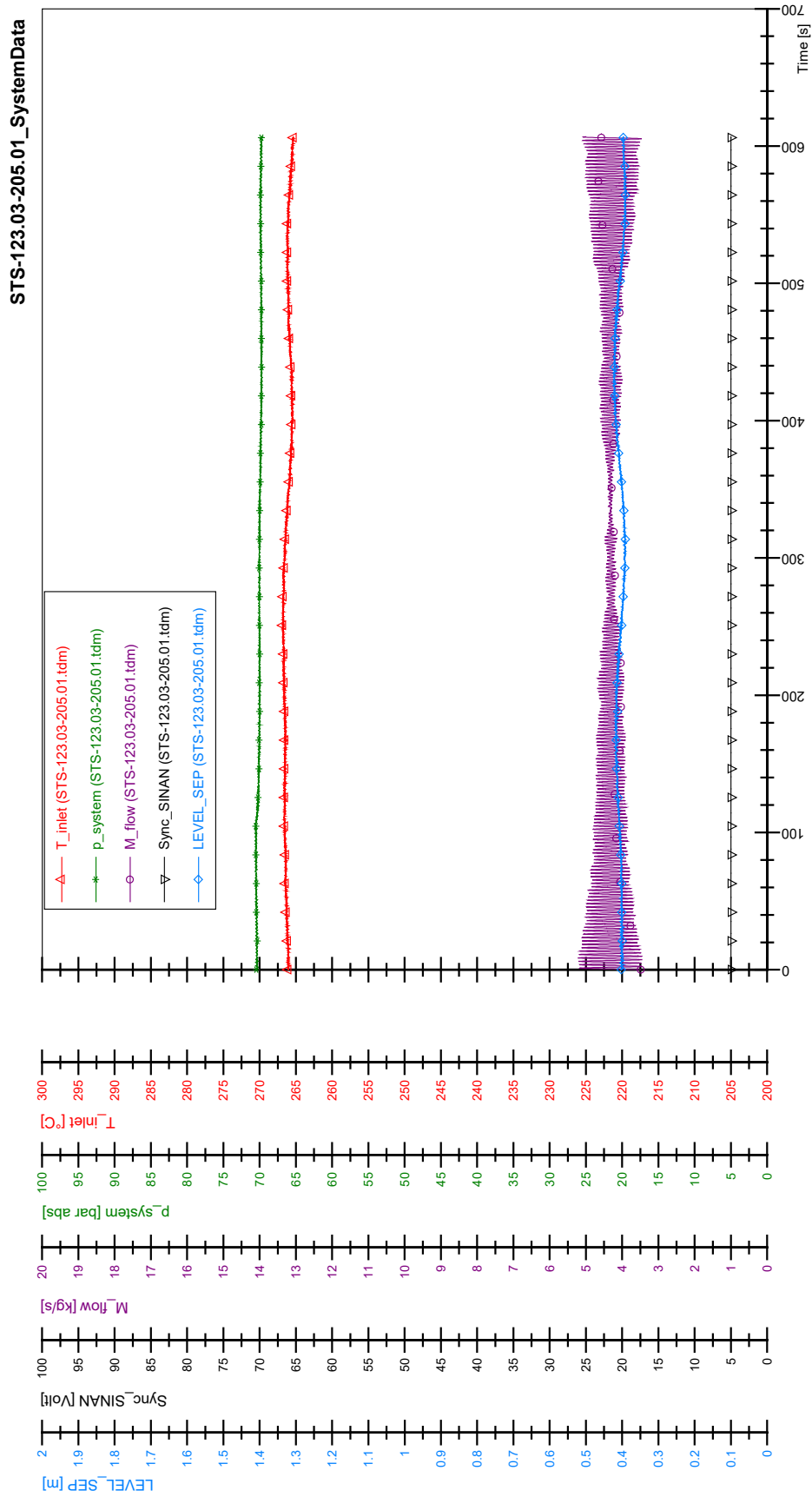
STS-123.03-204.01_Rod_87



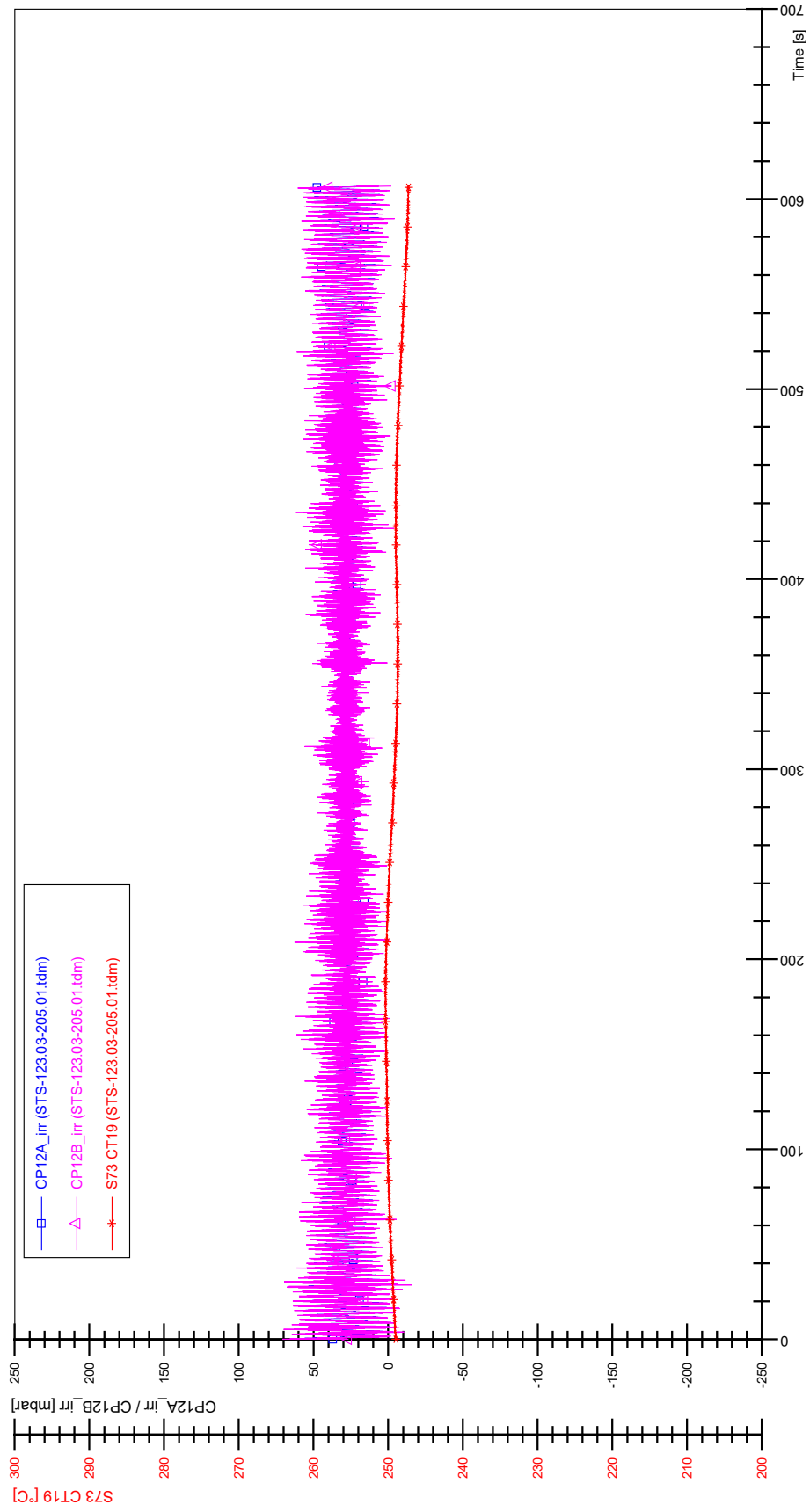
STS-123.03-204.01_Rod_88



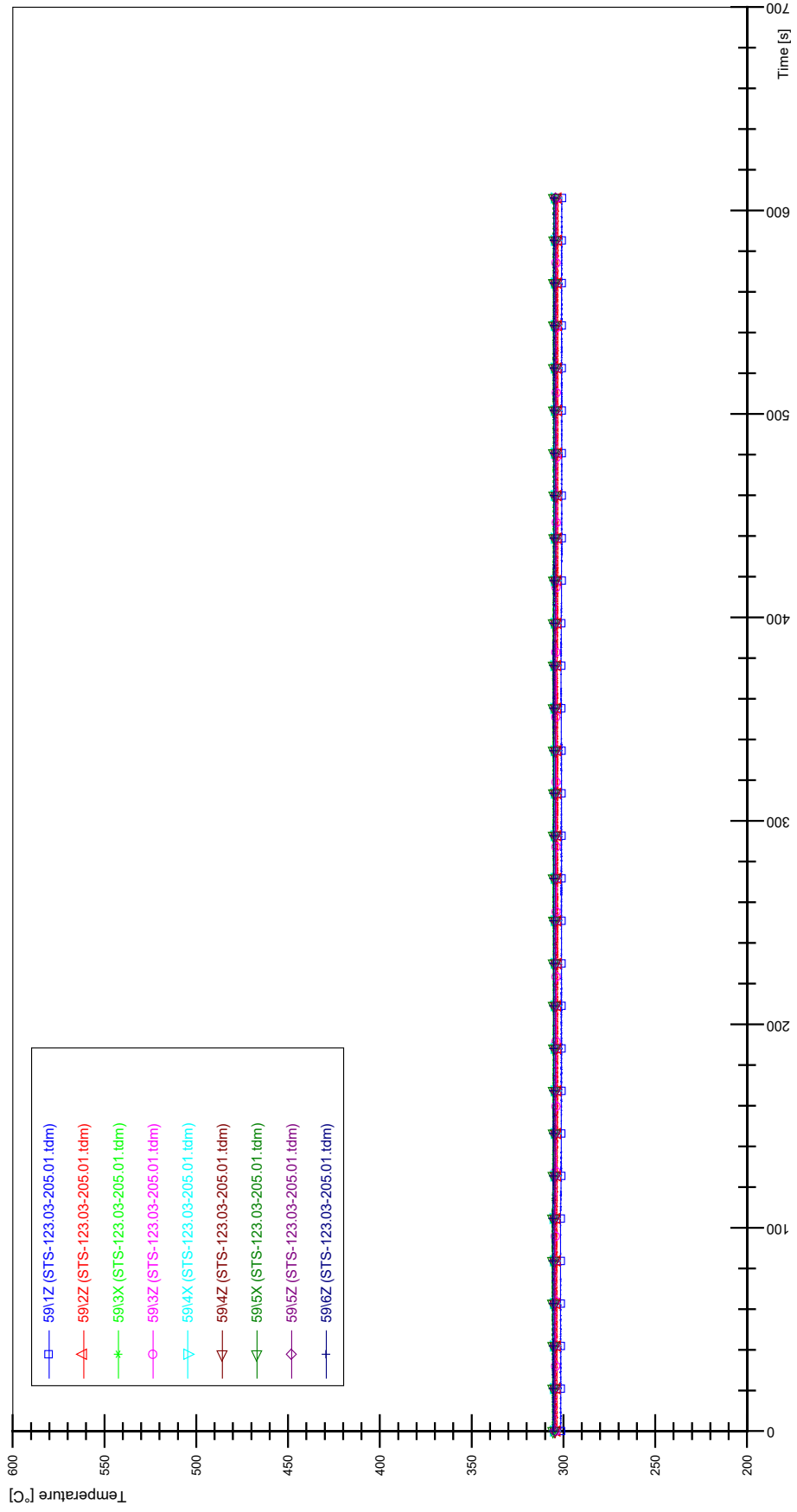
APPENDIX V PLOTS OF INSTABILITY TEST STS-123.03-205.01



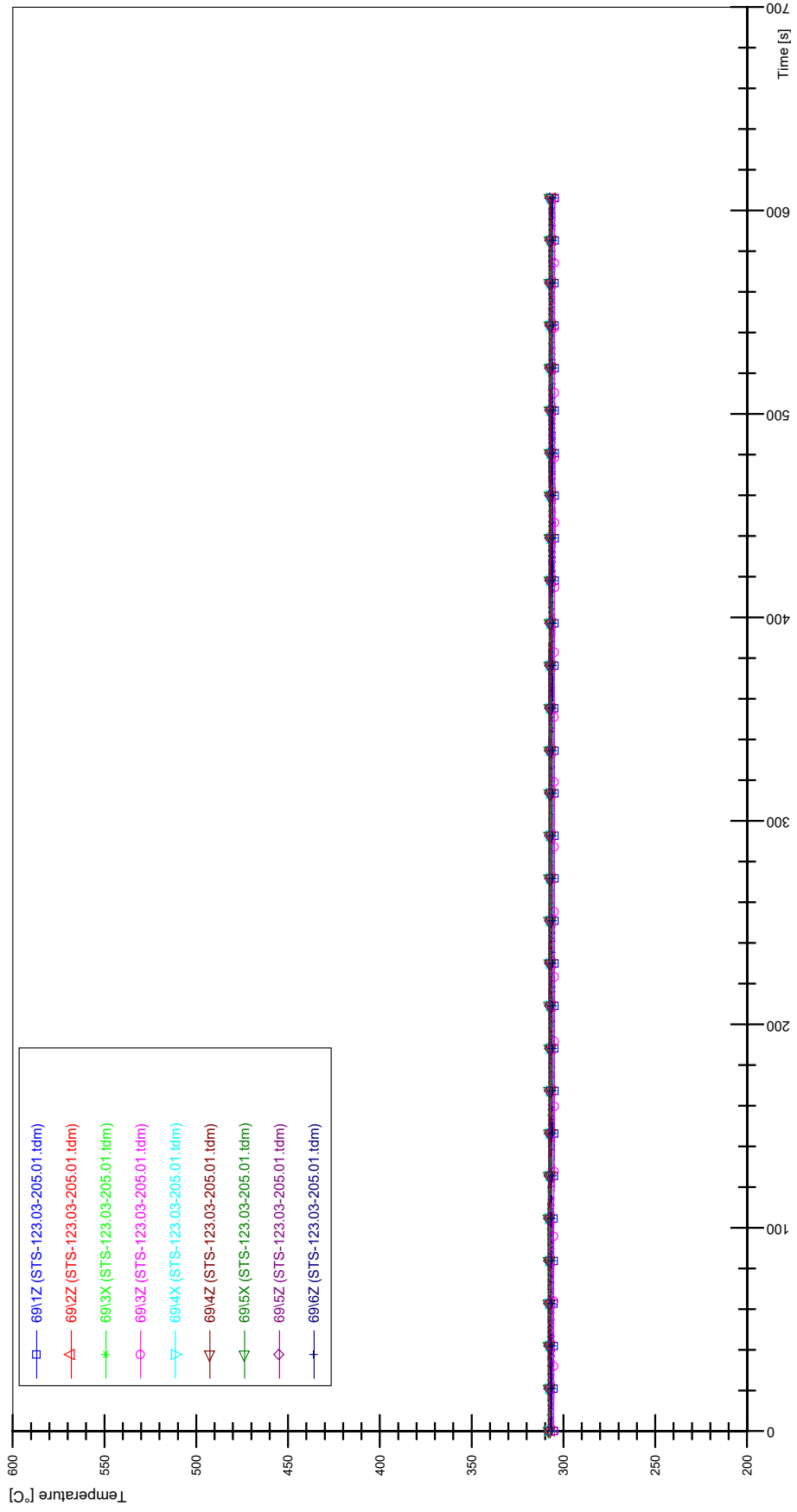
STS-123.03-205.01_CP12_CT19



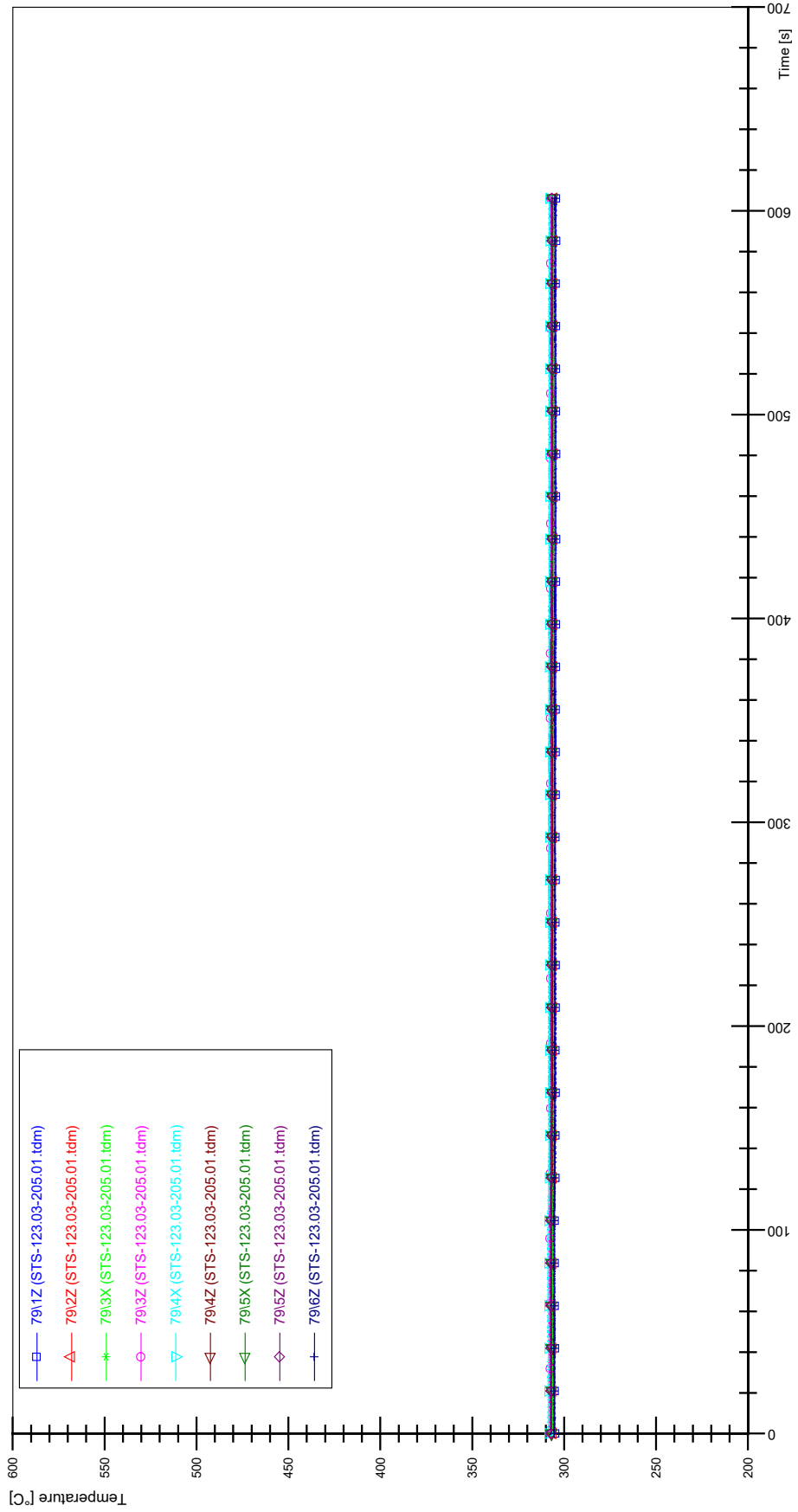
STS-123.03-205.01_Rod_59



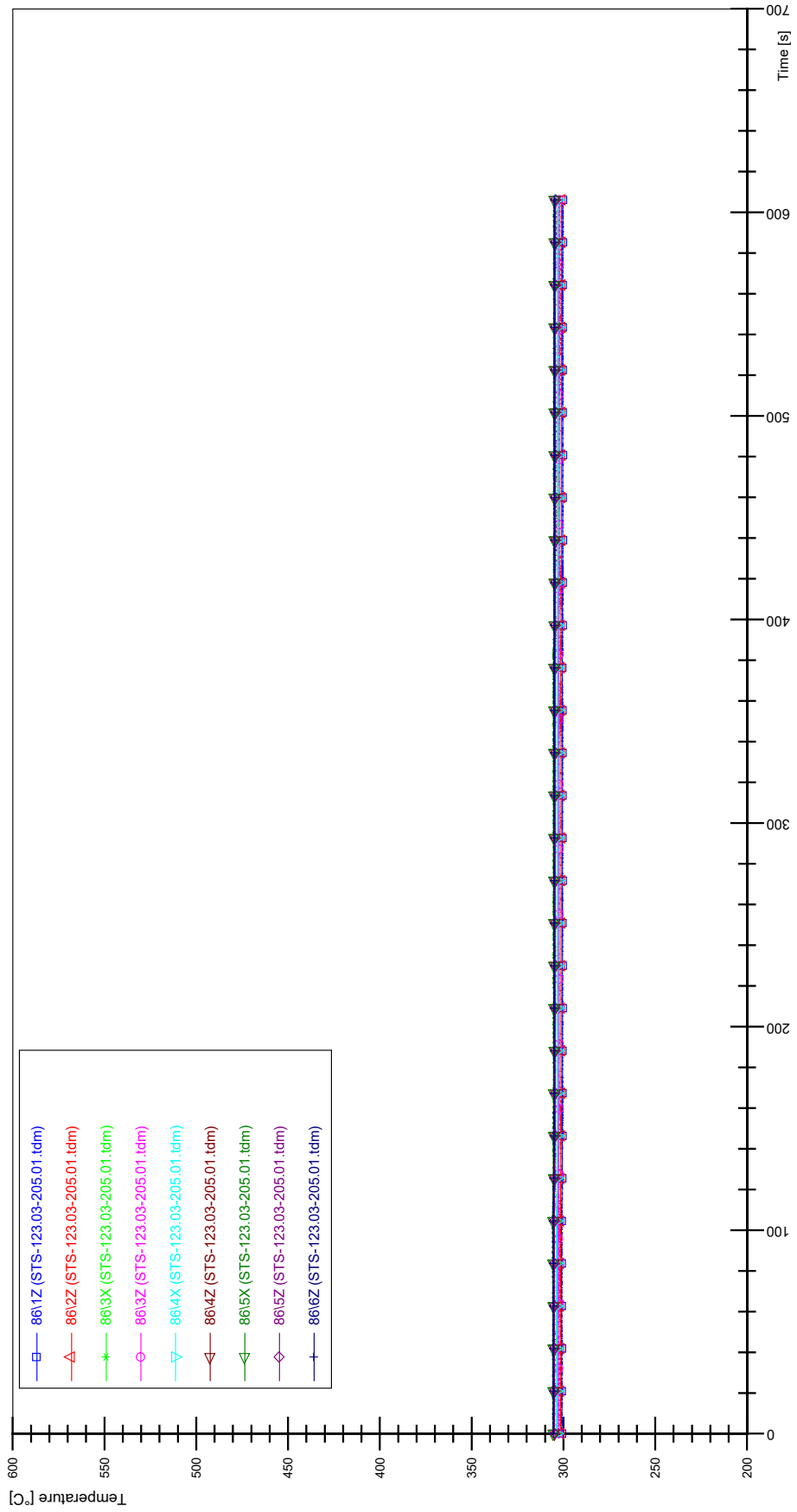
STS-123.03-205.01_Rod_69



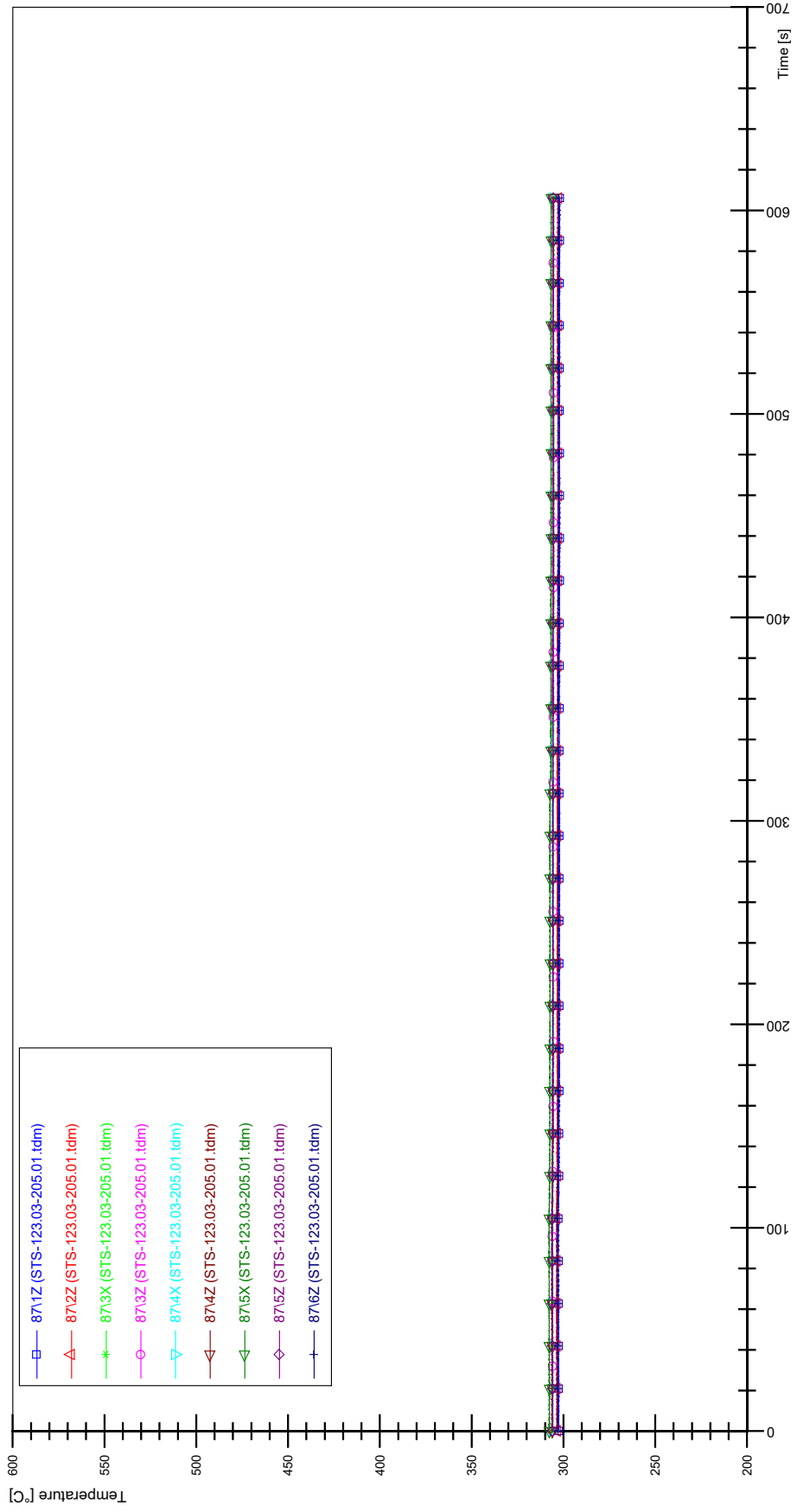
STS-123.03-205.01_Rod_79



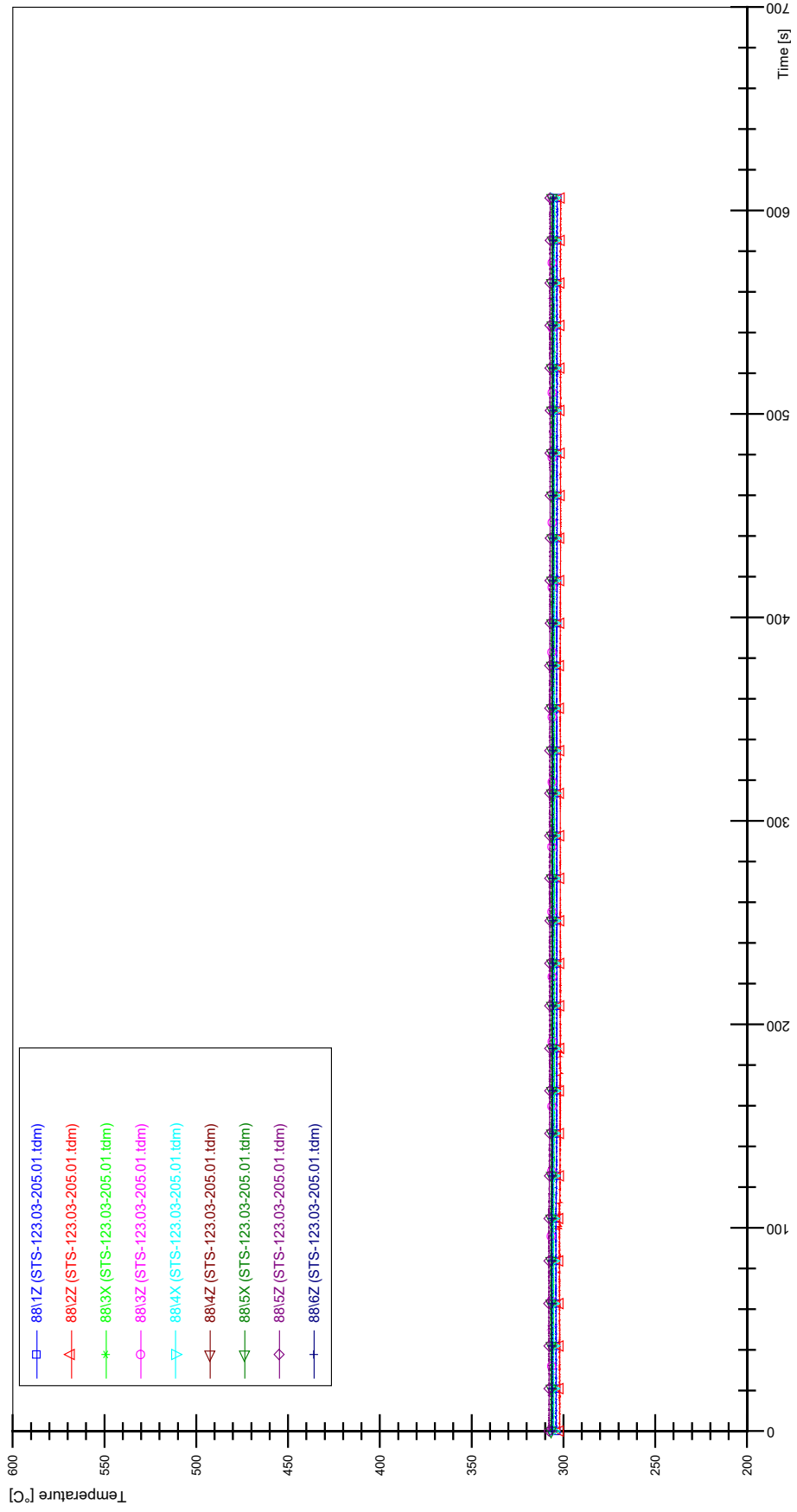
STS-123.03-205.01_Rod_86



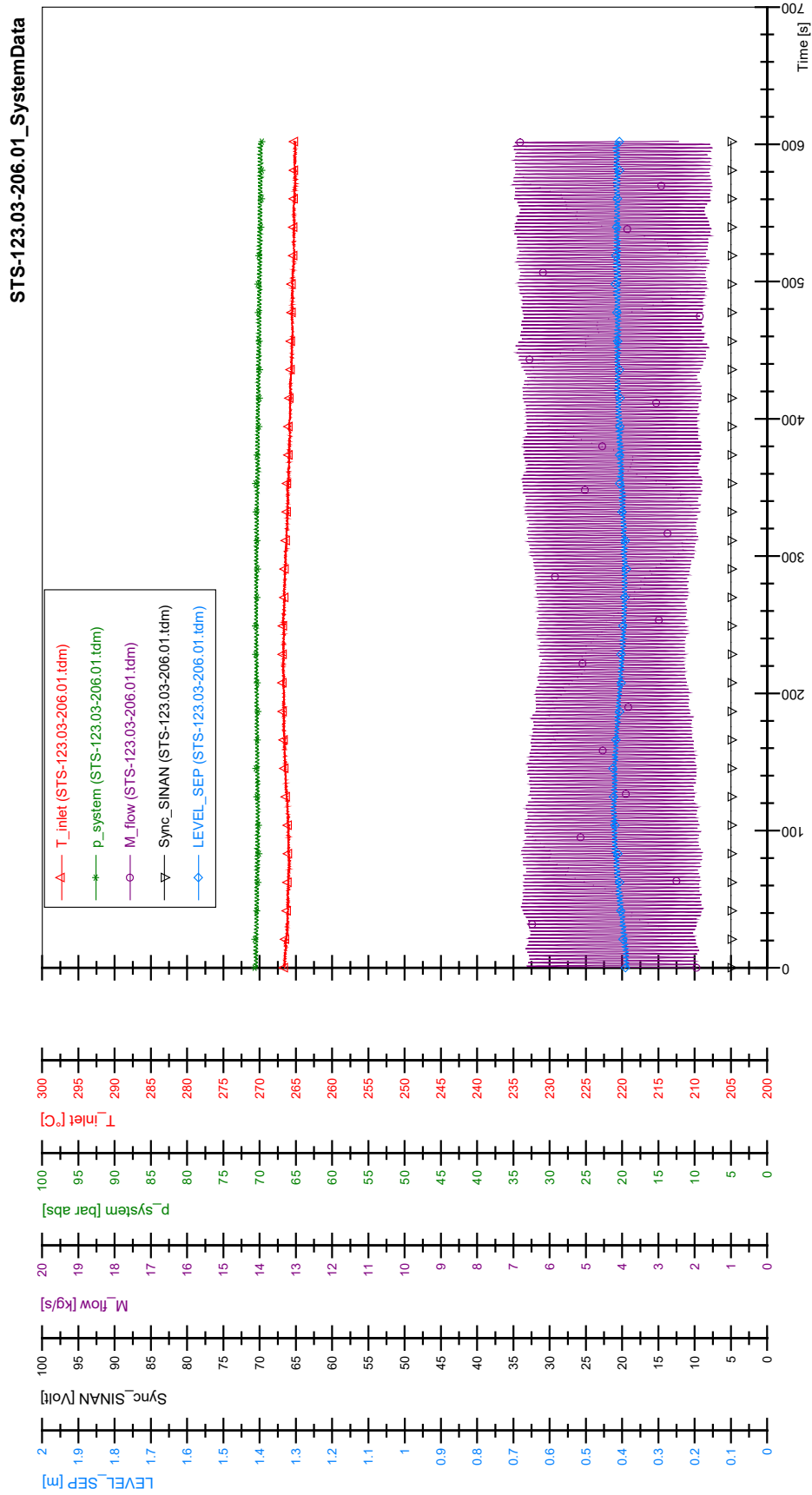
STS-123.03-205.01_Rod_87

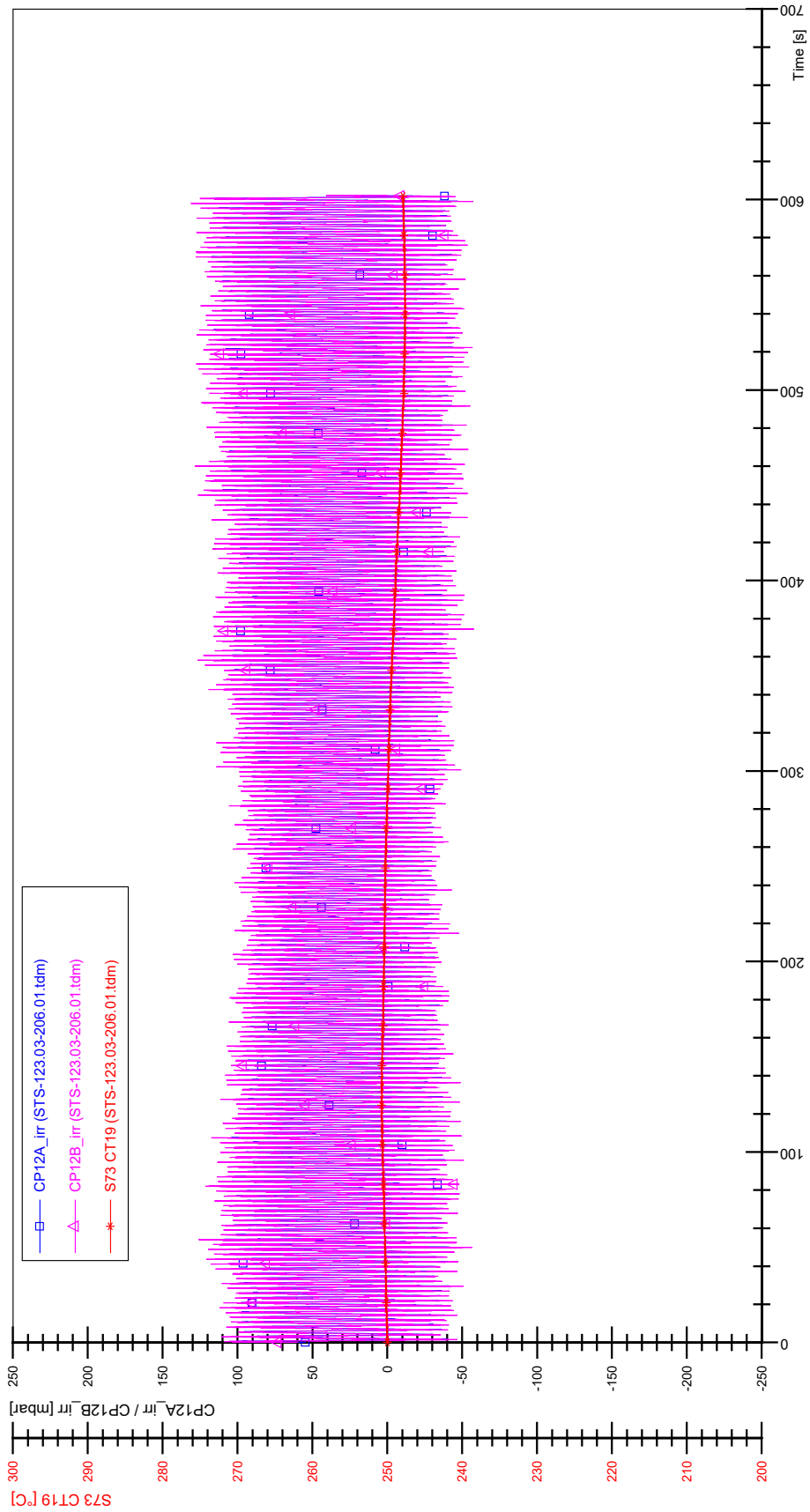


STS-123.03-205.01_Rod_88

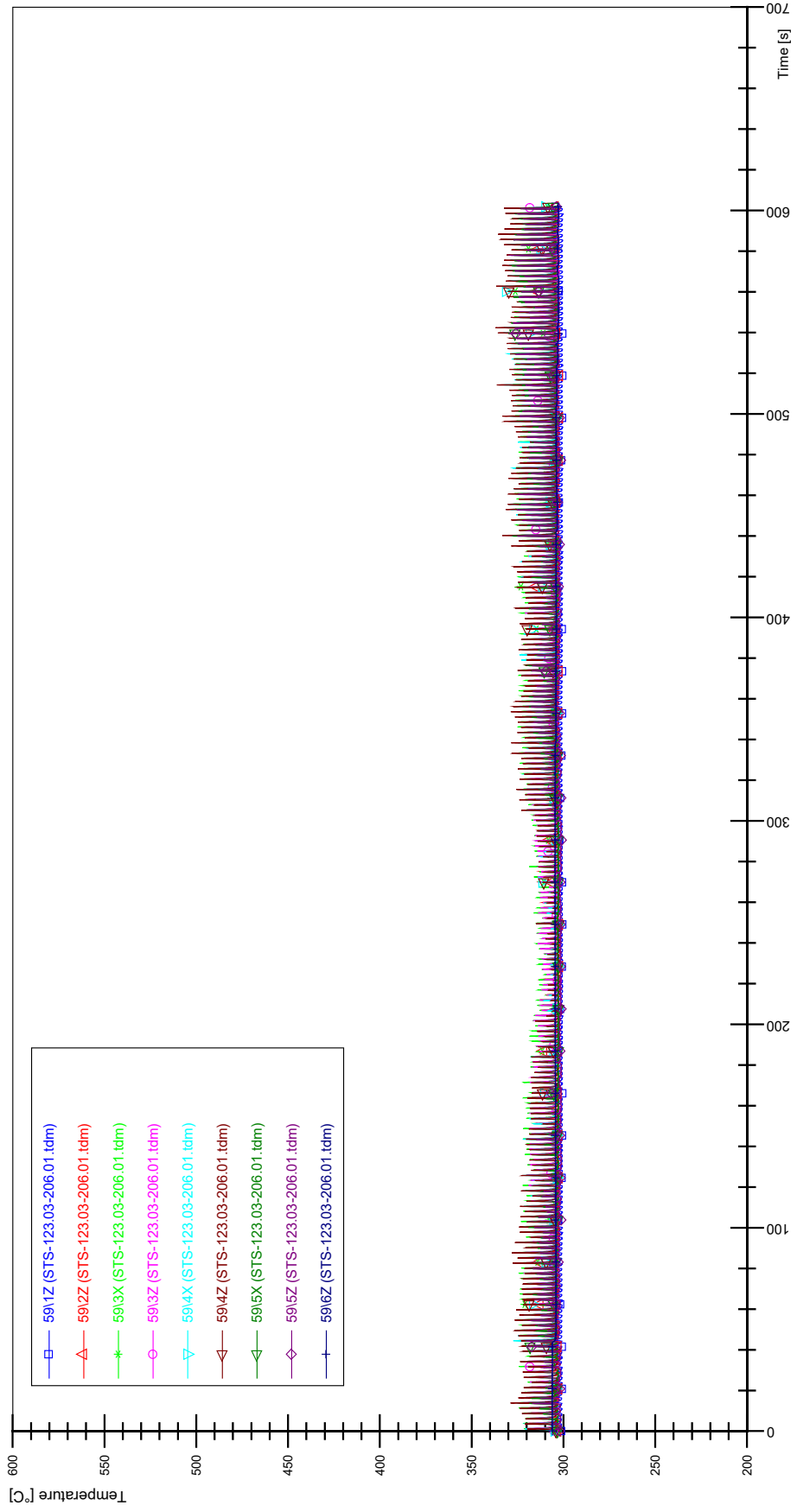


APPENDIX W PLOTS OF INSTABILITY TEST STS-123.03-206.01

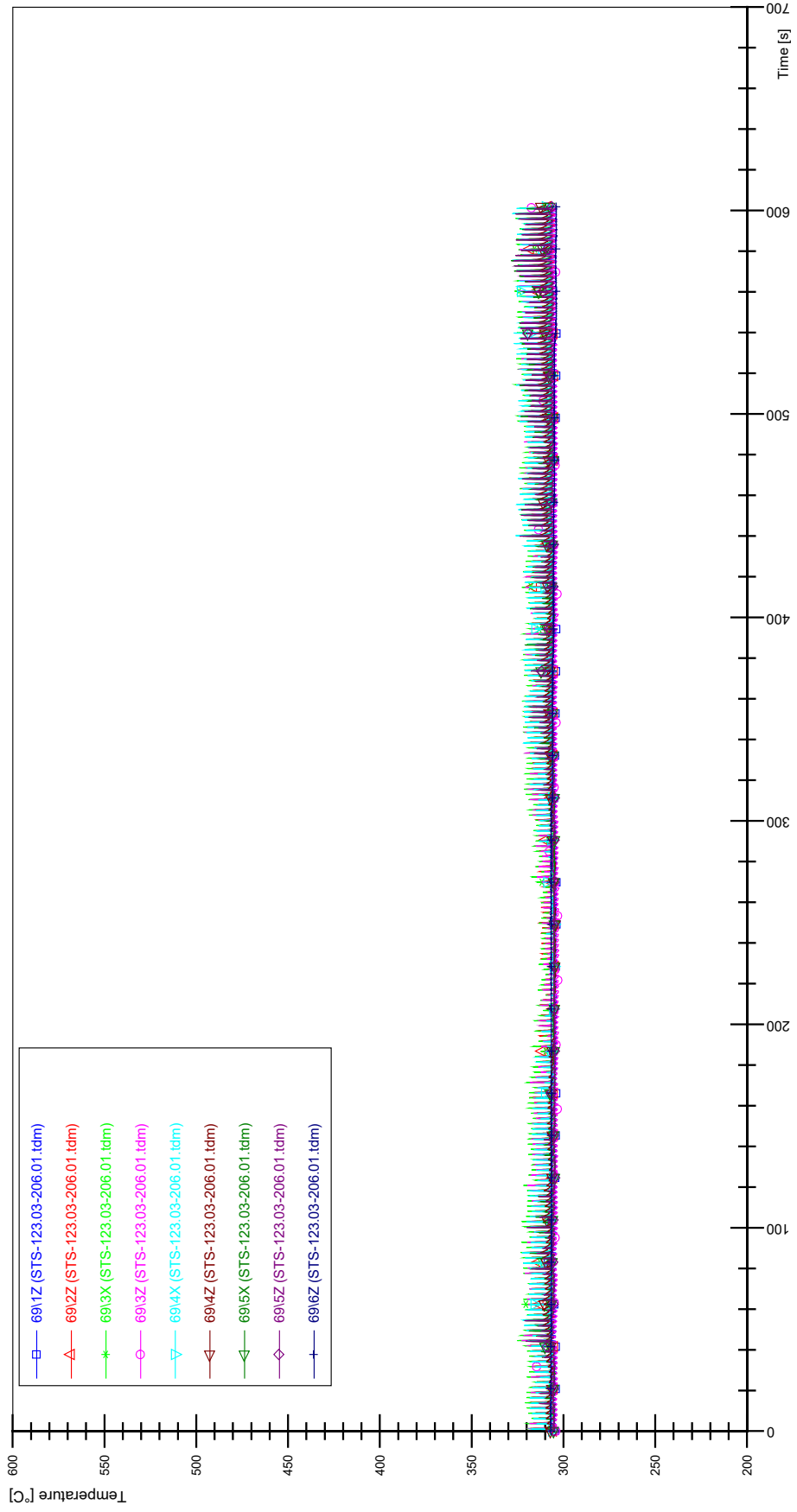




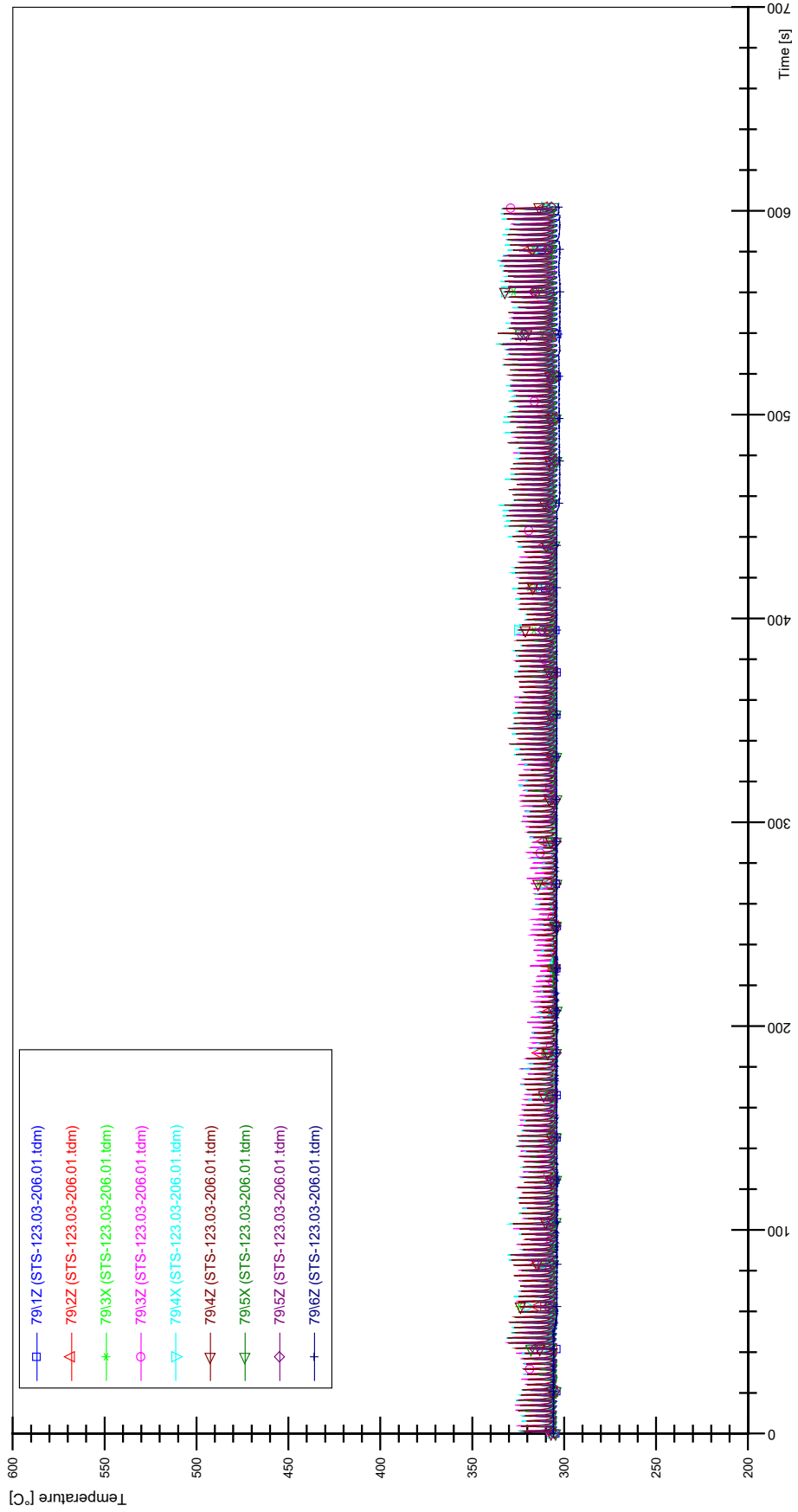
STS-123.03-206.01_Rod_59



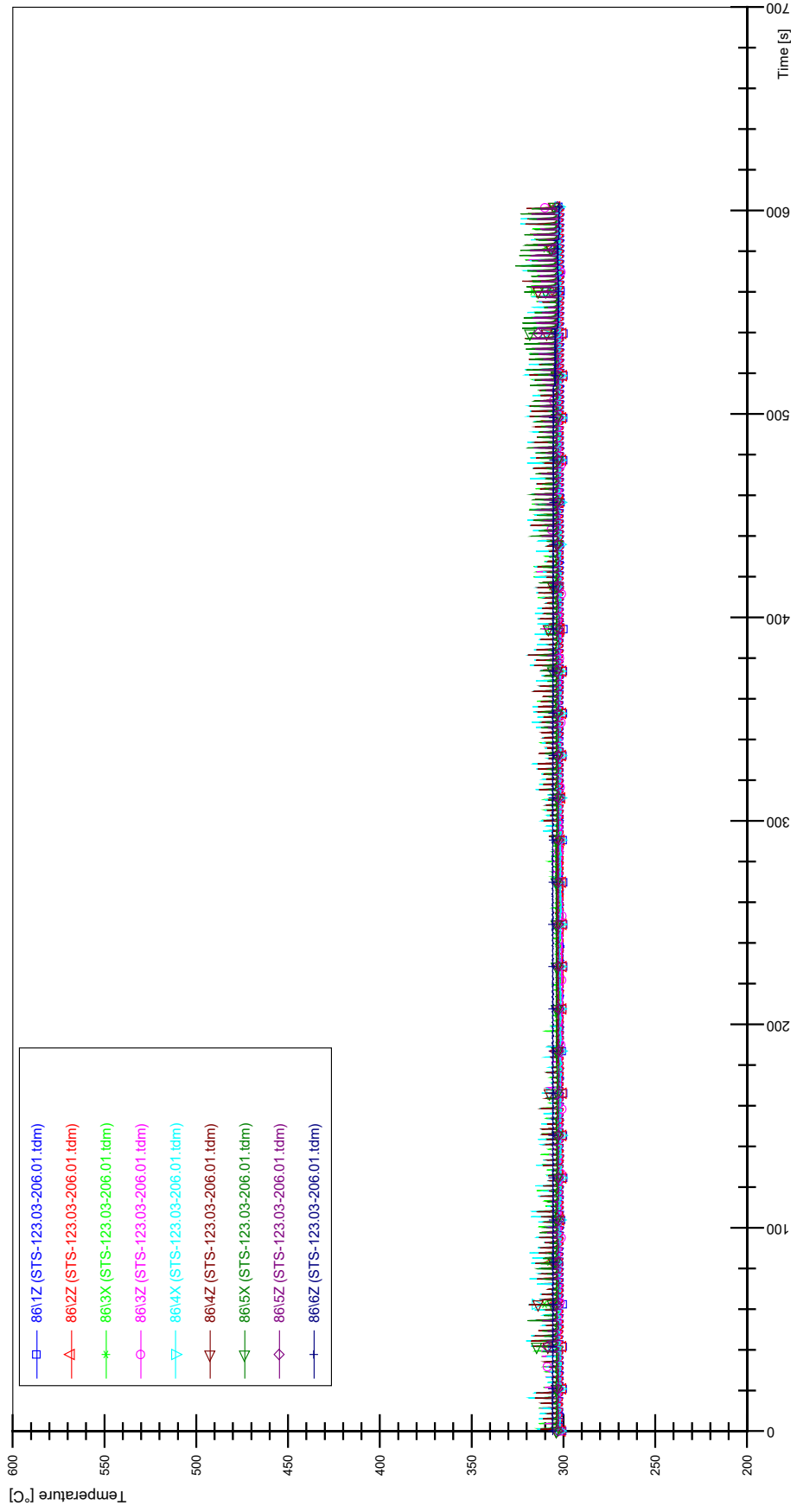
STS-123.03-206.01_Rod_69



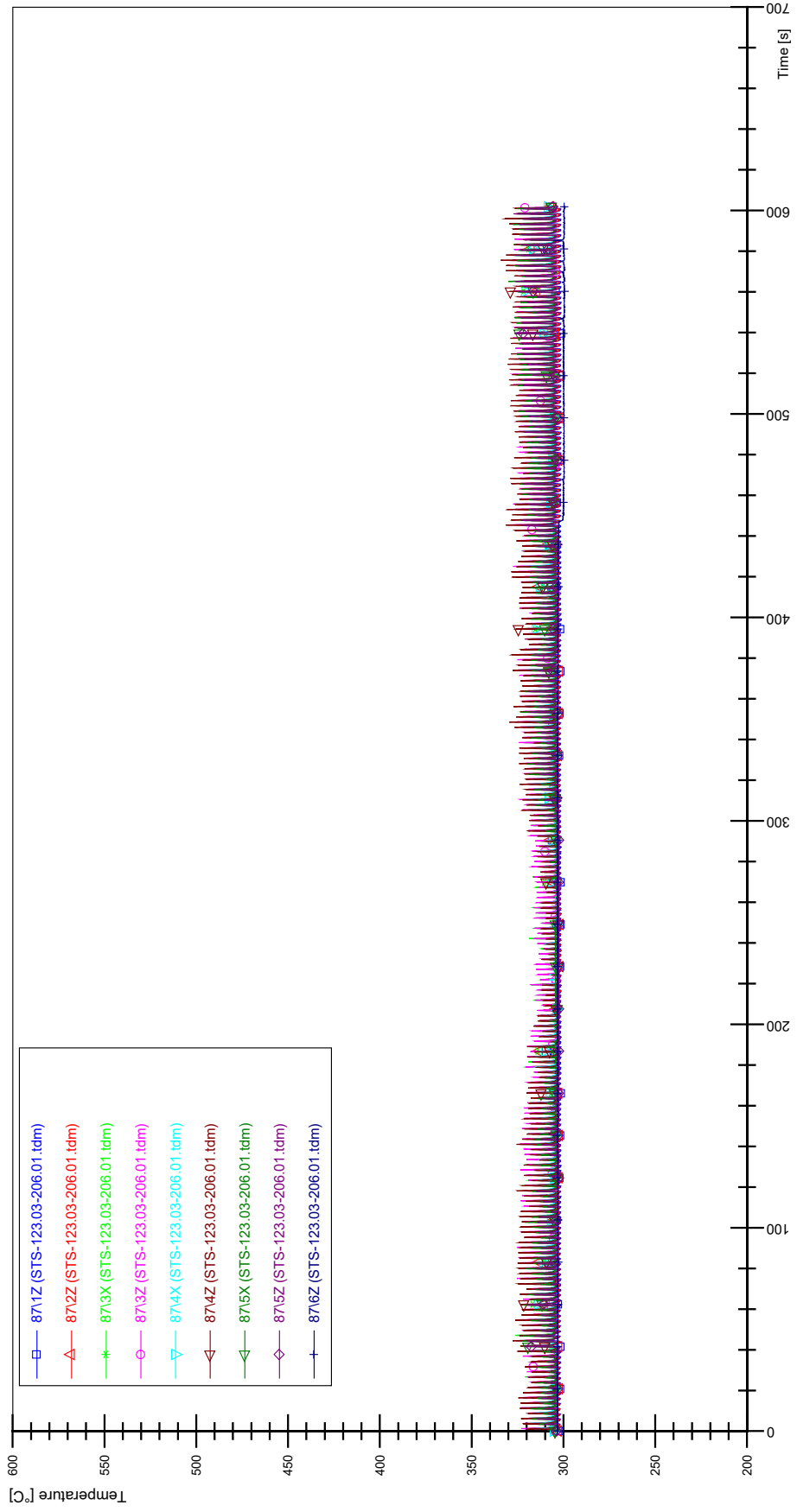
STS-123.03-206.01_Rod_79



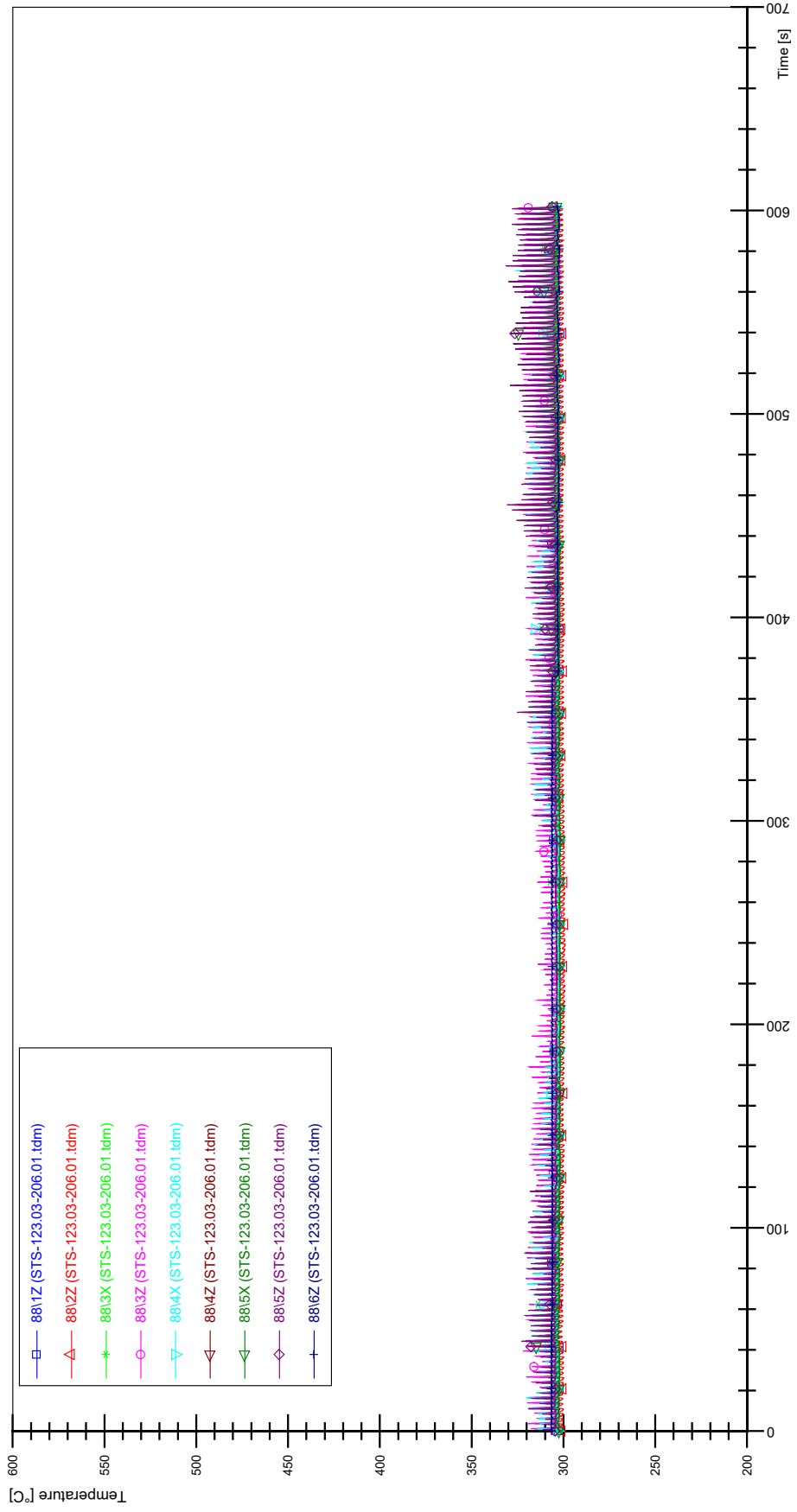
STS-123.03-206.01_Rod_86



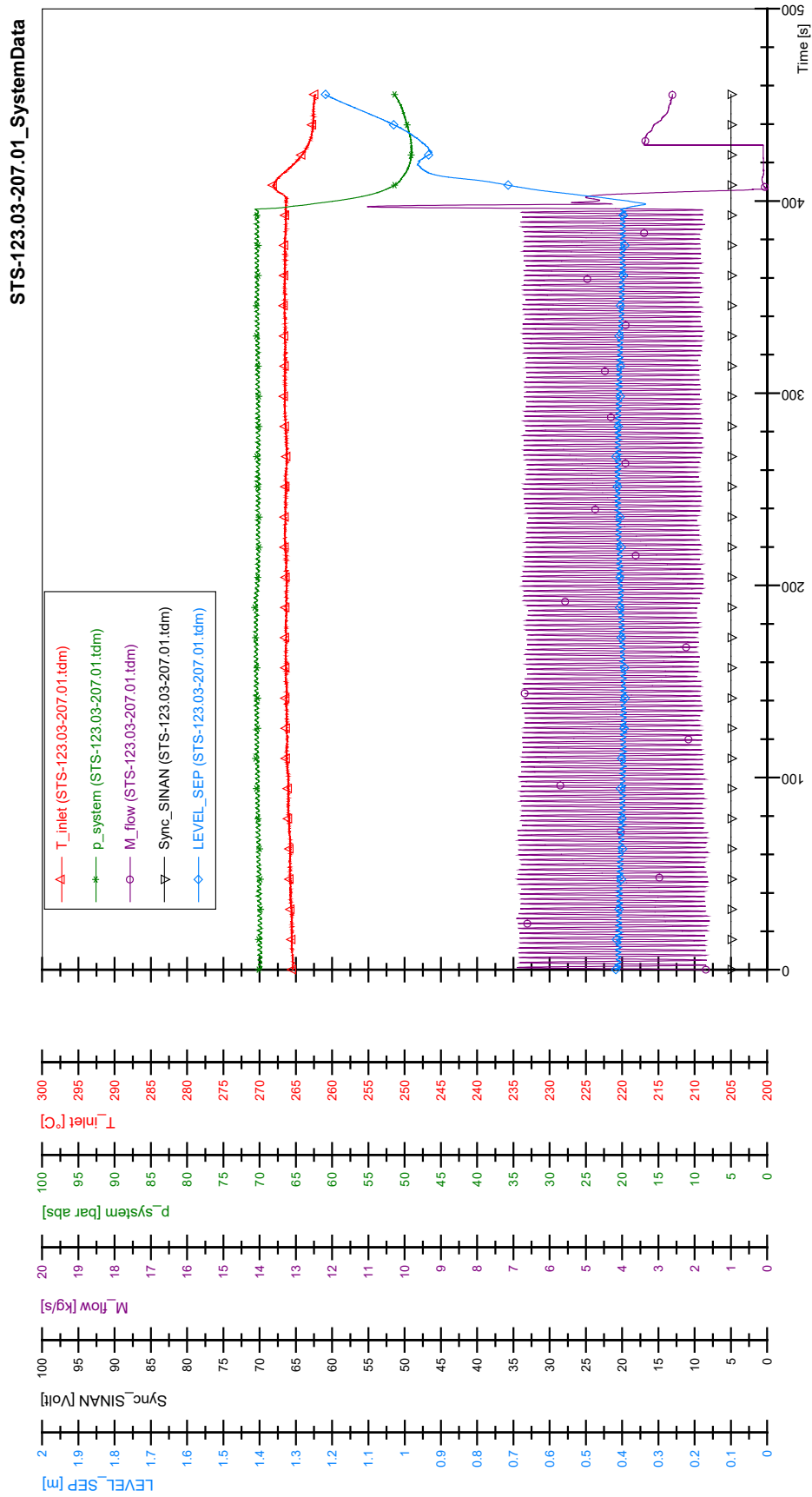
STS-123.03-206.01_Rod_87



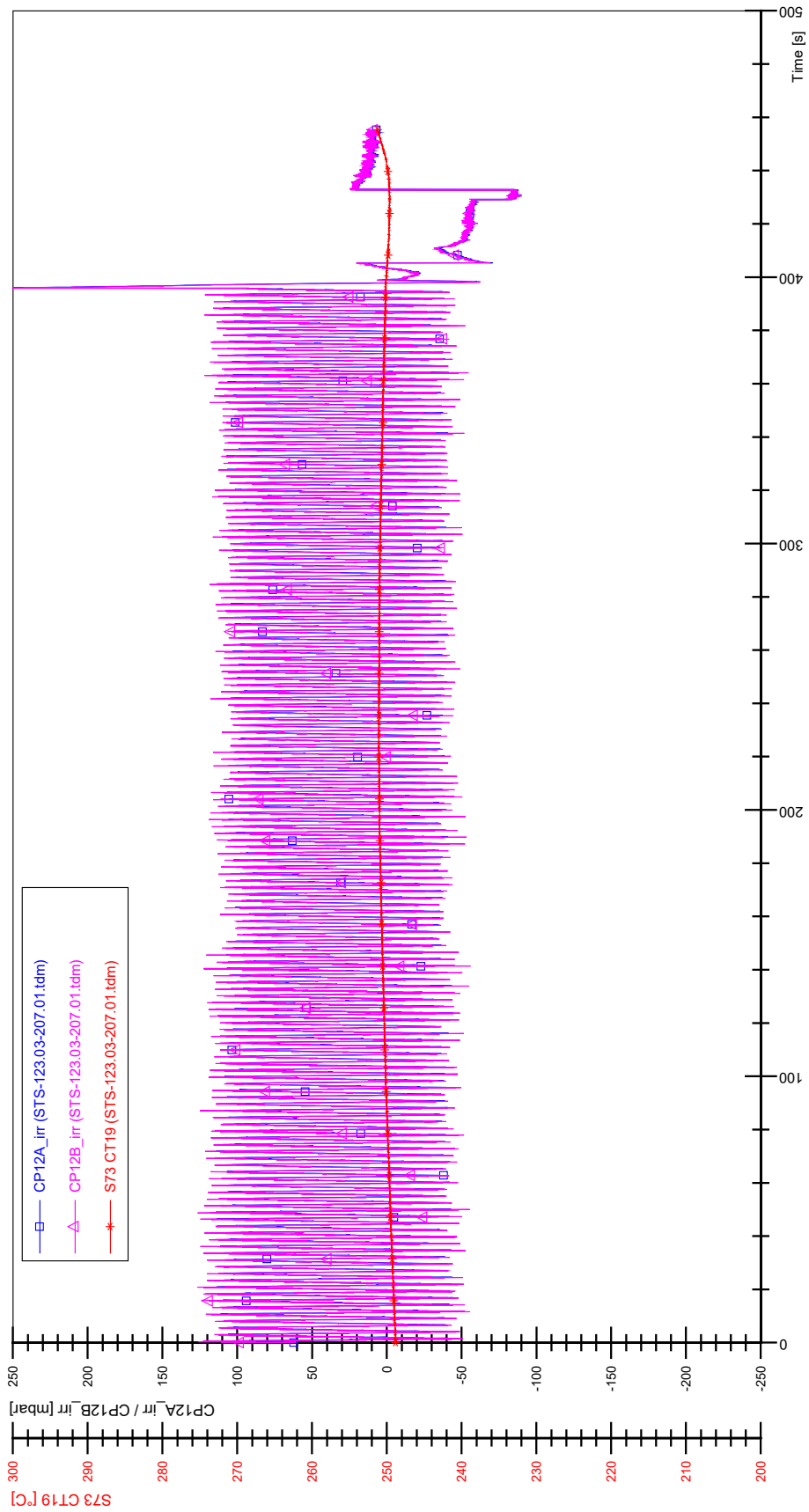
STS-123.03-206.01_Rod_88



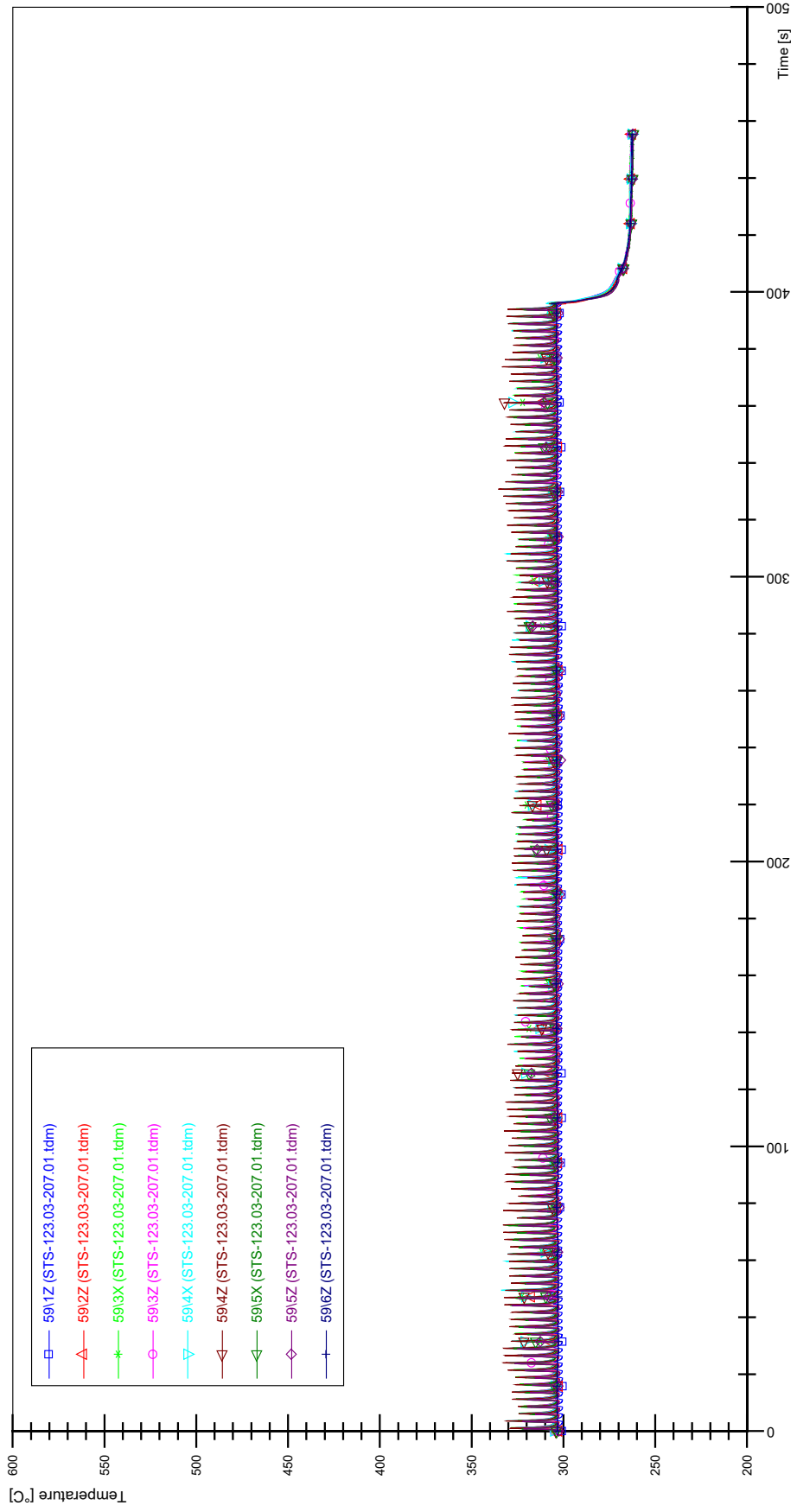
APPENDIX X PLOTS OF INSTABILITY TEST STS-123.03-207.01



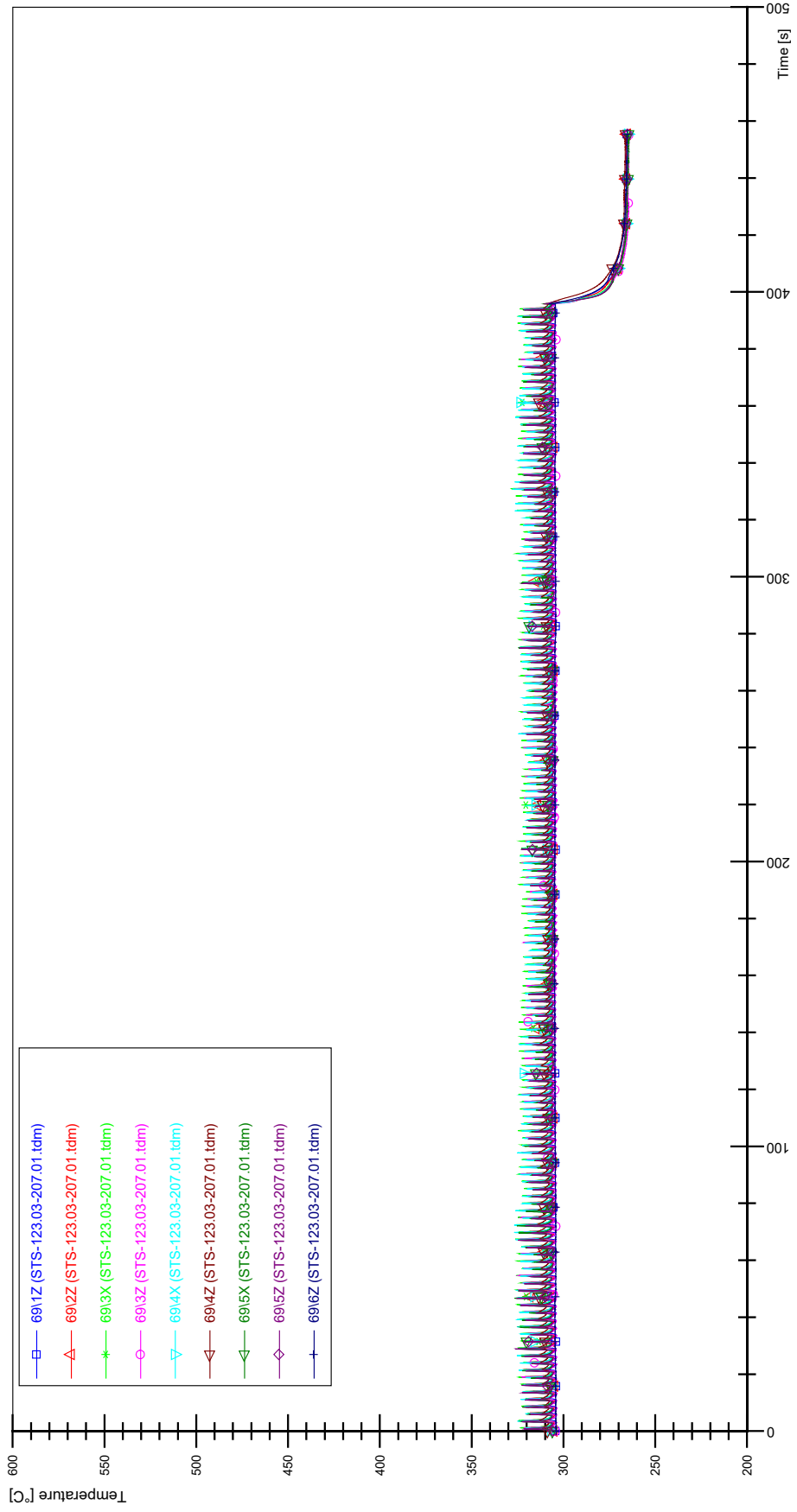
STS-123.03-207.01_CP12_CT19



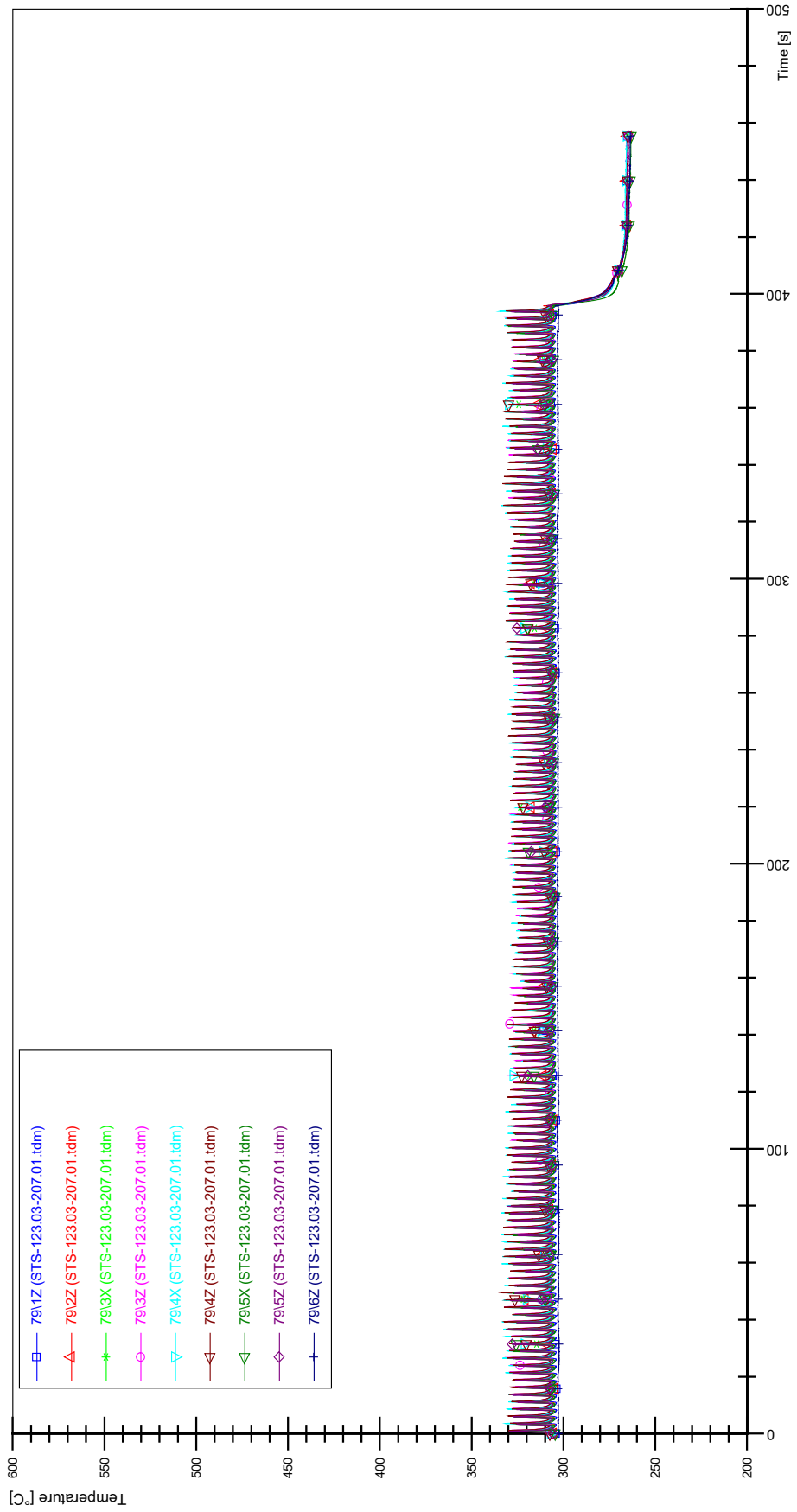
STS-123.03-207.01_Rod_59



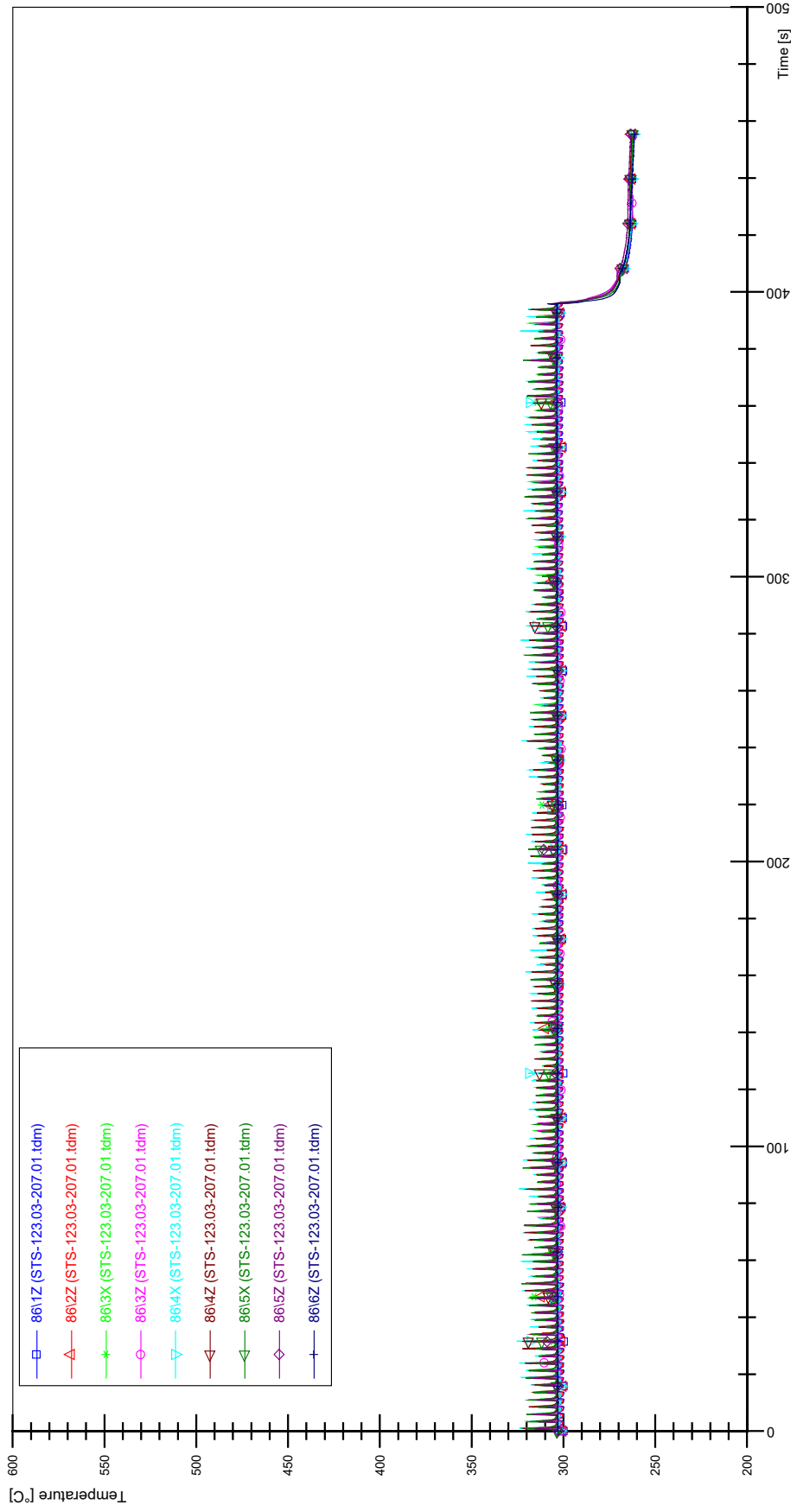
STS-123.03-207.01_Rod_69



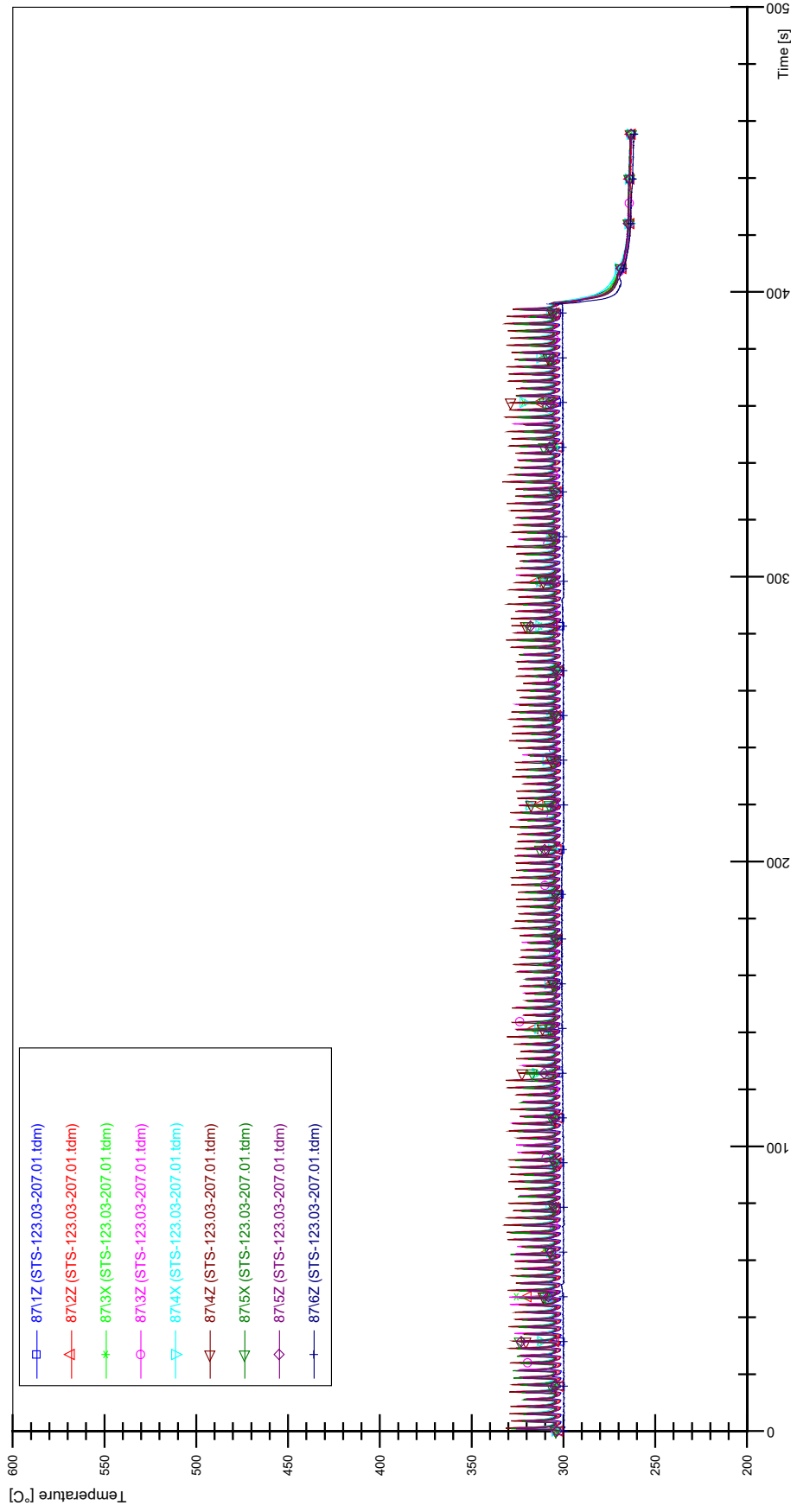
STS-123.03-207.01_Rod_79



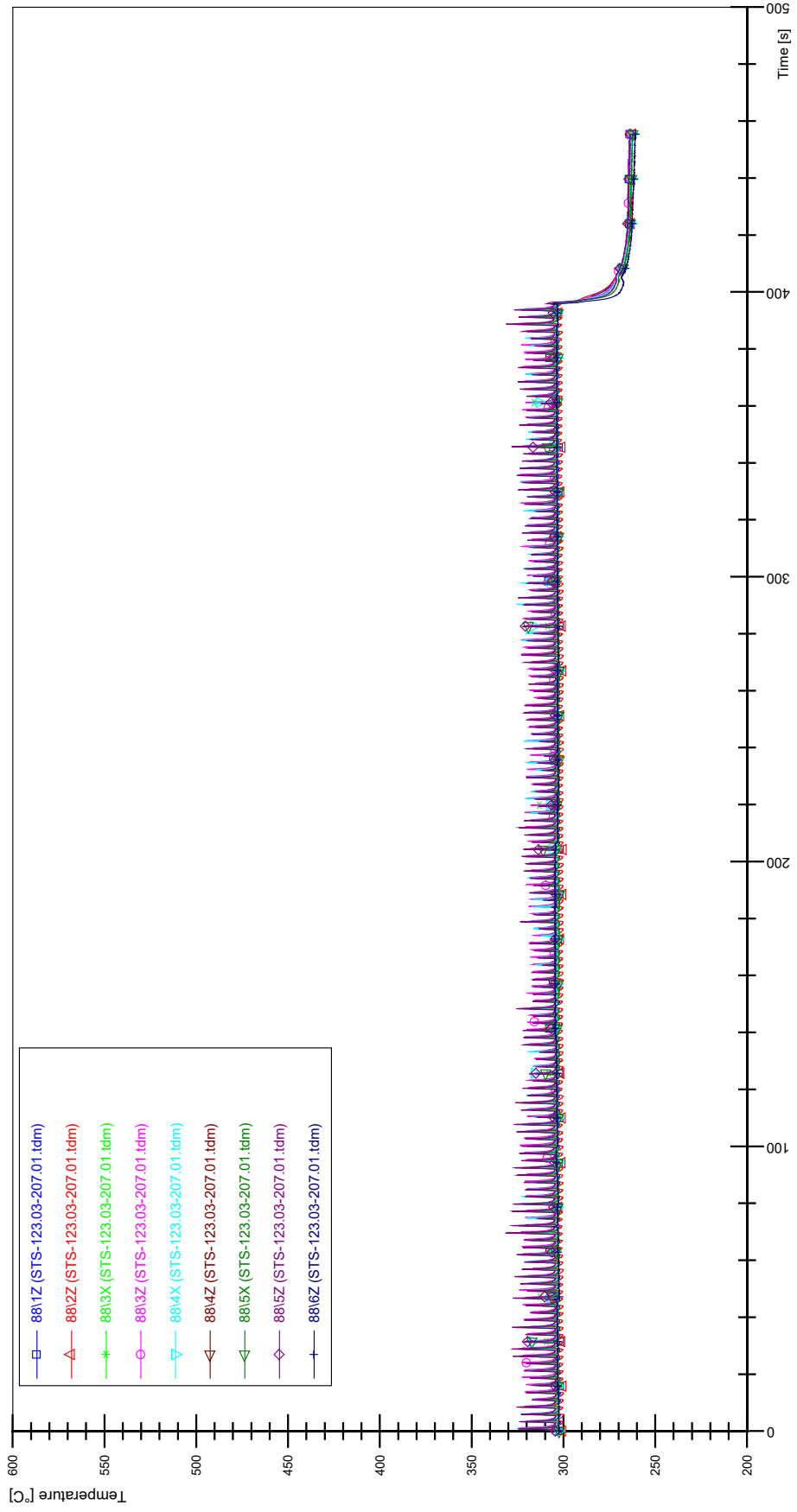
STS-123.03-207.01_Rod_86



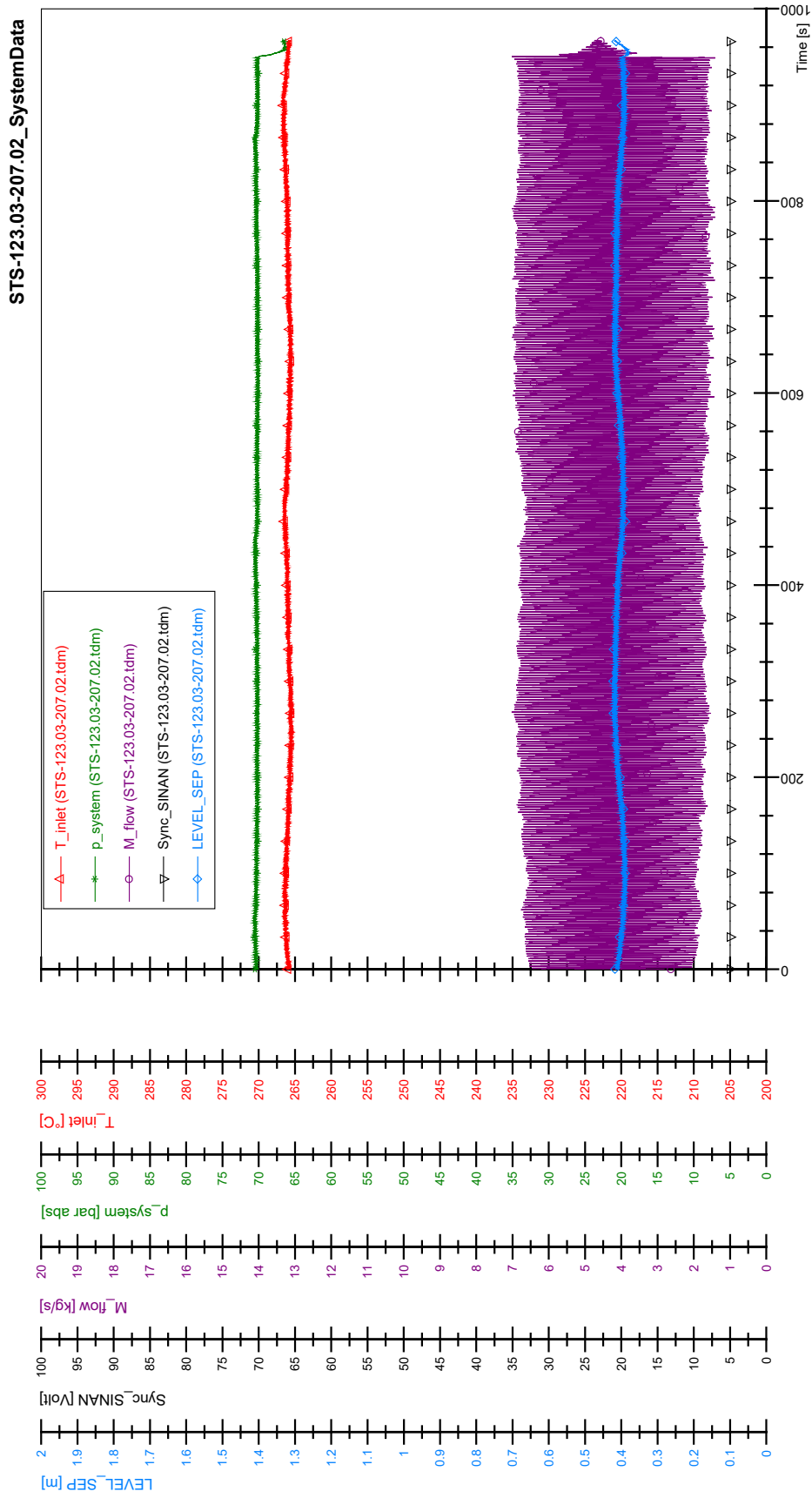
STS-123.03-207.01_Rod_87



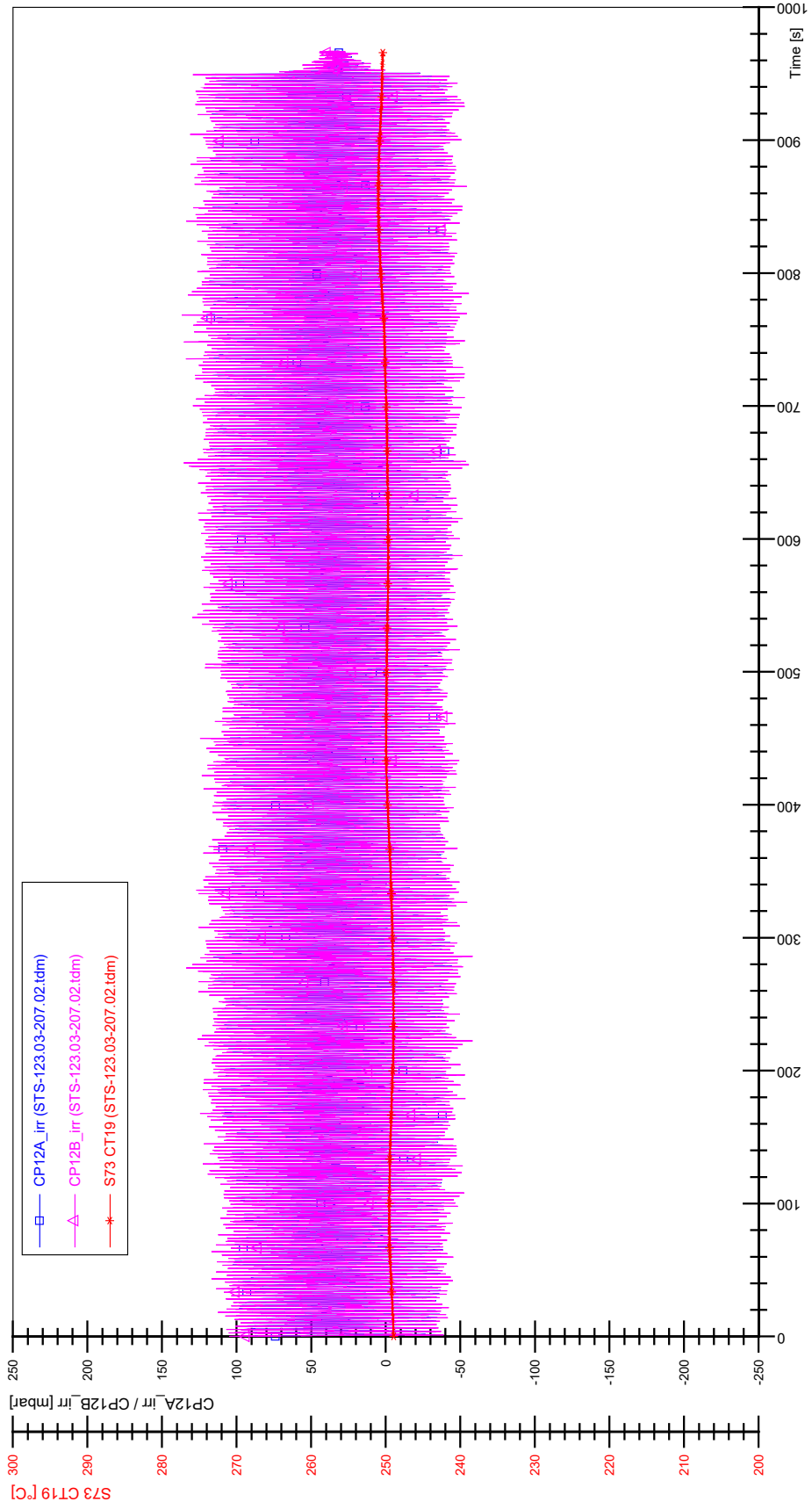
STS-123.03-207.01_Rod_88



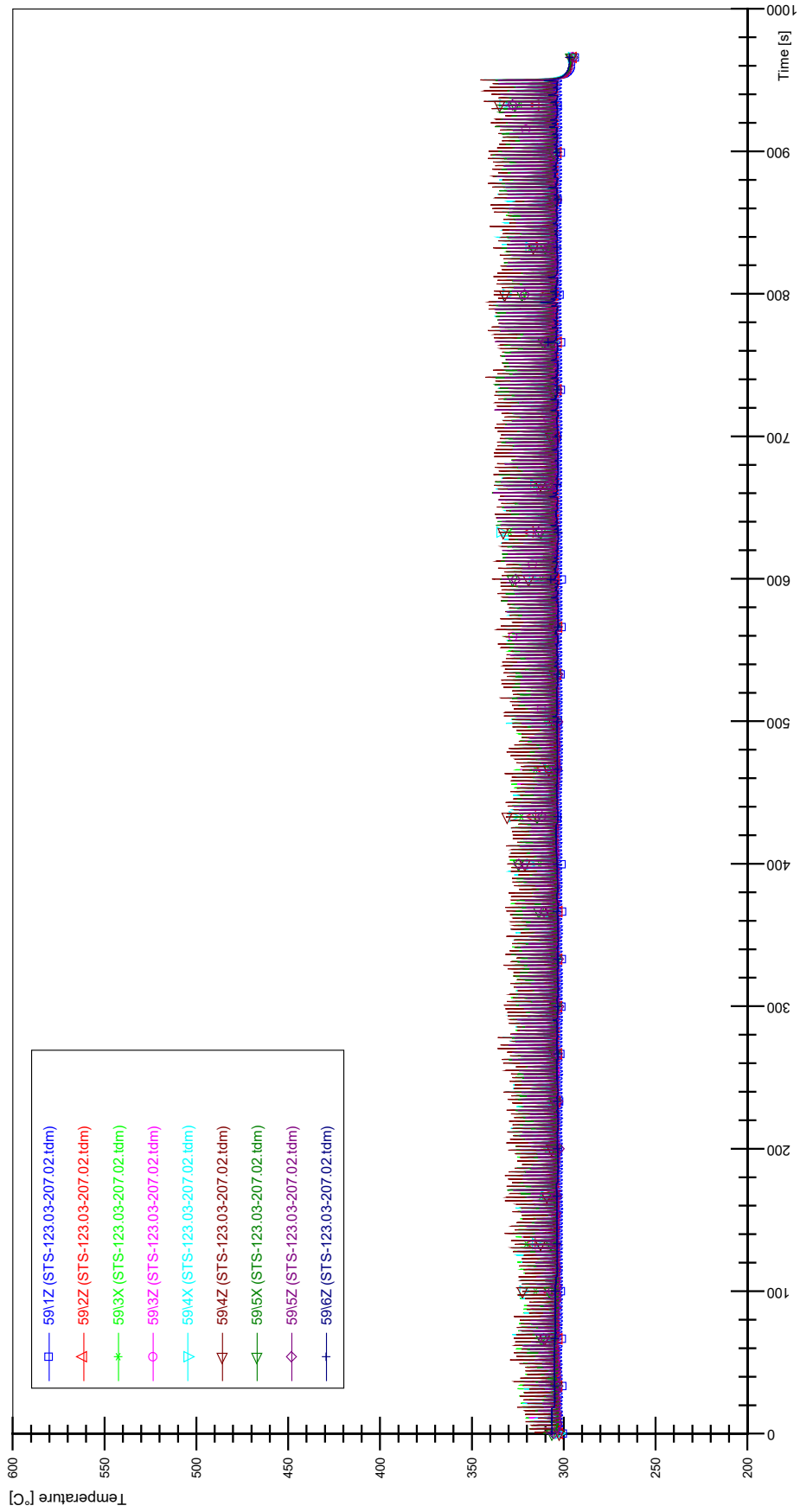
APPENDIX Y PLOTS OF INSTABILITY TEST STS-123.03-207.02



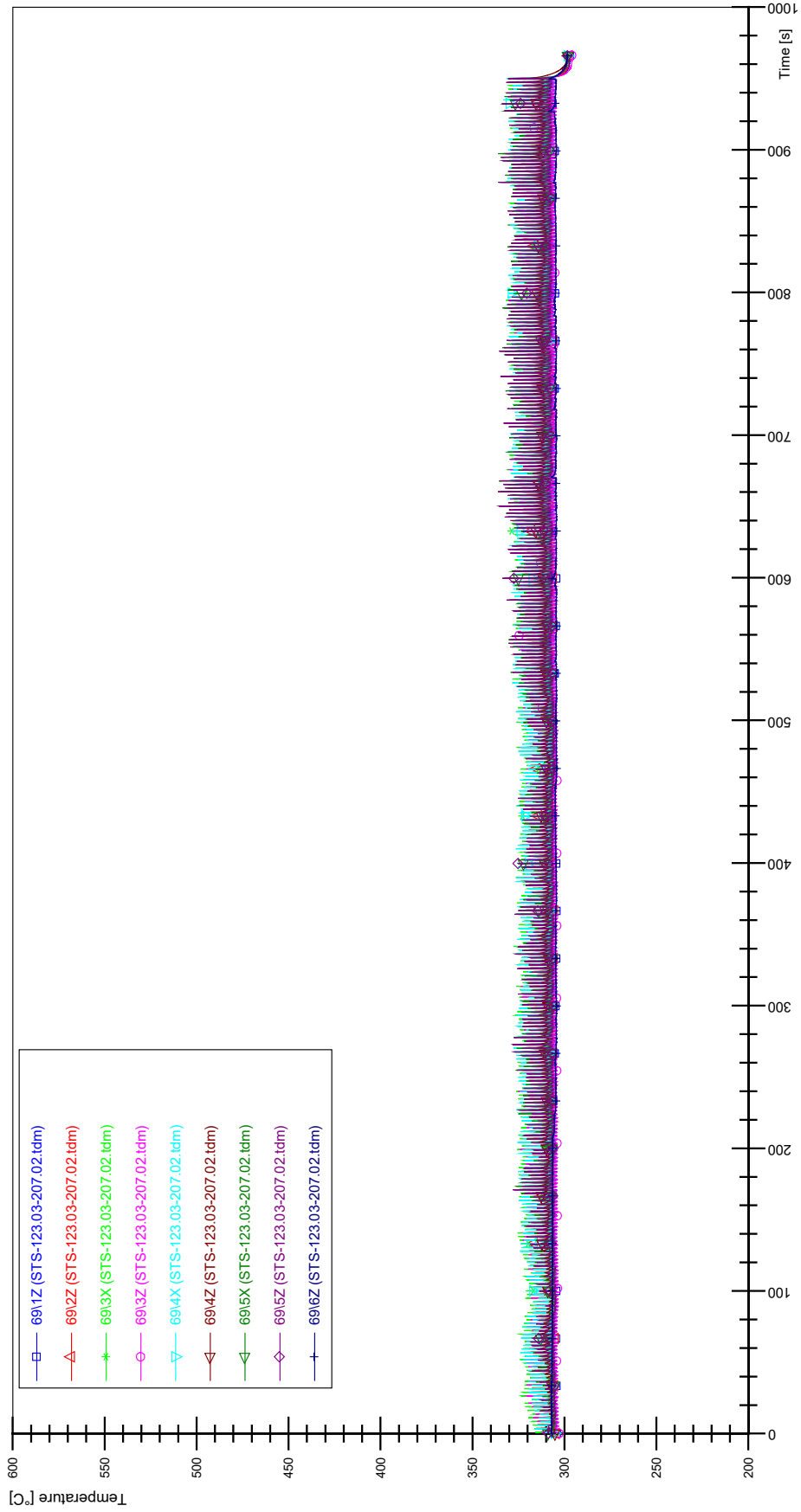
STS-123.03-207.02_CP12_CT19



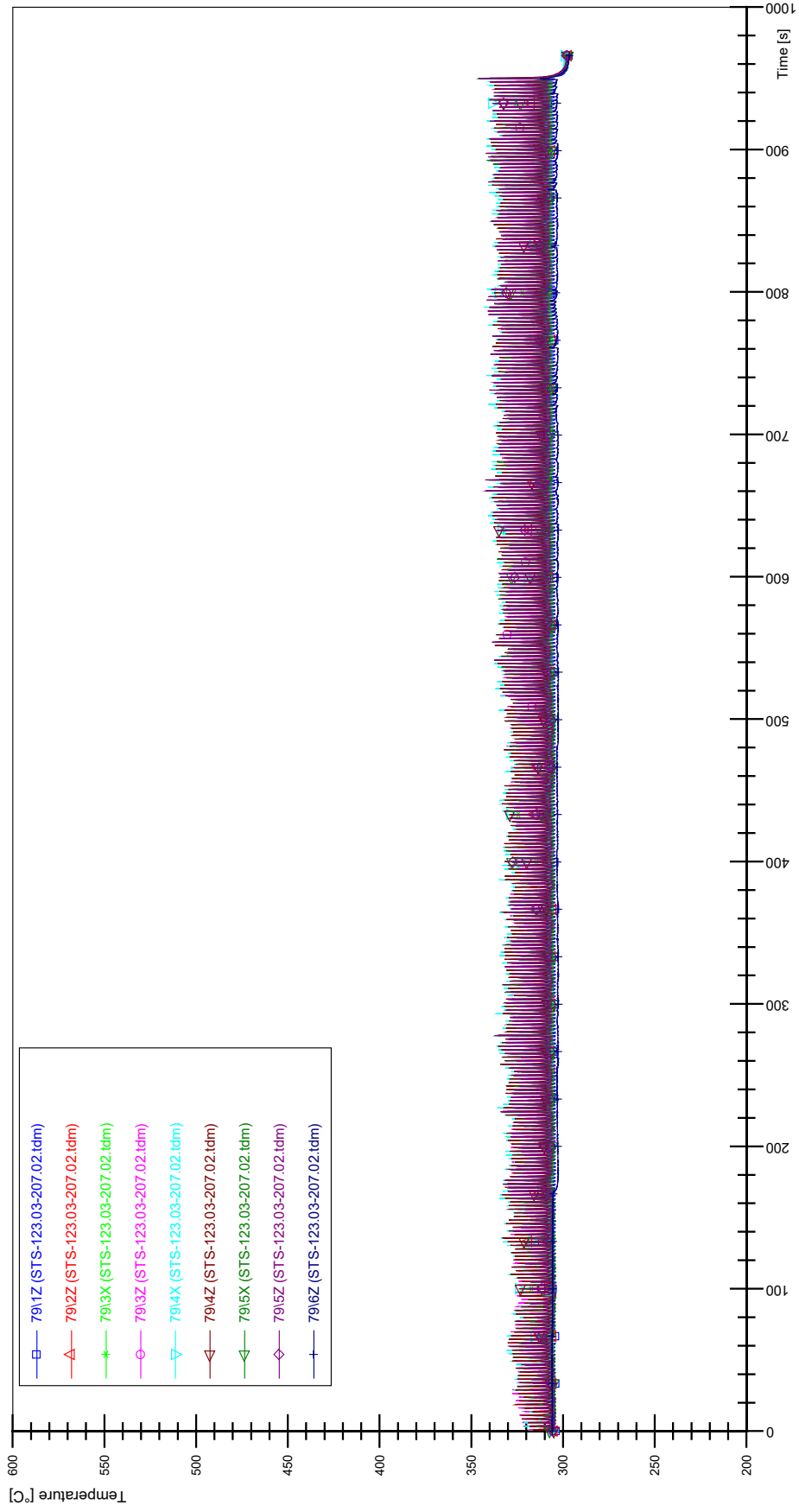
STS-123.03-207.02_Rod_59



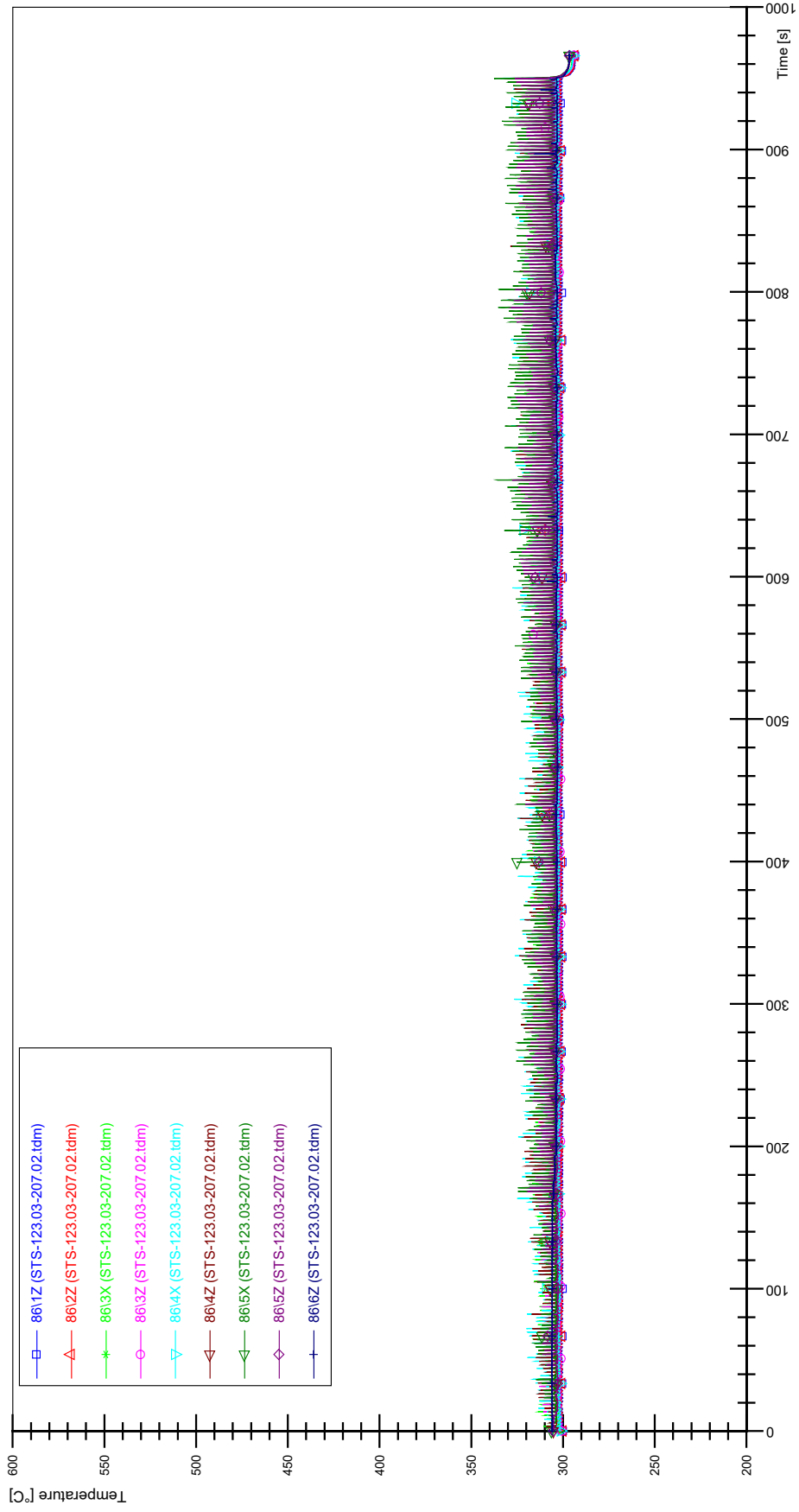
STS-123.03-207.02_Rod_69



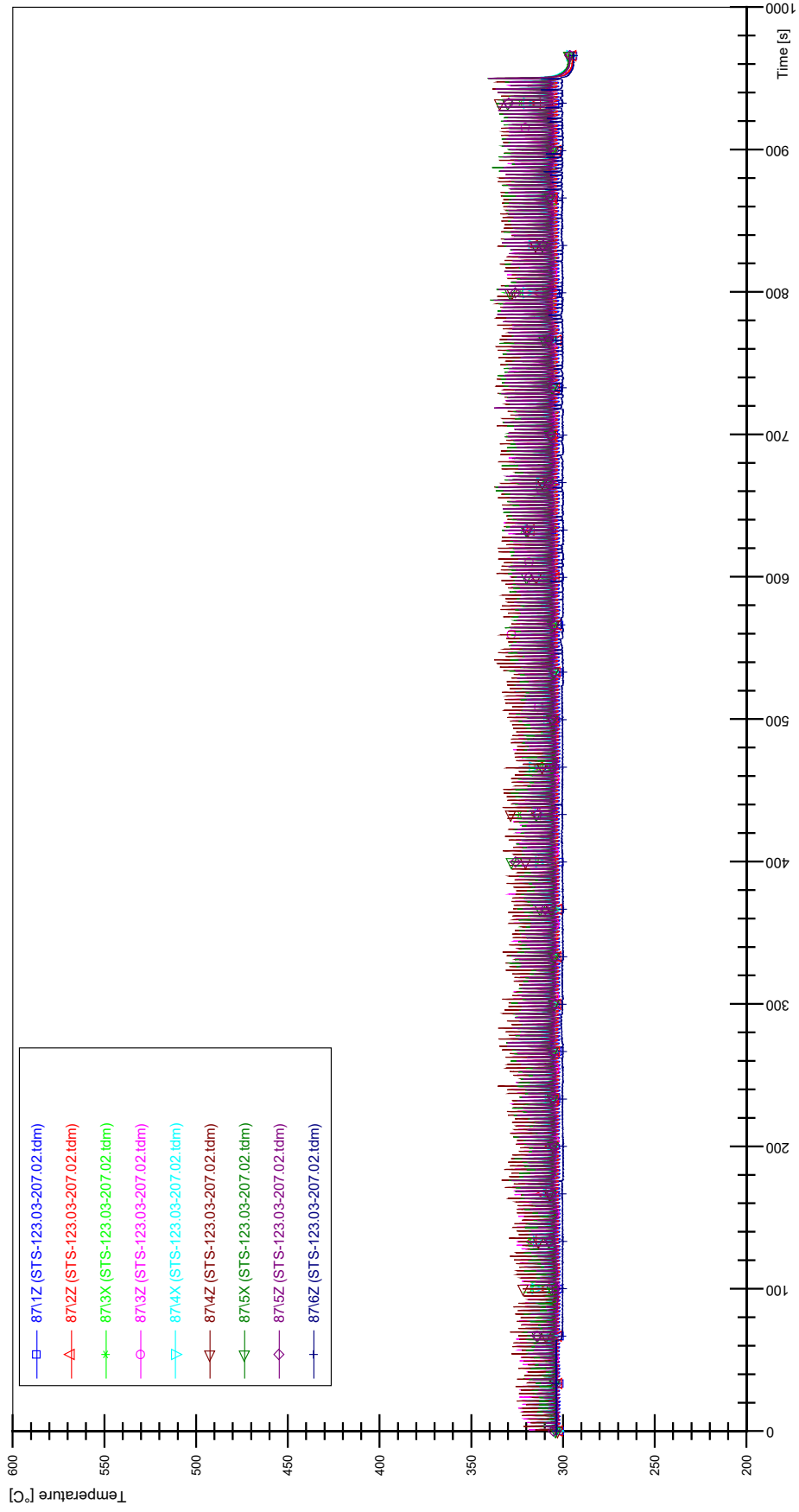
STS-123.03-207.02_Rod_79



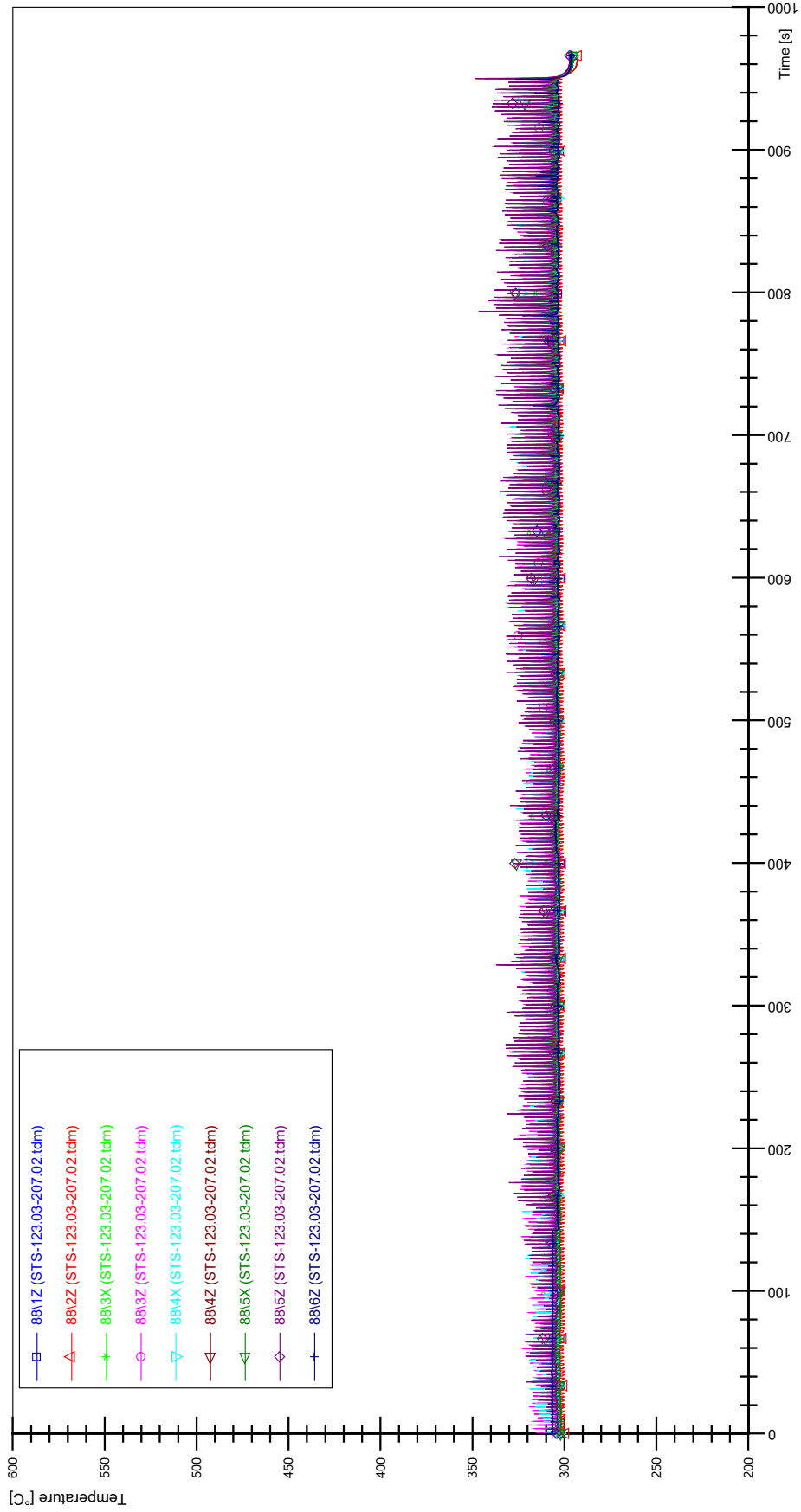
STS-123.03-207.02_Rod_86



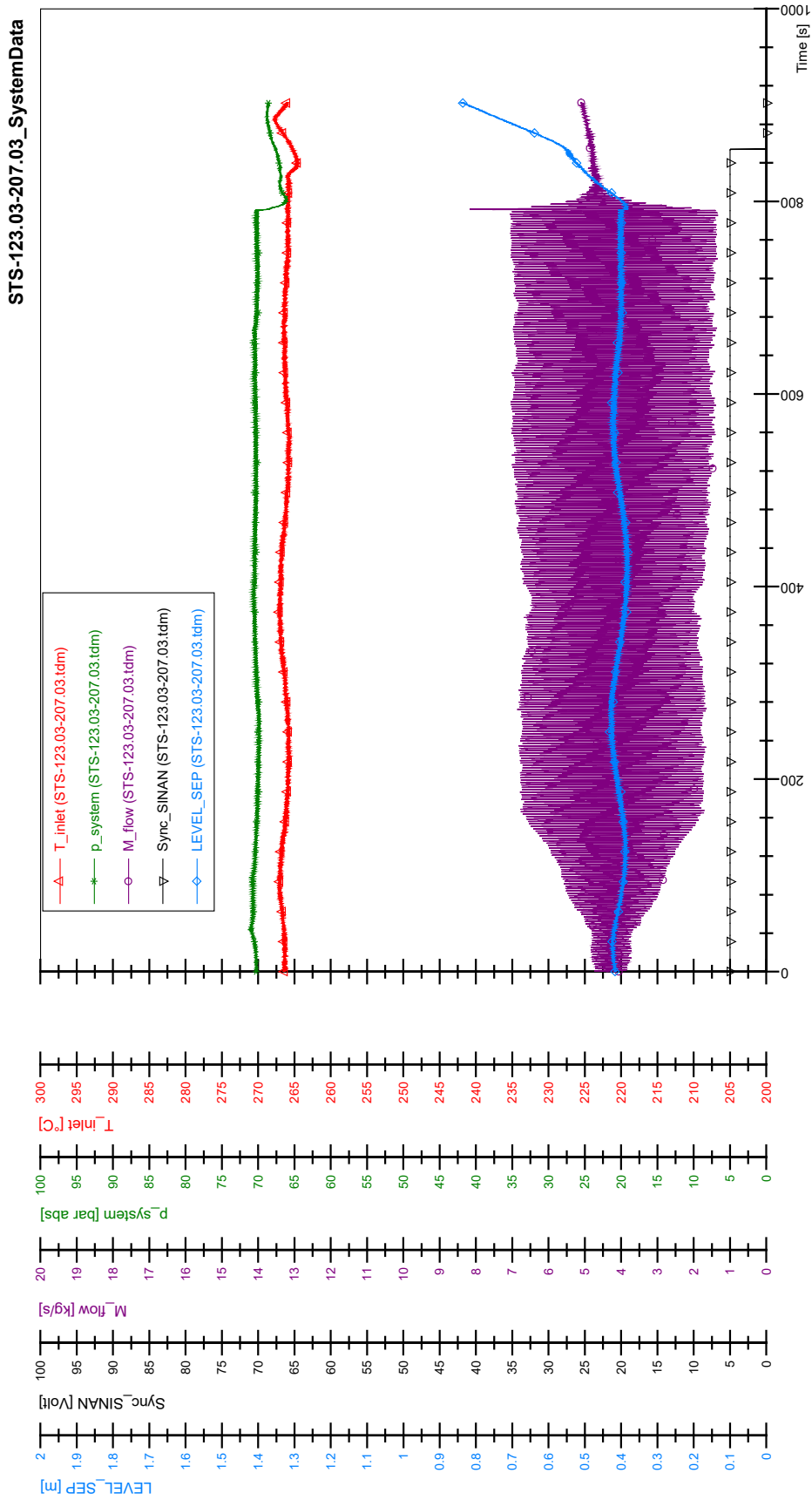
STS-123.03-207.02_Rod_87

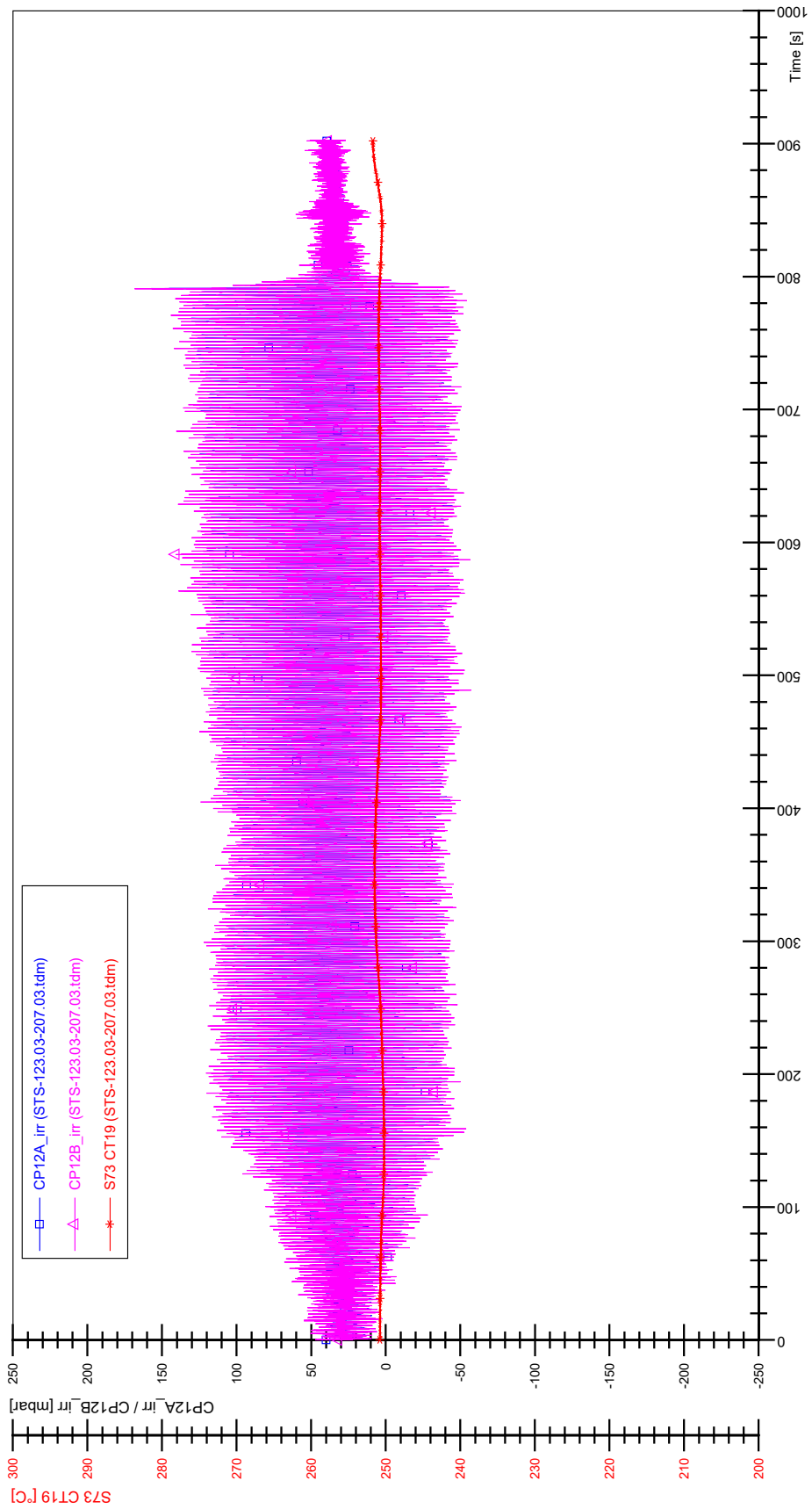


STS-123.03-207.02_Rod_88

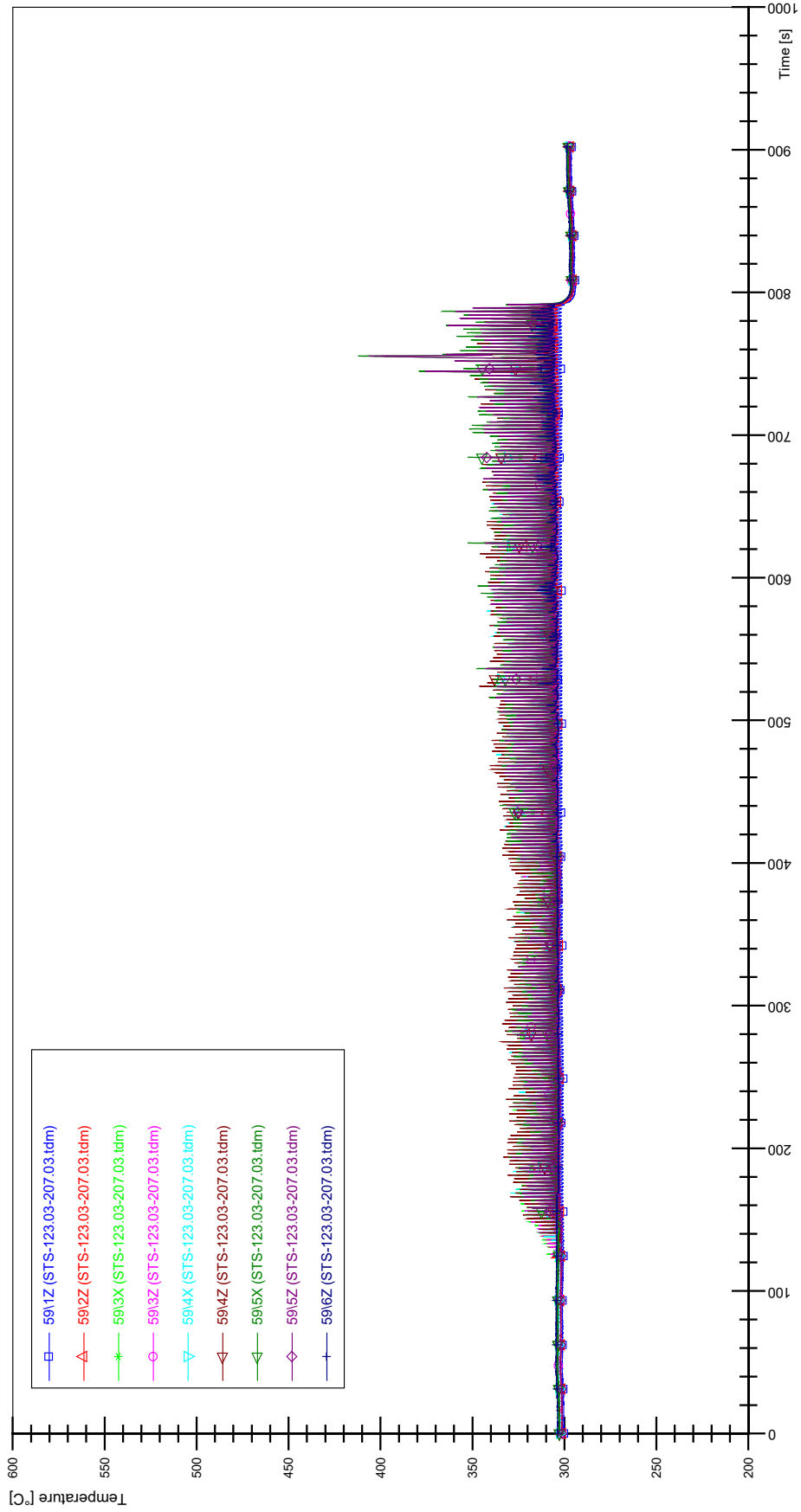


APPENDIX Z PLOTS OF INSTABILITY TEST STS-123.03-207.03

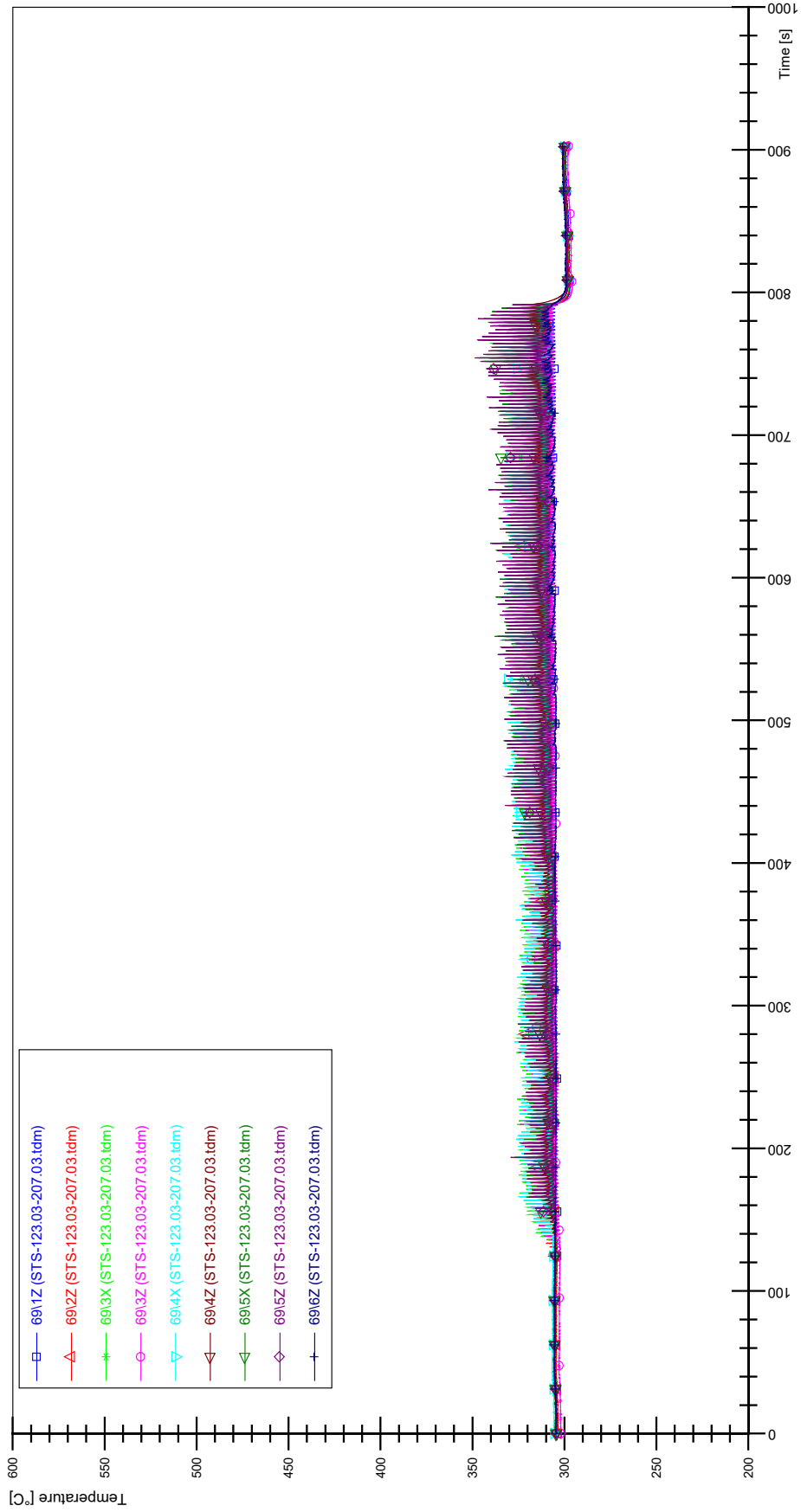




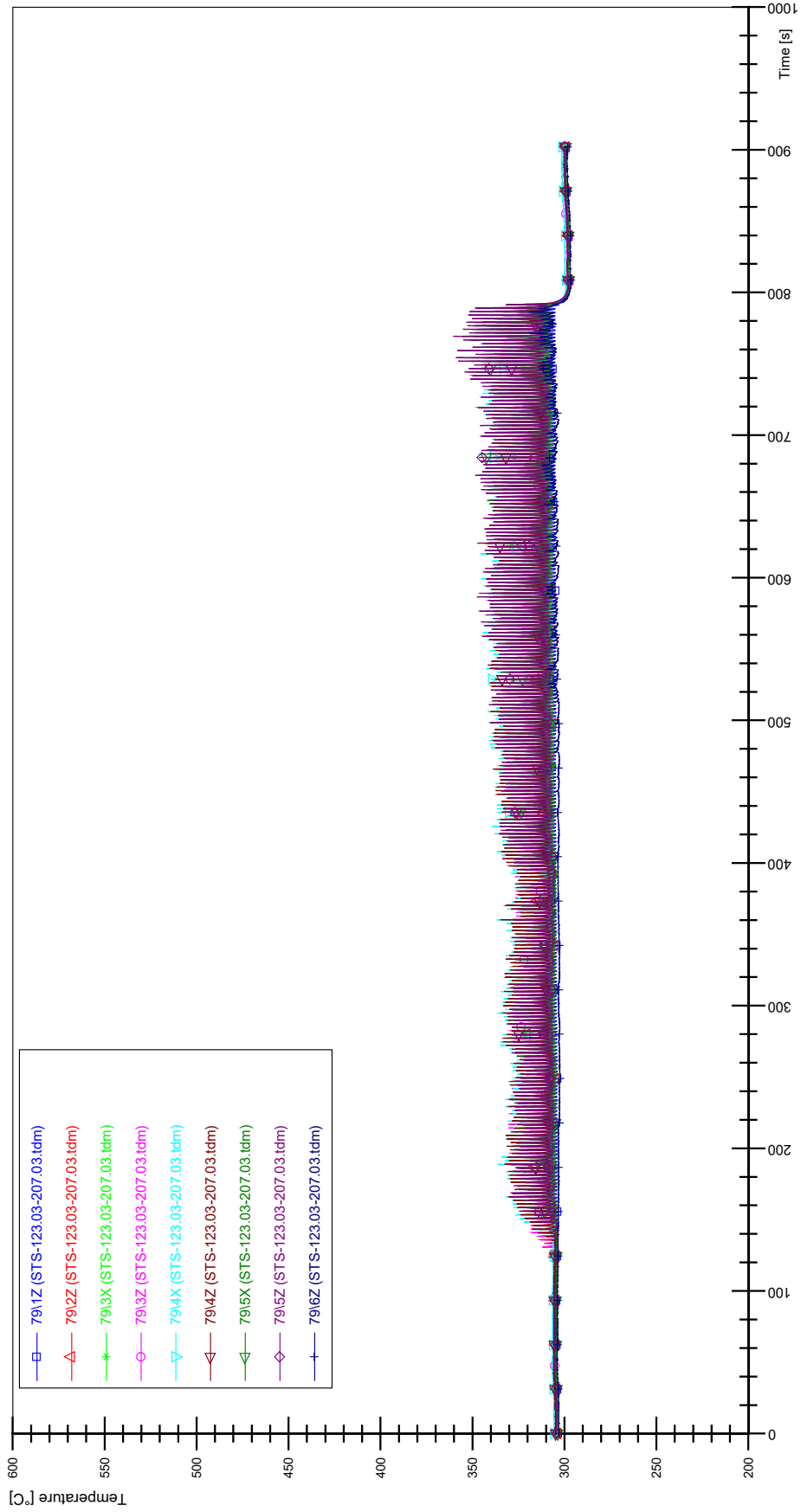
STS-123.03-207.03_Rod_59



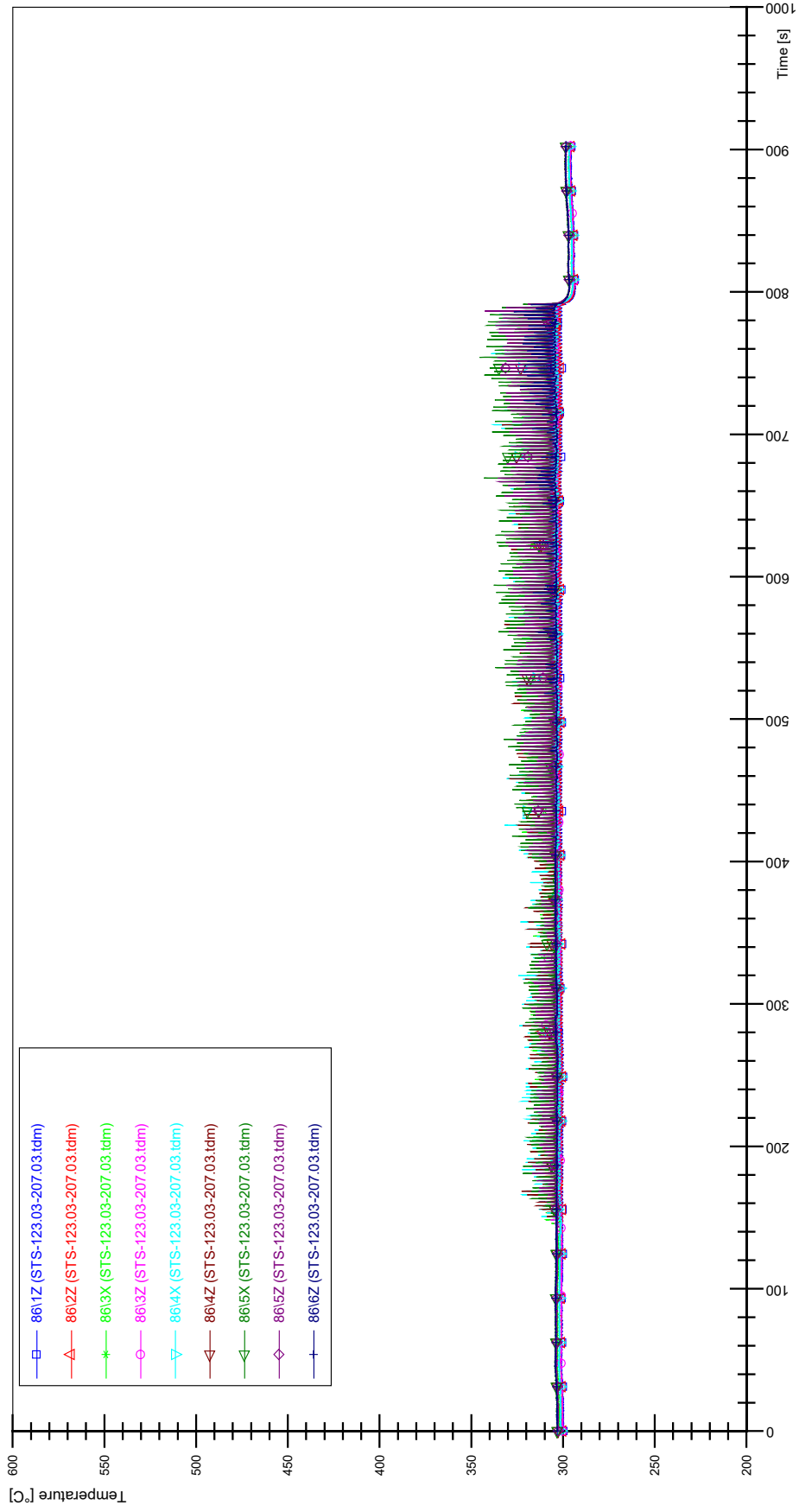
STS-123.03-207.03_Rod_69



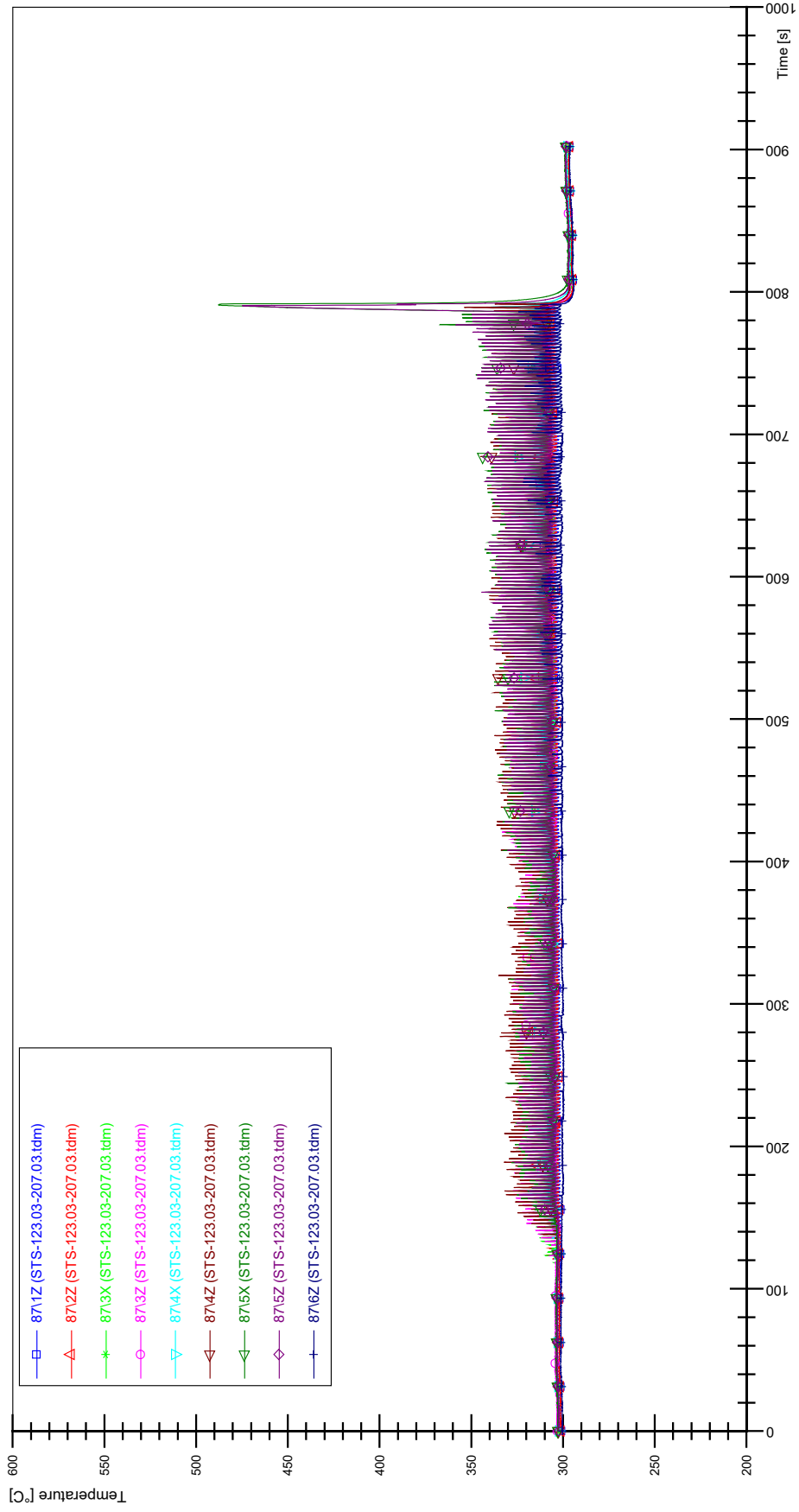
STS-123.03-207.03_Rod_79



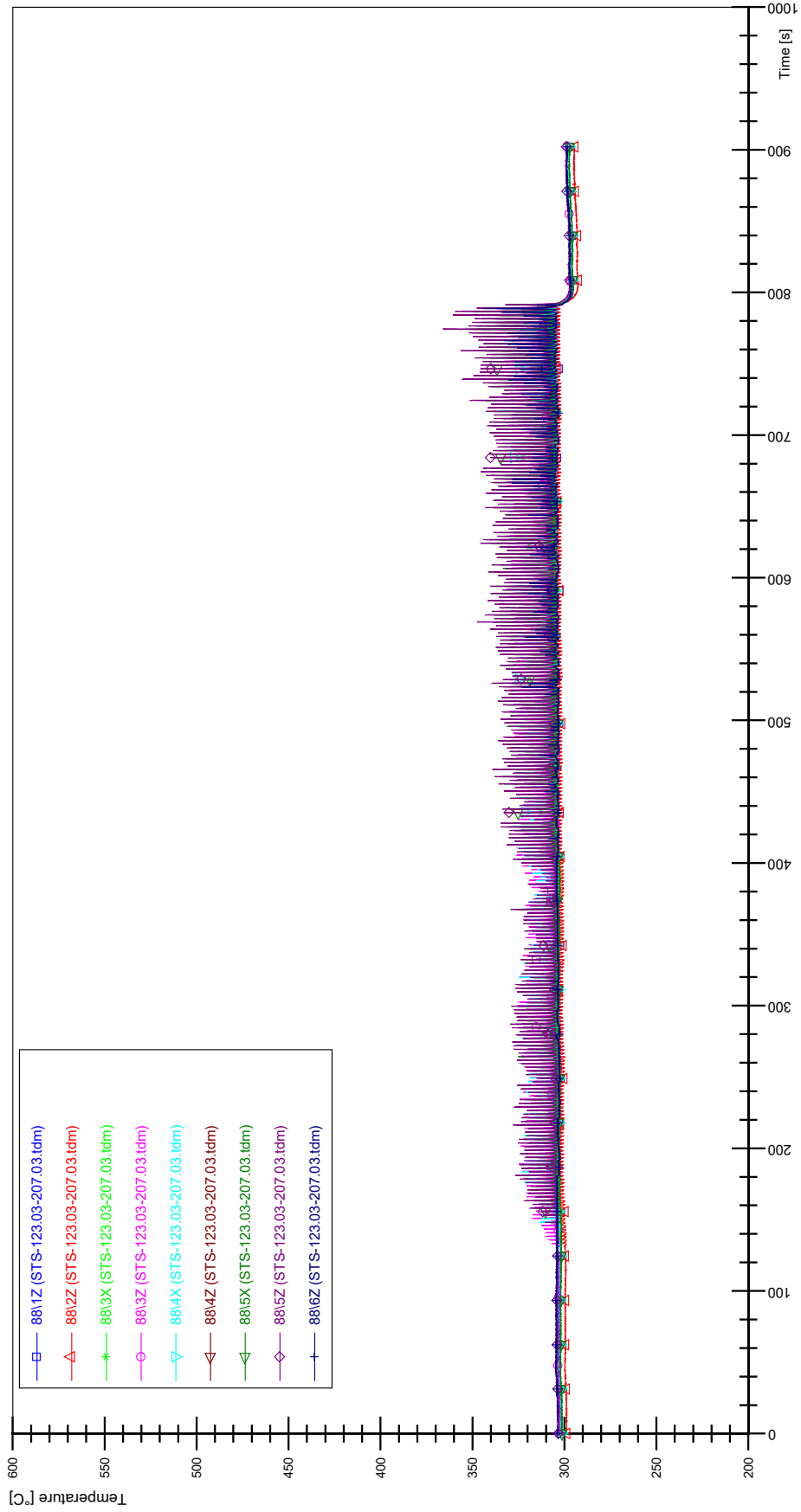
STS-123.03-207.03_Rod_86



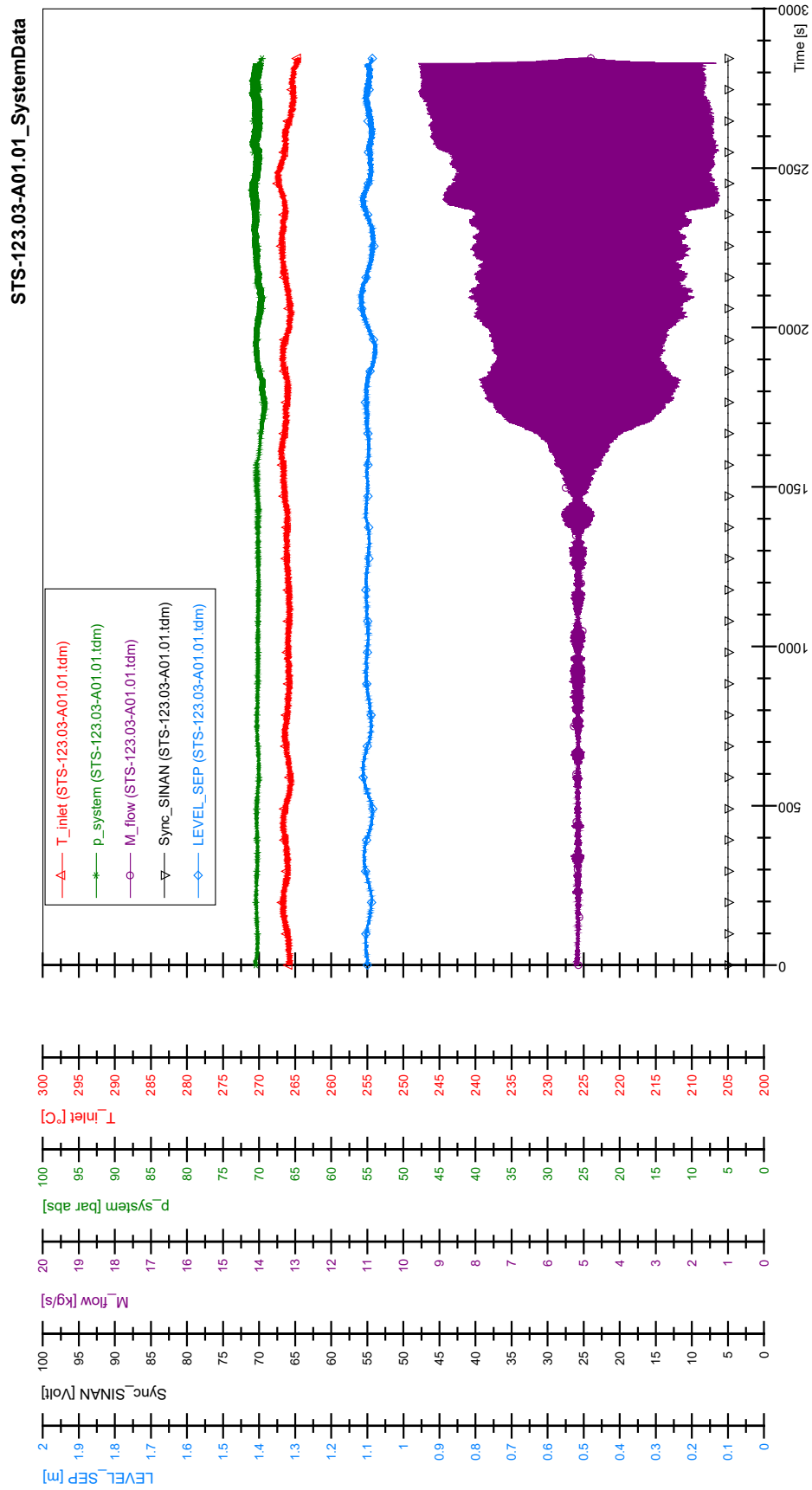
STS-123.03-207.03_Rod_87



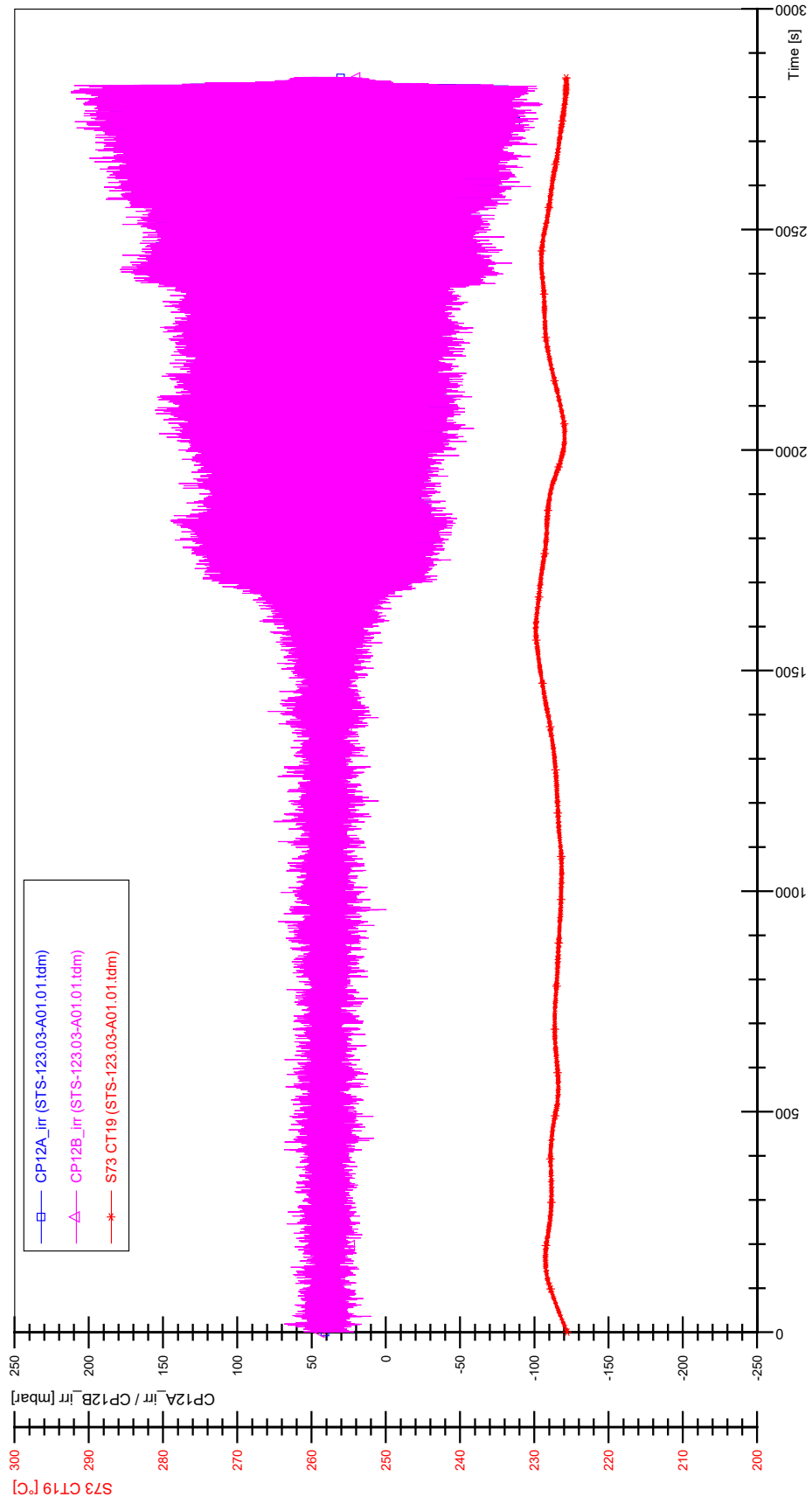
STS-123.03-207.03_Rod_88



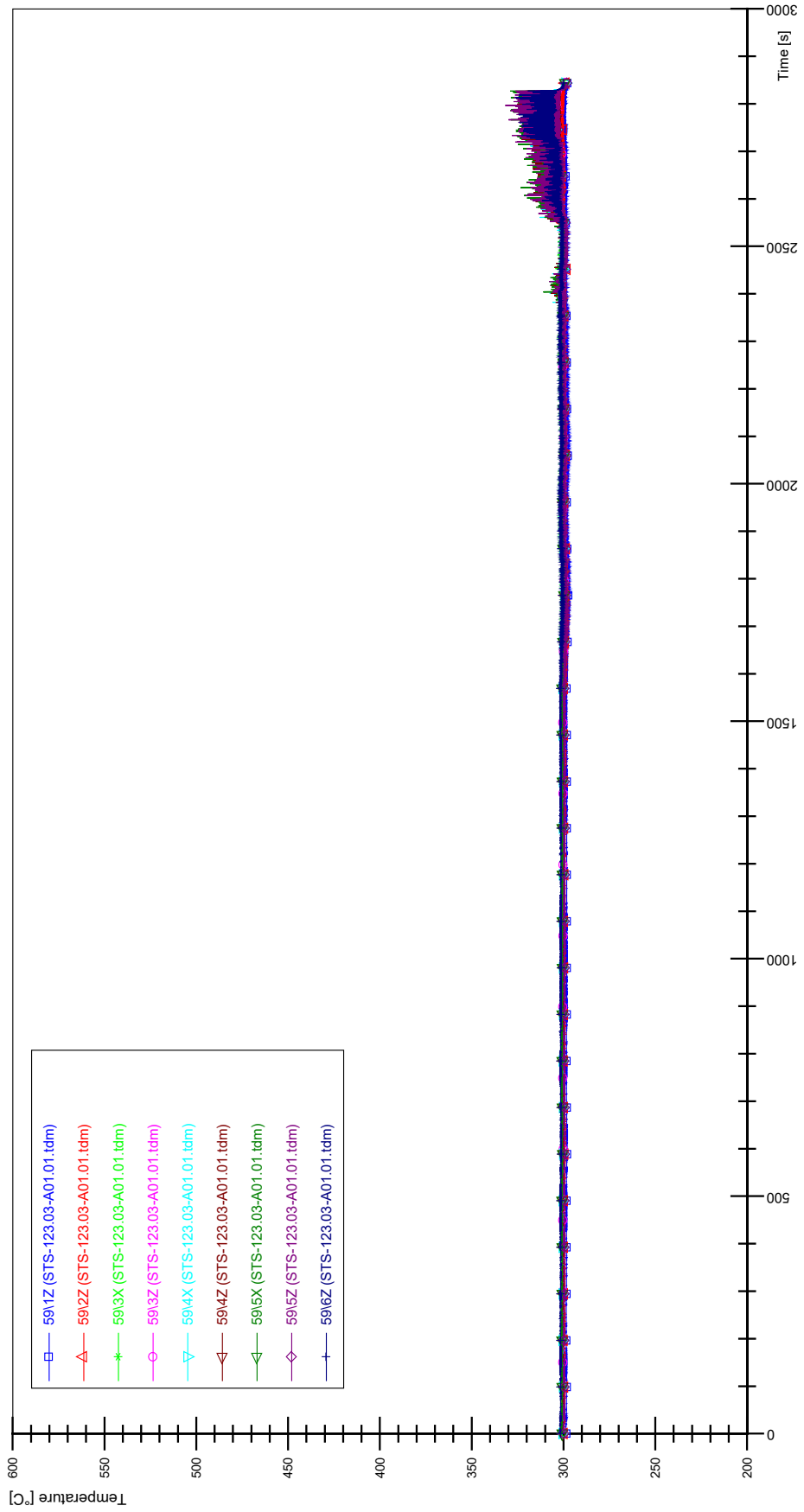
APPENDIX AA PLOTS OF INSTABILITY TEST STS-123.03-A01.01



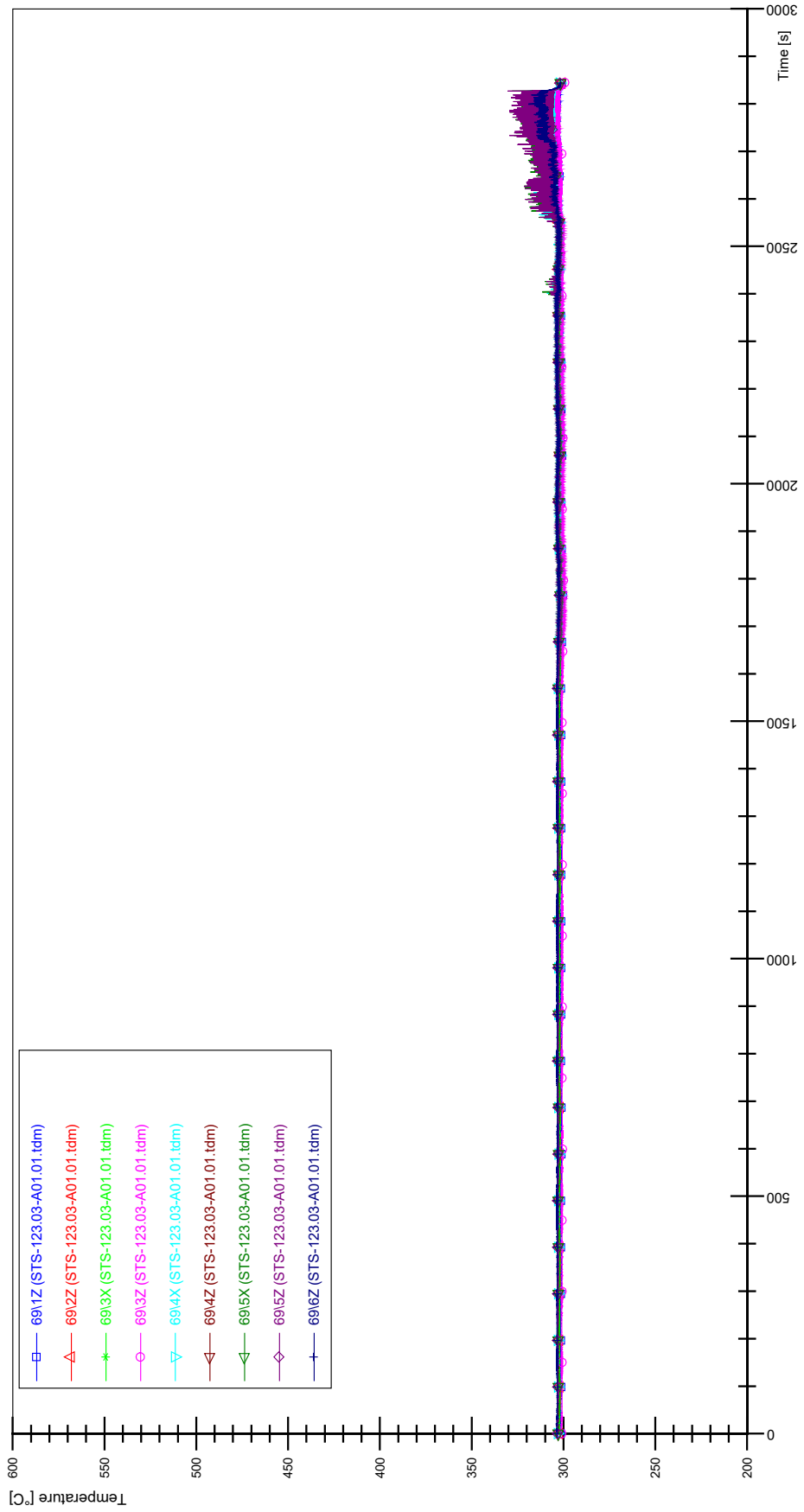
STS-123.03-A01.01_CP12_CT19



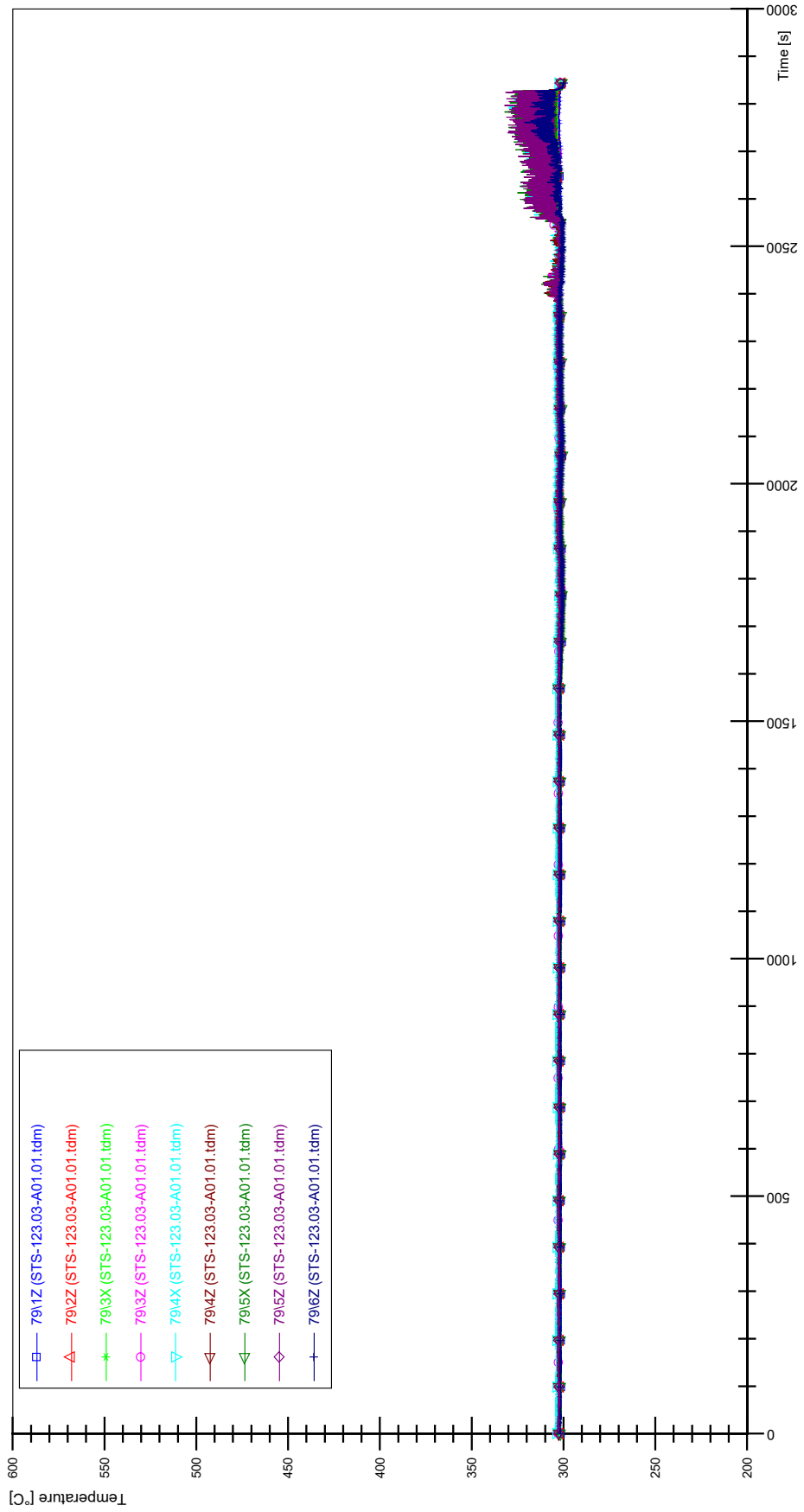
STS-123.03-A01.01_Rod_59



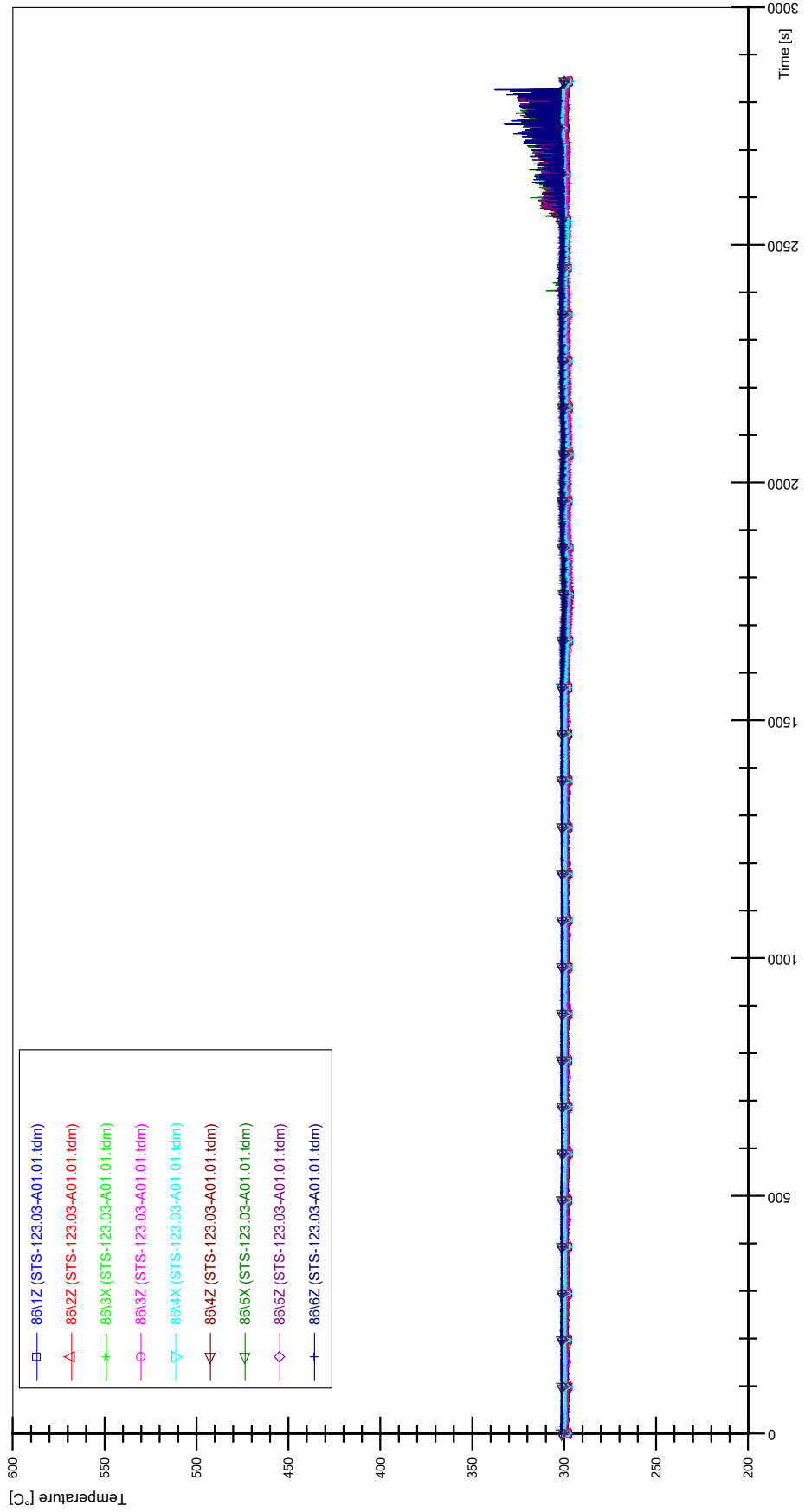
STS-123.03-A01.01_Rod_69



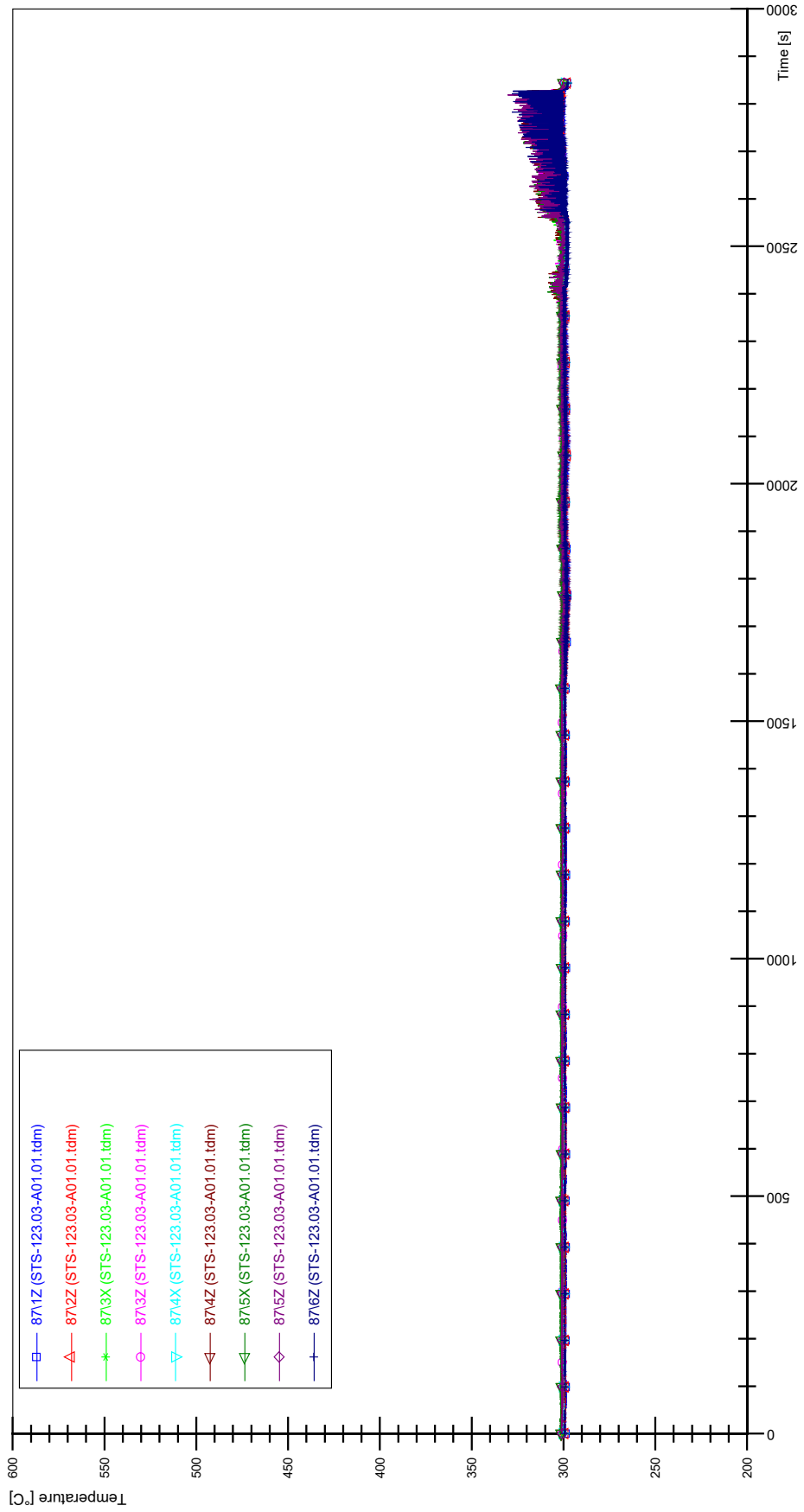
STS-123.03-A01.01_Rod_79



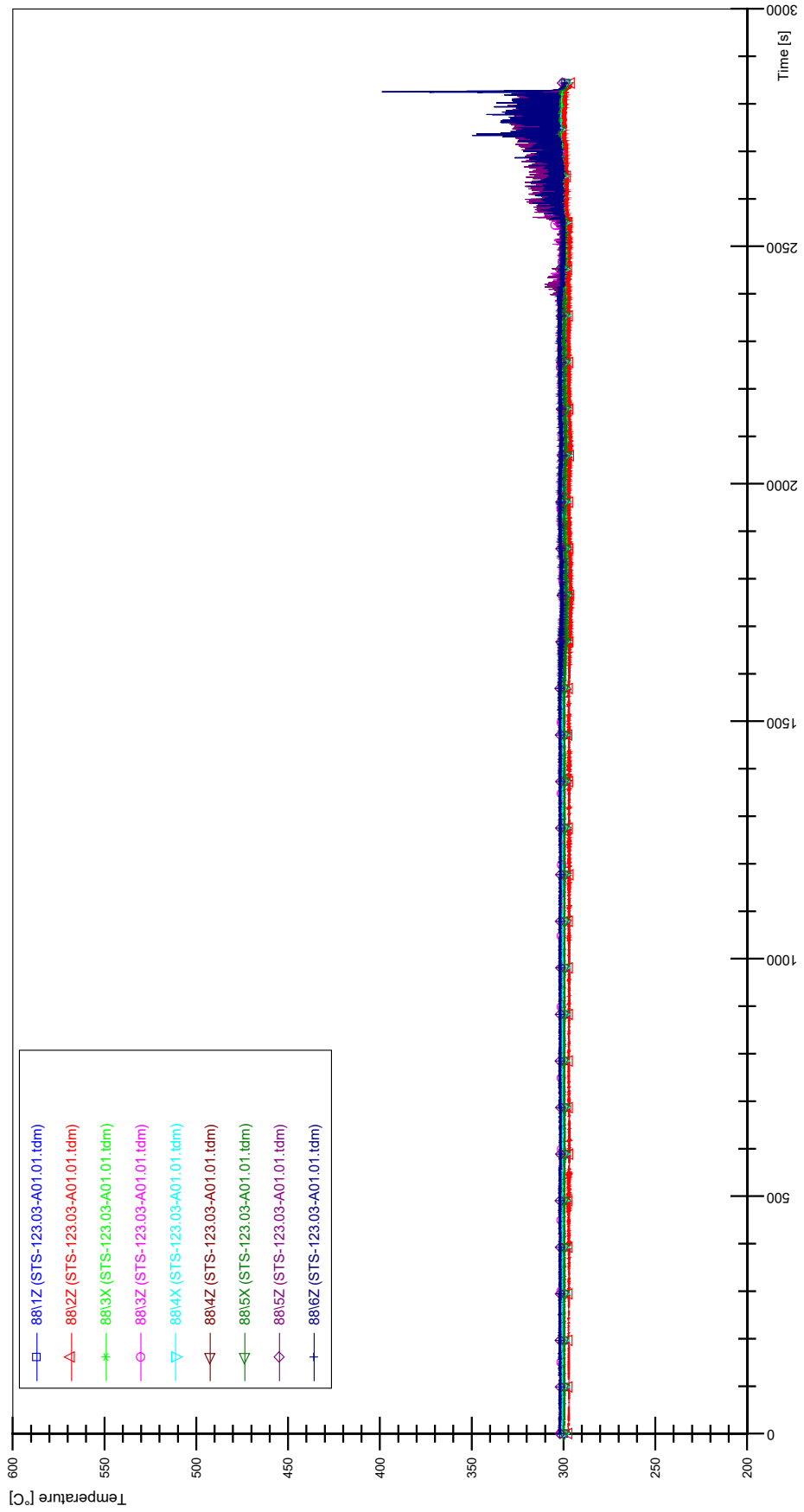
STS-123.03-A01.01_Rod_86



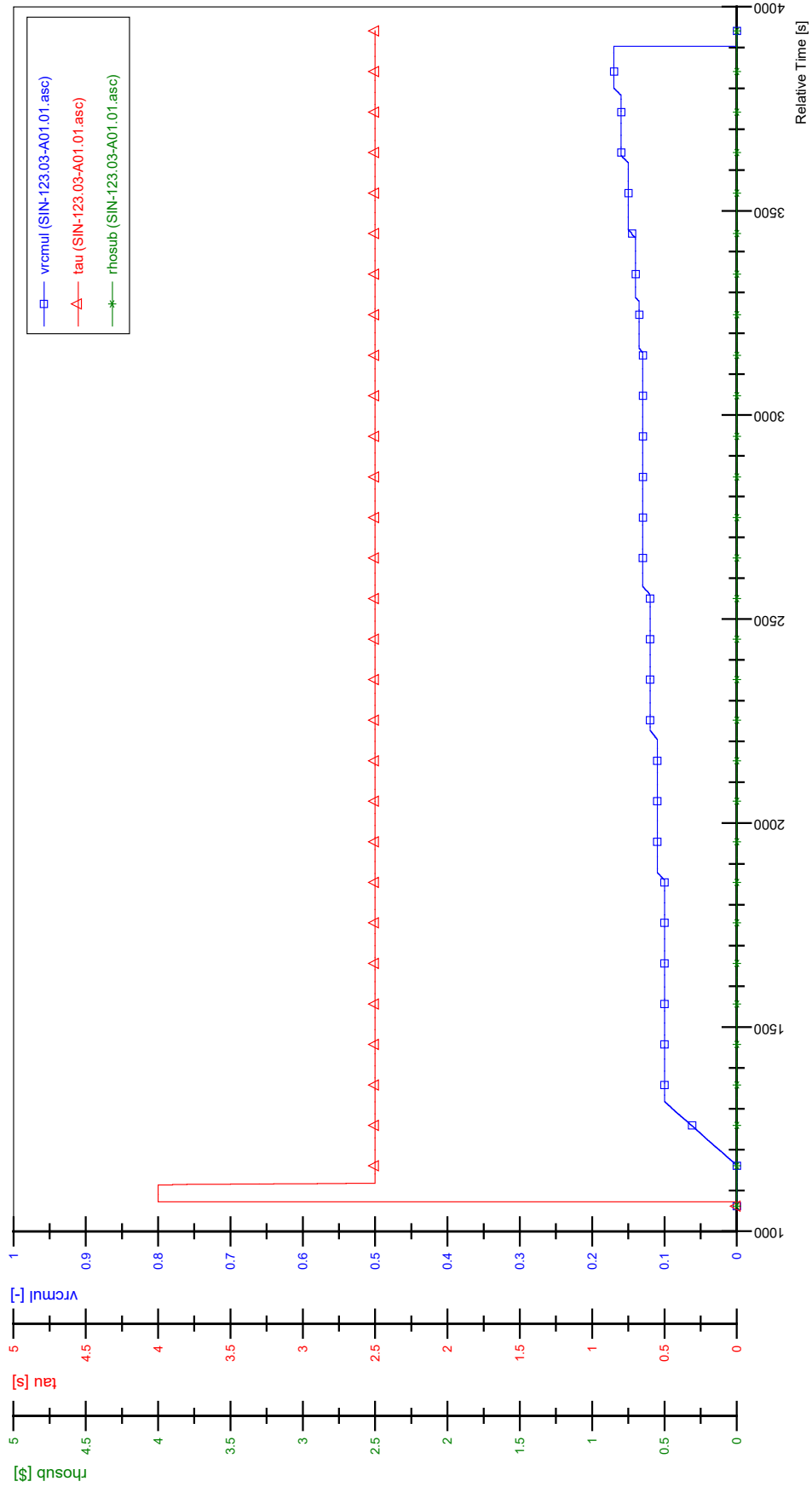
STS-123.03-A01.01_Rod_87



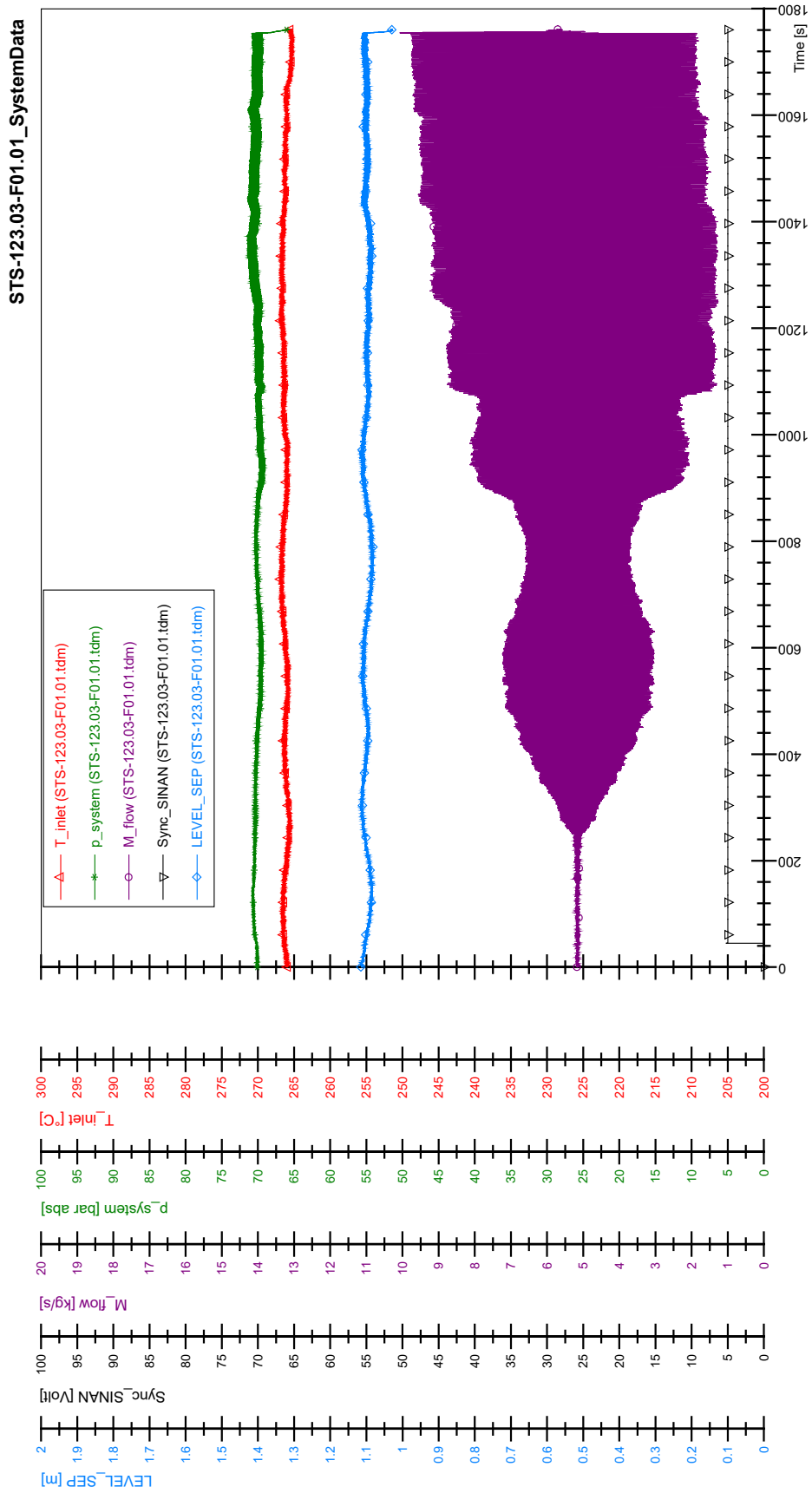
STS-123.03-A01.01_Rod_88



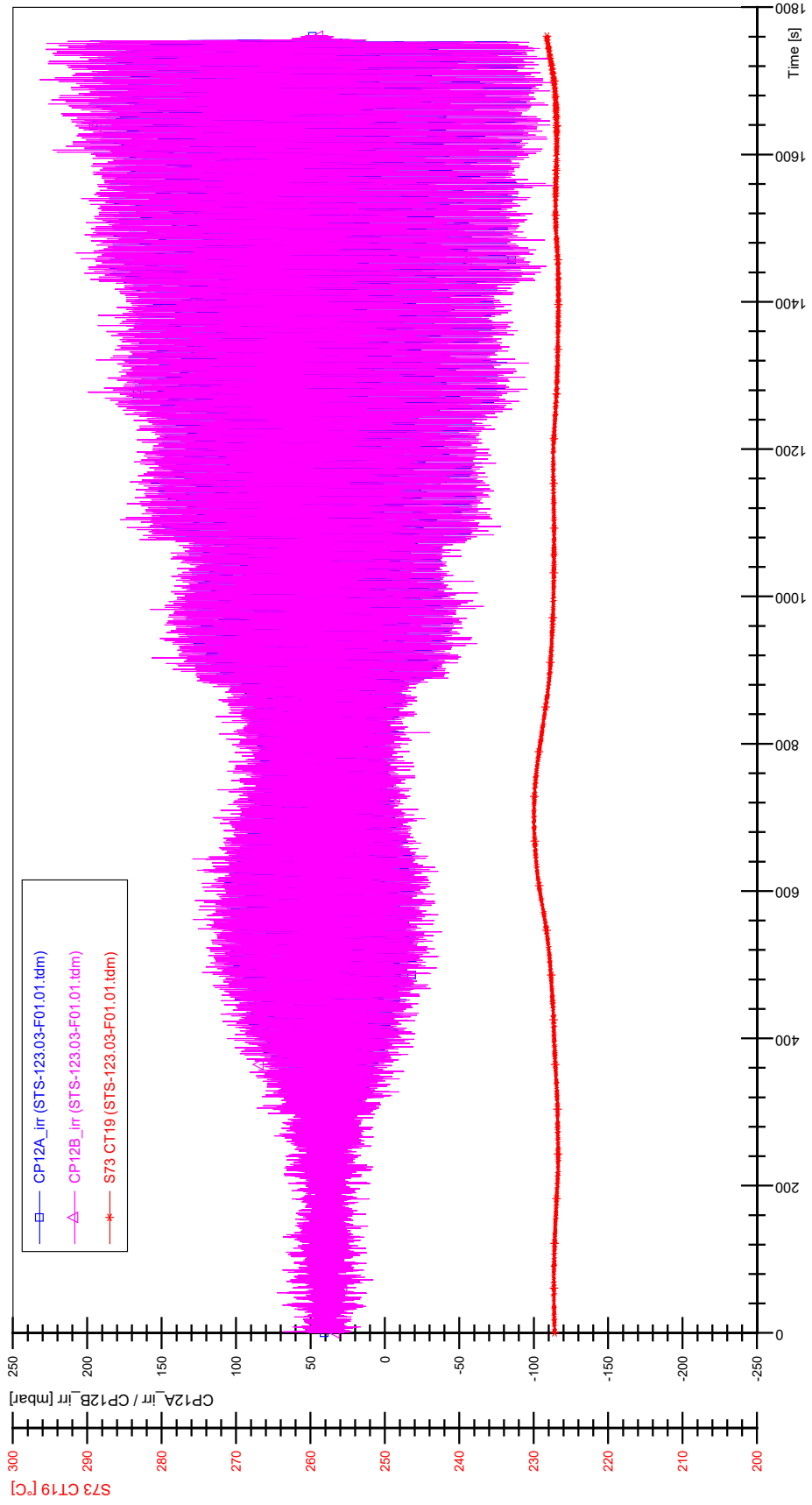
SIN-123.03-A01.01



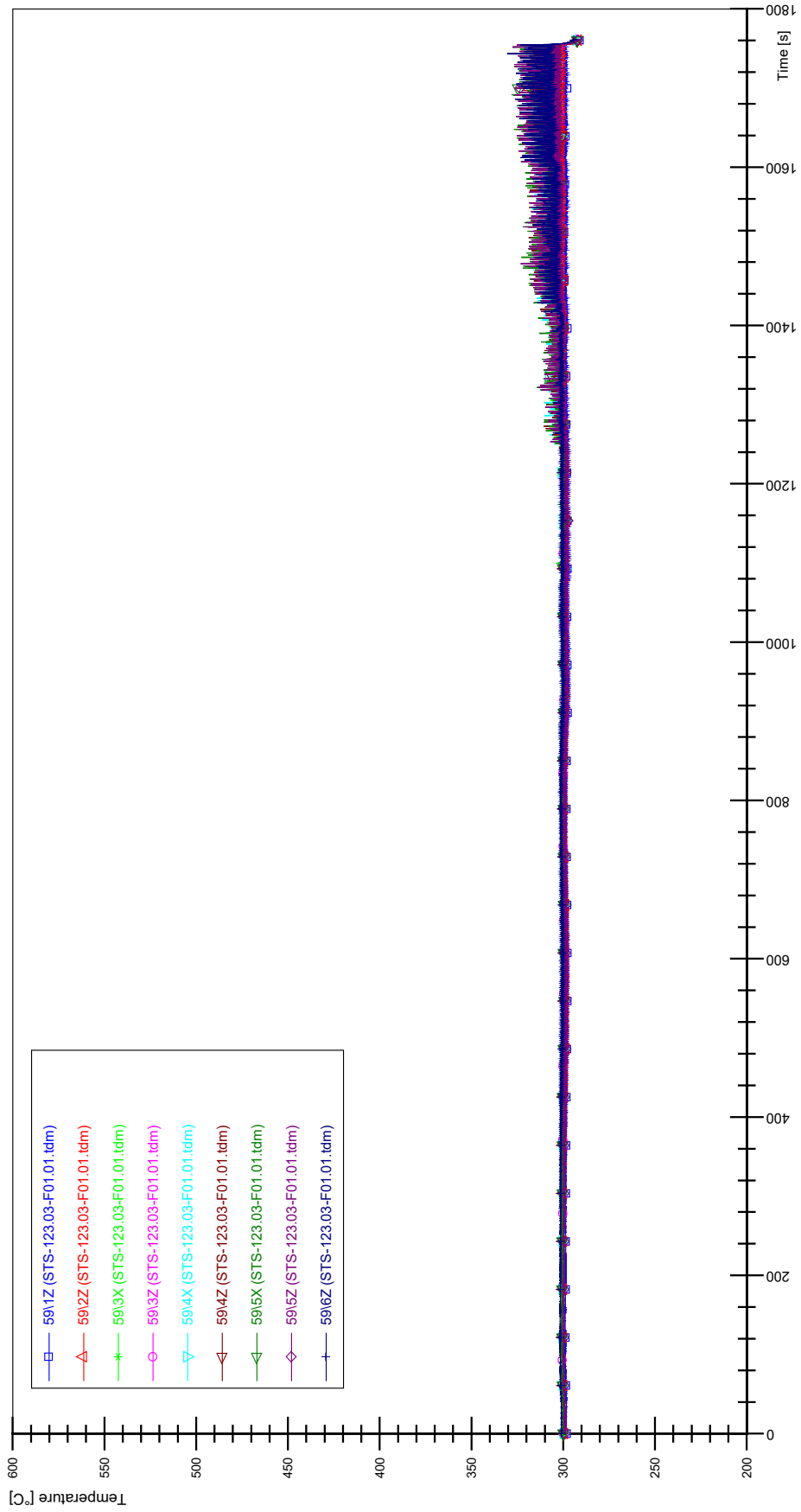
APPENDIX BB PLOTS OF INSTABILITY TEST STS-123.03-F01.01



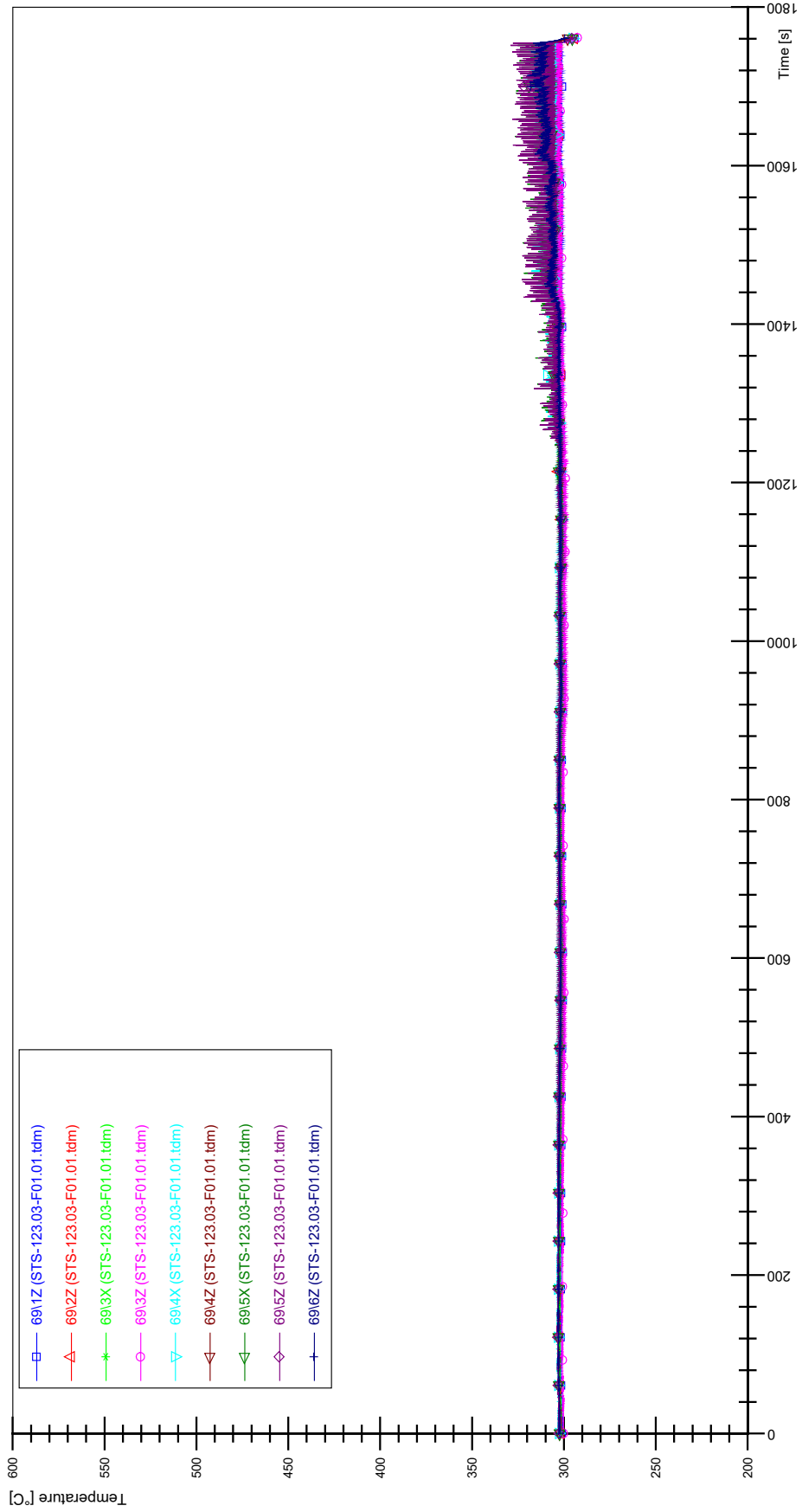
STS-123.03-F01.01_CP12_CT19



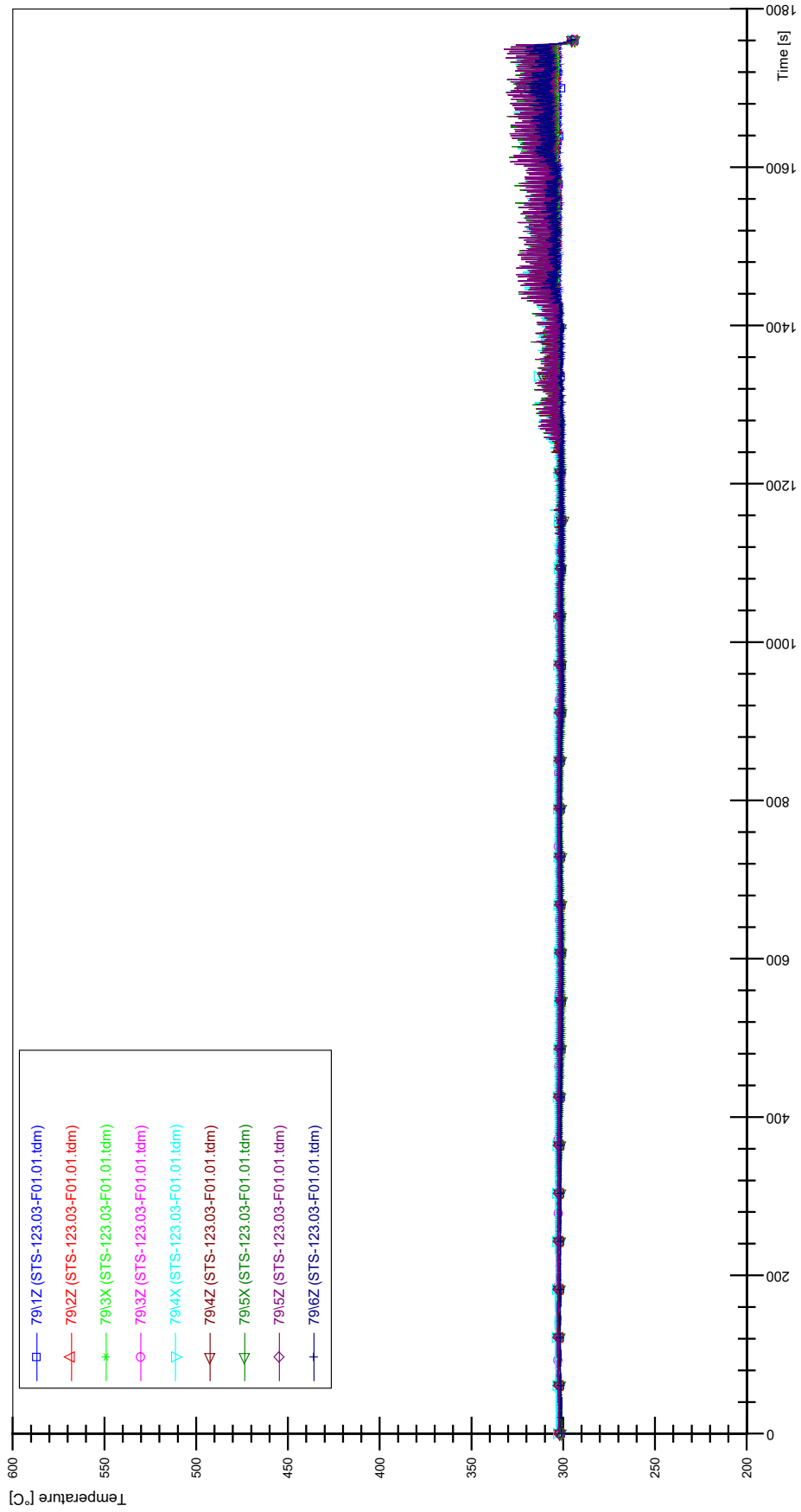
STS-123.03-F01.01_Rod_59



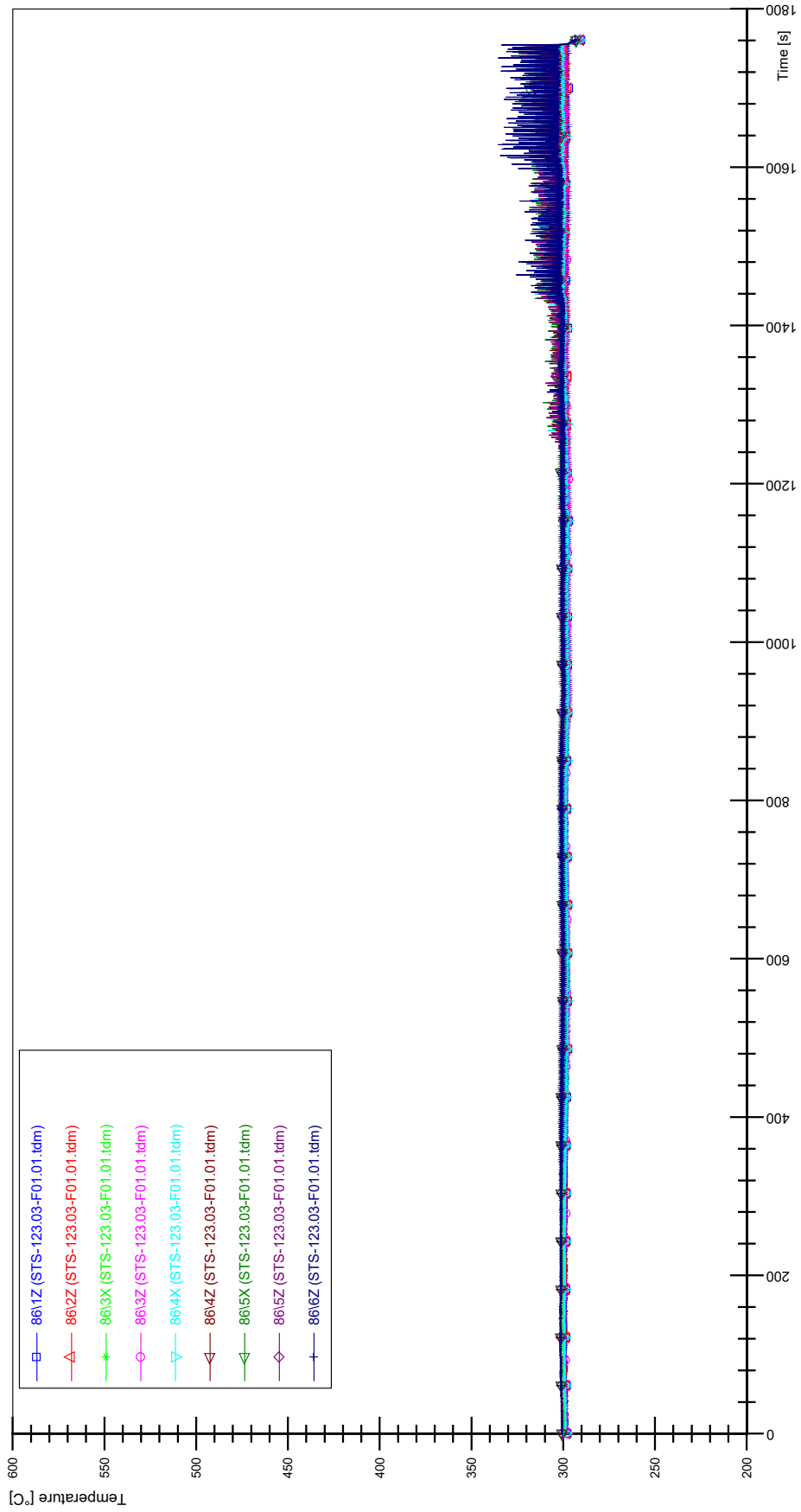
STS-123.03-F01.01_Rod_69



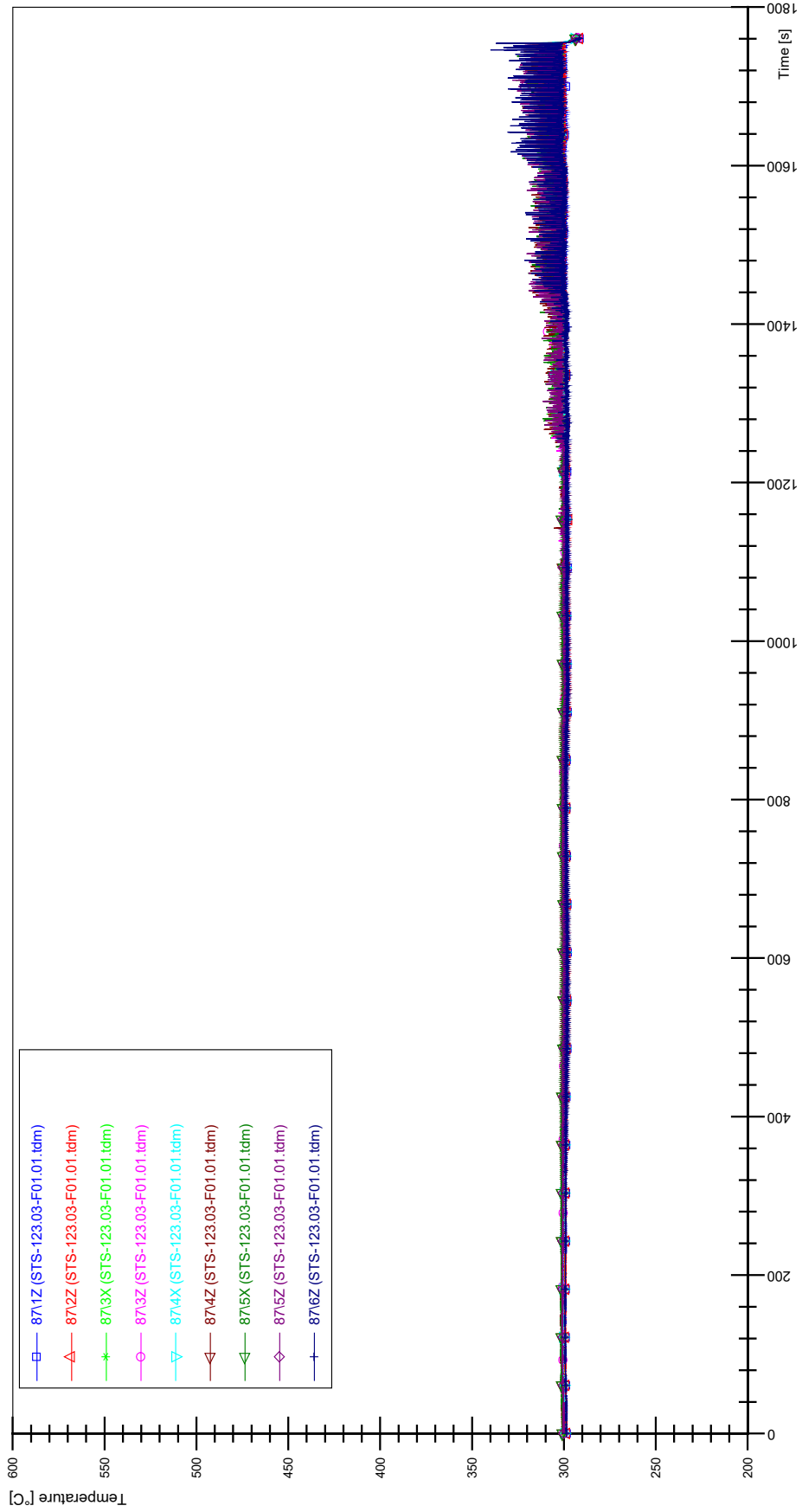
STS-123.03-F01.01_Rod_79



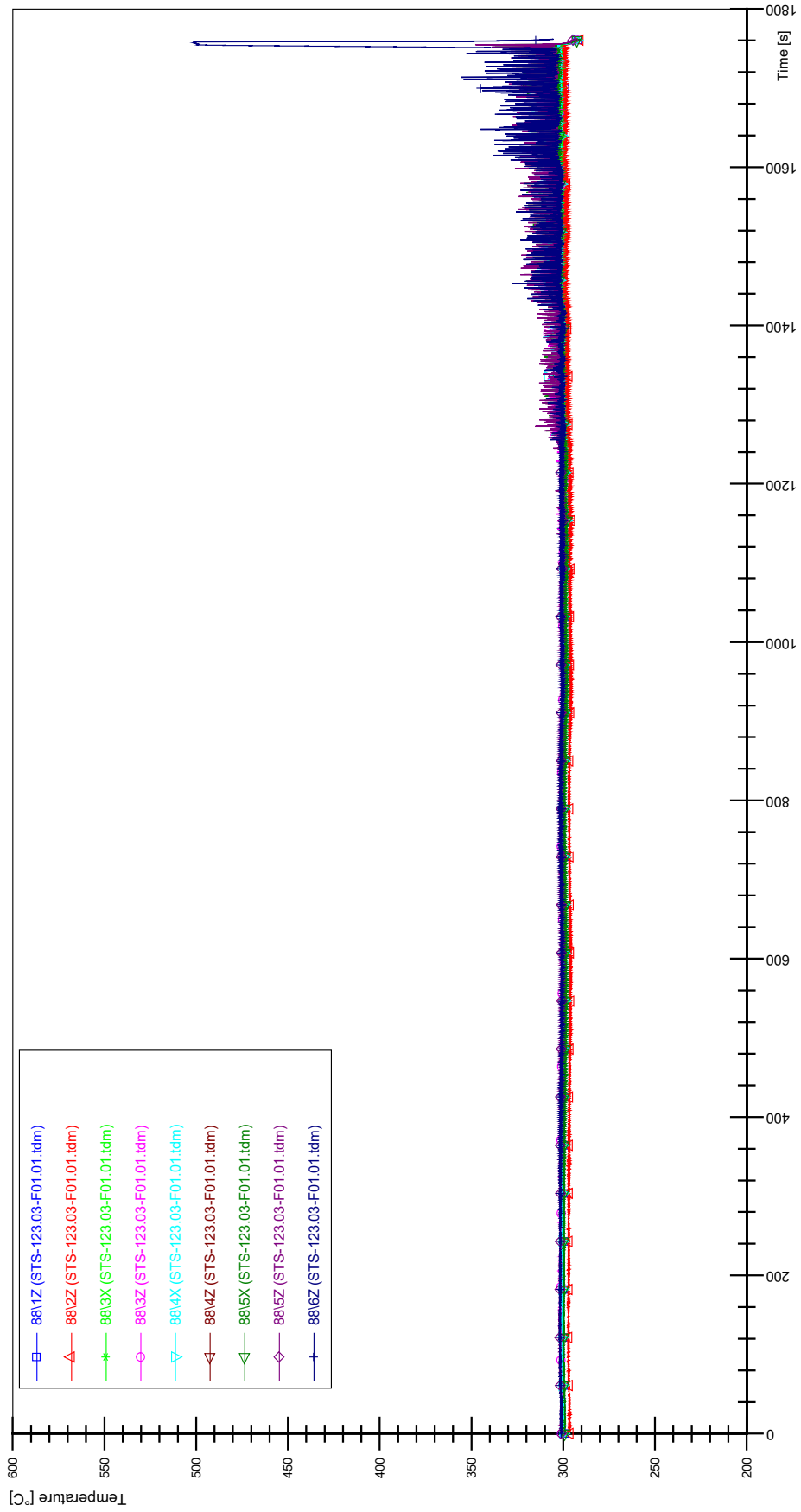
STS-123.03-F01.01_Rod_86



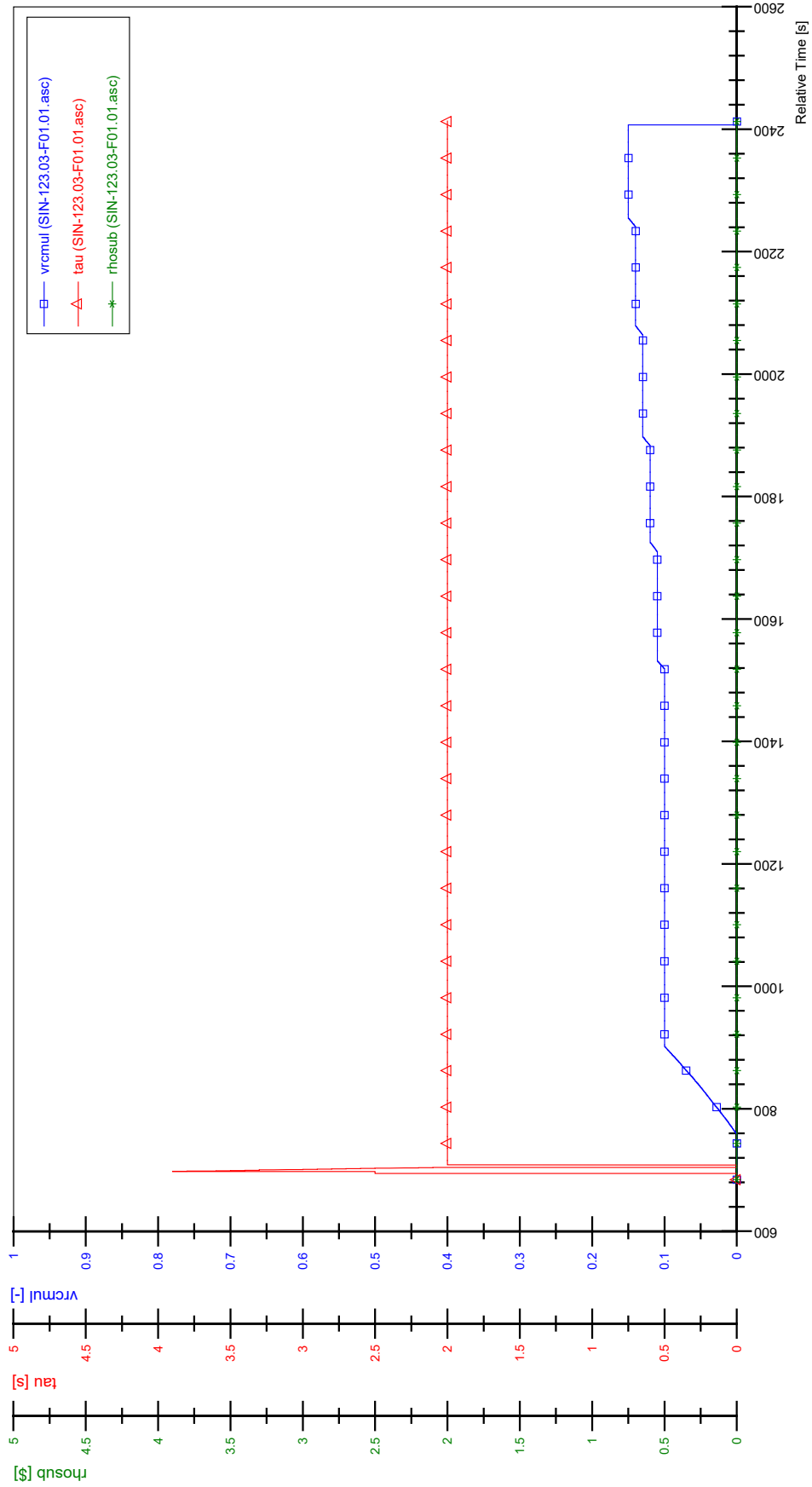
STS-123.03-F01.01_Rod_87



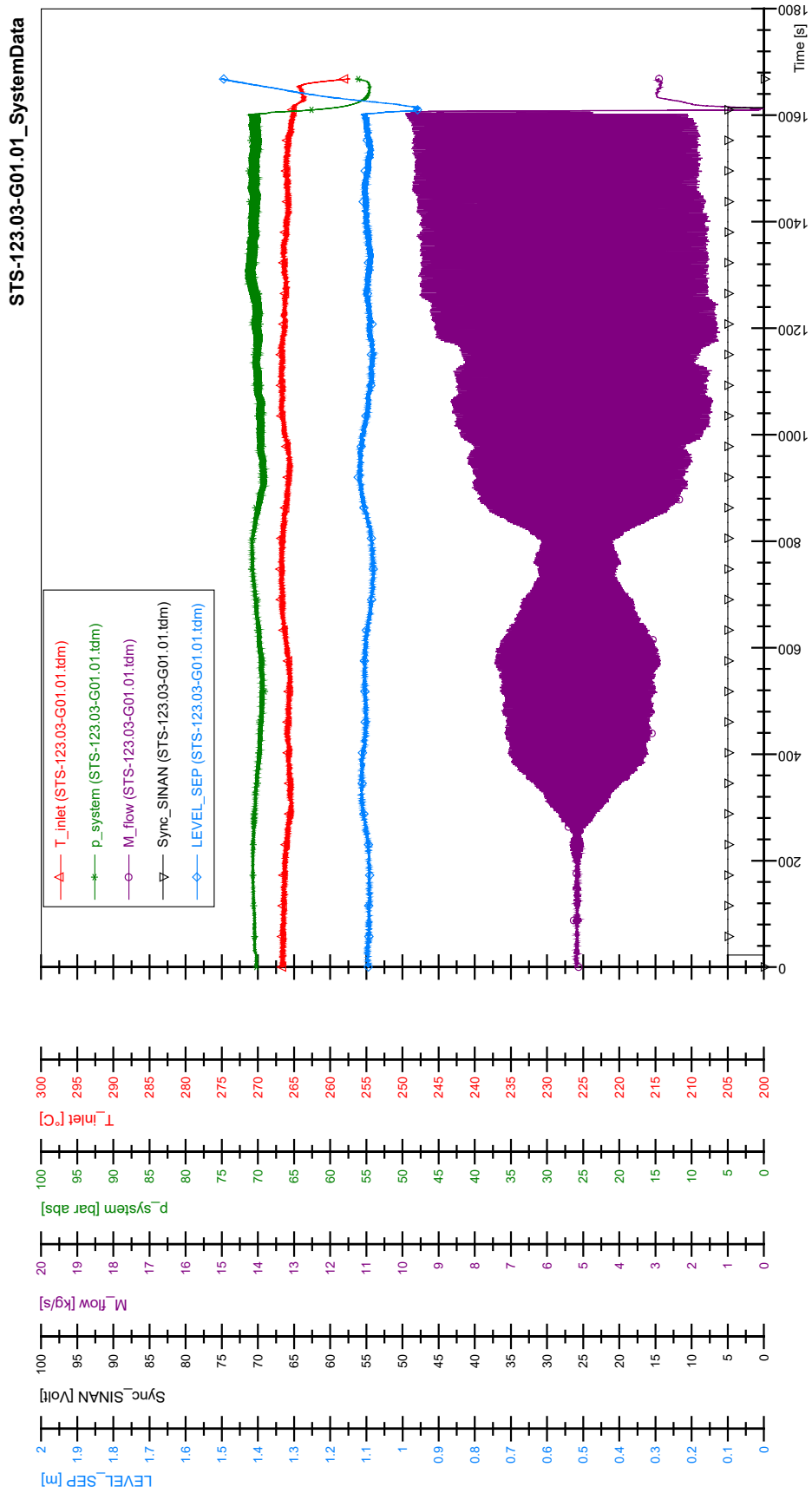
STS-123.03-F01.01_Rod_88



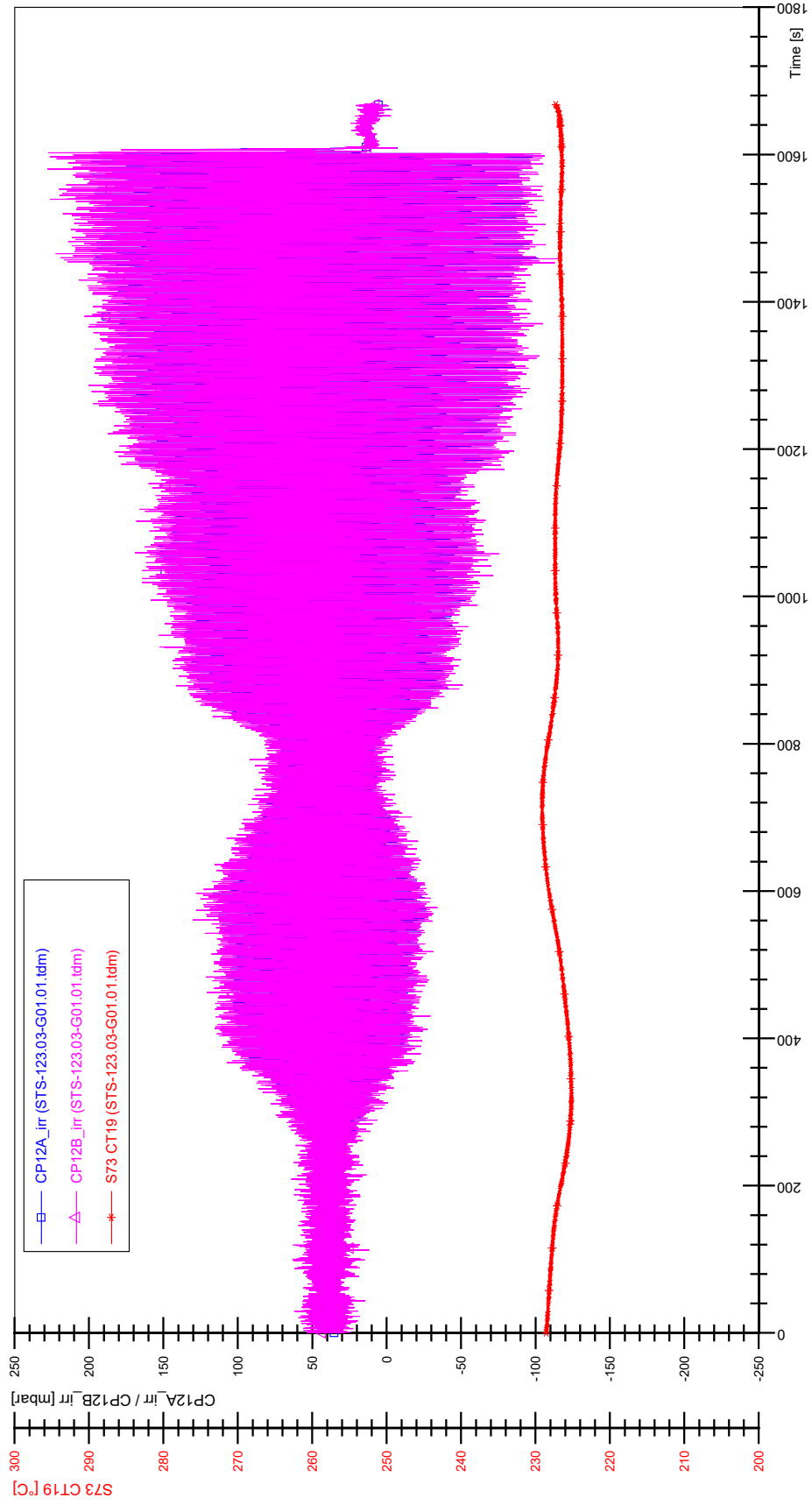
SIN-123.03-F01.01



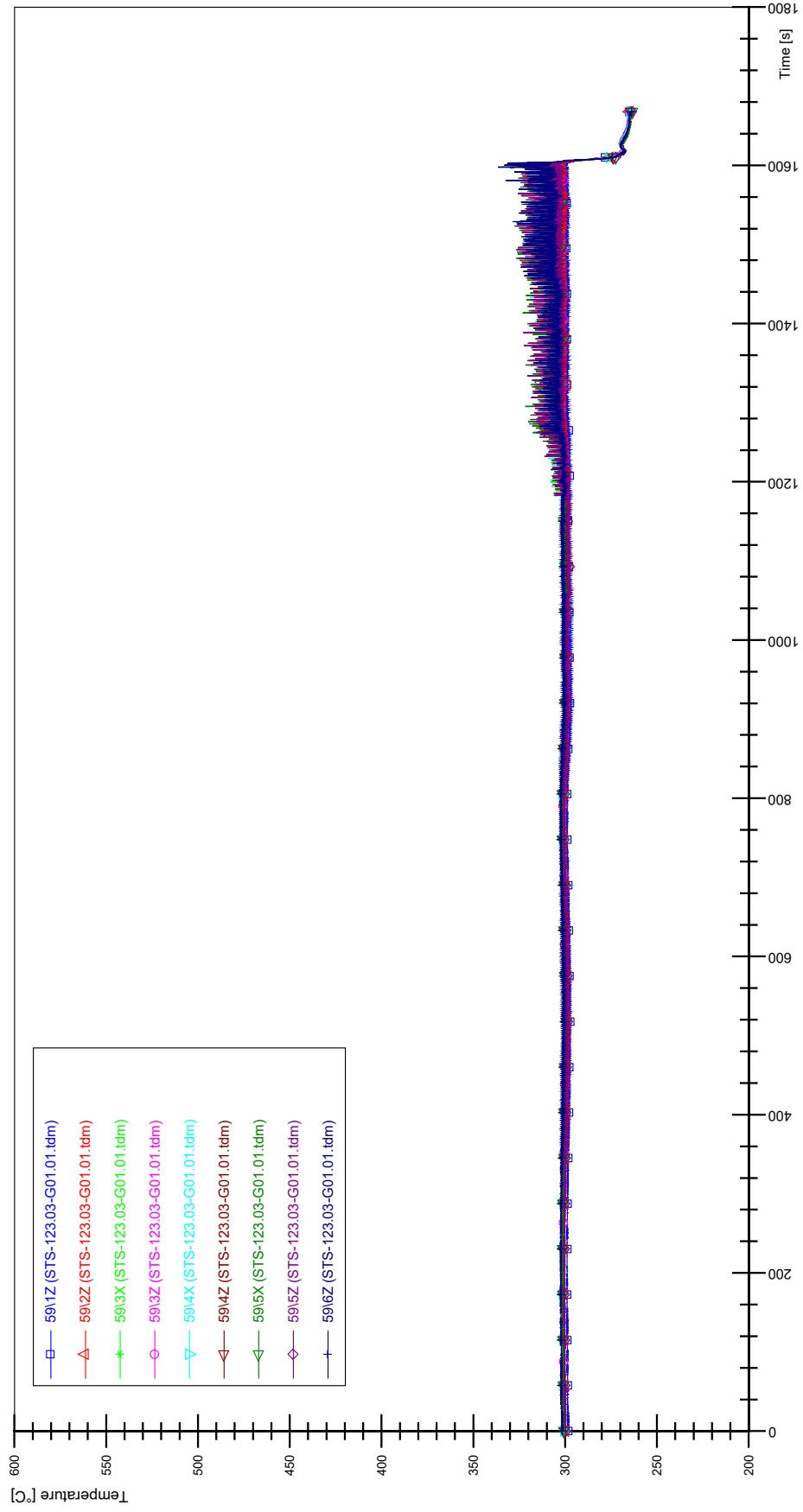
APPENDIX CC PLOTS OF INSTABILITY TEST STS-123.03-G01.01



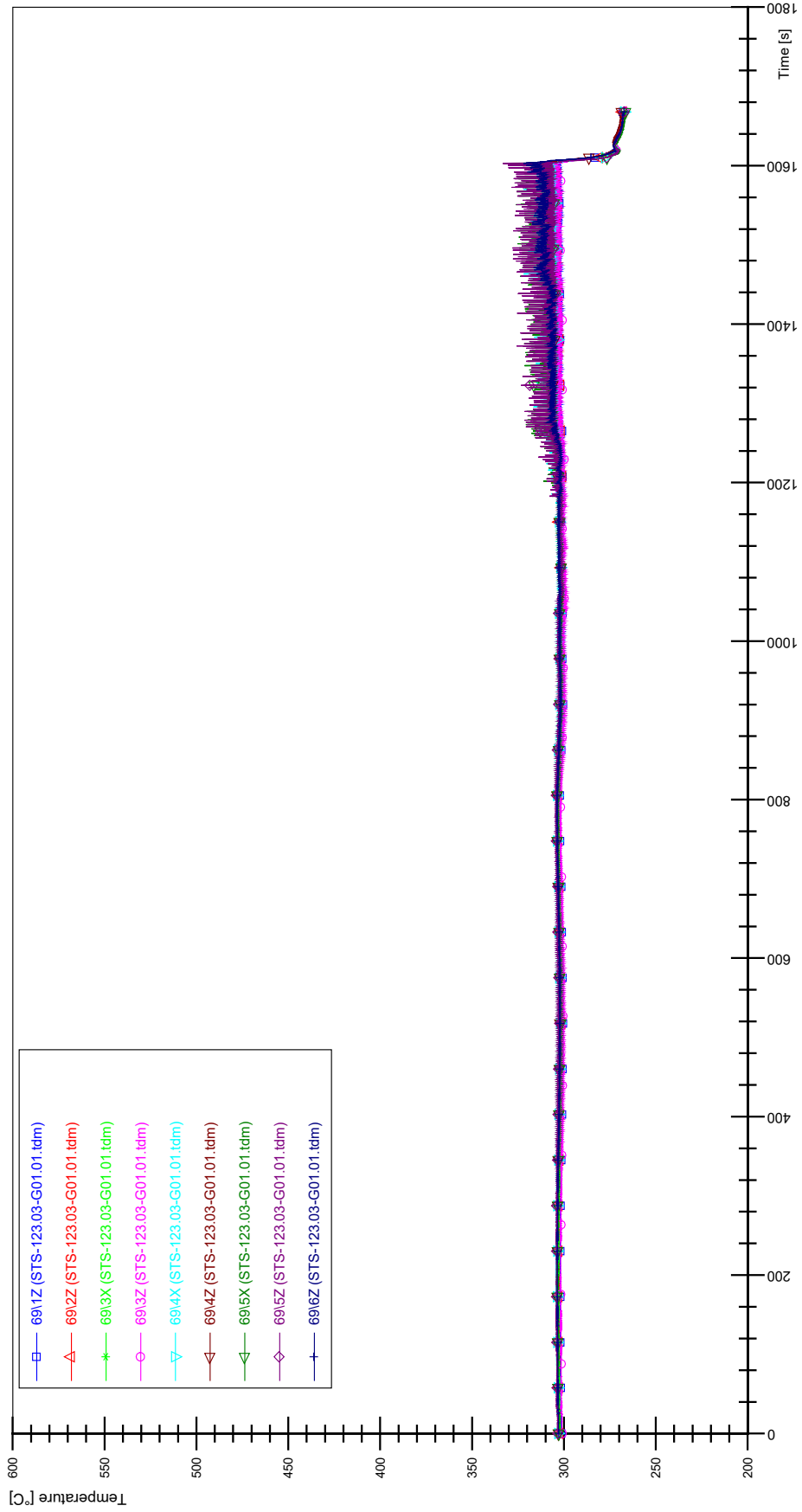
STS-123.03-G01.01_CP12_CT19



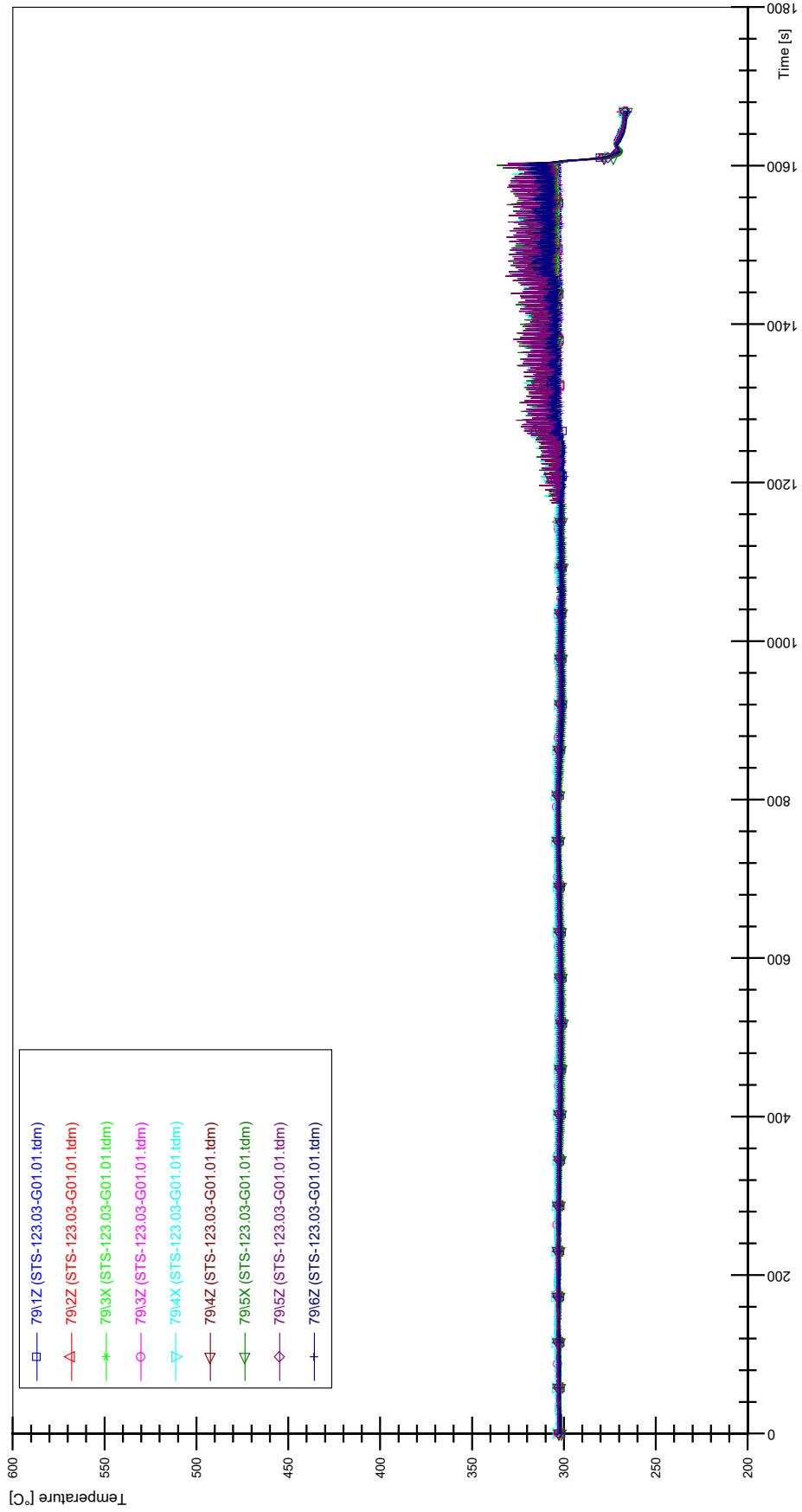
STS-123.03-G01.01_Rod_59



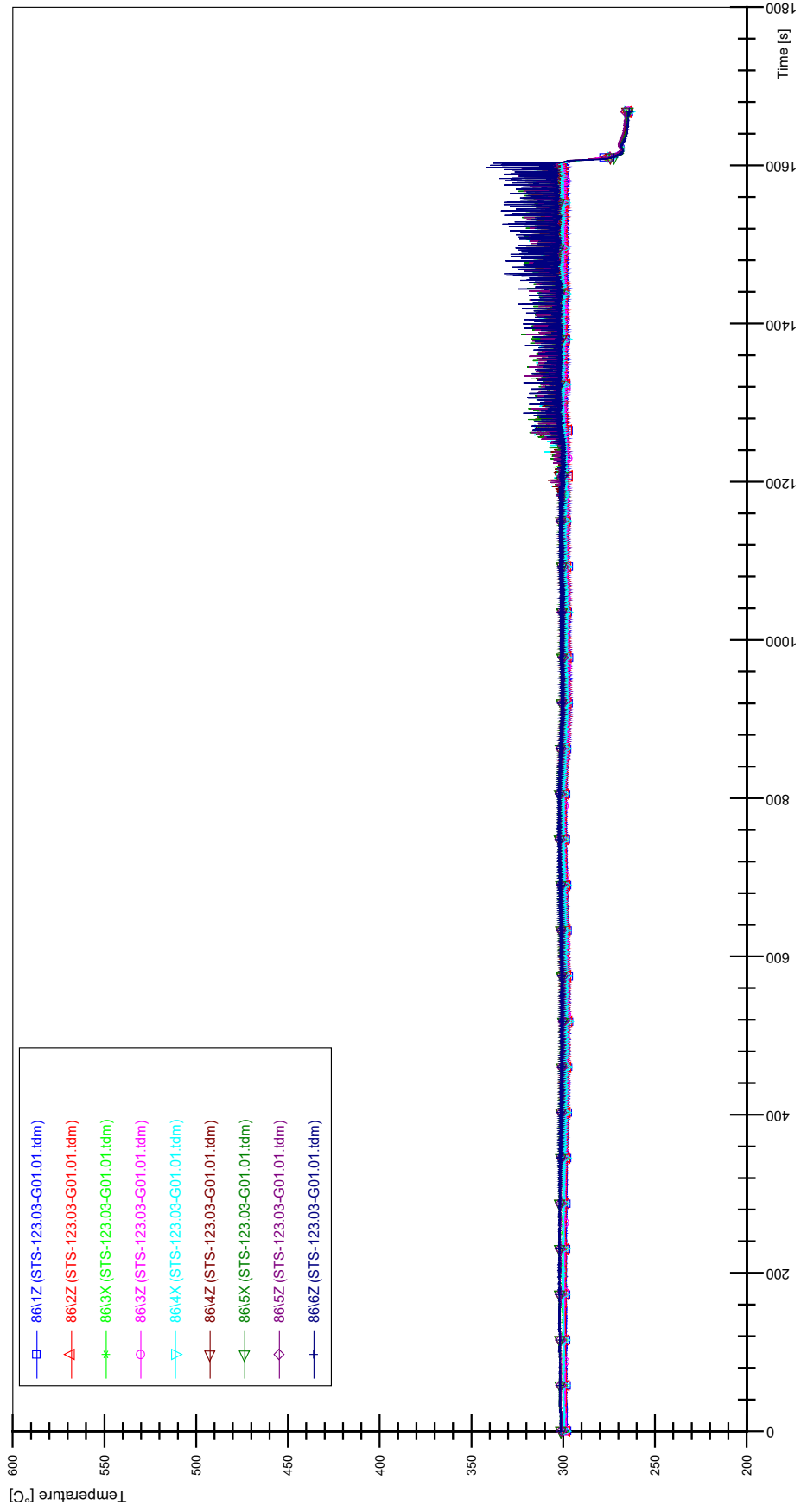
STS-123.03-G01.01_Rod_69



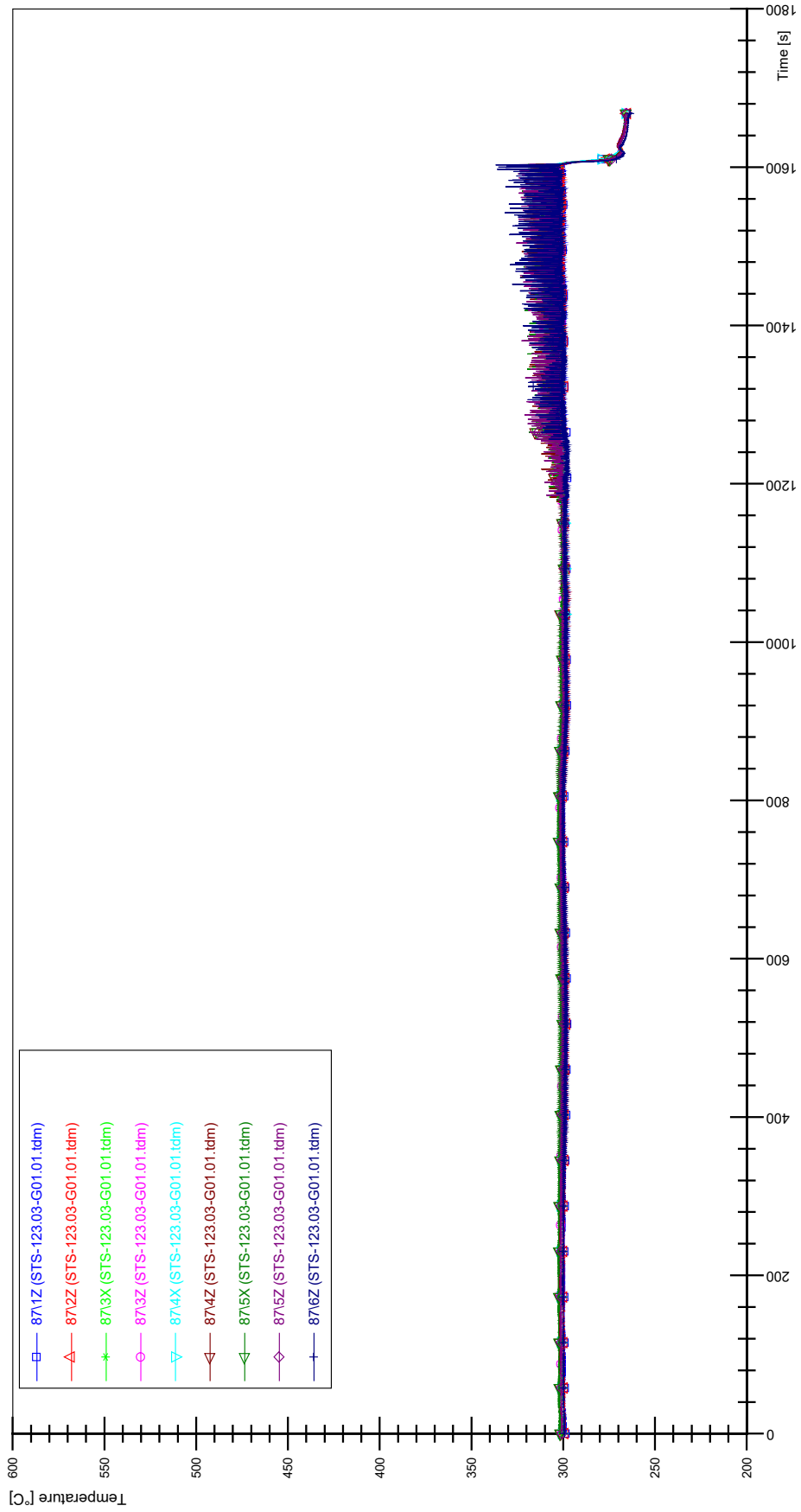
STS-123.03-G01.01_Rod_79



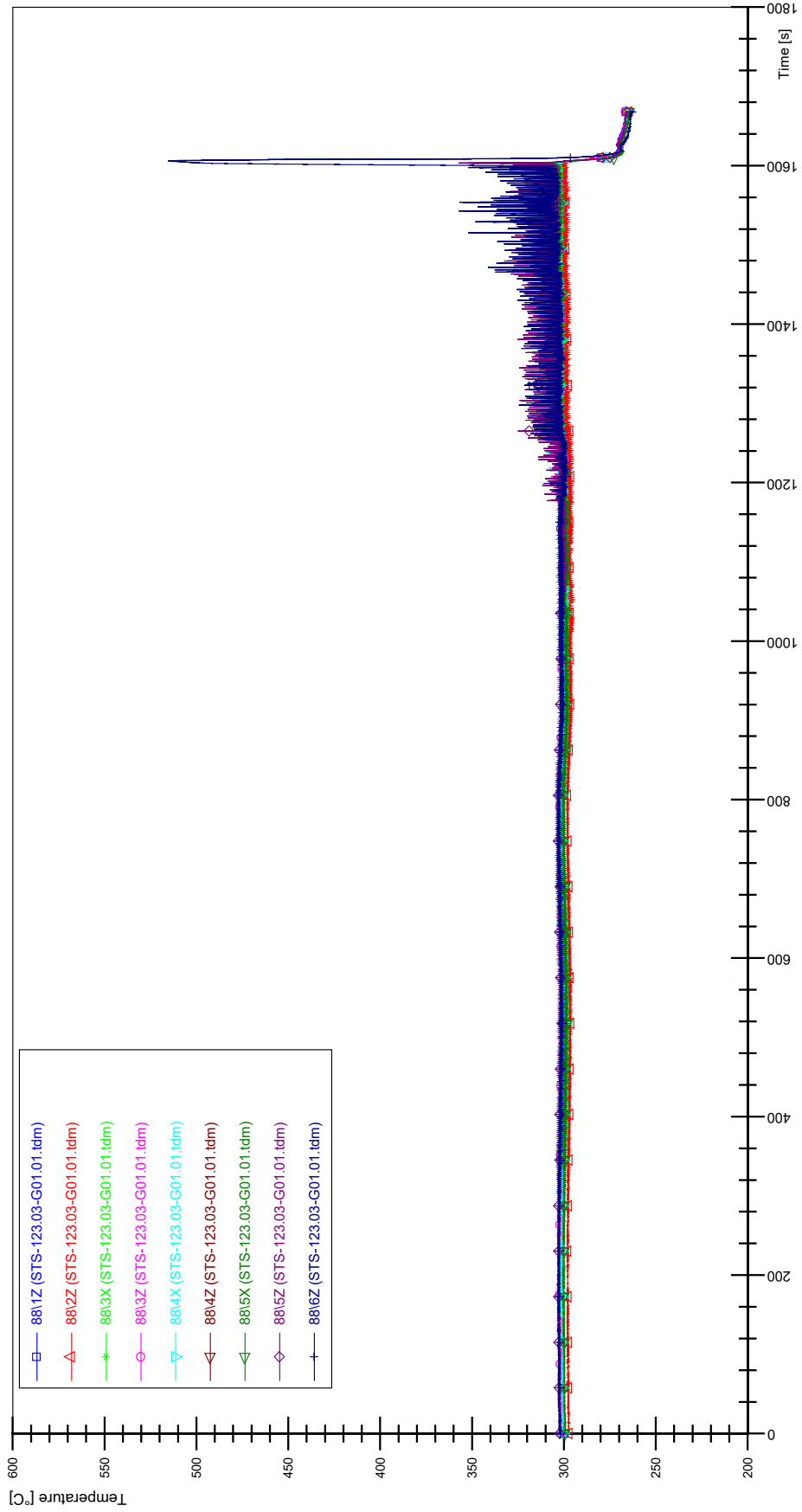
STS-123.03-G01.01_Rod_86



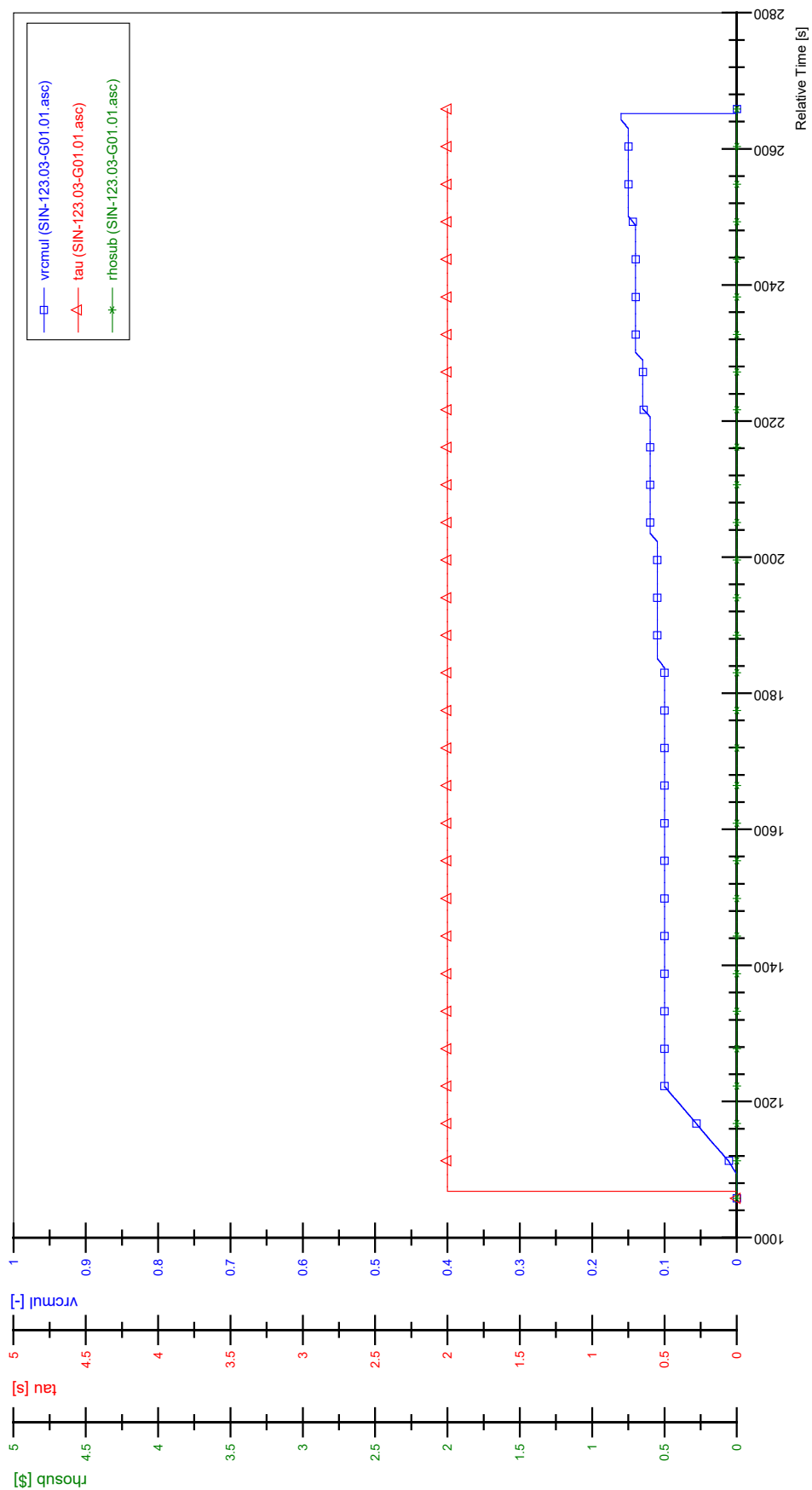
STS-123.03-G01.01_Rod_87



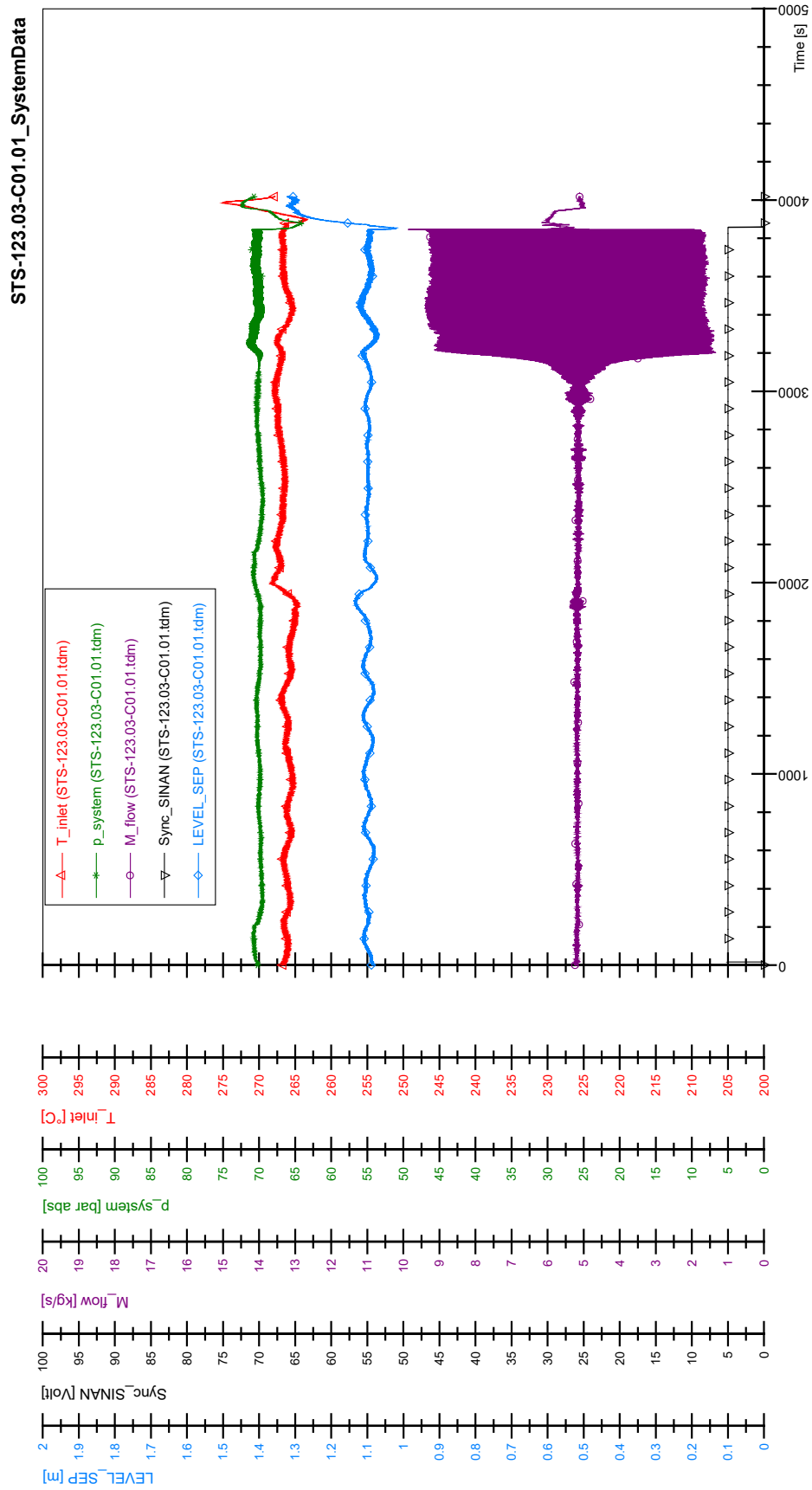
STS-123.03-G01.01_Rod_88



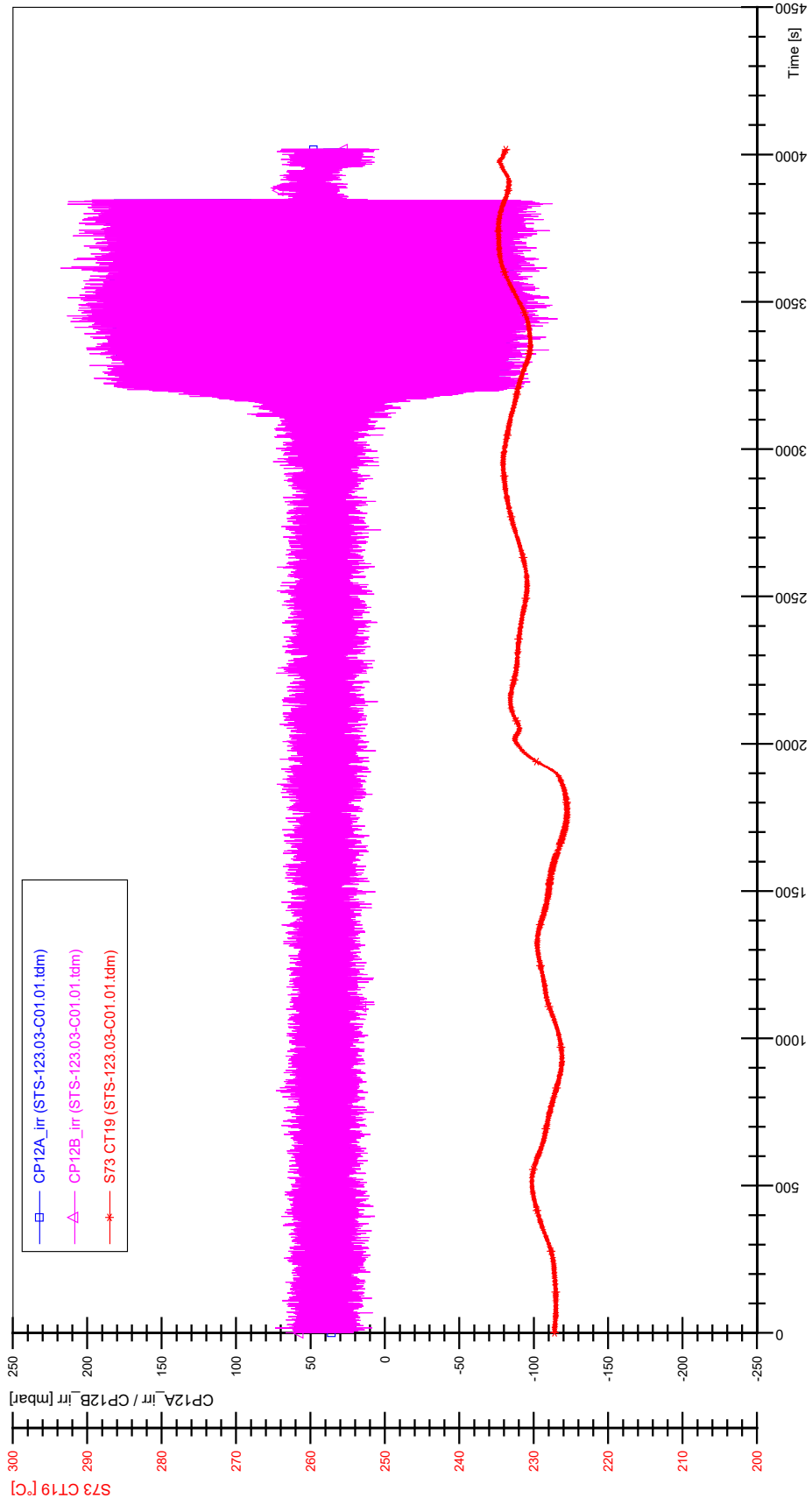
SIN-123.03-G01.01



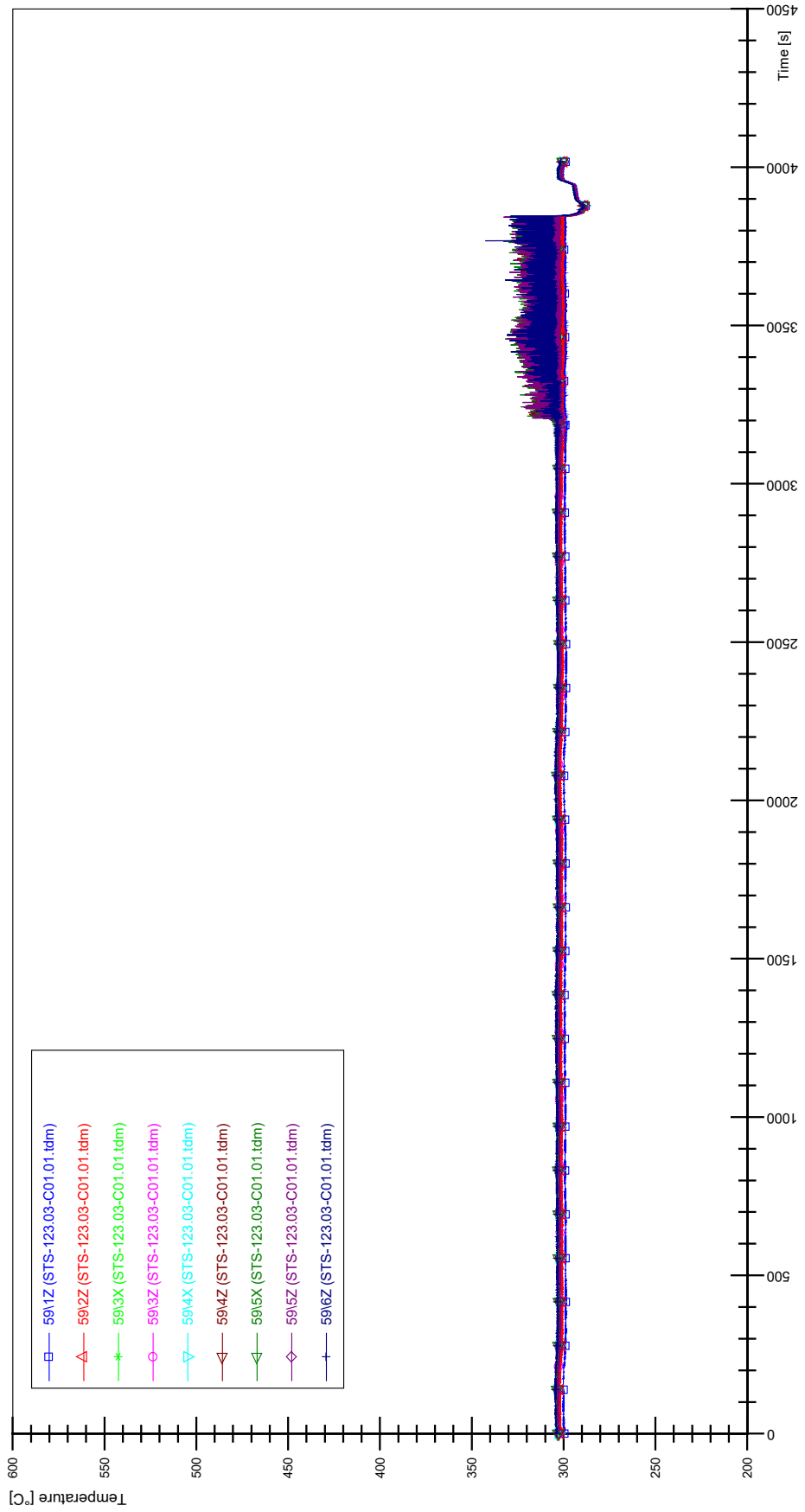
APPENDIX DD PLOTS OF INSTABILITY TEST STS-123.03-C01.01



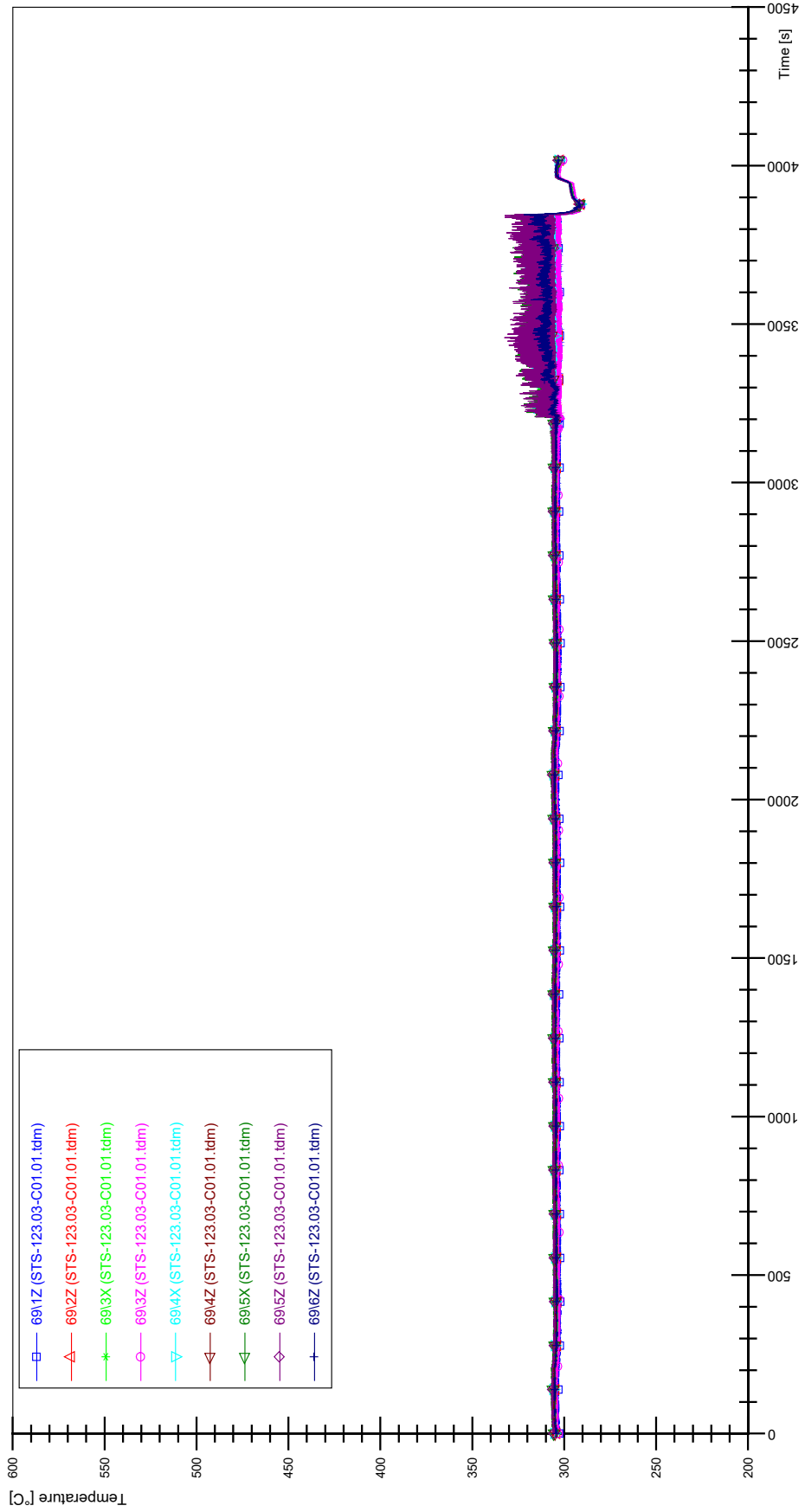
STS-123.03-C01.01_CP12_CT19



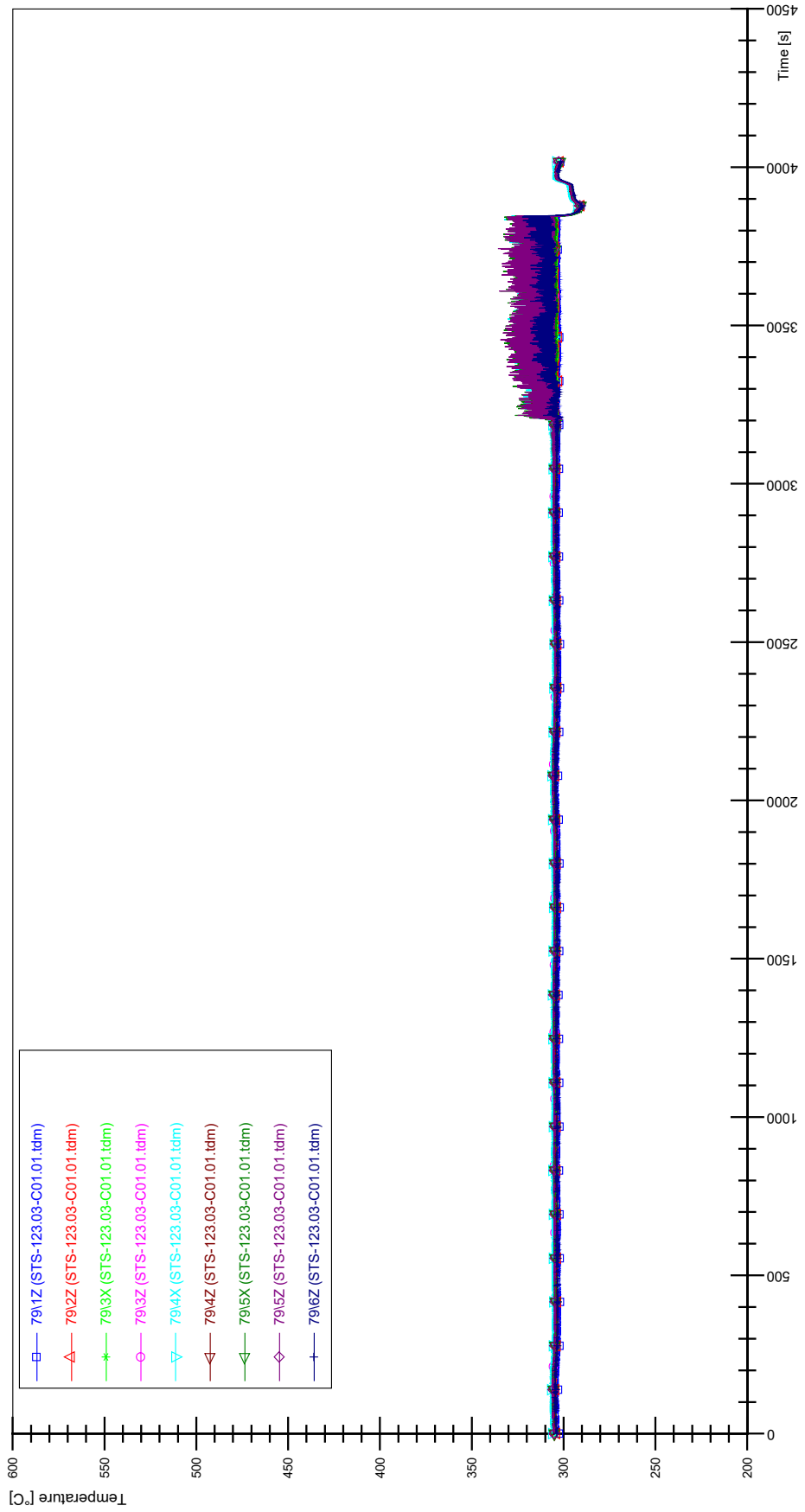
STS-123.03-C01.01_Rod_59



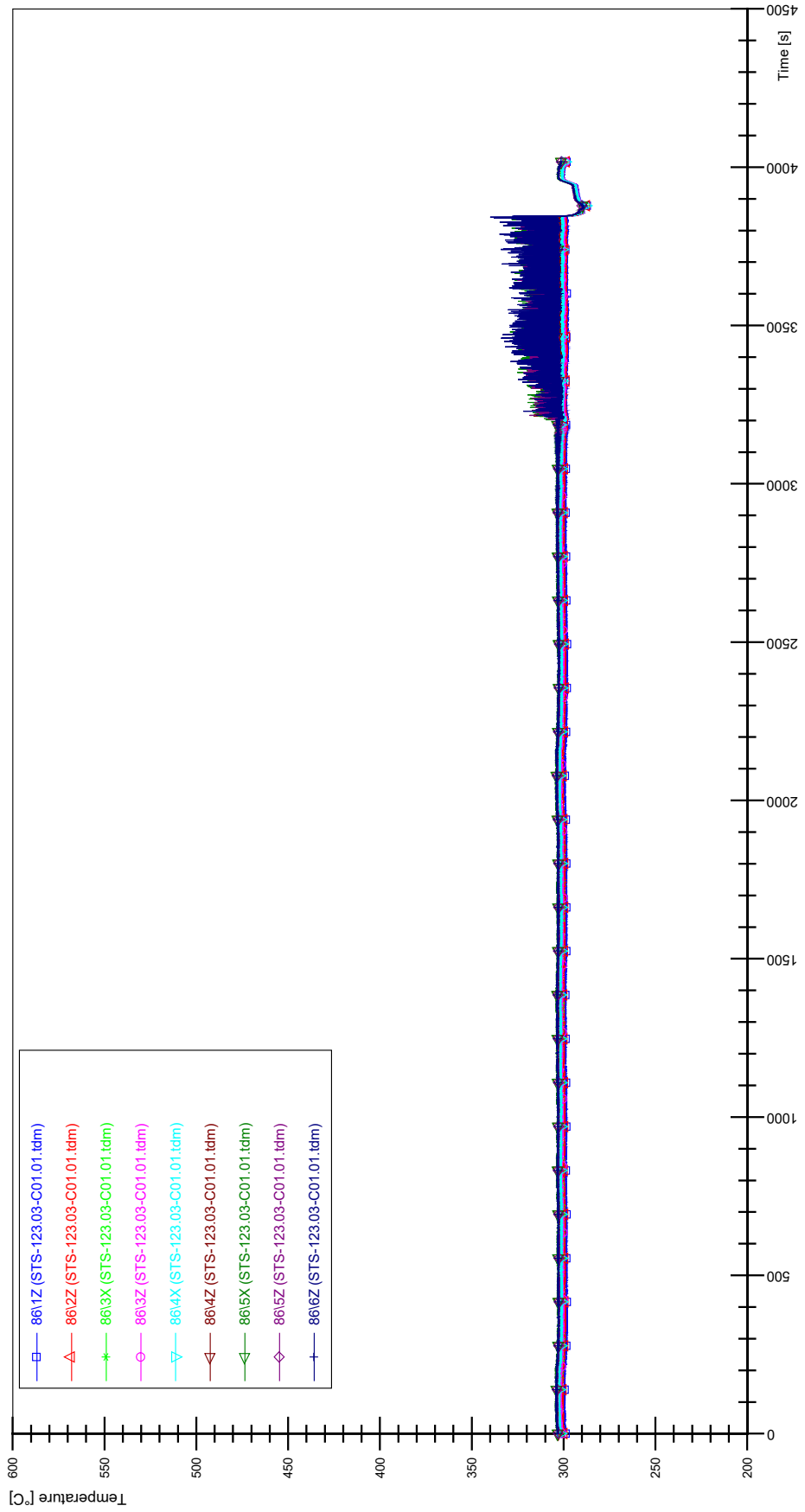
STS-123.03-C01.01_Rod_69



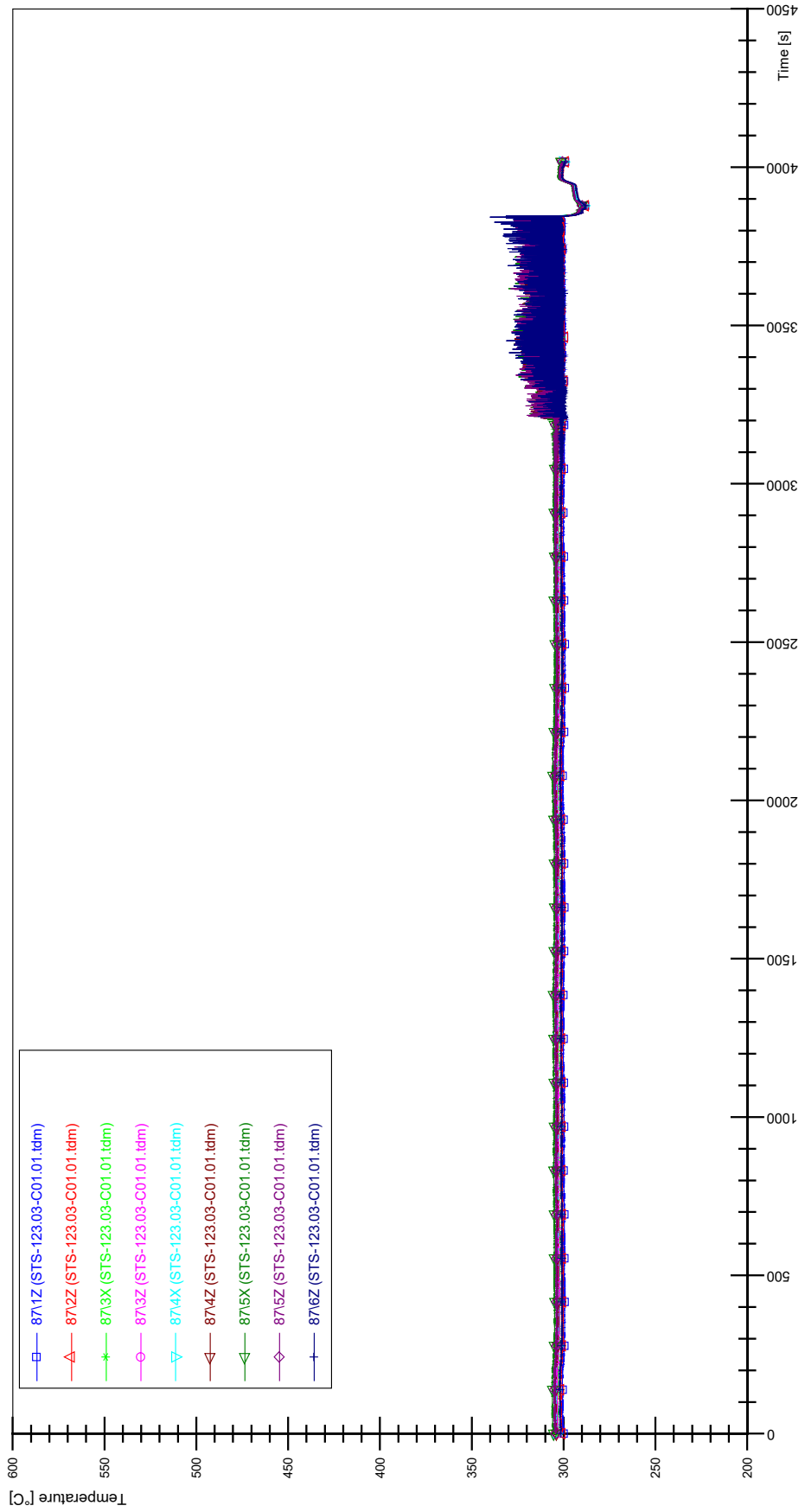
STS-123.03-C01.01_Rod_79



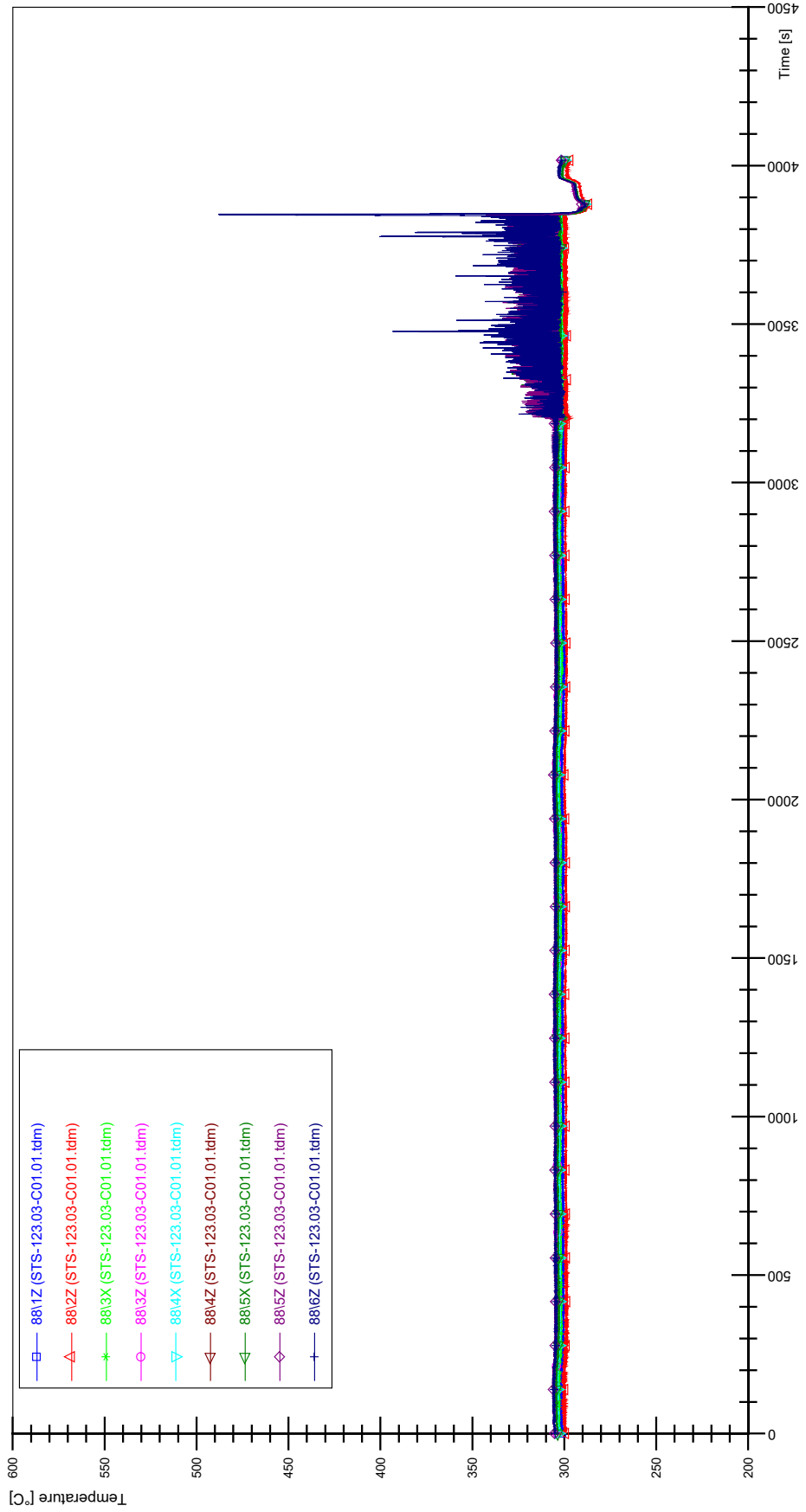
STS-123.03-C01.01_Rod_86



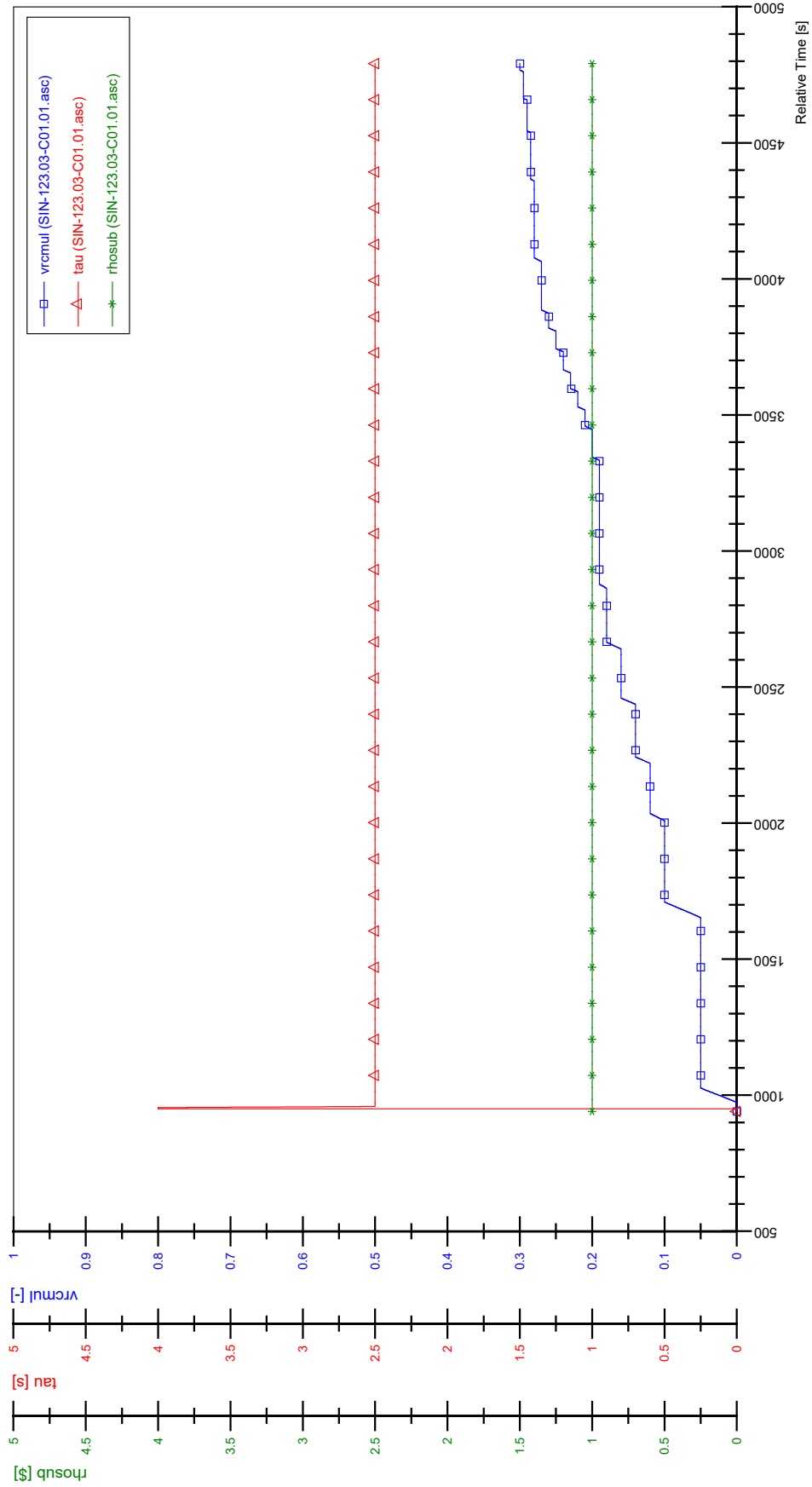
STS-123.03-C01.01_Rod_87



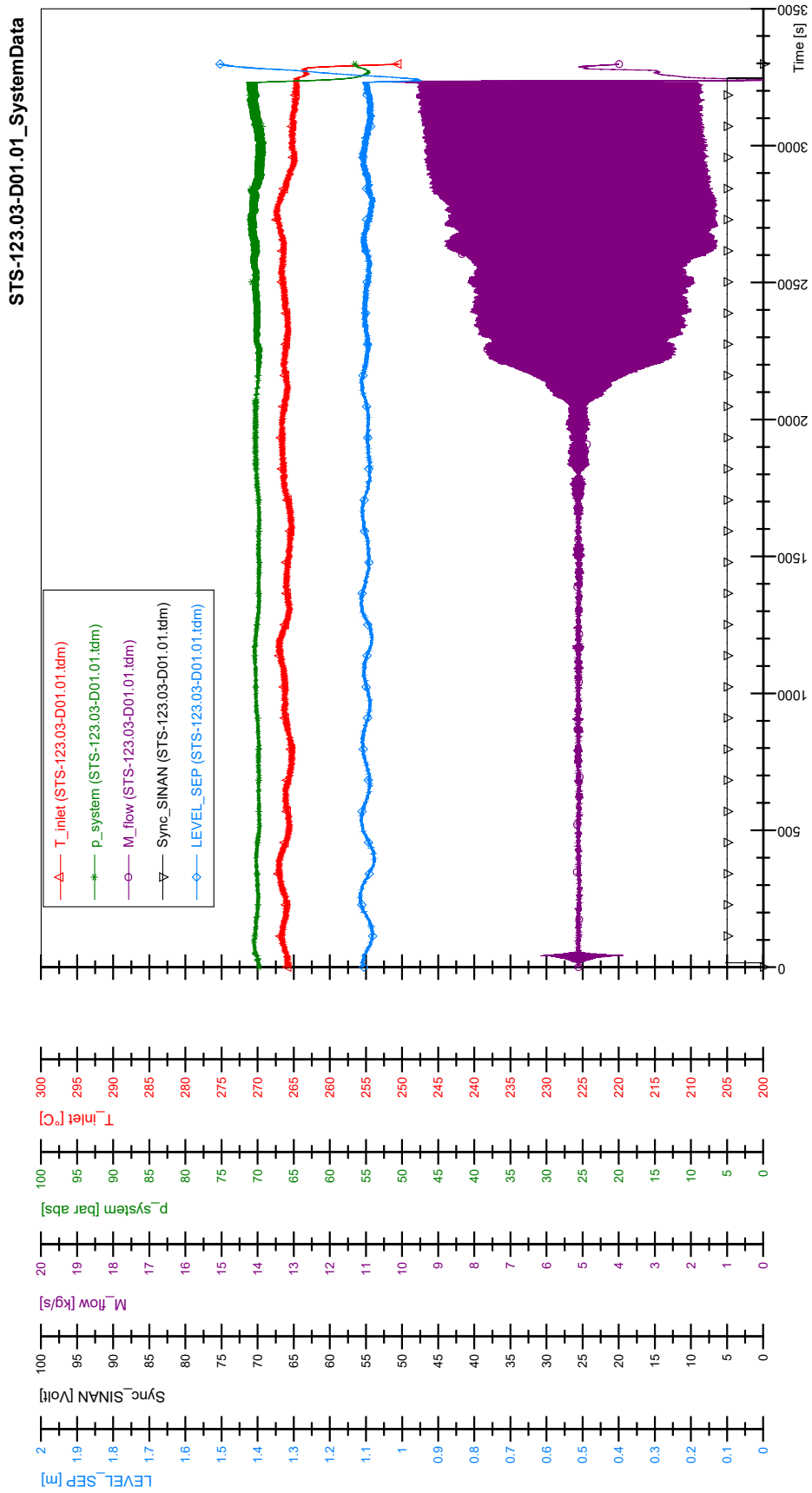
STS-123.03-C01.01_Rod_88



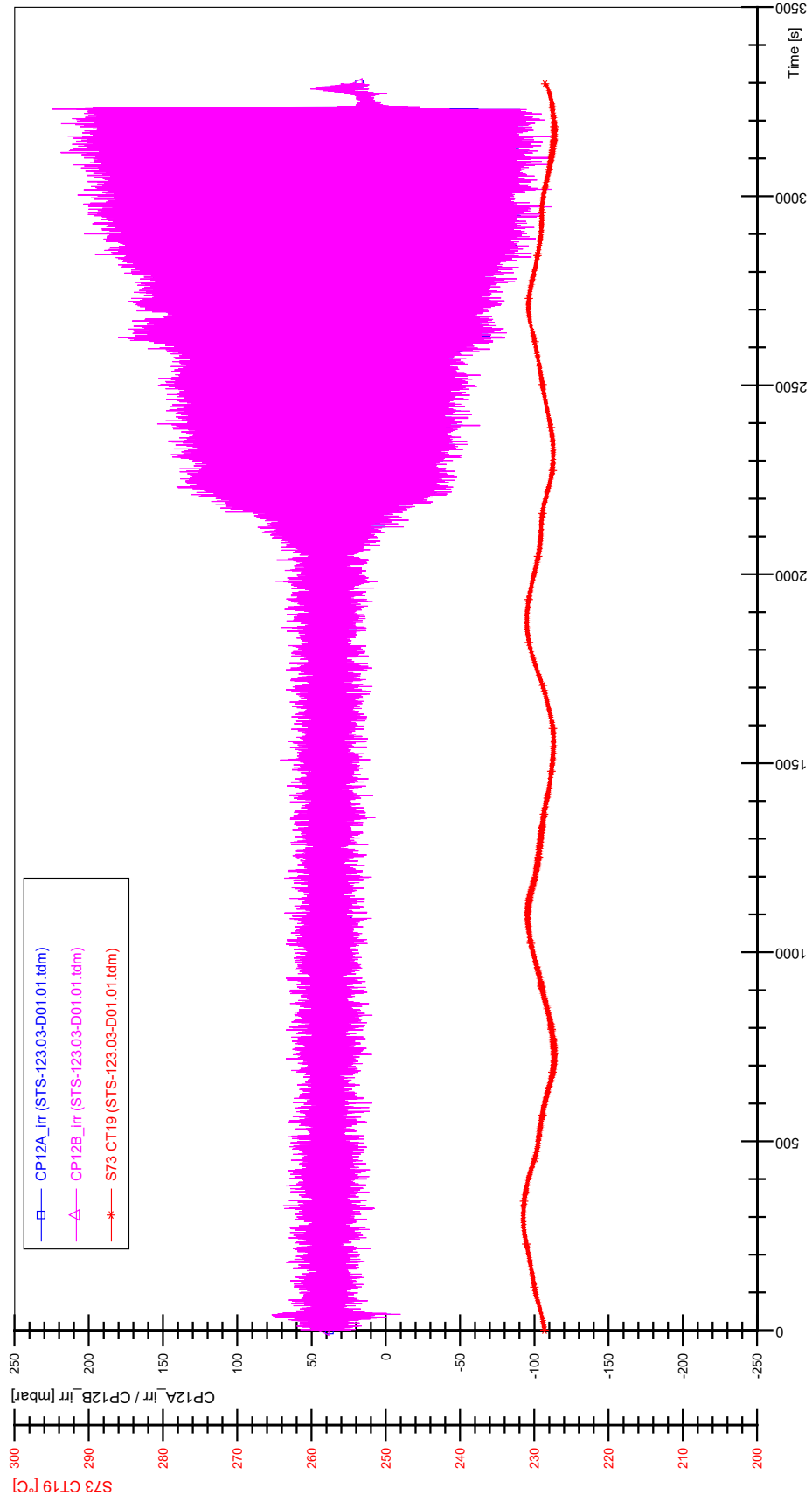
SIN-123.03-C01.01



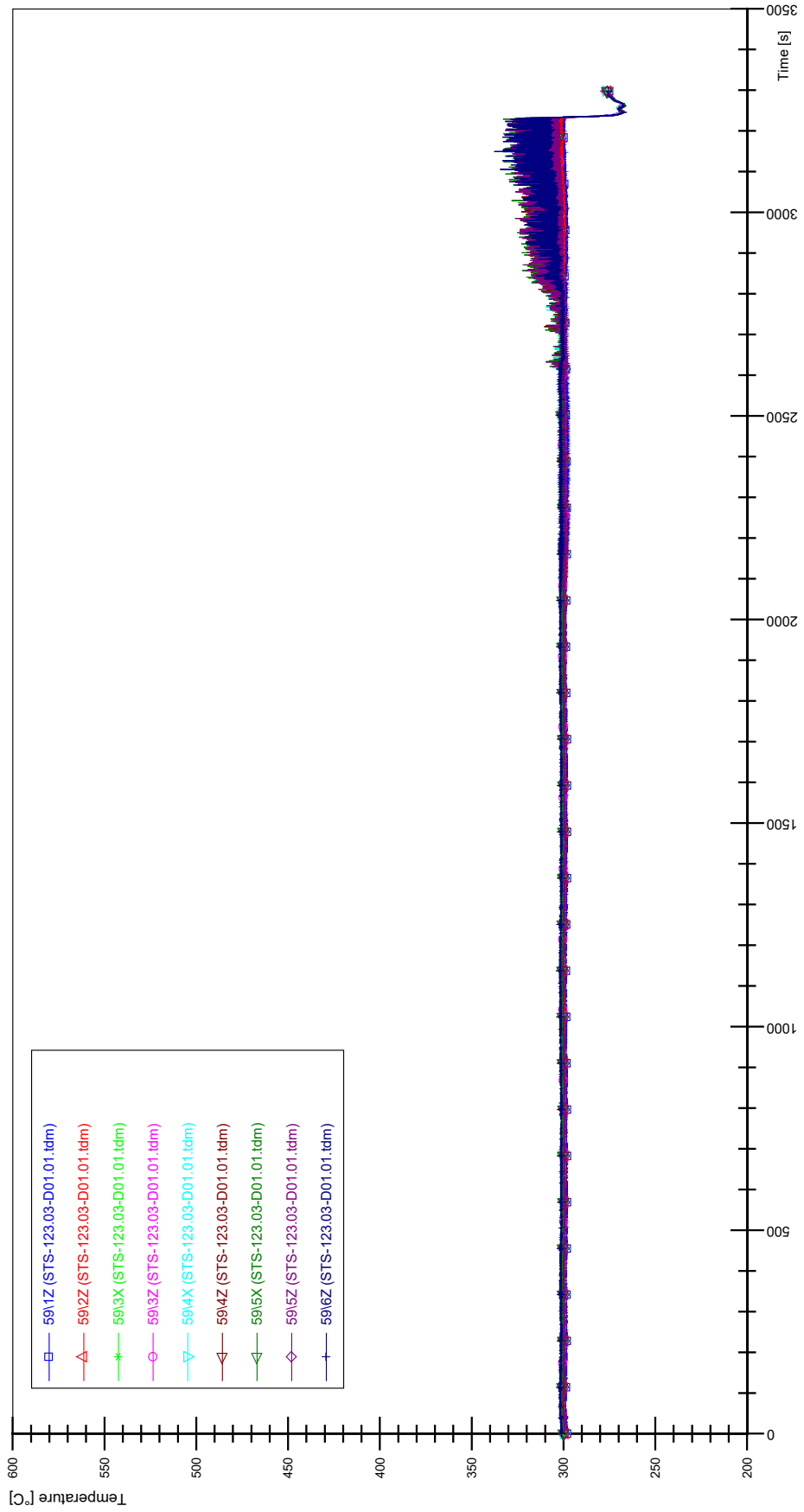
APPENDIX EE PLOTS OF INSTABILITY TEST STS-123.03-D01.01



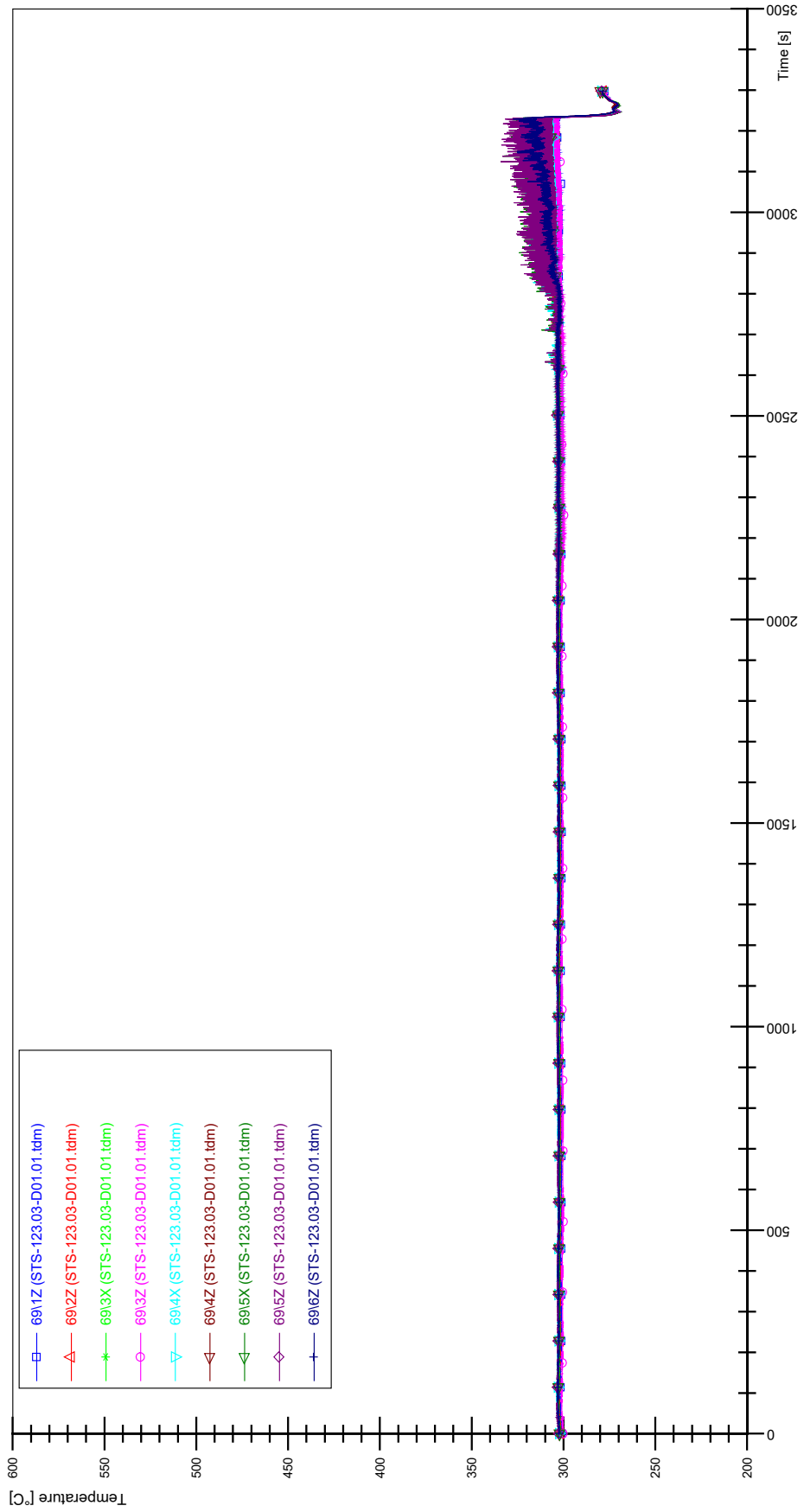
STS-123.03-D01.01_CP12_CT19



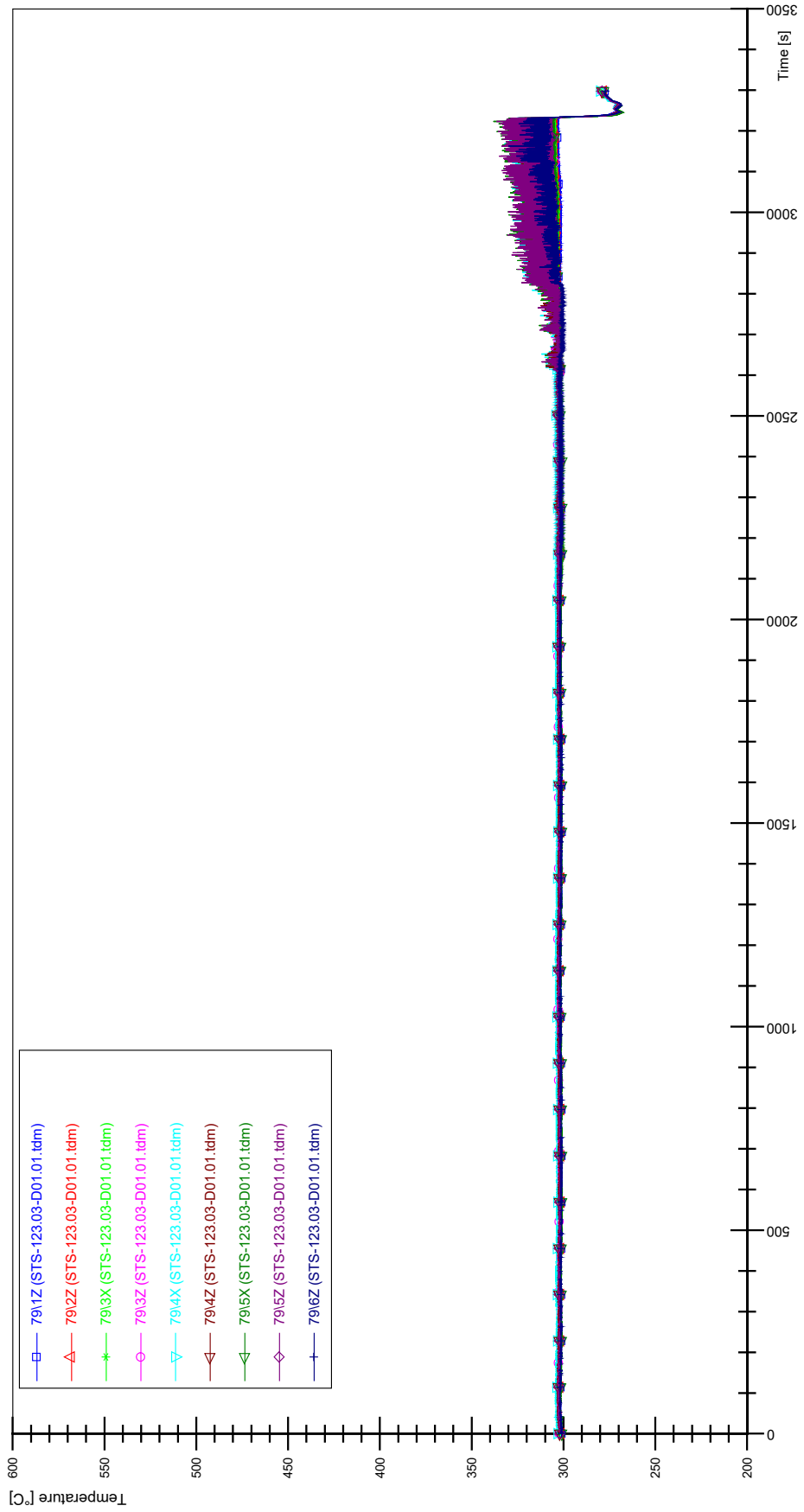
STS-123.03-D01.01_Rod_59



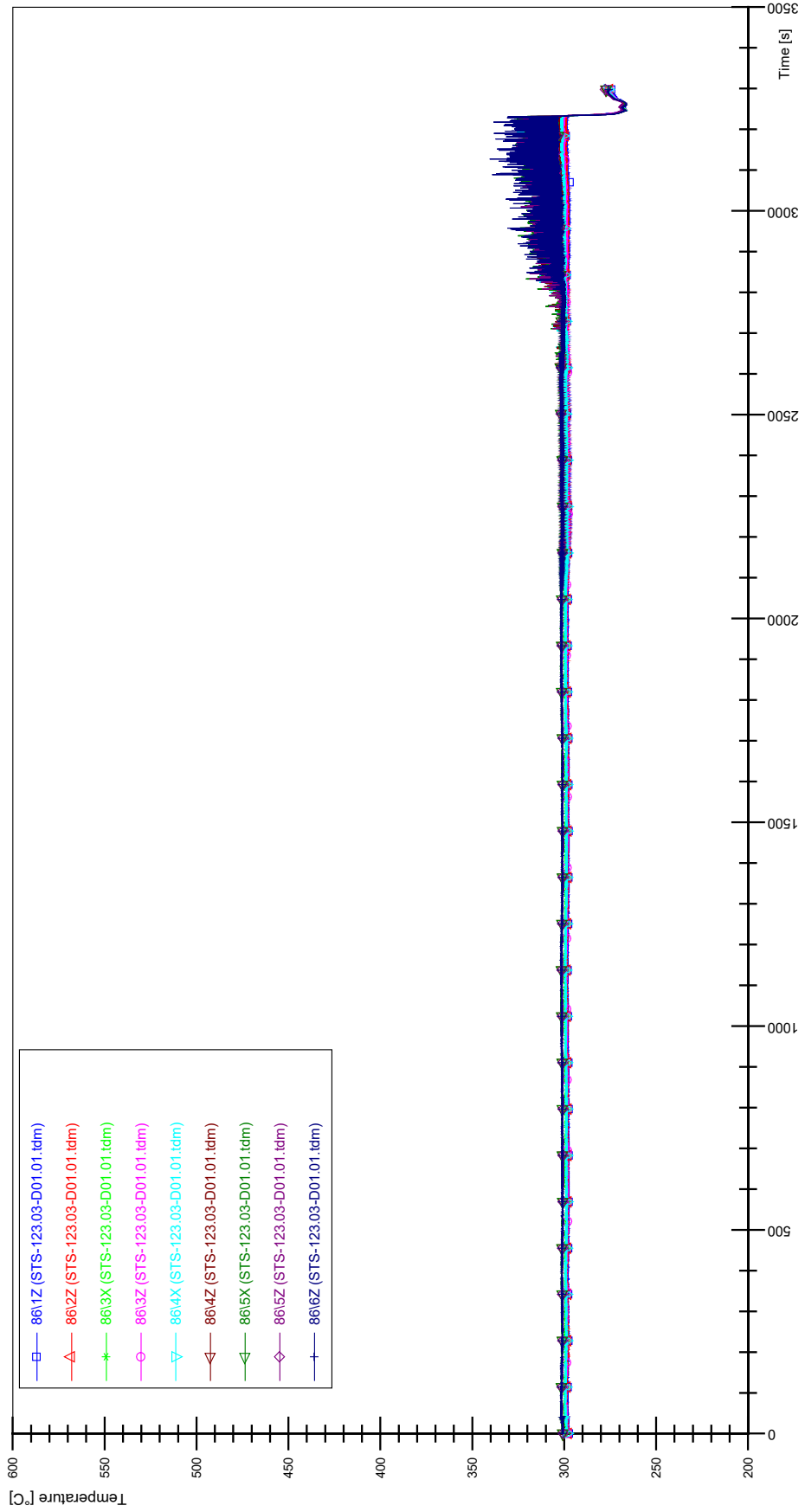
STS-123.03-D01.01_Rod_69



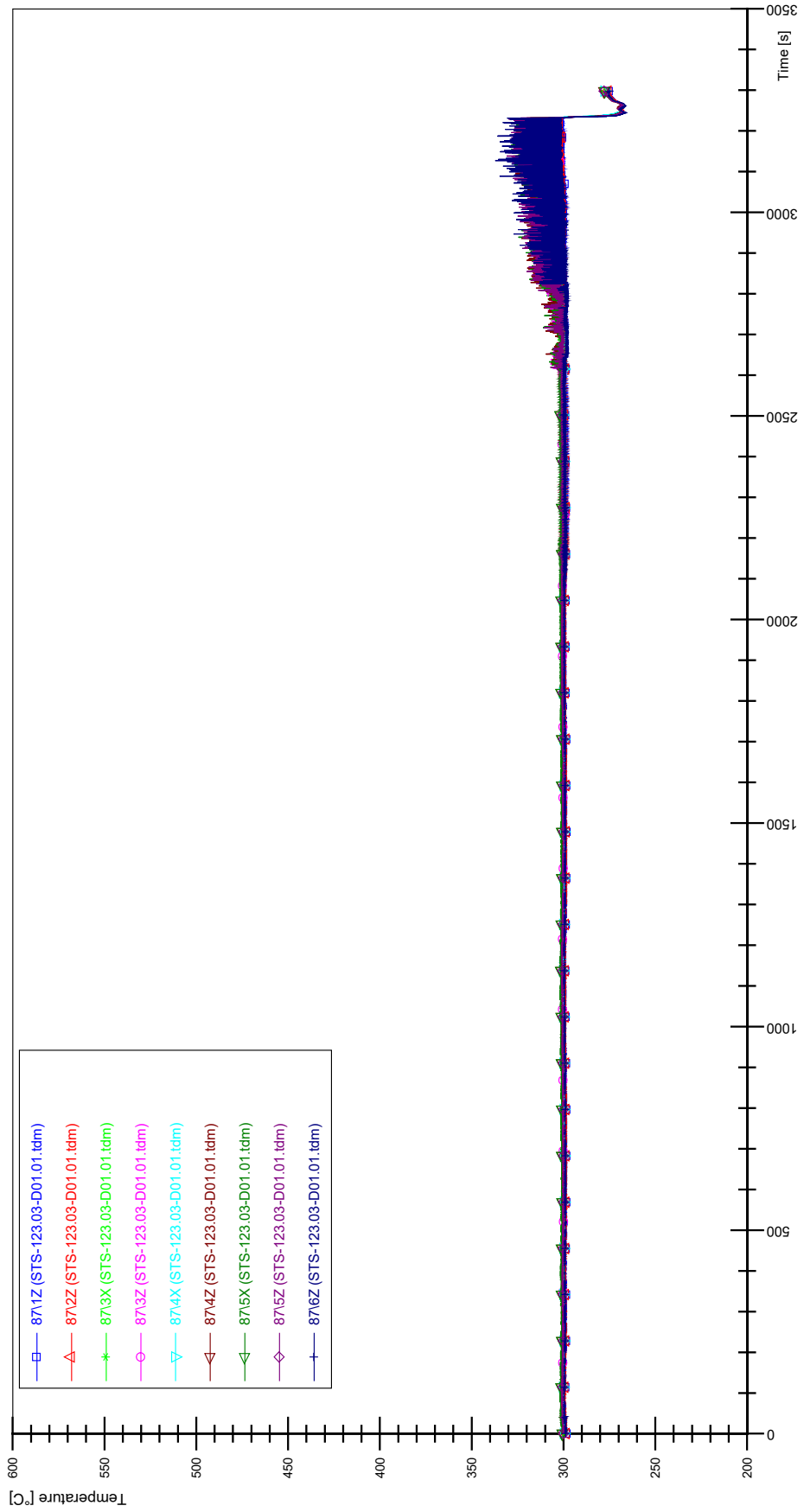
STS-123.03-D01.01_Rod_79



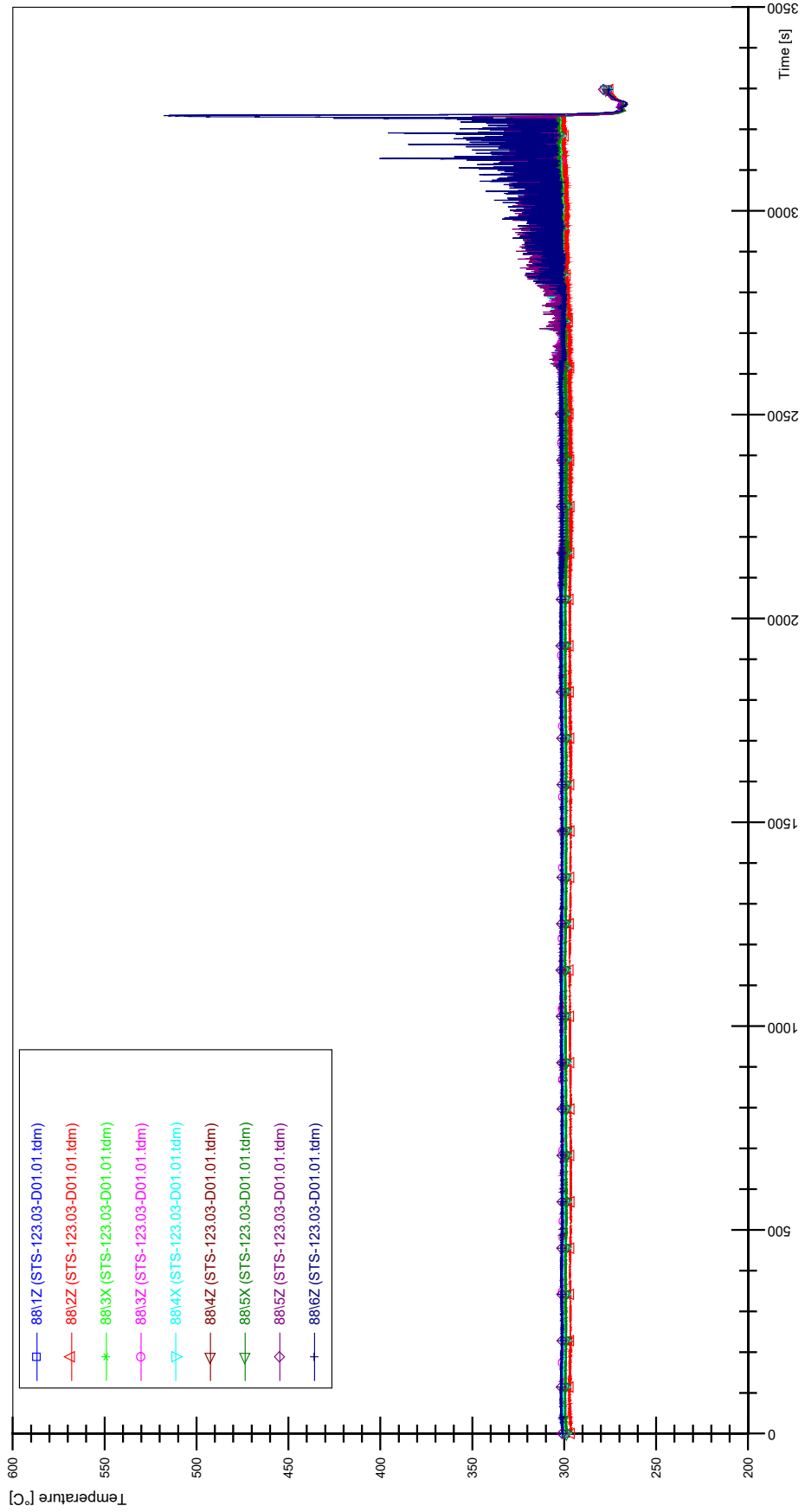
STS-123.03-D01.01_Rod_86



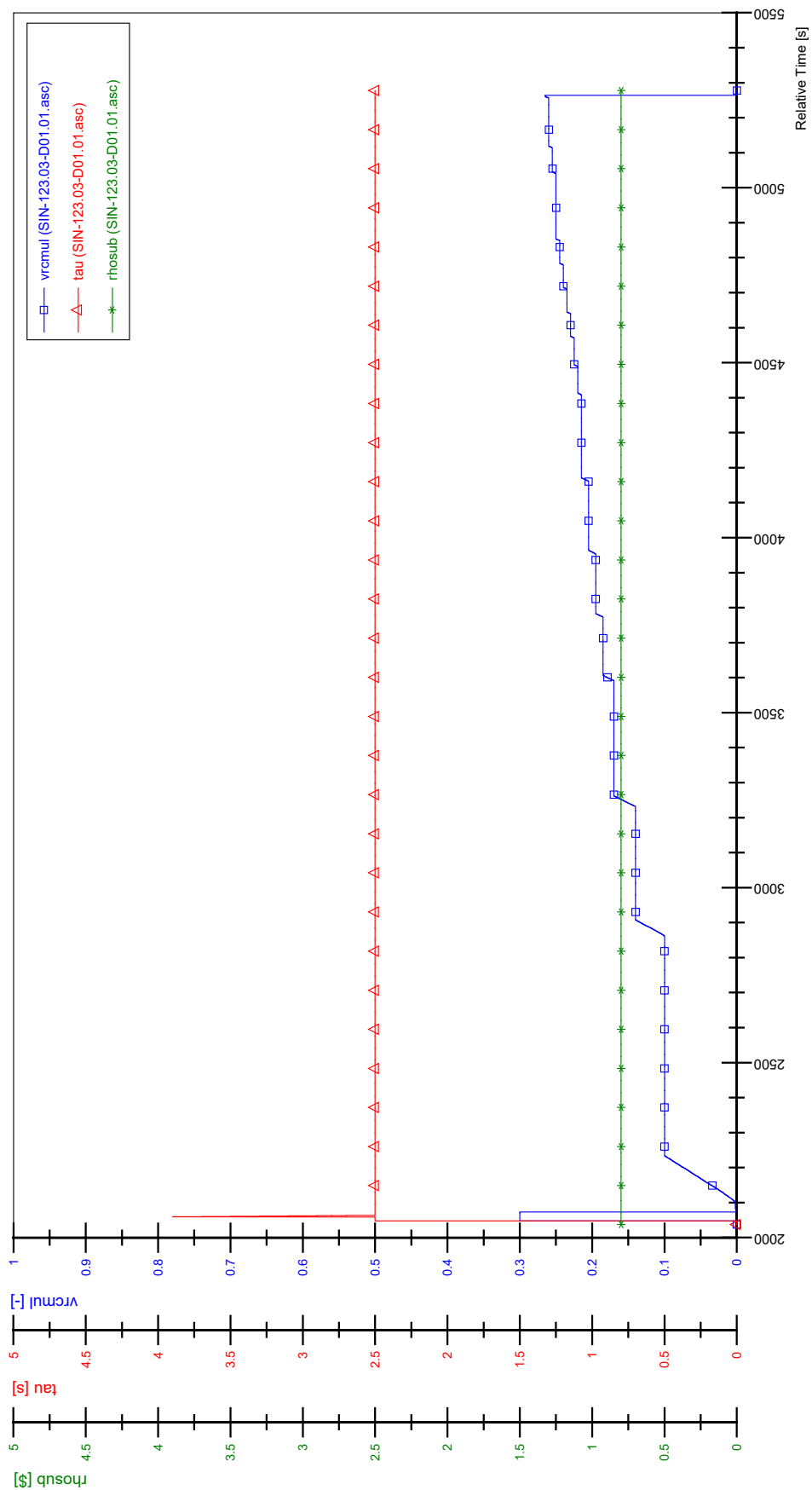
STS-123.03-D01.01_Rod_87



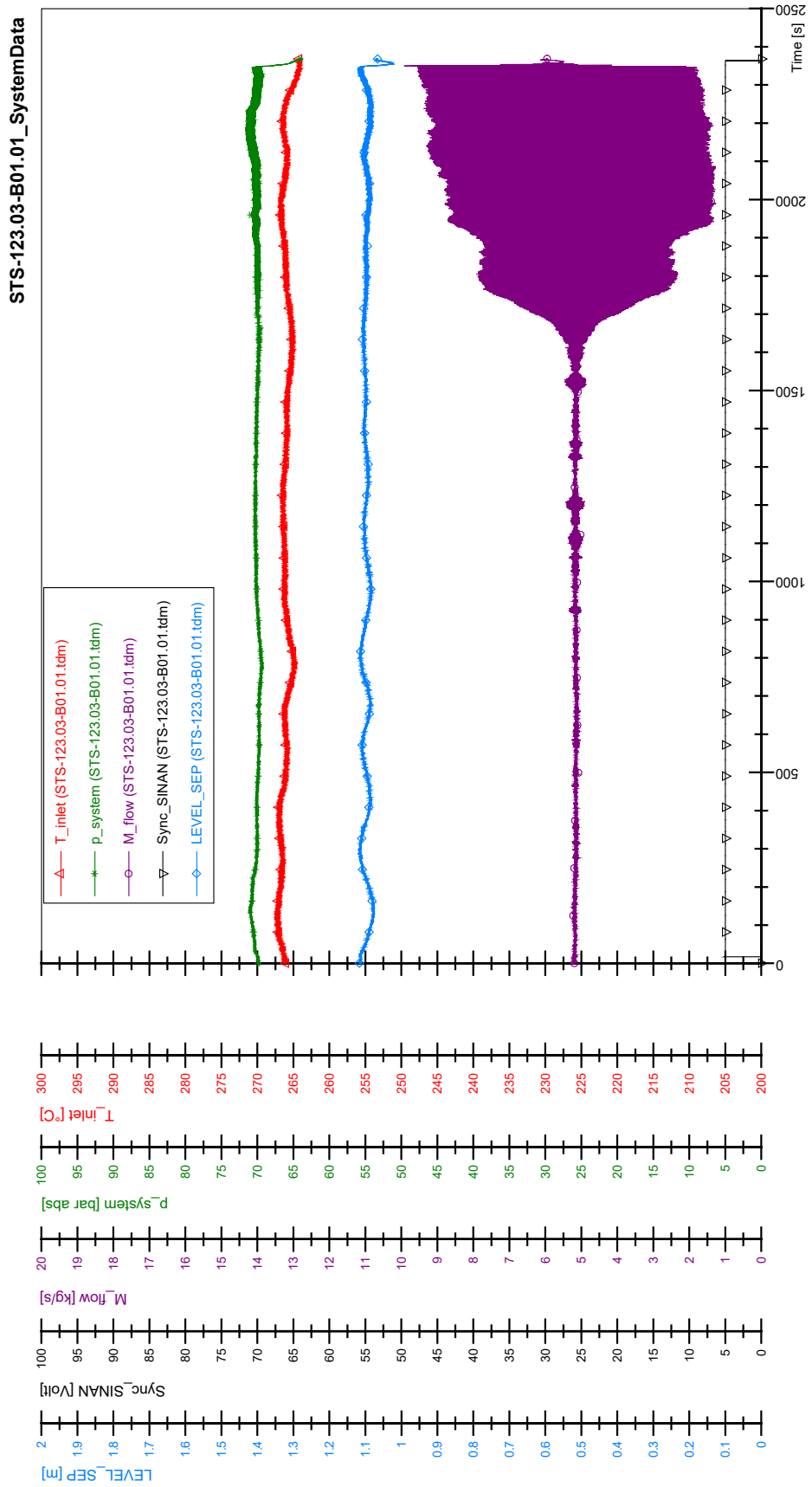
STS-123.03-D01.01_Rod_88



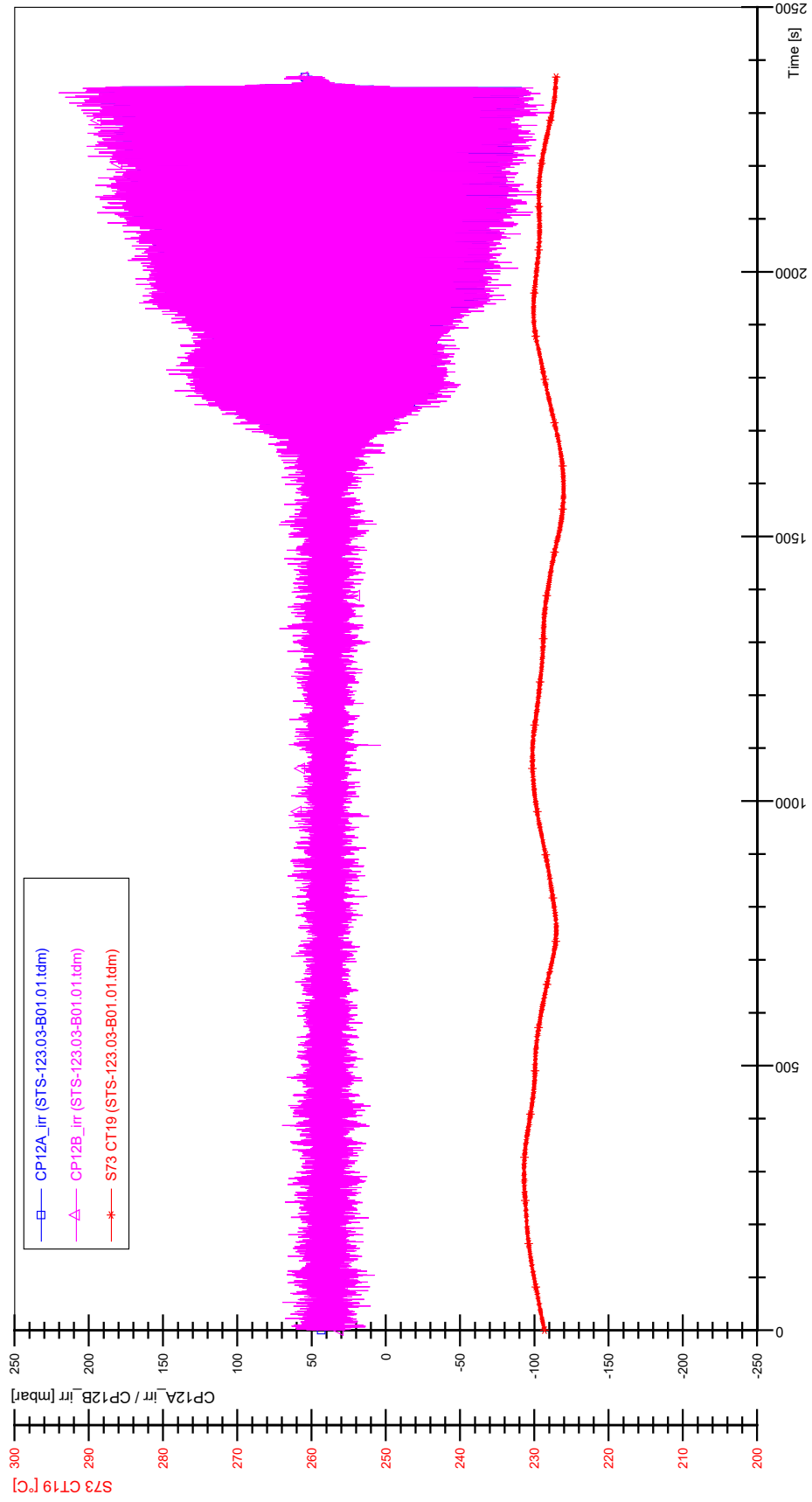
SIN-123.03-D01.01



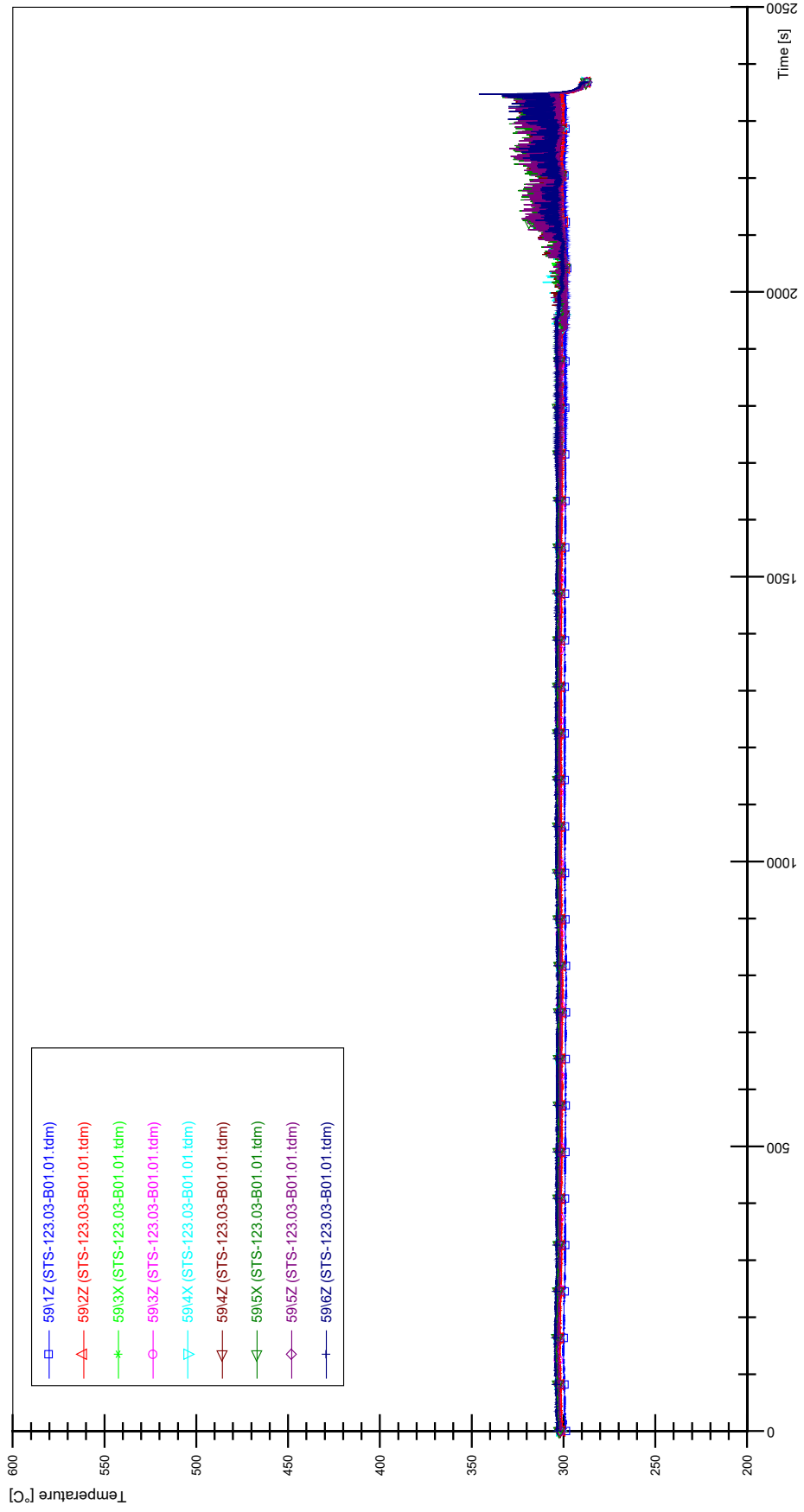
APPENDIX FF PLOTS OF INSTABILITY TEST STS-123.03-B01.01



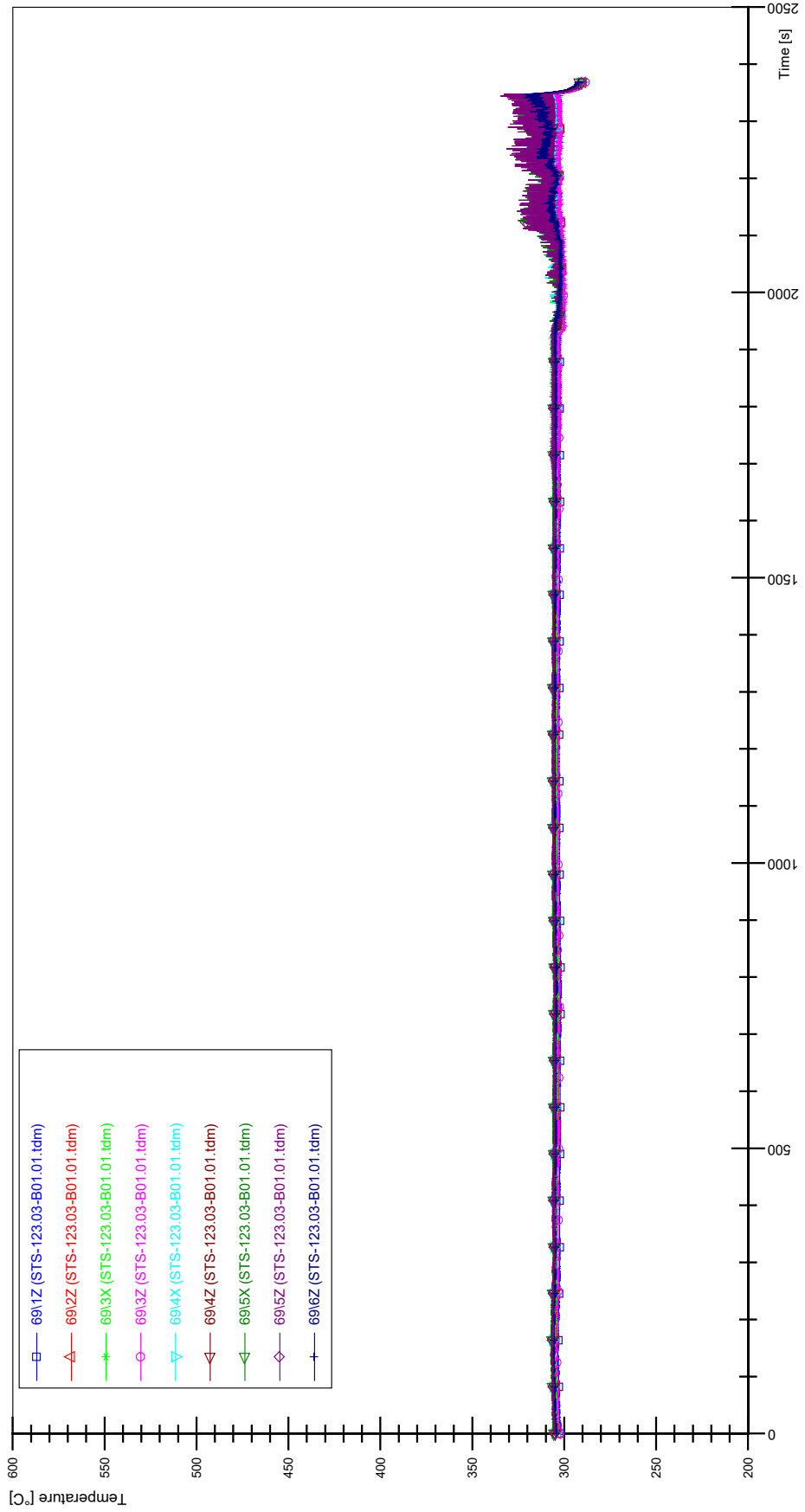
STS-123.03-B01.01_CP12_CT19



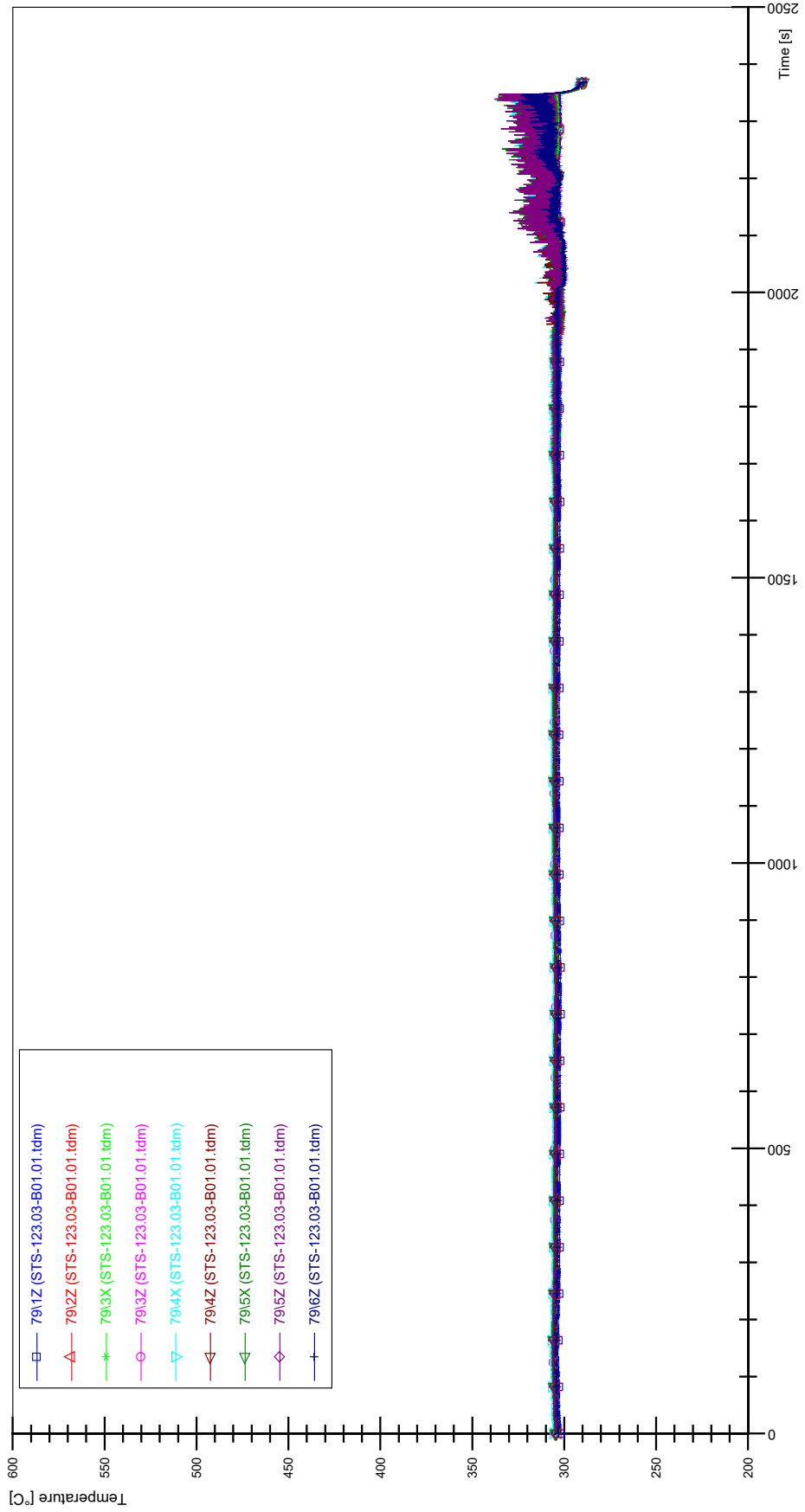
STS-123.03-B01.01_Rod_59



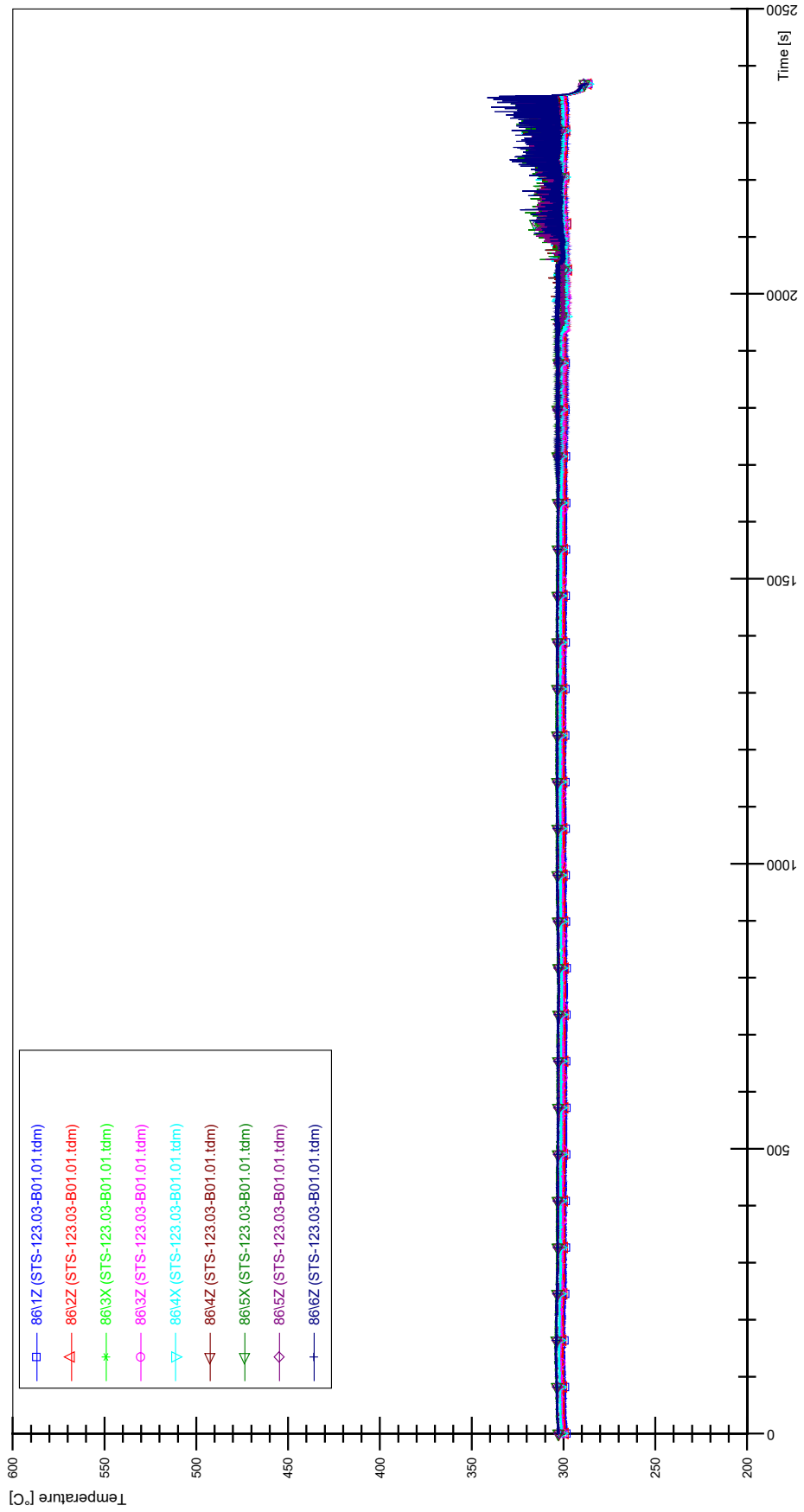
STS-123.03-B01.01_Rod_69



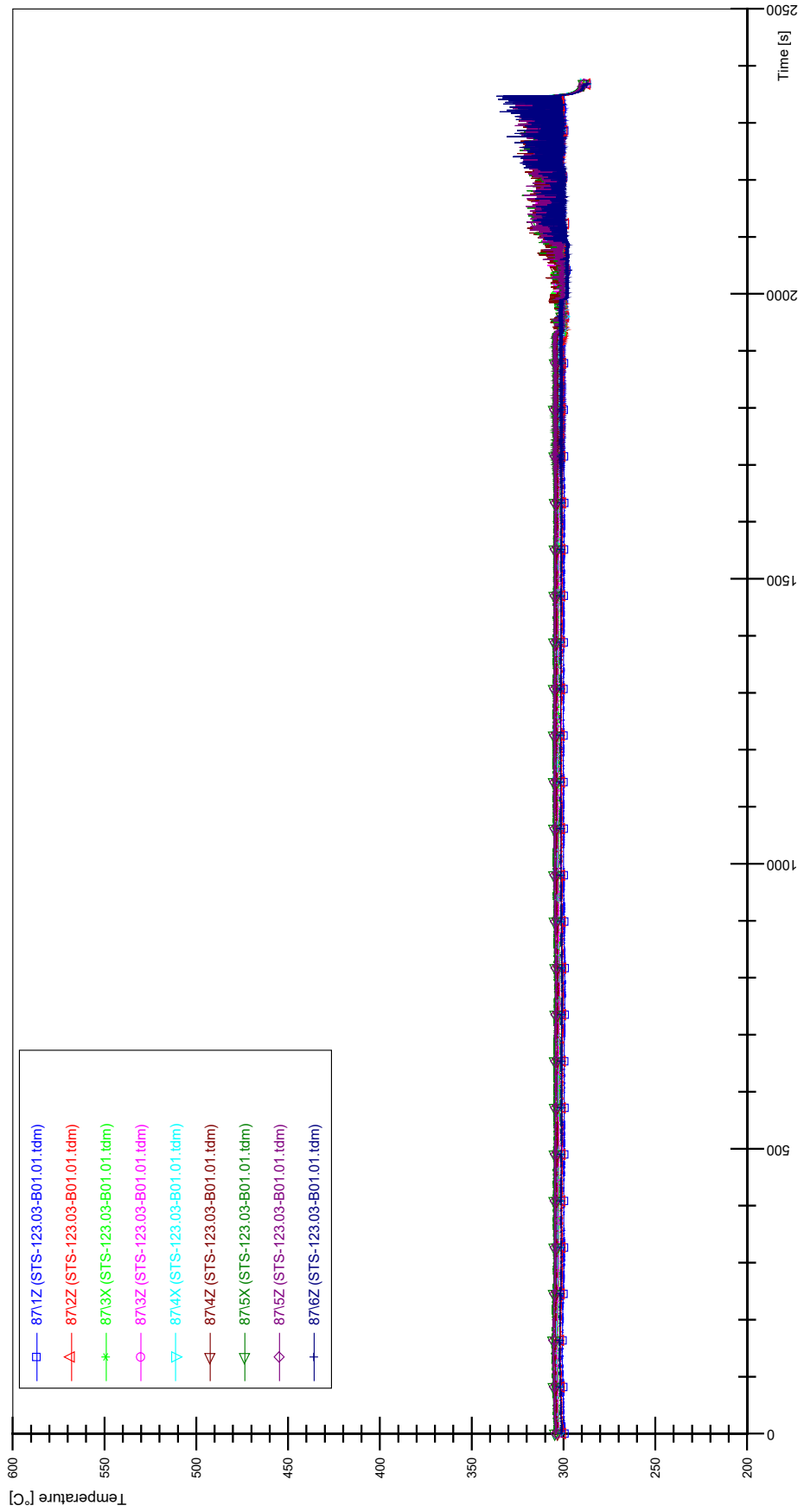
STS-123.03-B01.01_Rod_79



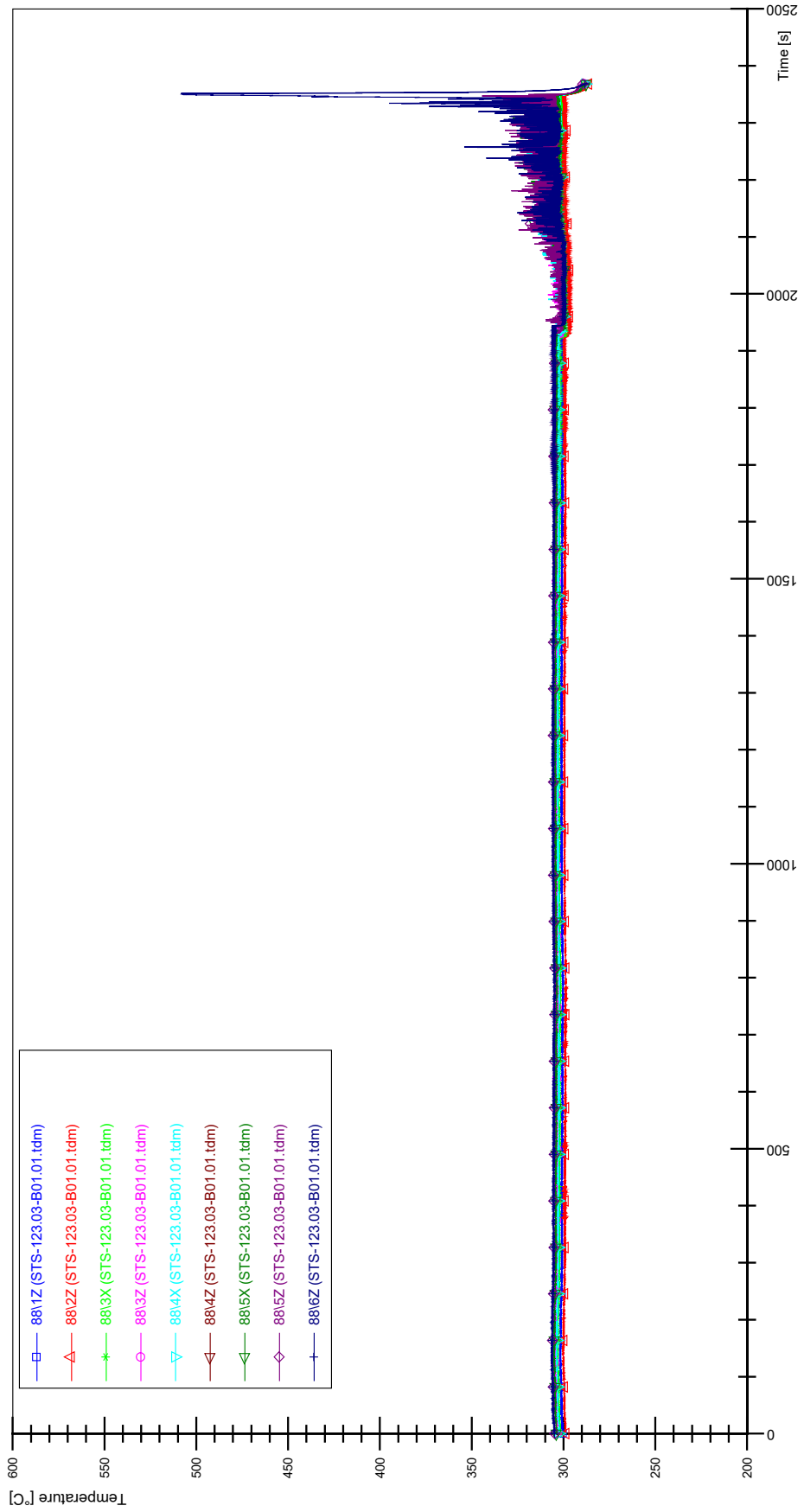
STS-123.03-B01.01_Rod_86



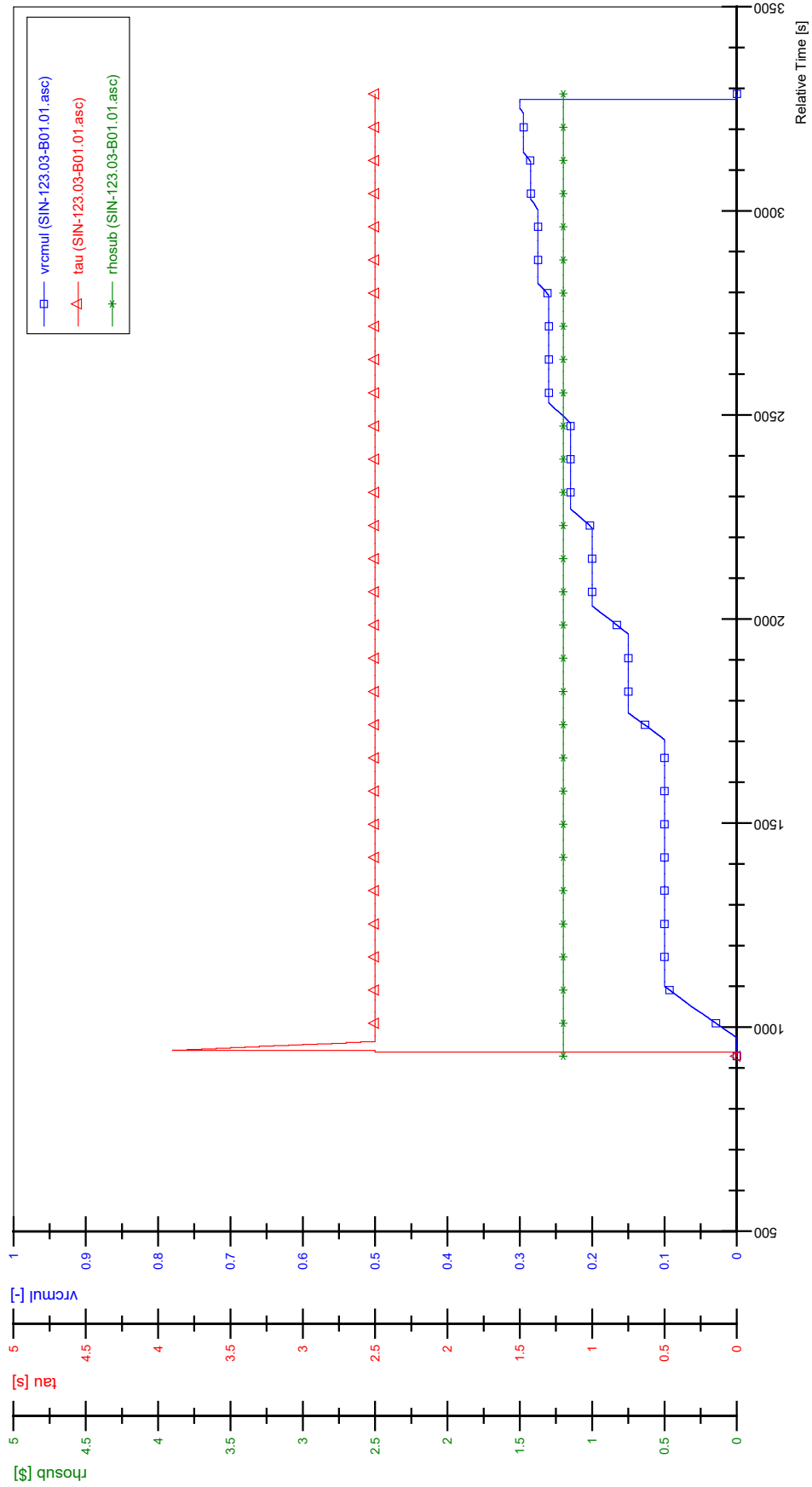
STS-123.03-B01.01_Rod_87



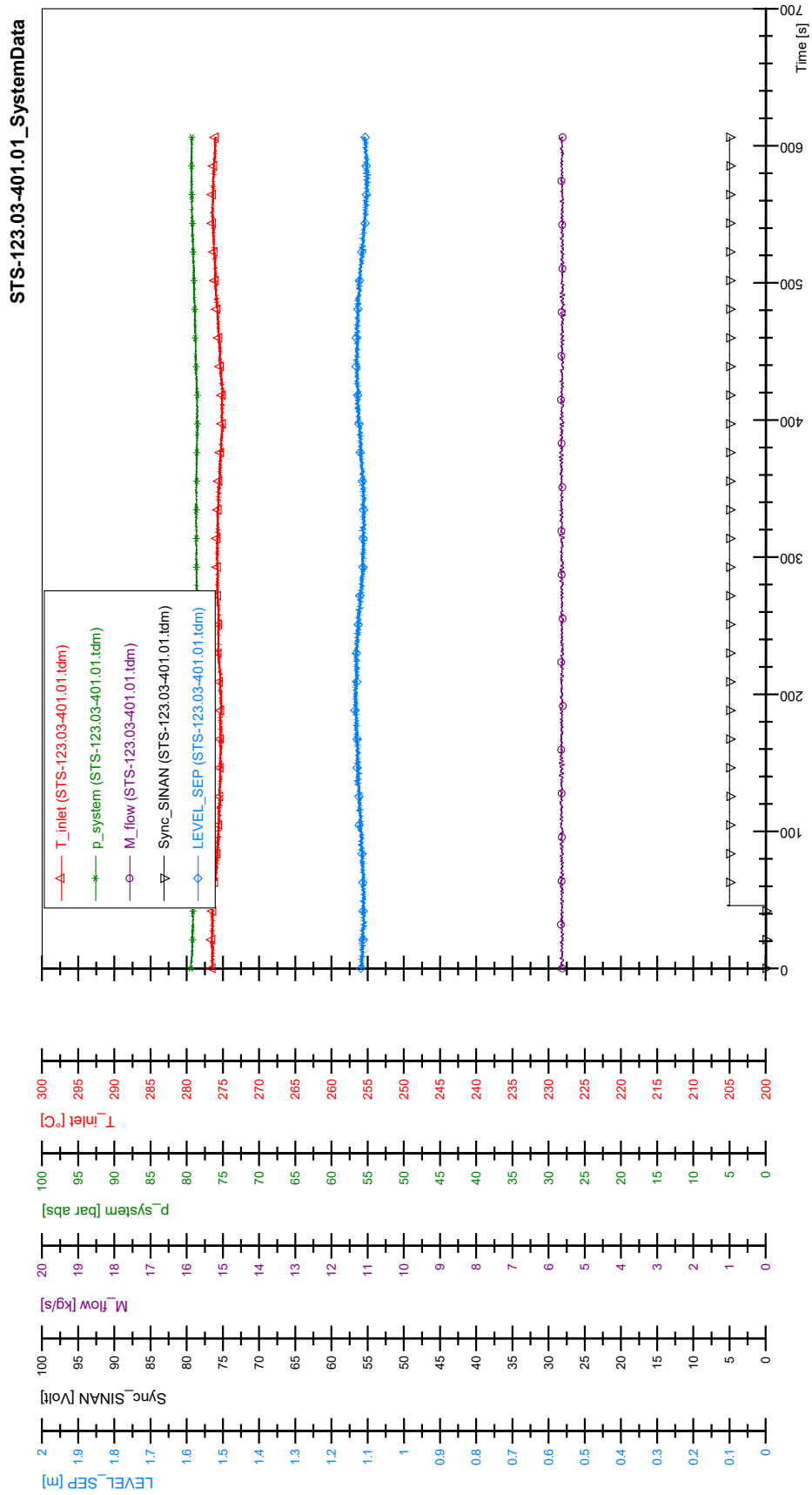
STS-123.03-B01.01_Rod_88



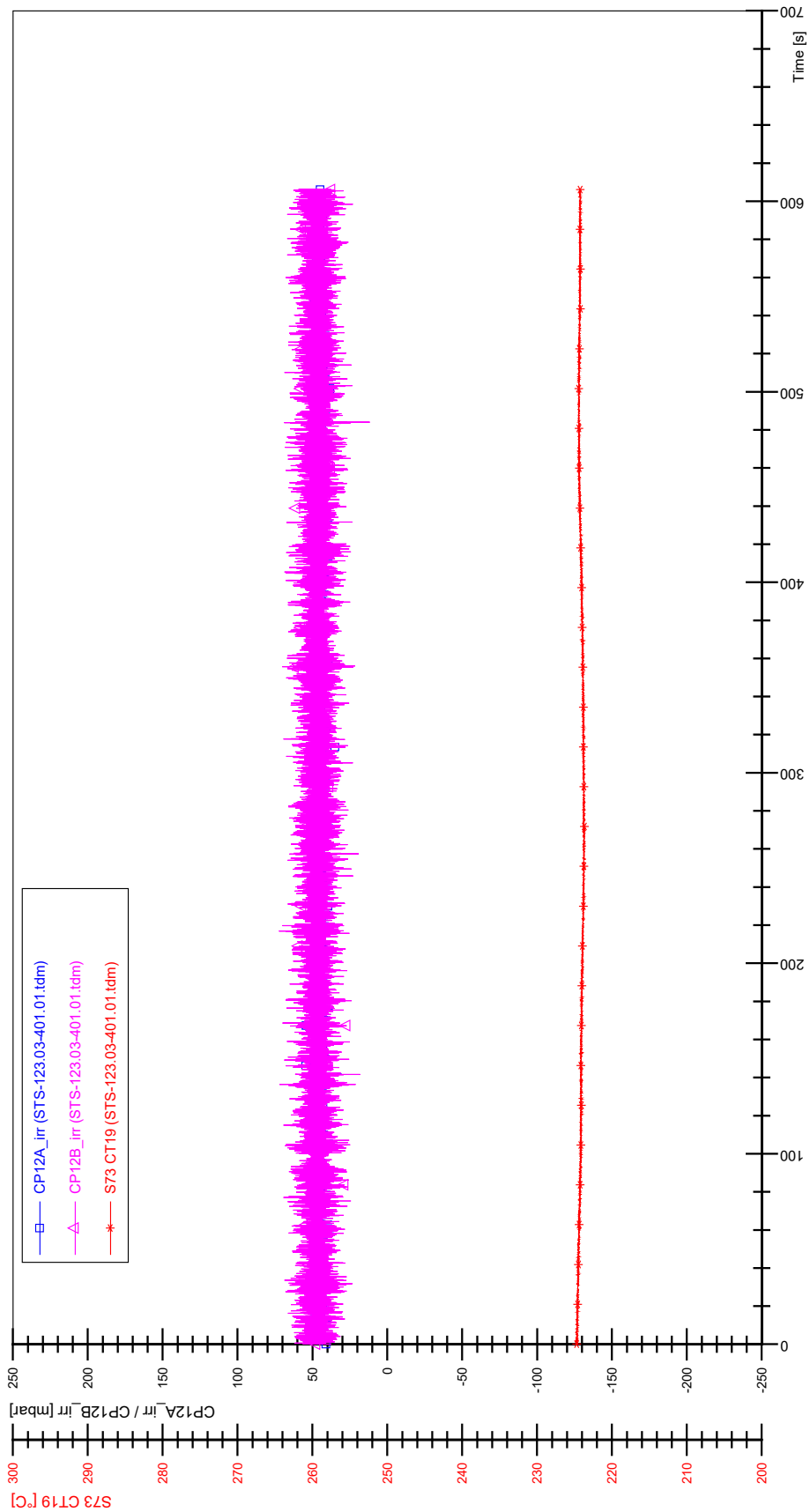
SIN-123.03-B01.01



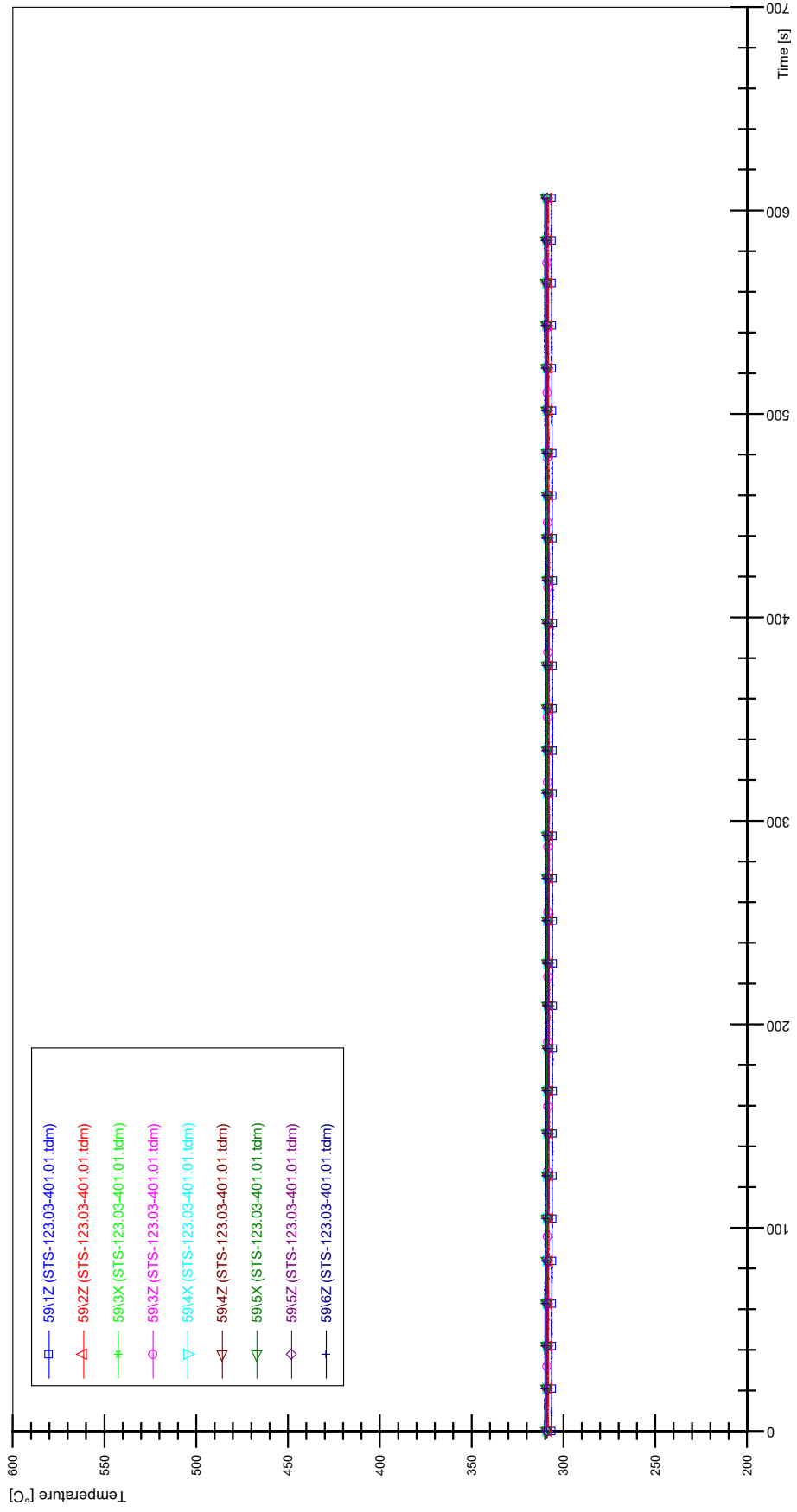
APPENDIX GG PLOTS OF INSTABILITY TEST STS-123.03-401.01



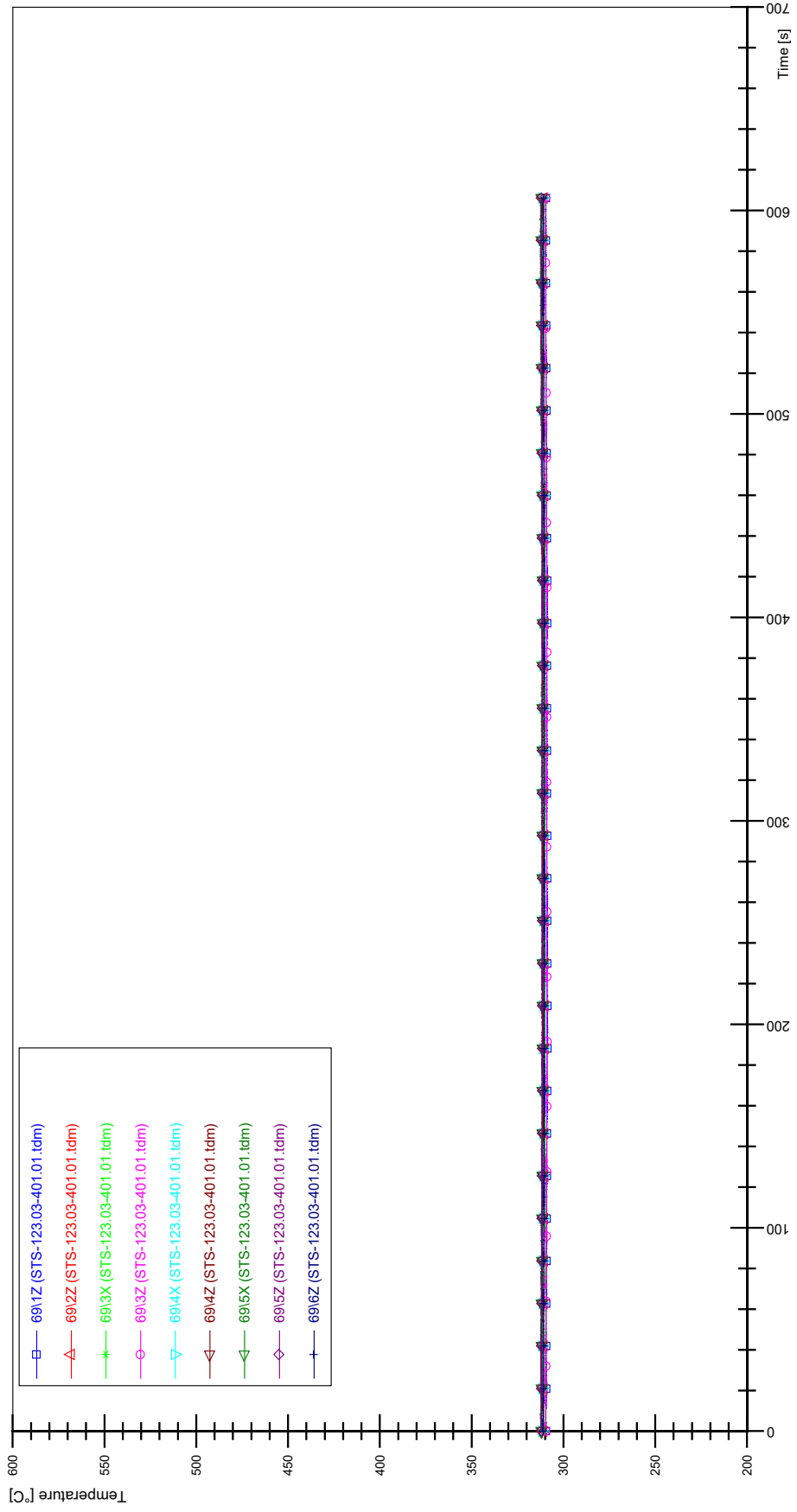
STS-123.03-401.01_CP12_CT19



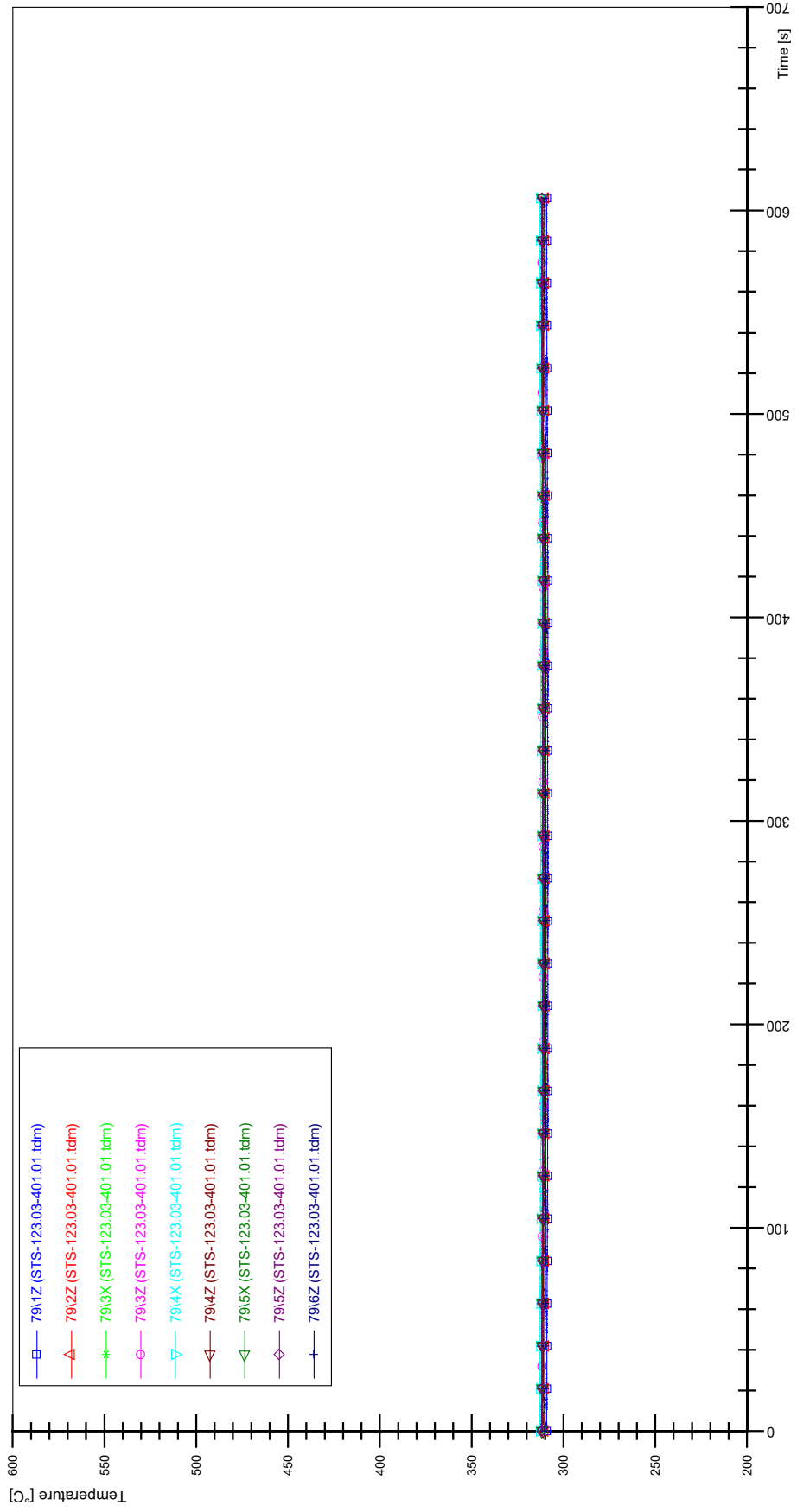
STS-123.03-401.01_Rod_59



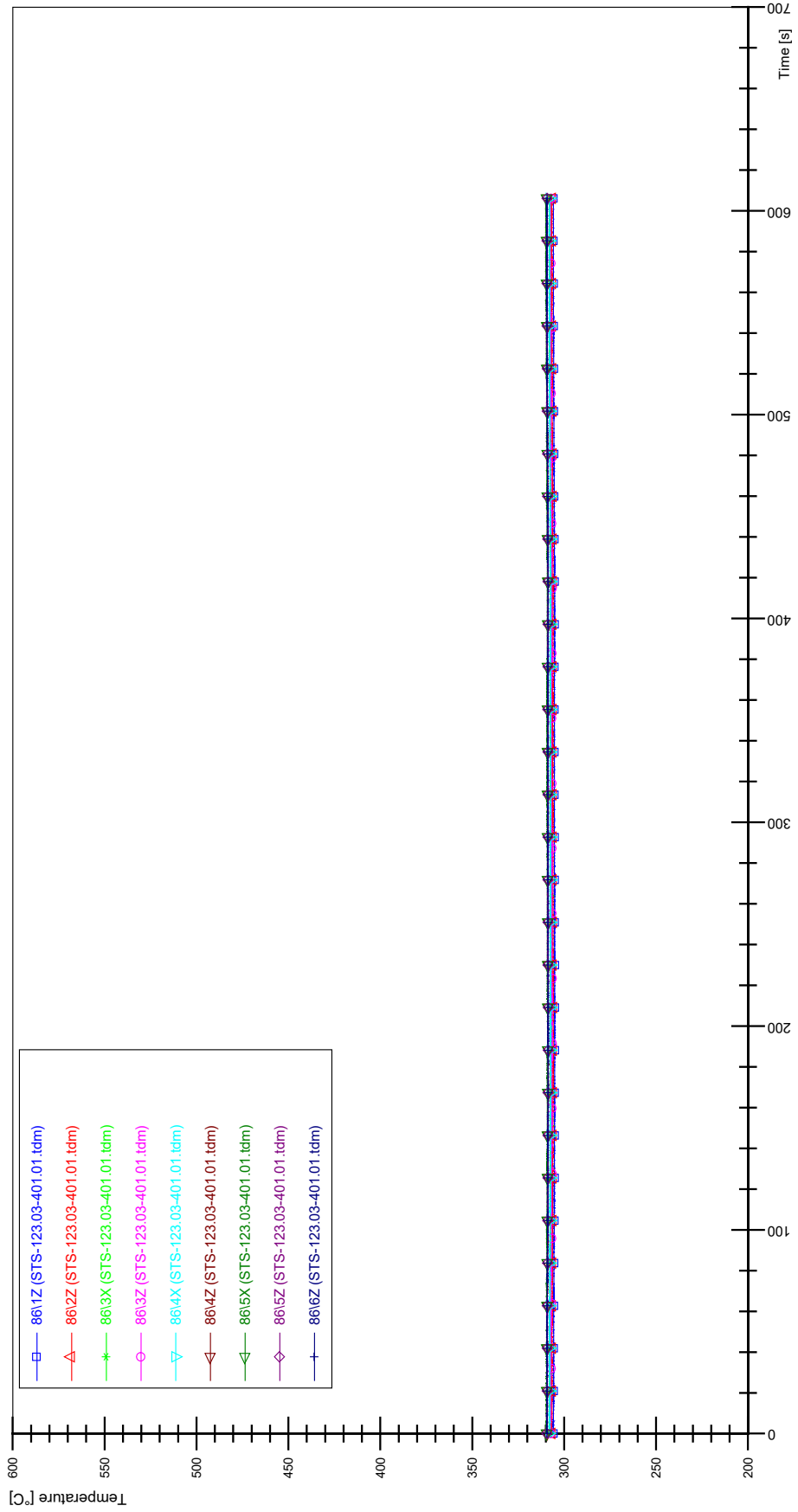
STS-123.03-401.01_Rod_69



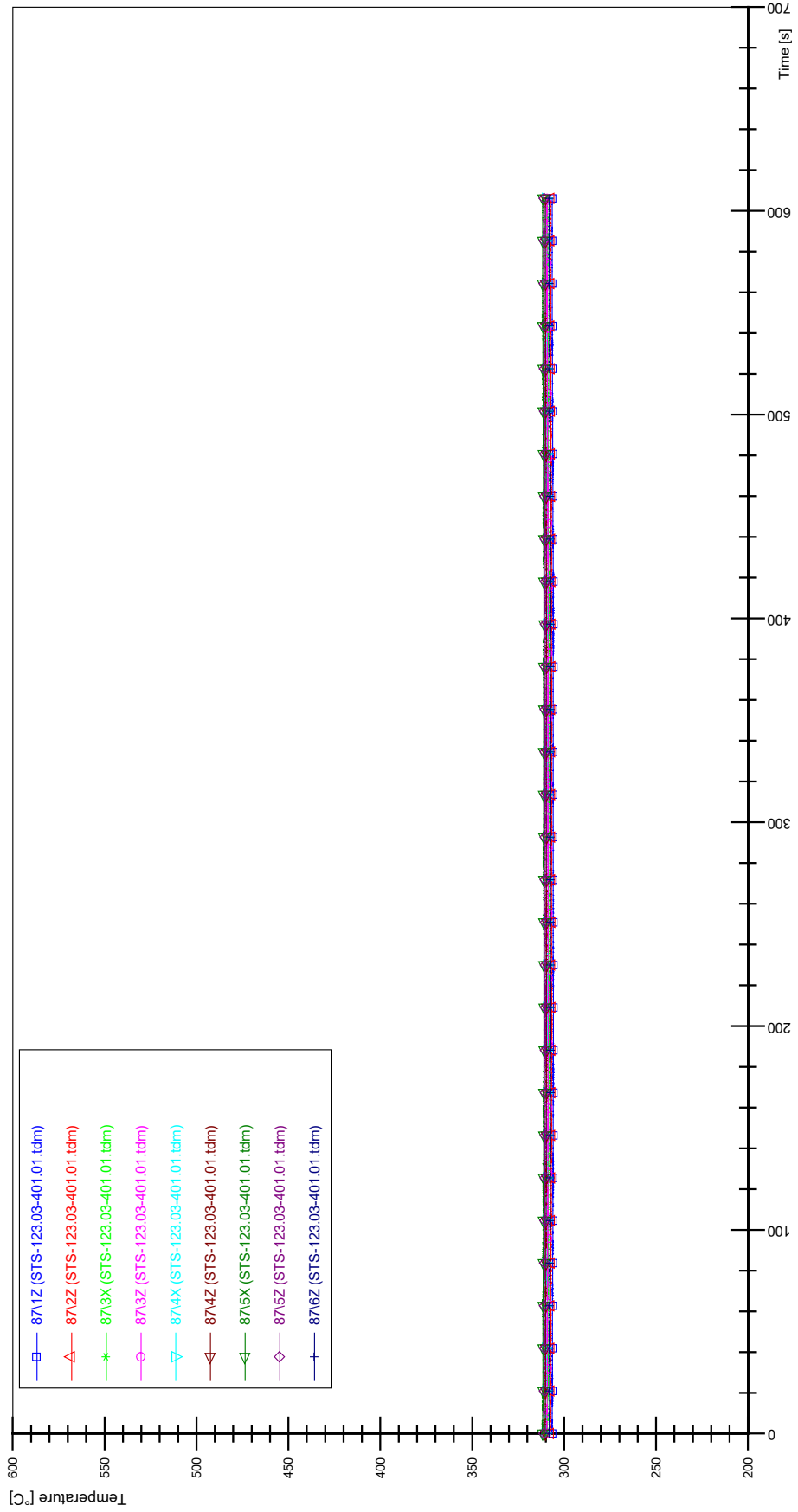
STS-123.03-401.01_Rod_79



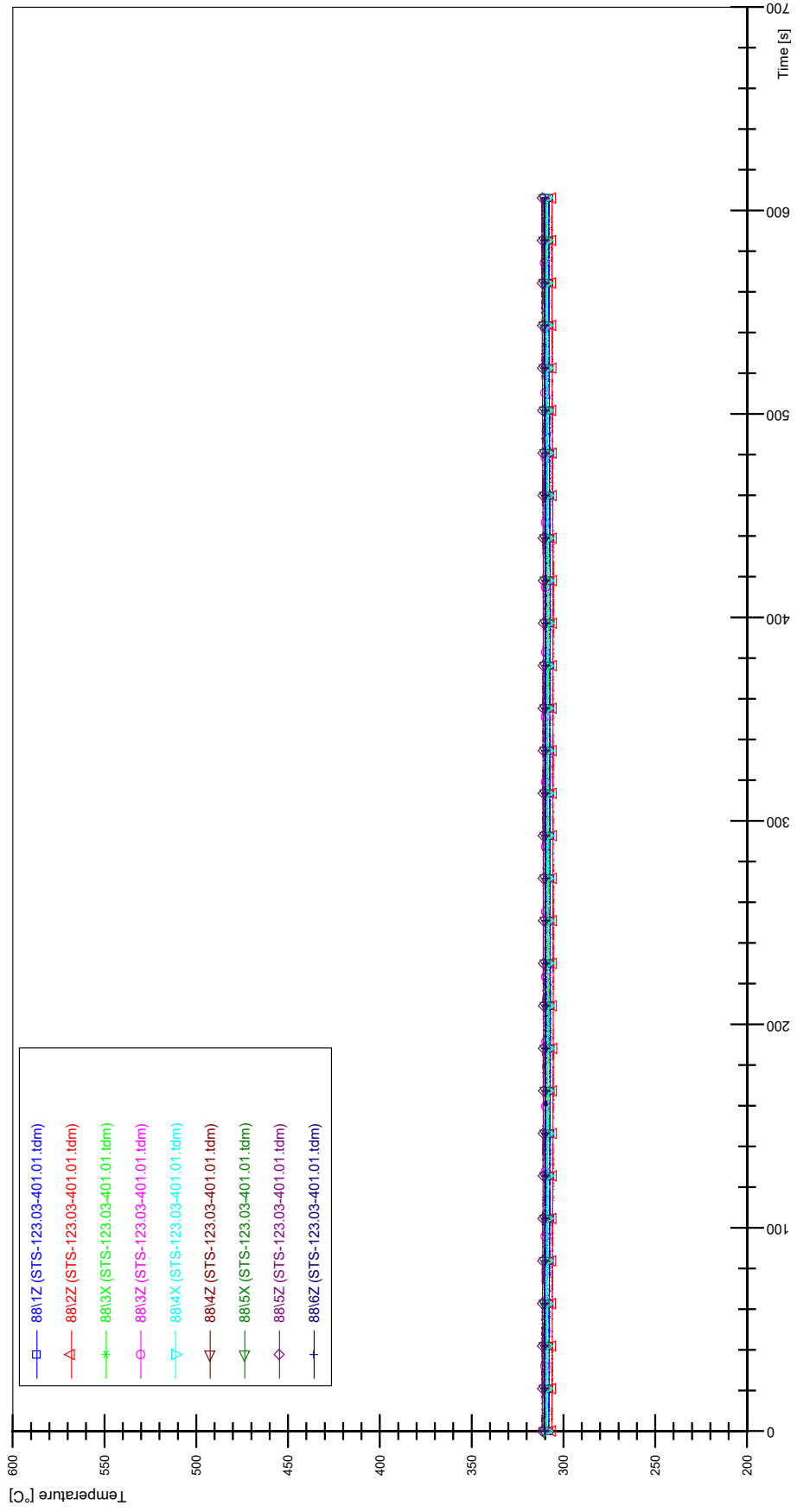
STS-123.03-401.01_Rod_86



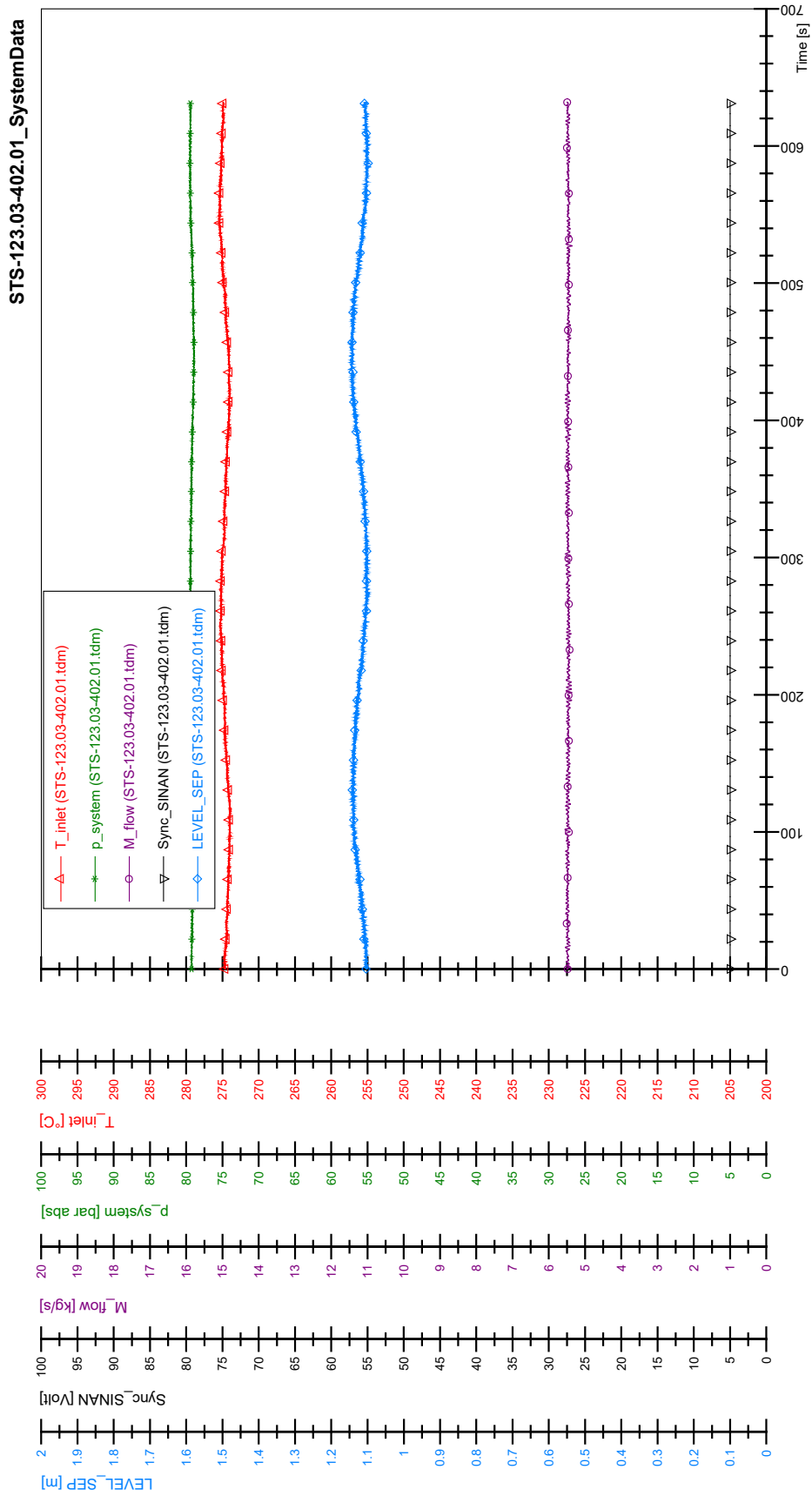
STS-123.03-401.01_Rod_87

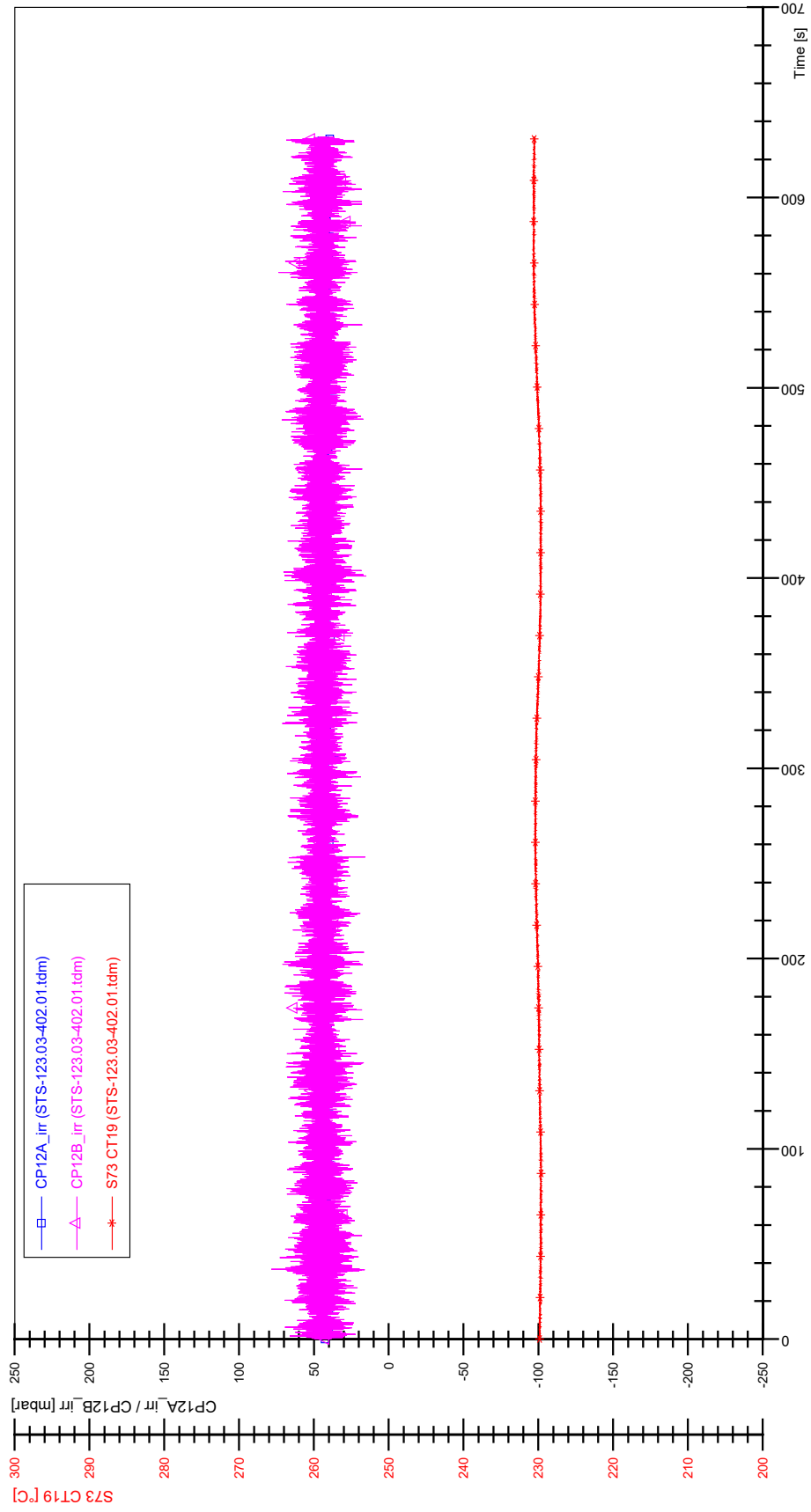


STS-123.03-401.01_Rod_88

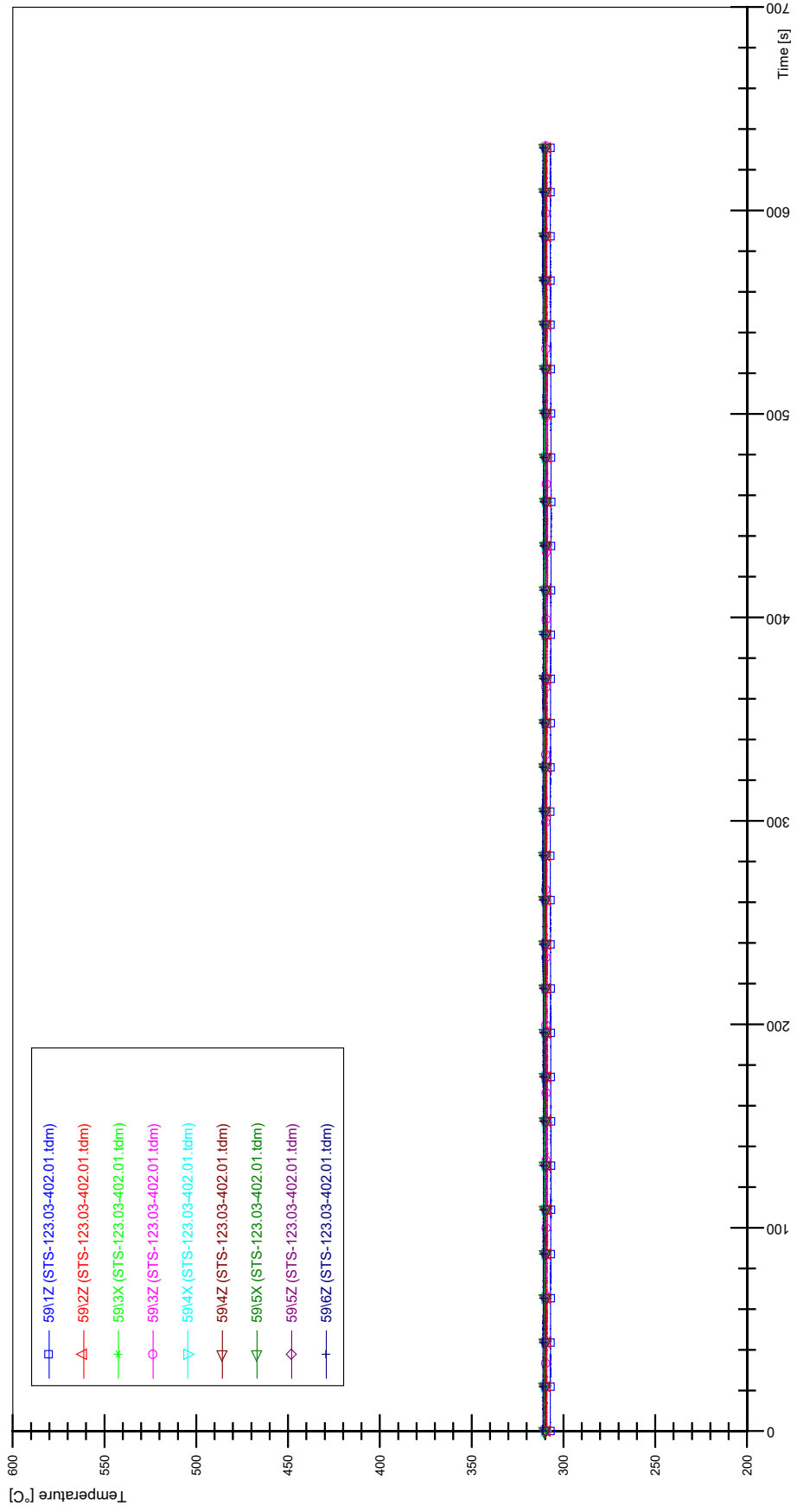


APPENDIX HH PLOTS OF INSTABILITY TEST STS-123.03-402.01

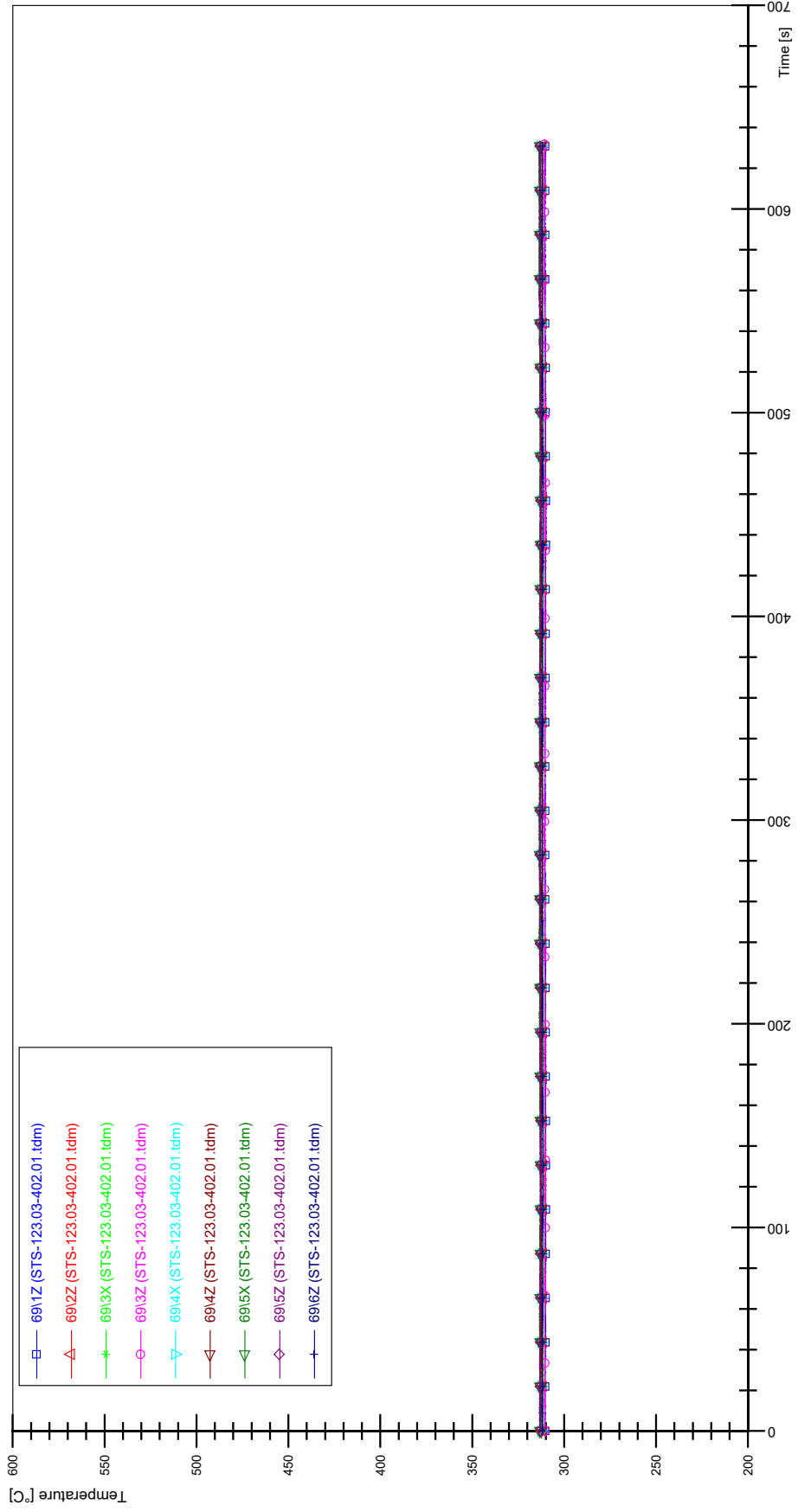




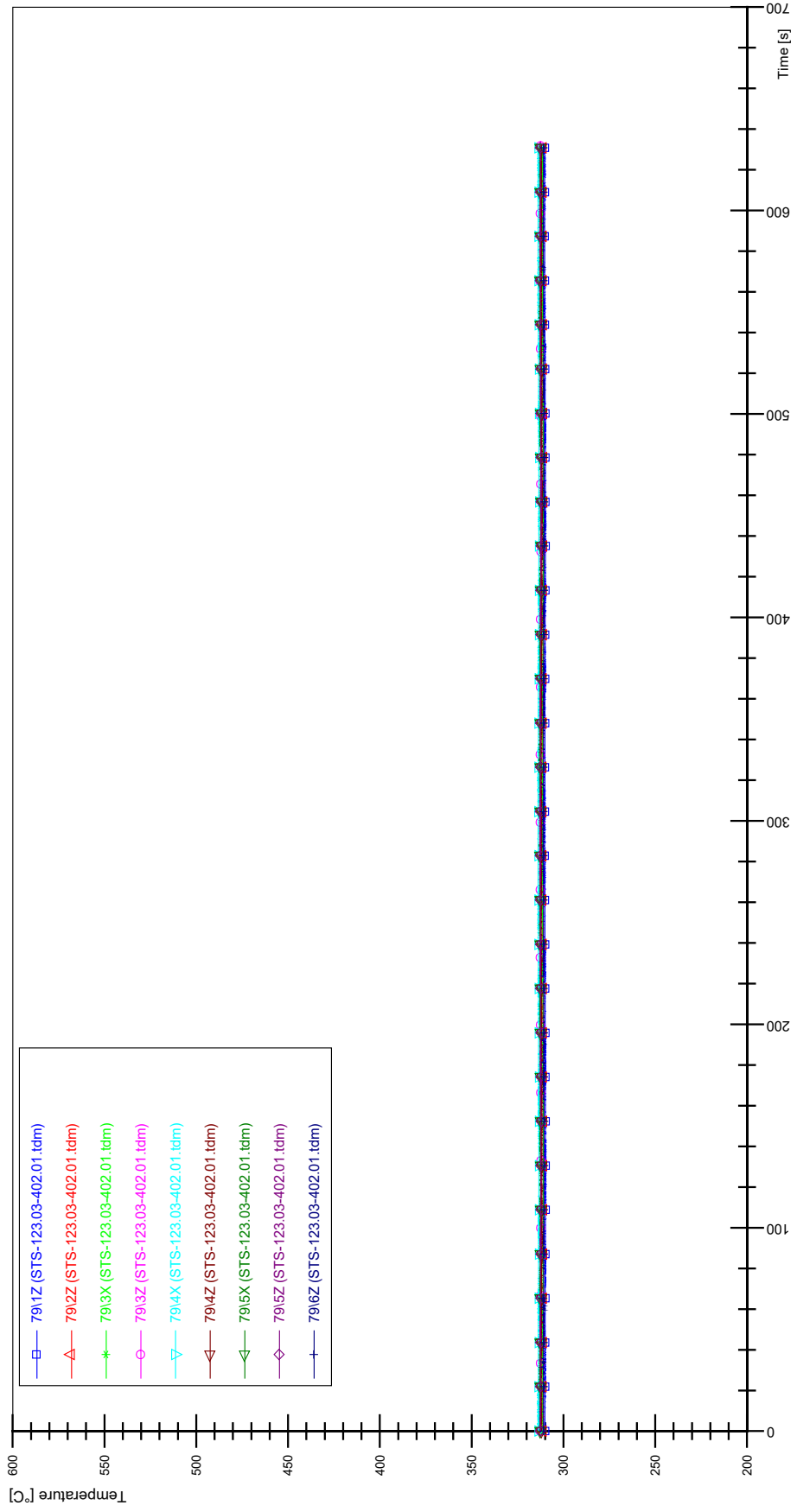
STS-123.03-402.01_Rod_59



STS-123.03-402.01_Rod_69

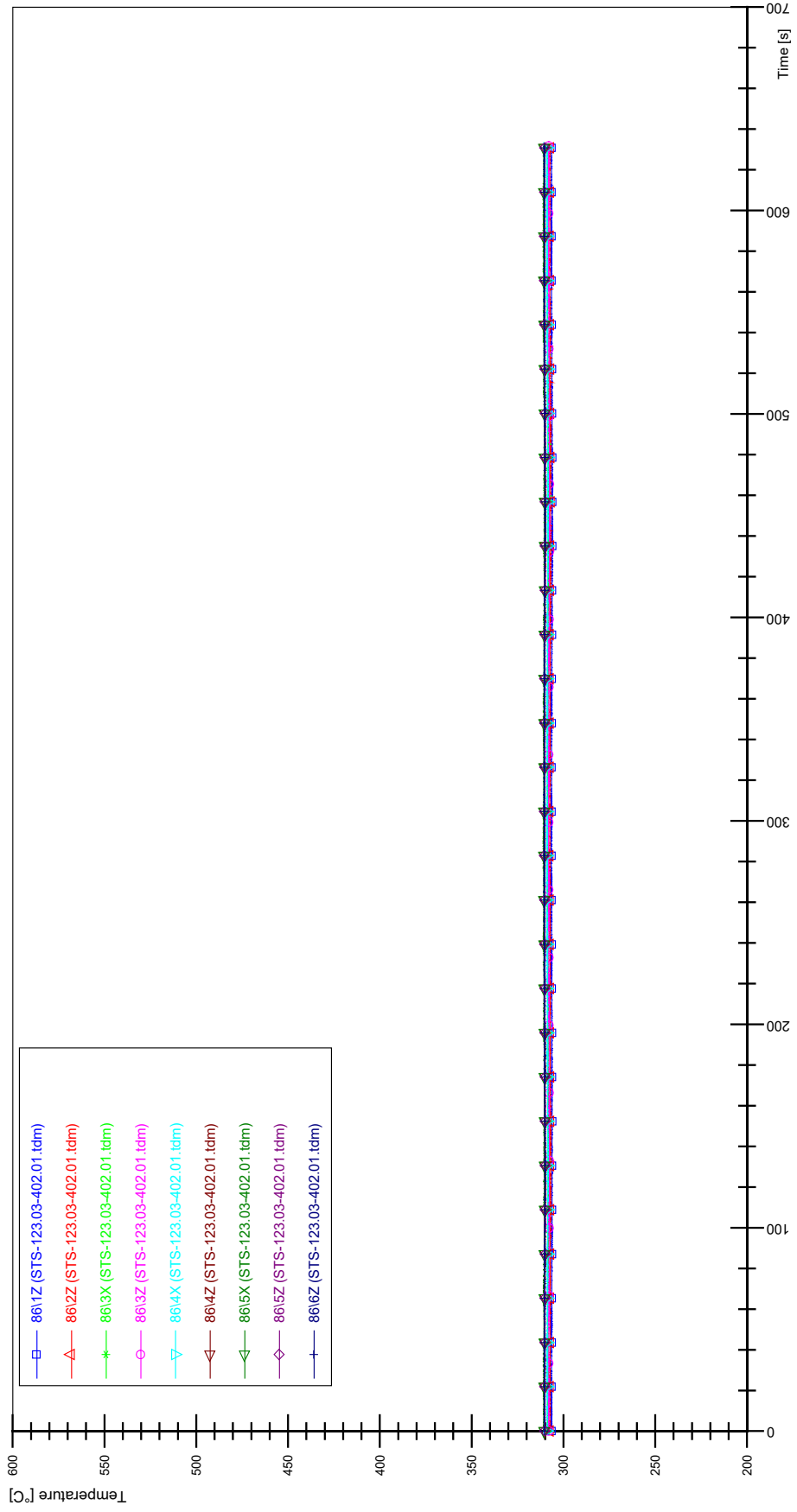


STS-123.03-402.01_Rod_79

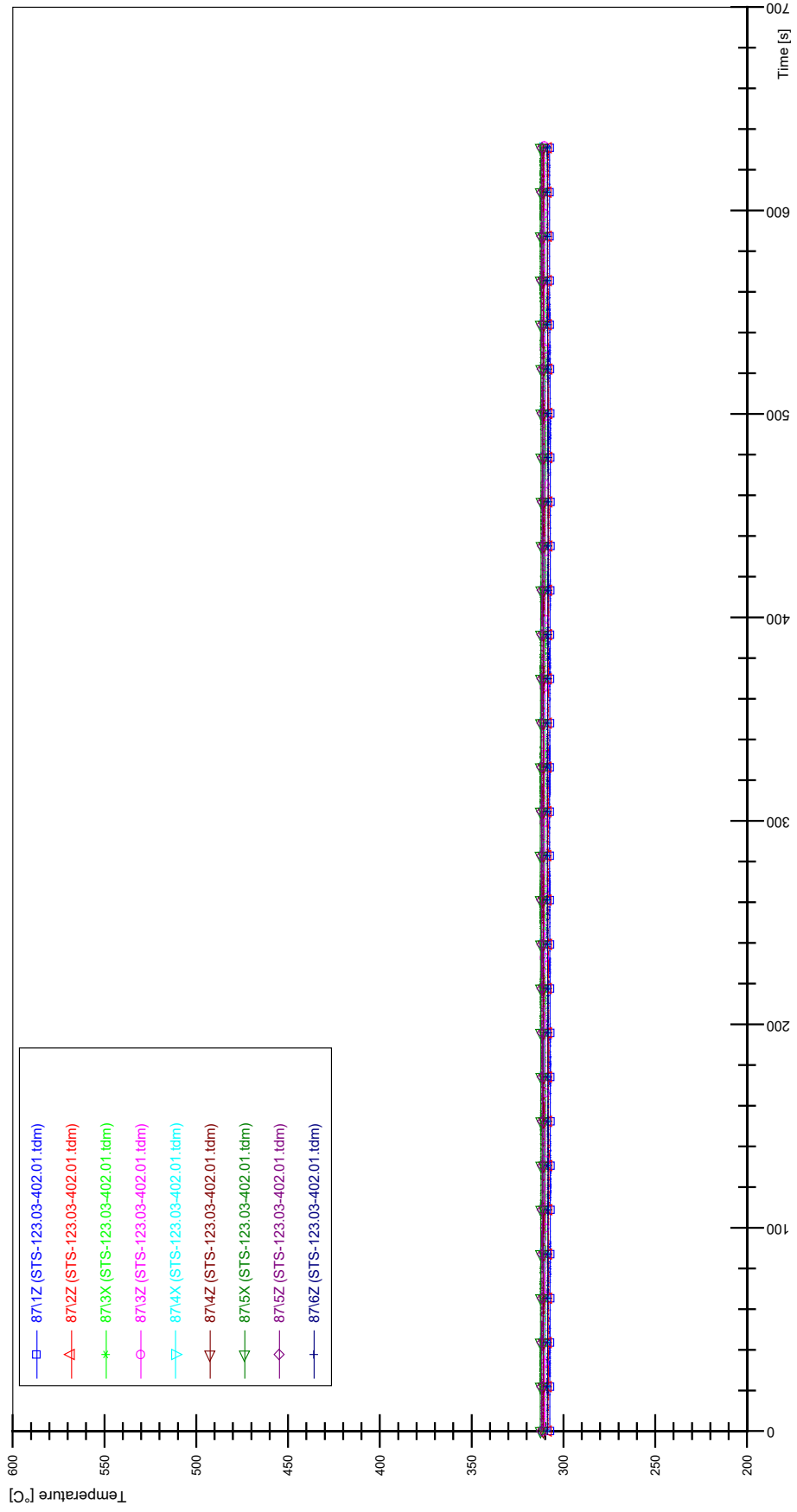


HH-5

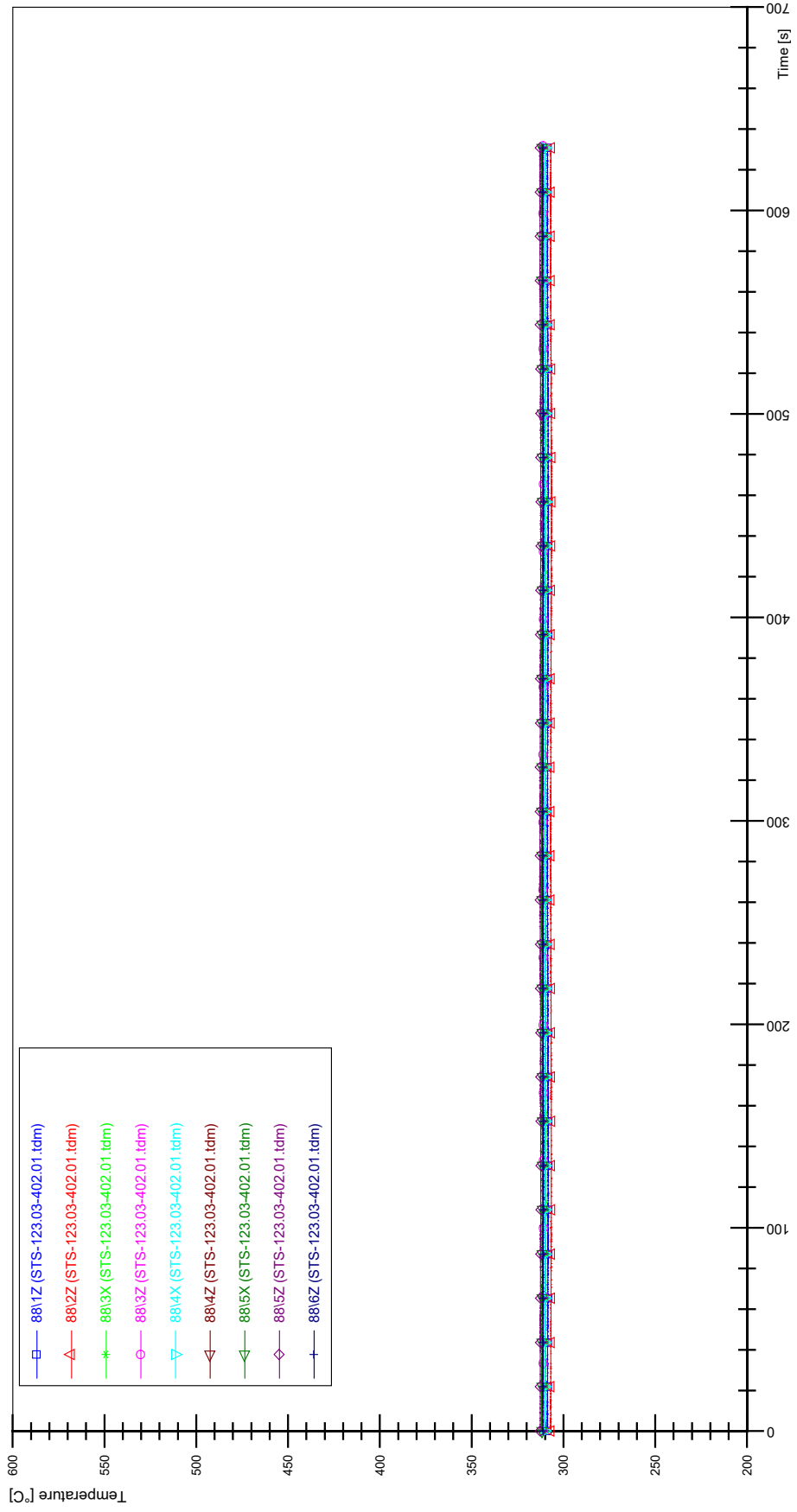
STS-123.03-402.01_Rod_86



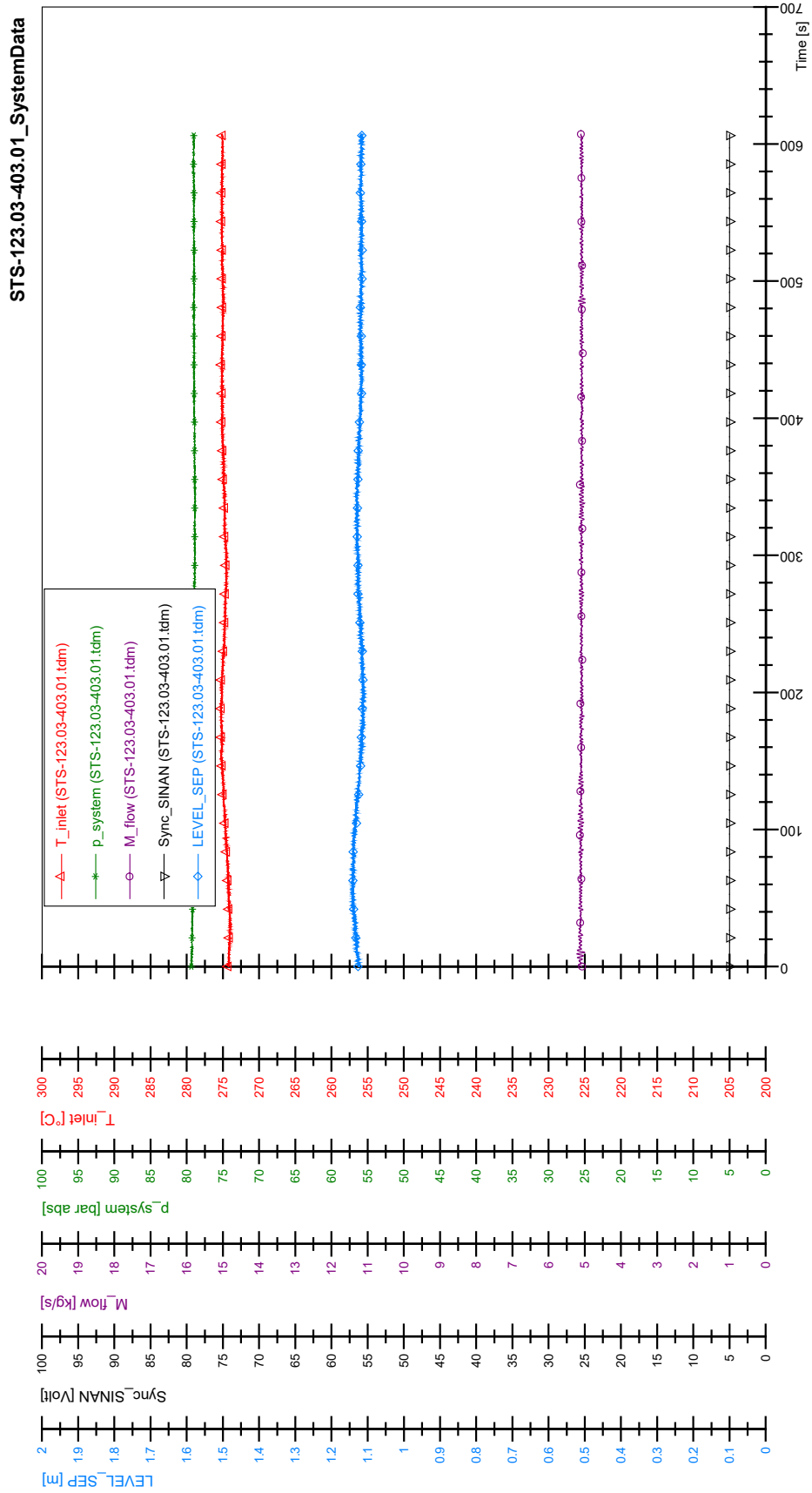
STS-123.03-402.01_Rod_87



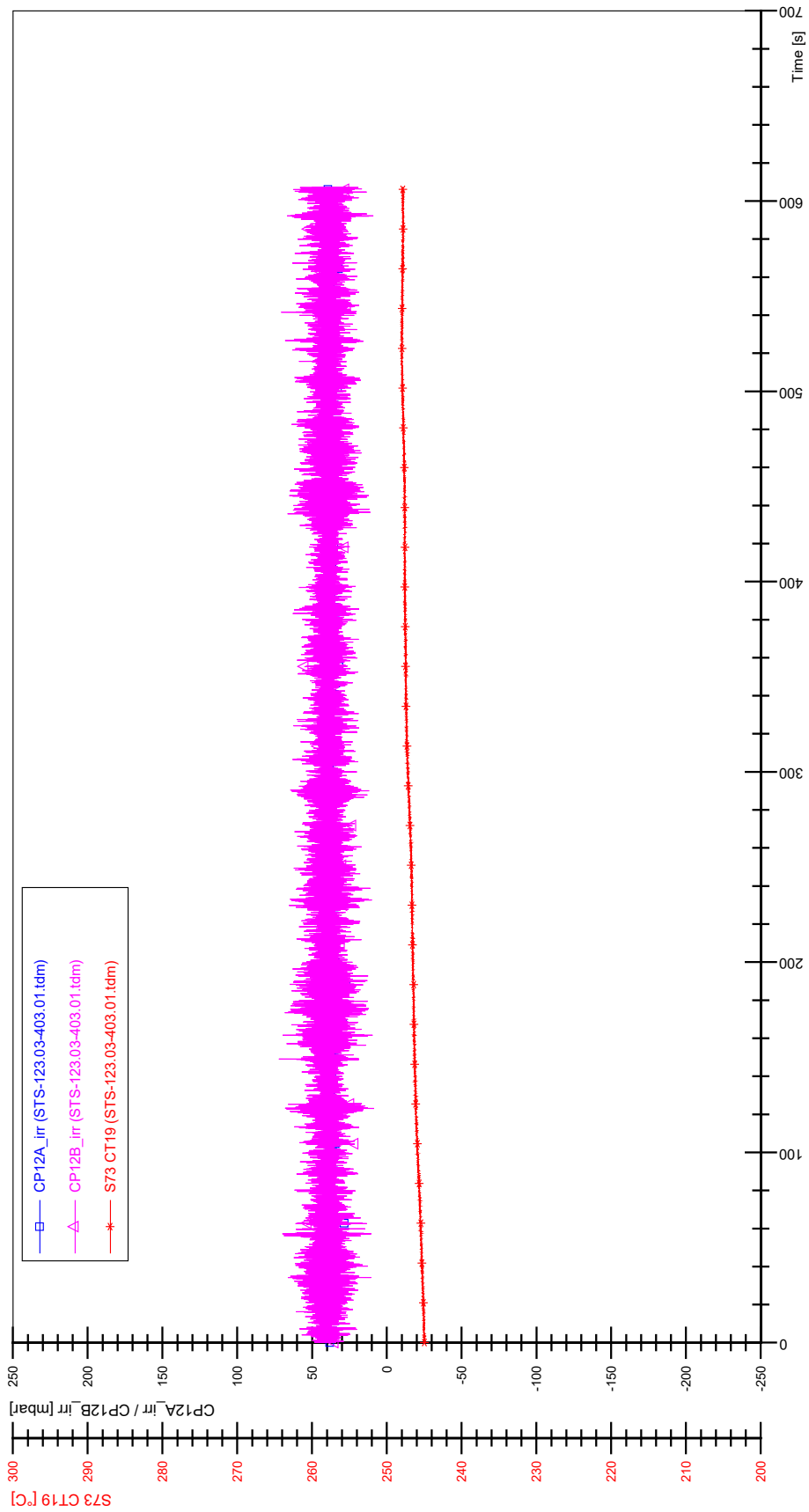
STS-123.03-402.01_Rod_88



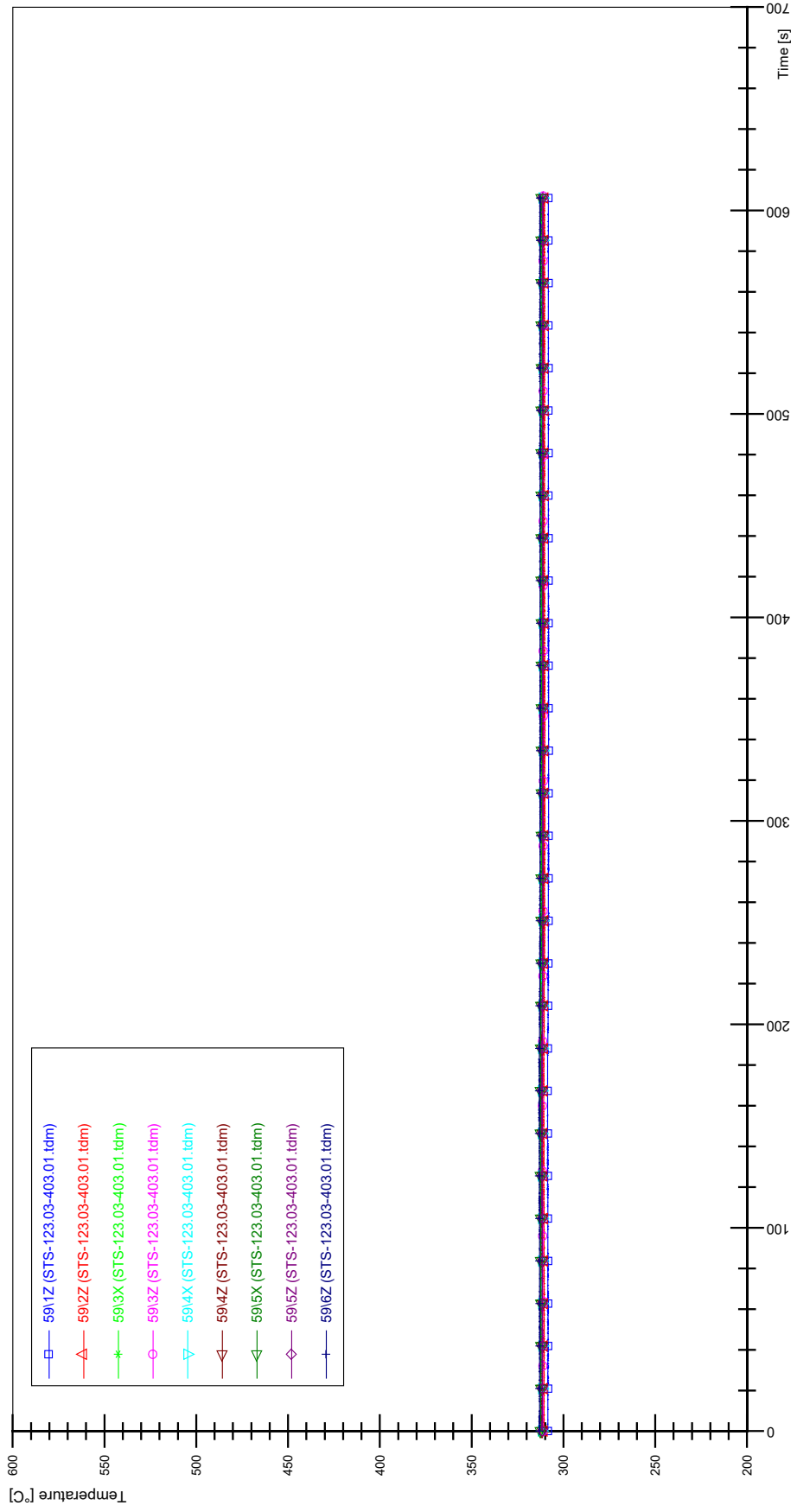
APPENDIX II PLOTS OF INSTABILITY TEST STS-123.03-403.01



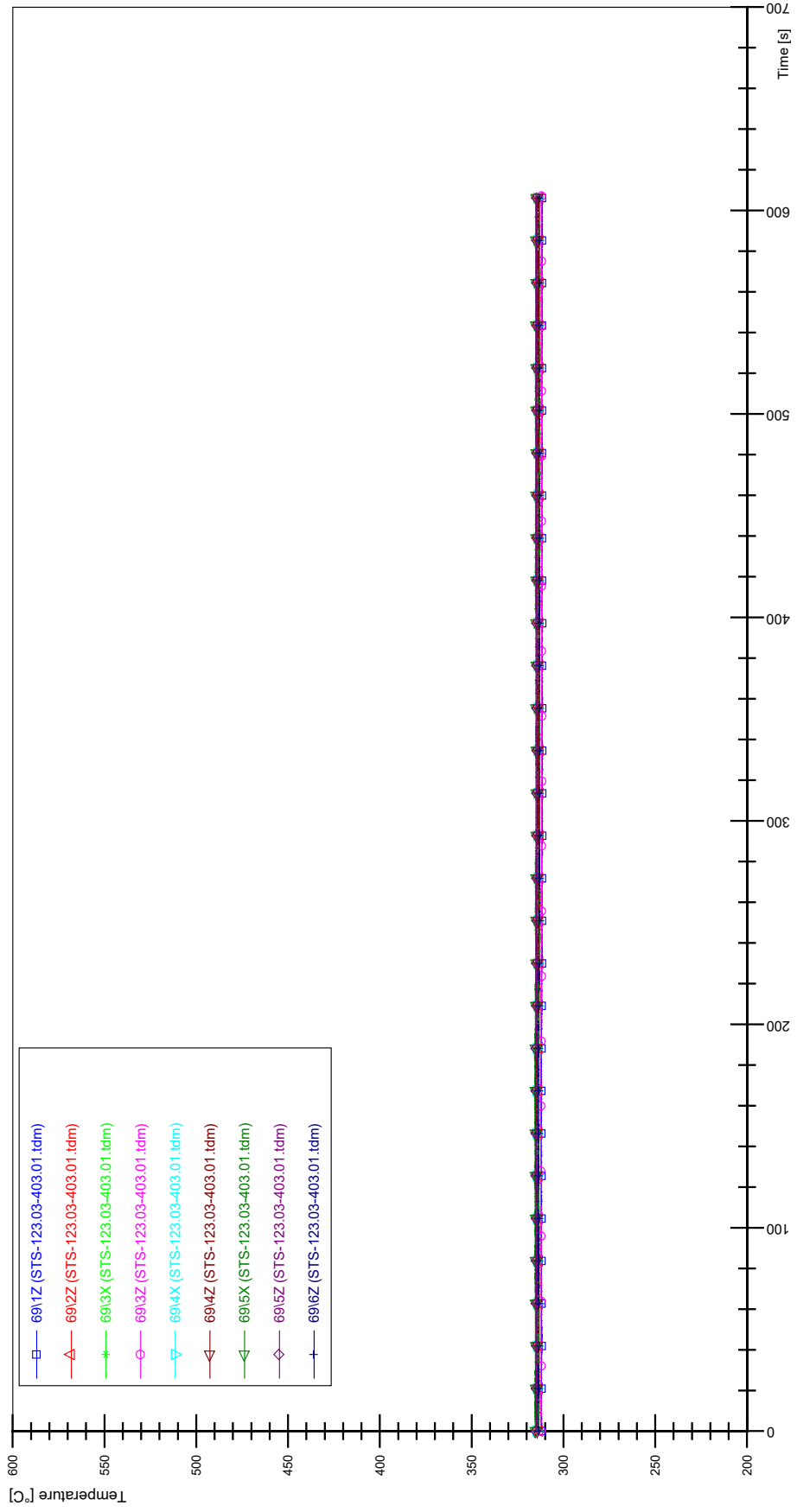
STS-123.03-403.01_CP12_CT19



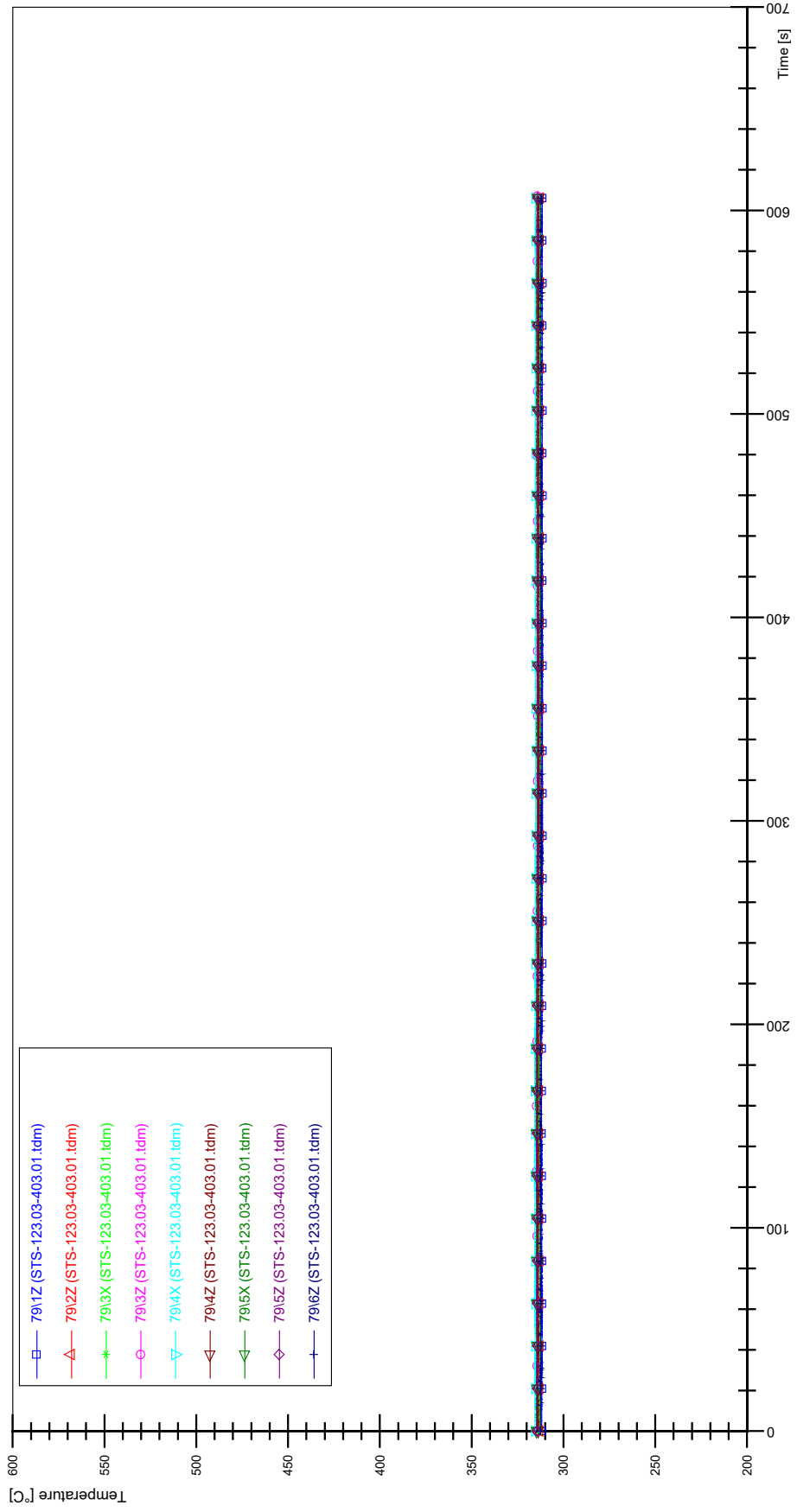
STS-123.03-403.01_Rod_59



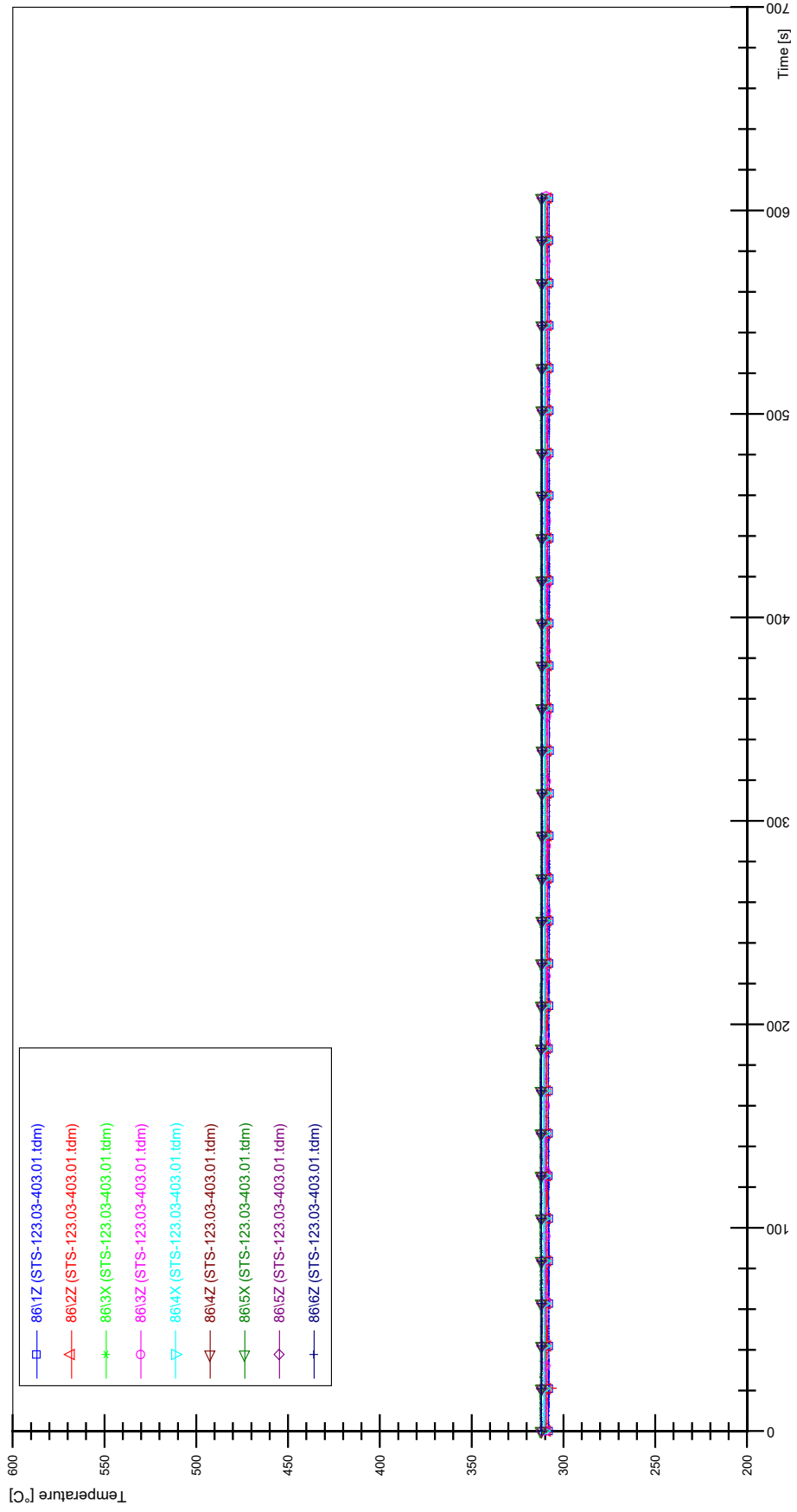
STS-123.03-403.01_Rod_69



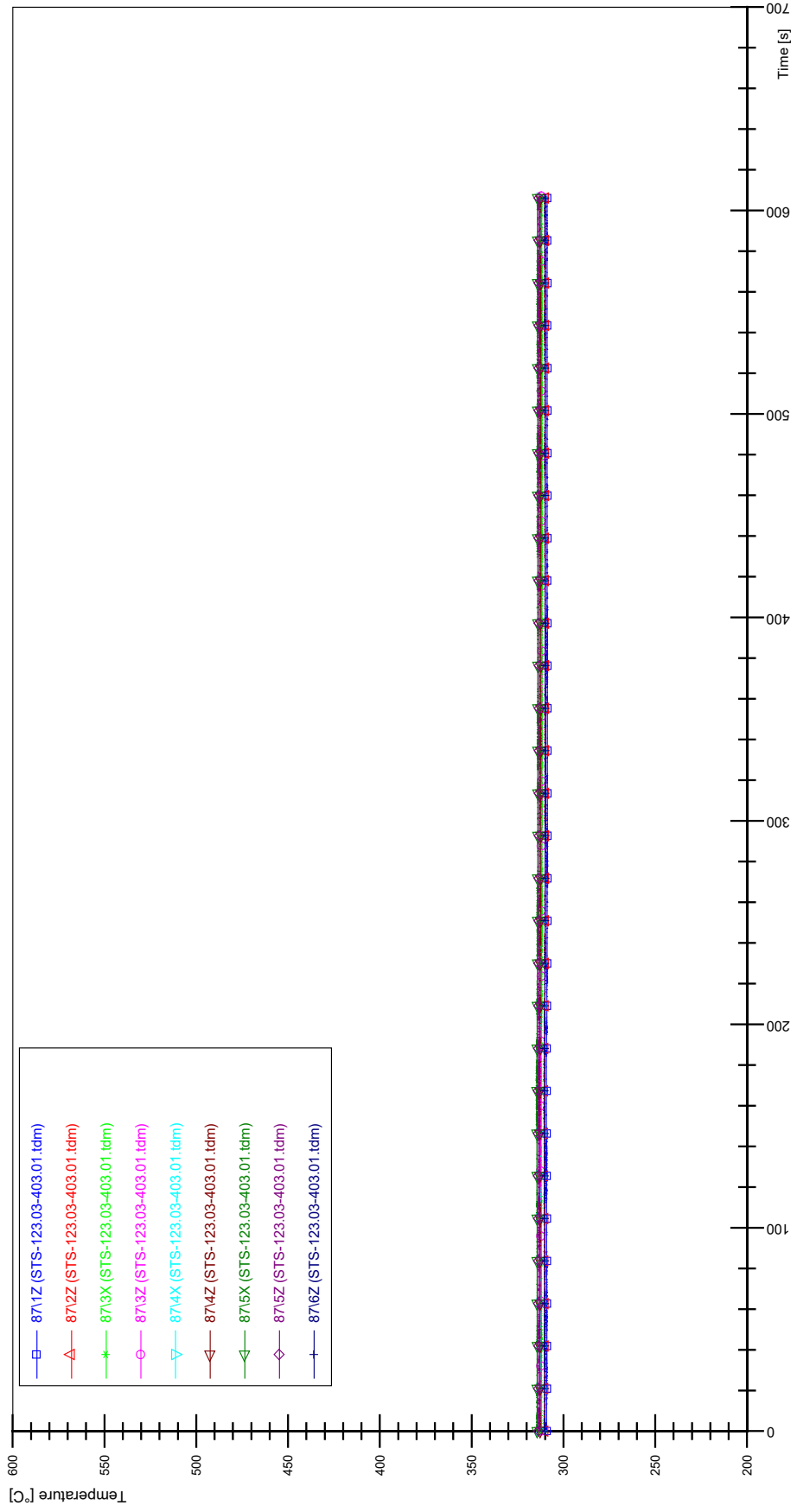
STS-123.03-403.01_Rod_79



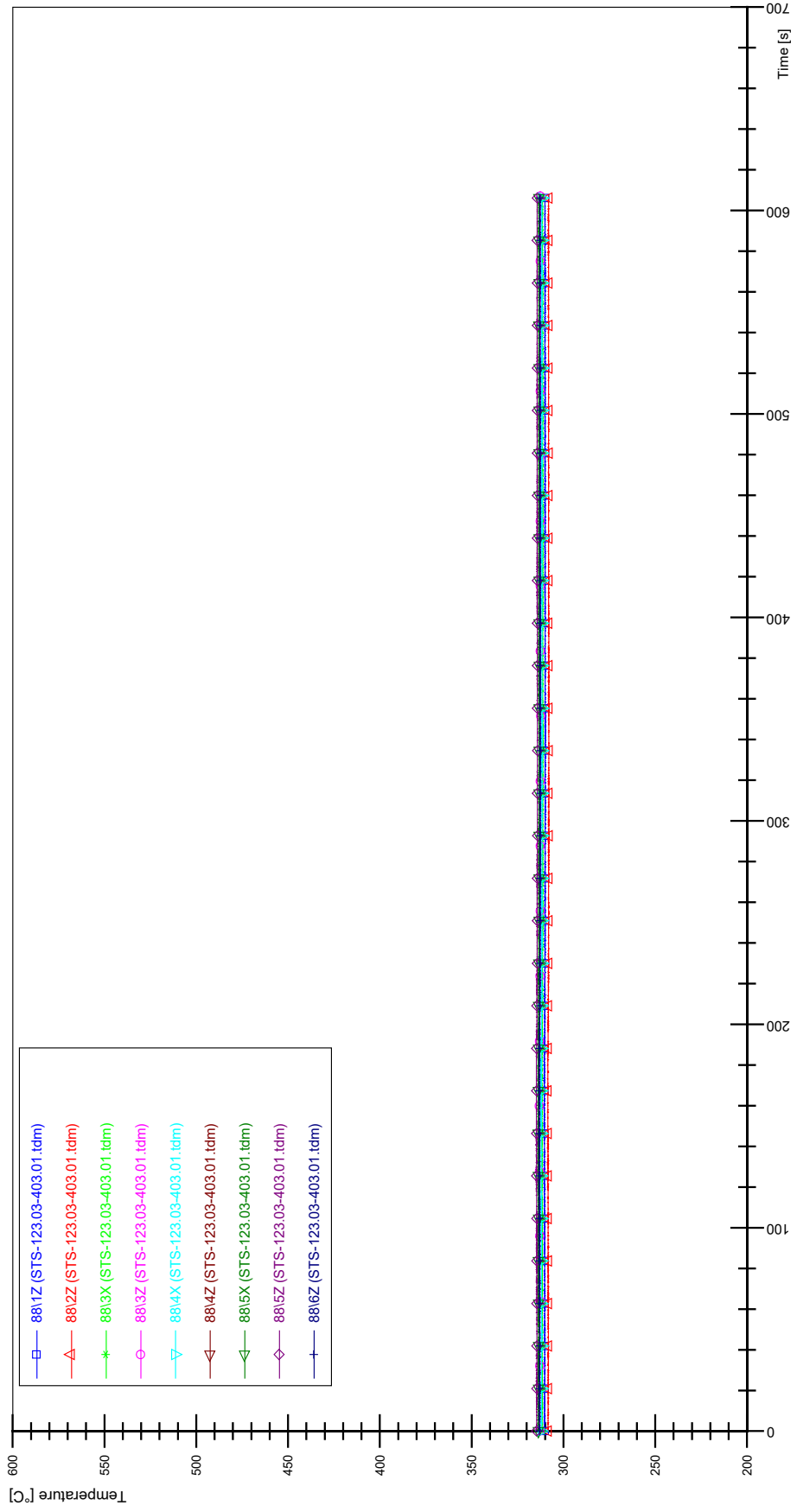
STS-123.03-403.01_Rod_86



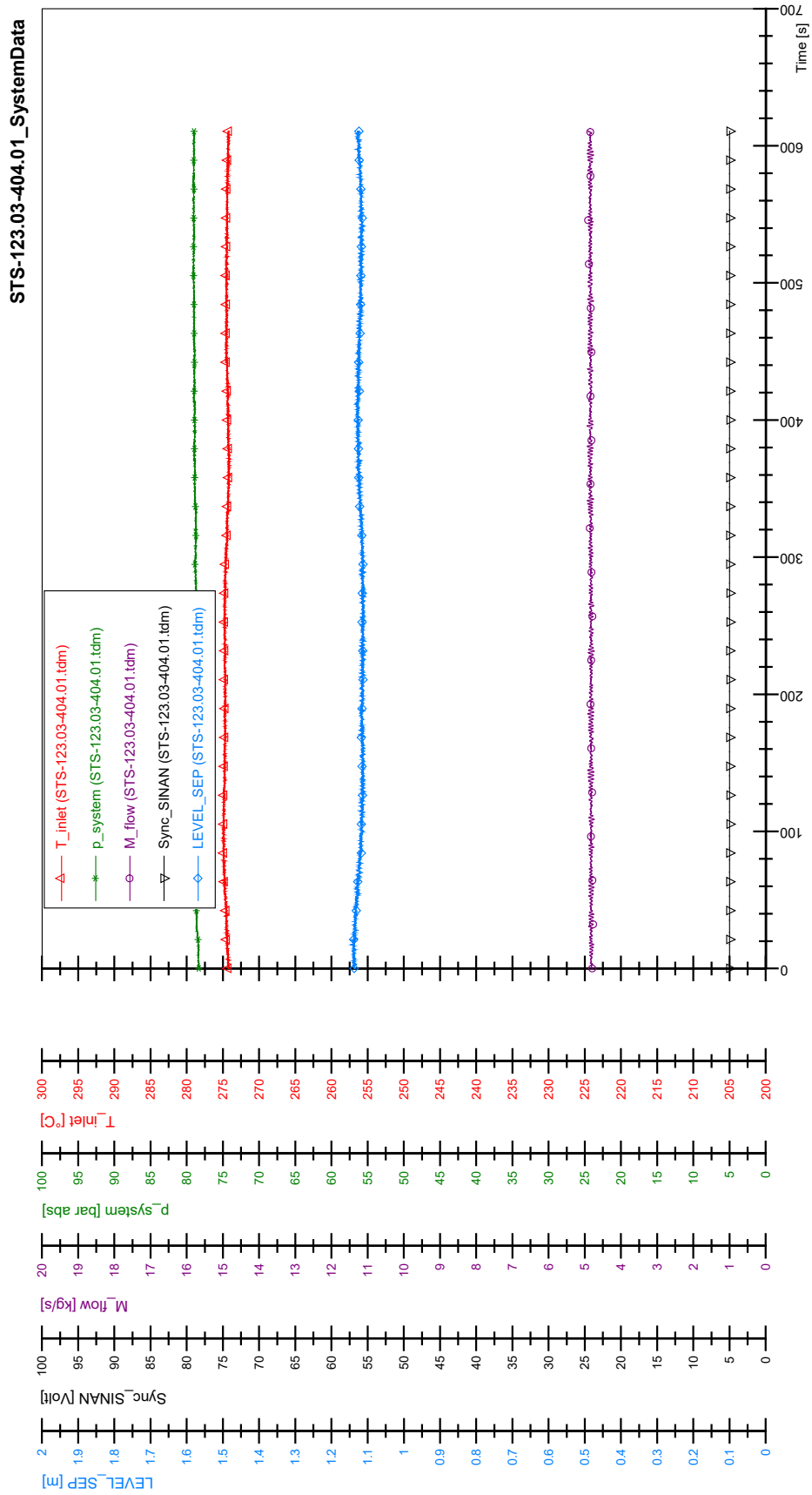
STS-123.03-403.01_Rod_87

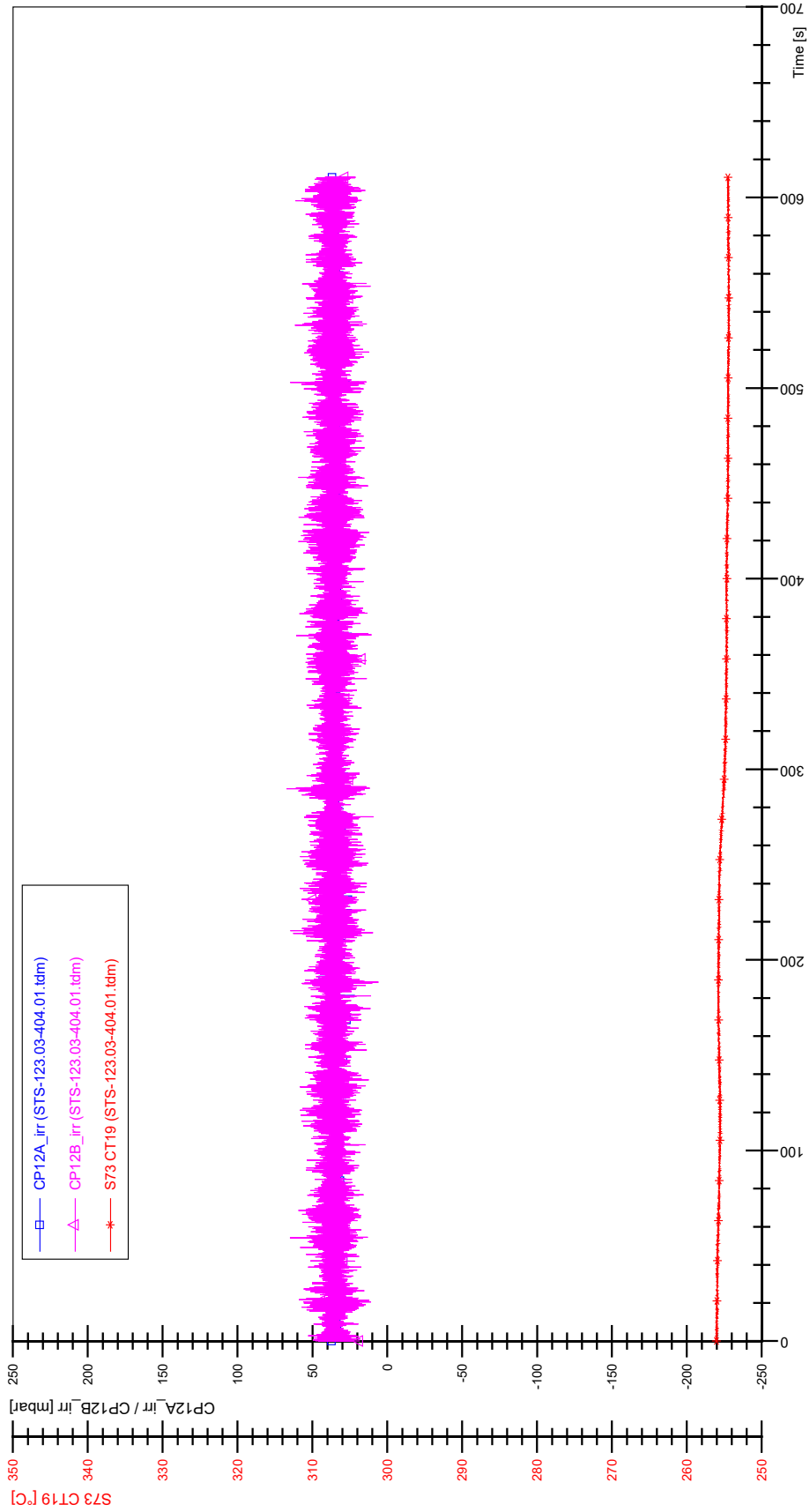


STS-123.03-403.01_Rod_88

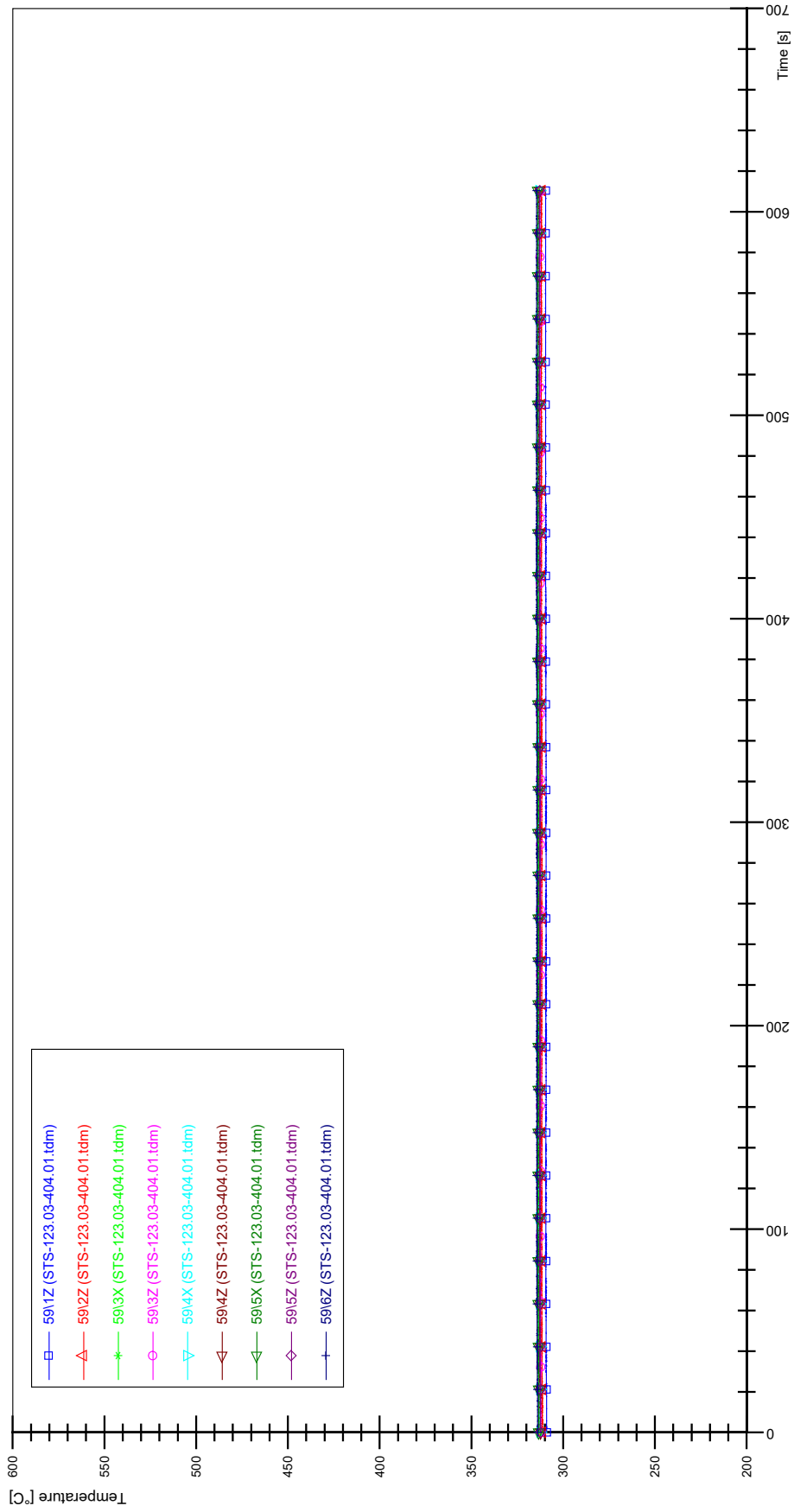


APPENDIX JJ PLOTS OF INSTABILITY TEST STS-123.03-404.01

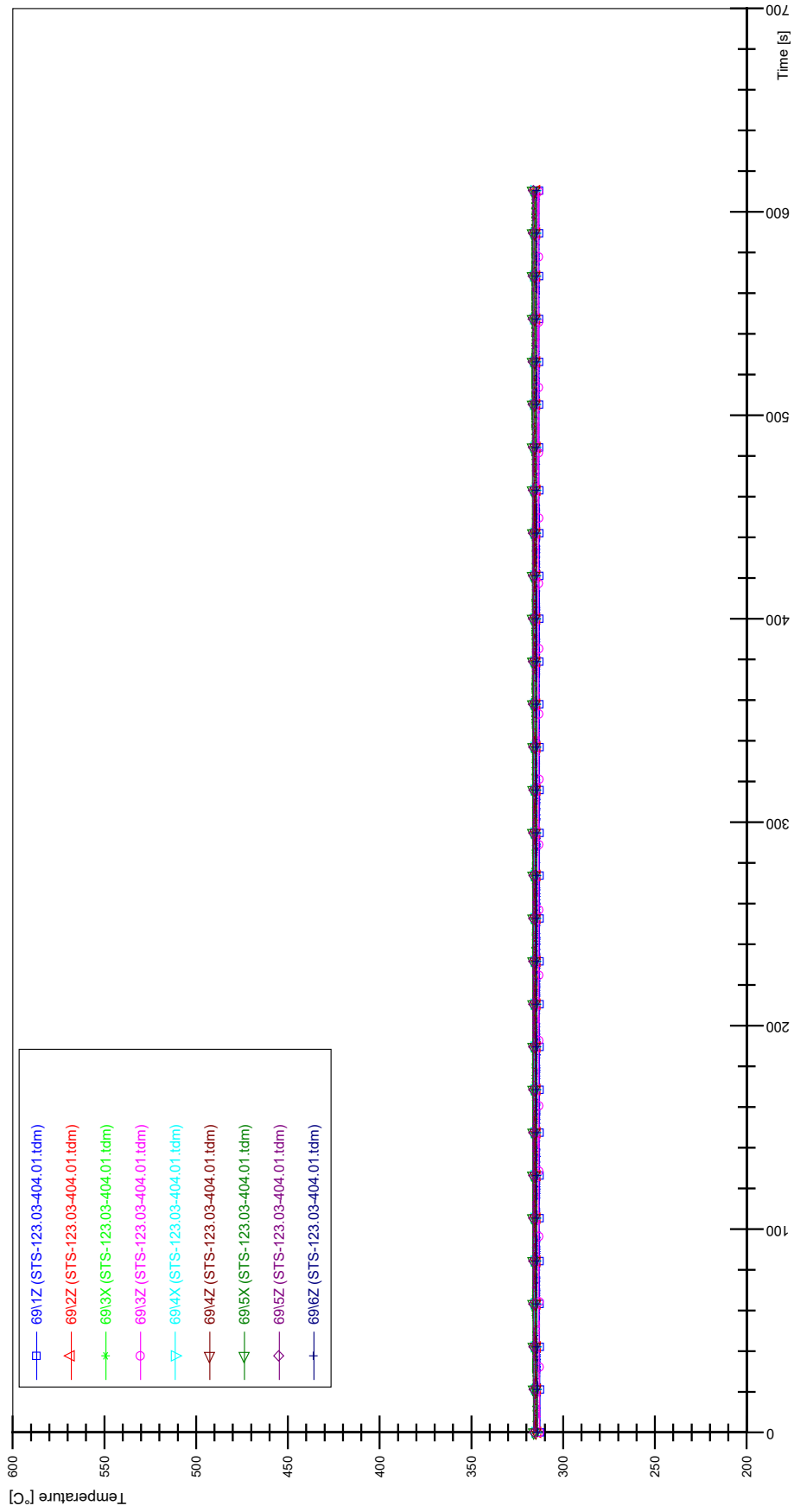




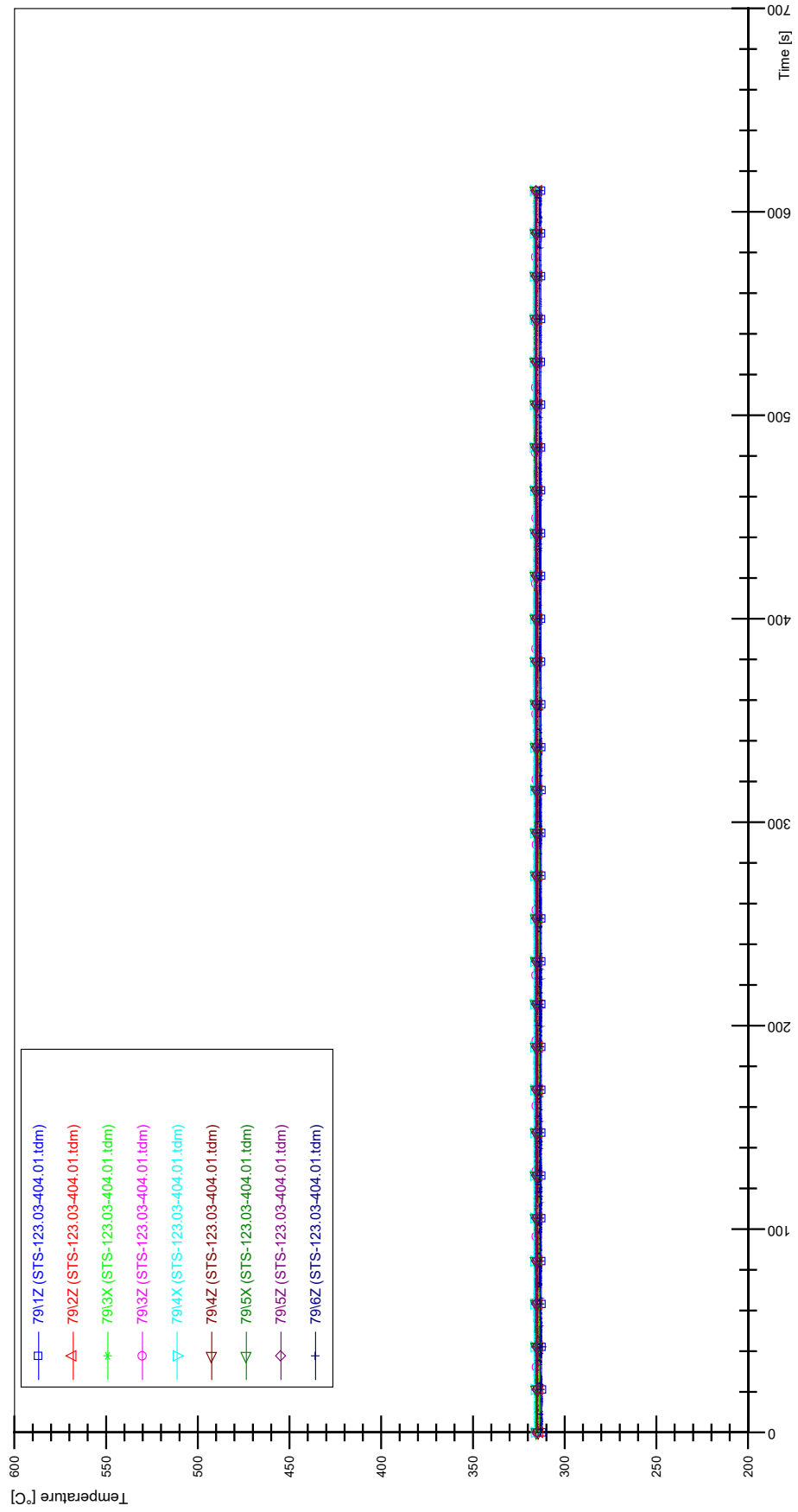
STS-123.03-404.01_Rod_59



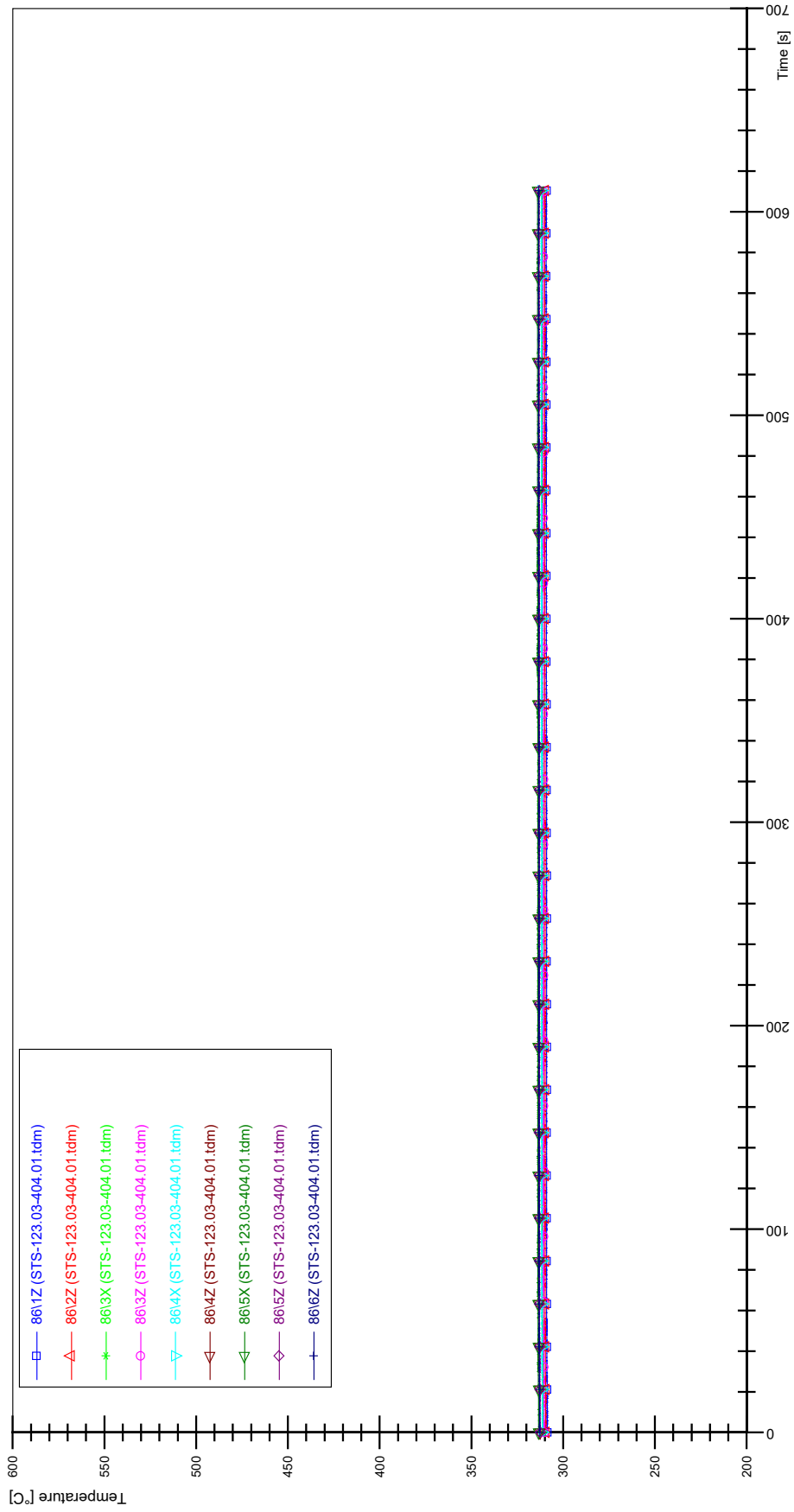
STS-123.03-404.01_Rod_69



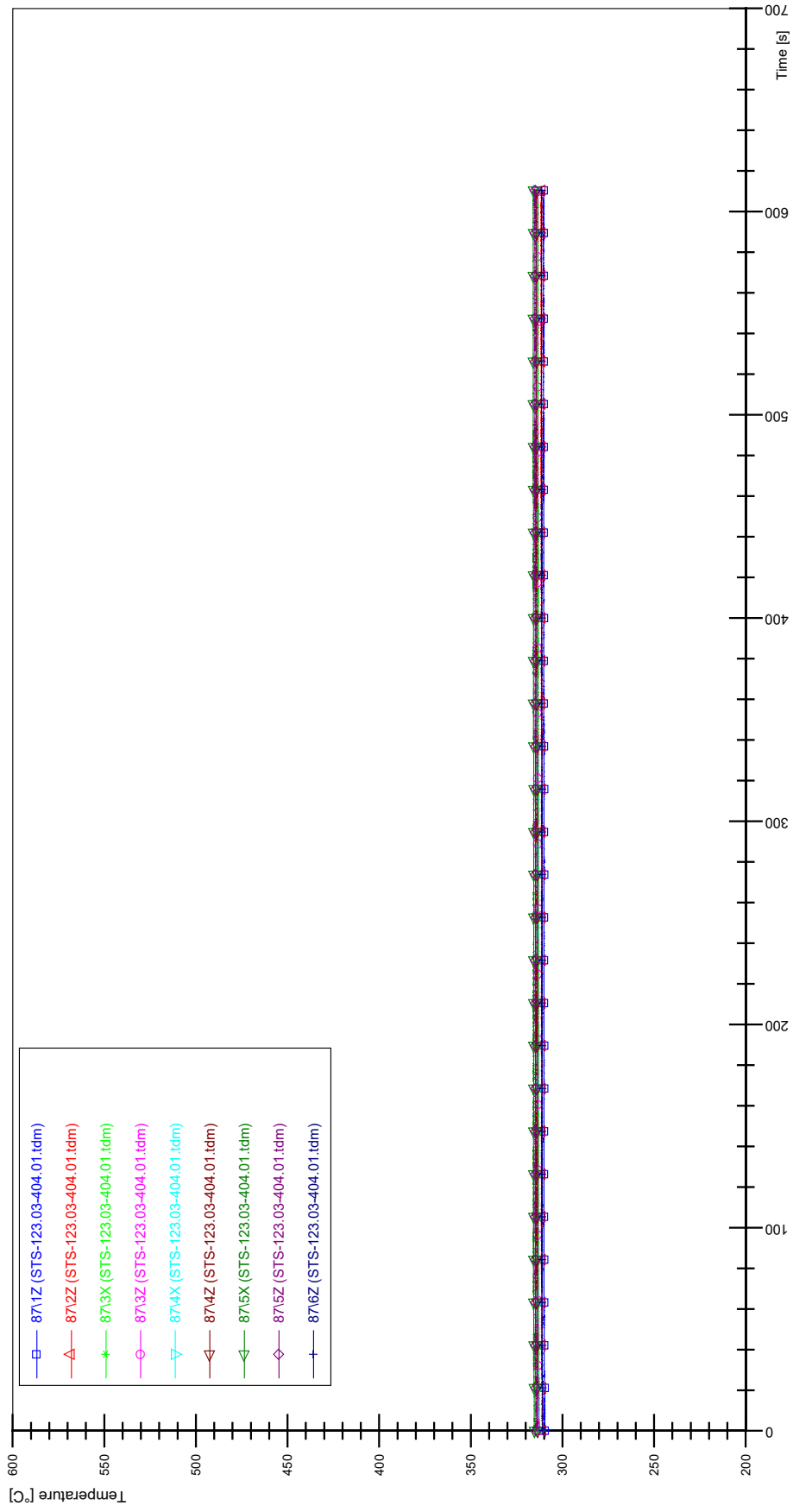
STS-123.03-404.01_Rod_79



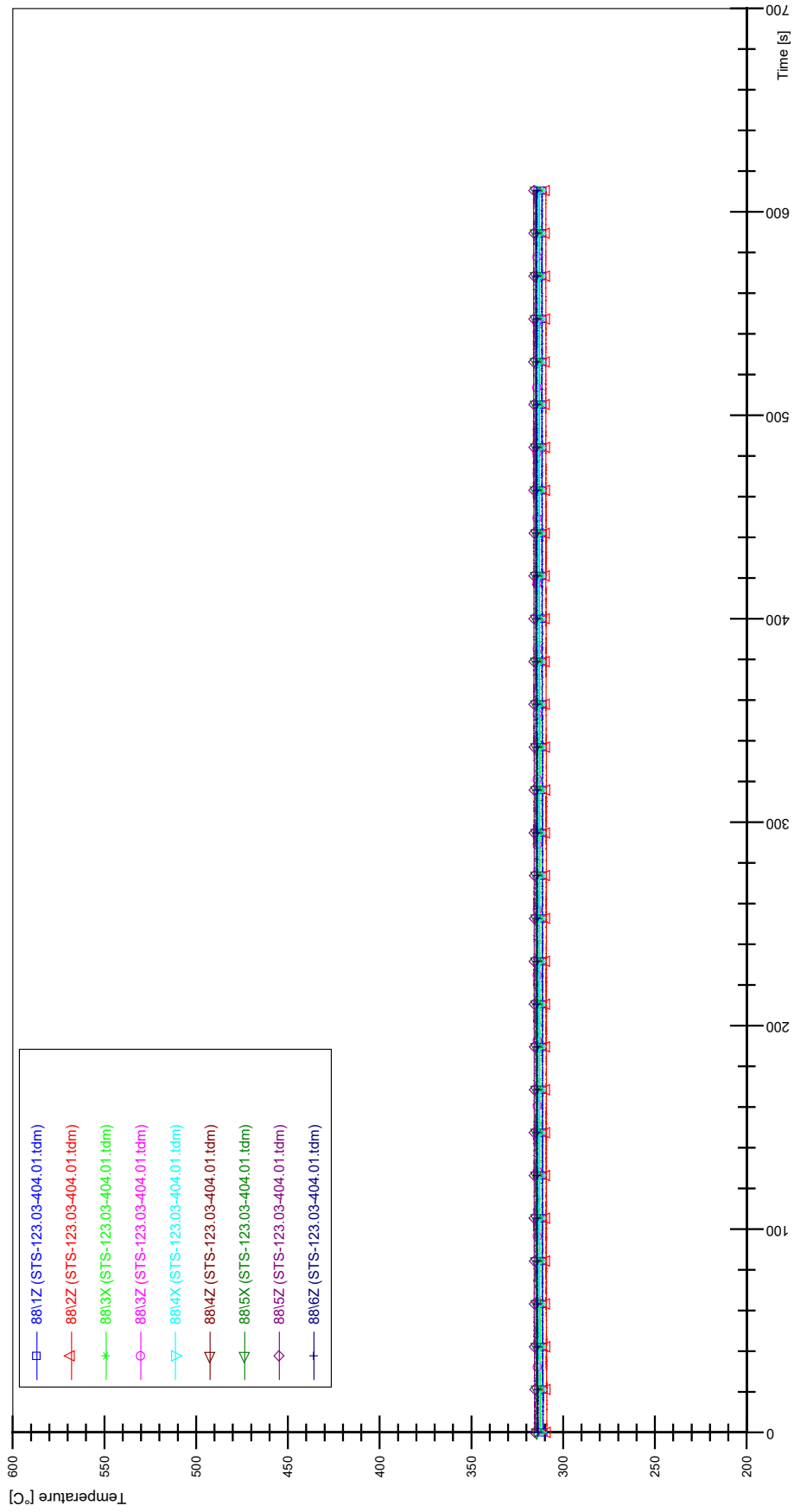
STS-123.03-404.01_Rod_86



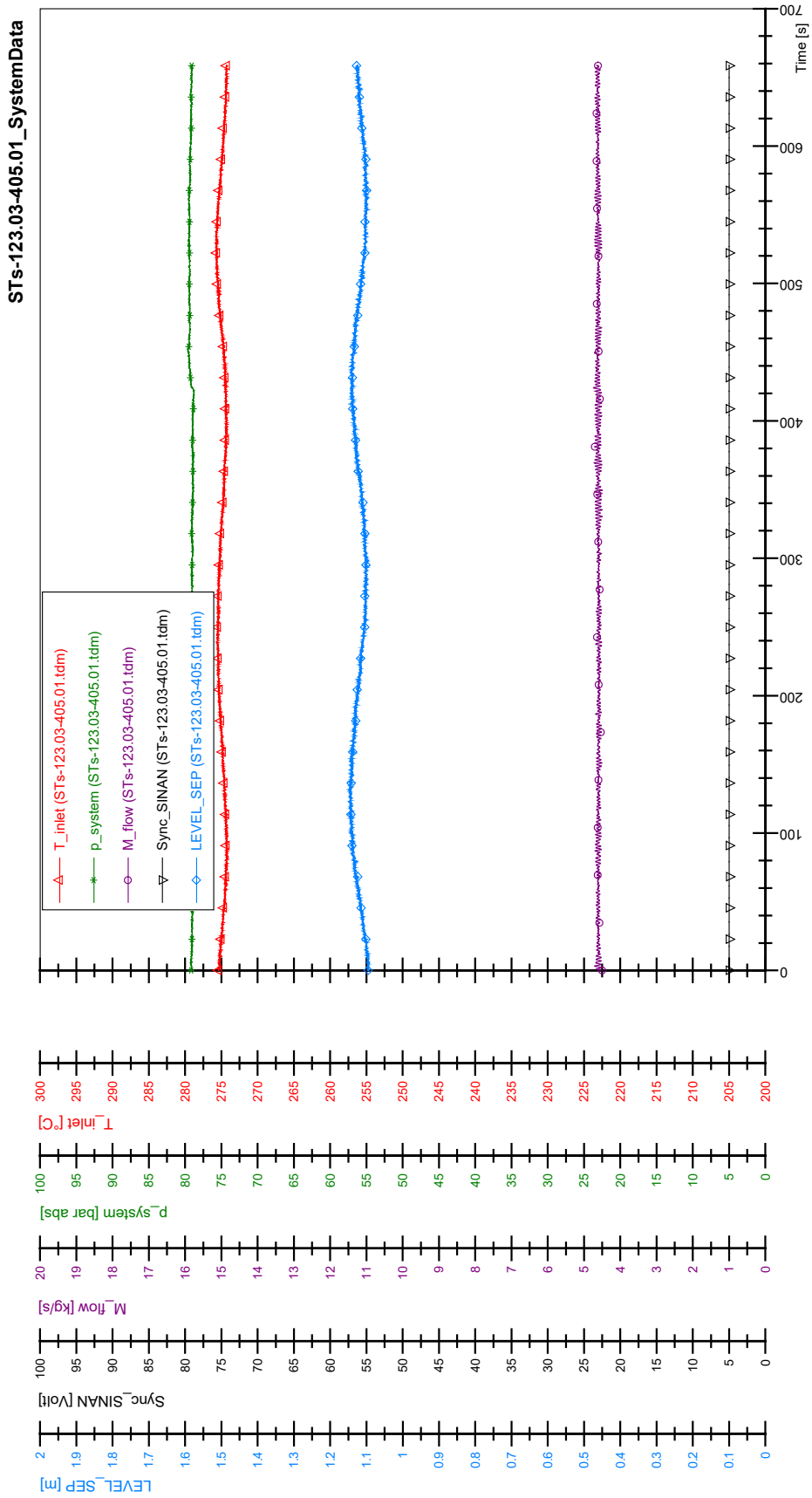
STS-123.03-404.01_Rod_87



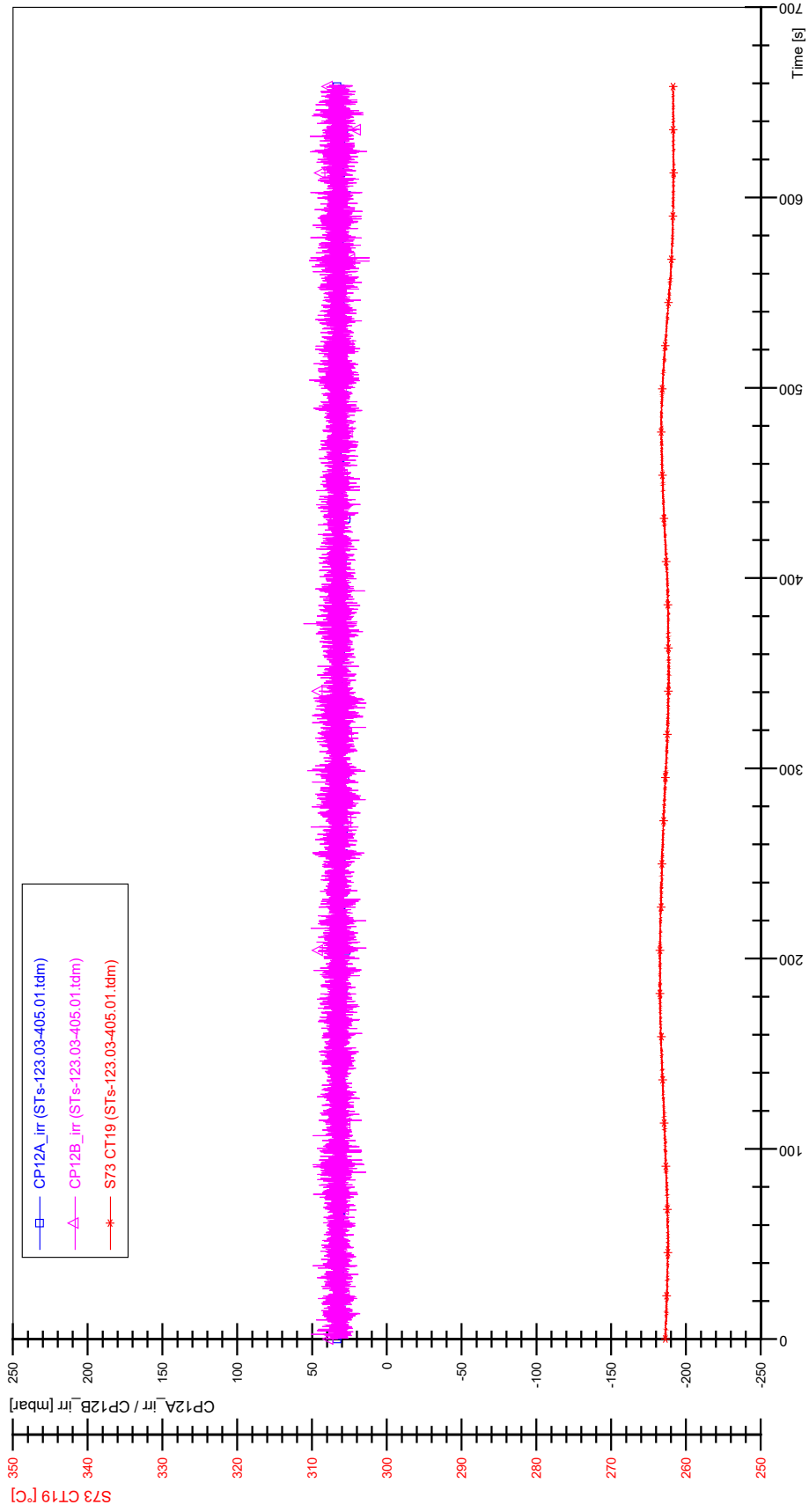
STS-123.03-404.01_Rod_88



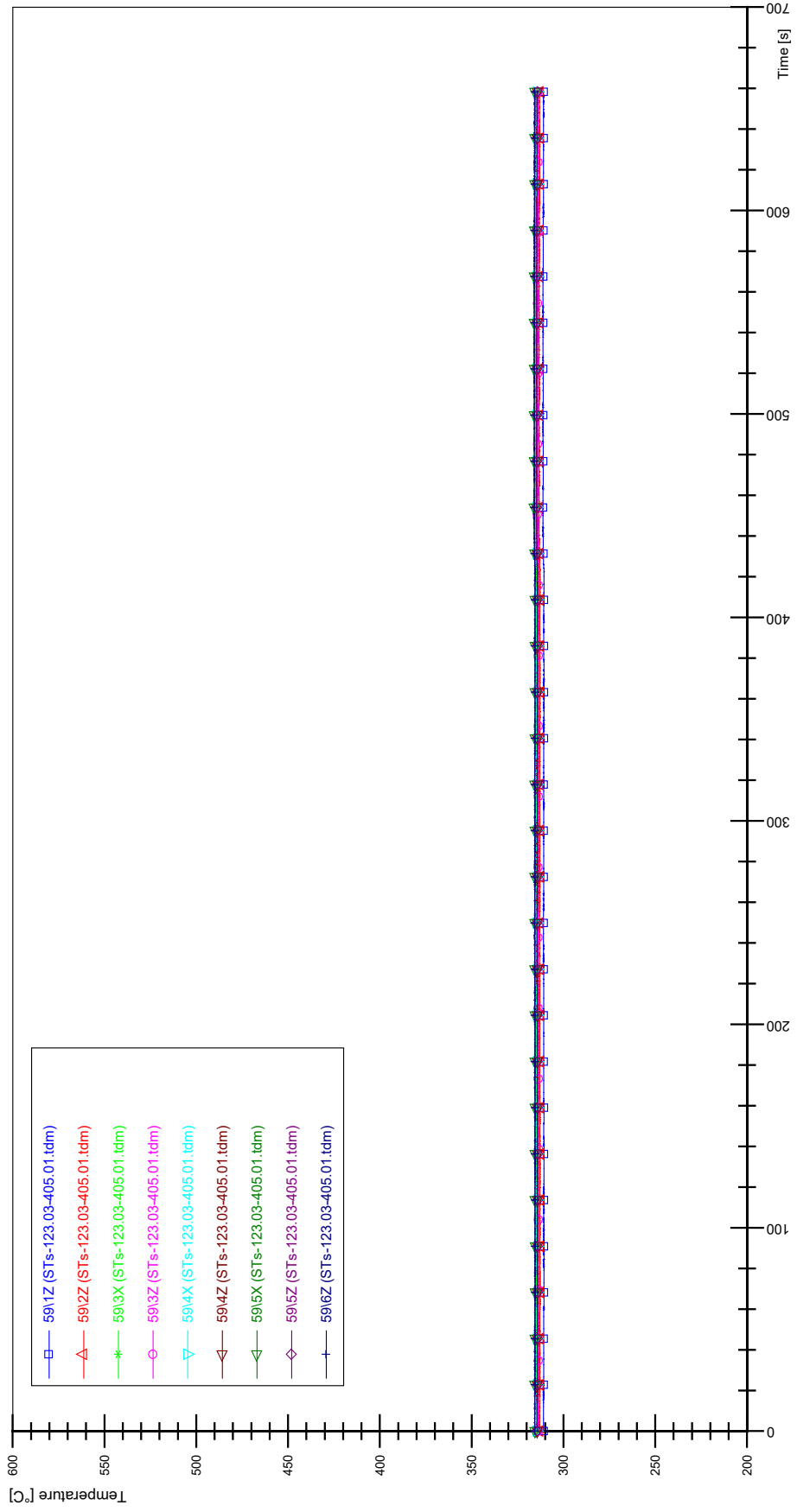
APPENDIX KK PLOTS OF INSTABILITY TEST STS-123.03-405.01



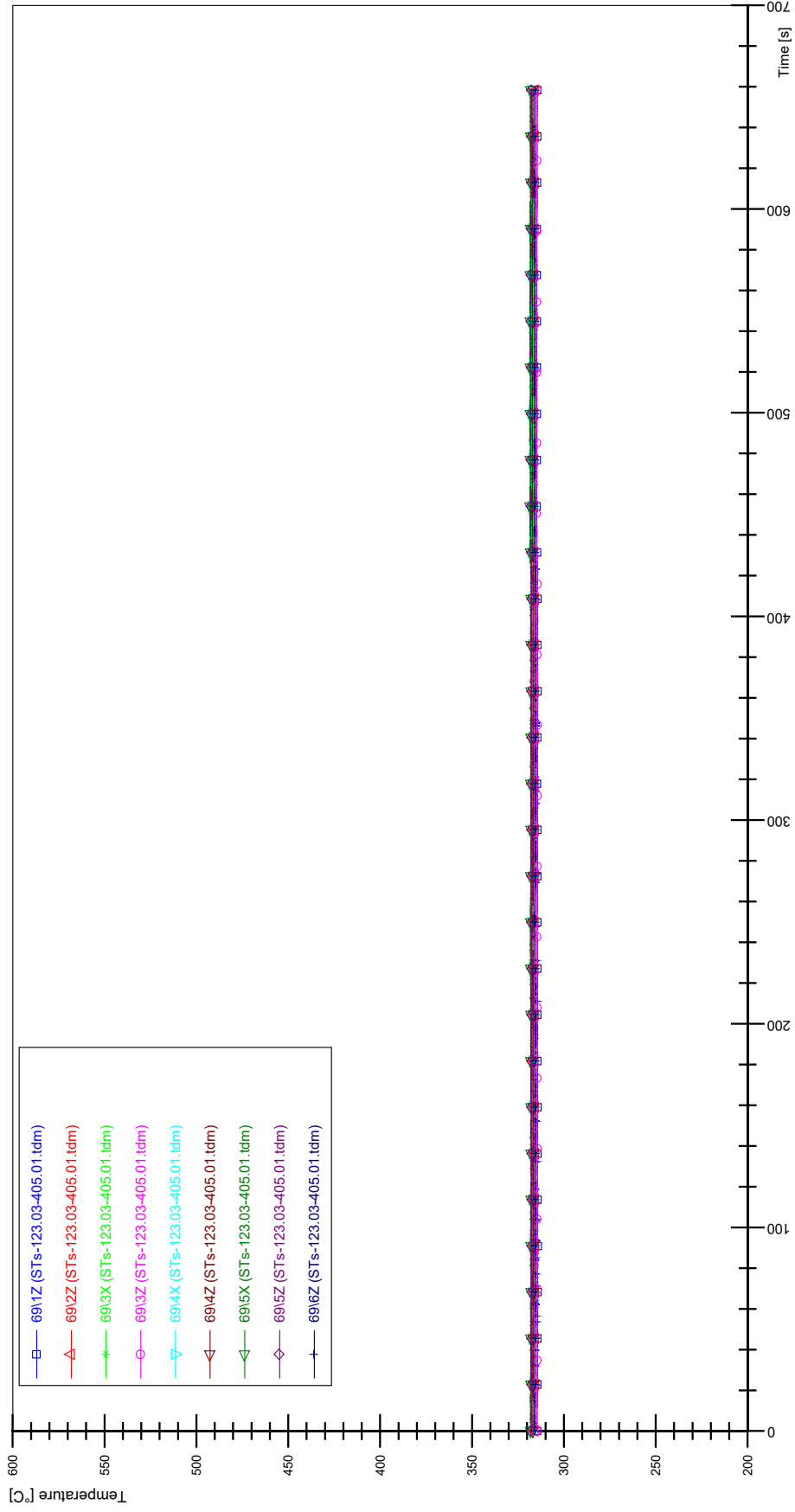
STs-123.03-405.01_CP12_CT19



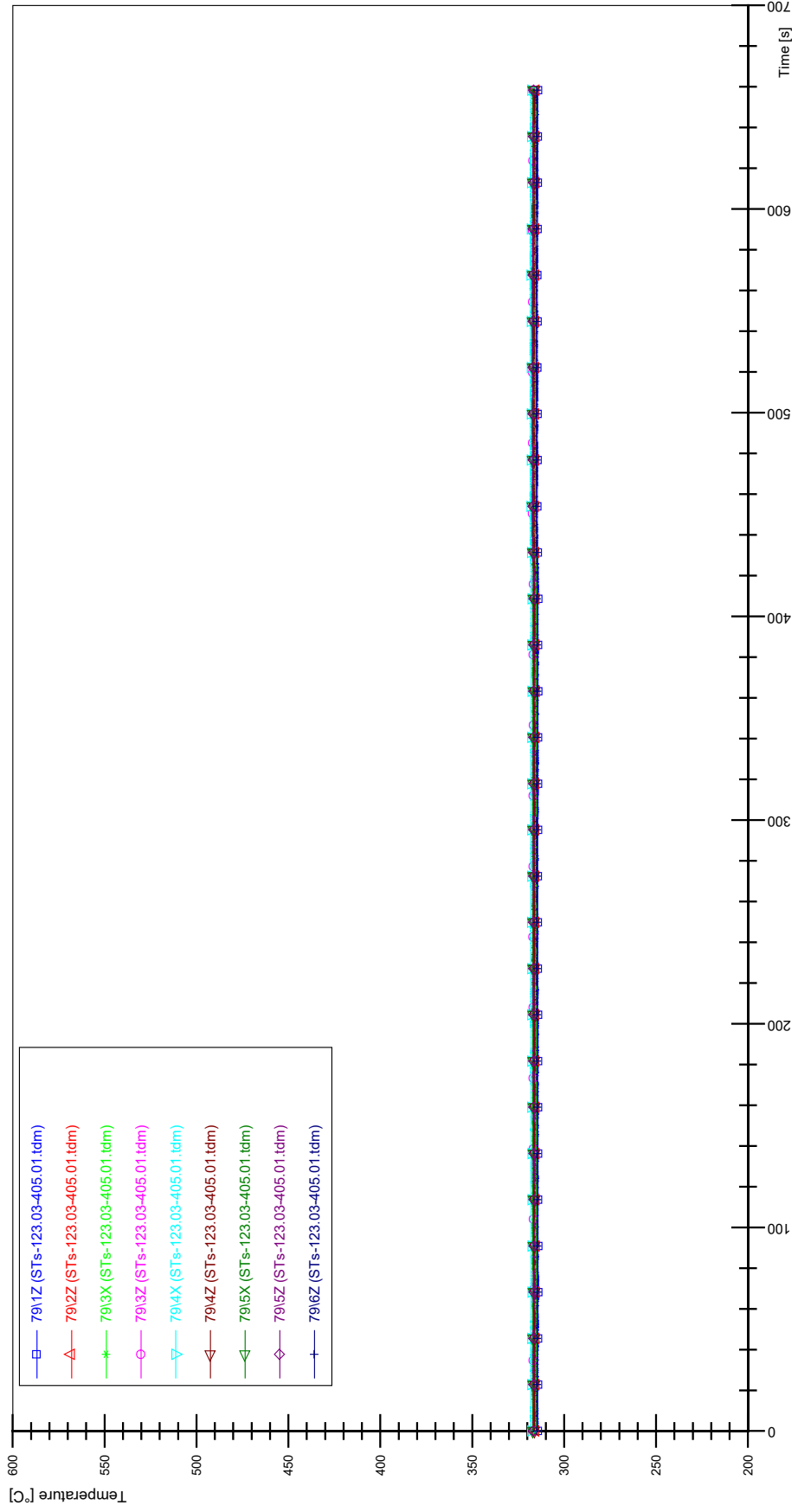
STs-123.03-405.01_Rod_59



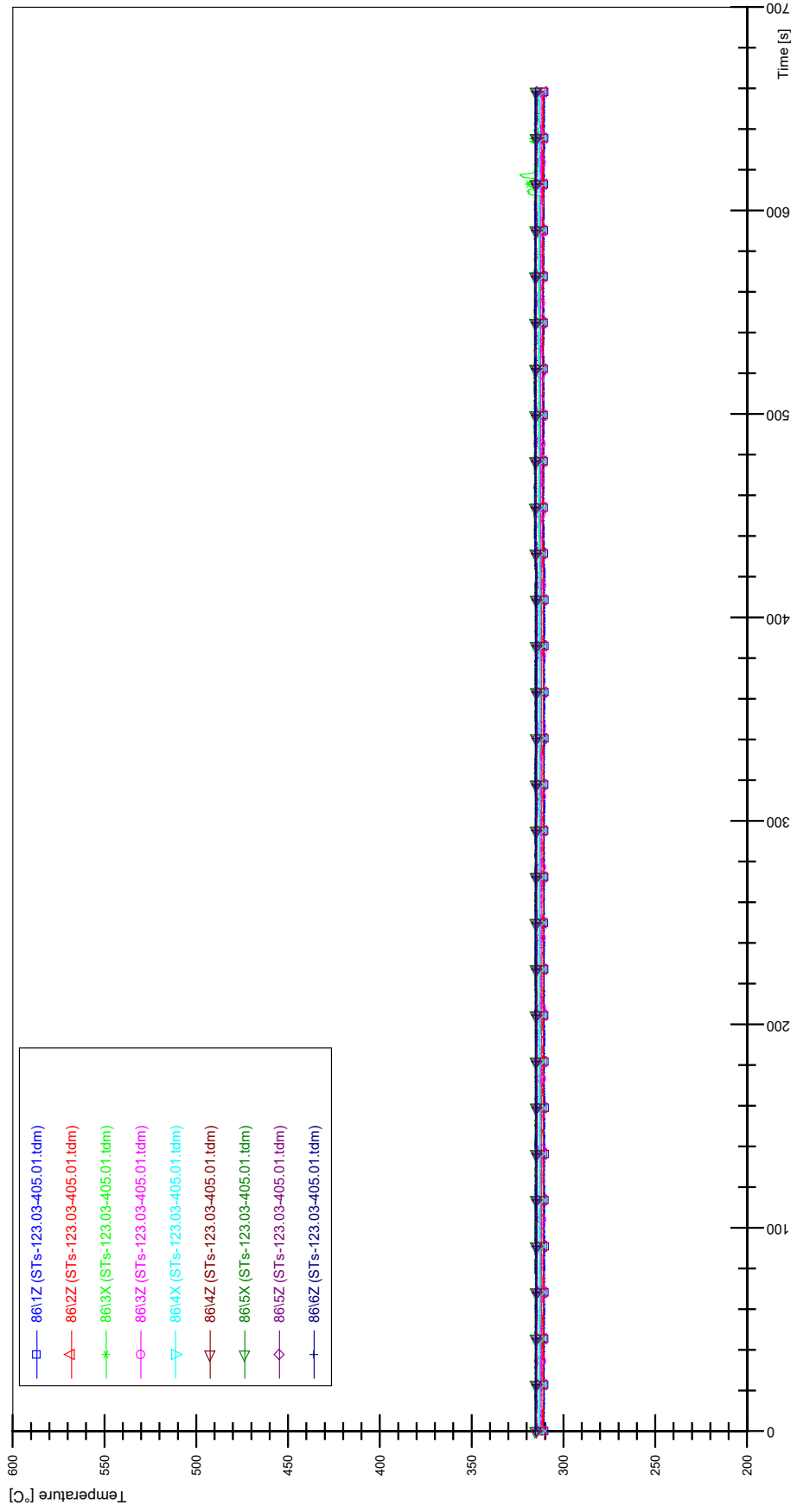
STs-123.03-405.01_Rod_69



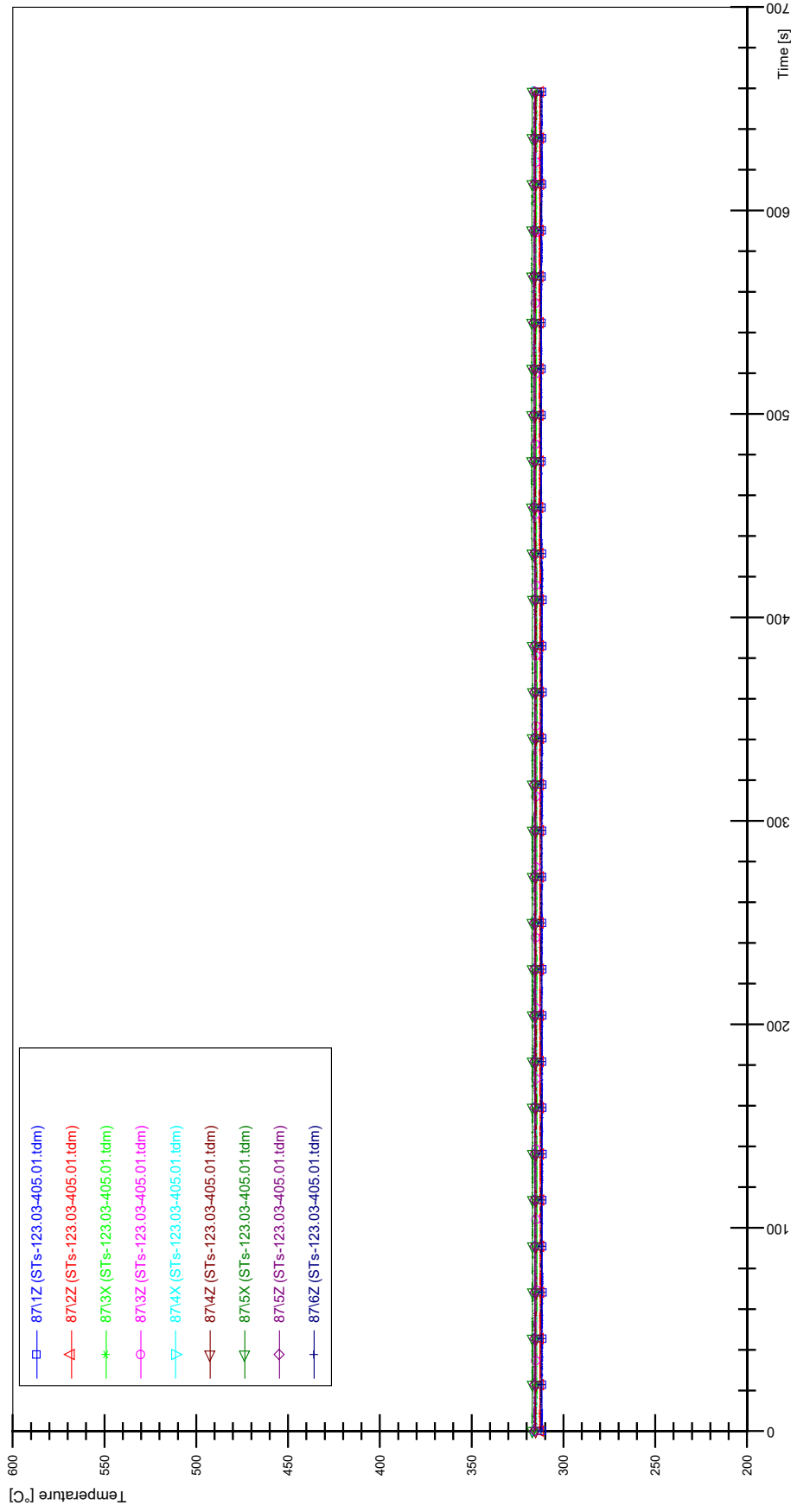
STs-123.03-405.01_Rod_79



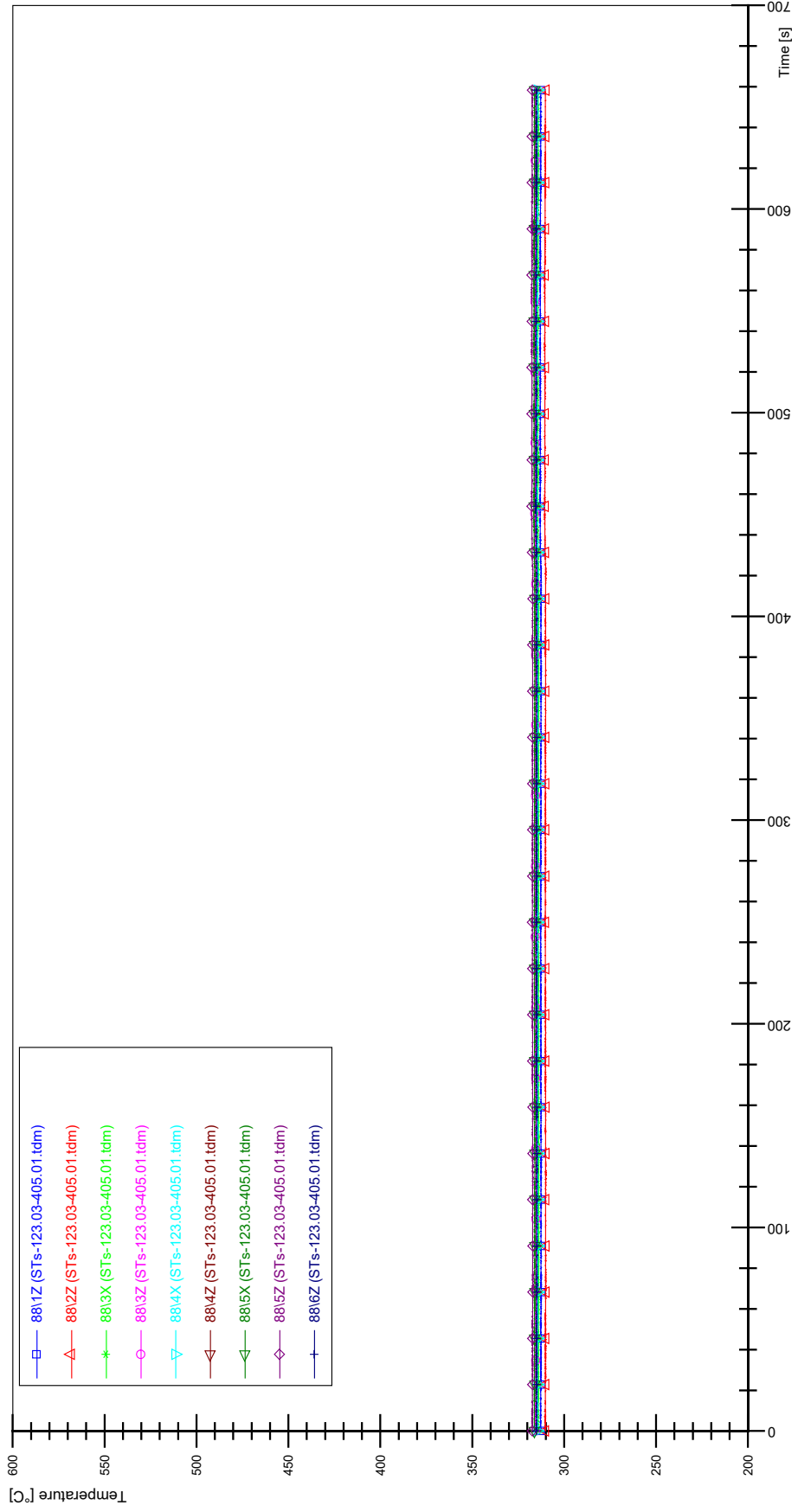
STs-123.03-405.01_Rod_86



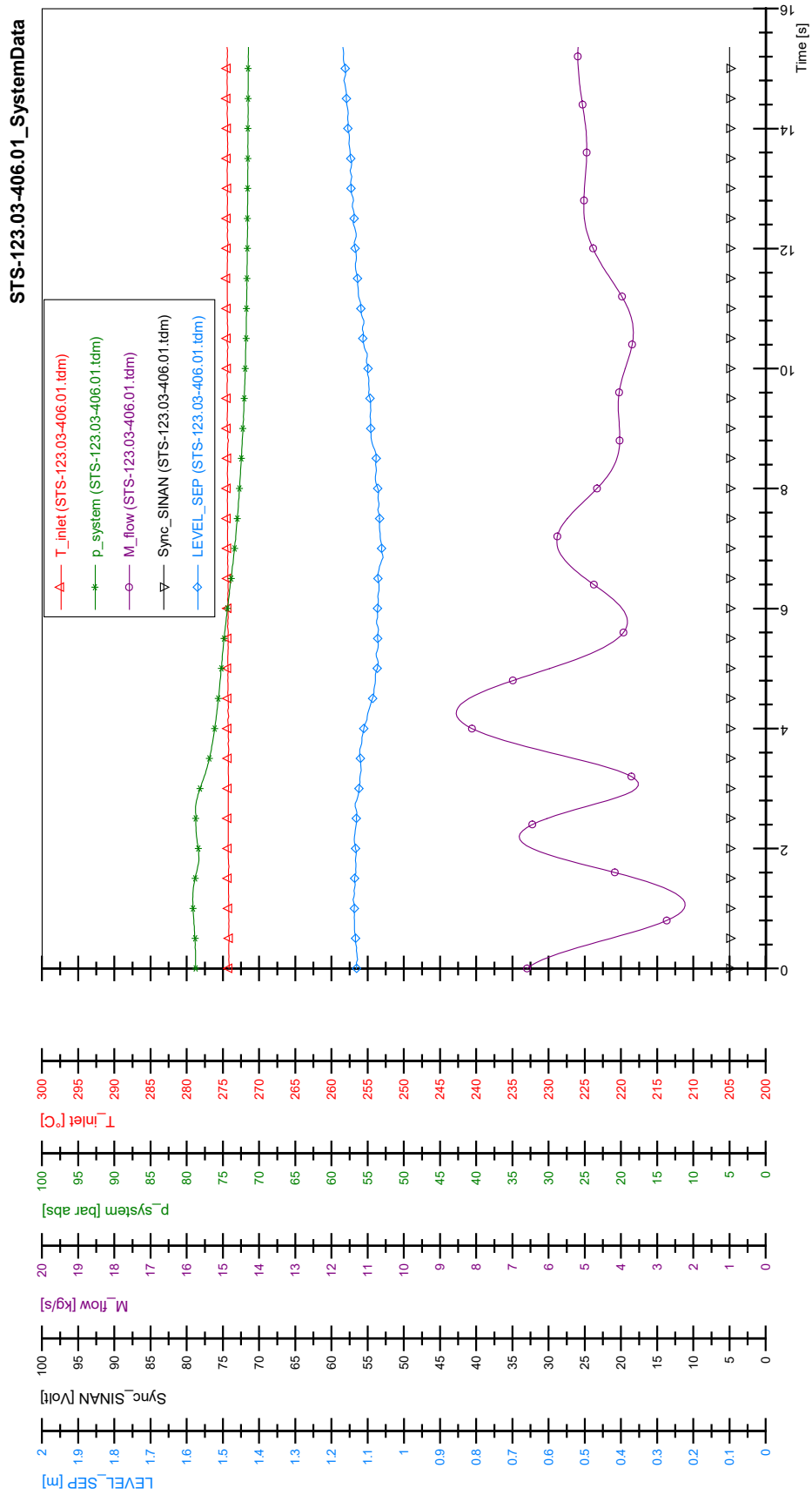
STs-123.03-405.01_Rod_87



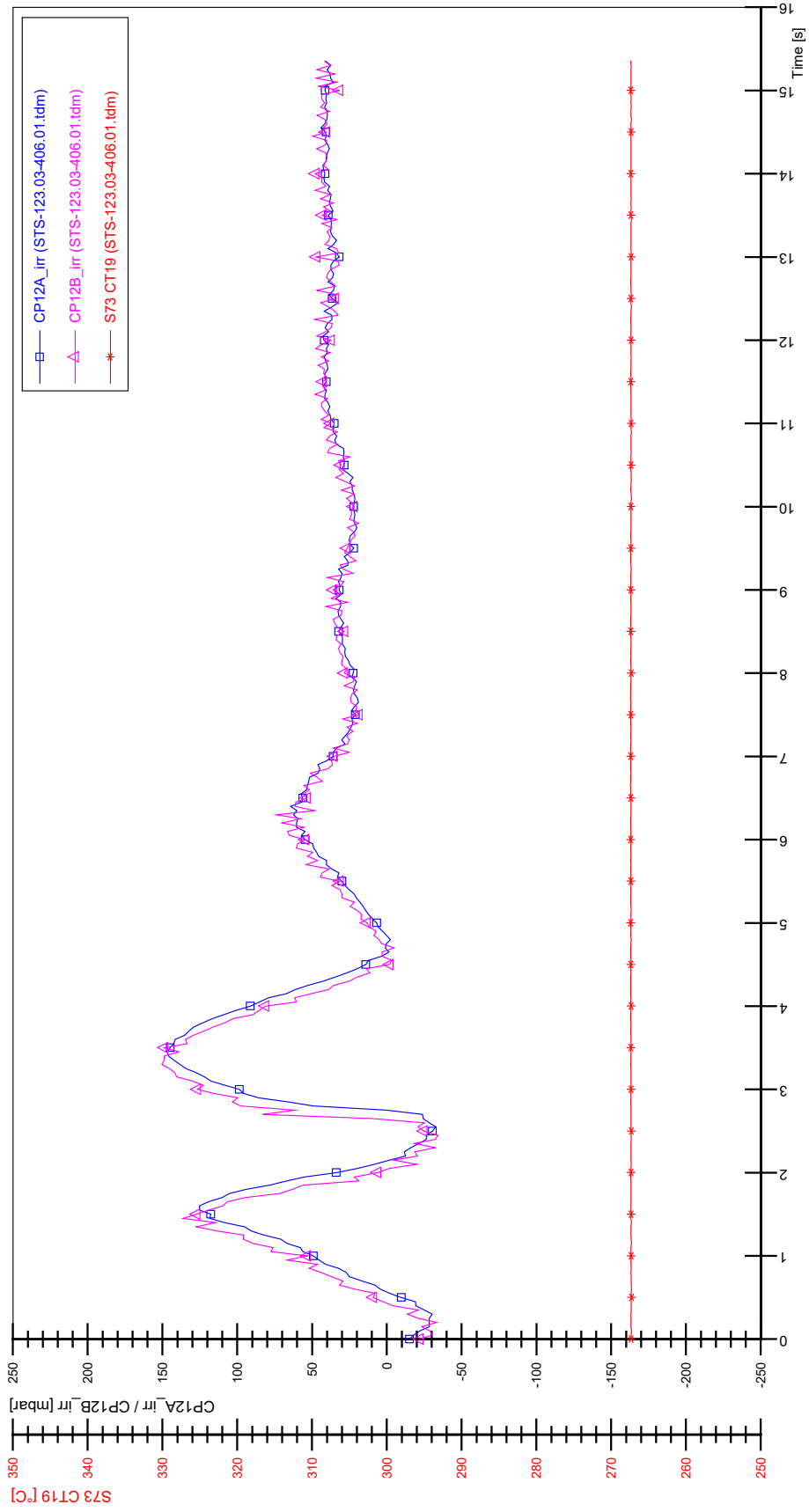
STs-123.03-405.01_Rod_88



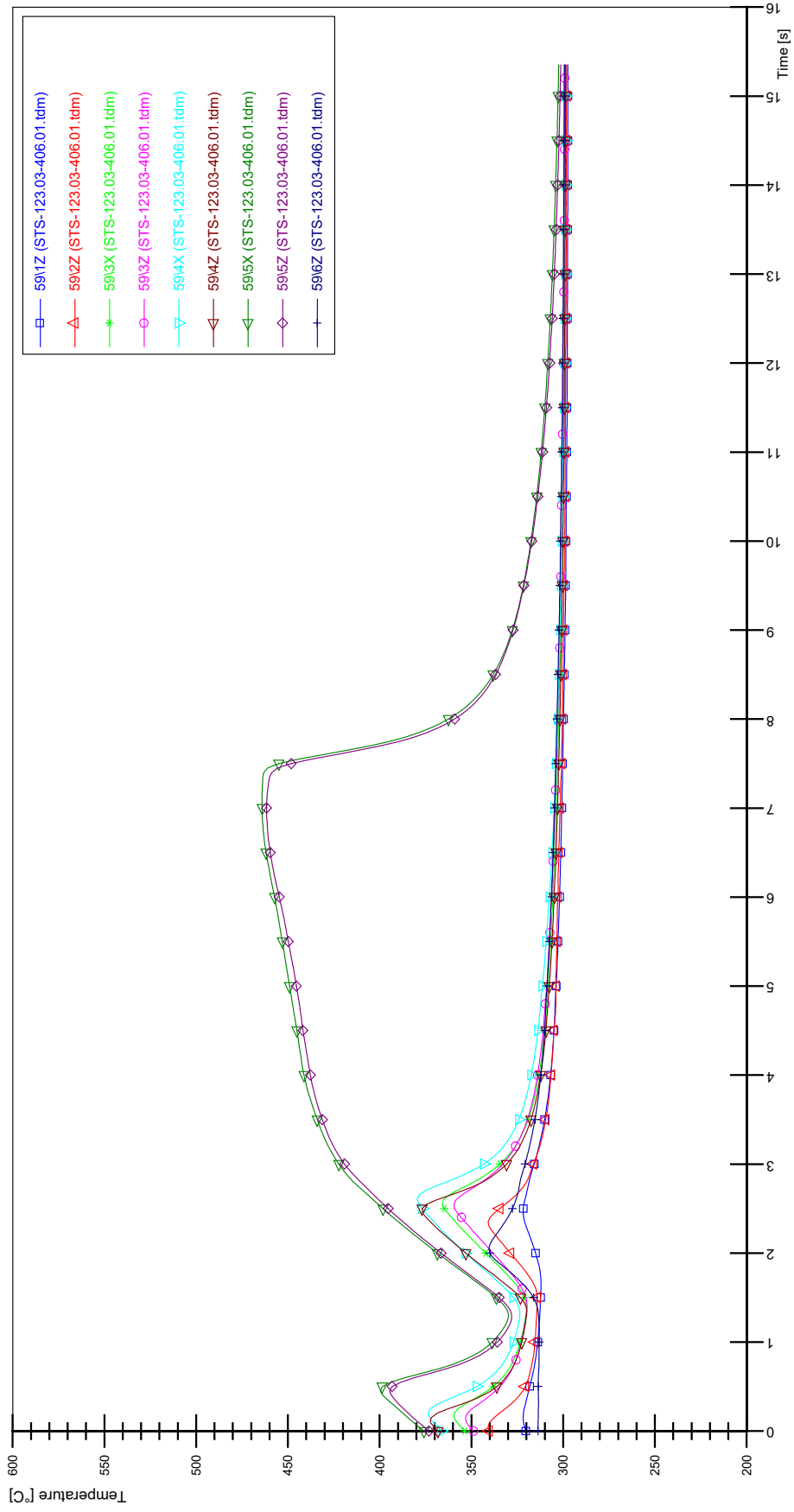
APPENDIX LL PLOTS OF INSTABILITY TEST STS-123.03-406.01



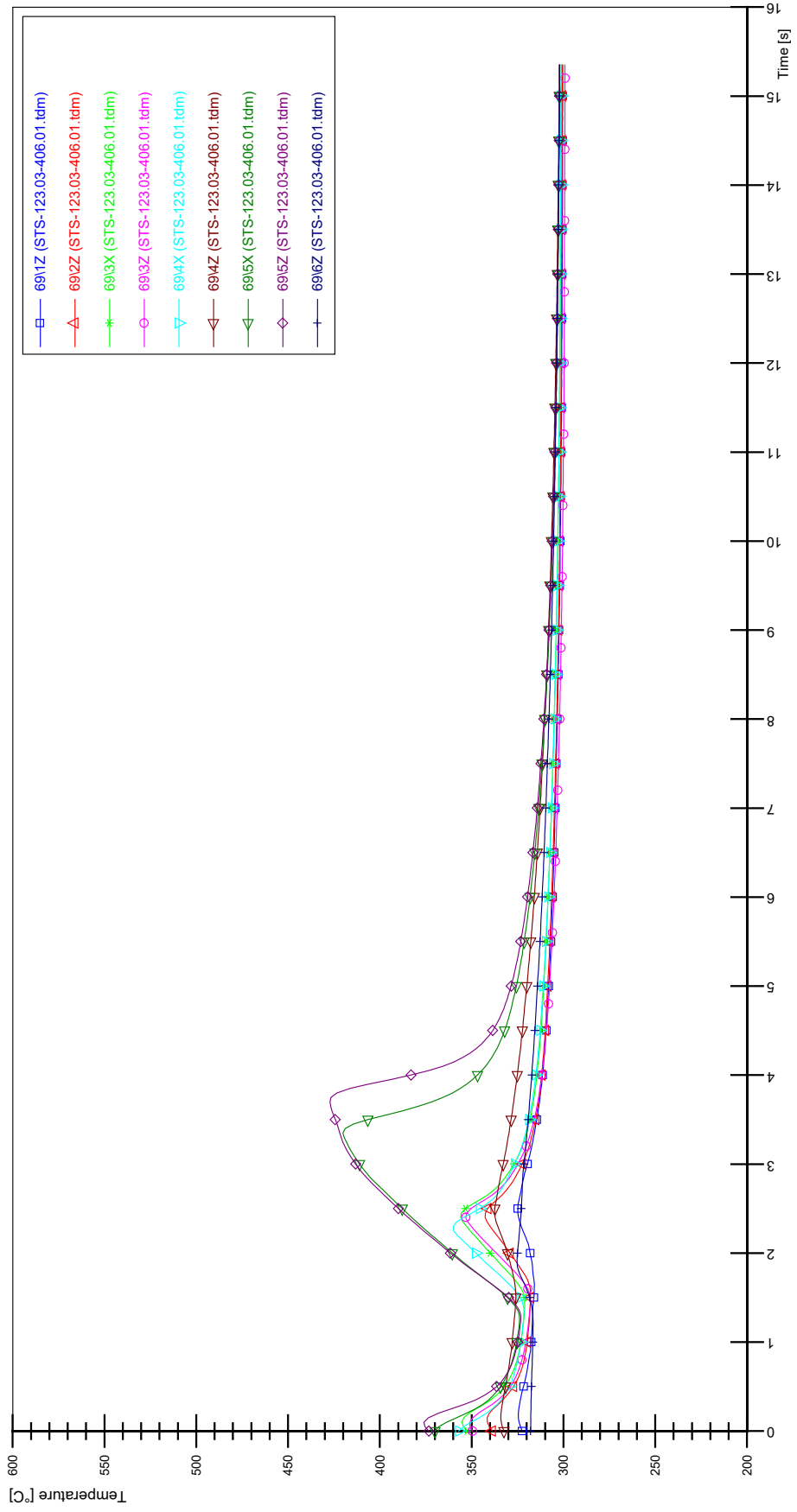
STS-123.03-406.01_CP12_CT19



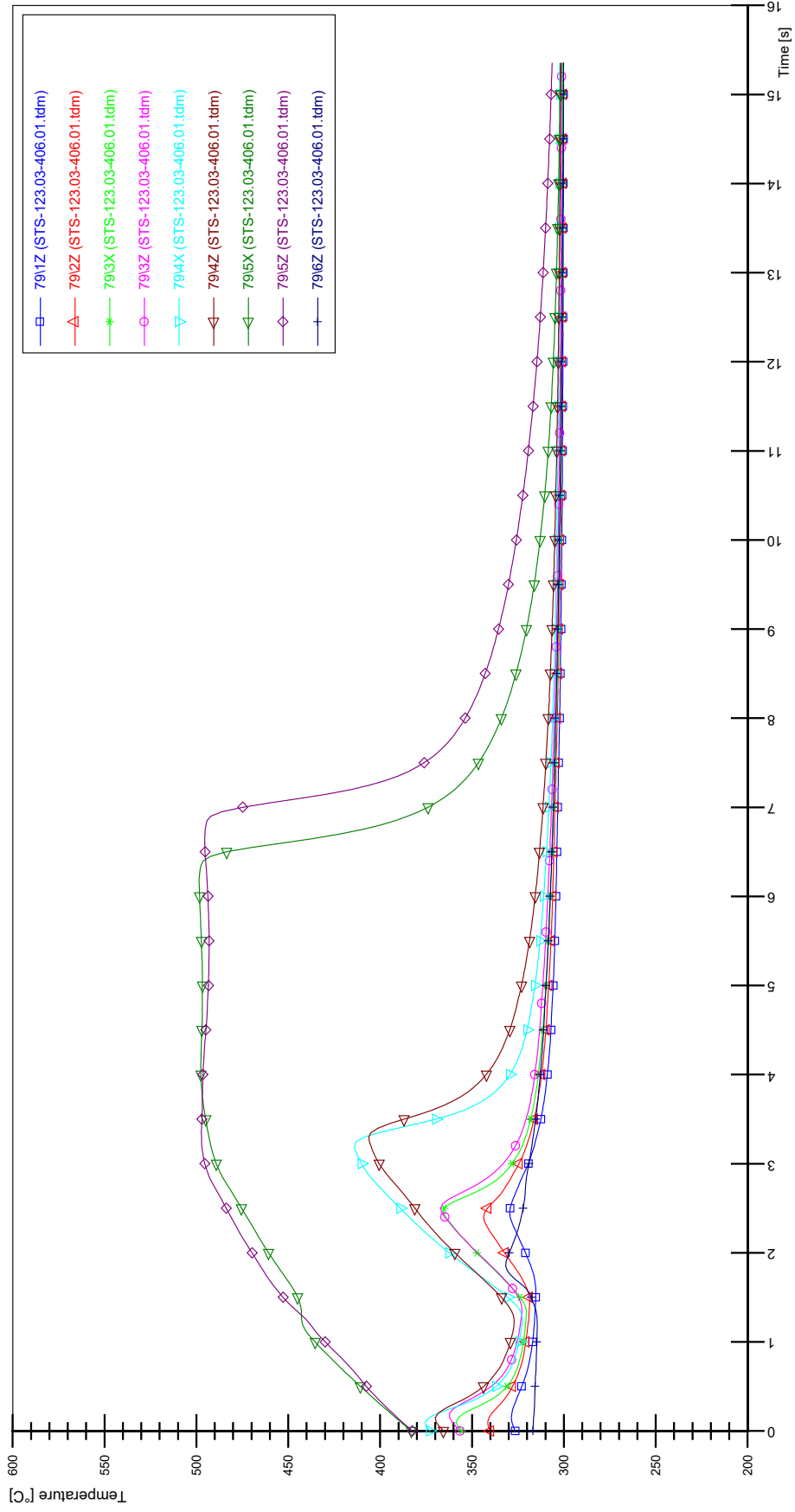
STS-123.03-406.01_Rod_59



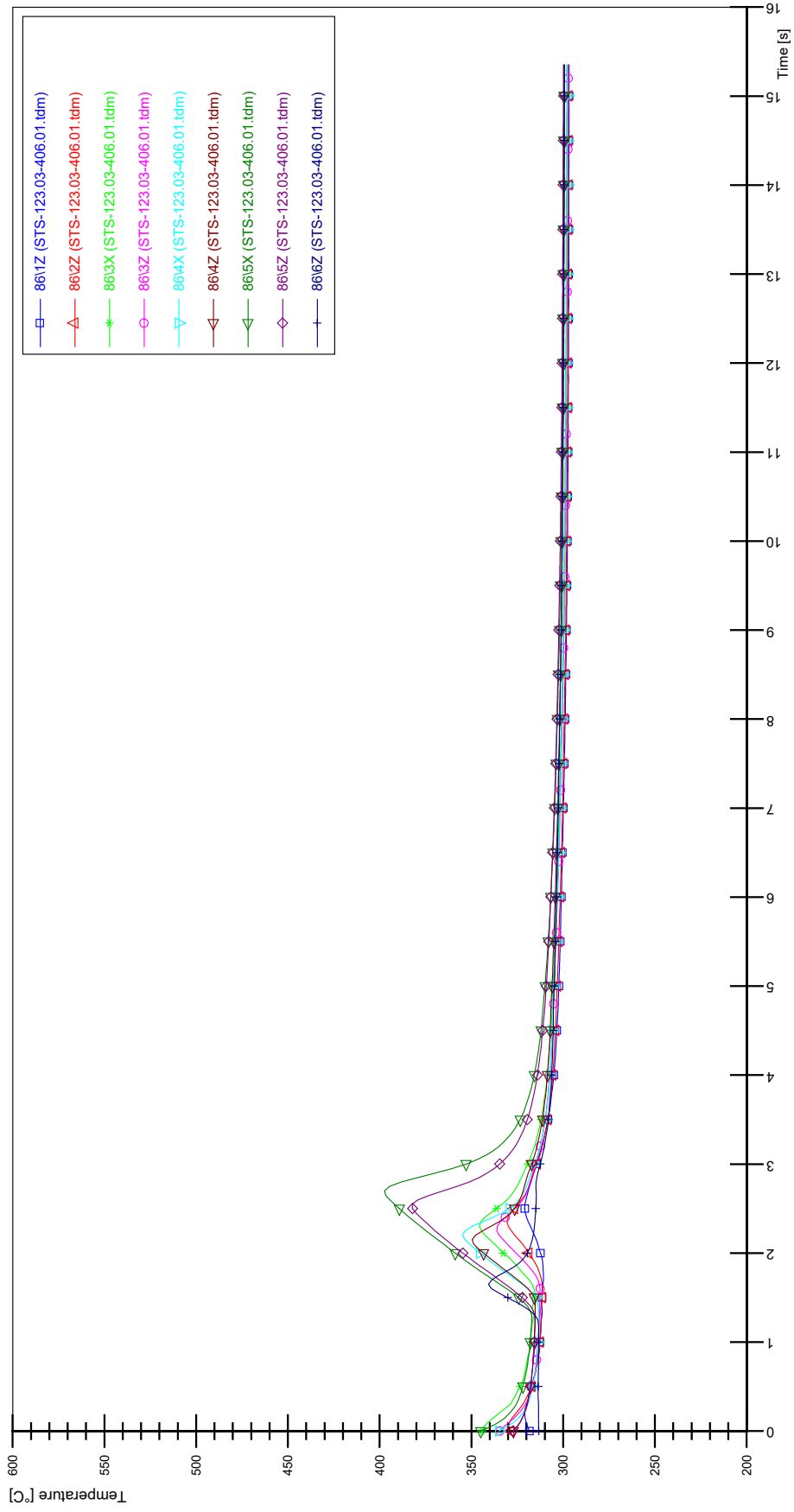
STS-123.03-406.01_Rod_69



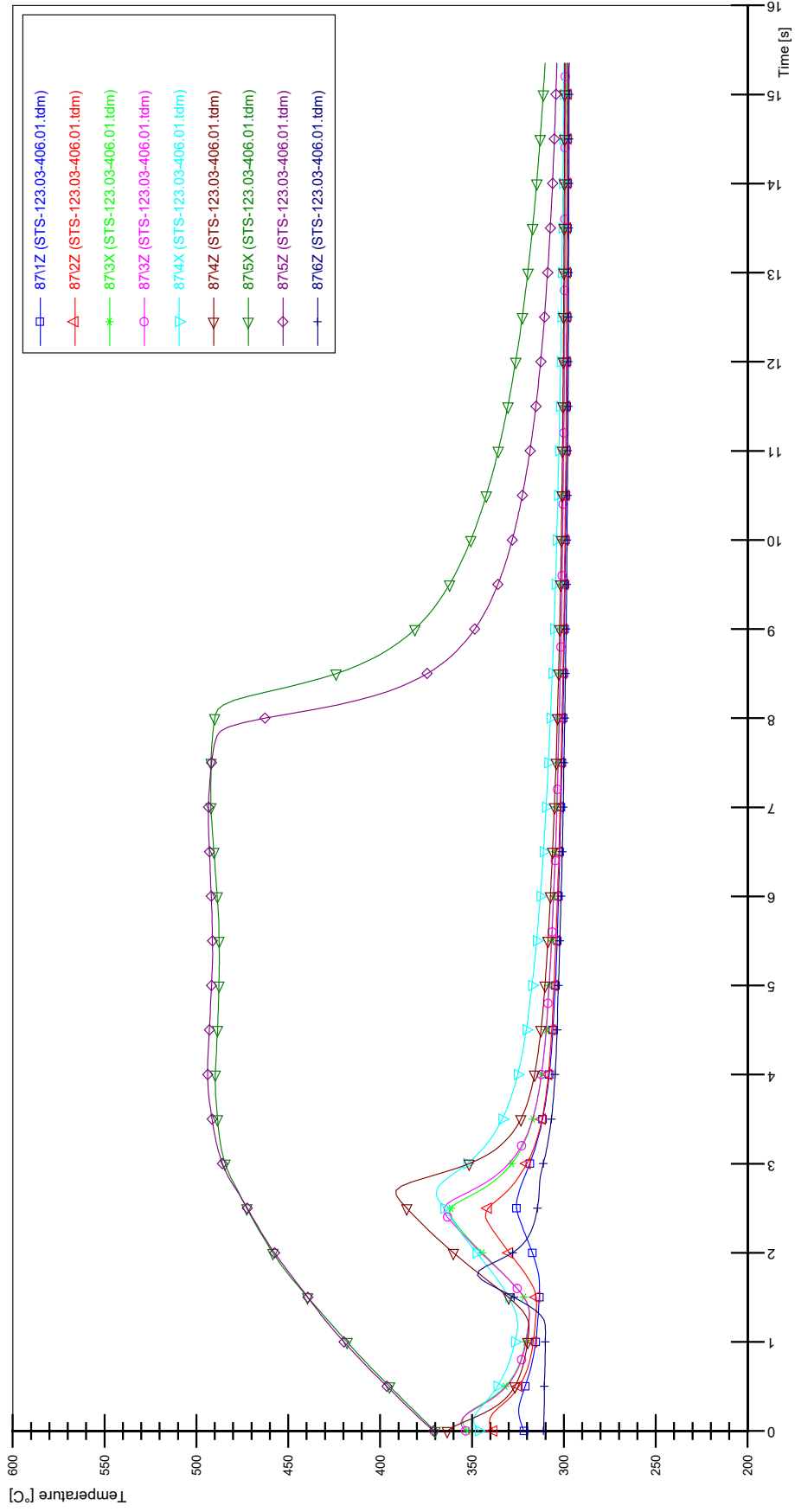
STS-123.03-406.01_Rod_79



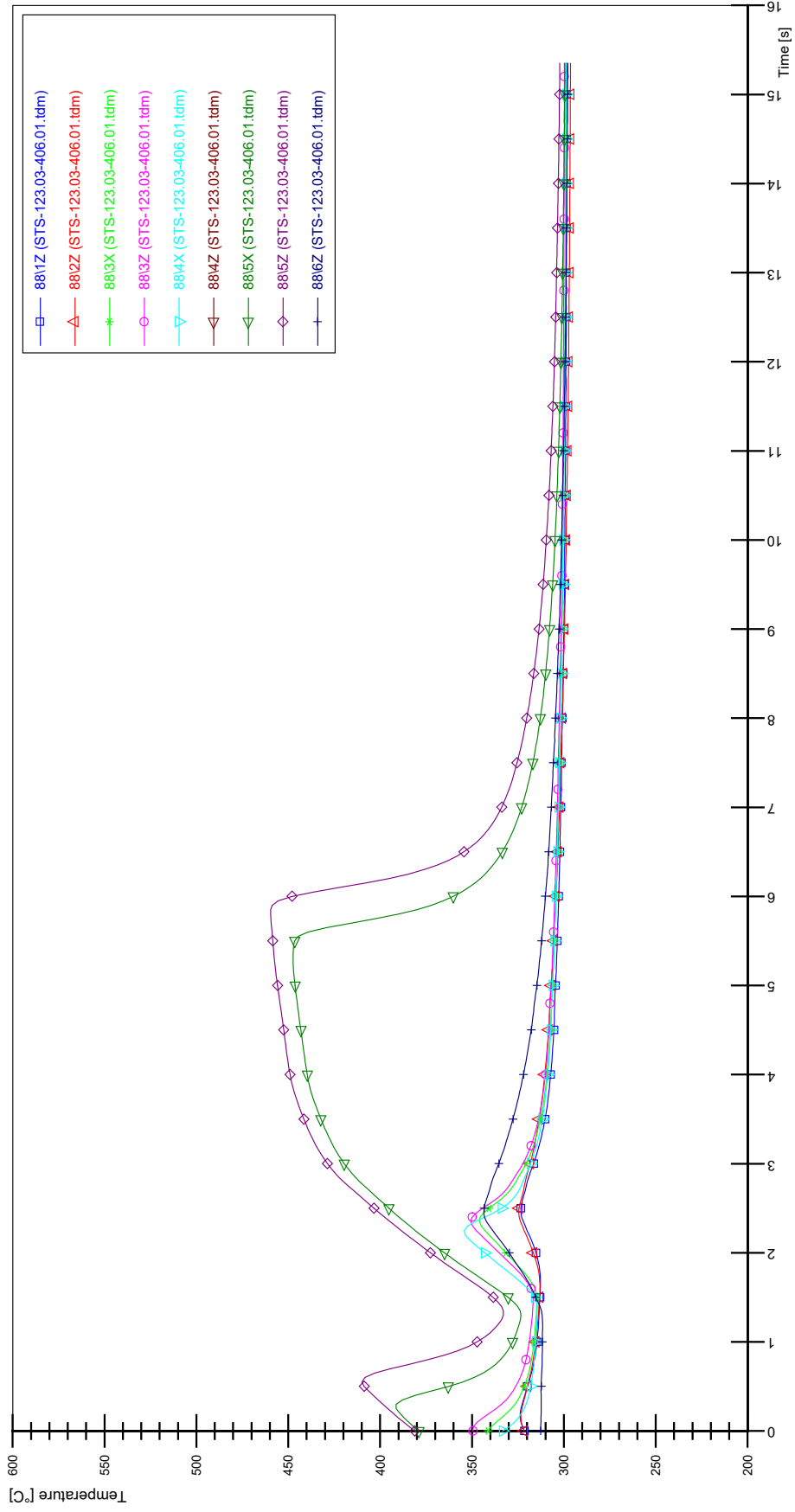
STS-123.03-406.01_Rod_86



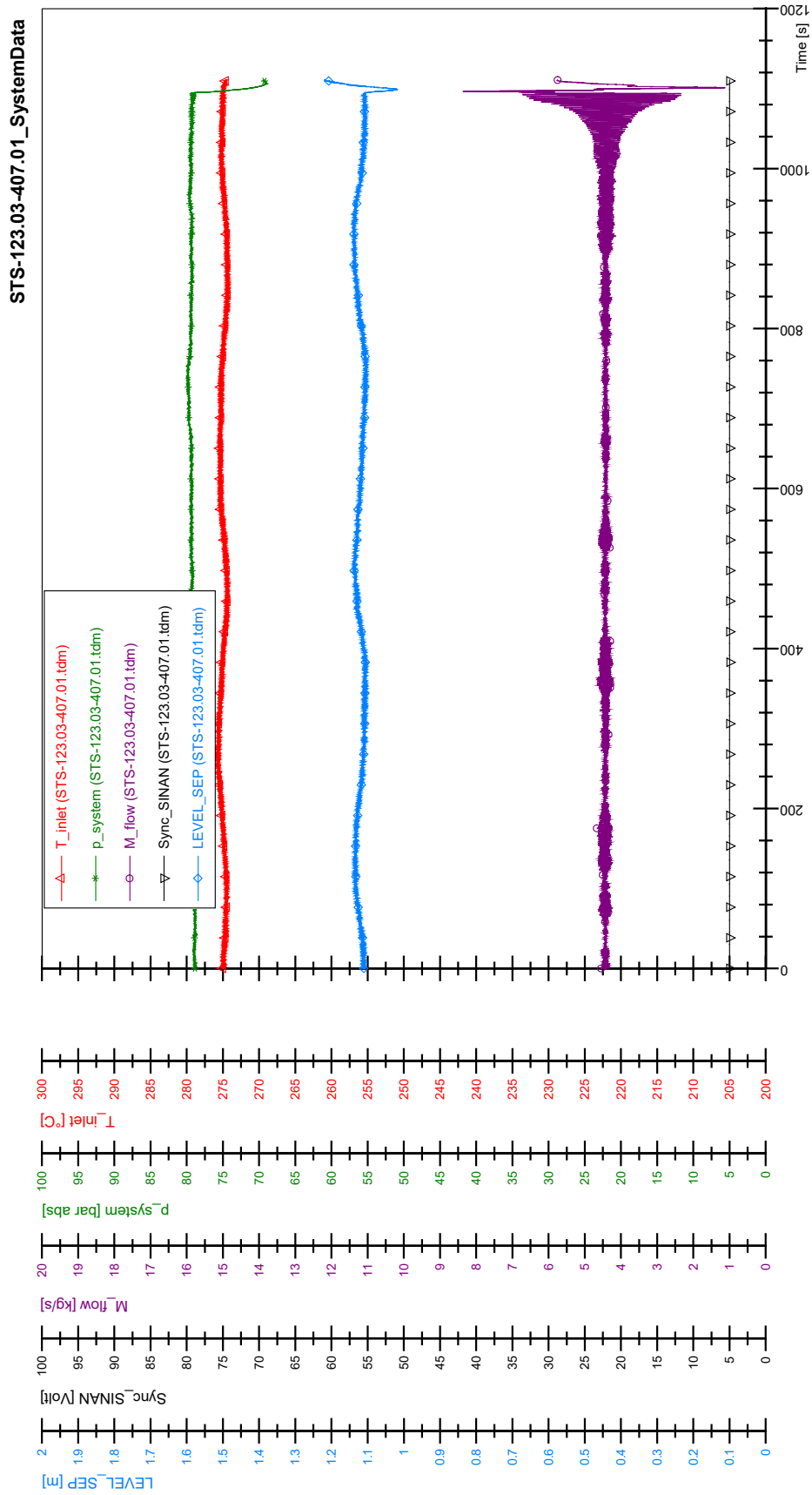
STS-123.03-406.01_Rod_87

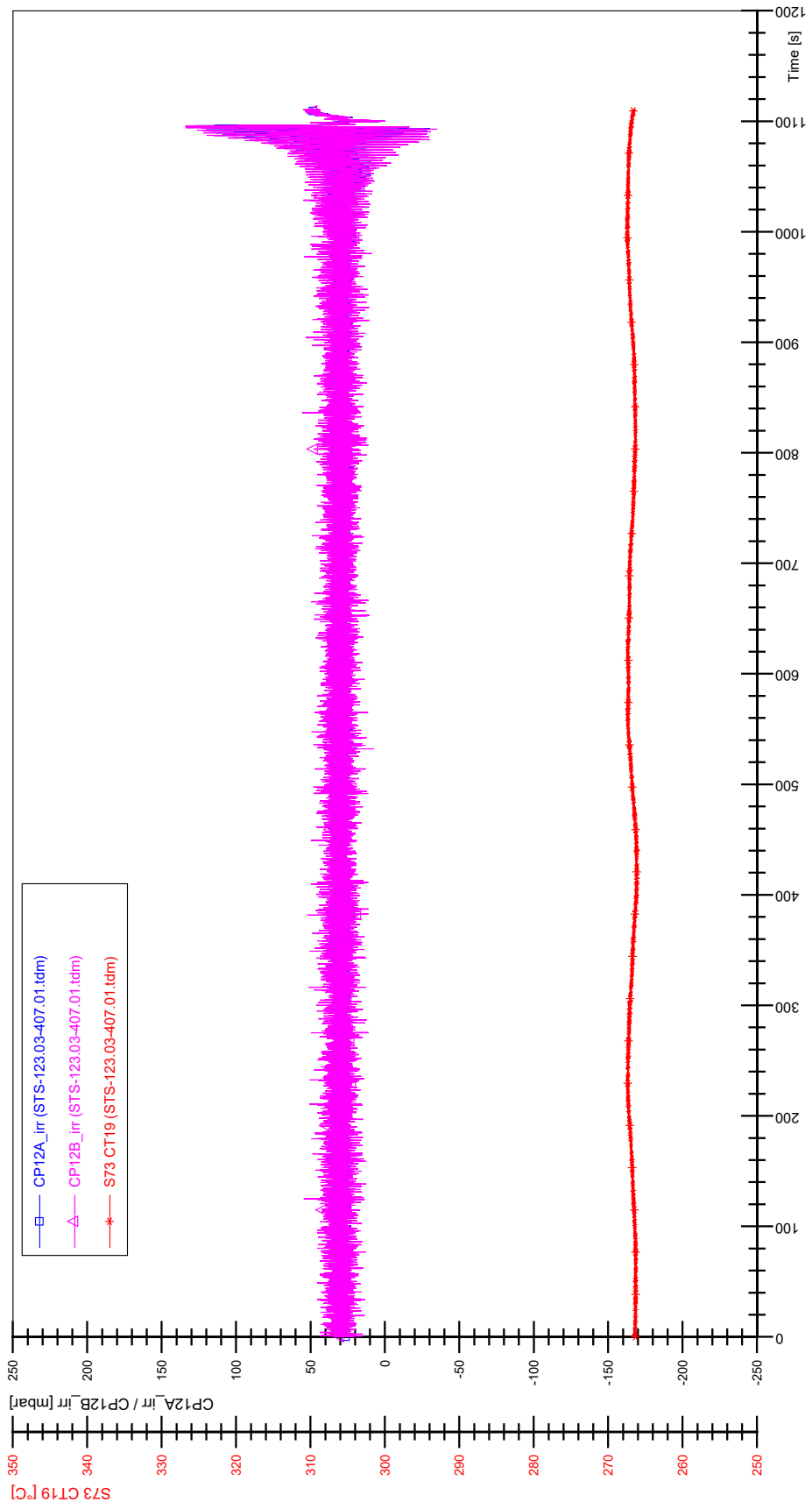


STS-123.03-406.01_Rod_88

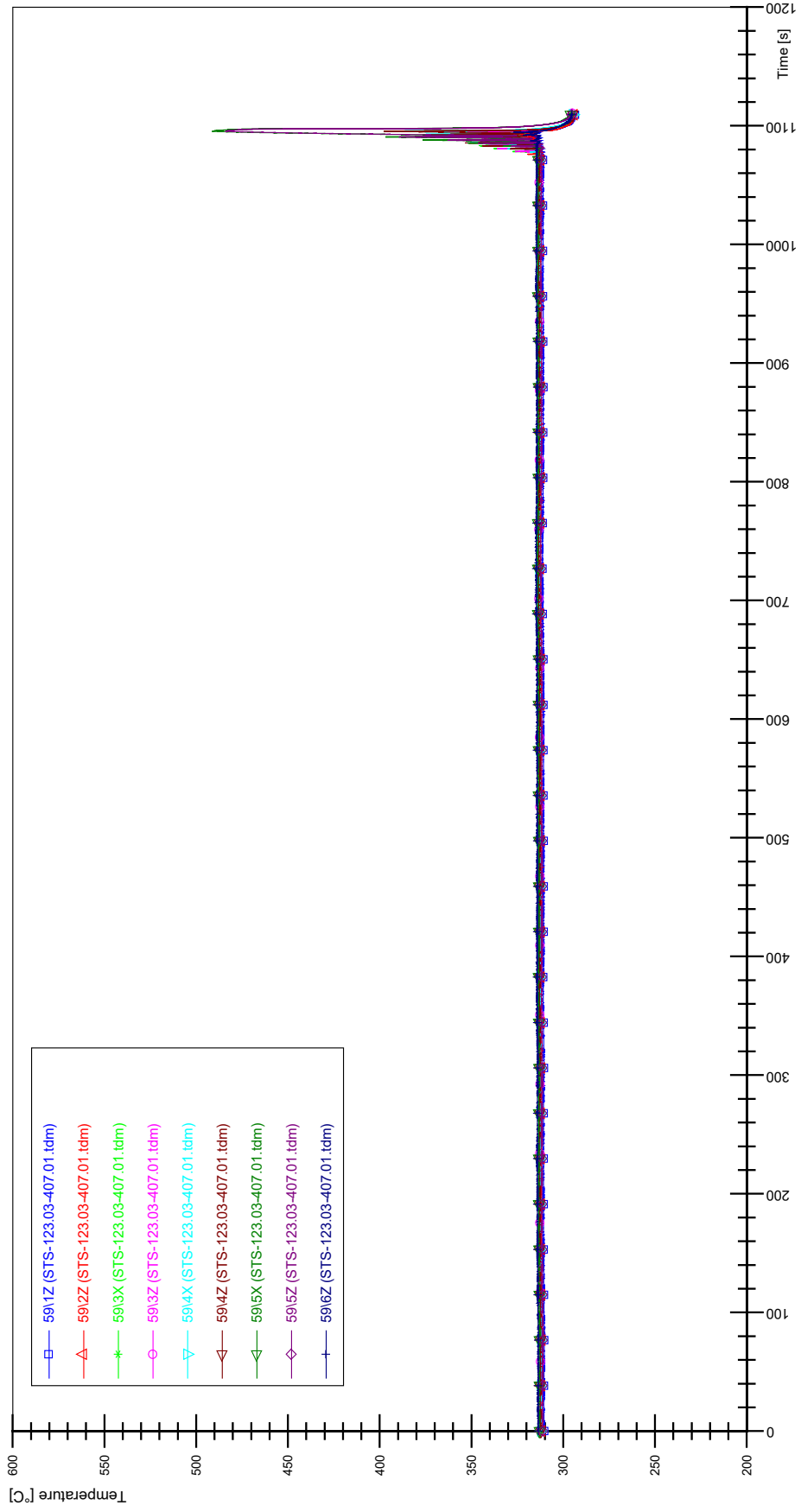


APPENDIX MM PLOTS OF INSTABILITY TEST STS-123.03-407.01

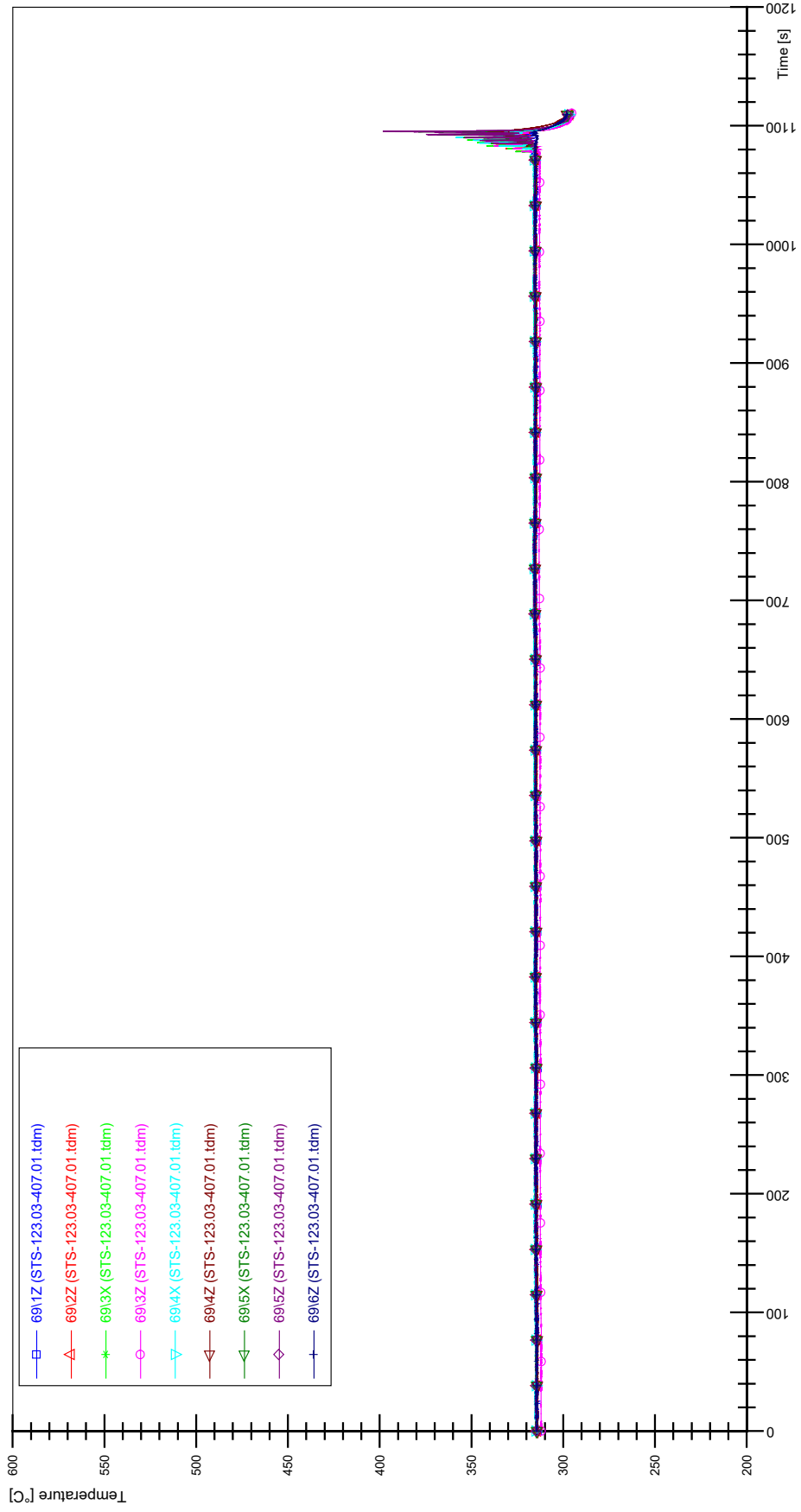




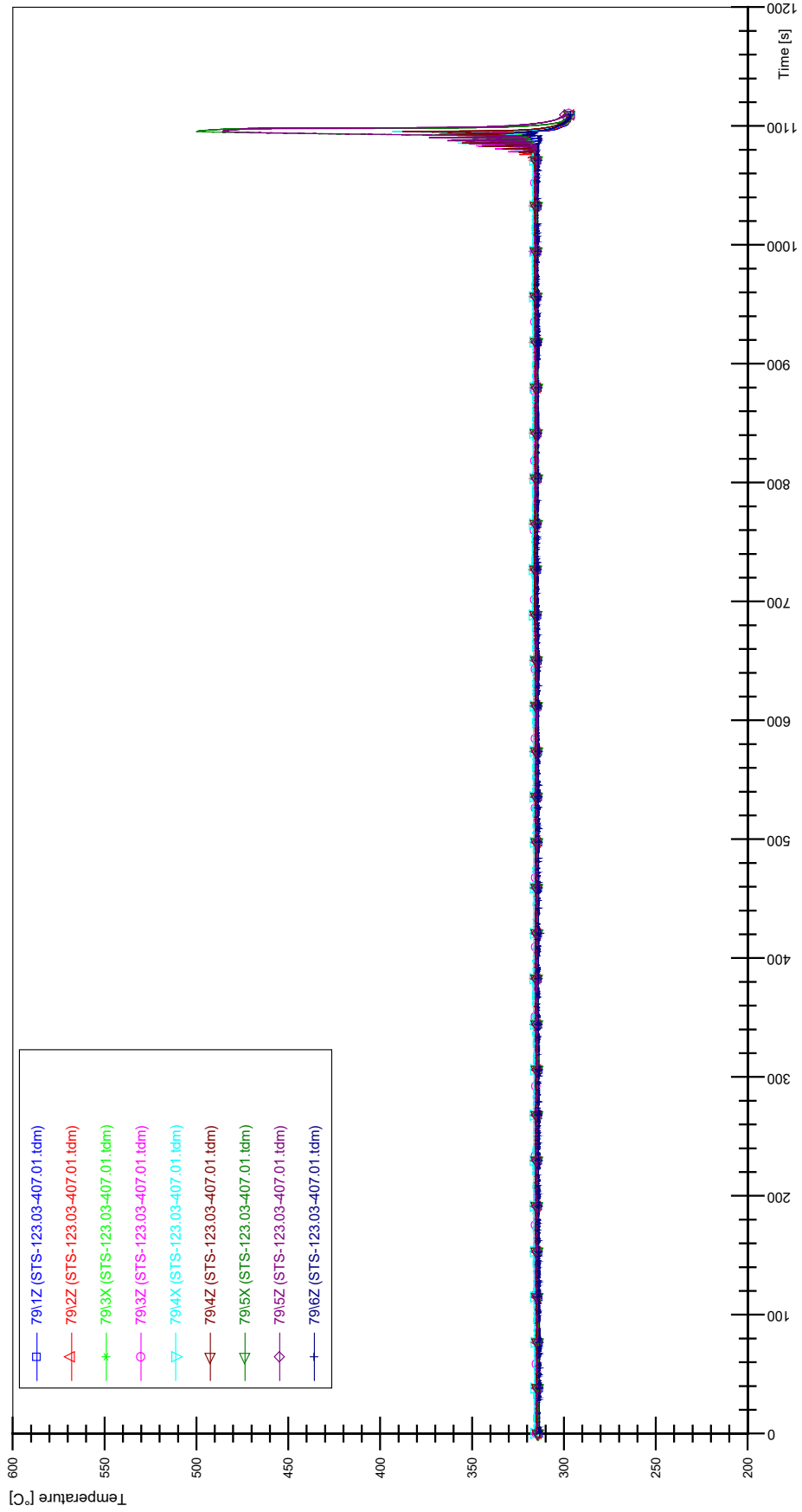
STS-123.03-407.01_Rod_59



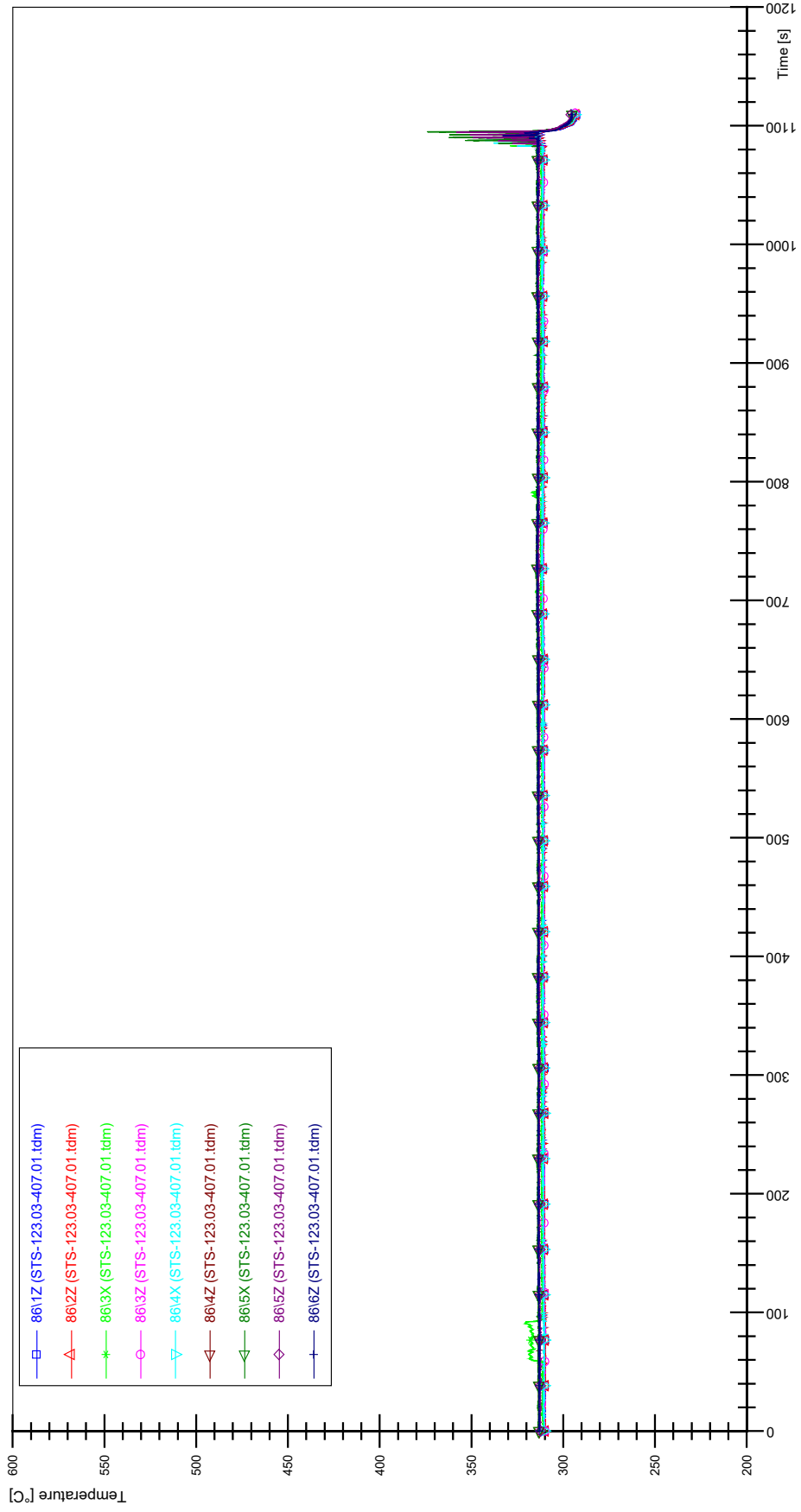
STS-123.03-407.01_Rod_69



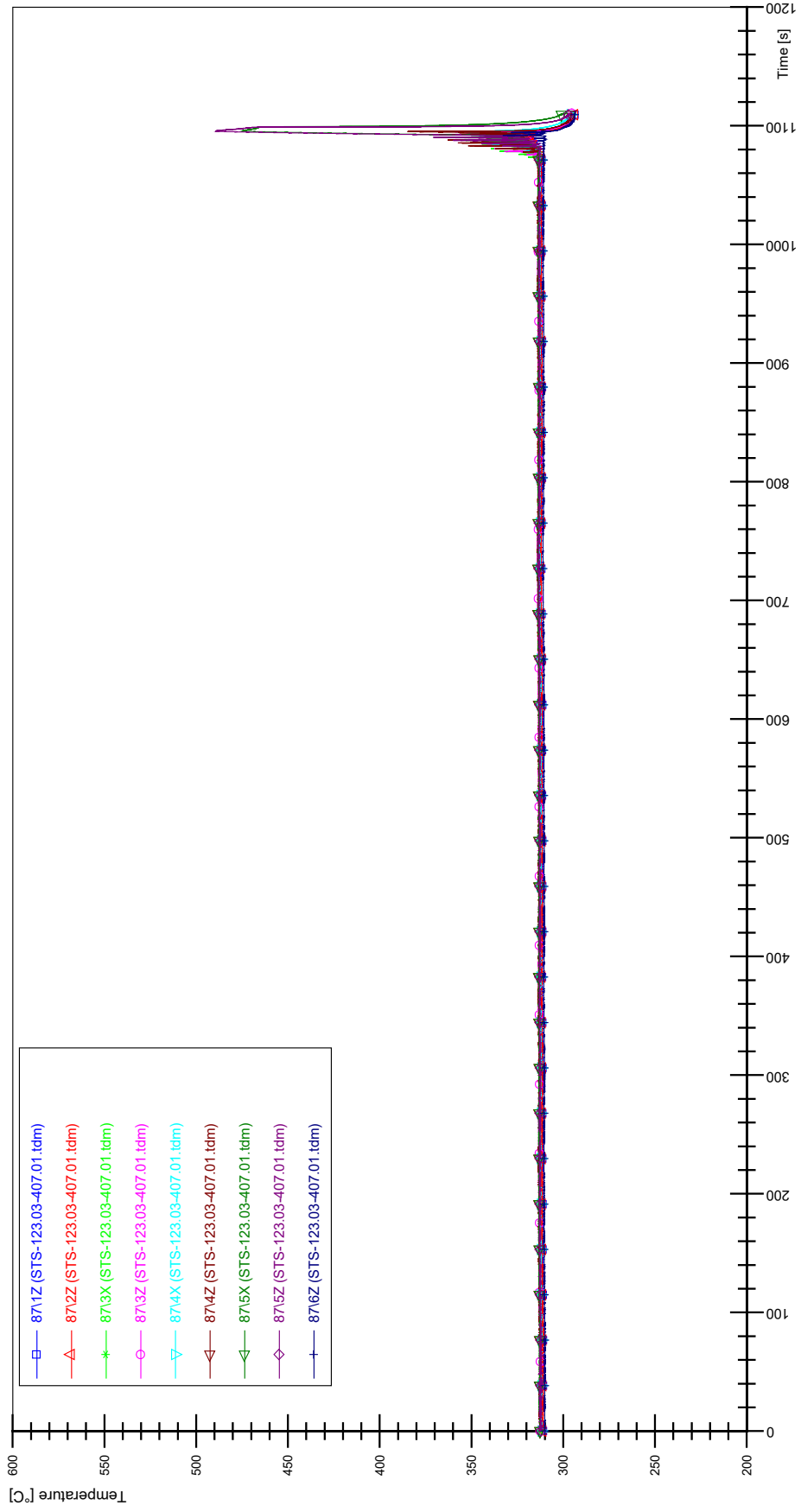
STS-123.03-407.01_Rod_79



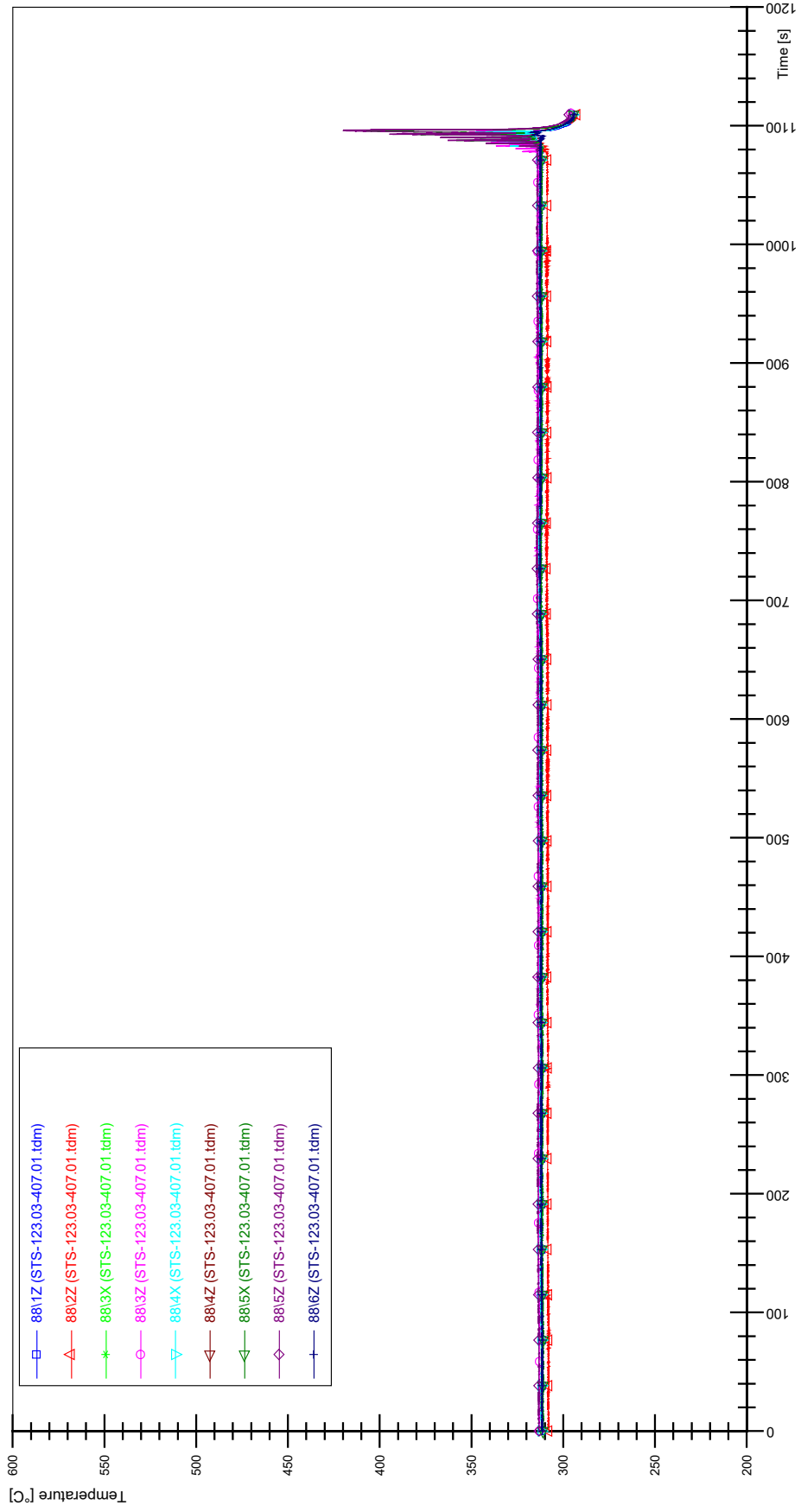
STS-123.03-407.01_Rod_86



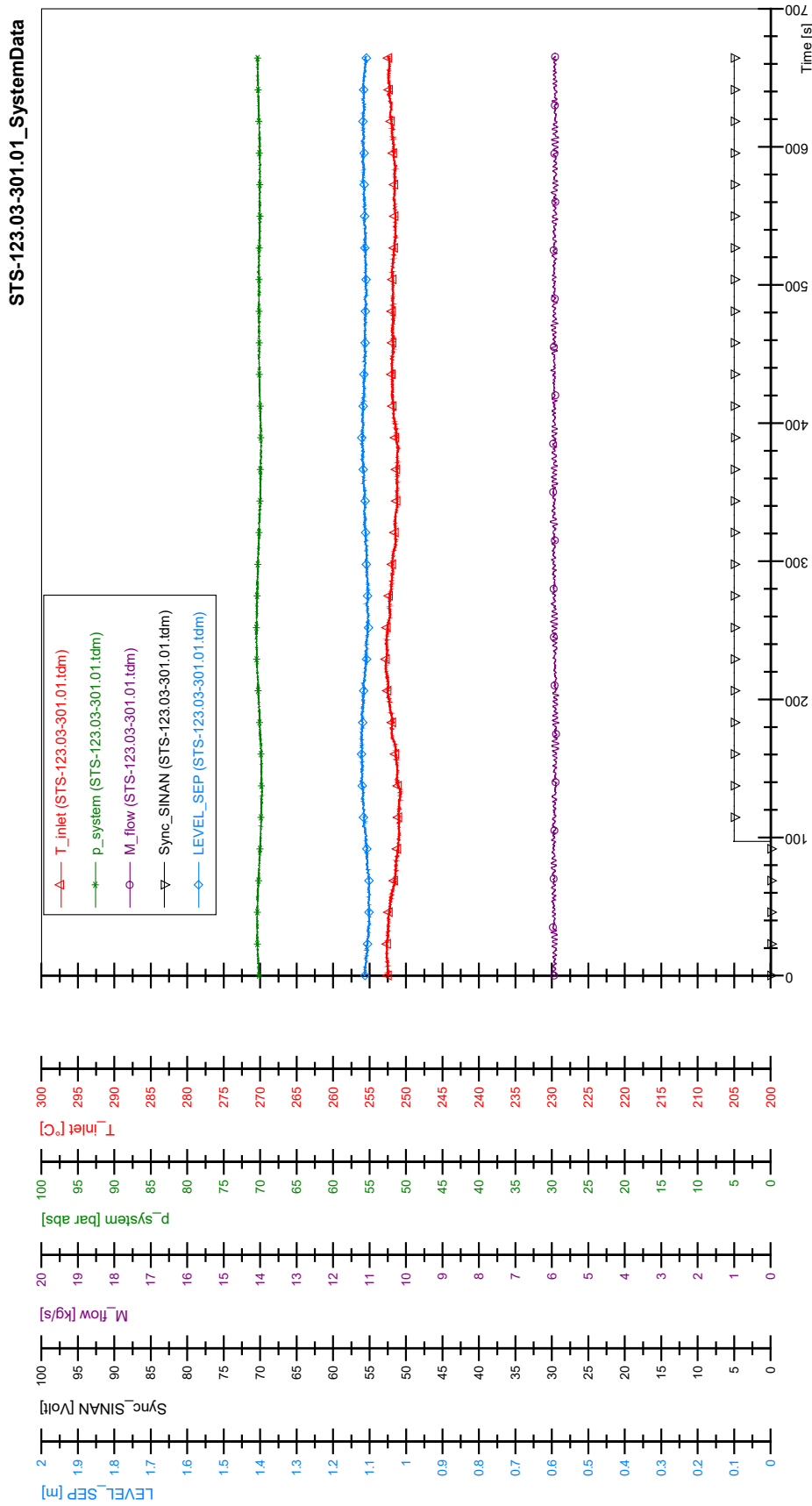
STS-123.03-407.01_Rod_87



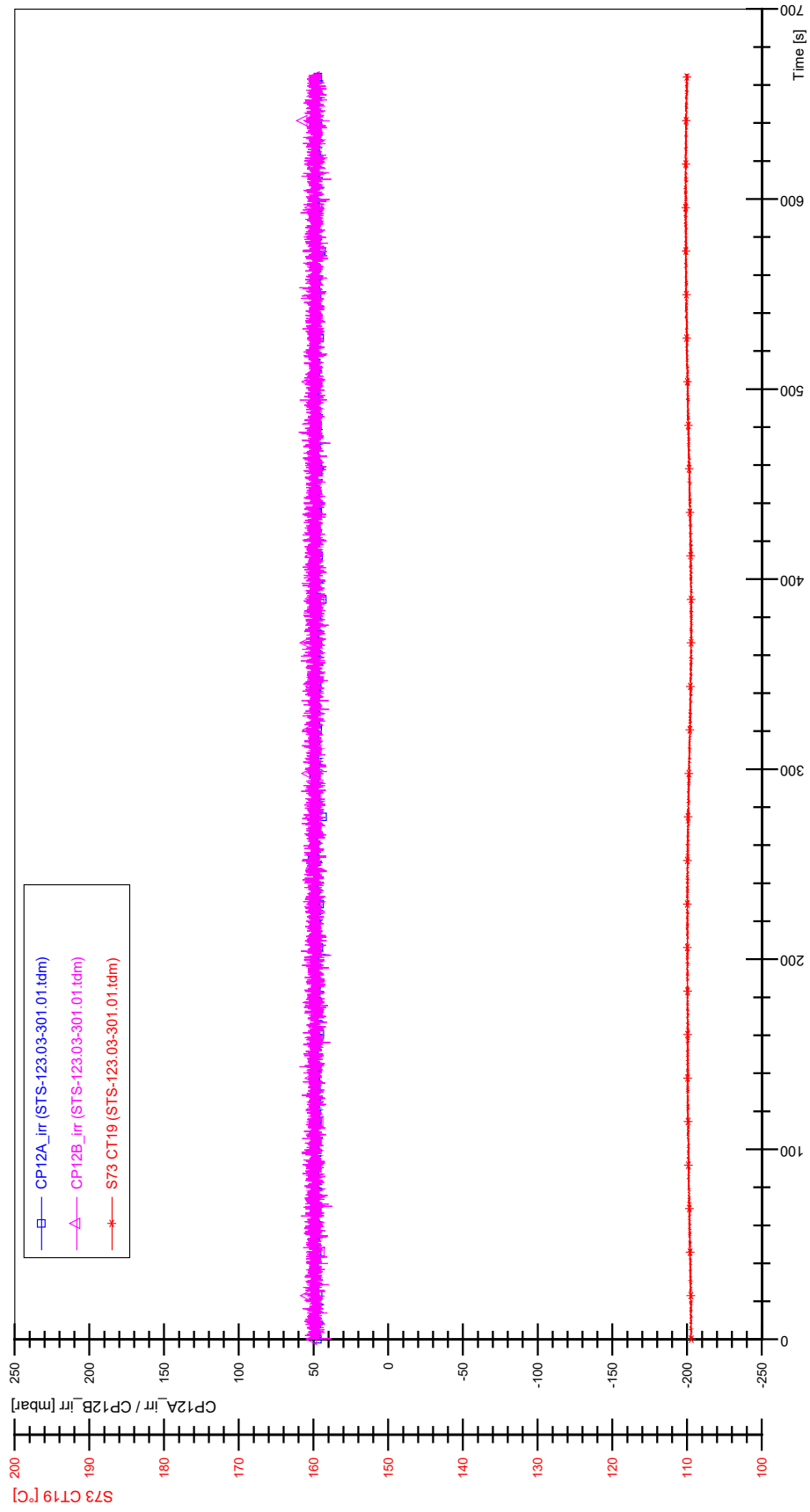
STS-123.03-407.01_Rod_88



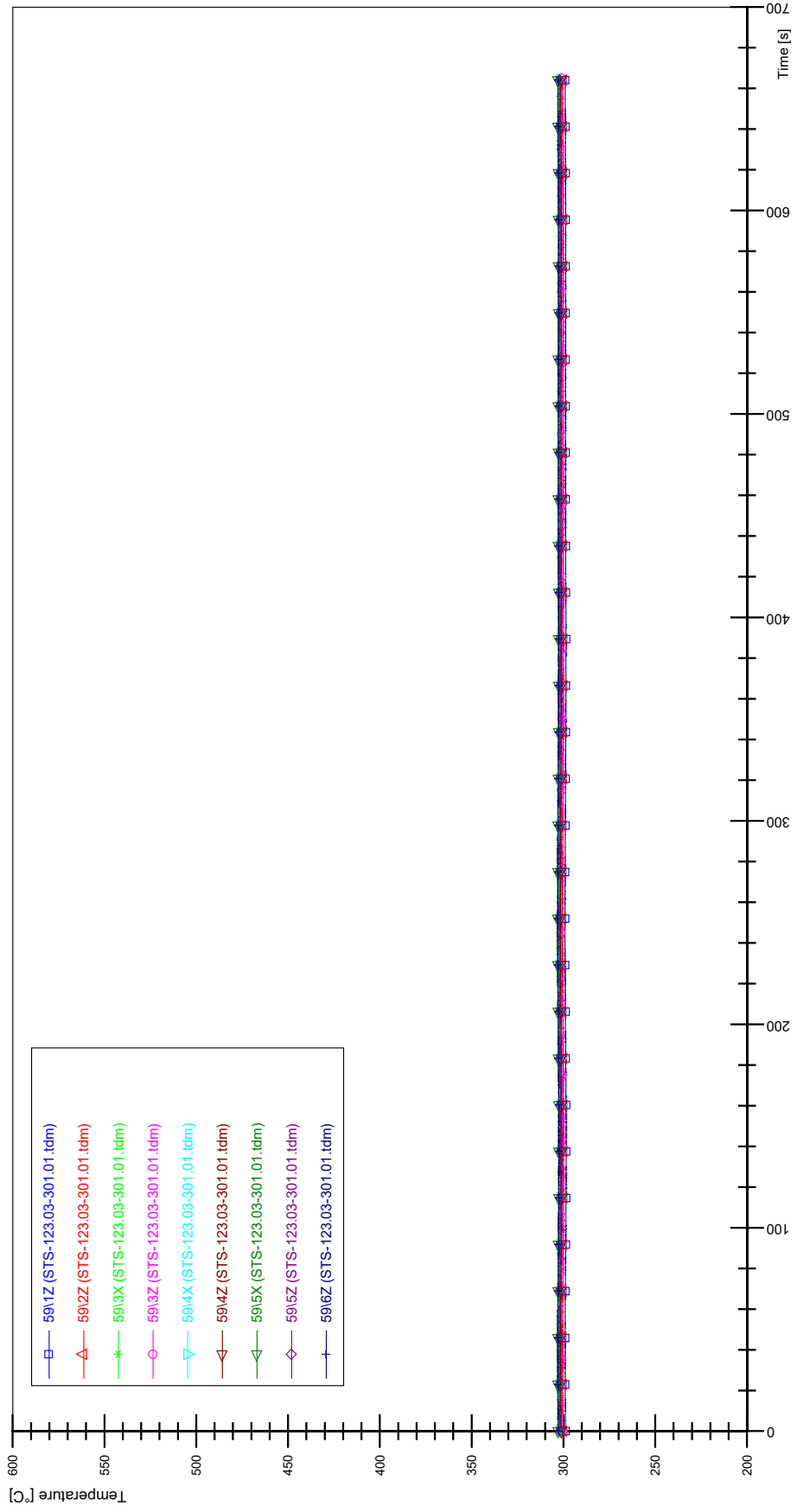
APPENDIX NN PLOTS OF INSTABILITY TEST STS-123.03-301.01



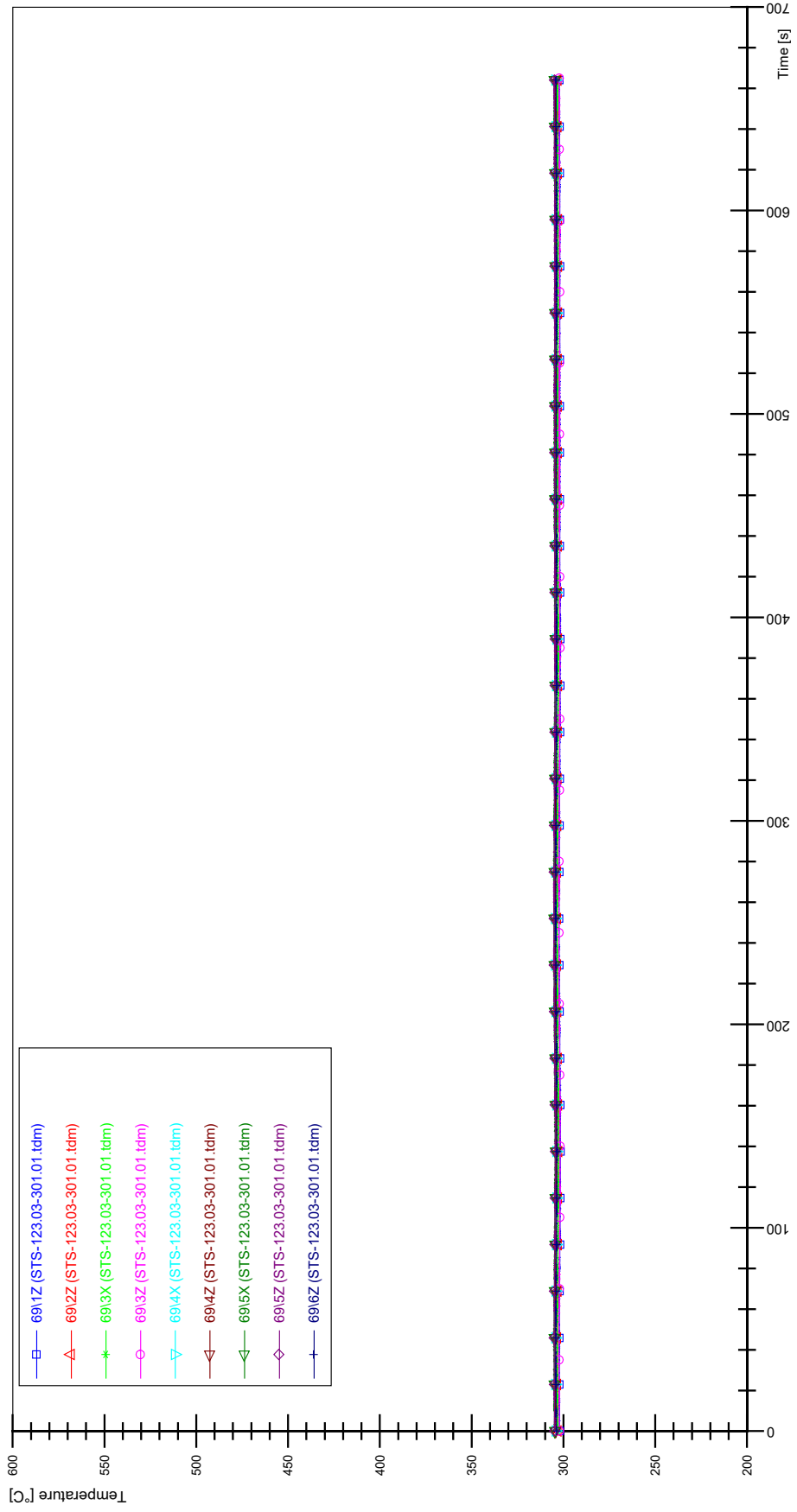
STS-123.03-301.01_CP12_CT19



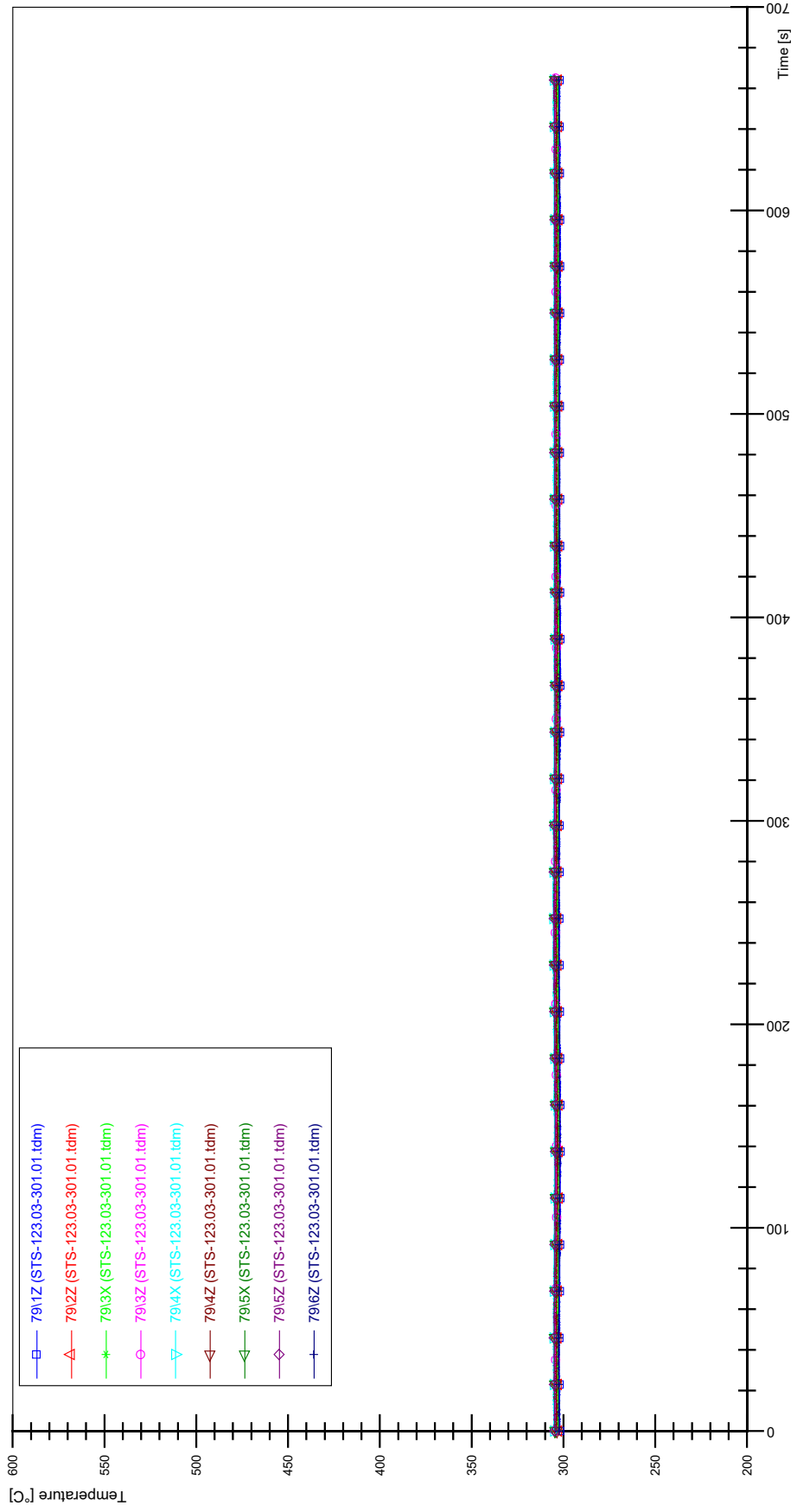
STS-123.03-301.01_Rod_59



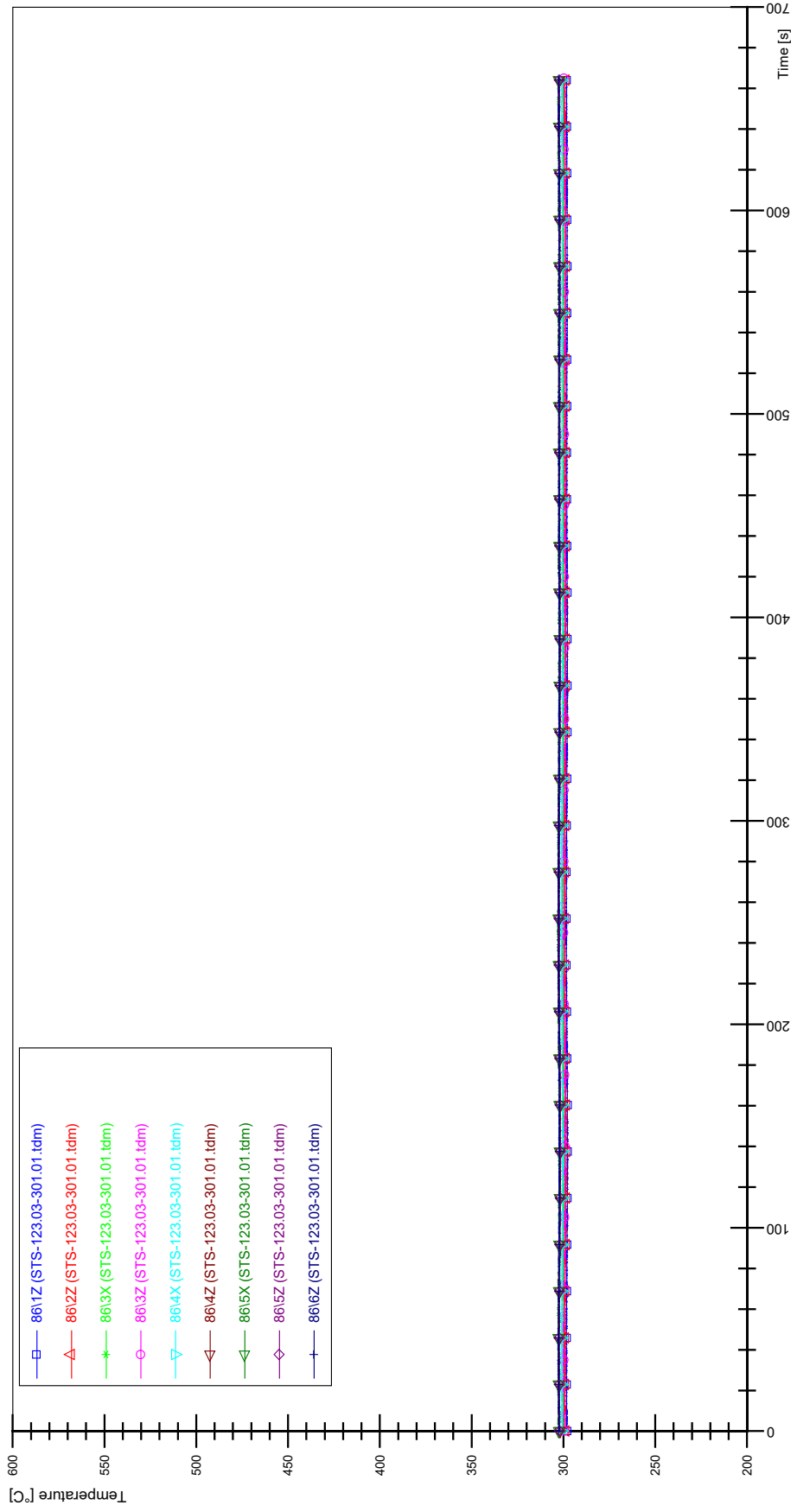
STS-123.03-301.01_Rod_69



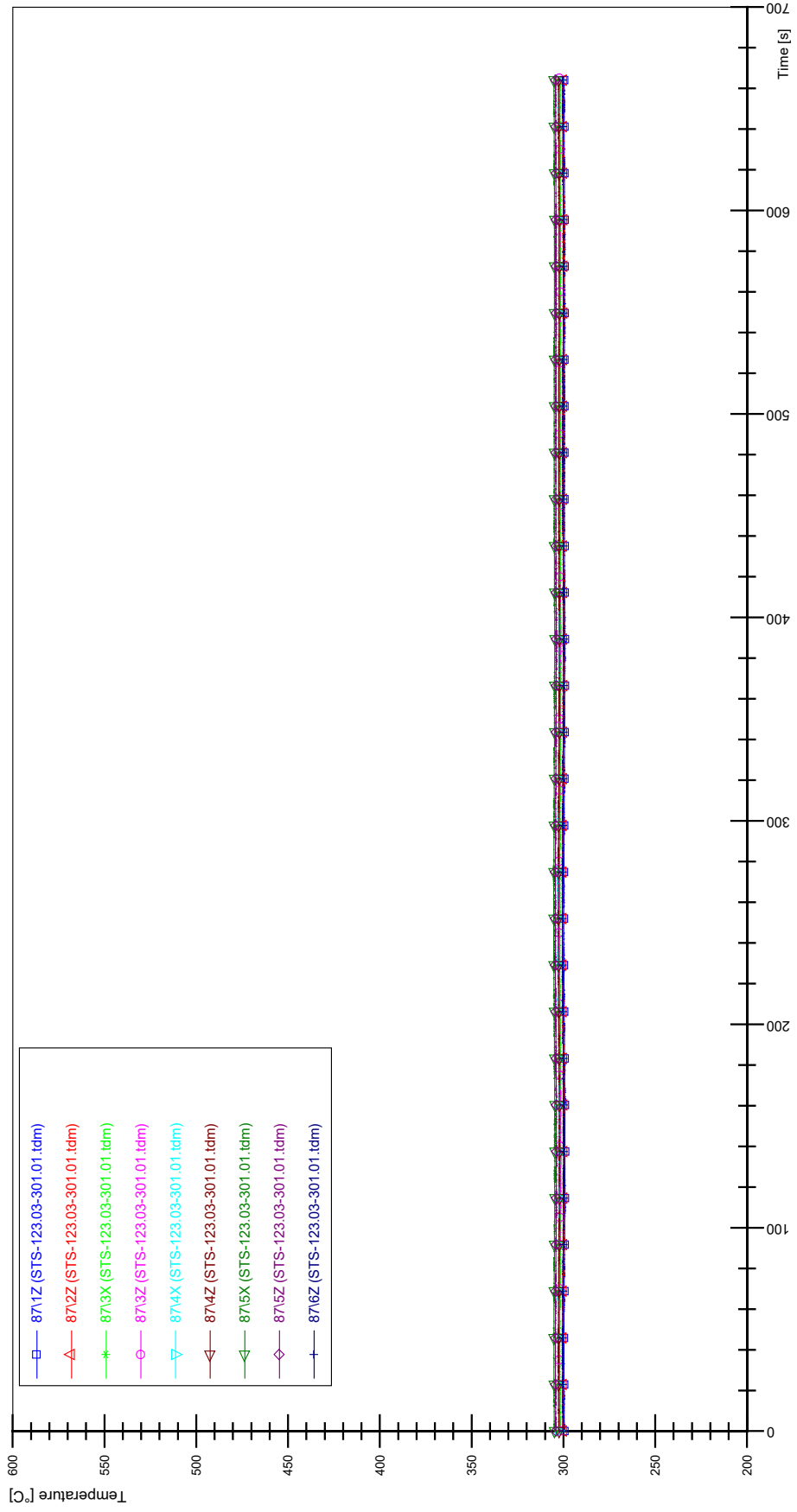
STS-123.03-301.01_Rod_79



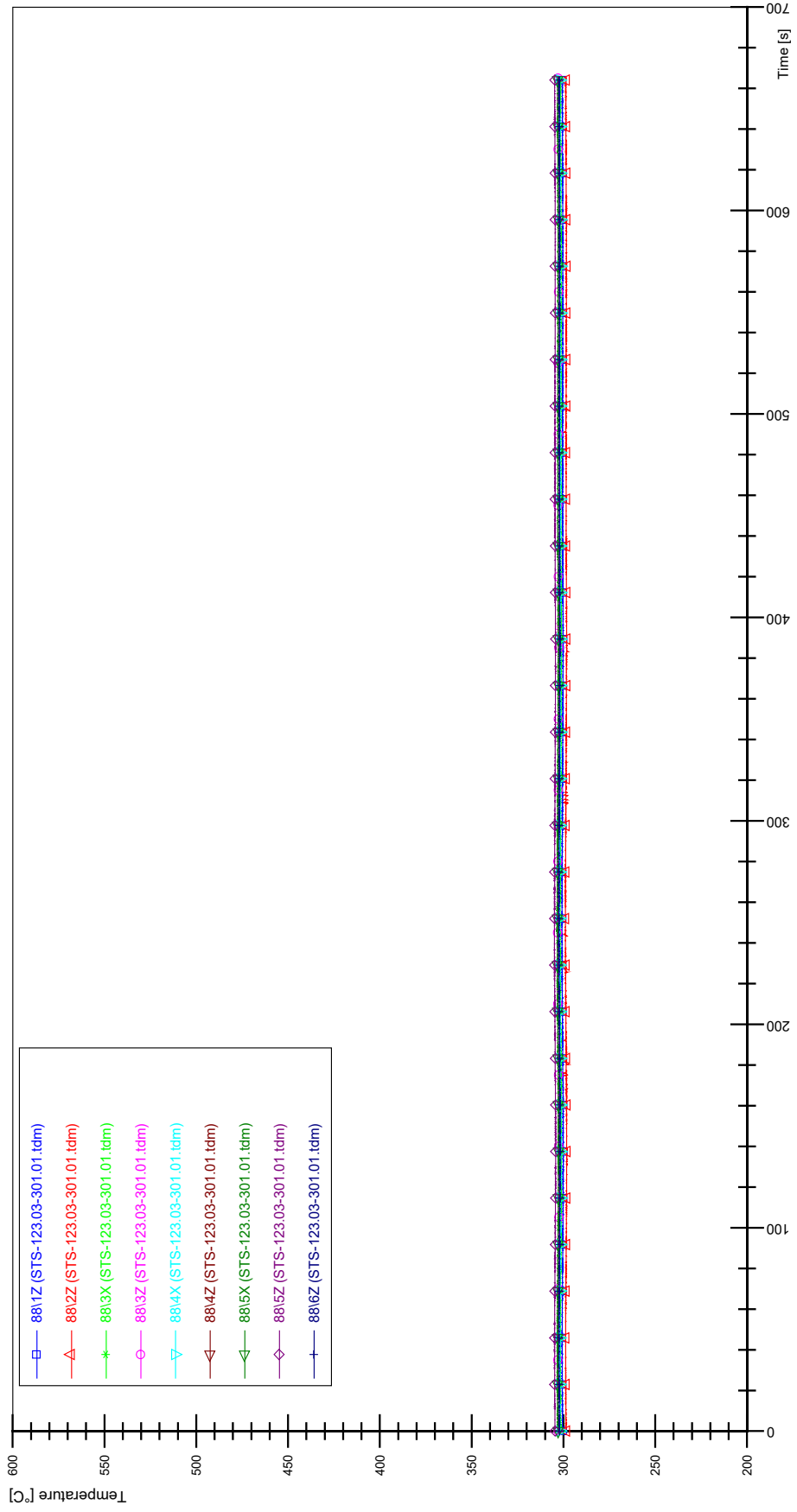
STS-123.03-301.01_Rod_86



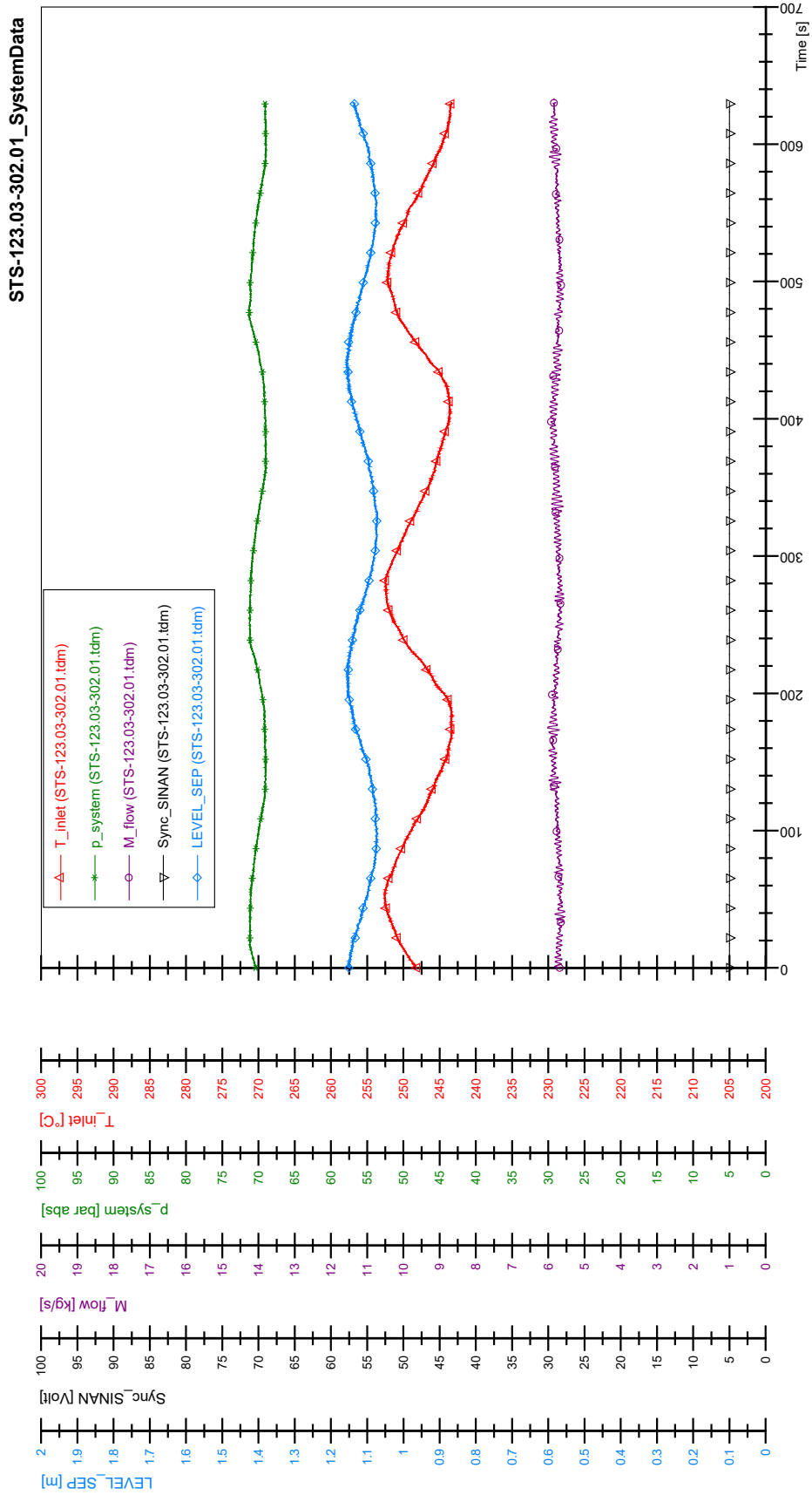
STS-123.03-301.01_Rod_87



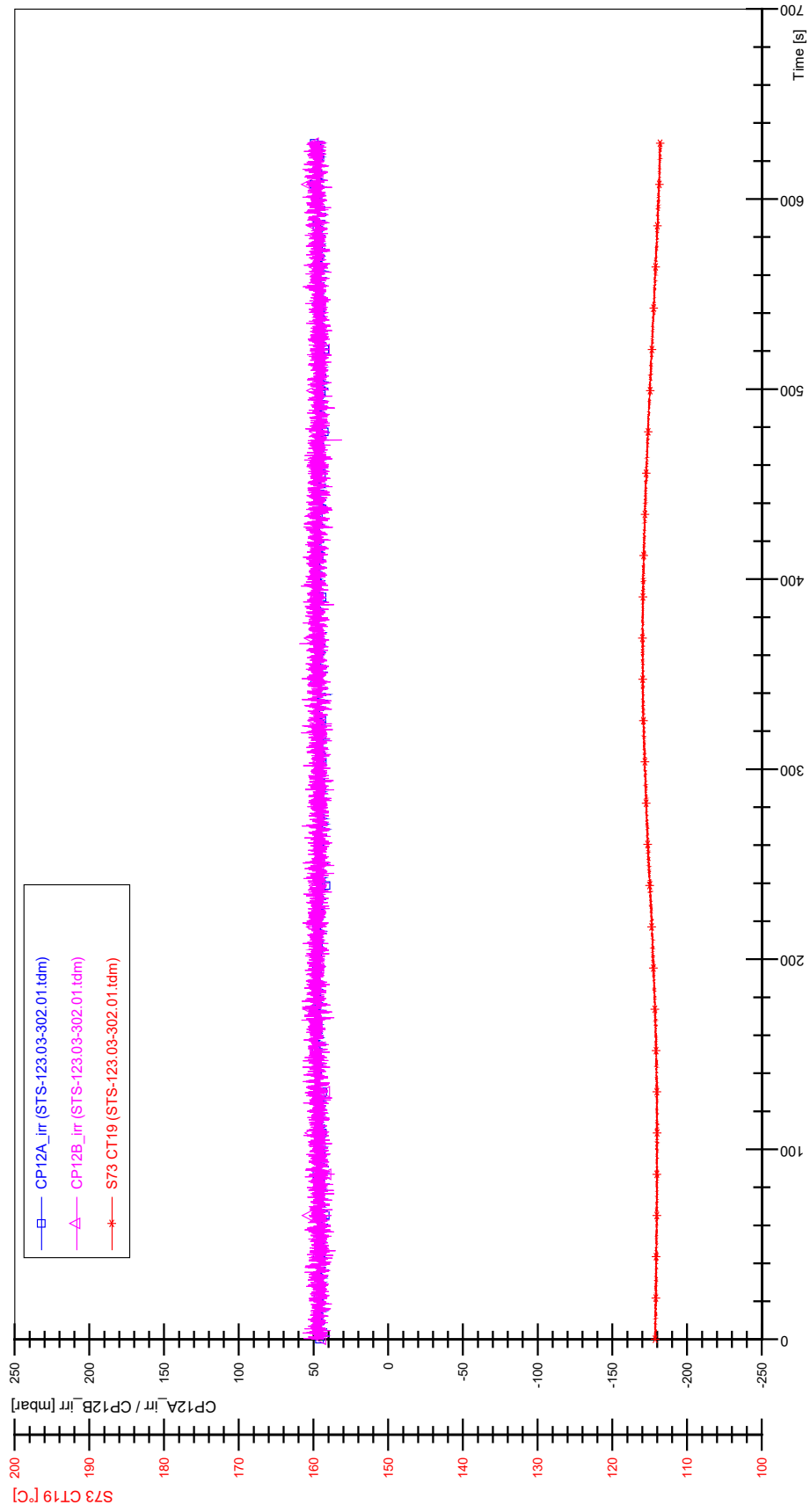
STS-123.03-301.01_Rod_88



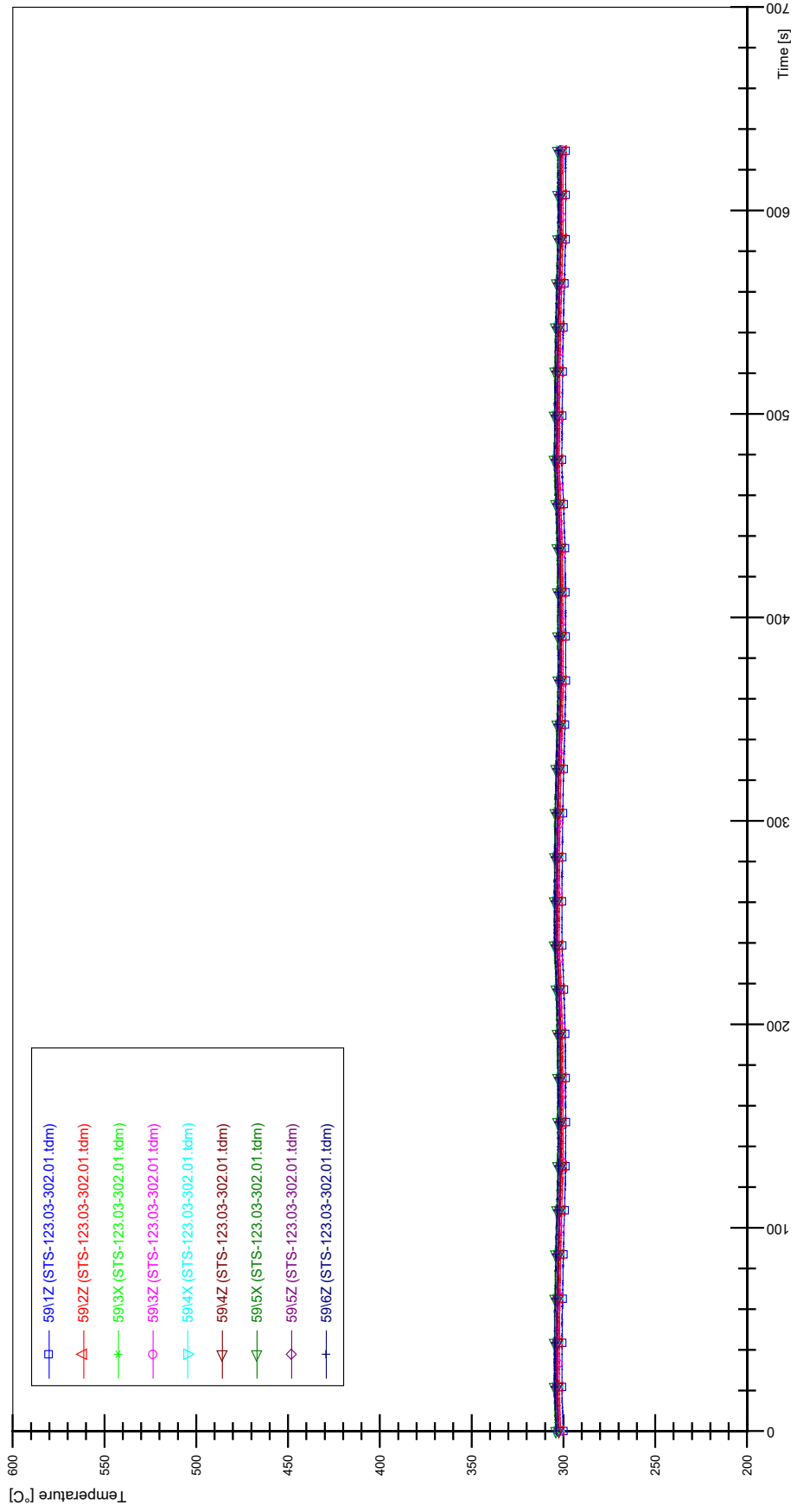
APPENDIX OO PLOTS OF INSTABILITY TEST STS-123.03-302.01



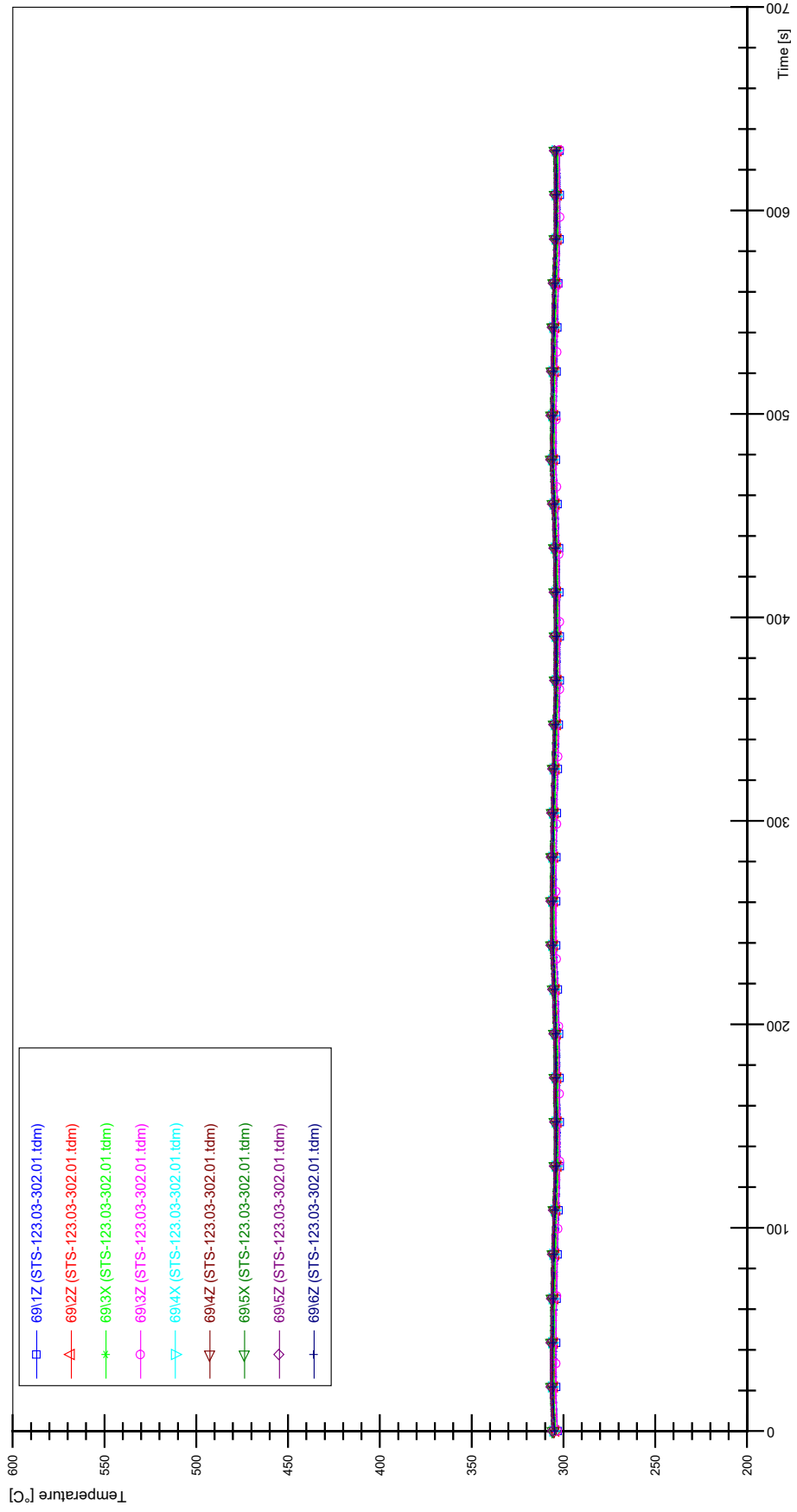
STS-123.03-302.01_CP12_CT19



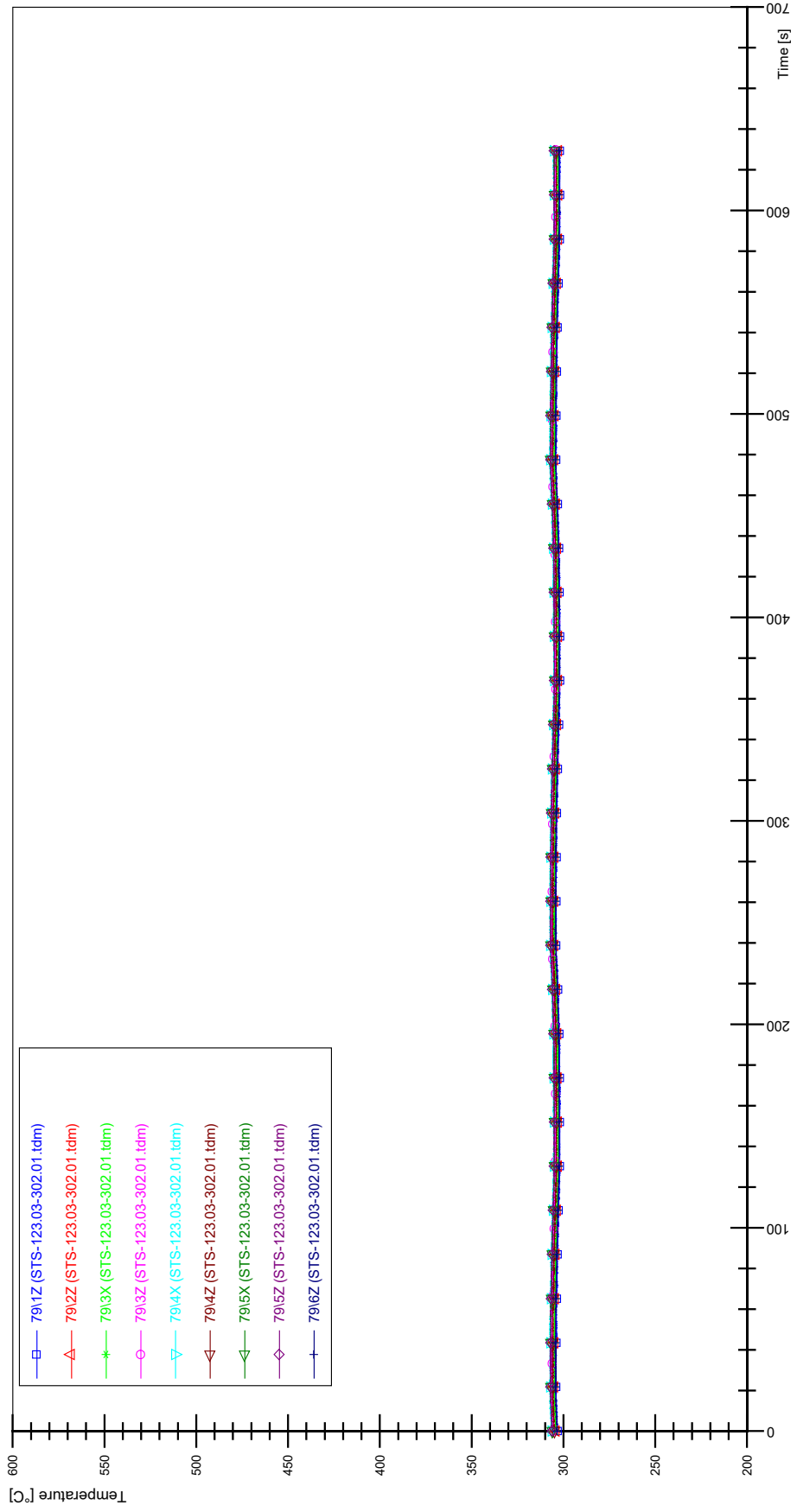
STS-123.03-302.01_Rod_59



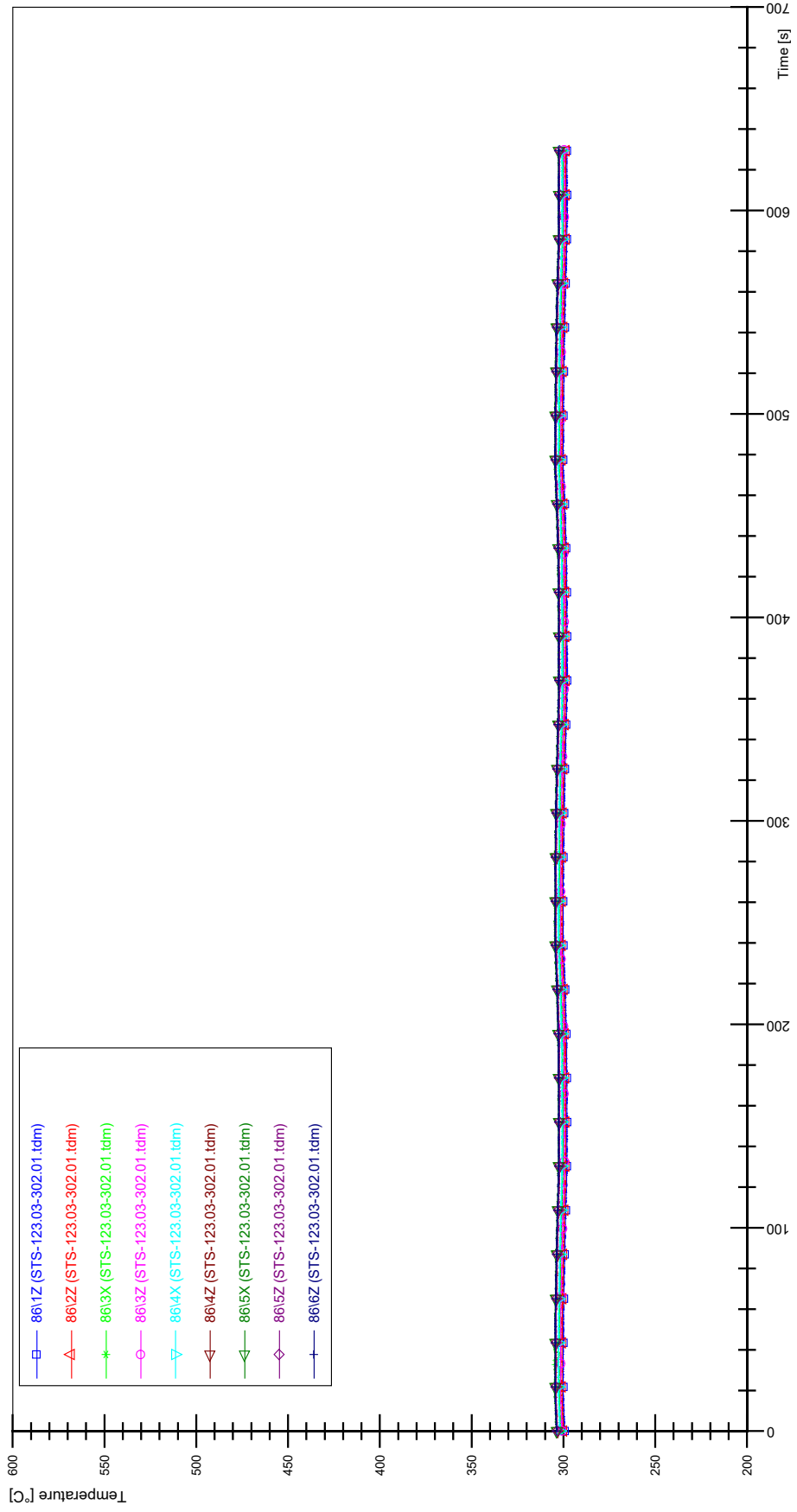
STS-123.03-302.01_Rod_69



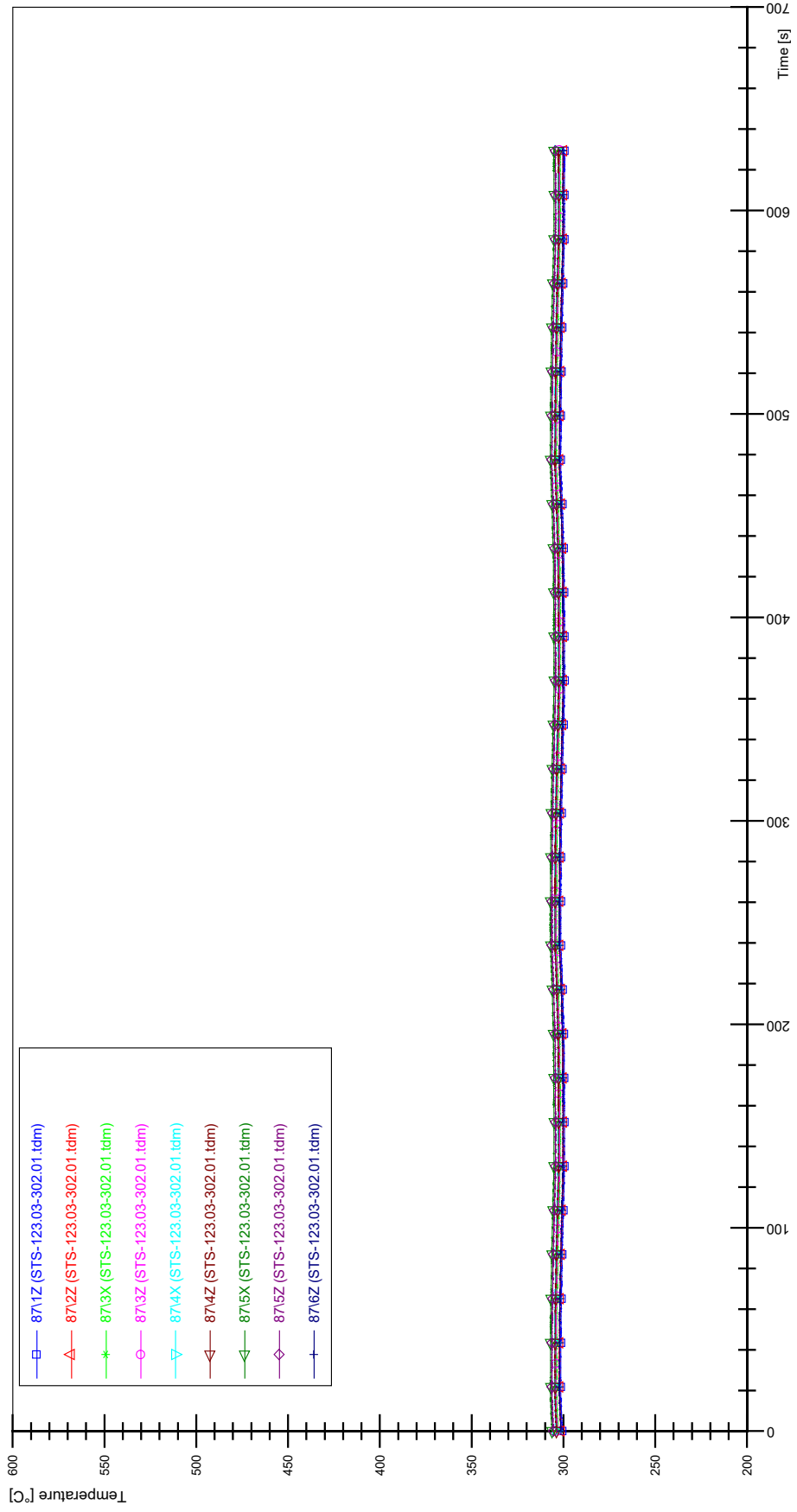
STS-123.03-302.01_Rod_79



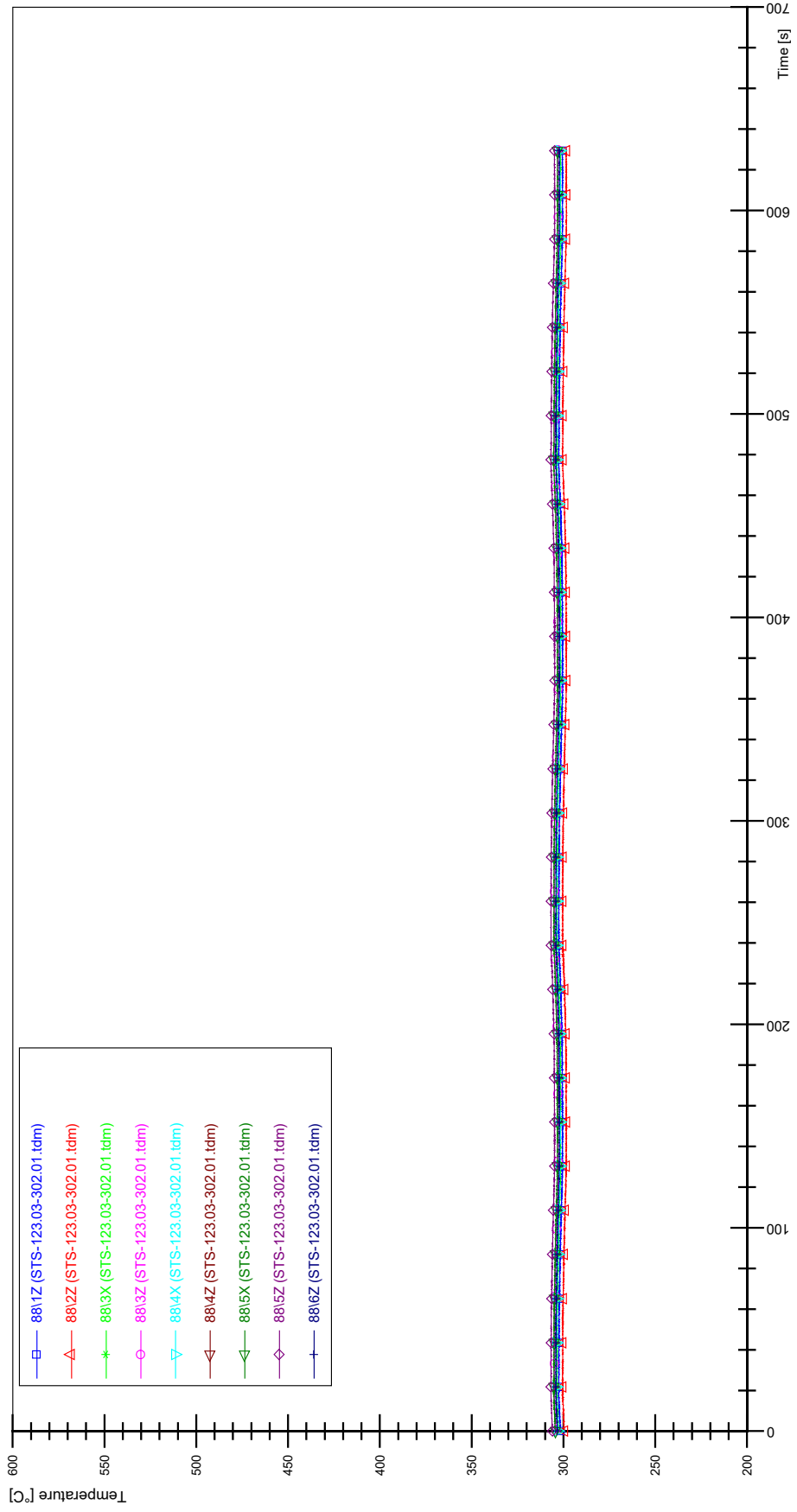
STS-123.03-302.01_Rod_86



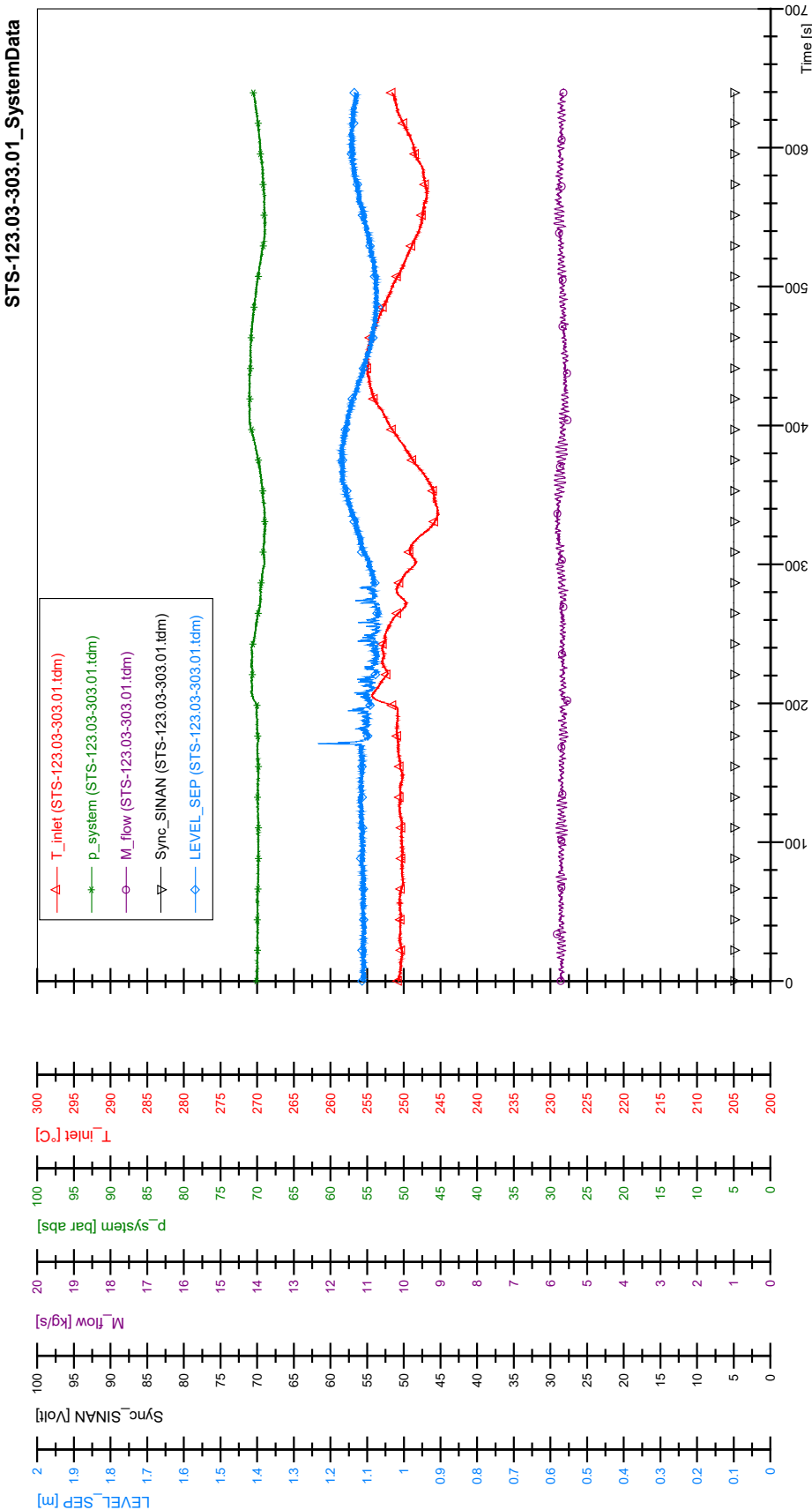
STS-123.03-302.01_Rod_87



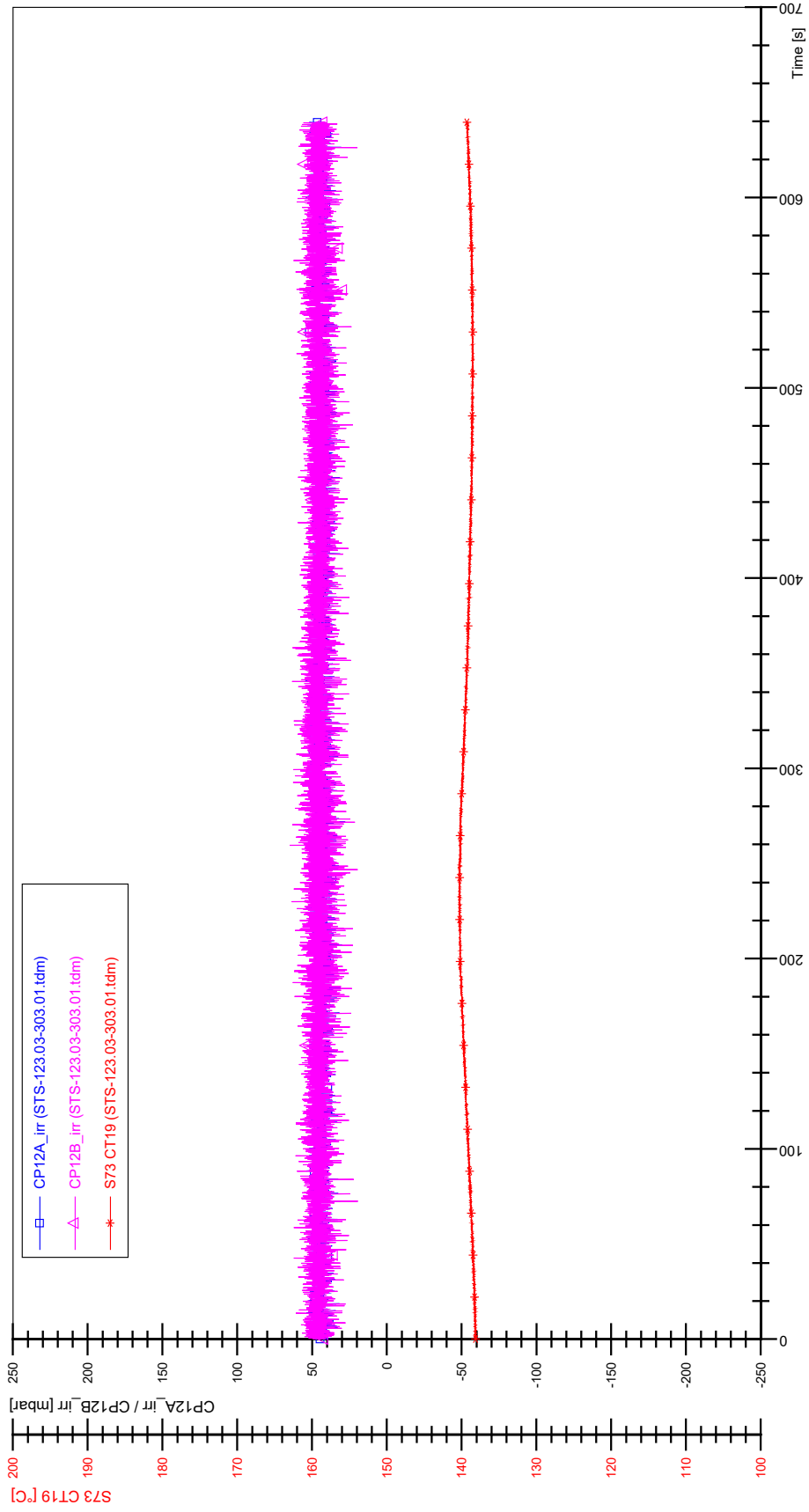
STS-123.03-302.01_Rod_88



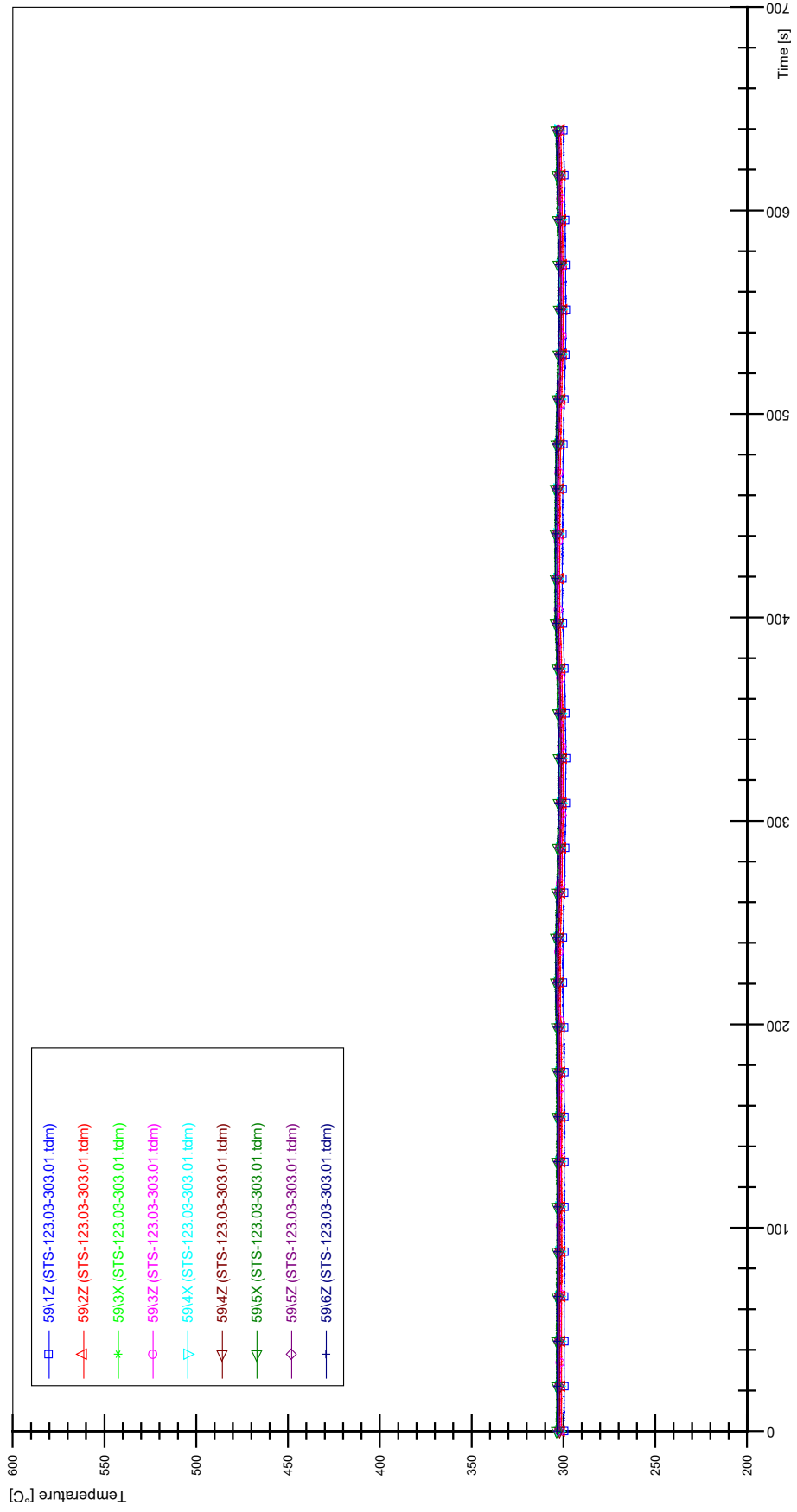
APPENDIX PP PLOTS OF INSTABILITY TEST STS-123.03-303.01



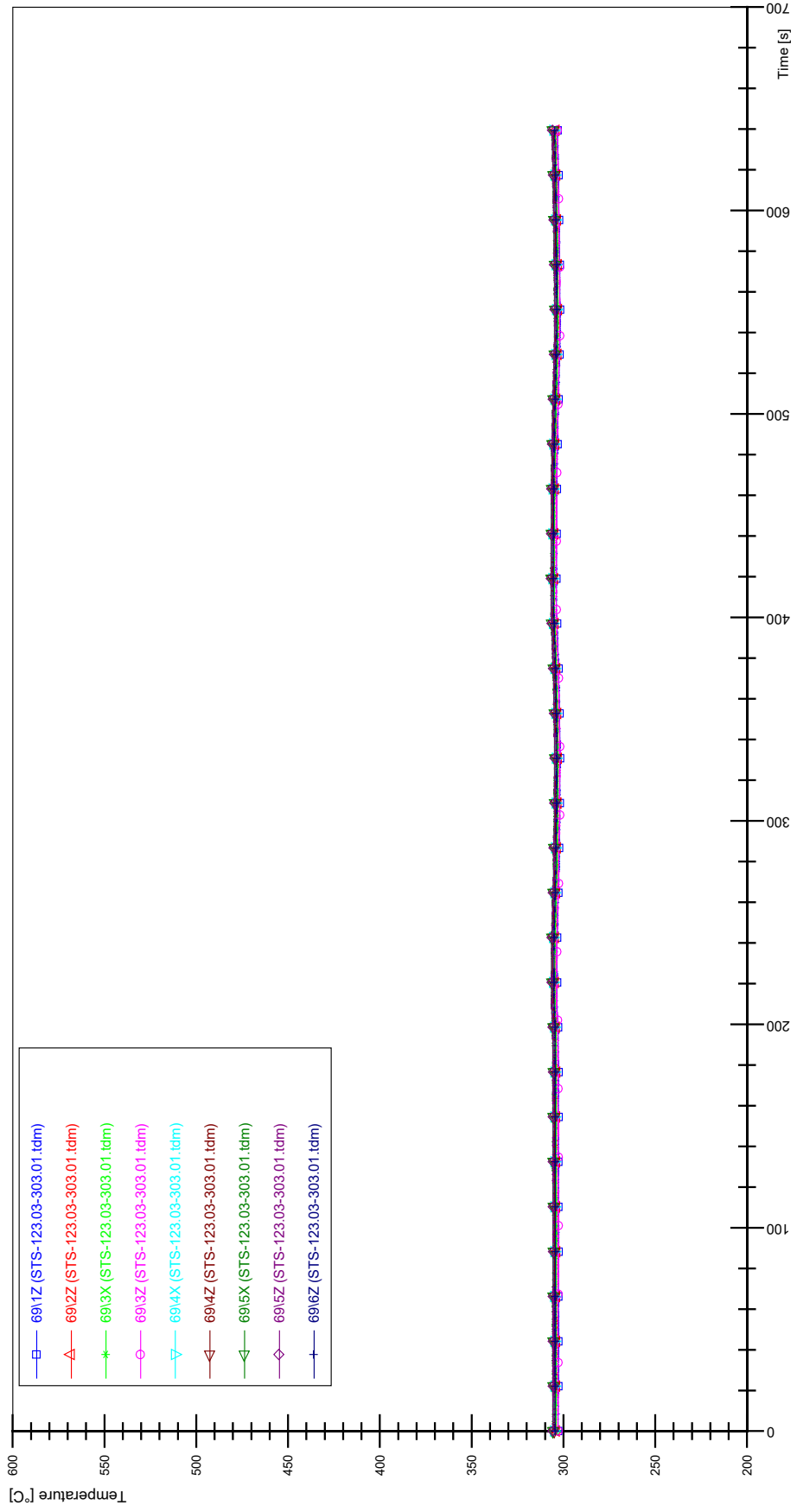
STS-123.03-303.01_CP12_CT19



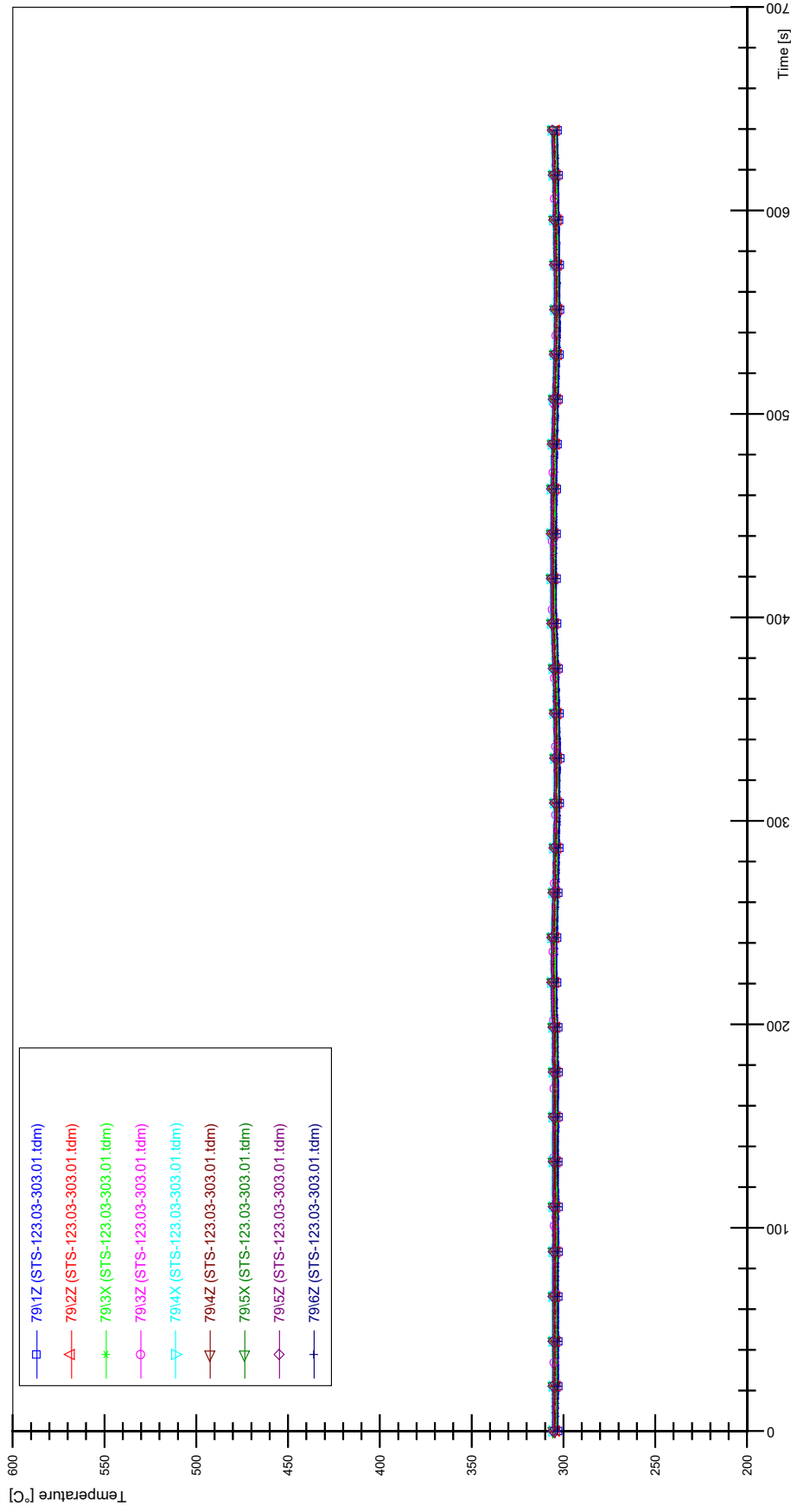
STS-123.03-303.01_Rod_59



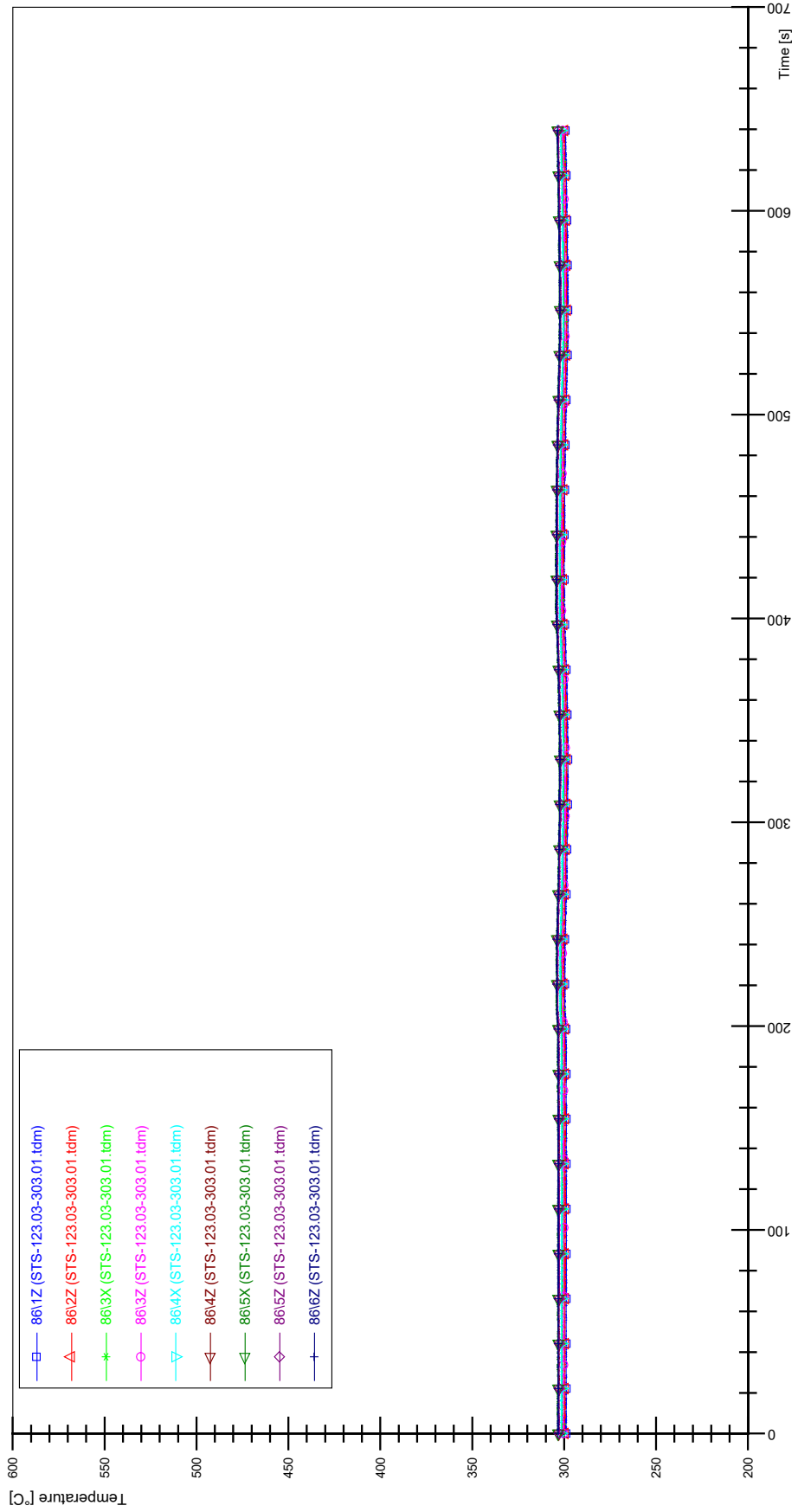
STS-123.03-303.01_Rod_69



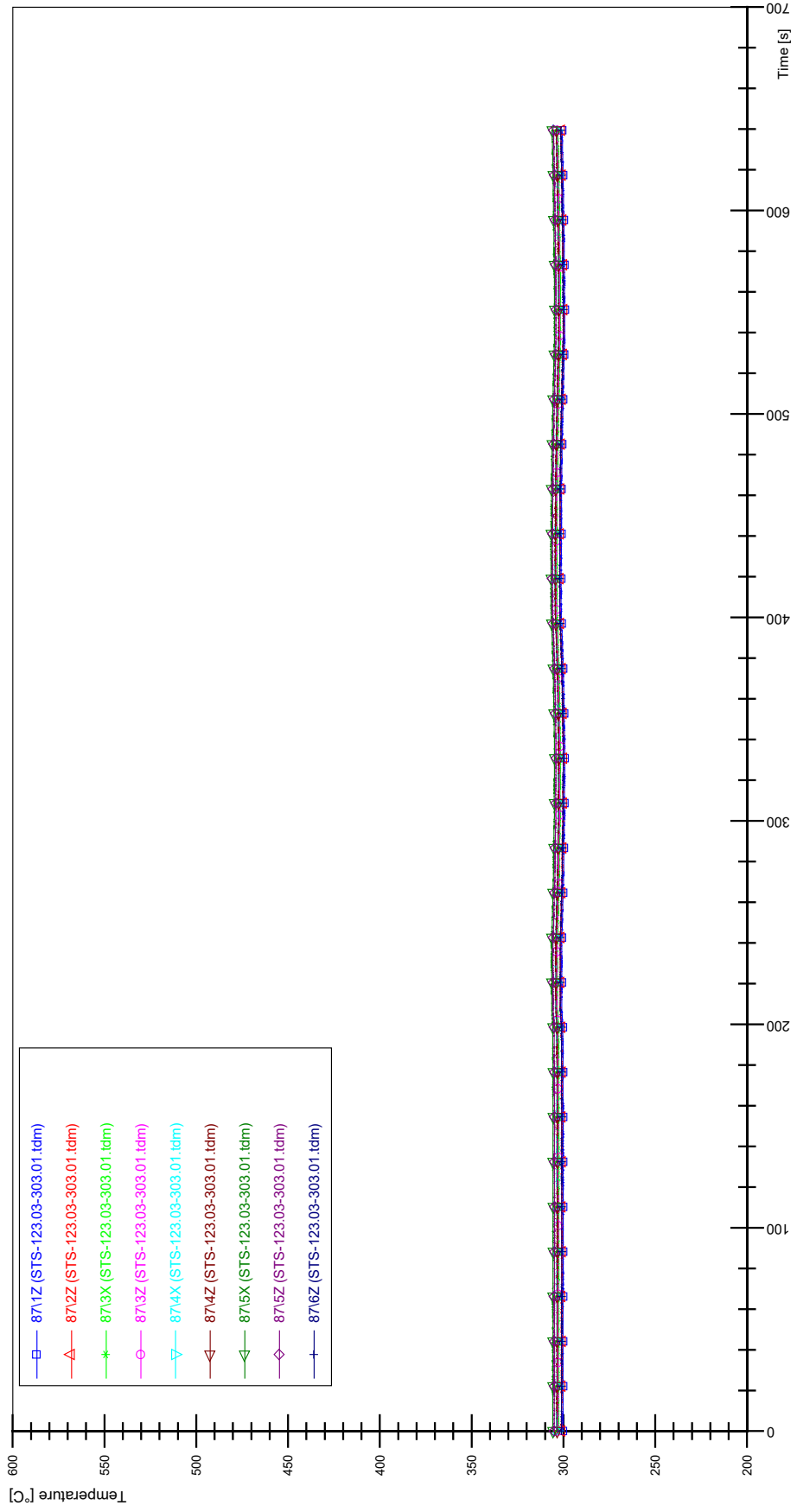
STS-123.03-303.01_Rod_79



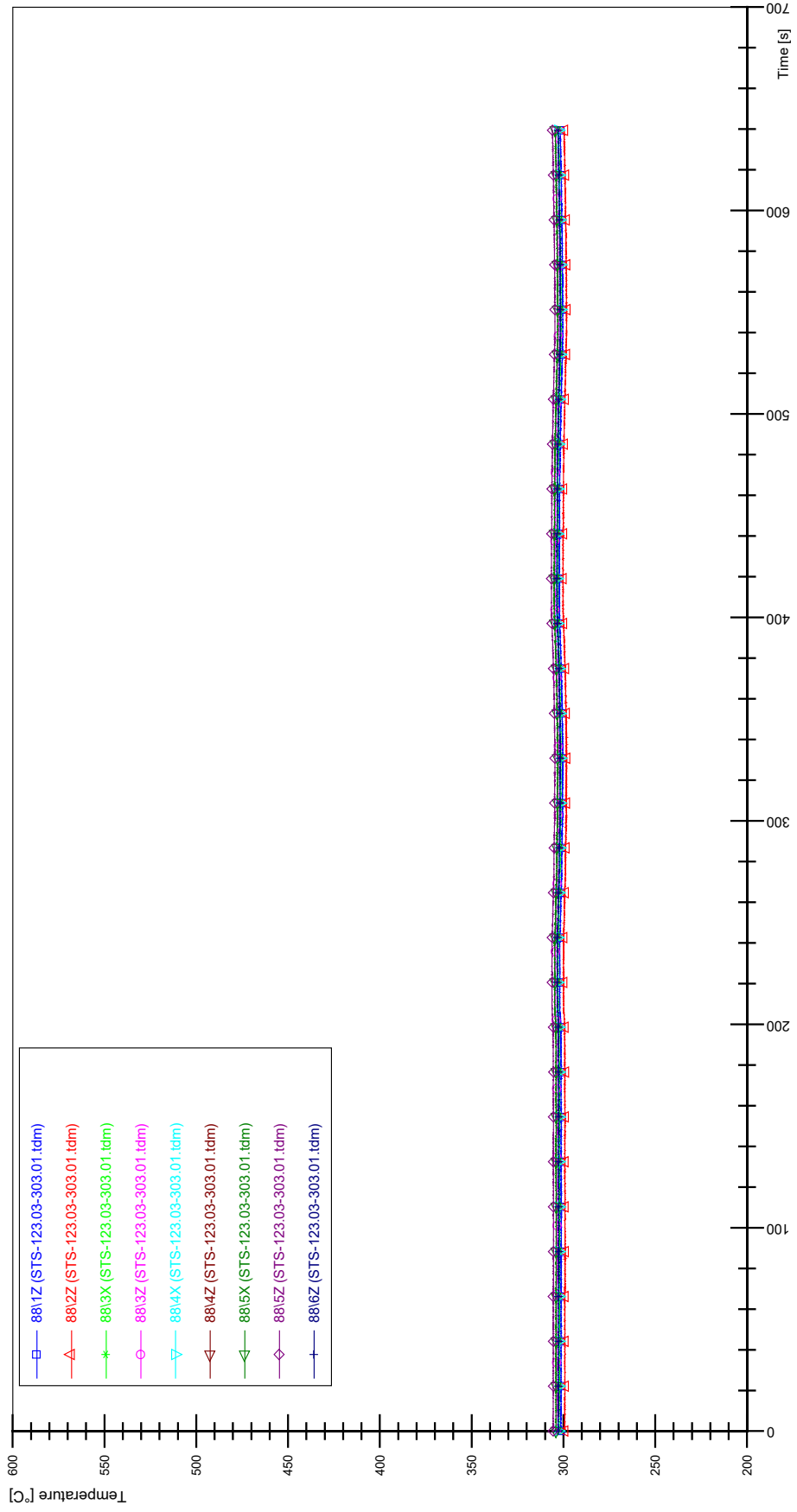
STS-123.03-303.01_Rod_86



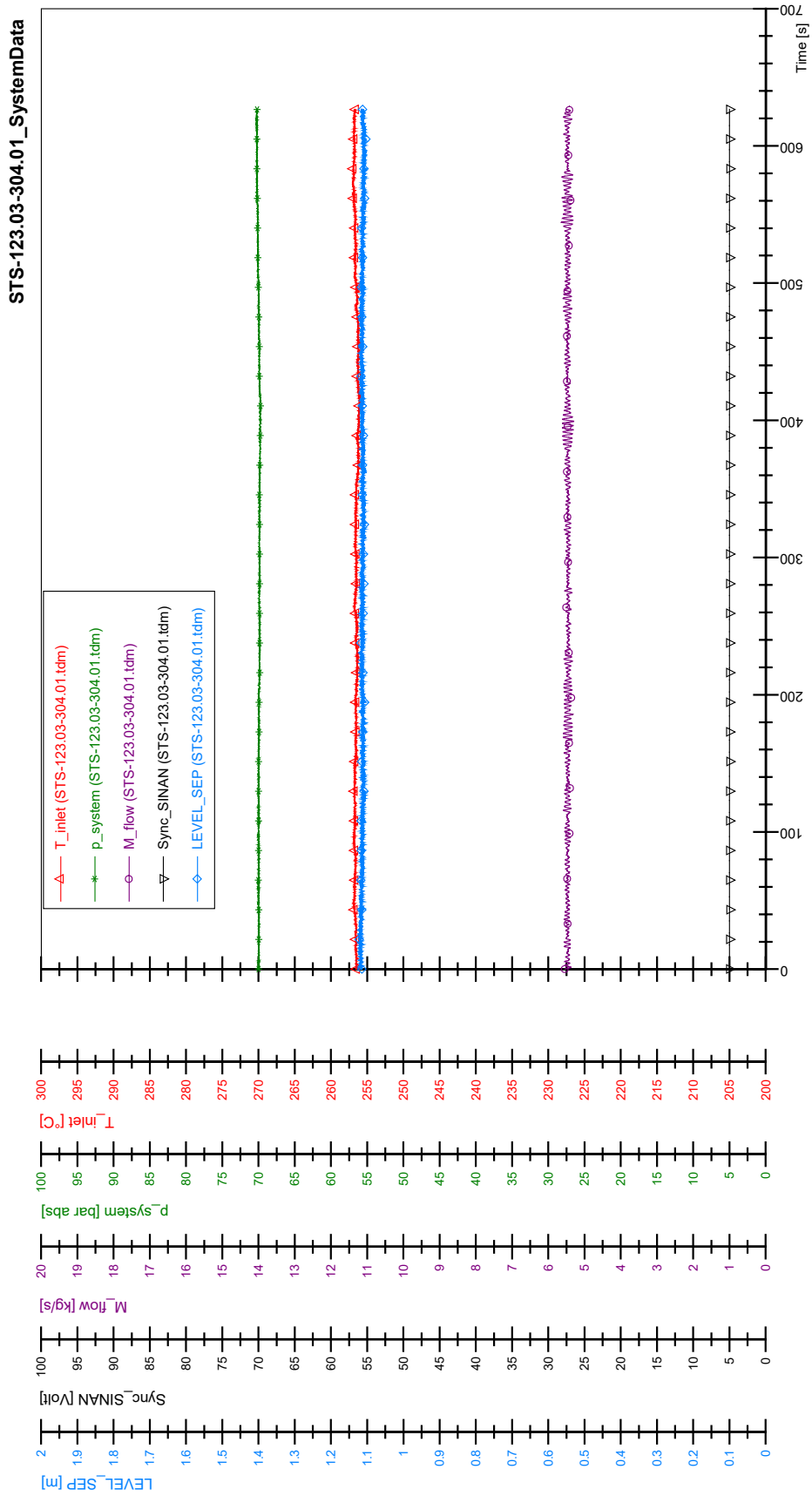
STS-123.03-303.01_Rod_87



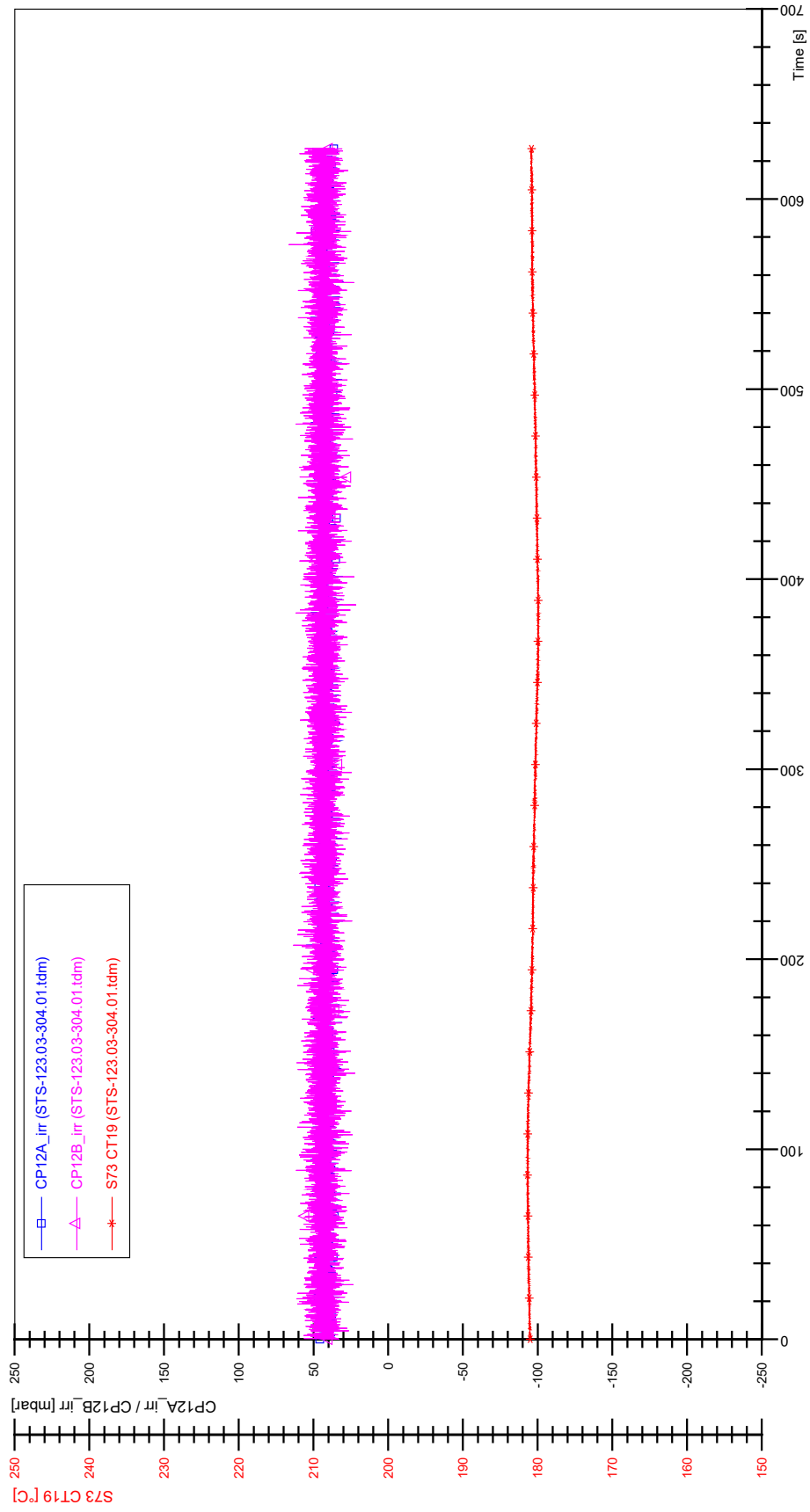
STS-123.03-303.01_Rod_88



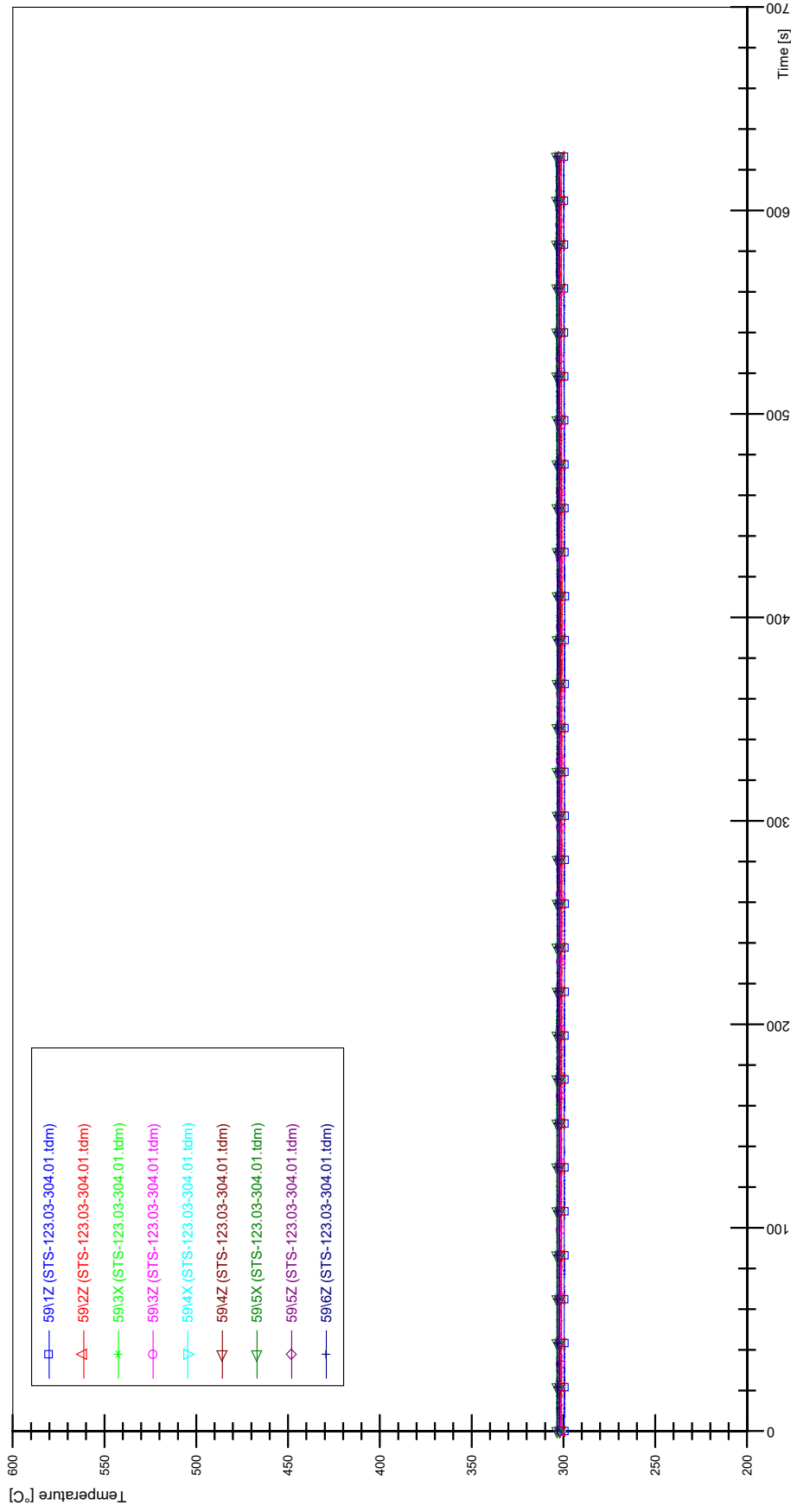
APPENDIX QQ PLOTS OF INSTABILITY TEST STS-123.03-304.01



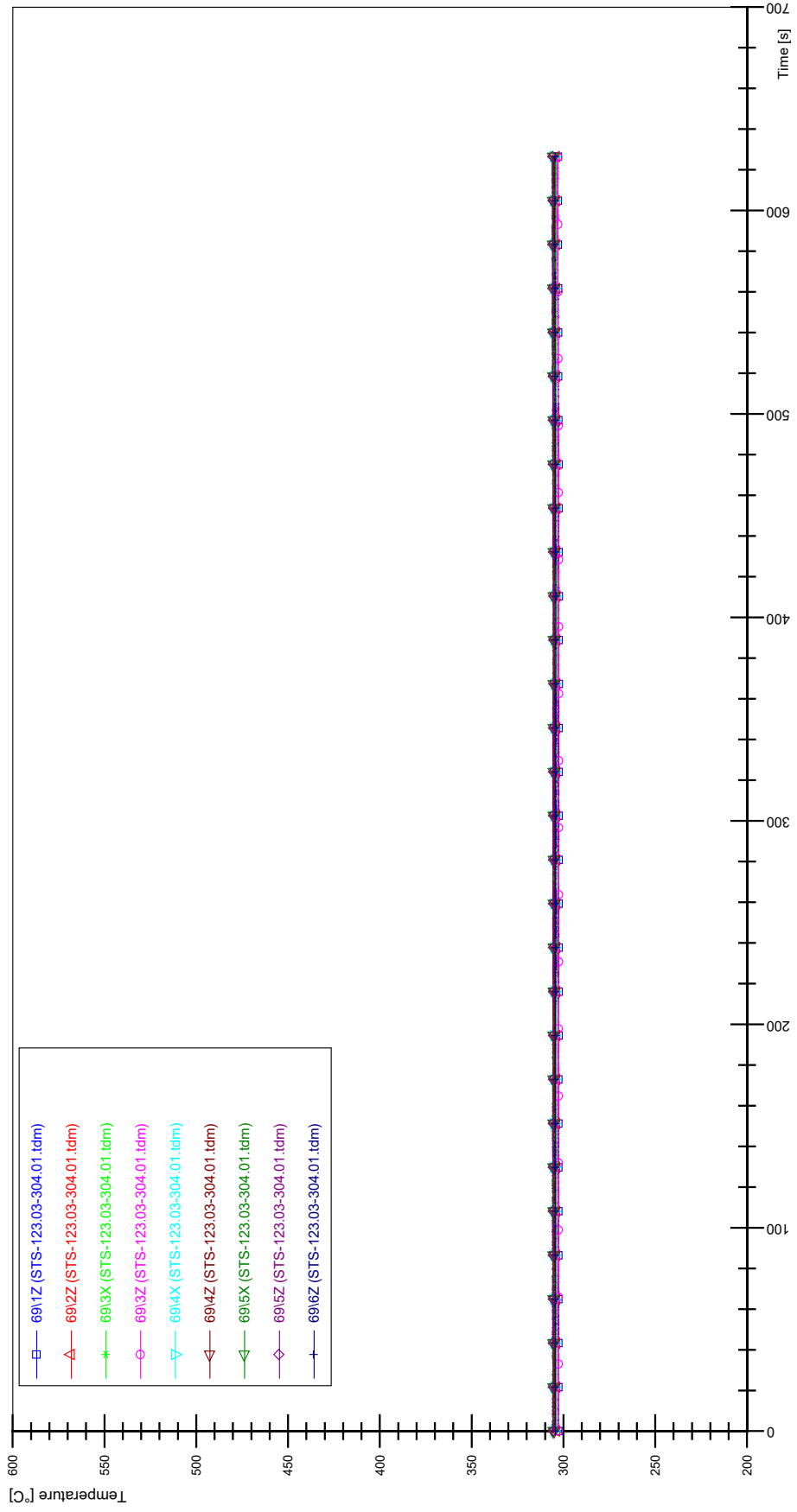
STS-123.03-304.01_CP12_CT19



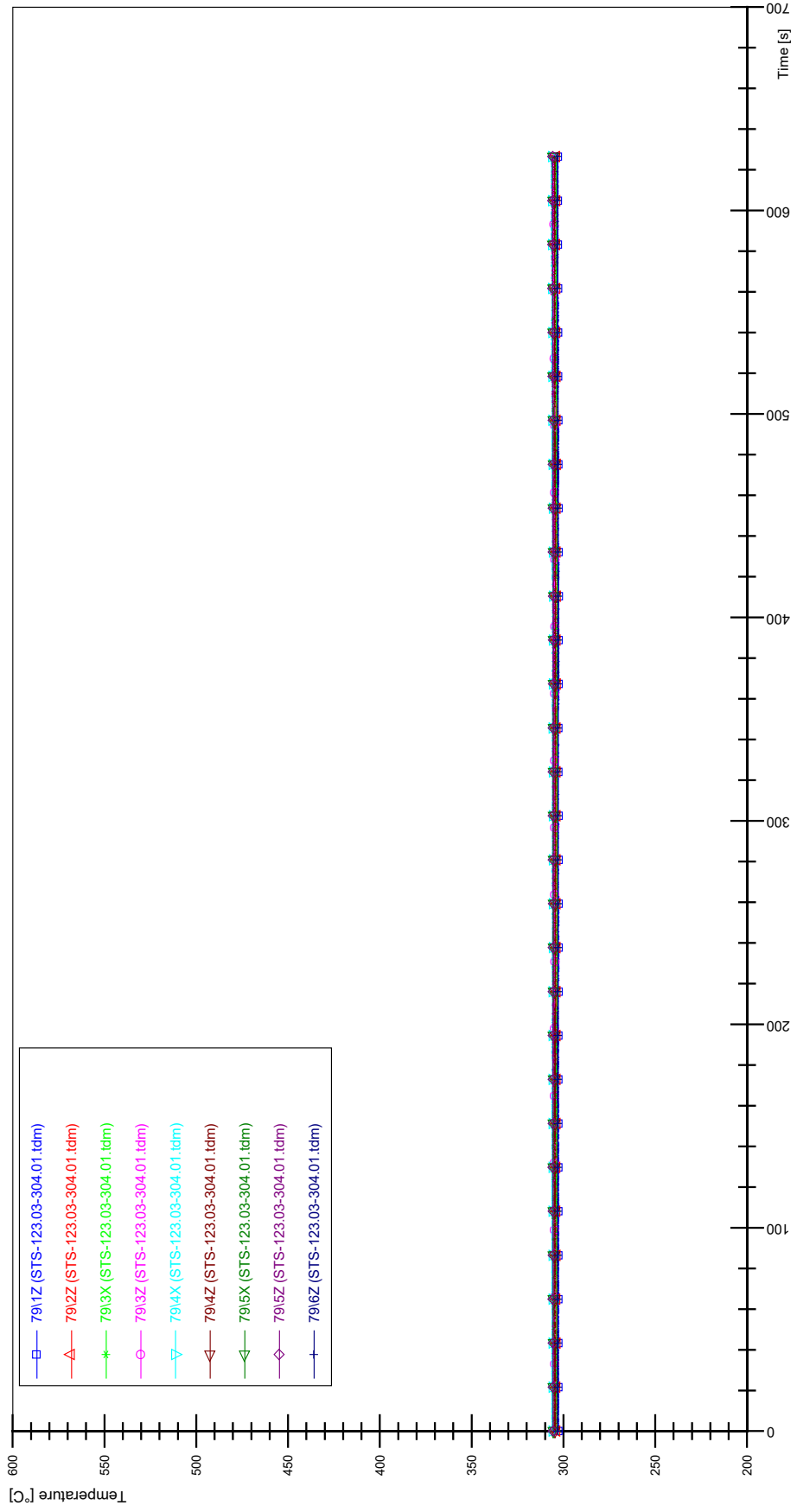
STS-123.03-304.01_Rod_59



STS-123.03-304.01_Rod_69

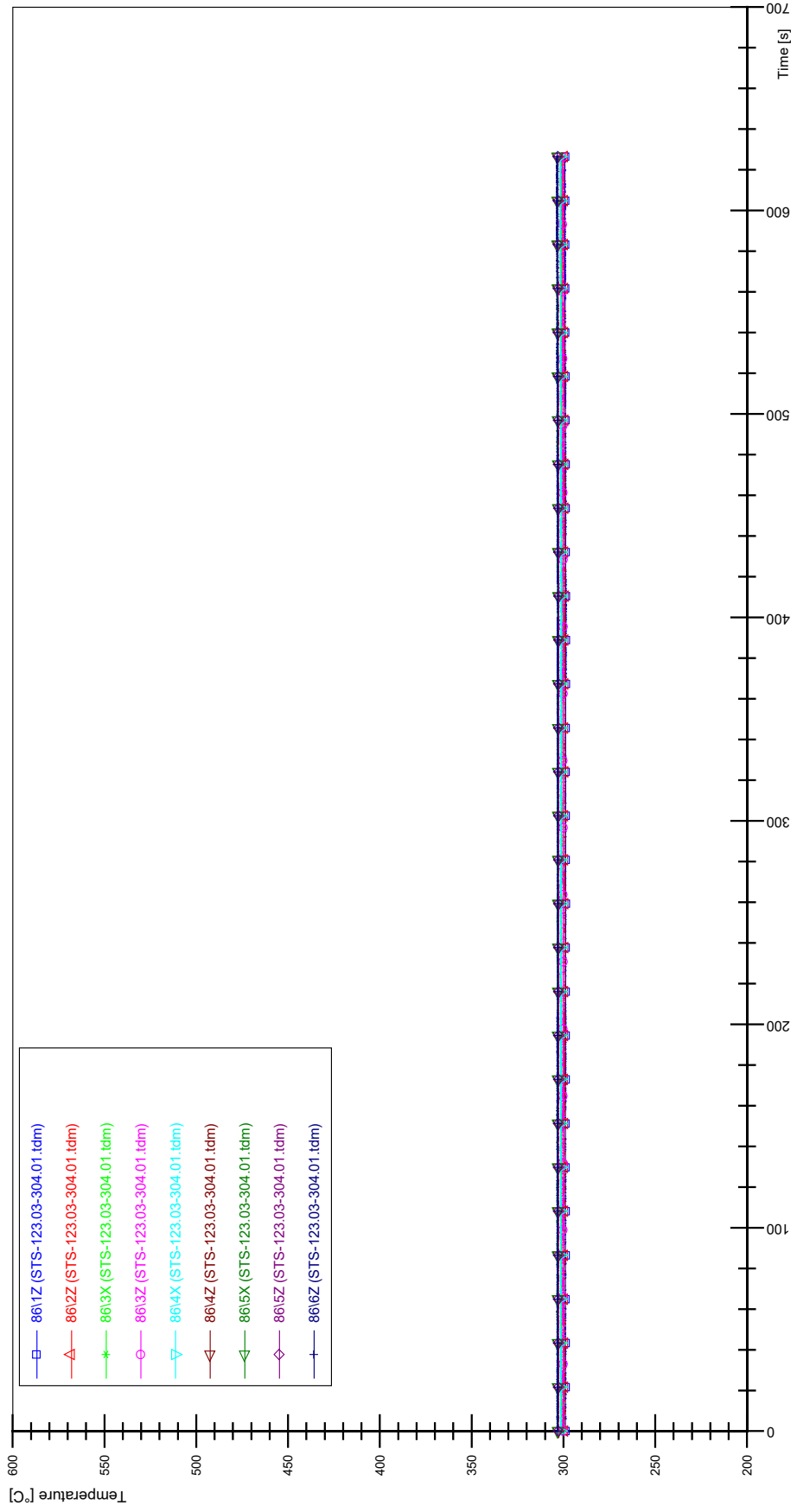


STS-123.03-304.01_Rod_79

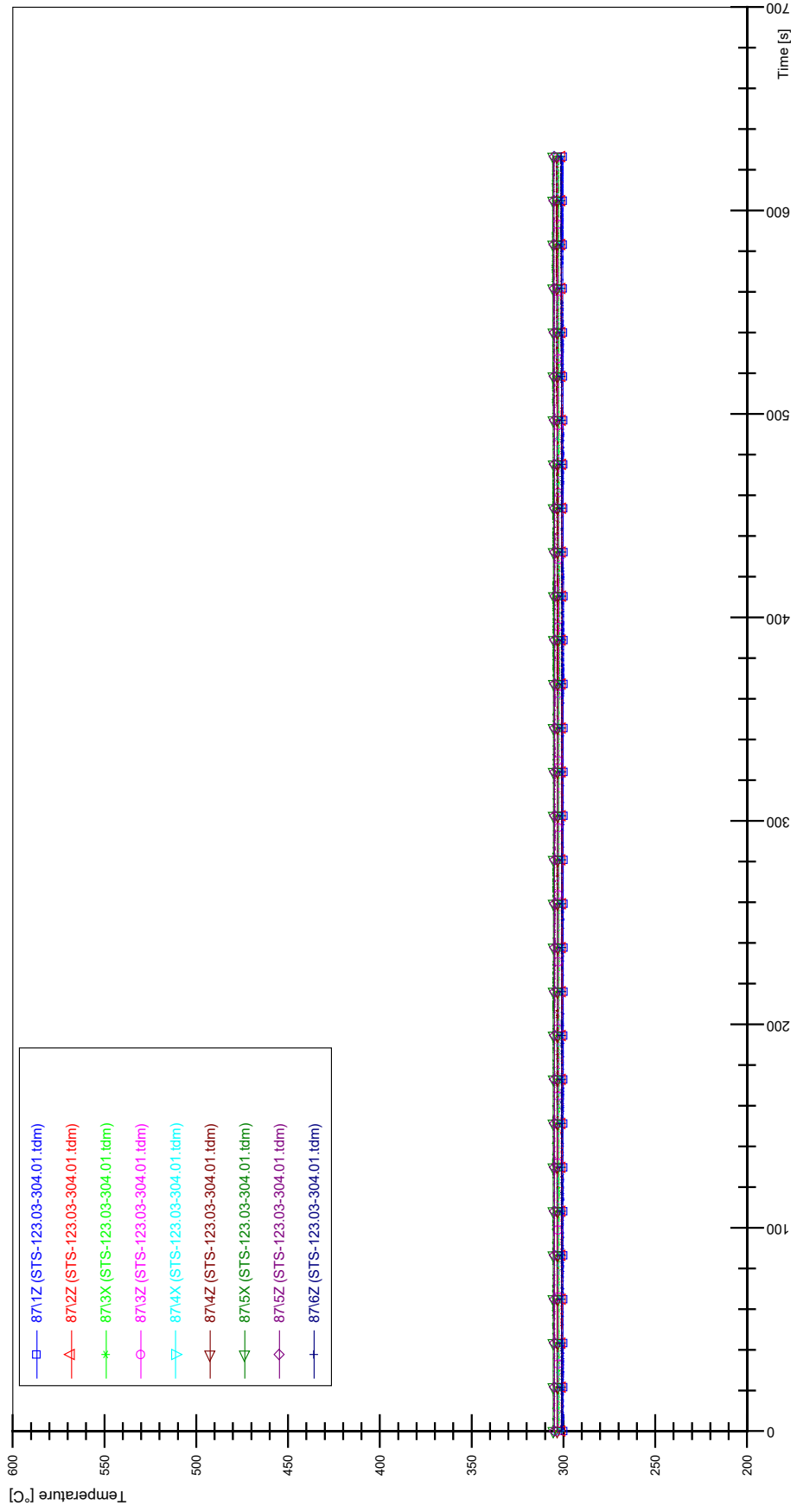


QQ-5

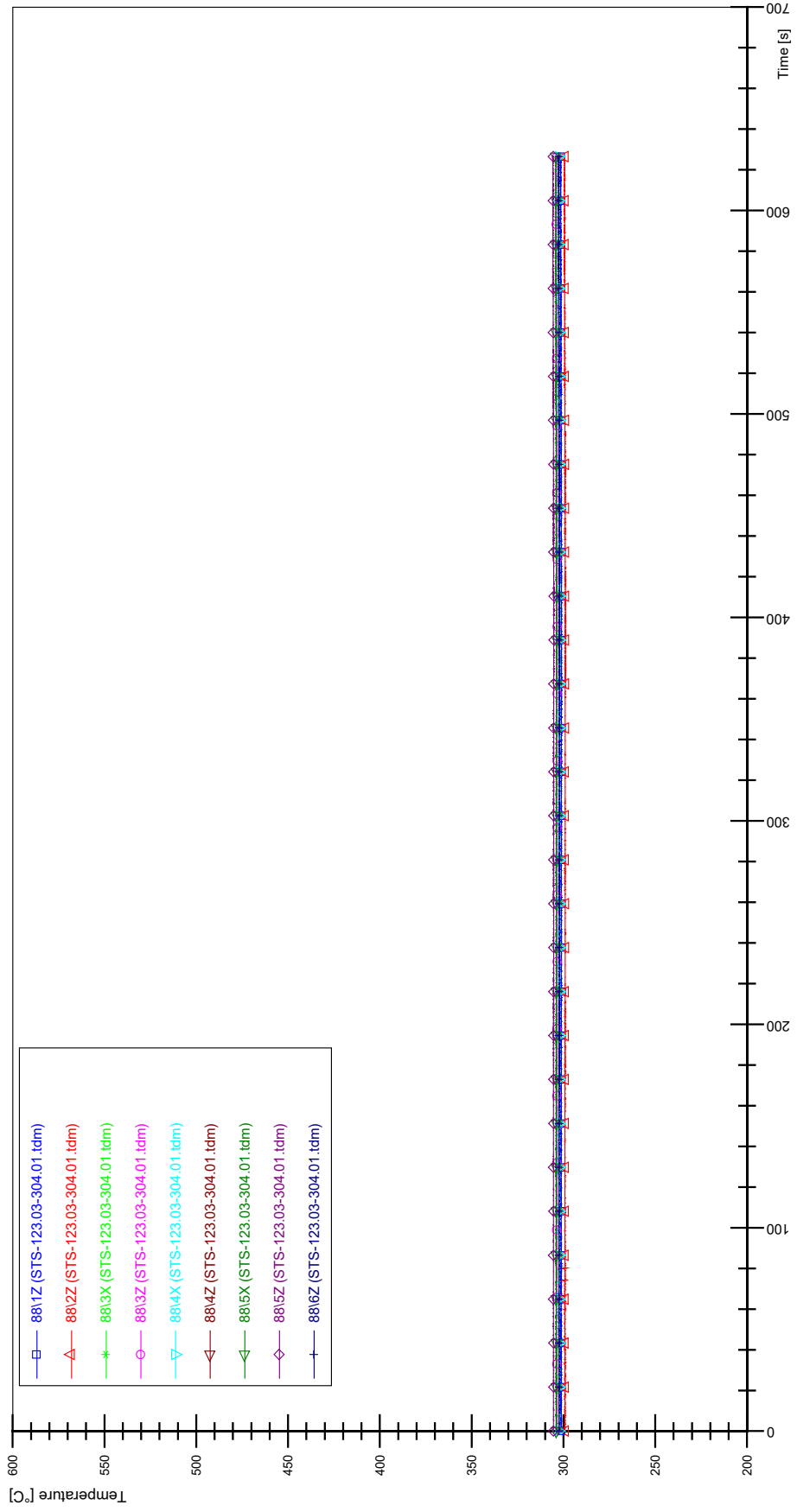
STS-123.03-304.01_Rod_86



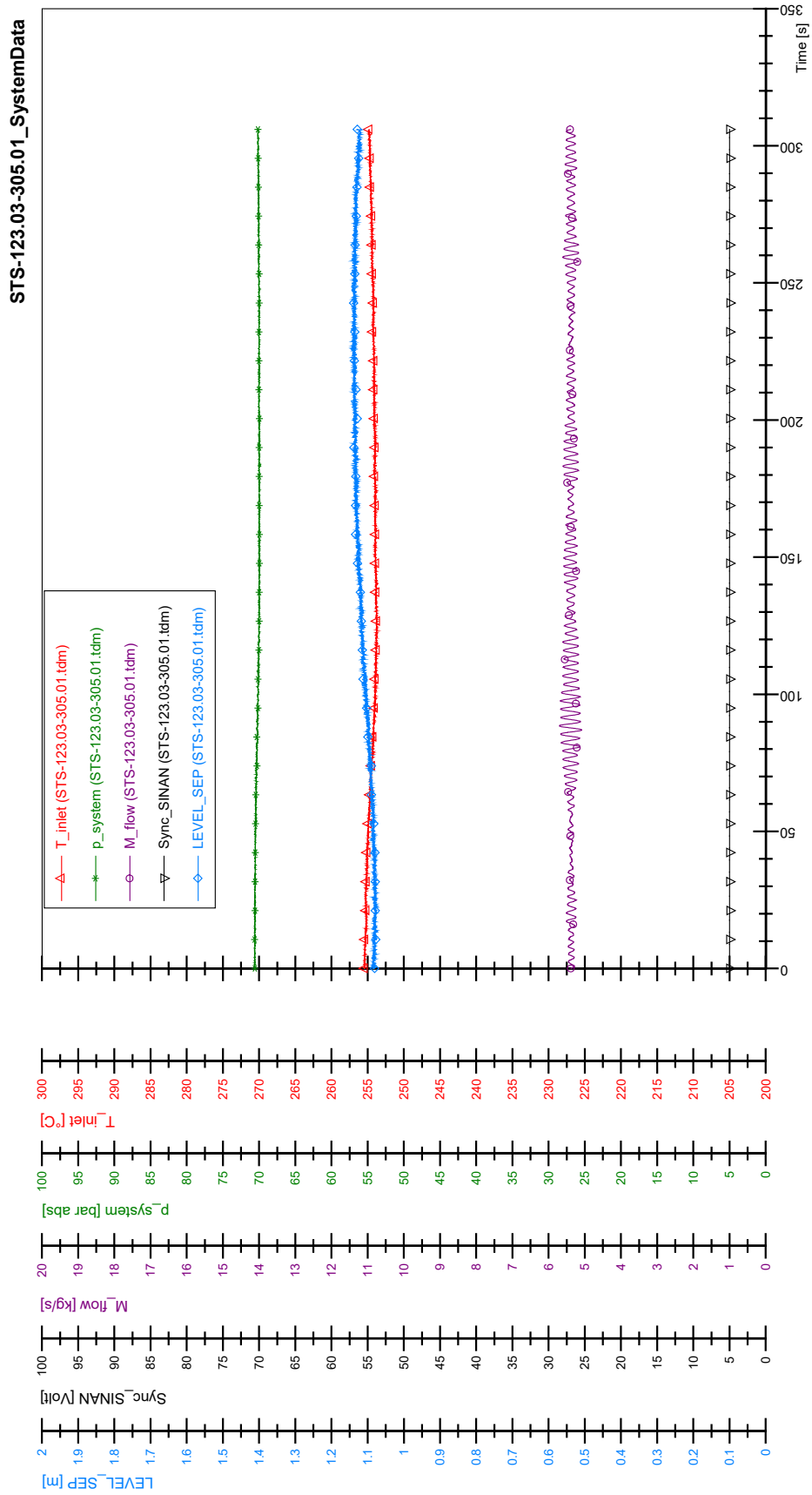
STS-123.03-304.01_Rod_87

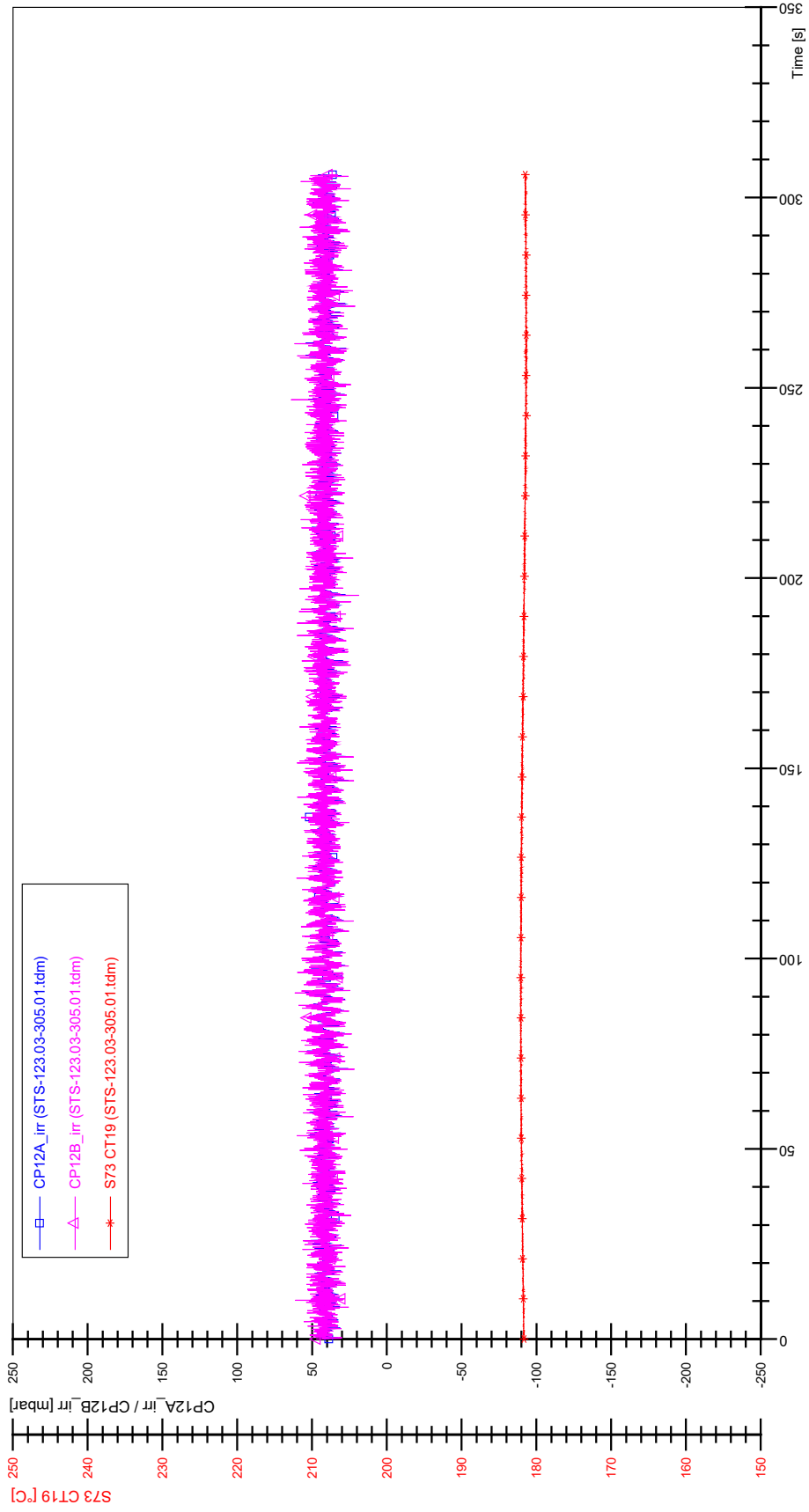


STS-123.03-304.01_Rod_88

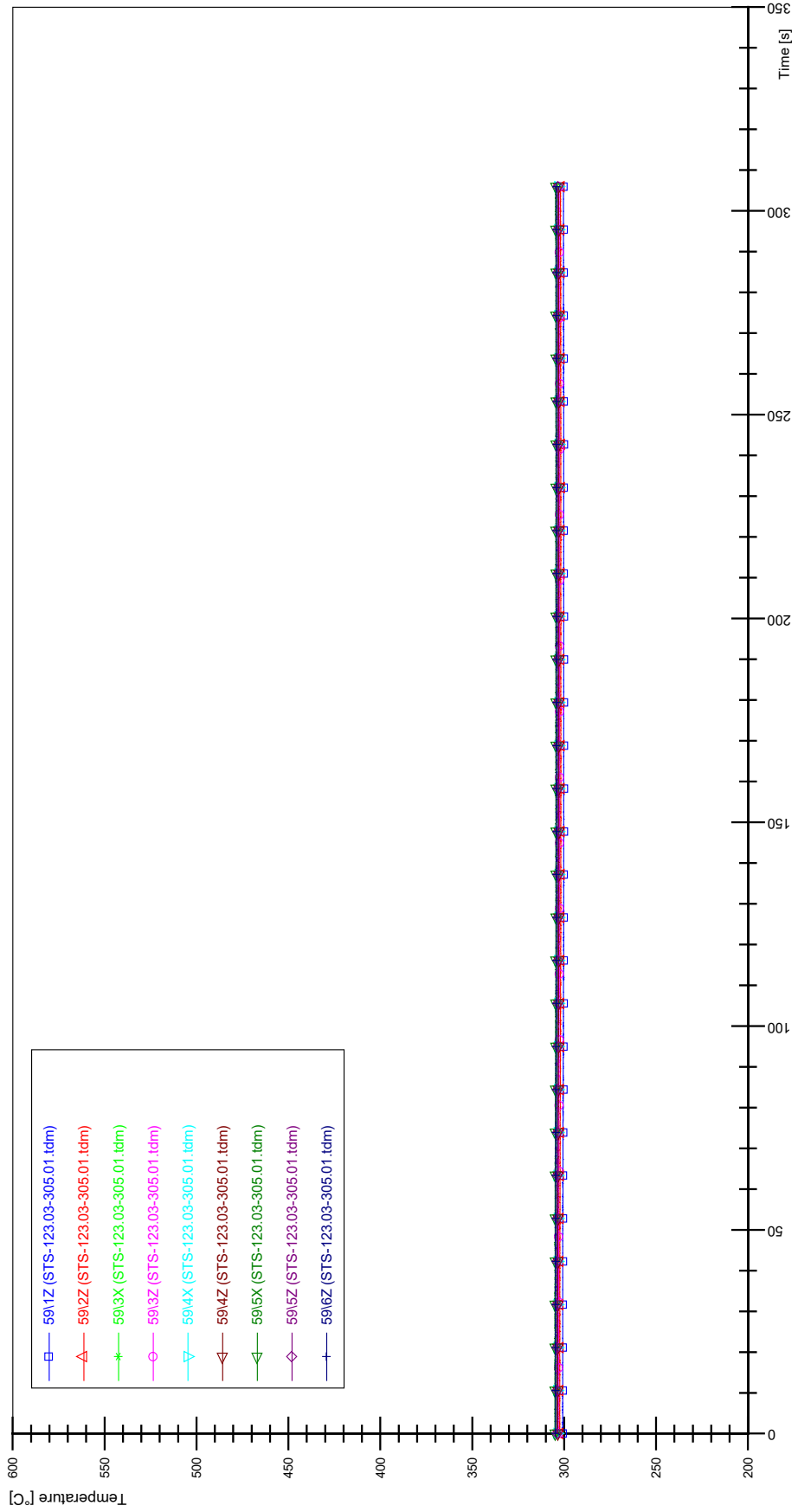


APPENDIX RR PLOTS OF INSTABILITY TEST STS-123.03-305.01

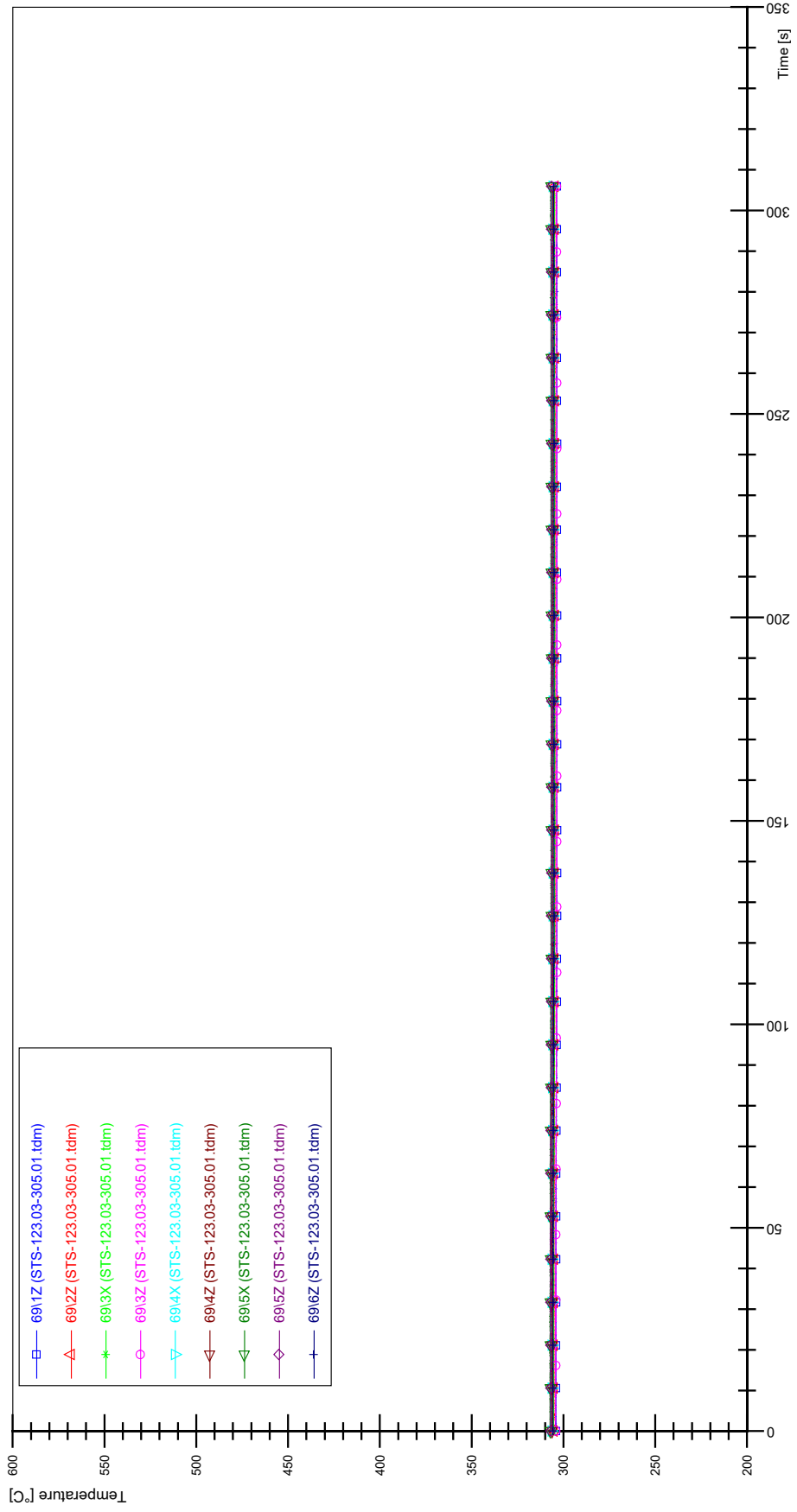




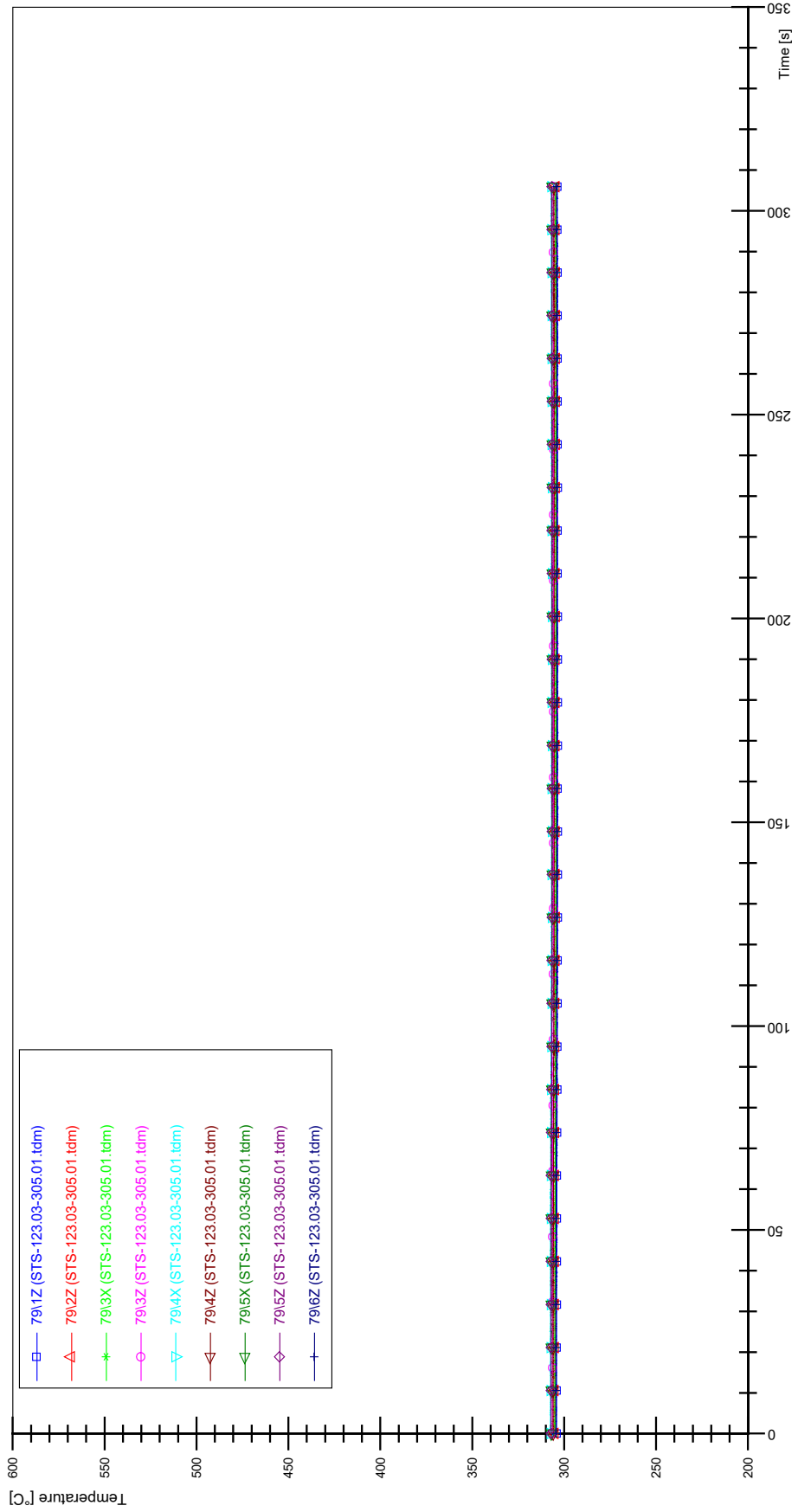
STS-123.03-305.01_Rod_59



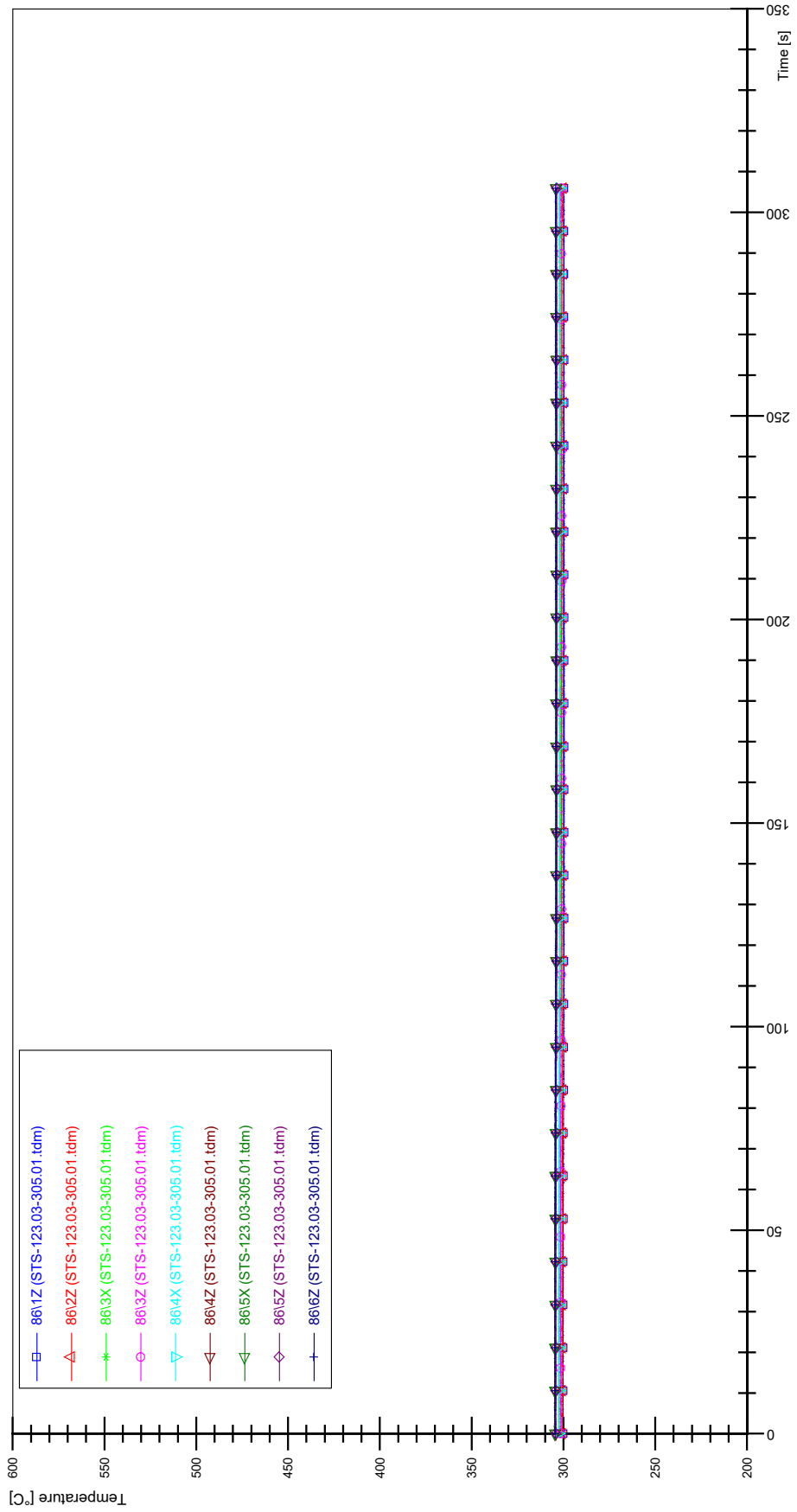
STS-123.03-305.01_Rod_69



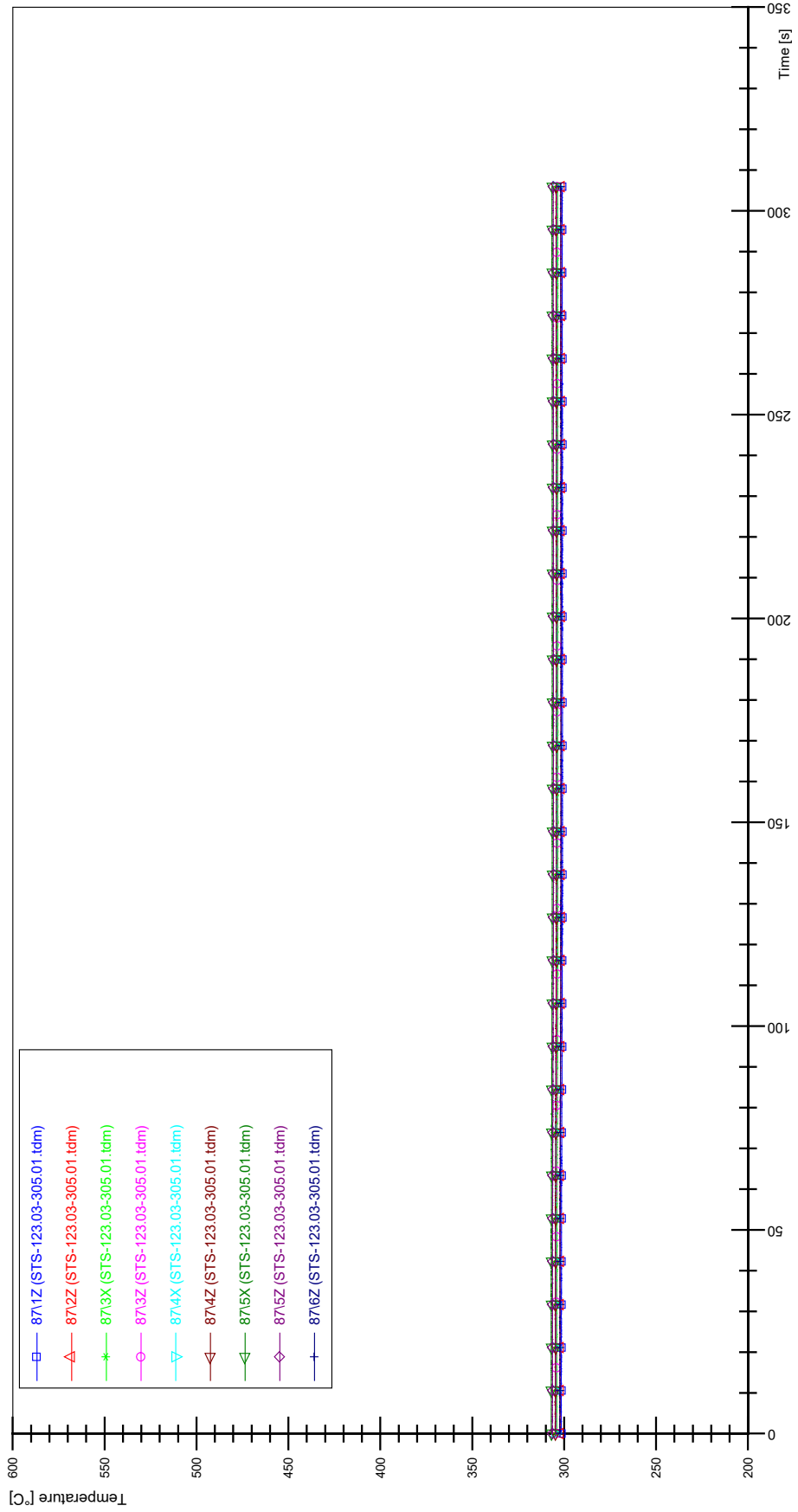
STS-123.03-305.01_Rod_79



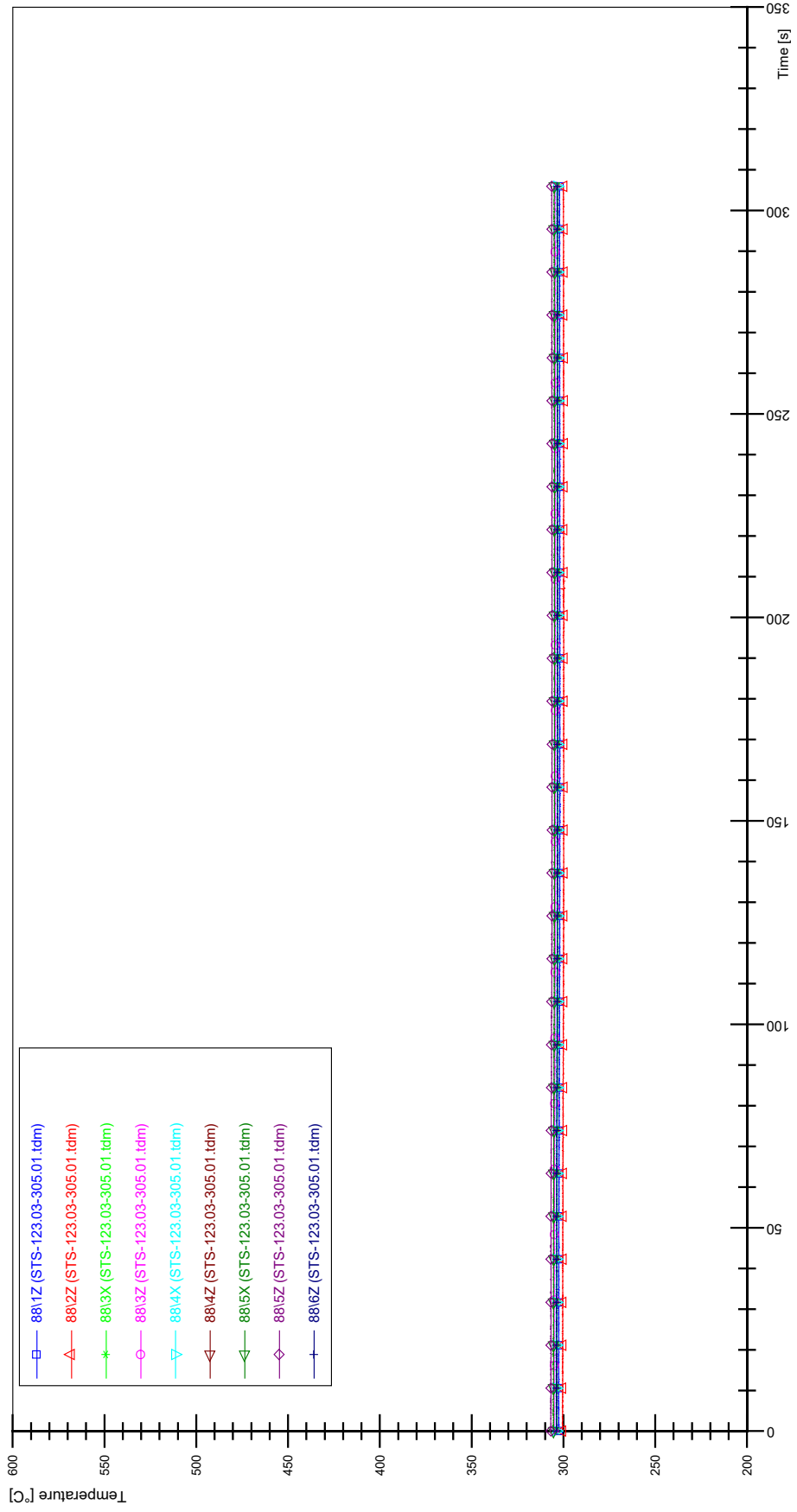
STS-123.03-305.01_Rod_86



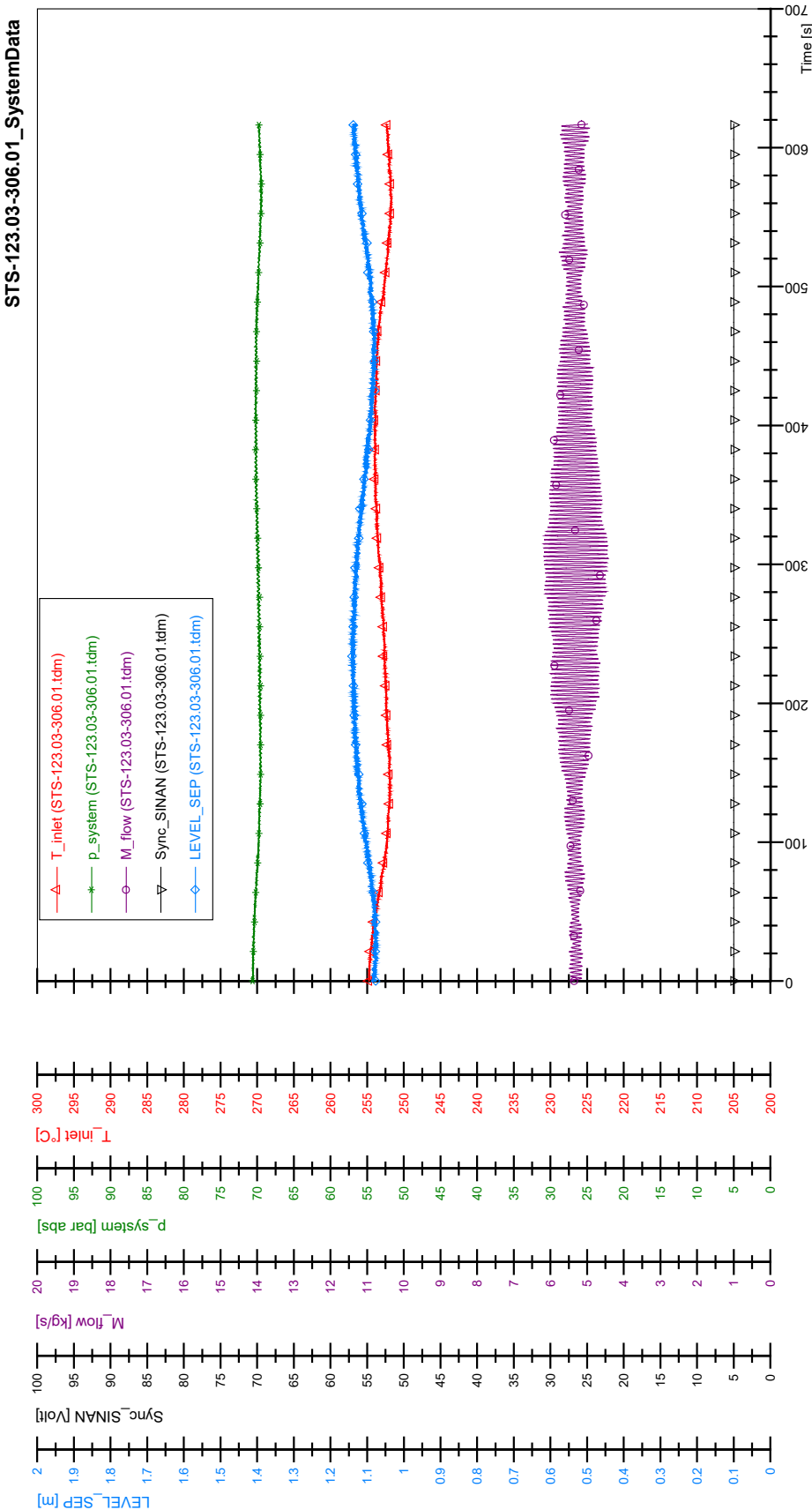
STS-123.03-305.01_Rod_87



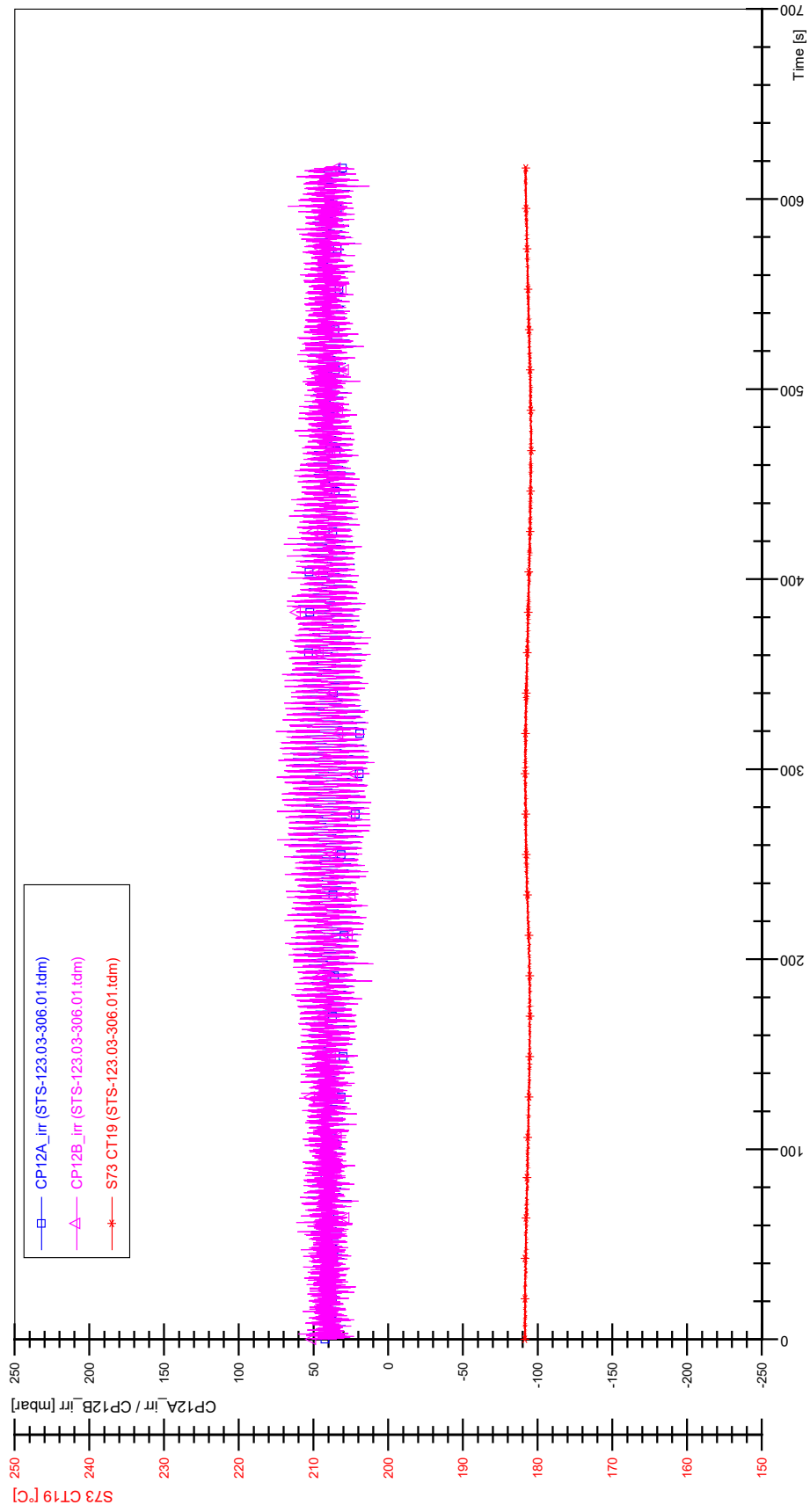
STS-123.03-305.01_Rod_88



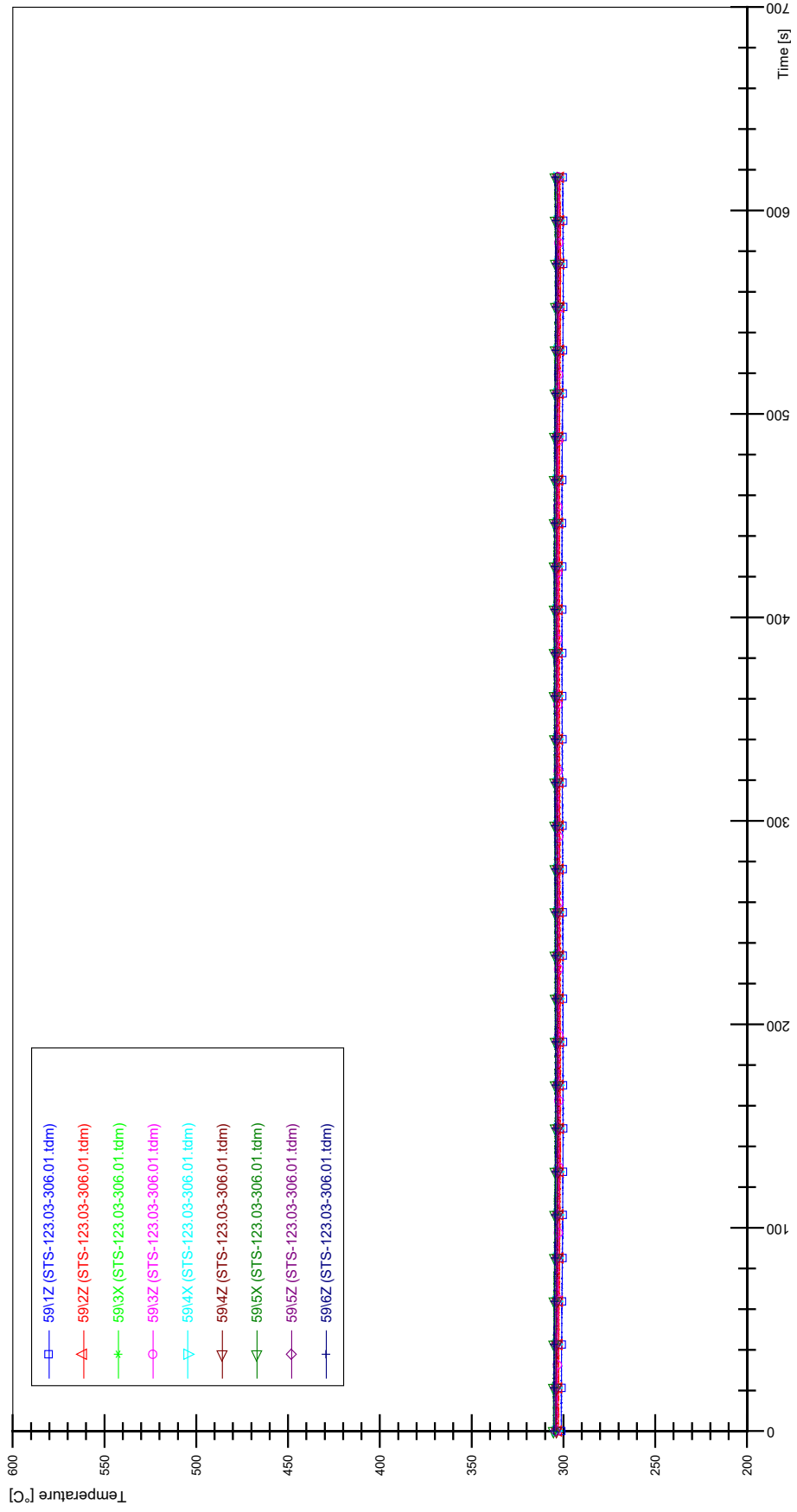
APPENDIX SS PLOTS OF INSTABILITY TEST STS-123.03-306.01



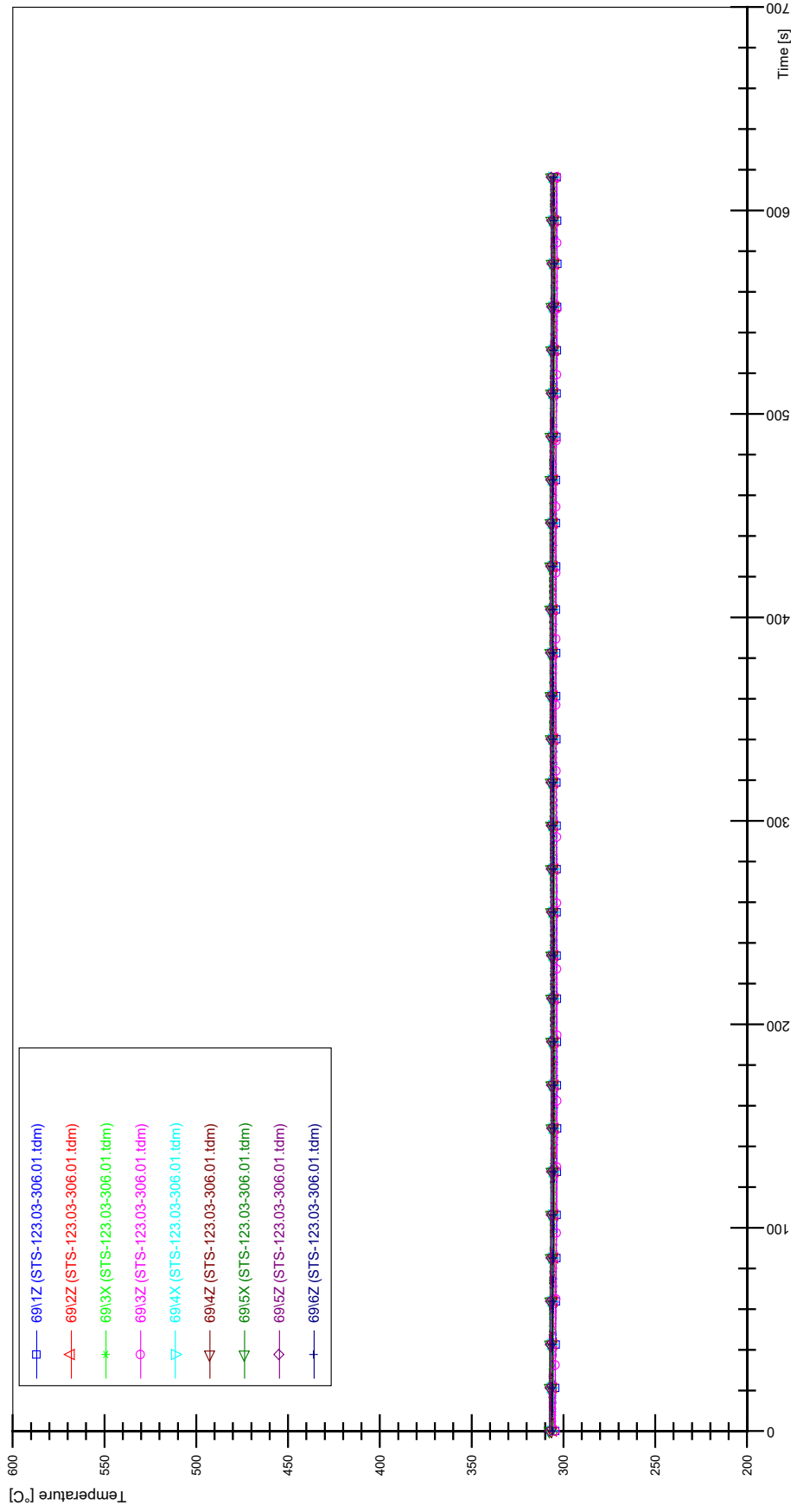
STS-123.03-306.01_CP12_CT19



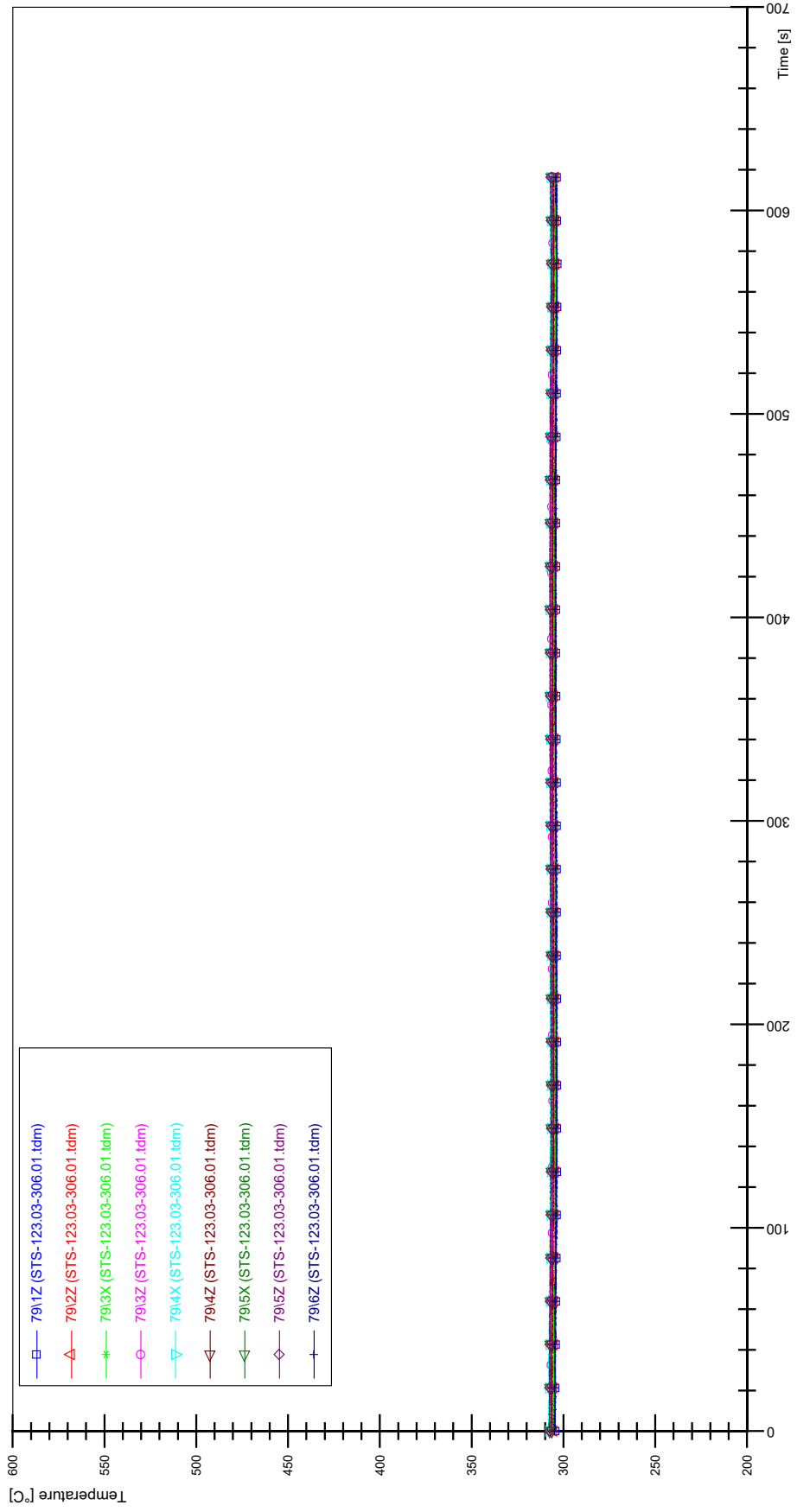
STS-123.03-306.01_Rod_59



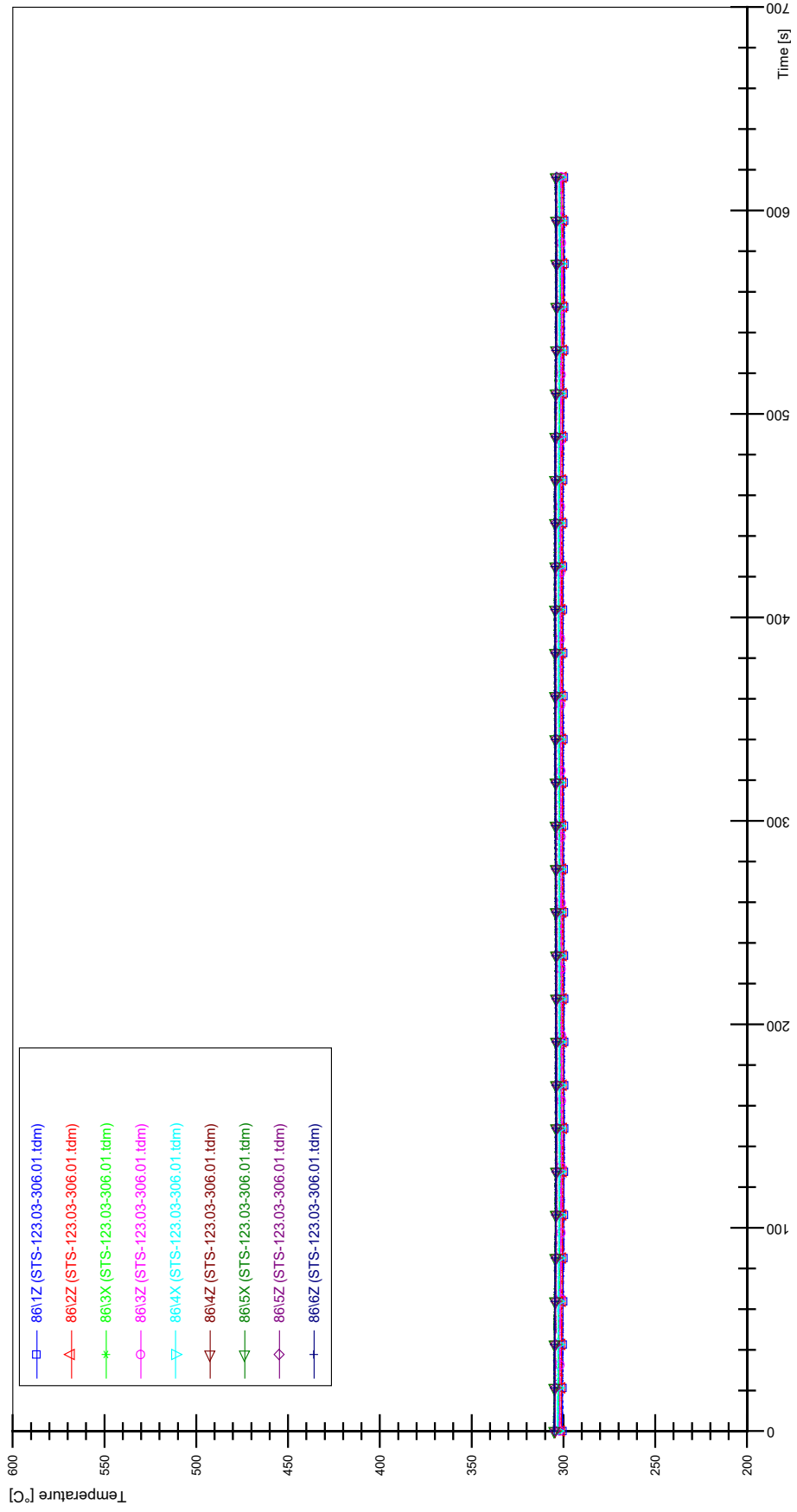
STS-123.03-306.01_Rod_69



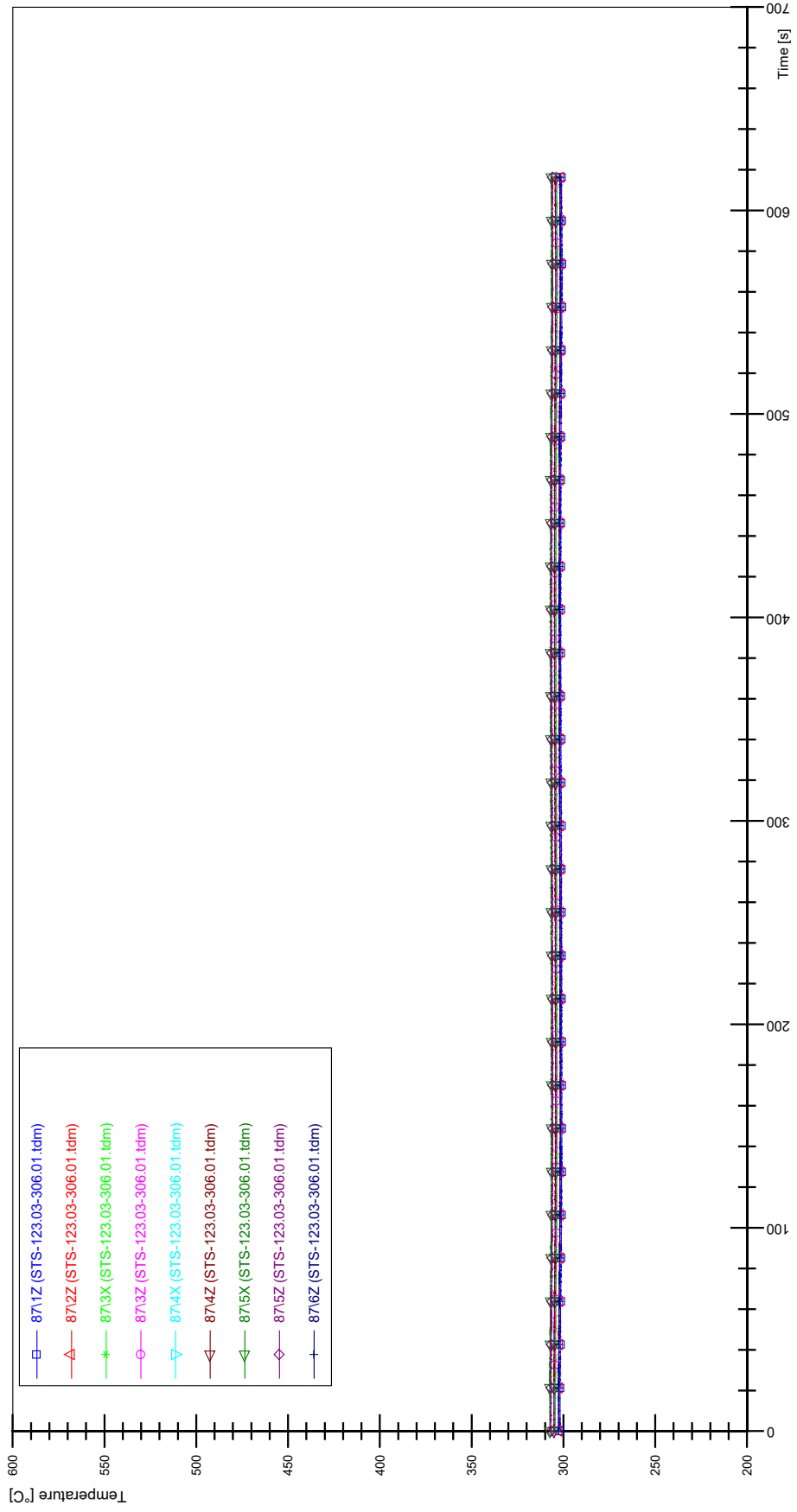
STS-123.03-306.01_Rod_79



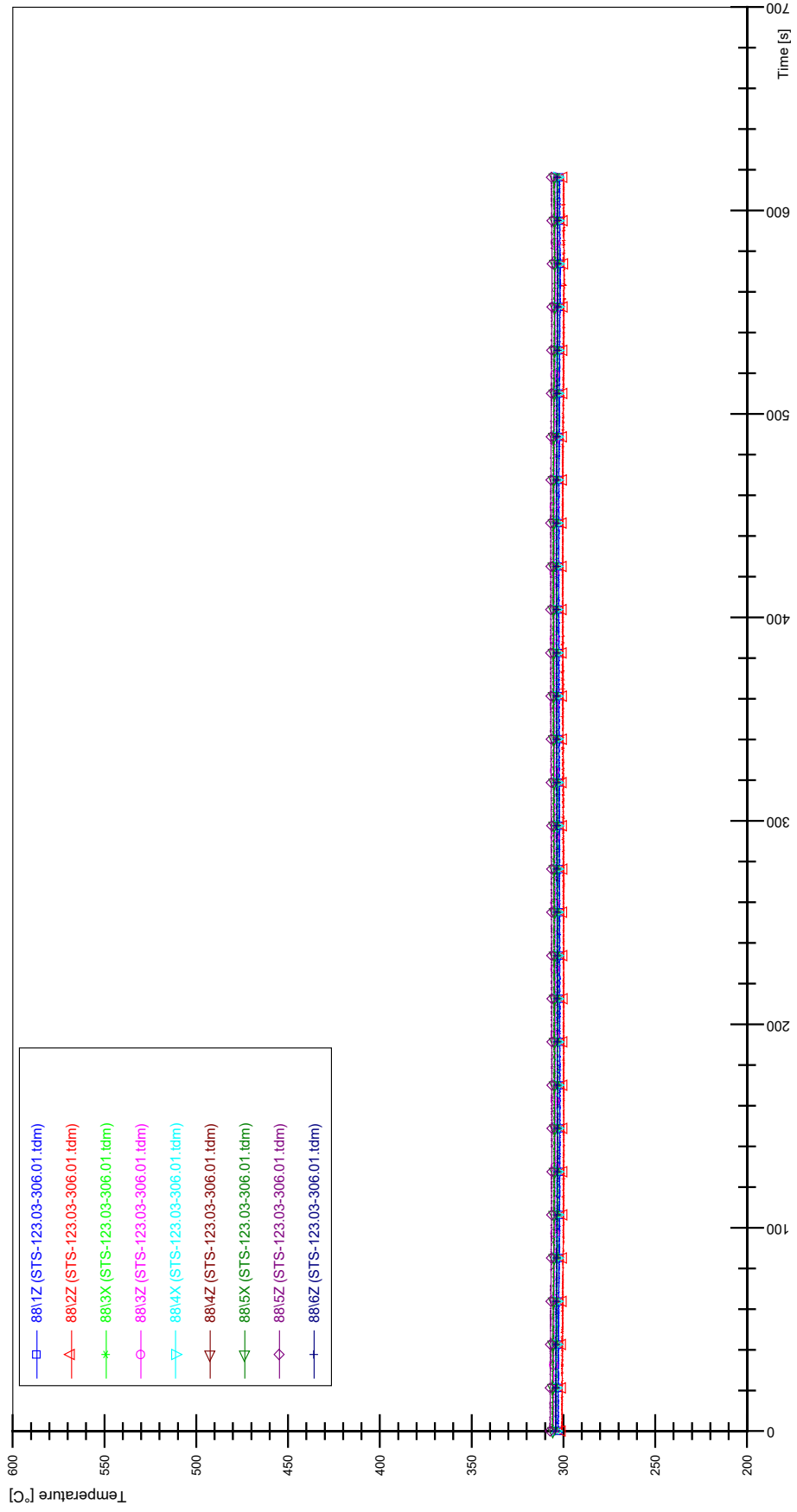
STS-123.03-306.01_Rod_86



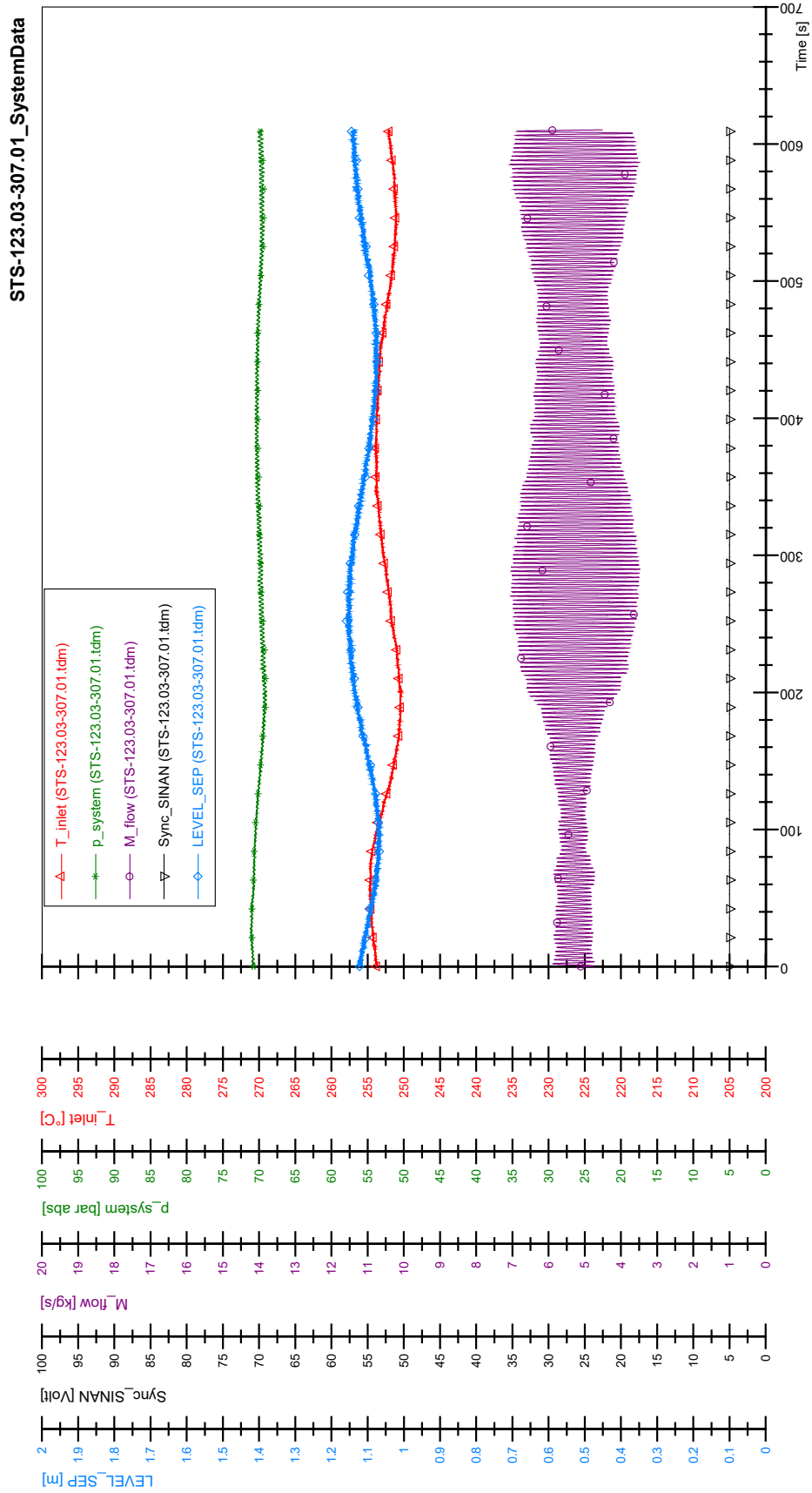
STS-123.03-306.01_Rod_87



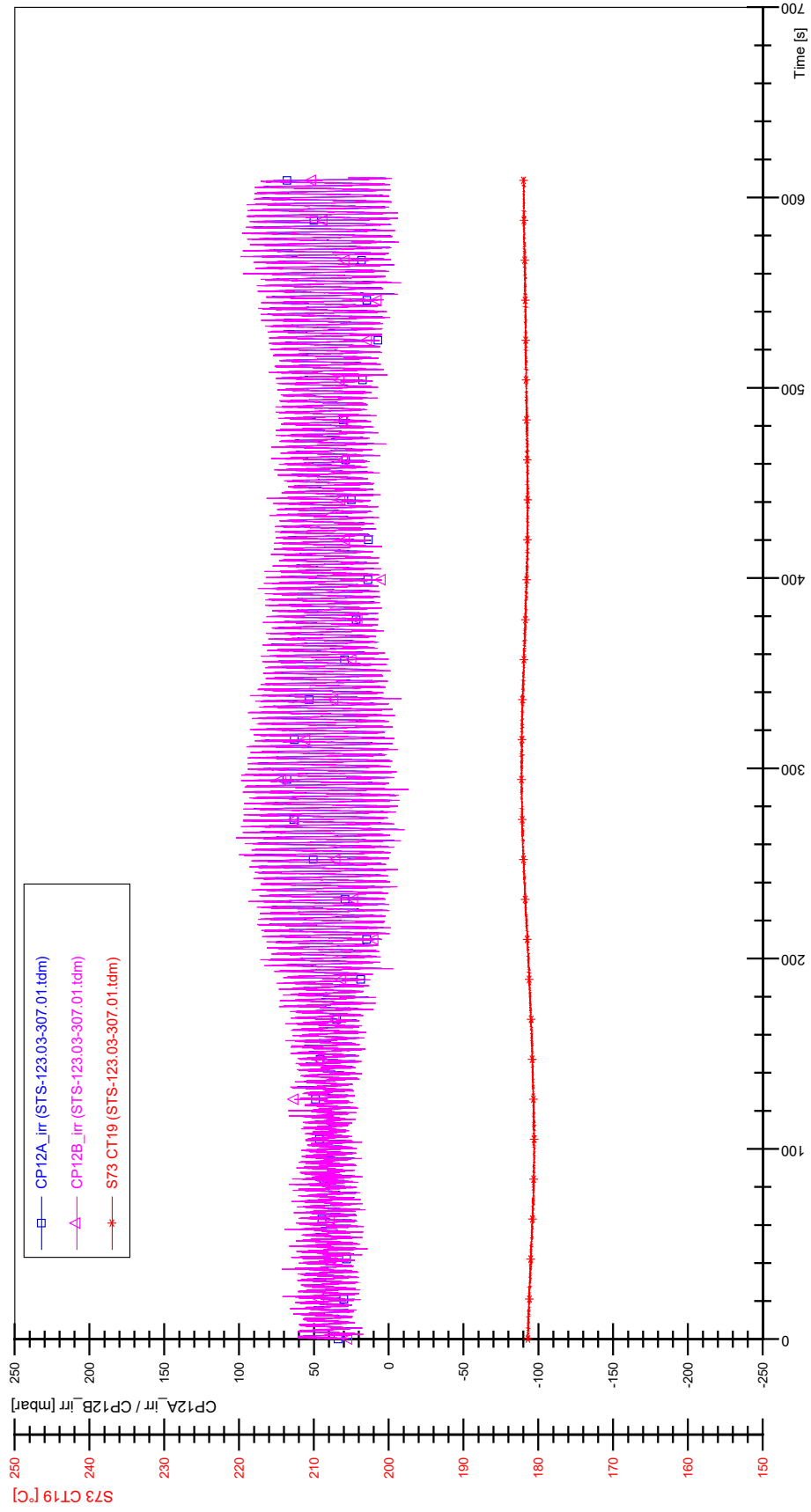
STS-123.03-306.01_Rod_88



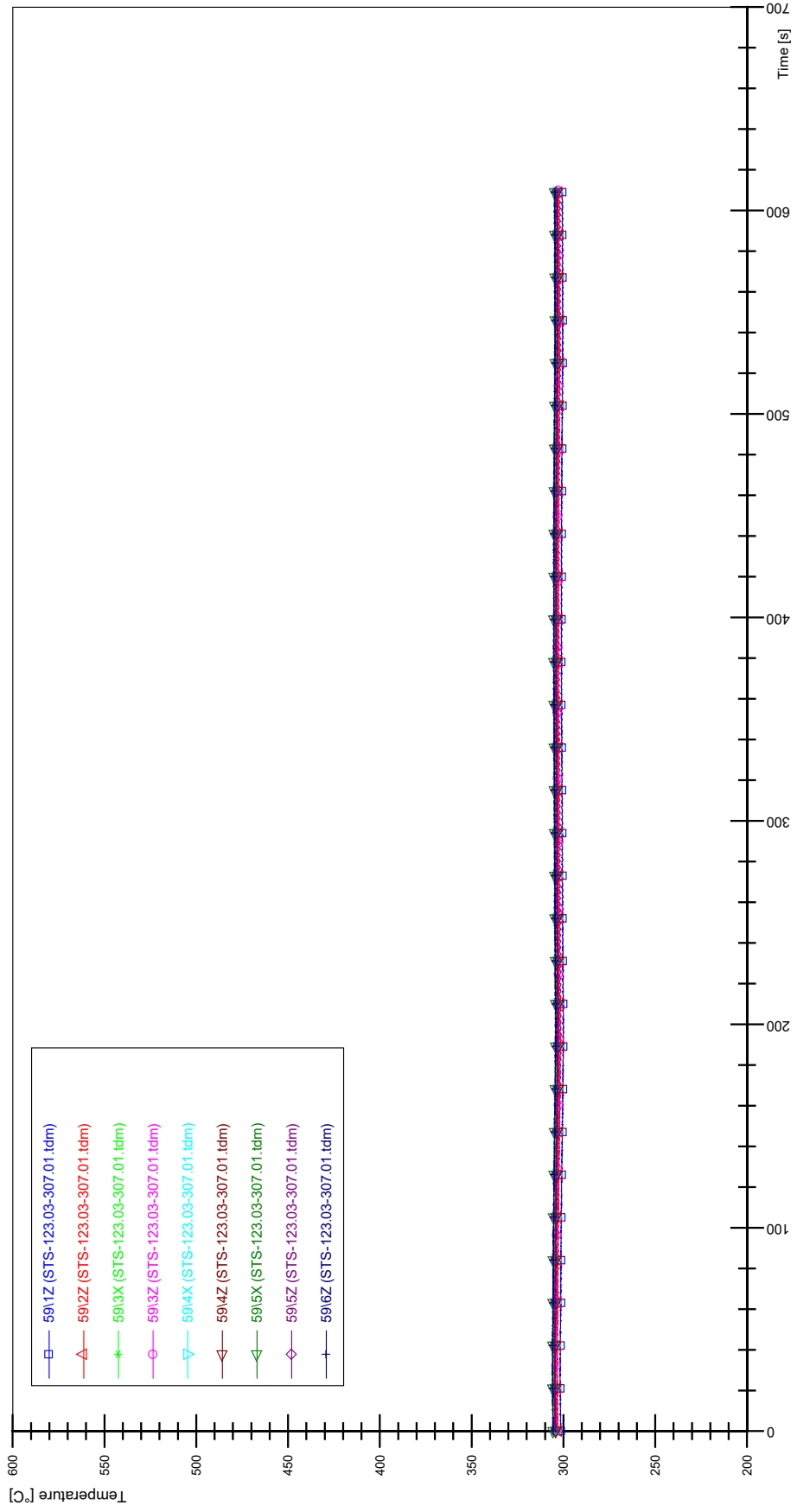
APPENDIX TT PLOTS OF INSTABILITY TEST STS-123.03-307.01



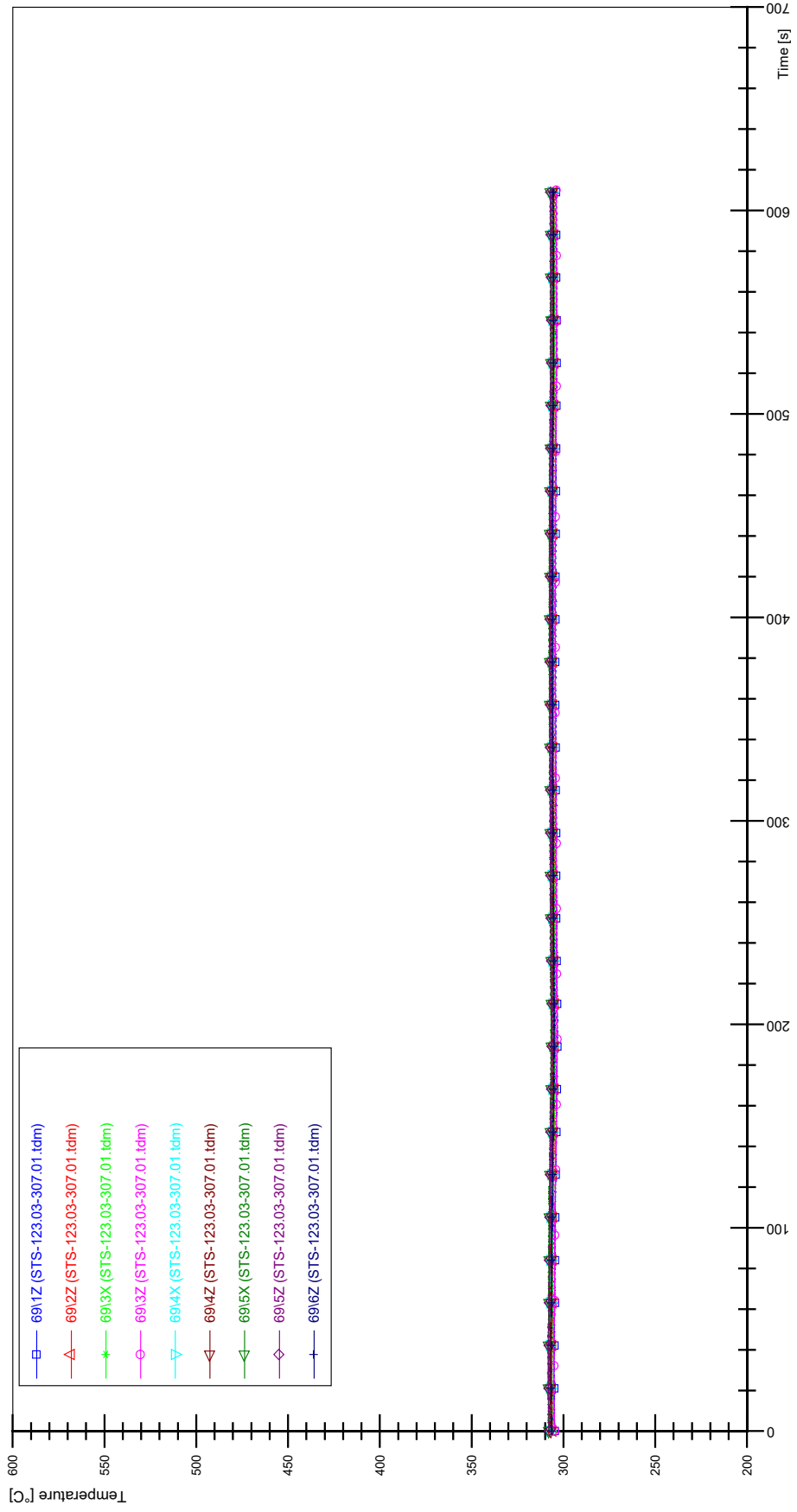
STS-123.03-307.01_CP12_CT19



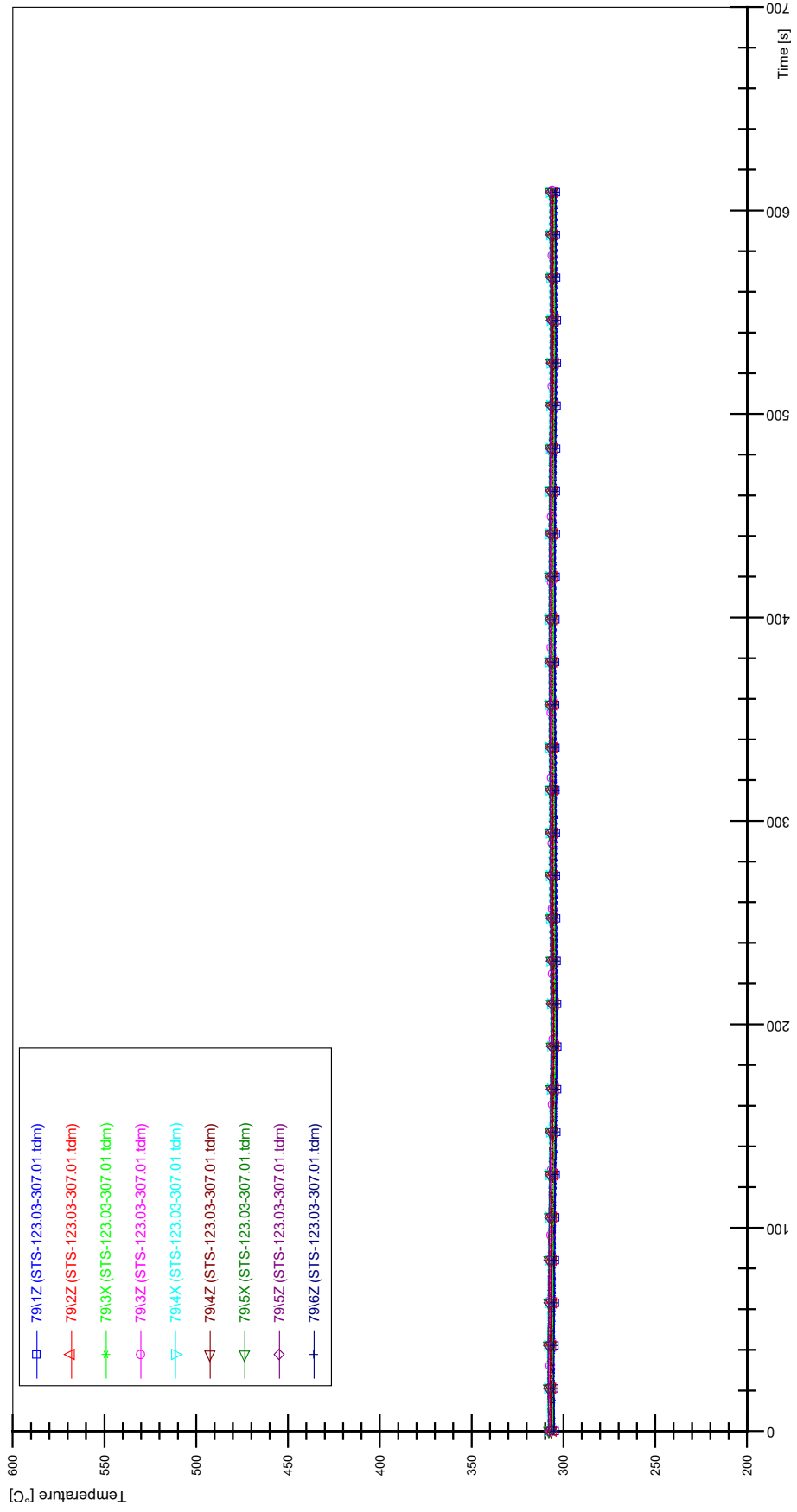
STS-123.03-307.01_Rod_59



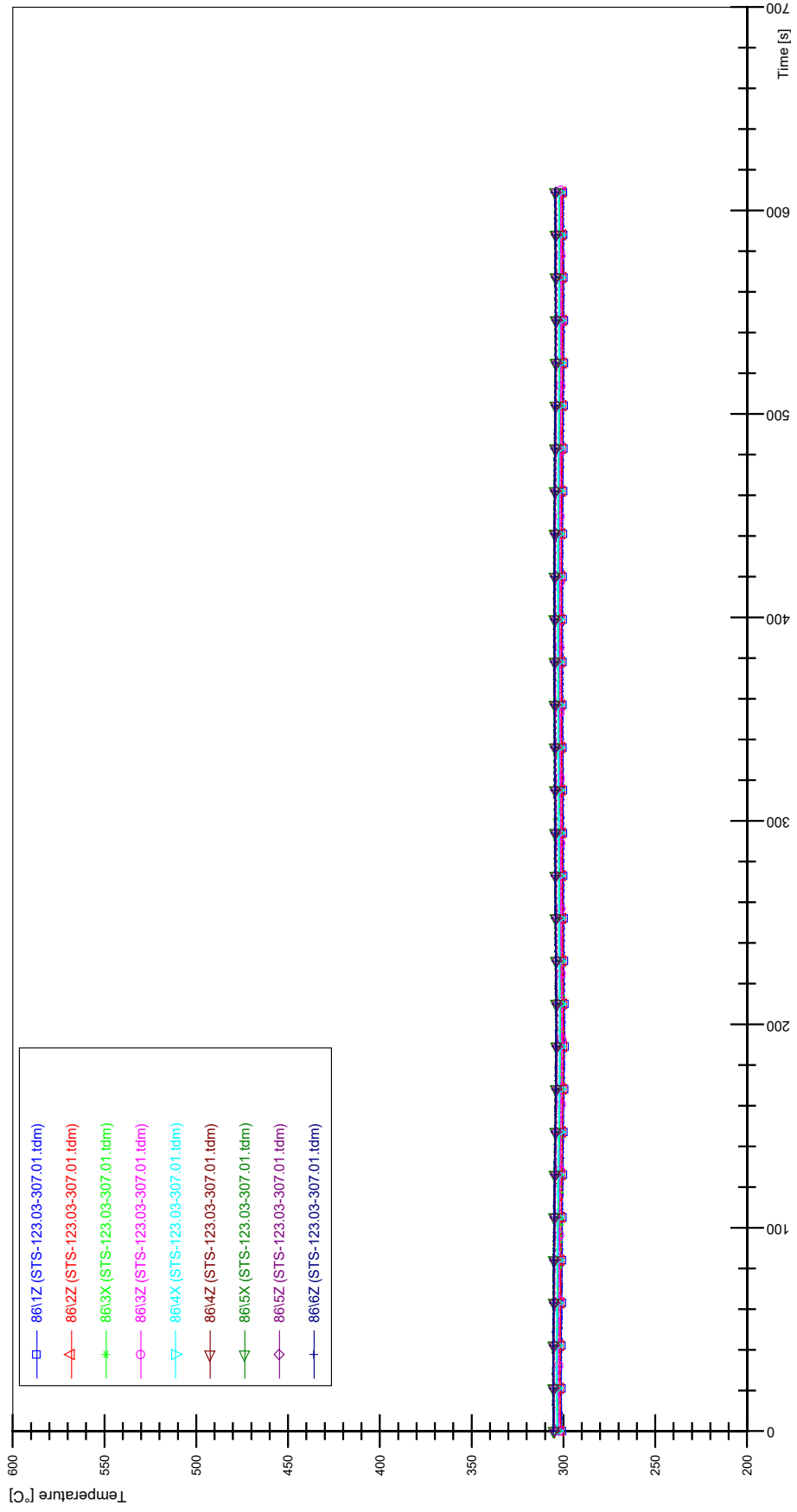
STS-123.03-307.01_Rod_69



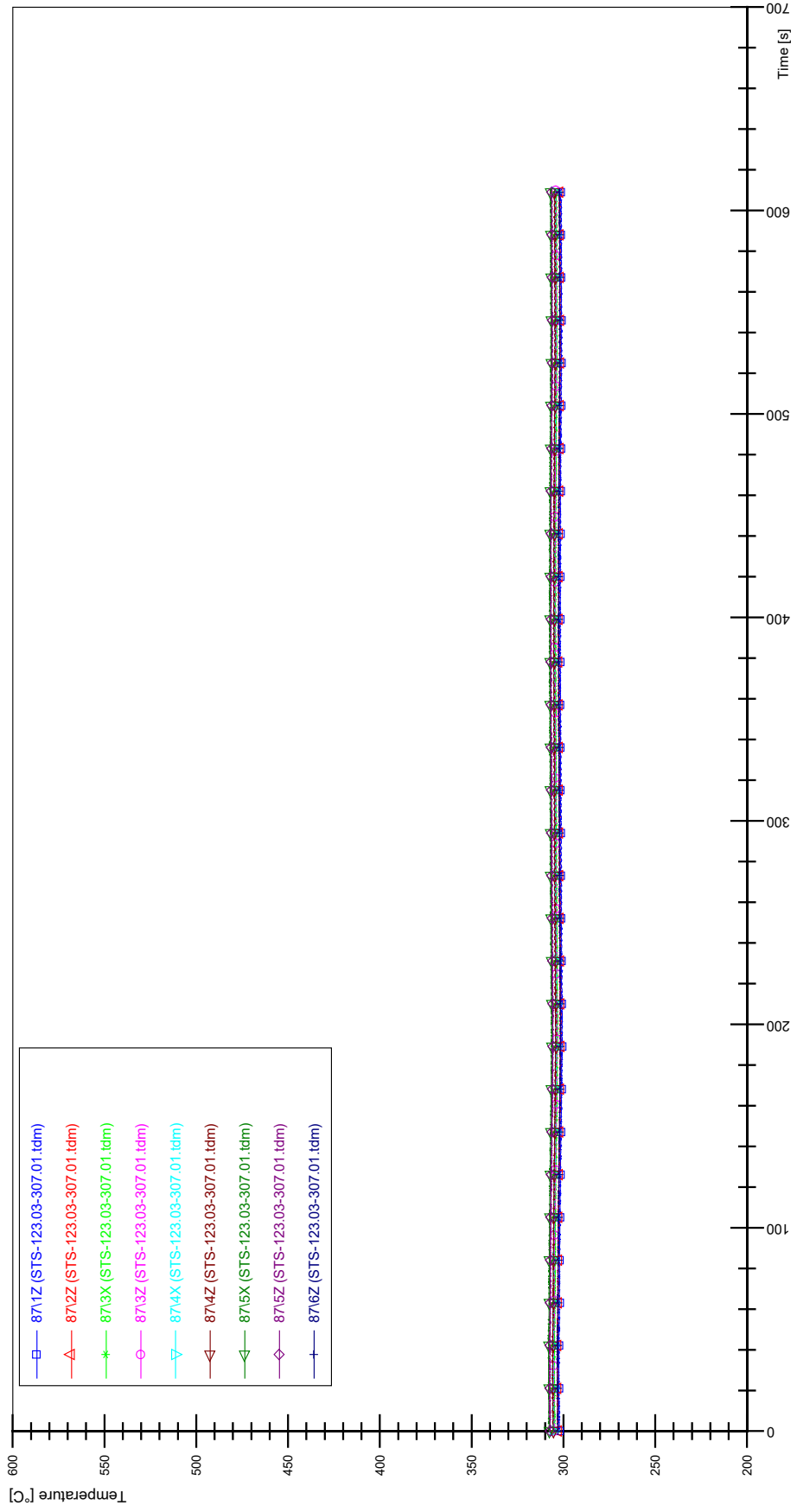
STS-123.03-307.01_Rod_79



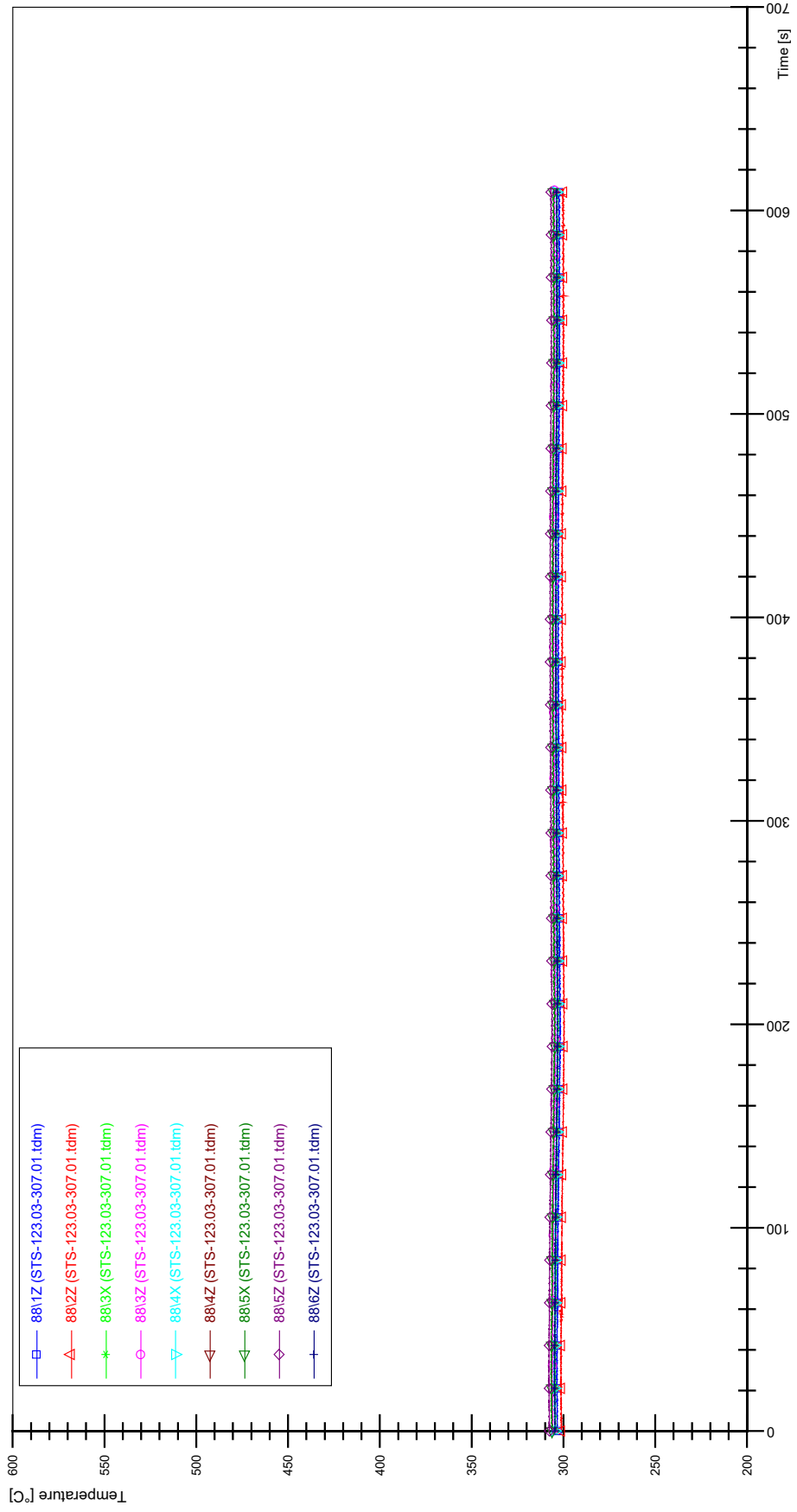
STS-123.03-307.01_Rod_86



STS-123.03-307.01_Rod_87

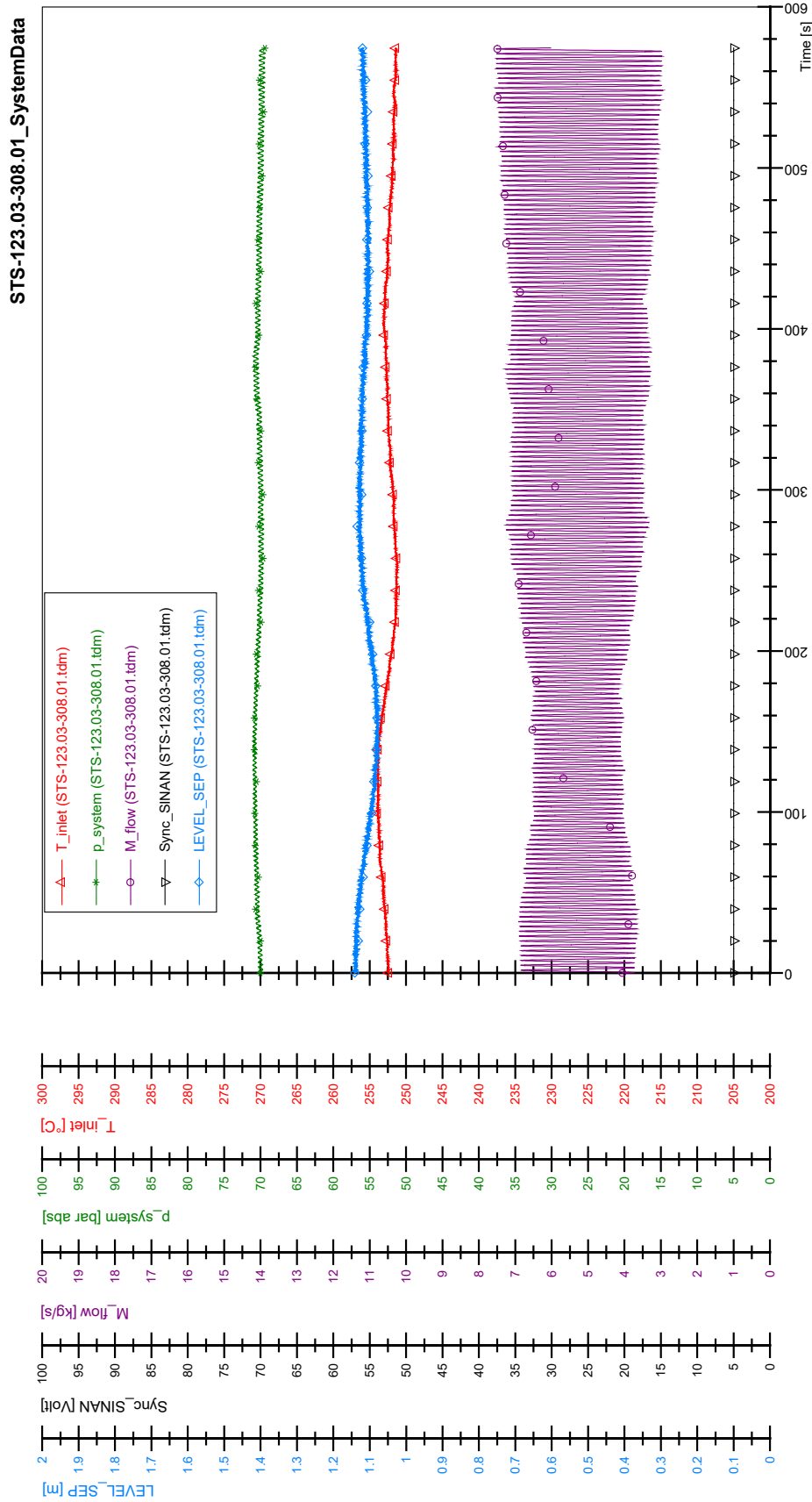


STS-123.03-307.01_Rod_88



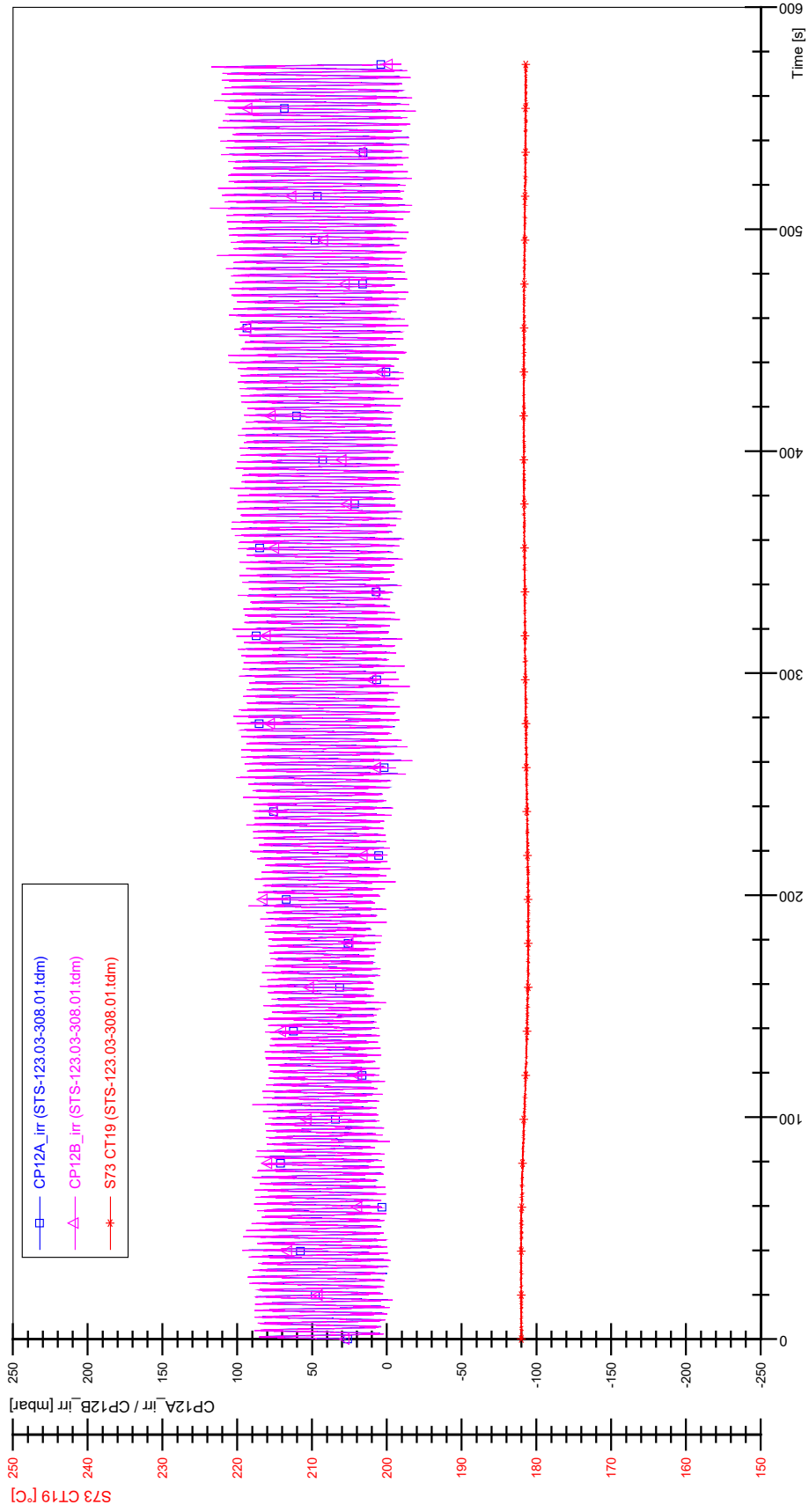
APPENDIX UU PLOTS OF INSTABILITY TEST STS-123.03-308.01

UU-1

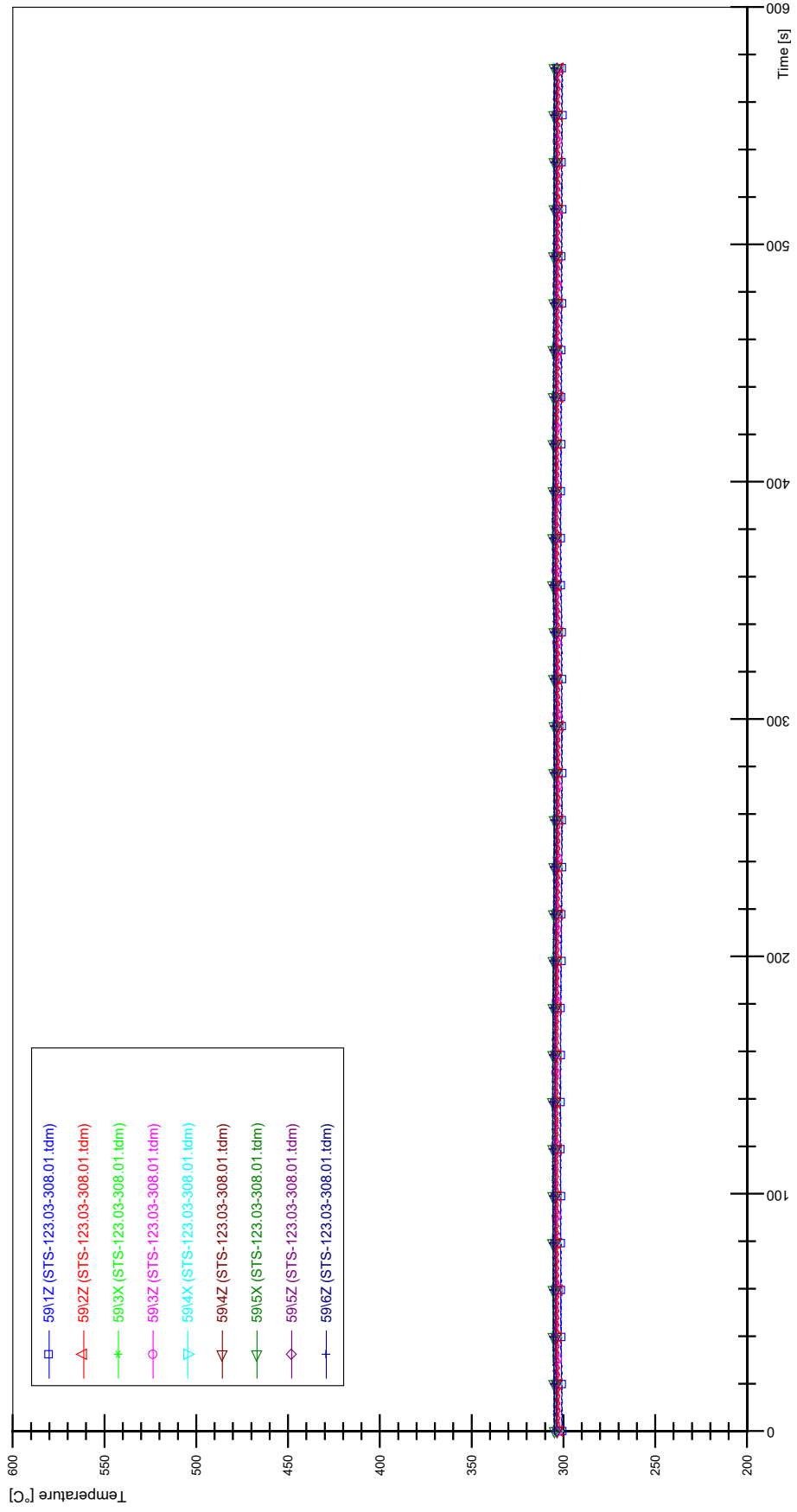


UU-1

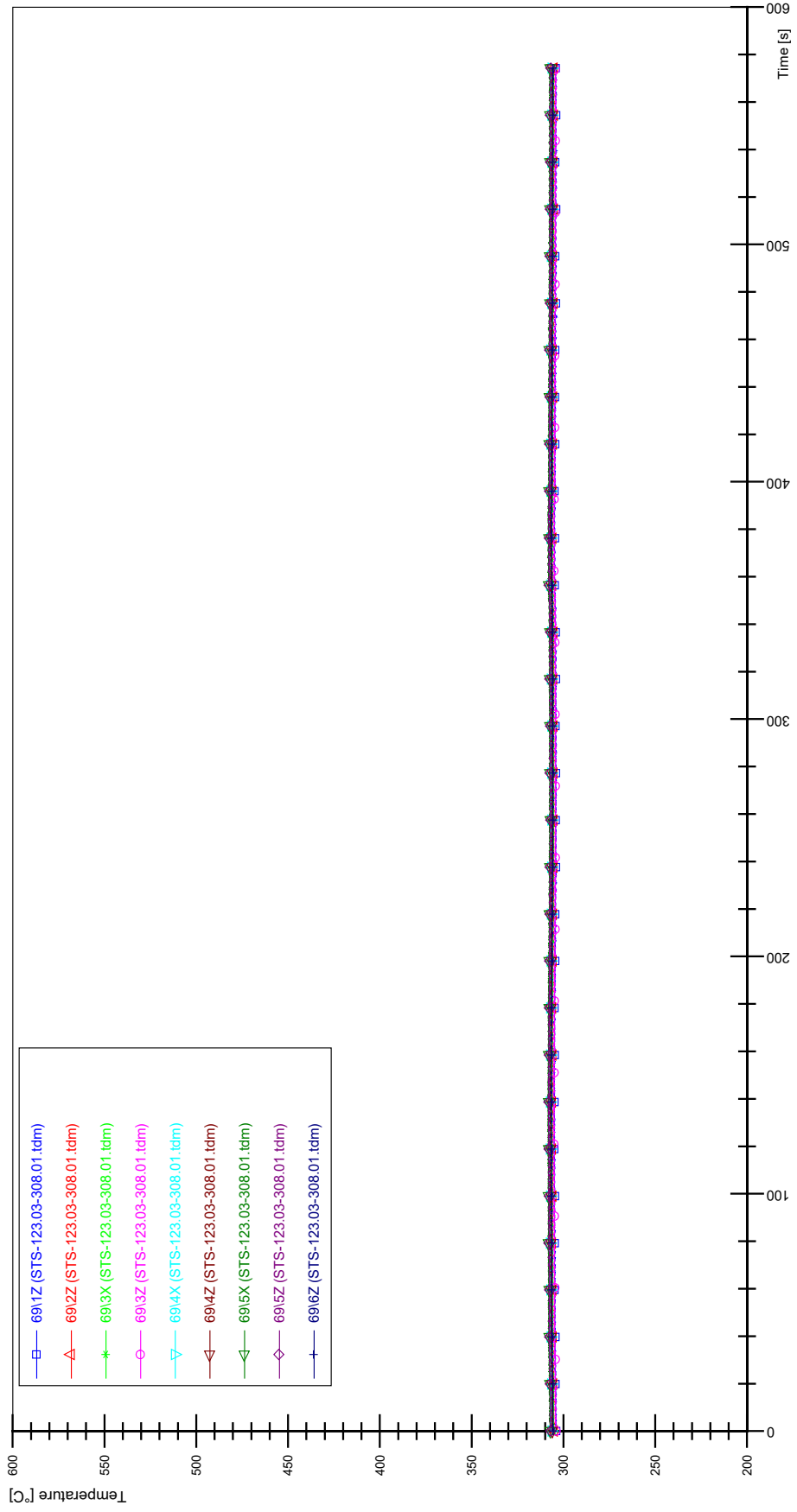
STS-123.03-308.01_CP12_CT19



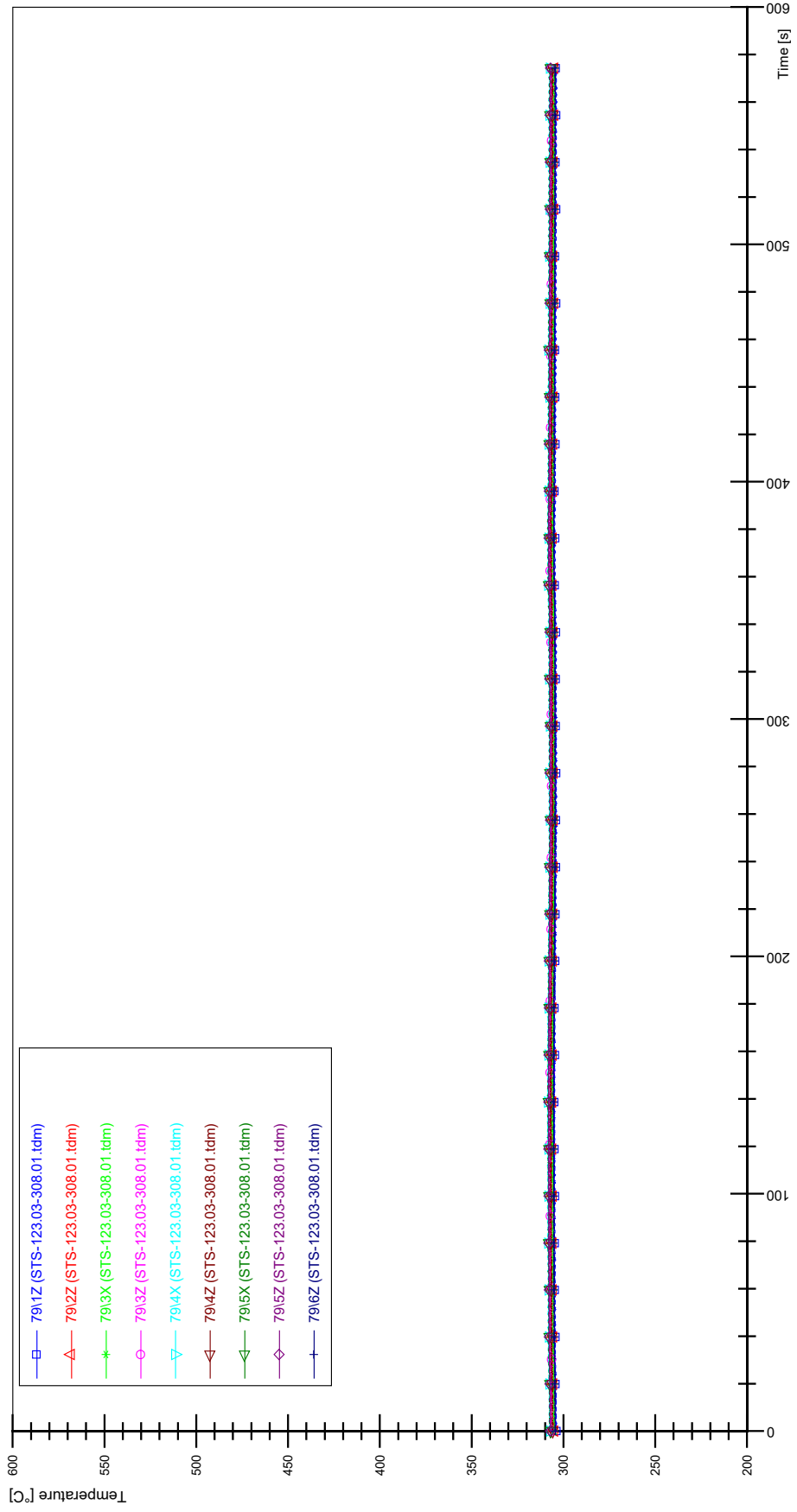
STS-123.03-308.01_Rod_59



STS-123.03-308.01_Rod_69

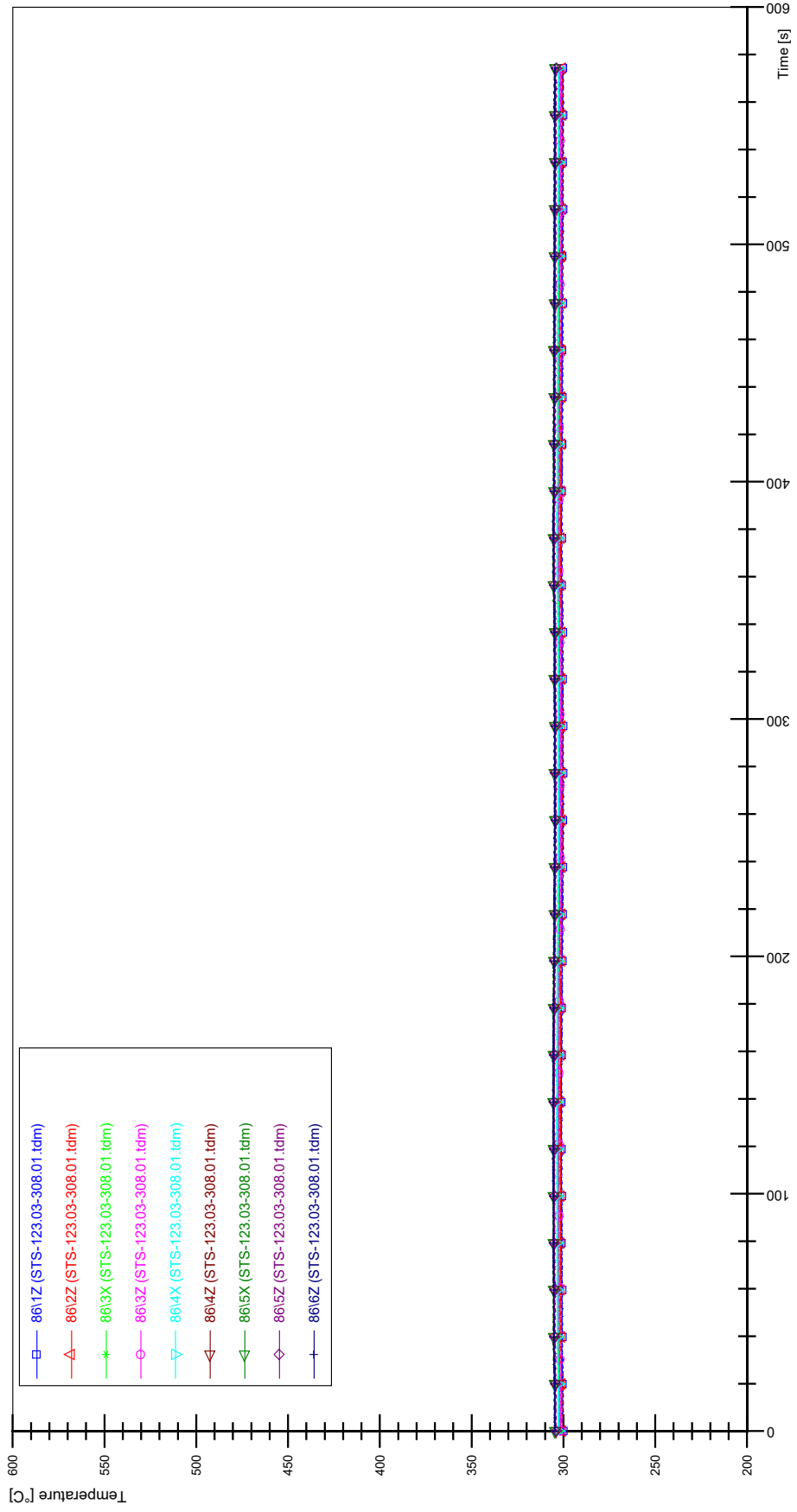


STS-123.03-308.01_Rod_79

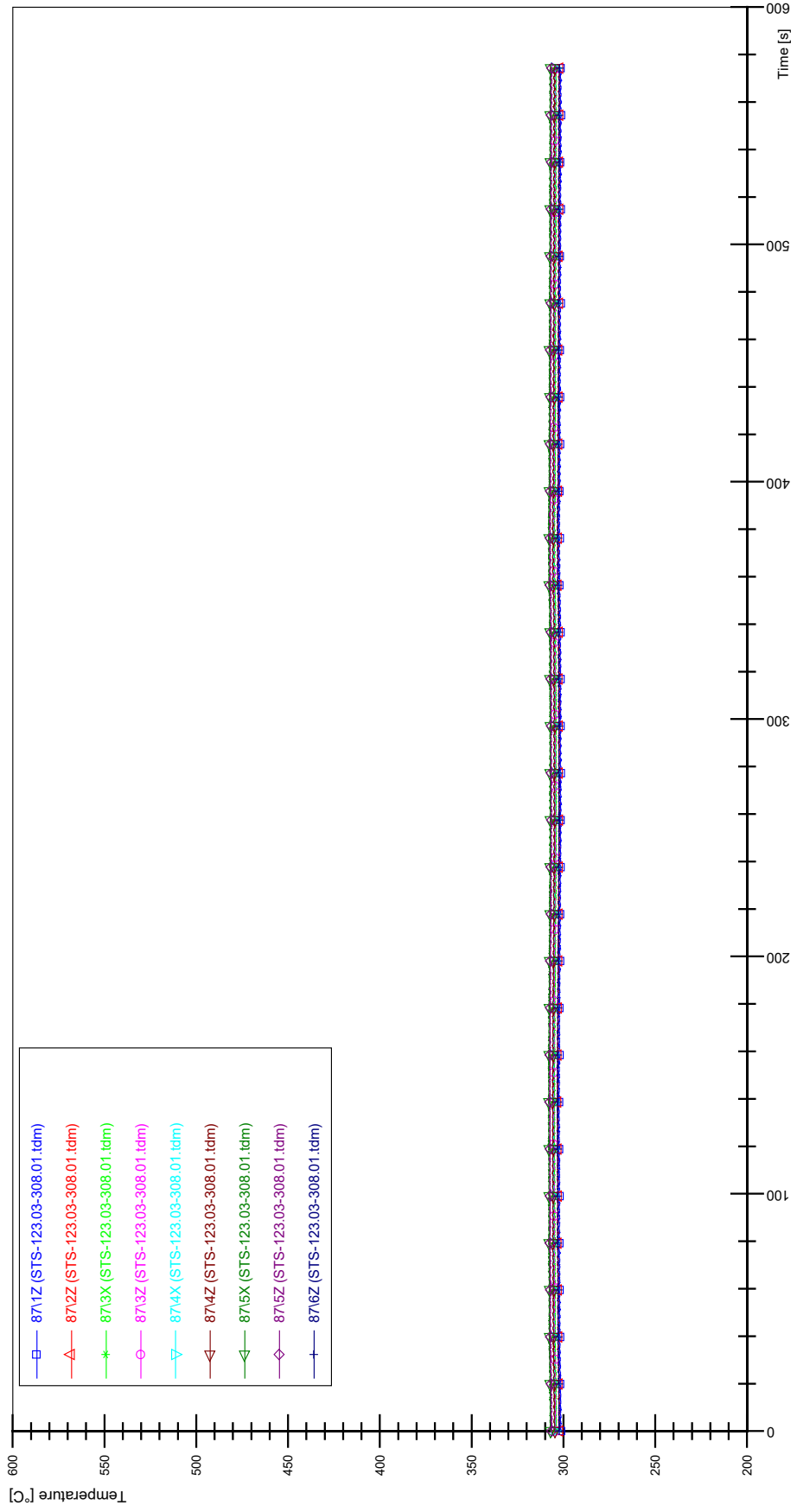


UU-5

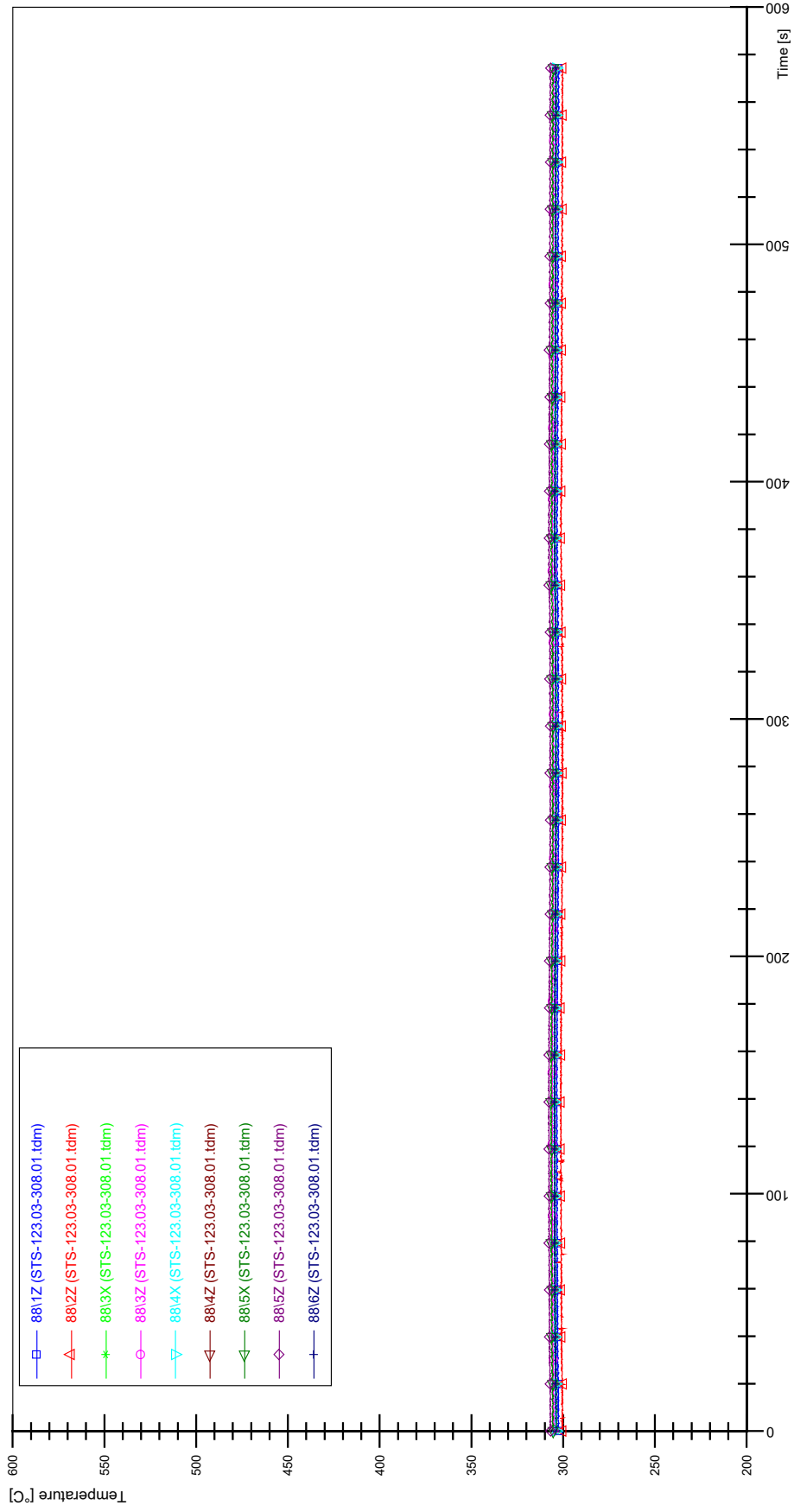
STS-123.03-308.01_Rod_86



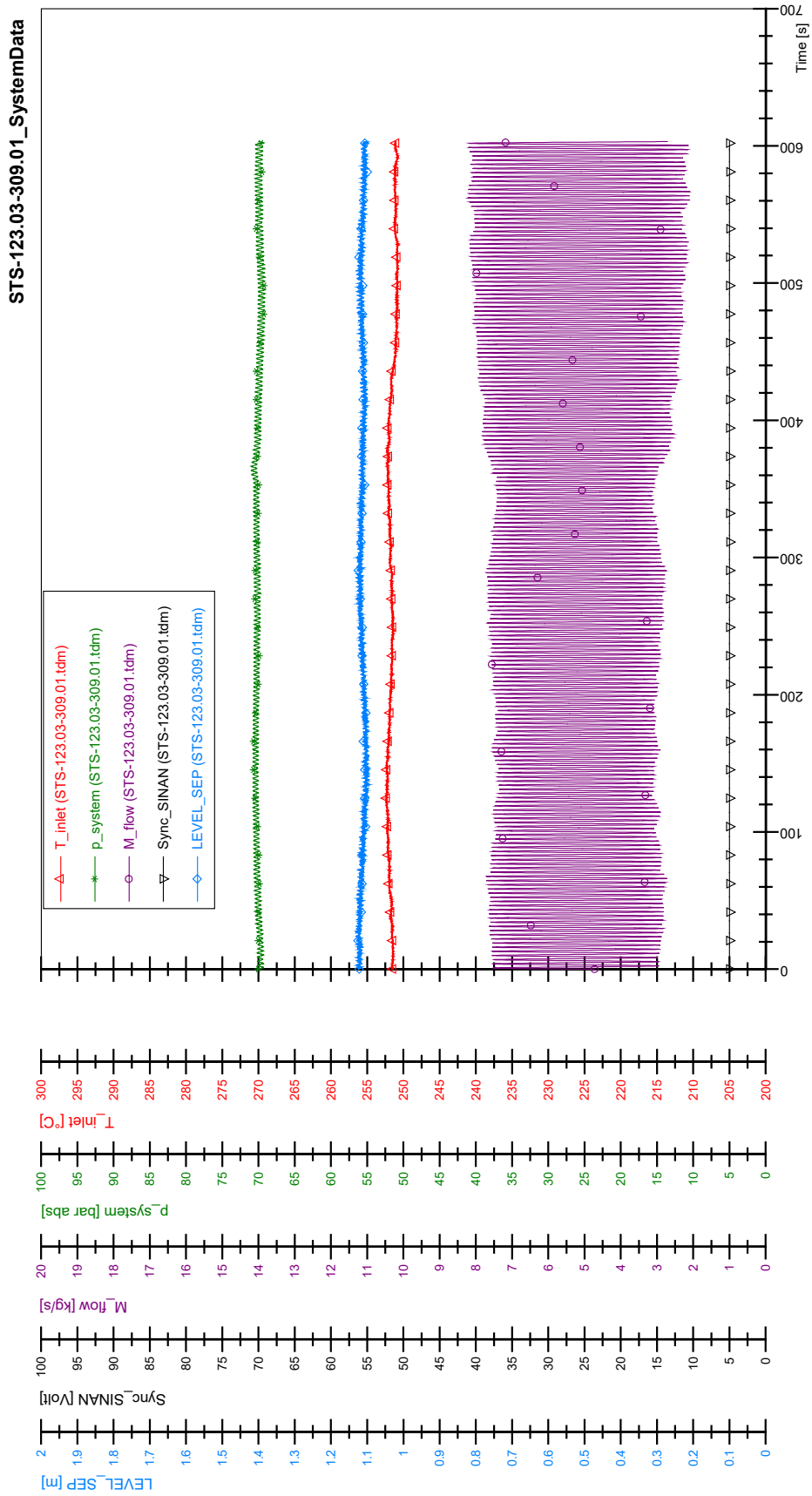
STS-123.03-308.01_Rod_87



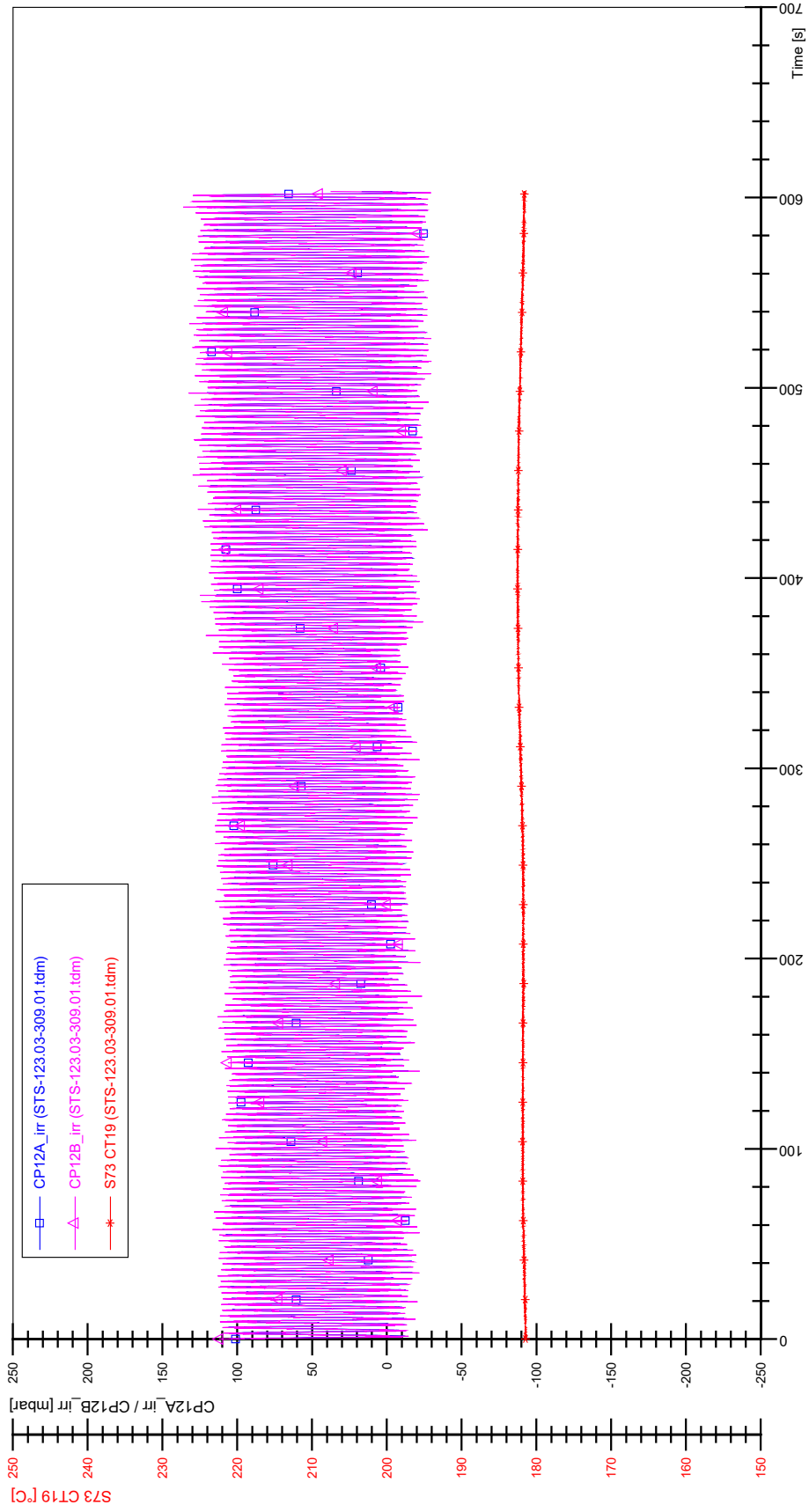
STS-123.03-308.01_Rod_88



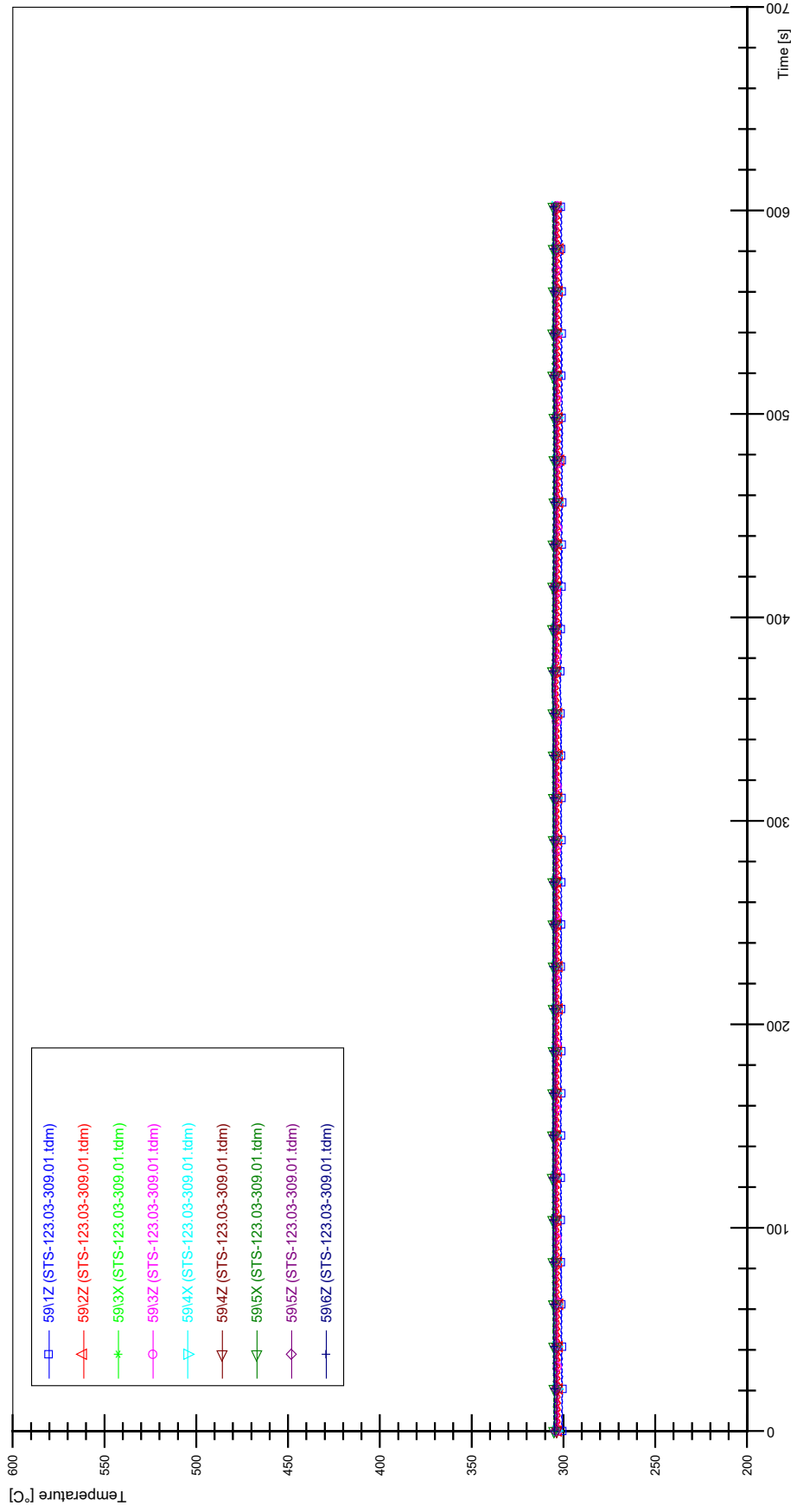
APPENDIX VV PLOTS OF INSTABILITY TEST STS-123.03-309.01



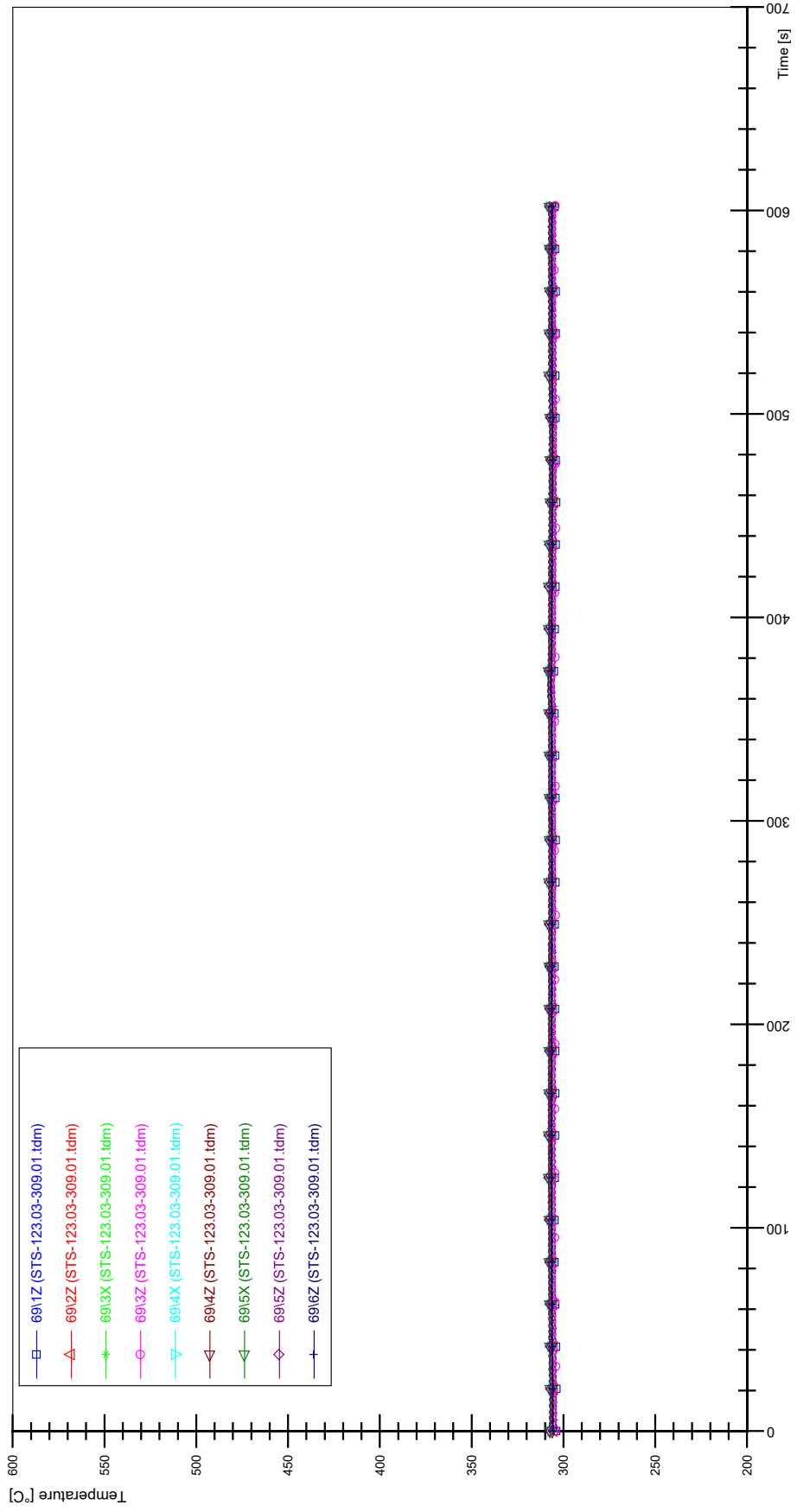
STS-123.03-309.01_CP12_CT19



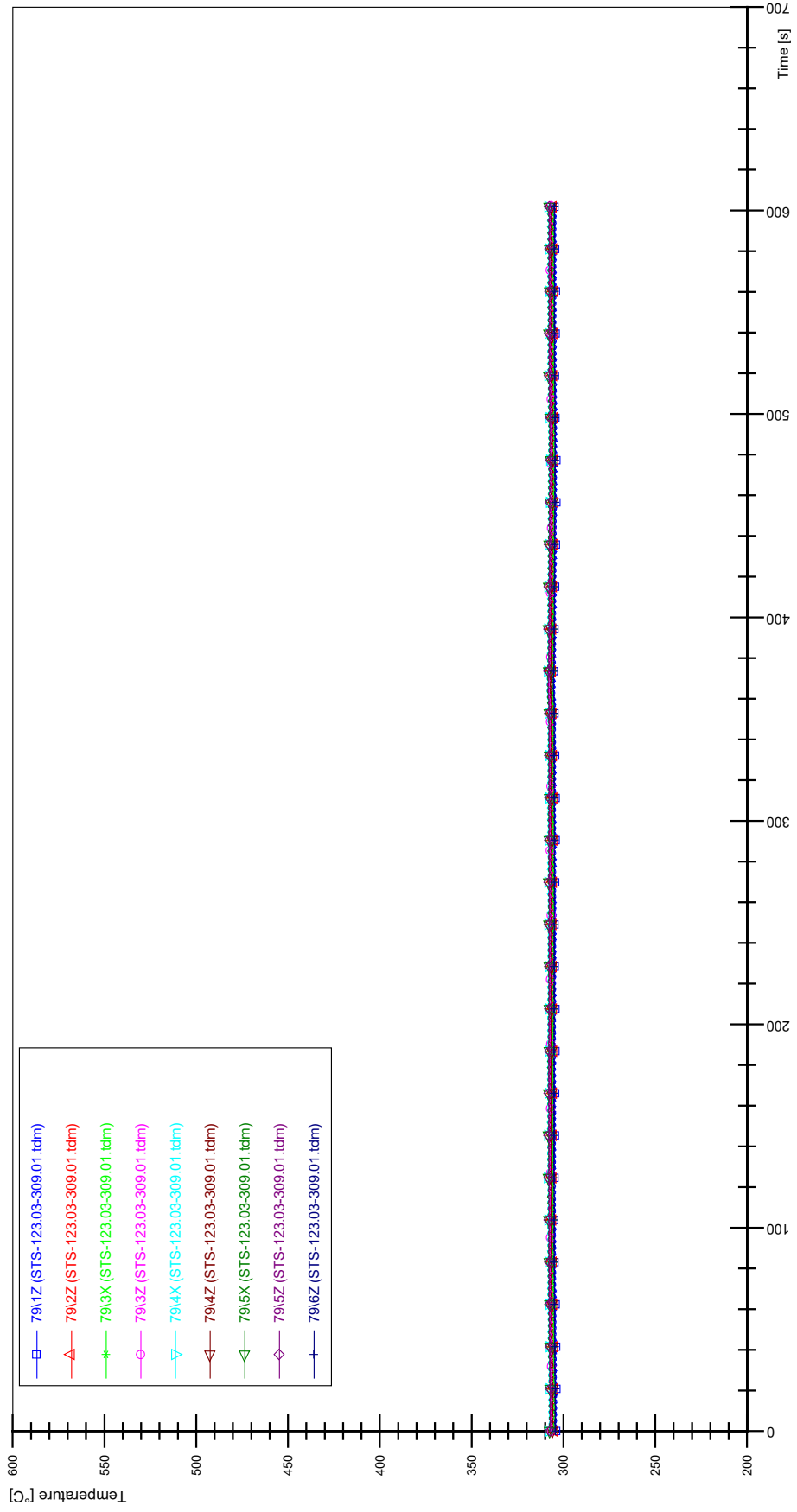
STS-123.03-309.01_Rod_59



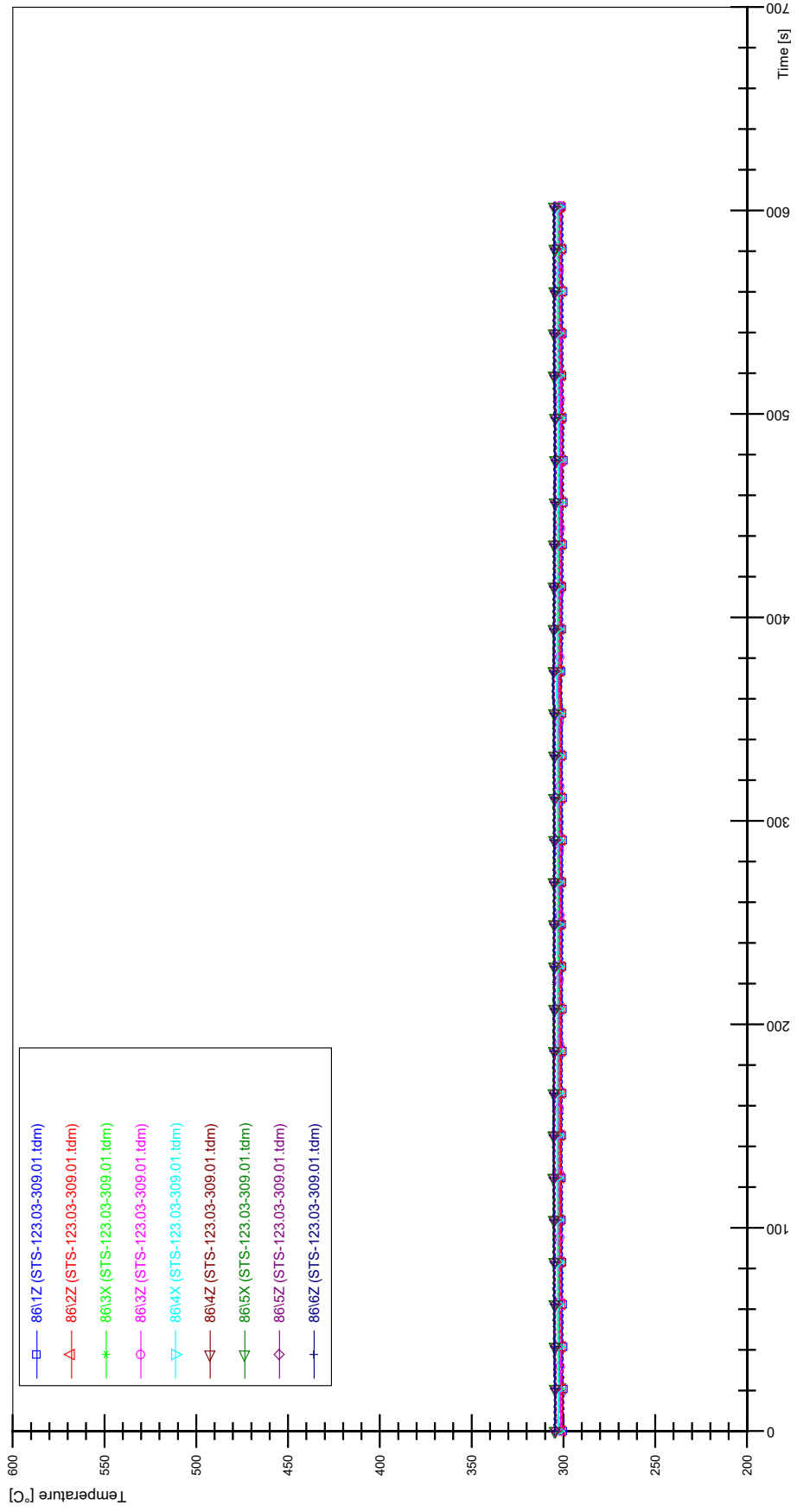
STS-123.03-309.01_Rod_69



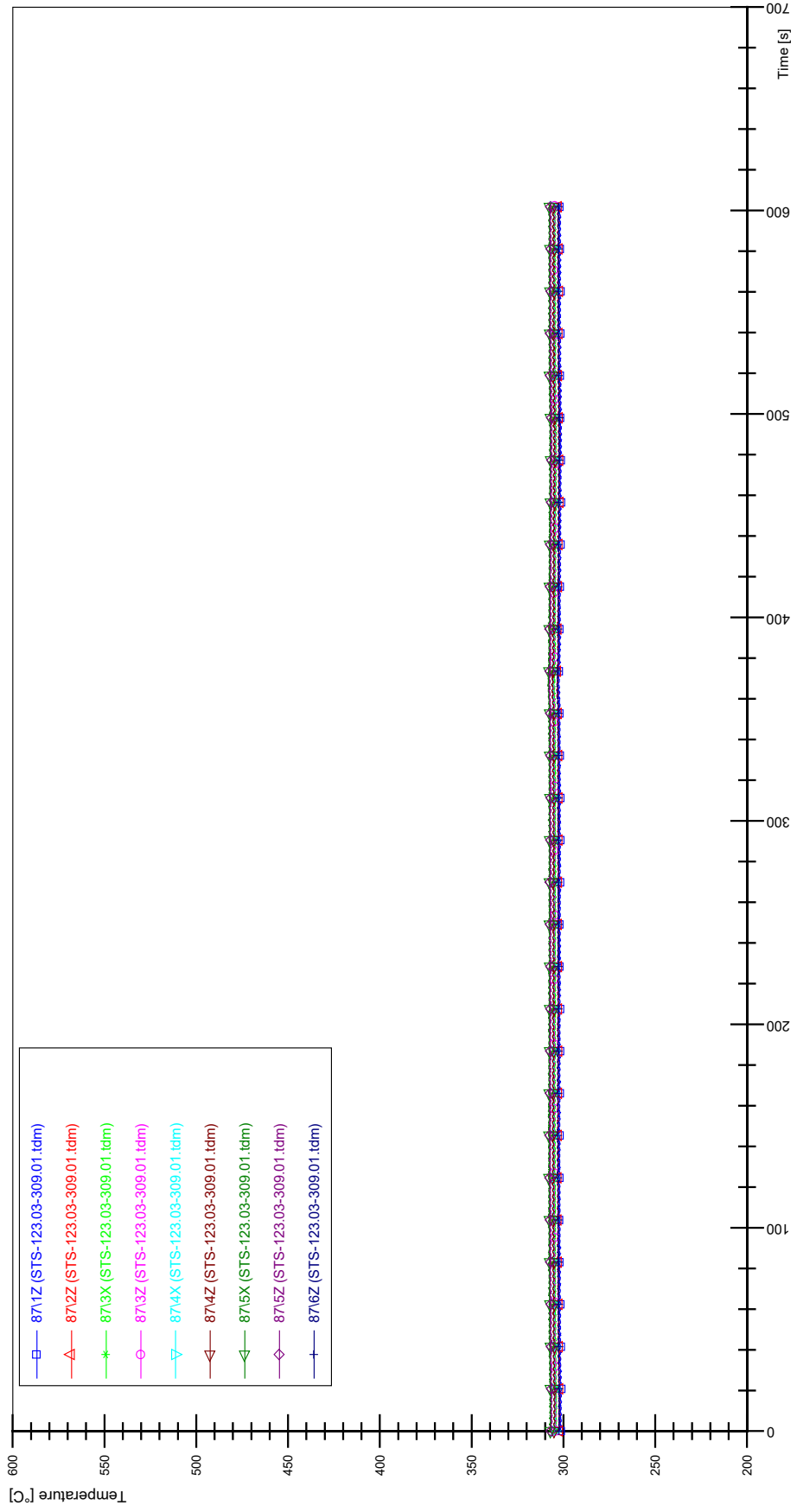
STS-123.03-309.01_Rod_79



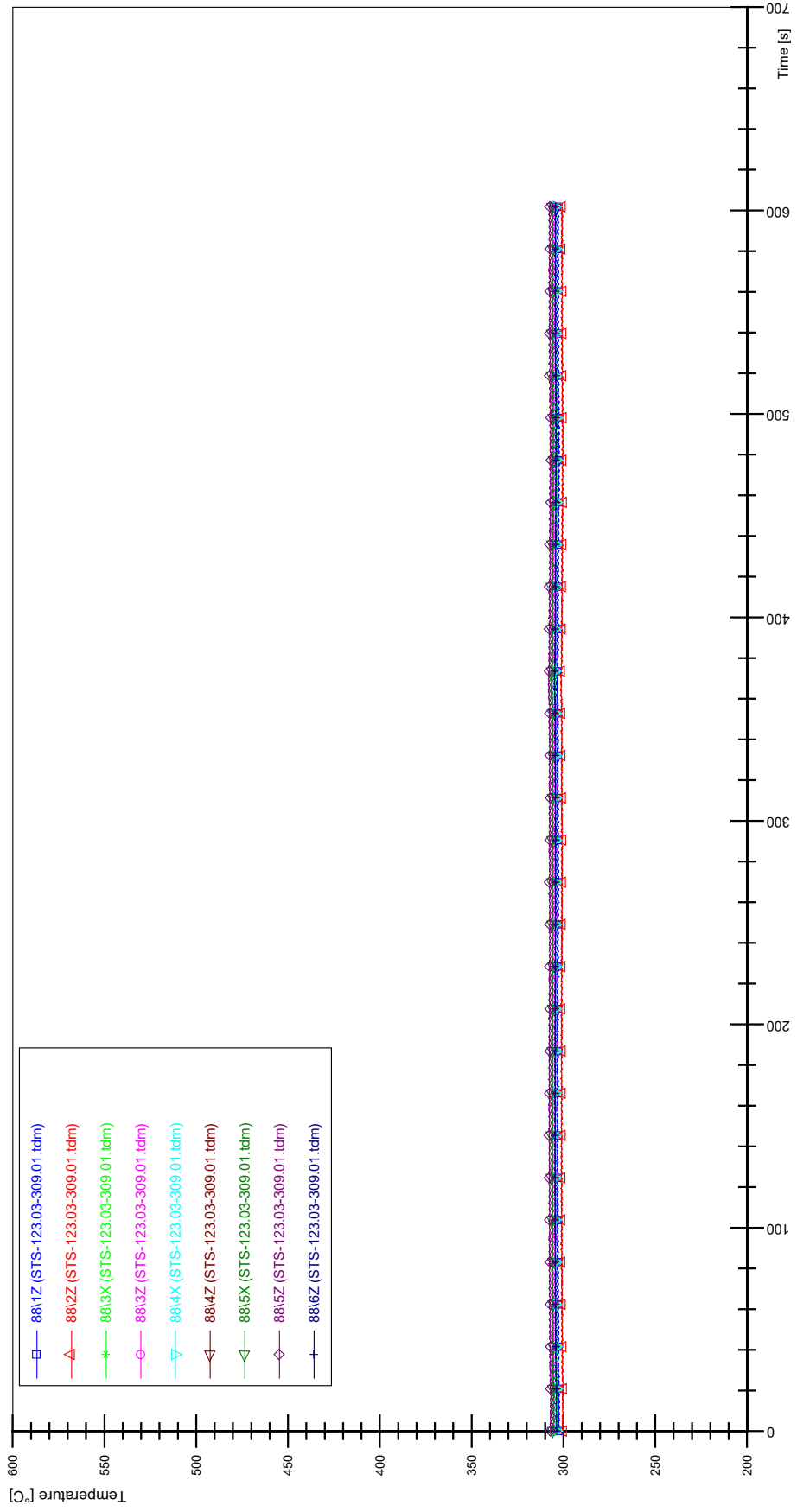
STS-123.03-309.01_Rod_86



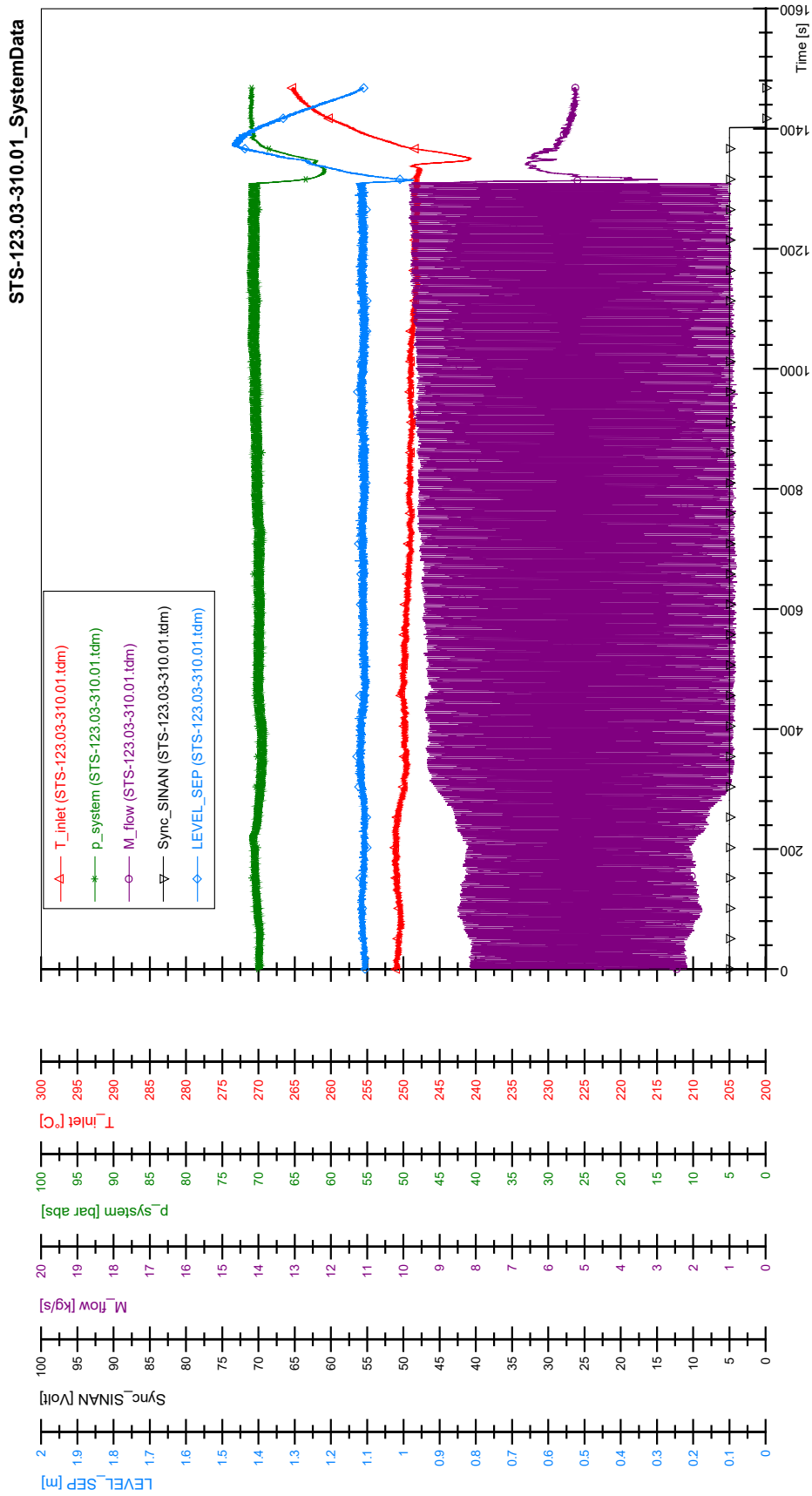
STS-123.03-309.01_Rod_87

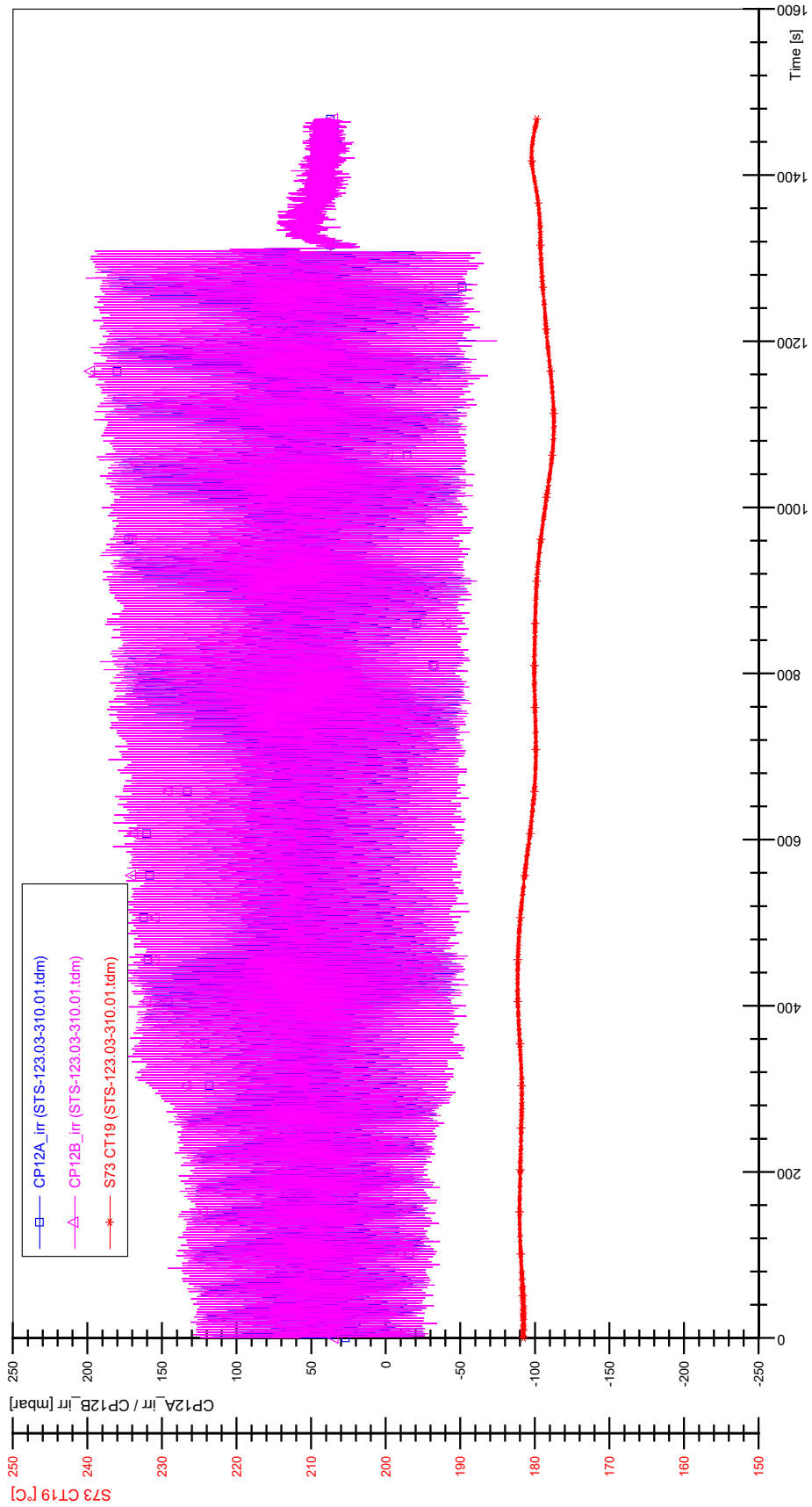


STS-123.03-309.01_Rod_88

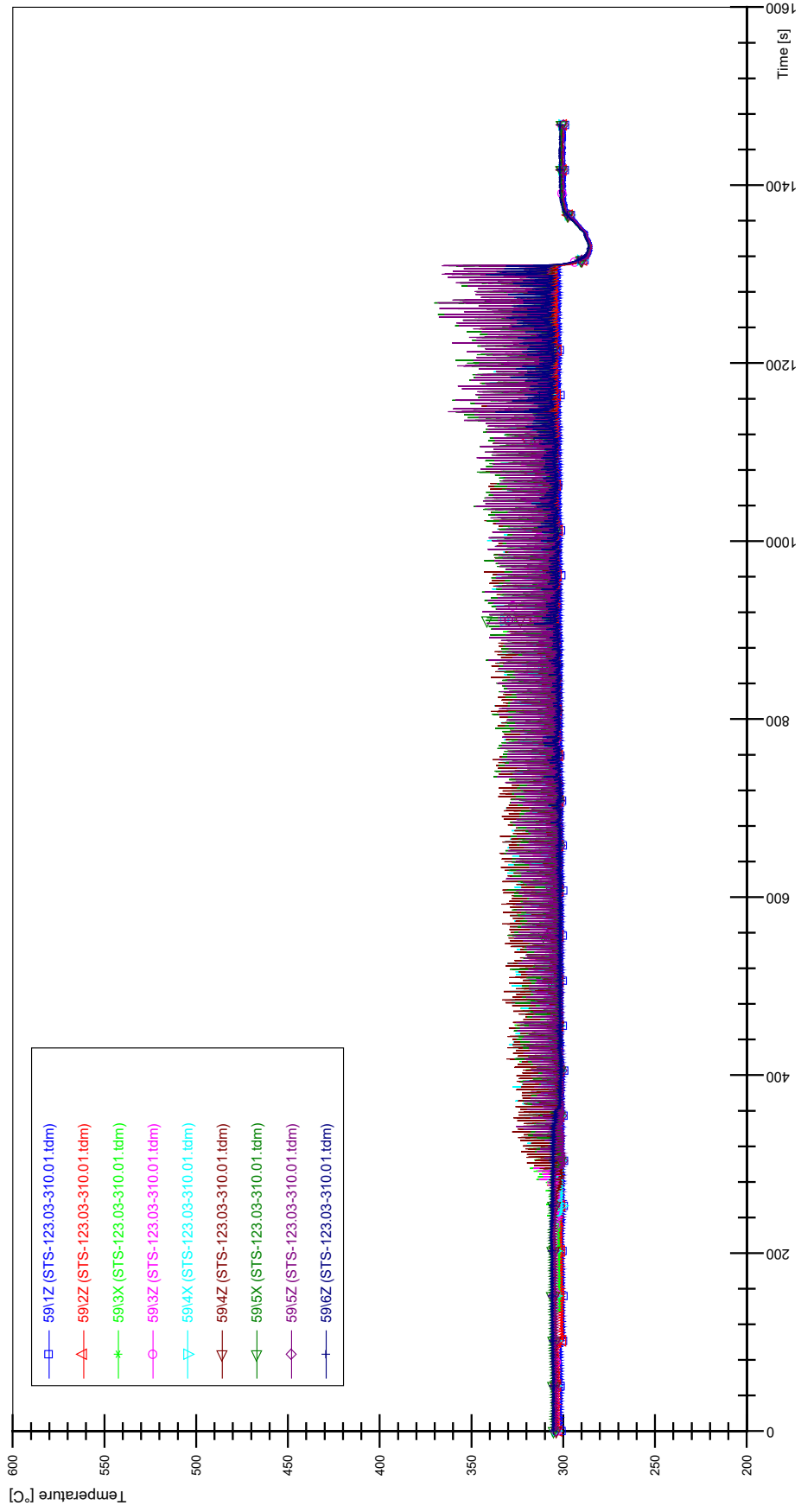


APPENDIX WW PLOTS OF INSTABILITY TEST STS-123.03-310.01

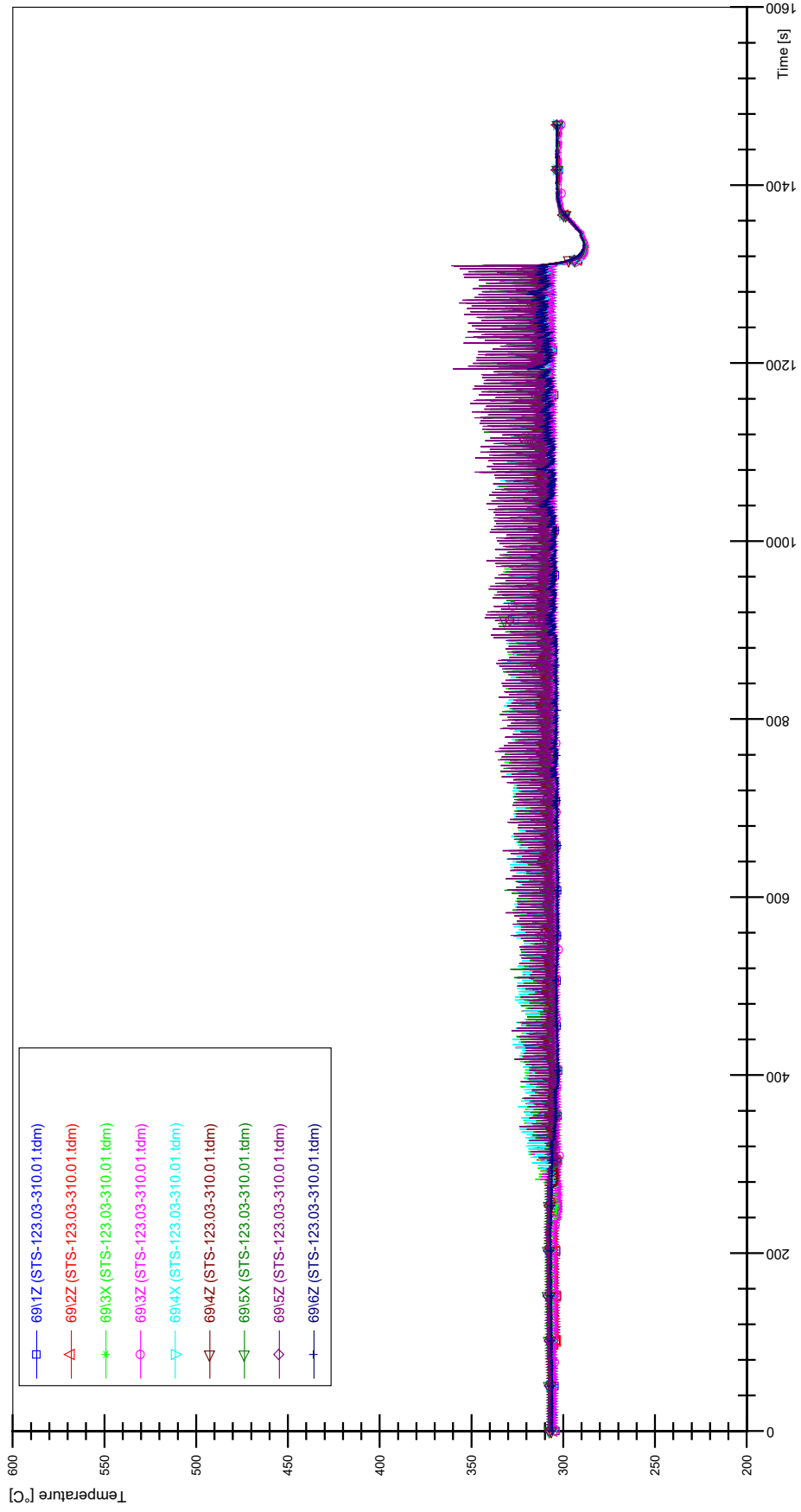




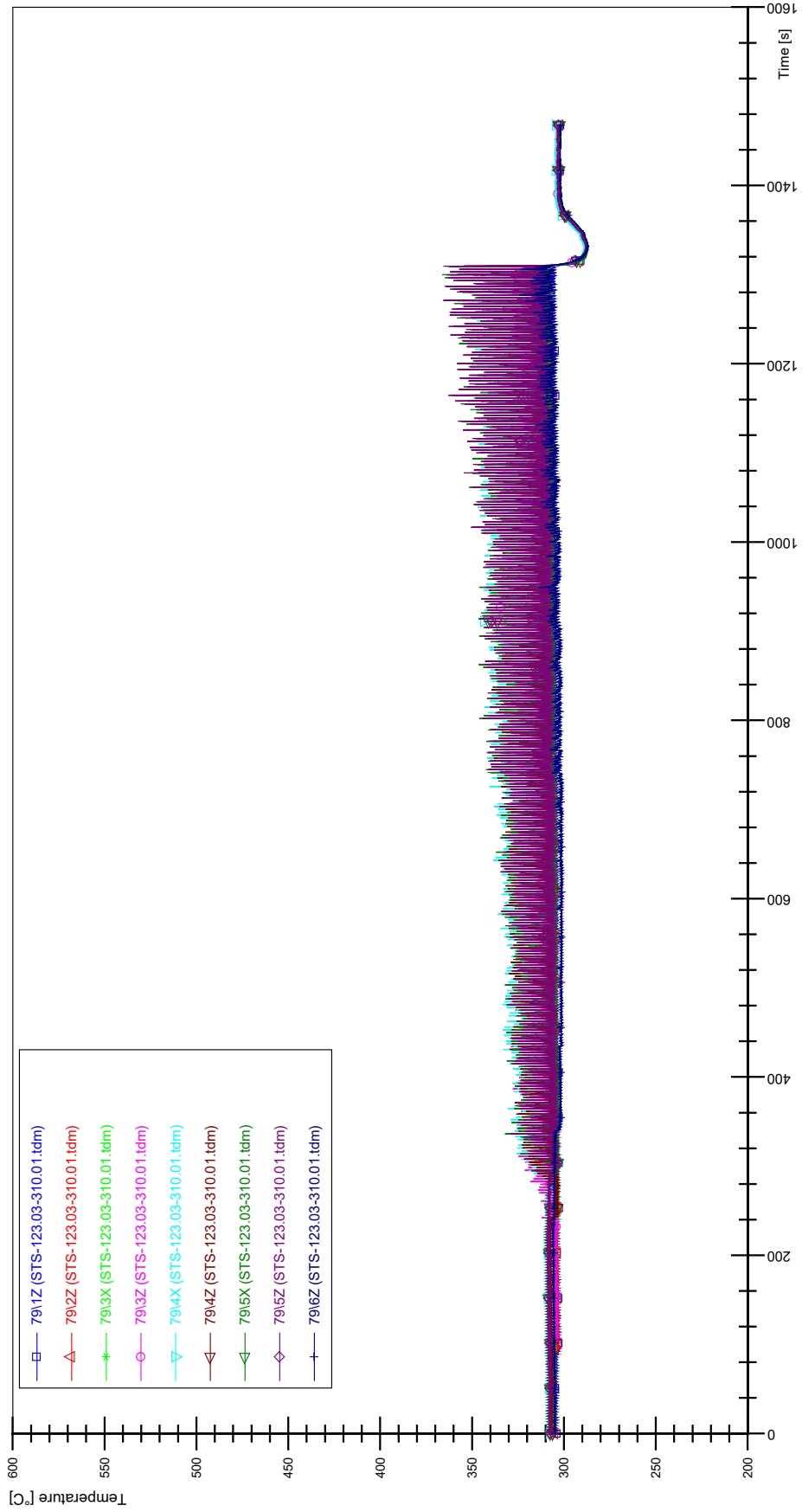
STS-123.03-310.01_Rod_59



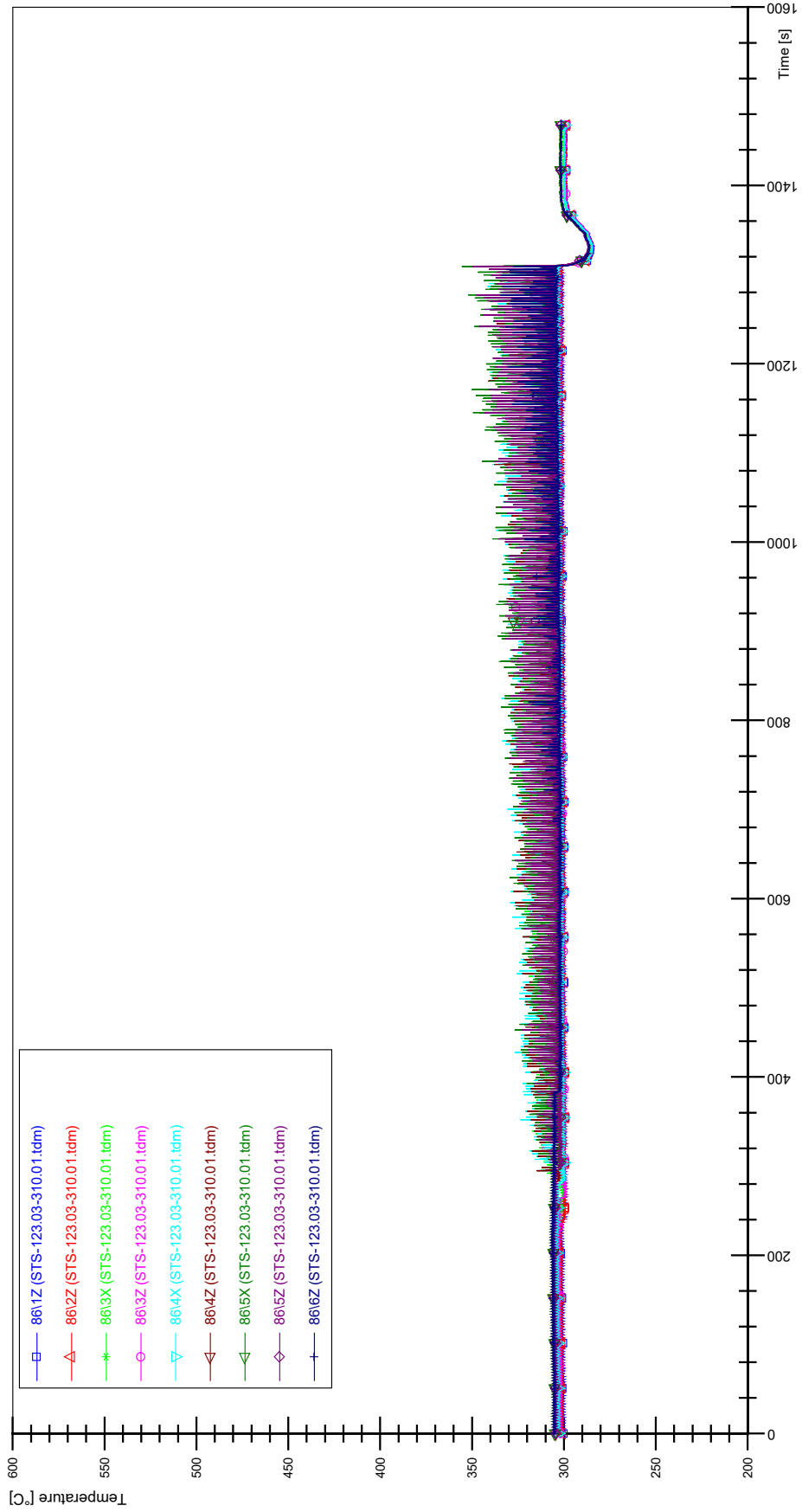
STS-123.03-310.01_Rod_69



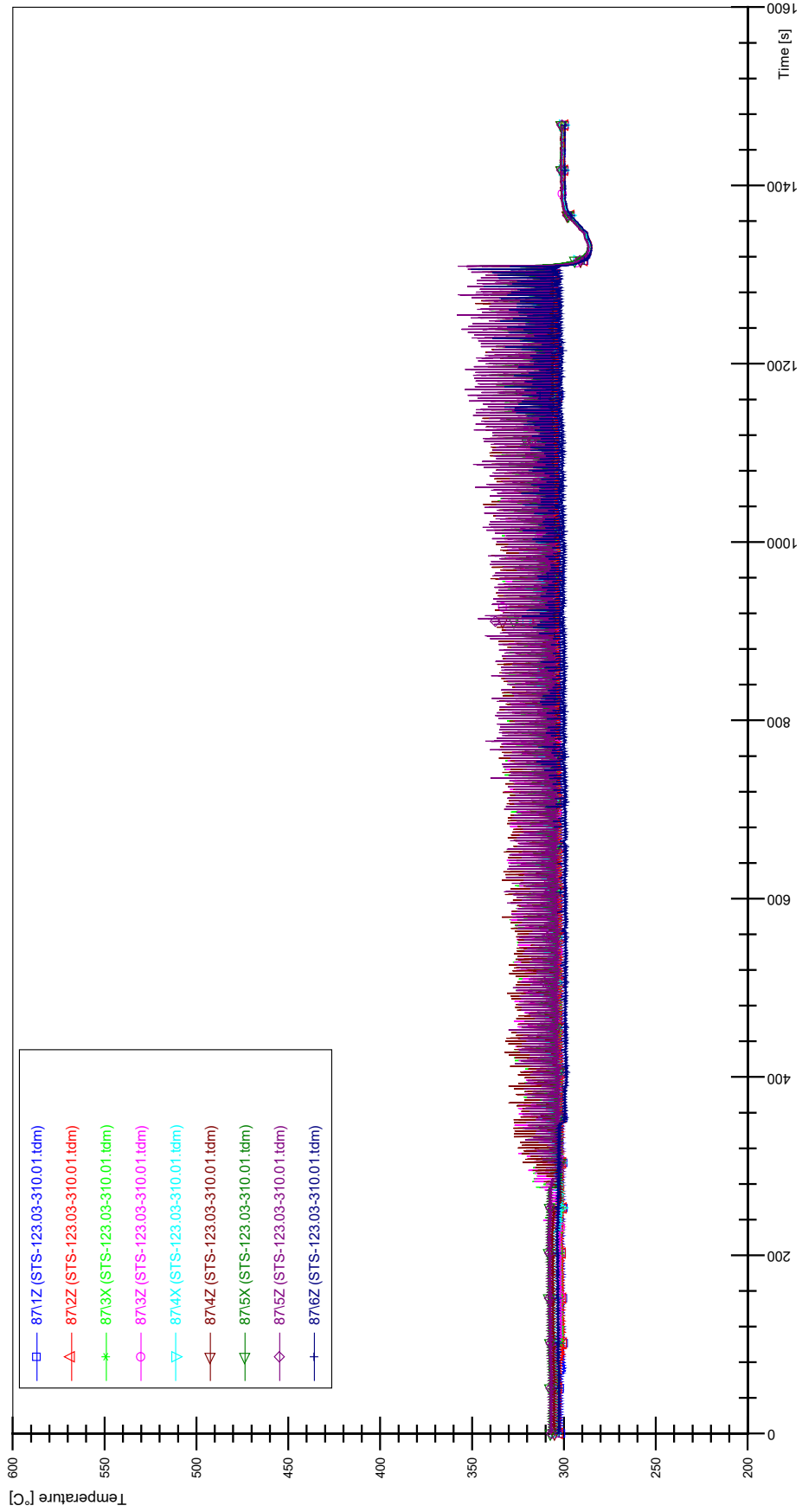
STS-123.03-310.01_Rod_79



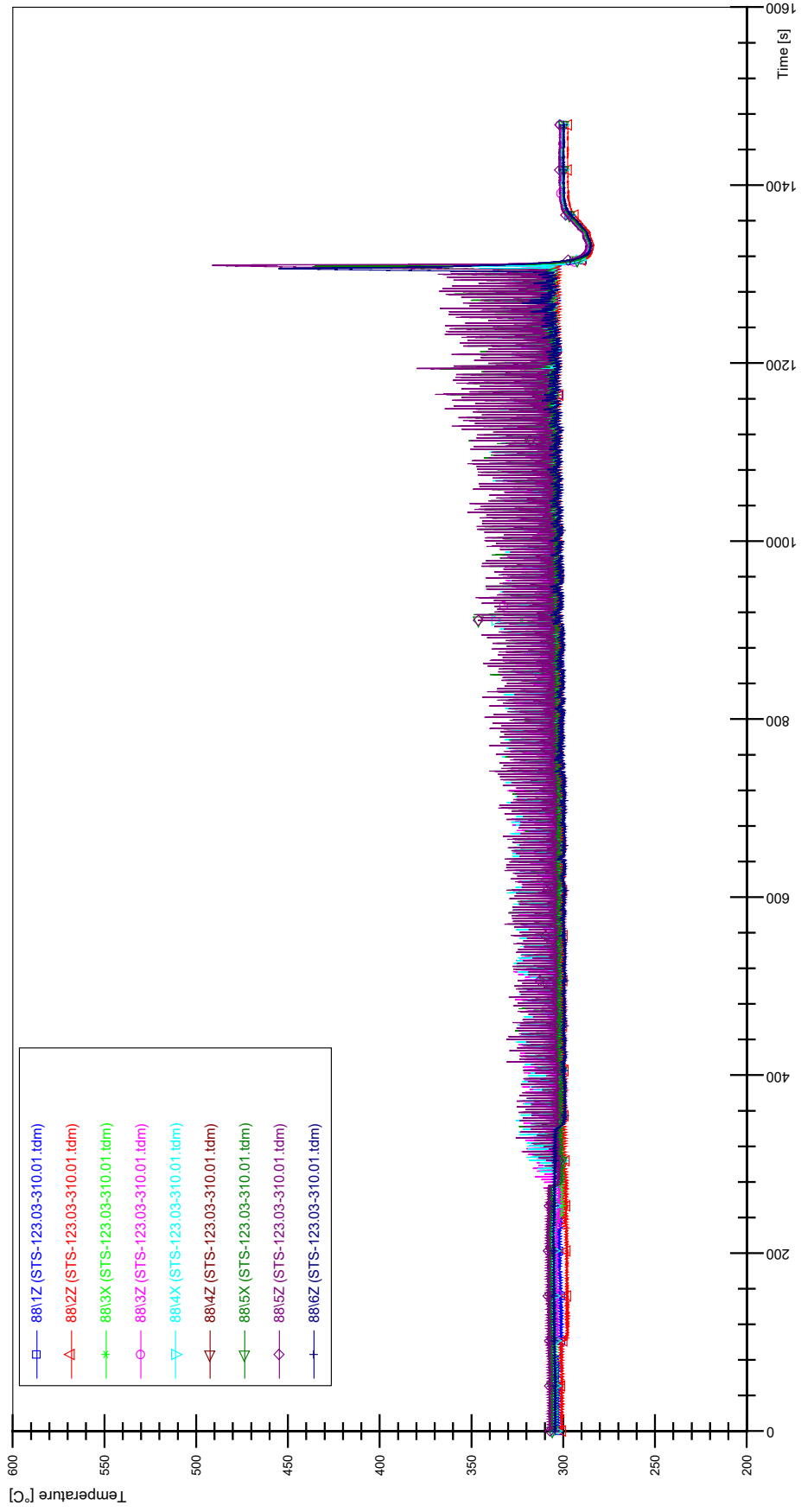
STS-123.03-310.01_Rod_86



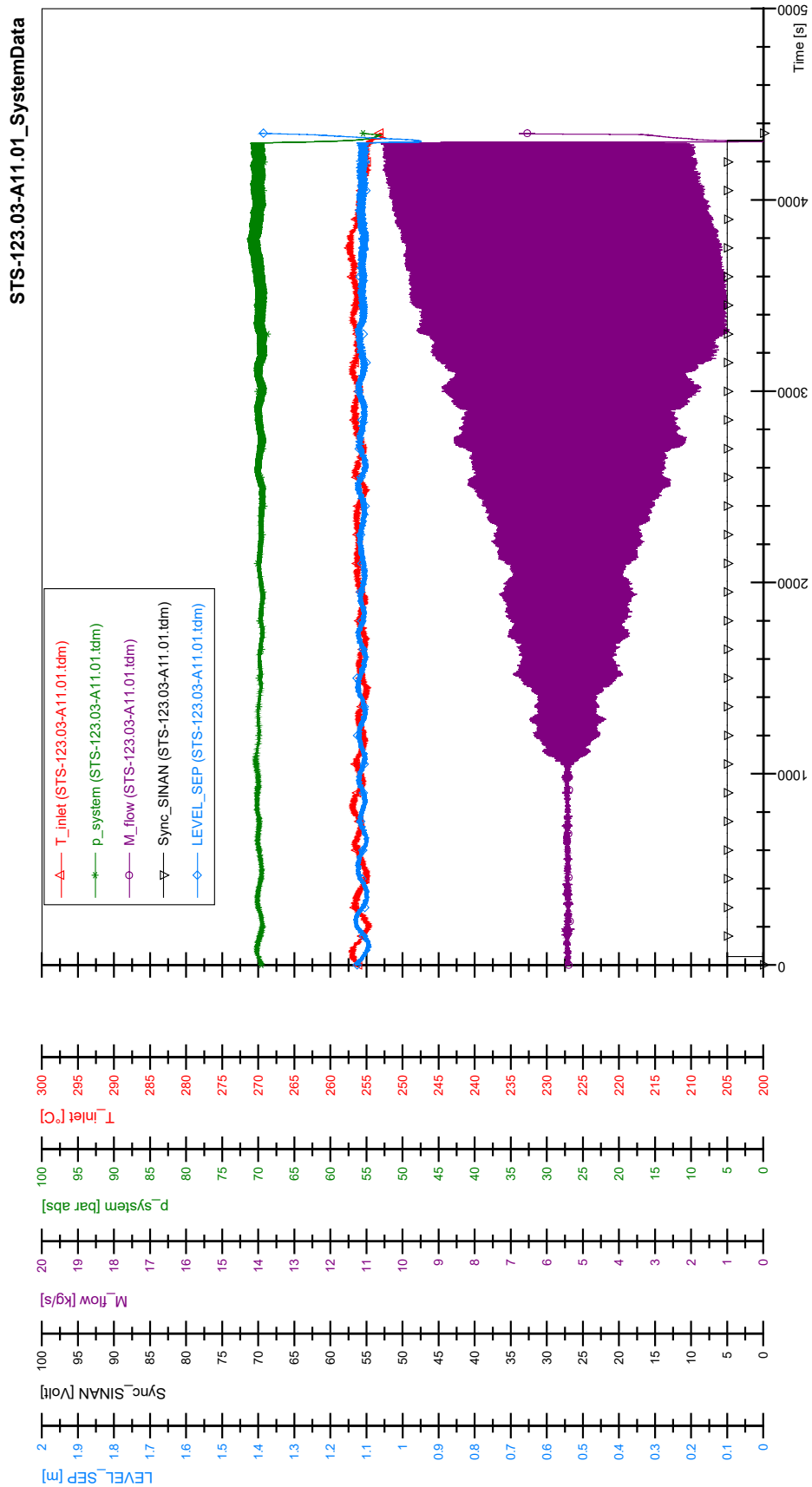
STS-123.03-310.01_Rod_87



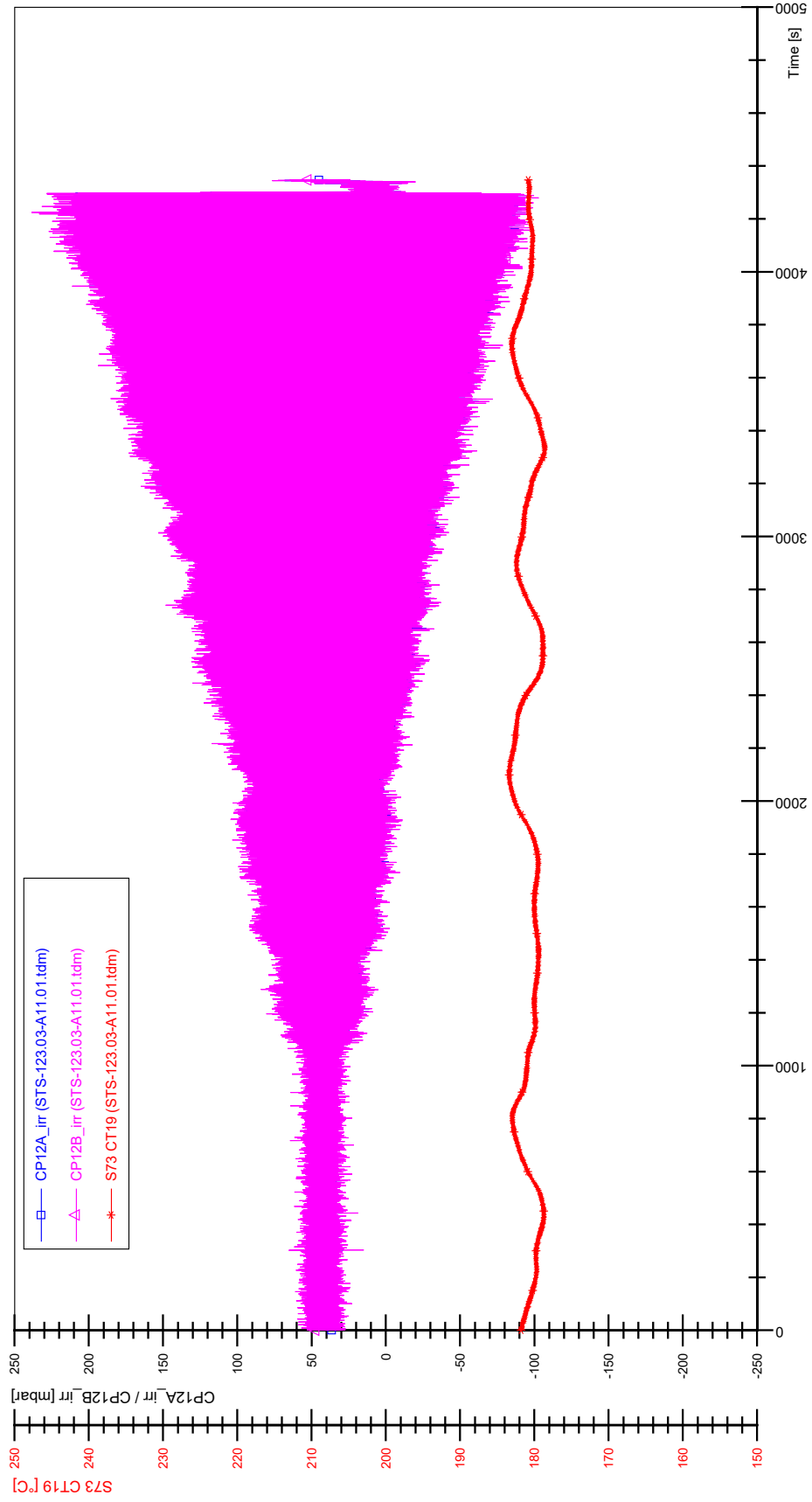
STS-123.03-310.01_Rod_88



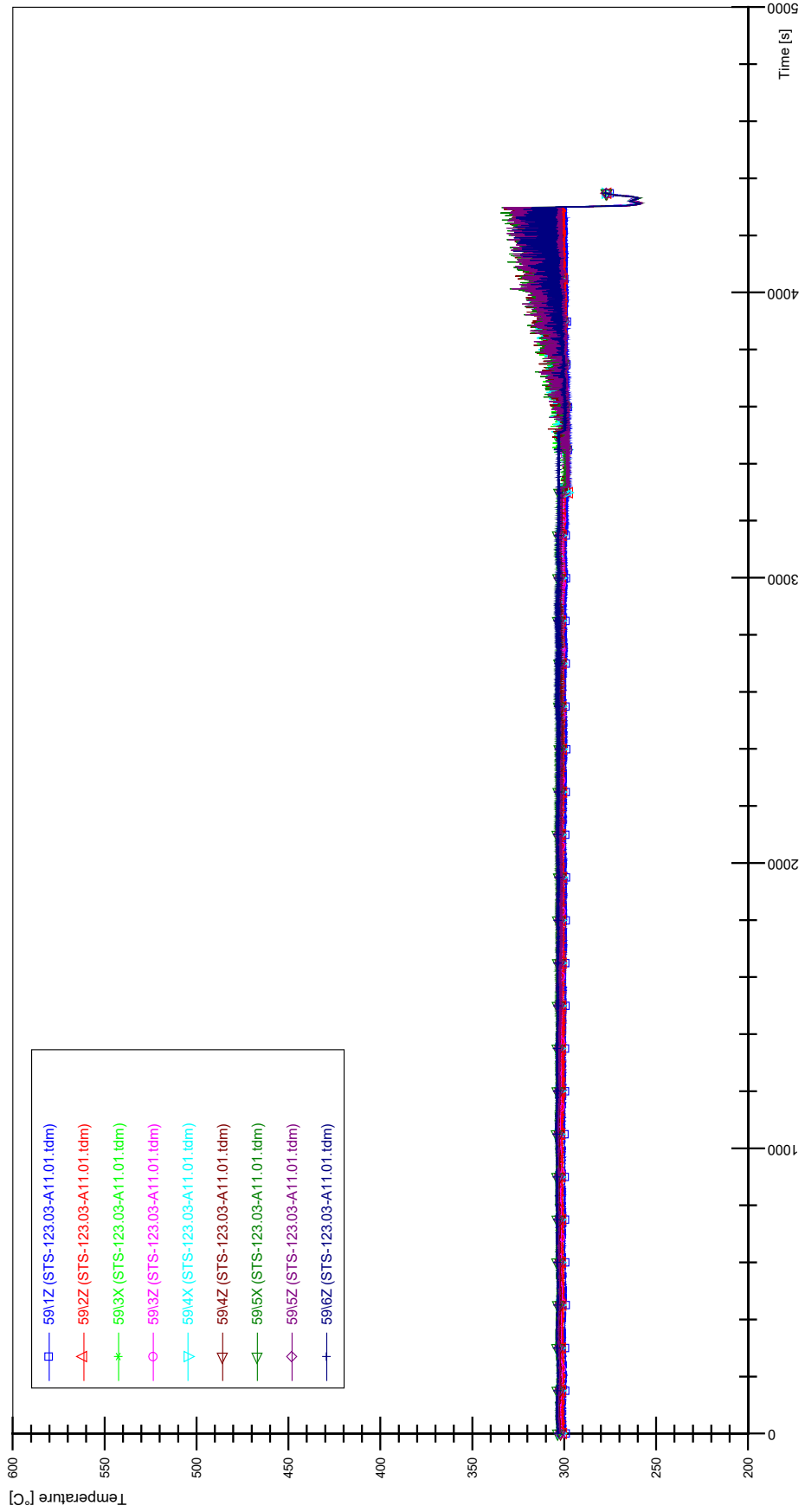
APPENDIX XX PLOTS OF INSTABILITY TEST STS-123.03-A11.01



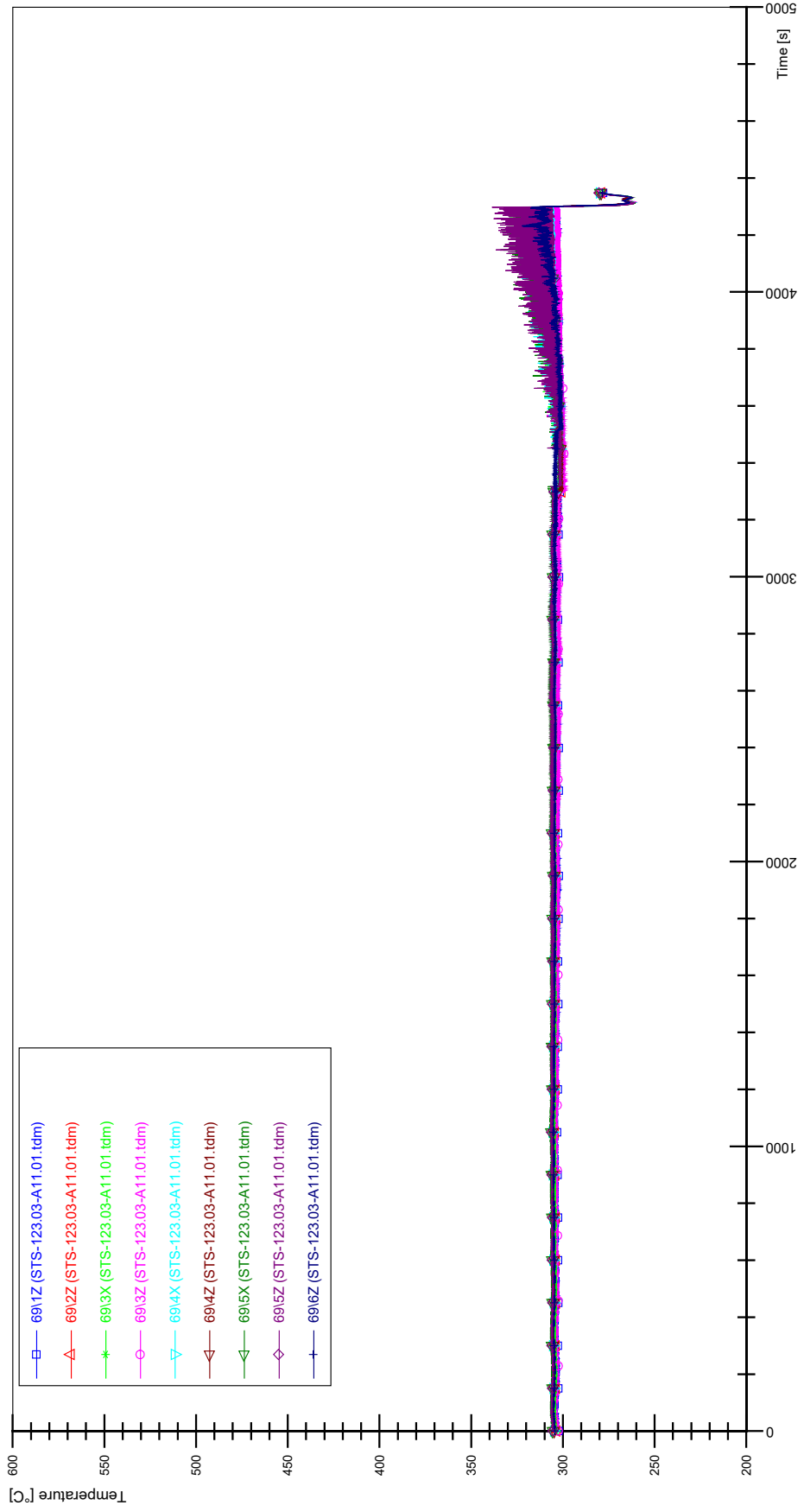
STS-123.03-A11.01_CP12_CT19



STS-123.03-A11.01_Rod_59

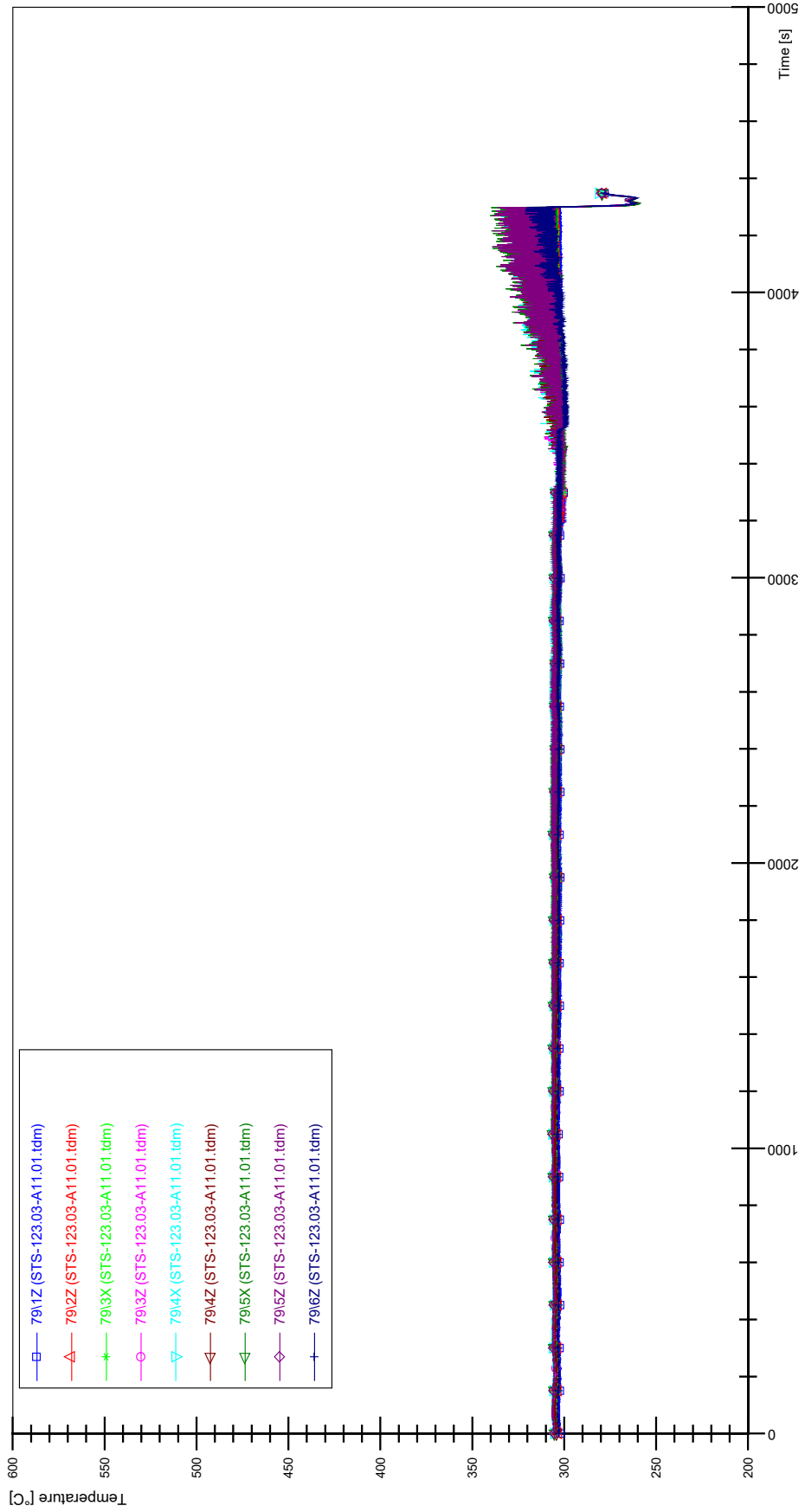


STS-123.03-A11.01_Rod_69

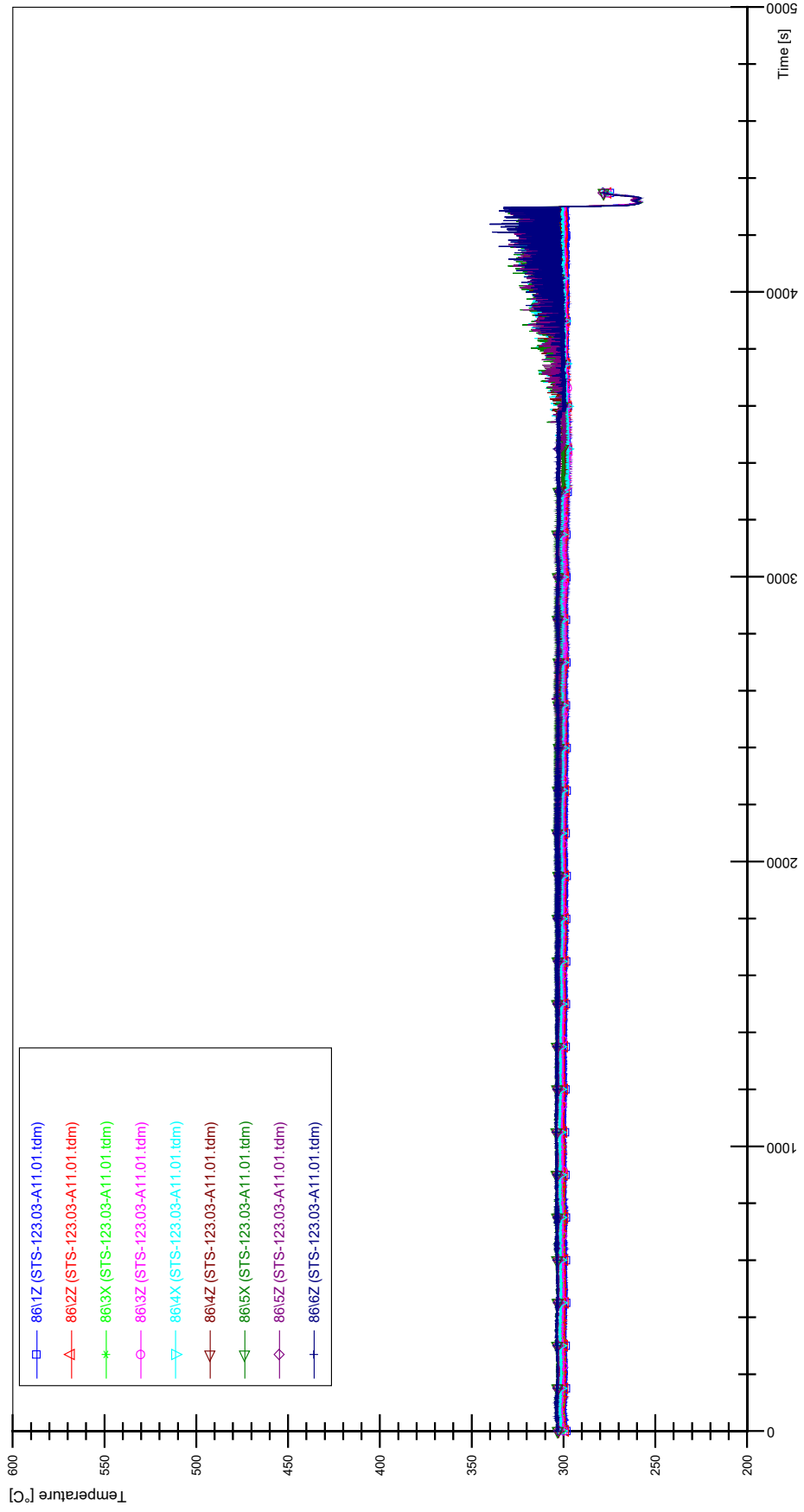


XX-4

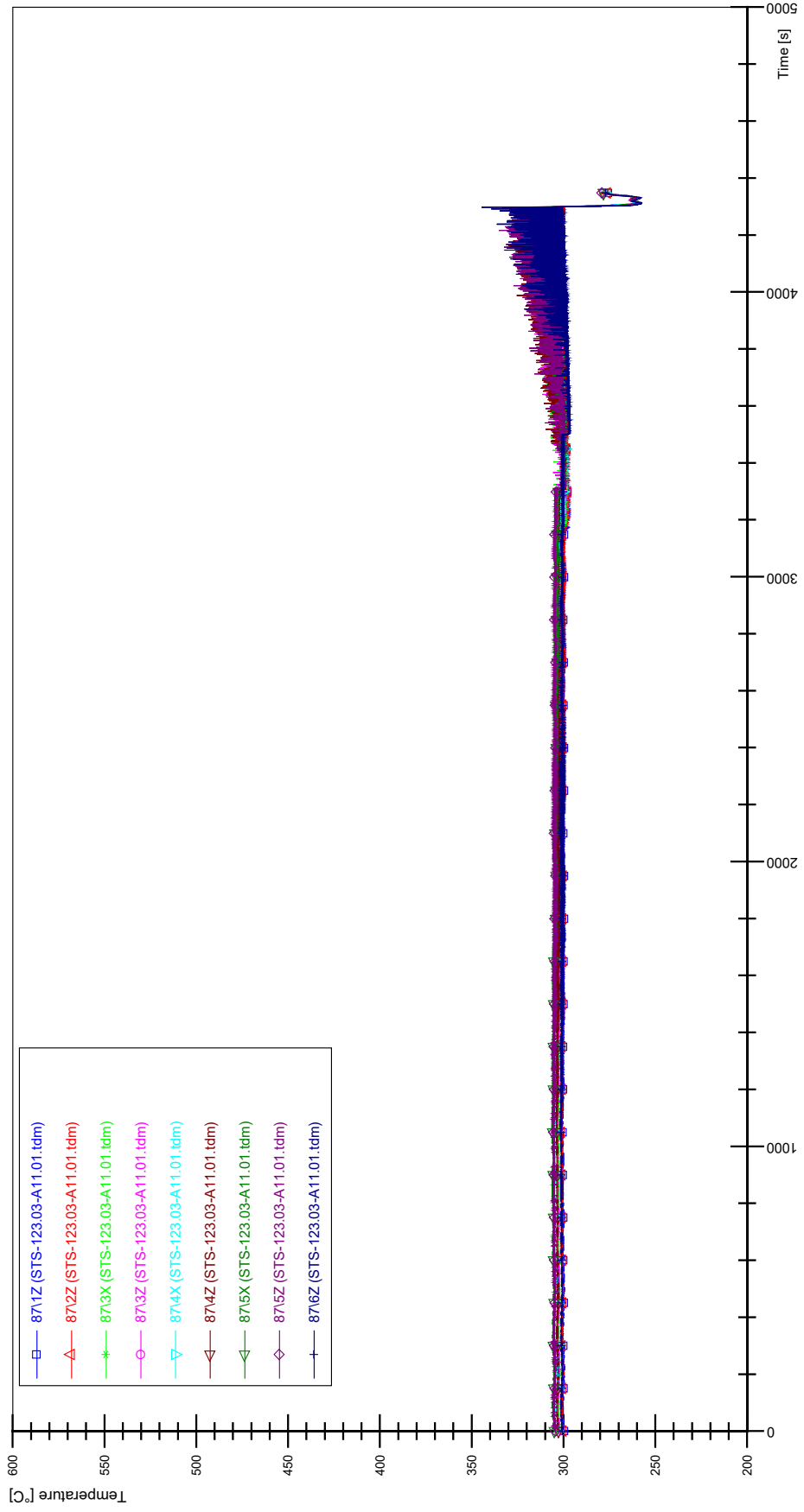
STS-123.03-A11.01_Rod_79



STS-123.03-A11.01_Rod_86

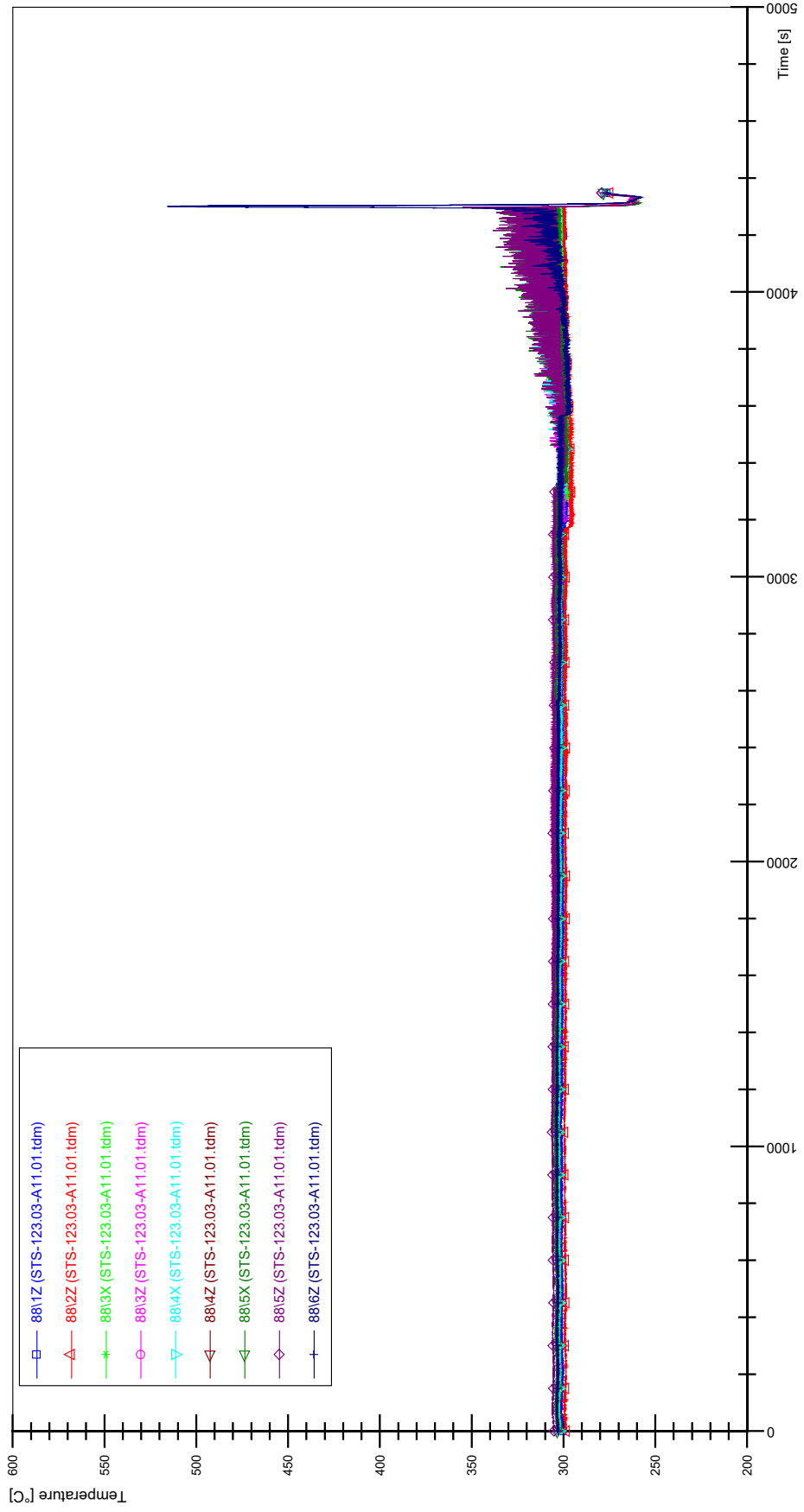


STS-123.03-A11.01_Rod_87

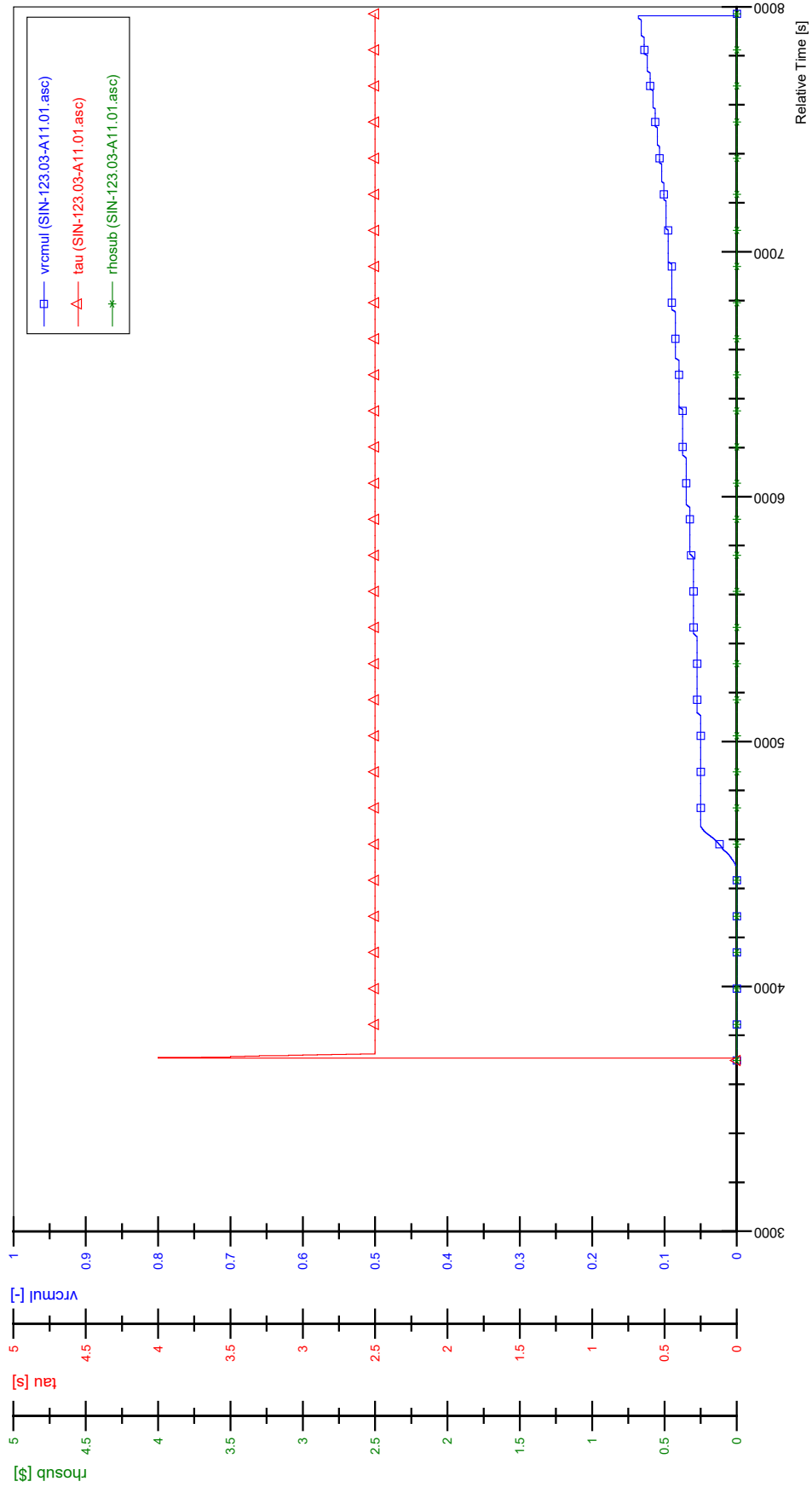


XX-7

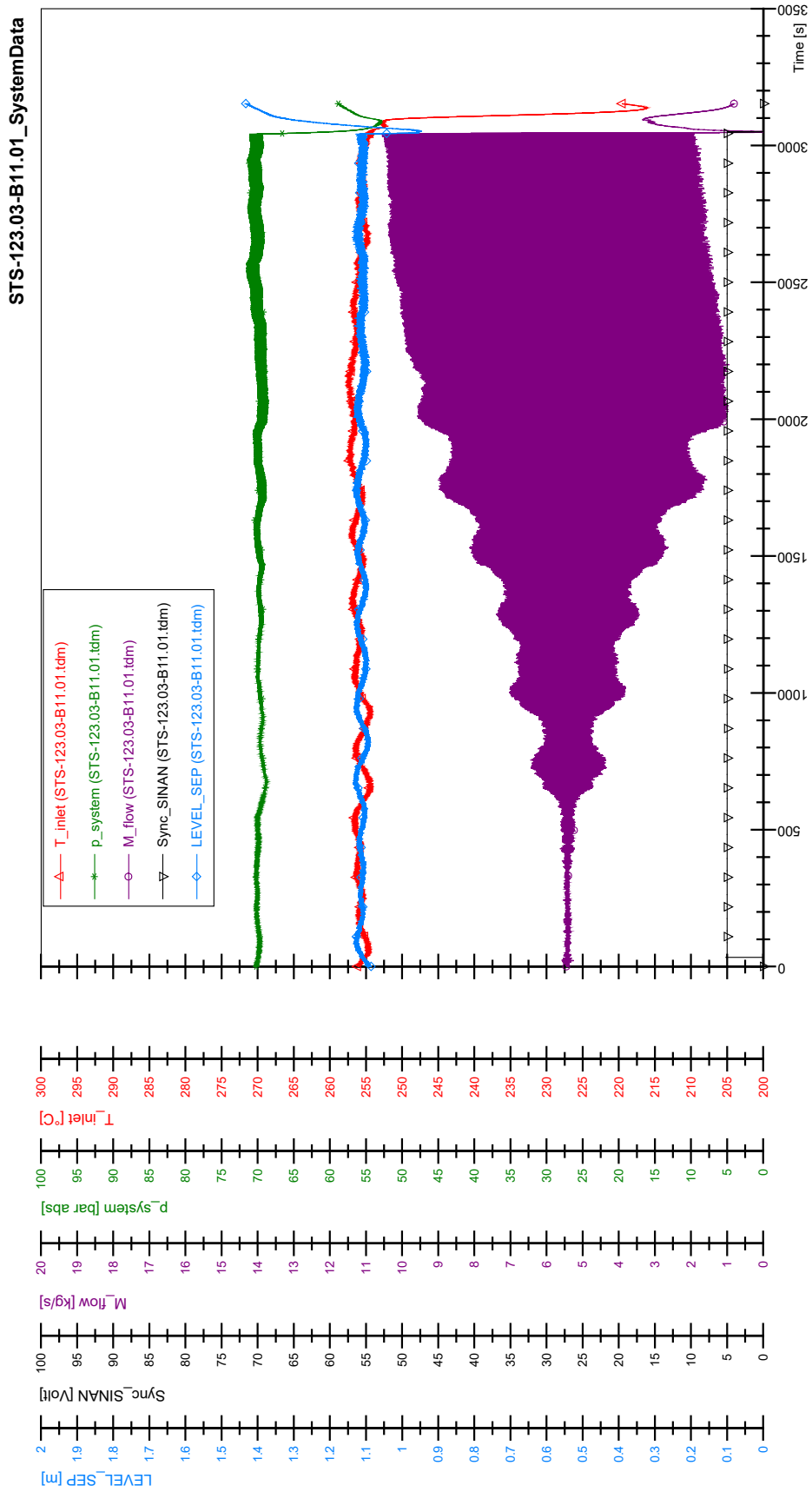
STS-123.03-A11.01_Rod_88



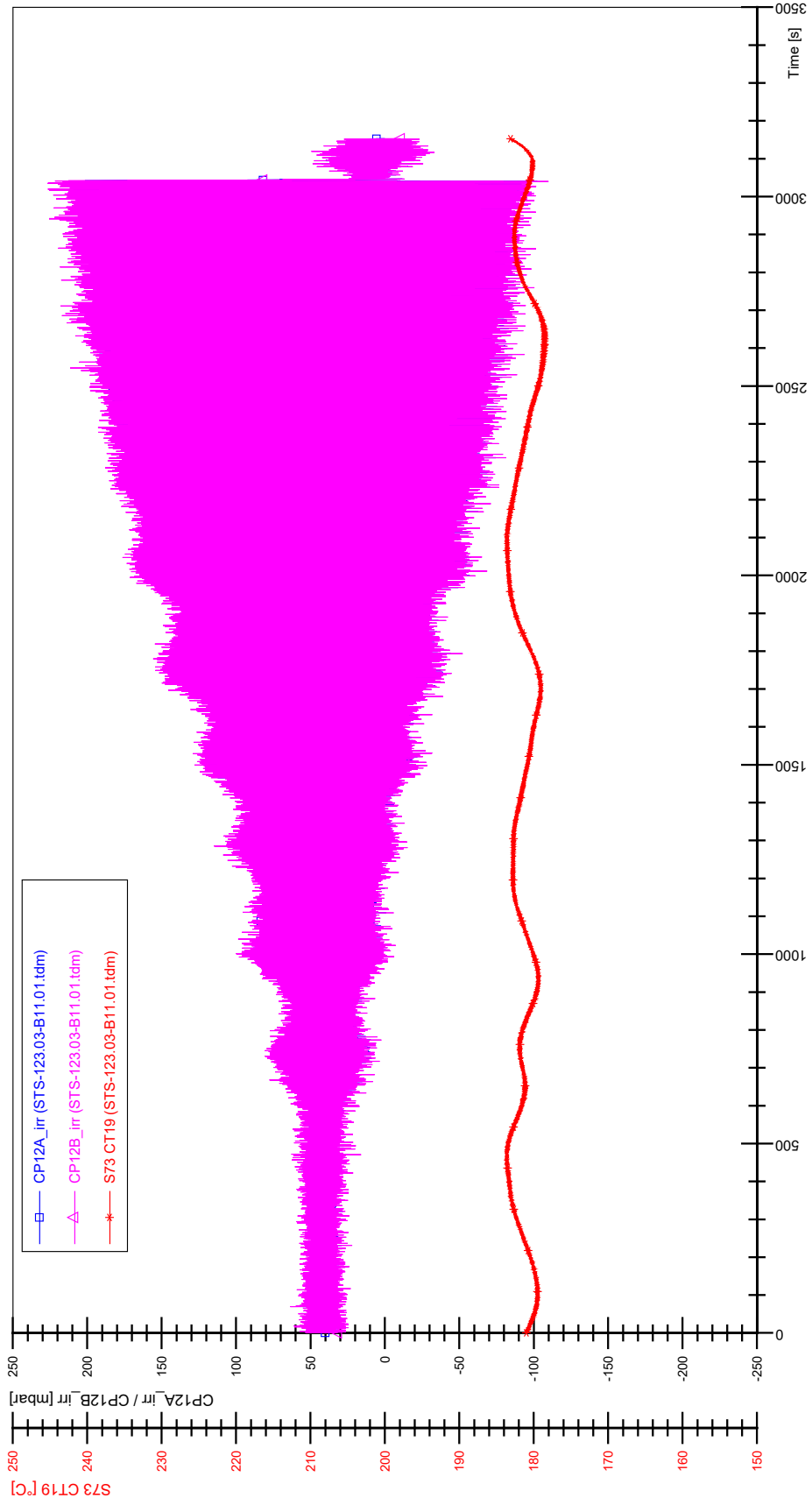
SIN-123.03-A11.01



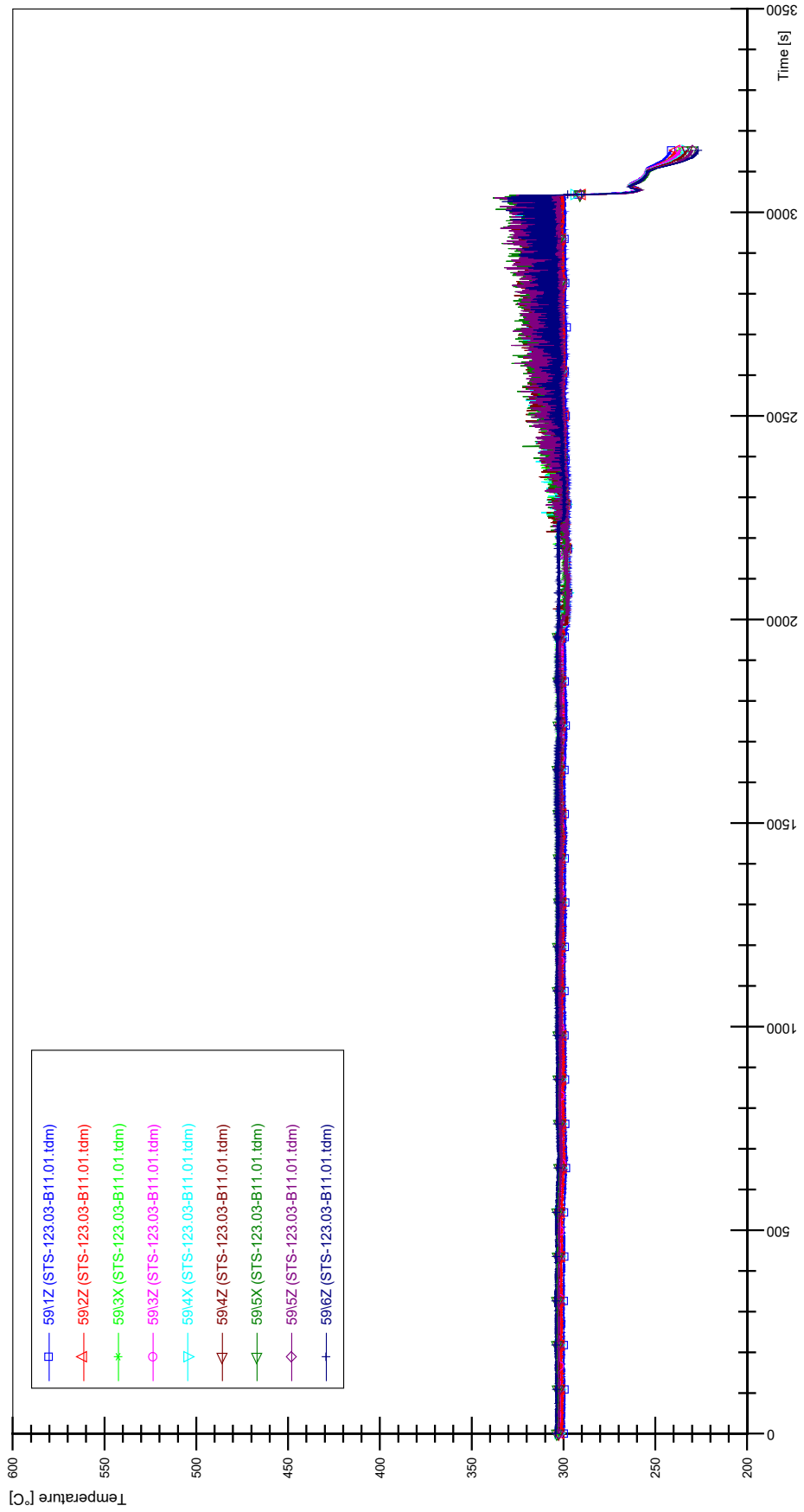
APPENDIX YY PLOTS OF INSTABILITY TEST STS-123.03-B11.01



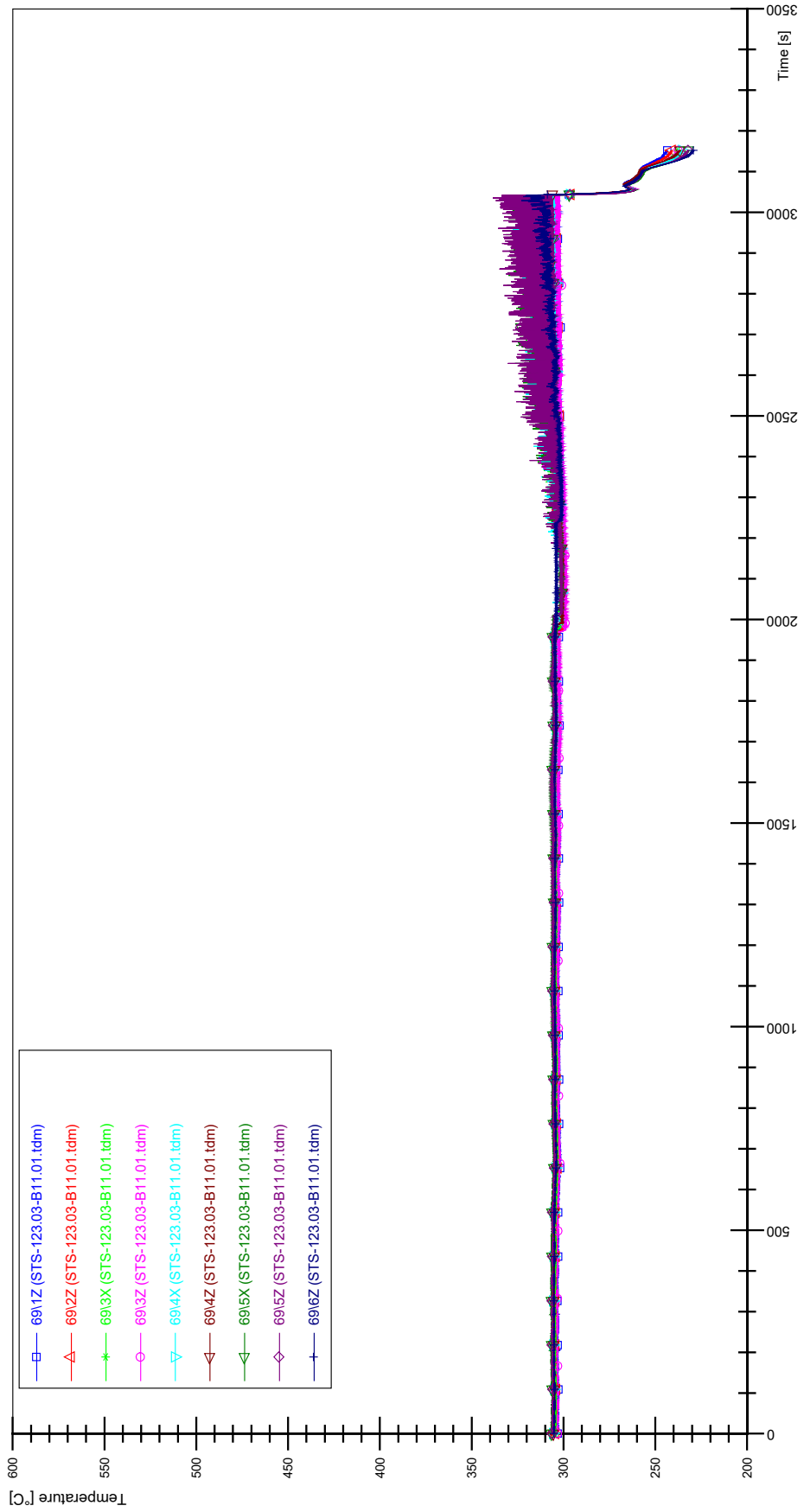
STS-123.03-B11.01_CP12_CT19



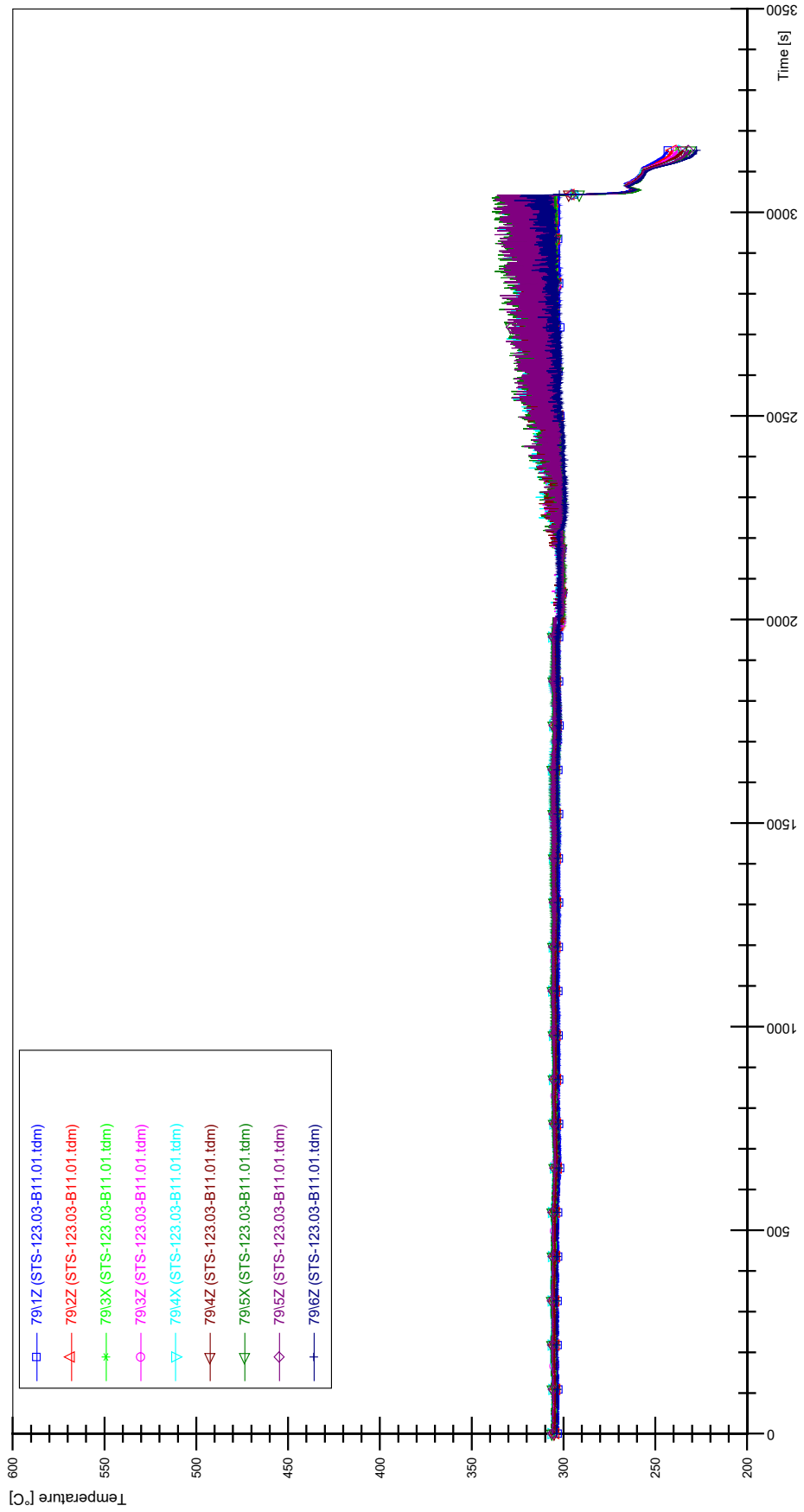
STS-123.03-B11.01_Rod_59



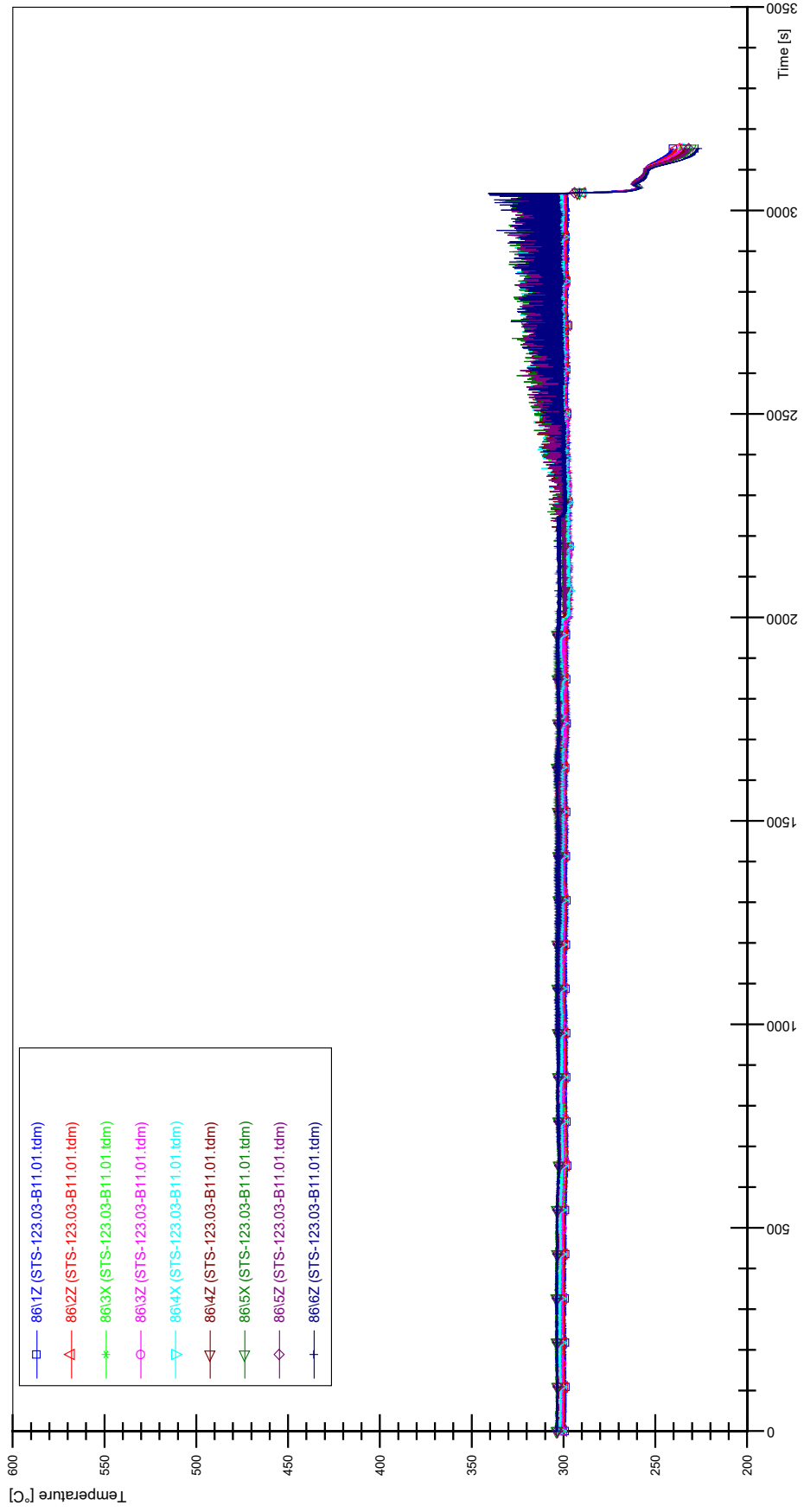
STS-123.03-B11.01_Rod_69



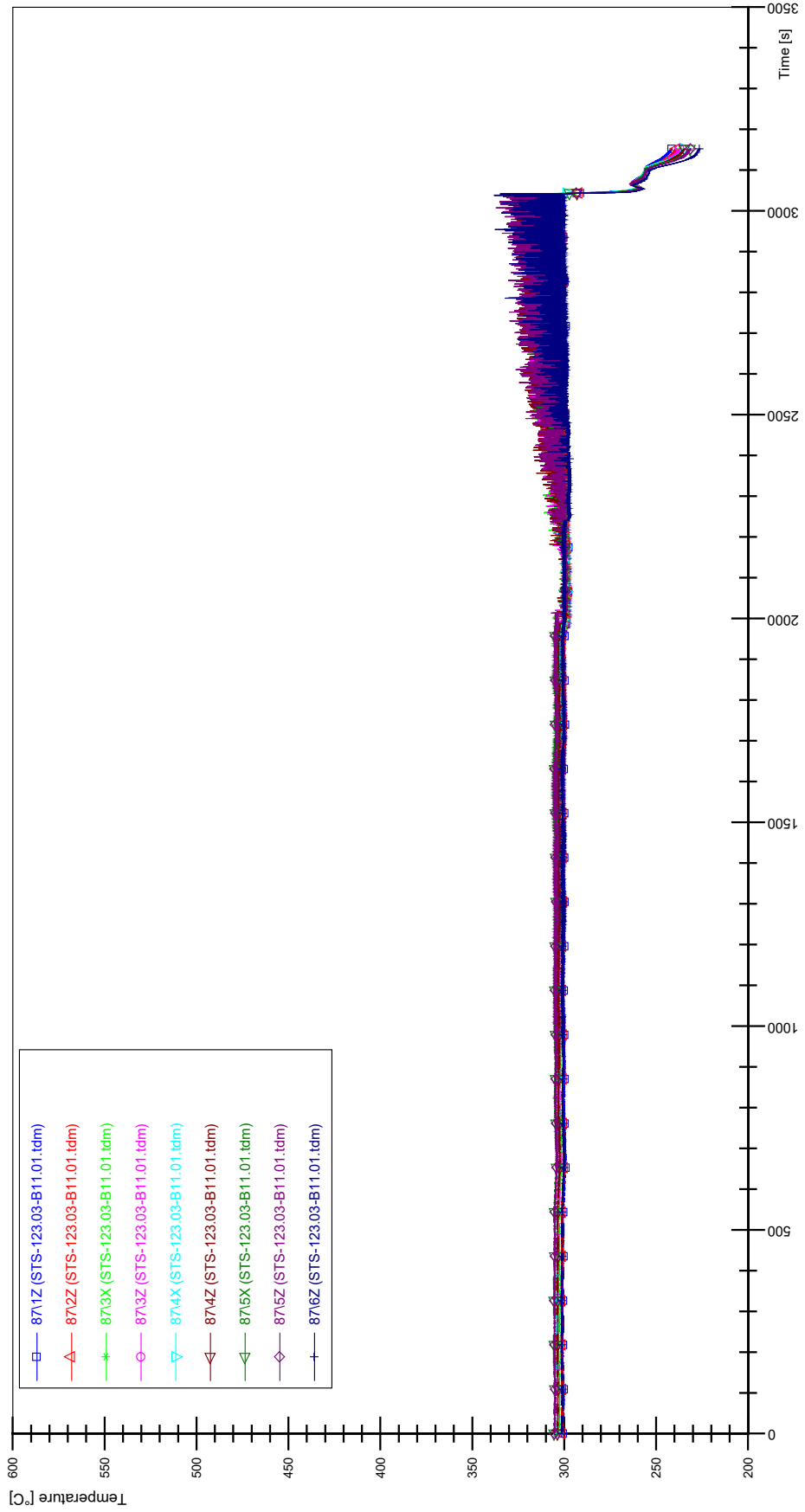
STS-123.03-B11.01_Rod_79



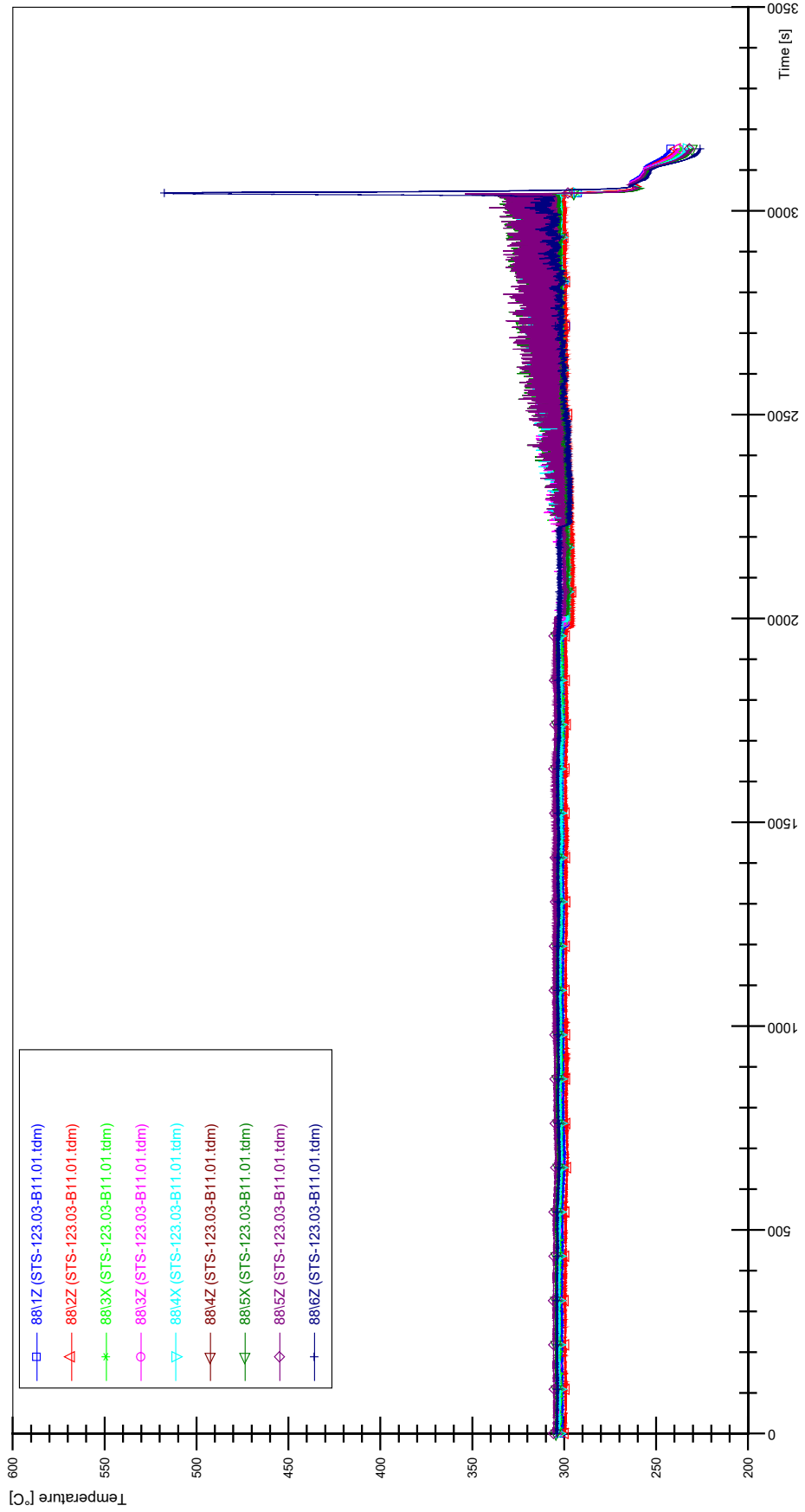
STS-123.03-B11.01_Rod_86



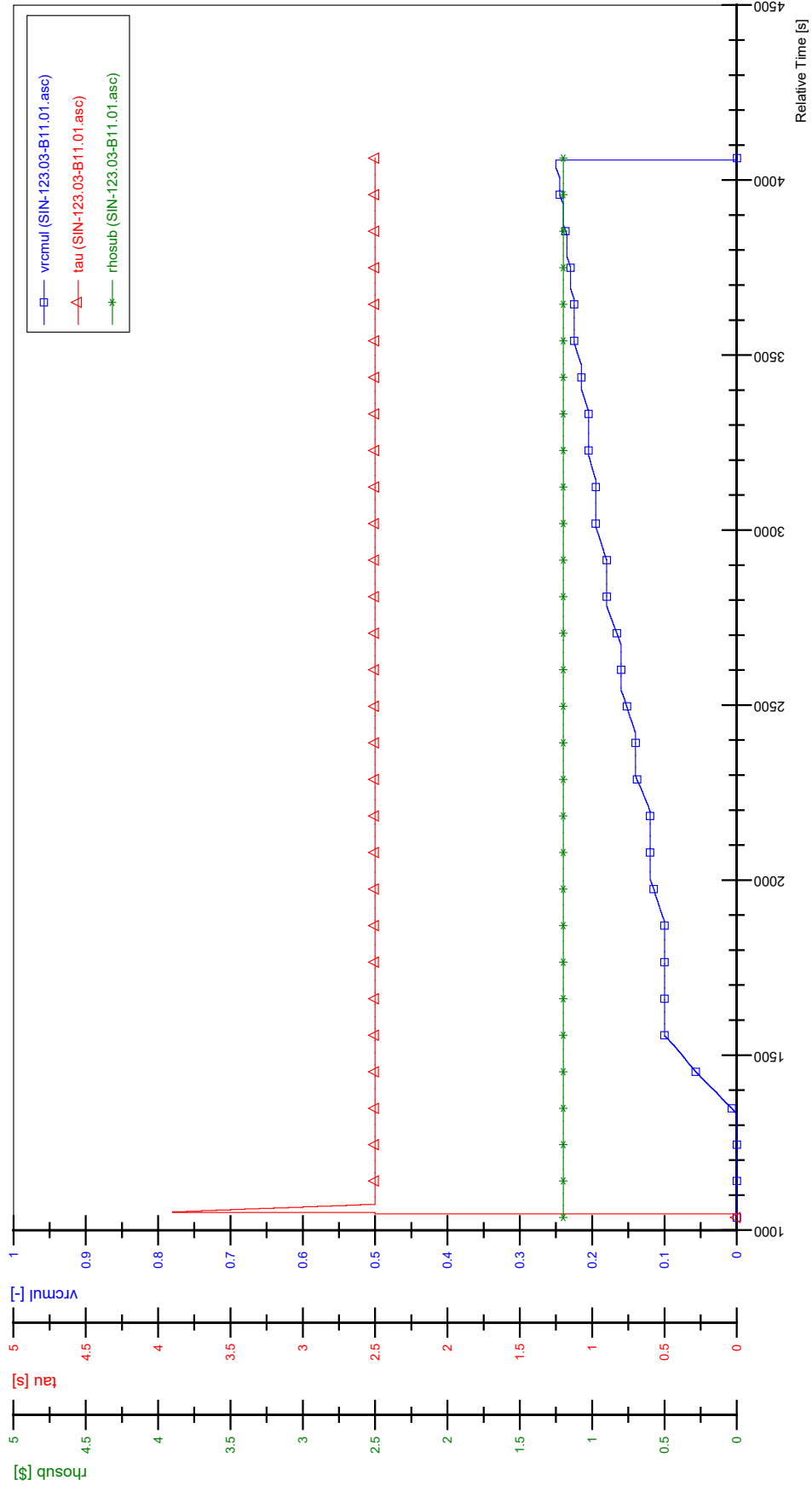
STS-123.03-B11.01_Rod_87



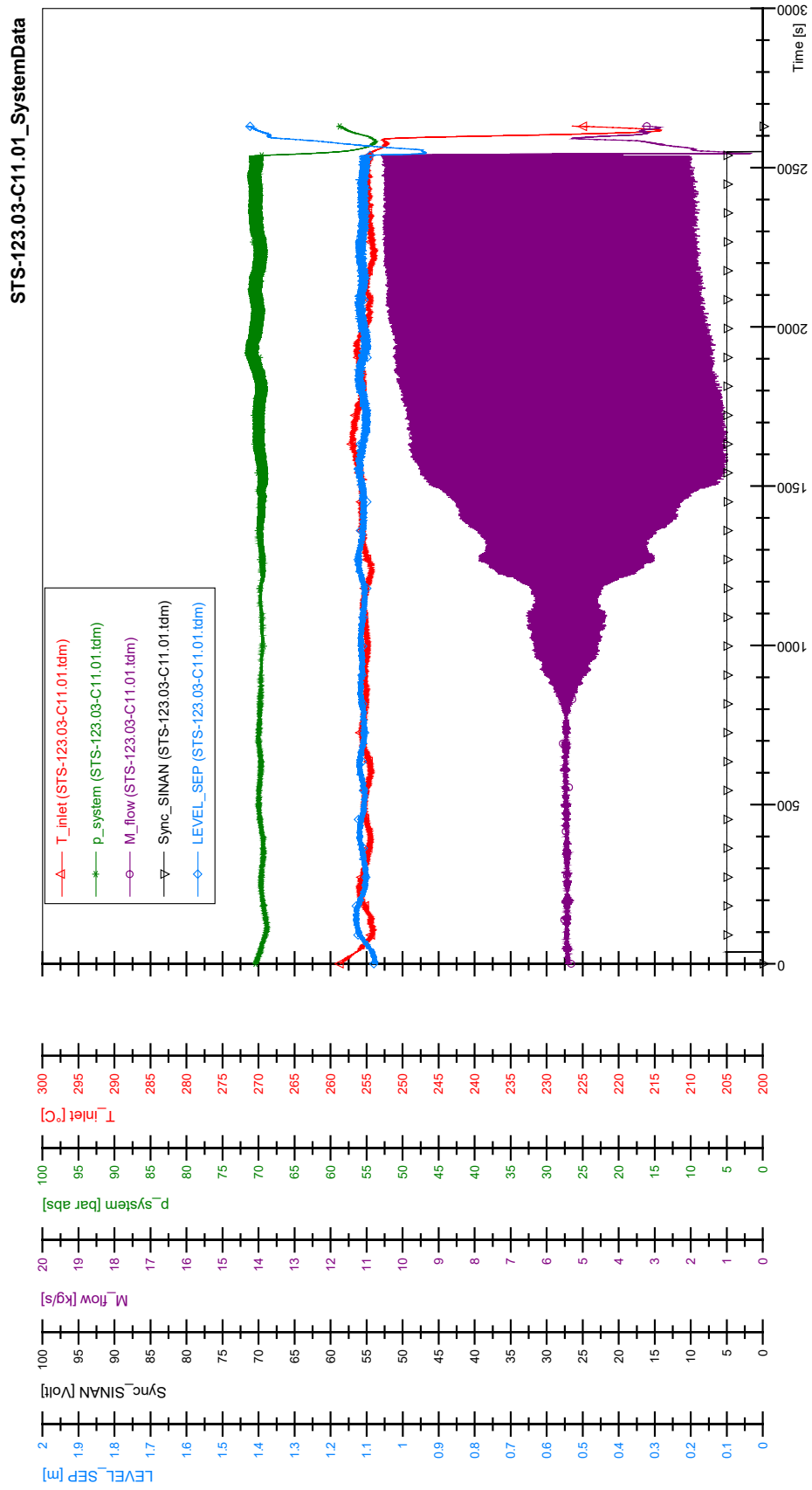
STS-123.03-B11.01_Rod_88



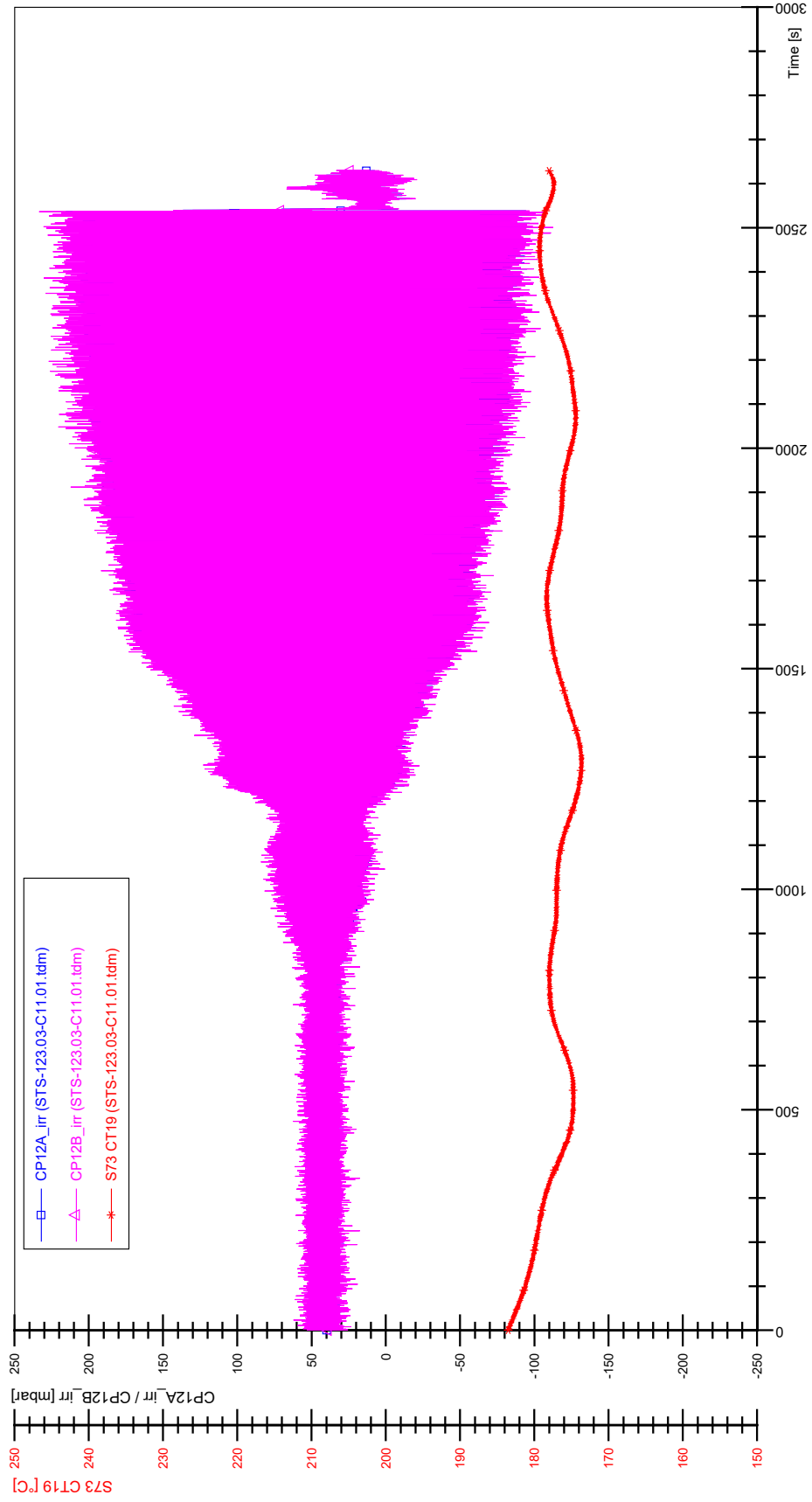
SIN-123.03-B11.01



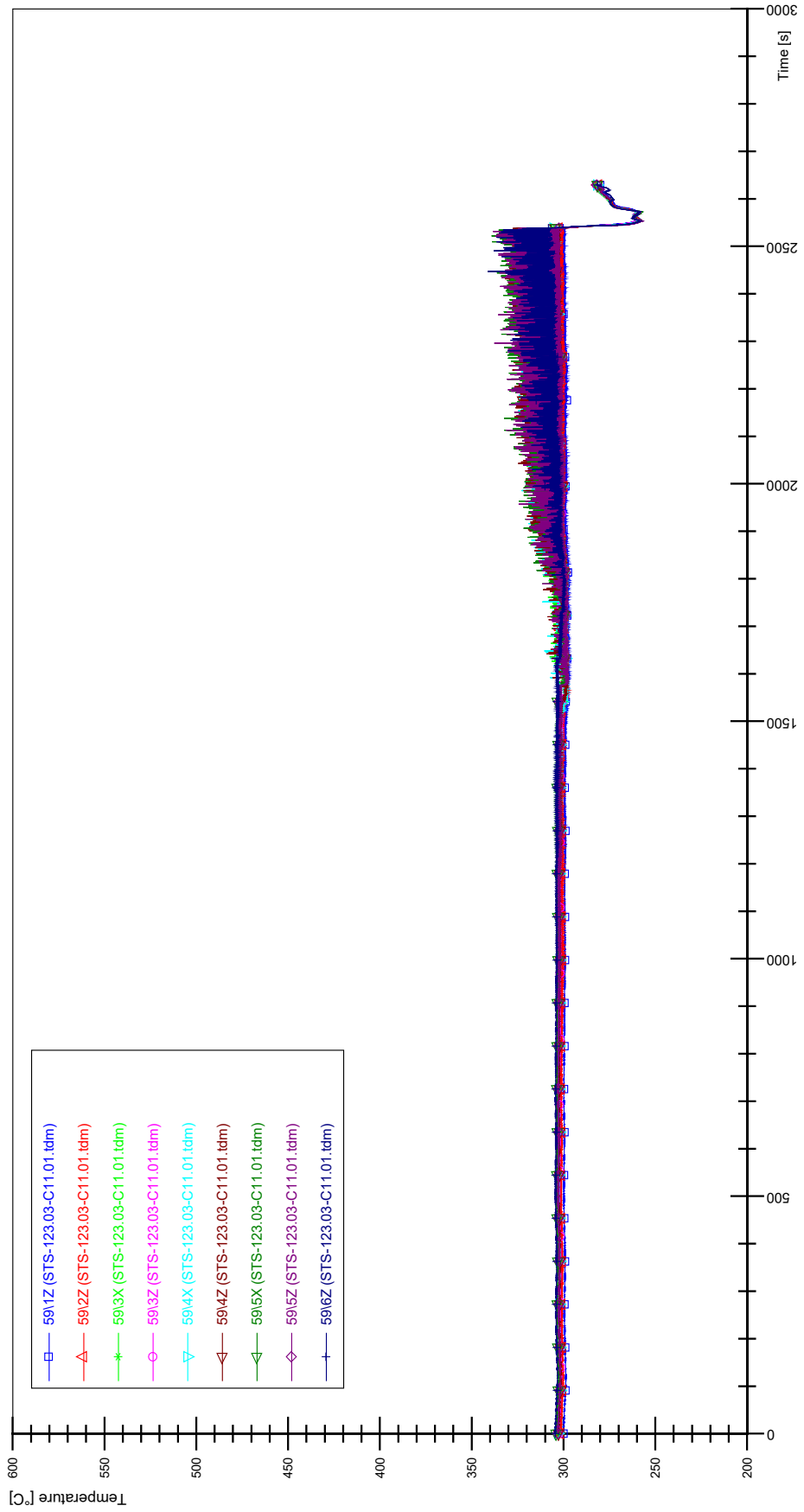
APPENDIX ZZ PLOTS OF INSTABILITY TEST STS-123.03-C11.01



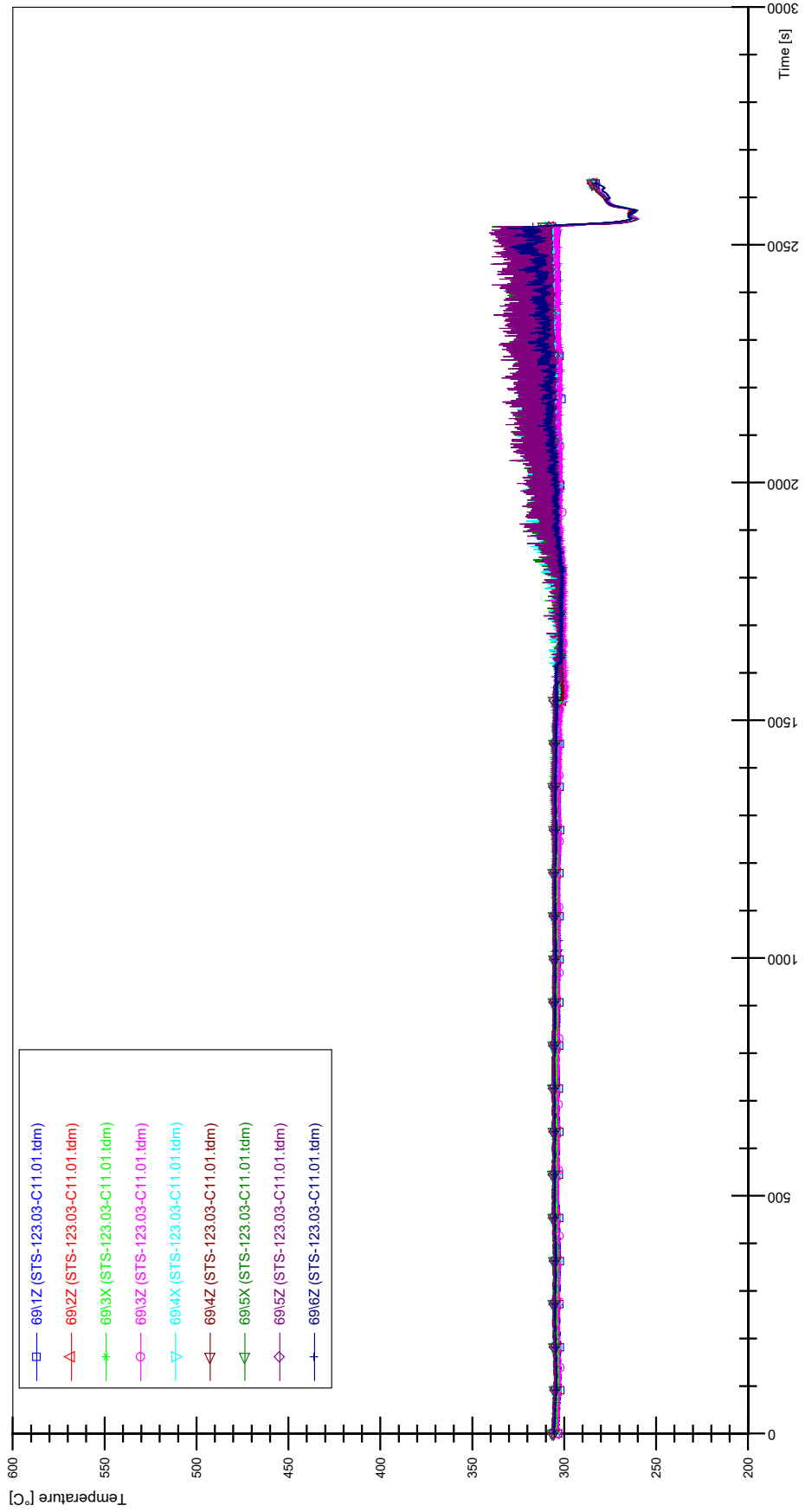
STS-123.03-C11.01_CP12_CT19



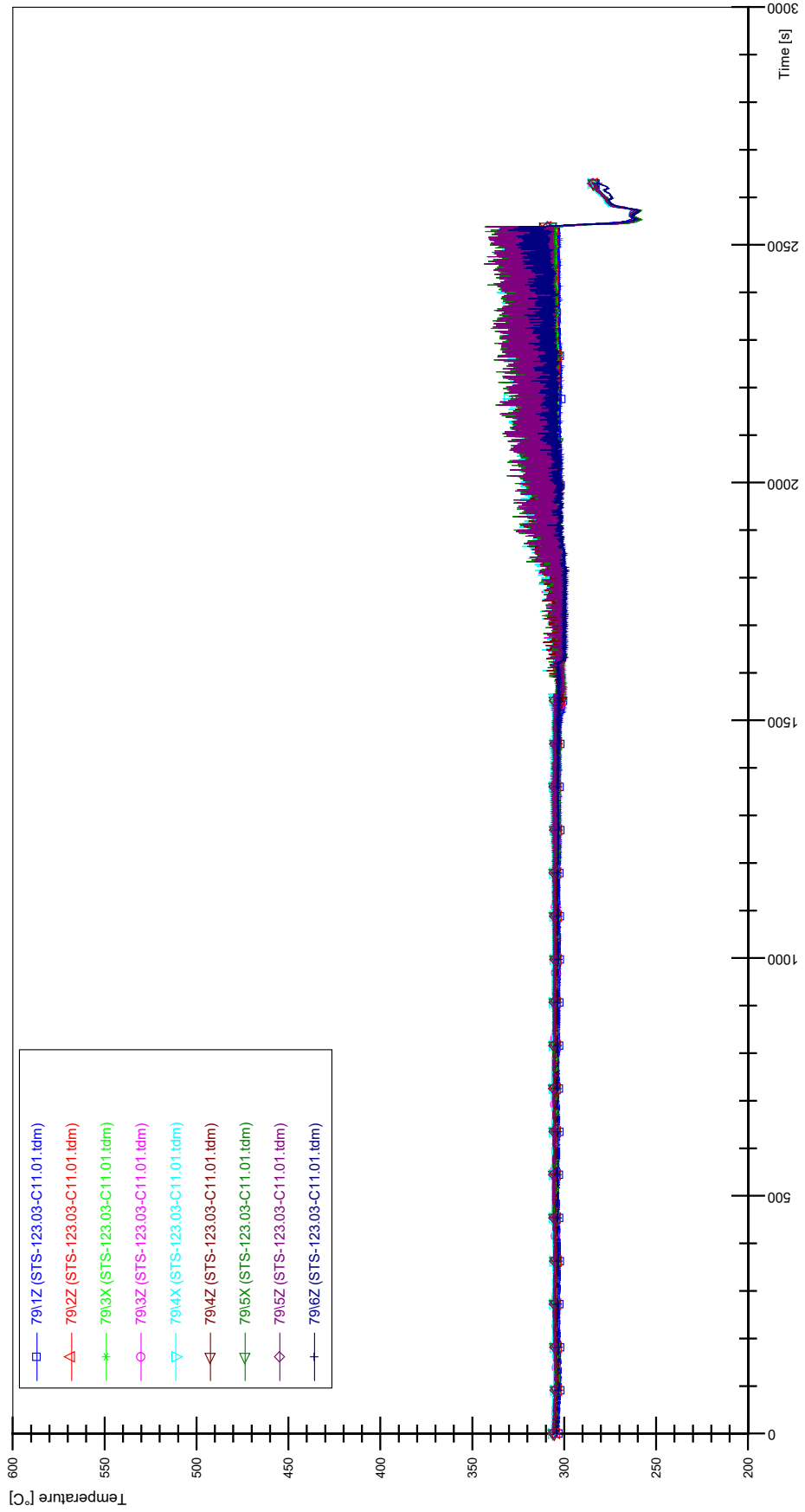
STS-123.03-C11.01_Rod_59



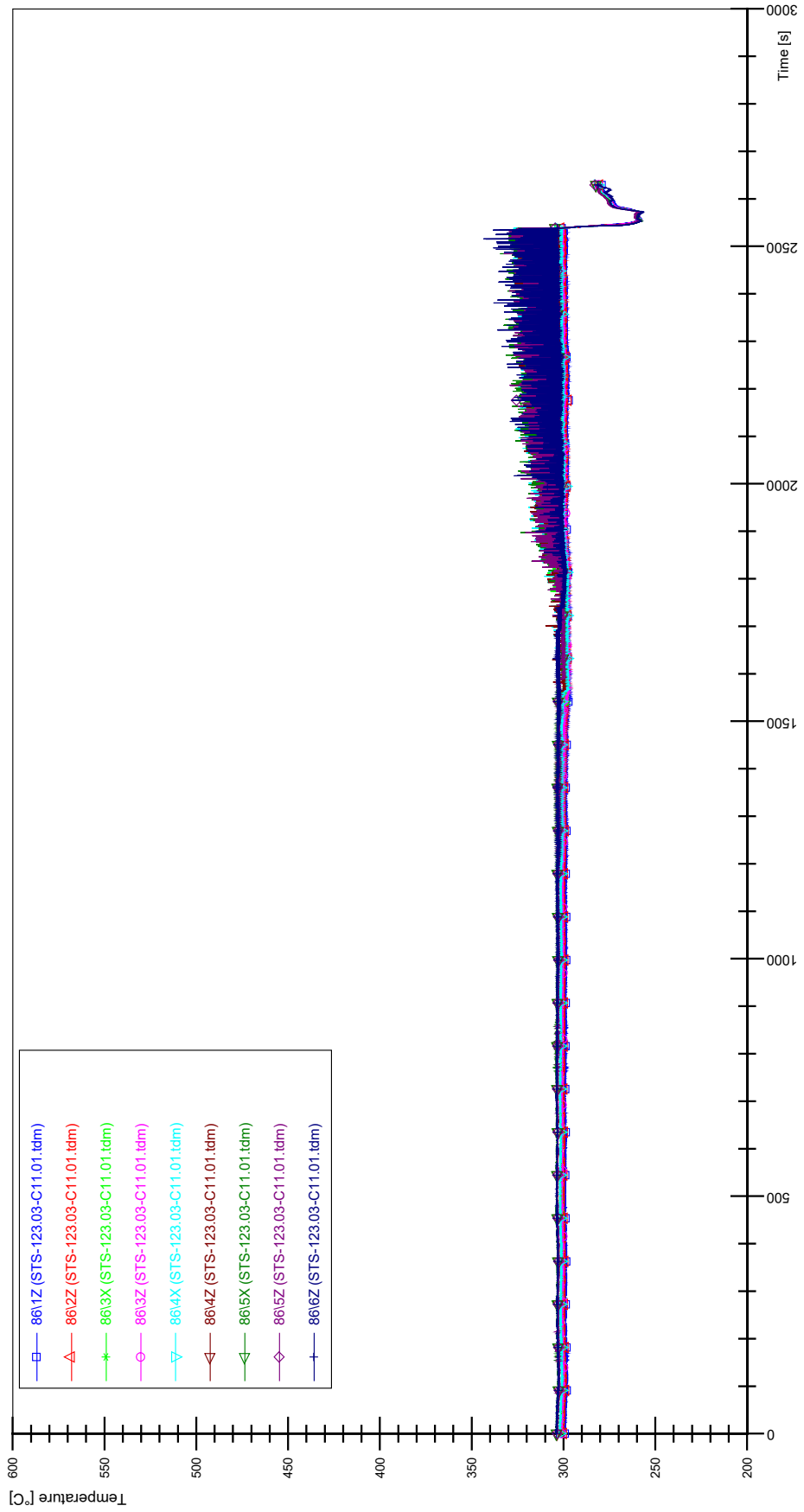
STS-123.03-C11.01_Rod_69



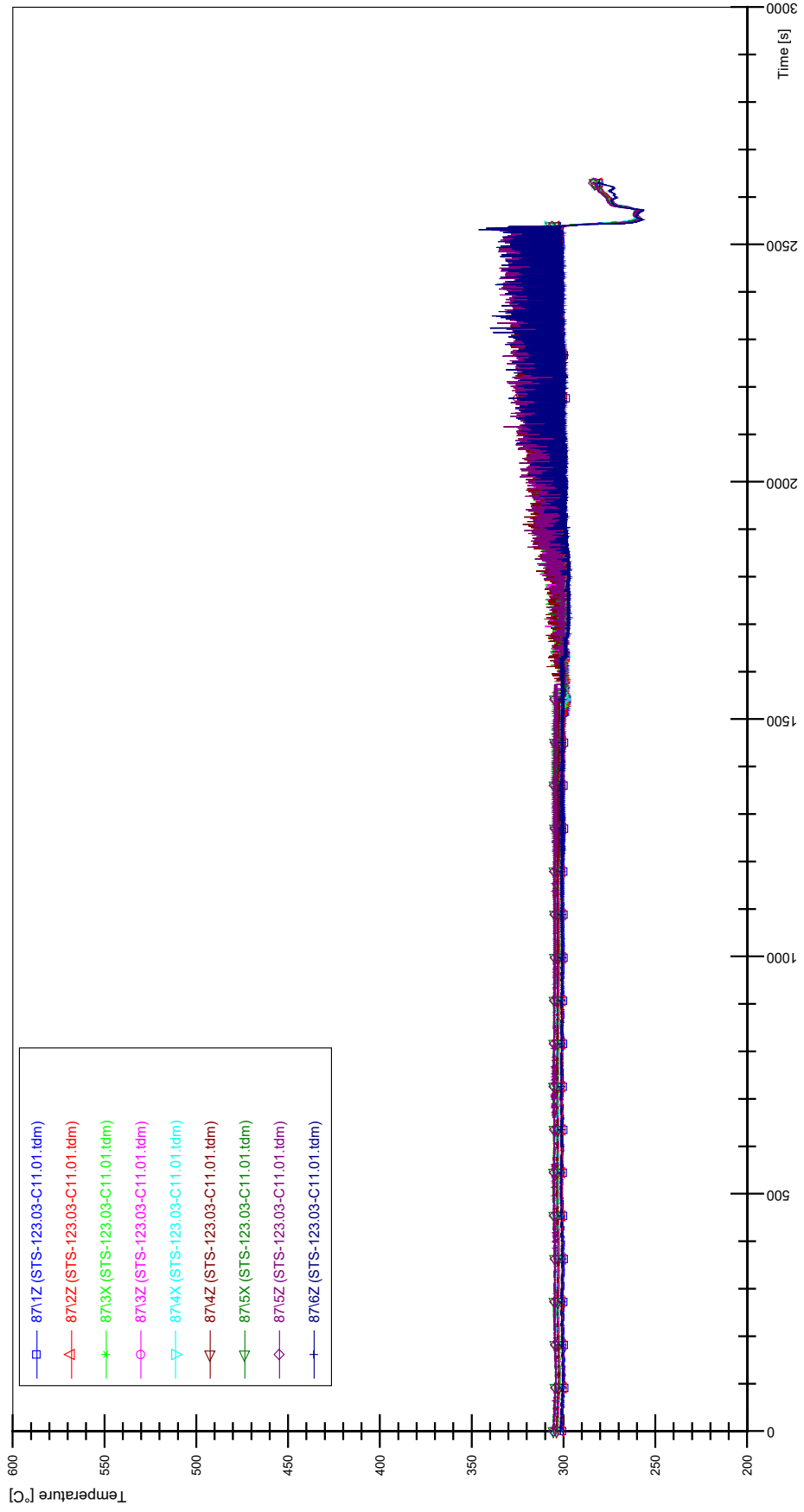
STS-123.03-C11.01_Rod_79



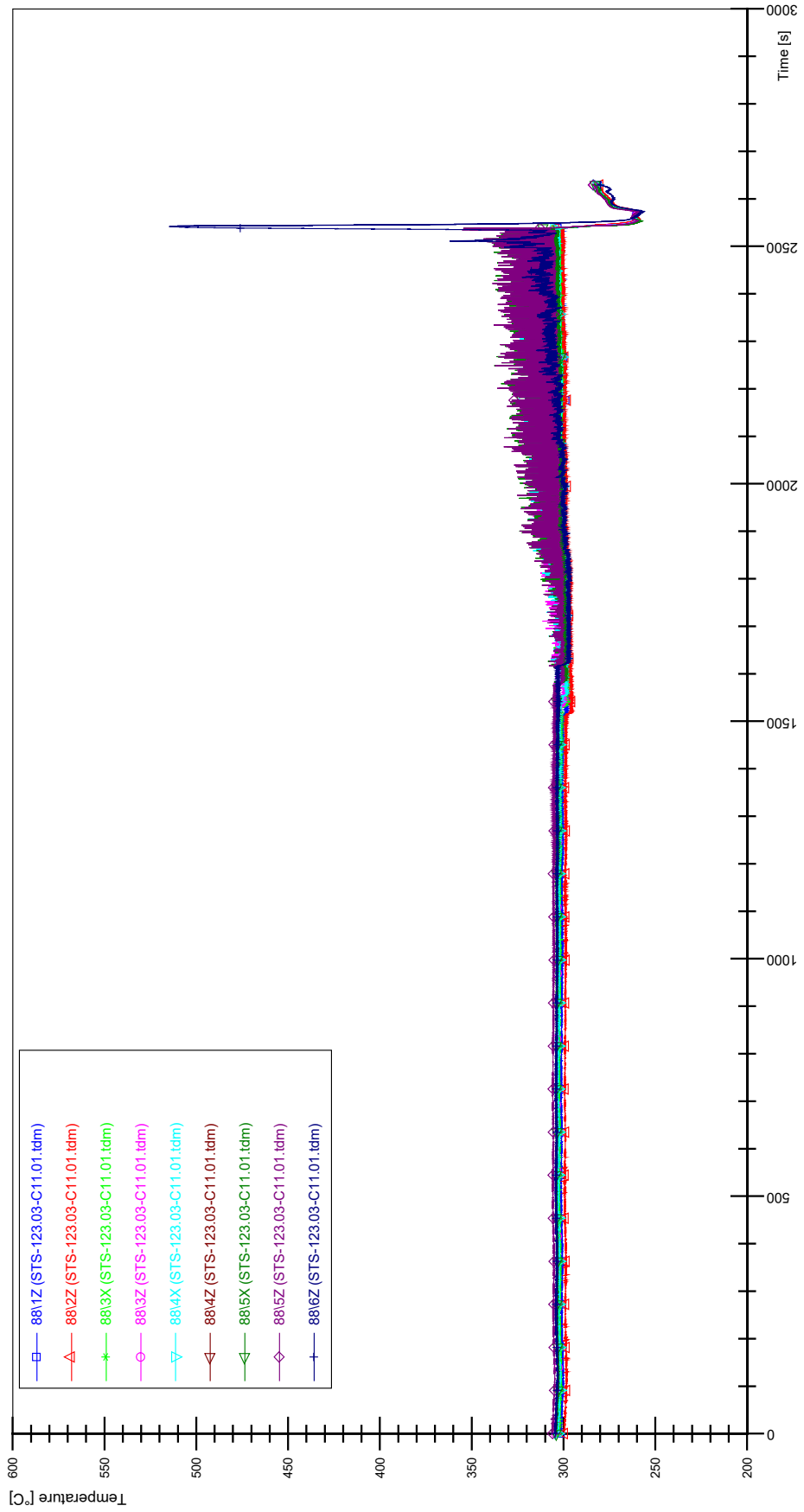
STS-123.03-C11.01_Rod_86



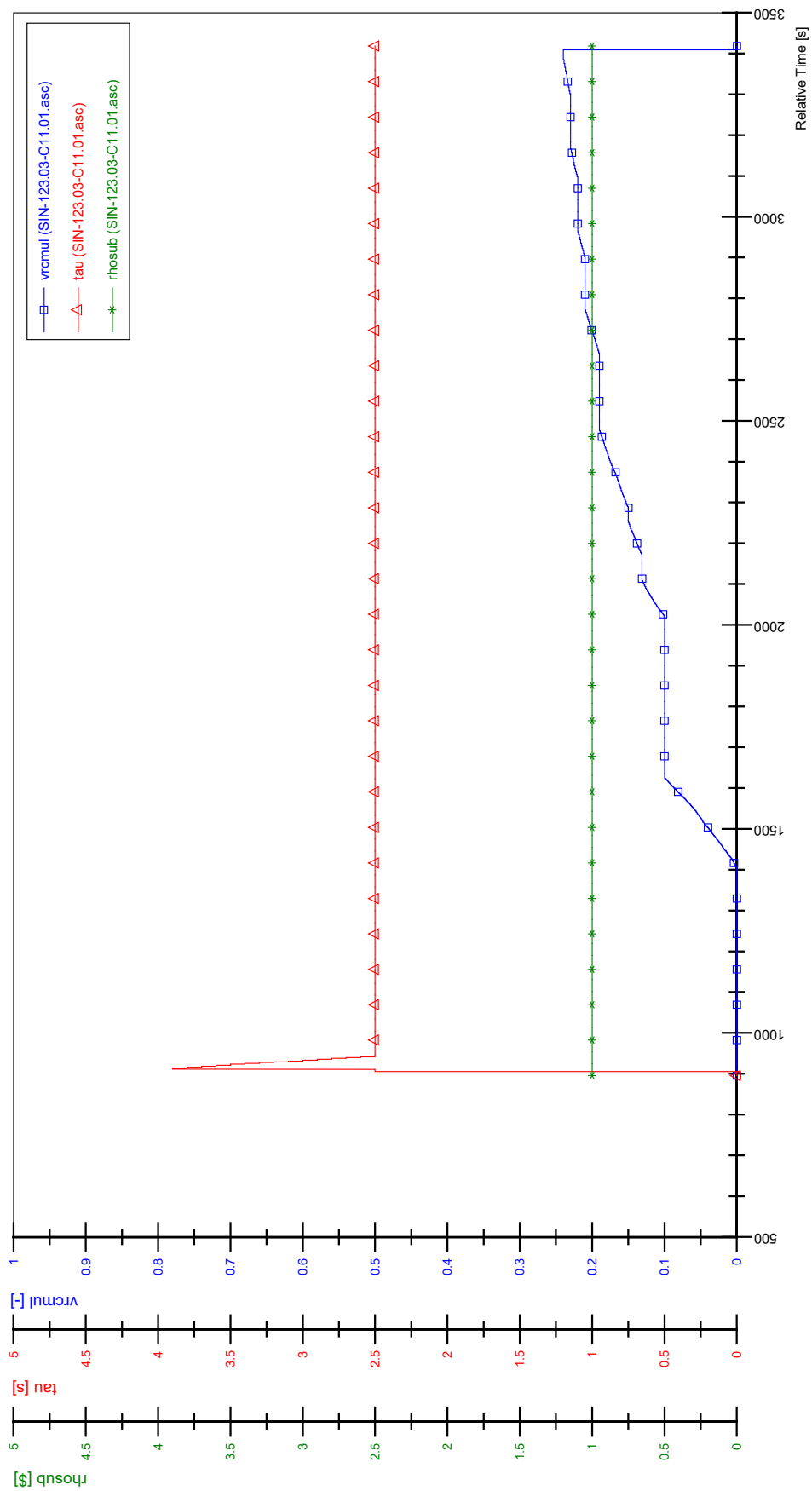
STS-123.03-C11.01_Rod_87



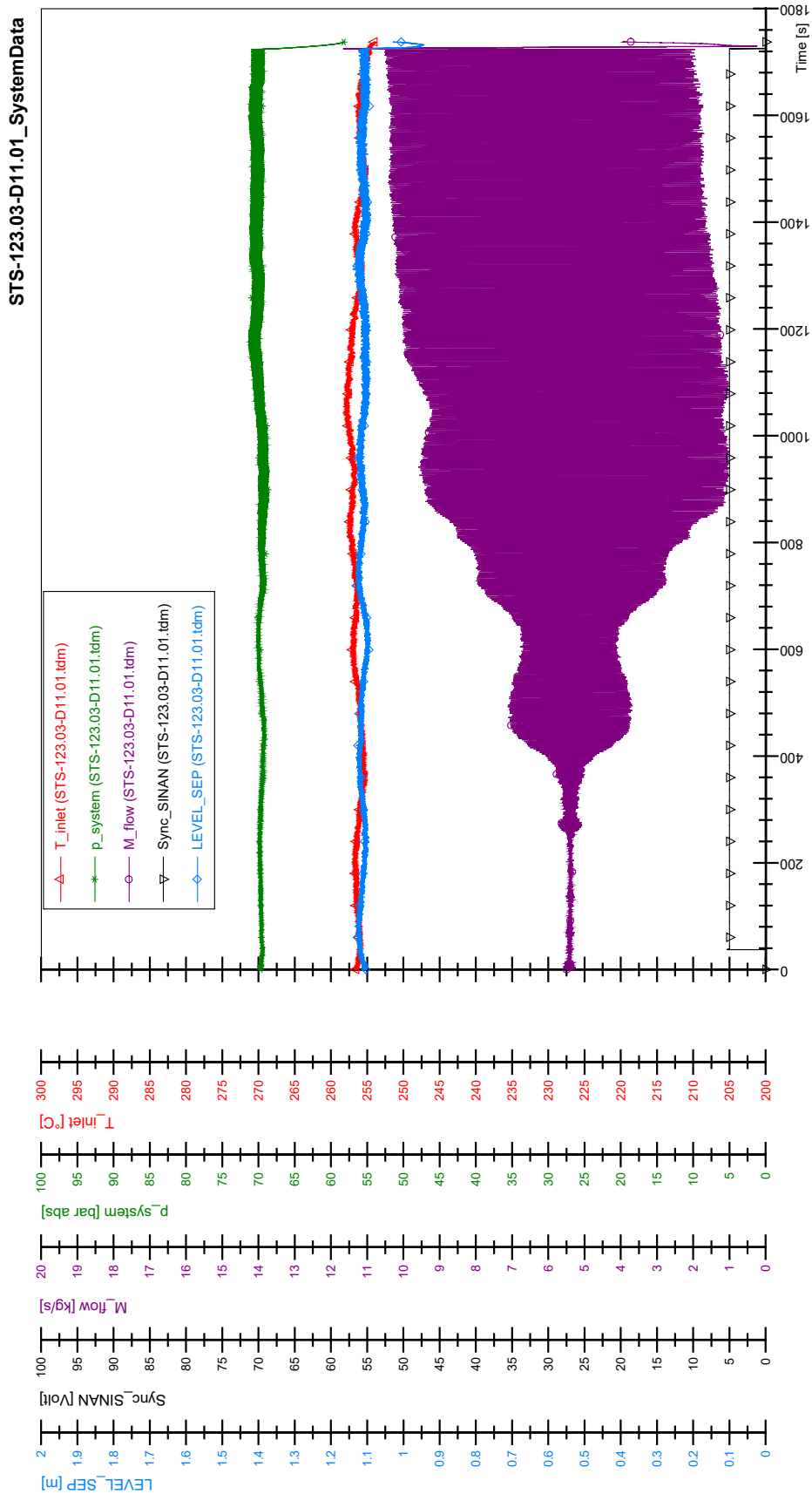
STS-123.03-C11.01_Rod_88



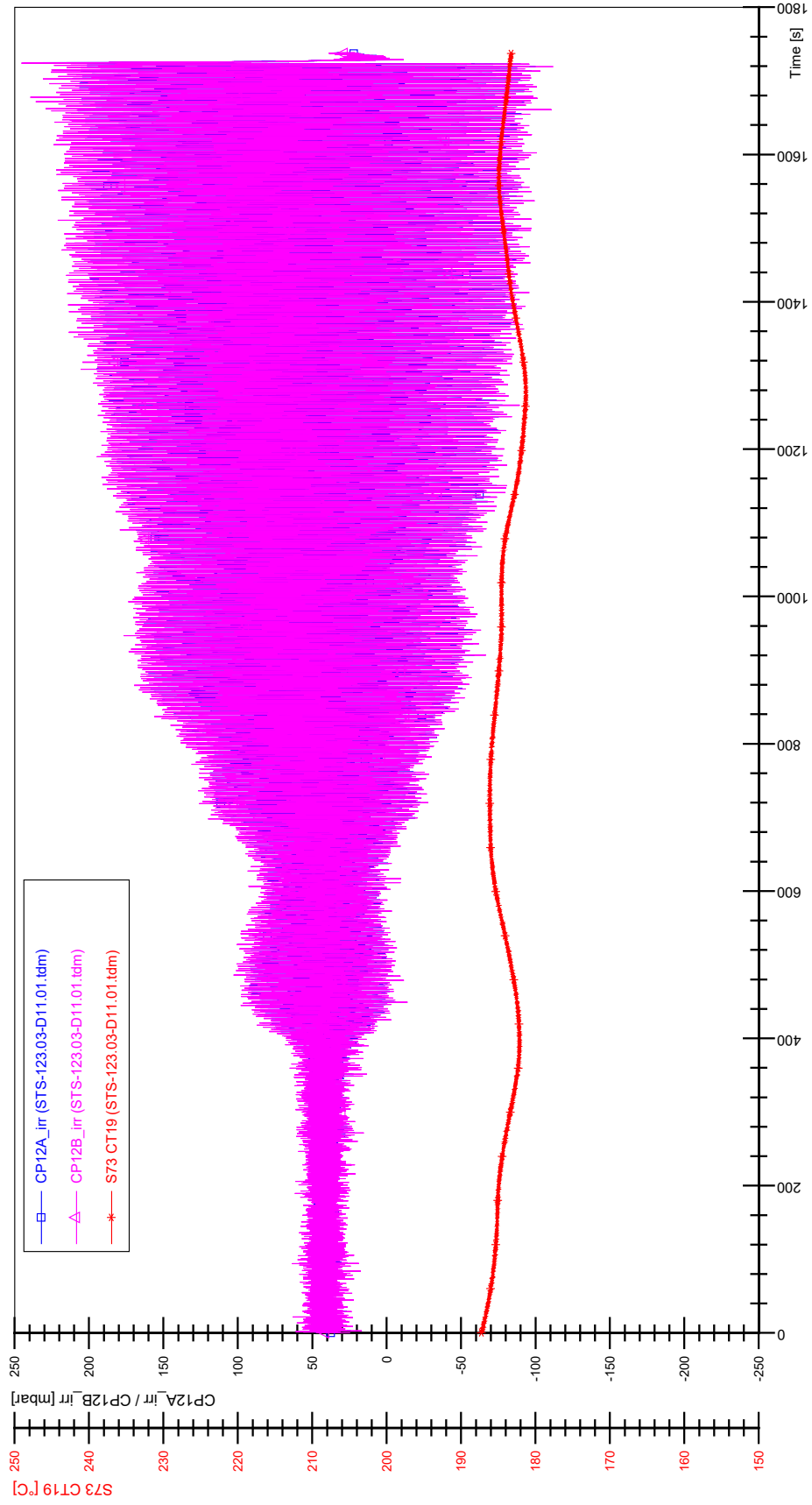
SIN-123.03-C11.01



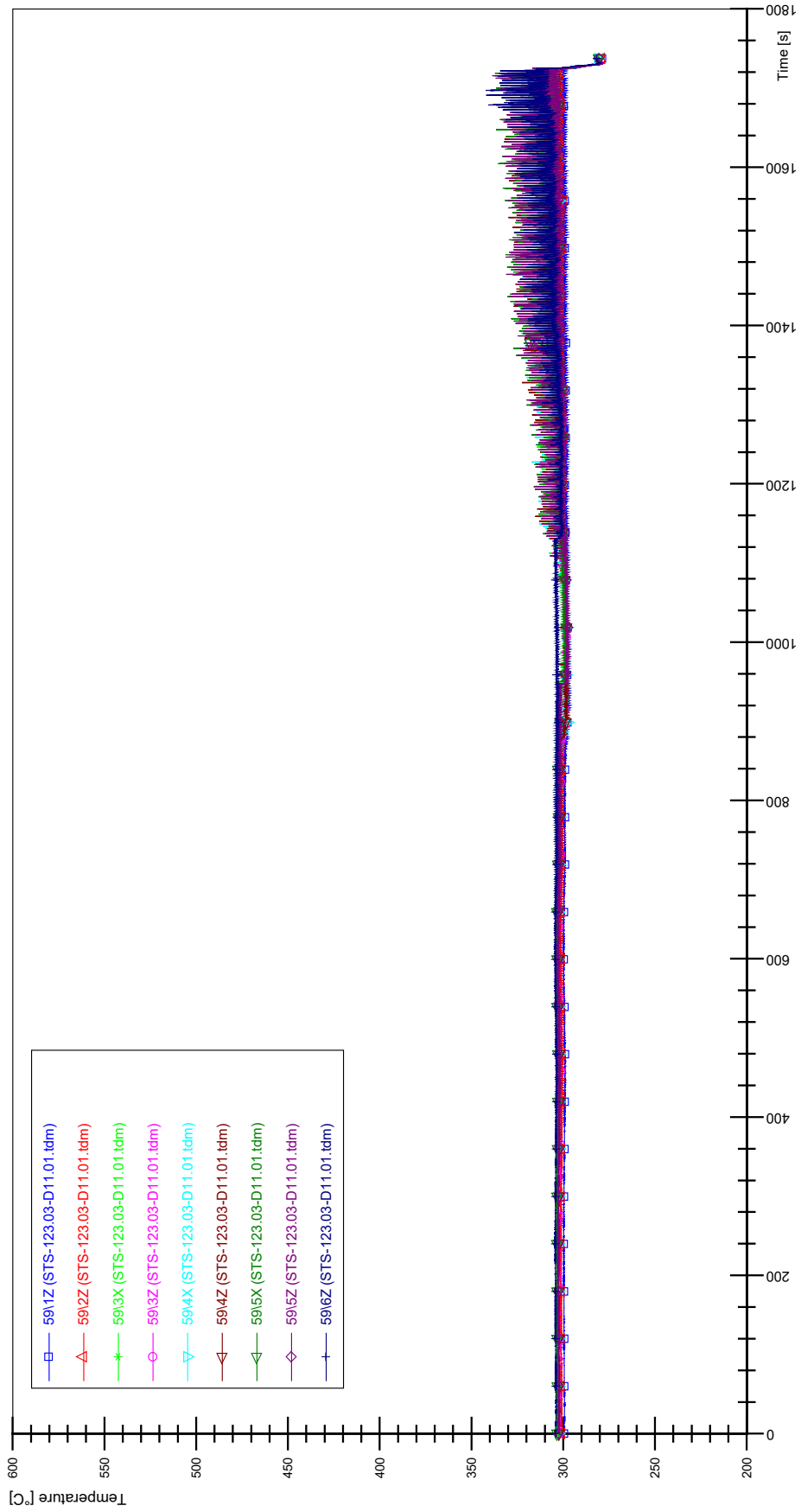
APPENDIX AAA PLOTS OF INSTABILITY TEST STS-123.03-D11.01



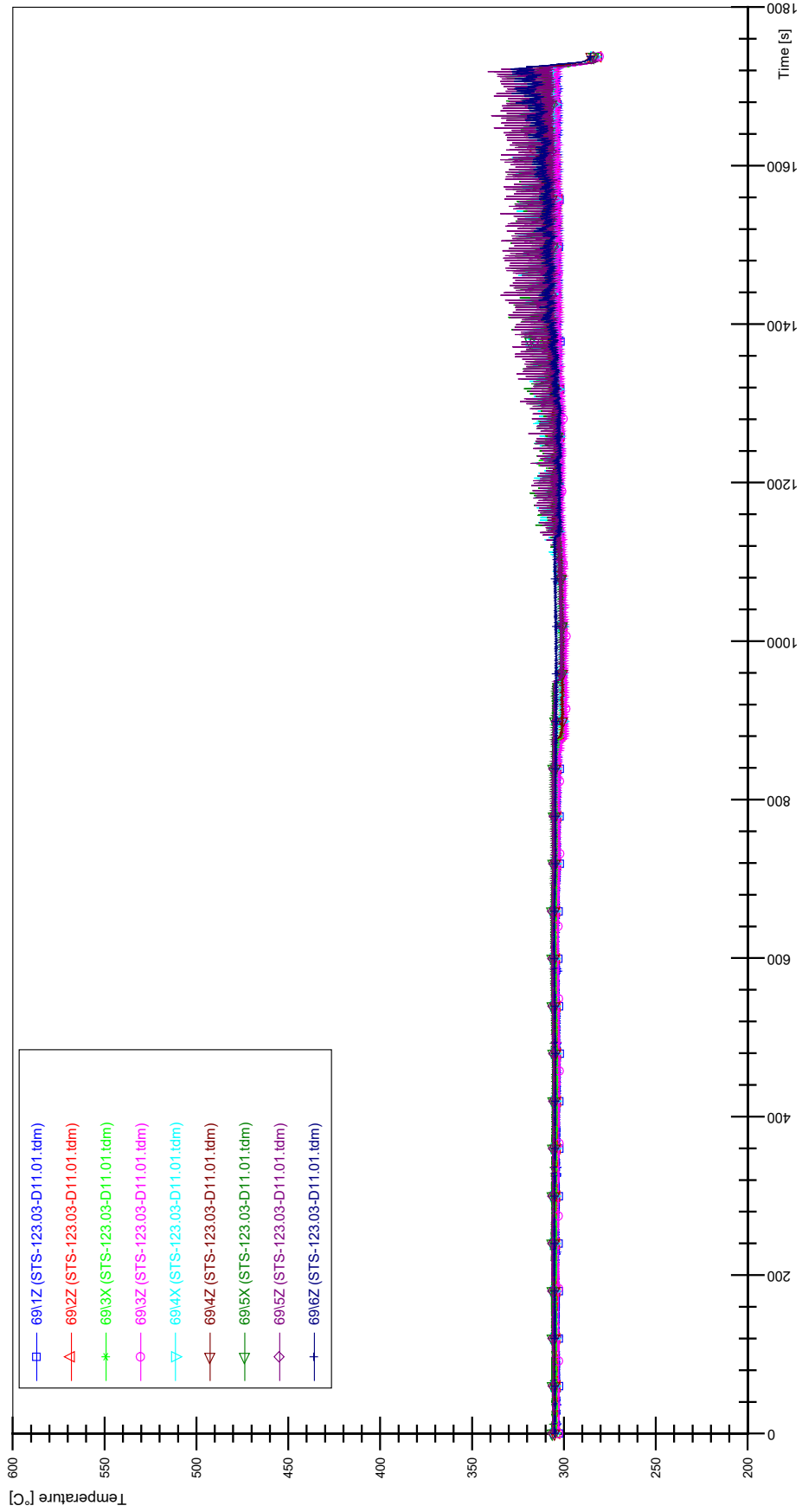
STS-123.03-D11.01_CP12_CT19



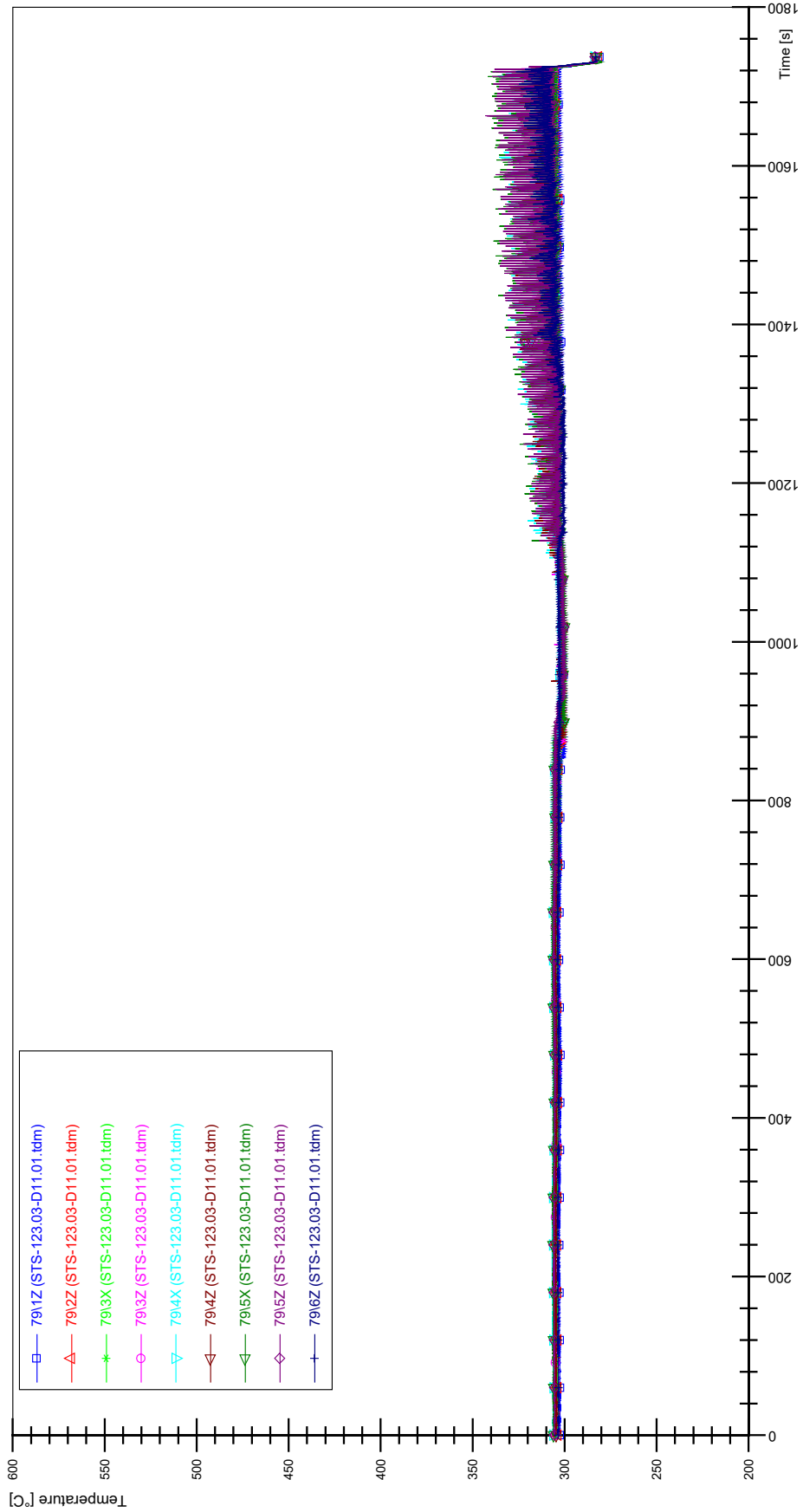
STS-123.03-D11.01_Rod_59



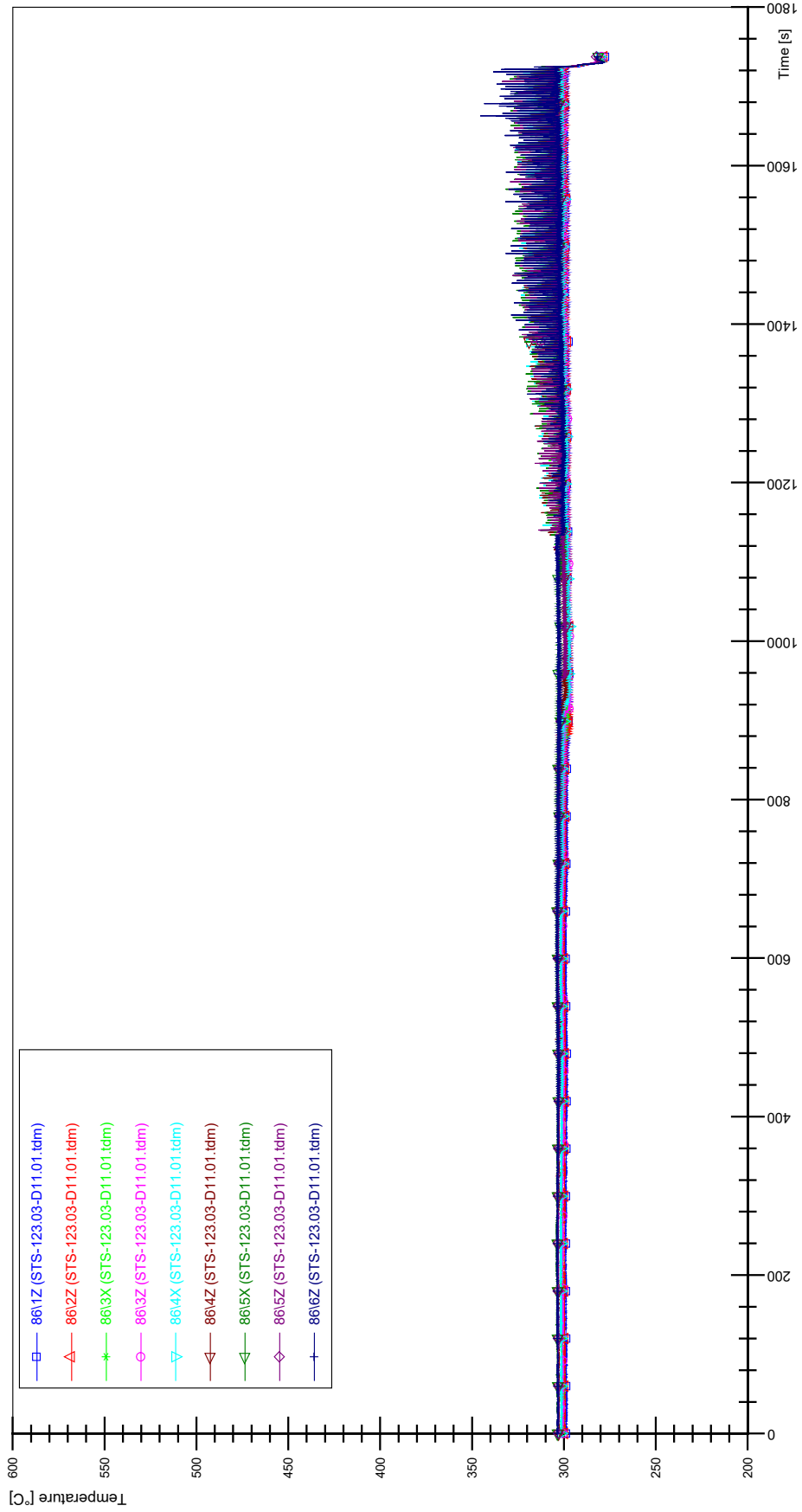
STS-123.03-D11.01_Rod_69



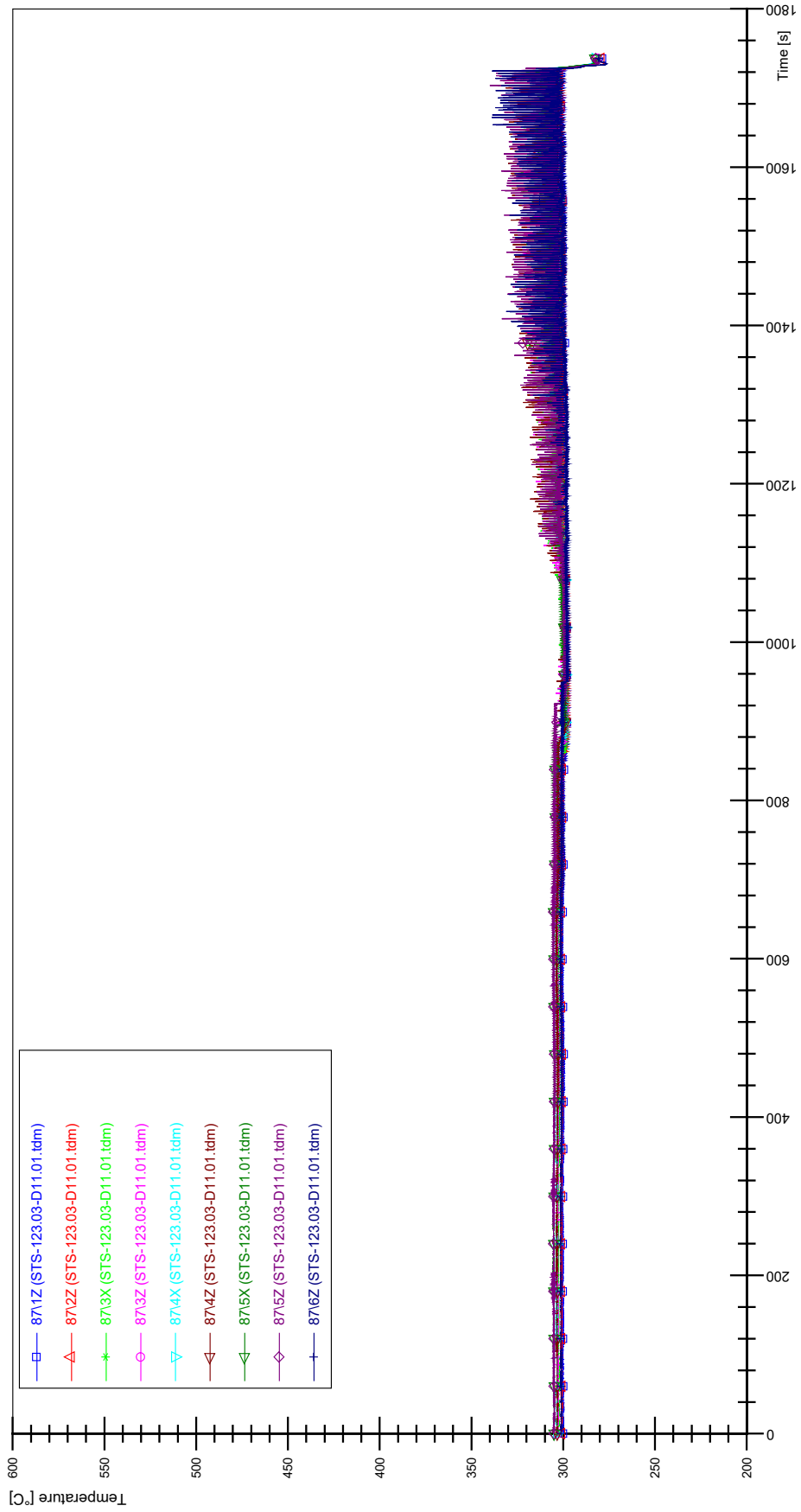
STS-123.03-D11.01_Rod_79



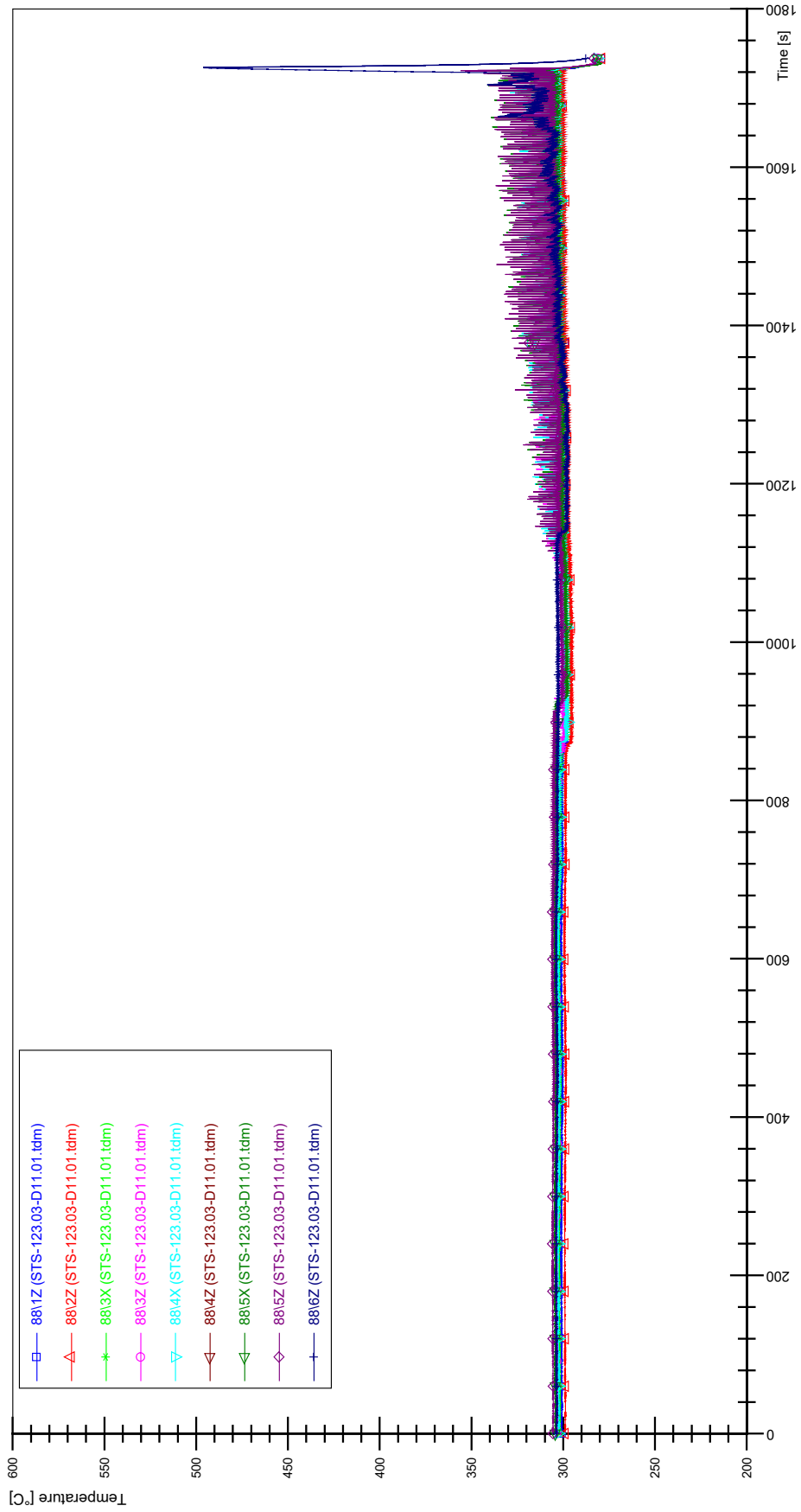
STS-123.03-D11.01_Rod_86



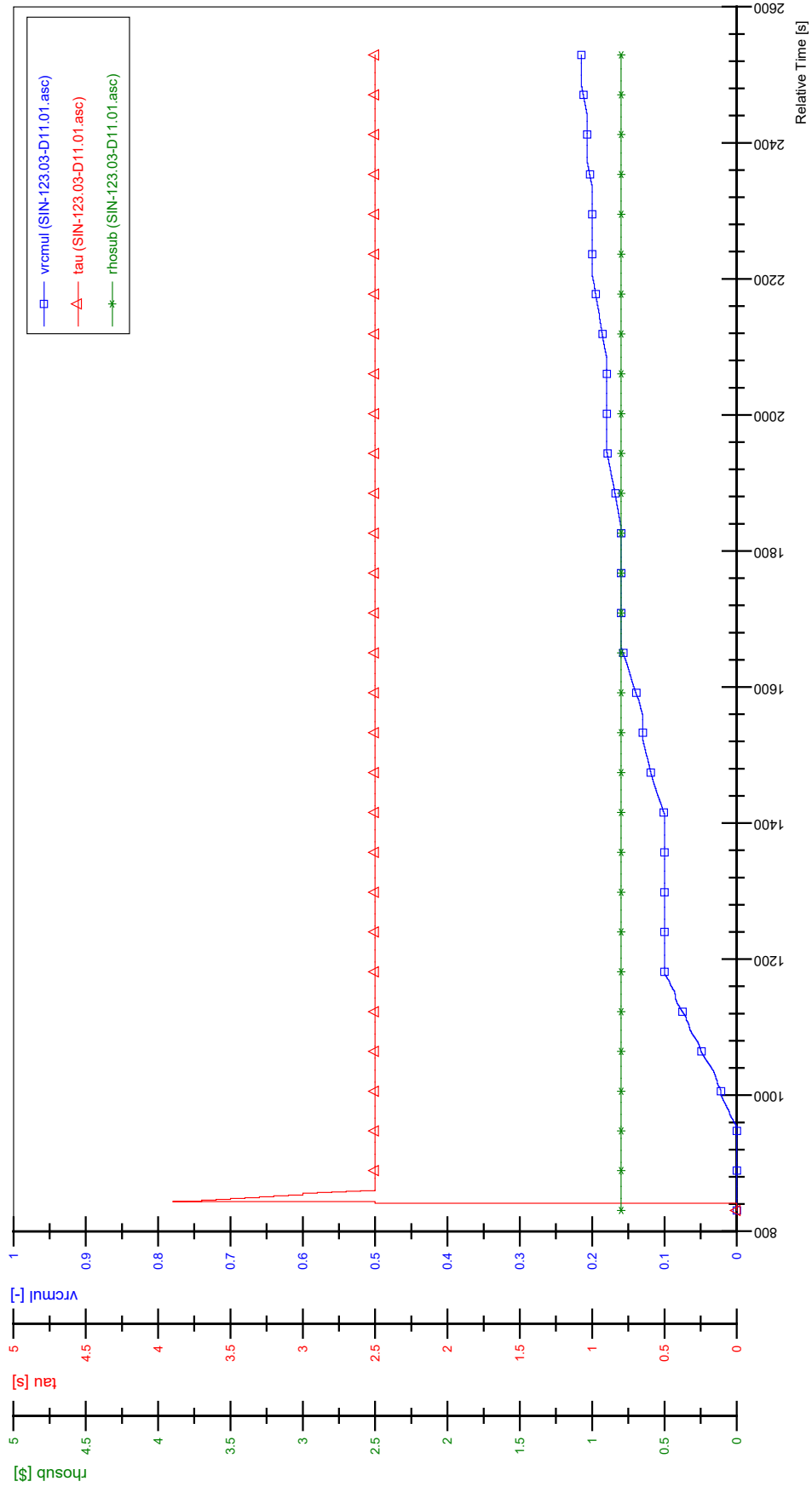
STS-123.03-D11.01_Rod_87



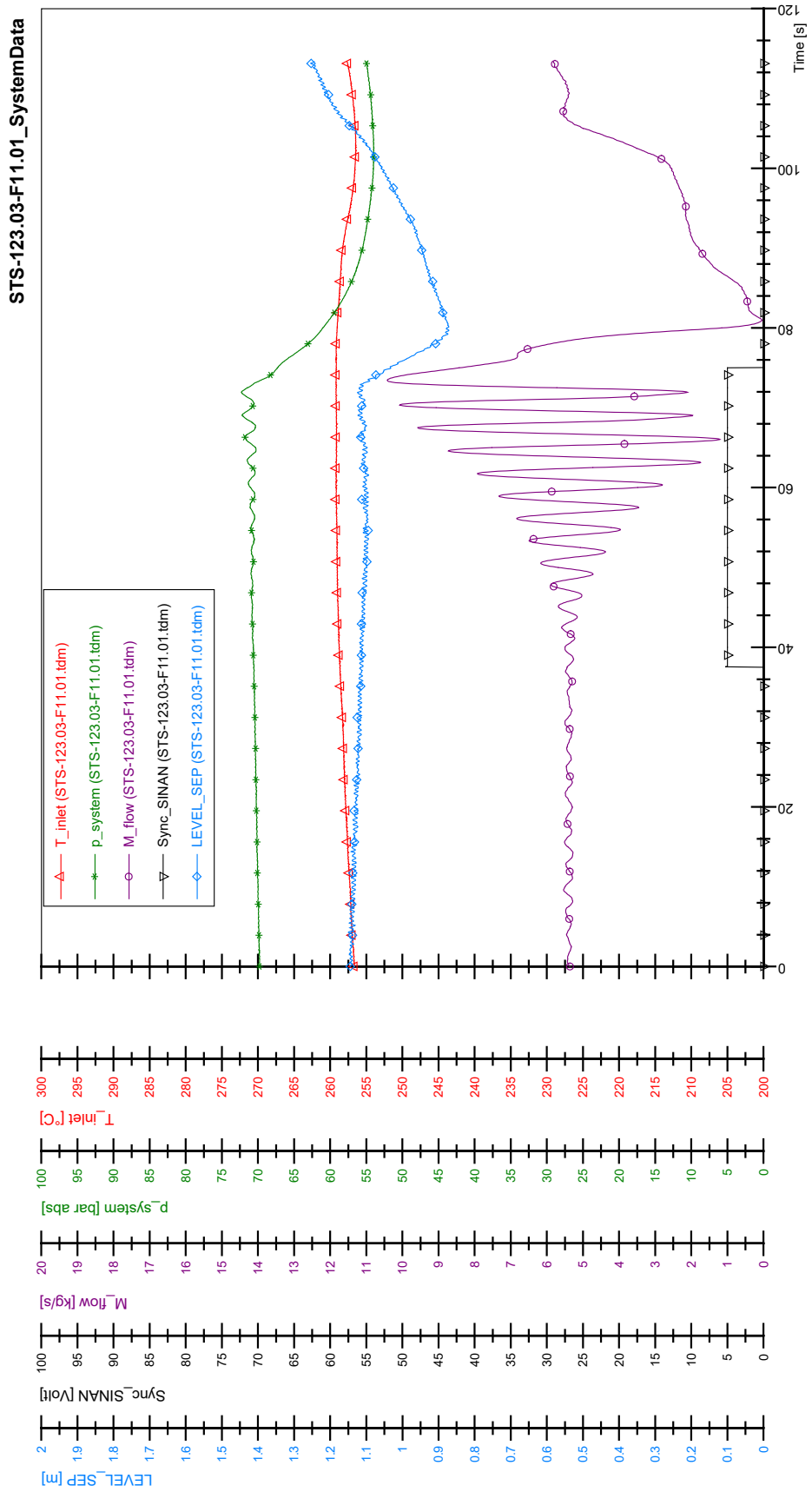
STS-123.03-D11.01_Rod_88



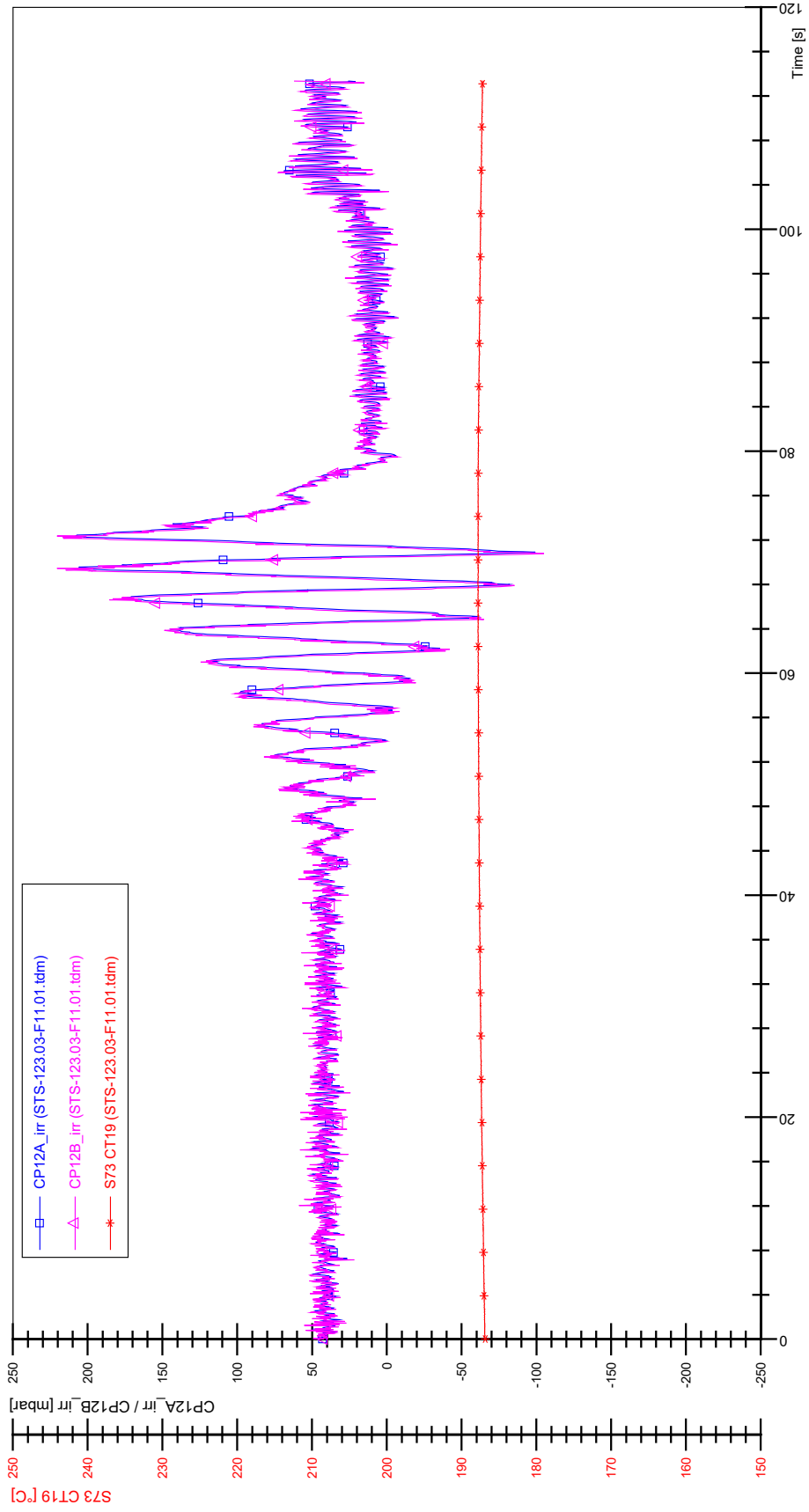
SIN-123.03-D11.01



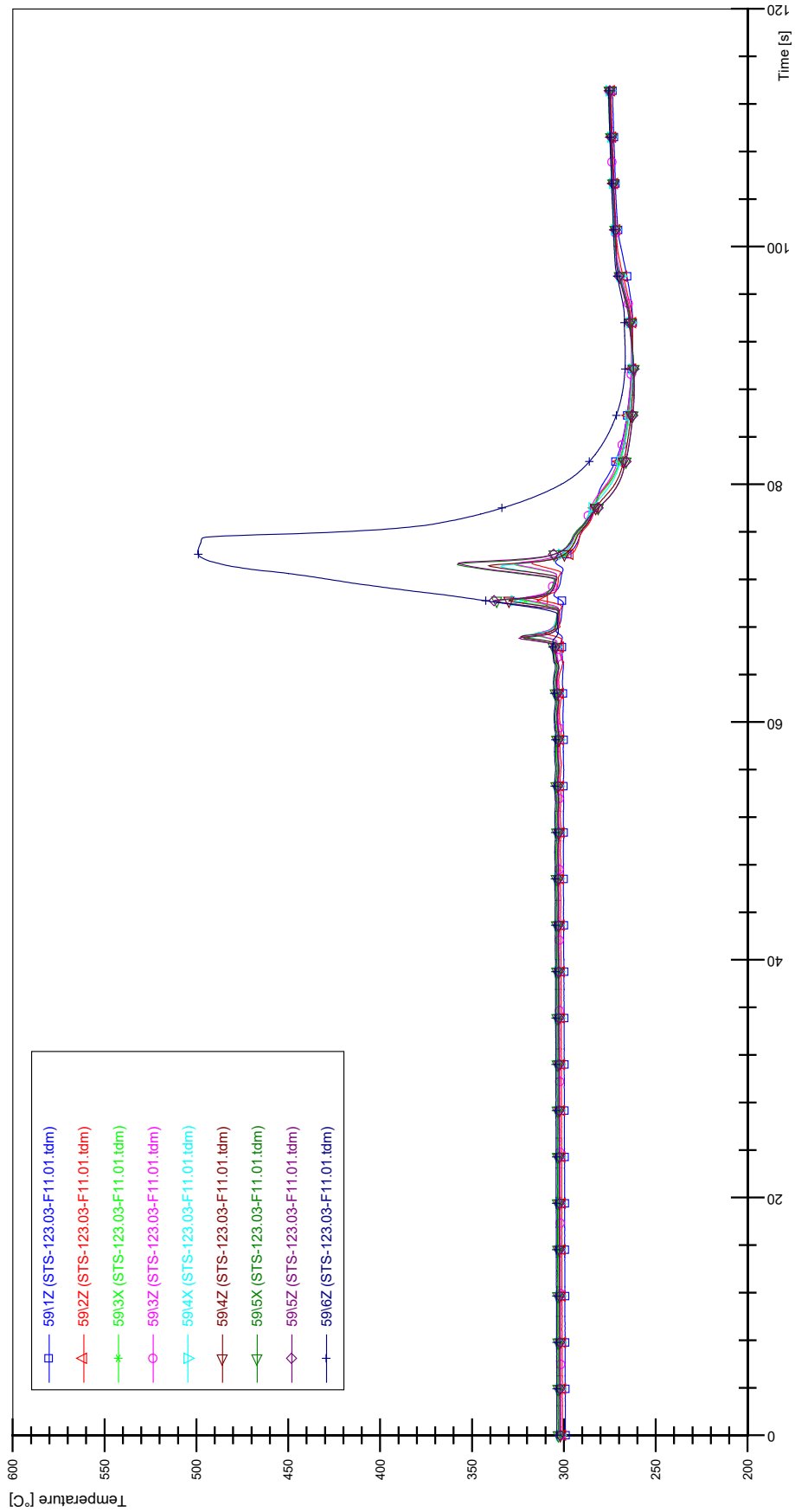
APPENDIX BBB PLOTS OF INSTABILITY TEST STS-123.03-F11.01



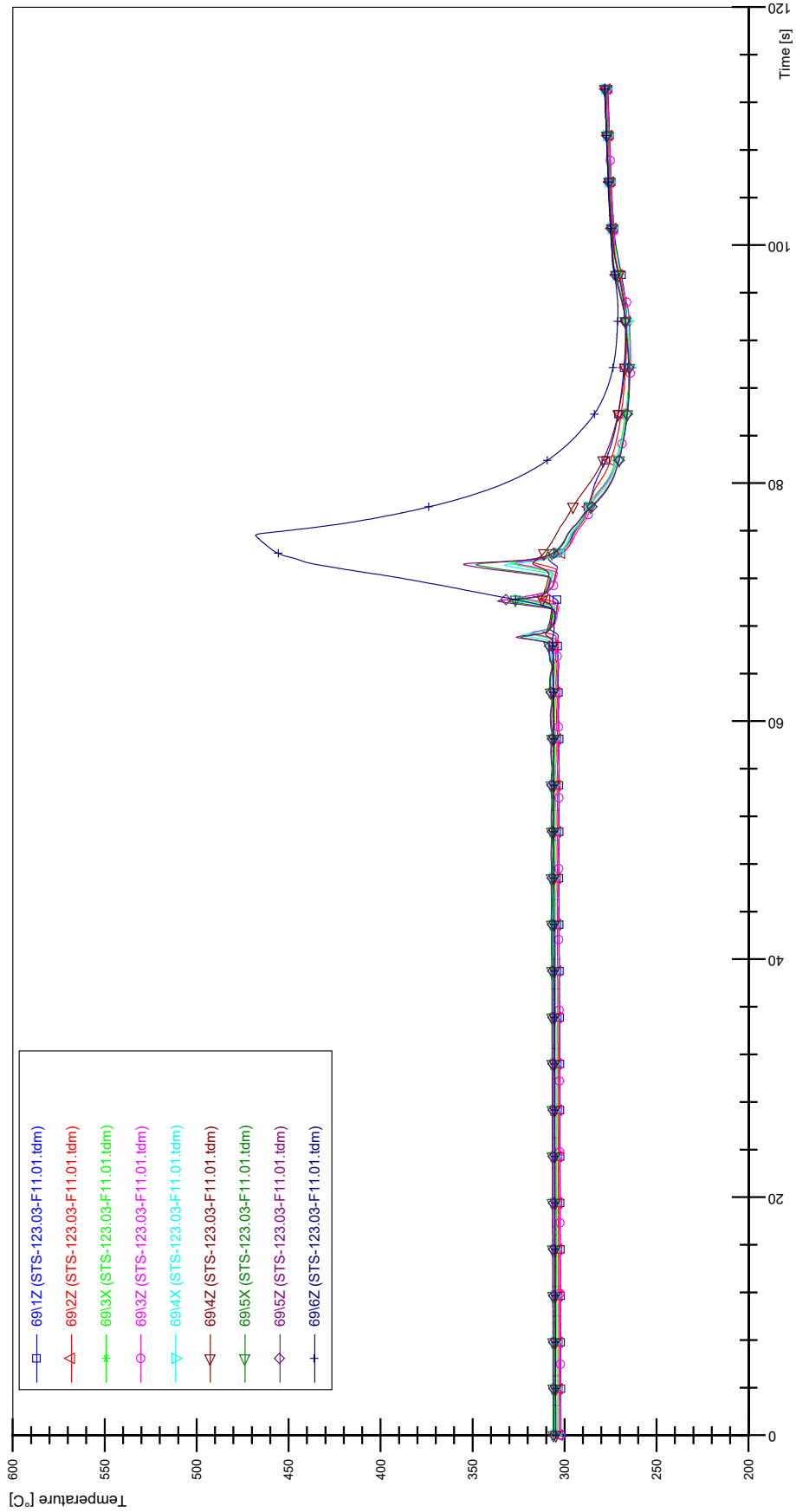
STS-123.03-F11.01_CP12_CT19



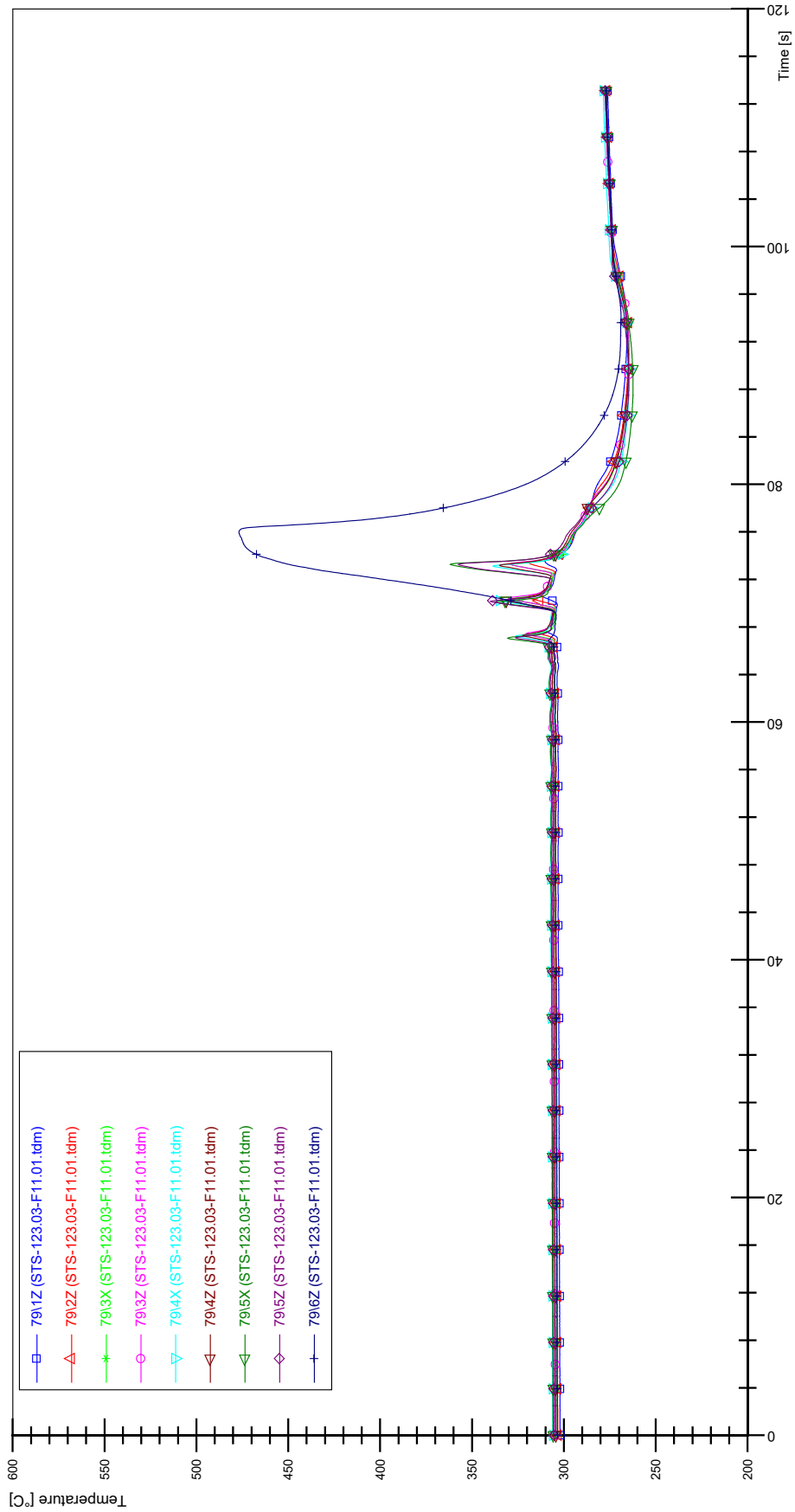
STS-123.03-F11.01_Rod_59



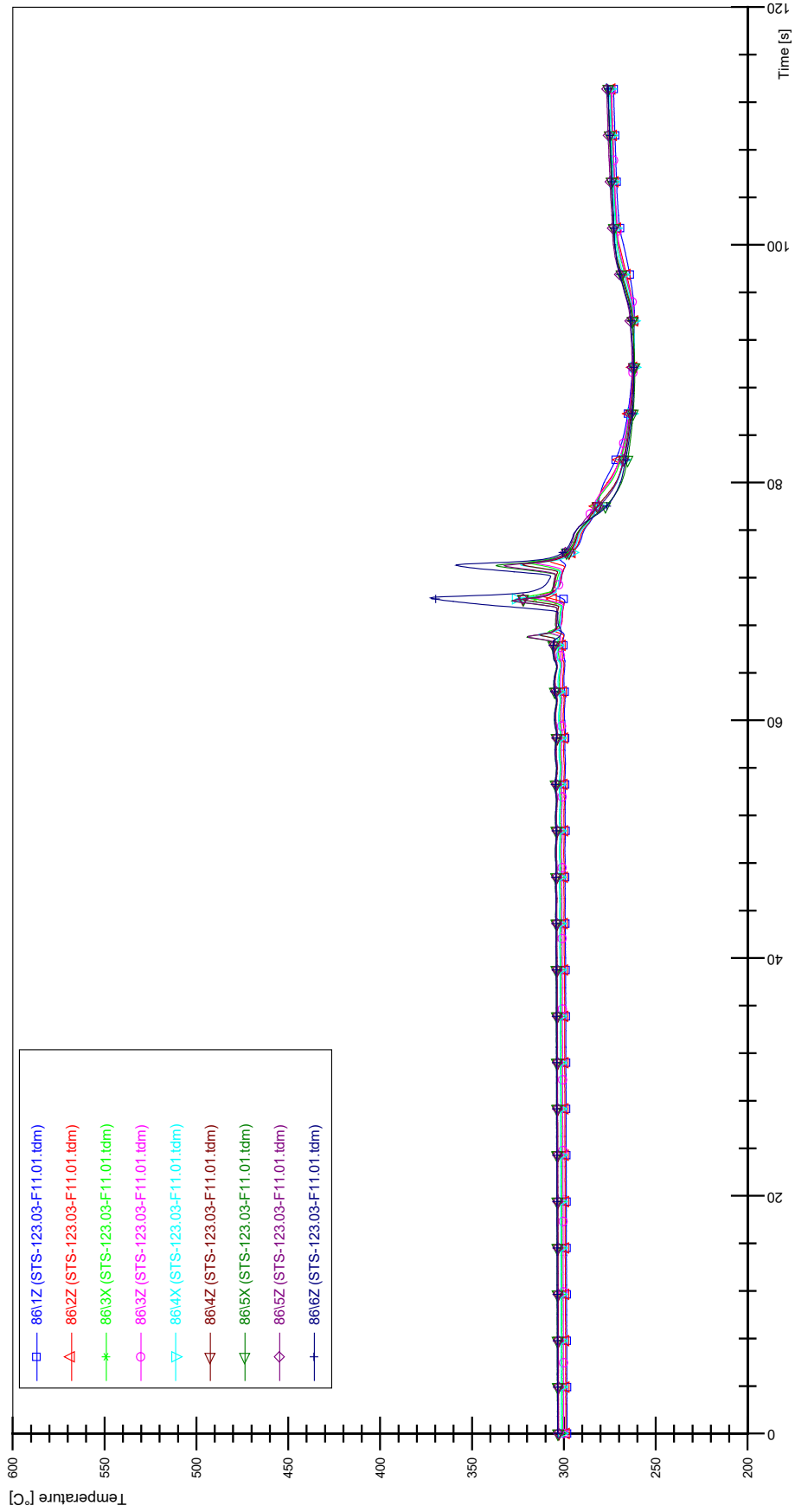
STS-123.03-F11.01_Rod_69



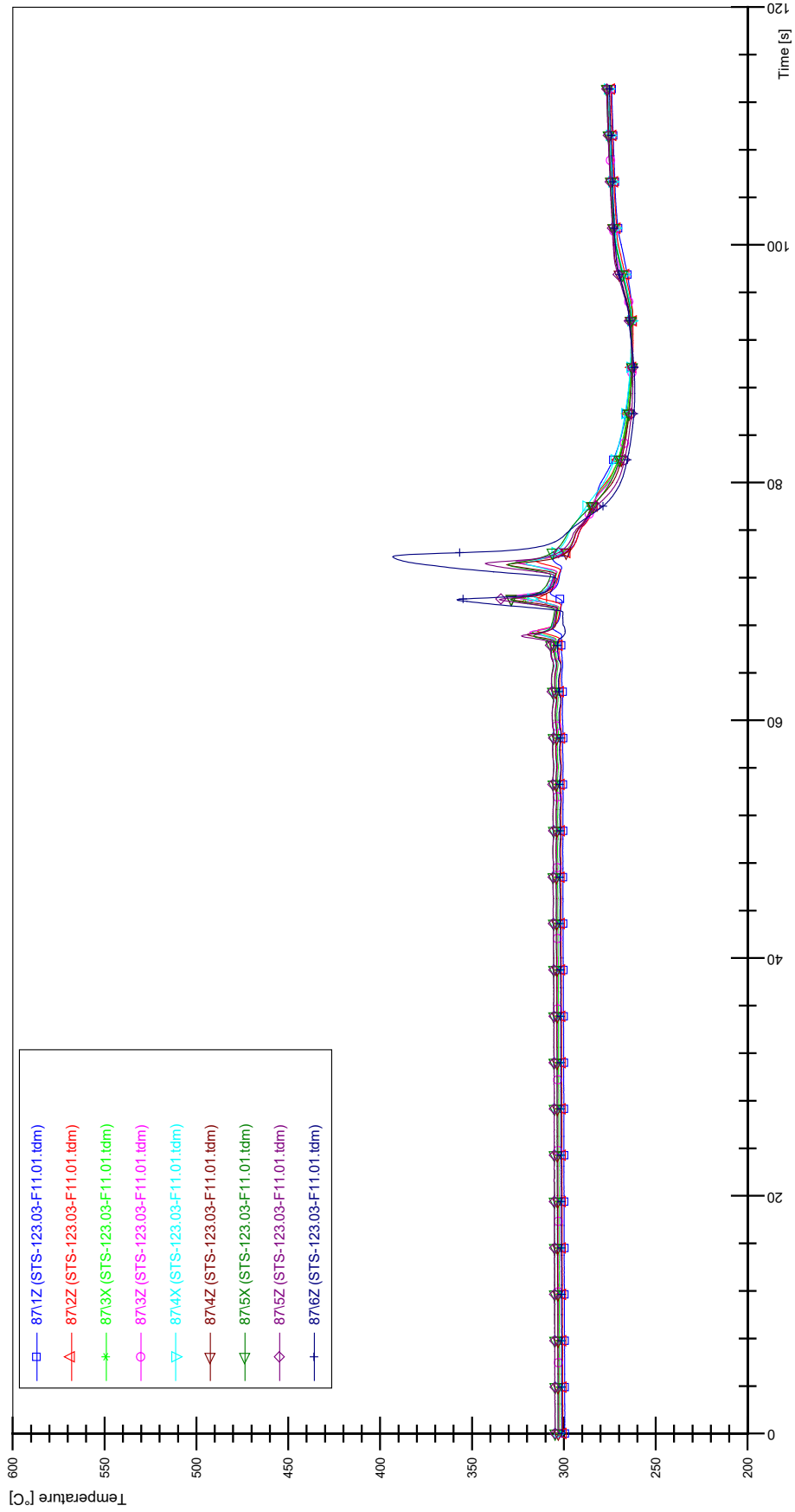
STS-123.03-F11.01_Rod_79



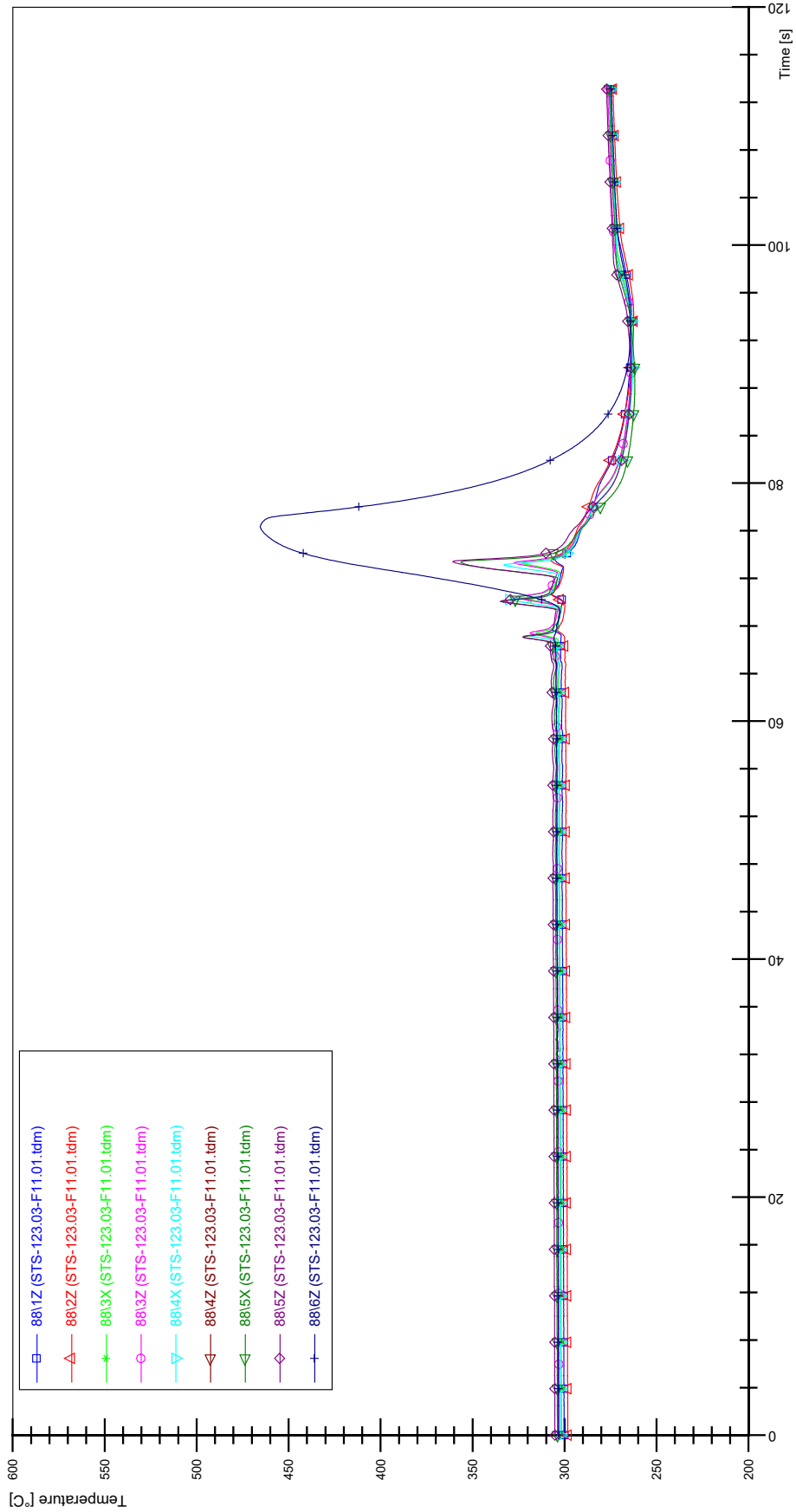
STS-123.03-F11.01_Rod_86



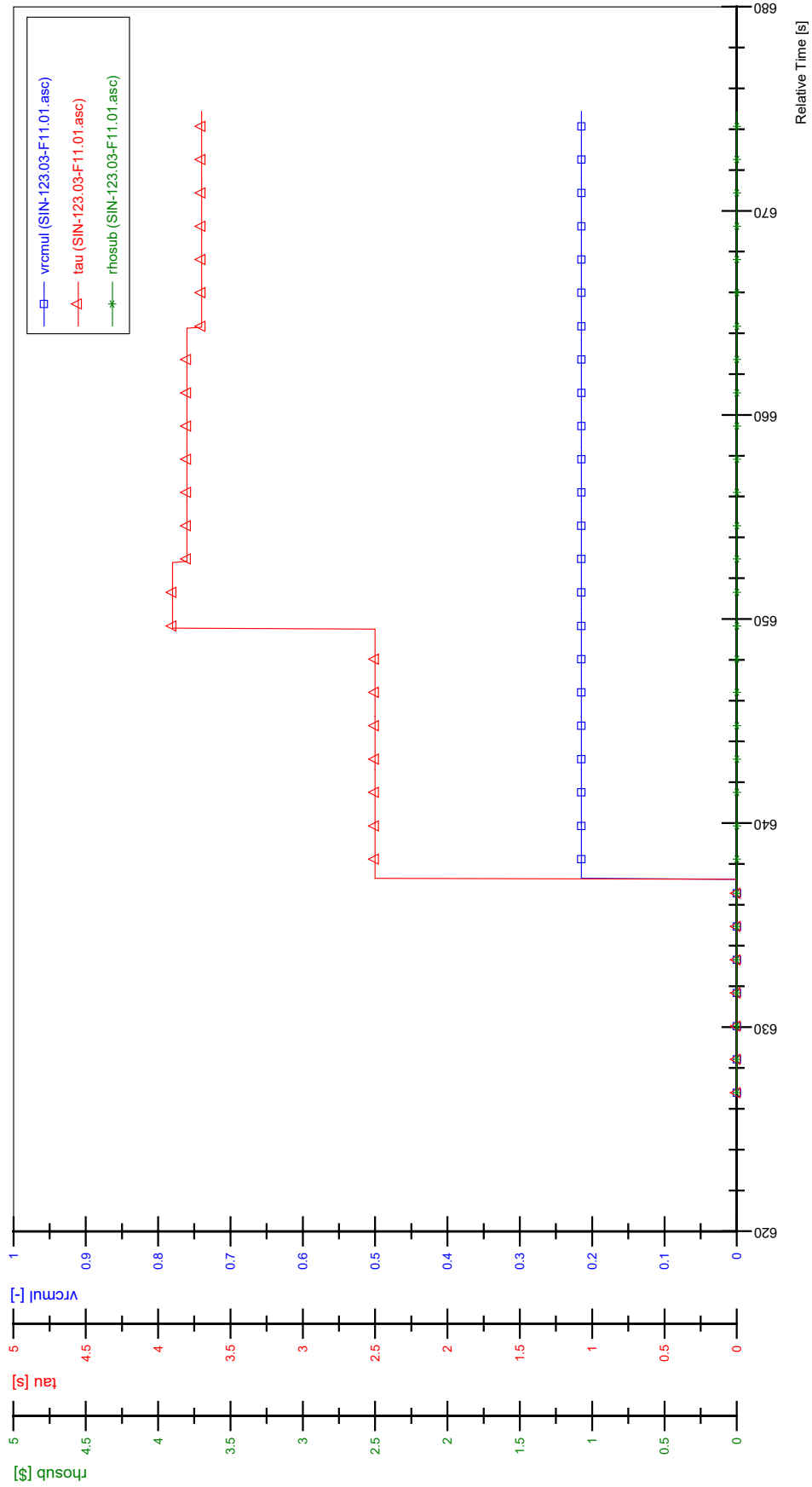
STS-123.03-F11.01_Rod_87



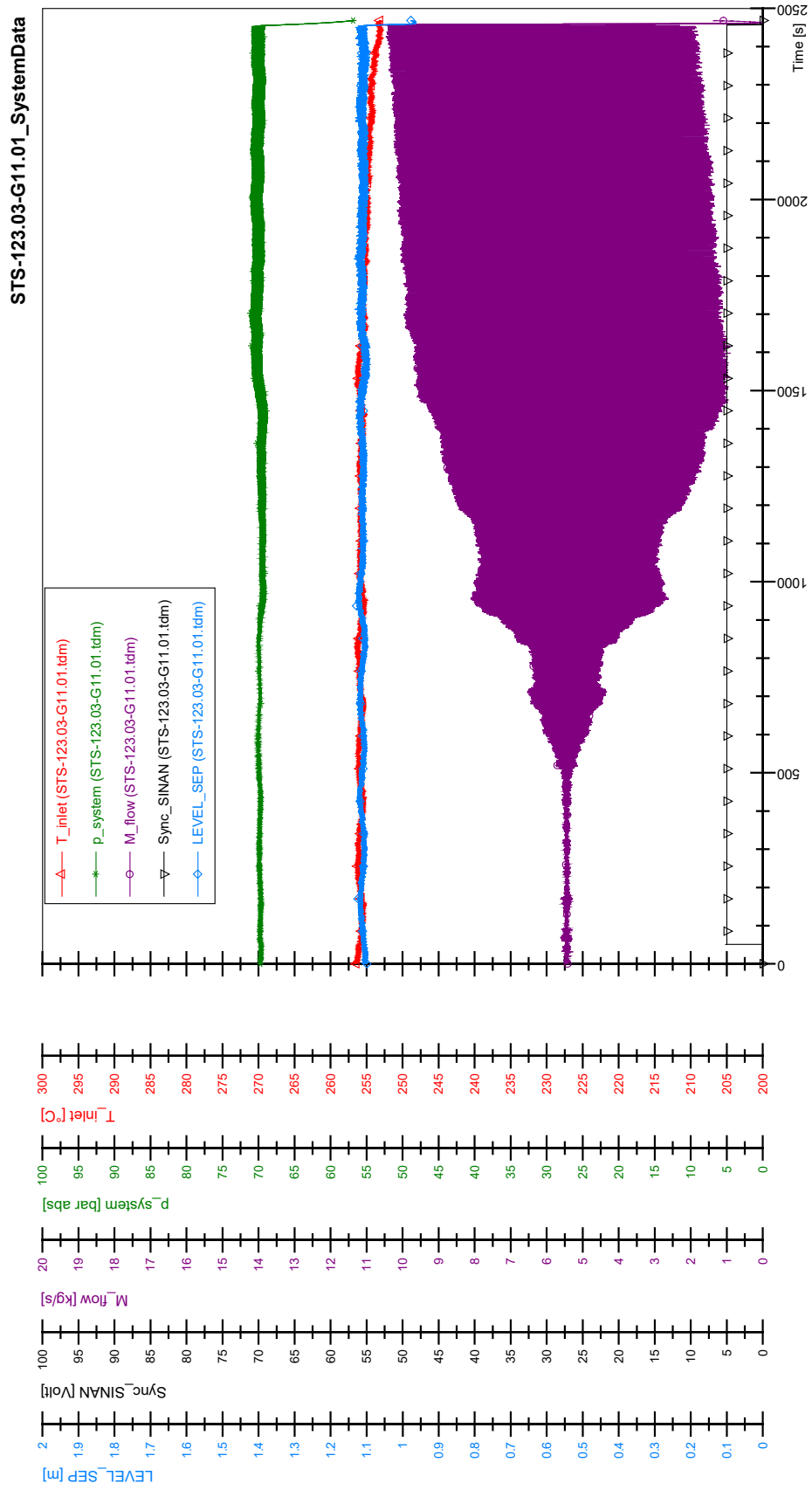
STS-123.03-F11.01_Rod_88



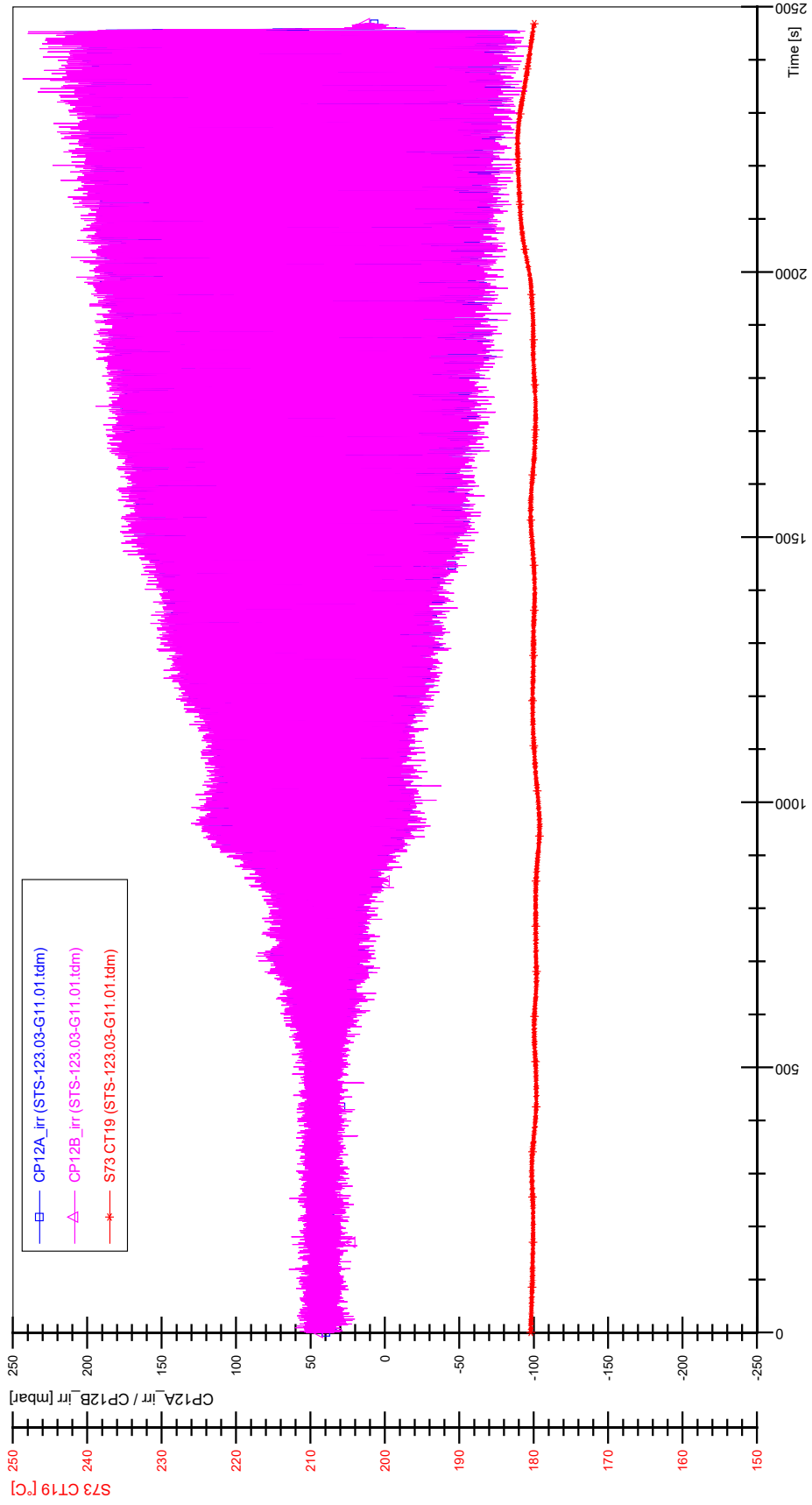
SIN-123.03-F11.01



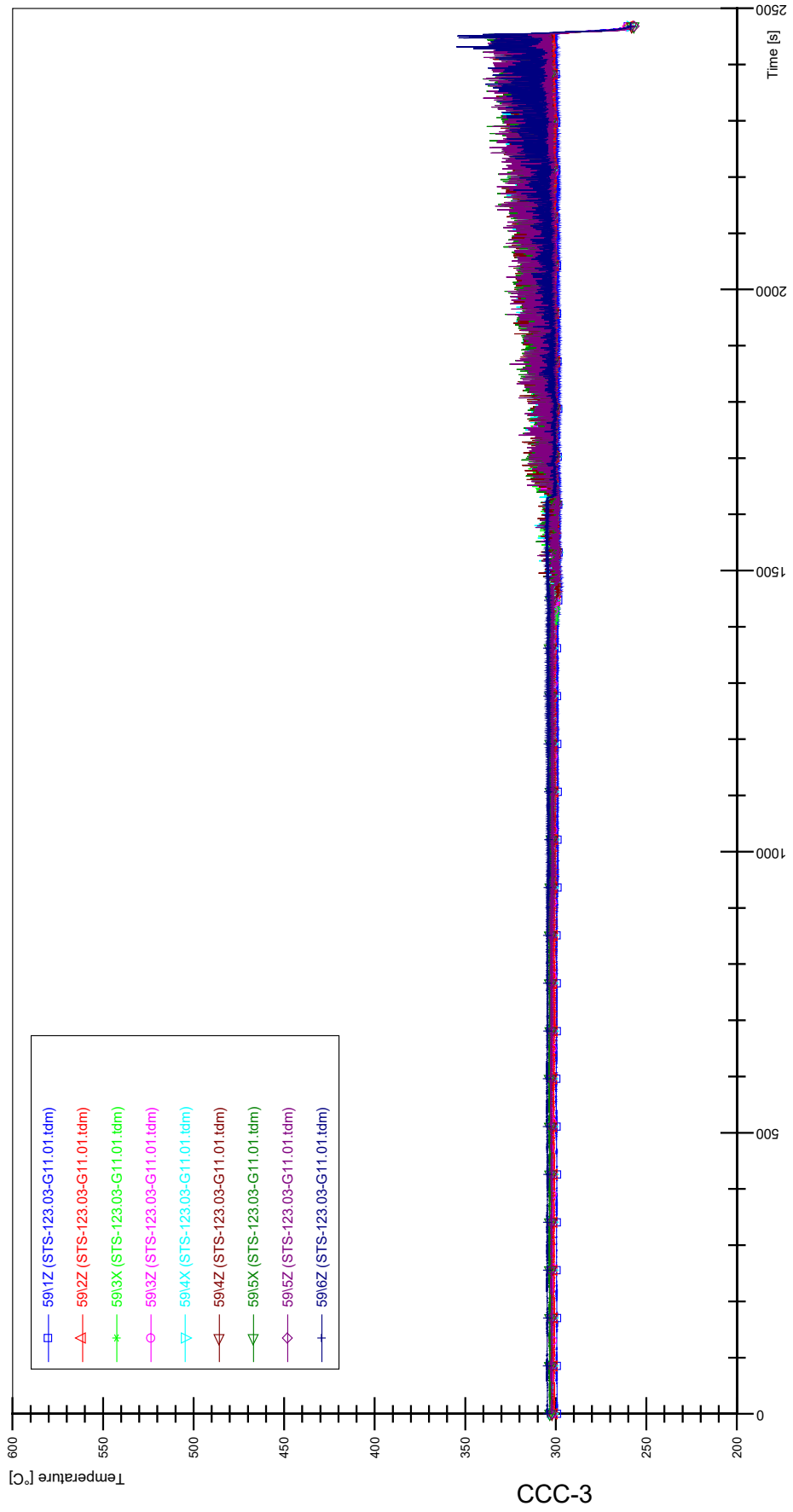
APPENDIX CCC PLOTS OF INSTABILITY TEST STS-123.03-G11.01



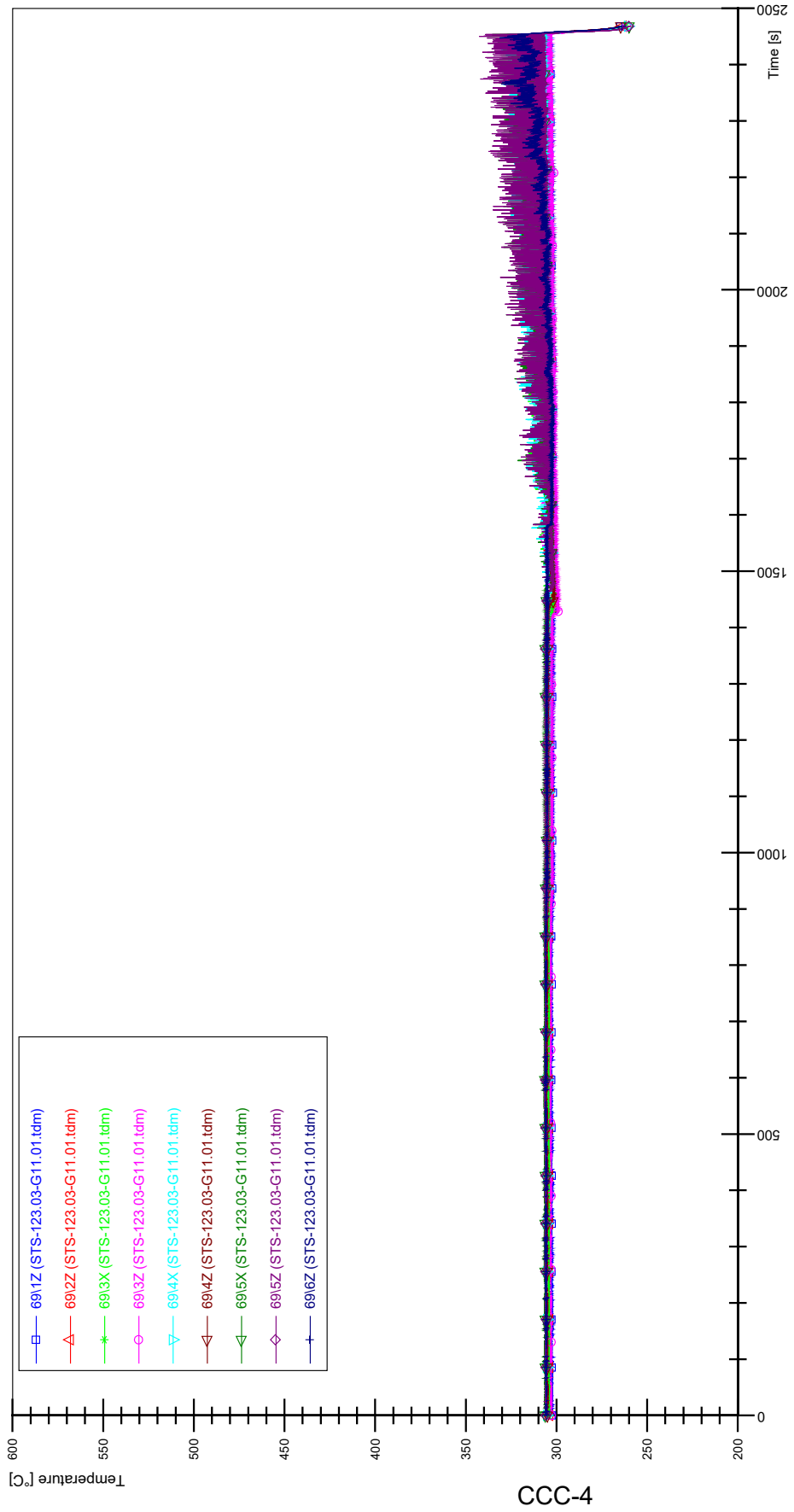
STS-123.03-G11.01_CP12_CT19



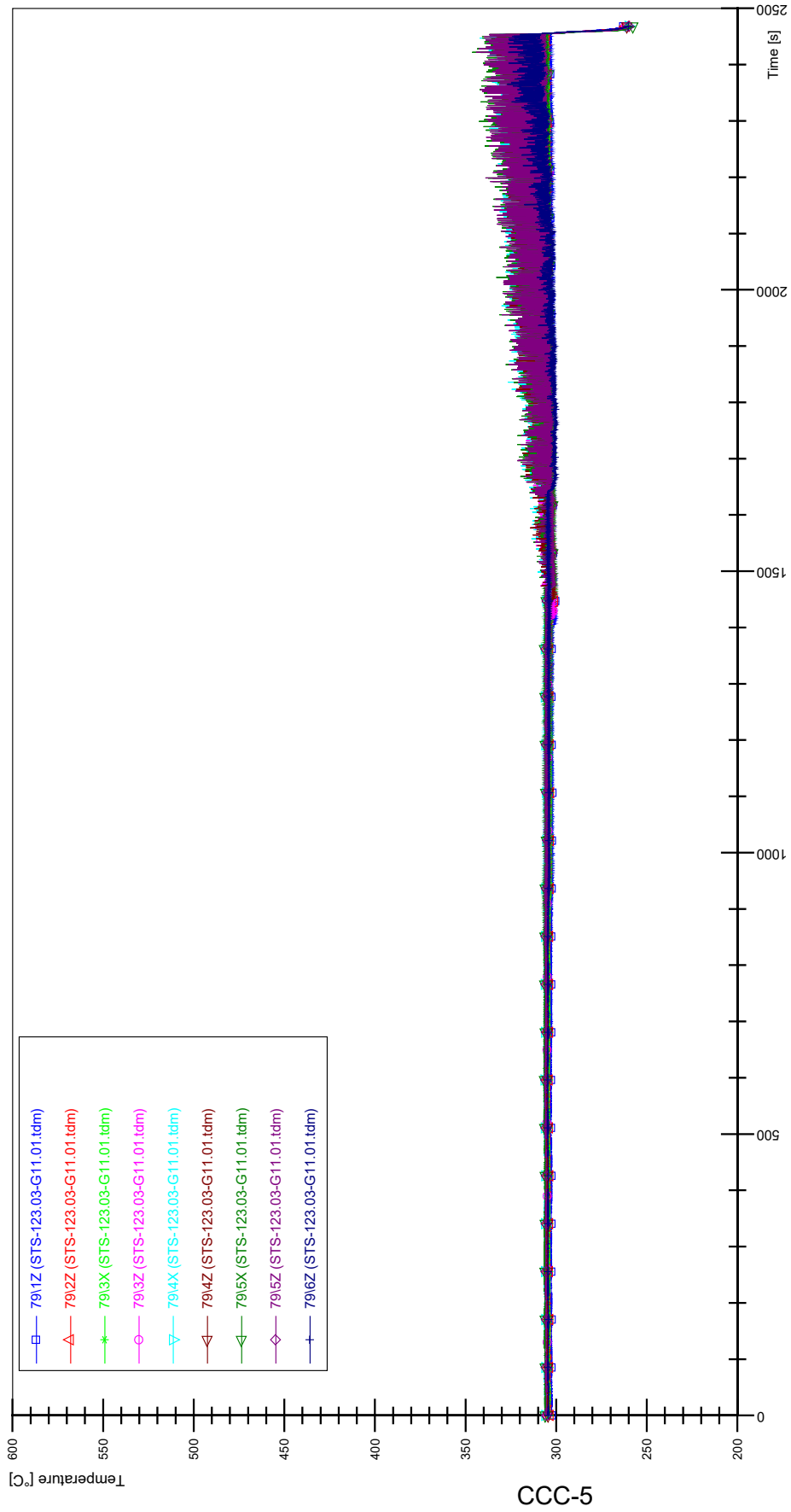
STS-123.03-G11.01_Rod_59



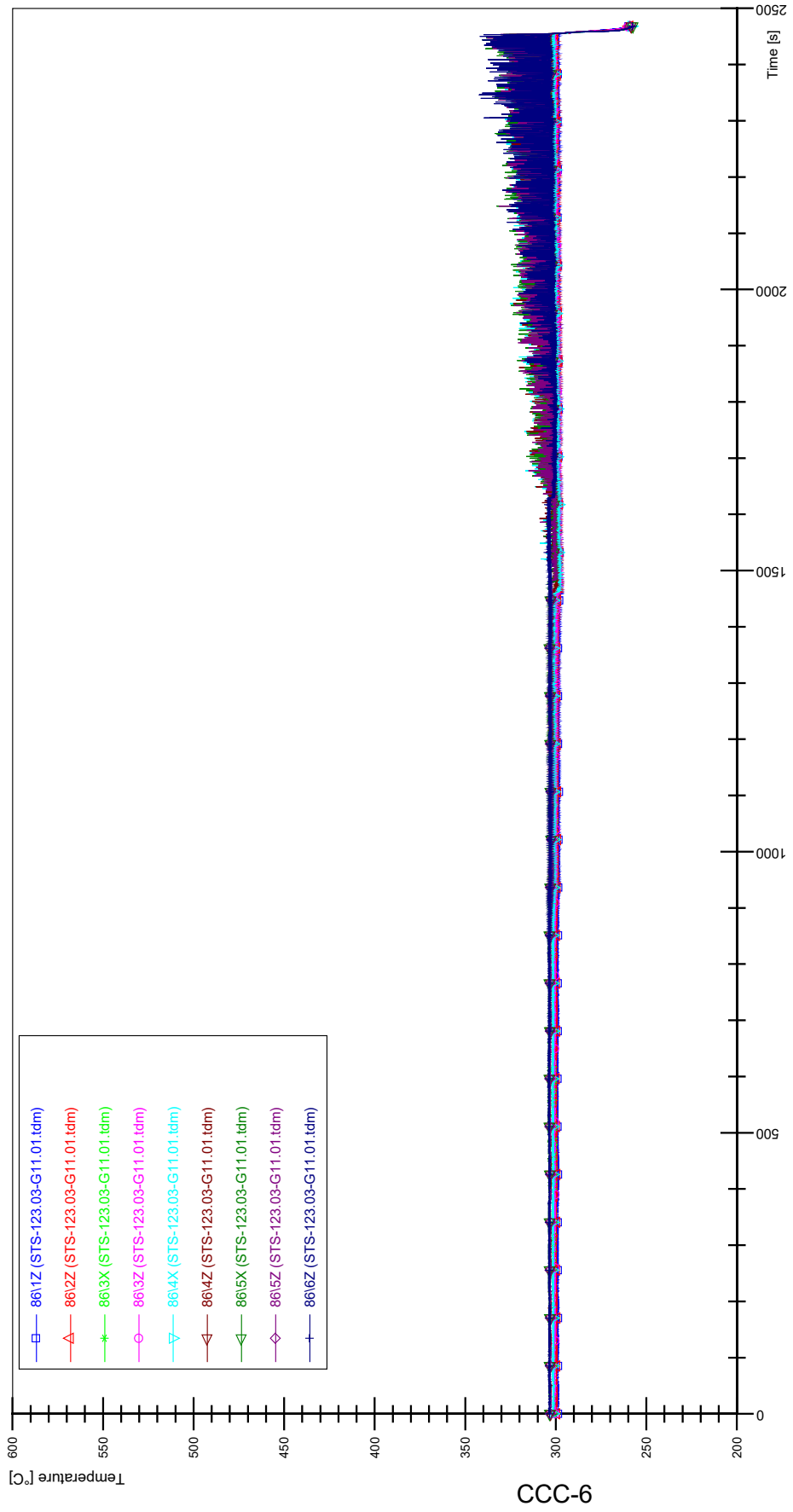
STS-123.03-G11.01_Rod_69



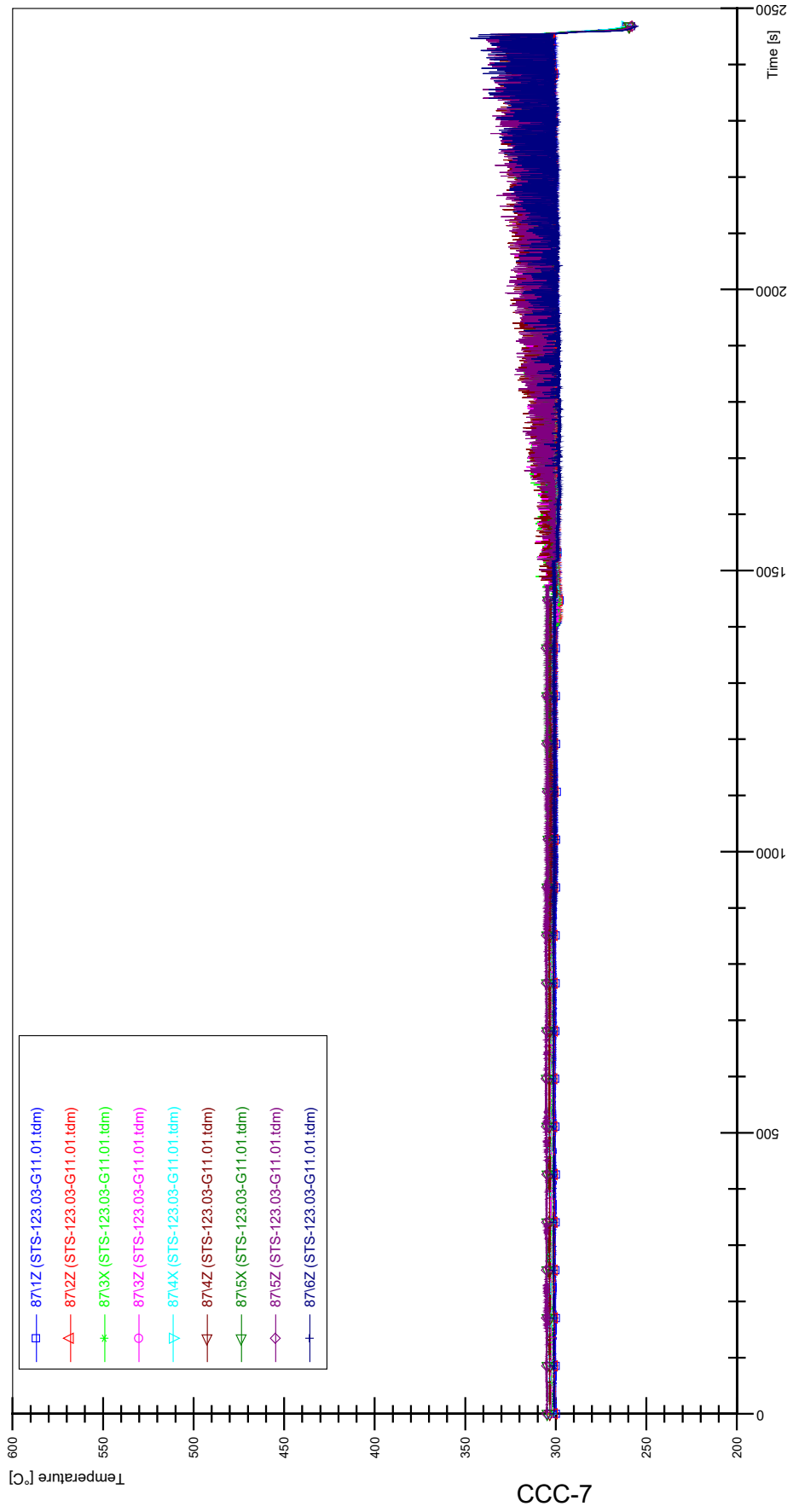
STS-123.03-G11.01_Rod_79



STS-123.03-G11.01_Rod_86

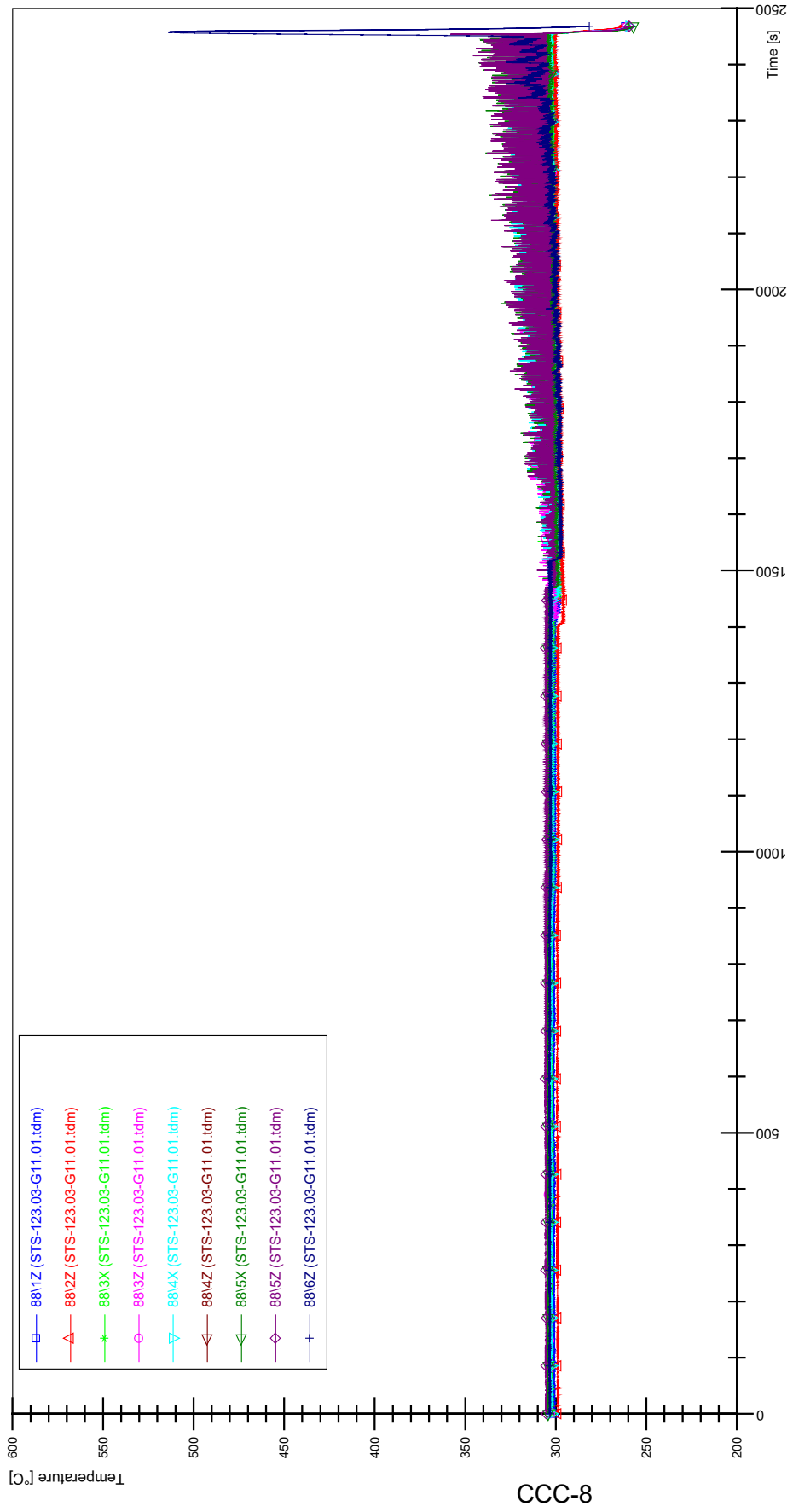


STS-123.03-G11.01_Rod_87

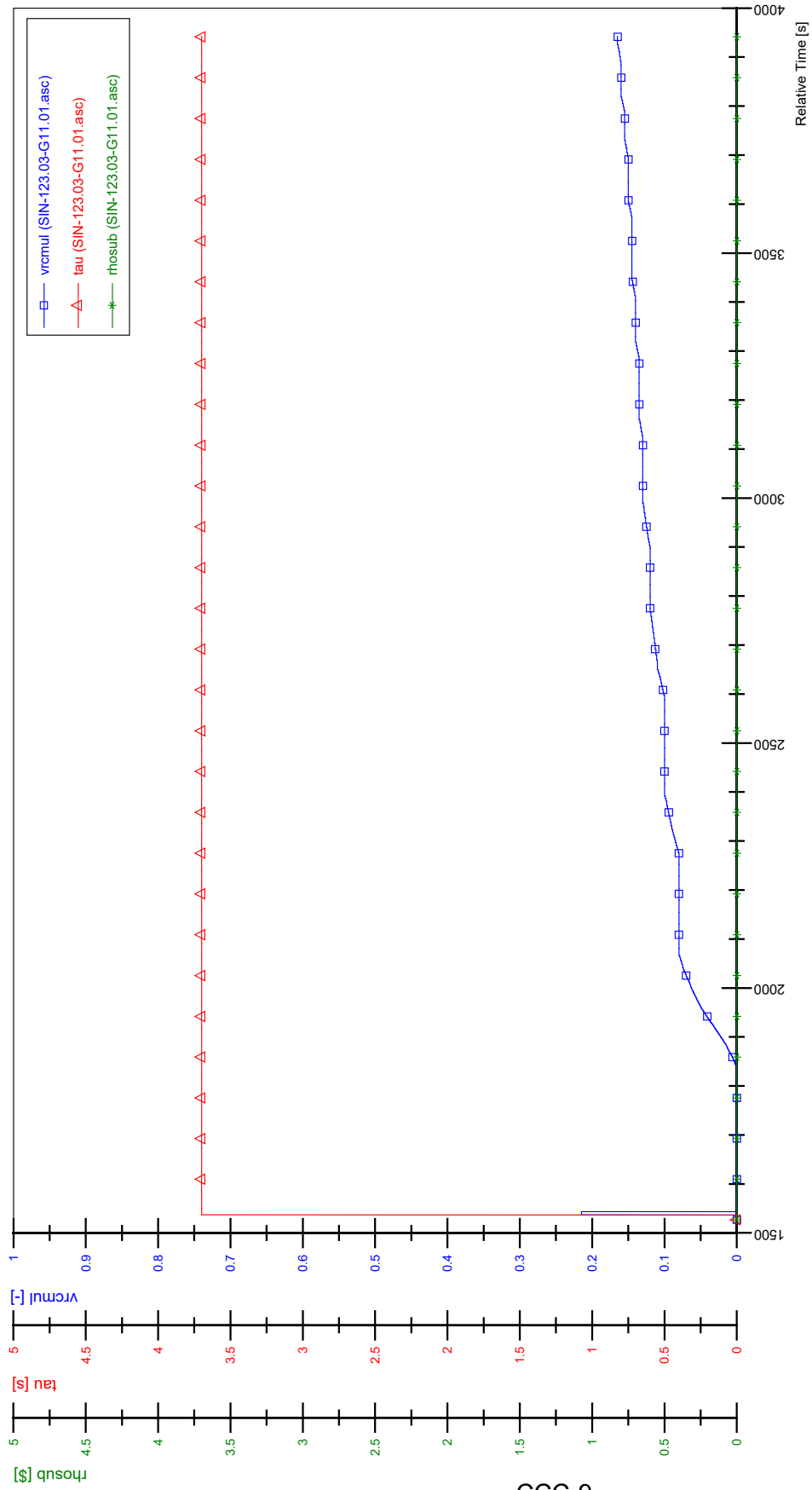


CCC-7

STS-123.03-G11.01_Rod_88

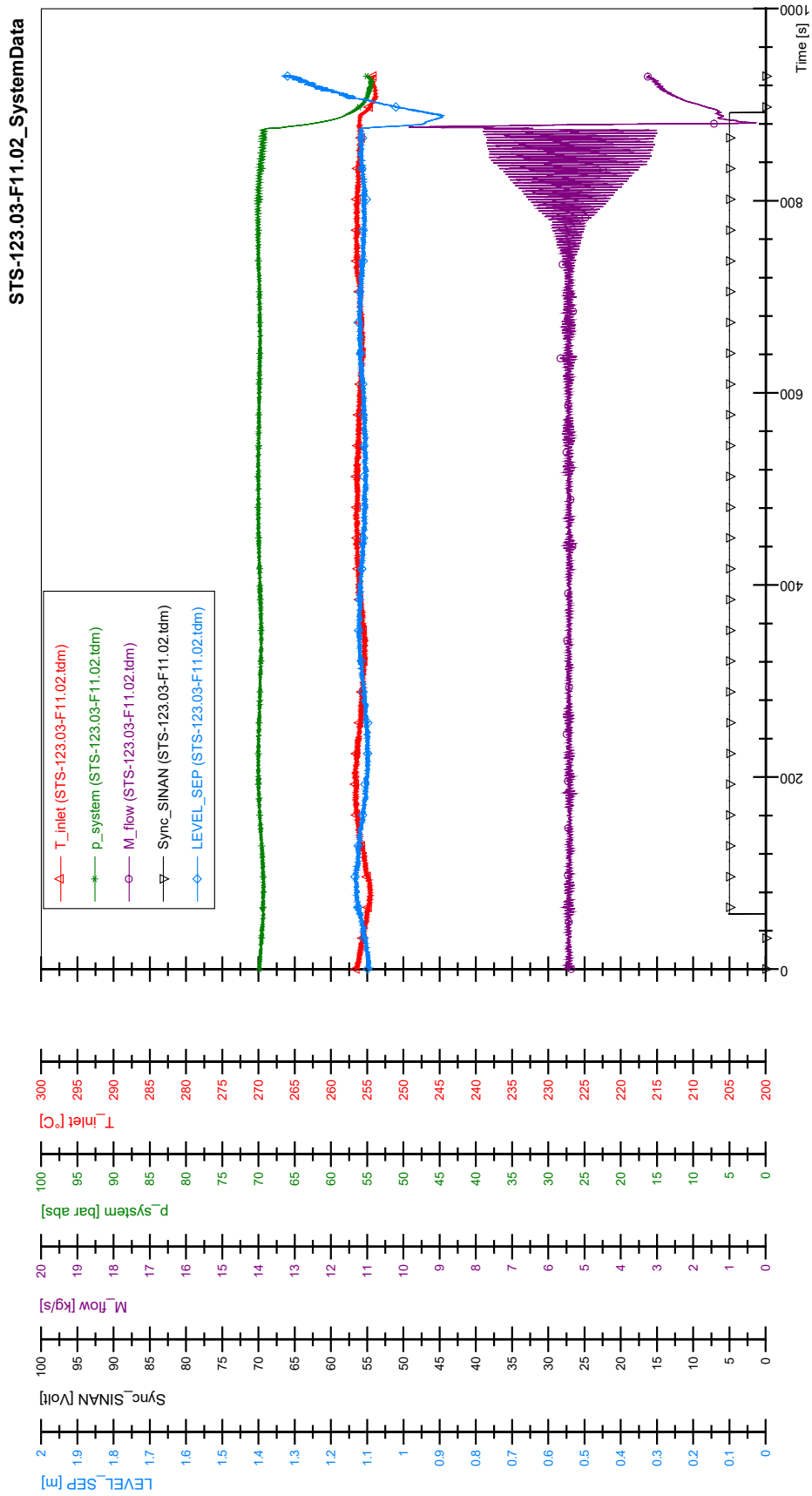


SIN-123.03-G11.01

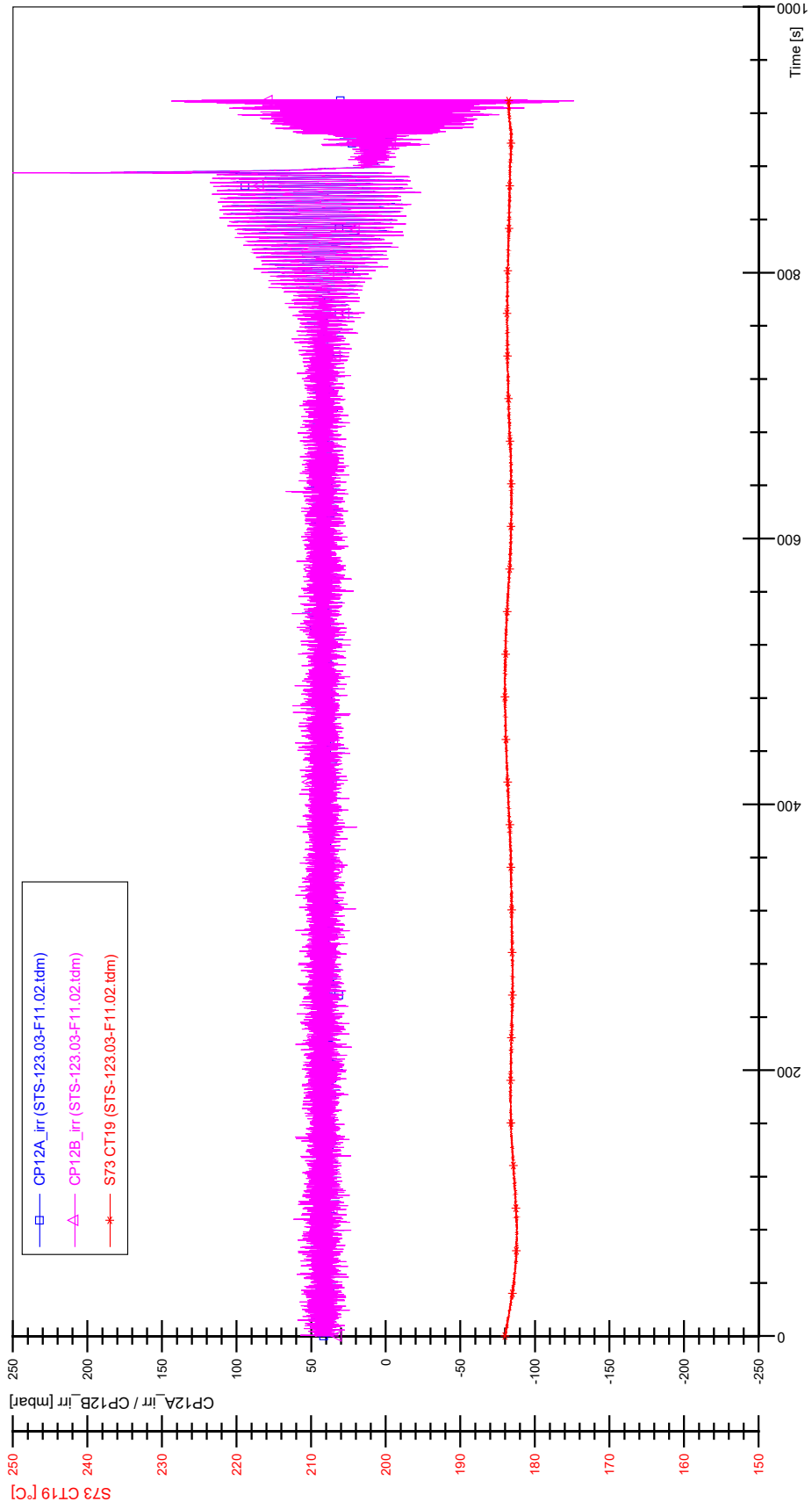


CCC-9

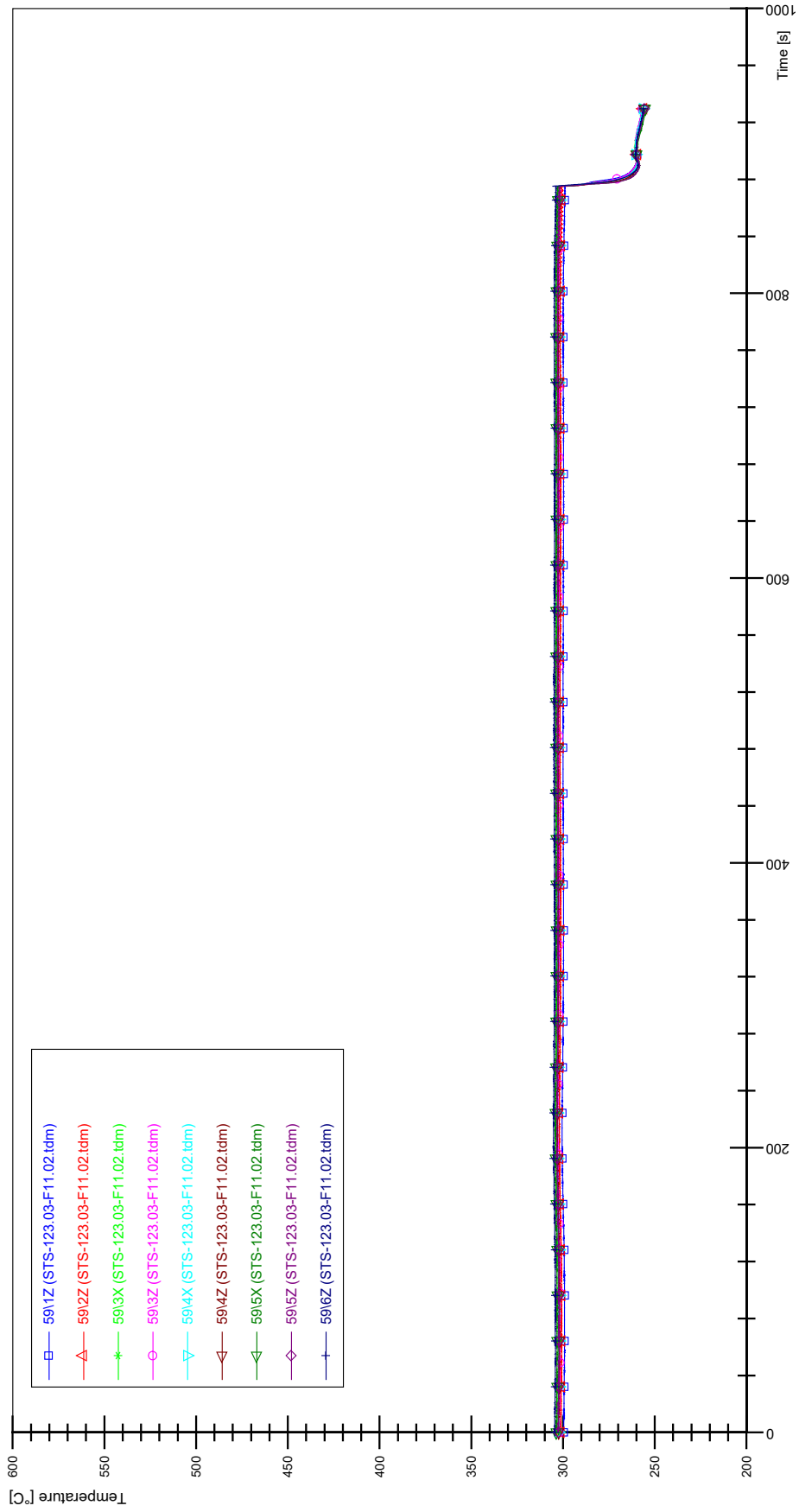
APPENDIX DDD PLOTS OF INSTABILITY TEST STS-123.03-F11.02



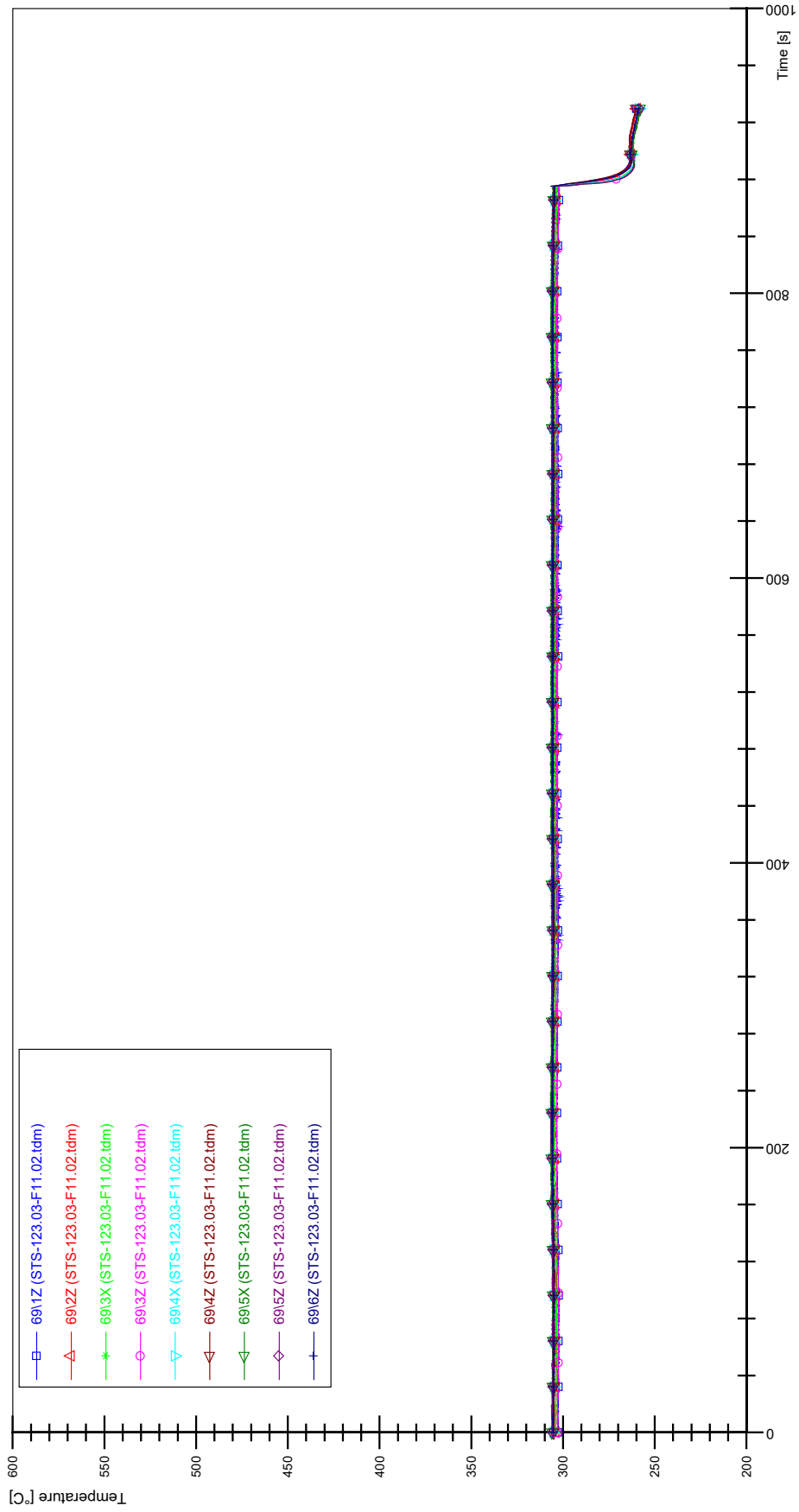
STS-123.03-F11.02_CP12_CT19



STS-123.03-F11.02_Rod_59

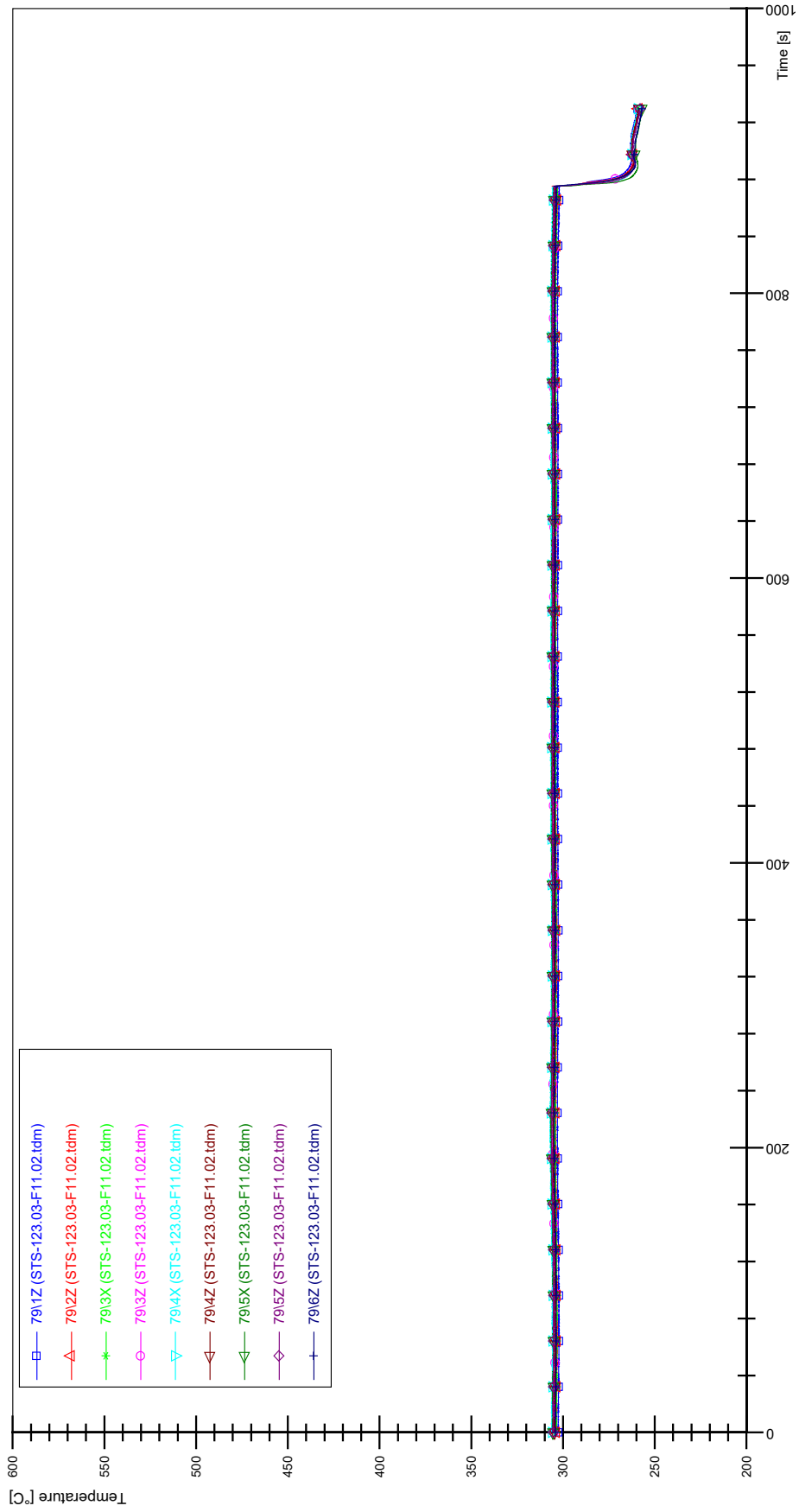


STS-123.03-F11.02_Rod_69



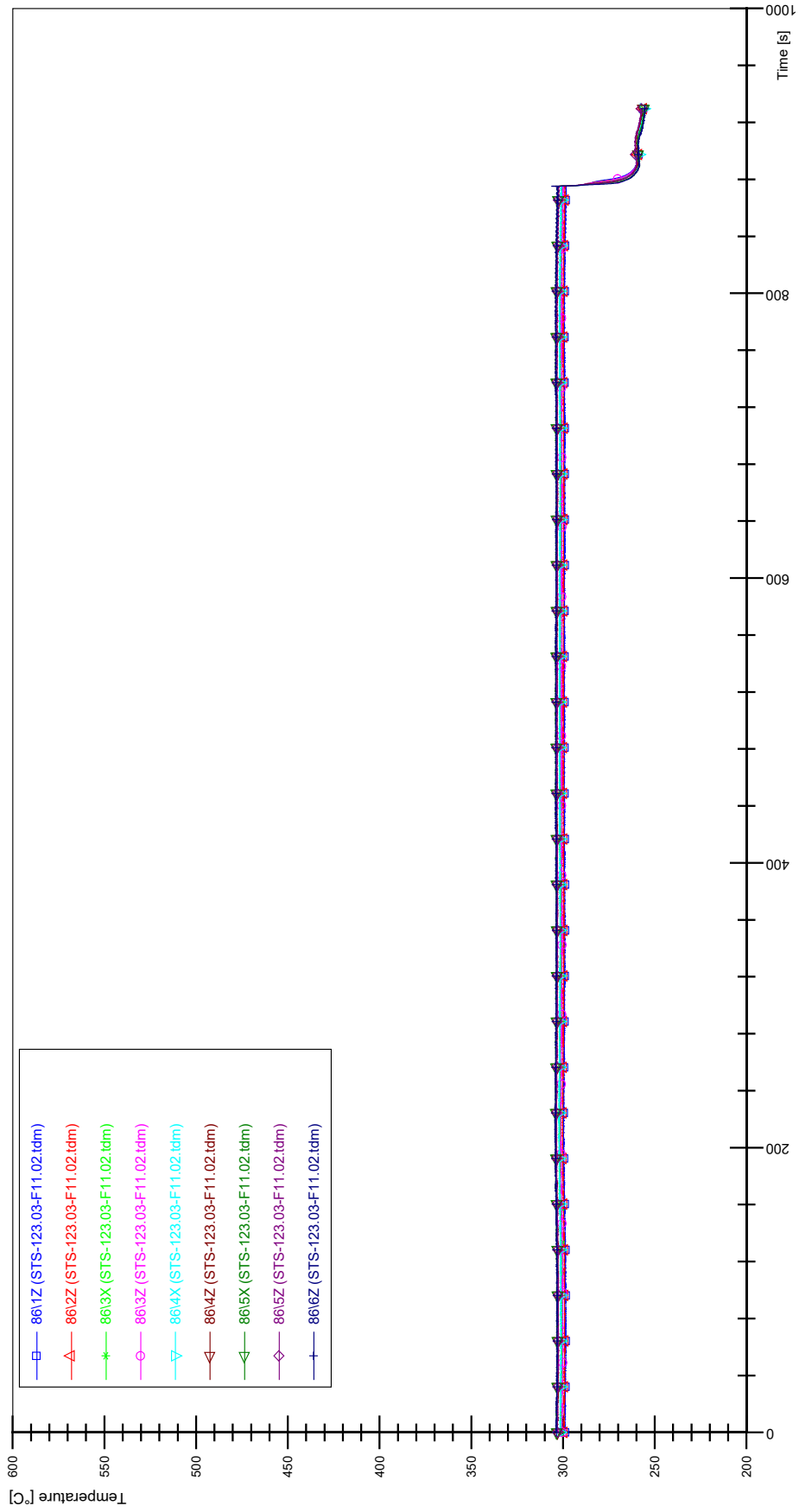
DDD-4

STS-123.03-F11.02_Rod_79

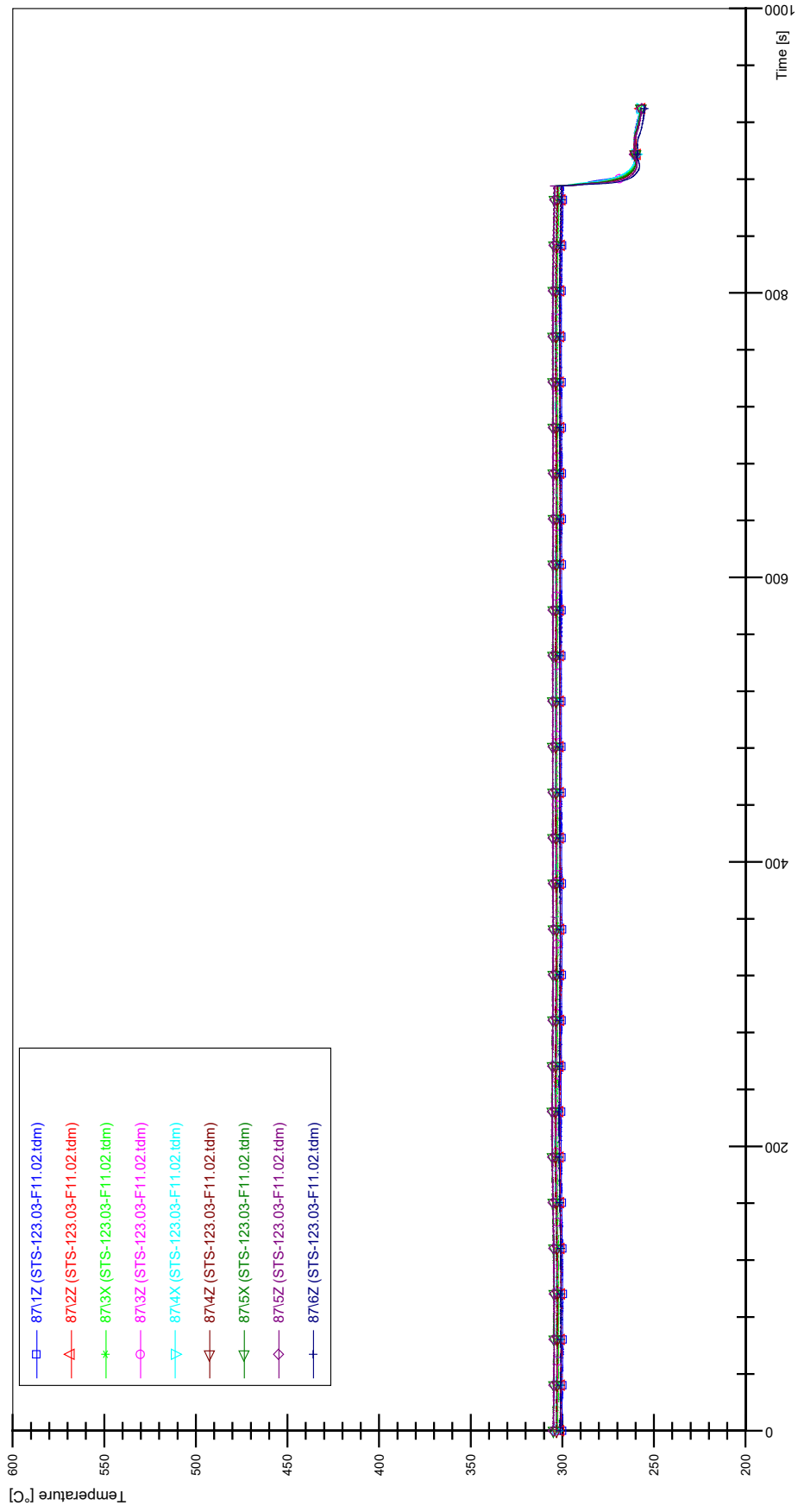


DDD-5

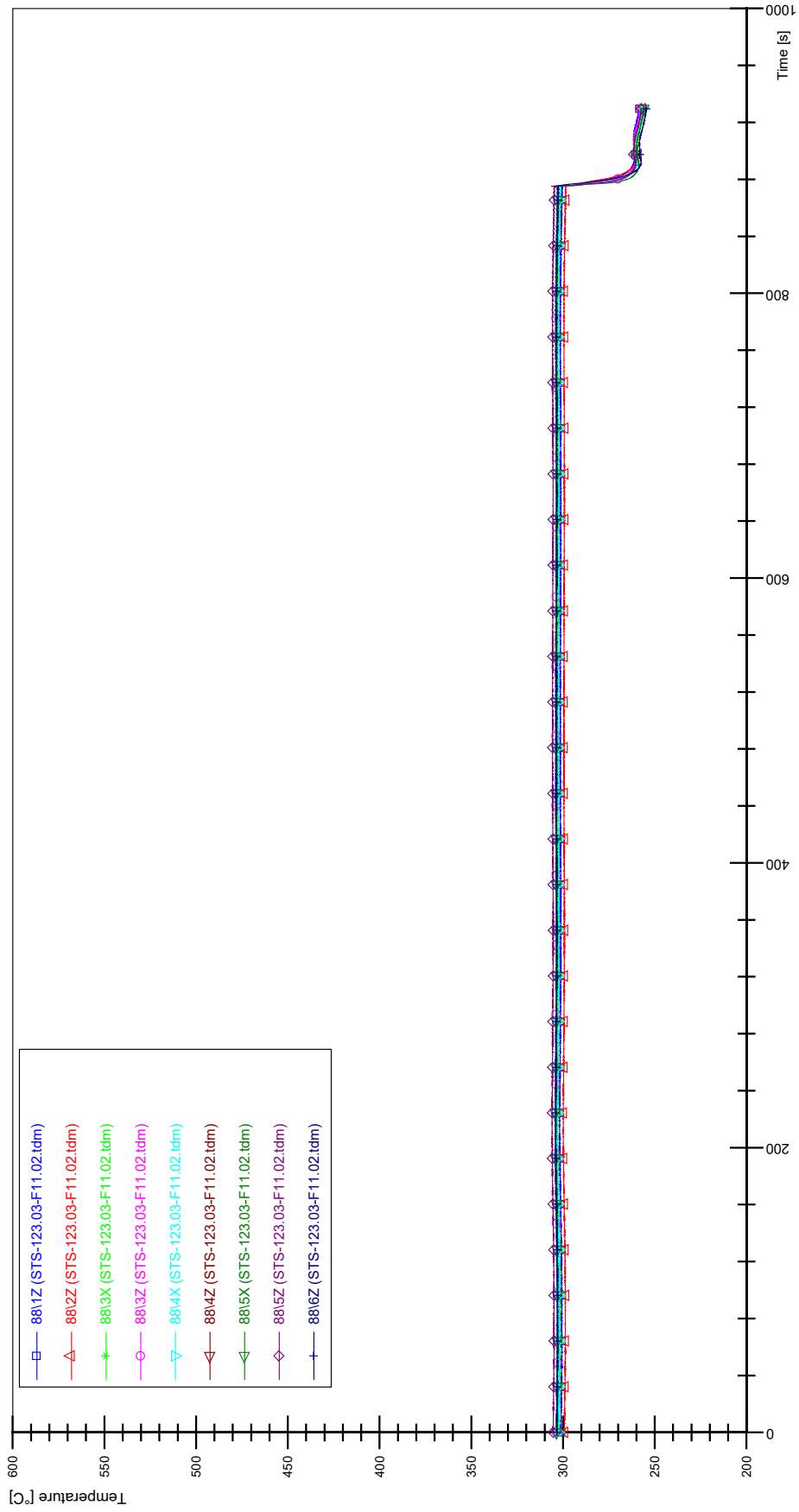
STS-123.03-F11.02_Rod_86



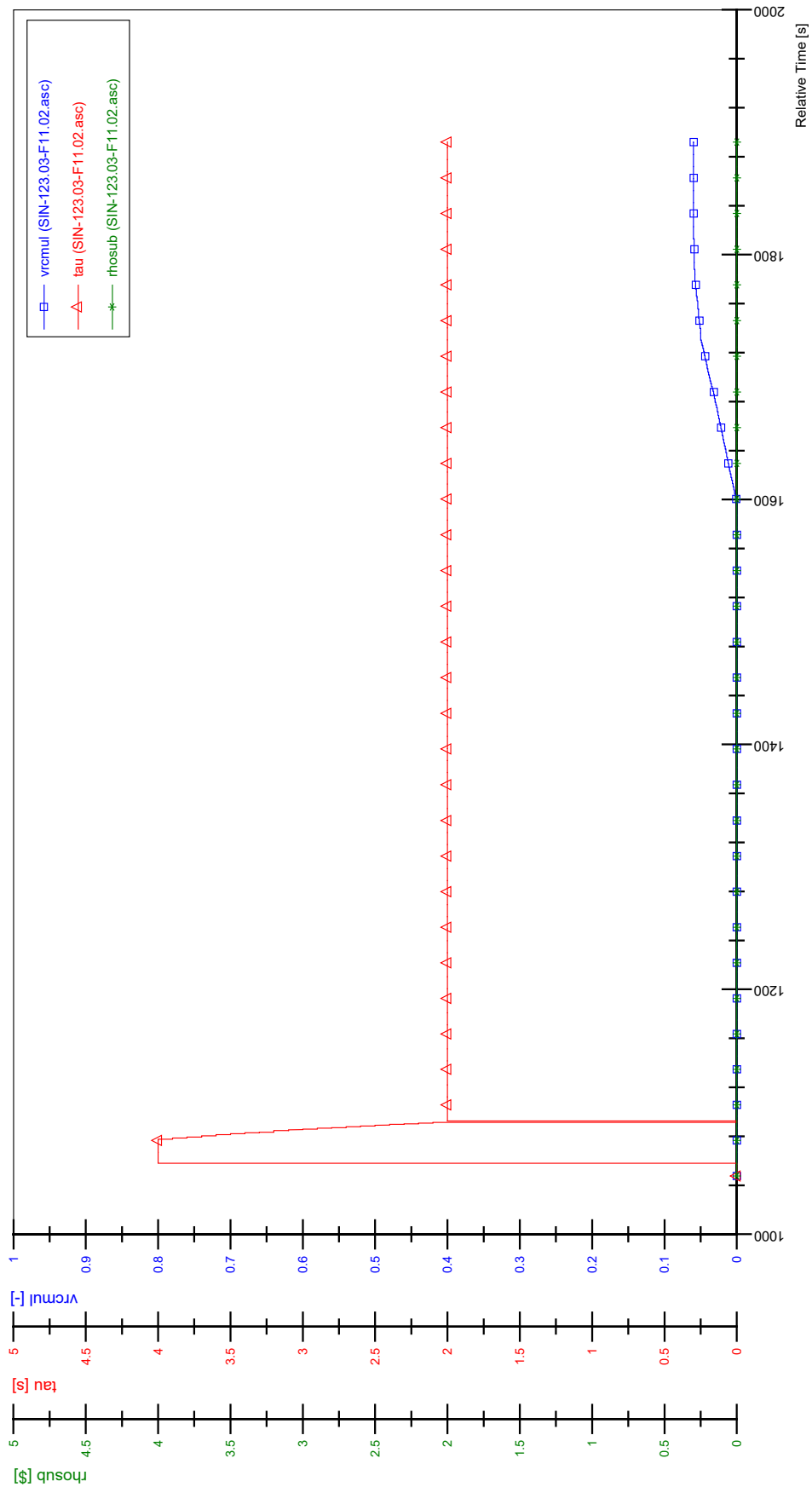
STS-123.03-F11.02_Rod_87



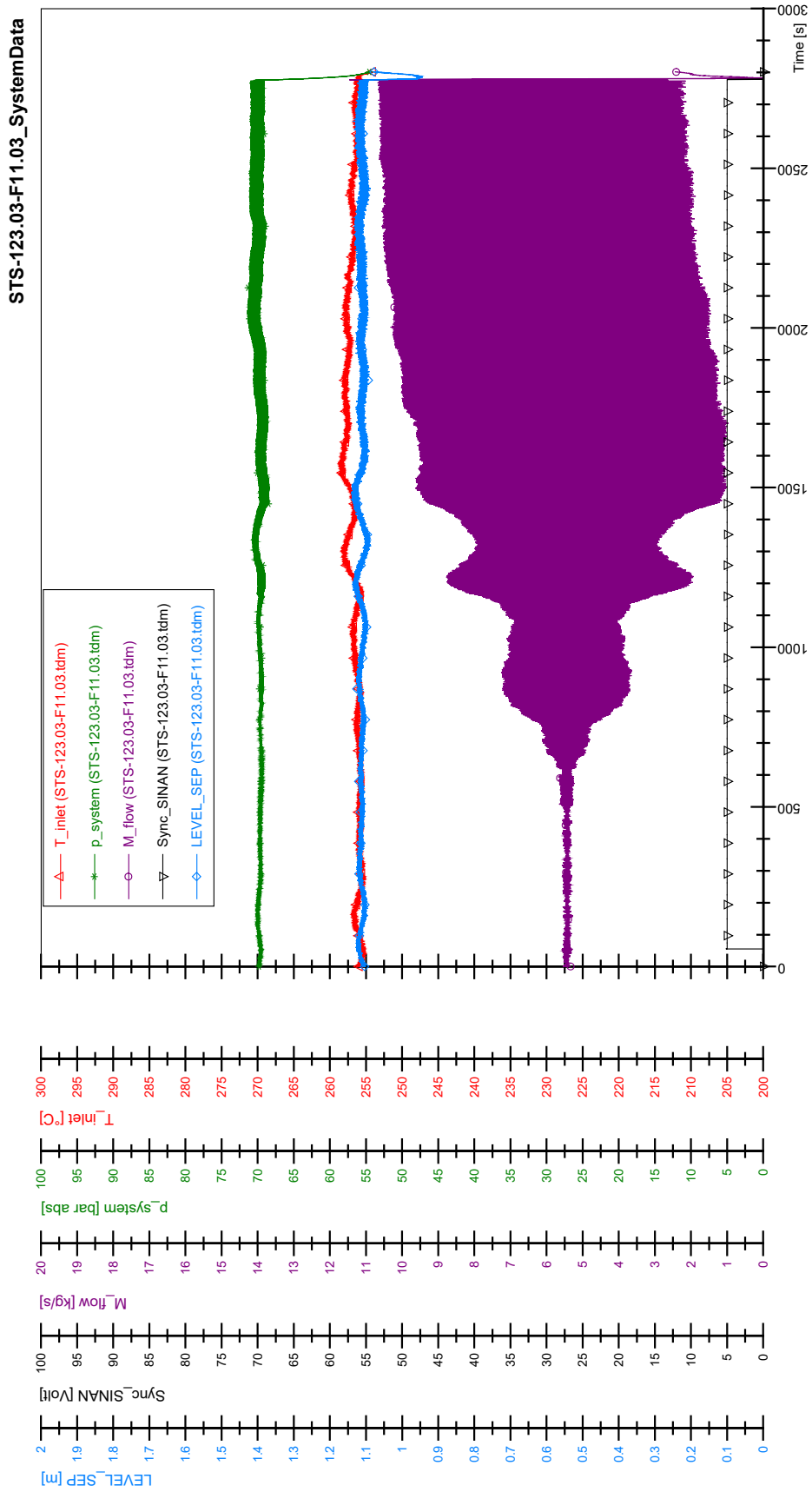
STS-123.03-F11.02_Rod_88

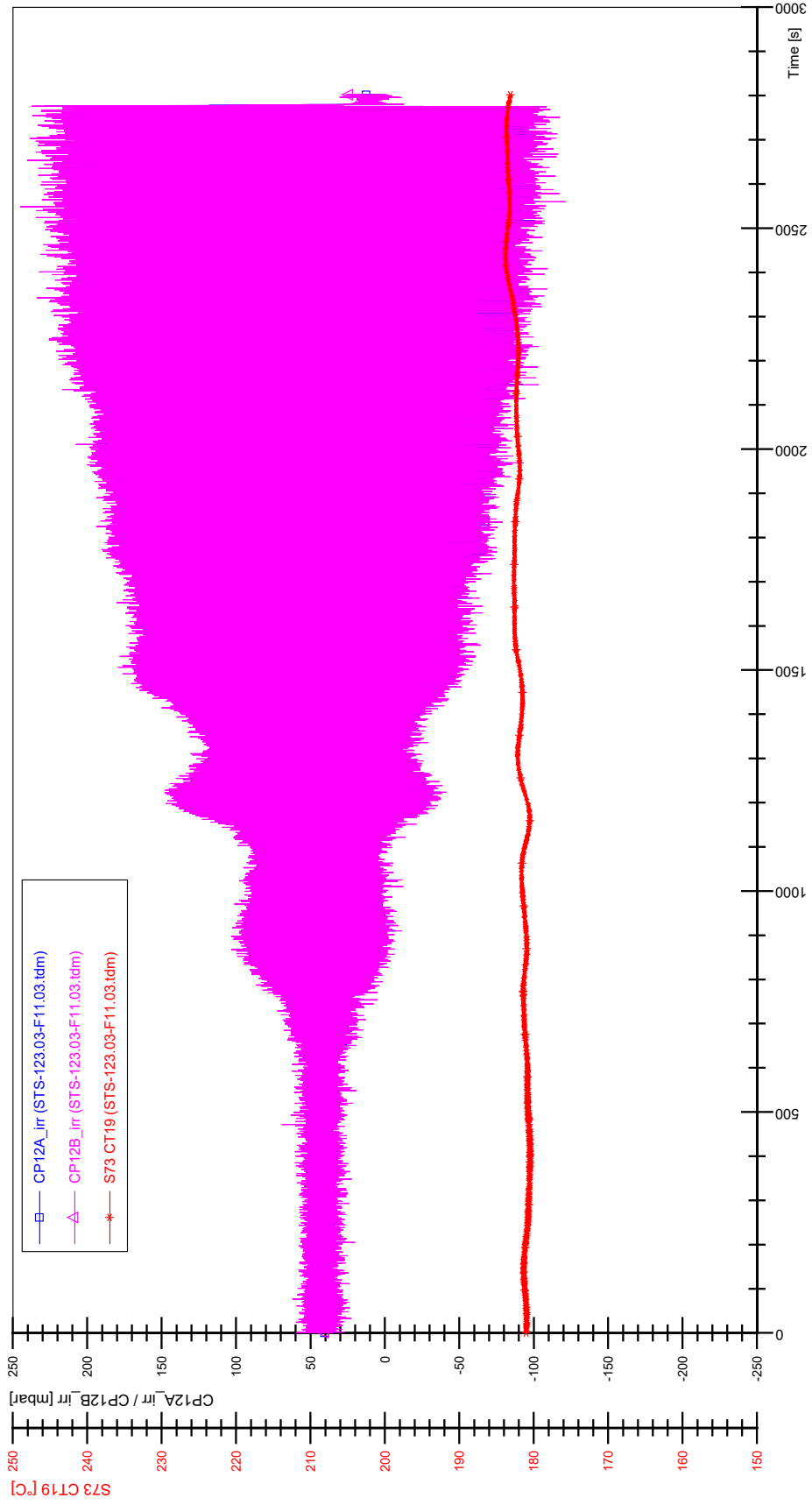


SIN-123.03-F11.02

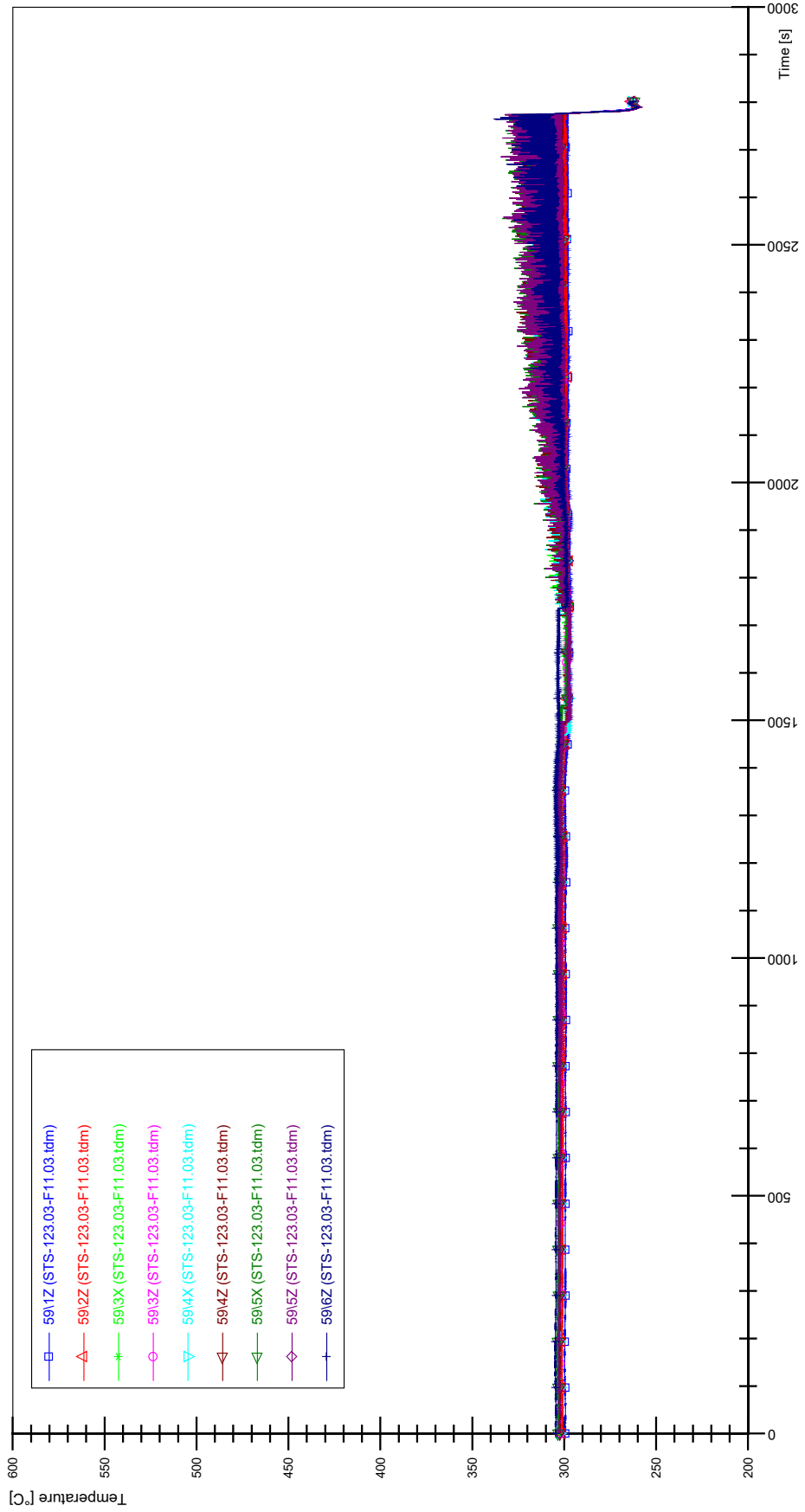


APPENDIX EEE PLOTS OF INSTABILITY TEST STS-123.03-F11.03

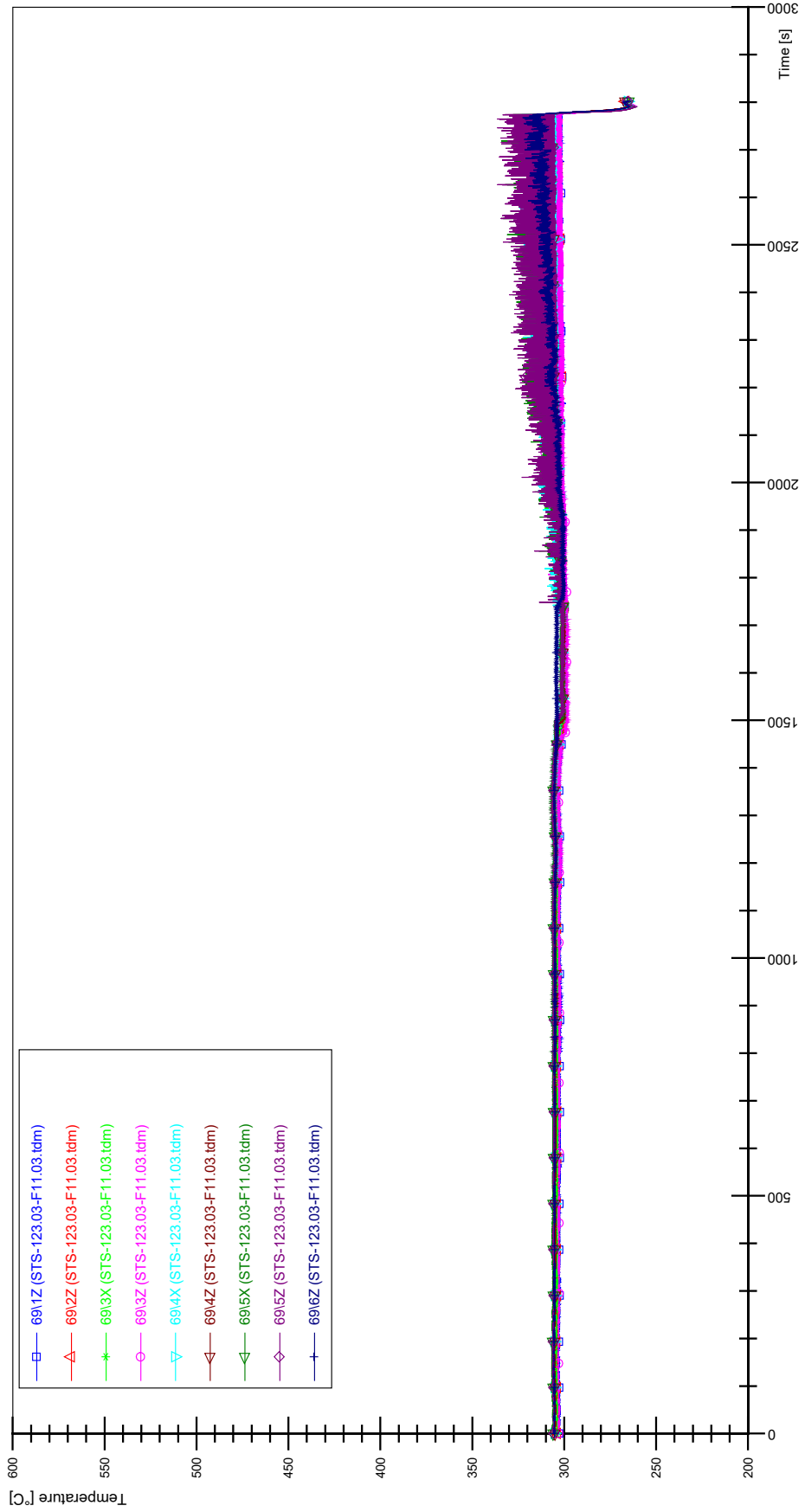




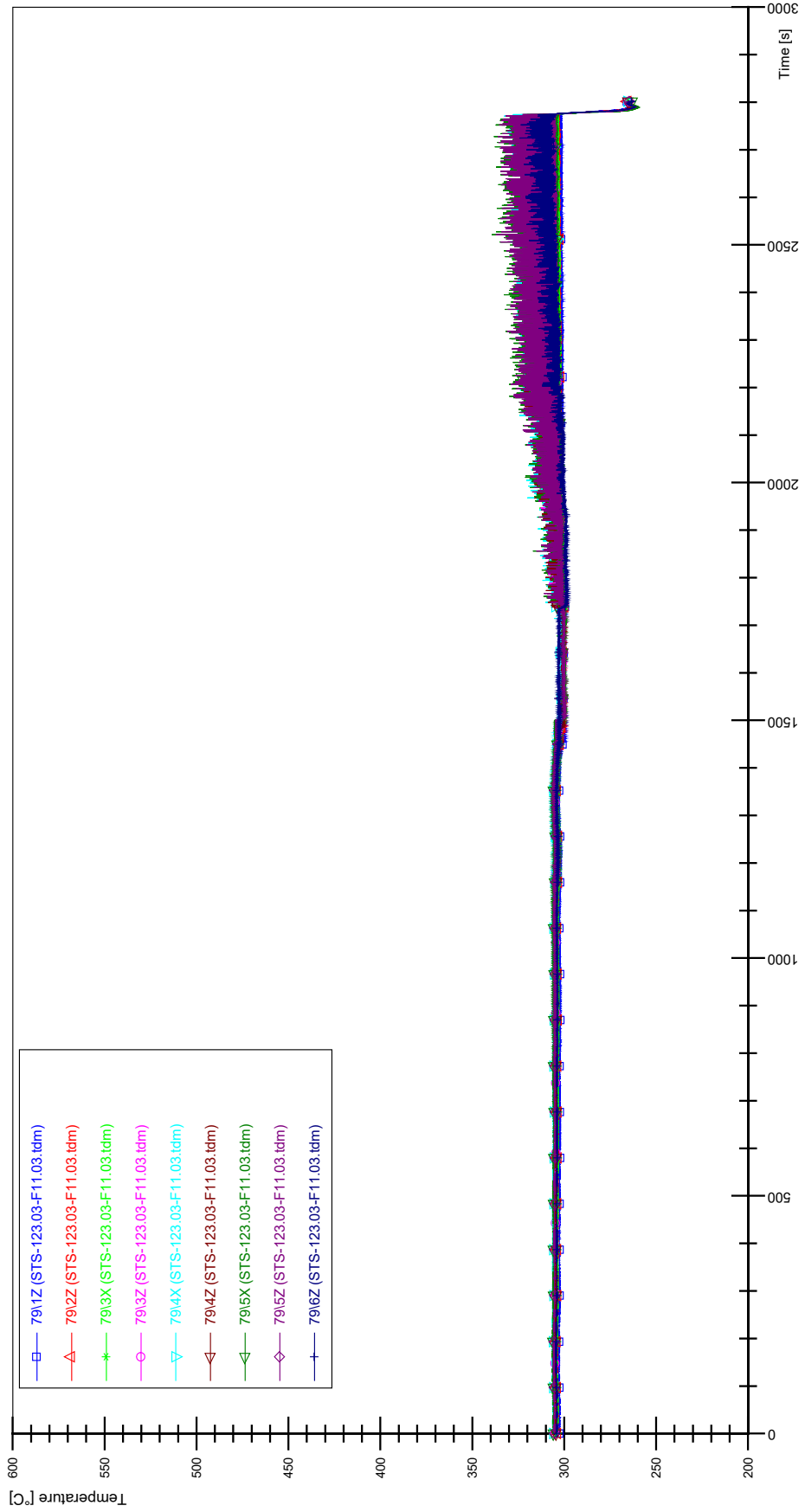
STS-123.03-F11.03_Rod_59



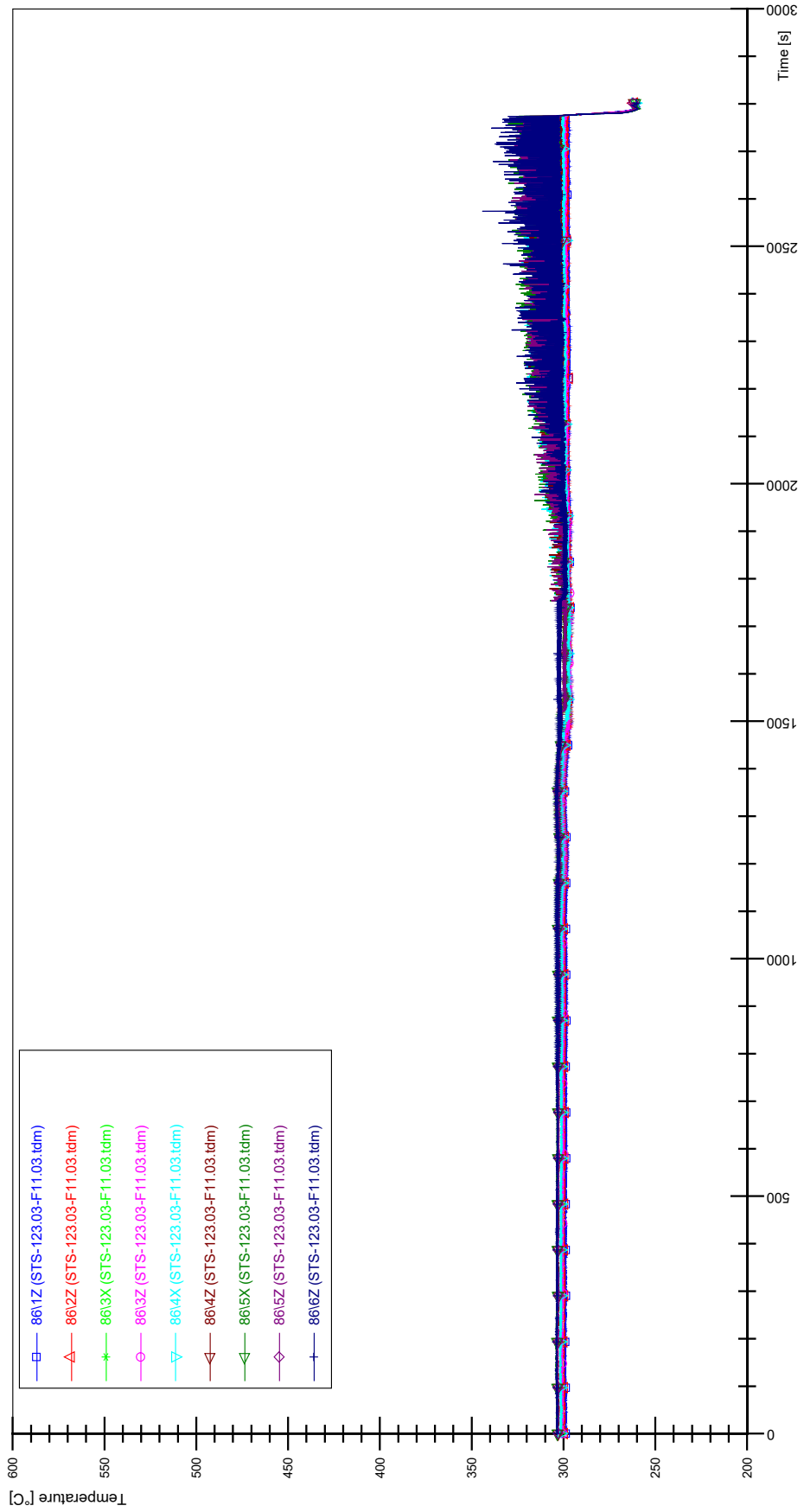
STS-123.03-F11.03_Rod_69



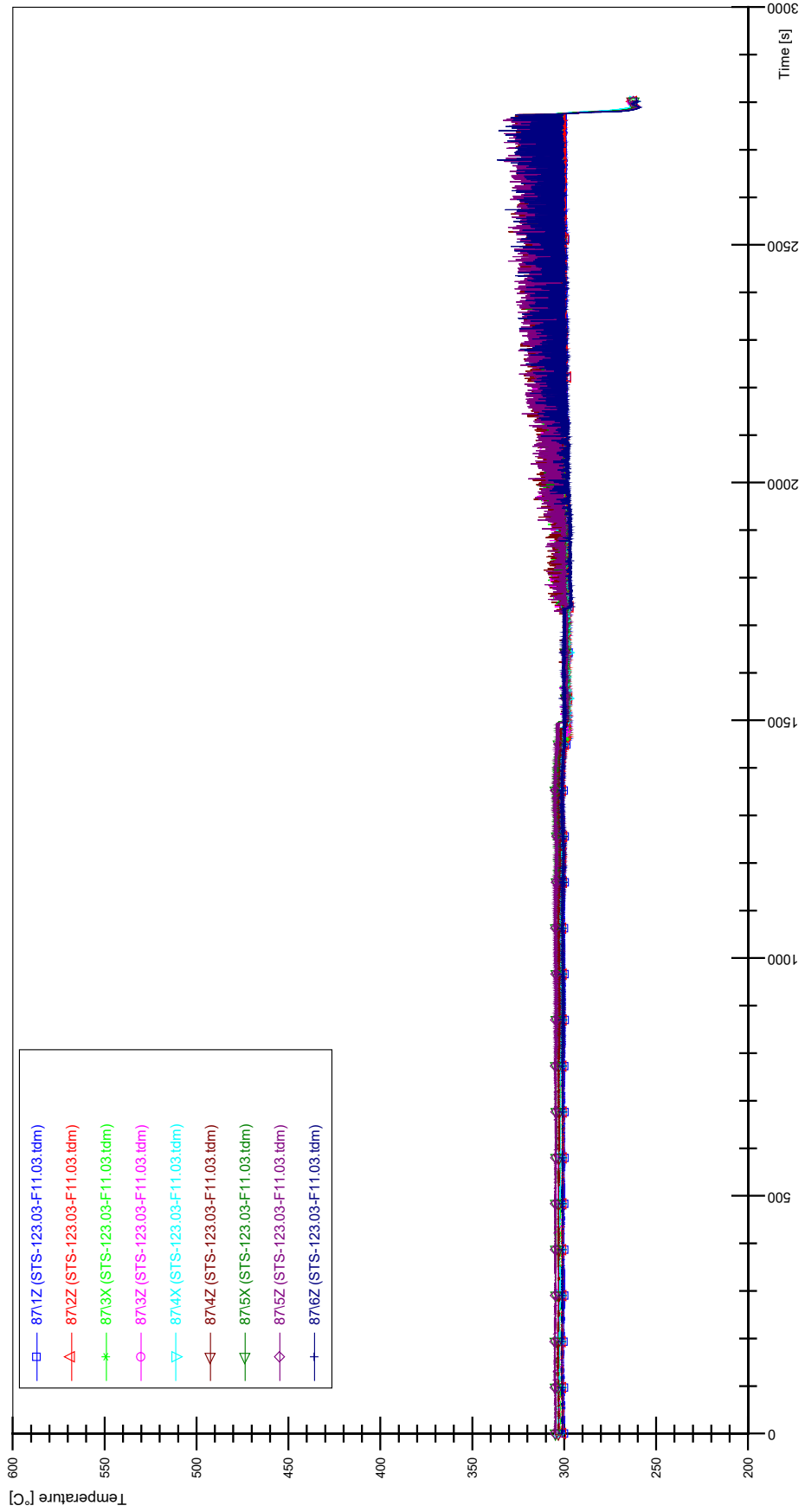
STS-123.03-F11.03_Rod_79



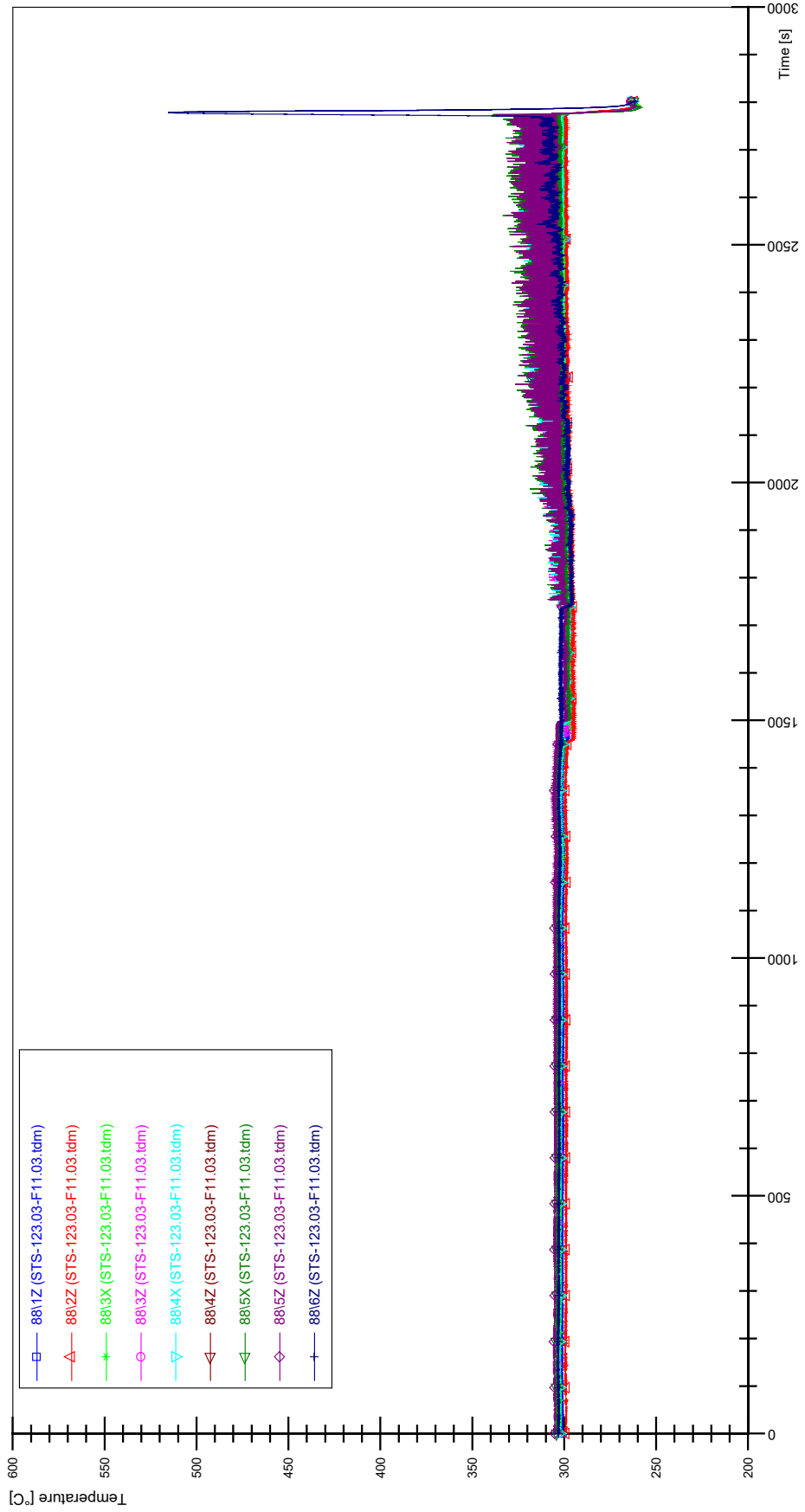
STS-123.03-F11.03_Rod_86



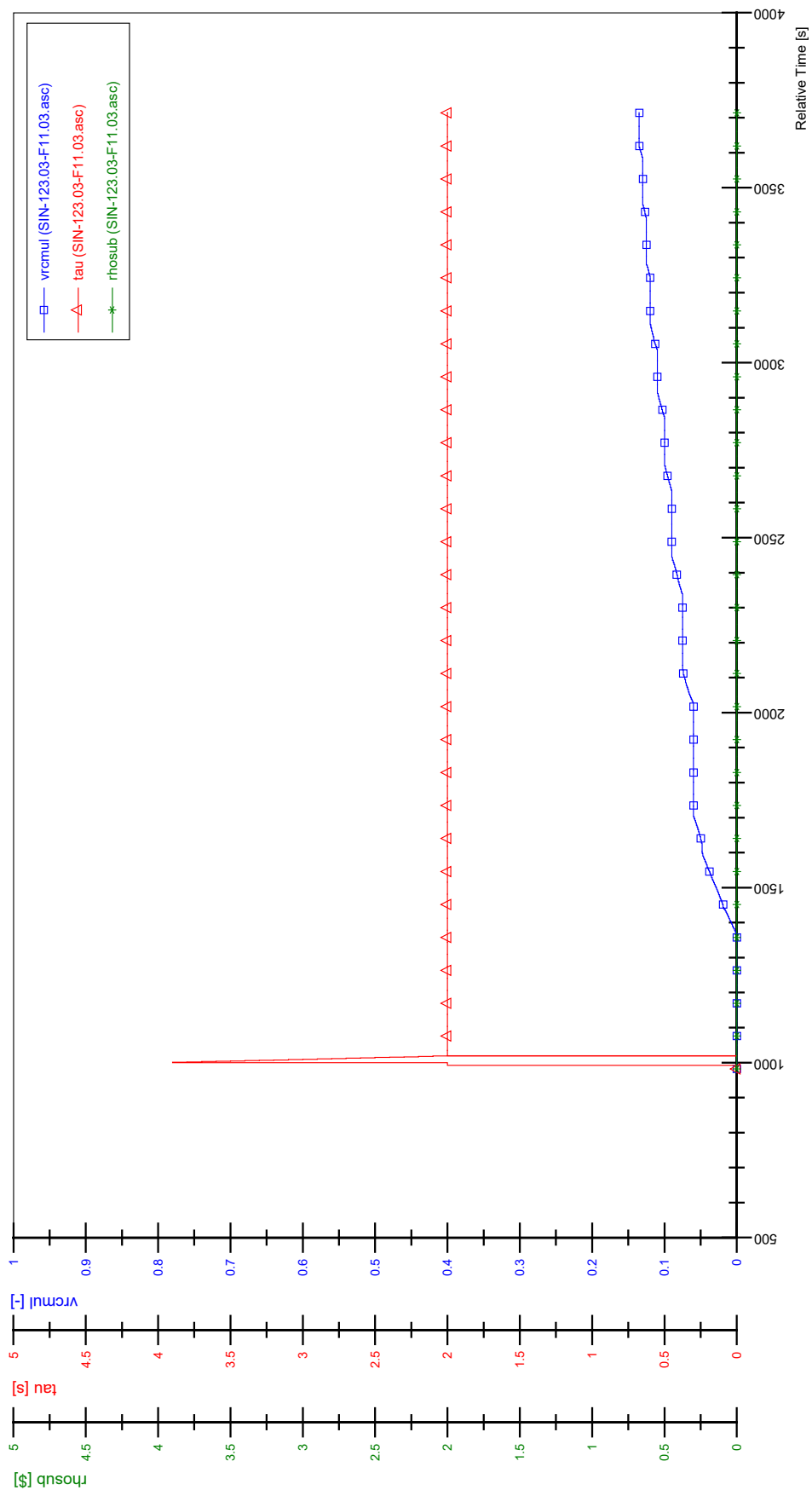
STS-123.03-F11.03_Rod_87



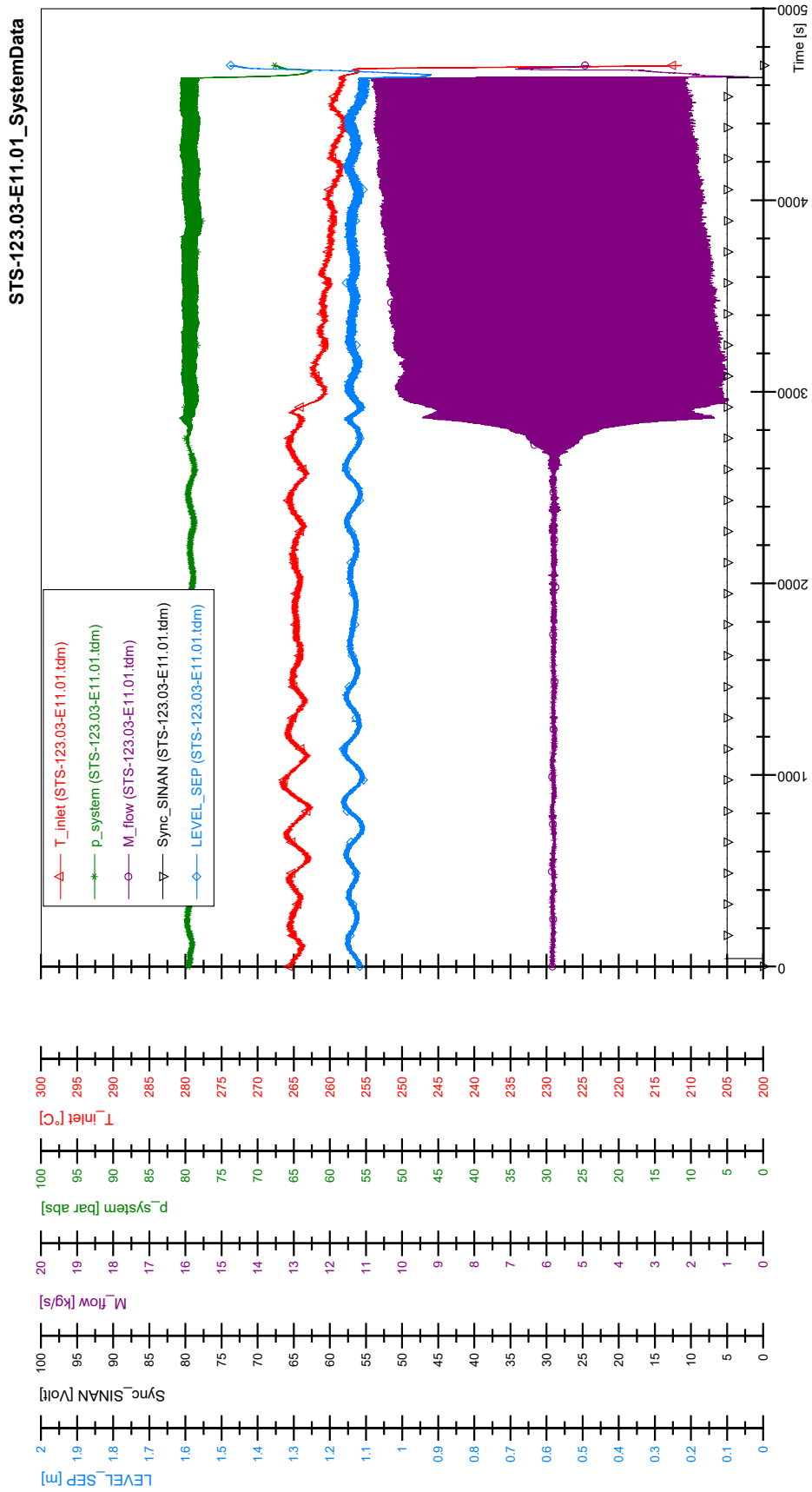
STS-123.03-F11.03_Rod_88



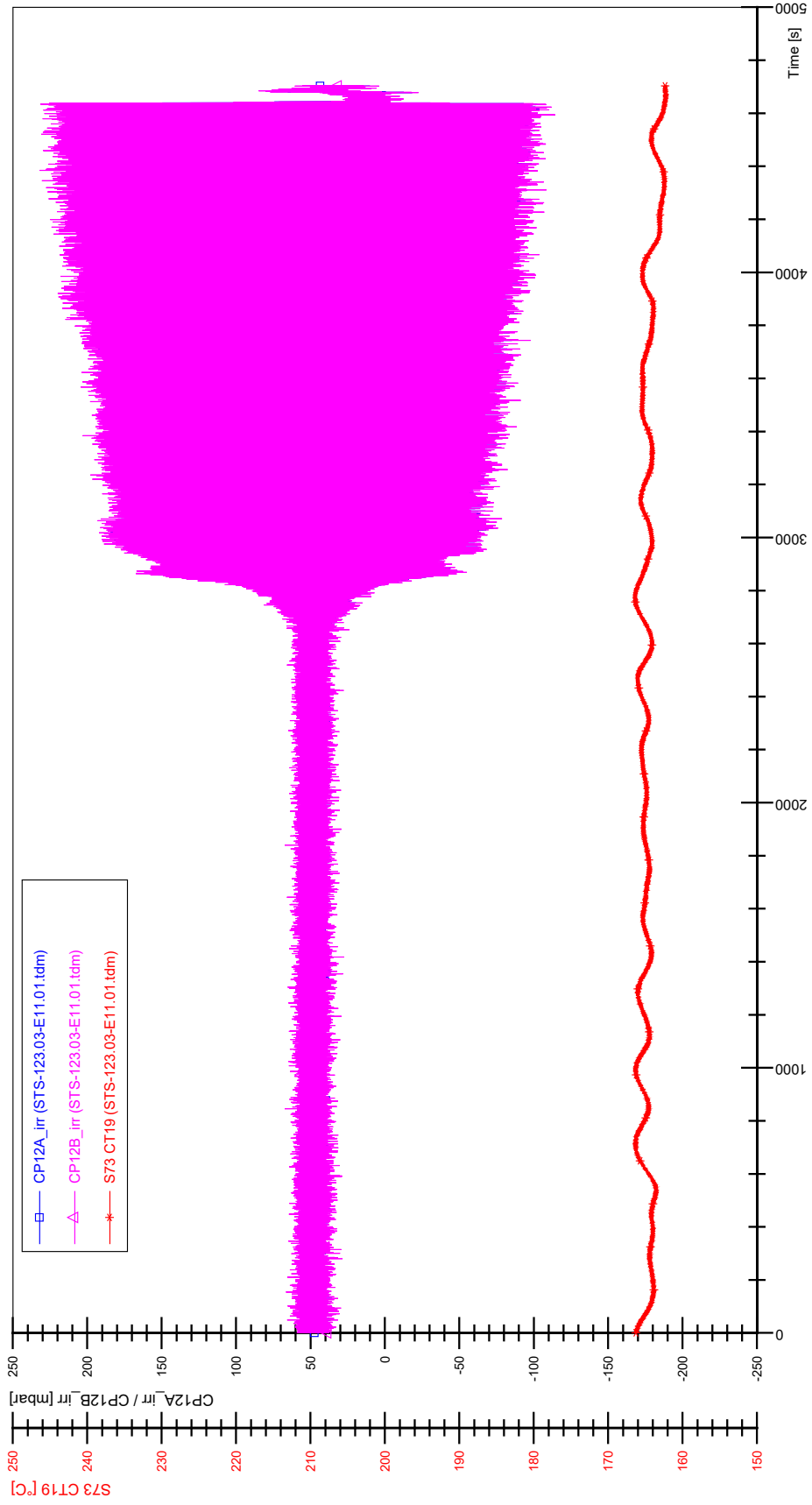
SIN-123.03-F11.03



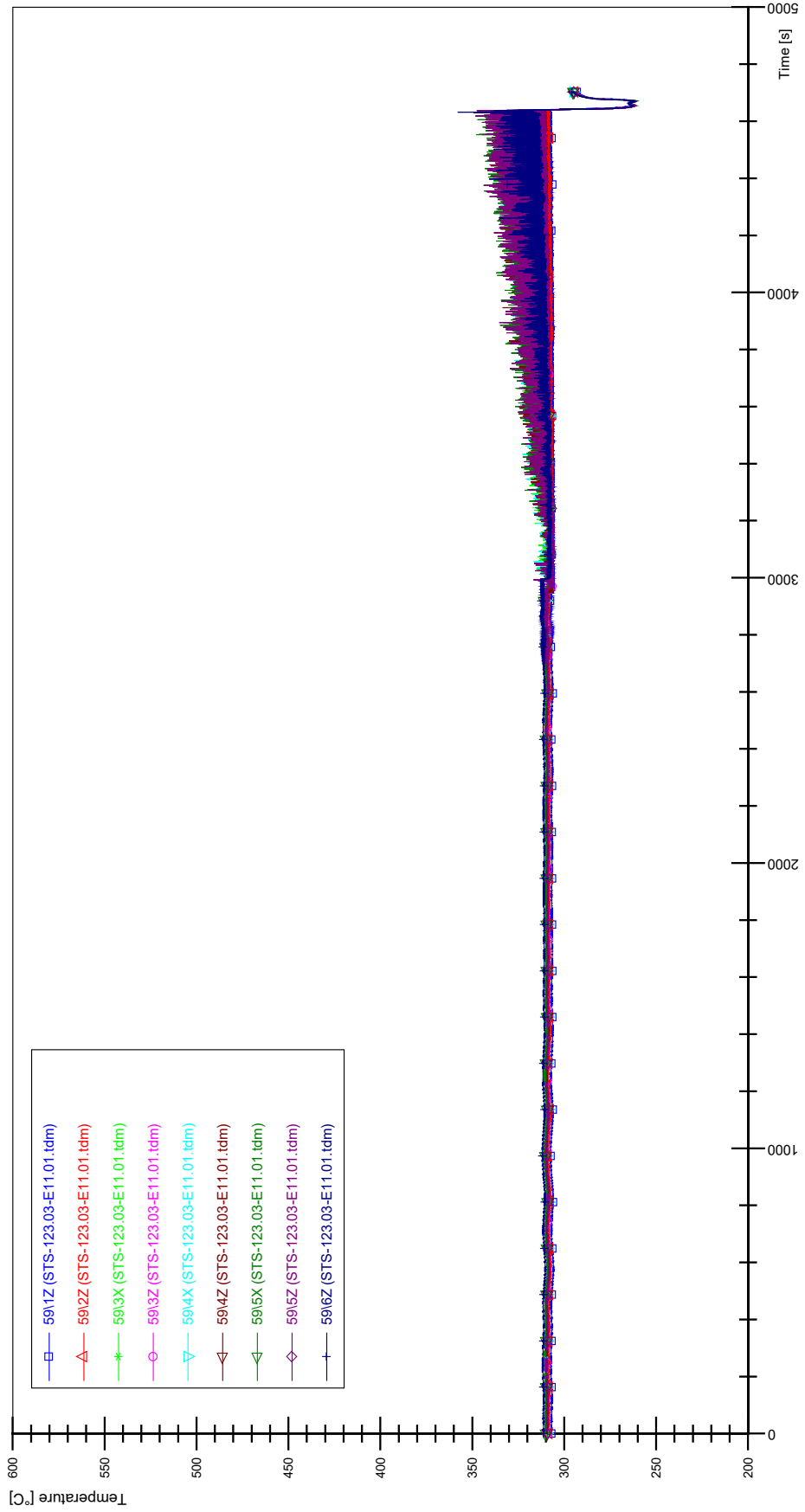
APPENDIX FFF PLOTS OF INSTABILITY TEST STS-123.03-E11.01



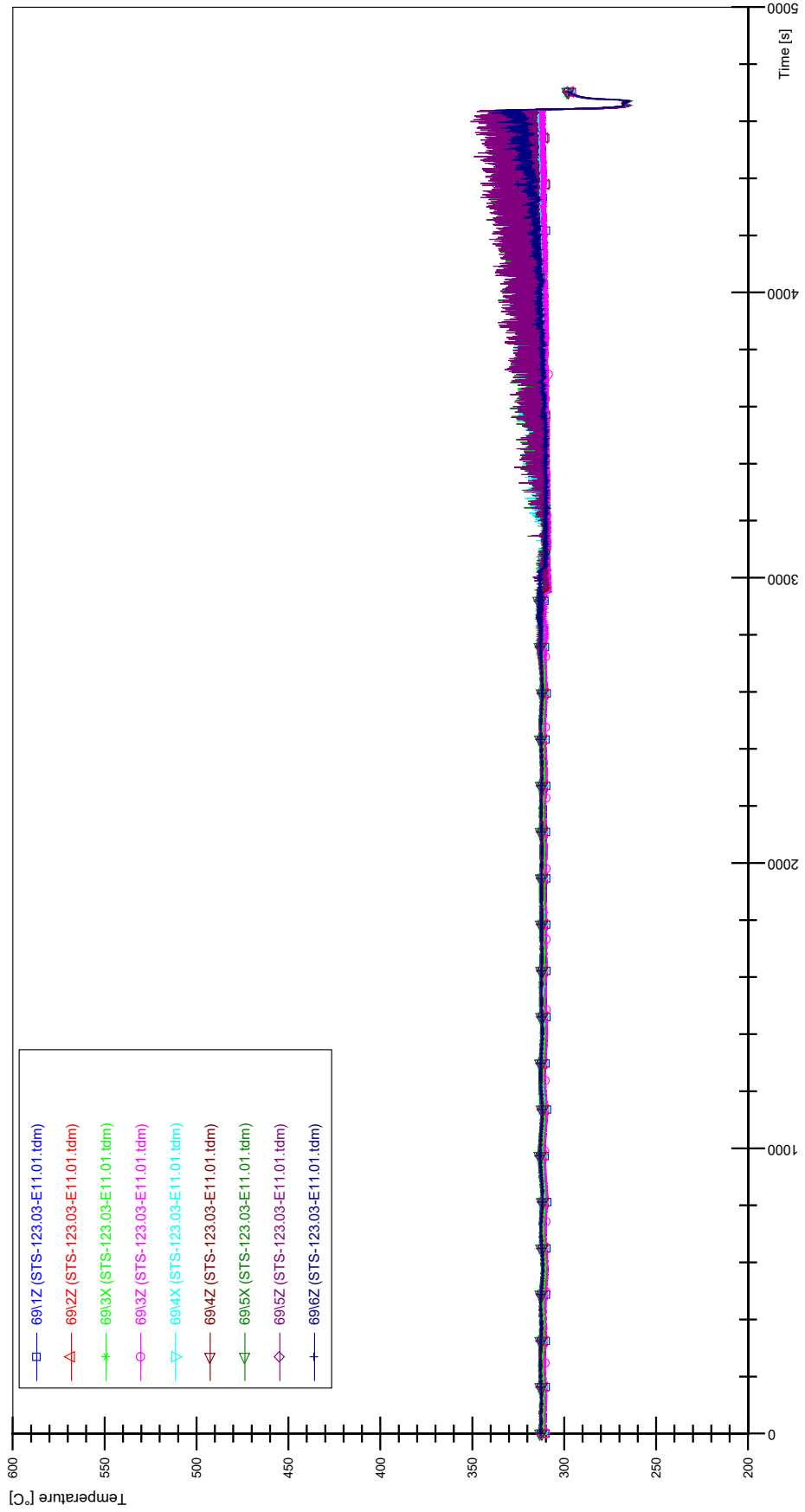
STS-123.03-E11.01_CP12_CT19



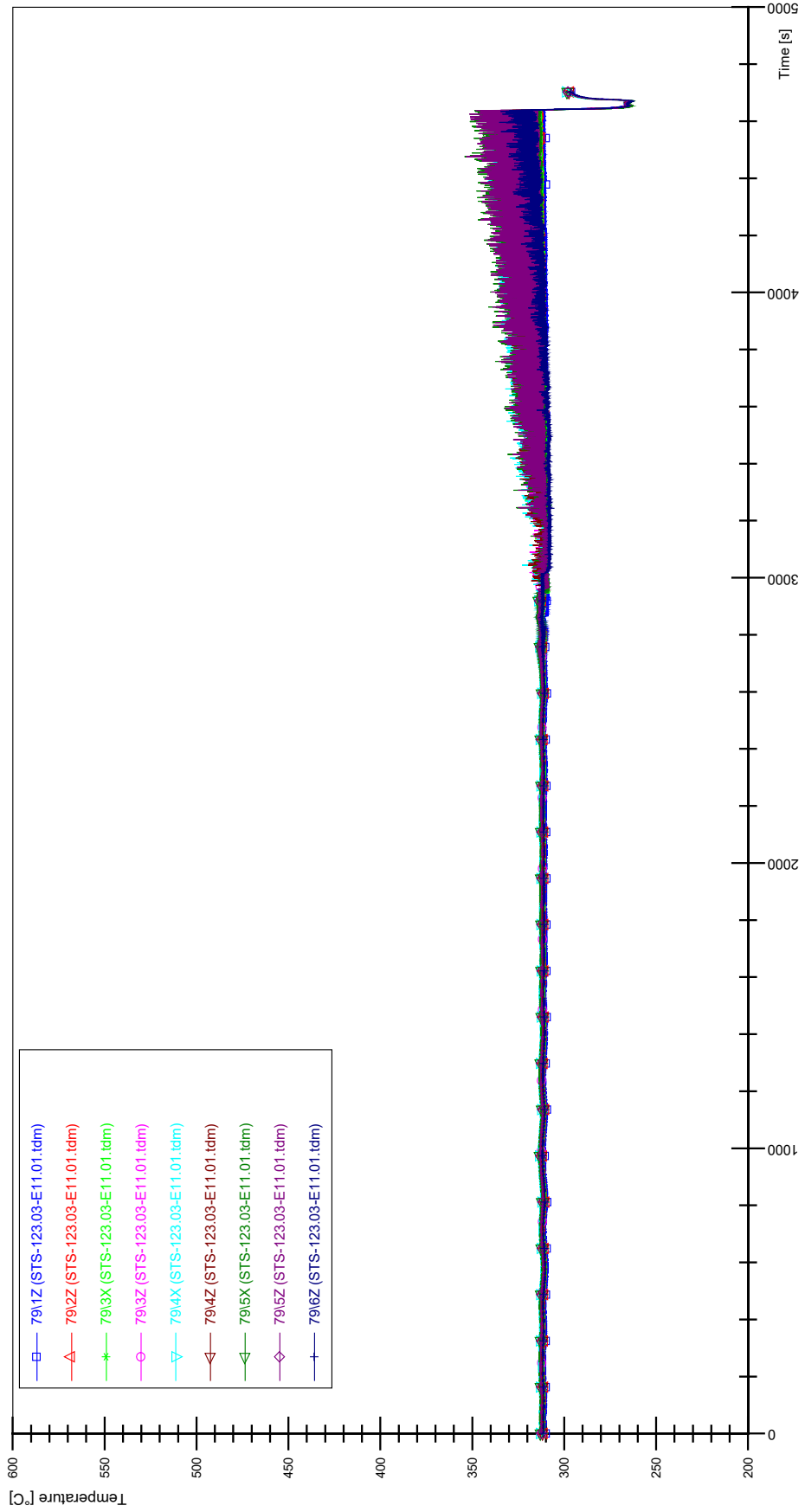
STS-123.03-E11.01_Rod_59



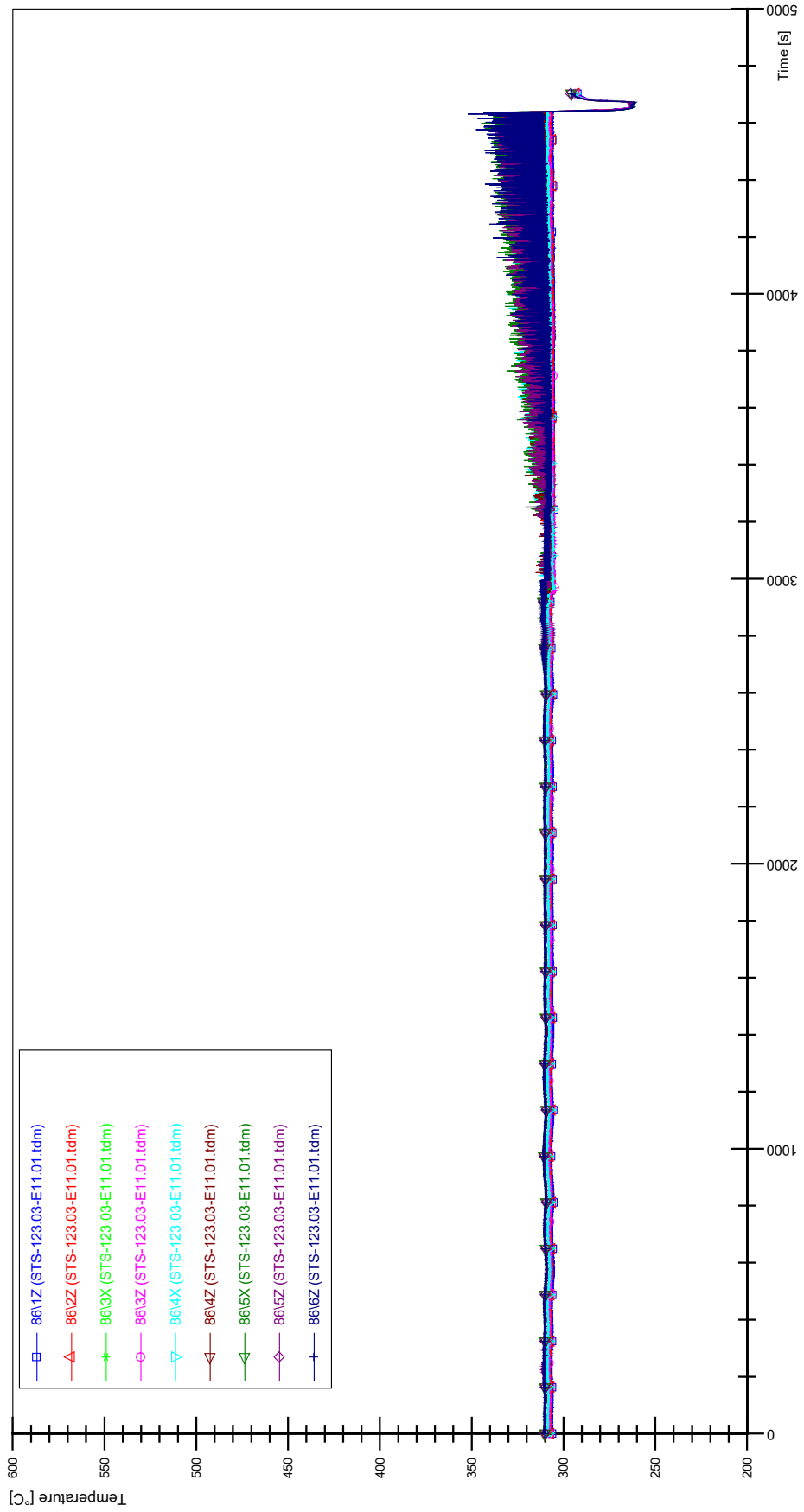
STS-123.03-E11.01_Rod_69



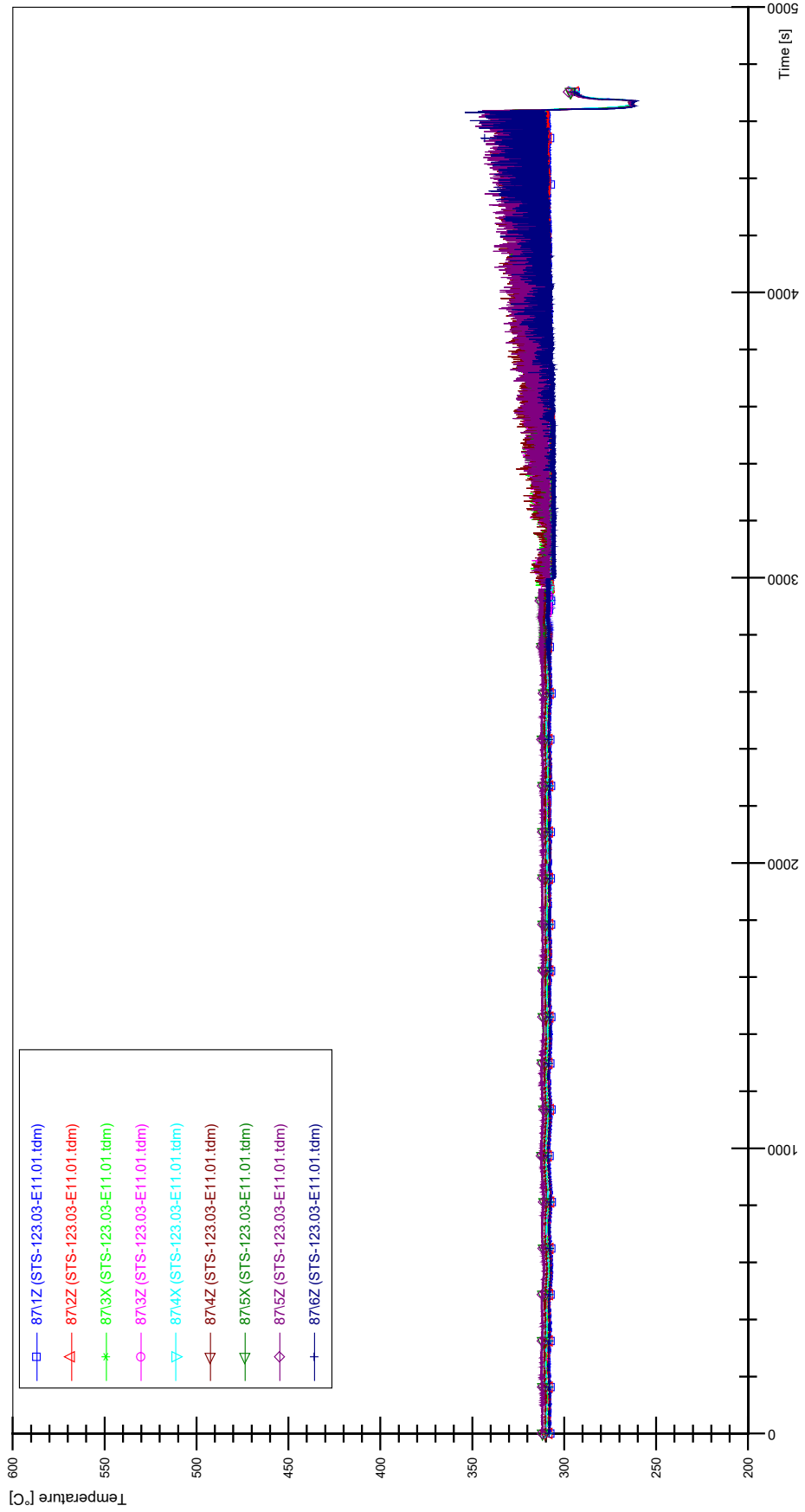
STS-123.03-E11.01_Rod_79



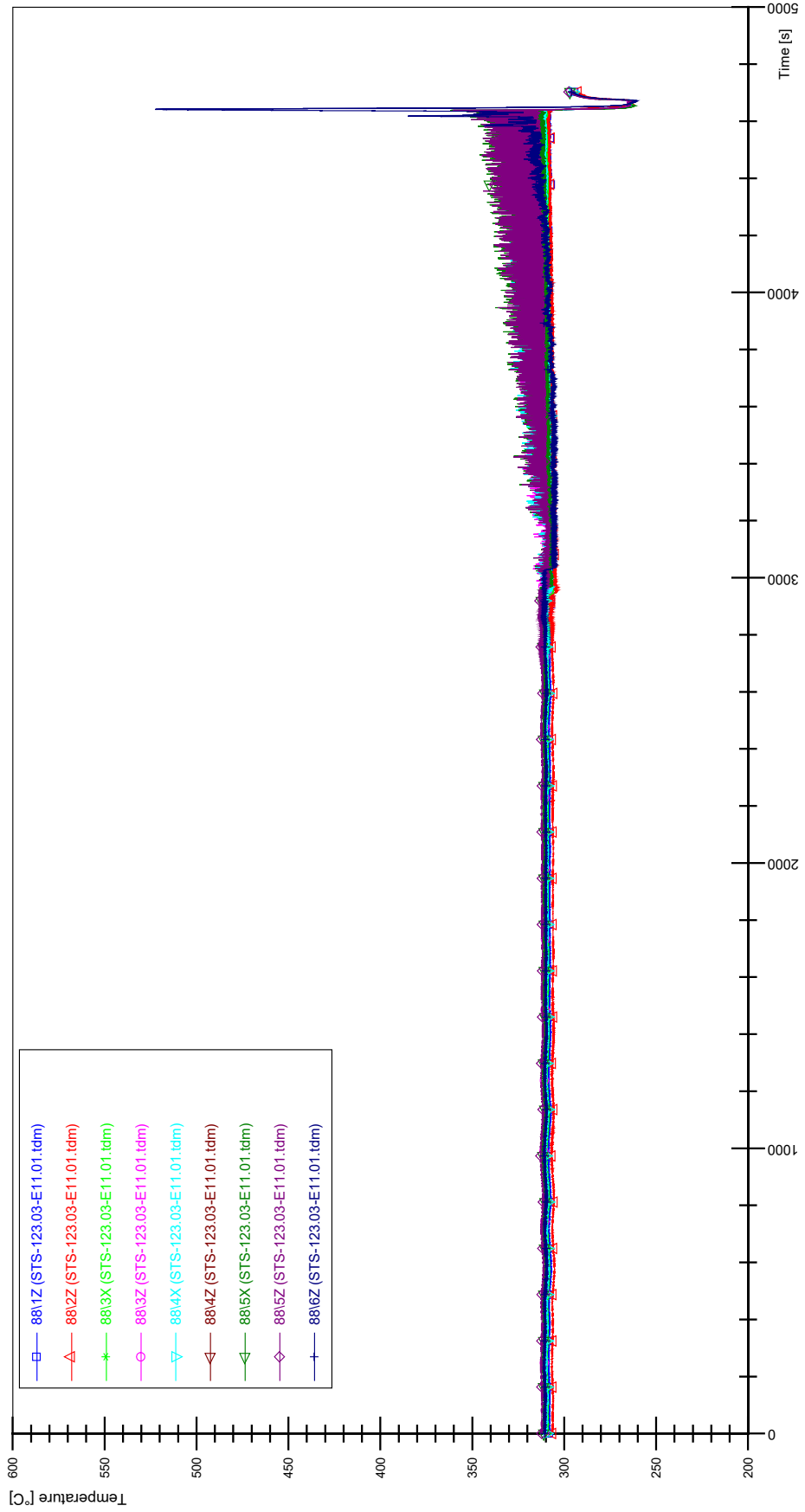
STS-123.03-E11.01_Rod_86



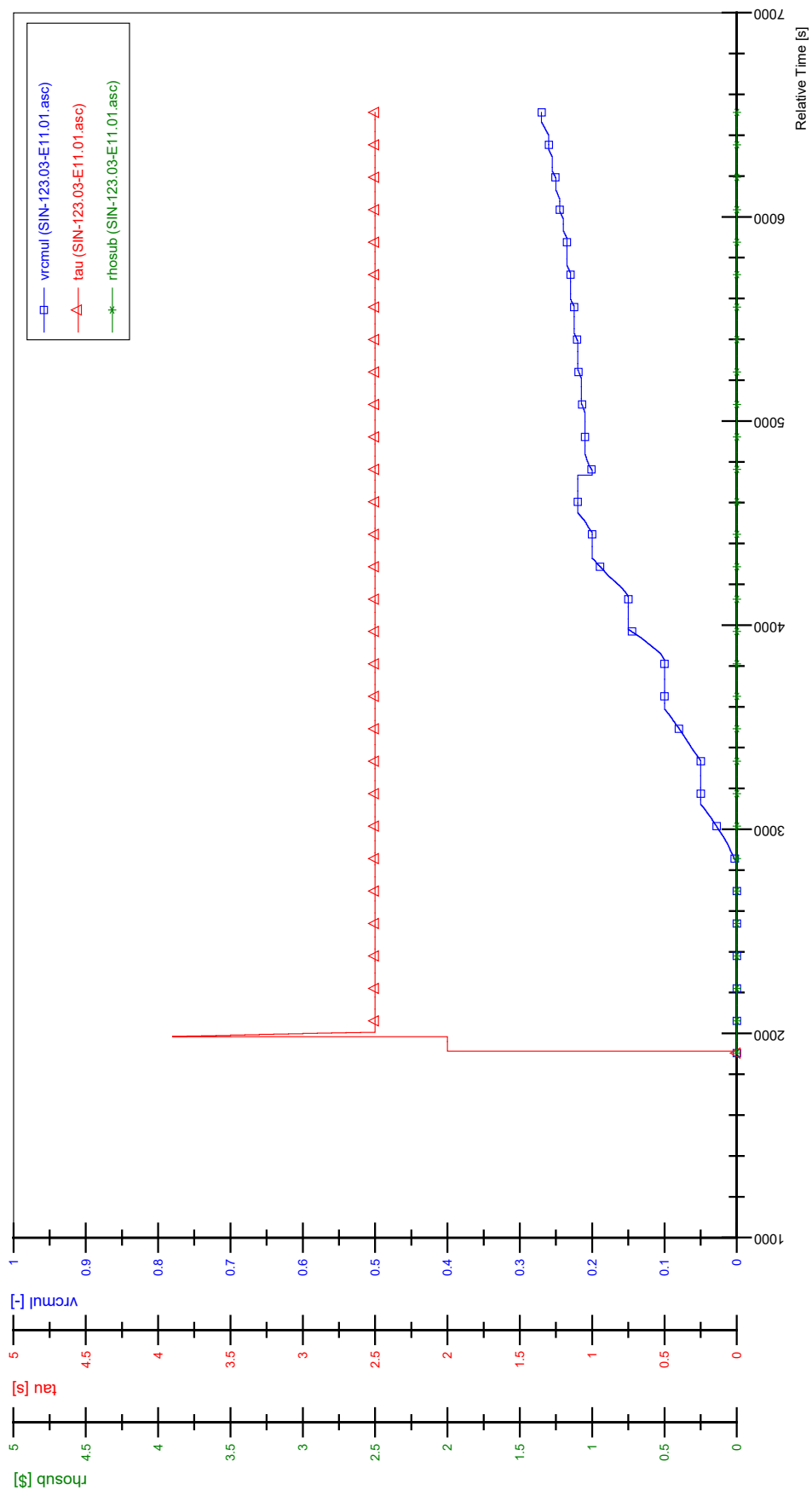
STS-123.03-E11.01_Rod_87



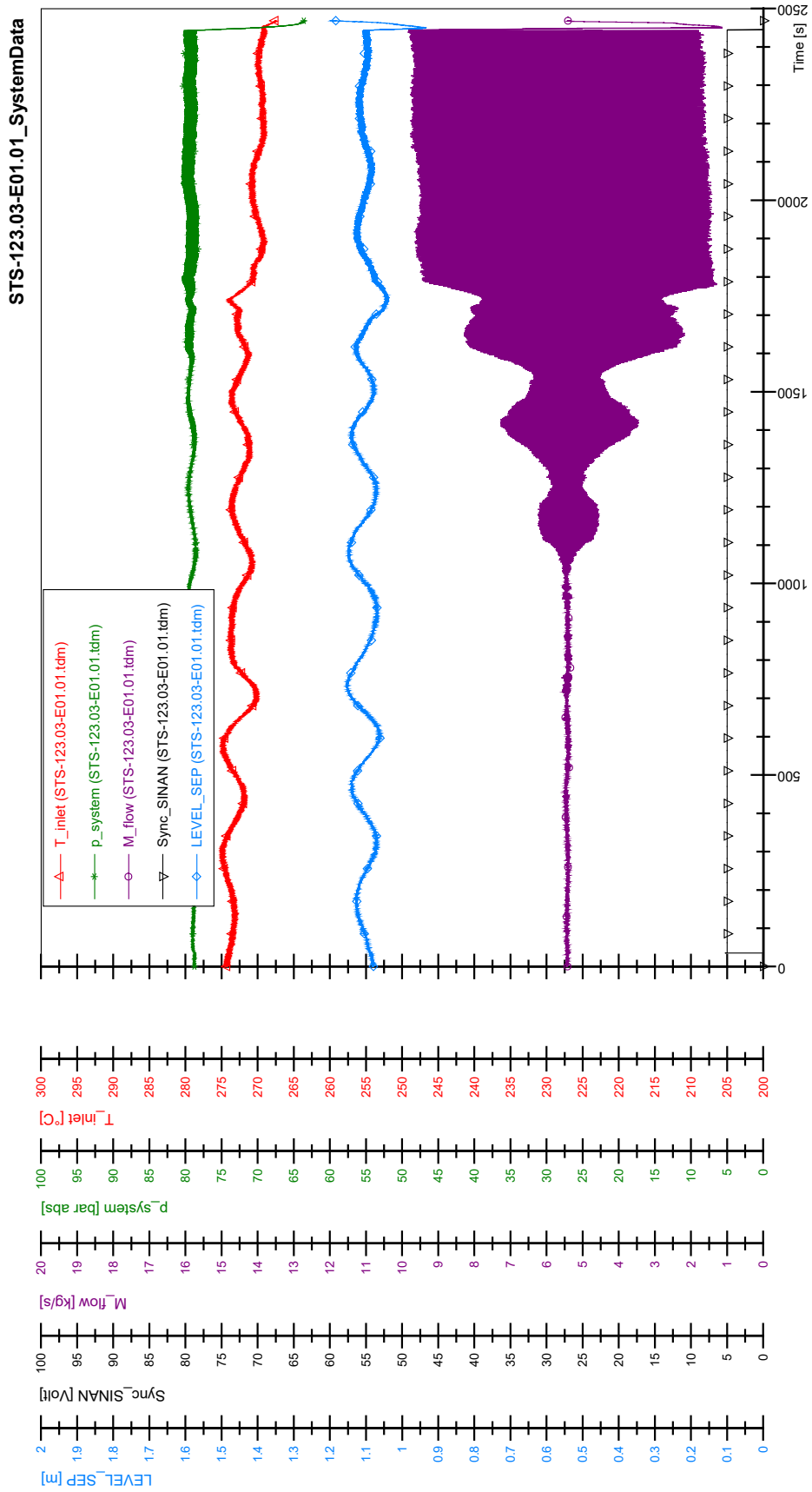
STS-123.03-E11.01_Rod_88



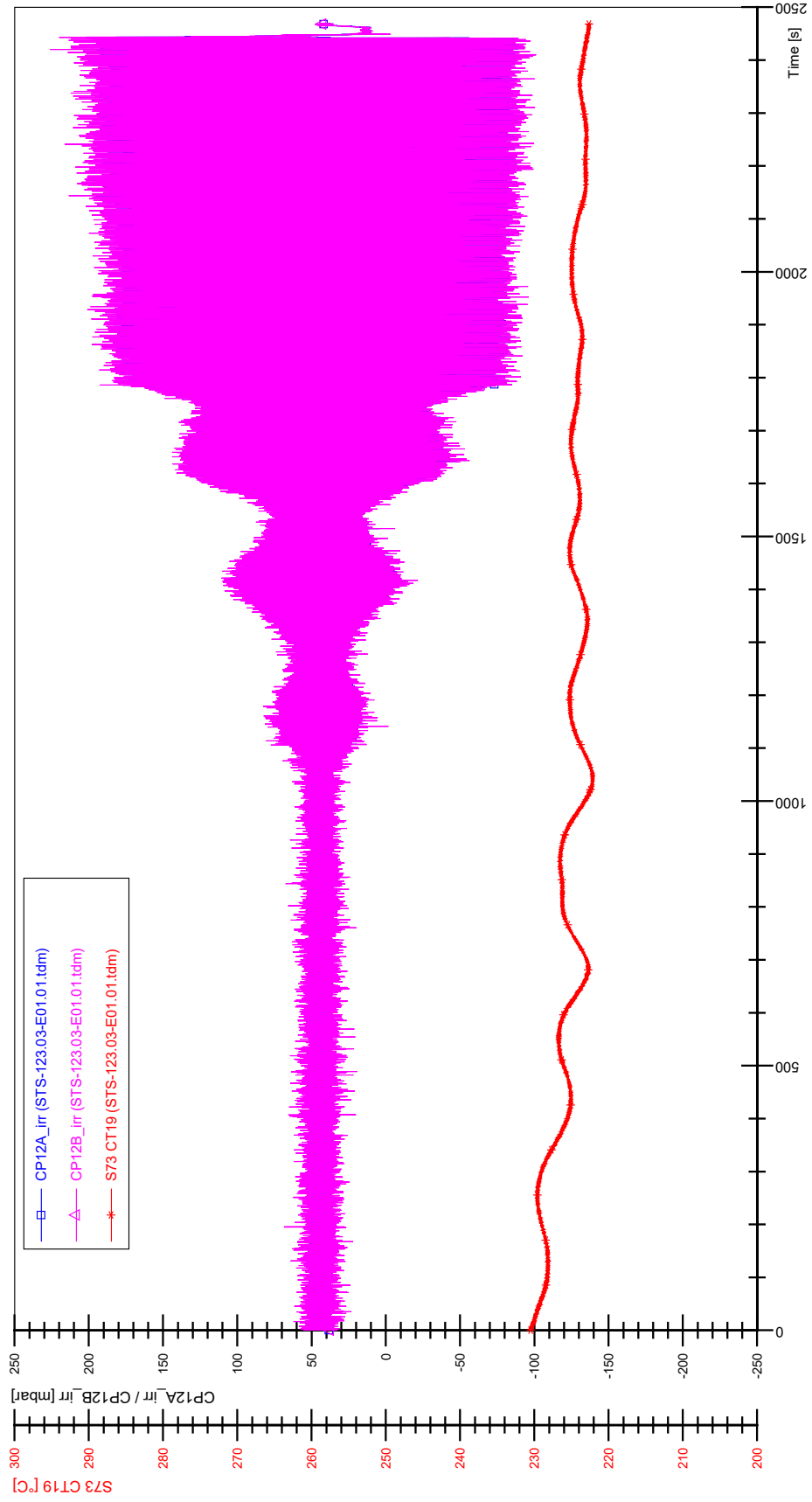
SIN-123.03-E11.01



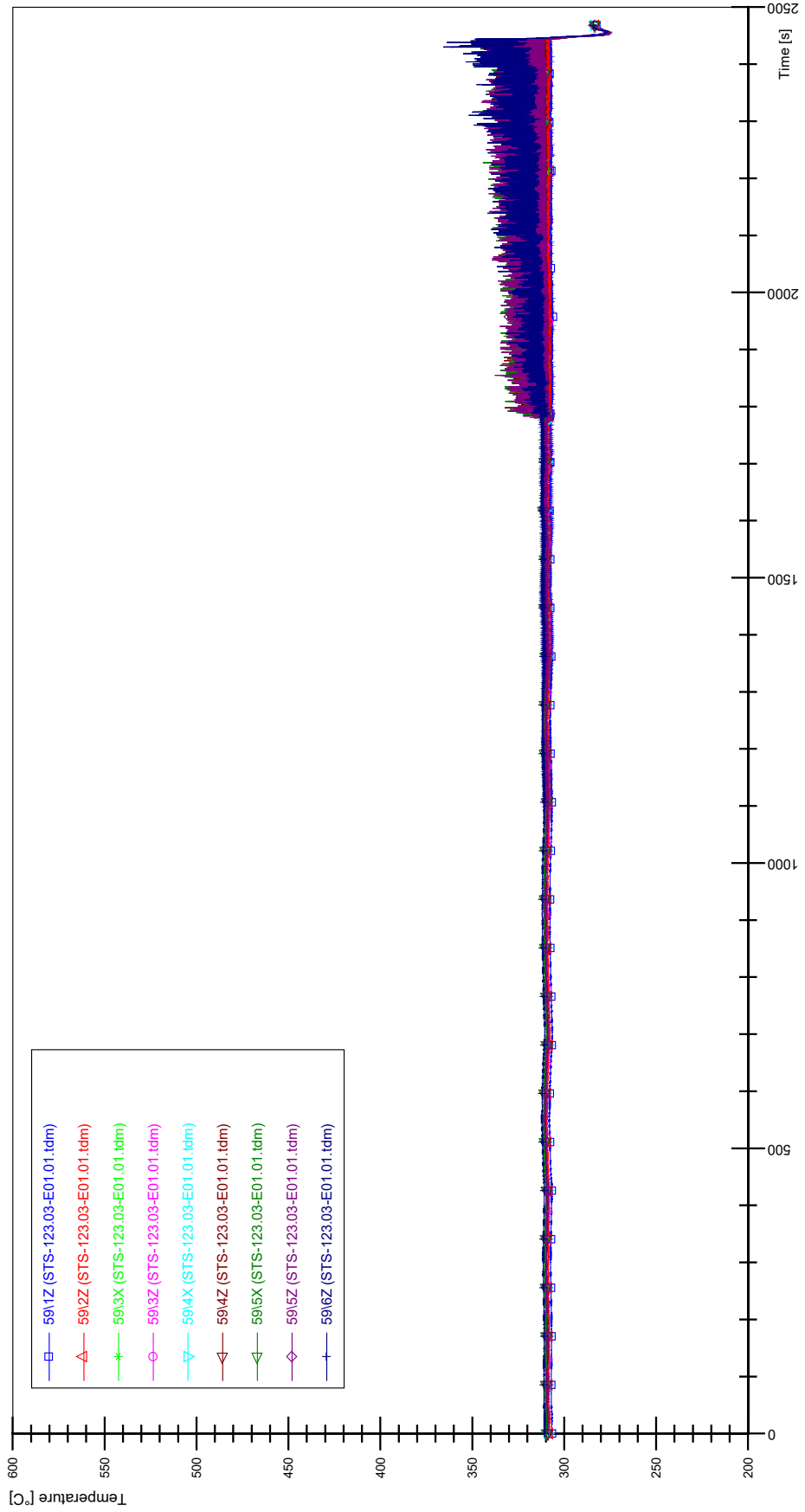
APPENDIX GGG PLOTS OF INSTABILITY TEST STS-123.03-E01.01



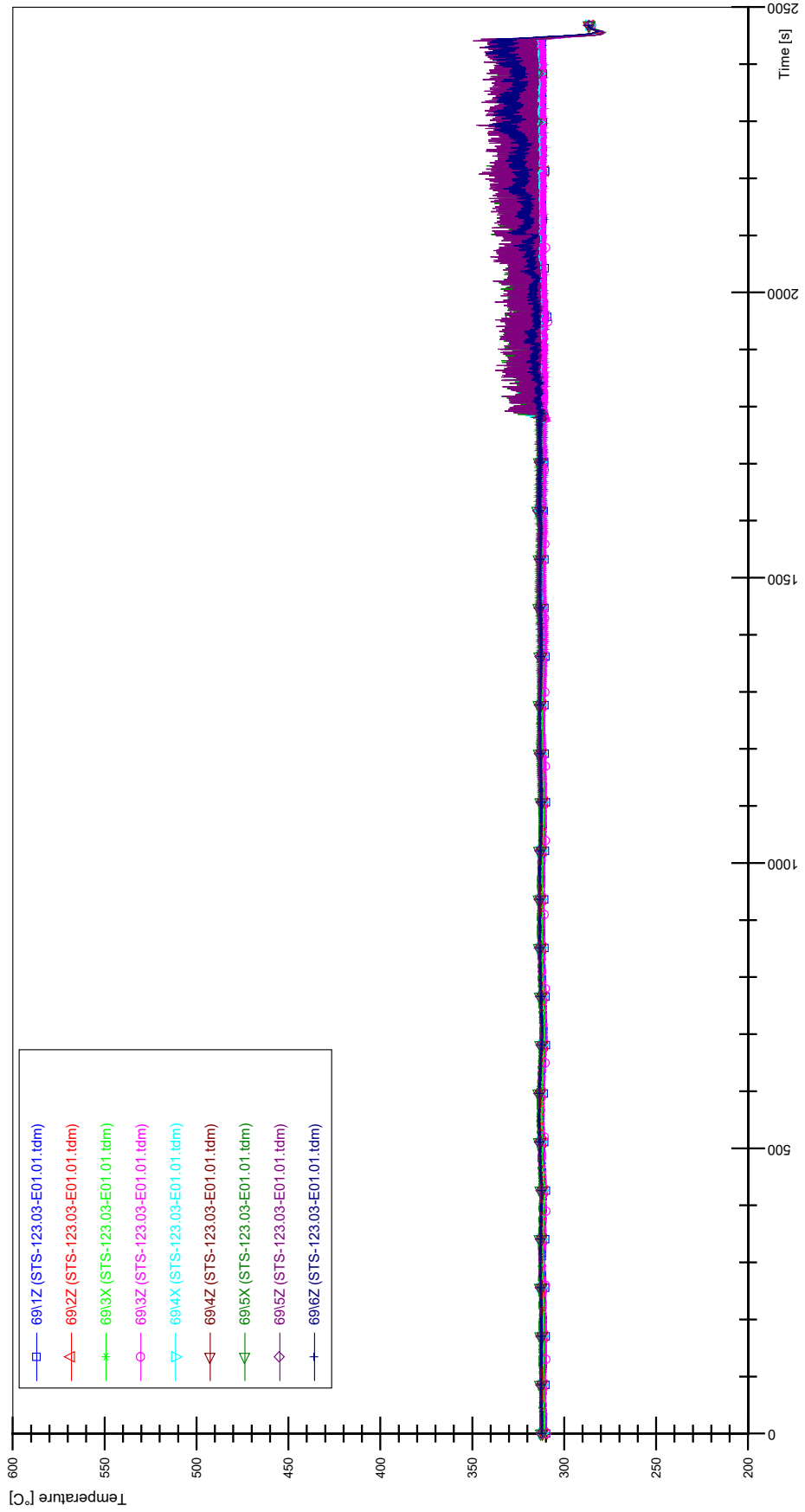
STS-123.03-E01.01_CP12_CT19



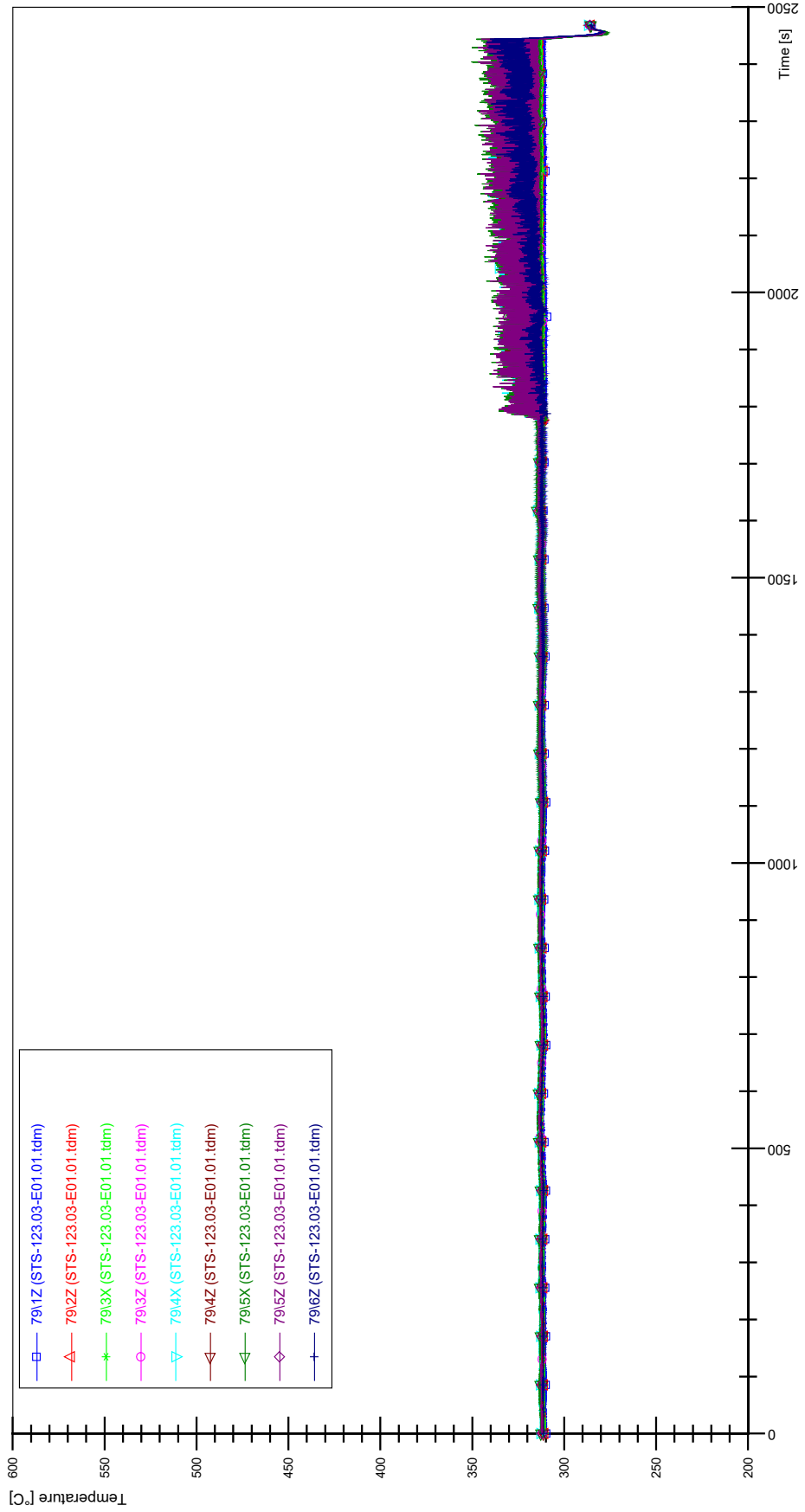
STS-123.03-E01.01_Rod_59



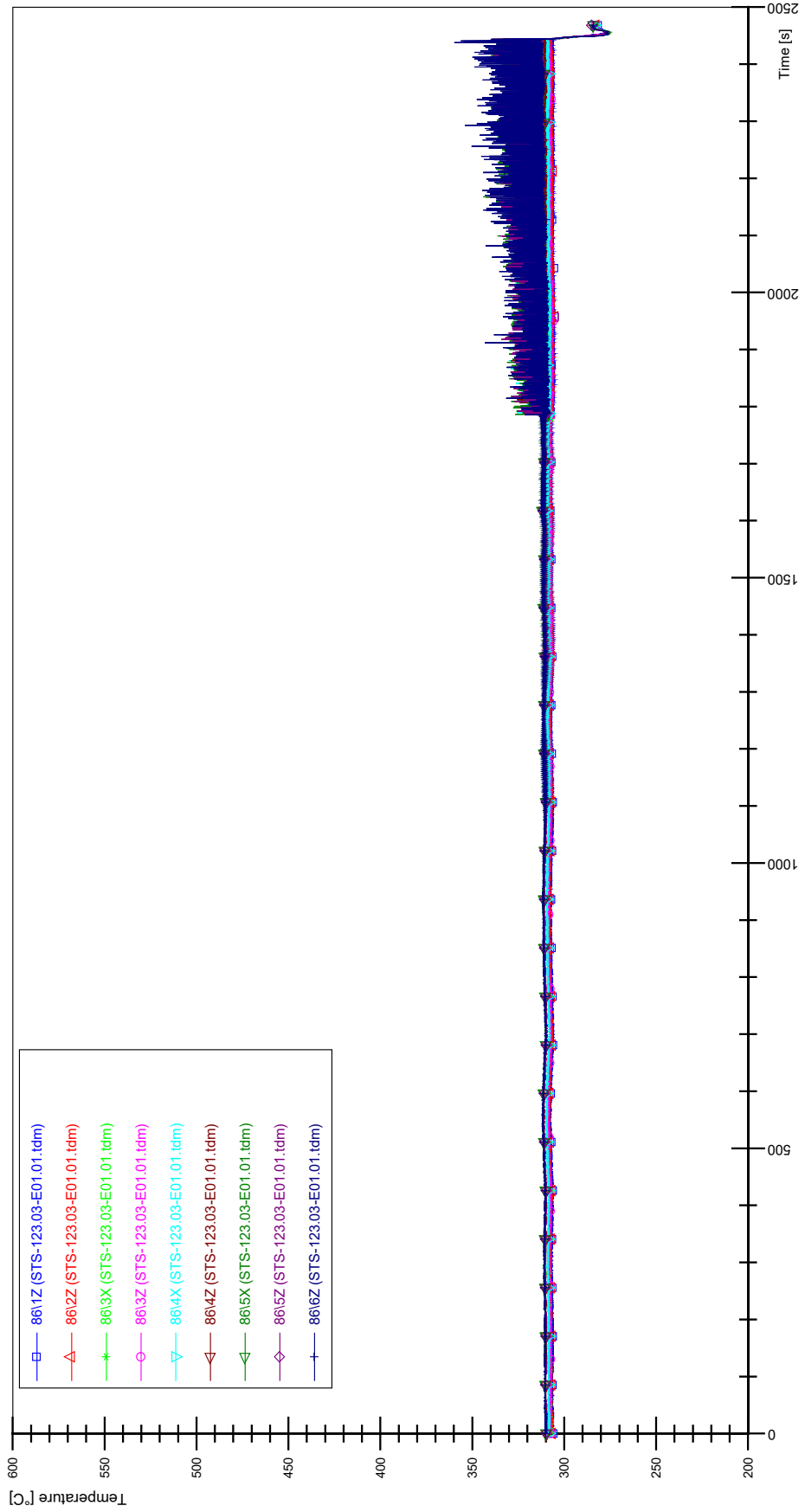
STS-123.03-E01.01_Rod_69



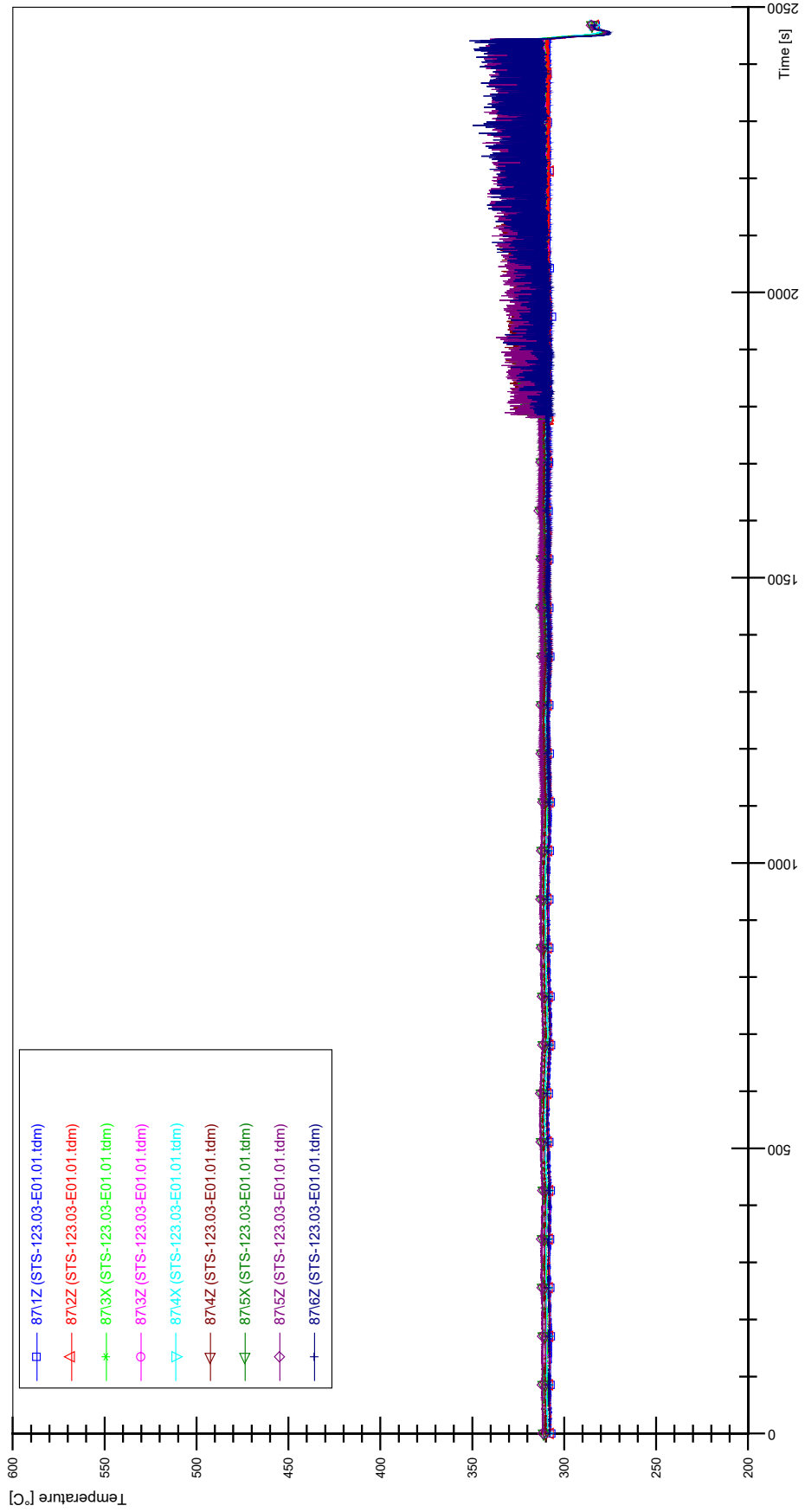
STS-123.03-E01.01_Rod_79



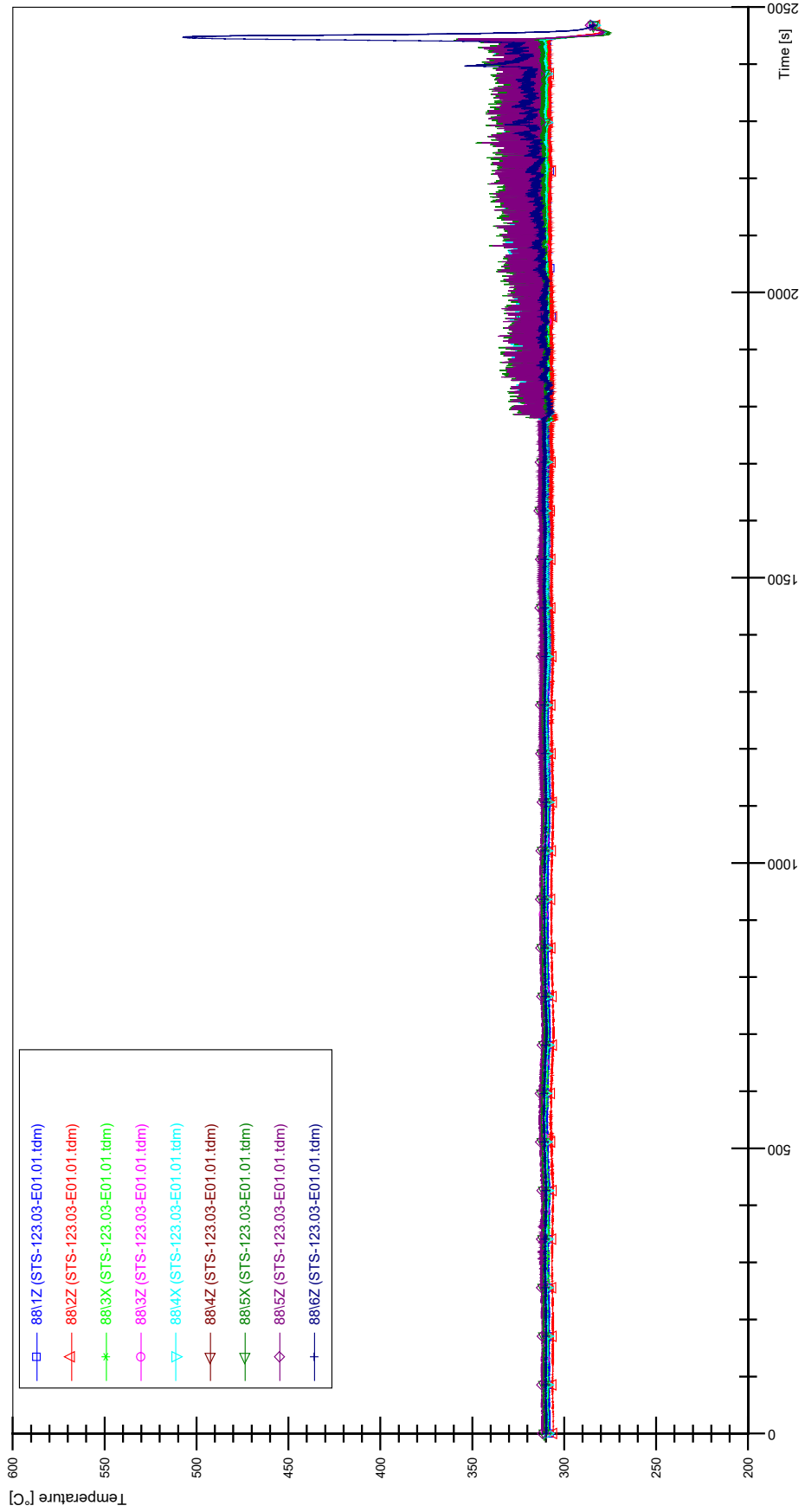
STS-123.03-E01.01_Rod_86



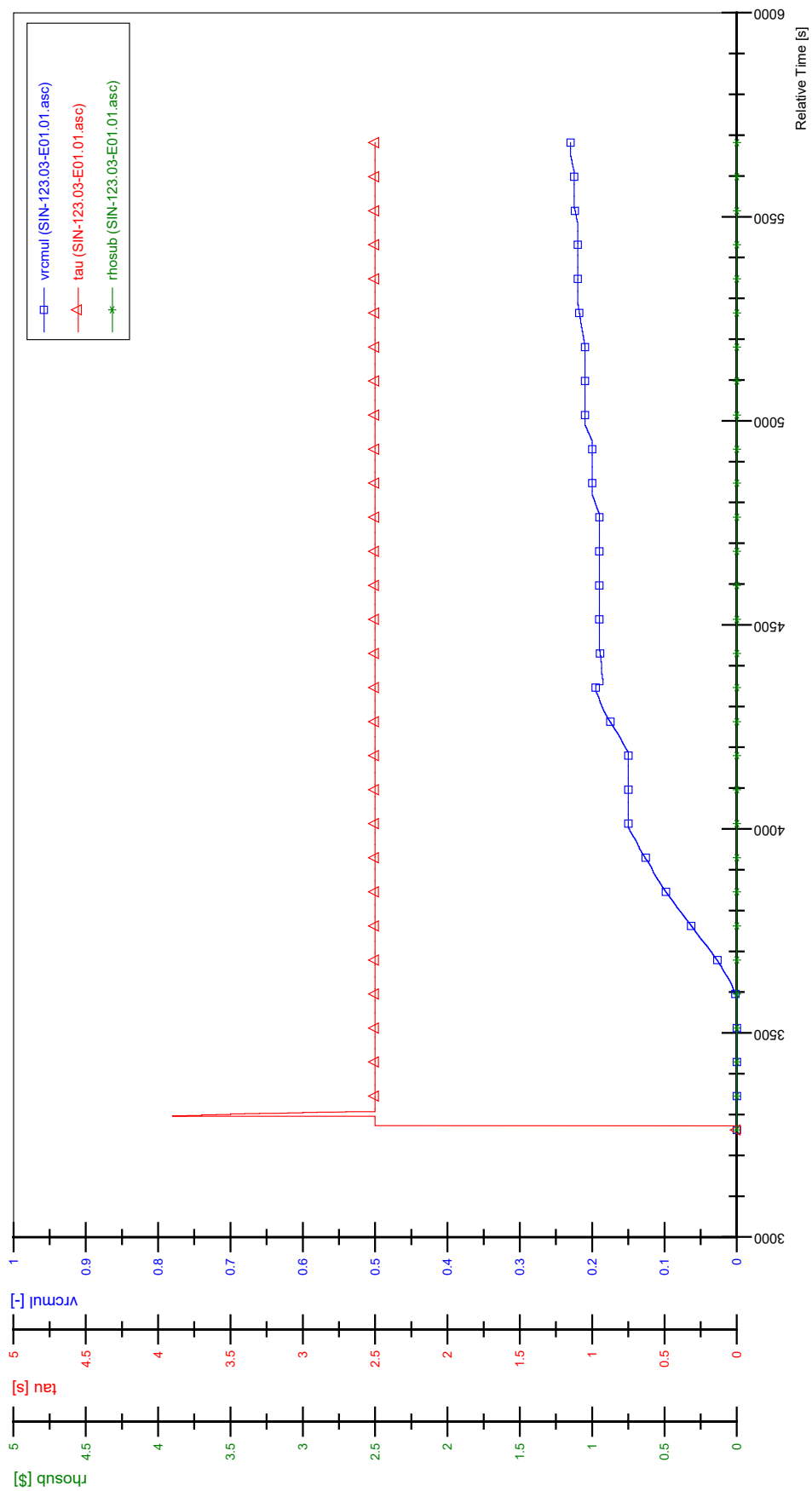
STS-123.03-E01.01_Rod_87



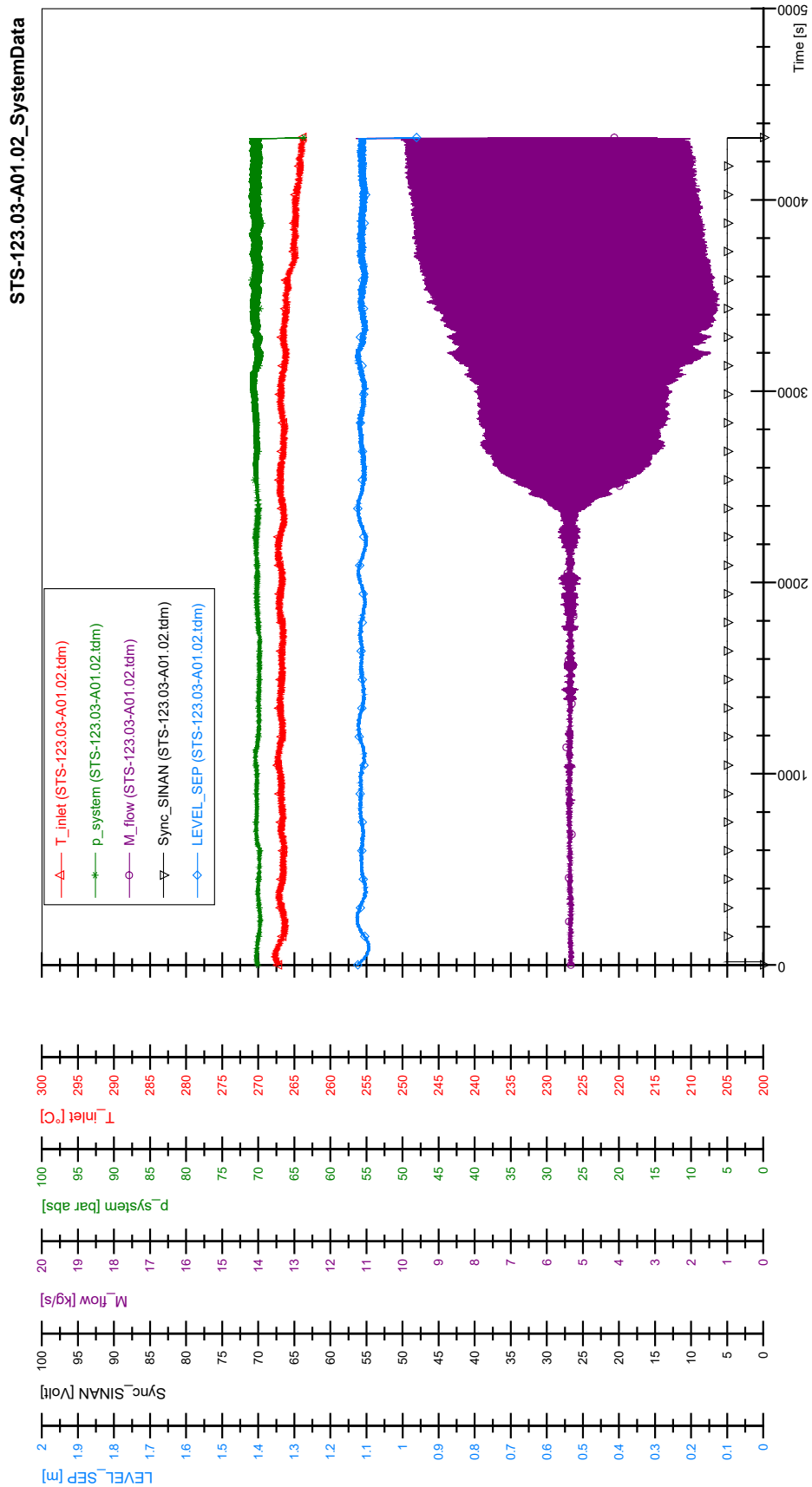
STS-123.03-E01.01_Rod_88



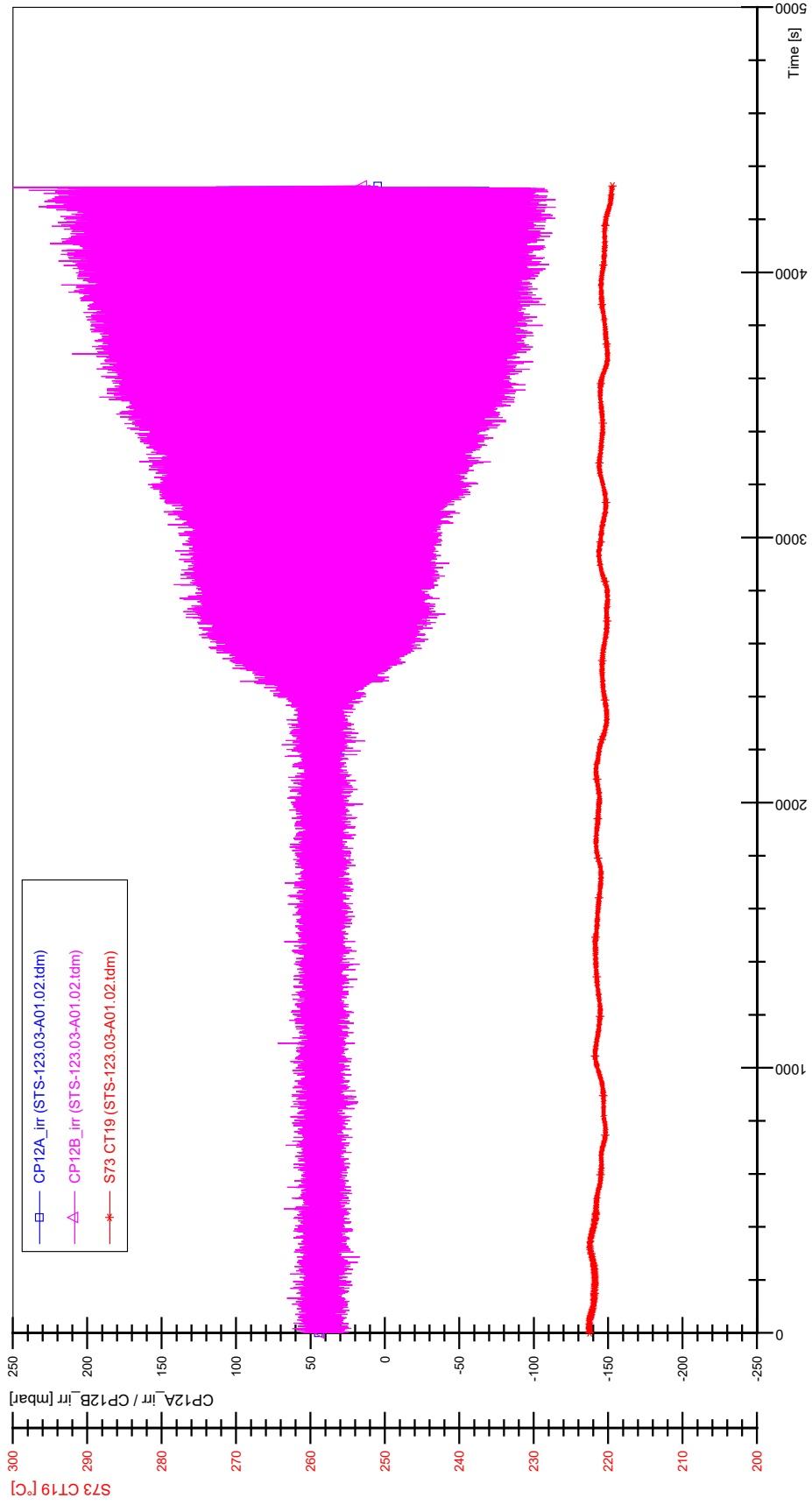
SIN-123.03-E01.01



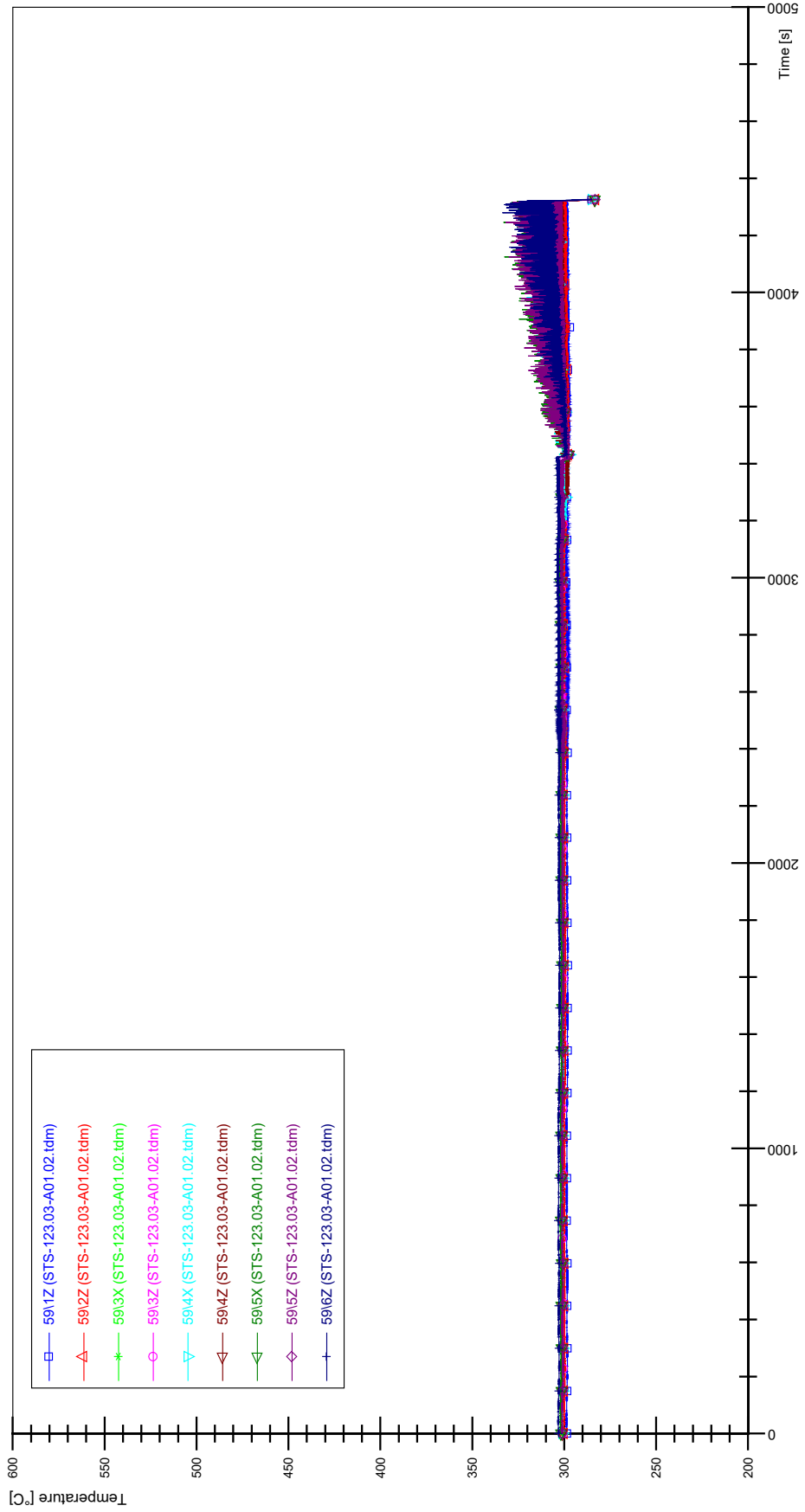
APPENDIX HHH PLOTS OF INSTABILITY TEST STS-123.03-A01.02



STS-123.03-A01.02_CP12_CT19

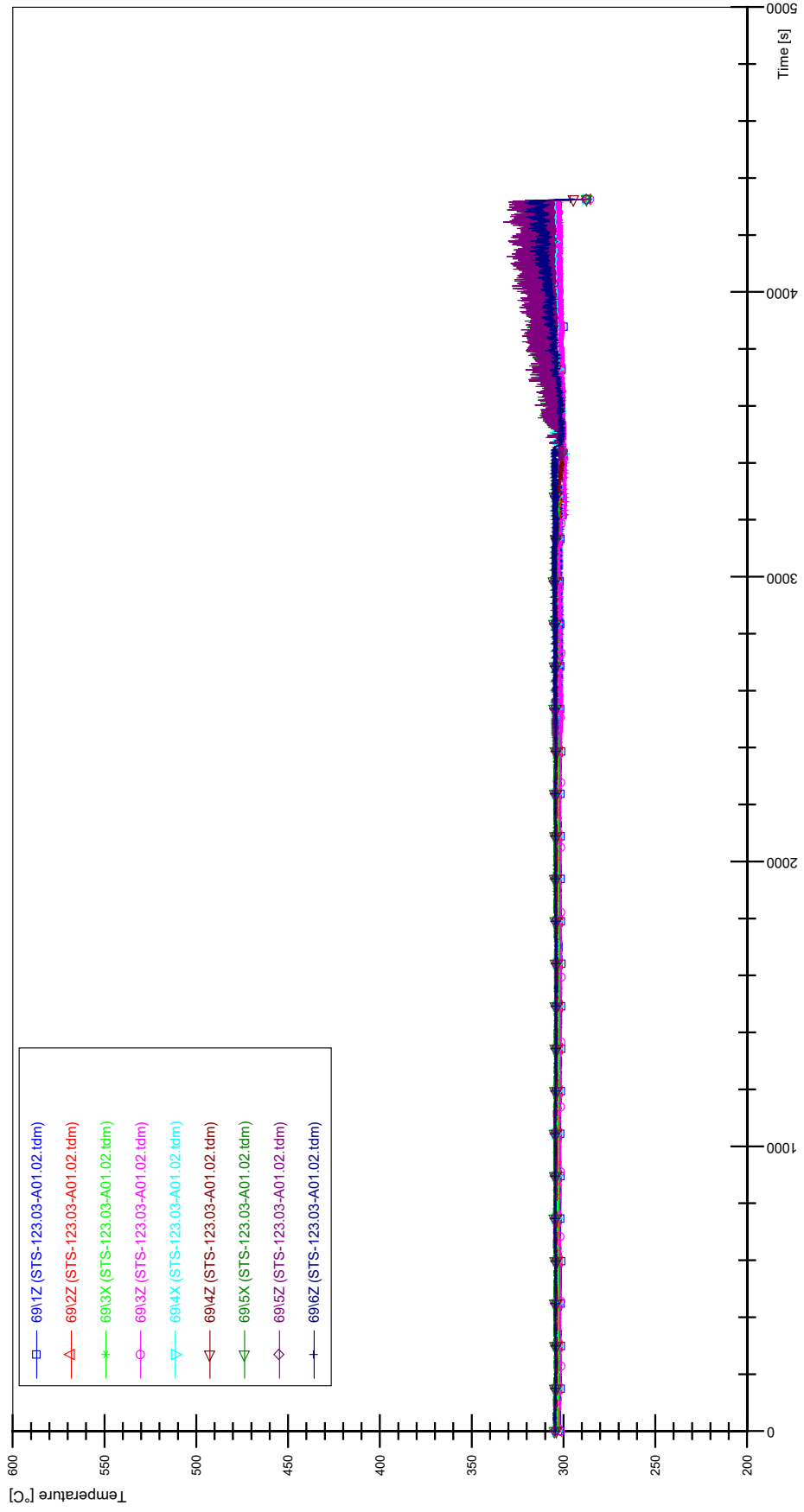


STS-123.03-A01.02_Rod_59

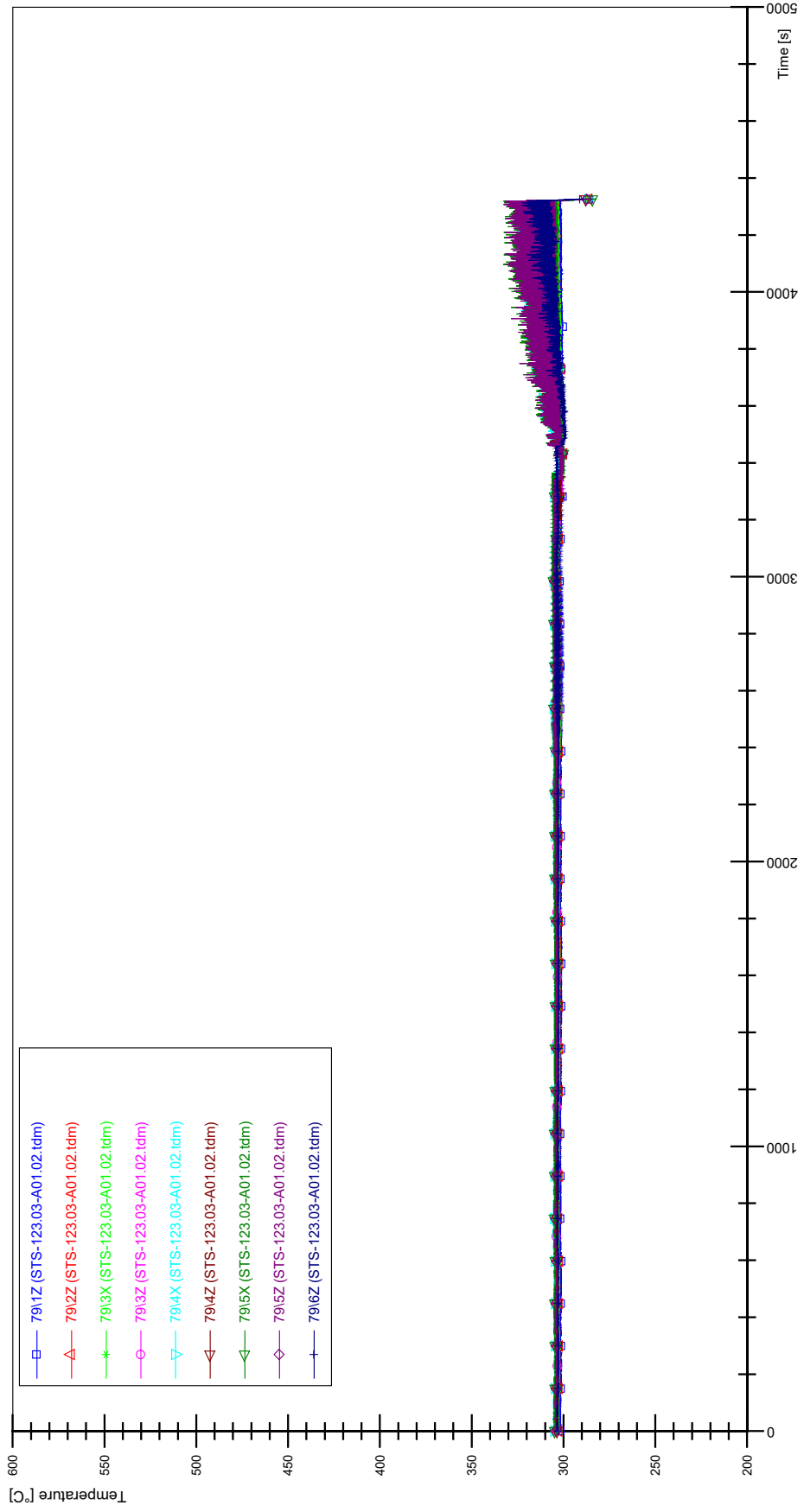


HHH-3

STS-123.03-A01.02_Rod_69

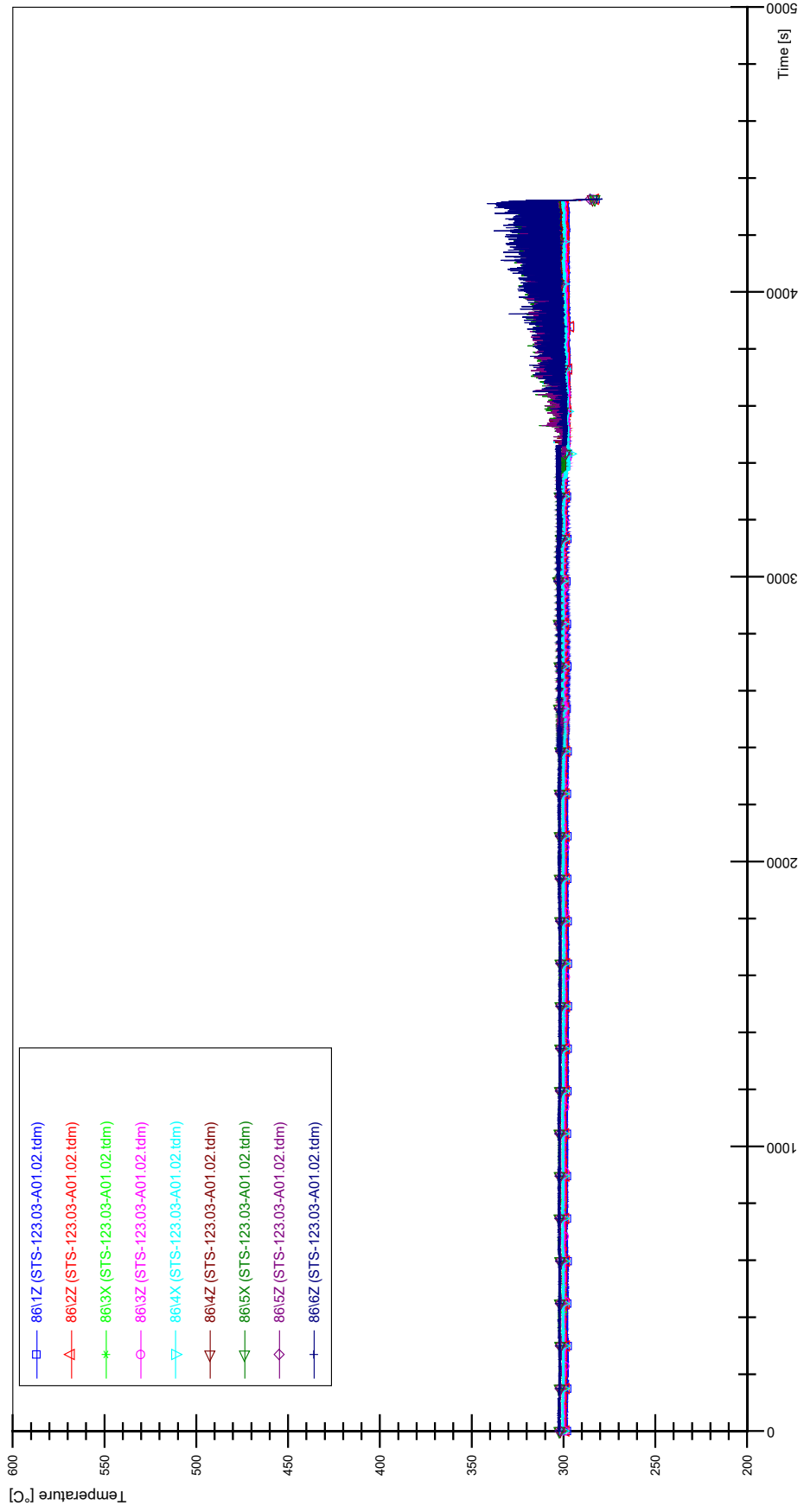


STS-123.03-A01.02_Rod_79

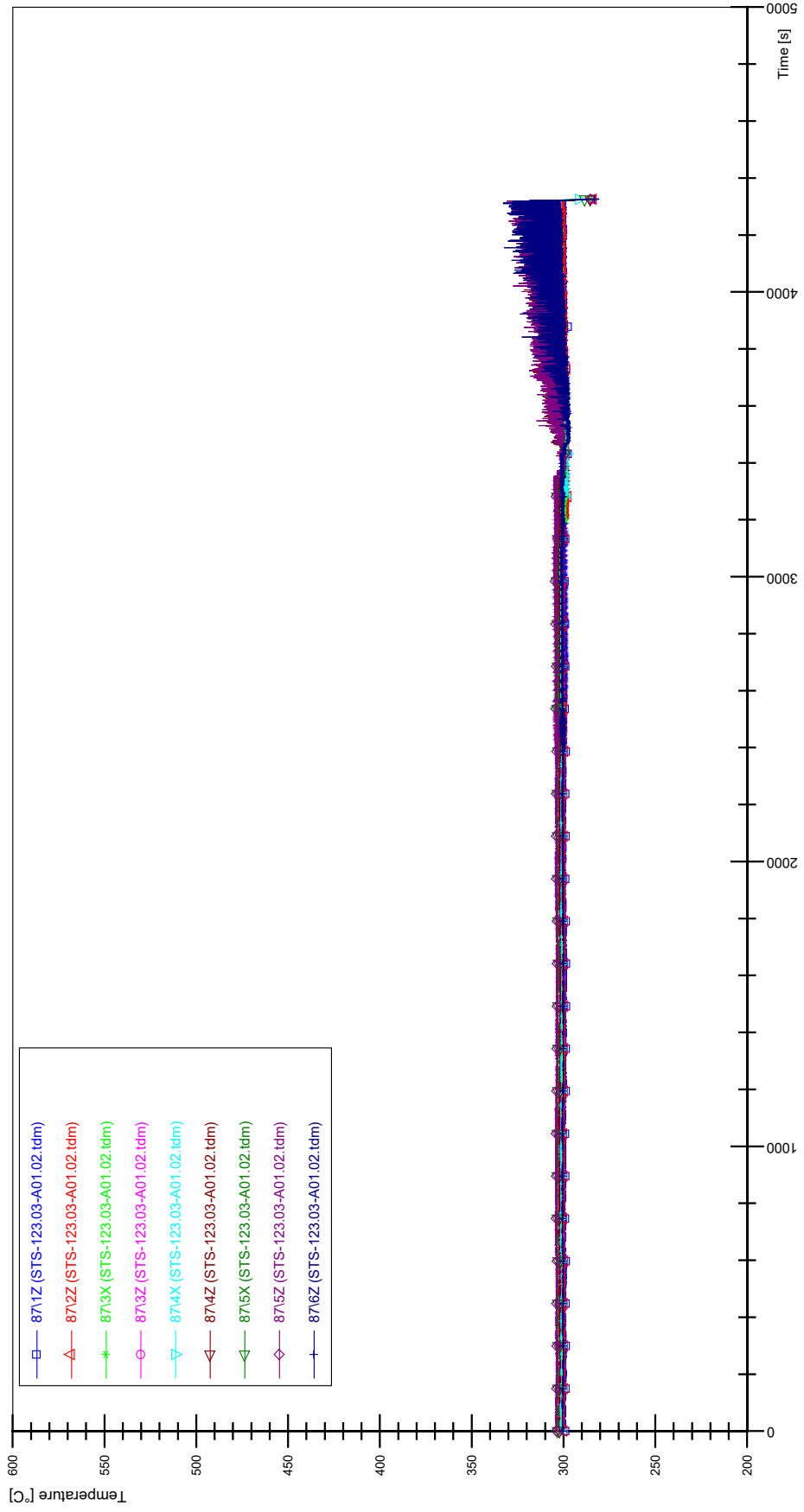


HHH-5

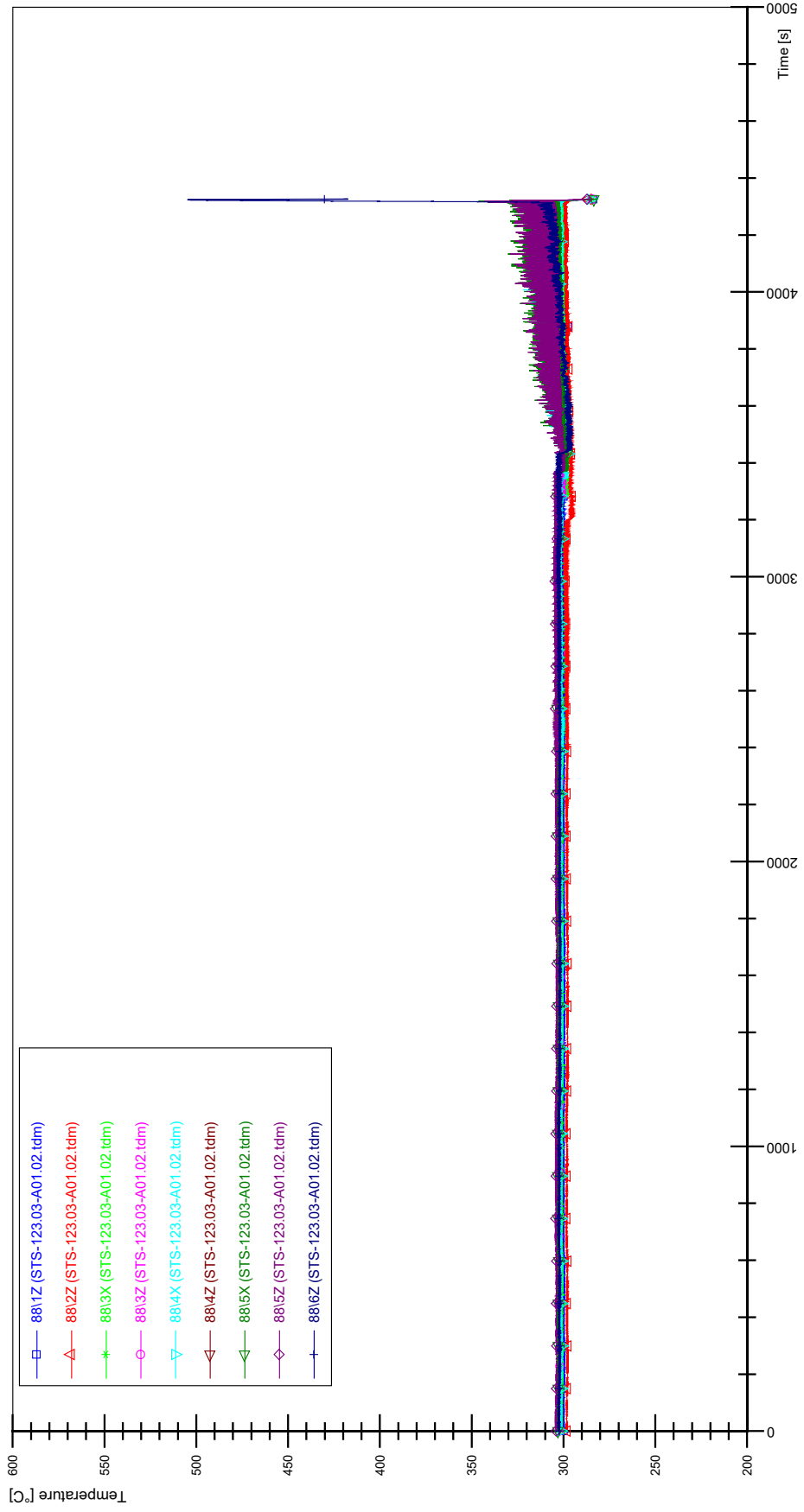
STS-123.03-A01.02_Rod_86



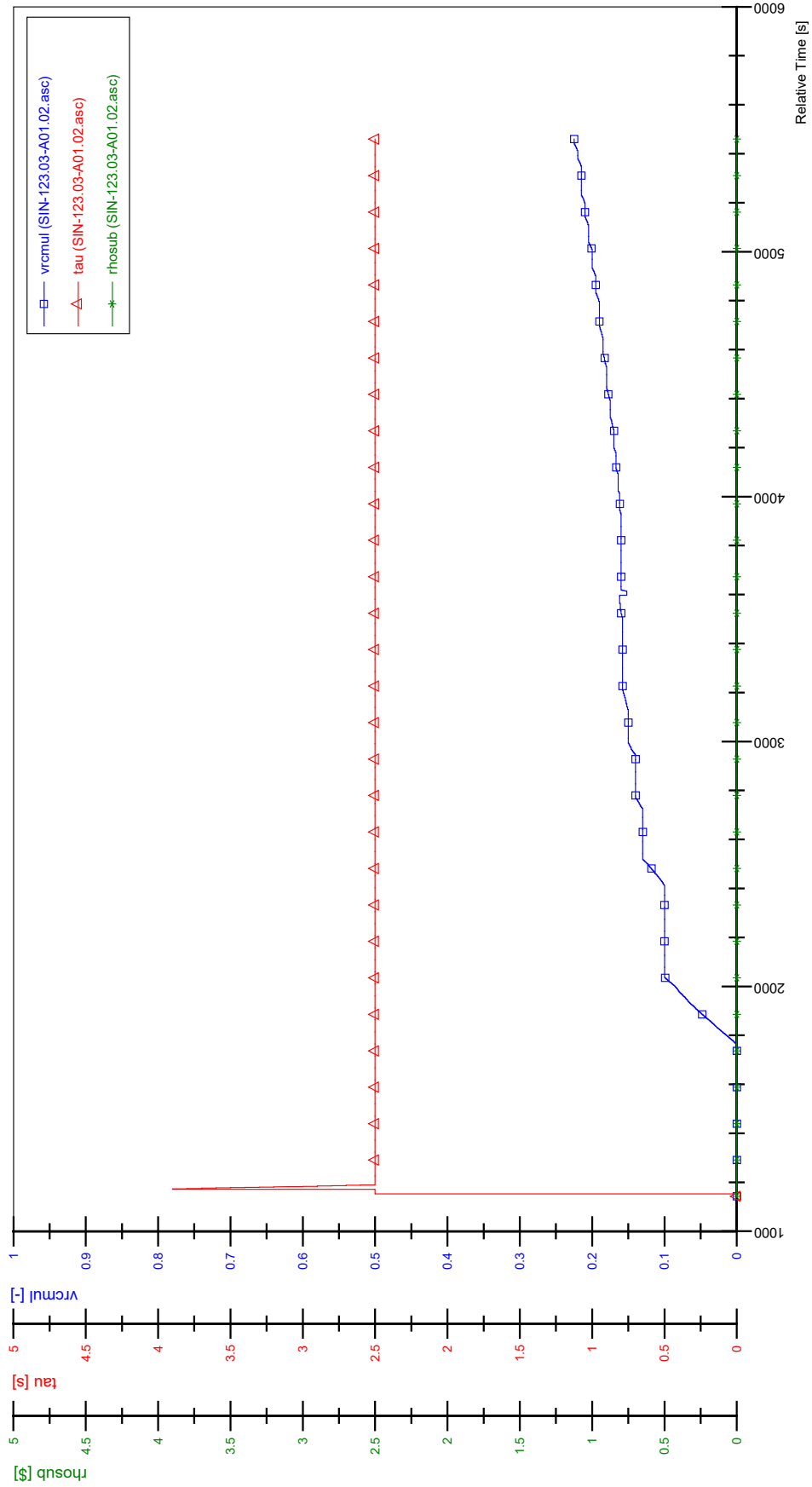
STS-123.03-A01.02_Rod_87



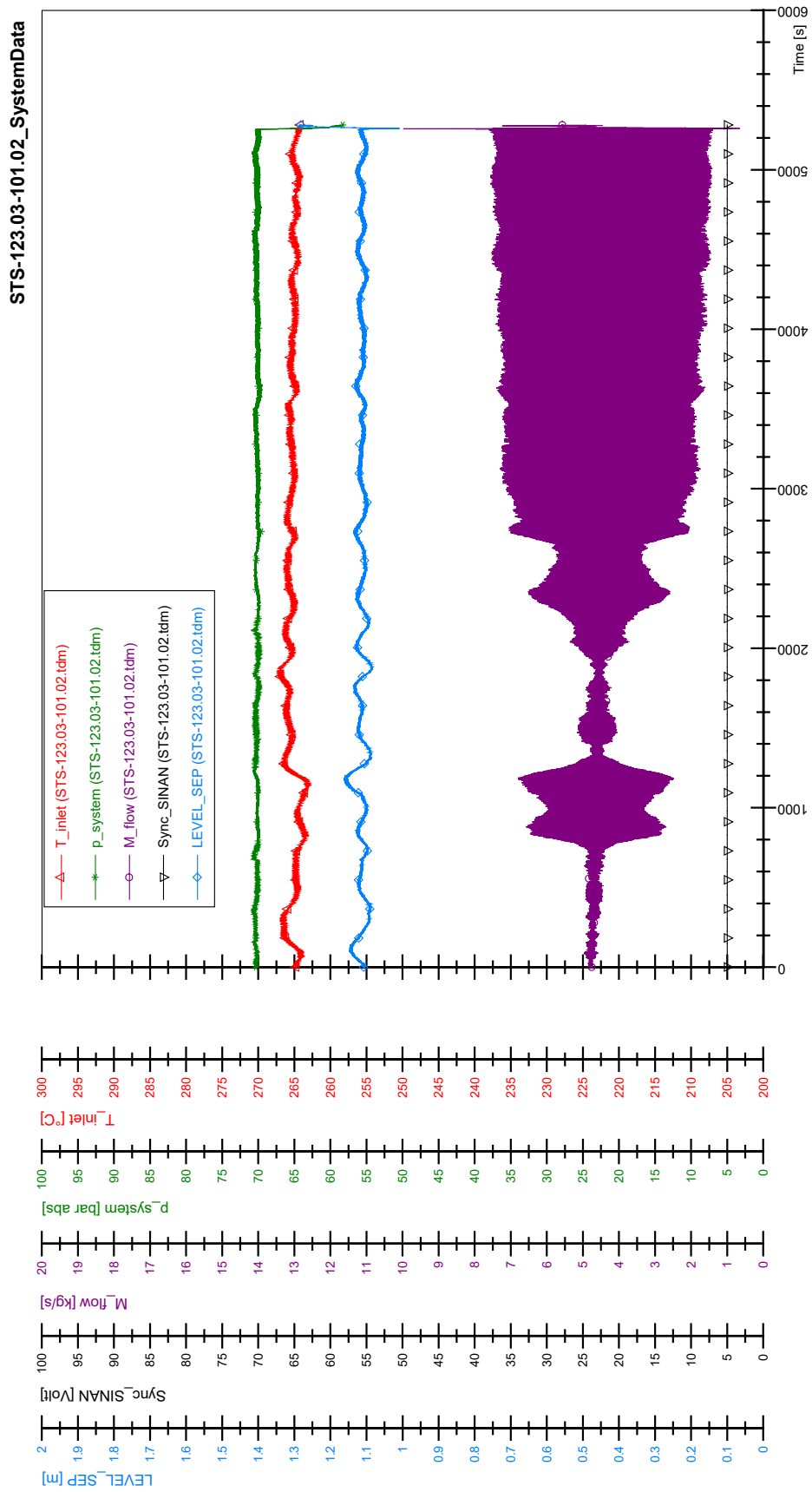
STS-123.03-A01.02_Rod_88



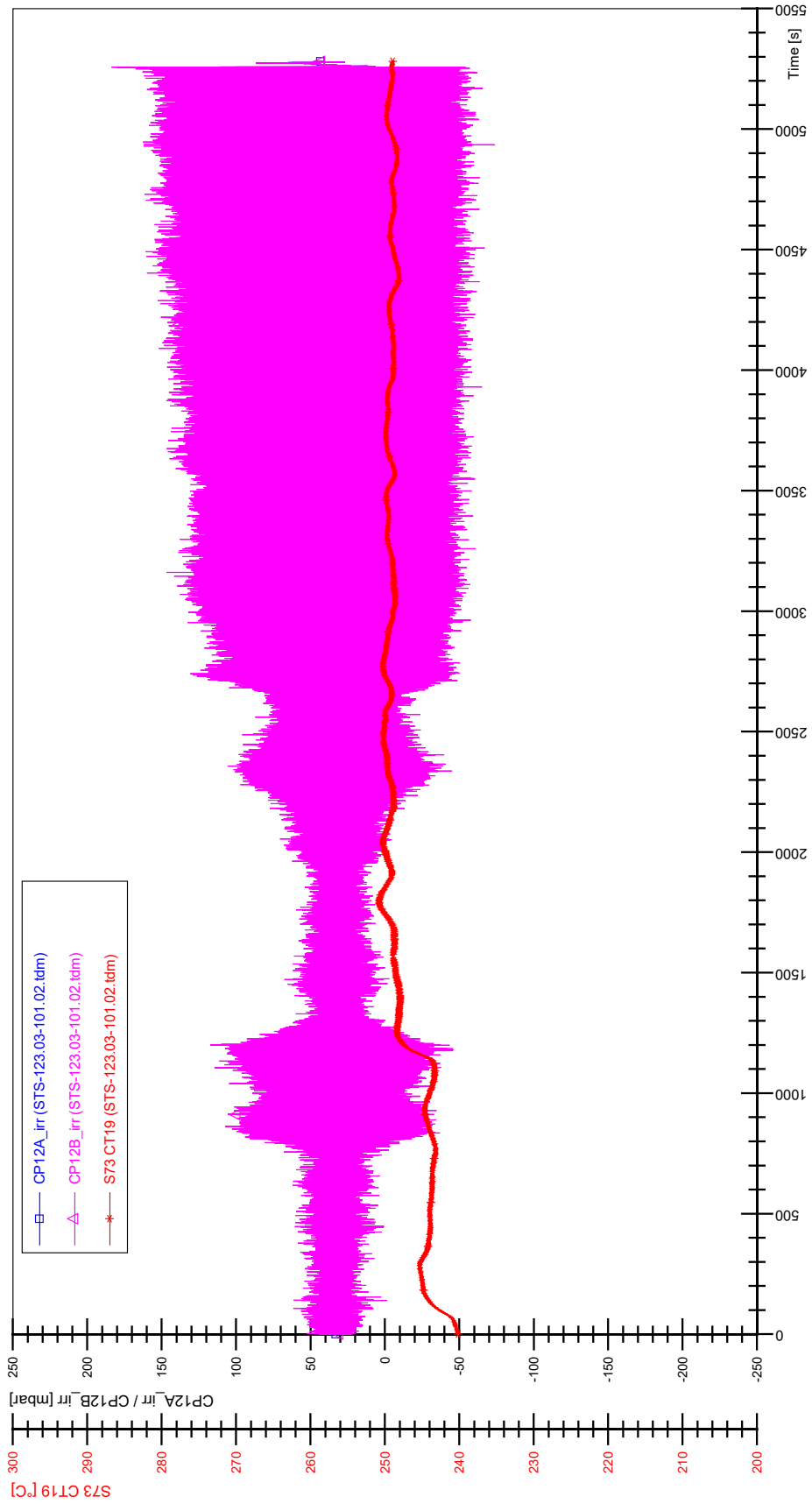
SIN-123.03-A01.02



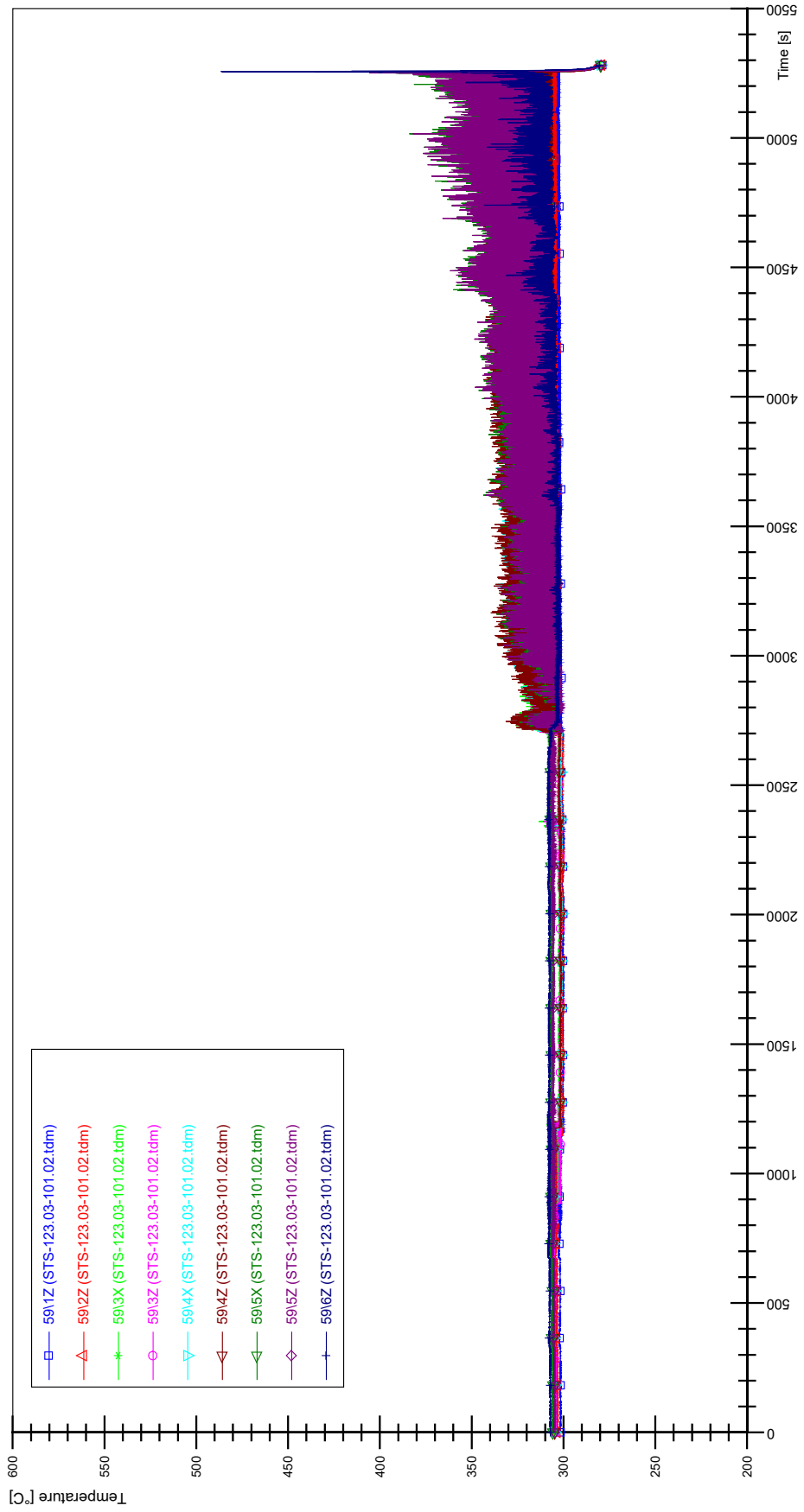
APPENDIX III PLOTS OF INSTABILITY TEST STS-123.03-101.02



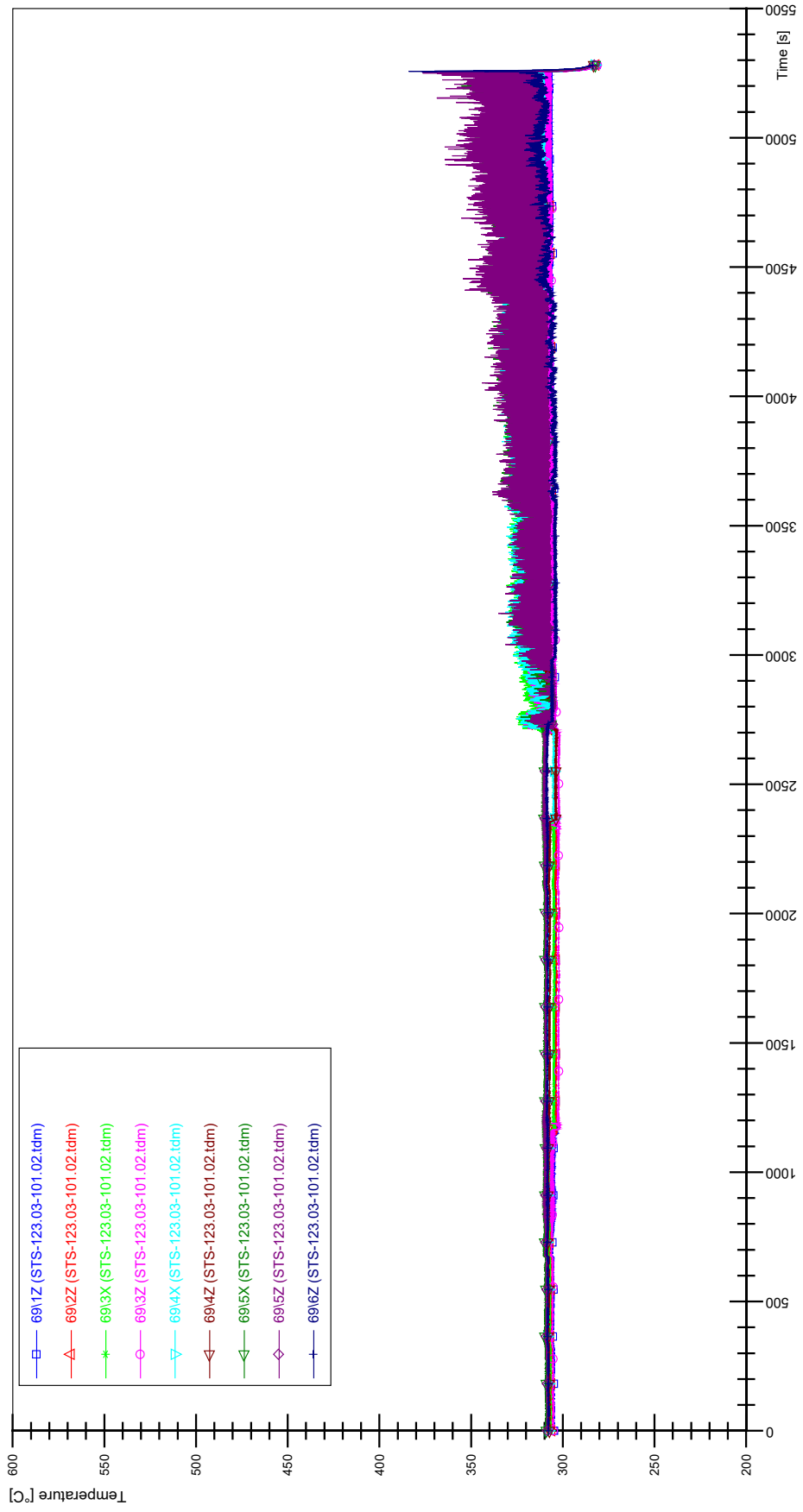
STS-123.03-101.02_CP12_CT19



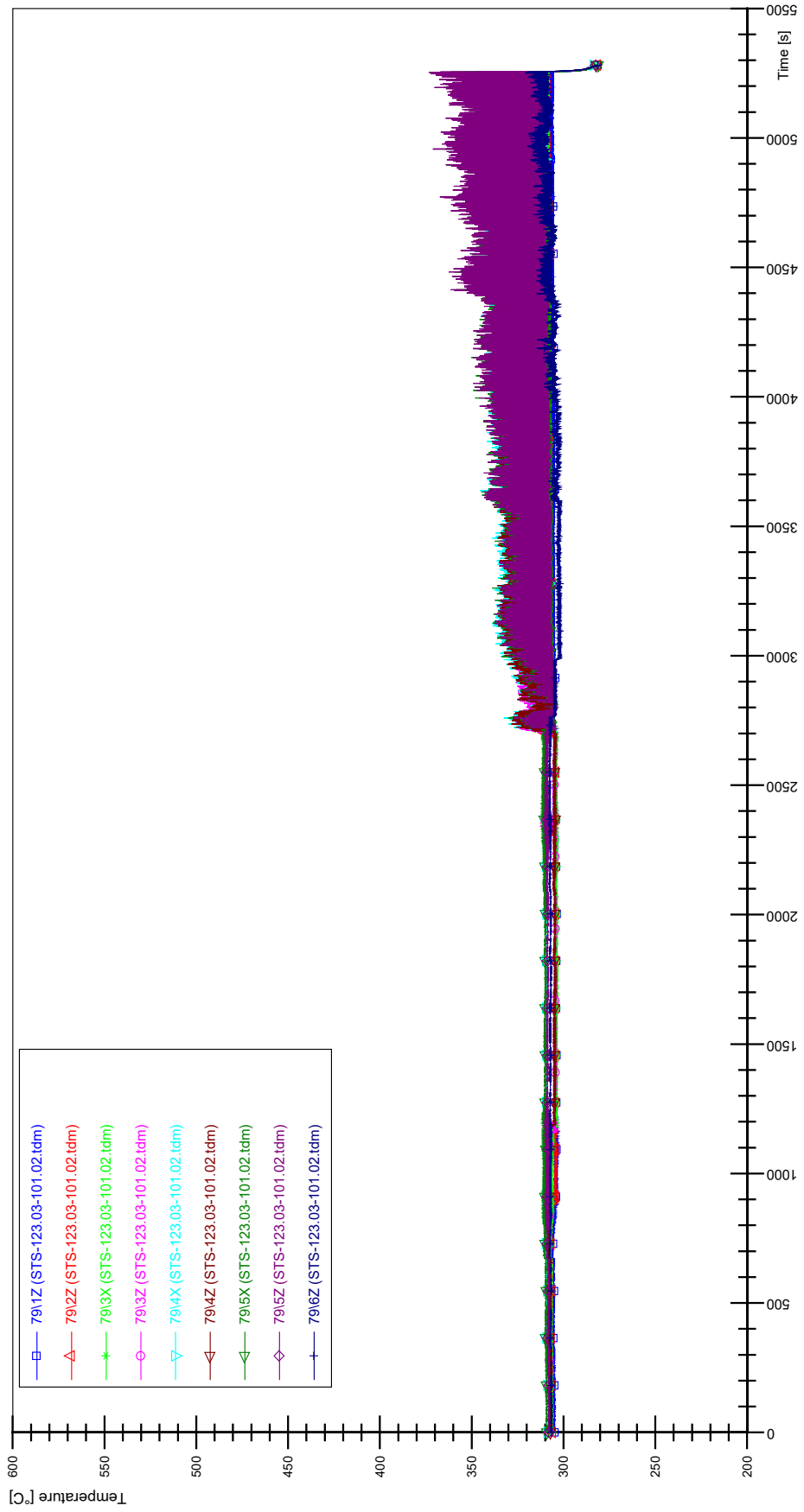
STS-123.03-101.02_Rod_59



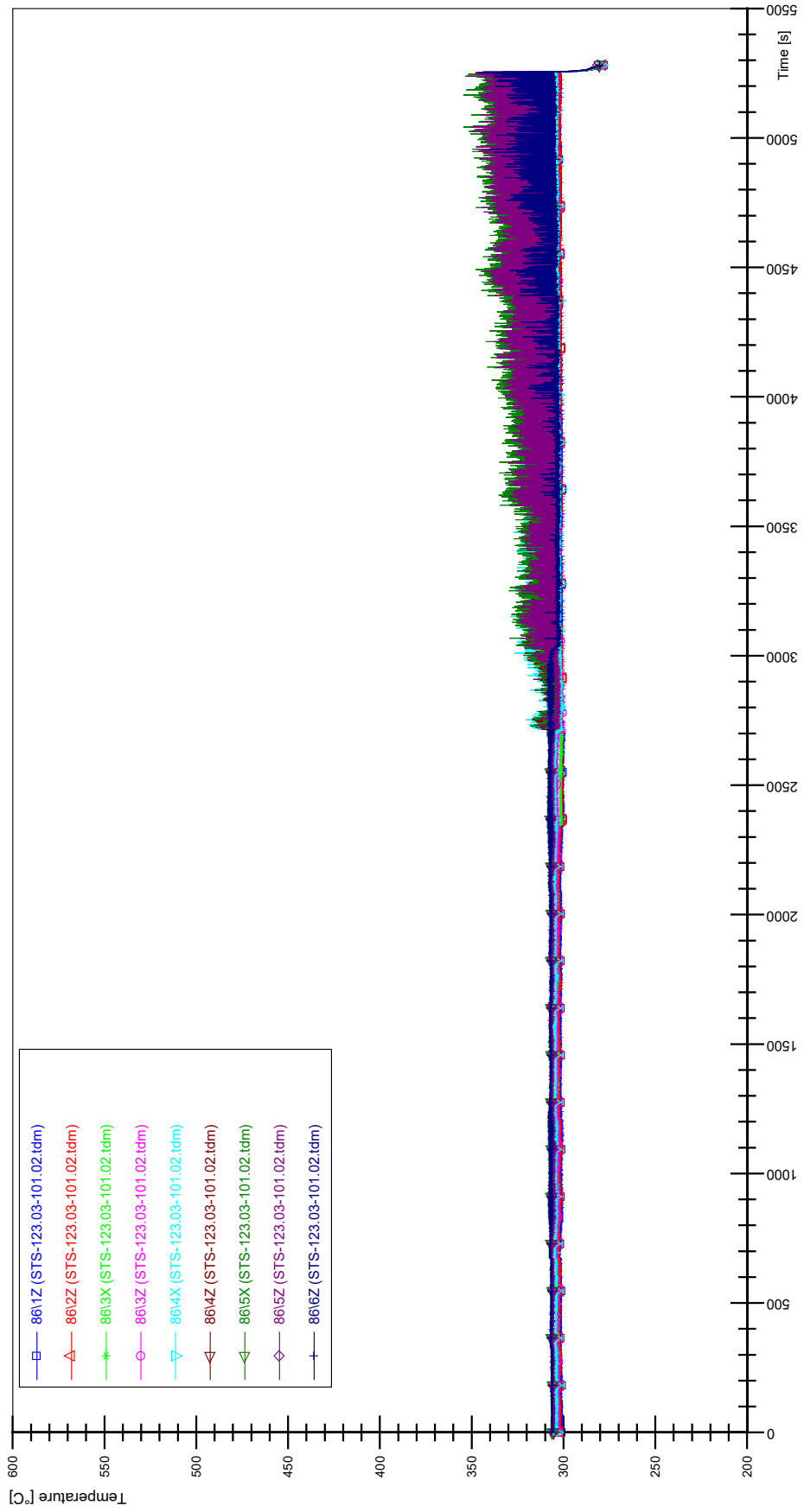
STS-123.03-101.02_Rod_69



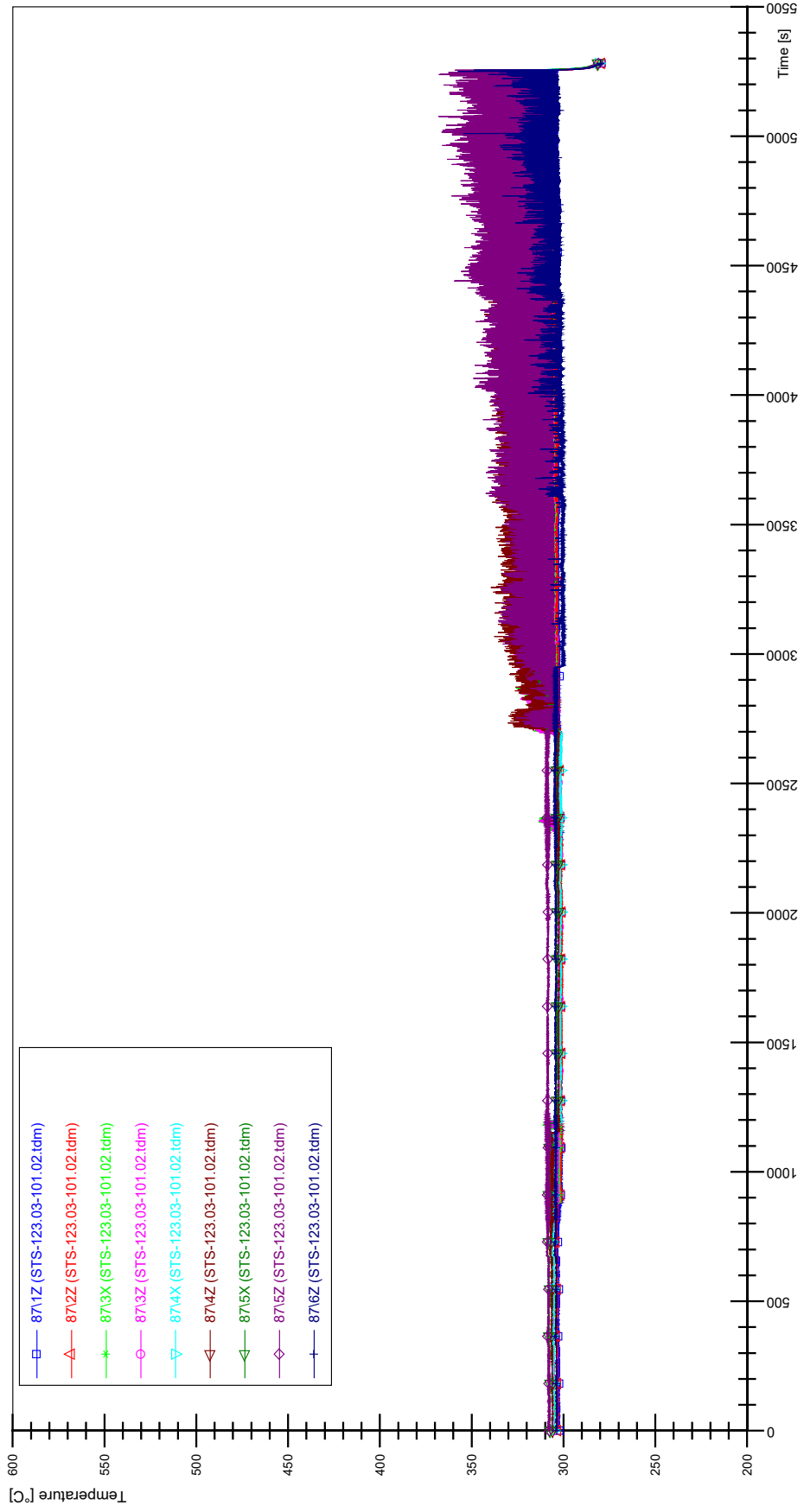
STS-123.03-101.02_Rod_79



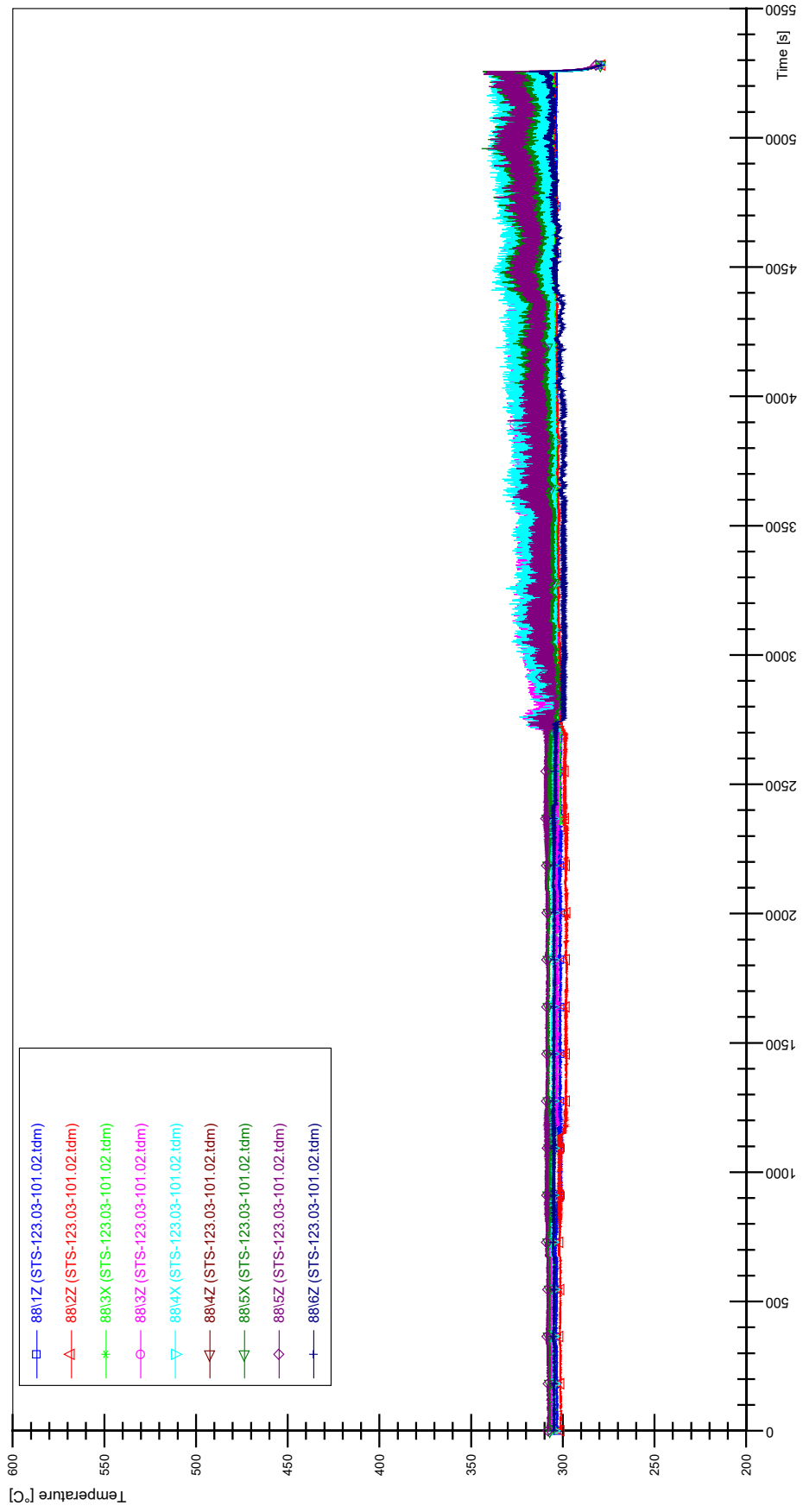
STS-123.03-101.02_Rod_86



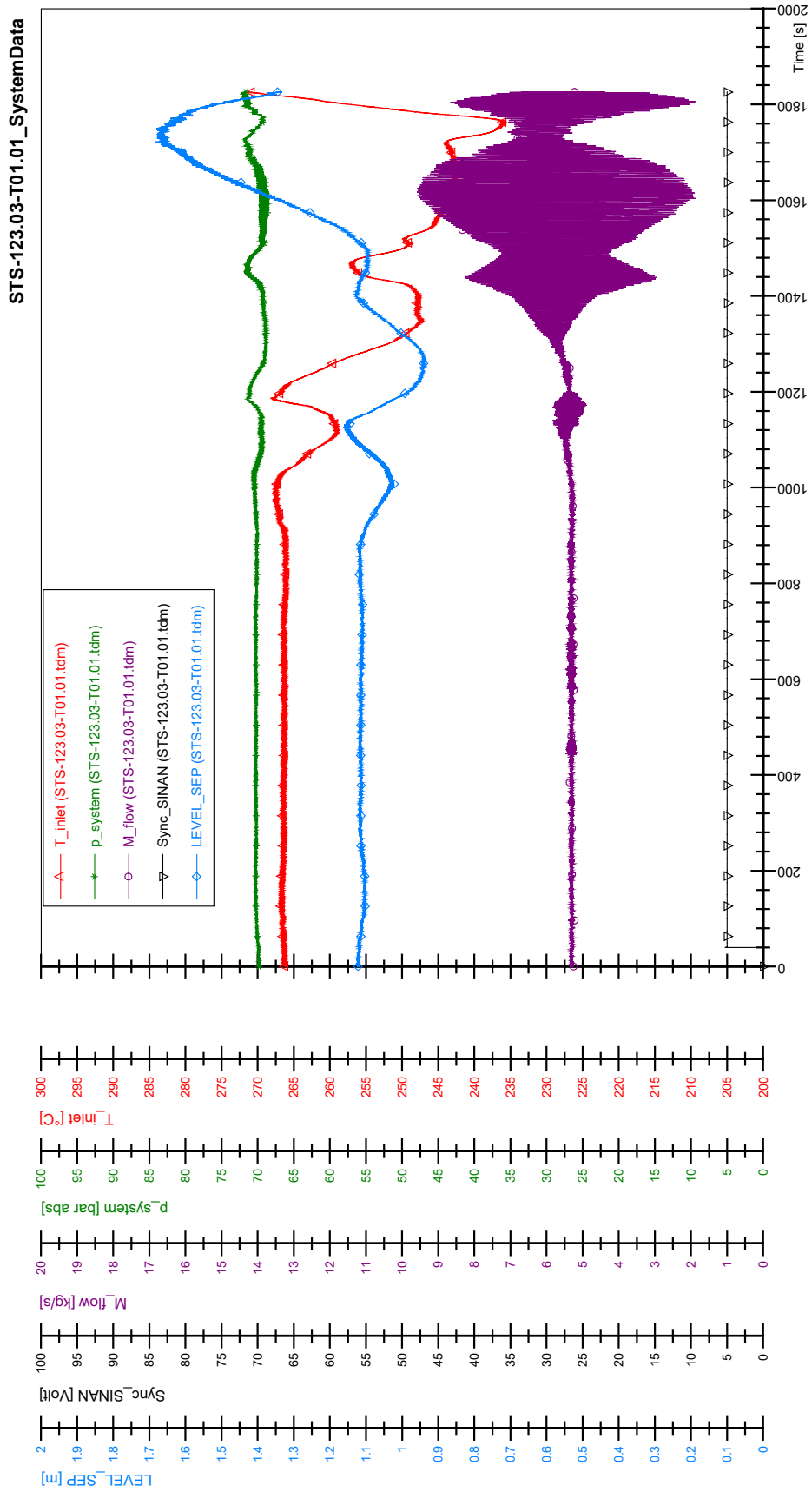
STS-123.03-101.02_Rod_87



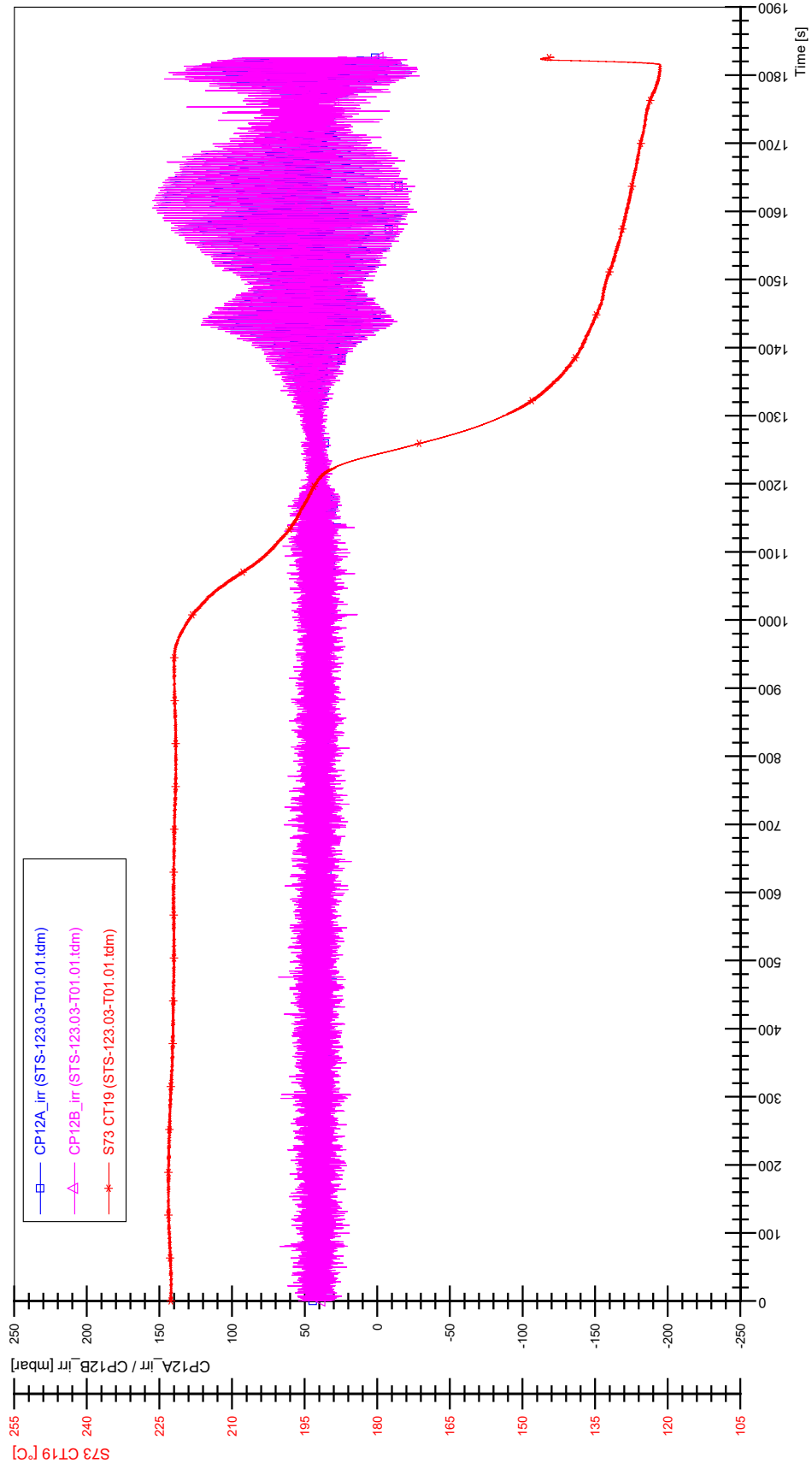
STS-123.03-101.02_Rod_88



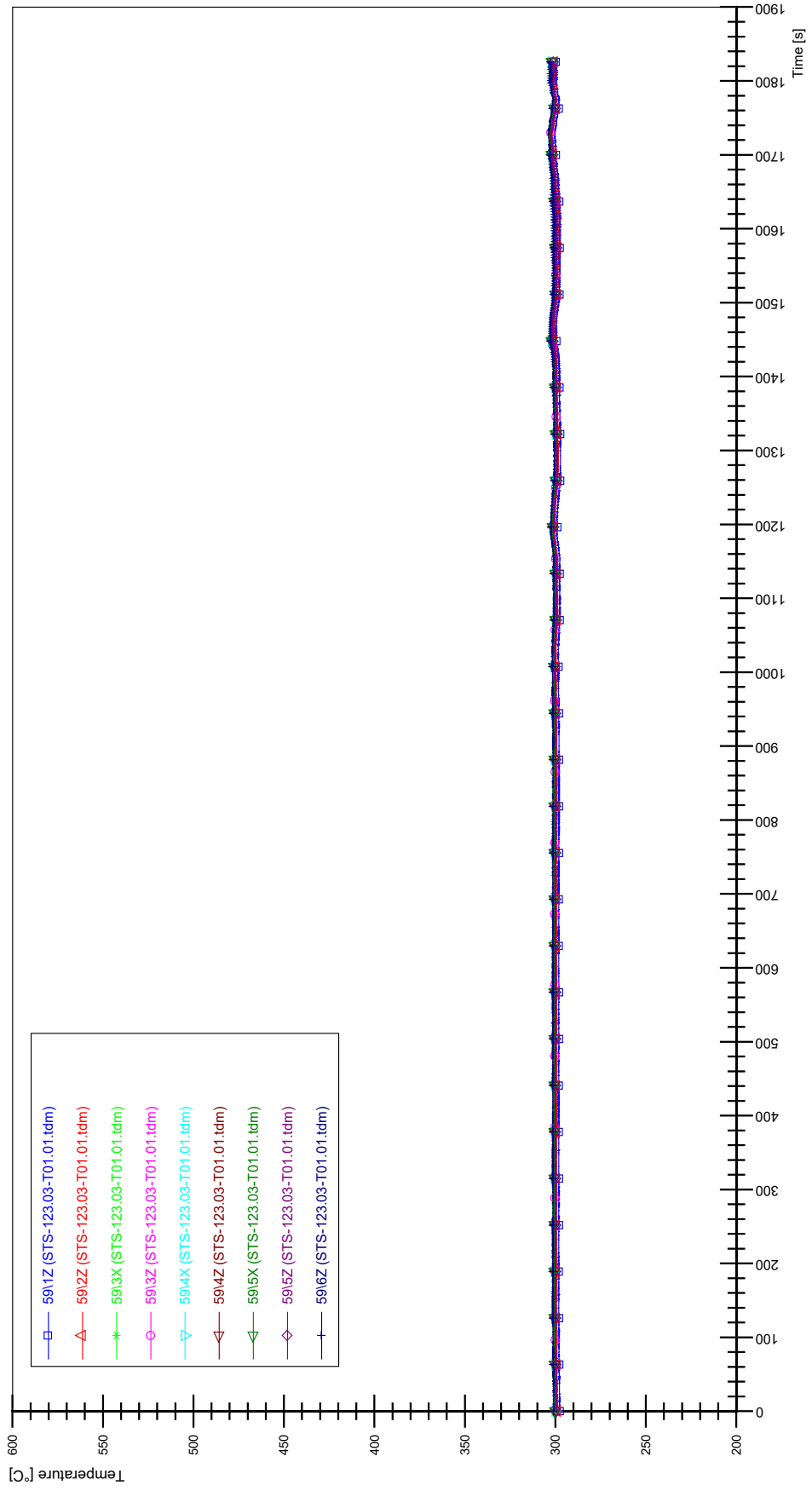
APPENDIX JJJ PLOTS OF INSTABILITY TEST STS-123.03-T01.01



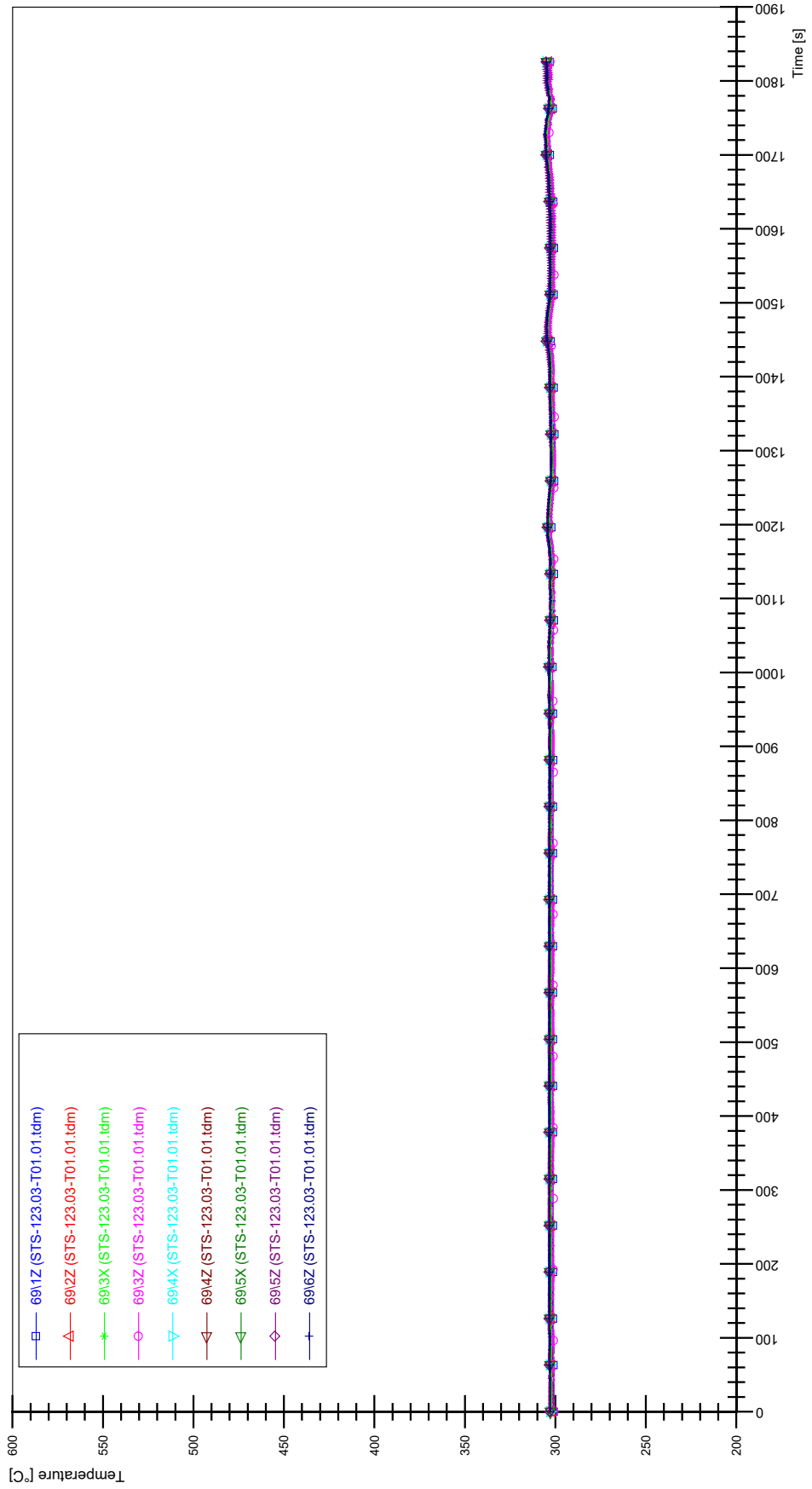
STS-123.03-T01.01_CP12_CT19



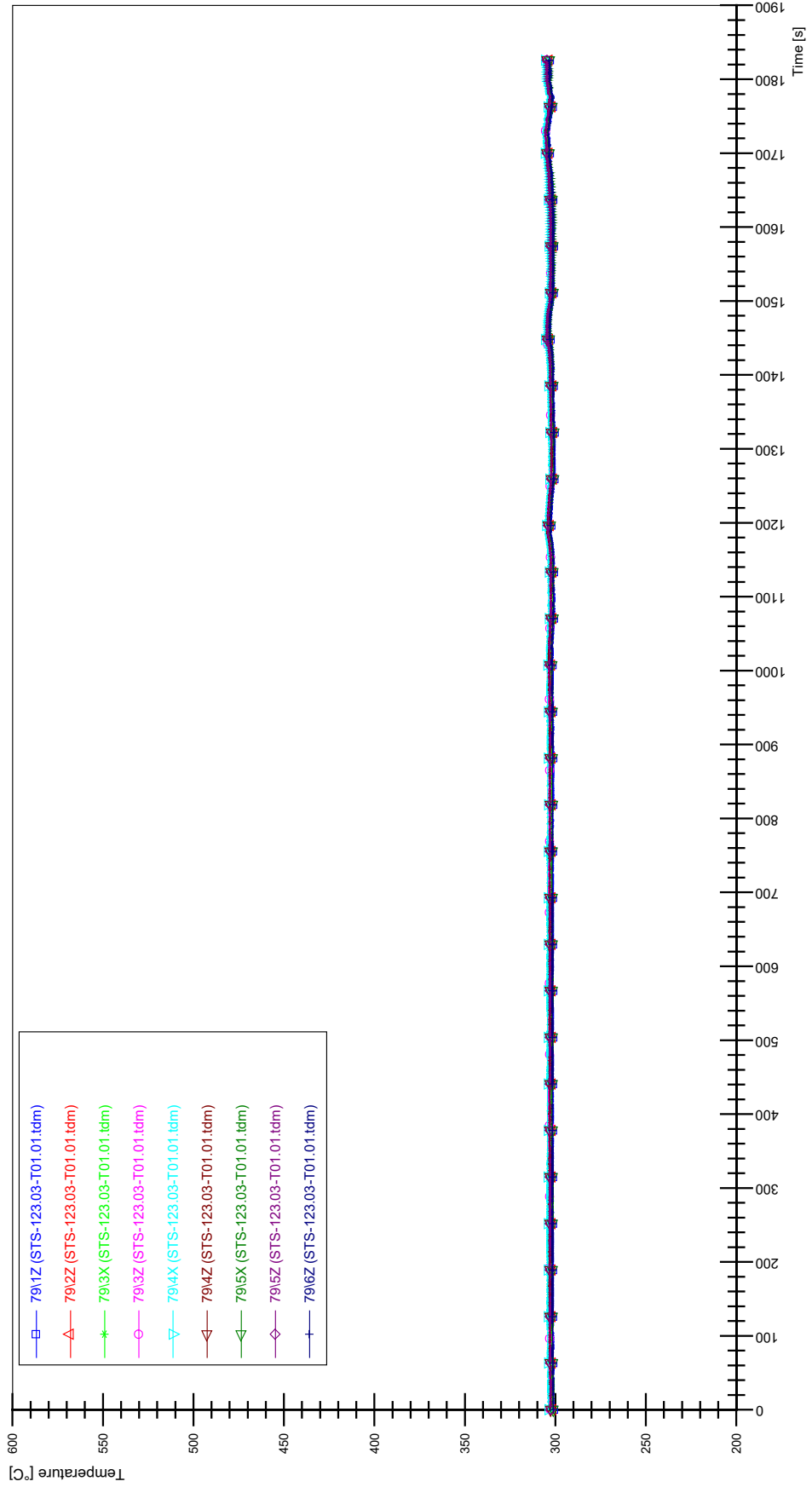
STS-123.03-T01.01_Rod_59



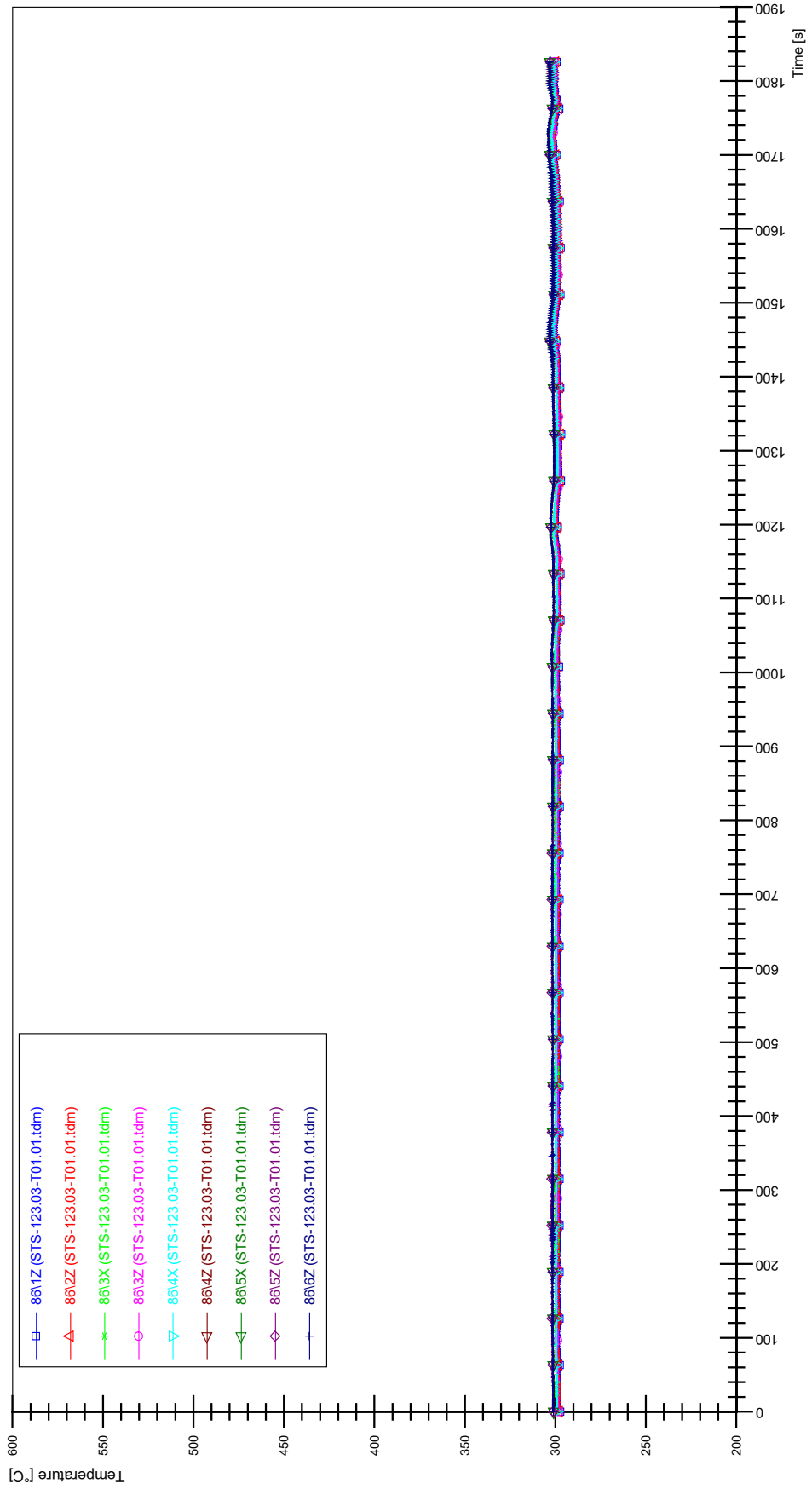
STS-123.03-T01.01_Rod_69



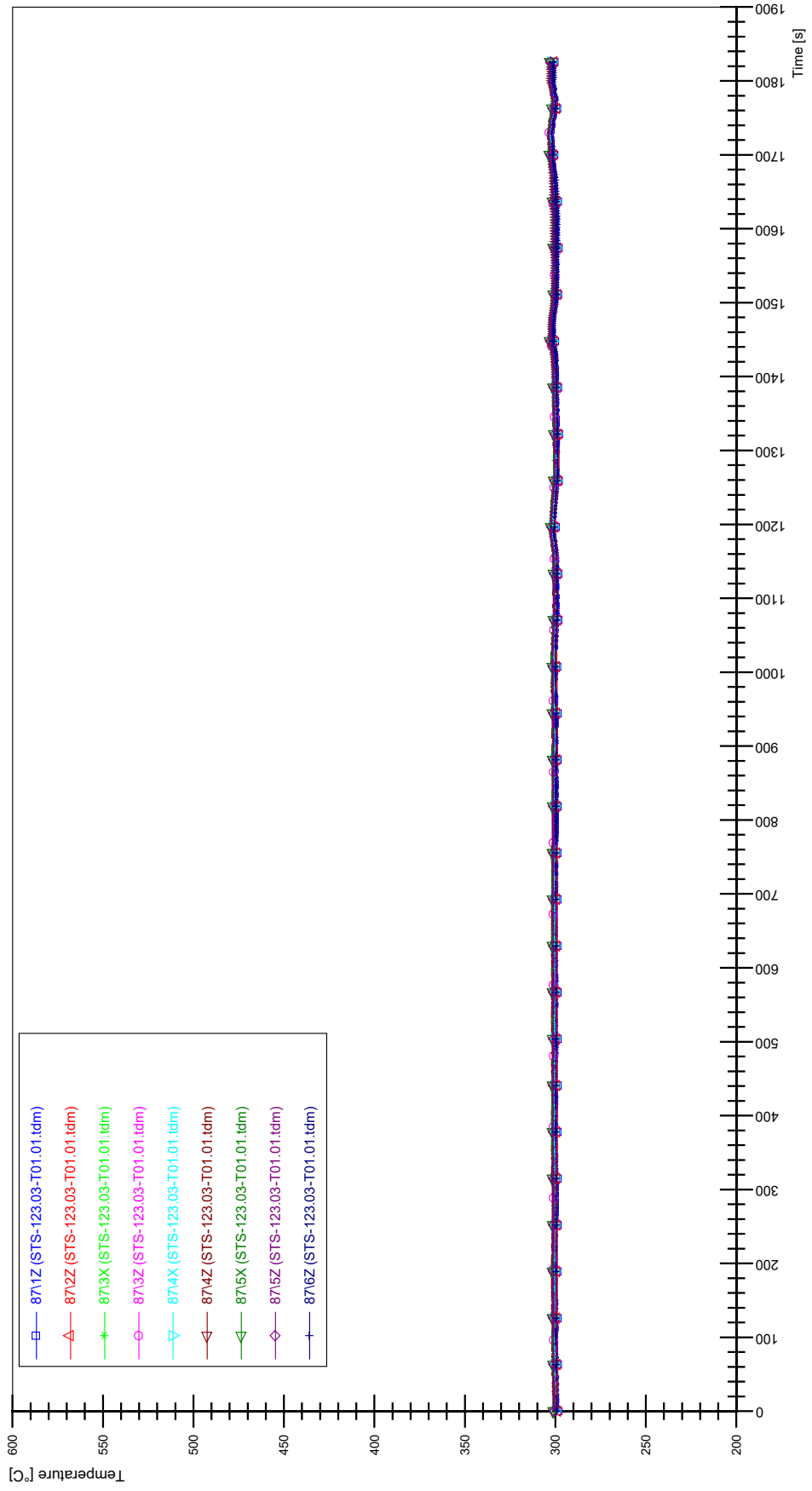
STS-123.03-T01.01_Rod_79



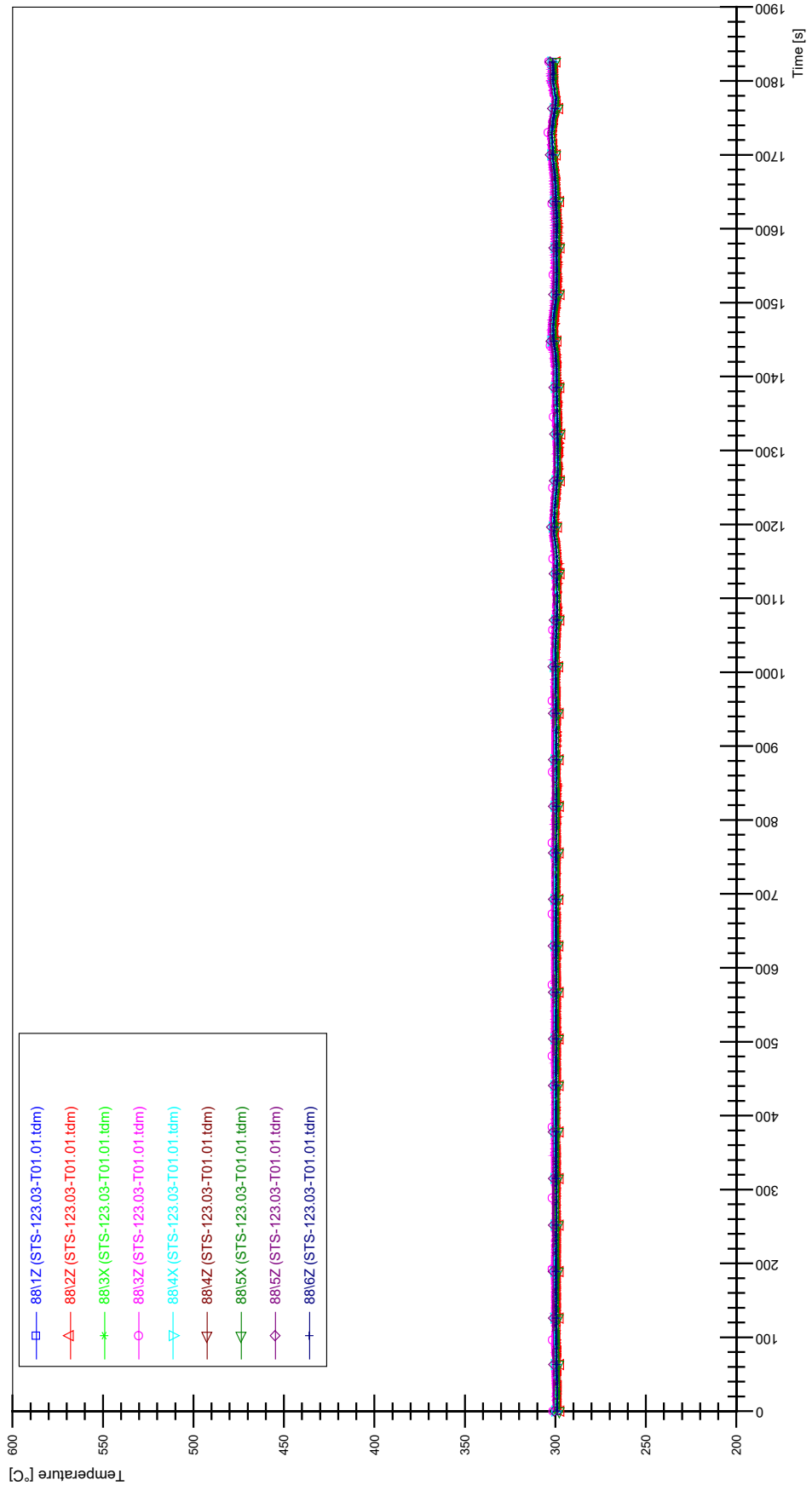
STS-123.03-T01.01_Rod_86



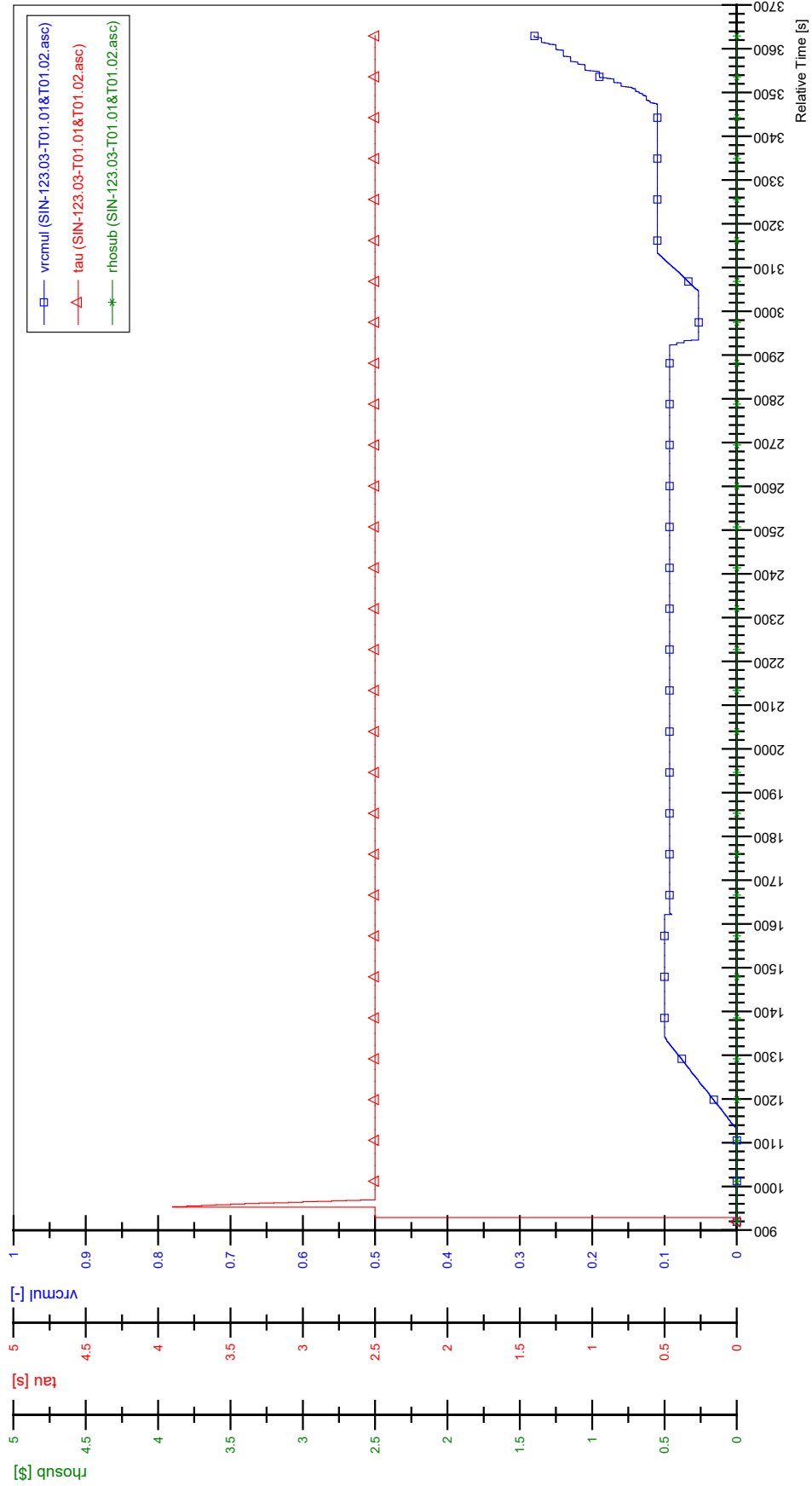
STS-123.03-T01.01_Rod_87



STS-123.03-T01.01_Rod_88

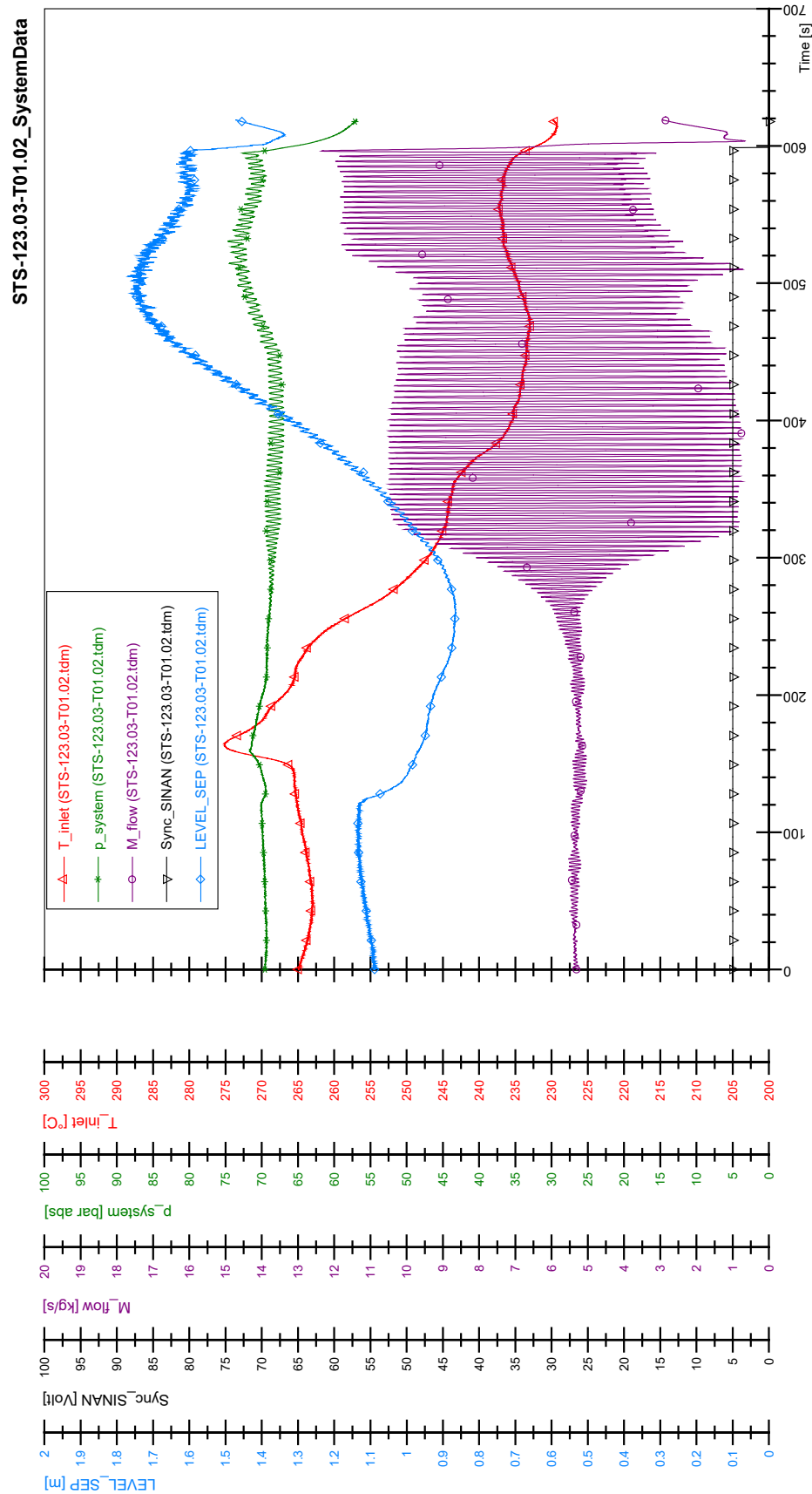


SIN-123.03-T01.01&T01.02

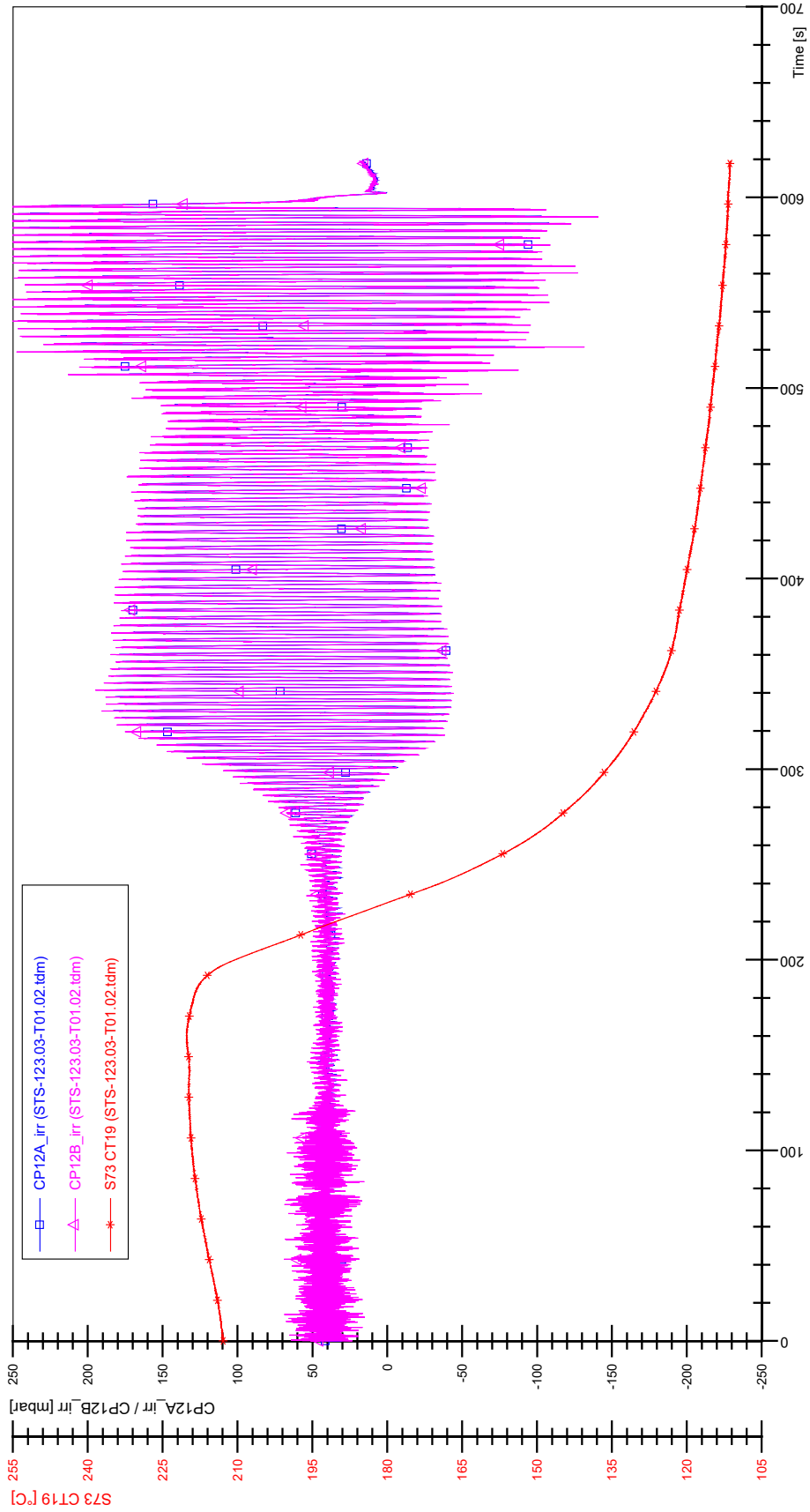


Remark:
 The file SIN-123.03-T01.01 includes the parameters (Vrcmul, Rhesub, Tau) versus time also for the test SIN-123.03-T01.02. The reason is that the data acquisition was running consecutively without interruption for both tests. Therefore, the left side displays for SIN-123.03-T01.01 and the right side displays for SIN-123.03-T01.2.

APPENDIX KKK PLOTS OF INSTABILITY TEST STS-123.03-T01.02

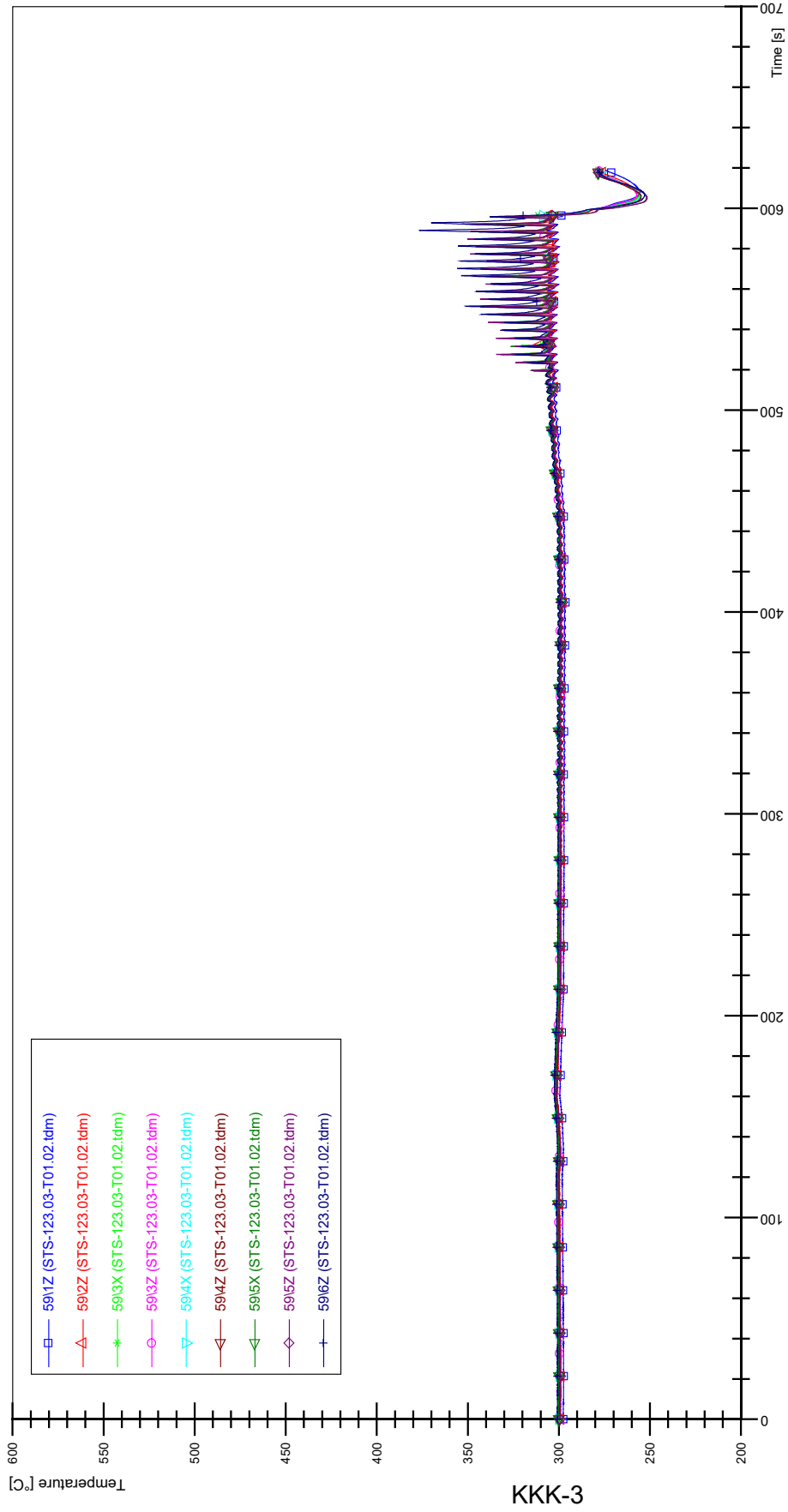


STS-123.03-T01.02_CP12_CT19

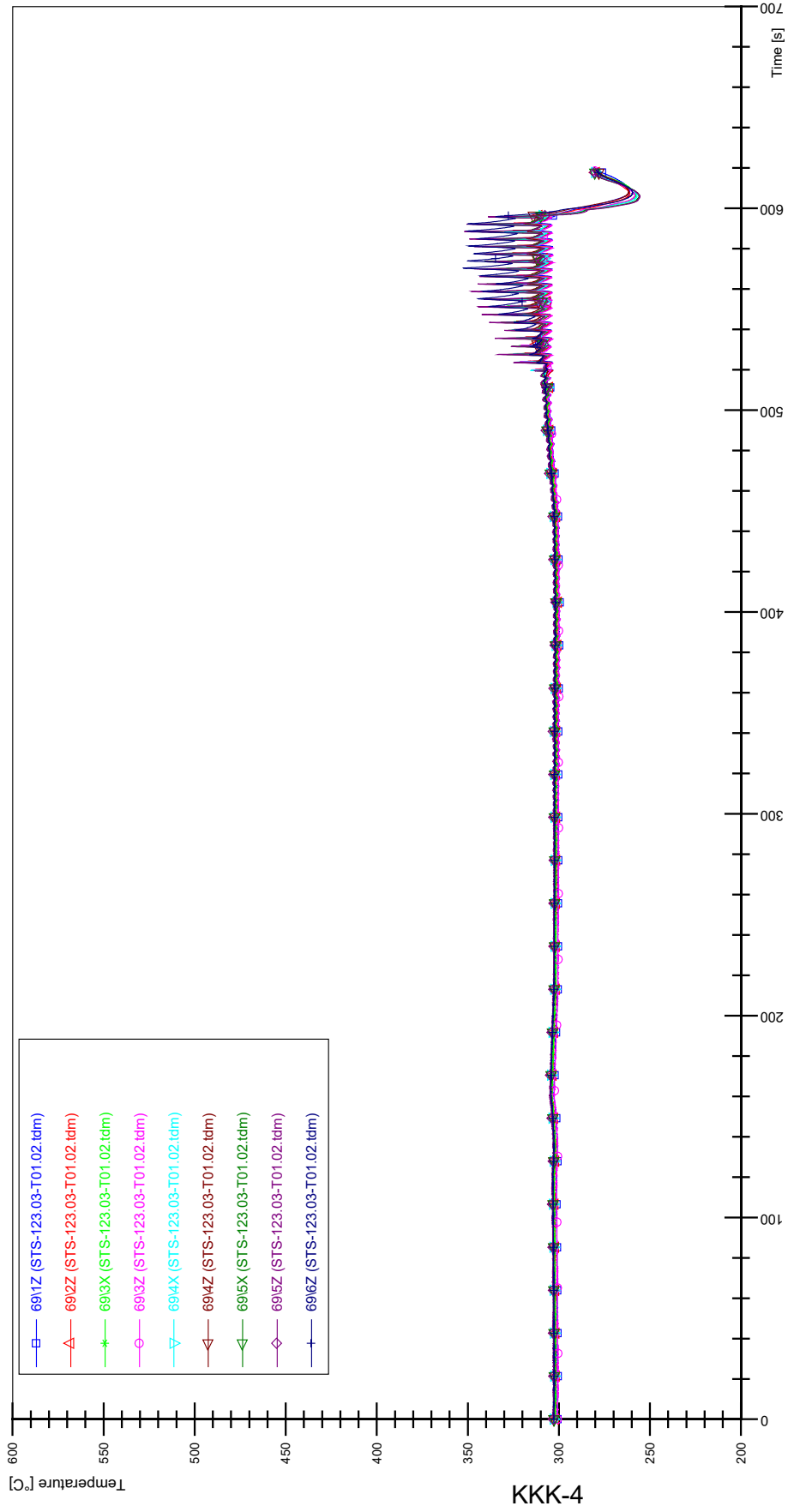


KKK-2

STS-123.03-T01.02_Rod_59

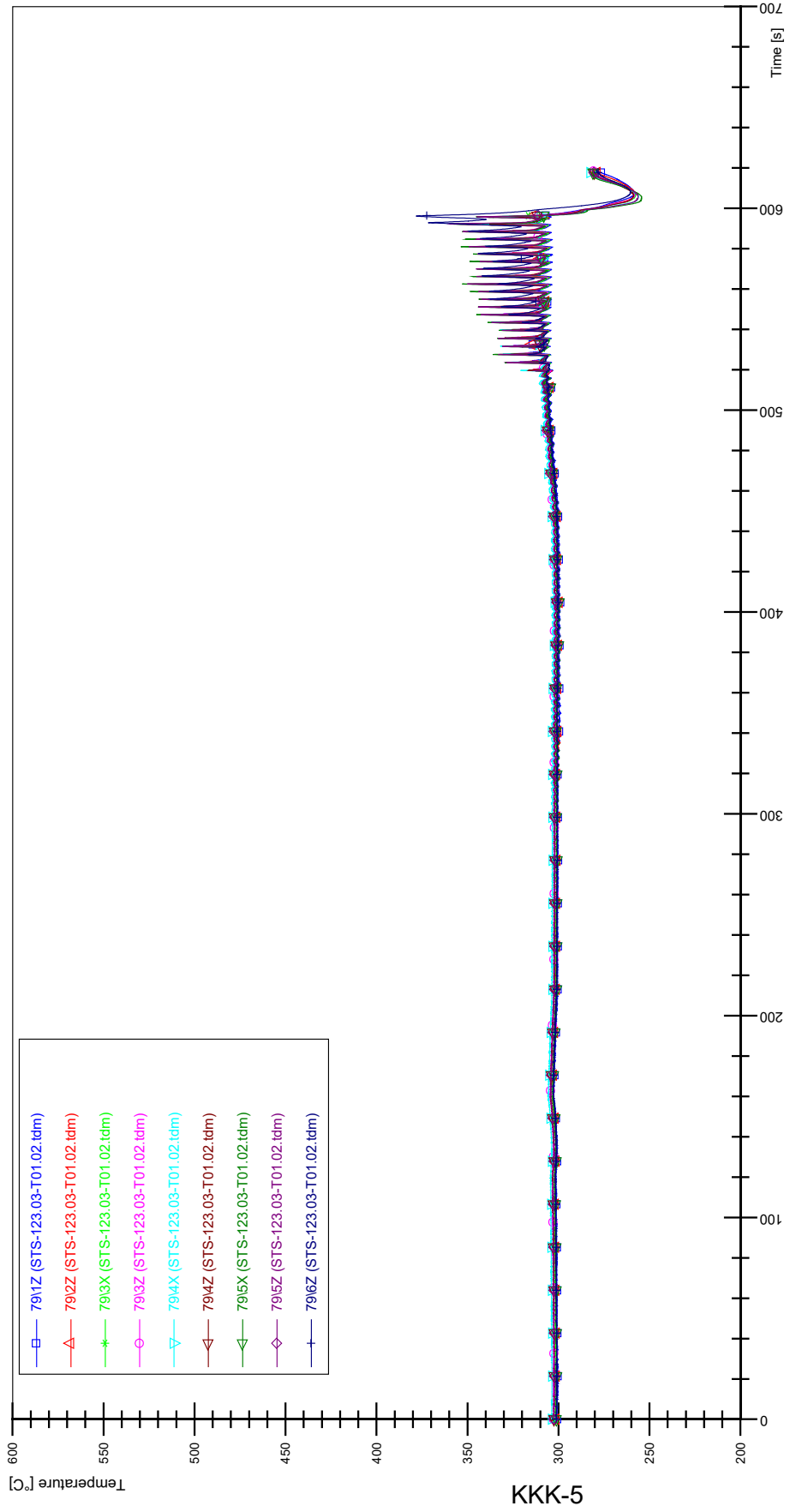


STS-123.03-T01.02_Rod_69

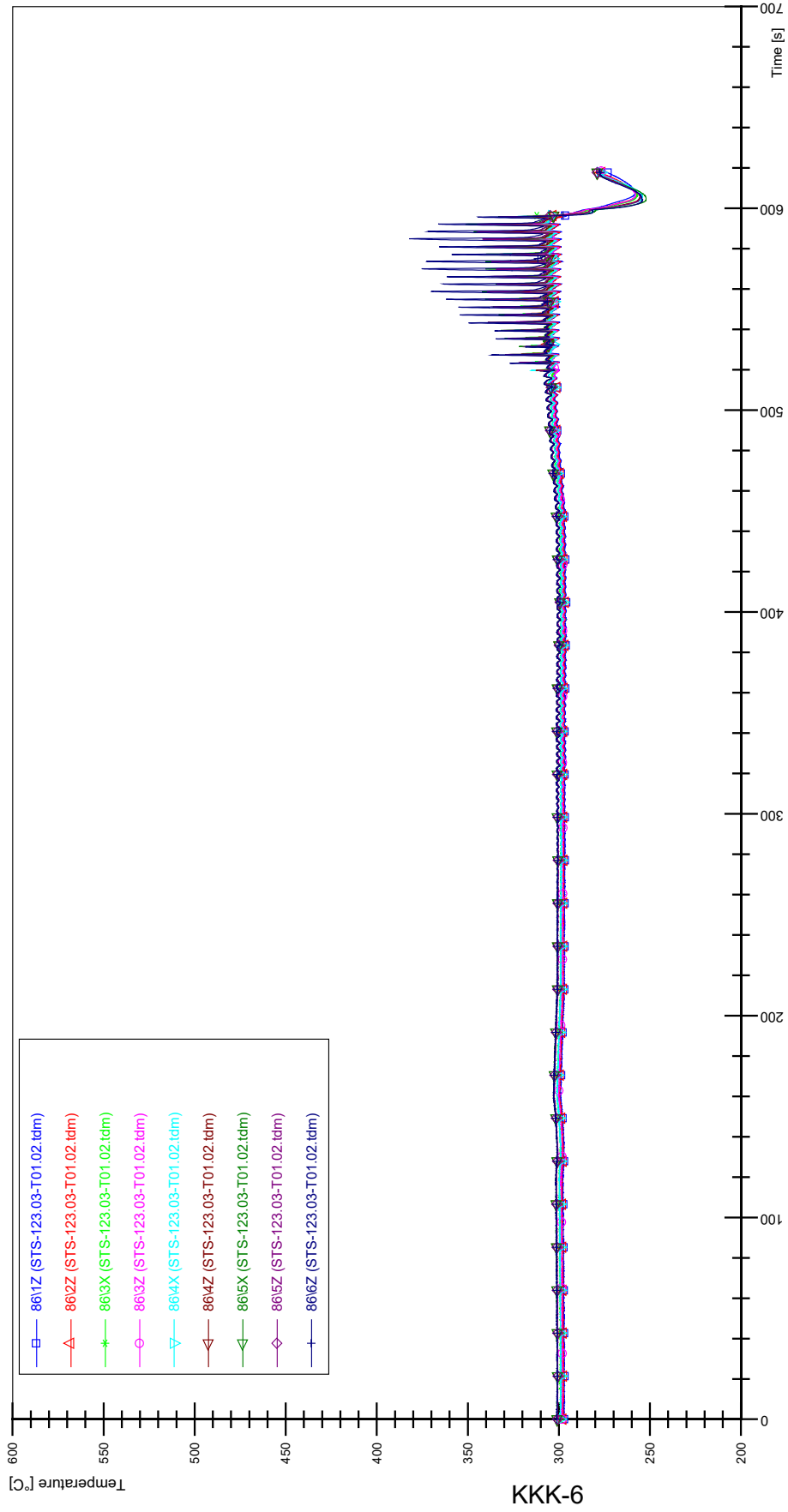


KKK-4

STS-123.03-T01.02_Rod_79

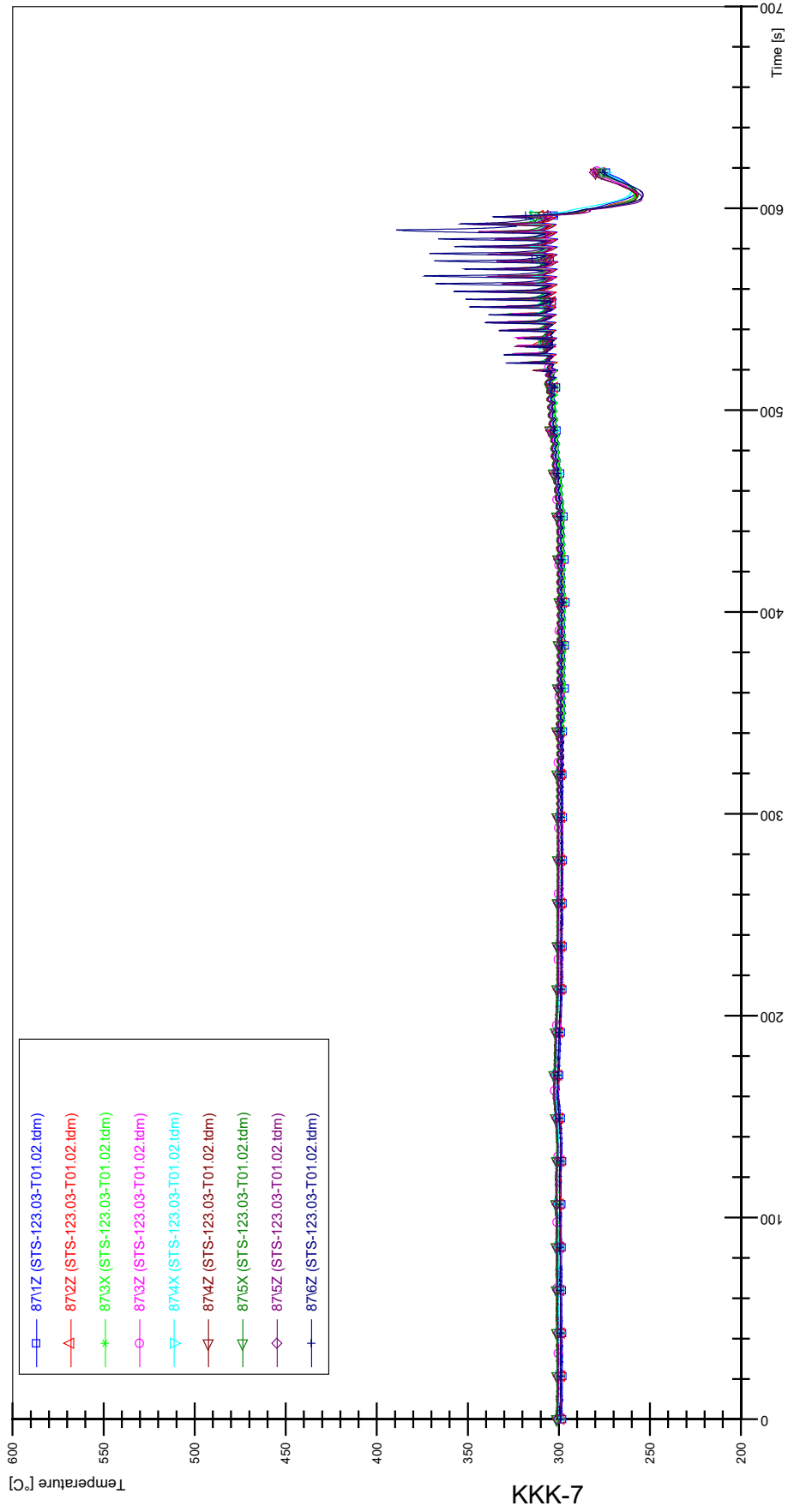


STS-123.03-T01.02_Rod_86

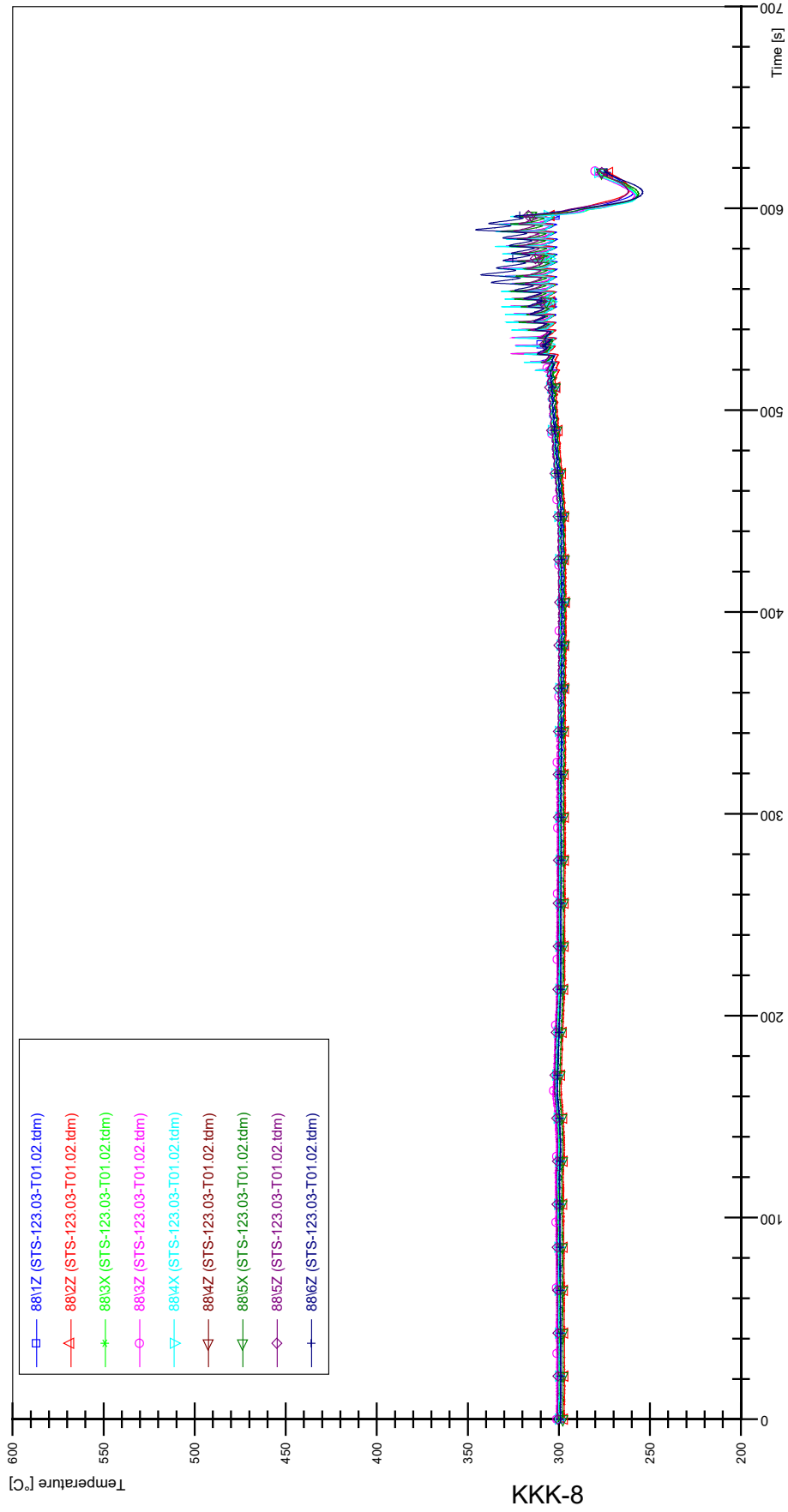


KKK-6

STS-123.03-T01.02_Rod_87

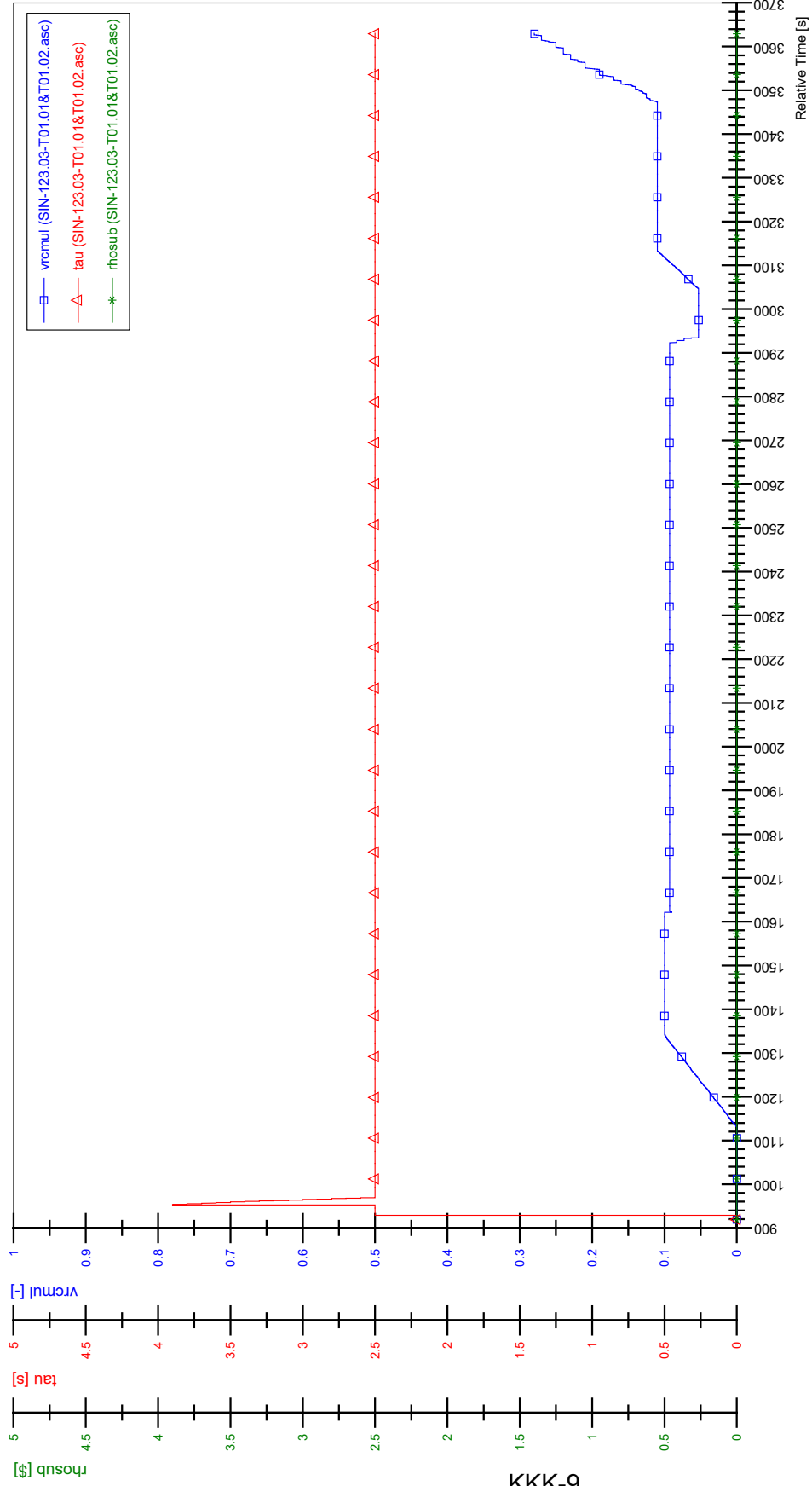


STS-123.03-T01.02_Rod_88



KKK-8

SIN-123.03-T01.01&T01.02

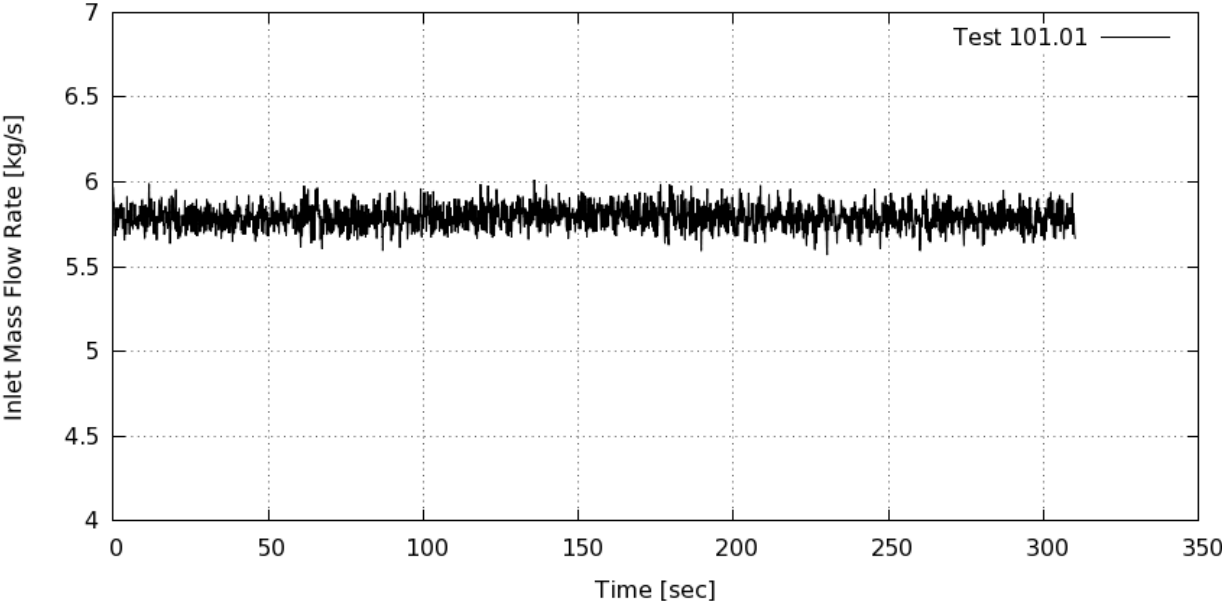


KKK-9

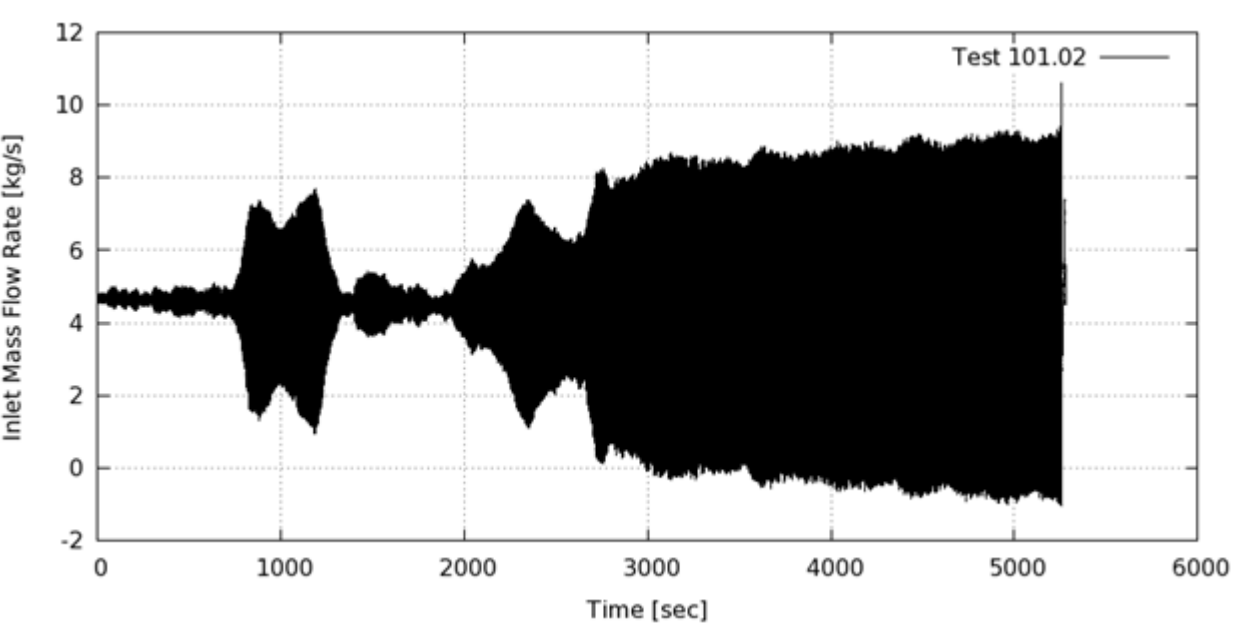
Remark:

The data set SIN-123.03-T01.01 includes the parameters (Vrcmul, Rhosub, Tau) versus time also for the test SIN-123.03-T01.02. The reason is that the data acquisition was running consecutively without interruption for both tests. Therefore, the left side displays for SIN-123.03-T01.01 and the right side displays for SIN-123.03-T01.02.

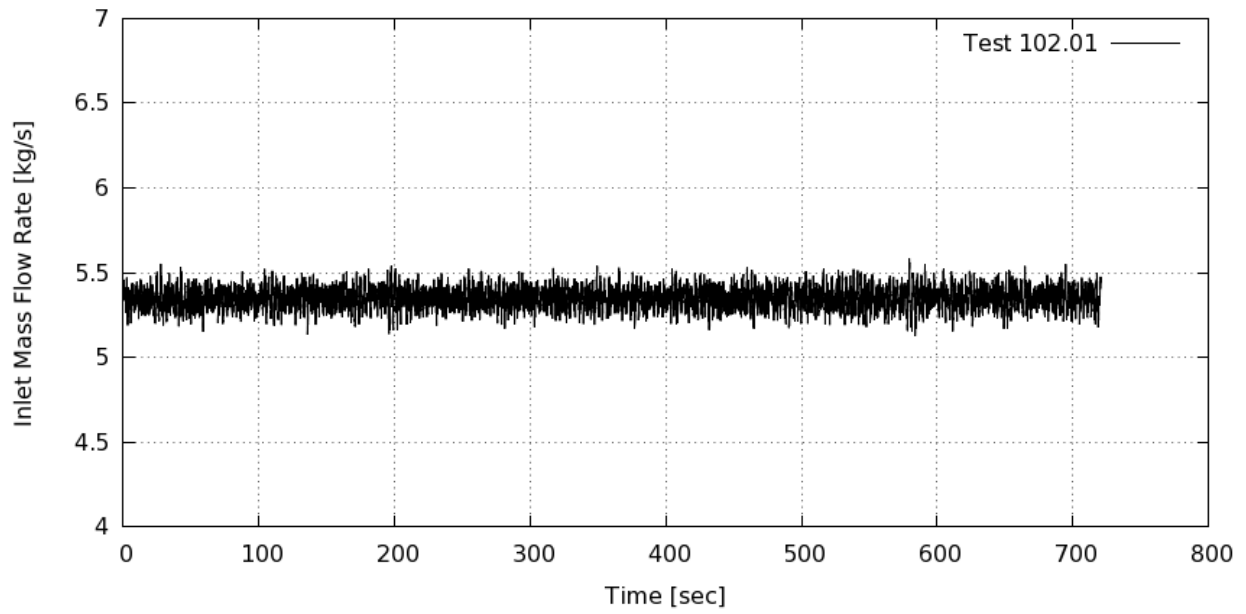
APPENDIX LLL MASS FLOW RATES FROM DP-INLET S73 CP12A



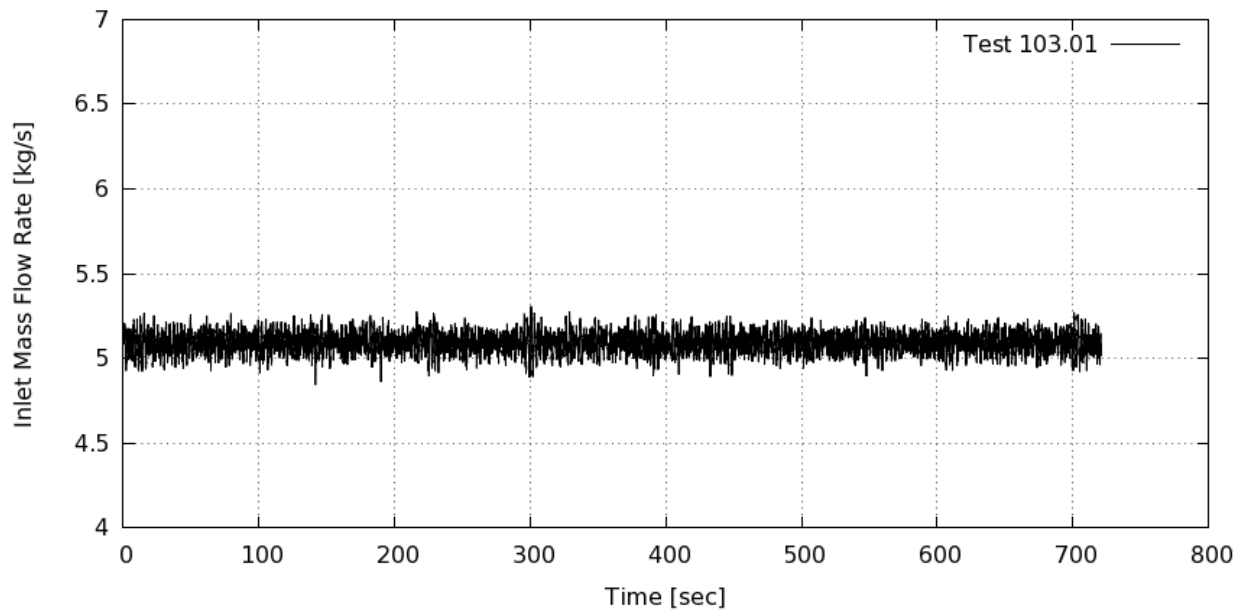
STS-123.03-101.01: Mass Flow Rate from DP-Inlet S73 CP12A



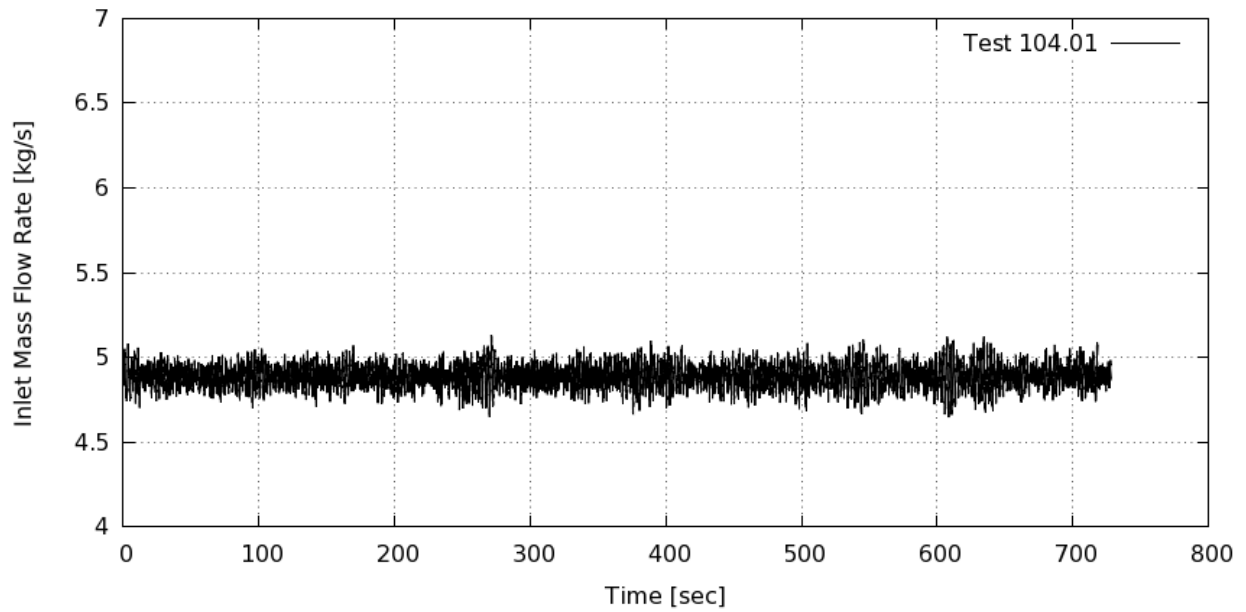
STS-123.03-101.02: Mass Flow Rate from DP-Inlet S73 CP12A



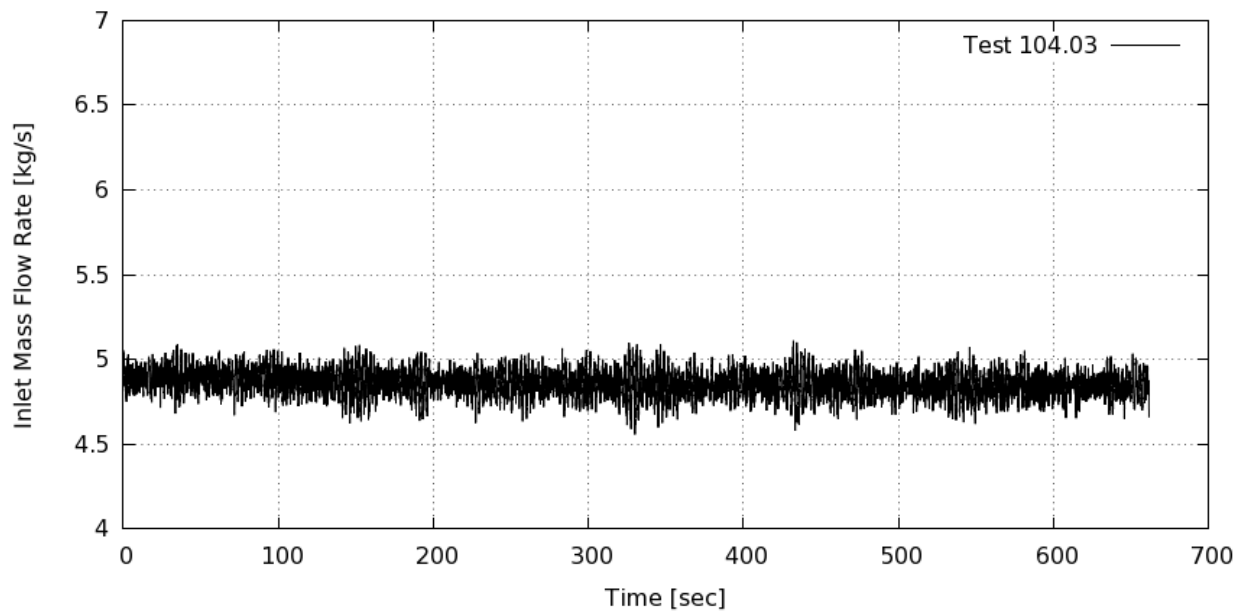
STS-123.03-102.01: Mass Flow Rate from DP-Inlet S73 CP12A



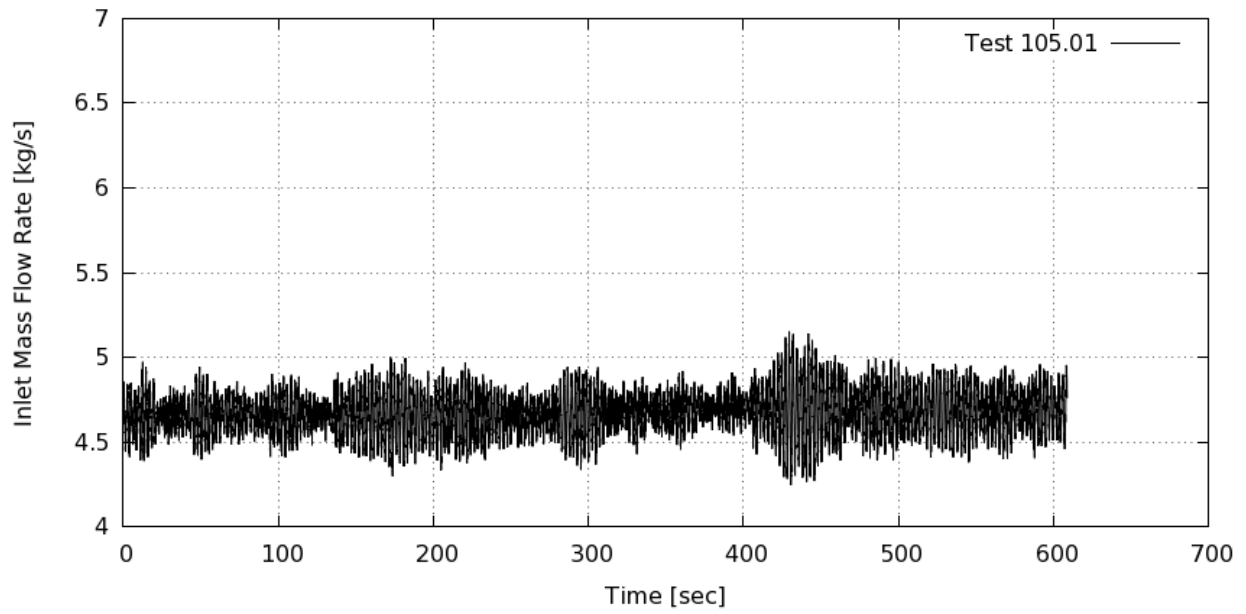
STS-123.03-103.01: Mass Flow Rate from DP-Inlet S73 CP12A



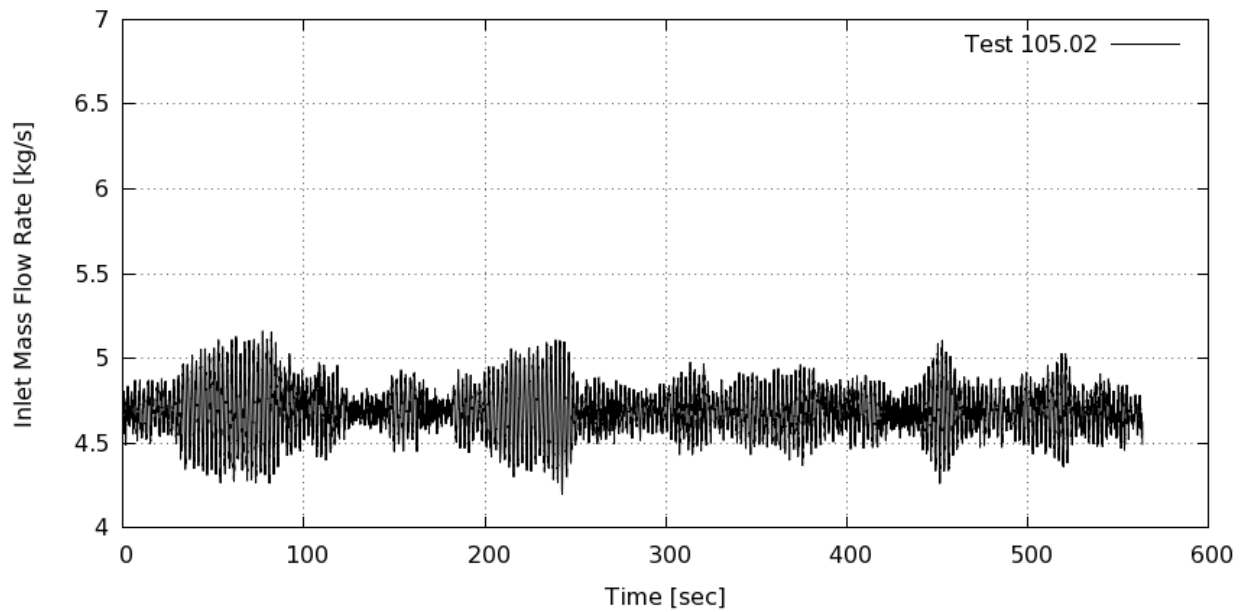
STS-123.03-104.01: Mass Flow Rate from DP-Inlet S73 CP12A



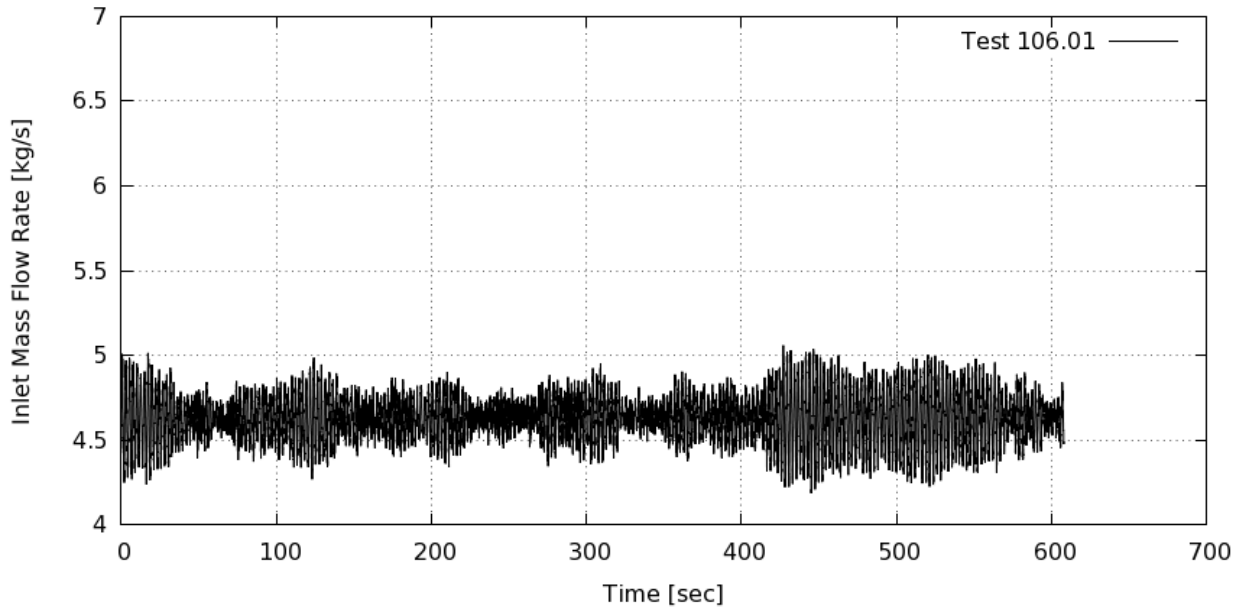
STS-123.03-104.03: Mass Flow Rate from DP-Inlet S73 CP12A



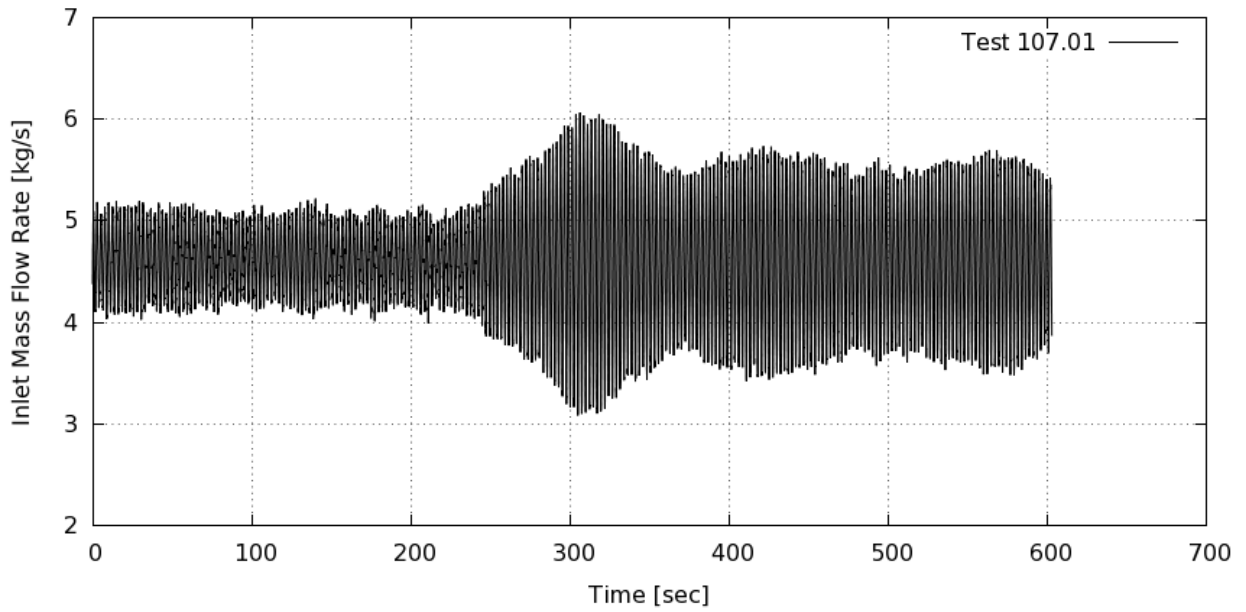
STS-123.03-105.01: Mass Flow Rate from DP-Inlet S73 CP12A



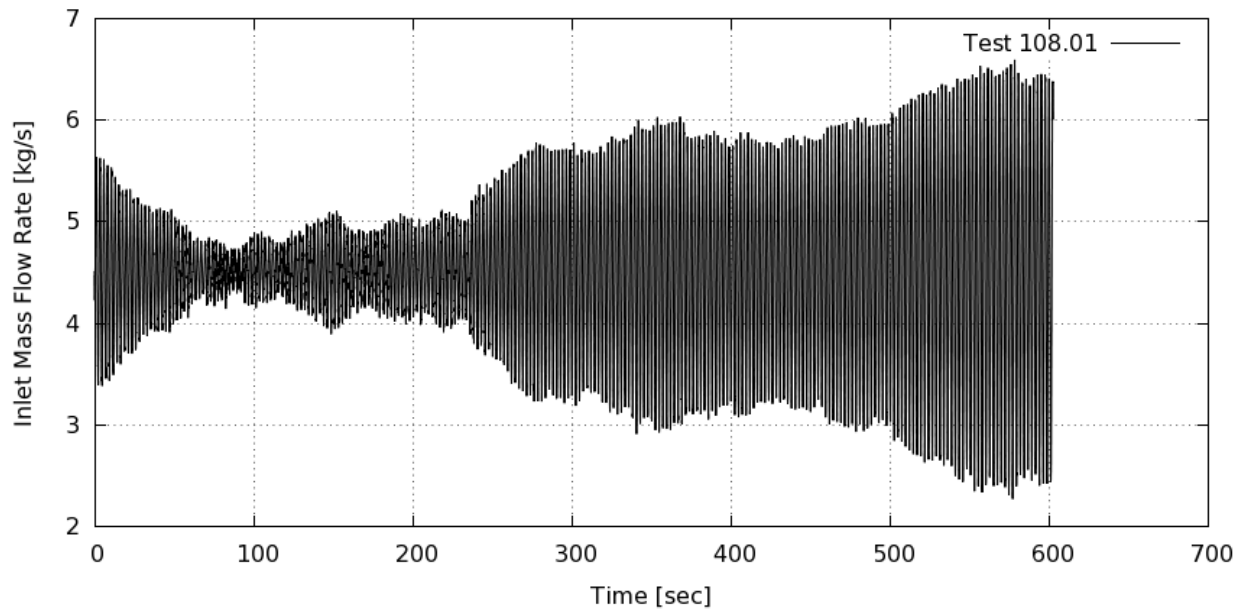
STS-123.03-105.02: Mass Flow Rate from DP-Inlet S73 CP12A



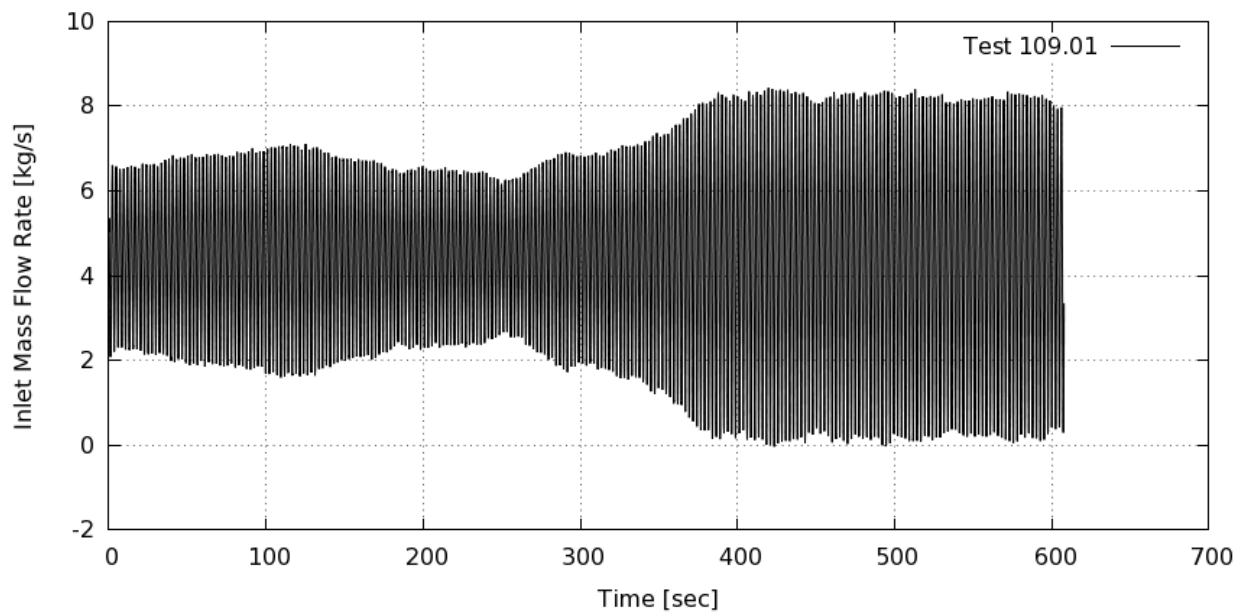
STS-123.03-106.01: Mass Flow Rate from DP-Inlet S73 CP12A



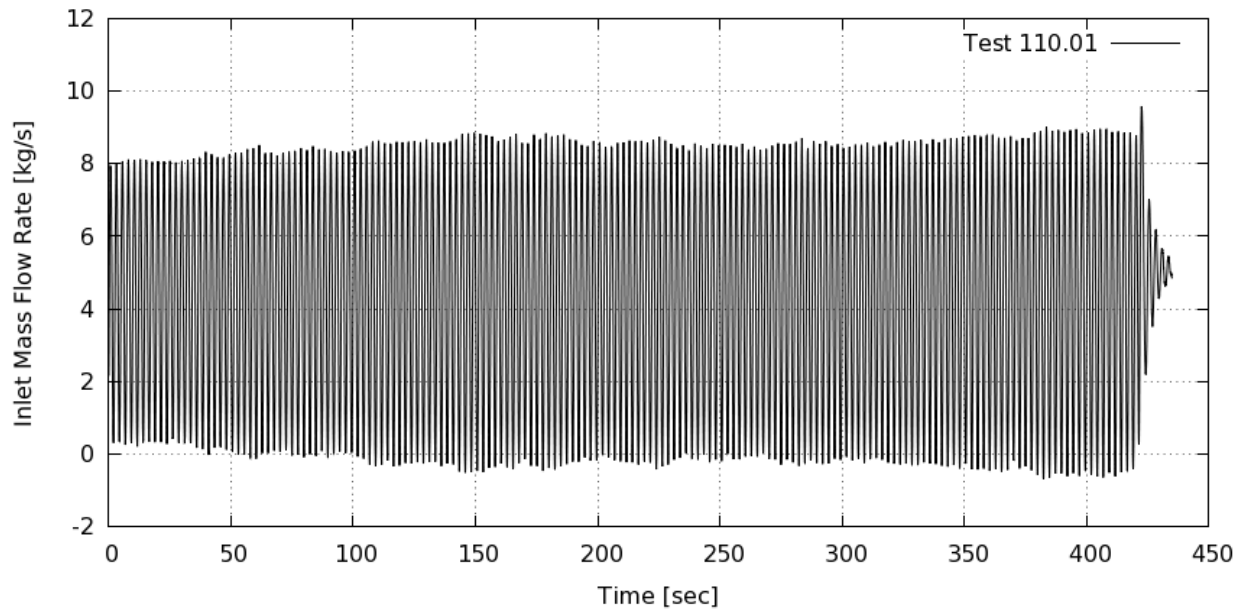
STS-123.03-107.01: Mass Flow Rate from DP-Inlet S73 CP12A



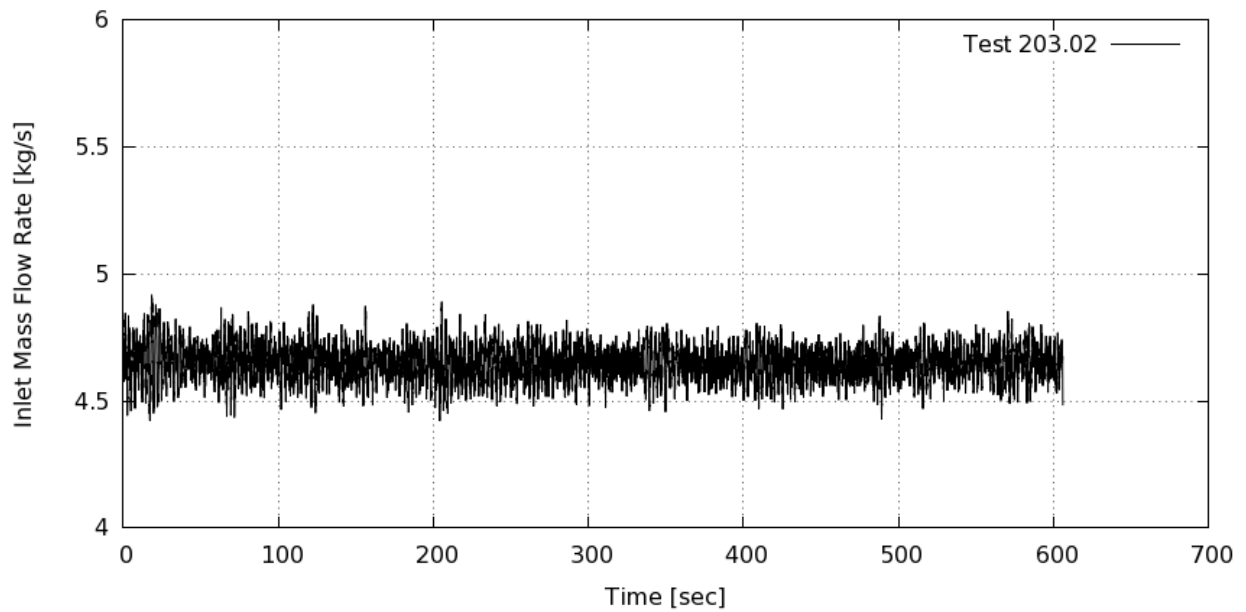
STS-123.03-108.01: Mass Flow Rate from DP-Inlet S73 CP12A



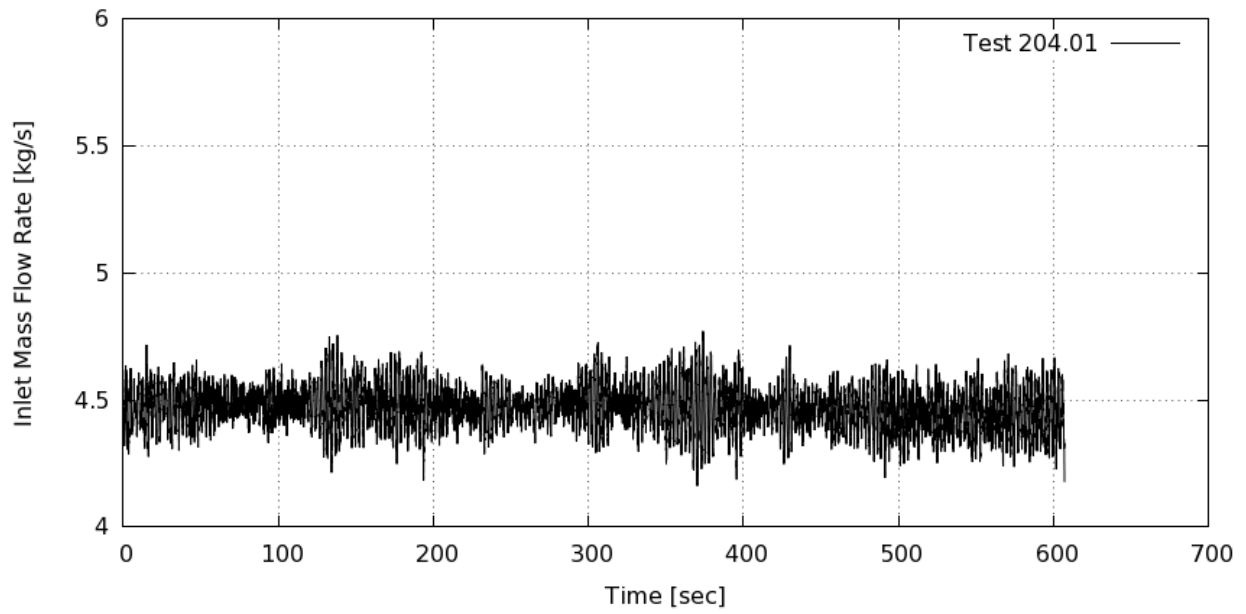
STS-123.03-109.01: Mass Flow Rate from DP-Inlet S73 CP12A



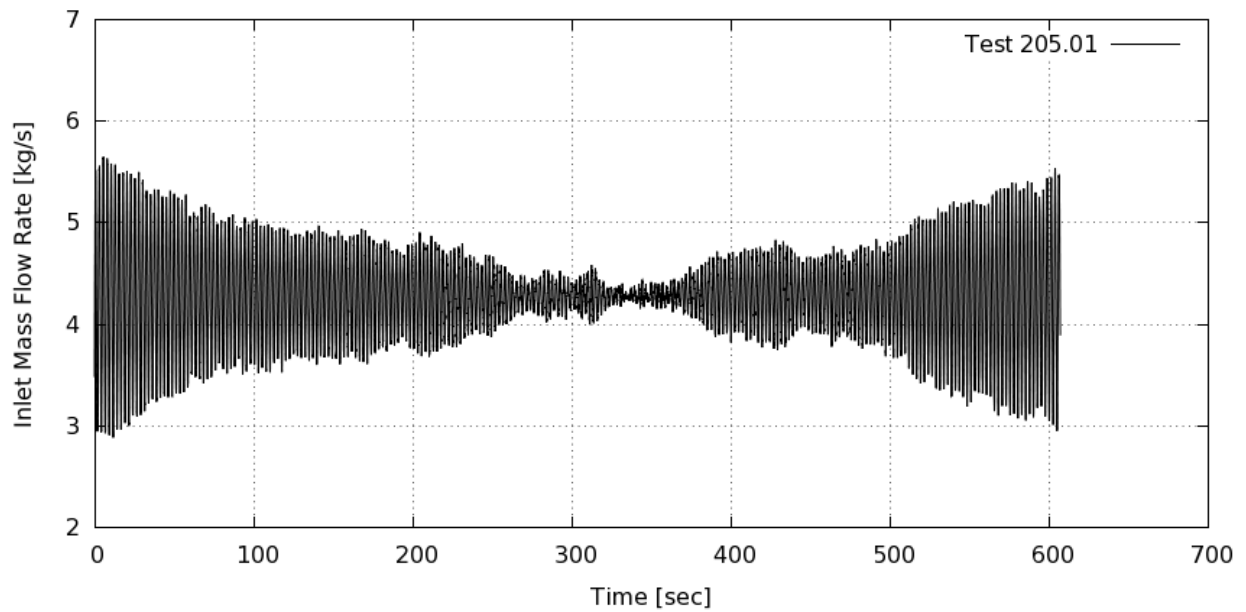
STS-123.03-110.01: Mass Flow Rate from DP-Inlet S73 CP12A



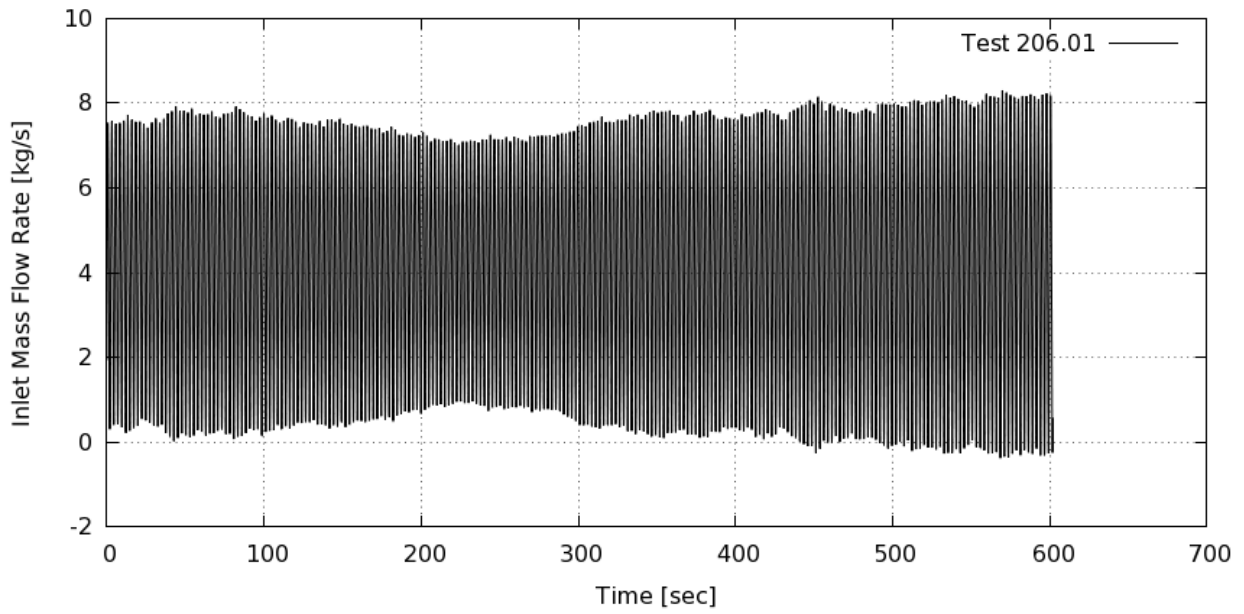
STS-123.03-203.02: Mass Flow Rate from DP-Inlet S73 CP12A



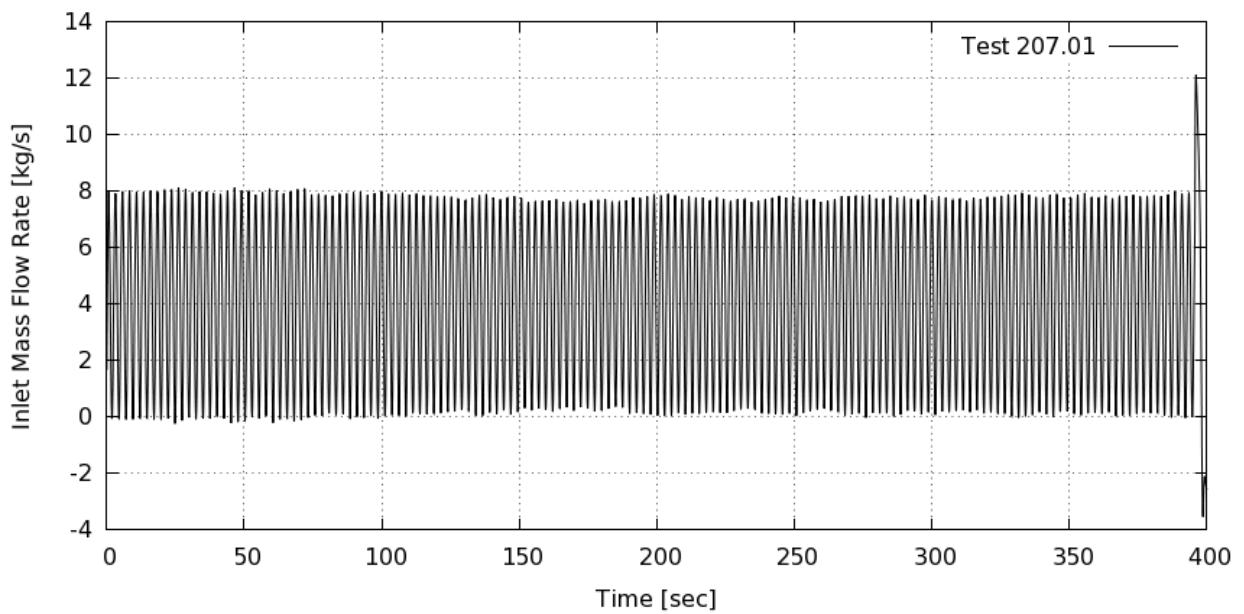
STS-123.03-204.01: Mass Flow Rate from DP-Inlet S73 CP12A



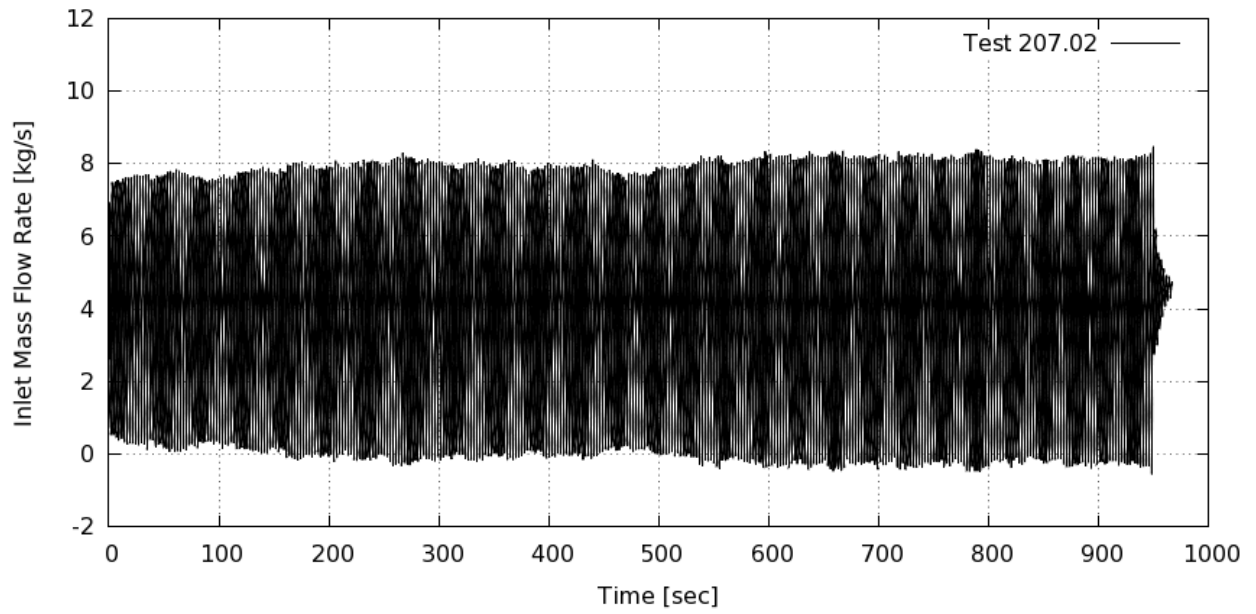
STS-123.03-205.01: Mass Flow Rate from DP-Inlet S73 CP12A



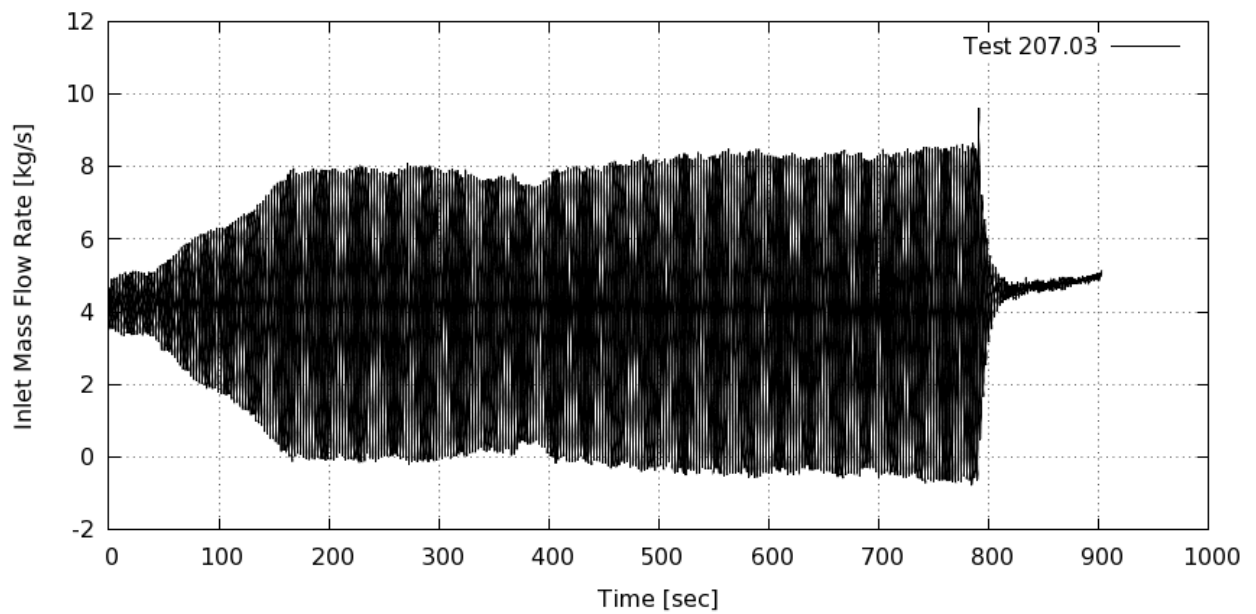
STS-123.03-206.01: Mass Flow Rate from DP-Inlet S73 CP12A



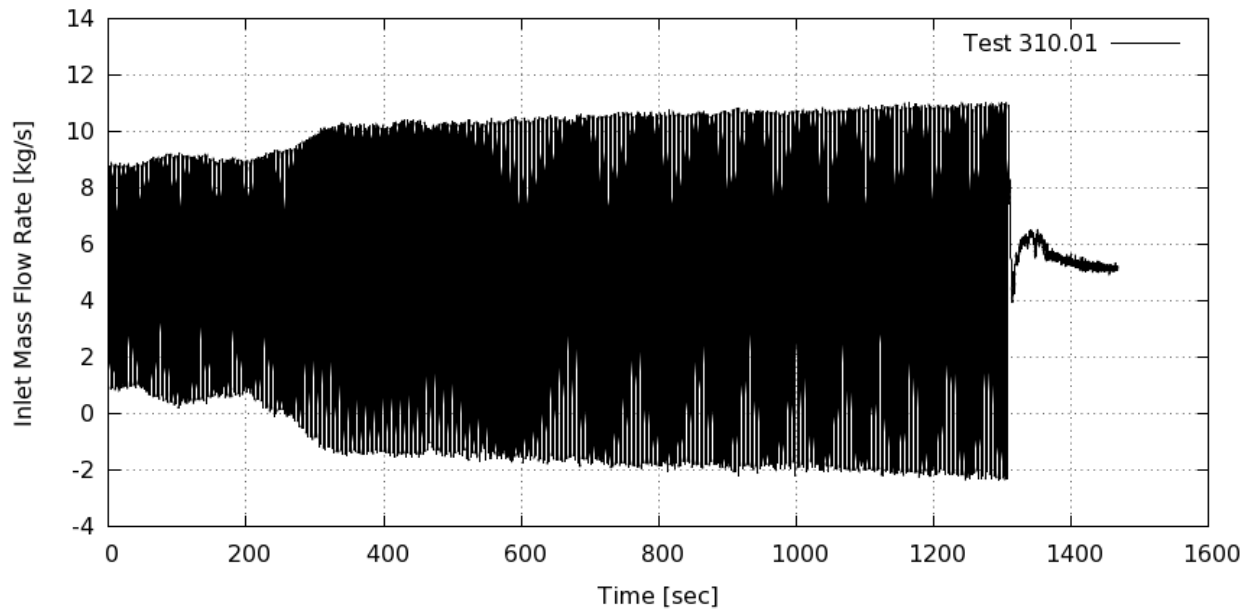
STS-123.03-207.01: Mass Flow Rate from DP-Inlet S73 CP12A



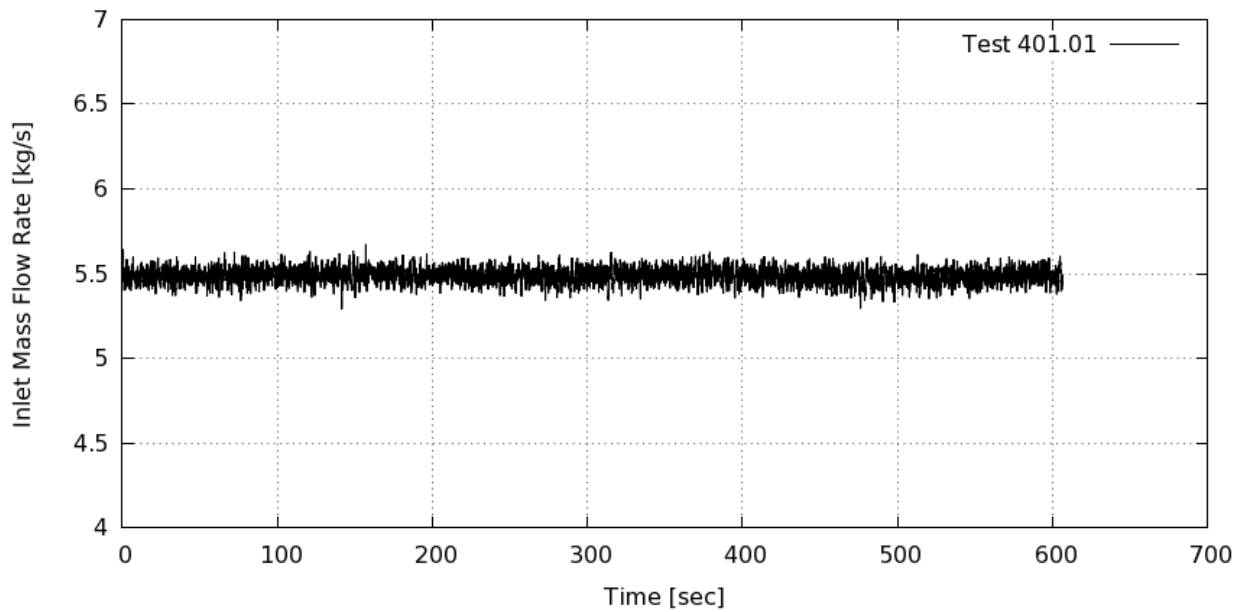
STS-123.03-207.02: Mass Flow Rate from DP-Inlet S73 CP12A



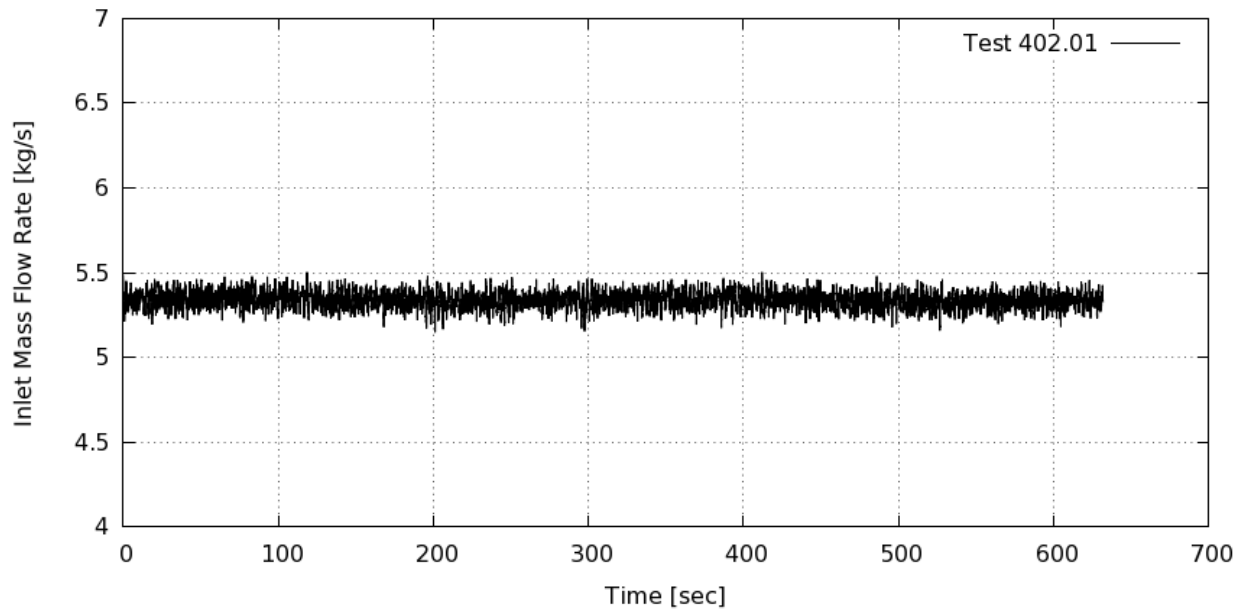
STS-123.03-207.03: Mass Flow Rate from DP-Inlet S73 CP12A



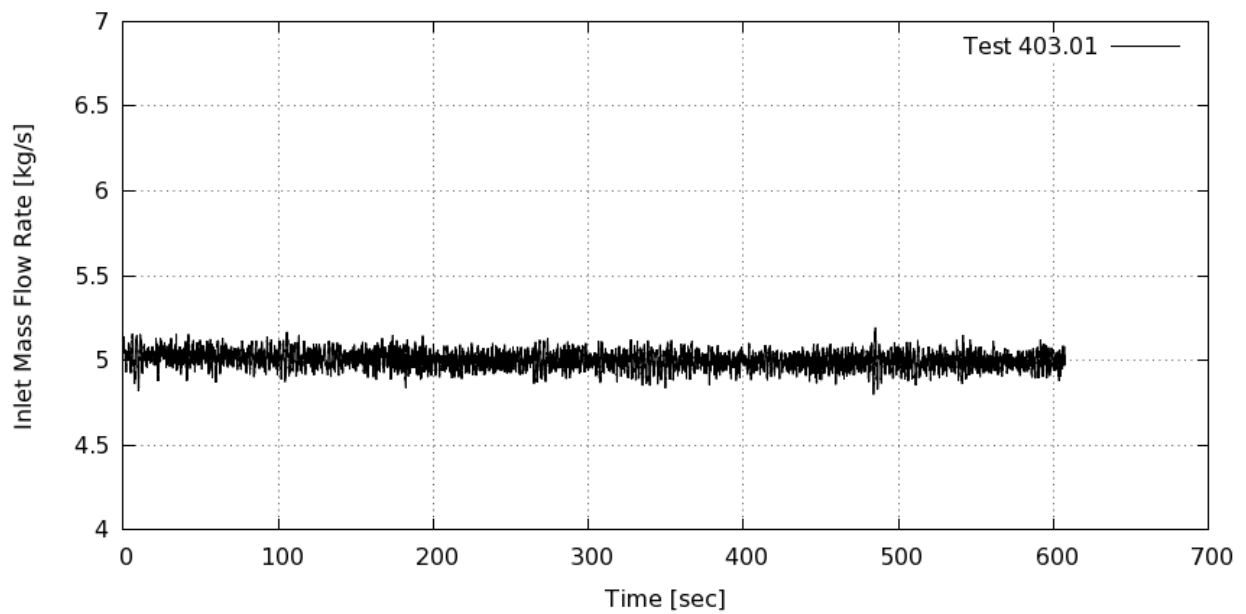
STS-123.03-310.01: Mass Flow Rate from DP-Inlet S73 CP12A



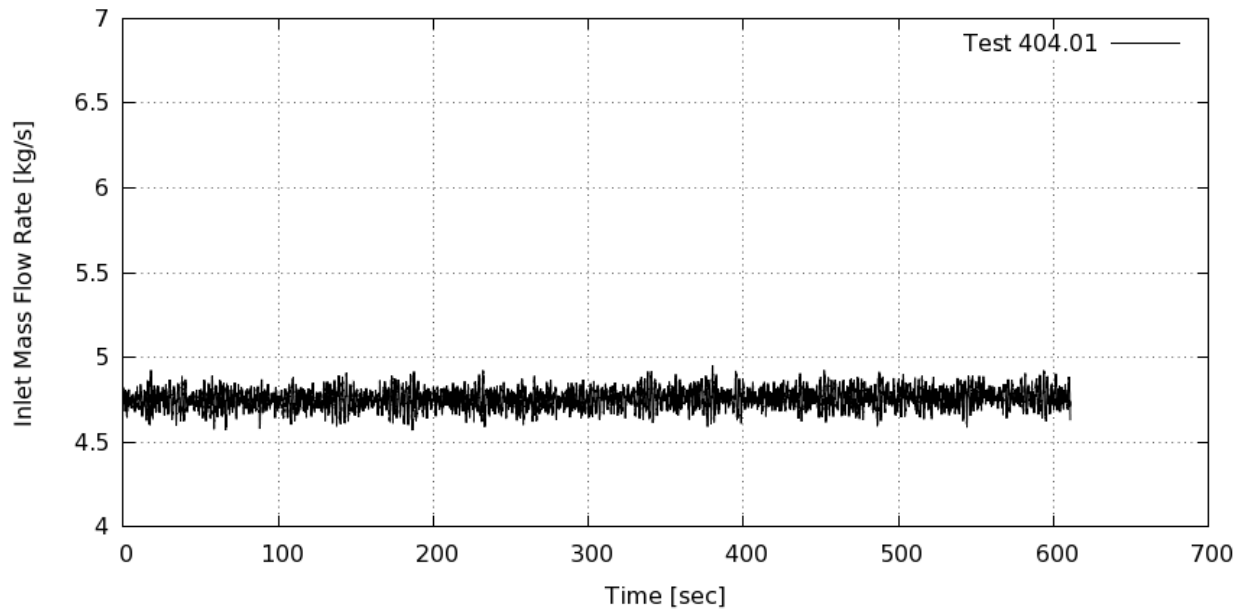
STS-123.03-401.01: Mass Flow Rate from DP-Inlet S73 CP12A



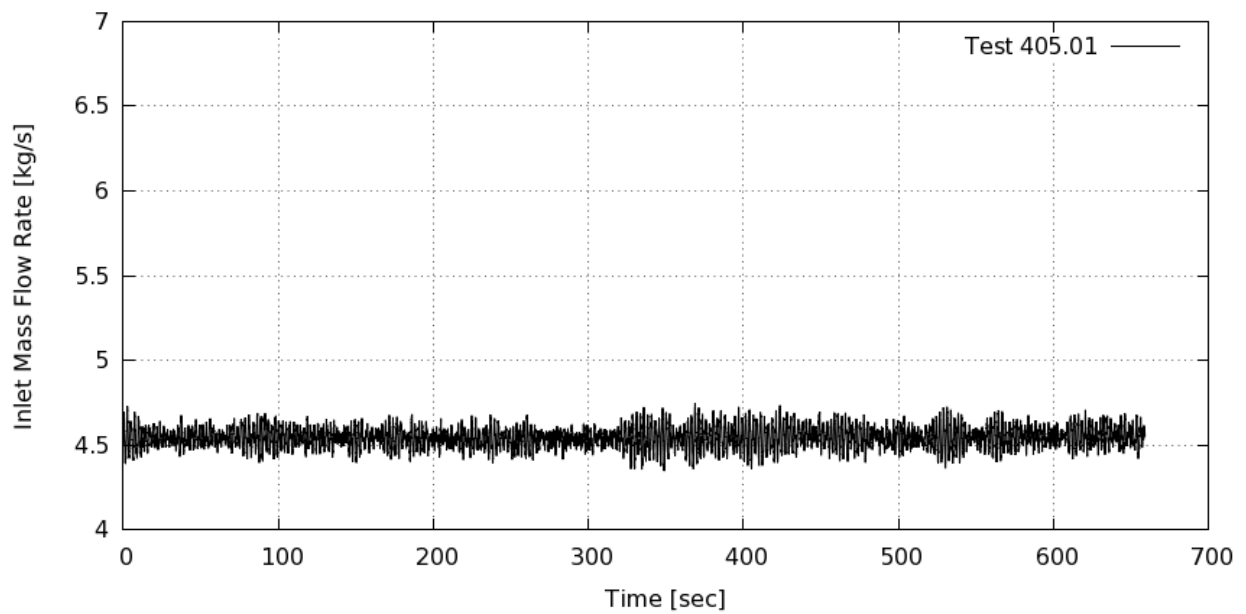
STS-123.03-402.01: Mass Flow Rate from DP-Inlet S73 CP12A



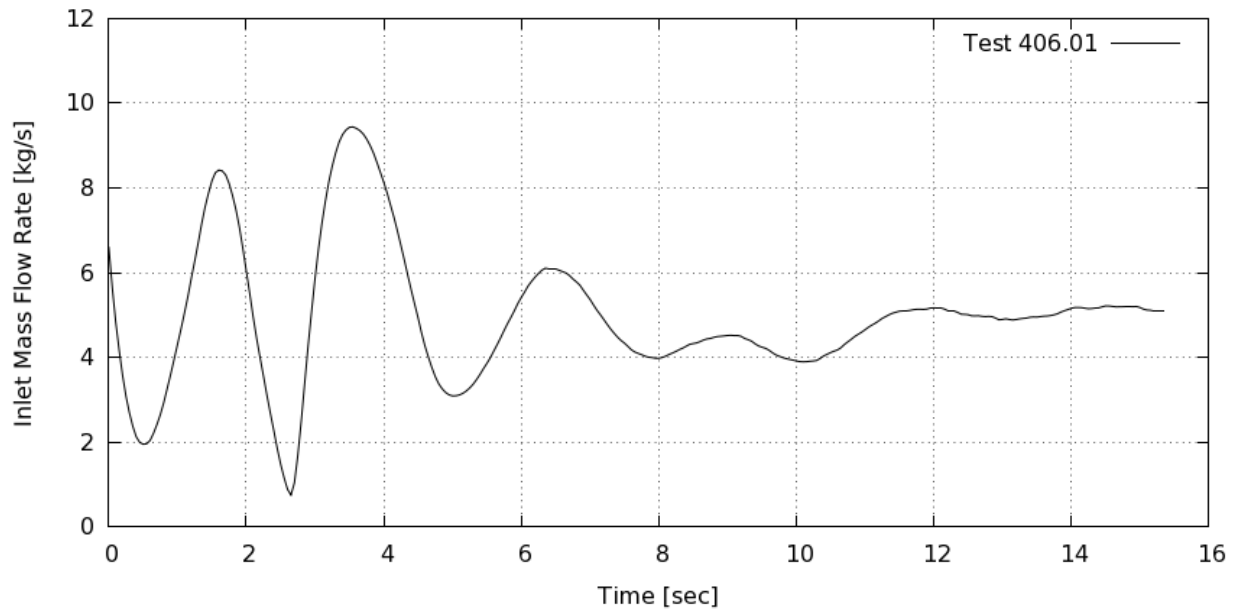
STS-123.03-403.01: Mass Flow Rate from DP-Inlet S73 CP12A



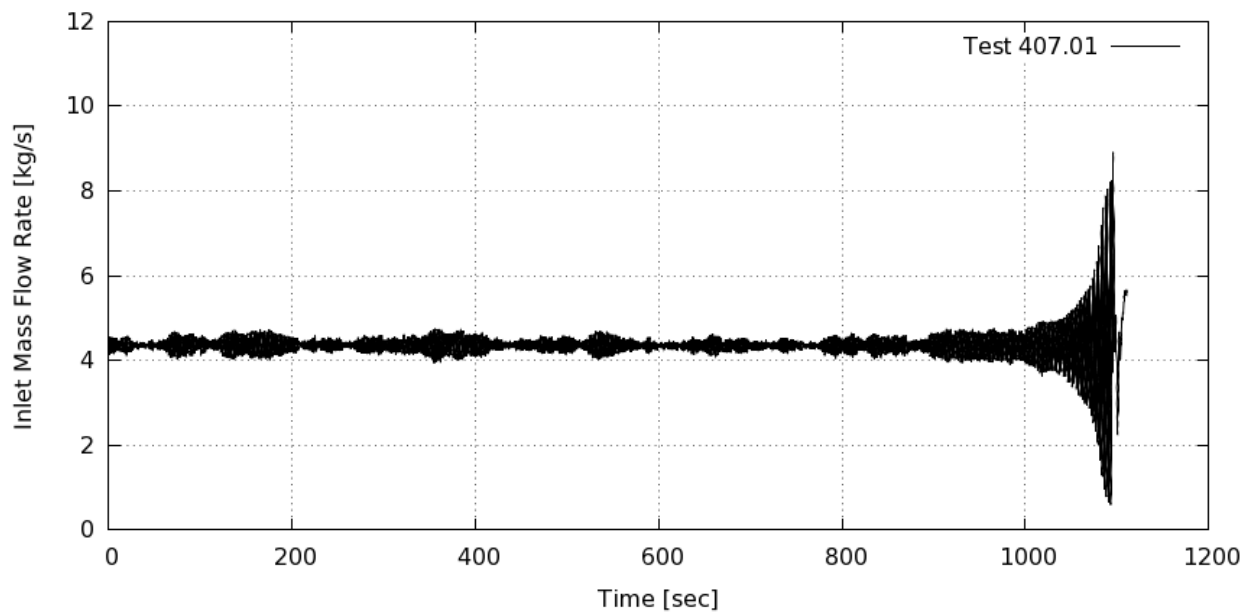
STS-123.03-404.01: Mass Flow Rate from DP-Inlet S73 CP12A



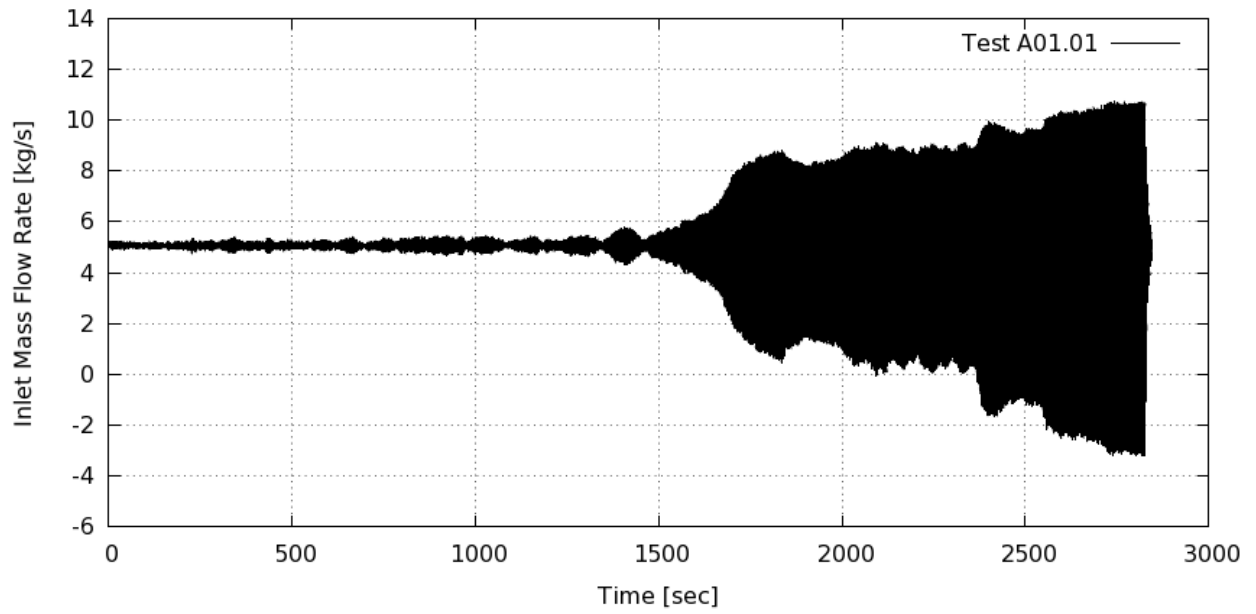
STS-123.03-405.01: Mass Flow Rate from DP-Inlet S73 CP12A



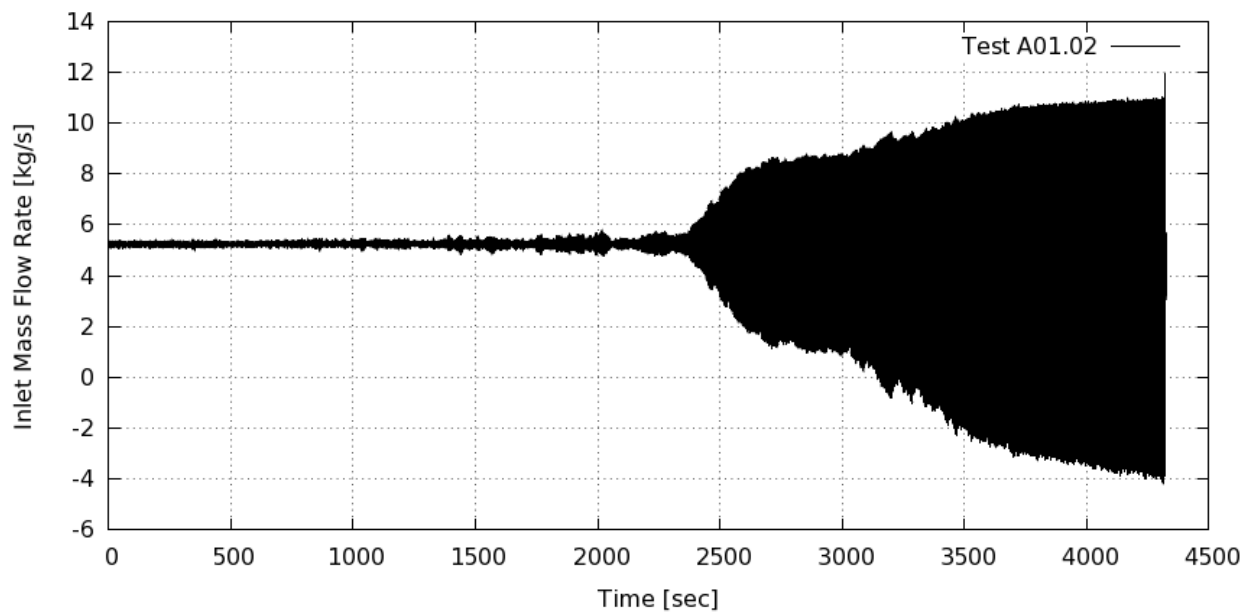
STS-123.03-406.01: Mass Flow Rate from DP-Inlet S73 CP12A



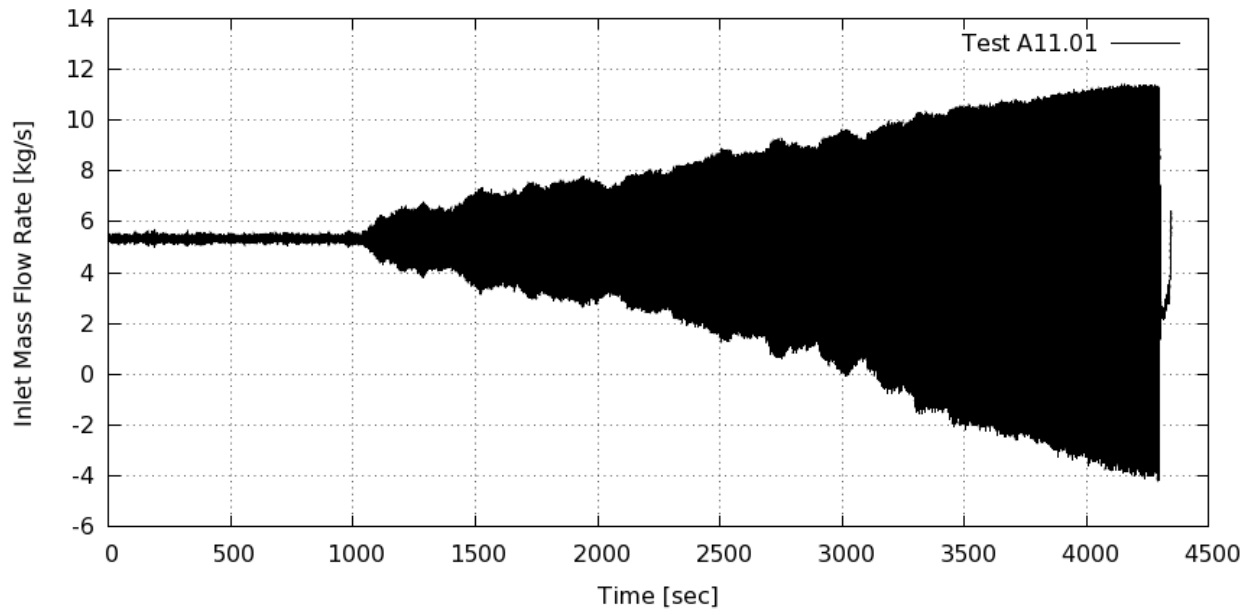
STS-123.03-407.01: Mass Flow Rate from DP-Inlet S73 CP12A



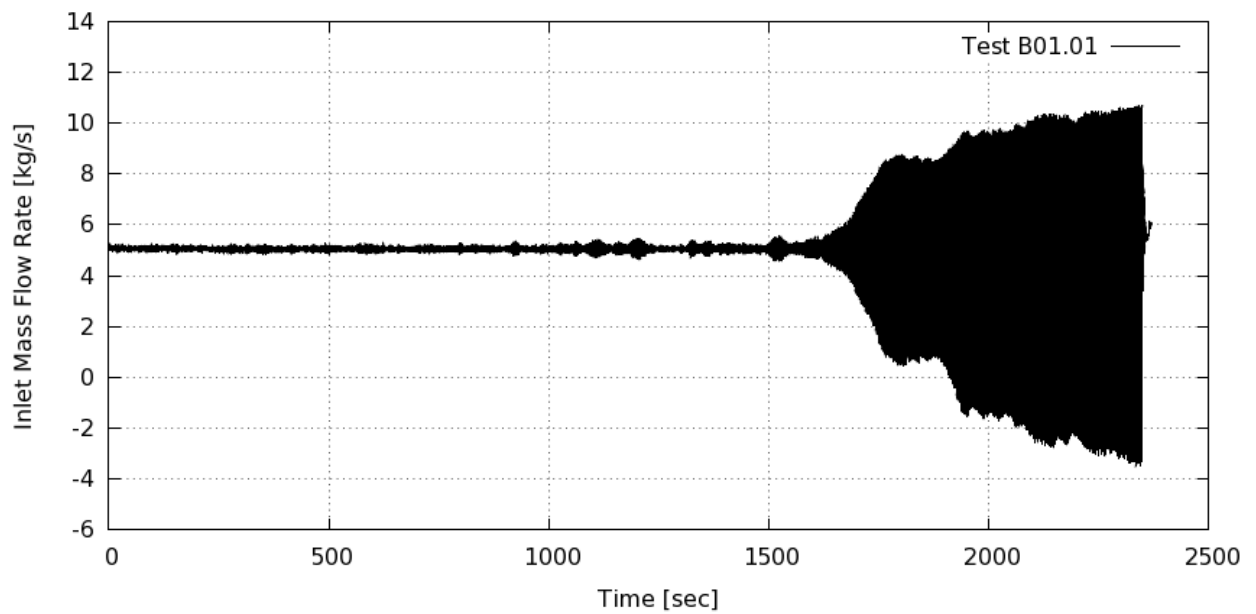
STS-123.03-A01.01: Mass Flow Rate from DP-Inlet S73 CP12A



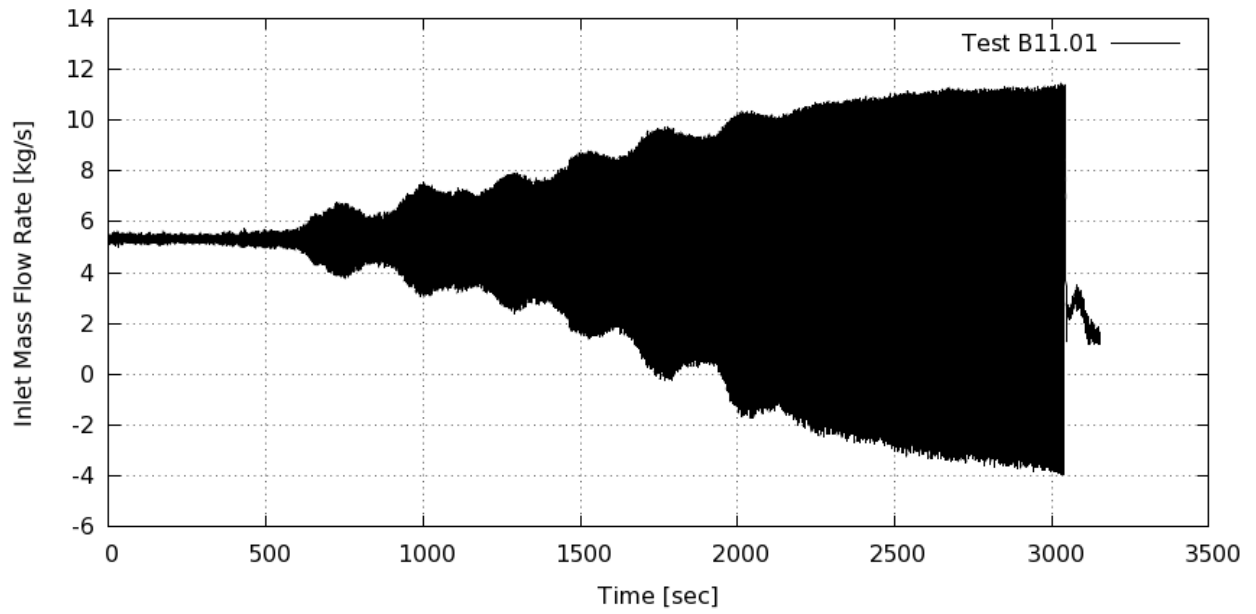
STS-123.03-A01.02: Mass Flow Rate from DP-Inlet S73 CP12A



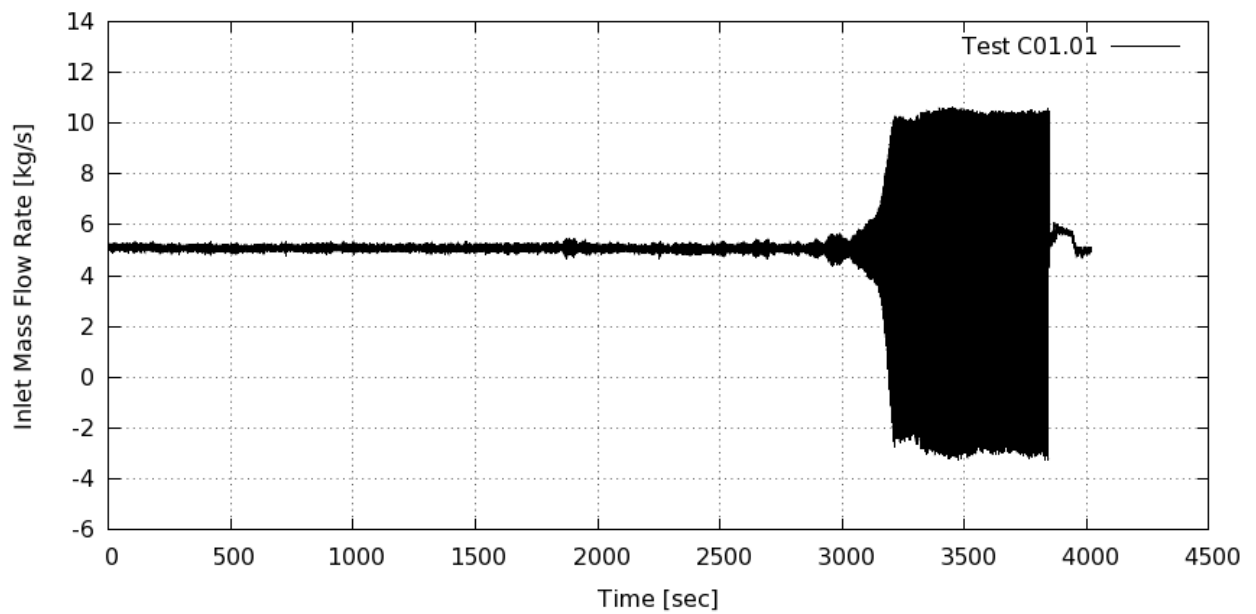
STS-123.03-A11.01: Mass Flow Rate from DP-Inlet S73 CP12A



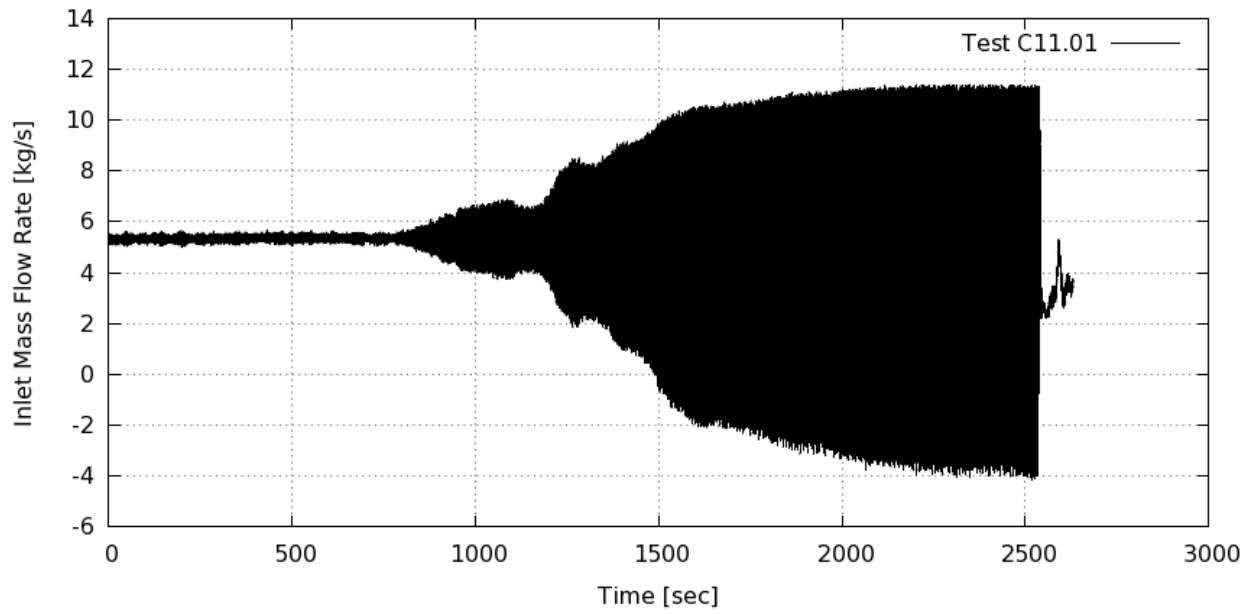
STS-123.03-B01.01: Mass Flow Rate from DP-Inlet S73 CP12A



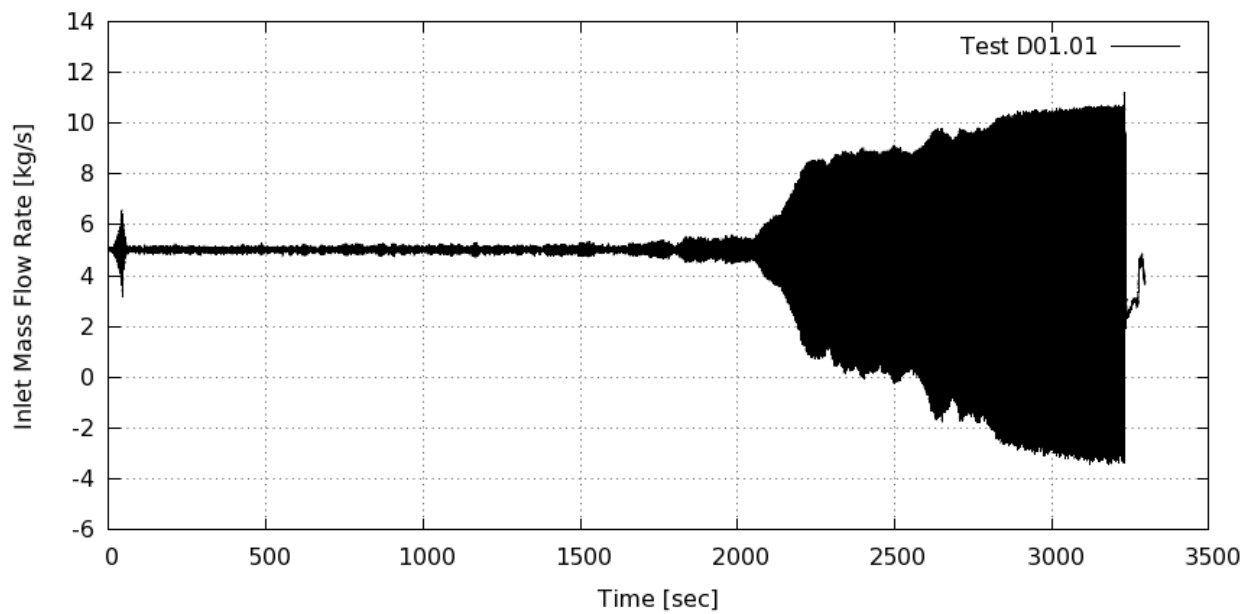
STS-123.03-B11.01: Mass Flow Rate from DP-Inlet S73 CP12A



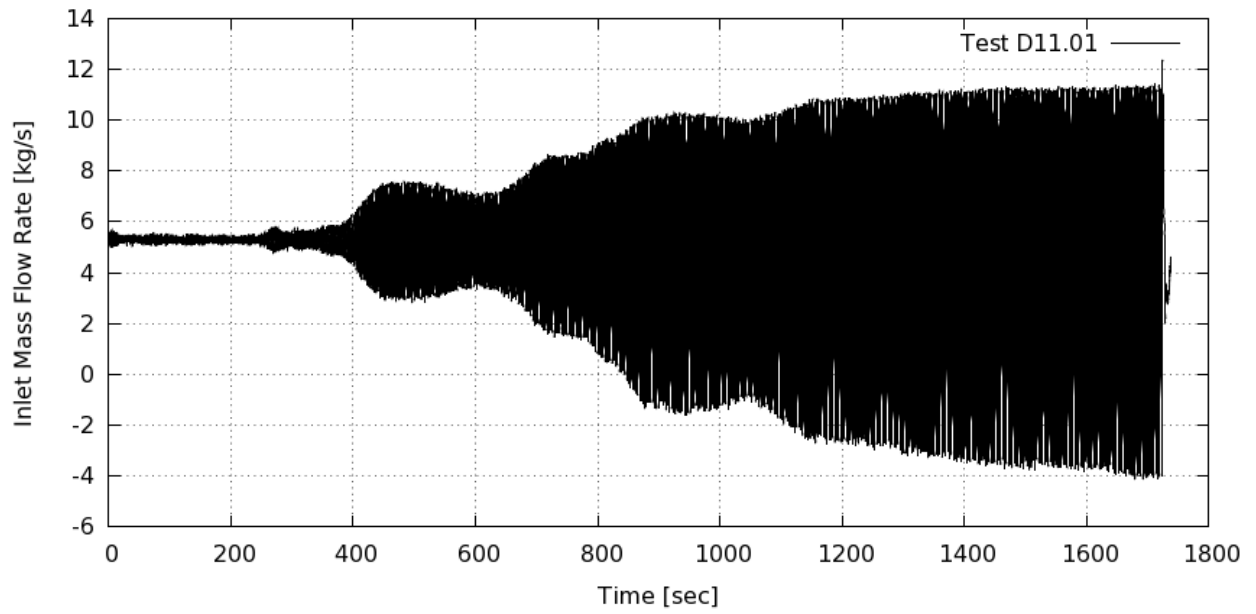
STS-123.03-C01.01: Mass Flow Rate from DP-Inlet S73 CP12A



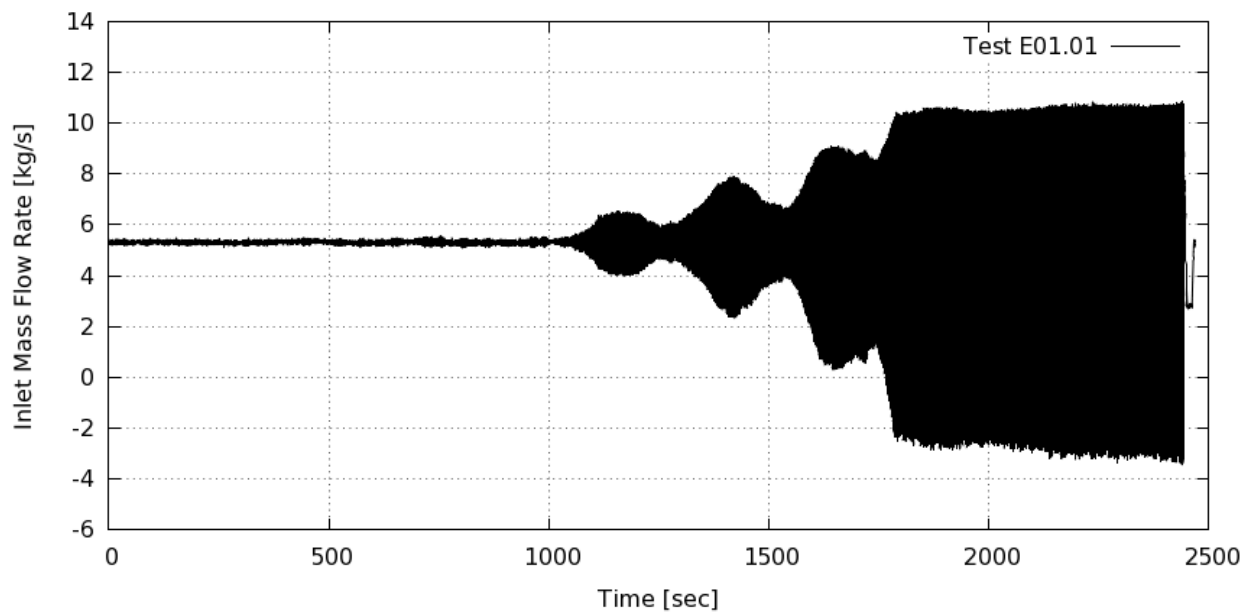
STS-123.03-C11.01: Mass Flow Rate from DP-Inlet S73 CP12A



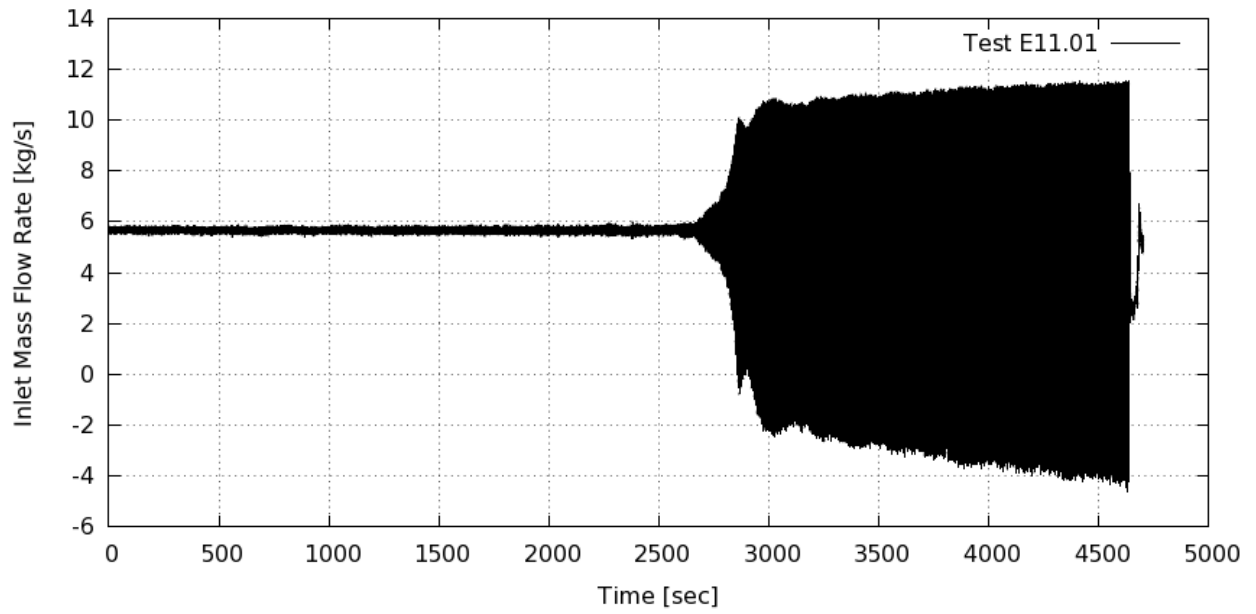
STS-123.03-D01.01: Mass Flow Rate from DP-Inlet S73 CP12A



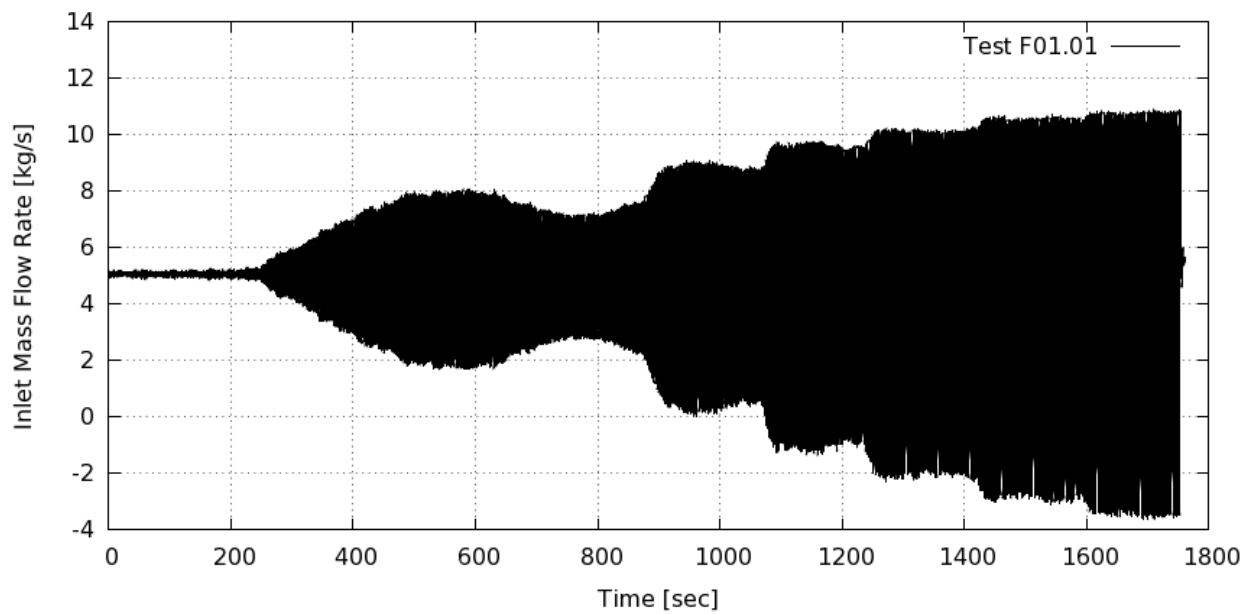
STS-123.03-D11.01: Mass Flow Rate from DP-Inlet S73 CP12A



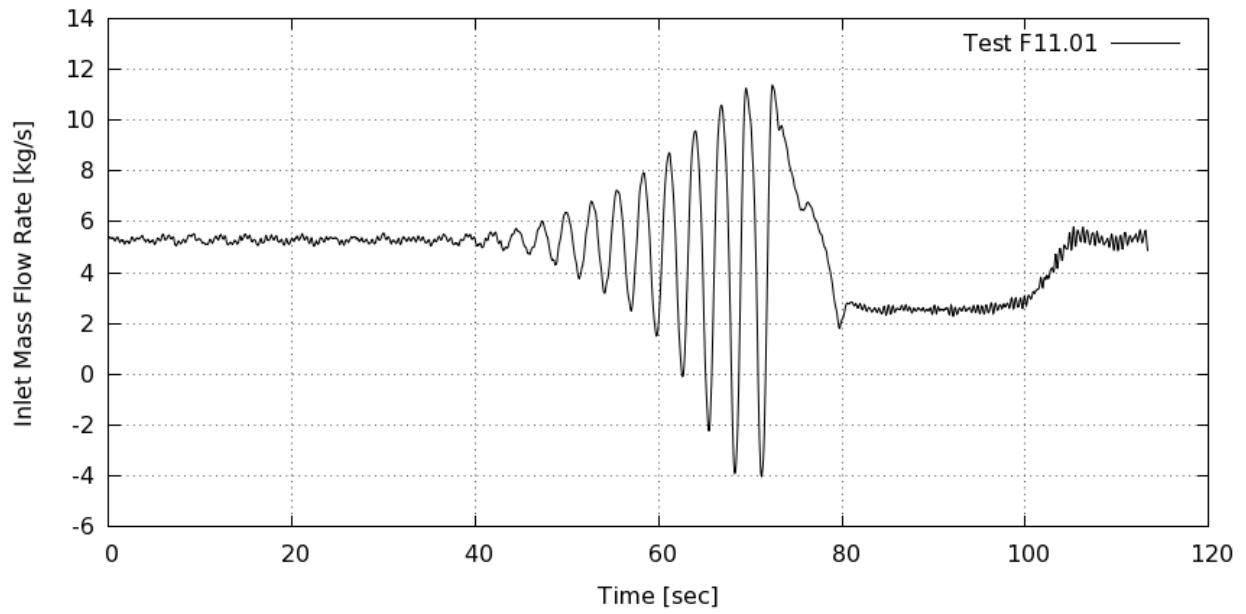
STS-123.03-E01.01: Mass Flow Rate from DP-Inlet S73 CP12A



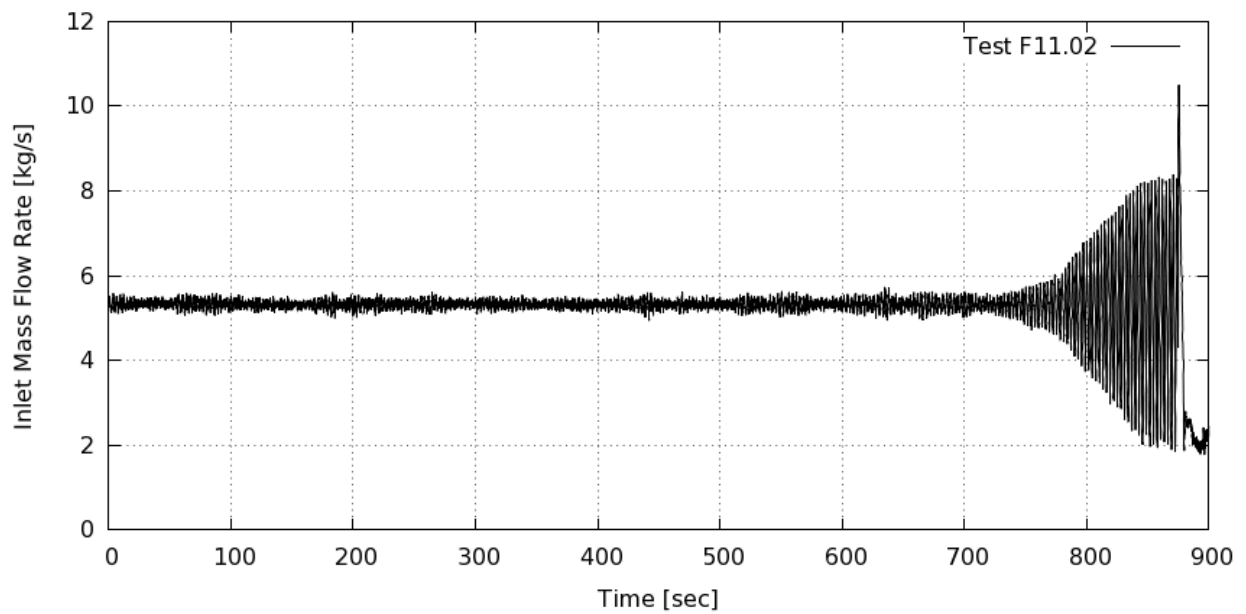
STS-123.03-E11.01: Mass Flow Rate from DP-Inlet S73 CP12A



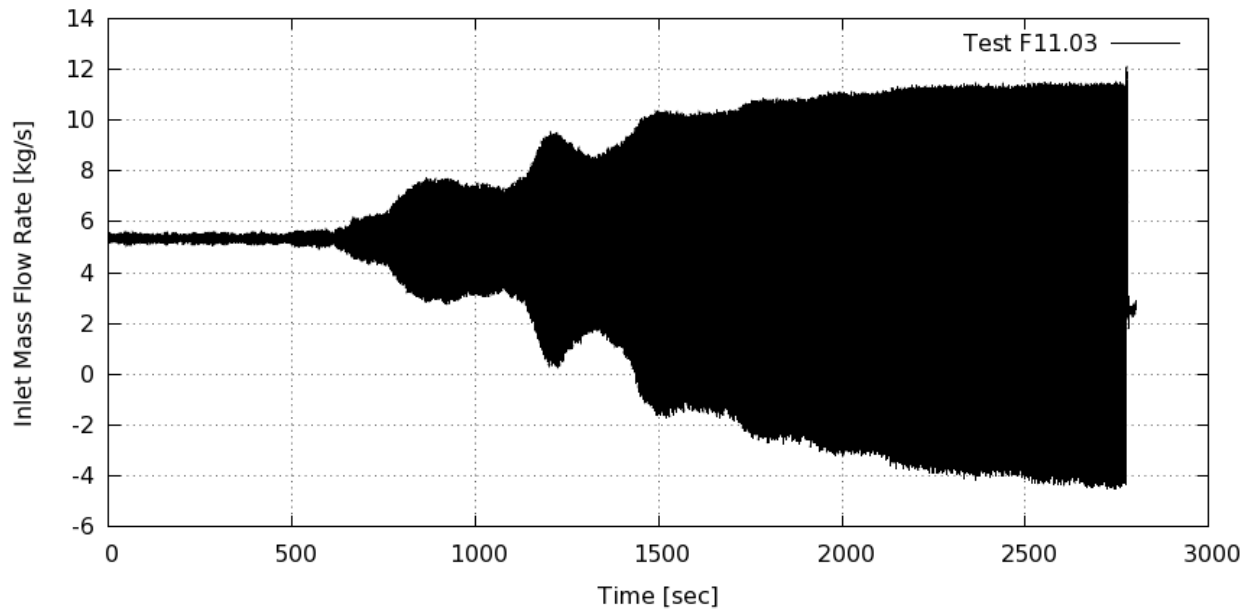
STS-123.03-F01.01: Mass Flow Rate from DP-Inlet S73 CP12A



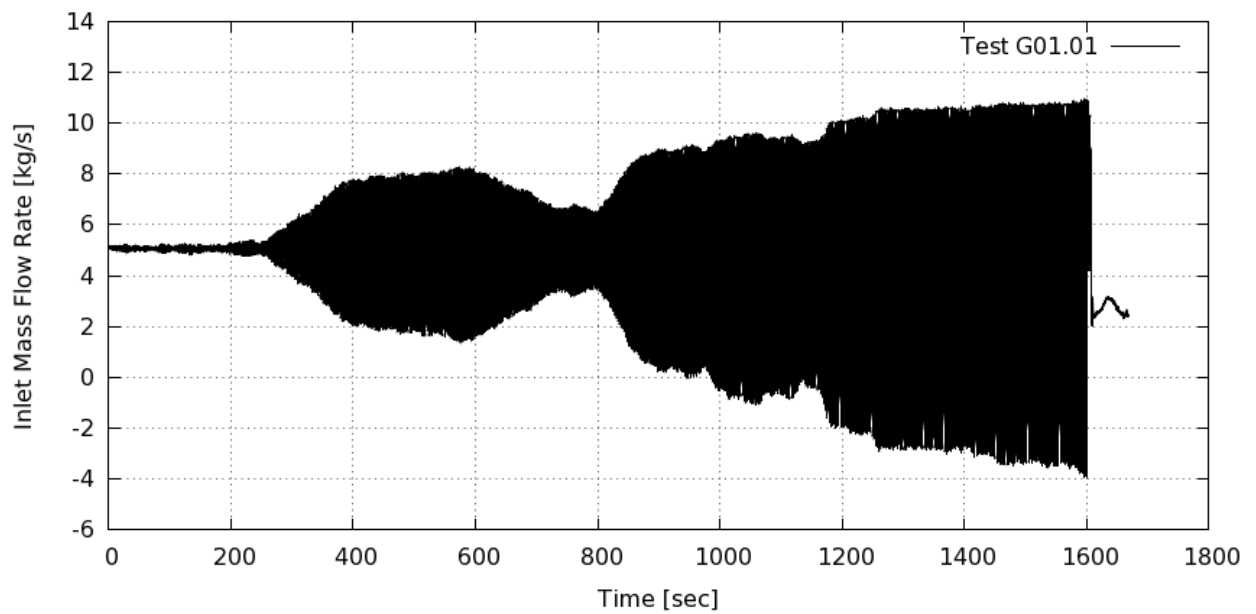
STS-123.03-F11.01: Mass Flow Rate from DP-Inlet S73 CP12A



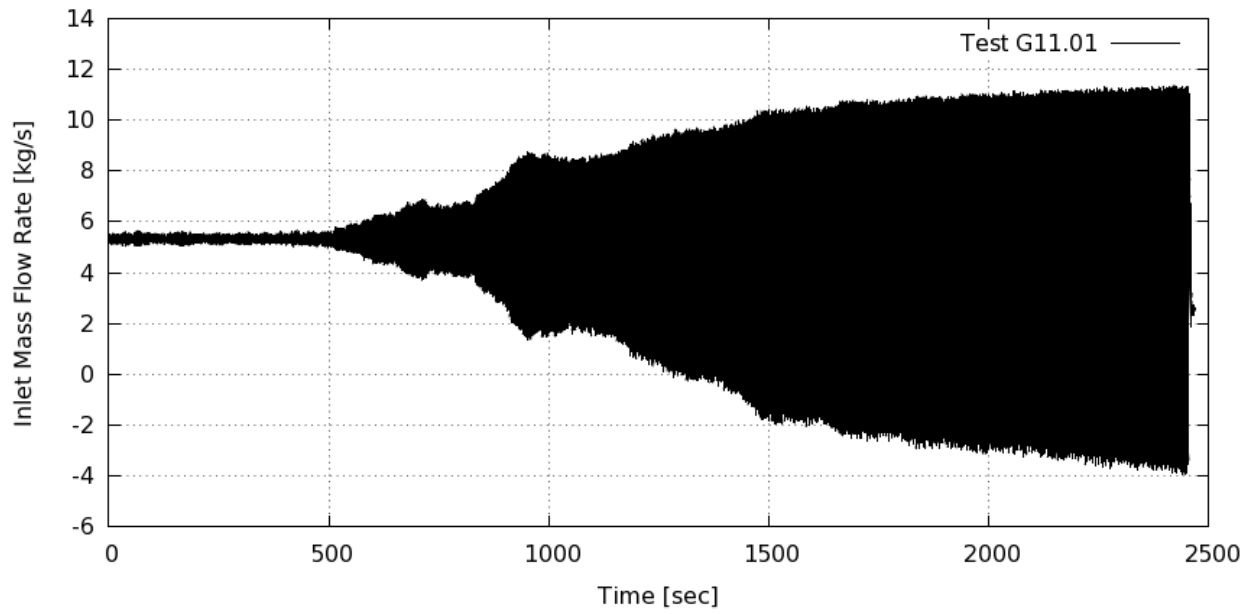
STS-123.03-F11.02: Mass Flow Rate from DP-Inlet S73 CP12A



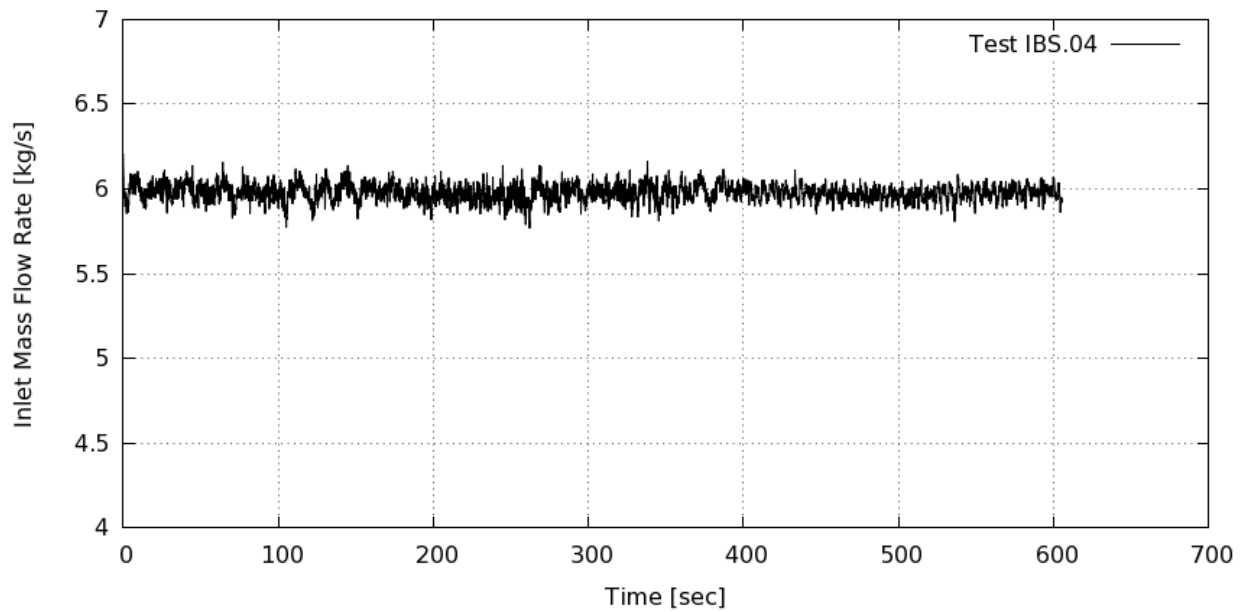
STS-123.03-F11.03: Mass Flow Rate from DP-Inlet S73 CP12A



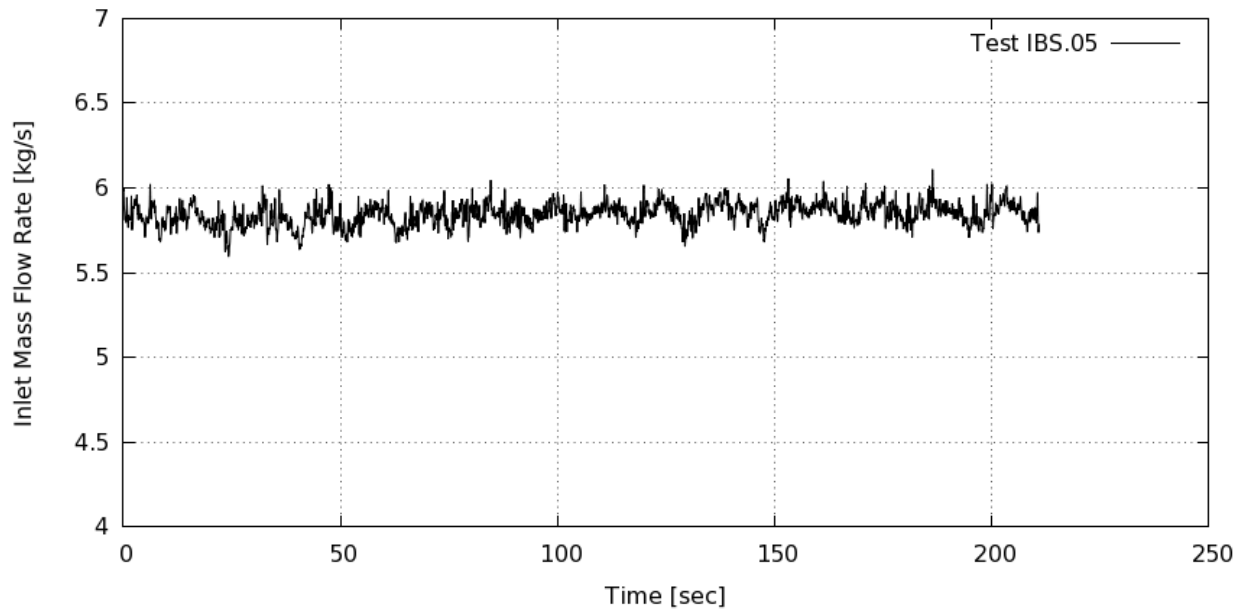
STS-123.03-G01.01: Mass Flow Rate from DP-Inlet S73 CP12A



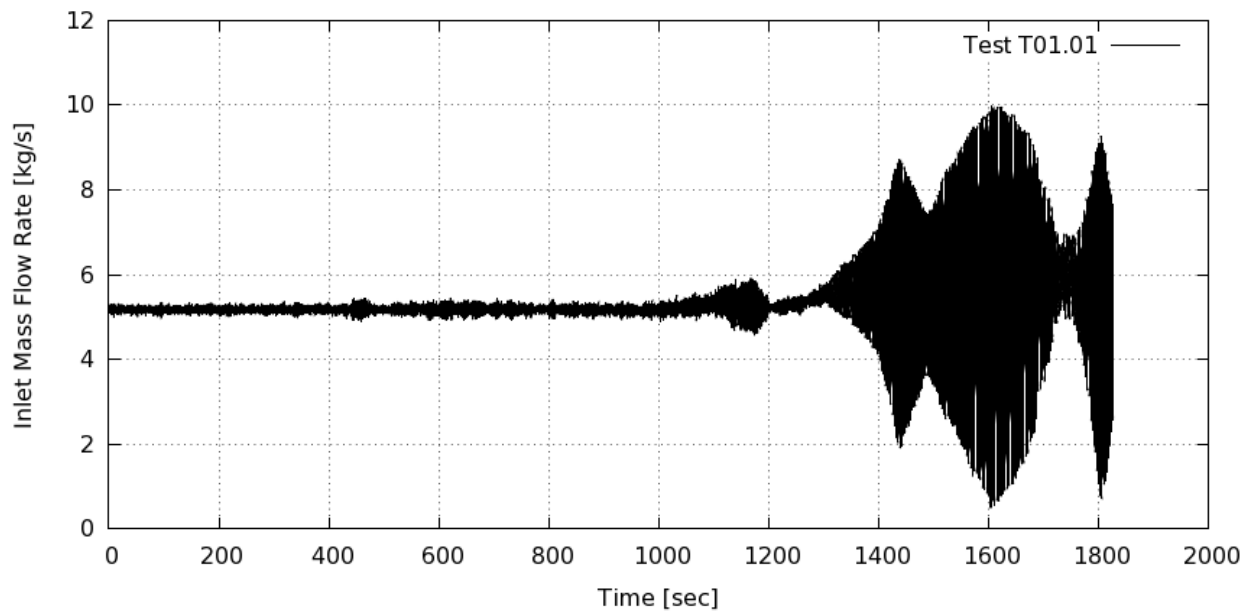
STS-123.03-G11.01: Mass Flow Rate from DP-Inlet S73 CP12A



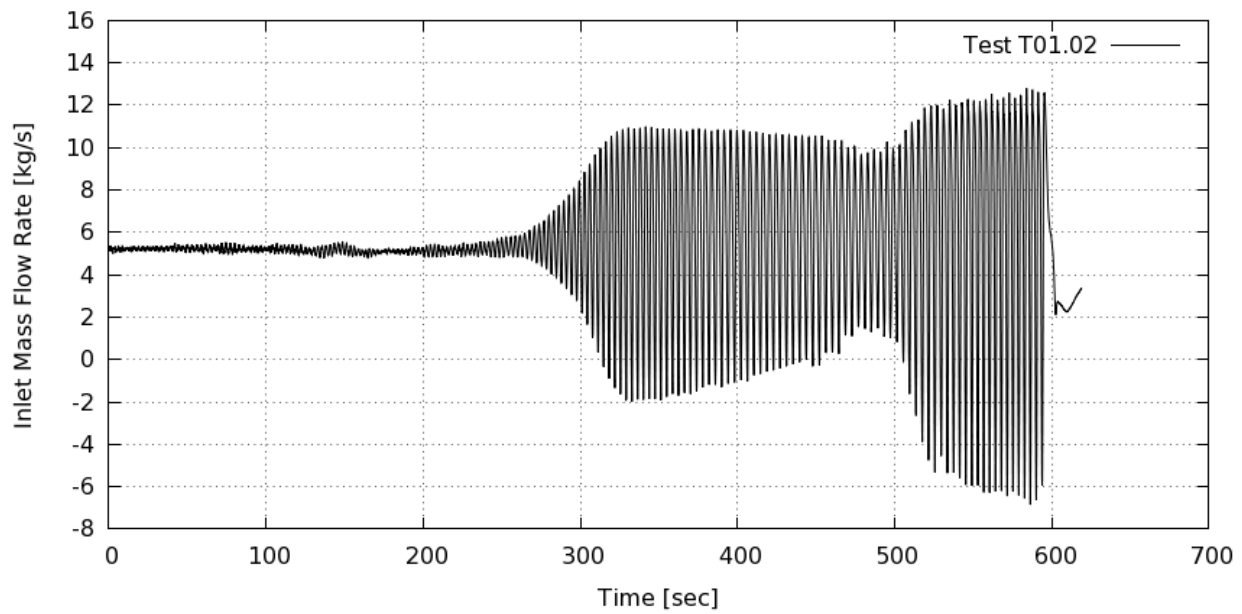
STS-123.03-IBS.04: Mass Flow Rate from DP-Inlet S73 CP12A



STS-123.03-IBS.05: Mass Flow Rate from DP-Inlet S73 CP12A



STS-123.03-T01.01: Mass Flow Rate from DP-Inlet S73 CP12A



STS-123.03-T01.02: Mass Flow Rate from DP-Inlet S73 CP12A

BIBLIOGRAPHIC DATA SHEET

(See instructions on the reverse)

NUREG/CR-7272

2. TITLE AND SUBTITLE

NRC ATWS-I Stability Tests with Downskew Axial Power Profile

KATHY Test Series STS123

3. DATE REPORT PUBLISHED

MONTH

September

YEAR

2020

4. FIN OR GRANT NUMBER

5. AUTHOR(S)

Daniel Tinkler, Kenneth Greene, Kevin Quick, Juris Kronenberg, Roger Velten, Franz Wehle, Achim Beisiegel, Thomas Berger, Fouad El Rharbaoui, Peter Yarsky

6. TYPE OF REPORT

Technical

7. PERIOD COVERED (Inclusive Dates)

8. PERFORMING ORGANIZATION - NAME AND ADDRESS (If NRC, provide Division, Office or Region, U. S. Nuclear Regulatory Commission, and mailing address; if contractor, provide name and mailing address.)

Framatome Inc.
2101 Horn Rapids Road
Richland, WA 99354

9. SPONSORING ORGANIZATION - NAME AND ADDRESS (If NRC, type "Same as above", if contractor, provide NRC Division, Office or Region, U. S. Nuclear Regulatory Commission, and mailing address.)

Division of System Analysis
Office of Nuclear Regulatory Research
U.S. Nuclear Regulatory Commission
Washington, DC 20555-0001

10. SUPPLEMENTARY NOTES

T. Zaki, NRC Project Manager

11. ABSTRACT (200 words or less)

Natural circulation instability tests were performed in the Multifunction Thermal Hydraulic Test Facility KATHY in Karlstein, Germany. One type of test involved stepping up test assembly power in oscillating flow until failure to rewet occurs based on temperature observation. A second type of test introduced a simulated neutronic feedback to dynamically change the power, again with flow oscillations up to the point of failure to rewet. Two tests featured a transient inlet temperature. The largest flow oscillations in the test program ranged from ~ -7 kg/s to 13 kg/s. The tests varied system pressure (7 and 8 MPa), water level in the steam-water separator (0.4 and 1.1 m), and inlet subcooling (20 K and 35 K). These tests simulated a full-scale boiling-water reactor rod bundle. Before the dynamic instability tests, the rod bundle was characterized with single-phase and two-phase pressure drop tests. Steady-state critical power tests were also performed to characterize the conditions under which steady-state dryout occurs. This report describes the tests performed as part of this program.

12. KEY WORDS/DESCRIPTORS (List words or phrases that will assist researchers in locating the report.)

Boiling-Water Reactor, Anticipated Transient Without SCRAM, Instability, Dryout, Critical Heat Flux, Pressure Drop, KATHY Loop

13. AVAILABILITY STATEMENT

unlimited

14. SECURITY CLASSIFICATION

(This Page)

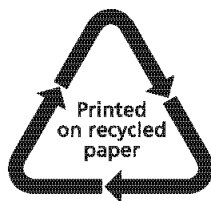
unclassified

(This Report)

unclassified

15. NUMBER OF PAGES

16. PRICE



Federal Recycling Program



**UNITED STATES
NUCLEAR REGULATORY COMMISSION
WASHINGTON, DC 20555-0001**

OFFICIAL BUSINESS



@NRCgov



NUREG/CR-7272

NRC ATWS-I Stability Tests with Downskew Axial Power Profile

September 2020